

THE DISCOVERY OF CHROMIUM-PHOTOCATALYZED RADICAL CATION REACTIONS AND  
EXPLOITS IN 1,6-ENYNE CYCLOISOMERIZATION

by

SUSAN MARIE STEVENSON

(Under the Direction of Eric M. Ferreira)

ABSTRACT

In recent years, the reemergence of photoredox catalysis has inspired exciting new prospects in the field of synthetic organic chemistry. Visible light-activated complexes of rare transition metals Ru and Ir have received considerable attention for their ability to efficiently incite these single-electron processes. In an effort to develop new and more sustainable photocatalysts, we have begun exploring synthetic applications of earth-abundant Cr-based photoredox catalysts. So far, these photooxidizing Cr complexes have been demonstrated to catalyze radical cation Diels-Alder reactions of electron-rich dienophiles. The critical roles of oxygen in this reaction have been investigated, revealing differential behavior between the Cr and Ru photocatalyst systems. Recent research has also uncovered a novel Cr-photocatalyzed radical cation [4+2] cycloaddition of electron-poor dienophiles. Remarkably, this approach provides access to [4+2] adducts of reversed regioselectivity compared to the adducts formed under conventional Diels-Alder conditions. Preliminary mechanistic results point to two competing pathways—a photochemical [2+2] cycloaddition followed by a radical cation vinylcyclobutane rearrangement, and exciplex formation followed by oxidation to generate a radical cation—that both lead to the reversed Diels-Alder products.

We have also explored C–C bond migration in the cycloisomerization of oxygen-tethered 1,6-enynes. Under Pt(II) or Ir(I) catalysis, cyclic and acyclic alkyl groups were found to undergo 1,2-shifts into metal carbenoids. Interestingly, this process does not appear to be driven by the release of ring strain, and thus provides access to large carbocyclic frameworks. The beneficial effect of CO on the Pt(II) and Ir(I) catalytic systems was also evaluated.

INDEX WORDS: Photocatalysis, Radical cation reaction, Diels-Alder cycloaddition, Alkyne activation, Cycloisomerization, Alkyl migration

THE DISCOVERY OF CHROMIUM-PHOTOCATALYZED RADICAL CATION REACTIONS AND  
EXPLOITS IN 1,6-ENYNE CYCLOISOMERIZATION

by

SUSAN MARIE STEVENSON

B.S., Hope College, 2011

A Dissertation Submitted to the Graduate Faculty of The University of Georgia in Partial Fulfillment of  
the Requirements for the Degree

DOCTOR OF PHILOSOPHY

ATHENS, GEORGIA

2016

© 2016

Susan Marie Stevenson

All Rights Reserved

THE DISCOVERY OF CHROMIUM-PHOTOCATALYZED RADICAL CATION REACTIONS AND  
EXPLOITS IN 1,6-ENYNE CYCLOISOMERIZATION

by

SUSAN MARIE STEVENSON

Major Professor:	Eric Ferreira
Committee:	Ryan Hili
	Robert Phillips

Electronic Version Approved:

Suzanne Barbour  
Dean of the Graduate School  
The University of Georgia  
August 2016

DEDICATION

*For my parents*

## ACKNOWLEDGMENTS

First and foremost, I would like to thank Eric. Without his guidance and encouragement, none of this would have been possible. Thank you for your confidence in my abilities and for your dedication to my development as a chemist. I hope I can make you proud at Caltech and beyond.

I would also like to acknowledge past and present members of the Ferreira Lab. Lil Mike, you were an amazing mentor to me since my first day in the lab, and even now you continue to be a valued source of advice. I can't believe you came to my defense—what a pleasant surprise. Thank you for constantly challenging me to learn more and work harder. Yes, I do remember that time I poured my ice bath into the trash. Thanks for bringing it up. Doug and Paul, thank you for being role models and leaders in the lab, and for generally being fun to work with. Except for that time Paul hid my fountain drink from me and I didn't notice for a week. I'm still upset about that. Tarik, I haven't used the hotline in a while, but you're still my C2B2F2. I miss our days playing softball with the Quantum Mechanics. It was awesome having you at my defense; the Ferreira Lab is not the same without you. Please don't let that make you sad. Phil, thank you for being such a great lab mate and friend these past two years in Georgia. I'm sorry I got you addicted to fountain drinks. Also, remember when we went to see the Decemberists and I locked my keys in the car? I'm sorry about that, too. But that was still a lot of fun. Lastly, thank you for sharing your Lifesaver gummies with me; I know how important they are to you. Francisco, thank you for your passion for the Cr photochemistry; I'm excited to see where you take the project next. Also, your enthusiasm for Corndog Queso Day was much appreciated. Tyler, Jeff, and Sheneika, it's been great getting to know all of you this past year. Great things are ahead for you, I'm sure. Good luck making the cookies, Willis. Last but not least, Sang, thank you for all your dedication and hard work, and for being patient with me while I've been writing this dissertation. Most importantly, thank you for letting us know where all the free food is. And for bringing us scones.

I have been very fortunate to be able to collaborate with an excellent group of graduate students and PI's at Colorado State University and the University of Colorado–Boulder. Robert, Steve, and Sam, thank you for your hard work and insight. Matt, Tony, and Niels, thank you for the enriching Skype discussions, which have greatly enhanced my understanding of our project and taught me to think about my research from different perspectives.

Darrin, best friend, thank you for always being down to get BFFFDs, TGIFDs, LJFDs (Fofos), MDFDs, SWFDs, BDFDs, etc., with me. And for being my BFF.

Alex, thank you for helping to make our time in graduate school some of my favorite years yet. I can't wait to travel the country with you and for our future adventures in Pasadena.

Lastly, I would like to thank all my friends and family. To my parents especially, I would not have been able to accomplish what I have today without your constant support and encouragement. This dissertation is for you. Thank you.

## TABLE OF CONTENTS

	Page
ACKNOWLEDGMENTS.....	v
LIST OF TABLES .....	x
LIST OF FIGURES.....	xi
LIST OF SCHEMES.....	xiii
CHAPTER	
1 1,6-ENYNE CYCLOISOMERIZATION AND ALKYL MIGRATIONS VIA ALKYNE ACTIVATION.....	1
1.1 Introduction: 1,6-Enyne Cycloisomerization .....	1
1.2 Brief Introduction to Alkyne Activation.....	2
1.3 Proposed Mechanism for Cycloisomerization of 1,6-Enynes.....	4
1.4 Cycloisomerization of 1,6-Enynes.....	5
1.5 1,2-Alkyl Migrations via Alkyne Activation .....	12
1.6 Project Proposal .....	15
Chapter 1 Notes and References .....	16
2 C-C BOND MIGRATION IN THE CYCLOISOMERIZATION OF 1,6-ENYNES.....	18
2.1 Introduction: Project Proposal .....	18
2.2 Preliminary Results .....	19
2.3 Reaction Optimization .....	19
2.4 Substrate Scope.....	27
2.5 Synthesis of Macrolactones from Cycloisomerization Products .....	34
2.6 Conclusion .....	34
2.7 Experimental Section .....	35

Chapter 2 Notes and References .....	97
3 PHOTSENSITIZED [2+2] AND [4+2] RADICAL CATION CYCLOADDITIONS.....	99
3.1 Introduction: Radical Cation Reactions of Alkenes.....	99
3.2 [2+2] Radical Cation Cycloadditions.....	102
3.3 [4+2] Radical Cation Cycloadditions.....	127
3.4 Competing [2+2] and [4+2] Mechanistic Pathways .....	146
3.5 Conclusion .....	157
Chapter 3 Notes and References .....	159
4 CHROMIUM-PHOTOCATALYZED RADICAL CATION DIELS-ALDER REACTIONS OF ELECTRON-RICH DIENOPHILES .....	166
4.1 Photooxidizing Chromium Catalysts .....	166
4.2 Preliminary Experiments.....	167
4.3 [4+2] Dimerization of 1,3-Cyclohexadiene .....	168
4.4 Cross [4+2] Cycloadditions .....	170
4.5 Mechanistic Studies .....	183
4.6 Stereoconvergence .....	192
4.7 Differential Reactivity in Intramolecular Cycloadditions.....	202
4.8 Conclusion .....	207
4.9 Experimental Section .....	208
Chapter 4 Notes and References .....	255
5 A CHROMIUM-PHOTOCATALYZED APPROACH TO DIELS-ALDER ADDUCTS OF REVERSED REGIOSELECTIVITY .....	260
5.1 Introduction: An Unlikely Result.....	260
5.2 Preliminary Results and Optimization .....	261
5.3 Substrate Scope .....	268
5.4 Stereoconvergence .....	277

5.5 Regioselectivity.....	279
5.6 Mechanistic Discussion.....	284
5.7 Diels-Alder Conditions vs. Cr Conditions .....	296
5.8 Efforts Towards an Enantioselective Cycloaddition.....	297
5.9 Attempted Vinylcyclopropane Rearrangement.....	301
5.10 Conclusion .....	302
5.11 Experimental Section .....	303
Chapter 5 Notes and References .....	369

## APPENDICES

A CRYSTALLOGRAPHIC DATA FOR PRODUCT <b>2-2</b> .....	375
B NMR SPECTRA RELEVANT TO CHAPTER 2 .....	382
C NMR SPECTRA RELEVANT TO CHAPTER 4 .....	479
D NMR SPECTRA RELEVANT TO CHAPTER 5 .....	528

## LIST OF TABLES

	Page
Table 2.1: (a) Initial catalyst optimization. (b) Solvent optimization for Zeise's dimer.....	20
Table 2.2: Application of Zeise's dimer conditions to differentially substituted enynes .....	21
Table 2.3: Effect of CO atmosphere.....	22
Table 2.4: Evaluation of Ir catalyst conditions under CO .....	24
Table 2.5: Comparison of CO vs. "CO, then Ar" atmospheres .....	25
Table 2.6: Evaluation of effect of removing excess ligand.....	27
Table 3.1: Relative rates of [2+2] cycloaddition of <i>N</i> -methyl- <i>N</i> -vinylacetamide with dienes .....	105
Table 3.2: Effect of different atmospheres on reaction efficiency .....	127
Table 3.3: Cost of catalyst for a reaction run on 1 mmol scale.....	157
Table 4.1: [4+2] Dimerization of 1,3-cyclohexadiene optimization.....	169
Table 4.2: Impact of solvent and atmosphere on Cr and Ru catalyzed cycloadditions.....	191
Table 5.1: Reaction optimization .....	266
Table 5.2: Cycloaddition of enone <b>5-56</b> .....	276
Table 5.3: Evaluation of photocatalysts .....	294
Table 5.4: Chiral oxazolidinone cycloaddition Lewis acid screen.....	299
Table 5.5: Cycloadditions with menthyl esters .....	301

## LIST OF FIGURES

	Page
Figure 1.1: Variety of rearrangement products that can form in the cycloisomerization of 1,6-enynes.....	1
Figure 1.2: Selection of chiral catalysts for the asymmetric cycloisomerization of 1,6-enynes.....	9
Figure 2.1: Structures and relative stabilities of three Ir(I) catalysts .....	26
Figure 2.2: Substrates that did not efficiently undergo the cycloisomerization.....	32
Figure 3.1: Common photosensitizers and excited state reduction potentials .....	101
Figure 3.2: Cyclobutane lignan natural products .....	123
Figure 4.1: Select Cr(III) complexes utilized in this chapter .....	166
Figure 4.2: Stern-Volmer plot showing the rate of <i>trans</i> -anethole oxidation with and without O <sub>2</sub> .....	187
Figure 4.3: Electronic absorption spectra showing a [Cr] <sup>2+</sup> degradation product in the absence of O <sub>2</sub> ....	189
Figure 4.4: <sup>1</sup> H NMR spectra of reaction mixture during lights on/off experiment.....	240
Figure 4.5: <sup>1</sup> H NMR spectrum of <i>anti/syn</i> - <b>4-12</b> mixture .....	248
Figure 4.6: Comparison of <sup>1</sup> H NMR chemical shifts of cycloadducts <b>4-101</b> and <b>4-102</b> to reported NMR data of similar cycloadducts <b>4-88</b> and <b>4-89</b> in order to determine the diastereomeric ratio. ....	252
Figure 5.1: Reaction rate constants in CHCl <sub>3</sub> for reaction with singlet oxygen (rate x 10 <sup>6</sup> M <sup>-1</sup> s <sup>-1</sup> ) .....	264
Figure 5.2: Unsuccessful dienophiles.....	270
Figure 5.3: Unsuccessful dienes.....	271
Figure 5.4: Reduction potentials of different functionalities .....	274
Figure 5.5: UV/Vis spectrum of electron-poor alkenes and their corresponding vinylcyclobutanes .....	288
Figure 5.6: COSY NMR of cyclohexene <b>5-22</b> .....	339
Figure 5.7: HMQC NMR of cyclohexene <b>5-22</b> .....	340
Figure 5.8: <sup>1</sup> H NMR decoupling experiment on cyclohexane <b>5-170</b> .....	342
Figure 5.9: Major and minor isomers from cycloaddition with isoprene.....	343

Figure 5.10: Identification of minor isomer <b>5-171</b> .....	344
Figure 5.11: Evaluation of the diastereomer <b>5-172</b> as possible minor isomer .....	345
Figure 5.12: 1D NOESY of vinylcyclobutane <b>5-5</b> .....	351

## LIST OF SCHEMES

	Page
Scheme 1.1: Activation of enyne through metal-alkyne coordination.....	2
Scheme 1.2: (a) General orbital diagram for metal-alkyne complex. (b) Slip from $\eta^2$ to $\eta^1$ coordination of the alkyne. (c) Pull/push reactivity demonstrated in acetylenic Schmidt reaction. ....	3
Scheme 1.3: Proposed 1,6-enyne cycloisomerization mechanism.....	4
Scheme 1.4: Deuterium-labeling experiments confirming 1,2-hydrogen migration into metal carbenoid...	5
Scheme 1.5: (a) Substrate scope of PtCl <sub>4</sub> cycloisomerization. (b) Demonstration of stereospecificity.....	6
Scheme 1.6: Fürstner's expansion of substrate scope with nitrogen-tethered enynes .....	6
Scheme 1.7: (a) Au(I)-catalyzed cycloisomerization of 1,6-enynes. (b) Cycloisomerization of alkoxy-substituted enynes and further synthetic modification of the product .....	7
Scheme 1.8: Use of cationic Ir(I) complexes for 1,6-enyne cycloisomerization .....	8
Scheme 1.9: Ir(I) conditions with no additives .....	9
Scheme 1.10: Chirality transfer in the cycloisomerization of 1,6-enynes .....	10
Scheme 1.11: (a) Racemic synthesis of GSK 1360707. (b) Asymmetric synthesis of GSK 1360707 .....	11
Scheme 1.12: Synthesis of Gelsenicine through cycloisomerization/Cope rearrangement sequence .....	11
Scheme 1.13: Ring expansions of cyclopropanols and cyclobutanols via alkyne activation .....	12
Scheme 1.14: Ring expansion vs. C–H insertion .....	13
Scheme 1.15: Oxygen-assisted ring expansion in the cycloisomerization of carbon-tethered 1,6-enynes.	13
Scheme 1.16: Alkyl migration in the rearrangement/cyclopropanation cascade of tethered diynes .....	14
Scheme 1.17: Example of acyclic alkyl migrations into metal carbenoids.....	15
Scheme 1.18: Proposed alkyl migration in the cycloisomerization of 1,6-enynes .....	15
Scheme 2.1: Proposed 1,2-alkyl migration into metal carbenoid .....	18
Scheme 2.2: Preliminary cycloisomerization/alkyl migration result .....	19

Scheme 2.3: Enyne synthesis .....	19
Scheme 2.4: (a) Fürstner's use of CO to accelerate the cycloisomerization of enyne <b>2-6</b> . (b) Proposed coordination of Pt-CO complex with enyne.....	22
Scheme 2.5: (a) Comparison of nitrogen- vs. oxygen-tethered enynes. (b) Comparison of reaction atmospheres.....	23
Scheme 2.6: Scope of alkene and alkyne variation.....	28
Scheme 2.7: Comparison of Pt(II) and Ir(I) catalyst systems for two similar substrates.....	29
Scheme 2.8: Scope of ring size variation .....	30
Scheme 2.9: (a) C–C migration vs. C–H insertion. (b) Ring strain energies.....	30
Scheme 2.10: Acyclic C–C bond migrations .....	31
Scheme 2.11: Decomposition of enyne <b>2-5</b> to aldehyde <b>2-51</b> .....	33
Scheme 2.12: Proposed deactivation of metal by terminal alkyne .....	33
Scheme 2.13: Proposed ionization of tethered ether.....	34
Scheme 2.14: Oxidative cleavage to access macrolactones.....	34
Scheme 3.1: General depiction of alkene radical cation formation through PET.....	99
Scheme 3.2: Approaches to cycloadditions of electron-rich alkenes.....	100
Scheme 3.3: General radical cation [2+2] cycloaddition .....	102
Scheme 3.4: [2+2] Dimerization of <i>N</i> -vinylcarbazole .....	103
Scheme 3.5: [2+2] Cycloaddition of <i>N</i> -methyl- <i>N</i> -vinylacetamide with dienes.....	104
Scheme 3.6: All possible alkene/radical cation combinations .....	104
Scheme 3.7: Proposed mechanism for cycloaddition of a diene with <i>N</i> -methyl- <i>N</i> -vinylacetamide.....	106
Scheme 3.8: Dimerization of phenyl vinyl ether catalyzed by dimethyl terephthalate.....	106
Scheme 3.9: Proposed mechanism for the dimerization of phenyl vinyl ether.....	107
Scheme 3.10: Cross [2+2] cycloadditions of vinyl ethers (syn/anti ratios in parentheses).....	107
Scheme 3.11: Mechanism for the crossed [2+2] cycloaddition of vinyl ethers .....	108
Scheme 3.12: Effect of concentration and temperature on syn/anti ratio and quantum yield.....	108

Scheme 3.13: Pathways to syn and anti cyclobutanes in the dimerization of phenyl vinyl ether.....	109
Scheme 3.14: Farid's chain propagation mechanism for the dimerization of phenyl vinyl ether.....	110
Scheme 3.15: Dimerization of indene.....	111
Scheme 3.16: Crossed [2+2] cycloadditions of indene and vinyl ethers.....	112
Scheme 3.17: Radical chain mechanism for the retrocyclobutanation of indene dimer.....	113
Scheme 3.18: [2+2] dimerization of 4-methoxystyrene.....	113
Scheme 3.19: Oxygen-mediated radical cation dimerization of 4-methoxystyrene.....	114
Scheme 3.20: Dimerization of <i>trans</i> -anethole.....	115
Scheme 3.21: Dimerization and isomerization of <i>cis</i> -anethole.....	116
Scheme 3.22: Solvent effects on stereoselectivity in the [2+2] cycloaddition of tethered vinyl ethers....	117
Scheme 3.23: Intramolecular [2+2] cycloaddition and rearrangement.....	118
Scheme 3.24: Yoon's oxidative intramolecular [2+2] cycloaddition.....	118
Scheme 3.25: Stereoconvergence in the intramolecular [2+2] cycloaddition.....	119
Scheme 3.26: Proposed mechanism for intramolecular radical cation [2+2] cycloaddition.....	119
Scheme 3.27: Yoon's intermolecular [2+2] cycloaddition.....	120
Scheme 3.28: Proposed mechanism for intermolecular [2+2] cycloaddition.....	121
Scheme 3.29: Cycloreversion under Ru photocatalysis.....	121
Scheme 3.30: Inhibition of cycloreversion using electron relay reagent.....	122
Scheme 3.31: Electron relay mechanism for dimerization of <i>trans</i> -anethole.....	123
Scheme 3.32: Chen's total synthesis of scep trin.....	124
Scheme 3.33: Further exploration toward the synthesis of dimeric pyrrole-imidazole alkaloids.....	125
Scheme 3.34: Proposed mechanism for the oxygen-mediated [2+2] cycloaddition of tethered alkenes..	126
Scheme 3.35: General radical cation [4+2] cycloaddition.....	127
Scheme 3.36: Dimerization of cyclohexadiene product distribution under different conditions.....	128
Scheme 3.37: Reaction of cyclohexadiene with DCA under direct irradiation in benzene.....	129
Scheme 3.38: Comparison of 1,3-cyclohexadiene dimerization mechanism in two different solvents....	130

Scheme 3.39: [4+2] Dimerization of other 1,3-dienes .....	131
Scheme 3.40: Possible products in a cross [4+2] radical cation cycloaddition.....	131
Scheme 3.41: Cross [4+2] cycloadditions of 1,3-cyclohexadiene .....	132
Scheme 3.42: Cross [4+2] cycloaddition of dienes with vinylbenzofurans.....	133
Scheme 3.43: Mechanism and origin of regioselectivity and endo selectivity .....	134
Scheme 3.44: [4+2] Cycloaddition of 1,3-cyclohexadiene and indole .....	134
Scheme 3.45: Scope of 1,3-cyclohexadiene cycloaddition partner.....	135
Scheme 3.46: Proposed mechanism for the cycloaddition of 1,3-cyclohexadienes with indole .....	135
Scheme 3.47: Cycloaddition of an exocyclic diene with indole .....	136
Scheme 3.48: Cycloaddition of a chiral exocyclic diene with indoles.....	137
Scheme 3.49: Cycloadditions with cleavable dienes .....	137
Scheme 3.50: Reductive cleavage of N–O bond.....	138
Scheme 3.51: [4+2] cycloaddition of furan and indene .....	138
Scheme 3.52: Radical cation cycloaddition with an allene .....	139
Scheme 3.53: Radical cation cycloaddition and rearrangement with a ketene .....	140
Scheme 3.54: [4+2] cycloaddition of thiobenzophenone.....	141
Scheme 3.55: Total synthesis of (–)-β-selinene through a radical cation [4+2] cycloaddition.....	141
Scheme 3.56: Representative substrates for the Ru-photocatalyzed radical cation Diels-Alder .....	142
Scheme 3.57: Mechanism for the Ru-photocatalyzed radical cation Diels-Alder .....	143
Scheme 3.58: Synthesis of heitziamide A through a radical cation Diels-Alder .....	144
Scheme 3.59: Yoon’s intramolecular radical cation Diels-Alder reaction.....	145
Scheme 3.60: Thermal intramolecular Diels-Alder reaction .....	145
Scheme 3.61: General depiction of competitive [2+2] and [4+2] radical cation cycloadditions.....	146
Scheme 3.62: Dimerization and cross cycloaddition of phenyl vinyl ethers .....	147
Scheme 3.63: Dimerization of styrene and α-methylstyrene .....	148
Scheme 3.64: [2+2] and [4+2] products of 1,1-diphenylethylene dimerization .....	148

Scheme 3.65: Proposed mechanism for the dimerization of 1,1-diphenylethylene .....	149
Scheme 3.66: Dimerization of 4-methoxystyrene .....	150
Scheme 3.67: Acyclic vs. long-bond radical cation intermediate .....	151
Scheme 3.68: Dimerization of 3-methoxystyrene .....	151
Scheme 3.69: Synthesis of natural products magnoshinin and magnosalin .....	152
Scheme 3.70: Periselectivity in cycloaddition between 1,1'-bicyclopentenyl diene and alkenes .....	153
Scheme 3.71: Explanation for periselectivity of 1,1'-bicyclopentenyl diene cycloadditions .....	153
Scheme 3.72: Cycloaddition of phenyl vinyl sulfide and 1,1'-bicyclopentenyl diene .....	154
Scheme 3.73: Three stages of the cycloaddition .....	154
Scheme 3.74: Explanation of periselectivity with reduction potentials .....	155
Scheme 4.1: Radical cation catalyzed [4+2] cyclodimerization of 1,3-cyclohexadiene .....	168
Scheme 4.2: Comparison of thermal and radical cation conditions for the Diels-Alder cycloaddition of electron-rich alkenes .....	171
Scheme 4.3: (a) Cross cycloaddition of <b>4-1</b> with <b>4-3</b> . (b) Kinetic data. (c) Kinetic explanation for feasibility of Cr-catalyzed dimerization of 1,3-cyclohexadiene .....	172
Scheme 4.4: Reduction potentials for common dienes .....	173
Scheme 4.5: Scope of diene component .....	174
Scheme 4.6: Scope of the dienophile component .....	175
Scheme 4.7: Evaluation of different irradiation sources .....	176
Scheme 4.8: Dienes and dienophiles that were not successful substrates .....	177
Scheme 4.9: Proposed formation of myrcene peroxide dimer .....	178
Scheme 4.10: Relative rates of <b>4-3</b> vs. <b>4-33</b> in a radical cation cycloaddition with diene <b>4-7</b> .....	179
Scheme 4.11: Reduction potentials and cycloaddition yields for reaction with isoprene .....	179
Scheme 4.12: Dimerization of 4-methoxystyrene .....	180
Scheme 4.13: Dimerization of $\alpha$ -methylstyrene <b>4-40</b> .....	181
Scheme 4.14: Bauld's cycloaddition of 4-chloro- <i>trans</i> -stilbene with diene <b>4-7</b> .....	181

Scheme 4.15: (a) Proposed stabilization of radical cation with alcohol. (b) Nicewicz's anti-Markovnikov addition of alcohols to alkenes .....	182
Scheme 4.16: Initial proposed mechanism for Cr-photocatalyzed radical cation Diels-Alder .....	183
Scheme 4.17: Discontinuous irradiation experiment .....	184
Scheme 4.18: Preliminary experiments exploring the effect of air on reactivity .....	185
Scheme 4.19: Proposed mechanism showing roles of O <sub>2</sub> .....	186
Scheme 4.20: Proposed formation of <i>para</i> -anisaldehyde from <i>trans</i> -anethole .....	187
Scheme 4.21: Formation of endoperoxide through [4+2] with <sup>1</sup> O <sub>2</sub> .....	188
Scheme 4.22: Cycloaddition of isomeric mixture of alkene <b>4-76</b> .....	192
Scheme 4.23: Cr-catalyzed cycloaddition of <i>cis</i> -anethole .....	193
Scheme 4.24: Isomerization of <i>cis</i> -anethole to <i>trans</i> -anethole .....	193
Scheme 4.25: Aminium salt-catalyzed cycloaddition of cyclopentadiene with <i>trans</i> - and <i>cis</i> -anethole ..	194
Scheme 4.26: Proposed mechanism for formation of anti products from <i>cis</i> -anethole .....	195
Scheme 4.27: Isomerization of syn cycloadducts to anti cycloadducts .....	196
Scheme 4.28: Cycloaddition of <i>cis</i> -anethole with isoprene under the aminium salt conditions .....	197
Scheme 4.29: Cr-catalyzed cycloaddition of <i>cis</i> -anethole with other dienes .....	198
Scheme 4.30: Proposed experiment to detect <i>cis</i> - to <i>trans</i> -anethole isomerization .....	199
Scheme 4.31: Detection of <i>cis</i> -anethole isomerization before cycloaddition .....	200
Scheme 4.32: Cycloaddition of cyclohexene <b>4-85</b> .....	202
Scheme 4.33: [4+2] vs. [2+2] cycloadditions in the triplex Diels-Alder reaction .....	203
Scheme 4.34: Photosensitized dimerization of 1,3-cyclobutadiene .....	204
Scheme 4.35: Examples from Yoon of selective photosensitization of alkenes .....	205
Scheme 4.36: Radical cation intramolecular Diels-Alder reaction .....	206
Scheme 4.37: Intramolecular [2+2] cycloaddition under photooxidizing conditions .....	207
Scheme 5.1: Unexpected cycloaddition result with electron-poor alkene .....	260
Scheme 5.2: Preliminary experiments implicating vinylcyclobutane <b>5-5</b> as a reaction intermediate .....	261

Scheme 5.3: Early mechanistic hypothesis .....	262
Scheme 5.4: Schenck-ene reaction of singlet oxygen with cycloadduct <b>5-7</b> .....	263
Scheme 5.5: Formation of oxidized product over time .....	267
Scheme 5.6: Scope of electron-poor alkenes .....	268
Scheme 5.7: Scope of diene .....	269
Scheme 5.8: Cycloaddition of bicyclopentenyl diene <b>5-50</b> .....	272
Scheme 5.9: Cycloaddition of vinyl enones.....	273
Scheme 5.10: Possible side products that could form under photooxidative conditions .....	274
Scheme 5.11: Other attempted substrates .....	277
Scheme 5.12: (a) Formation of <i>anti</i> -cyclohexene from <i>cis</i> -enone. (b) Isomerization of <i>cis</i> -enone.....	278
Scheme 5.13: Unsuccessful ( <i>Z</i> )-diene .....	279
Scheme 5.14: General explanation of enone/alkene [2+2] regioselectivity .....	279
Scheme 5.15: Possible regiochemical explanation .....	280
Scheme 5.16: Reversed regioselectivity through radical cation mechanism .....	280
Scheme 5.17: Proposed regiochemical explanation for 1-substituted dienes .....	281
Scheme 5.18: Possible regiochemical explanation for 1-substituted dienes.....	281
Scheme 5.19: Regiochemical comparison to traditional Diels-Alder conditions .....	283
Scheme 5.20: Oxidative cleavage of PMP group.....	283
Scheme 5.21: Regioselectivity in the Diels-Alder reaction of acrylic acid <b>5-100</b> .....	284
Scheme 5.22: Reaction progress with and without catalyst .....	285
Scheme 5.23: Two possible mechanistic pathways .....	285
Scheme 5.24: Attempts at triplet sensitized [2+2] cycloaddition.....	286
Scheme 5.25: Trapping experiments.....	287
Scheme 5.26: Working mechanistic hypothesis involving an enone dimer or exciplex.....	289
Scheme 5.27: Validation of dimer <b>5-105</b> as a reaction intermediate .....	290
Scheme 5.28: Radical cation cyclopropanation of 4-methoxychalcone .....	291

Scheme 5.29: Regioselectivity of full cycloaddition vs. stepwise [2+2]/rearrangement .....	292
Scheme 5.30: Competition experiment between <i>trans</i> -anethole and 4-methoxychalcone .....	293
Scheme 5.31: Cycloaddition with an aminium radical cation salt .....	295
Scheme 5.32: Cr-photocatalyzed vs. thermal Diels-Alder conditions .....	297
Scheme 5.33: Cycloaddition of oxazolidinone substrate .....	298
Scheme 5.34: Cycloaddition of chiral oxazolidinones .....	299
Scheme 5.35: Enantioselective [2+2] cycloadditions with menthyl cyclohexene carboxylates .....	300
Scheme 5.36: [3+2] cycloaddition of cyclopropane vinylcyclopropane and oxygen .....	302

## CHAPTER 1

### 1,6-ENYNE CYCLOISOMERIZATION AND ALKYL MIGRATIONS VIA ALKYNE ACTIVATION

#### 1.1 Introduction: 1,6-Enyne Cycloisomerization

Enyne cycloisomerization through metal-catalyzed alkyne activation is a widely studied reaction class that enables the efficient construction of complex molecular frameworks from relatively simple starting materials.<sup>1</sup> In the case of 1,6-enynes, a variety of skeletally diverse products can be accessed depending on the substitution of the enyne, the enyne tether, and the chosen reaction conditions (Figure 1.1).<sup>2</sup> Our lab has been specifically interested in the cycloisomerization of oxygen-tethered 1,6-enynes to give bicyclo[4.1.0]heptene derivatives. This chapter will provide the necessary background concerning this transformation and the basic principles of metal catalyzed alkyne activation chemistry.

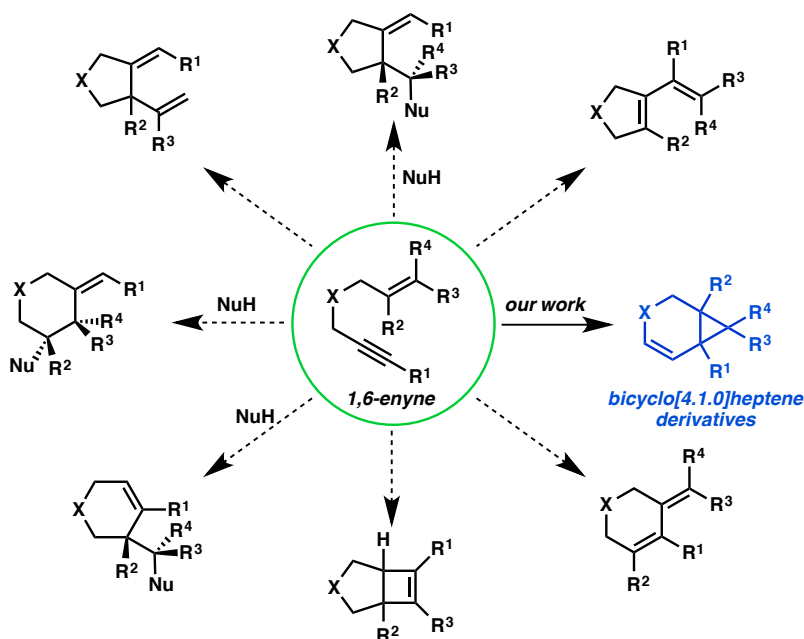
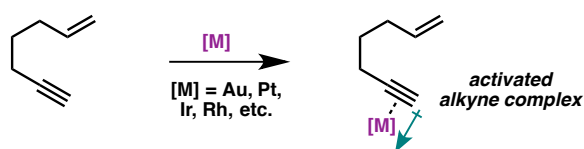


Figure 1.1. Variety of rearrangement products that can form in the cycloisomerization of 1,6-enynes.

## 1.2 Brief Introduction to Alkyne Activation

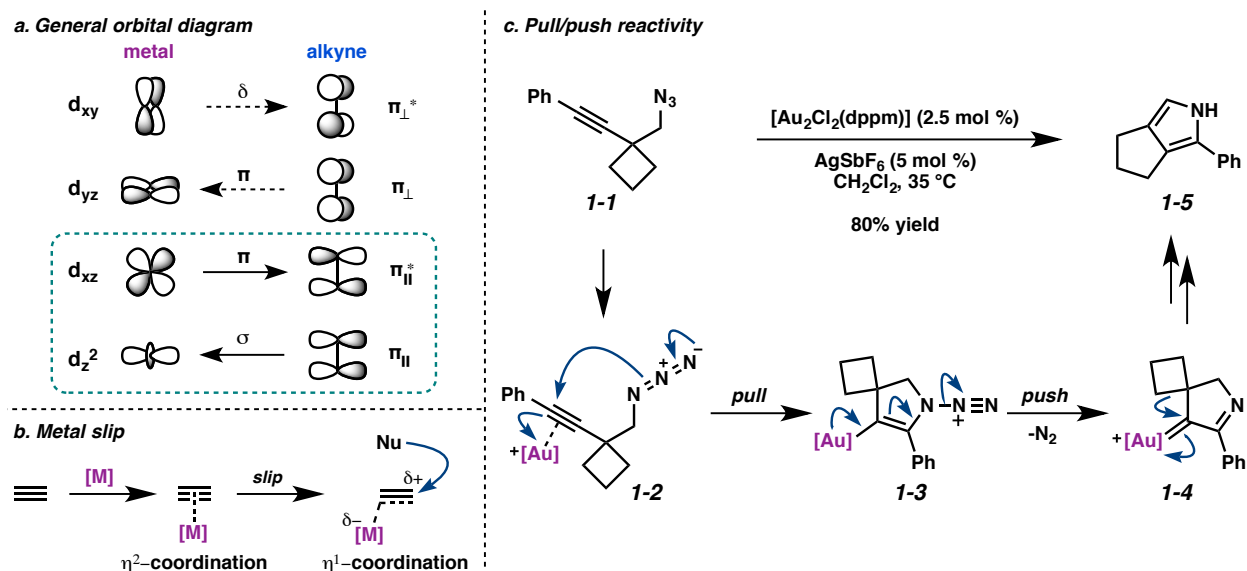
Many enyne cycloisomerization reactions are initiated by activation of the alkyne through metal coordination (Scheme 1.1). Metals that activate alkynes through  $\pi$ -coordination are known as alkynophilic metals. These can include Au, Pt, Ir, Rh, and others. The high alkynophilicity of these metals is due in part to relativistic effects, which cause the contraction of the 6s orbital.<sup>3</sup> This contraction results in the lowest unoccupied molecular orbital (LUMO) of the metal being lower in energy, rendering it more  $\pi$ -acidic. In addition, the contraction of the 6s orbital causes the metal's 5d orbital to expand due to shielding. This expansion lowers the highest occupied molecular orbital (HOMO) of the metal, meaning the metal is less nucleophilic and does not display significant backbonding with the alkyne ligand.



*Scheme 1.1.* Activation of enyne through metal-alkyne coordination.

A generic orbital diagram for the metal-alkyne complex is depicted in Scheme 1.2a. Four of the metal's  $d$  orbitals have the appropriate symmetry to interact with the alkyne.<sup>4</sup> The main orbital interaction is  $\sigma$ -donation from the in-plane  $\pi$ -orbital of the alkyne into the  $d_z^2$  orbital of the metal. The next strongest interaction is a back-bonding  $\pi$ -donation from the  $d_{xz}$  orbital of the metal to the in-plane  $\pi^*$ -orbital of the alkyne. Donation can also occur from the out-of-plane alkyne  $\pi$ -orbital into the  $d_{yz}$  orbital of the metal, and from the  $d_{xy}$  metal orbital into the out-of-plane  $\pi^*$ -orbital; however, in most cases, these orbital contributions are relatively minor. Overall, when interacting with alkynophilic metals, alkynes act as strong  $\sigma$ -donors, but weak  $\pi$ -acceptors, resulting in the high electrophilicity of the alkyne in these metal-alkyne complexes.

Further, it is well-accepted that when approached by a nucleophile, the metal-alkyne complex will “slip” along the axis of the alkyne, going from  $\eta^2$  to  $\eta^1$  coordination (Scheme 1.2b). This slippage enhances the electrophilicity of the metal-alkyne complex.<sup>4</sup>

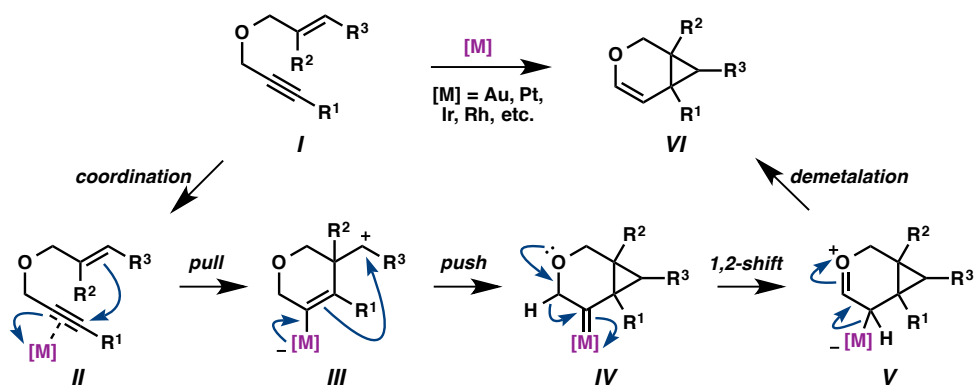


Scheme 1.2. (a) General orbital diagram for metal-alkyne complex.<sup>4</sup> (b) Metal slip from  $\eta^2$  to  $\eta^1$  coordination of the alkyne. (c) Pull/push reactivity demonstrated in acetylenic Schmidt reaction.

Another aspect of metal alkyne activation involving the nucleophile is referred to as the “pull-push” mechanism. A prime example of this concept is illustrated in the Au(I)-catalyzed acetylenic Schmidt reaction of homopropargyl azides reported by Toste in 2005 (Scheme 1.2c).<sup>5</sup> In the first step, the Au catalyst can be thought to “pull” on the alkyne (**1-2**), or pull electron density away from the alkyne, inciting the attack of the azide (**1-2**  $\rightarrow$  **1-3**). In the next step, the Au can “push” electron density back in to form the Au-carbenoid (**1-4**) and expel  $\text{N}_2$  gas. A 1,2-alkyl migration into the Au-carbenoid, followed by rearomatization provides the pyrrole product (**1-5**). A similar pull-push mechanism is represented in the mechanism of 1,6-enyne cycloisomerization described below.

### 1.3 Proposed Mechanism for Cycloisomerization of 1,6-Enynes

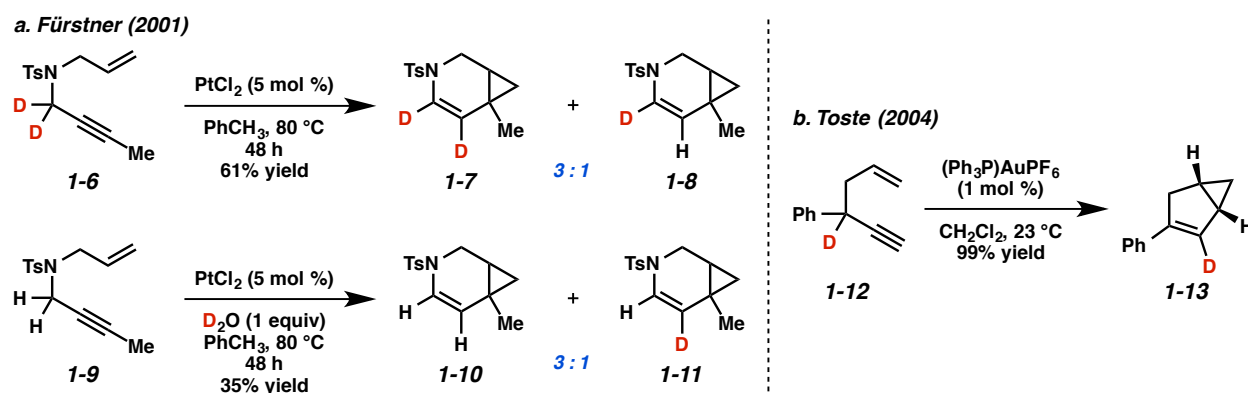
The cycloisomerization of 1,6-enynes is proposed to proceed by the general mechanism shown in Scheme 1.3. As described above, first the  $\pi$ -acidic metal coordinates to the alkyne (**I**  $\rightarrow$  **II**). This complexation renders the alkyne electrophilic, inciting the attack of the alkene nucleophile (*pull*) (**II**  $\rightarrow$  **III**). In the next step, the metal quenches the carbocation to form the cyclopropane ring and the metal carbenoid (*push*) (**III**  $\rightarrow$  **IV**).



Scheme 1.3. Proposed 1,6-enyne cycloisomerization mechanism.

Next, an oxygen-assisted 1,2-hydrogen migration occurs into the metal carbenoid (**IV**  $\rightarrow$  **V**), then demetalation gives the product (**V**  $\rightarrow$  **VI**). Evidence for this 1,2-hydrogen shift was provided by Fürstner and coworkers through a deuterium labeling experiment (Scheme 1.4a).<sup>6</sup> When the  $\text{PtCl}_2$ -catalyzed cycloisomerization of deuterium-labeled nitrogen-tethered 1,6-enyne **1-6** was performed, the deuterium-shifted product (**1-7**) was observed, along with protonated product **1-8** in a 3:1 ratio. They hypothesized that the hydrogen in the minor product might be coming from traces of water in toluene. To test this theory, they performed the cycloisomerization of enyne **1-9** with 1 equiv of  $\text{D}_2\text{O}$  added. Here, they observed the 1,2-hydrogen shift product (**1-10**), as well as the deuterium-incorporated product (**1-11**), indicating that the proton in the first reaction was likely a result of wet toluene. Ultimately, they

demonstrated that 1,2-migration into the metal carbenoid is the dominant pathway, occurring preferentially over competing insertion of the carbenoid into water or D<sub>2</sub>O. In a different example, Toste and coworkers also observed a 1,2-deuterium shift in the Au(I)-catalyzed cycloisomerization of carbon-tethered 1,5-enyne **1-12**, further validating the proposed mechanism (Scheme 1.4b).<sup>7</sup>

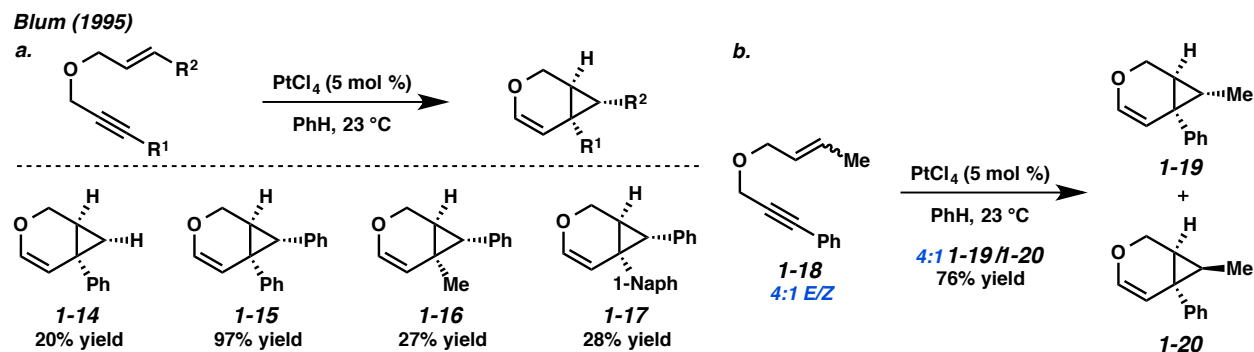


Scheme 1.4. Deuterium-labeling experiments confirming 1,2-hydrogen migration into metal carbenoid.

## 1.4 Cycloisomerization of 1,6-Enynes

### 1.4.1 Blum's Seminal Report

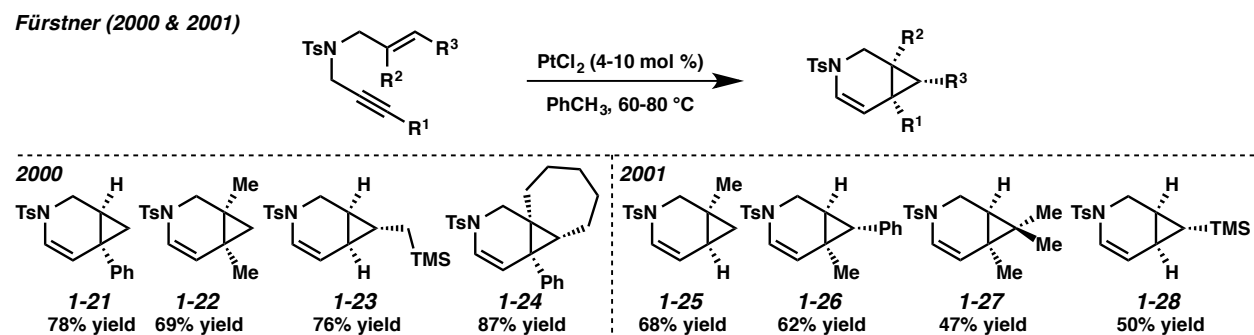
In 1995, Blum and coworkers reported that oxygen-tethered 1,6-enynes could rearrange to oxabicyclo[4.1.0]heptenes under PtCl<sub>4</sub>-catalysis (Scheme 1.5).<sup>8</sup> Five enyne substrates were examined and variable yields of the cycloisomerization products were obtained. Interestingly, the cycloisomerization was found to be stereospecific. Cyclopropanes **1-14–1-17** were formed as one diastereomer, and when a 4:1 E/Z mixture of alkene **1-18** was exposed to the reaction conditions, a 4:1 mixture of diastereomers was obtained (**1-19:1-20**) (Scheme 1.5b). This reinforces that, upon attack of the alkene on the activated alkyne, subsequent cyclopropane formation must occur quickly, or else a mixture of diastereomers would be observed.



Scheme 1.5. (a) Substrate scope of  $\text{PtCl}_4$  cycloisomerization. (b) Demonstration of stereospecificity.

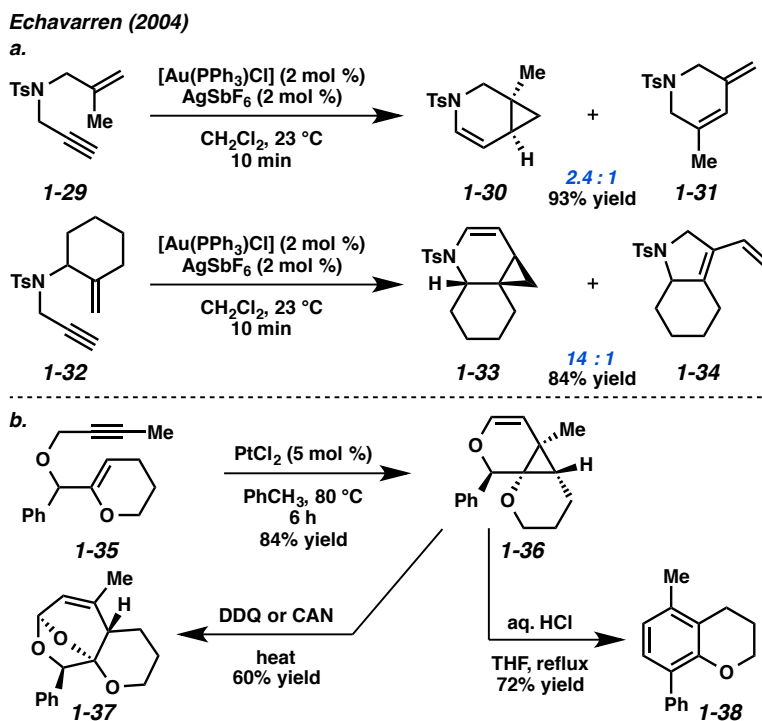
## 1.4.2 Further Exploration

Since Blum's initial account, a number of examples have been reported for the cycloisomerization of 1,6-enynes to bicyclo[4.1.0]heptene derivatives. Five years later, Fürstner and coworkers further explored the cycloisomerization of 1,6-enynes using  $\text{PtCl}_2$ .<sup>9</sup> A variety of differentially substituted enynes, including allylsilanes, underwent the rearrangement in moderate to high yields (**1-21**–**1-24**) (Scheme 1.6). Notably, nitrogen-tethered enynes were revealed as viable cycloisomerization substrates. A subsequent publication from Fürstner in 2001 expanded this substrate scope, employing enynes possessing a wider range of alkene substitution patterns, as well as a vinylsilane (**1-28**) (Scheme 1.6).<sup>6</sup>



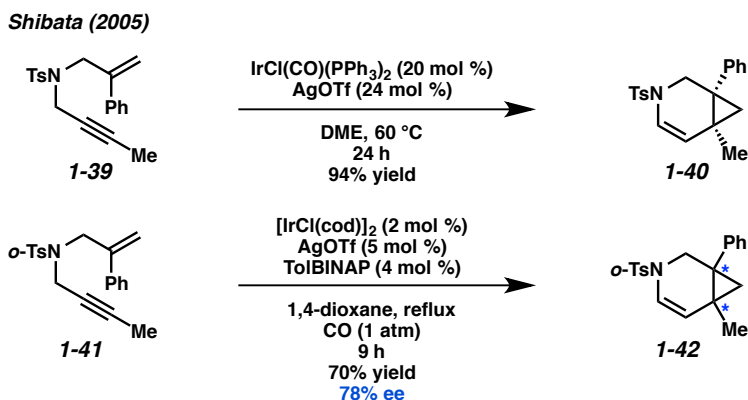
Scheme 1.6. Fürstner's expansion of substrate scope with nitrogen-tethered enynes.

A report by Echavarren and coworkers in 2004 demonstrated the use of a Au(I) catalyst for the cycloisomerization of 1,6-enynes.<sup>10</sup> Only two examples are given, but the mild cationic Au conditions showed selectivity for the formation of the azabicyclo[4.1.0]heptene derivatives (**1-30** and **1-33**) over other possible rearrangement products (**1-31** and **1-34**) (Scheme 1.7a). Echavarren later studied the PtCl<sub>2</sub>-catalyzed cycloisomerization of enynes with alkoxy-substituted alkenes, such as **1-35** (Scheme 1.7b).<sup>11</sup> The intent was to generate electron-rich fused cyclopropanes that could undergo further structural modification. Under oxidative conditions (DDQ or CAN), cleavage of the cyclopropane occurred to give double acetal **1-37** in good yield. Alternately, heating the oxabicyclo[4.1.0]heptene (**1-36**) in acid gave 3,4-dihydro-2*H*-chromene **1-38** through a new benzannulation reaction. These unique transformations showcase the versatility of the bicyclo[4.1.0]heptene products as reactive intermediates in organic synthesis.



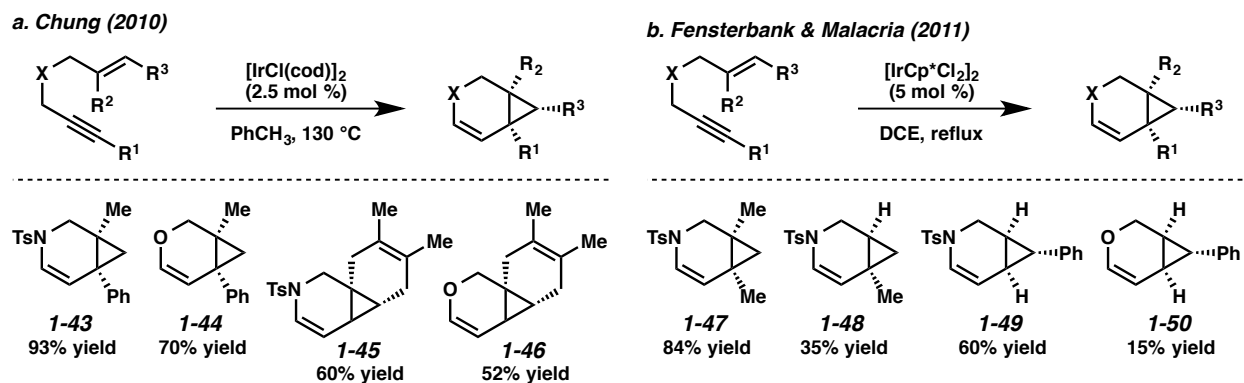
*Scheme 1.7.* (a) Au(I)-catalyzed cycloisomerization of 1,6-enynes. (b) Cycloisomerization of alkoxy-substituted enynes and further synthetic modification of the product.

The first instance of Ir(I)-catalysis for the cycloisomerization of 1,6-enynes was reported by Shibata and coworkers in 2005.<sup>12</sup> Cationic Ir(I) conditions with  $\text{IrCl}(\text{CO})(\text{PPh}_3)_2$  (Vaska's complex) or  $[\text{Ir}(\text{cod})\text{Cl}]_2$  with Ag salts were explored (Scheme 1.8). Although the substrate scope in this report was somewhat limited, the cycloisomerization could be performed asymmetrically by employing chiral diphosphine ligands. An enantiomeric excess of up to 78% was obtained (**1-42**). The authors also noted the advantageous impact of CO on the reaction, an effect which will be discussed further in Chapter 2.



*Scheme 1.8.* Use of cationic Ir(I) complexes for 1,6-enyne cycloisomerization.

Simpler Ir(I) conditions were reported by Chung and coworkers in 2010 for similar nitrogen- and oxygen-tethered 1,6-enyne cycloisomerizations.<sup>13</sup> Exposing the enynes to catalytic  $[\text{Ir}(\text{cod})\text{Cl}]_2$  in toluene at 130 °C without any additives afforded the corresponding bicyclo[4.1.0]heptenes in good yields (Scheme 1.9a). Fensterbank, Malacria, and coworkers also demonstrated the utility of  $[\text{IrCp}^*\text{Cl}_2]_2$  as a catalyst for 1,6-enyne cycloisomerization.<sup>14</sup> Yields ranged from high to relatively poor (Scheme 1.9b). In both of these reports, as in many others, the oxygen-tethered substrates gave significantly lower yields and longer reaction times than the analogous nitrogen-tethered substrates. Presumably, oxygen-tethered enynes are more susceptible to decomposition under the reaction conditions.



Scheme 1.9. Ir(I) conditions with no additives.

### 1.4.3 Asymmetric Variants

Since Shibata's attempt at developing an enantioselective cycloisomerization reaction using cationic Ir(I) and chiral diphosphine ligands, a number of more successful asymmetric variants have been reported.<sup>15</sup> Noteworthy approaches include the use of chiral Au(I) phosphine complexes (**1-51**),<sup>16</sup> N-heterocyclic carbene-phosphine-Pt(II) (**1-52**),<sup>17</sup> Ir(I) complexes formed in situ from chiral silver phosphate salts and Vaska's complex (**1-53**),<sup>18</sup> and Rh(I)-chiral diene complexes (**1-54**) (Figure 1.2).<sup>19</sup>

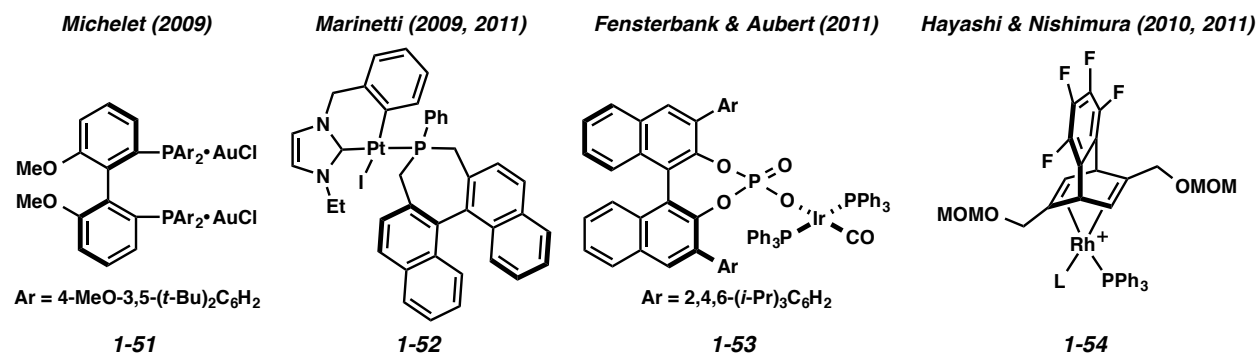
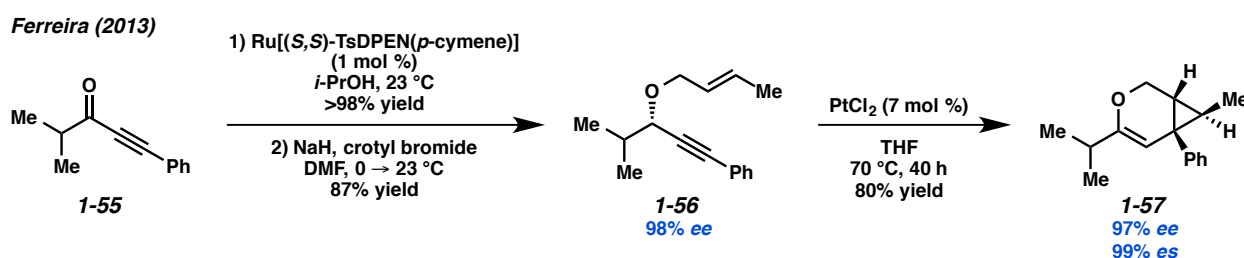


Figure 1.2. Selection of chiral catalysts for the asymmetric cycloisomerization of 1,6-enynes.

A novel method for the enantiospecific cycloisomerization of 1,6-enynes that does not require a chiral catalyst was developed by our lab in 2013.<sup>20</sup> In this approach, the stereochemistry of the product

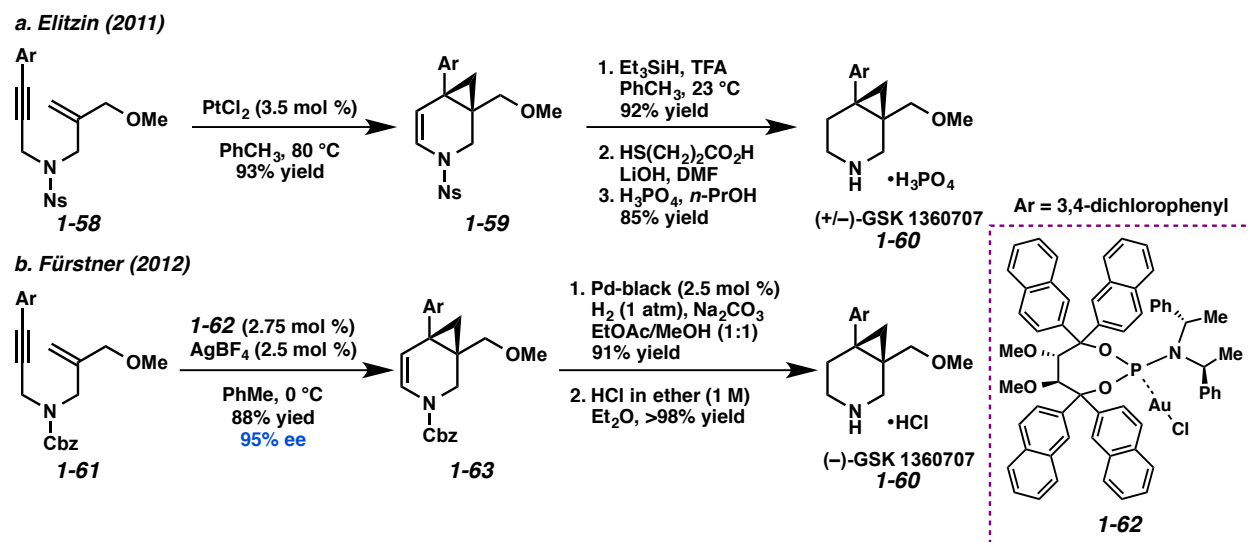
originates from the chiral enyne, which can readily be synthesized from the Noyori reduction of an ynone, followed by alkylation (Scheme 1.10). This PtCl<sub>2</sub>-catalyzed chirality transfer method was successfully applied to a variety of oxygen-tethered 1,6-enynes, giving the stereodefined cyclopropanes in high yields and enantiospecificities. For example, chiral enyne **1-56** (98% ee) underwent the cycloisomerization to give cyclopropane **1-57** in 80% yield and 97% ee, indicating that the stereochemistry of the enyne was almost completely conserved in the transformation (99% es). Additionally, the effectiveness of this approach provides insight into the cycloisomerization mechanism; in order for the chirality of the enyne to be transferred to the product, cyclopropane formation must be complete before the loss of the ether stereocenter. The transfer of chirality demonstrated in this report offers further evidence for the proposed mechanism (Scheme 1.3).



*Scheme 1.10.* Chirality transfer in the cycloisomerization of 1,6-enynes.

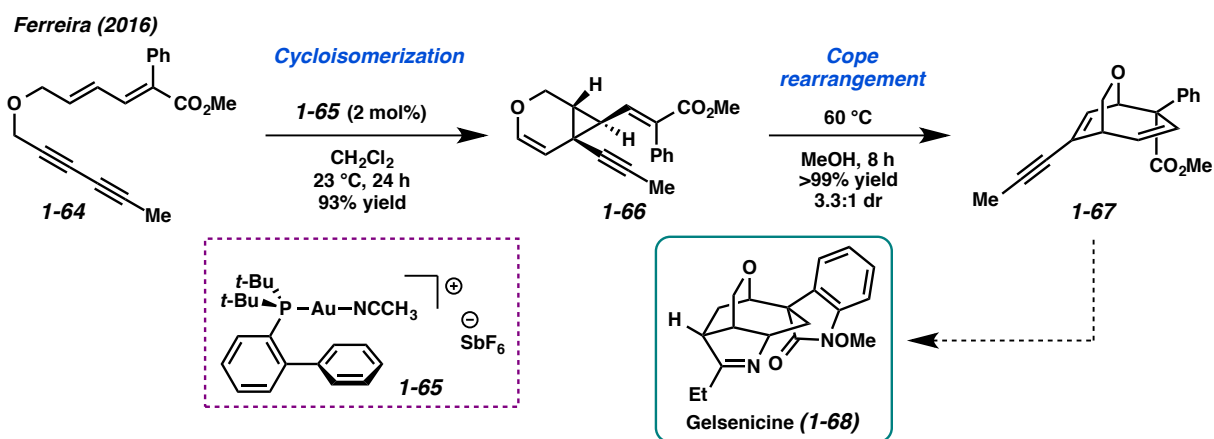
### 1.4.5 Application to Natural Product Synthesis

The cycloisomerization of 1,6-enynes has also been utilized in natural product synthesis. For instance, the total synthesis of antidepressive agent (–)-GSK 1360707 (**1-60**) has been reported using a nitrogen-tethered 1,6-enyne cycloisomerization as the key step. A racemic synthesis was devised by Elitzin and coworkers in 2011 utilizing PtCl<sub>2</sub> catalysis (Scheme 1.11a).<sup>21</sup> A year later, Fürstner devised an asymmetric synthesis of the same molecule using chiral cationic Au(I) catalyst **1-62** (Scheme 1.11b).<sup>16b</sup>



Scheme 1.11. (a) Racemic synthesis of GSK 1360707. (b) Asymmetric synthesis of GSK 1360707.

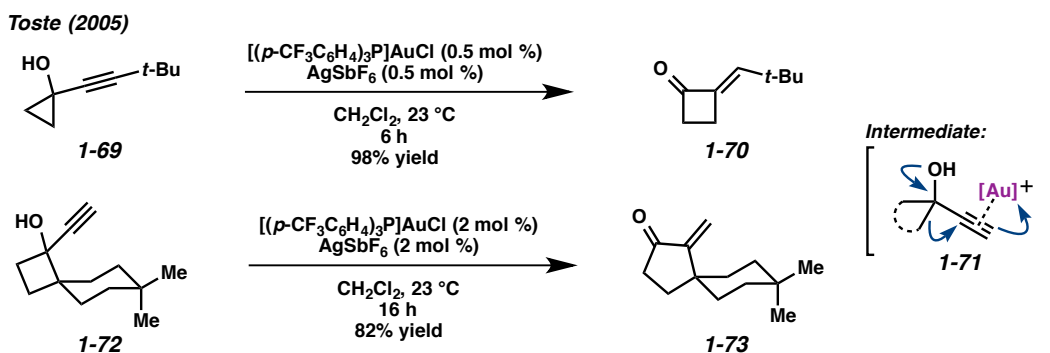
Our lab has also showcased the synthetic utility of 1,6-enyne cycloisomerization in the total synthesis of Gelsenicine (**1-67**) (Scheme 1.12). A Au(I)-catalyzed 1,6-enyne cycloisomerization/thermal Cope rearrangement sequence of substrate **1-64** was exploited to access the core of the natural product (**1-66**).<sup>22</sup> The total synthesis was then completed in just 13 total steps, representing one of the shortest total synthesis to date of a Gelsemium alkaloid. In addition, this cycloisomerization/Cope cascade strategy provides a unified approach to a broad array of members in the Gelsemium family.



Scheme 1.12. Synthesis of Gelsenicine through cycloisomerization/Cope rearrangement sequence.

## 1.5 1,2-Alkyl Migrations via Alkyne Activation

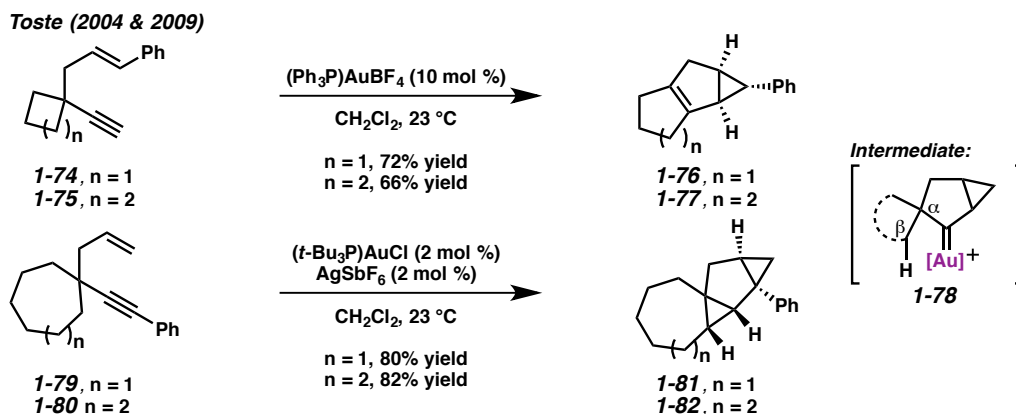
Though C–H bond migration is more common, alkyl groups have also been demonstrated to undergo 1,2-migrations into metal carbenoids generated through 1,6-enyne cycloisomerization and other alkyne activation reactions.<sup>23</sup> In addition to the acetylenic Schmidt reaction already discussed (Scheme 1.2), in 2005, Toste and coworkers reported the Au(I)-catalyzed ring expansion of cyclopropanols (**1-69** → **1-70**) (Scheme 1.13).<sup>24</sup> As shown in intermediate **1-71**, this reaction proceeds by activation of the alkyne with Au(I), inciting an oxygen-assisted alkyl shift to give the ring-expanded ketone product. Alkynylcyclobutanols also underwent a ring expansion under the same conditions to give 2-methylene-cyclopentanones (**1-72** → **1-73**). Notably, the more substituted carbon of the cyclobutanol was observed to migrate selectively.



Scheme 1.13. Ring expansions of cyclopropanols and cyclobutanols in alkyne activation chemistry.

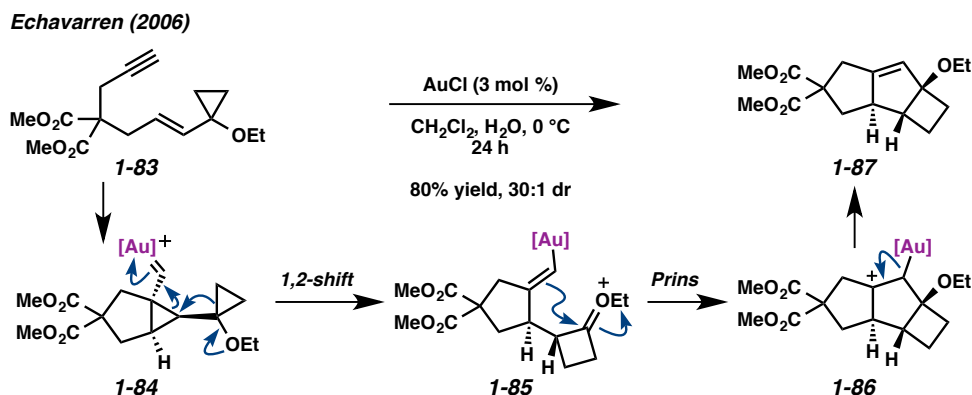
Toste and coworkers also explored alkyl migrations in the Au(I)-catalyzed cycloisomerization of carbon-tethered 1,5-enynes, which proceed through metal carbenoid intermediate **1-78** (Scheme 1.14). Interestingly, the researchers found that when the adjacent carbocycle was a 4- or 5-membered ring (**1-74** and **1-75**), a 1,2-alkyl migration occurred into the carbenoid to give the ring-expanded products (**1-76** and **1-77**).<sup>25</sup> If the adjacent ring was 7- or 8-membered (**1-79** and **1-80**), however, the carbenoid instead

inserted into the  $\beta$ -C–H bond to generate dicyclopropanated products (**1-81** and **1-82**).<sup>26</sup> They proposed that the flexibility of the larger rings favors an intramolecular C–H insertion pathway over ring expansion.



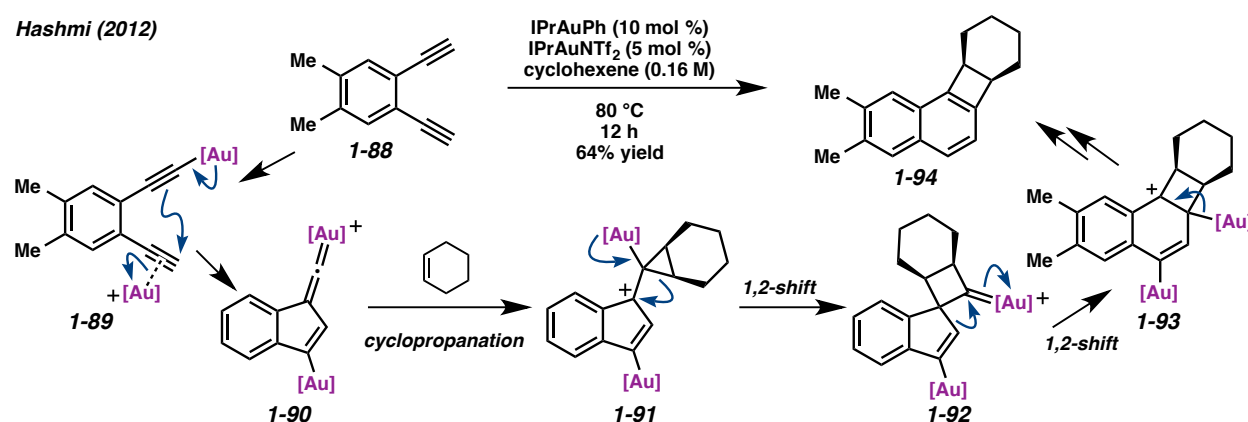
Scheme 1.14. Ring expansion vs. C–H insertion.

Another cycloisomerization/1,2-alkyl migration was reported by Echavarren and coworkers in 2006.<sup>27</sup> In this example, carbon-tethered 1,6-enyne **1-83** with an allylic cyclopropane undergoes a Au(I)-catalyzed cycloisomerization to give carbenoid **1-84** (Scheme 1.15). Next, an oxygen-assisted ring expansion occurs to relieve the carbenoid and form cyclobutane **1-85**. This intermediate undergoes an intramolecular Prins cyclization to generate tricycle **1-86**. Demetalation gives product **1-87**, the skeleton of which maps on to several sesquiterpene natural products.



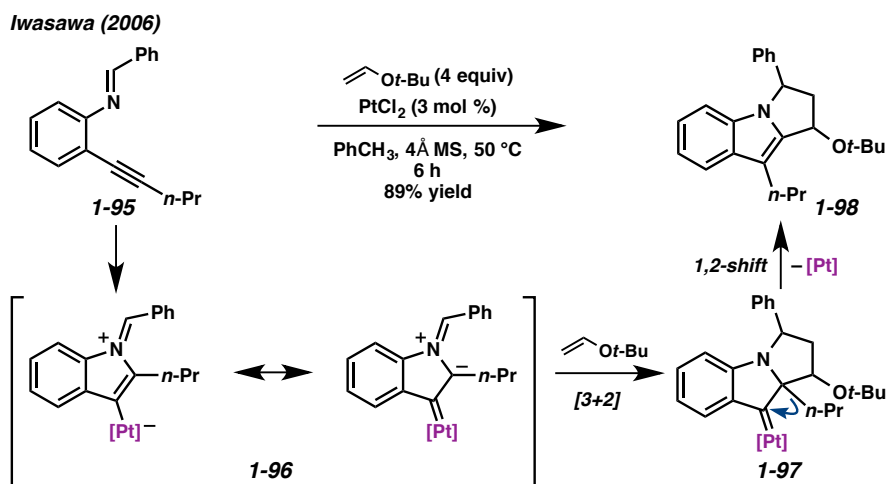
Scheme 1.15. Oxygen-assisted ring expansion in the cycloisomerization of carbon-tethered 1,6-enynes.

In 2012, Hashmi and coworkers reported the Au(I)-catalyzed rearrangement/intermolecular cyclopropanation reaction of benzene-tethered diynes and alkenes involving two sequential ring expansion events (Scheme 1.16).<sup>28</sup> Interesting about this transformation is the dual role of Au: one Au catalyst coordinates to the alkyne, while the other inserts in the terminal alkyne C–H bond, generating intermediate **1-89**. This species closes down to vinylidene intermediate **1-90**, which reacts with cyclohexene to give cyclopropane **1-91**. Next, Au-assisted cyclopropane expansion occurs to quench the carbocation, generating carbenoid **1-92**, which undergoes another ring expansion to form cyclobutane **1-93**. Elimination to regain aromaticity, followed by catalyst transfer to another equivalent of **1-88** gives the product (**1-94**).



Scheme 1.16. Alkyl migration in the rearrangement/cyclopropanation cascade of tethered diynes.

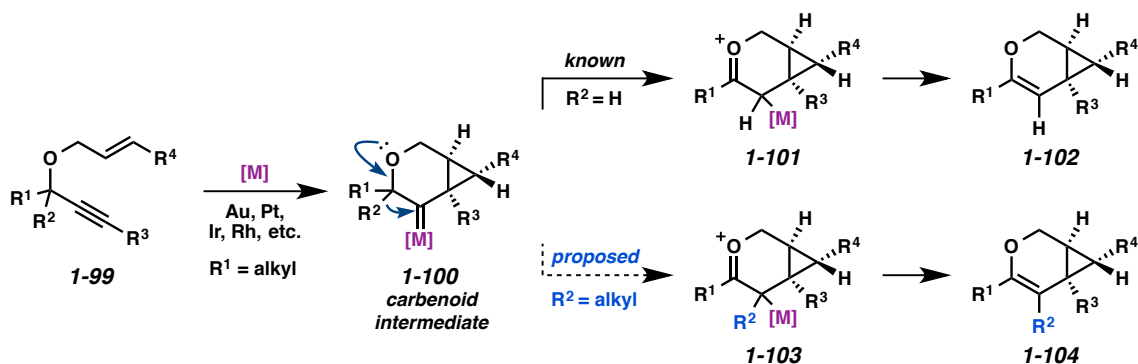
Migrations of acyclic alkyl groups have also been reported. In 2006, Iwasawa and coworkers reported a Au(I)- or Pt(II)-catalyzed [3+2] cycloaddition that proceeded with alkyl migration (Scheme 1.17).<sup>29</sup> Reaction of alkyne **1-95** and PtCl<sub>2</sub> generates azomethine ylide **1-96**, which then undergoes a [3+2] cycloaddition with *tert*-butyl vinyl ether. The resulting carbenoid (**1-97**) can undergo a 1,2-alkyl shift, with proposed assistance by the adjacent nitrogen, followed by elimination to give the tricyclic product (**1-98**). In addition to *n*-Pr, other groups were also observed to migrate. These included methyl, cyclohexyl, siloxymethyl, and phenyl.



Scheme 1.17. Example of acyclic alkyl migrations into metal carbenoids.

## 1.6 Project Proposal

Although the cycloisomerization of 1,6-enynes to bicyclo[4.1.0]heptene derivatives is typically terminated in a 1,2-hydrogen migration (**1-100**  $\rightarrow$  **1-102**), based on the precedents for C–C bond migration in alkyne activation chemistry, we hypothesized that a 1,2-alkyl shift might also be possible in substrates containing a fully substituted propargylic carbon center (Scheme 1.18,  $\text{R}^2 = \text{alkyl}$ , **1-100**  $\rightarrow$  **1-104**).<sup>30</sup> Our studies in this area will be discussed in Chapter 2.



Scheme 1.18. Proposed alkyl migration in the cycloisomerization of 1,6-enynes.

## Chapter 1 Notes and References

---

- <sup>1</sup> (a) Nieto-Oberhuber, C.; López, S.; Jiménez-Núñez, E.; Echavarren, A. M. *Chem. Eur. J.* **2006**, *12*, 5916-5923. (b) Michelet, V.; Toullec, P. Y.; Genêt, J.-P. *Angew. Chem., Int. Ed.* **2008**, *47*, 4268-4315.
- <sup>2</sup> (a) Zhang, L.; Sun, J.; Kozmin, S. A. *Adv. Synth. Catal.* **2006**, *348*, 2271-2296. (b) Jiménez-Núñez, E.; Echavarren, A. M. *Chem. Rev.* **2008**, *108*, 3326-3350.
- <sup>3</sup> Gorin, D. J.; Toste, F. D. *Nature* **2007**, *446*, 395-403.
- <sup>4</sup> Fürstner, A.; Davies, P. W. *Angew. Chem., Int. Ed.* **2007**, *46*, 3410-3449.
- <sup>5</sup> Gorin, D. J.; Davis, N. R.; Toste, F. D. *J. Am. Chem. Soc.* **2005**, *127*, 11260-11261.
- <sup>6</sup> Fürstner, A.; Stelzer, F.; Szillat, H. *J. Am. Chem. Soc.* **2001**, *123*, 11863-11869.
- <sup>7</sup> Luzing, M. R.; Markham, J. P.; Toste, F. D. *J. Am. Chem. Soc.* **2004**, *126*, 10858-10859.
- <sup>8</sup> Blum, J.; Beer-Kraft, H.; Badrieh, Y. *J. Org. Chem.* **1995**, *60*, 5567-5569.
- <sup>9</sup> Fürstner, A.; Szillat, H.; Stelzer, F. *J. Am. Chem. Soc.* **2000**, *122*, 6785-6786.
- <sup>10</sup> Nieto-Oberhuber, C.; Muñoz, M. P.; Buñuel, E.; Nevado, C.; Cárdenas, D. J.; Echavarren, A. M. *Angew. Chem., Int. Ed.* **2004**, *43*, 2402-2406.
- <sup>11</sup> Nevado, C.; Ferrer, C.; Echavarren, A. M. *Org. Lett.* **2004**, *6*, 3191-3194.
- <sup>12</sup> Shibata, T.; Kobayashi, Y.; Maekawa, S.; Toshida, N.; Takagi, K. *Tetrahedron* **2005**, *61*, 9018-9024.
- <sup>13</sup> Sim, S. H.; Lee, S. I.; Park, J. H.; Chung, Y. K. *Adv. Synth. Catal.* **2010**, *352*, 317-322.
- <sup>14</sup> Benedetti, E.; Simonneau, A.; Hours, A.; Amouri, H.; Penoni, A.; Palmisano, G.; Malacria, M.; Goddard, J.-P.; Fensterbank, L. *Adv. Synth. Catal.* **2011**, *353*, 1908-1912.
- <sup>15</sup> Watson, I.; Toste, F. D. *Chem. Sci.* **2012**, *3*, 2899-2919.
- <sup>16</sup> (a) Chao, C.-M.; Beltrami, D.; Toullec, P. Y.; Michelet, V. *Chem. Commun.* **2009**, 6988-6990. (b) Teller, H.; Corbet, M.; Mantilli, L.; Gopakumar, G.; Goddard, R.; Thiel, W.; Fürstner, A. *J. Am. Chem. Soc.* **2012**, *134*, 15331-15342.
- <sup>17</sup> (a) Brissy, D.; Skander, M.; Jullien, H.; Retailleau, P.; Marinetti, A. *Org. Lett.* **2009**, *11*, 2137-2139. (b) Brissy, D.; Skander, M.; Retailleau, P.; Frison, G.; Marinetti, A. *Organometallics* **2009**, *28*, 140-151. (c)

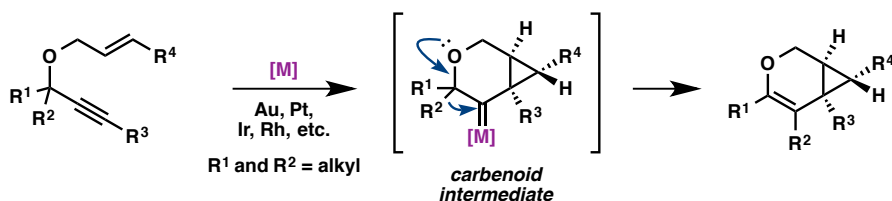
- 
- Jullien, H.; Brissy, D.; Sylvain, R.; Retailleau, P.; Naubron, J.-V.; Gladiali, S.; Marinetti, A. *Adv. Synth. Catal.* **2011**, *353*, 1109-1124.
- <sup>18</sup> Barbazanges, M.; Augé, M.; Moussa, J.; Amouri, H.; Aubert, C.; Desmarets, C.; Fensterbank, L.; Gandon, V.; Malacria, M.; Ollivier, C. *Chem. Eur. J.* **2011**, *17*, 13789-13794.
- <sup>19</sup> (a) Nishimura, T.; Kawamoto, T.; Nagaosa, M.; Kumamoto, H.; Hayashi, T. *Angew. Chem., Int. Ed.* **2010**, *49*, 1638-1641. (b) Nishimura, T.; Maeda, Y.; Hayashi, T. *Org. Lett.* **2011**, *13*, 3674-3677.
- <sup>20</sup> Newcomb, E. T.; Ferreira, E. M. *Org. Lett.* **2013**, *15*, 1772-1775.
- <sup>21</sup> (a) Deschamps, N. M.; Elitzin, V. I.; Liu, B.; Mitchell, M. B.; Sharp, M. J.; Tabet, E. A. *J. Org. Chem.* **2011**, *76*, 712-715. (b) Elitzin, V.; Liu, B.; Sharp, M.; Tabet, E. *Tetrahedron Lett.* **2011**, *52*, 3518-3520.
- <sup>22</sup> Newcomb, E. T.; Knutson, P. C.; Pedersen, B. A.; Ferreira, E. M. *J. Am. Chem. Soc.* **2016**, *138*, 108-111.
- <sup>23</sup> (a) Crone, B.; Kirsch, S. F. *Chem. Eur. J.* **2008**, *14*, 3514-3522. (b) Mack, D. J.; Njardarson, J. T. *ACS Catal.* **2013**, *3*, 272-286.
- <sup>24</sup> Markham, J. P.; Staben, S. T.; Toste, F. D. *J. Am. Chem. Soc.* **2005**, *127*, 9708-9709.
- <sup>25</sup> Luzung, M. R.; Markham, J. P.; Toste, F. D. *J. Am. Chem. Soc.* **2004**, *126*, 10858-10859.
- <sup>26</sup> Horino, Y.; Yamamoto, T.; Uedo, K.; Kuroda, S.; Toste, F. D. *J. Am. Chem. Soc.* **2009**, *131*, 2809-2811.
- <sup>27</sup> Jiménez-Núñez, E.; Claverie, C. K.; Nieto-Oberhuber, C.; Echavarren, A. M. *Angew. Chem., Int. Ed.* **2006**, *45*, 5452-5455.
- <sup>28</sup> Hashmi, A. S. K.; Wieteck, M.; Braun, I.; Rudolph, M.; Rominger, F. *Angew. Chem., Int. Ed.* **2012**, *51*, 10633-10637.
- <sup>29</sup> Kusama, H.; Miyashita, Y.; Takaya, J.; Iwasawa, N. *Org. Lett.* **2006**, *8*, 289-292.
- <sup>30</sup> As we were nearing the completion of this project, a similar transformation was reported: Simonneau, A.; Harrak, Y.; Jeanne-Julien, L.; Lemiére, G.; Mouriès-Mansuy, V.; Goddard, J.-P.; Malacria, M.; Fensterbank, L. *ChemCatChem* **2013**, *5*, 1096-1099.

## CHAPTER 2

### C–C BOND MIGRATION IN THE CYCLOISOMERIZATION OF 1,6-ENYNES

#### 2.1 Introduction: Project Proposal

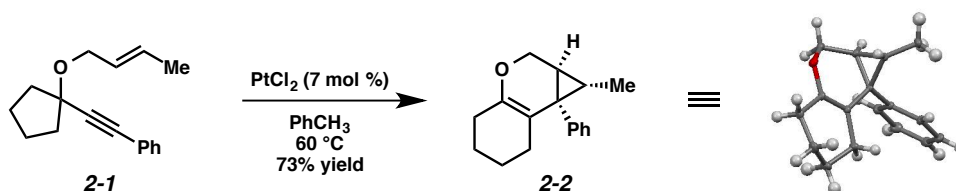
As exhibited in Chapter 1, enyne cycloisomerization is an important strategy for attaining structural complexity from simple, easily accessed starting materials. Though enyne cycloisomerization has been extensively explored, new aspects of this chemistry are still regularly reported. As mentioned previously, our lab has been interested in the cycloisomerization of 1,6-enynes to form bicyclo[4.1.0]heptene derivatives.<sup>1</sup> A large majority of the research in our lab has also focused on the synthetic utility of Pt-generated carbenoid intermediates.<sup>2</sup> In an effort to further explore the synthetic utility of metal carbenoid intermediates, we proposed to explore the propensity for alkyl migration in the context of 1,6-enyne cycloisomerization (Scheme 2.1). Fensterbank and Malacria have published a similar transformation utilizing Au catalysis; however, a relatively narrow substrate scope was reported with respect to the migrating alkyl group.<sup>3</sup> This chapter will discuss our investigation of C–C bond migration in the cycloisomerization of 1,6-enynes employing both Pt(II) and Ir(I) catalysis.<sup>4</sup>



*Scheme 2.1.* Proposed 1,2-alkyl migration into metal carbenoid.

## 2.2 Preliminary Results

A former group member, Dr. Eric Newcomb, performed the preliminary experiment for this project. When he exposed enyne **2-1** containing a fully substituted propargylic carbon to catalytic  $\text{PtCl}_2$  in toluene at 60 °C, the desired ring expanded product formed (**2-2**) (Scheme 2.2), indicating that C–C bond migration was a plausible outcome of this transformation. The structure of product **2-2** was later confirmed by X-ray crystallography.<sup>5</sup>

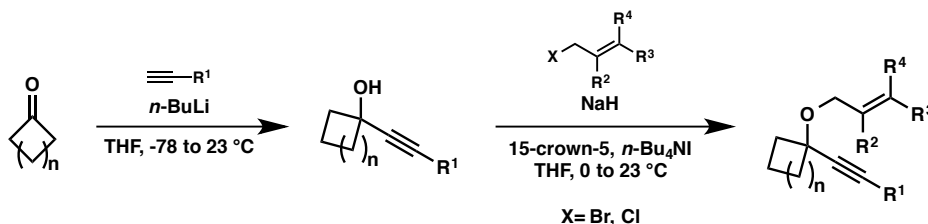


Scheme 2.2. Preliminary cycloisomerization/alkyl migration result.

## 2.3 Reaction Optimization

### 2.3.1 Initial Catalyst Screens

A variety of enyne starting materials were synthesized by nucleophilic addition of an alkyne into a cyclic ketone, followed by etherification with an allylic halide (Scheme 2.3).



Scheme 2.3. Enyne synthesis.

We began our optimization studies on enyne **2-1** with catalysts that had been previously reported to initiate 1,6-enyne cycloisomerizations (Table 2.1a). Platinum complexes, PtCl<sub>2</sub> and PtCl<sub>4</sub>, were both effective catalysts for this transformation, yielding product **2-2** in 73% and 78% yield, respectively (entries 1 and 2). An increase to 86% yield was observed with the more reactive [(C<sub>2</sub>H<sub>4</sub>)PtCl<sub>2</sub>]<sub>2</sub> (Zeise's dimer) at ambient temperature (entry 3). The use of (PhCN)<sub>2</sub>PtCl<sub>2</sub> and (Ph<sub>3</sub>P)<sub>2</sub>PtCl<sub>2</sub> resulted in only trace amounts of the cycloisomerized product (entries 4 and 5), perhaps because these complexes are more coordinatively saturated, making them less π-acidic. Catalysts of metals other than Pt were also tested. A cationic Au complex, (Ph<sub>3</sub>P)Au(NTf<sub>2</sub>), was able to effect this transformation in 63% yield (entry 6). When the cycloisomerization was attempted with [Rh(CO)<sub>2</sub>Cl]<sub>2</sub>, however, a complex mixture of products was obtained (entry 7).

Table 2.1. (a) Initial catalyst optimization. (b) Solvent optimization for Zeise's dimer.

a. Catalyst optimization					b. Solvent optimization			
Entry	Catalyst (mol %)	Temperature (°C)	Time (h)	Yield (%) <sup>a</sup>	Entry	Solvent	Time (h)	Yield (%) <sup>a</sup>
1	PtCl <sub>2</sub> (7)	60	2.5	73	1	PhCH <sub>3</sub>	3.5	86
2	PtCl <sub>4</sub> (7)	60	3	78	2	xylenes	16	62
3	[(C <sub>2</sub> H <sub>4</sub> )PtCl <sub>2</sub> ] <sub>2</sub> (2.5)	23	3.5	86	3	THF	16	47
4	(PhCN) <sub>2</sub> PtCl <sub>2</sub> (2.5)	23	2	<5	4	1,4-dioxane	20	83
5	(Ph <sub>3</sub> P) <sub>2</sub> PtCl <sub>2</sub> (2.5)	80	20	<5	5	Et <sub>2</sub> O	16	80
6	(Ph <sub>3</sub> P)Au(NTf <sub>2</sub> ) (3)	-78 to 23	12	63	6	CH <sub>2</sub> Cl <sub>2</sub>	6	63
7	[Rh(CO) <sub>2</sub> Cl] <sub>2</sub> (2.5)	80	23	— <sup>b</sup>	7	CHCl <sub>3</sub>	20	74
					8	1,2-dichloroethane	18	64
					9	hexanes	16	73
					10	CH <sub>3</sub> NO <sub>2</sub>	20	12
					11	EtOAc	18	58

<sup>a</sup> GC yields using 4,4'-di-*tert*-butylbiphenyl as internal standard  
<sup>b</sup> Complex mixture obtained

<sup>a</sup> GC yields using 4,4'-di-*tert*-butylbiphenyl as internal standard

Next a solvent screen was performed with Zeise's dimer (Table 2.1b). Both polar and nonpolar solvents provided the product in good yields, but none gave better reactivity than the original solvent

choice of toluene (entry 1). Overall, Zeise's dimer in toluene at ambient temperature seemed to give us the best results for this substrate.

When these optimized reaction conditions were applied to other enyne substrates, however, results varied (Table 2.2). For example, disubstituted alkene substrate **2-3** underwent the cycloisomerization with Zeise's dimer at ambient temperature in 70% isolated yield, which was comparable to what was observed under these reaction conditions with enyne **2-1** (Table 2.1a, entry 3). In contrast, increased substitution on the alkene (enyne **2-4** and **2-5**) required elevated temperatures in order for full conversion to be achieved, and even then product yields were poor, perhaps due to steric effects. Clearly, further optimization was needed in order to encompass a broader scope of substrates.

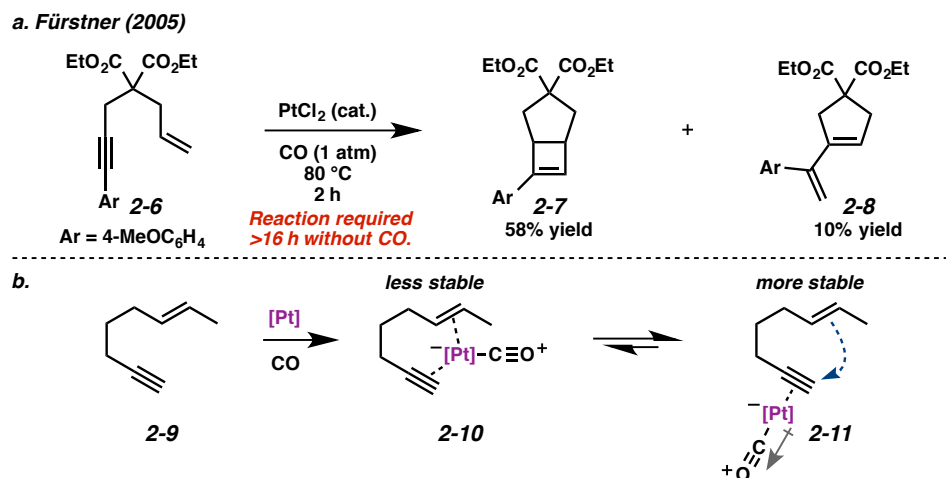
Table 2.2. Application of Zeise's dimer conditions to differentially substituted enynes.

Entry	Enyne	R <sup>1</sup>	R <sup>2</sup>	R <sup>3</sup>	R <sup>4</sup>	Temperature (°C)	Yield (%) <sup>a</sup>
1	<b>2-3</b>	Ph	H	Ph	H	23	70
2	<b>2-4</b>	<i>n</i> -Bu	Me	Me	H	60	26
3	<b>2-5</b>	<i>n</i> -Bu	H	Me	Me	60	11

<sup>a</sup> Isolated

### 2.3.2 Effect of CO

In 2005, Fürstner and coworkers reported the use of carbon monoxide to increase reaction rates in Pt(II)-catalyzed cycloisomerizations of carbon-tethered 1,6-enyne **2-6** (Scheme 2.4a).<sup>6</sup> They propose that this beneficial effect may be due to the increased electrophilicity of the metal catalyst through coordination of a  $\pi$ -accepting ligand (Scheme 2.4b). Computational experiments also suggest that the formation of the Pt-CO complex increases the preference of the metal for mono-coordination (**2-11**) of the alkyne as opposed to alkene-alkyne bis-coordination (**2-10**), the former enabling a more facile reaction.<sup>7</sup>



*Scheme 2.4.* (a) Fürstner's use of CO to accelerate the cycloisomerization of enyne **2-6**. (b) Proposed coordination of Pt-CO complex with enyne.

Hoping to see a similar increase in reaction rate and yield, we evaluated the effect of CO on the cycloisomerization of enyne **2-12**, a substrate which had previously performed mediocrely when exposed to Zeise's dimer under Ar (Table 2.3, entry 3). Encouragingly, the PtCl<sub>2</sub>-catalyzed cycloisomerization run under CO proceeded in 75% yield and in a shorter reaction time than the same reaction run under Ar (entries 1 and 2). Likewise, Zeise's dimer in the presence of CO gave product **2-13** in 88% yield, compared to 63% yield under Ar (entries 3 and 4). Thus, our final optimized Zeise's dimer conditions were concluded to be 2.5 mol % catalyst in toluene at 60 °C under CO.

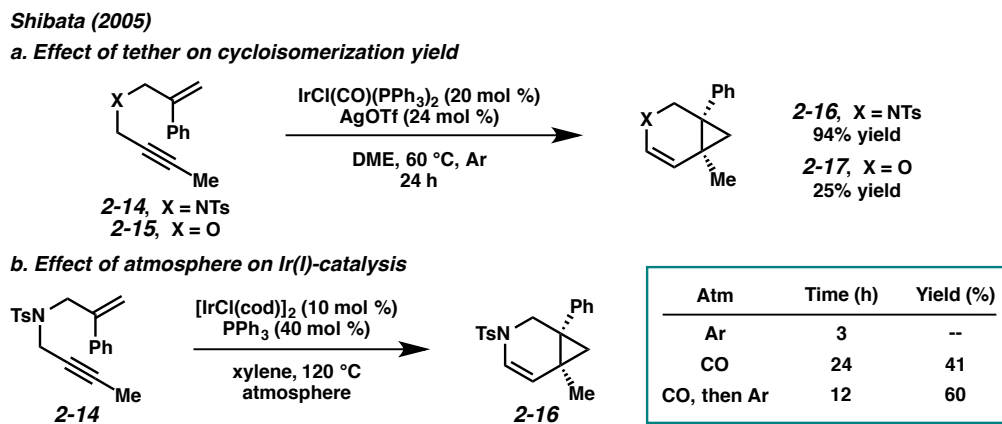
*Table 2.3.* Effect of CO atmosphere.

Entry	Catalyst (mol %)	Atmosphere	Time (h)	Yield (%) <sup>a</sup>
1	PtCl <sub>2</sub> (7)	Ar	43	54
2	PtCl <sub>2</sub> (7)	CO (1 atm)	25	75
3	[(C <sub>2</sub> H <sub>4</sub> )PtCl <sub>2</sub> ] <sub>2</sub> (2.5)	Ar	43	63
4	[(C <sub>2</sub> H <sub>4</sub> )PtCl <sub>2</sub> ] <sub>2</sub> (2.5)	CO (1 atm)	30	88

<sup>a</sup> Isolated

### 2.3.4 Optimization of Ir(I) Conditions

A report by Shibata and coworkers in 2005 described the use of Ir(I) complexes with CO in the cycloisomerization of mainly nitrogen-tethered 1,6-enynes (Scheme 2.5).<sup>8</sup> In light of the success of our Pt(II)/CO system, we thought it worthwhile to examine Ir(I)/CO catalyst systems with our oxygen-tethered enyne cycloisomerization.<sup>9</sup>



Scheme 2.5. (a) Comparison of nitrogen- vs. oxygen-tethered enynes. (b) Comparison of reaction atmospheres.

One catalyst employed in Shibata's report was IrCl(CO)(PPh<sub>3</sub>)<sub>2</sub> (Vaska's complex);<sup>10</sup> however, we saw very little reactivity with this catalyst, either under an Ar or CO atmosphere (Table 2.4, entries 1 and 2). In the report, mostly nitrogen-tethered substrates were evaluated. Their one oxygen-tethered enyne example reacted in significantly lower yield than the analogous nitrogen-tethered substrates (Scheme 2.5a, **2-16** vs. **2-17**), suggesting that Vaska's complex may be more suited for cycloisomerizations of nitrogen-tethered enynes. Other Ir complexes, Ir<sub>4</sub>(CO)<sub>12</sub>, Ir(CO)<sub>2</sub>(acac), and a chiral Ir salt, [Ir(dbcot)(L)]<sup>+</sup>, all performed poorly as well, giving low conversions after extended reaction times (entries 3-5). Initially, [Ir(cod)Cl]<sub>2</sub> also showed low reactivity, with only 24% of product **2-13** forming in 60 hours under Ar (entry 6). When [Ir(cod)Cl]<sub>2</sub> was prepared under CO, but the reaction was run under

Ar, an increase in yield to 37% was observed with a shorter reaction time as well (entry 7). Utilizing this same technique with  $[\text{Ir}(\text{dbcot})\text{Cl}]_2$  resulted in 68% yield of product **2-13** in only 3 h (entry 8). This method of “CO, then Ar” was described in Shibata’s report as sometimes resulting in higher yields than simply running the reaction under CO (Scheme 2.5b), but this effect was not elaborated upon. Experimentally, the reactions under an atmosphere of CO were performed by bubbling CO through the reaction mixture, and then running the reaction with a balloon of CO attached. The “CO, then Ar” experiments were performed by bubbling CO through the reaction mixture, and then bubbling Ar through the reaction mixture and sealing the vessel.

Table 2.4. Evaluation of Ir catalyst conditions under CO.

Entry	R	Catalyst (mol %)	Atmosphere	Time (h)	Result (%) <sup>a</sup>
1	CH <sub>2</sub> OBn	$\text{IrCl}(\text{CO})(\text{PPh}_3)_2$ (10)	Ar	16	<5% conversion
2	CH <sub>2</sub> OBn	$\text{IrCl}(\text{CO})(\text{PPh}_3)_2$ (5)	CO (1 atm)	16	<5% conversion
3	<i>n</i> -Bu	$[\text{Ir}(\text{dbcot})(\text{L})]^+\text{SbF}_6^-$ (5)	CO (1 atm)	16	<5% conversion
4	<i>n</i> -Bu	$\text{Ir}_4(\text{CO})_{12}$ (3)	CO, then Ar	40	50% conversion
5	<i>n</i> -Bu	$\text{Ir}(\text{CO})_2(\text{acac})$ (5)	CO, then Ar	40	<10% conversion
6	<i>n</i> -Bu	$[\text{Ir}(\text{cod})\text{Cl}]_2$ (2.5)	Ar	60	24% yield
7	<i>n</i> -Bu	$[\text{Ir}(\text{cod})\text{Cl}]_2$ (2.5)	CO, then Ar	16	37% yield
8	<i>n</i> -Bu	$[\text{Ir}(\text{dbcot})\text{Cl}]_2$ (2.5)	CO, then Ar	3	68% yield

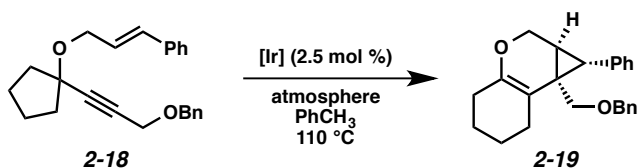
<sup>a</sup> Conversions are approximated by <sup>1</sup>H NMR; yields are isolated.

### 2.3.5 CO vs. “CO, then Ar”

Intrigued by the “CO, then Ar” technique, we investigated further. Table 2.5 compares the yields of cycloisomerization product **2-19** with three different Ir(I) catalysts both under a CO atmosphere and the “CO, then Ar” atmosphere. For  $[\text{Ir}(\text{dbcot})\text{Cl}]_2$  and  $[\text{Ir}(\text{cod})\text{Cl}]_2$ , the yield of product **2-19** increased from

72% to 87% and from 63% to 81% yield, respectively, when the “CO, then Ar” conditions were applied versus when the reactions were just performed under CO (entries 1 and 2). An increase in yield was also observed for  $[\text{Ir}(\text{coe})_2\text{Cl}]_2$ ; however, the effect was less pronounced (entry 3).

Table 2.5. Comparison of CO vs. “CO, then Ar” atmospheres.



Entry	[Ir]	Yield (%) <sup>a</sup>	
		CO (1 atm)	CO, then Ar
1	$[\text{Ir}(\text{dbcot})\text{Cl}]_2$	72	87
2	$[\text{Ir}(\text{cod})\text{Cl}]_2$	63	81
3	$[\text{Ir}(\text{coe})_2\text{Cl}]_2$	47	50

<sup>a</sup> Isolated

### 2.3.6 Active Ir Catalyst

Interestingly, when CO was bubbled through a solution of bright yellow  $[\text{Ir}(\text{dbcot})\text{Cl}]_2$ ,  $[\text{Ir}(\text{cod})\text{Cl}]_2$ , or  $[\text{Ir}(\text{coe})_2\text{Cl}]_2$  in toluene, a dark blue solid precipitated out on the sides of the reaction vessel. This solid dissolved in toluene when heated. Similar observations were made by Roberto and coworkers in 1994 when they exposed  $[\text{Ir}(\text{coe})_2\text{Cl}]_2$  to CO: the metal complex changed from bright yellow to dark blue.<sup>11</sup> Through IR experiments, they proposed that the dark blue compound being formed was an  $[\text{Ir}(\text{CO})_2\text{Cl}]_n$  polymeric complex. Based on this report and our observations, we believe the actual active catalyst in the reactions where  $[\text{Ir}(\text{dbcot})\text{Cl}]_2$ ,  $[\text{Ir}(\text{cod})\text{Cl}]_2$ , or  $[\text{Ir}(\text{coe})_2\text{Cl}]_2$  are performed with CO is the same  $[\text{Ir}(\text{CO})_2\text{Cl}]_n$  polymeric complex.

If this theory is correct and the active Ir catalyst is being formed *in situ* through reaction with CO, then it would seem as if the starting Ir complex does not matter. In the cycloisomerization of enyne **2-18**,

however, we observed a slight variance in yield between  $[\text{Ir}(\text{dbcot})\text{Cl}]_2$  and  $[\text{Ir}(\text{cod})\text{Cl}]_2$ , and a more significant difference between these two and  $[\text{Ir}(\text{coe})_2\text{Cl}]_2$  (Table 2.5).

We considered that the differential reactivity between the three Ir(I) catalysts may simply be attributed to the ease of  $[\text{Ir}(\text{CO})_2\text{Cl}]_n$  formation from  $[\text{Ir}(\text{dbcot})\text{Cl}]_2$  and  $[\text{Ir}(\text{cod})\text{Cl}]_2$  compared to  $[\text{Ir}(\text{coe})_2\text{Cl}]_2$ . When comparing the stability of each complex and their metal-ligand bond strengths, however, this explanation is insufficient. Of the three ligands, the bidentate chelation of dbcot and cod should render the  $[\text{Ir}(\text{dbcot})\text{Cl}]_2$  and  $[\text{Ir}(\text{cod})\text{Cl}]_2$  complexes more stable than  $[\text{Ir}(\text{coe})_2\text{Cl}]_2$  due to the chelate effect.<sup>12</sup> Further, comparing the dbcot and cod ligands, dbcot should bind more strongly to the metal due to its greater  $\pi$ -accepting character.<sup>13</sup> This suggests that the  $[\text{Ir}(\text{CO})_2\text{Cl}]_n$  complex should form the least efficiently from  $[\text{Ir}(\text{dbcot})\text{Cl}]_2$  and the most efficiently from  $[\text{Ir}(\text{coe})_2\text{Cl}]_2$ ; however, the effect we observe with respect to yields is the exact opposite (Figure 2.1). This led us to wonder whether the displaced ligand may be playing a role in the reactivity of the metal.

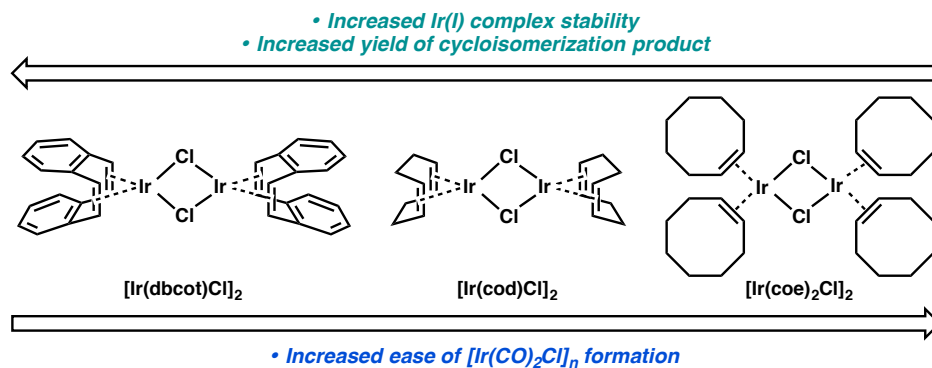
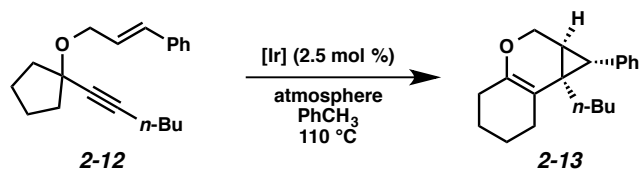


Figure 2.1. Structures and relative stabilities of three Ir(I) catalysts.

To better understand the catalyst system and to probe whether or not the displaced ligand could be influencing the reactivity of the metal, experiments were performed where the displaced ligand was removed from the reaction mixture prior to addition of the enyne. For these experiments, the Ir(I) catalyst was taken up in toluene and CO was bubbled through the solution, causing the dark blue  $[\text{Ir}(\text{CO})_2\text{Cl}]_n$  precipitate to form. The toluene, which contained the displaced ligand (confirmed by  $^1\text{H}$  NMR), was then

removed from the flask as thoroughly as possible, leaving the solid behind. The dark blue solid was then taken up in fresh toluene, enyne **2-12** was added, and the reaction was performed as usual. The yields of product **2-13** with the displaced ligand still present and with the ligand removed were compared (Table 2.6). A small decrease in yield from 68% to 64% was observed when dbcot was removed from reaction mixture (entry 1), but almost no change in yield was observed for the  $[\text{Ir}(\text{cod})\text{Cl}]_2$  with and without excess ligand present (entry 2). In the case of  $[\text{Ir}(\text{coe})_2\text{Cl}]_2$ , a slightly larger decrease in yield was observed when the excess coe was removed from the reaction mixture (entry 3). Ultimately, the yield changes observed when the excess ligand was removed from the reaction mixture are not substantial enough to conclusively indicate whether or not the displaced ligand has an effect on reactivity. It remains possible, however, that when the displaced ligand is still present, some kind of beneficial competitive binding between the ligand and the  $[\text{Ir}(\text{CO})_2\text{Cl}]_n$  complex with the enyne substrate may be operative.

Table 2.6. Evaluation of effect of removing excess ligand.



Entry	[Ir]	Yield (%) <sup>a</sup>	
		CO, then Ar	CO, then Ar <sup>b</sup>
1	$[\text{Ir}(\text{dbcot})\text{Cl}]_2$	68	64
2	$[\text{Ir}(\text{cod})\text{Cl}]_2$	37	38
3	$[\text{Ir}(\text{coe})_2\text{Cl}]_2$	49	39

<sup>a</sup> Isolated

<sup>b</sup> Excess ligand removed

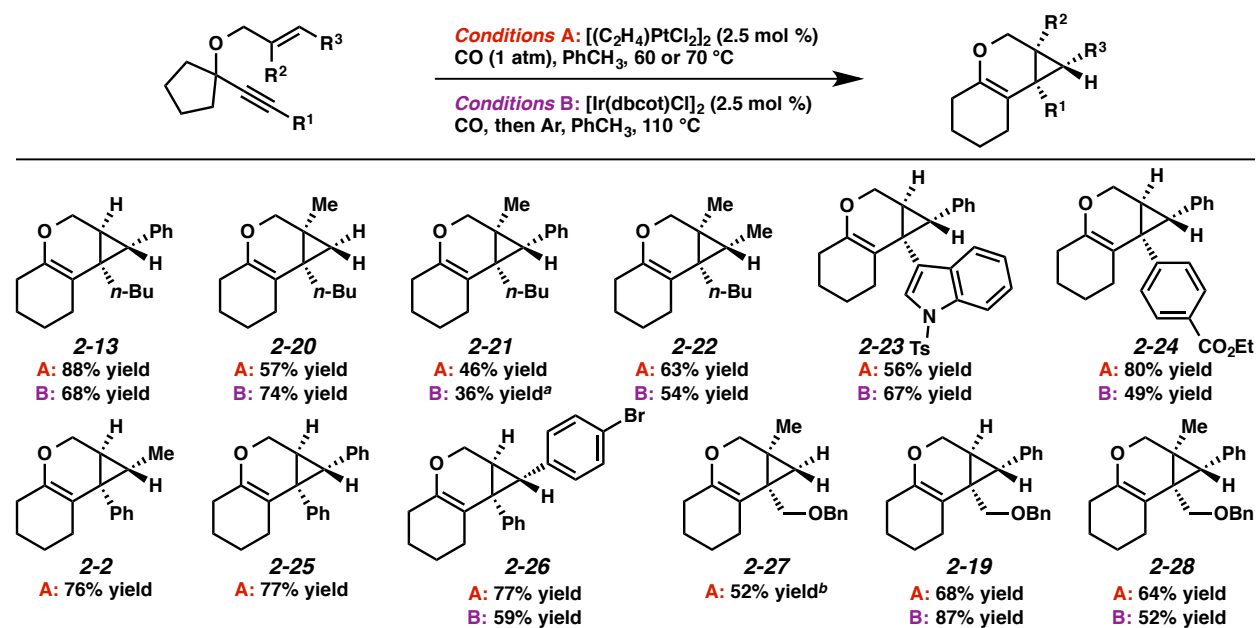
## 2.4 Substrate Scope

In the interest of exploring new reaction conditions and comparing the Pt(II) and Ir(I) systems for different substrates, we investigated the substrate scope of this transformation using both our optimized

Zeise's dimer and  $[\text{Ir}(\text{dbcot})\text{Cl}]_2$  conditions.  $\text{PtCl}_2$  was also employed, specifically for the different ring-size substrates.

### 2.4.1 Alkene and Alkyne Variation

Overall, yields ranged from moderate to very good. With respect to alkene substitution, both alkyl and aryl substituents were tolerated (Scheme 2.6). Substitution at the terminus of the alkene (position  $\text{R}^3$ ) resulted in higher yields than internal substitution (position  $\text{R}^2$ ). This could be due to the increased stabilization of the short-lived carbocation intermediate upon nucleophilic attack of the alkene. Trisubstituted alkenes **2-21**, **2-22**, and **2-28** reacted in lower yields than the disubstituted alkenes with both Pt(II) and Ir(I) conditions, likely due to sterics. Both alkyl and aryl substituents were also tolerated on the alkyne. Notably, both electron-rich and electron-poor alkynes efficiently underwent the cycloisomerization (**2-23** and **2-24**).

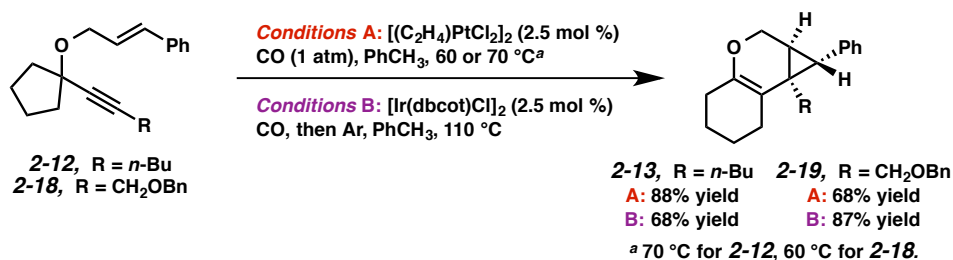


<sup>a</sup> Run under CO (1 atm)

<sup>b</sup> Run under Ar

Scheme 2.6. Scope of alkene and alkyne variation.

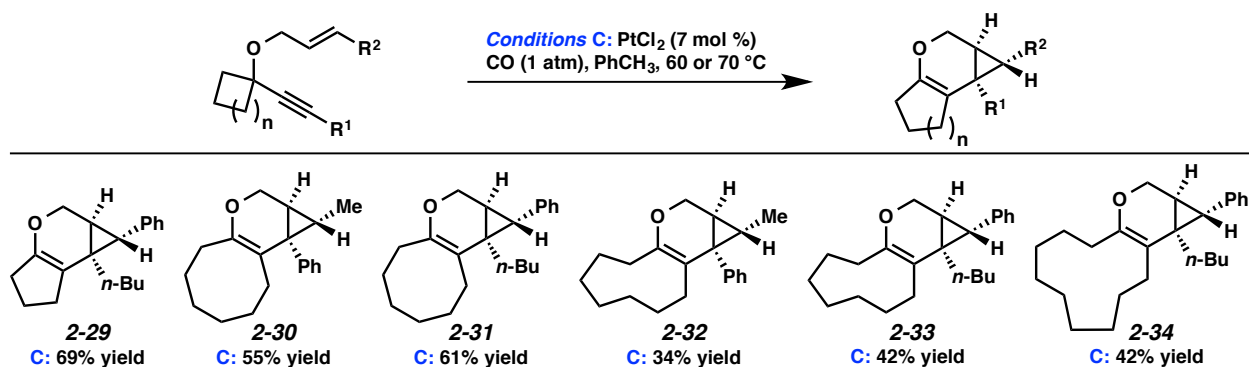
In terms of the Pt(II) vs. Ir(I) conditions, we were not able to draw any conclusions about why one set of conditions seemed to work better than the other; patterns in yields were hard to discern. For example, the Pt(II) conditions seemed to work better for enyne **2-12** with a Ph-substituted alkene and *n*-Bu-substituted alkyne, giving the product (**2-13**) in 88% yield vs. 68% yield with the Ir(I) conditions (Scheme 2.7). With Ph-substituted alkene **2-18**, however, which also contained an alkyl-substituted alkyne (–CH<sub>2</sub>OBn), essentially opposite reactivity was observed: Pt(II) catalysis gave the product (**2-19**) in 68% yield, while Ir(I) catalysis gave 87% yield. Ultimately, optimal reaction conditions seemed to be fairly substrate-dependent.



Scheme 2.7. Comparison of Pt(II) and Ir(I) catalyst systems for two similar substrates.

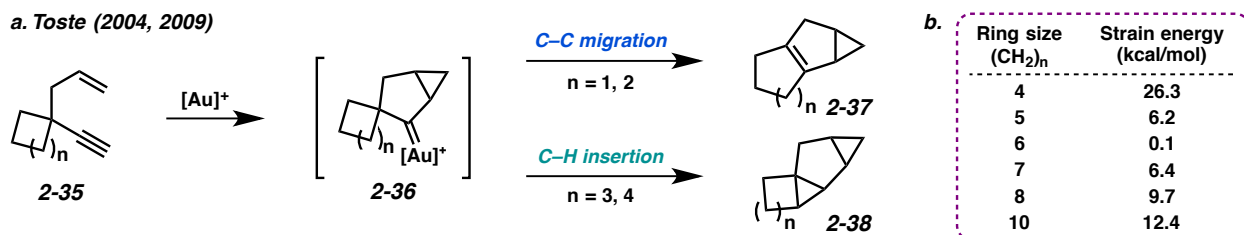
## 2.4.2 Ring Size Variation

Next, we explored the propensity for alkyl shifts in substrates with larger and smaller cycloalkanes at the propargylic position (Scheme 2.8). Not surprisingly, under PtCl<sub>2</sub>-catalysis a four-membered ring was observed to expand to give five-membered ring product **2-29**. Medium sized rings (7- and 8-membered) also underwent the cycloisomerization/alkyl shift to yield products **2-30–2-33**, albeit in lower yields. Even an 11-membered ring product (**2-34**) was formed in 42% yield. This finding is significant, considering that few methods exist to access large carbocyclic frameworks.



Scheme 2.8. Scope of ring size variation.

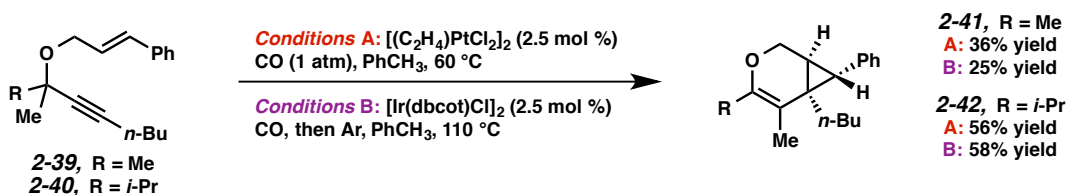
These results are in contrast to previous reports by Toste and coworkers where, in the Au-catalyzed cycloisomerization of carbon-tethered 1,5-enynes, 4- and 5-membered rings underwent a ring expansion into the Au-carbenoid (**2-36**  $\rightarrow$  **2-37**), while 6- and 7-membered rings underwent a C–H insertion (**2-36**  $\rightarrow$  **2-38**) (Scheme 2.9a).<sup>14</sup> Though this variance in reactivity may simply be catalyst- or substrate-dependent, both transformations are thought to proceed through similar carbenoid intermediates. Perhaps, in our oxygen-tethered case, stabilization by the adjacent oxygen atom through oxocarbenium formation promotes the alkyl migration for the larger ring substrates. Ring strain may also be playing a role; 4- and 5-membered rings have higher strain energies than 6- and 7-membered rings (though the 5- and 7-membered ring strains are very close),<sup>15</sup> thus the smaller rings will more readily undergo ring expansion (Scheme 2.9b). This would imply that in Toste’s Au-catalyzed 1,5-enyne cycloisomerization, product formation is driven by release of ring strain, but in our 1,6-enyne Pt(II)-catalyzed system, the release of ring strain may not be playing a significant role.



Scheme 2.9. (a) C–C migration vs. C–H insertion. (b) Ring strain energies.

### 2.4.3 Acyclic C–C Bond Migration

Lastly, since release of ring strain did not seem to be necessary for migration into the carbenoid, we hypothesized that acyclic alkyl groups could shift as well. Indeed, we observed methyl-migration into both Pt(II)- and Ir(I)-generated carbenoids to afford products **2-41** and **2-42** in moderate yields (Scheme 2.10). In the case of cycloisomerization product **2-42**, the methyl group shifted exclusively over the larger isopropyl group.



Scheme 2.10. Acyclic C–C bond migrations.

### 2.4.4 Unsuccessful Substrates

Enynes that were not effective substrates for the cycloisomerization are depicted in Figure 2.2. Terminal alkene **2-43** was likely an inefficient substrate due to the lower nucleophilicity of the alkene. Conversely, tetrasubstituted olefin **2-44** also did not undergo the cycloisomerization. This alkene may have been too sterically encumbered for efficient nucleophilic attack on the alkyne. Allylic benzyl ether **2-45** did not yield any cycloisomerization product, which was unexpected considering that the propargylic benzyl ether was well tolerated in this transformation. Vinylsilane (**2-46**) was also not an effective substrate, despite this functionality having been employed in past cycloisomerization literature.<sup>16</sup> Curiously, cyclohexyl enyne **2-47** was not an efficient substrate for the cycloisomerization. When enyne **2-47** was exposed to the reaction conditions, a complex mixture of products was obtained, in which neither the ring-expanded product or the C–H insertion product could be identified.

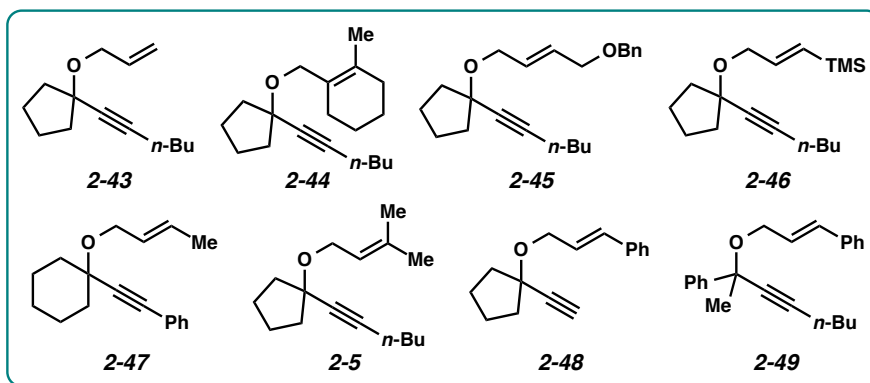


Figure 2.2. Substrates that did not efficiently undergo the cycloisomerization.

In the case of enyne **2-5**, we observed that the enyne was being consumed under the cycloisomerization conditions, yet the yield of the desired product was very low. This was somewhat surprising considering the carbocation intermediate that would result from nucleophilic attack of the geminal dimethyl alkene would be relatively stable. To try to explain this consumption of starting material but low yield, we wondered if product decomposition may be occurring. Probing this hypothesis, we exposed cycloisomerization product **2-50** to the reaction conditions (Zeise's dimer,  $\text{PhCH}_3$ , 70-105 °C, ~18 h), but no product decomposition was observed by TLC or  $^1\text{H}$  NMR.

We also considered that some kind of catalyst inhibition could be occurring where product generated during the reaction could be inhibiting the cycloisomerization through complexation of the catalyst by the enol ether moiety. To test this hypothesis, the cycloisomerization of prenyl substrate **2-5** was performed with 0.5 equivalents of product **2-50** also included in the initial reaction mixture. This reaction proceeded to completion despite the presence of the additional enol ether, so product inhibition was disproved as well.

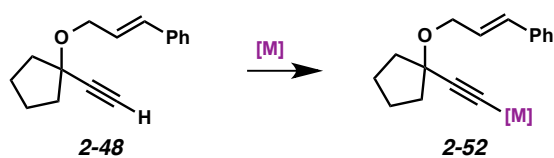
Lastly, the cycloisomerization of enyne **2-5** was performed in an NMR tube to ascertain side products in the reaction mixture that could have been removed through the workup procedure. The  $^1\text{H}$  NMR experiment on the cycloisomerization of prenyl substrate **2-5** revealed a peak at ~9.76 ppm, indicative of an aldehyde in the crude product mixture. Aldehyde **2-51** could arise from ionization of

enyne **2-5** to give the propargyl cation and oxygen anion, then oxidation of the resulting alcohol (Scheme 2.11). The formation of this aldehyde may explain why the starting material was consumed, but a low yield of product **2-50** was obtained. In addition, we believe this ether ionization/aldehyde formation is also likely occurring in some of our more modest yielding cycloisomerizations.



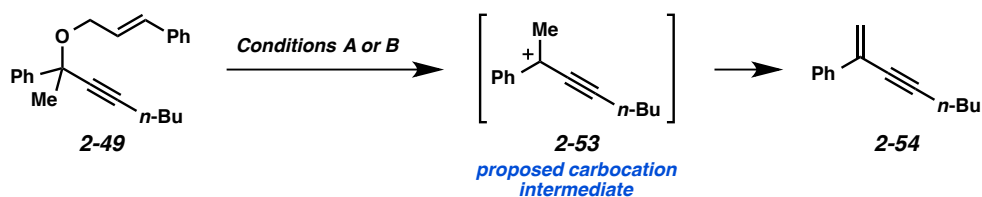
*Scheme 2.11.* Decomposition of enyne **2-5** to aldehyde **2-51**.

Terminal alkyne substrate **2-48** also did not undergo the cycloisomerization. This is not uncommon in the enyne cycloisomerization literature, although certain approaches to terminal alkyne substrates have seen success, particularly with Ir(I) catalysis.<sup>17</sup> A possible explanation for this lack of reactivity could be deprotonation or C–H insertion of the metal at the terminus of the alkyne (**2-52**), rendering the catalyst incapable of facilitating the cycloisomerization (Scheme 2.12).



*Scheme 2.12.* Proposed deactivation of metal by terminal alkyne.

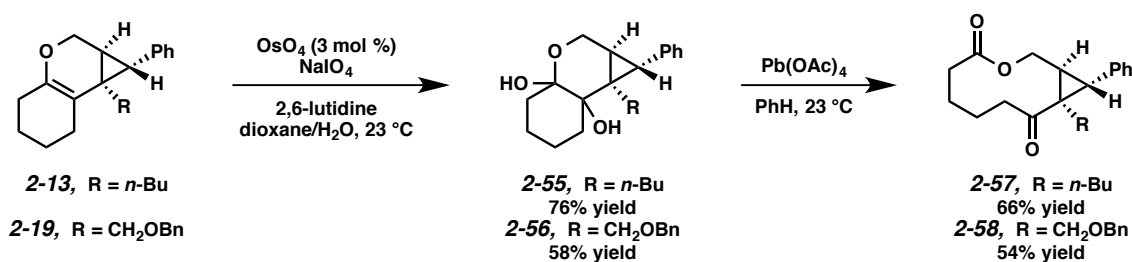
Lastly, acyclic substrate **2-49** with phenyl substitution at the propargylic position also did not undergo the cycloisomerization, perhaps due to the stability of benzylic carbocation (**2-53**) upon ionization of the tethered ether (Scheme 2.13).



Scheme 2.13. Proposed ionization of tethered ether.

## 2.5 Synthesis of Macrolactones from Cycloisomerization Products

Macrocyclic synthesis is of increasing interest in the natural product community due to the prevalence of this motif in biologically active molecules.<sup>18</sup> We envisioned that our cycloisomerization/ring expansion process could provide access to macrolactones via oxidative cleavage of the cyclic enol ether of the products. With this in mind, a two-step method to convert the tricyclic products into macrolactones was devised (Scheme 2.14). Reaction of tricycles **2-13** and **2-19** with catalytic  $\text{OsO}_4$  gave diols **2-55** and **2-56** in 76% and 58% yield, respectively. The resulting diols were then cleaved with  $\text{Pb}(\text{OAc})_4$  to give macrolactones **2-57** and **2-58**.



Scheme 2.14. Oxidative cleavage to access macrolactones.

## 2.6 Conclusion

We have developed a Pt(II)- or Ir(I)-catalyzed enyne cycloisomerization/C–C bond migration reaction that provides access to tricyclic enol ethers. A variety of substituted enyne substrates undergo the

cycloisomerization, and both cyclic and acyclic alkyl groups are able to migrate into the carbenoid intermediates. The influence of CO on both the Pt(II)- and Ir(I)-catalyst systems was also explored. The cycloisomerization products can also be cleaved to generate macrolactones. Ultimately, this ring expansion process provides access to large carbocycles, which are traditionally synthetically challenging.

## 2.7 Experimental Section

### 2.7.1 Materials and Methods

Reactions were performed under an argon atmosphere unless otherwise noted. Tetrahydrofuran, toluene, and benzene were purified by passing through activated alumina columns. All other reagents were used as received unless otherwise noted. Commercially available chemicals were purchased from Alfa Aesar (Ward Hill, MA), Sigma-Aldrich (St. Louis, MO), Oakwood Products, (West Columbia, SC), Strem (Newburyport, MA) and TCI America (Portland, OR). Qualitative TLC analysis was performed on 250 mm thick, 60 Å, glass backed, F254 silica (Silicycle, Quebec City, Canada). Visualization was accomplished with UV light and exposure to *p*-anisaldehyde or ceric ammonium molybdate (CAM) solutions followed by heating. Flash chromatography was performed using Silicycle silica gel (230-400 mesh). NMR spectra were acquired at both the Colorado State University Central Instrument Facility on an Agilent (Varian) 400-MR and at the University of Georgia Chemical Sciences Magnetic Resonance Facility on a Varian Mercury Plus 400 MHz NMR. <sup>1</sup>H NMR spectra were acquired at 400 MHz and are reported relative to SiMe<sub>4</sub> (δ 0.00). <sup>13</sup>C NMR spectra were at 100 MHz and are reported relative to SiMe<sub>4</sub> (δ 0.0). All IR spectra were obtained on NaCl plates (film) with a Bruker Tensor 27. Gas chromatography was performed on a Varian CP-3800 gas chromatograph. High resolution mass spectrometry data were acquired by the Colorado State University Central Instrument Facility on an Agilent 6210 TOF LC/MS and by the Proteomics and Mass Spectrometry Facility at the University of Georgia on a Thermo Orbitrap Elite.

## 2.7.2 Enyne Cycloisomerizations

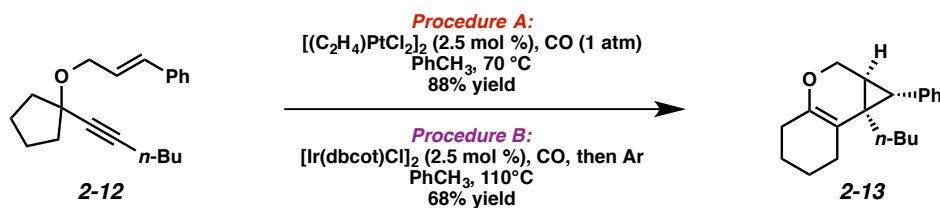
**General Notes:** All solvents used were anhydrous and all reactions were performed in flame-dried glassware. Without the addition of triethylamine to the flash chromatography eluent, decreased yields were observed. In the cycloisomerizations run with  $[\text{Ir}(\text{dbcot})\text{Cl}]_2$ , 1,3-bis(diphenylphosphino)propane (dppp) was added in the work up to chelate the iridium. NMR spectra for the cycloisomerization products were taken in  $d_6$ -benzene, since the products decomposed in  $\text{CDCl}_3$ .

**A. General procedure for the cycloisomerization of oxygen-tethered 1,6-enynes catalyzed by Zeise's dimer ( $[(\text{C}_2\text{H}_4)\text{PtCl}_2]_2$ ).** To a solution of the 1,6-enyne (1 equiv) in toluene (0.06 M) in a 2-dram vial under argon was quickly added Zeise's dimer (2.5 mol %). CO was bubbled through the solution using a balloon and needle outlet (ca. 30 s). The balloon and outlet were then removed and the solution was stirred at the described temperature until all of the starting material was consumed, as determined by TLC. The reaction was allowed to cool to ambient temperature and diluted with an approximately equal amount of hexanes. The mixture was stirred for 15 min, then passed through a small plug of  $\text{Al}_2\text{O}_3$  (hexanes  $\rightarrow$  1:1 hexanes/EtOAc eluent). The volatile materials were removed by rotary evaporation and the resulting residue was purified by flash chromatography.

**General procedure for the *scaled-up* cycloisomerization of oxygen-tethered 1,6-enynes catalyzed by Zeise's dimer ( $[(\text{C}_2\text{H}_4)\text{PtCl}_2]_2$ ).** To a solution of the 1,6-enyne (1 equiv) in toluene (0.15 M) in a 16 x 125 mm glass culture tube under argon was quickly added Zeise's dimer (2.5 mol %). CO was bubbled through the solution using a balloon and needle outlet (ca. 30 s). The balloon and outlet were then removed and the solution was stirred at the described temperature until all of the starting material was consumed, as determined by TLC. The reaction was allowed to cool to ambient temperature and the volatile materials were removed by rotary evaporation. The resulting residue was purified by flash chromatography.

**B. General procedure for the cycloisomerization of oxygen-tethered 1,6-enynes catalyzed by [Ir(dbcot)Cl]<sub>2</sub>.** To a solution of the 1,6-enyne (1 equiv) in toluene (0.06 M) in a 16 x 125 mm glass culture tube under argon was quickly added [Ir(dbcot)Cl]<sub>2</sub> (2.5 mol %). CO was bubbled through the solution using a balloon and needle outlet (ca. 30 s), during which time the reaction mixture turned a dark-blue/black color. The balloon was removed and argon was bubbled through the reaction mixture in the same manner. The septum was quickly replaced with a Teflon cap and the reaction mixture was stirred at 110 °C until all of the starting material was consumed, as determined by TLC. The reaction was allowed to cool to ambient temperature and diluted with an approximately equal amount of hexanes. 1,3-Bis(diphenylphosphino)propane (dppp) (0.25 equiv) was also added to the mixture. The mixture was stirred for 15 min, then passed through a small plug of Al<sub>2</sub>O<sub>3</sub> (hexanes → 1:1 hexanes/EtOAc eluent). The volatile materials were removed by rotary evaporation and the resulting residue was purified by flash chromatography.

**C. General procedure for the cycloisomerization of oxygen-tethered 1,6-enynes catalyzed by PtCl<sub>2</sub>.** To a solution of the 1,6-enyne (1 equiv) in toluene (0.06 M) in a 2-dram vial under argon was quickly added PtCl<sub>2</sub> (7 mol %). CO was bubbled through the solution using a balloon and needle outlet (ca. 30 s). The balloon and outlet were then removed and the solution was stirred at the described temperature until all of the starting material was consumed, as determined by TLC. The reaction was allowed to cool to ambient temperature and diluted with an approximately equal amount of hexanes. The mixture was stirred for 15 min, then passed through a small plug of Al<sub>2</sub>O<sub>3</sub> (hexanes → 1:1 hexanes/EtOAc eluent). The volatile materials were removed by rotary evaporation and the resulting residue was purified by flash chromatography.

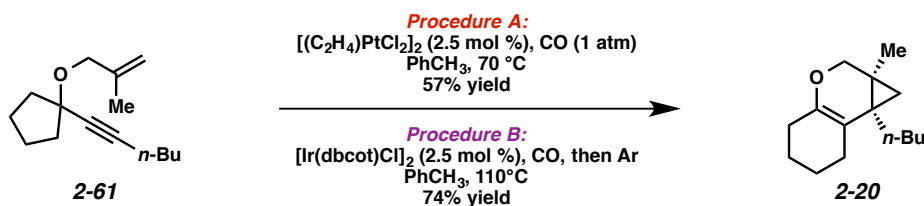


**Tricyclic 2-13. Procedure A:** To a solution of enyne **2-12** (16.0 mg, 56.7  $\mu$ mol) in toluene (0.92 mL) in a 2-dram vial under argon was quickly added  $[(C_2H_4)PtCl_2]_2$  (0.9 mg, 1.53  $\mu$ mol). CO was bubbled through the solution using a balloon and needle outlet (ca. 30 s). The balloon and outlet were then removed and the solution was stirred at 70 °C for 43 h. The reaction was allowed to cool to ambient temperature and was diluted with an approximately equal amount of hexanes. The mixture was stirred for 15 min, then passed through a small plug of Al<sub>2</sub>O<sub>3</sub> (hexanes  $\rightarrow$  1:1 hexanes/EtOAc eluent). The volatile materials were removed by rotary evaporation and the resulting residue was purified by flash chromatography (99:1 hexanes/CH<sub>2</sub>Cl<sub>2</sub> w/ 0.5% Et<sub>3</sub>N  $\rightarrow$  5:1 hexanes/CH<sub>2</sub>Cl<sub>2</sub> w/ 0.5% Et<sub>3</sub>N eluent) affording tricyclic **2-13** (14.1 mg, 88% yield, R<sub>f</sub> = 0.70 in 2:1 CH<sub>2</sub>Cl<sub>2</sub>/hexanes, stained red with *p*-anisaldehyde) as a yellow oil.

**Procedure B:** To a solution of enyne **2-12** (16.9 mg, 59.8  $\mu$ mol) in toluene (0.92 mL) in a 16 x 125 mm glass culture tube under argon was quickly added  $[Ir(dbcot)Cl]_2$  (1.3 mg, 1.53  $\mu$ mol). CO was bubbled through the solution using a balloon and needle outlet (ca. 30 s), during which time the reaction mixture turned a dark-blue/black color. The balloon was removed and argon was bubbled through the reaction mixture in the same manner. The septum was quickly replaced with a Teflon cap and the reaction mixture was stirred at 110 °C for 15.5 h. The reaction was allowed to cool to ambient temperature and was diluted with an approximately equal amount of hexanes. 1,3-Bis(diphenylphosphino)propane (dppp) (6.2 mg, 15.0  $\mu$ mol) was also added to the mixture. The mixture was stirred for 15 min, then passed through a small plug of Al<sub>2</sub>O<sub>3</sub> (hexanes  $\rightarrow$  1:1 hexanes/EtOAc eluent). The volatile materials were removed by rotary evaporation and the resulting residue was purified by flash chromatography (99:1 hexanes/CH<sub>2</sub>Cl<sub>2</sub>

w/ 0.5% Et<sub>3</sub>N → 5:1 hexanes/CH<sub>2</sub>Cl<sub>2</sub>w/ 0.5% Et<sub>3</sub>N eluent) affording tricycle **2-13** (11.5 mg, 68% yield) as a yellow oil.

**Tricycle 2-13:** <sup>1</sup>H NMR (400 MHz; C<sub>6</sub>D<sub>6</sub>): δ 7.21-7.18 (m, 1H), 7.15 (d, *J* = 2.3 Hz, 1H), 7.09-7.04 (m, 3H), 4.08 (dd, *J* = 10.8, 4.5 Hz, 1H), 3.92 (dd, *J* = 10.9, 2.4 Hz, 1H), 2.29 (d, *J* = 5.5 Hz, 1H), 2.26-2.02 (m, 4H), 1.65-1.09 (m, 10H), 0.82 (d, *J* = 14.6 Hz, 3H), 0.62 (ddd, *J* = 14.0, 11.1, 5.7 Hz, 1H); <sup>13</sup>C NMR (100 MHz; C<sub>6</sub>D<sub>6</sub>): δ 147.8, 139.1, 129.4, 128.4, 126.2, 110.8, 64.5, 38.4, 30.2, 29.3, 28.1, 26.4, 25.6, 25.3, 23.8, 23.4, 23.3, 14.5; IR (film) 2929, 2858, 1673, 1447, 1145 cm<sup>-1</sup>; HRMS (ESI+) *m/z* calc'd for (M + H)<sup>+</sup> [C<sub>20</sub>H<sub>26</sub>O + H]<sup>+</sup>: 283.2056, found 283.2045.

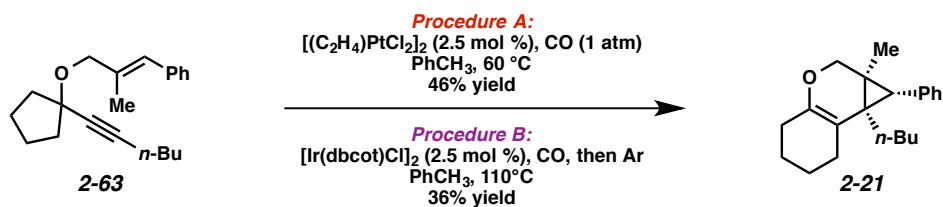


**Tricycle 2-20. Procedure A:** To a solution of enyne **2-61** (31.5 mg, 143 μmol) in toluene (2.5 mL) in a 2-dram vial under argon was quickly added [(C<sub>2</sub>H<sub>4</sub>)PtCl<sub>2</sub>]<sub>2</sub> (2.2 mg, 3.74 μmol). CO was bubbled through the solution using a balloon and needle outlet (ca. 30 s). The balloon and outlet were then removed and the solution was stirred at 70 °C for 19 h. The reaction was allowed to cool to ambient temperature and was diluted with an approximately equal amount of hexanes. The mixture was stirred for 15 min, then passed through a small plug of Al<sub>2</sub>O<sub>3</sub> (hexanes → 1:1 hexanes/EtOAc eluent). The volatile materials were removed by rotary evaporation and the resulting residue was purified by flash chromatography (hexanes w/ 0.5% Et<sub>3</sub>N → 20:1 hexanes/CH<sub>2</sub>Cl<sub>2</sub> w/ 0.5% Et<sub>3</sub>N eluent) affording tricycle **2-20** (17.9 mg, 57% yield, R<sub>f</sub> = 0.81 in 2:1 CH<sub>2</sub>Cl<sub>2</sub>/hexanes, stained orange with *p*-anisaldehyde) as a colorless oil.

**Procedure B:** To a solution of enyne **2-61** (13.3 mg, 60.4 μmol) in toluene (0.92 mL) in a 16 x 125 mm glass culture tube under argon was quickly added [Ir(dbcot)Cl]<sub>2</sub> (1.3 mg, 1.50 μmol). CO was bubbled through the solution using a balloon and needle outlet (ca. 30 s), during which time the reaction mixture

turned a dark-blue/black color. The balloon was removed and argon was bubbled through the reaction mixture in the same manner. The septum was quickly replaced with a Teflon cap and the reaction mixture was stirred at 110 °C for 15.5 h. The reaction was allowed to cool to ambient temperature and was diluted with an approximately equal amount of hexanes. 1,3-Bis(diphenylphosphino)propane (dppp) (6.2 mg, 15.0 μmol) was also added to the mixture. The mixture was stirred for 15 min, then passed through a small plug of Al<sub>2</sub>O<sub>3</sub> (hexanes → 1:1 hexanes/EtOAc eluent). The volatile materials were removed by rotary evaporation and the resulting residue was purified by flash chromatography (99:1 hexanes/CH<sub>2</sub>Cl<sub>2</sub> w/ 0.5% Et<sub>3</sub>N → 20:1 hexanes/CH<sub>2</sub>Cl<sub>2</sub> w/ 0.5% Et<sub>3</sub>N eluent) affording tricycle **2-20** (9.9 mg, 74% yield) as a colorless oil.

**Tricycle 2-20:** <sup>1</sup>H NMR (400 MHz; C<sub>6</sub>D<sub>6</sub>): δ 3.74 (q, *J* = 12.4 Hz, 2H), 2.27-2.06 (m, 4H), 1.95-1.87 (m, 2H), 1.60-1.40 (m, 4H), 1.33-1.23 (m, 4H), 0.97 (d, *J* = 4.6 Hz, 3H), 0.93-0.91 (m, 3H), 0.41 (s, 1H), 0.35 (d, *J* = 3.6 Hz, 1H); <sup>13</sup>C NMR (100 MHz; C<sub>6</sub>D<sub>6</sub>): δ 147.5, 110.9, 70.5, 31.2, 30.6, 30.2, 28.1, 26.8, 25.5, 23.9, 23.8, 23.6, 23.3, 17.2, 14.4; IR (film) 2930, 2860, 1674, 1457, 1158 cm<sup>-1</sup>; HRMS (ESI+) *m/z* calc'd for (M + H)<sup>+</sup> [C<sub>15</sub>H<sub>24</sub>O + H]<sup>+</sup>: 221.1900, found 221.1894.

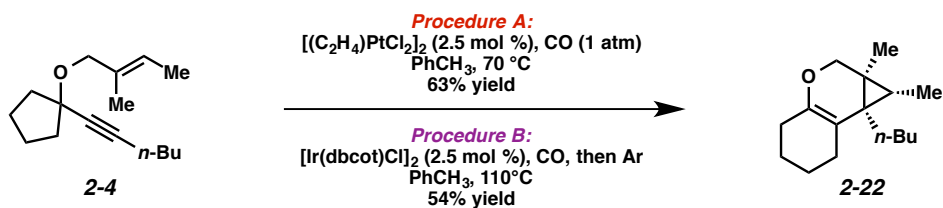


**Tricycle 2-21. Procedure A:** To a solution of enyne **2-63** (29.3 mg, 98.8 μmol) in toluene (1.5 mL) in a 2-dram vial under argon was quickly added [(C<sub>2</sub>H<sub>4</sub>)PtCl<sub>2</sub>]<sub>2</sub> (1.5 mg, 2.55 μmol). CO was bubbled through the solution using a balloon and needle outlet (ca. 30 s). The balloon and outlet were then removed and the solution was stirred at 60 °C for 24 h. The reaction was allowed to cool to ambient temperature and was diluted with an approximately equal amount of hexanes. The mixture was stirred for 15 min, then passed through a small plug of Al<sub>2</sub>O<sub>3</sub> (hexanes → 1:1 hexanes/EtOAc eluent). The volatile materials were

removed by rotary evaporation and the resulting residue was purified by flash chromatography (99:1 hexanes/CH<sub>2</sub>Cl<sub>2</sub> w/ 0.5% Et<sub>3</sub>N → 6:1 hexanes/CH<sub>2</sub>Cl<sub>2</sub> w/ 0.5% Et<sub>3</sub>N eluent) affording tricycle **2-21** (13.4 mg, 46% yield, R<sub>f</sub> = 0.75 in 1:1 CH<sub>2</sub>Cl<sub>2</sub>/hexanes, stained orange with *p*-anisaldehyde) as a colorless oil.

**Procedure B:** To a solution of enyne **2-63** (23.6 mg, 79.6 μmol) in toluene (1.2 mL) in a 16 x 125 mm glass culture tube under argon was quickly added [Ir(dbcot)Cl]<sub>2</sub> (1.7 mg, 1.97 μmol). CO was bubbled through the solution using a balloon and needle outlet (ca. 30 s), during which time the reaction mixture turned a dark-blue/black color. The balloon was removed and argon was bubbled through the reaction mixture in the same manner. The septum was quickly replaced with a Teflon cap and the reaction mixture was stirred at 110 °C for 27 h. The reaction was allowed to cool to ambient temperature and was diluted with an approximately equal amount of hexanes. The mixture was stirred for 15 min, then passed through a small plug of Al<sub>2</sub>O<sub>3</sub> (hexanes → 1:1 hexanes/EtOAc eluent). The volatile materials were removed by rotary evaporation and the resulting residue was purified by flash chromatography (99:1 hexanes/CH<sub>2</sub>Cl<sub>2</sub> w/ 0.5% Et<sub>3</sub>N → 2:1 hexanes/CH<sub>2</sub>Cl<sub>2</sub> w/ 0.5% Et<sub>3</sub>N eluent) affording tricycle **2-21** (8.4 mg, 36% yield) as a colorless oil.

**Tricycle 2-21:** <sup>1</sup>H NMR (400 MHz; C<sub>6</sub>D<sub>6</sub>): δ 7.27-7.07 (m, 5H), 3.86 (ABq, J<sub>AB</sub> = 10.8 Hz, Δν<sub>AB</sub> = 49.6 Hz, 2H), 2.31-2.24 (m, 1H), 2.22-2.12 (m, 2H), 1.90-1.80 (m, 1H), 1.65-1.42 (m, 6H), 1.39-1.27 (m, 1H), 1.22-1.12 (m, 2H), 0.99 (s, 3H), 0.98-0.91 (m, 1H), 0.83-0.79 (m, 3H); <sup>13</sup>C NMR (100 MHz; C<sub>6</sub>D<sub>6</sub>): δ 147.8, 138.0, 131.2, 130.2, 128.5, 126.4, 111.6, 71.2, 38.5, 29.9, 28.8, 28.1, 27.8, 27.4, 25.6, 23.9, 23.6, 23.3, 14.5, 14.4; IR (film) 2930, 2859, 1497, 1156, 1156 cm<sup>-1</sup>; HRMS (ESI+) *m/z* calc'd for (M + H)<sup>+</sup> [C<sub>21</sub>H<sub>28</sub>O + H]<sup>+</sup>: 297.2213, found 297.2212.

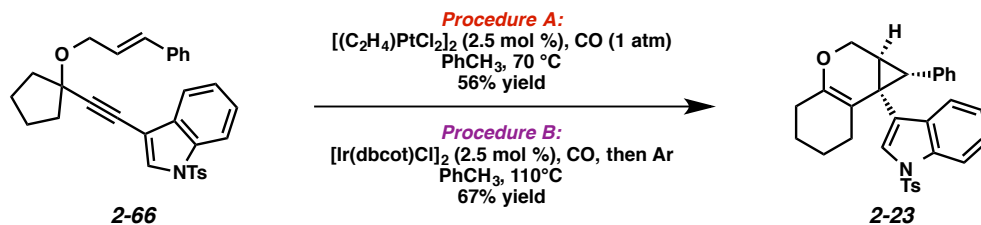


**Tricycle 2-22. Procedure A:** To a solution of enyne **2-4** (15.5 mg, 66.1  $\mu\text{mol}$ ) in toluene (1.1 mL) in a 2-dram vial under argon was quickly added  $[(\text{C}_2\text{H}_4)\text{PtCl}_2]_2$  (1.0 mg, 1.65  $\mu\text{mol}$ ). CO was bubbled through the solution using a balloon and needle outlet (ca. 30 s). The balloon and outlet were then removed and the solution was stirred at 70  $^\circ\text{C}$  for 17 h. The reaction was allowed to cool to ambient temperature and was diluted with an approximately equal amount of hexanes. The mixture was stirred for 15 min, then passed through a small plug of  $\text{Al}_2\text{O}_3$  (hexanes  $\rightarrow$  1:1 hexanes/EtOAc eluent). The volatile materials were removed by rotary evaporation and the resulting residue was purified by flash chromatography (hexanes w/ 0.5%  $\text{Et}_3\text{N}$   $\rightarrow$  10:1 hexanes/ $\text{CH}_2\text{Cl}_2$  w/ 0.5%  $\text{Et}_3\text{N}$  eluent) affording tricycle **2-22** (9.8 mg, 63% yield,  $R_f = 0.84$  in 2:1  $\text{CH}_2\text{Cl}_2$ /hexanes, stained orange with *p*-anisaldehyde) as a colorless oil.

**Procedure B:** To a solution of enyne **2-4** (14.4 mg, 61.4  $\mu\text{mol}$ ) in toluene (0.92 mL) in a 16 x 125 mm glass culture tube under argon was quickly added  $[\text{Ir}(\text{dbcot})\text{Cl}]_2$  (1.3 mg, 1.50  $\mu\text{mol}$ ). CO was bubbled through the solution using a balloon and needle outlet (ca. 30 s), during which time the reaction mixture turned a dark-blue/black color. The balloon was removed and argon was bubbled through the reaction mixture in the same manner. The septum was quickly replaced with a Teflon cap and the reaction mixture was stirred at 110  $^\circ\text{C}$  for 15.5 h. The reaction was allowed to cool to ambient temperature and was diluted with an approximately equal amount of hexanes. 1,3-Bis(diphenylphosphino)propane (dppp) (6.2 mg, 15.0  $\mu\text{mol}$ ) was also added to the mixture. The mixture was stirred for 15 min, then passed through a small plug of  $\text{Al}_2\text{O}_3$  (hexanes  $\rightarrow$  1:1 hexanes/EtOAc eluent). The volatile materials were removed by rotary evaporation and the resulting residue was purified by flash chromatography (99:1 hexanes/ $\text{CH}_2\text{Cl}_2$  w/ 0.5%  $\text{Et}_3\text{N}$   $\rightarrow$  50:1 hexanes/ $\text{CH}_2\text{Cl}_2$  w/ 0.5%  $\text{Et}_3\text{N}$  eluent) affording tricycle **2-22** (7.8 mg, 54% yield) as a colorless oil.

**Tricycle 2-22:**  $^1\text{H}$  NMR (400 MHz;  $\text{C}_6\text{D}_6$ ):  $\delta$  3.74 (q,  $J = 10.8$  Hz, 2H), 2.24-2.04 (m, 4H), 1.98-1.91 (m, 1H), 1.56-1.44 (m, 4H), 1.34-1.28 (m, 4H), 1.02 (t,  $J = 3.1$  Hz, 2H), 0.92 (t,  $J = 7.0$  Hz, 6H), 0.88 (s, 3H);  $^{13}\text{C}$  NMR (100 MHz;  $\text{C}_6\text{D}_6$ ):  $\delta$  147.2, 112.4, 71.2, 30.0, 28.2, 27.7, 26.9, 25.6, 24.9, 23.9, 23.8, 23.3, 20.6,

14.4, 12.0, 9.0; IR (film) 2926, 2956, 1457, 1157  $\text{cm}^{-1}$ ; HRMS (ESI+)  $m/z$  calc'd for  $(\text{M} + \text{H})^+$   $[\text{C}_{16}\text{H}_{26}\text{O} + \text{H}]^+$ : 235.2056, found 235.2050.

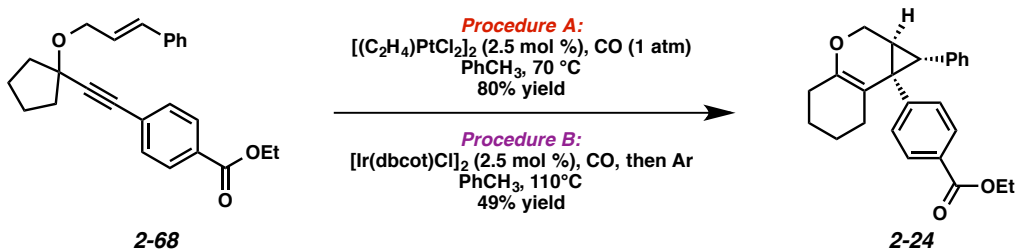


**Tricycle 2-23. Procedure A:** To a solution of enyne **2-66** (78.0 mg, 157  $\mu\text{mol}$ ) in toluene (2.5 mL) in a 2-dram vial under argon was quickly added  $[(\text{C}_2\text{H}_4)\text{PtCl}_2]_2$  (2.2 mg, 3.75  $\mu\text{mol}$ ). CO was bubbled through the solution using a balloon and needle outlet (ca. 30 s). The balloon and outlet were then removed and the solution was stirred at 70 °C for 20.5 h. The reaction was allowed to cool to ambient temperature and was diluted with an approximately equal amount of hexanes. The mixture was stirred for 15 min, then passed through a small plug of  $\text{Al}_2\text{O}_3$  (hexanes  $\rightarrow$  1:1 hexanes/EtOAc eluent). The volatile materials were removed by rotary evaporation and the resulting residue was purified by flash chromatography (hexanes w/ 0.5%  $\text{Et}_3\text{N}$   $\rightarrow$  10:1 hexanes/ $\text{CH}_2\text{Cl}_2$  w/ 0.5%  $\text{Et}_3\text{N}$  eluent) affording tricycle **2-23** (43.6 mg, 56% yield,  $R_f = 0.67$  in 2:1  $\text{CH}_2\text{Cl}_2$ /hexanes, stained purple with *p*-anisaldehyde) as a colorless oil.

**Procedure B:** To a solution of enyne **2-66** (49.7 mg, 99.9  $\mu\text{mol}$ ) in toluene (1.7 mL) in a 16 x 125 mm glass culture tube under argon was quickly added  $[\text{Ir}(\text{dbcot})\text{Cl}]_2$  (2.2 mg, 2.55  $\mu\text{mol}$ ). CO was bubbled through the solution using a balloon and needle outlet (ca. 30 s), during which time the reaction mixture turned a dark-blue/black color. The balloon was removed and argon was bubbled through the reaction mixture in the same manner. The septum was quickly replaced with a Teflon cap and the reaction mixture was stirred at 110 °C for 15 h. The reaction was allowed to cool to ambient temperature and was diluted with an approximately equal amount of hexanes. The mixture was stirred for 15 min, then passed through a small plug of  $\text{Al}_2\text{O}_3$  (hexanes  $\rightarrow$  1:1 hexanes/EtOAc eluent). The volatile materials were removed by

rotary evaporation and the resulting residue was purified by flash chromatography (hexanes w/ 0.5% Et<sub>3</sub>N → 9:1 hexanes/CH<sub>2</sub>Cl<sub>2</sub> w/ 0.5% Et<sub>3</sub>N eluent) affording tricycle **2-23** (33.1 mg, 67% yield, R<sub>f</sub> = 0.56 in 2:1 CH<sub>2</sub>Cl<sub>2</sub>/hexanes, stained purple with *p*-anisaldehyde) as a colorless oil.

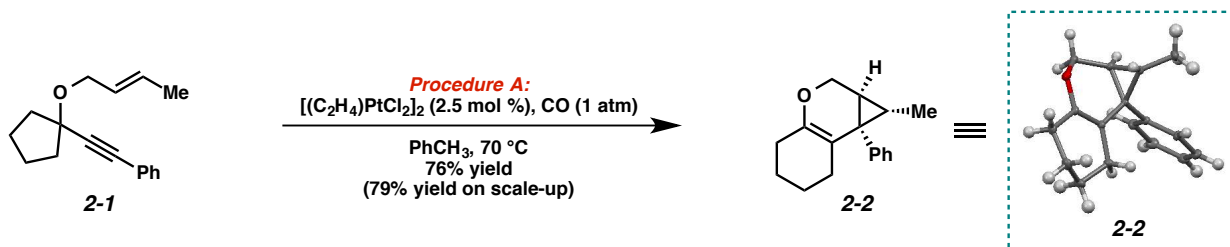
**Tricycle 2-23:** <sup>1</sup>H NMR (400 MHz; C<sub>6</sub>D<sub>6</sub>): δ 8.15 (d, *J* = 8.2 Hz, 1H), 7.54-7.52 (m, 1H), 7.42 (d, *J* = 8.3 Hz, 2H), 7.07-6.96 (m, 2H), 6.92-6.85 (m, 4H), 6.68 (d, *J* = 7.0 Hz, 2H), 6.51 (d, *J* = 8.1 Hz, 2H), 3.98-3.91 (m, 2H), 2.71 (d, *J* = 6.0 Hz, 1H), 2.19-2.00 (m, 3H), 1.84 (dt, *J* = 5.8, 2.8 Hz, 1H), 1.68 (s, 3H), 1.53-1.44 (m, 2H), 1.41-1.11 (m, 5H), 0.38-0.34 (m, 2H); <sup>13</sup>C NMR (100 MHz; C<sub>6</sub>D<sub>6</sub>): δ 179.4, 144.2, 138.8, 132.6, 129.7, 128.5, 128.2, 127.9, 127.2, 126.1, 124.9, 123.4, 114.2, 62.9, 28.2, 26.5, 23.6, 23.2, 21.1; IR (film) 2929, 2858, 1447, 1188 cm<sup>-1</sup>; HRMS (ESI+) *m/z* calc'd for (M + H)<sup>+</sup> [C<sub>31</sub>H<sub>29</sub>NO<sub>3</sub>S + H]<sup>+</sup>: 496.1941, found 496.1926.



**Tricycle 2-24. Procedure A:** To a solution of enyne **2-68** (55.7 mg, 149 μmol) in toluene (2.5 mL) in a 2-dram vial under argon was quickly added [(C<sub>2</sub>H<sub>4</sub>)PtCl<sub>2</sub>]<sub>2</sub> (2.2 mg, 3.75 μmol). CO was bubbled through the solution using a balloon and needle outlet (ca. 30 s). The balloon and outlet were then removed and the solution was stirred at 70 °C for 20.5 h. The reaction was allowed to cool to ambient temperature and was diluted with an approximately equal amount of hexanes. The mixture was stirred for 15 min, then passed through a small plug of Al<sub>2</sub>O<sub>3</sub> (hexanes → 1:1 hexanes/EtOAc eluent). The volatile materials were removed by rotary evaporation and the resulting residue was purified by flash chromatography (hexanes w/ 0.5% Et<sub>3</sub>N → 10:1 hexanes/CH<sub>2</sub>Cl<sub>2</sub> w/ 0.5% Et<sub>3</sub>N eluent) affording tricycle **2-24** (44.6 mg, 80% yield, R<sub>f</sub> = 0.55 in 2:1 CH<sub>2</sub>Cl<sub>2</sub>/hexanes, stained purple with *p*-anisaldehyde) as a yellow oil.

**Procedure B:** To a solution of enyne **2-68** (34.6 mg, 99.6  $\mu\text{mol}$ ) in toluene (1.7 mL) in a 16 x 125 mm glass culture tube under argon was quickly added  $[\text{Ir}(\text{dbcot})\text{Cl}]_2$  (2.2 mg, 2.55  $\mu\text{mol}$ ). CO was bubbled through the solution using a balloon and needle outlet (ca. 30 s), during which time the reaction mixture turned a dark-blue/black color. The balloon was removed and argon was bubbled through the reaction mixture in the same manner. The septum was quickly replaced with a Teflon cap and the reaction mixture was stirred at 110  $^\circ\text{C}$  for 15 h. The reaction was allowed to cool to ambient temperature and was diluted with an approximately equal amount of hexanes. The mixture was stirred for 15 min, then passed through a small plug of  $\text{Al}_2\text{O}_3$  (hexanes  $\rightarrow$  1:1 hexanes/EtOAc eluent). The volatile materials were removed by rotary evaporation and the resulting residue was purified by flash chromatography (hexanes w/ 0.5%  $\text{Et}_3\text{N}$   $\rightarrow$  2:1 hexanes/ $\text{CH}_2\text{Cl}_2$  w/ 0.5%  $\text{Et}_3\text{N}$  eluent) affording tricycle **2-24** (16.8 mg, 49% yield) as a yellow oil.

**Tricycle 2-24:**  $^1\text{H}$  NMR (400 MHz;  $\text{C}_6\text{D}_6$ ):  $\delta$  8.02 (d,  $J = 8.3$  Hz, 2H), 6.97-6.91 (m, 5H), 6.59 (dd,  $J = 7.6, 1.9$  Hz, 2H), 4.12-4.05 (m, 2H), 4.04-3.92 (m, 2H), 2.74 (d,  $J = 5.8$  Hz, 1H), 2.27-2.05 (m, 2H), 1.93-1.91 (m, 1H), 1.90-1.86 (m, 1H), 1.61-1.58 (m, 1H), 1.46-1.39 (m, 3H), 1.31-1.23 (m, 1H), 0.98 (t,  $J = 7.1$  Hz, 3H);  $^{13}\text{C}$  NMR (100 MHz;  $\text{C}_6\text{D}_6$ ):  $\delta$  166.2, 146.5, 144.4, 138.6, 132.5, 129.4, 126.0, 111.4, 62.5, 60.7, 36.7, 34.7, 30.8, 28.2, 27.0, 23.5, 23.1, 14.3; IR (film) 2931, 2859, 1716, 1274, 1101  $\text{cm}^{-1}$ ; HRMS (ESI+)  $m/z$  calc'd for  $(\text{M} + \text{H})^+ [\text{C}_{25}\text{H}_{26}\text{O}_3 + \text{H}]^+$ : 375.1955, found 375.1943.

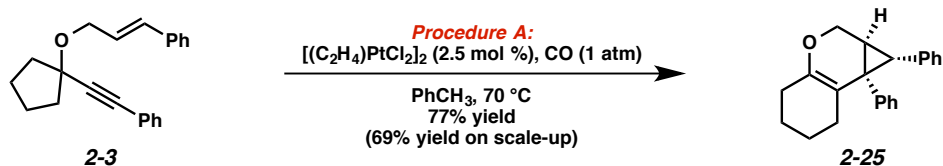


**Tricycle 2-2. Procedure A:** To a solution of enyne **2-1** (36.7 mg, 153  $\mu\text{mol}$ ) in toluene (2.5 mL) in a 2-dram vial under argon was quickly added  $[(\text{C}_2\text{H}_4)\text{PtCl}_2]_2$  (2.2 mg, 3.74  $\mu\text{mol}$ ). CO was bubbled through the solution using a balloon and needle outlet (ca. 30 s). The balloon and outlet were then removed and

the solution was stirred at 70 °C for 19 h. The reaction was allowed to cool to ambient temperature and was diluted with an approximately equal amount of hexanes. The mixture was stirred for 15 min, then passed through a small plug of Al<sub>2</sub>O<sub>3</sub> (hexanes → 1:1 hexanes/EtOAc eluent). The volatile materials were removed by rotary evaporation and the resulting residue was purified by flash chromatography (hexanes w/ 0.5% Et<sub>3</sub>N → 20:1 hexanes/CH<sub>2</sub>Cl<sub>2</sub> w/ 0.5% Et<sub>3</sub>N eluent) affording tricycle **2-2** (27.9 mg, 76% yield, R<sub>f</sub> = 0.81 in 2:1 CH<sub>2</sub>Cl<sub>2</sub>/hexanes, stained red with *p*-anisaldehyde) as a colorless oil.

**Procedure A (Scale-up):** To a solution of enyne **2-1** (0.2715 g, 1.13 mmol) in toluene (7.5 mL) in a 16 x 125 mm glass culture tube under argon was quickly added [(C<sub>2</sub>H<sub>4</sub>)PtCl<sub>2</sub>]<sub>2</sub> (16.6 mg, 0.0283 mmol). CO was bubbled through the solution using a balloon and needle outlet (ca. 30 s). The balloon and outlet were then removed and the solution was stirred at 70 °C for 20 h. The reaction was allowed to cool to ambient temperature and the volatile materials were removed by rotary evaporation. The resulting residue was purified by flash chromatography (hexanes w/ 0.5% Et<sub>3</sub>N → 10:1 hexanes/CH<sub>2</sub>Cl<sub>2</sub> w/ 0.5% Et<sub>3</sub>N eluent) affording tricycle **2-2** (0.2151 g, 79% yield) as a colorless oil.

**Tricycle 2-2:** <sup>1</sup>H NMR (400 MHz; C<sub>6</sub>D<sub>6</sub>): δ 7.22-7.17 (m, 4H), 7.10 (tt, *J* = 6.8, 2.2 Hz, 1H), 4.05-3.94 (m, 2H), 2.22-1.95 (m, 4H), 1.73 (dq, *J* = 15.4, 4.0 Hz, 1H), 1.45-1.35 (m, 4H), 1.13 (td, *J* = 4.9, 2.3 Hz, 1H), 0.86 (d, *J* = 6.3 Hz, 3H); <sup>13</sup>C NMR (100 MHz; C<sub>6</sub>D<sub>6</sub>): δ 145.5, 141.0, 132.0, 128.3, 126.6, 112.3, 63.2, 31.8, 29.9, 28.2, 27.4, 25.8, 23.7, 23.3, 16.1; IR (film) 2928, 2858, 1670, 1445, 1150 cm<sup>-1</sup>; HRMS (ESI<sup>+</sup>) *m/z* calc'd for (M + H)<sup>+</sup> [C<sub>17</sub>H<sub>20</sub>O + H]<sup>+</sup>: 241.1587, found 241.1583.

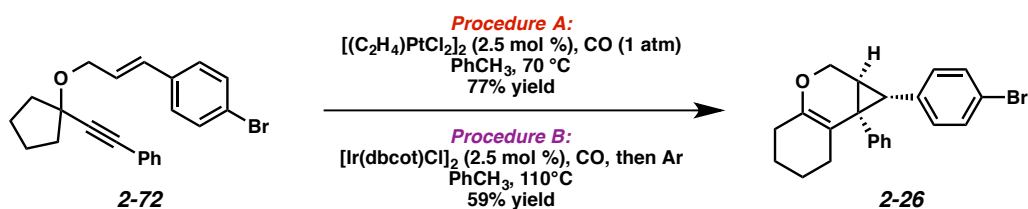


**Tricycle 2-25. Procedure A:** To a solution of enyne **2-3** (45.1 mg, 149 μmol) in toluene (2.5 mL) in a 2-dram vial under argon was quickly added [(C<sub>2</sub>H<sub>4</sub>)PtCl<sub>2</sub>]<sub>2</sub> (2.2 mg, 3.75 μmol). CO was bubbled through

the solution using a balloon and needle outlet (ca. 30 s). The balloon and outlet were then removed and the solution was stirred at 70 °C for 18 h. The reaction was allowed to cool to ambient temperature and was diluted with an approximately equal amount of hexanes. The mixture was stirred for 15 min, then passed through a small plug of Al<sub>2</sub>O<sub>3</sub> (hexanes → 1:1 hexanes/EtOAc eluent). The volatile materials were removed by rotary evaporation and the resulting residue was purified by flash chromatography (hexanes w/ 0.5% Et<sub>3</sub>N → 20:1 hexanes/CH<sub>2</sub>Cl<sub>2</sub> w/ 0.5% Et<sub>3</sub>N eluent) affording tricycle **2-25** (34.7 mg, 77% yield, R<sub>f</sub> = 0.80 in 2:1 CH<sub>2</sub>Cl<sub>2</sub>/hexanes, stained red with *p*-anisaldehyde) as a yellow oil.

**Procedure A (Scale-up):** To a solution of enyne **2-3** (0.1271 g, 420 μmol) in toluene (2.8 mL) in a 16 x 125 mm glass culture tube under argon was quickly added [(C<sub>2</sub>H<sub>4</sub>)PtCl<sub>2</sub>]<sub>2</sub> (6.2 mg, 10.5 μmol). CO was bubbled through the solution using a balloon and needle outlet (ca. 30 s). The balloon and outlet were then removed and the solution was stirred at 70 °C for 41 h. The reaction was allowed to cool to ambient temperature and the volatile materials were removed by rotary evaporation. The resulting residue was purified by flash chromatography (hexanes w/ 0.5% Et<sub>3</sub>N → 20:1 hexanes/CH<sub>2</sub>Cl<sub>2</sub> w/ 0.5% Et<sub>3</sub>N eluent) affording tricycle **2-25** (87.5 mg, 69% yield) as a yellow oil.

**Tricycle 2-25:** <sup>1</sup>H NMR (400 MHz; C<sub>6</sub>D<sub>6</sub>): δ 6.99-6.91 (m, 8H), 6.65 (dd, *J* = 7.7, 1.6 Hz, 2H), 4.09-3.99 (m, 2H), 2.75 (d, *J* = 5.8 Hz, 1H), 2.28-2.07 (m, 2H), 2.02-1.95 (m, 2H), 1.72-1.66 (m, 1H), 1.46-1.38 (m, 3H), 1.31-1.25 (m, 1H); <sup>13</sup>C NMR (100 MHz; C<sub>6</sub>D<sub>6</sub>): δ 146.1, 139.2, 132.4, 128.1, 127.9, 126.7, 125.7, 112.3, 62.7, 36.7, 34.9, 31.3, 28.3, 27.2, 23.6, 23.2; IR (film) 2928, 1666, 1496, 1191 cm<sup>-1</sup>; HRMS (ESI+) *m/z* calc'd for (M + H)<sup>+</sup> [C<sub>22</sub>H<sub>22</sub>O + H]<sup>+</sup>: 303.1743, found 303.1740.

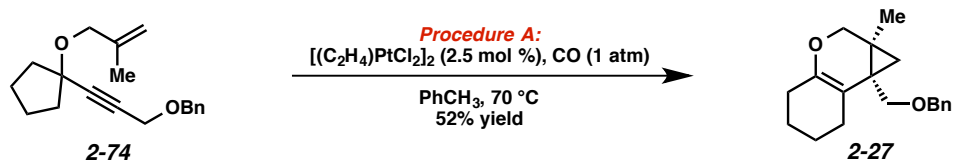


**Tricycle 2-26. Procedure A:** To a solution of enyne **2-72** (16.4 mg, 43.0  $\mu\text{mol}$ ) in toluene (0.70 mL) in a 2-dram vial under argon was quickly added  $[(\text{C}_2\text{H}_4)\text{PtCl}_2]_2$  (0.6 mg, 1.02  $\mu\text{mol}$ ). CO was bubbled through the solution using a balloon and needle outlet (ca. 30 s). The balloon and outlet were then removed and the solution was stirred at 70  $^\circ\text{C}$  for 18 h. The reaction was allowed to cool to ambient temperature and was diluted with an approximately equal amount of hexanes. The mixture was stirred for 15 min, then passed through a small plug of  $\text{Al}_2\text{O}_3$  (hexanes  $\rightarrow$  1:1 hexanes/EtOAc eluent). The volatile materials were removed by rotary evaporation and the resulting residue was purified by flash chromatography (hexanes w/ 0.5%  $\text{Et}_3\text{N}$   $\rightarrow$  20:1 hexanes/ $\text{CH}_2\text{Cl}_2$  w/ 0.5%  $\text{Et}_3\text{N}$  eluent) affording tricycle **2-26** (12.7 mg, 77% yield,  $R_f = 0.79$  in 2:1  $\text{CH}_2\text{Cl}_2$ /hexanes, stained red with *p*-anisaldehyde) as a colorless oil.

**Procedure B:** To a solution of enyne **2-72** (20.5 mg, 53.8  $\mu\text{mol}$ ) in toluene (0.92 mL) in a 16 x 125 mm glass culture tube under argon was quickly added  $[\text{Ir}(\text{dbcot})\text{Cl}]_2$  (1.3 mg, 1.50  $\mu\text{mol}$ ). CO was bubbled through the solution using a balloon and needle outlet (ca. 30 s), during which time the reaction mixture turned a dark-blue/black color. The balloon was removed and argon was bubbled through the reaction mixture in the same manner. The septum was quickly replaced with a Teflon cap and the reaction mixture was stirred at 110  $^\circ\text{C}$  for 6 h. The reaction was allowed to cool to ambient temperature and was diluted with an approximately equal amount of hexanes. 1,3-Bis(diphenylphosphino)propane (dppp) (7.4 mg, 17.9  $\mu\text{mol}$ ) was also added to the mixture. The mixture was stirred for 15 min, then passed through a small plug of  $\text{Al}_2\text{O}_3$  (hexanes  $\rightarrow$  1:1 hexanes/EtOAc eluent). The volatile materials were removed by rotary evaporation and the resulting residue was purified by flash chromatography (99:1 hexanes/ $\text{CH}_2\text{Cl}_2$  w/ 0.5%  $\text{Et}_3\text{N}$   $\rightarrow$  5:1 hexanes/ $\text{CH}_2\text{Cl}_2$  w/ 0.5%  $\text{Et}_3\text{N}$  eluent) affording tricycle **2-26** (12.0 mg, 59% yield,  $R_f = 0.79$  in 2:1  $\text{CH}_2\text{Cl}_2$ /hexanes, stained red with *p*-anisaldehyde) as a colorless oil.

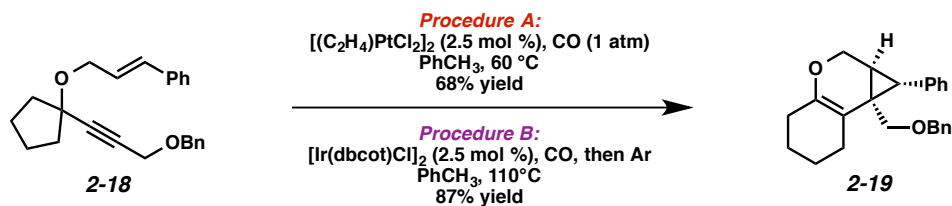
**Tricycle 2-26:**  $^1\text{H}$  NMR (400 MHz;  $\text{C}_6\text{D}_6$ ):  $\delta$  7.04-7.02 (m, 2H), 6.97-6.95 (m, 3H), 6.89-6.87 (m, 2H), 6.27-6.25 (m, 2H), 4.03-3.92 (m, 2H), 2.57 (d,  $J = 5.8$  Hz, 1H), 2.26-2.05 (m, 2H), 1.98-1.89 (m, 1H), 1.83-1.79 (m, 1H), 1.70-1.60 (m, 1H), 1.46-1.37 (m, 3H), 1.30-1.21 (m, 1H);  $^{13}\text{C}$  NMR (100 MHz;  $\text{C}_6\text{D}_6$ ):  $\delta$  146.2, 138.6, 138.3, 132.3, 130.9, 129.7, 126.9, 119.5, 112.0, 62.5, 35.9, 35.0, 31.5, 28.2, 27.1, 23.5,

23.2; IR (film) 2928, 2858, 1668, 1491, 1145  $\text{cm}^{-1}$ ; HRMS (ESI+)  $m/z$  calc'd for  $(\text{M} + \text{H})^+$   $[\text{C}_{22}\text{H}_{21}\text{BrO} + \text{H}]^+$ : 381.0849, found 381.0842.



**Tricyclic 2-27. Procedure A:** To a solution of enyne **2-74** (24.8 mg, 87.2  $\mu\text{mol}$ ) in toluene (1.3 mL) in a 2-dram vial under argon was quickly added  $[(\text{C}_2\text{H}_4)\text{PtCl}_2]_2$  (1.3 mg, 2.21  $\mu\text{mol}$ ). The solution was stirred at 70 °C for 23 h. The reaction was allowed to cool to ambient temperature and was diluted with an approximately equal amount of hexanes. The mixture was stirred for 15 min, then passed through a small plug of  $\text{Al}_2\text{O}_3$  (hexanes  $\rightarrow$  1:1 hexanes/EtOAc eluent). The volatile materials were removed by rotary evaporation and the resulting residue was purified by flash chromatography (99:1 hexanes/ $\text{CH}_2\text{Cl}_2$  w/ 0.5%  $\text{Et}_3\text{N}$   $\rightarrow$  2:1 hexanes/ $\text{CH}_2\text{Cl}_2$  w/ 0.5%  $\text{Et}_3\text{N}$  eluent) affording tricyclic **2-27** (12.8 mg, 52% yield,  $R_f = 0.30$  in 2:1  $\text{CH}_2\text{Cl}_2$ /hexanes, stained blue with *p*-anisaldehyde) as a colorless oil.

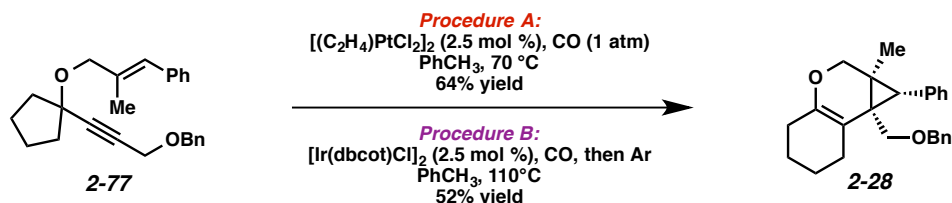
**Tricyclic 2-27:**  $^1\text{H}$  NMR (400 MHz;  $\text{C}_6\text{D}_6$ ):  $\delta$  7.30-7.28 (m, 2H), 7.18-7.15 (m, 2H), 7.11-7.07 (m, 1H), 4.28 (ABq,  $J_{\text{AB}} = 12.0$  Hz,  $\Delta\nu_{\text{AB}} = 42.0$  Hz, 2H), 3.77 (d,  $J = 10.4$  Hz, 1H), 3.72 (ABq,  $J_{\text{AB}} = 10.2$  Hz,  $\Delta\nu_{\text{AB}} = 65.7$  Hz, 2H), 2.91 (d,  $J = 10.4$  Hz, 1H), 2.57-2.50 (m, 1H), 2.22-2.05 (m, 3H), 1.63-1.38 (m, 4H), 1.23-1.20 (m, 1H), 0.99 (s, 3H), 0.41-0.40 (m, 1H);  $^{13}\text{C}$  NMR (100 MHz;  $\text{C}_6\text{D}_6$ ):  $\delta$  146.2, 139.2, 128.5, 128.2, 127.7, 110.7, 73.1, 71.3, 68.0, 28.1, 28.0, 25.0, 24.5, 23.6, 23.2, 22.9, 16.0; IR (film) 2929, 2856, 1678, 1454, 1075  $\text{cm}^{-1}$ ; HRMS (ESI+)  $m/z$  calc'd for  $(\text{M} + \text{H})^+$   $[\text{C}_{19}\text{H}_{24}\text{O}_2 + \text{H}]^+$ : 285.1849, found 285.1848.



**Tricyclic 2-19. Procedure A:** To a solution of enyne **2-18** (34.5 mg, 99.6  $\mu$ mol) in toluene (1.5 mL) in a 2-dram vial under argon was quickly added  $[(C_2H_4)PtCl_2]_2$  (1.5 mg, 2.55  $\mu$ mol). CO was bubbled through the solution using a balloon and needle outlet (ca. 30 s). The balloon and outlet were then removed and the solution was stirred at 60 °C for 20 h. The reaction was allowed to cool to ambient temperature and was diluted with an approximately equal amount of hexanes. The mixture was stirred for 15 min, then passed through a small plug of  $Al_2O_3$  (hexanes  $\rightarrow$  1:1 hexanes/EtOAc eluent). The volatile materials were removed by rotary evaporation and the resulting residue was purified by flash chromatography (99:1 hexanes/ $CH_2Cl_2$  w/ 0.5%  $Et_3N$   $\rightarrow$  20:1 hexanes/ $CH_2Cl_2$  w/ 0.5%  $Et_3N$  eluent) affording tricyclic **2-19** (23.4 mg, 68% yield,  $R_f = 0.46$  (2:1  $CH_2Cl_2$ /hexanes), stained blue with *p*-anisaldehyde) as a colorless oil.

**Procedure B:** To a solution of enyne **2-18** (17.5 mg, 50.5  $\mu$ mol) in toluene (0.77 mL) in a 16 x 125 mm glass culture tube under argon was quickly added  $[Ir(dbcot)Cl]_2$  (1.1 mg, 1.25  $\mu$ mol). CO was bubbled through the solution using a balloon and needle outlet (ca. 30 s), during which time the reaction mixture turned a dark-blue/black color. The balloon was removed and argon was bubbled through the reaction mixture in the same manner. The septum was quickly replaced with a Teflon cap and the reaction mixture was stirred at 110 °C for 16 h. The reaction was allowed to cool to ambient temperature and was diluted with an approximately equal amount of hexanes. 1,3-Bis(diphenylphosphino)propane (dppp) (6.2 mg, 1.50  $\mu$ mol) was also added to the mixture. The mixture was stirred for 15 min, then passed through a small plug of  $Al_2O_3$  (hexanes  $\rightarrow$  1:1 hexanes/EtOAc eluent). The volatile materials were removed by rotary evaporation and the resulting residue was purified by flash chromatography (99:1 hexanes/ $CH_2Cl_2$  w/ 0.5%  $Et_3N$   $\rightarrow$  10:1 hexanes/ $CH_2Cl_2$  w/ 0.5%  $Et_3N$  eluent) affording tricyclic **2-19** (15.2 mg, 87% yield,  $R_f = 0.46$  (2:1  $CH_2Cl_2$ /hexanes), stained blue with *p*-anisaldehyde) as a colorless oil.

**Tricyclic 2-19:**  $^1\text{H}$  NMR (400 MHz;  $\text{C}_6\text{D}_6$ ):  $\delta$  7.14-7.02 (m, 10H), 4.10 (ABq,  $J_{\text{AB}} = 12.0$  Hz,  $\Delta\nu_{\text{AB}} = 30.2$  Hz, 2H), 4.01-3.91 (m, 2H), 3.50 (d,  $J = 10.5$  Hz, 1H), 2.94 (d,  $J = 10.5$  Hz, 1H), 2.60 (d,  $J = 5.9$  Hz, 1H), 2.57-2.50 (m, 1H), 2.31-2.07 (m, 3H), 1.80-1.77 (m, 1H), 1.61-1.49 (m, 4H);  $^{13}\text{C}$  NMR (100 MHz;  $\text{C}_6\text{D}_6$ ):  $\delta$  146.7, 139.3, 138.3, 129.3, 128.5, 128.2, 127.9, 127.5, 126.4, 111.2, 72.8, 71.1, 62.5, 35.2, 28.2, 27.3, 26.5, 25.4, 23.7, 23.3; IR (film) 3028, 2929, 2858, 1672, 1453, 1096  $\text{cm}^{-1}$ ; HRMS (ESI+)  $m/z$  calc'd for  $(\text{M} + \text{H})^+ [\text{C}_{24}\text{H}_{26}\text{O}_2 + \text{H}]^+$ : 347.2006, found 347.2009.

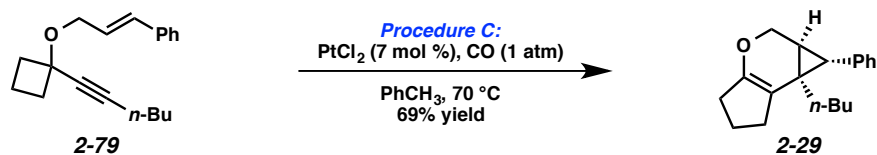


**Tricyclic 2-28. Procedure A:** To a solution of enyne **2-77** (52.9 mg, 148  $\mu\text{mol}$ ) in toluene (2.5 mL) in a 2-dram vial under argon was quickly added  $[(\text{C}_2\text{H}_4)\text{PtCl}_2]_2$  (2.2 mg, 3.75  $\mu\text{mol}$ ). CO was bubbled through the solution using a balloon and needle outlet (ca. 30 s). The balloon and outlet were then removed and the solution was stirred at 70 °C for 18 h. The reaction was allowed to cool to ambient temperature and was diluted with an approximately equal amount of hexanes. The mixture was stirred for 15 min, then passed through a small plug of  $\text{Al}_2\text{O}_3$  (hexanes  $\rightarrow$  1:1 hexanes/EtOAc eluent). The volatile materials were removed by rotary evaporation and the resulting residue was purified by flash chromatography (hexanes w/ 0.5%  $\text{Et}_3\text{N}$   $\rightarrow$  20:1 hexanes/ $\text{CH}_2\text{Cl}_2$  w/ 0.5%  $\text{Et}_3\text{N}$  eluent) affording tricyclic **2-28** (34.1 mg, 64% yield,  $R_f = 0.42$  in 2:1  $\text{CH}_2\text{Cl}_2$ /hexanes, stained red with *p*-anisaldehyde) as a yellow oil.

**Procedure B:** To a solution of enyne **2-77** (28.1 mg, 77.9  $\mu\text{mol}$ ) in toluene (1.2 mL) in a 16 x 125 mm glass culture tube under argon was quickly added  $[\text{Ir}(\text{dbcot})\text{Cl}]_2$  (1.7 mg, 1.97  $\mu\text{mol}$ ). CO was bubbled through the solution using a balloon and needle outlet (ca. 30 s), during which time the reaction mixture turned a dark-blue/black color. The balloon was removed and argon was bubbled through the reaction mixture in the same manner. The septum was quickly replaced with a Teflon cap and the reaction mixture

was stirred at 110 °C for 16 h. The reaction was allowed to cool to ambient temperature and was diluted with an approximately equal amount of hexanes. The mixture was stirred for 15 min, then passed through a small plug of Al<sub>2</sub>O<sub>3</sub> (hexanes → 1:1 hexanes/EtOAc eluent). The volatile materials were removed by rotary evaporation and the resulting residue was purified by flash chromatography (99:1 hexanes/CH<sub>2</sub>Cl<sub>2</sub> w/ 0.5% Et<sub>3</sub>N → 2:1 hexanes/CH<sub>2</sub>Cl<sub>2</sub> w/ 0.5% Et<sub>3</sub>N eluent) affording tricycle **2-28** (14.5 mg, 52% yield) as a yellow oil.

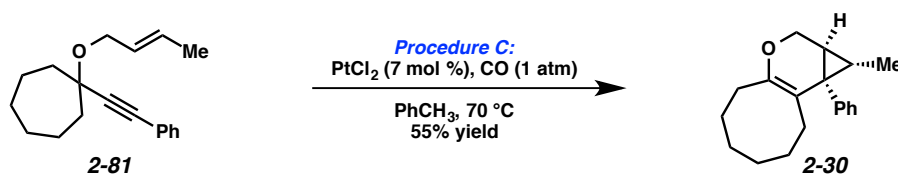
**Tricycle 2-28:** <sup>1</sup>H NMR (400 MHz; C<sub>6</sub>D<sub>6</sub>): δ 7.22 (d, *J* = 7.2 Hz, 2H), 7.13 (dt, *J* = 5.9, 2.1 Hz, 4H), 7.10-7.02 (m, 4H), 4.09 (ABq, *J*<sub>AB</sub> = 12.0 Hz, Δ*v*<sub>AB</sub> = 26.4 Hz, 2H), 3.85 (d, *J* = 10.0 Hz, 1H), 3.79 (ABq, *J*<sub>AB</sub> = 10.0 Hz, Δ*v*<sub>AB</sub> = 120.1 Hz, 2H), 3.00 (d, *J* = 10.0 Hz, 1H), 2.84 (s, 1H), 2.64-2.57 (m, 1H), 2.32-2.25 (m, 1H), 2.19-2.13 (m, 2H), 1.65-1.45 (m, 4H), 1.09 (s, 3H); <sup>13</sup>C NMR (100 MHz; C<sub>6</sub>D<sub>6</sub>): δ 146.5, 139.2, 137.6, 130.8, 128.6, 128.5, 127.9, 127.6, 126.5, 111.5, 73.3, 69.2, 68.4, 36.5, 31.9, 28.1, 27.7, 25.1, 23.7, 23.6, 23.1, 13.1; IR (film) 2930, 2856, 1678, 1445, 1155 cm<sup>-1</sup>; HRMS (ESI+) *m/z* calc'd for (M + H)<sup>+</sup> [C<sub>25</sub>H<sub>28</sub>O<sub>2</sub> + H]<sup>+</sup>: 361.2162, found 361.2169.



**Tricycle 2-29. Procedure C:** To a solution of enyne **2-79** (40.6 mg, 151 μmol) in toluene (2.5 mL) in a 2-dram vial under argon was quickly added PtCl<sub>2</sub> (2.8 mg, 1.05 μmol). CO was bubbled through the solution using a balloon and needle outlet (ca. 30 s). The balloon and outlet were then removed and the solution was stirred at 70 °C for 16 h. The reaction was allowed to cool to ambient temperature and was diluted with an approximately equal amount of hexanes. The mixture was stirred for 15 min, then passed through a small plug of Al<sub>2</sub>O<sub>3</sub> (hexanes → 1:1 hexanes/EtOAc eluent). The volatile materials were removed by rotary evaporation and the resulting residue was purified by flash chromatography (hexanes

w/ 0.5% Et<sub>3</sub>N → 2:1 hexanes/CH<sub>2</sub>Cl<sub>2</sub> w/ 0.5% Et<sub>3</sub>N eluent) affording tricycle **2-29** (27.9 mg, 69% yield, R<sub>f</sub> = 0.86 in 2:1 CH<sub>2</sub>Cl<sub>2</sub>/hexanes, stained brown with *p*-anisaldehyde) as a colorless oil.

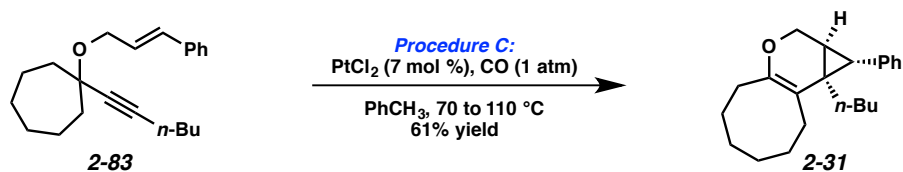
**Tricycle 2-29:** <sup>1</sup>H NMR (400 MHz; C<sub>6</sub>D<sub>6</sub>): δ 7.20-7.13 (m, 2H), 7.06 (dd, *J* = 7.3, 5.0 Hz, 3H), 4.19-4.16 (m, 1H), 4.01 (dd, *J* = 10.7, 2.9 Hz, 1H), 2.54-2.32 (m, 4H), 1.94-1.84 (m, 1H), 1.75-1.66 (m, 2H), 1.59-1.52 (m, 1H), 1.41-1.07 (m, 8H), 0.81 (t, *J* = 7.3 Hz, 3H); <sup>13</sup>C NMR (100 MHz; C<sub>6</sub>D<sub>6</sub>): δ 150.3, 138.9, 129.2, 128.4, 126.2, 113.1, 64.2, 37.4, 31.8, 30.6, 29.9, 29.8, 26.5, 26.0, 23.2, 19.5, 14.4; IR (film) 3026, 2960, 1682, 1464, 1152, 698 cm<sup>-1</sup>; HRMS (ESI+) *m/z* calc'd for (M + H)<sup>+</sup> [C<sub>19</sub>H<sub>24</sub>O + H]<sup>+</sup>: 269.1900, found 269.1910.



**Tricycle 2-30. Procedure C:** To a solution of enyne **2-81** (40.9 mg, 152 μmol) in toluene (2.5 mL) in a 2-dram vial under argon was quickly added PtCl<sub>2</sub> (2.8 mg, 1.05 μmol). CO was bubbled through the solution using a balloon and needle outlet (ca. 30 s). The balloon and outlet were then removed and the solution was stirred at 70 °C for 16 h. The reaction was allowed to cool to ambient temperature and was diluted with an approximately equal amount of hexanes. The mixture was stirred for 15 min, then passed through a small plug of Al<sub>2</sub>O<sub>3</sub> (hexanes → 1:1 hexanes/EtOAc eluent). The volatile materials were removed by rotary evaporation and the resulting residue was purified by flash chromatography (hexanes w/ 0.5% Et<sub>3</sub>N → 1:1 hexanes/CH<sub>2</sub>Cl<sub>2</sub> w/ 0.5% Et<sub>3</sub>N eluent) affording tricycle **2-30** (22.5 mg, 55% yield, R<sub>f</sub> = 0.85 in 2:1 CH<sub>2</sub>Cl<sub>2</sub>/hexanes, stained blue with *p*-anisaldehyde) as a colorless oil.

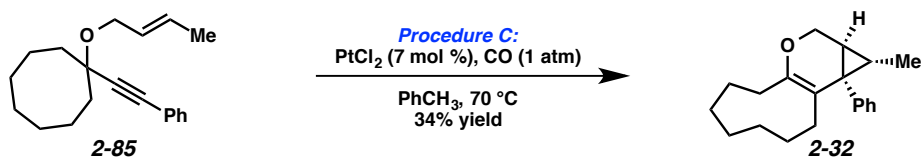
**Tricycle 2-30:** <sup>1</sup>H NMR (400 MHz; C<sub>6</sub>D<sub>6</sub>): δ 7.26-7.24 (m, 2H), 7.16 (d, *J* = 14.8 Hz, 2H), 7.08 (dd, *J* = 8.5, 6.1 Hz, 1H), 4.05-3.93 (m, 2H), 2.33-2.16 (m, 2H), 2.08 (d, *J* = 6.3 Hz, 1H), 1.67-1.33 (m, 8H), 1.20-1.13 (m, 2H), 1.05 (dt, *J* = 5.3, 2.6 Hz, 1H), 0.90 (d, *J* = 6.4 Hz, 3H); <sup>13</sup>C NMR (100 MHz; C<sub>6</sub>D<sub>6</sub>): δ

148.0, 141.6, 132.0, 127.9, 126.6, 112.9, 63.4, 31.7, 31.3, 30.3, 29.6, 29.3, 27.53, 27.51, 26.8, 25.8, 16.3; IR (film) 2923, 2851, 1658, 1493, 1164, 703  $\text{cm}^{-1}$ ; HRMS (ESI+)  $m/z$  calc'd for  $(M + H)^+$  [ $\text{C}_{19}\text{H}_{24}\text{O} + \text{H}$ ] $^+$ : 269.1900, found 269.1897.



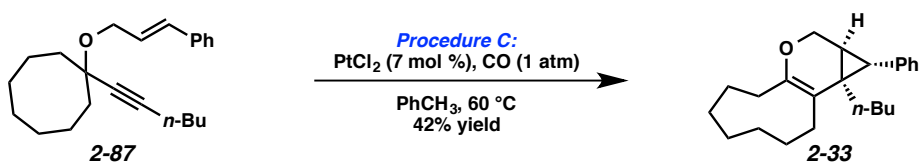
**Tricyclic 2-31. Procedure C:** To a solution of enyne **2-83** (12.7 mg, 40.9  $\mu\text{mol}$ ) in toluene (0.67 mL) in a 2-dram vial under argon was quickly added  $\text{PtCl}_2$  (0.7 mg, 2.63  $\mu\text{mol}$ ). CO was bubbled through the solution using a balloon and needle outlet (ca. 30 s). The balloon and outlet were then removed and the solution was stirred at 70 °C for 21 h, then at 110 °C for 24 h. The reaction was allowed to cool to ambient temperature and was diluted with an approximately equal amount of hexanes. The mixture was stirred for 15 min, then passed through a small plug of  $\text{Al}_2\text{O}_3$  (hexanes  $\rightarrow$  1:1 hexanes/ $\text{EtOAc}$  eluent). The volatile materials were removed by rotary evaporation and the resulting residue was purified by flash chromatography (99:1 hexanes/ $\text{CH}_2\text{Cl}_2$  w/ 0.5%  $\text{Et}_3\text{N}$   $\rightarrow$  5:1 hexanes/ $\text{CH}_2\text{Cl}_2$  w/ 0.5%  $\text{Et}_3\text{N}$  eluent) affording tricyclic **2-31** (7.7 mg, 61% yield,  $R_f = 0.84$  in 2:1  $\text{CH}_2\text{Cl}_2$ /hexanes, stained purple with *p*-anisaldehyde) as a yellow oil.

**Tricyclic 2-31:**  $^1\text{H}$  NMR (400 MHz;  $\text{C}_6\text{D}_6$ ):  $\delta$  7.19-7.17 (m, 2H), 7.13-7.11 (m, 2H), 7.09-7.05 (m, 1H), 4.04-3.97 (m, 2H), 2.42 (d,  $J = 5.7$  Hz, 1H), 2.39-2.14 (m, 4H), 1.79-1.10 (m, 14H), 0.82 (t,  $J = 7.3$  Hz, 3H), 0.58 (ddd,  $J = 14.1, 11.1, 5.8$  Hz, 1H);  $^{13}\text{C}$  NMR (100 MHz;  $\text{C}_6\text{D}_6$ ):  $\delta$  139.1, 129.3, 128.4, 126.2, 110.4, 63.5, 36.3, 31.6, 30.4, 30.3, 30.1, 29.5, 27.6, 26.9, 25.7, 25.6, 25.4, 23.2, 14.5; IR (film) 2924, 2854, 1660, 1447, 1128, 698  $\text{cm}^{-1}$ ; HRMS (ESI+)  $m/z$  calc'd for  $(M + H)^+$  [ $\text{C}_{22}\text{H}_{30}\text{O} + \text{H}$ ] $^+$ : 311.2369, found 311.2355.



**Tricyclic 2-32. Procedure C:** To a solution of enyne **2-85** (42.8 mg, 152  $\mu\text{mol}$ ) in toluene (2.5 mL) in a 2-dram vial under argon was quickly added  $\text{PtCl}_2$  (2.8 mg, 1.05  $\mu\text{mol}$ ). CO was bubbled through the solution using a balloon and needle outlet (ca. 30 s). The balloon and outlet were then removed and the solution was stirred at 70  $^\circ\text{C}$  for 20.5 h. The reaction was allowed to cool to ambient temperature and was diluted with an approximately equal amount of hexanes. The mixture was stirred for 15 min, then passed through a small plug of  $\text{Al}_2\text{O}_3$  (hexanes  $\rightarrow$  1:1 hexanes/EtOAc eluent). The volatile materials were removed by rotary evaporation and the resulting residue was purified by flash chromatography (hexanes w/ 0.5%  $\text{Et}_3\text{N}$   $\rightarrow$  10:1 hexanes/ $\text{CH}_2\text{Cl}_2$  w/ 0.5%  $\text{Et}_3\text{N}$  eluent) affording tricyclic **2-32** (13.6 mg, 34% yield,  $R_f = 0.85$  in 2:1  $\text{CH}_2\text{Cl}_2$ /hexanes, stained blue with *p*-anisaldehyde) as a yellow oil.

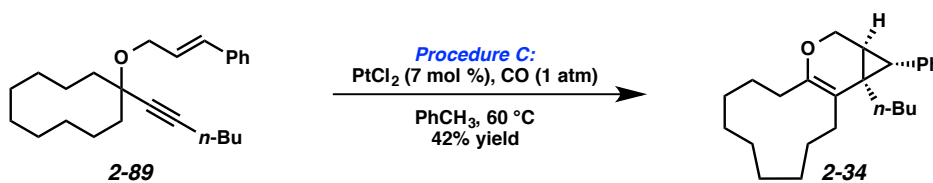
**Tricyclic 2-32:**  $^1\text{H}$  NMR (400 MHz;  $\text{C}_6\text{D}_6$ ):  $\delta$  7.28-7.26 (m, 2H), 7.18-7.15 (m, 2H), 7.11-7.06 (m, 1H), 3.99 (qd,  $J = 11.3, 3.2$  Hz, 2H), 2.33-2.17 (m, 2H), 2.11 (dd,  $J = 4.2, 3.1$  Hz, 1H), 1.69-1.59 (m, 2H), 1.51-1.30 (m, 10H), 1.08 (dd,  $J = 3.1, 2.1$  Hz, 1H), 0.91 (d,  $J = 6.4$  Hz, 3H);  $^{13}\text{C}$  NMR (100 MHz;  $\text{C}_6\text{D}_6$ ):  $\delta$  148.6, 141.8, 132.1, 128.2, 126.6, 114.6, 64.2, 31.0, 30.4, 29.7, 28.2, 26.8, 26.5, 26.2, 25.7, 25.5, 25.4, 16.3; IR (film) 2926, 2853, 1653, 1493, 1146, 704  $\text{cm}^{-1}$ ; HRMS (ESI+)  $m/z$  calc'd for  $(\text{M} + \text{H})^+ [\text{C}_{20}\text{H}_{26}\text{O} + \text{H}]^+$ : 283.2056, found 283.2056.



**Tricyclic 2-33. Procedure C:** To a solution of enyne **2-87** (19.6 mg, 60.4  $\mu\text{mol}$ ) in toluene (1.0 mL) in a 2-dram vial under argon was quickly added  $\text{PtCl}_2$  (1.2 mg, 4.51  $\mu\text{mol}$ ). CO was bubbled through the

solution using a balloon and needle outlet (ca. 30 s). The balloon and outlet were then removed and the solution was stirred at 60 °C for 21 h. The reaction was allowed to cool to ambient temperature and was diluted with an approximately equal amount of hexanes. The mixture was stirred for 15 min, then passed through a small plug of Al<sub>2</sub>O<sub>3</sub> (hexanes → 1:1 hexanes/EtOAc eluent). The volatile materials were removed by rotary evaporation and the resulting residue was purified by flash chromatography (99:1 hexanes/CH<sub>2</sub>Cl<sub>2</sub> w/ 0.5% Et<sub>3</sub>N → 20:1 hexanes/CH<sub>2</sub>Cl<sub>2</sub> w/ 0.5% Et<sub>3</sub>N eluent) affording tricycle **2-33** (8.3 mg, 42% yield, R<sub>f</sub> = 0.87 in 2:1 CH<sub>2</sub>Cl<sub>2</sub>/hexanes, stained blue with *p*-anisaldehyde) as a yellow oil.

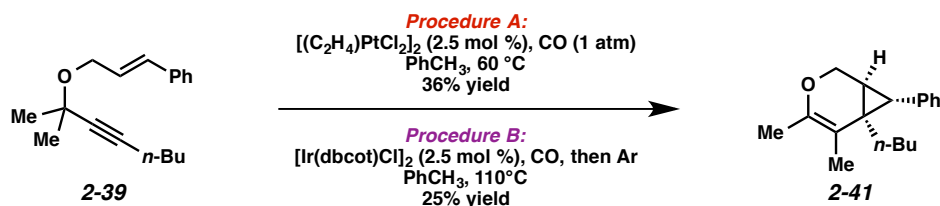
**Tricycle 2-33:** <sup>1</sup>H NMR (400 MHz; C<sub>6</sub>D<sub>6</sub>): δ 7.20-7.17 (m, 1H), 7.15-7.13 (m, 2H), 7.10-7.06 (m, 1H), 4.04 (dd, *J* = 10.7, 4.0 Hz, 1H), 3.98-3.94 (m, 1H), 2.42 (d, *J* = 5.7 Hz, 1H), 2.39-2.30 (m, 3H), 2.21-2.15 (m, 1H), 1.81-1.08 (m, 19H), 0.82 (t, *J* = 7.3 Hz, 3H), 0.60 (ddd, *J* = 14.1, 11.2, 5.7 Hz, 1H); <sup>13</sup>C NMR (100 MHz; C<sub>6</sub>D<sub>6</sub>): δ 150.8, 139.1, 129.3, 128.4, 126.3, 111.3, 64.1, 37.0, 30.6, 30.4, 29.7, 27.1, 26.9, 26.5, 26.2, 25.6, 25.5, 24.9, 24.3, 23.3, 14.5; IR (film) 2926, 2856, 1654, 1497, 1183 cm<sup>-1</sup>; HRMS (ESI+) *m/z* calc'd for (M + H)<sup>+</sup> [C<sub>23</sub>H<sub>32</sub>O + H]<sup>+</sup>: 325.2526, found 325.2517.



**Tricycle 2-34. Procedure C:** To a solution of enyne **2-89** (21.1 mg, 59.8 μmol) in toluene (1.0 mL) in a 2-dram vial under argon was quickly added PtCl<sub>2</sub> (1.2 mg, 4.51 μmol). CO was bubbled through the solution using a balloon and needle outlet (ca. 30 s). The balloon and outlet were then removed and the solution was stirred at 60 °C for 21 h. The reaction was allowed to cool to ambient temperature and was diluted with an approximately equal amount of hexanes. The mixture was stirred for 15 min, then passed through a small plug of Al<sub>2</sub>O<sub>3</sub> (hexanes → 1:1 hexanes/EtOAc eluent). The volatile materials were removed by rotary evaporation and the resulting residue was purified by flash chromatography (99:1

hexanes/CH<sub>2</sub>Cl<sub>2</sub> w/ 0.5% Et<sub>3</sub>N → 10:1 hexanes/CH<sub>2</sub>Cl<sub>2</sub> w/ 0.5% Et<sub>3</sub>N eluent) affording tricycle **2-34** (8.9 mg, 42% yield, R<sub>f</sub> = 0.86 in 2:1 CH<sub>2</sub>Cl<sub>2</sub>/hexanes, stained brown/blue in *p*-anisaldehyde) as a colorless oil.

**Tricycle 2-34:** <sup>1</sup>H NMR (400 MHz; C<sub>6</sub>D<sub>6</sub>): δ 7.22-7.19 (m, 4H), 7.11-7.07 (m, 1H), 4.26 (dd, *J* = 11.3, 6.3 Hz, 1H), 3.62 (dd, *J* = 11.4, 4.6 Hz, 1H), 2.54-2.39 (m, 2H), 2.30-2.21 (m, 2H), 2.18 (d, *J* = 5.2 Hz, 1H), 2.00-1.89 (m, 2H), 1.74-1.08 (m, 18H), 0.80 (t, *J* = 7.3 Hz, 3H), 0.69 (ddd, *J* = 14.0, 11.1, 5.7 Hz, 1H); <sup>13</sup>C NMR (100 MHz; C<sub>6</sub>D<sub>6</sub>): δ 151.3, 139.1, 129.1, 128.4, 126.3, 112.4, 66.9, 39.5, 29.9, 29.7, 29.3, 27.8, 26.8, 26.44, 26.4, 26.3, 25.8, 25.53, 25.48, 25.2, 23.2, 22.4, 14.4; IR (film) 2927, 2857, 1498, 1154, 721 cm<sup>-1</sup>; HRMS (ESI+) *m/z* calc'd for (M + H)<sup>+</sup> [C<sub>25</sub>H<sub>36</sub>O + H]<sup>+</sup>: 353.2839, found 353.2831.

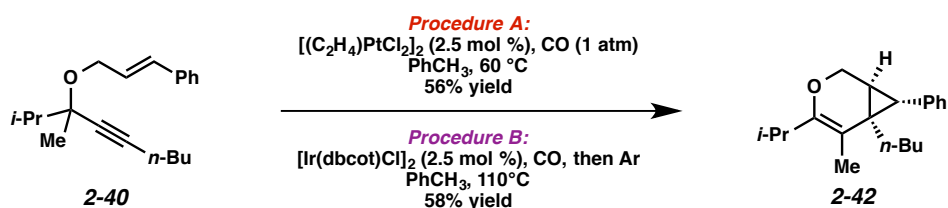


**Bicycle 2-41. Procedure A:** To a solution of enyne **2-39** (20.6 mg, 80.3 μmol) in toluene (1.2 mL) in a 2-dram vial under argon was quickly added  $[(C_2H_4)PtCl_2]_2$  (1.2 mg, 2.04 μmol). CO was bubbled through the solution using a balloon and needle outlet (ca. 30 s). The balloon and outlet were then removed and the solution was stirred at 60 °C for 19.5 h. The reaction was allowed to cool to ambient temperature and was diluted with an approximately equal amount of hexanes. The mixture was stirred for 15 min, then passed through a small plug of Al<sub>2</sub>O<sub>3</sub> (hexanes → 1:1 hexanes/EtOAc eluent). The volatile materials were removed by rotary evaporation and the resulting residue was purified by flash chromatography (50:1 hexanes/CH<sub>2</sub>Cl<sub>2</sub> w/ 0.5% Et<sub>3</sub>N → 2:1 hexanes/CH<sub>2</sub>Cl<sub>2</sub> w/ 0.5% Et<sub>3</sub>N eluent) affording bicycle **2-41** (7.5 mg, 36% yield, R<sub>f</sub> = 0.78 in 2:1 CH<sub>2</sub>Cl<sub>2</sub>/hexanes, stained orange with *p*-anisaldehyde) as a yellow oil.

**Procedure B:** To a solution of enyne **2-39** (15.6 mg, 60.8 μmol) in toluene (0.92 mL) in a 16 x 125 mm glass culture tube under argon was quickly added  $[Ir(dbcot)Cl]_2$  (1.3 mg, 1.50 μmol). CO was bubbled through the solution using a balloon and needle outlet (ca. 30 s), during which time the reaction mixture

turned a dark-blue/black color. The balloon was removed and argon was bubbled through the reaction mixture in the same manner. The septum was quickly replaced with a Teflon cap and the reaction mixture was stirred at 110 °C for 18 h. The reaction was allowed to cool to ambient temperature and was diluted with an approximately equal amount of hexanes. 1,3-Bis(diphenylphosphino)propane (dppp) (6.2 mg, 15.0 μmol) was also added to the mixture. The mixture was stirred for 15 min, then passed through a small plug of Al<sub>2</sub>O<sub>3</sub> (hexanes → 1:1 hexanes/EtOAc eluent). The volatile materials were removed by rotary evaporation and the resulting residue was purified by flash chromatography (99:1 hexanes/CH<sub>2</sub>Cl<sub>2</sub> w/ 0.5% Et<sub>3</sub>N → 50:1 hexanes/CH<sub>2</sub>Cl<sub>2</sub> w/ 0.5% Et<sub>3</sub>N eluent) affording bicycle **2-41** (3.9 mg, 25% yield) as a yellow oil.

**Bicycle 2-41:** <sup>1</sup>H NMR (400 MHz; C<sub>6</sub>D<sub>6</sub>): δ 7.16 (d, *J* = 14.7 Hz, 3H), 7.08-7.06 (m, 2H), 4.10 (dd, *J* = 11.0, 5.1 Hz, 1H), 3.80 (dd, *J* = 11.0, 3.4 Hz, 1H), 2.17 (d, *J* = 5.4 Hz, 1H), 1.79 (d, *J* = 0.9 Hz, 3H), 1.70 (d, *J* = 0.9 Hz, 3H), 1.65-1.58 (m, 1H), 1.47 (td, *J* = 5.3, 3.4 Hz, 1H), 1.36-1.09 (m, 4H), 0.81 (t, *J* = 7.3 Hz, 3H), 0.61 (ddd, *J* = 14.0, 10.9, 5.9 Hz, 1H); <sup>13</sup>C NMR (100 MHz; C<sub>6</sub>D<sub>6</sub>): δ 146.2, 139.1, 129.4, 126.2, 108.5, 65.4, 38.7, 30.0, 27.2, 25.4, 23.2, 16.8, 14.4, 14.0; IR (film) 2956, 2859, 2017, 1948, 1384, 1150 cm<sup>-1</sup>; HRMS (ESI+) *m/z* calc'd for (M + H)<sup>+</sup> [C<sub>18</sub>H<sub>24</sub>O + H]<sup>+</sup>: 257.1900, found 257.1888.



**Bicycle 2-42. Procedure A:** To a solution of enyne **2-40** (42.2 mg, 148 μmol) in toluene (2.5 mL) in a 2-dram vial under argon was quickly added  $[(C_2H_4)PtCl_2]_2$  (2.2 mg, 3.74 μmol). CO was bubbled through the solution using a balloon and needle outlet (ca. 30 s). The balloon and outlet were then removed and the solution was stirred at 60 °C for 20 h. The reaction was allowed to cool to ambient temperature and was diluted with an approximately equal amount of hexanes. The mixture was stirred for 15 min, then

passed through a small plug of Al<sub>2</sub>O<sub>3</sub> (hexanes → 1:1 hexanes/EtOAc eluent). The volatile materials were removed by rotary evaporation and the resulting residue was purified by flash chromatography (hexanes w/ 0.5% Et<sub>3</sub>N → 9:1 hexanes/CH<sub>2</sub>Cl<sub>2</sub> w/ 0.5% Et<sub>3</sub>N eluent) affording bicycle **2-42** (23.8 mg, 56% yield, R<sub>f</sub> = 0.78 in 2:1 CH<sub>2</sub>Cl<sub>2</sub>/hexanes, stained orange with *p*-anisaldehyde) as a yellow oil.

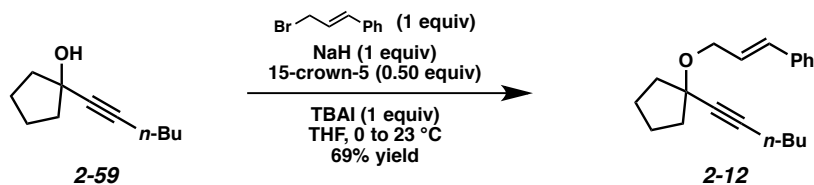
**Procedure B:** To a solution of enyne **2-40** (28.9 mg, 102 μmol) in toluene (1.5 mL) in a 16 x 125 mm glass culture tube under argon was quickly added [Ir(dbcot)Cl]<sub>2</sub> (2.2 mg, 2.55 μmol). CO was bubbled through the solution using a balloon and needle outlet (ca. 30 s), during which time the reaction mixture turned a dark-blue/black color. The balloon was removed and argon was bubbled through the reaction mixture in the same manner. The septum was quickly replaced with a Teflon cap and the reaction mixture was stirred at 110 °C for 23 h. The reaction was allowed to cool to ambient temperature and was diluted with an approximately equal amount of hexanes. 1,3-Bis(diphenylphosphino)propane (dppp) (10.3 mg, 25.0 μmol) was also added to the mixture. The mixture was stirred for 15 min, then passed through a small plug of Al<sub>2</sub>O<sub>3</sub> (hexanes → 1:1 hexanes/EtOAc eluent). The volatile materials were removed by rotary evaporation and the resulting residue was purified by flash chromatography (99:1 hexanes/CH<sub>2</sub>Cl<sub>2</sub> w/ 0.5% Et<sub>3</sub>N → 20:1 hexanes/CH<sub>2</sub>Cl<sub>2</sub> w/ 0.5% Et<sub>3</sub>N eluent) affording bicycle **2-42** (16.9 mg, 58% yield) as a yellow oil.

**Bicycle 2-42:** <sup>1</sup>H NMR (400 MHz; C<sub>6</sub>D<sub>6</sub>): δ 7.18-7.14 (m, 2H), 7.08-7.06 (m, 3H), 4.19 (ddd, *J* = 11.1, 5.9, 0.9 Hz, 1H), 3.65 (dd, *J* = 11.1, 4.1 Hz, 1H), 2.80-2.69 (m, 1H), 2.05 (d, *J* = 5.1 Hz, 1H), 1.73 (d, *J* = 1.0 Hz, 3H), 1.65-1.58 (m, 1H), 1.52-1.48 (m, 1H), 1.40-1.21 (m, 4H), 1.18 (dd, *J* = 6.8, 1.1 Hz, 3H), 1.13 (dd, *J* = 6.8, 1.0 Hz, 3H), 0.81 (t, *J* = 7.3 Hz, 3H), 0.64-0.57 (m, 1H); <sup>13</sup>C NMR (100 MHz; C<sub>6</sub>D<sub>6</sub>): δ 154.6, 139.1, 133.7, 129.4, 127.1, 126.2, 107.4, 67.3, 39.2, 30.2, 30.0, 29.8, 29.0, 27.4, 25.0, 23.1, 20.3, 20.2, 14.4, 13.3; IR (film) 2929, 2859, 1454, 1094, 698 cm<sup>-1</sup>; HRMS (ESI+) *m/z* calc'd for (M + H)<sup>+</sup> [C<sub>20</sub>H<sub>28</sub>O + H]<sup>+</sup>: 285.2213, found 285.2201.

### 2.7.3 Substrate Synthesis

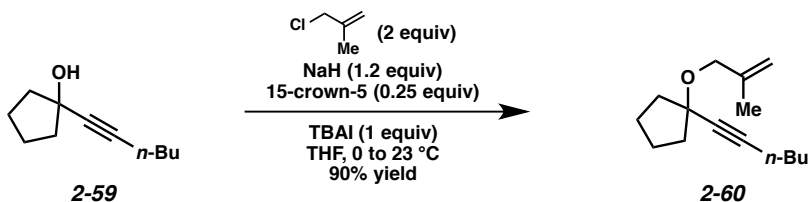
**General procedure for the synthesis of tertiary propargyl alcohols.** To a solution of the terminal alkyne (1.1 equiv) in THF (0.30 M) at 0 °C was slowly added *n*-BuLi (2.5 M in hexane, 1 equiv). The reaction mixture was stirred at 0 °C for 30 min, then the ketone (1 equiv) was added. The reaction mixture was allowed to warm to ambient temperature and was stirred until the ketone was consumed, as determined by TLC. The reaction mixture was then diluted with aq. 1 M HCl and the mixture was transferred to a separatory funnel. The layers were separated and the aqueous layer was extracted with Et<sub>2</sub>O (3x). The combined organic layers were washed with brine, then dried over MgSO<sub>4</sub>. The volatile materials were removed by rotary evaporation and the crude residue was purified by flash chromatography.

**General procedure for the alkylation of tertiary propargyl alcohols to give oxygen-tethered 1,6-enynes.** To a solution of the tertiary propargyl alcohol (1 equiv) in THF (0.20 M) in a flame-dried flask under argon at 0 °C was added NaH (1.2 equiv, 60% dispersion in mineral oil). The reaction mixture was allowed to warm to ambient temperature and was stirred until gas evolution was visibly complete. To this suspension was added sequentially 15-crown-5 (0.25 equiv), tetrabutylammonium iodide (TBAI) (1 equiv), and the allylic halide (1 equiv). The resulting mixture was stirred at ambient temperature until completion, as determined by TLC. The reaction was quenched with sat. aq. NH<sub>4</sub>Cl. The layers were separated, and the aqueous layer was extracted with Et<sub>2</sub>O (3x). The combined organic layers were washed with brine, then dried over MgSO<sub>4</sub>. The volatile materials were removed by rotary evaporation and the resulting residue was purified by flash chromatography.



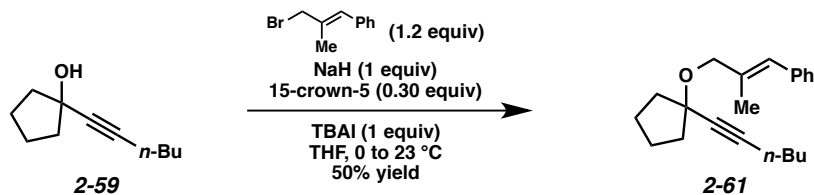
**Enyne 2-12.** To a solution of tertiary propargyl alcohol **2-59** (0.166 g, 1.00 mmol) in THF (5.0 mL) at 0 °C was added NaH (40.0 mg, 60% dispersion in mineral oil, 1.00 mmol). The reaction mixture was allowed to warm to ambient temperature and was stirred until gas evolution was visibly complete. To this suspension was added sequentially 15-crown-5 (99.0  $\mu$ L, 0.500 mmol), tetrabutylammonium iodide (0.369 g, 1.00 mmol), and cinnamyl bromide (0.197 g, 1.00 mmol). The resulting mixture was stirred at ambient temperature for 16 h. The reaction was quenched with sat. aq.  $\text{NH}_4\text{Cl}$  (10 mL). The layers were separated, and the aqueous layer was extracted with  $\text{Et}_2\text{O}$  (3 x 10 mL). The combined organic layers were washed with brine (25 mL), then dried over  $\text{MgSO}_4$ . The volatile materials were removed by rotary evaporation and the resulting residue was purified by flash chromatography (99:1 hexanes/ $\text{CH}_2\text{Cl}_2$   $\rightarrow$  2:1 hexanes/ $\text{CH}_2\text{Cl}_2$  eluent), affording enyne **2-12** (0.195 g, 69% yield,  $R_f$  = 0.67 in 1:1 hexanes/ $\text{CH}_2\text{Cl}_2$ , stained blue with *p*-anisidine) as a yellow oil.

**Enyne 2-12:**  $^1\text{H}$  NMR (400 MHz;  $\text{CDCl}_3$ ):  $\delta$  7.39-7.37 (m, 2H), 7.32-7.28 (m, 2H), 7.24-7.19 (m, 1H), 6.61 (d,  $J$  = 15.9 Hz, 1H), 6.33 (dt,  $J$  = 15.9, 6.0 Hz, 1H), 4.23 (dd,  $J$  = 6.0, 1.5 Hz, 2H), 2.24 (t,  $J$  = 7.0 Hz, 2H), 2.06-1.99 (m, 2H), 1.92-1.85 (m, 2H), 1.80-1.69 (m, 4H), 1.55-1.40 (m, 4H), 0.92 (d,  $J$  = 14.5 Hz, 3H);  $^{13}\text{C}$  NMR (100 MHz;  $\text{CDCl}_3$ ):  $\delta$  137.2, 131.6, 128.6, 127.5, 127.3, 126.6, 85.6, 81.7, 80.8, 65.7, 39.9, 31.1, 23.5, 22.1, 18.6, 13.8; IR (film) 2959, 2872, 1496, 1053, 964  $\text{cm}^{-1}$ ; HRMS (ESI+)  $m/z$  calc'd for  $(\text{M} + \text{H})^+$  [ $\text{C}_{20}\text{H}_{26}\text{O} + \text{H}$ ] $^+$ : 283.2056, found 283.2056.



**Enyne 2-60.** To a solution of tertiary propargyl alcohol **2-59** (0.415 g, 2.49 mmol) in THF (13 mL) at 0 °C was added NaH (0.125 g, 60% dispersion in mineral oil, 3.14 mmol). The reaction mixture was allowed to warm to ambient temperature and was stirred until gas evolution was visibly complete. To this suspension was added sequentially 15-crown-5 (0.120 mL, 0.625 mmol), tetrabutylammonium iodide (0.924 g, 2.50 mmol), and methallyl chloride (0.550 mL, 5.57 mmol). The resulting mixture was stirred at ambient temperature for 19.5 h. The reaction was quenched with sat. aq. NH<sub>4</sub>Cl (15 mL). The layers were separated, and the aqueous layer was extracted with Et<sub>2</sub>O (3 x 15 mL). The combined organic layers were washed with brine (40 mL), then dried over MgSO<sub>4</sub>. The volatile materials were removed by rotary evaporation and the resulting residue was purified by flash chromatography (100% hexanes → 5:1 hexanes/EtOAc eluent), affording enyne **2-60** (0.470 g, 90% yield, R<sub>f</sub> = 0.85 in 1:1 hexanes/CH<sub>2</sub>Cl<sub>2</sub>, stained blue with *p*-anisaldehyde) as a colorless oil.

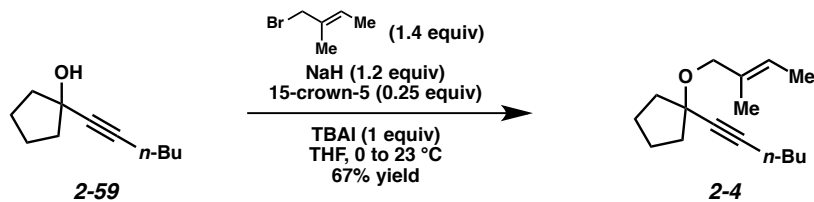
**Enyne 2-60:** <sup>1</sup>H NMR (400 MHz; CDCl<sub>3</sub>): δ 4.98 (dd, *J* = 2.2, 0.9 Hz, 1H), 4.84 (t, *J* = 1.1 Hz, 1H), 3.94 (s, 2H), 2.21 (t, *J* = 6.9 Hz, 2H), 2.03-1.96 (m, 2H), 1.88-1.78 (m, 2H), 1.75 (s, 3H), 1.74-1.65 (m, 4H), 1.53-1.38 (m, 4H), 0.91 (t, *J* = 7.2 Hz, 3H); <sup>13</sup>C NMR (100 MHz; CDCl<sub>3</sub>): δ 143.3, 111.4, 85.2, 81.8, 80.6, 77.2, 68.7, 39.8, 31.1, 23.5, 22.1, 20.0, 18.6, 13.8; IR (film) 2960, 2873, 1452, 1094 cm<sup>-1</sup>; HRMS (ESI+) *m/z* calc'd for (M + H)<sup>+</sup> [C<sub>15</sub>H<sub>24</sub>O + H]<sup>+</sup>: 221.1900, found 221.1902.



**Enyne 2-61.** To a solution of tertiary propargyl alcohol **2-59** (0.167 g, 1.00 mmol) in THF (5.0 mL) at 0 °C was added NaH (40.0 mg, 60% dispersion in mineral oil, 1.00 mmol). The reaction mixture was allowed to warm to ambient temperature and was stirred until gas evolution was visibly complete. To this suspension was added sequentially 15-crown-5 (60.0 μL, 0.303 mmol), tetrabutylammonium iodide

(0.369 g, 1.00 mmol), and 3-bromo-2-methyl-1-phenyl-1-propene (0.258 g, 1.22 mmol). The resulting mixture was stirred at ambient temperature for 20 h. The reaction was quenched with sat. aq. NH<sub>4</sub>Cl (10 mL). The layers were separated, and the aqueous layer was extracted with Et<sub>2</sub>O (3 x 10 mL). The combined organic layers were washed with brine (25 mL), then dried over MgSO<sub>4</sub>. The volatile materials were removed by rotary evaporation and the resulting residue was purified by flash chromatography (20:1 hexanes/CH<sub>2</sub>Cl<sub>2</sub> → 1:1 hexanes/CH<sub>2</sub>Cl<sub>2</sub> eluent), affording enyne **2-61** (0.148 g, 50% yield, R<sub>f</sub> = 0.63 in 1:1 hexanes/CH<sub>2</sub>Cl<sub>2</sub>, stained blue with *p*-anisaldehyde) as a colorless oil.

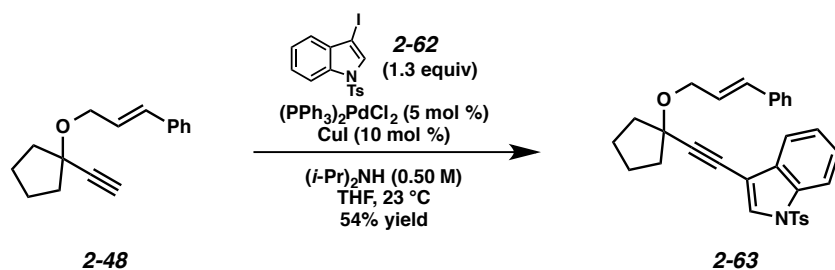
**Enyne 2-61:** <sup>1</sup>H NMR (400 MHz; CDCl<sub>3</sub>): δ 7.34-7.27 (m, 4H), 7.21-7.17 (m, 1H), 6.53 (s, 1H), 4.09 (s, 2H), 2.24 (t, *J* = 6.9 Hz, 2H), 2.08-2.01 (m, 2H), 1.90 (s, 3H), 1.88-1.84 (m, 2H), 1.82-1.69 (m, 4H), 1.53-1.40 (m, 4H), 0.92 (t, *J* = 7.2 Hz, 3H); <sup>13</sup>C NMR (100 MHz; CDCl<sub>3</sub>): δ 138.1, 136.2, 129.1, 128.1, 126.3, 126.1, 98.8, 85.4, 81.8, 80.8, 70.9, 39.9, 31.1, 23.5, 22.1, 18.6, 15.9, 13.8; IR (film) 2959, 2872, 1446, 1047 cm<sup>-1</sup>; HRMS (ESI+) *m/z* calc'd for (M + H)<sup>+</sup> [C<sub>21</sub>H<sub>28</sub>O + H]<sup>+</sup>: 297.2213, found 297.2208.



**Enyne 2-4.** To a solution of tertiary propargyl alcohol **2-59** (0.166 g, 0.996 mmol) in THF (5.0 mL) at 0 °C was added NaH (40.0 mg, 60% dispersion in mineral oil, 1.00 mmol). The reaction mixture was allowed to warm to ambient temperature and was stirred until gas evolution was visibly complete. To this suspension was added sequentially 15-crown-5 (60.0 μL, 0.303 mmol), tetrabutylammonium iodide (0.369 g, 1.00 mmol), and 3-bromo-2-methyl-1-methyl-1-propene (0.208 g, 1.40 mmol). The resulting mixture was stirred at ambient temperature for 16 h. The reaction was quenched with sat. aq. NH<sub>4</sub>Cl (10 mL). The layers were separated, and the aqueous layer was extracted with Et<sub>2</sub>O (3 x 10 mL). The combined organic layers were washed with brine (40 mL), then dried over MgSO<sub>4</sub>. The volatile materials

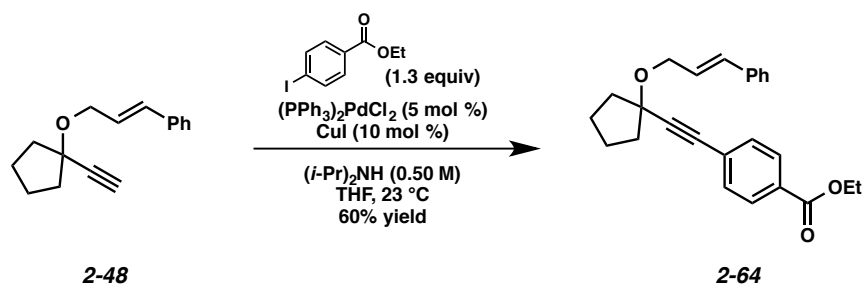
were removed by rotary evaporation and the resulting residue was purified by flash chromatography (hexanes  $\rightarrow$  1:1 hexanes/CH<sub>2</sub>Cl<sub>2</sub> eluent), affording enyne **2-4** (0.158 g, 67% yield, R<sub>f</sub> = 0.71 in 1:1 hexanes/CH<sub>2</sub>Cl<sub>2</sub>, stained blue with *p*-anisaldehyde) as a colorless oil.

**Enyne 2-4:** <sup>1</sup>H NMR (400 MHz; CDCl<sub>3</sub>): δ 5.51 (q, *J* = 6.28 Hz, 1H), 3.90 (s, 2H), 2.22 (t, *J* = 6.9 Hz, 2H), 2.02-1.96 (m, 2H), 1.86-1.78 (m, 2H), 1.76-1.67 (m, 4H), 1.65 (d, *J* = 1.0 Hz, 3H), 1.61 (dt, *J* = 6.7, 0.9 Hz, 3H), 1.51-1.39 (m, 4H), 0.91 (t, *J* = 7.2 Hz, 3H); <sup>13</sup>C NMR (100 MHz; CDCl<sub>3</sub>): δ 133.8, 121.9, 85.1, 82.0, 80.5, 70.9, 39.8, 31.1, 23.4, 22.1, 18.6, 14.0, 13.8, 13.4; IR (film) 2960, 2934, 2861, 1449, 1046 cm<sup>-1</sup>; HRMS (ESI+) *m/z* calc'd for (M + H)<sup>+</sup> [C<sub>16</sub>H<sub>26</sub>O + H]<sup>+</sup>: 235.2056, found 235.2050.



**Enyne 2-63.** To (PPh<sub>3</sub>)<sub>2</sub>PdCl<sub>2</sub> (52.7 mg, 75.1 μmol) and CuI (28.6 mg, 0.150 mmol) under argon was added (i-Pr)<sub>2</sub>NH (3.0 mL). The reaction mixture was stirred for 5 min, then 3-iodo-1-tosylindole (**2-62**) (0.775 g, 1.95 mmol) was added and the mixture was stirred for 5 more min. Terminal alkyne **2-48** (0.339 g, 1.50 mmol) was then added as a 0.50 M solution in THF. Additional THF (ca. 3.0 mL) was added to maintain dissolution. The mixture was stirred for 14 h, after which the reaction mixture was partitioned between 1 M HCl (10 mL) and Et<sub>2</sub>O (5.0 mL). The layers were separated and the aqueous layer was extracted with Et<sub>2</sub>O (3 x 5.0 mL). The combined organic layers were washed with brine (20 mL), then dried over MgSO<sub>4</sub>. The volatile materials were removed by rotary evaporation and the resulting residue was purified by flash chromatography (100% hexanes  $\rightarrow$  9:1 hexanes/EtOAc eluent), affording enyne **2-63** (0.406 g, 54% yield, R<sub>f</sub> = 0.33 in 9:1 hexanes/EtOAc, stained blue with *p*-anisaldehyde) as a brown amorphous solid.

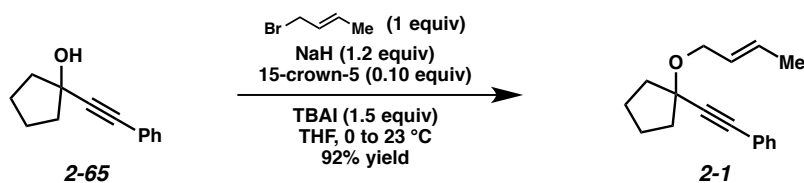
**Enyne 2-63:**  $^1\text{H}$  NMR (400 MHz;  $\text{CDCl}_3$ ):  $\delta$  7.97 (d,  $J = 8.3$  Hz, 1H), 7.79 (d,  $J = 8.3$  Hz, 2H), 7.72 (s, 1H), 7.61 (d,  $J = 7.7$  Hz, 1H), 7.38 (t,  $J = 8.2$  Hz, 3H), 7.34-7.28 (m, 3H), 7.23 (t,  $J = 8.3$  Hz, 3H), 6.65 (d,  $J = 16.1$  Hz, 1H), 6.40-6.33 (m, 1H), 4.36-4.34 (m, 2H), 2.35 (s, 3H), 2.22-2.04 (m, 4H), 1.90-1.78 (m, 4H);  $^{13}\text{C}$  NMR (100 MHz;  $\text{CDCl}_3$ ):  $\delta$  145.4, 135.1, 134.3, 131.9, 130.2, 128.8, 128.6, 127.7, 127.1, 127.0, 126.6, 125.6, 123.8, 120.6, 113.7, 95.5, 81.2, 77.4, 66.1, 40.1, 23.6, 21.7; IR (film) 2966, 1376, 1175, 964  $\text{cm}^{-1}$ ; HRMS (ESI+)  $m/z$  calc'd for  $(\text{M} + \text{H})^+$  [ $\text{C}_{31}\text{H}_{29}\text{NO}_3\text{S} + \text{H}$ ] $^+$ : 496.1941, found 496.1960.



**Enyne 2-64.** To  $(\text{PPh}_3)_2\text{PdCl}_2$  (52.7 mg, 75.1  $\mu\text{mol}$ ) and  $\text{CuI}$  (28.6 mg, 0.150 mmol) under argon was added  $(i\text{-Pr})_2\text{NH}$  (3.0 mL). The reaction mixture was stirred for 5 min, then 4-iodoethylbenzoate (0.330 mL, 1.95 mmol) was added and the mixture was stirred for 5 min. Terminal alkyne **2-48** (0.339 g, 1.50 mmol) was then added as a 0.50 M solution in THF. Additional THF (ca. 3.0 mL) was added to maintain dissolution. The mixture was stirred for 14 h, after which the reaction mixture was partitioned between 1 M  $\text{HCl}$  (10 mL) and  $\text{Et}_2\text{O}$  (5.0 mL). The layers were separated and the aqueous layer was extracted with  $\text{Et}_2\text{O}$  (3 x 5.0 mL). The combined organic layers were washed with brine (20 mL), then dried over  $\text{MgSO}_4$ . The volatile materials were removed by rotary evaporation and the resulting residue was purified by flash chromatography (100% hexanes  $\rightarrow$  9:1 hexanes/ $\text{EtOAc}$  eluent), affording enyne **2-64** (0.338 g, 60% yield,  $R_f = 0.42$  in 9:1 hexanes/ $\text{EtOAc}$ , stained blue with *p*-anisaldehyde) as a colorless oil.

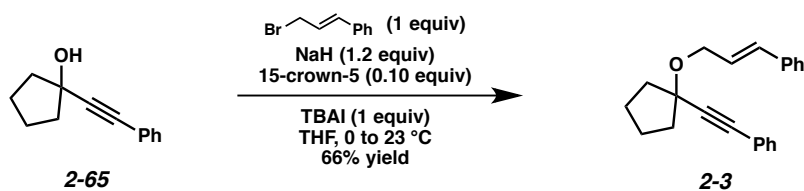
**Enyne 2-64:**  $^1\text{H}$  NMR (400 MHz;  $\text{CDCl}_3$ ):  $\delta$  7.99-7.97 (m, 2H), 7.50-7.48 (m, 2H), 7.40-7.38 (m, 2H), 7.30 (dd,  $J = 8.1, 6.7$  Hz, 2H), 7.24-7.20 (m, 1H), 6.63 (t,  $J = 14.3$  Hz, 1H), 6.39-6.27 (m, 1H), 4.38 (q,  $J = 7.1$  Hz, 2H), 4.32 (dd,  $J = 5.9, 1.4$  Hz, 1H), 2.20-2.01 (m, 4H), 1.88-1.75 (m, 4H), 1.40 (d,  $J = 14.3$  Hz,

3H);  $^{13}\text{C}$  NMR (100 MHz;  $\text{CDCl}_3$ ):  $\delta$  131.9, 131.7, 129.5, 128.6, 127.7, 126.6, 94.2, 84.6, 81.0, 66.1, 61.3, 39.9, 23.6, 14.5; IR (film) 2965, 1719, 1272, 1106  $\text{cm}^{-1}$ ; HRMS (ESI+)  $m/z$  calc'd for  $(\text{M} + \text{H})^+$   $[\text{C}_{25}\text{H}_{26}\text{O}_3 + \text{H}]^+$ : 375.1955, found 375.1935.



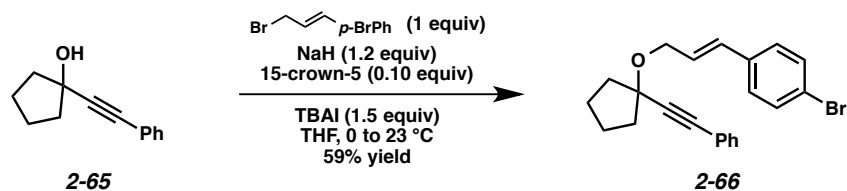
**Enyne 2-1.** To a solution of tertiary propargyl alcohol **2-65** (0.150 g, 0.805 mmol) in THF (4.0 mL) at 0 °C was added NaH (38.9 mg, 60% dispersion in mineral oil, 0.973 mmol). The reaction mixture was allowed to warm to ambient temperature and was stirred until gas evolution was visibly complete. To this suspension was added sequentially 15-crown-5 (16.0  $\mu\text{L}$ , 81.0  $\mu\text{mol}$ ), tetrabutylammonium iodide (0.451 g, 1.22 mmol), and crotyl bromide (83.3  $\mu\text{L}$ , 0.810 mmol). The resulting mixture was stirred at ambient temperature for 24 h. The reaction was quenched with sat. aq.  $\text{NH}_4\text{Cl}$  (10 mL). The layers were separated, and the aqueous layer was extracted with  $\text{Et}_2\text{O}$  (3 x 10 mL). The combined organic layers were washed with brine (30 mL), then dried over  $\text{MgSO}_4$ . The volatile materials were removed by rotary evaporation and the resulting residue was purified by flash chromatography (100% hexanes  $\rightarrow$  9:1 hexanes/ $\text{Et}_2\text{O}$  eluent), affording enyne **2-1** (0.179 g, 92% yield,  $R_f = 0.71$  in 4:1 hexanes/ $\text{EtOAc}$ , stained blue with *p*-anisaldehyde) as a colorless oil.

**Enyne 2-1:**  $^1\text{H}$  NMR (400 MHz;  $\text{CDCl}_3$ ):  $\delta$  7.43 (td,  $J = 3.8, 1.7$  Hz, 2H), 7.30 (t,  $J = 3.2$  Hz, 3H), 5.79-5.60 (m, 2H), 4.08 (d,  $J = 6.1$  Hz, 2H), 2.13-1.96 (m, 4H), 1.86-1.74 (m, 4H), 1.71 (dd,  $J = 6.2, 0.9$  Hz, 3H);  $^{13}\text{C}$  NMR (100 MHz;  $\text{CDCl}_3$ ):  $\delta$  131.8, 129.1, 128.36, 128.35, 128.2, 126.6, 91.2, 84.9, 80.8, 66.1, 39.9, 23.6, 18.0; IR (film) 2965, 2857, 1443, 1088  $\text{cm}^{-1}$ ; HRMS (ESI+)  $m/z$  calc'd for  $(\text{M} + \text{H})^+$   $[\text{C}_{17}\text{H}_{20}\text{O} + \text{H}]^+$ : 241.1587, found 241.1587.



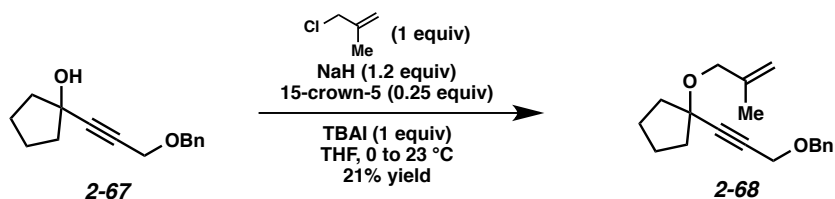
**Enyne 2-3.** To a solution of tertiary propargyl alcohol **2-65** (0.187 g, 1.00 mmol) in THF (5.0 mL) at 0 °C was added NaH (48.0 mg, 60% dispersion in mineral oil, 1.20 mmol). The reaction mixture was allowed to warm to ambient temperature and was stirred until gas evolution was visibly complete. To this suspension was added sequentially 15-crown-5 (20.0  $\mu$ L, 0.101 mmol), tetrabutylammonium iodide (0.369 g, 1.00 mmol), and cinnamyl bromide (0.198 g, 1.00 mmol). The resulting mixture was stirred at ambient temperature for 20 h. The reaction was quenched with sat. aq.  $\text{NH}_4\text{Cl}$  (10 mL). The layers were separated, and the aqueous layer was extracted with  $\text{Et}_2\text{O}$  (3 x 10 mL). The combined organic layers were washed with brine (30 mL), then dried over  $\text{MgSO}_4$ . The volatile materials were removed by rotary evaporation and the resulting residue was purified by flash chromatography (100% hexanes  $\rightarrow$  1:1 hexanes/ $\text{CH}_2\text{Cl}_2$  eluent), affording enyne **2-3** (0.201 g, 66% yield,  $R_f = 0.62$  in 1:1 hexanes/ $\text{CH}_2\text{Cl}_2$ , stained blue with *p*-anisaldehyde) as a colorless oil.

**Enyne 2-3:**  $^1\text{H}$  NMR (400 MHz;  $\text{CDCl}_3$ ):  $\delta$  7.45-7.43 (m, 2H), 7.40-7.38 (m, 2H), 7.30 (dd,  $J = 8.5, 5.3$  Hz, 5H), 7.24-7.20 (m, 1H), 6.64 (d,  $J = 15.9$  Hz, 1H), 6.36 (dt,  $J = 15.9, 5.9$  Hz, 1H), 4.33 (dd,  $J = 6.0, 1.5$  Hz, 2H), 2.19-2.01 (m, 4H), 1.89-1.76 (m, 4H);  $^{13}\text{C}$  NMR (100 MHz;  $\text{CDCl}_3$ ):  $\delta$  137.2, 131.9, 131.8, 128.6, 128.4, 128.3, 127.6, 127.1, 126.6, 123.2, 91.0, 85.2, 81.1, 66.0, 39.9, 23.6; IR (film) 2965, 1598, 1445, 1048  $\text{cm}^{-1}$ ; HRMS (ESI+)  $m/z$  calc'd for  $(\text{M} + \text{H})^+$  [ $\text{C}_{22}\text{H}_{22}\text{O} + \text{H}$ ] $^+$ : 303.1743, found 303.1743.



**Enyne 2-66.** To a solution of tertiary propargyl alcohol **2-65** (0.140 g, 0.750 mmol) in THF (3.8 mL) at 0 °C was added NaH (36.0 mg, 60% dispersion in mineral oil, 0.900 mmol). The reaction mixture was allowed to warm to ambient temperature and was stirred until gas evolution was visibly complete. To this suspension was added sequentially 15-crown-5 (15.0  $\mu$ L, 75.8  $\mu$ mol), tetrabutylammonium iodide (0.420 g, 1.14 mmol), and *p*-bromocinnamyl bromide (0.207 g, 0.750 mmol). The resulting mixture was stirred at ambient temperature for 14 h. The reaction was quenched with sat. aq. NH<sub>4</sub>Cl (10 mL). The layers were separated, and the aqueous layer was extracted with Et<sub>2</sub>O (3 x 10 mL). The combined organic layers were washed with brine (30 mL), then dried over MgSO<sub>4</sub>. The volatile materials were removed by rotary evaporation and the resulting residue was purified by flash chromatography (100% hexanes  $\rightarrow$  1:1 hexanes/CH<sub>2</sub>Cl<sub>2</sub> eluent), affording enyne **2-66** (0.169 g, 59% yield, R<sub>f</sub> = 0.71 in 4:1 hexanes/EtOAc, stained blue with *p*-anisaldehyde) as a colorless oil.

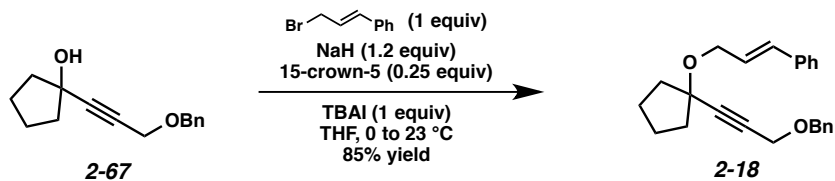
**Enyne 2-66:** <sup>1</sup>H NMR (400 MHz; CDCl<sub>3</sub>):  $\delta$  7.44-7.41 (m, 4H), 7.31 (t, *J* = 3.2 Hz, 3H), 7.24 (d, *J* = 8.5 Hz, 2H), 6.58 (d, *J* = 15.8 Hz, 1H), 6.35 (dt, *J* = 15.8, 5.9 Hz, 1H), 4.31 (dd, *J* = 5.8, 1.2 Hz, 2H), 2.17-1.99 (m, 4H), 1.85-1.76 (m, 4H); <sup>13</sup>C NMR (100 MHz; CDCl<sub>3</sub>):  $\delta$  136.1, 131.8, 131.7, 128.4, 128.3, 128.1, 128.0, 98.8, 77.4, 77.0, 69.9, 39.9, 23.6; IR (film) 2965, 1488, 1071 cm<sup>-1</sup>; HRMS (ESI+) *m/z* calc'd for (M + H)<sup>+</sup> [C<sub>22</sub>H<sub>21</sub>BrO + H]<sup>+</sup>: 381.0849, found 381.0844.



**Enyne 2-68.** To a solution of tertiary propargyl alcohol **2-67** (0.150 g, 0.652 mmol) in THF (3.3 mL) at 0 °C was added NaH (31.2 mg, 60% dispersion in mineral oil, 0.780 mmol). The reaction mixture was allowed to warm to ambient temperature and was stirred until gas evolution was visibly complete. To this suspension was added sequentially 15-crown-5 (32.0  $\mu$ L, 0.163 mmol), tetrabutylammonium iodide

(0.240 g, 0.650 mmol), and methallyl chloride (64.2  $\mu$ L, 0.650 mmol). The resulting mixture was stirred at ambient temperature for 22 h. The reaction was quenched with sat. aq.  $\text{NH}_4\text{Cl}$  (10 mL). The layers were separated, and the aqueous layer was extracted with  $\text{Et}_2\text{O}$  (3 x 10 mL). The combined organic layers were washed with brine (30 mL), then dried over  $\text{MgSO}_4$ . The volatile materials were removed by rotary evaporation and the resulting residue was purified by flash chromatography (100% hexanes  $\rightarrow$  10:1 hexanes/EtOAc eluent), affording enyne **2-68** (38.3 mg, 21% yield,  $R_f = 0.81$  in 3:1 hexanes/EtOAc, stained blue with *p*-anisaldehyde) as a colorless oil.

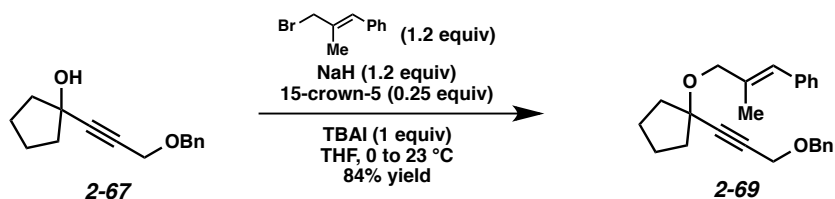
**Enyne 2-68:**  $^1\text{H}$  NMR (400 MHz;  $\text{CDCl}_3$ ):  $\delta$  7.36 (d,  $J = 4.4$  Hz, 4H), 7.31 (td,  $J = 6.6, 3.7$  Hz, 1H), 5.00 (s, 1H), 4.86 (s, 1H), 4.61 (s, 2H), 4.23 (s, 2H), 3.97 (s, 2H), 2.06 (td,  $J = 10.8, 4.4$  Hz, 2H), 1.95-1.88 (m, 2H), 1.81-1.70 (m, 7H);  $^{13}\text{C}$  NMR (100 MHz;  $\text{CDCl}_3$ ):  $\delta$  143.0, 137.6, 128.6, 128.2, 128.0, 111.5, 88.5, 80.6, 80.5, 71.5, 68.9, 57.6, 39.7, 23.5, 20.0; IR (film) 2969, 2856, 1496, 1091  $\text{cm}^{-1}$ ; HRMS (ESI+)  $m/z$  calc'd for  $(\text{M} + \text{H})^+ [\text{C}_{19}\text{H}_{24}\text{O}_2 + \text{H}]^+$ : 285.1849, found 285.1851.



**Enyne 2-18.** To a solution of tertiary propargyl alcohol **2-67** (0.172 g, 0.749 mmol) in THF (3.8 mL) at 0  $^\circ\text{C}$  was added NaH (36.0 mg, 60% dispersion in mineral oil, 0.900 mmol). The reaction mixture was allowed to warm to ambient temperature and was stirred until gas evolution was visibly complete. To this suspension was added sequentially 15-crown-5 (37.6  $\mu$ L, 0.190 mmol), tetrabutylammonium iodide (0.280 g, 0.758 mmol), and cinnamyl bromide (0.147 g, 0.746 mmol). The resulting mixture was stirred at ambient temperature for 22 h. The reaction was quenched with sat. aq.  $\text{NH}_4\text{Cl}$  (10 mL). The layers were separated, and the aqueous layer was extracted with  $\text{Et}_2\text{O}$  (3 x 10 mL). The combined organic layers were washed with brine (30 mL), then dried over  $\text{MgSO}_4$ . The volatile materials were removed by rotary

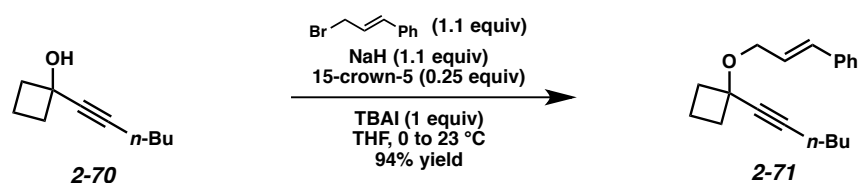
evaporation and the resulting residue was purified by flash chromatography (100% hexanes → 9:1 hexanes/EtOAc eluent), affording enyne **2-18** (0.221 g, 85% yield,  $R_f = 0.77$  (3:1 hexanes/EtOAc), stained blue with *p*-anisaldehyde) as a colorless oil.

**Enyne 2-18:**  $^1\text{H-NMR}$  (400 MHz;  $\text{CDCl}_3$ ):  $\delta$  7.39-7.34 (m, 5H), 7.31 (t,  $J = 7.5$  Hz, 3H), 7.23 (dd,  $J = 8.3, 6.1$  Hz, 2H), 6.63 (d,  $J = 15.9$  Hz, 1H), 6.33 (dt,  $J = 15.9, 5.9$  Hz, 1H), 4.62 (s, 2H), 4.27-4.26 (m, 4H), 2.12-2.05 (m, 2H), 2.00-1.92 (m, 2H), 1.84-1.72 (m, 4H);  $^{13}\text{C NMR}$  (100 MHz;  $\text{CDCl}_3$ ):  $\delta$  137.6, 137.1, 131.8, 128.6, 128.2, 128.0, 127.6, 126.9, 126.6, 88.4, 80.9, 80.6, 71.6, 65.9, 57.7, 39.8, 23.5; IR (film) 2963, 2856, 1496, 1073  $\text{cm}^{-1}$ ; HRMS (ESI+)  $m/z$  calc'd for  $(\text{M} + \text{H})^+ [\text{C}_{24}\text{H}_{26}\text{O}_2 + \text{H}]^+$ : 347.2006, found 347.2011.



**Enyne 2-69.** To a solution of tertiary propargyl alcohol **2-67** (0.110 g, 0.475 mmol) in THF (2.4 mL) at 0 °C was added NaH (23.0 g, 60% dispersion in mineral oil, 0.571 mmol). The reaction mixture was allowed to warm to ambient temperature and was stirred until gas evolution was visibly complete. To this suspension was added sequentially 15-crown-5 (23.8  $\mu\text{L}$ , 0.120 mmol), tetrabutylammonium iodide (0.175 g, 0.475 mmol), and 3-bromo-2-methyl-1-phenyl-1-propene (0.101 g, 0.475 mmol). The resulting mixture was stirred at ambient temperature for 15 h. The reaction was quenched with sat. aq.  $\text{NH}_4\text{Cl}$  (10 mL). The layers were separated, and the aqueous layer was extracted with  $\text{Et}_2\text{O}$  (3 x 10 mL). The combined organic layers were washed with brine (30 mL), then dried over  $\text{MgSO}_4$ . The volatile materials were removed by rotary evaporation and the resulting residue was purified by flash chromatography (100% hexanes → 1:1 hexanes/ $\text{CH}_2\text{Cl}_2$  eluent), affording enyne **2-69** (0.144 g, 84% yield,  $R_f = 0.55$  in 1:1 hexanes/ $\text{CH}_2\text{Cl}_2$ , stained blue with *p*-anisaldehyde) as a colorless oil.

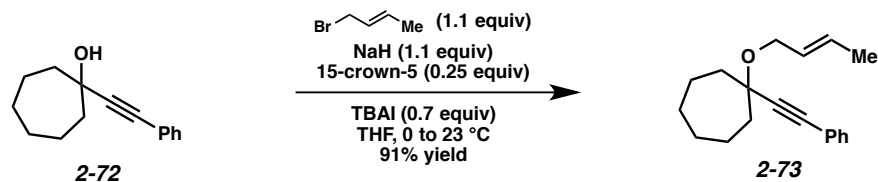
**Enyne 2-69:**  $^1\text{H}$  NMR (400 MHz;  $\text{CDCl}_3$ ):  $\delta$  7.35 (dd,  $J = 6.0, 4.0$  Hz, 3H), 7.30 (dt,  $J = 12.7, 6.1$  Hz, 5H), 7.22-7.18 (m, 1H), 6.54 (s, 1H), 4.62 (s, 2H), 4.25 (s, 2H), 4.12 (s, 2H), 2.14-1.92 (m, 4H), 1.92 (s, 3H), 1.84-1.72 (m, 4H);  $^{13}\text{C}$  NMR (100 MHz;  $\text{CDCl}_3$ ):  $\delta$  138.0, 137.6, 135.9, 129.1, 128.6, 128.3, 128.2, 128.0, 126.4, 126.3, 88.5, 80.8, 80.6, 71.6, 71.2, 57.6, 39.8, 23.5, 15.9; IR (film) 2964, 2855, 1683, 1493, 1089  $\text{cm}^{-1}$ ; HRMS (ESI+)  $m/z$  calc'd for  $(\text{M} + \text{H})^+$  [ $\text{C}_{25}\text{H}_{28}\text{O}_2 + \text{H}$ ] $^+$ : 361.2162, found 361.2162.



**Enyne 2-71.** To a solution of tertiary propargyl alcohol **2-70** (0.378 g, 2.48 mmol) in THF (10 mL) at 0  $^\circ\text{C}$  was added NaH (0.111 g, 60% dispersion in mineral oil, 2.75 mmol). The reaction mixture was allowed to warm to ambient temperature and was stirred until gas evolution was visibly complete. To this suspension was added sequentially 15-crown-5 (0.120 mL, 0.625 mmol), tetrabutylammonium iodide (0.646 g, 1.75 mmol), and cinnamyl bromide (0.542 g, 2.75 mmol). The resulting mixture was stirred at ambient temperature for 19 h. The reaction was quenched with sat. aq.  $\text{NH}_4\text{Cl}$  (15 mL). The layers were separated, and the aqueous layer was extracted with  $\text{Et}_2\text{O}$  (3 x 10 mL). The combined organic layers were washed with brine (20 mL), then dried over  $\text{MgSO}_4$ . The volatile materials were removed by rotary evaporation and the resulting residue was purified by flash chromatography (100% hexanes  $\rightarrow$  9:1 hexanes/EtOAc eluent), affording enyne **2-71** (0.629 g, 94% yield,  $R_f = 0.58$  in 9:1 hexanes/EtOAc, stained blue with *p*-anisaldehyde) as a colorless oil.

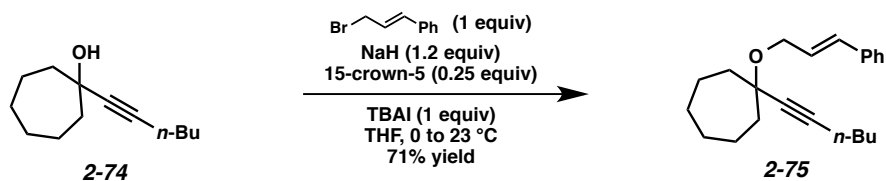
**Enyne 2-71:**  $^1\text{H}$  NMR (400 MHz;  $\text{CDCl}_3$ ):  $\delta$  7.40-7.38 (m, 2H), 7.30 (t,  $J = 7.6$  Hz, 2H), 7.24-7.20 (m, 1H), 6.63 (d,  $J = 15.9$  Hz, 1H), 6.33 (dt,  $J = 15.9, 6.1$  Hz, 1H), 4.17 (dd,  $J = 6.1, 1.2$  Hz, 2H), 2.35-2.24 (m, 6H), 1.93-1.78 (m, 2H), 1.57-1.40 (m, 4H), 0.93 (t,  $J = 7.2$  Hz, 3H);  $^{13}\text{C}$  NMR (100 MHz;  $\text{CDCl}_3$ ):  $\delta$  137.1, 132.2, 128.6, 127.6, 126.7, 126.6, 85.8, 81.6, 73.1, 65.3, 36.5, 31.1, 22.1, 18.7, 13.8, 13.5; IR

(film) 2935, 2861, 1450, 1128, 735  $\text{cm}^{-1}$ ; HRMS (ESI+)  $m/z$  calc'd for  $(M + H)^+$   $[\text{C}_{19}\text{H}_{24}\text{O} + \text{H}]^+$ : 269.1900, found 269.1901.



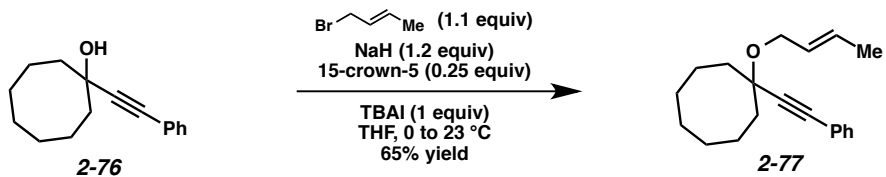
**Enyne 2-73.** To a solution of tertiary propargyl alcohol **2-72** (2.14 g, 10.0 mmol) in THF (40 mL) at 0 °C was added NaH (0.442 g, 60% dispersion in mineral oil, 11.1 mmol). The reaction mixture was allowed to warm to ambient temperature and was stirred until gas evolution was visibly complete. To this suspension was added sequentially 15-crown-5 (0.495 mL, 2.50 mmol), tetrabutylammonium iodide (2.58 g, 6.98 mmol), and crotyl bromide (1.13 mL, 11.0 mmol). The resulting mixture was stirred at ambient temperature for 19 h. The reaction was quenched with sat. aq.  $\text{NH}_4\text{Cl}$  (50 mL). The layers were separated, and the aqueous layer was extracted with  $\text{Et}_2\text{O}$  (3 x 40 mL). The combined organic layers were washed with brine (100 mL), then dried over  $\text{MgSO}_4$ . The volatile materials were removed by rotary evaporation and the resulting residue was purified by flash chromatography (100% hexanes  $\rightarrow$  9:1 hexanes/ $\text{EtOAc}$  eluent), affording enyne **2-73** (2.44 g, 91% yield,  $R_f = 0.75$  in 9:1 hexanes/ $\text{EtOAc}$ , stained blue with *p*-anisaldehyde) as a colorless oil.

**Enyne 2-73:**  $^1\text{H}$  NMR (400 MHz;  $\text{CDCl}_3$ ):  $\delta$  7.44-7.42 (m, 2H), 7.30 (t,  $J = 3.3$  Hz, 3H), 5.79-5.60 (m, 2H), 4.10 (d,  $J = 6.0$  Hz, 2H), 2.09 (dd,  $J = 13.9, 8.0$  Hz, 2H), 1.98-1.92 (m, 2H), 1.71 (d,  $J = 6.2$  Hz, 3H), 1.69-1.56 (m, 8H);  $^{13}\text{C}$  NMR (100 MHz;  $\text{CDCl}_3$ ):  $\delta$  131.8, 128.8, 128.6, 128.4, 128.2, 123.3, 98.9, 92.0, 77.5, 65.0, 40.3, 28.5, 22.3, 18.0; IR (film) 2929, 2856, 1444, 1041, 755  $\text{cm}^{-1}$ ; HRMS (ESI+)  $m/z$  calc'd for  $(M + H)^+$   $[\text{C}_{19}\text{H}_{24}\text{O} + \text{H}]^+$ : 269.1900, found 269.1900.



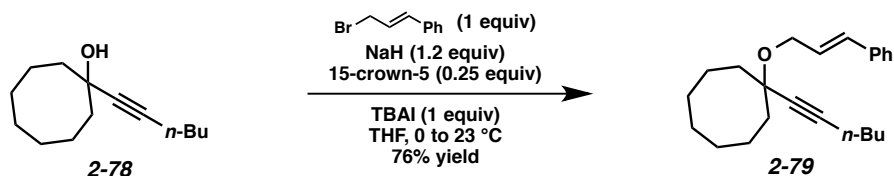
**Enyne 2-75.** To a solution of tertiary propargyl alcohol **2-74** (0.505 g, 2.21 mmol) in THF (11 mL) at 0 °C was added NaH (0.104 g, 60% dispersion in mineral oil, 2.60 mmol). The reaction mixture was allowed to warm to ambient temperature and was stirred until gas evolution was visibly complete. To this suspension was added sequentially 15-crown-5 (43.5  $\mu$ L, 0.220 mmol), tetrabutylammonium iodide (0.815 g, 2.21 mmol), and crotyl bromide (0.235 mL, 2.28 mmol). The resulting mixture was stirred at ambient temperature for 18 h. The reaction was quenched with sat. aq.  $\text{NH}_4\text{Cl}$  (15 mL). The layers were separated, and the aqueous layer was extracted with  $\text{Et}_2\text{O}$  (3 x 10 mL). The combined organic layers were washed with brine (30 mL), then dried over  $\text{MgSO}_4$ . The volatile materials were removed by rotary evaporation and the resulting residue was purified by flash chromatography (hexanes  $\rightarrow$  4:1 hexanes/ $\text{Et}_2\text{O}$  eluent), affording enyne **2-75** (0.406 g, 65% yield,  $R_f = 0.79$  in 4:1 hexanes/ $\text{EtOAc}$ , stained blue with *p*-anisaldehyde) as a colorless oil.

**Enyne 2-75:**  $^1\text{H}$  NMR (400 MHz;  $\text{CDCl}_3$ ):  $\delta$  7.44-7.41 (m, 2H), 7.30 (t,  $J = 3.2$  Hz, 3H), 5.78-5.60 (m, 2H), 4.08 (d,  $J = 6.0$  Hz, 2H), 2.10-1.95 (m, 4H), 1.71 (dd,  $J = 6.2, 0.9$  Hz, 3H), 1.68-1.56 (m, 10H);  $^{13}\text{C}$  NMR (100 MHz;  $\text{CDCl}_3$ ):  $\delta$  131.8, 128.7, 128.6, 128.4, 128.2, 123.3, 91.9, 85.2, 77.3, 64.8, 35.1, 28.2, 24.7, 21.9, 18.0; IR (film) 2923, 2855, 1444, 1038, 755  $\text{cm}^{-1}$ ; HRMS (ESI+)  $m/z$  calc'd for  $(\text{M} + \text{H})^+$  [ $\text{C}_{20}\text{H}_{26}\text{O} + \text{H}$ ] $^+$ : 283.2056, found 283.2053.



**Enyne 2-77.** To a solution of tertiary propargyl alcohol **2-76** (0.194 g, 0.999 mmol) in THF (5.0 mL) at 0 °C was added NaH (48.0 mg, 60% dispersion in mineral oil, 1.20 mmol). The reaction mixture was allowed to warm to ambient temperature and was stirred until gas evolution was visibly complete. To this suspension was added sequentially 15-crown-5 (49.5  $\mu$ L, 0.250 mmol), tetrabutylammonium iodide (0.369 g, 1.00 mmol), and cinnamyl bromide (0.197 g, 1.00 mmol). The resulting mixture was stirred at ambient temperature for 14 h. The reaction was quenched with sat. aq.  $\text{NH}_4\text{Cl}$  (10 mL). The layers were separated, and the aqueous layer was extracted with  $\text{Et}_2\text{O}$  (3 x 10 mL). The combined organic layers were washed with brine (20 mL), then dried over  $\text{MgSO}_4$ . The volatile materials were removed by rotary evaporation and the resulting residue was purified by flash chromatography (100% hexanes  $\rightarrow$  1:1 hexanes/ $\text{CH}_2\text{Cl}_2$  eluent), affording enyne **2-77** (0.220 g, 71% yield,  $R_f = 0.82$  in 2:1  $\text{CH}_2\text{Cl}_2$ /hexanes, stained blue with *p*-anisaldehyde) as a yellow oil.

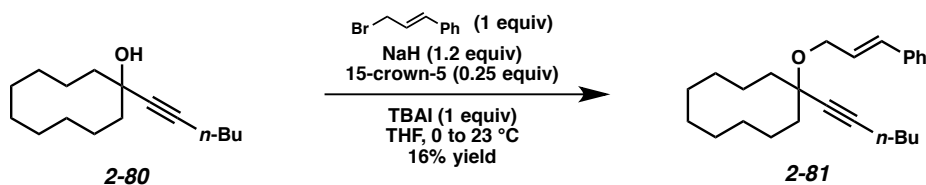
**Enyne 2-77:**  $^1\text{H}$  NMR (400 MHz;  $\text{CDCl}_3$ ):  $\delta$  7.38 (d,  $J = 7.5$  Hz, 2H), 7.30 (t,  $J = 7.6$  Hz, 2H), 7.21 (dd,  $J = 8.2, 6.3$  Hz, 1H), 6.61 (d,  $J = 16.0$  Hz, 1H), 6.33 (dt,  $J = 15.8, 5.9$  Hz, 1H), 4.25 (dd,  $J = 5.9, 1.1$  Hz, 2H), 2.24 (t,  $J = 6.9$  Hz, 2H), 2.01-1.85 (m, 4H), 1.70-1.39 (m, 12H), 0.92 (t,  $J = 7.2$  Hz, 3H);  $^{13}\text{C}$  NMR (100 MHz;  $\text{CDCl}_3$ ):  $\delta$  137.3, 131.3, 128.6, 127.7, 127.5, 126.6, 86.0, 82.6, 77.6, 64.6, 40.6, 31.1, 28.5, 22.2, 22.1, 18.6, 13.8; IR (film) 2932, 2859, 1496, 1058, 964  $\text{cm}^{-1}$ ; HRMS (ESI+)  $m/z$  calc'd for  $(\text{M} + \text{H})^+$  [ $\text{C}_{22}\text{H}_{30}\text{O} + \text{H}$ ] $^+$ : 311.2369, found 311.2362.



**Enyne 2-79.** To a solution of tertiary propargyl alcohol **2-78** (0.209 g, 1.00 mmol) in THF (5.0 mL) at 0 °C was added NaH (48.0 mg, 60% dispersion in mineral oil, 1.20 mmol). The reaction mixture was allowed to warm to ambient temperature and was stirred until gas evolution was visibly complete. To this

suspension was added sequentially 15-crown-5 (49.5  $\mu\text{L}$ , 0.250 mmol), tetrabutylammonium iodide (0.369 g, 1.00 mmol), and cinnamyl bromide (0.197 g, 1.00 mmol). The resulting mixture was stirred at ambient temperature for 14 h. The reaction was quenched with sat. aq.  $\text{NH}_4\text{Cl}$  (10 mL). The layers were separated, and the aqueous layer was extracted with  $\text{Et}_2\text{O}$  (3 x 10 mL). The combined organic layers were washed with brine (20 mL), then dried over  $\text{MgSO}_4$ . The volatile materials were removed by rotary evaporation and the resulting residue was purified by flash chromatography (100% hexanes  $\rightarrow$  1:1 hexanes/ $\text{CH}_2\text{Cl}_2$  eluent), affording enyne **2-79** (0.247 g, 76% yield,  $R_f = 0.86$  in 2:1  $\text{CH}_2\text{Cl}_2$ /hexanes, stained blue with *p*-anisaldehyde) as a yellow oil.

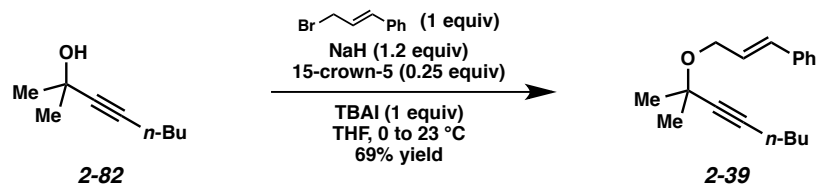
**Enyne 2-79:**  $^1\text{H}$  NMR (400 MHz;  $\text{CDCl}_3$ ):  $\delta$  7.39-7.37 (m, 2H), 7.31-7.27 (m, 2H), 7.23-7.19 (m, 1H), 6.60 (d,  $J = 15.9$  Hz, 1H), 6.32 (dt,  $J = 15.9, 5.9$  Hz, 1H), 4.23 (dd,  $J = 5.9, 1.5$  Hz, 2H), 2.23 (t,  $J = 6.9$  Hz, 2H), 2.03-1.84 (m, 4H), 1.69-1.40 (m, 14H), 0.92 (t,  $J = 7.2$  Hz, 3H);  $^{13}\text{C}$  NMR (100 MHz;  $\text{CDCl}_3$ ):  $\delta$  137.3, 131.3, 128.6, 127.4, 126.6, 98.9, 85.7, 82.4, 64.4, 35.3, 31.1, 28.3, 24.7, 22.1, 21.9, 18.5, 13.8; IR (film) 2927, 2857, 1496, 1111, 963  $\text{cm}^{-1}$ ; HRMS (ESI+)  $m/z$  calc'd for  $(\text{M} + \text{H})^+$  [ $\text{C}_{23}\text{H}_{32}\text{O} + \text{H}$ ] $^+$ : 325.2526, found 325.2517.



**Enyne 2-81.** To a solution of tertiary propargyl alcohol **2-80** (0.298 g, 1.26 mmol) in THF (6.3 mL) at 0 °C was added NaH (60.4 mg, 60% dispersion in mineral oil, 1.51 mmol). The reaction mixture was allowed to warm to ambient temperature and was stirred until gas evolution was visibly complete. To this suspension was added sequentially 15-crown-5 (63.3  $\mu\text{L}$ , 0.320 mmol), tetrabutylammonium iodide (0.465 g, 1.26 mmol), and cinnamyl bromide (0.249 g, 1.26 mmol). The resulting mixture was stirred at ambient temperature for 14 h. The reaction was quenched with sat. aq.  $\text{NH}_4\text{Cl}$  (15 mL). The layers were

separated, and the aqueous layer was extracted with Et<sub>2</sub>O (3 x 15 mL). The combined organic layers were washed with brine (30 mL), then dried over MgSO<sub>4</sub>. The volatile materials were removed by rotary evaporation and the resulting residue was purified by flash chromatography (10:1 hexanes/CH<sub>2</sub>Cl<sub>2</sub> → 1:1 hexanes/CH<sub>2</sub>Cl<sub>2</sub> eluent), affording enyne **2-81** (72.7 mg, 16% yield, R<sub>f</sub> = 0.89 in 2:1 CH<sub>2</sub>Cl<sub>2</sub>/hexanes, stained blue with *p*-anisaldehyde) as a yellow oil.

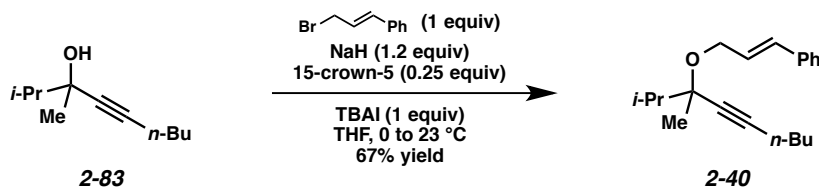
**Enyne 2-81:** <sup>1</sup>H NMR (400 MHz; CDCl<sub>3</sub>): δ 7.39-7.37 (m, 2H), 7.31-7.27 (m, 2H), 7.23-7.19 (m, 1H), 6.60 (d, *J* = 15.9 Hz, 1H), 6.33 (dt, *J* = 15.9, 5.9 Hz, 1H), 4.23 (dd, *J* = 5.9, 1.4 Hz, 2H), 2.23 (t, *J* = 6.9 Hz, 2H), 2.04-1.97 (m, 2H), 1.82 (dt, *J* = 14.2, 6.9 Hz, 2H), 1.71-1.38 (m, 18H), 0.92 (t, *J* = 7.2 Hz, 3H); <sup>13</sup>C NMR (100 MHz; CDCl<sub>3</sub>): δ 137.3, 131.5, 128.6, 127.5, 126.6, 86.1, 82.0, 77.7, 64.3, 33.3, 31.2, 26.5, 26.0, 23.9, 22.1, 21.4, 18.5, 13.8; IR (film) 2924, 1446, 1054, 962 cm<sup>-1</sup>; HRMS (ESI+) *m/z* calc'd for (M + H)<sup>+</sup> [C<sub>25</sub>H<sub>36</sub>O + H]<sup>+</sup>: 353.2839, found 353.2828.



**Enyne 2-39.** To a solution of tertiary propargyl alcohol **2-82** (0.140 g, 0.998 mmol) in THF (5.0 mL) at 0 °C was added NaH (48.0 mg, 60% dispersion in mineral oil, 1.20 mmol). The reaction mixture was allowed to warm to ambient temperature and was stirred until gas evolution was visibly complete. To this suspension was added sequentially 15-crown-5 (49.5 μL, 0.250 mmol), tetrabutylammonium iodide (0.369 g, 1.00 mmol), and cinnamyl bromide (0.197 g, 1.00 mmol). The resulting mixture was stirred at ambient temperature for 19 h. The reaction was quenched with sat. aq. NH<sub>4</sub>Cl (10 mL). The layers were separated, and the aqueous layer was extracted with Et<sub>2</sub>O (3 x 10 mL). The combined organic layers were washed with brine (25 mL), then dried over MgSO<sub>4</sub>. The volatile materials were removed by rotary evaporation and the resulting residue was purified by flash chromatography (hexanes → 1:1

hexanes/CH<sub>2</sub>Cl<sub>2</sub> → 1:1:1 hexanes/CH<sub>2</sub>Cl<sub>2</sub>/EtOAc eluent), affording enyne **2-39** (0.183 g, 69% yield, R<sub>f</sub> = 0.71 in 2:1 CH<sub>2</sub>Cl<sub>2</sub>/hexanes, stained blue with *p*-anisaldehyde) as a colorless oil.

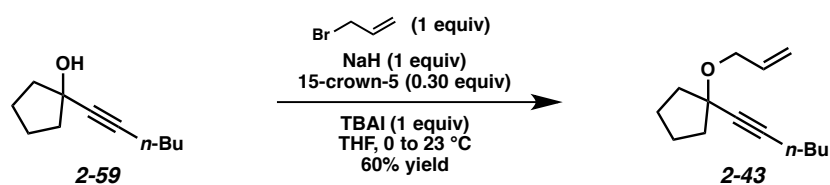
**Enyne 2-39:** <sup>1</sup>H NMR (400 MHz; CDCl<sub>3</sub>): δ 7.40-7.38 (m, 2H), 7.30 (dd, *J* = 8.2, 6.8 Hz, 2H), 7.24-7.22 (m, 1H), 6.62 (d, *J* = 15.9 Hz, 1H), 6.33 (dt, *J* = 15.9, 6.0 Hz, 1H), 4.26 (dd, *J* = 6.0, 1.5 Hz, 2H), 2.22 (t, *J* = 7.0 Hz, 2H), 1.49 (s, 6H), 1.54-1.39 (m, 10H), 0.92 (t, *J* = 7.2 Hz, 3H); <sup>13</sup>C NMR (100 MHz; CDCl<sub>3</sub>): δ 137.2, 131.7, 128.6, 127.5, 127.3, 126.6, 84.9, 82.4, 70.7, 65.1, 31.0, 29.4, 22.1, 18.5, 13.8; IR (film) 2932, 2862, 1449, 1185 cm<sup>-1</sup>; HRMS (ESI+) *m/z* calc'd for (M + H)<sup>+</sup> [C<sub>18</sub>H<sub>24</sub>O + H]<sup>+</sup>: 257.1900, found 257.1888.



**Enyne 2-40.** To a solution of tertiary propargyl alcohol **2-83** (0.706 g, 4.20 mmol) in THF (21 mL) at 0 °C was added NaH (0.201 g, 60% dispersion in mineral oil, 5.04 mmol). The reaction mixture was allowed to warm to ambient temperature and was stirred until gas evolution was visibly complete. To this suspension was added sequentially 15-crown-5 (0.208 mL, 1.05 mmol), tetrabutylammonium iodide (1.55 g, 4.20 mmol), and cinnamyl bromide (0.827 g, 4.20 mmol). The resulting mixture was stirred at ambient temperature for 16.5 h. The reaction was quenched with sat. aq. NH<sub>4</sub>Cl (25 mL). The layers were separated, and the aqueous layer was extracted with Et<sub>2</sub>O (3 x 20 mL). The combined organic layers were washed with brine (50 mL), then dried over MgSO<sub>4</sub>. The volatile materials were removed by rotary evaporation and the resulting residue was purified by flash chromatography (100% hexanes → 1:1 hexanes/CH<sub>2</sub>Cl<sub>2</sub> eluent), affording enyne **2-40** (0.800 g, 67% yield, R<sub>f</sub> = 0.86 in 2:1 hexanes/CH<sub>2</sub>Cl<sub>2</sub>, stained blue with *p*-anisaldehyde) as a yellow oil.

**Enyne 2-40:**  $^1\text{H}$  NMR (400 MHz;  $\text{CDCl}_3$ ):  $\delta$  7.38 (dd,  $J = 8.3, 1.1$  Hz, 2H), 7.30 (dd,  $J = 8.2, 6.8$  Hz, 2H), 7.23-7.19 (m, 1H), 6.61 (d,  $J = 15.9$  Hz, 1H), 6.33 (dt,  $J = 15.9, 5.8$  Hz, 1H), 4.32-4.19 (m, 2H), 2.24 (t,  $J = 6.9$  Hz, 2H), 1.93 (dt,  $J = 13.5, 6.8$  Hz, 1H), 1.55-1.40 (m, 4H), 1.36 (s, 3H), 1.04 (d,  $J = 6.8$  Hz, 3H), 0.98 (d,  $J = 6.8$  Hz, 3H), 0.92 (t,  $J = 7.2$  Hz, 3H);  $^{13}\text{C}$  NMR (100 MHz;  $\text{CDCl}_3$ ):  $\delta$  137.3, 131.1, 128.6, 127.7, 127.4, 126.6, 86.5, 80.8, 77.4, 64.6, 37.5, 31.1, 23.2, 22.1, 18.5, 18.3, 17.4, 13.8; IR (film) 2961, 2933, 1496, 1205, 964  $\text{cm}^{-1}$ ; HRMS (ESI+)  $m/z$  calc'd for  $(\text{M} + \text{H})^+$  [ $\text{C}_{20}\text{H}_{28}\text{O} + \text{H}$ ] $^+$ : 285.2213, found 285.2205.

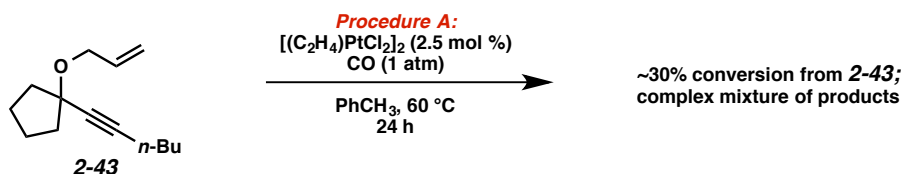
#### 2.7.4 Unsuccessful Substrates



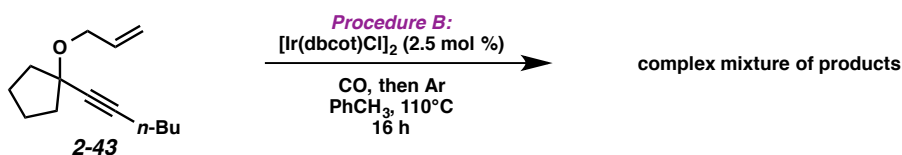
**Enyne 2-43.** To a solution of tertiary propargyl alcohol **2-59** (0.168 g, 1.00 mmol) in THF (5.0 mL) at 0 °C was added NaH (40.0 mg, 60% dispersion in mineral oil, 1.00 mmol). The reaction mixture was allowed to warm to ambient temperature and was stirred until gas evolution was visibly complete. To this suspension was added sequentially 15-crown-5 (60.0  $\mu\text{L}$ , 0.300 mmol), tetrabutylammonium iodide (0.369 g, 1.00 mmol), and allyl bromide (86.0  $\mu\text{L}$ , 1.00 mmol). The resulting mixture was stirred at ambient temperature for 20 h. The reaction was quenched with sat. aq.  $\text{NH}_4\text{Cl}$  (10 mL). The layers were separated, and the aqueous layer was extracted with  $\text{Et}_2\text{O}$  (3 x 10 mL). The combined organic layers were washed with brine (25 mL), then dried over  $\text{MgSO}_4$ . The volatile materials were removed by rotary evaporation and the resulting residue was purified by flash chromatography (20:1 hexanes/ $\text{CH}_2\text{Cl}_2 \rightarrow$  4:1 hexanes/ $\text{CH}_2\text{Cl}_2$  eluent), affording enyne **2-43** (0.124, 60% yield,  $R_f = 0.55$  in 1:1 hexanes/ $\text{CH}_2\text{Cl}_2$ ,

stained blue with *p*-anisaldehyde) as a colorless oil. All spectroscopic data were consistent with previously reported values.<sup>3</sup>

#### Attempted Cycloisomerization of Enyne 2-43:

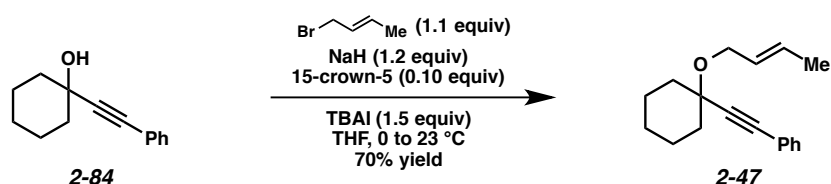


**Procedure A:** To a solution of enyne **2-43** (20.7 mg, 0.100 mmol) in toluene (1.54 mL) in a 2-dram vial under argon was quickly added  $[(C_2H_4)PtCl_2]_2$  (1.5 mg, 0.00250 mmol). CO was bubbled through the solution using a balloon and needle outlet (ca. 30 s). The balloon and outlet were then removed and the solution was stirred at 60 °C for 24 h. The reaction was allowed to cool to ambient temperature and was diluted with an approximately equal amount of hexanes. The mixture was stirred for 15 min, then passed through a small plug of  $Al_2O_3$  (hexanes  $\rightarrow$  1:1 hexanes/EtOAc eluent). The volatile materials were removed by rotary evaporation and the resulting residue was analyzed by  $^1H$  NMR. Enyne **2-43** was partly consumed, but the desired product was not detected.



**Procedure B:** To a solution of enyne **2-43** (12.0 mg, 60.0  $\mu$ mol) in toluene (0.920 mL) in a 16 x 125 mm glass culture tube under argon was quickly added  $[Ir(dbcot)Cl]_2$  (1.3 mg, 1.50  $\mu$ mol). CO was bubbled through the solution using a balloon and needle outlet (ca. 30 s), during which time the solution turned a dark-blue/black color. The balloon was removed and argon was bubbled through the solution in the same

manner. The septum was quickly replaced with a Teflon cap and the solution was stirred at 110 °C for 16 h. The reaction was allowed to cool to ambient temperature and was diluted with an approximately equal amount of hexanes. The mixture was stirred for 15 min, then passed through a small plug of Al<sub>2</sub>O<sub>3</sub> (hexanes → 1:1 hexanes/EtOAc eluent). The volatile materials were removed by rotary evaporation and the resulting residue was analyzed by <sup>1</sup>H NMR. Enyne **2-43** was completely consumed, but the desired product was not detected.

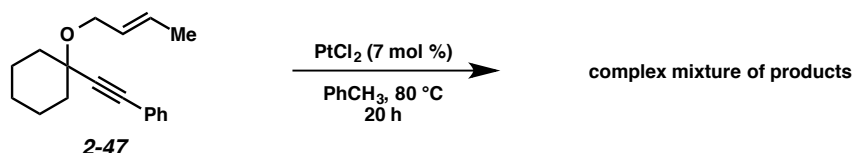


**Enyne 2-47.** To a solution of tertiary propargyl alcohol **2-84** (0.200 g, 0.998 mmol) in THF (5.0 mL) at 0 °C was added NaH (48.0 mg, 60% dispersion in mineral oil, 1.20 mmol). The reaction mixture was allowed to warm to ambient temperature and was stirred until gas evolution was visibly complete. To this suspension was added sequentially 15-crown-5 (0.020 mL, 0.0998 mmol), tetrabutylammonium iodide (0.369 g, 0.998 mmol), and cinnamyl bromide (0.11 mL, 1.10 mmol). The resulting mixture was stirred at ambient temperature for 20 h. The reaction was quenched with sat. aq. NH<sub>4</sub>Cl (10 mL). The layers were separated, and the aqueous layer was extracted with Et<sub>2</sub>O (3 x 10 mL). The combined organic layers were washed with brine (25 mL), then dried over MgSO<sub>4</sub>. The volatile materials were removed by rotary evaporation and the resulting residue was purified by flash chromatography (99:1 hexanes/EtOAc → 20:1 hexanes/EtOAc eluent), affording enyne **2-47** (0.176, 70% yield, R<sub>f</sub> = 0.90 in 3:1 hexanes/EtOAc, visualized by UV) as a pale yellow oil.

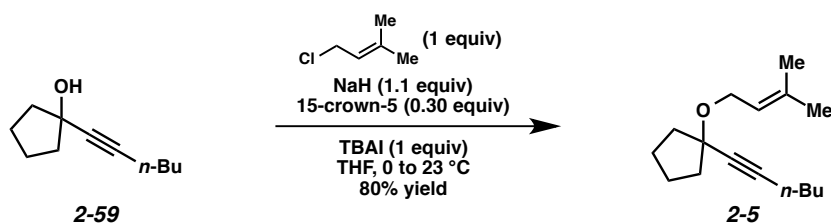
**Enyne 2-47:** <sup>1</sup>H NMR (400 MHz; CDCl<sub>3</sub>): δ 7.45-7.43 (m, 2H), 7.31-7.30 (m, 3H), 5.80-5.72 (m, 1H), 5.69-5.62 (m, 1H), 4.13 (dt, *J* = 6.2, 1.0 Hz, 2H), 2.05-2.00 (m, 2H), 1.71 (dd, *J* = 6.2, 1.2 Hz, 3H), 1.66-1.54 (comp. m, 7H), 1.35-1.25 (m, 1H); <sup>13</sup>C NMR (100 MHz; CDCl<sub>3</sub>): δ 131.7, 128.4, 128.2, 128.1,

123.3, 123.1, 90.7, 86.1, 75.8, 64.3, 37.4, 25.5, 23.0, 17.9; HRMS (ESI+)  $m/z$  calc'd for  $(M + Na)^+$   $[C_{18}H_{22}O + Na]^+$ : 277.1563, found 277.1549.

#### Attempted Cycloisomerization of Enyne 2-47:



To a solution of enyne **2-47** (0.2552 mg, 1.00 mmol) in toluene (17.5 mL) in a 2-dram vial under argon was quickly added  $\text{PtCl}_2$  (18.6 mg, 0.0700 mmol). The reaction mixture was stirred at 80 °C for 20 h. The reaction was allowed to cool to ambient temperature and was diluted with an approximately equal amount of hexanes. The mixture was stirred for 15 min, then passed through a small plug of  $\text{Al}_2\text{O}_3$  (hexanes  $\rightarrow$  1:1 hexanes/EtOAc eluent). The volatile materials were removed by rotary evaporation and the resulting residue was analyzed by  $^1\text{H}$  NMR. Enyne **2-47** was completely consumed, but the majority of the crude product was a complex mixture from which the desired product could not be detected. The reaction was also performed at 60 °C. The same results were obtained.

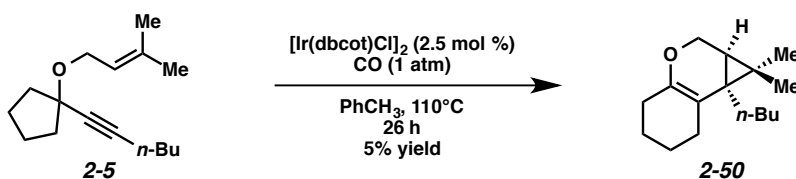


**Enyne 2-5.** To a solution of tertiary propargyl alcohol **2-59** (1.67 g, 10.0 mmol) in THF (50 mL) at 0 °C was added NaH (0.450 g, 60% dispersion in mineral oil, 11.0 mmol). The reaction mixture was allowed to warm to ambient temperature and was stirred until gas evolution was visibly complete. To this

suspension was added sequentially 15-crown-5 (0.60 mL, 3.00 mmol), tetrabutylammonium iodide (3.69 g, 10.0 mmol), and prenyl chloride (1.13 mL, 10.0 mmol). The resulting mixture was stirred at ambient temperature for 20 h. The reaction was quenched with sat. aq. NH<sub>4</sub>Cl (50 mL). The layers were separated, and the aqueous layer was extracted with Et<sub>2</sub>O (3 x 50 mL). The combined organic layers were washed with brine (100 mL), then dried over MgSO<sub>4</sub>. The volatile materials were removed by rotary evaporation and the resulting residue was purified by flash chromatography (99:1 hexanes/CH<sub>2</sub>Cl<sub>2</sub> → 1:1 hexanes/CH<sub>2</sub>Cl<sub>2</sub> eluent), affording enyne **2-5** (1.874 g, 80% yield, R<sub>f</sub> = 0.67 in 1:1 hexanes/CH<sub>2</sub>Cl<sub>2</sub>, stained blue with *p*-anisidine) as a yellow oil.

**Enyne 2-5:** <sup>1</sup>H NMR (400 MHz; CDCl<sub>3</sub>): δ 5.37-5.33 (m, 1H), 4.03 (d, *J* = 7.0 Hz, 2H), 2.22 (t, *J* = 6.9 Hz, 2H), 2.00-1.78 (comp. m, 4H), 1.73 (s, 3H), 1.68 (s, 3H), 1.51-1.31 (comp. m, 8H), 0.91 (t, *J* = 7.2 Hz, 3H); <sup>13</sup>C NMR (100 MHz; CDCl<sub>3</sub>): δ 123.3, 121.7, 85.1, 80.2, 75.8, 61.2, 42.6, 39.7, 30.9, 25.9, 23.2, 21.9, 18.4, 13.6; HRMS (ESI+) *m/z* calc'd for (M + H)<sup>+</sup> [C<sub>16</sub>H<sub>26</sub>O + H]<sup>+</sup>: 235.2056, found 235.2044.

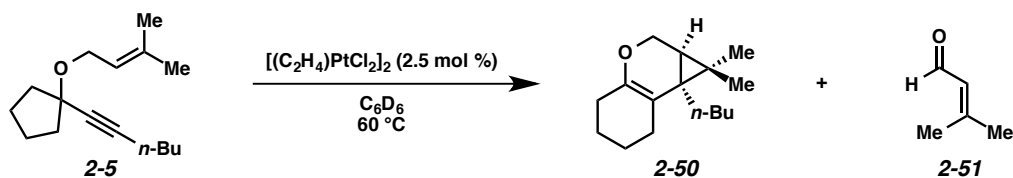
#### Attempted Cycloisomerization of Enyne 2-5:



To a solution of enyne **2-5** (28.5 mg, 0.120 mmol) in toluene (2.60 mL) in a 16 x 125 mm glass culture tube under argon was quickly added [Ir(dbcot)Cl]<sub>2</sub> (2.6 mg, 0.00300 mmol). CO was bubbled through the solution using a balloon and needle outlet (ca. 30 s) and the vessel was sealed. The reaction mixture was stirred at 110 °C for 26 h, then reaction was allowed to cool to ambient temperature and was diluted with an approximately equal amount of hexanes. The mixture was stirred for 15 min, then passed through a small plug of Al<sub>2</sub>O<sub>3</sub> (hexanes → 1:1 hexanes/EtOAc eluent). The volatile materials were removed by

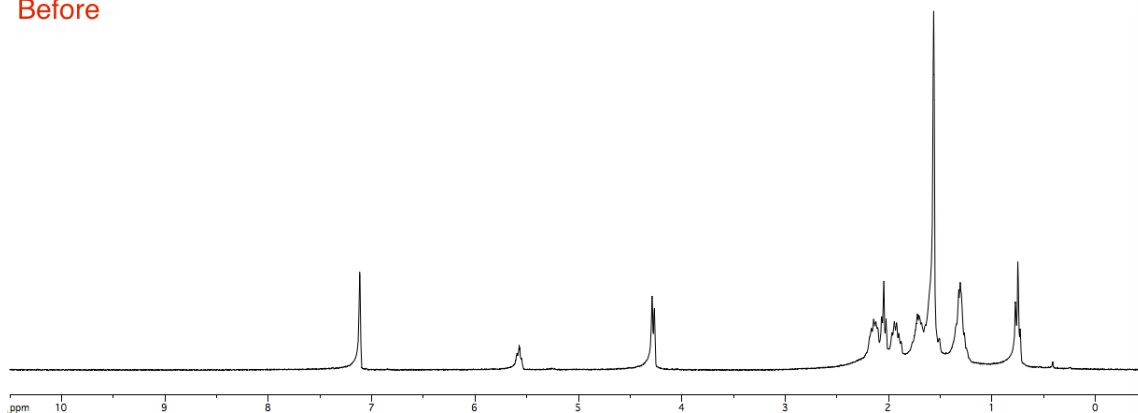
rotary evaporation and the resulting residue was purified by flash chromatography (99:1 hexanes/CH<sub>2</sub>Cl<sub>2</sub> → 6:1 hexanes/CH<sub>2</sub>Cl<sub>2</sub> eluent), affording tricycle **2-50** (1.4 mg, 5% yield, R<sub>f</sub> = 0.66 in 1:1 hexanes/CH<sub>2</sub>Cl<sub>2</sub>, stained orange with *p*-anisidine) as a yellow oil.

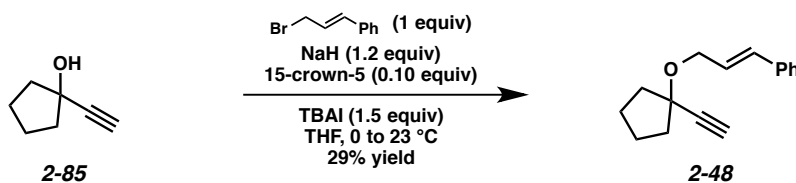
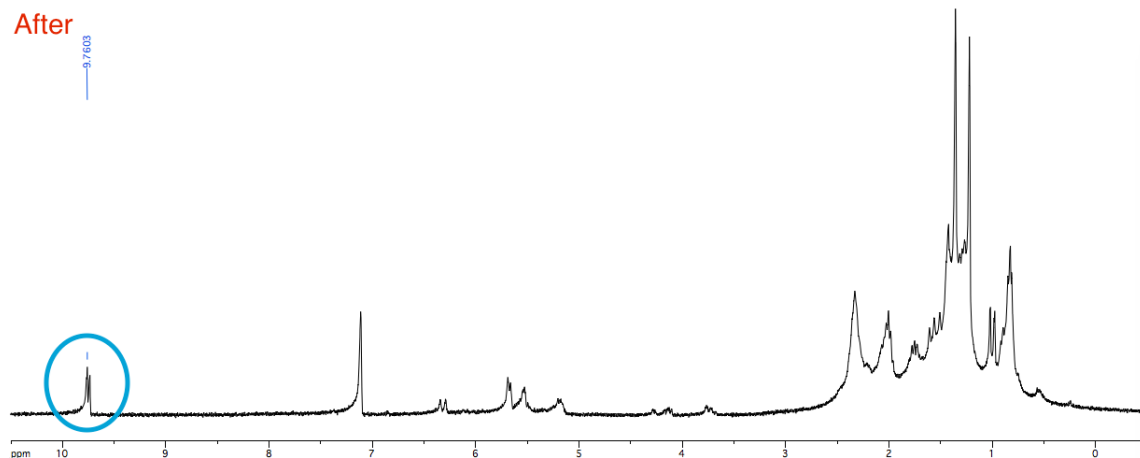
Also see: **Preliminary Results with Zeise's Dimer (Table 2.2)**



*NMR Experiment:* To enyne **2-5** (8.6 mg, 0.0300 mmol) in C<sub>6</sub>D<sub>6</sub> (0.460 mL) was added [(C<sub>2</sub>H<sub>4</sub>)PtCl<sub>2</sub>]<sub>2</sub> (0.5 mg, 0.000750 mmol). The reaction mixture was transferred to an NMR tube. An <sup>1</sup>H NMR was taken of the starting reaction mixture. The NMR tube was then heated at 60 °C for 21 h and a second <sup>1</sup>H NMR was taken that revealed the formation of an aldehyde peak at 9.76 ppm.

Before

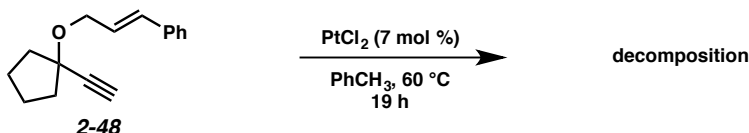




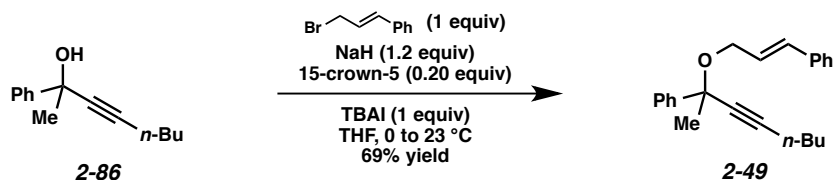
**Enyne 2-48.** To a solution of tertiary propargyl alcohol **2-85** (0.992 g, 9.00 mmol) in THF (45 mL) at 0 °C was added NaH (0.432 g, 60% dispersion in mineral oil, 10.8 mmol). The reaction mixture was allowed to warm to ambient temperature and was stirred until gas evolution was visibly complete. To this suspension was added sequentially 15-crown-5 (0.18 mL, 0.900 mmol), tetrabutylammonium iodide (4.99 g, 13.5 mmol), and cinnamyl bromide (1.77 g, 9.00 mmol). The resulting mixture was stirred at ambient temperature for 14 h. The reaction was quenched with sat. aq.  $\text{NH}_4\text{Cl}$  (40 mL). The layers were separated, and the aqueous layer was extracted with  $\text{Et}_2\text{O}$  (3 x 40 mL). The combined organic layers were washed with brine (80 mL), then dried over  $\text{MgSO}_4$ . The volatile materials were removed by rotary evaporation and the resulting residue was purified by flash chromatography (99:1 hexanes/ $\text{Et}_2\text{O}$  → 4:1 hexanes/ $\text{Et}_2\text{O}$  eluent), affording enyne **2-48** (0.598 g, 29% yield,  $R_f = 0.85$  in 3:1 hexanes/ $\text{EtOAc}$ , visualized by UV) as a colorless oil.

**Enyne 2-48:**  $^1\text{H}$  NMR (400 MHz;  $\text{CDCl}_3$ ):  $\delta$  7.38 (d,  $J = 7.2$  Hz, 2H), 7.30 (t,  $J = 7.2$  Hz, 2H), 7.22 (t,  $J = 7.2$  Hz, 1H), 6.62 (d,  $J = 15.9$  Hz, 1H), 6.32 (dt,  $J = 15.9, 6.0$  Hz, 1H), 4.25 (dd,  $J = 6.0, 1.4$  Hz, 2H), 2.51 (s, 1H), 2.11-2.05 (m, 2H), 1.99-1.93 (m, 2H), 1.84-1.71 (m, 4H);  $^{13}\text{C}$  NMR (100 MHz;  $\text{CDCl}_3$ ):  $\delta$  136.9, 131.7, 128.4, 127.5, 126.6, 126.5, 85.5, 80.2, 72.9, 65.7, 39.6, 23.3; HRMS (ESI+)  $m/z$  calc'd for  $(\text{M} + \text{Na})^+$   $[\text{C}_{16}\text{H}_{18}\text{O} + \text{Na}]^+$ : 249.1250, found 249.1237.

#### Attempted Cycloisomerization of Enyne 2-48:



To a solution of enyne **2-48** (90.5 mg, 0.400 mmol) in toluene (4.0 mL) in a 2-dram vial under argon was quickly added  $\text{PtCl}_2$  (7.5 mg, 0.0280 mmol). The reaction mixture was stirred at  $60^\circ\text{C}$  for 19 h. The reaction was allowed to cool to ambient temperature and was diluted with an approximately equal amount of hexanes. The mixture was stirred for 15 min, then passed through a small plug of  $\text{Al}_2\text{O}_3$  (hexanes  $\rightarrow$  1:1 hexanes/EtOAc eluent). The volatile materials were removed by rotary evaporation and the resulting residue was analyzed by  $^1\text{H}$  NMR. Enyne **2-48** was not completely consumed, but the majority of the crude product mixture was decomposition products.

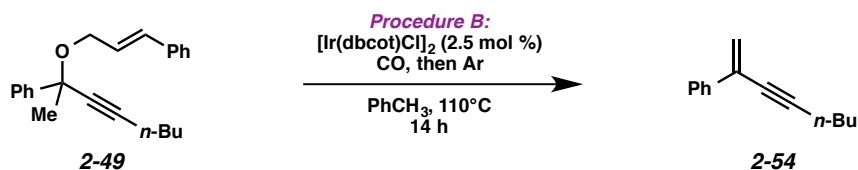


**Enyne 2-49.** To a solution of tertiary propargyl alcohol **2-86** (0.202 g, 1.00 mmol) in THF (5.00 mL) at  $0^\circ\text{C}$  was added NaH (48.0 mg, 60% dispersion in mineral oil, 1.20 mmol). The reaction mixture was

allowed to warm to ambient temperature and was stirred until gas evolution was visibly complete. To this suspension was added sequentially 15-crown-5 (0.050 mL, 0.250 mmol), tetrabutylammonium iodide (0.369 g, 1.00 mmol), and cinnamyl bromide (0.197 g, 1.00 mmol). The resulting mixture was stirred at ambient temperature for 19 h. The reaction was quenched with sat. aq.  $\text{NH}_4\text{Cl}$  (10 mL). The layers were separated, and the aqueous layer was extracted with  $\text{Et}_2\text{O}$  (3 x 10 mL). The combined organic layers were washed with brine (25 mL), then dried over  $\text{MgSO}_4$ . The volatile materials were removed by rotary evaporation and the resulting residue was purified by flash chromatography (99:1 hexanes/ $\text{CH}_2\text{Cl}_2 \rightarrow$  1:1 hexanes/ $\text{CH}_2\text{Cl}_2$  eluent), affording enyne **2-49** (0.192 g, 60% yield,  $R_f = 0.85$  in 1:2 hexanes/ $\text{CH}_2\text{Cl}_2$ , stained purple with *p*-anisidine) as a yellow oil.

**Enyne 2-49:**  $^1\text{H}$  NMR (400 MHz;  $\text{CDCl}_3$ ):  $\delta$  7.65 (dd,  $J = 8.2, 1.2$  Hz, 2H), 7.39-7.36 (comp. m, 4H), 7.32-7.28 (comp. m, 3H), 7.24-7.20 (m, 1H), 6.59 (d,  $J = 15.9$  Hz, 1H), 6.31 (dt,  $J = 15.9, 6.0$  Hz, 1H), 4.27 (ddd,  $J = 12.2, 6.0, 1.4$  Hz, 1H), 3.79 (ddd,  $J = 12.2, 6.0, 1.4$  Hz, 1H), 2.37 (t,  $J = 7.0$  Hz, 2H), 1.75 (s, 3H), 1.62-1.56 (m, 2H), 1.49 (m, 2H), 0.95 (t,  $J = 7.3$  Hz, 3H);  $^{13}\text{C}$  NMR (100 MHz;  $\text{CDCl}_3$ ):  $\delta$  131.6, 128.4, 128.2, 127.6, 127.4, 126.6, 126.4, 126.0, 88.3, 83.7, 80.2, 76.2, 75.8, 65.7, 33.3, 30.9, 22.0, 18.5, 13.6; HRMS (ESI+)  $m/z$  calc'd for  $(\text{M} + \text{Na})^+ [\text{C}_{23}\text{H}_{26}\text{O} + \text{Na}]^+$ : 341.1876, found 341.1859.

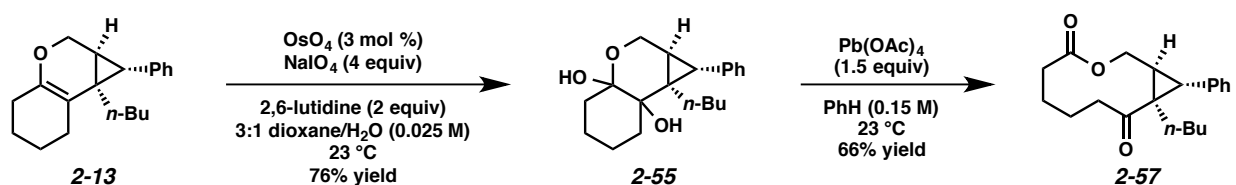
#### Attempted Cycloisomerization of Enyne 2-49:



**Procedure B:** To a solution of enyne **2-49** (15.4 mg, 50.0  $\mu\text{mol}$ ) in toluene (0.770 mL) in a 16 x 125 mm glass culture tube under argon was quickly added  $[\text{Ir}(\text{dbcot})\text{Cl}]_2$  (1.1 mg, 1.25  $\mu\text{mol}$ ). CO was bubbled through the solution using a balloon and needle outlet (ca. 30 s), during which time the solution turned a

dark-blue/black color. The balloon was removed and argon was bubbled through the solution in the same manner. The septum was quickly replaced with a Teflon cap and the solution was stirred at 110 °C for 14 h. The reaction was allowed to cool to ambient temperature and was diluted with an approximately equal amount of hexanes. The mixture was stirred for 15 min, then passed through a small plug of Al<sub>2</sub>O<sub>3</sub> (hexanes → 1:1 hexanes/EtOAc eluent). The volatile materials were removed by rotary evaporation and the resulting residue was analyzed by <sup>1</sup>H NMR. Enyne **2-49** was completely consumed and alkene **2-54** was the major product. All spectroscopic data were consistent with previously reported values.<sup>19</sup>

### 2.7.5 Oxidative Cleavage to Macrolactones



**Diol 2-55.** To tricyclic **2-13** (67.6 mg, 0.239 mmol) in dioxane (7.5 mL) was added OsO<sub>4</sub> (50.0 μL, 4% solution in H<sub>2</sub>O, 0.00750 mmol), followed by 2,6-lutidine (57.6 μL, 0.500 mmol). The reaction mixture was stirred for 5 min, then NaIO<sub>4</sub> (0.2139 g, 1.00 mmol) was added as a solution in H<sub>2</sub>O (2.5 mL). The resulting mixture was stirred at ambient temperature for 1.5 d, after which the mixture was quenched with 1 M HCl (5 mL) and diluted with EtOAc (5 mL). The layers were separated and the aqueous layer was extracted with EtOAc (1 x 5 mL). The combined organic layers were washed with sat. Na<sub>2</sub>S<sub>2</sub>O<sub>3</sub> (10 mL) and brine (10 mL), then dried over MgSO<sub>4</sub>. The volatile materials were removed by rotary evaporation and the resulting residue was purified by flash chromatography (100% hexanes → 1:1 hexanes/CH<sub>2</sub>Cl<sub>2</sub> → EtOAc eluent), affording diol **2-55** (57.4 mg, 76% yield, R<sub>f</sub> = 0.77 in 1:1 hexanes/EtOAc, stained with CAM) as a green oil.



**Diol 2-56.** To tricycle **2-19** (34.5 mg, 0.0907 mmol) in dioxane (3.0 mL) was added OsO<sub>4</sub> (19.0 μL, 4% solution in H<sub>2</sub>O, 2.72 μmol), followed by 2,6-lutidine (20.9 μL, 0.0194 mmol). The reaction mixture was stirred for 5 min, then NaIO<sub>4</sub> (85.6 mg, 0.400 mmol) was added as a solution in H<sub>2</sub>O (1.0 mL). The resulting mixture was stirred at ambient temperature for 3 d, after which the mixture was quenched with 1 M HCl (3 mL) and diluted with EtOAc (3 mL). The layers were separated and the aqueous layer was extracted with EtOAc (1 x 3 mL). The combined organic layers were washed with sat. Na<sub>2</sub>S<sub>2</sub>O<sub>3</sub> (5 mL) and brine (5 mL), then dried over MgSO<sub>4</sub>. The volatile materials were removed by rotary evaporation and the resulting residue was purified by flash chromatography (100% hexanes → 1:1 hexanes/EtOAc eluent), affording diol **2-56** (20.0 mg, 58% yield, R<sub>f</sub> = 0.66 in 1:1 hexanes/EtOAc, stained with CAM) as a green oil.

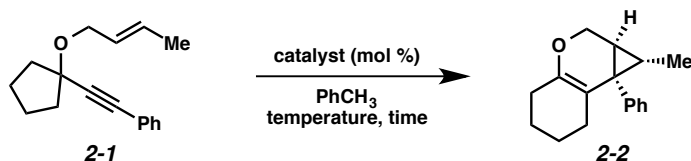
**Diol 2-56:** <sup>1</sup>H NMR (400 MHz; C<sub>6</sub>D<sub>6</sub>): δ 7.14-6.95 (m, 10H), 4.42 (dd, *J* = 11.1, 4.5 Hz, 1H), 3.87-3.80 (m, 2H), 3.75 (d, *J* = 11.2 Hz, 2H), 3.36 (d, *J* = 9.5 Hz, 1H), 2.80 (d, *J* = 9.5 Hz, 1H), 2.32 (d, *J* = 6.3 Hz, 1H), 2.15-2.02 (m, 2H), 1.91-1.84 (m, 2H), 1.65-1.52 (m, 2H), 1.47-1.41 (m, 1H), 1.12 (dd, *J* = 6.2, 4.6 Hz, 1H); <sup>13</sup>C NMR (100 MHz; C<sub>6</sub>D<sub>6</sub>): δ 138.2, 137.9, 129.4, 128.7, 128.4, 128.0, 127.9, 126.6, 94.1, 73.1, 72.3, 71.0, 58.9, 36.2, 35.3, 33.5, 30.8, 22.9, 21.2, 19.9; IR (film) 3449, 2933, 2865, 1498, 1071 cm<sup>-1</sup>; HRMS (ESI+) *m/z* calc'd for (M + Na)<sup>+</sup> [C<sub>24</sub>H<sub>28</sub>O<sub>4</sub> + Na]<sup>+</sup>: 403.1885, found 403.1889.

**Macrolactone 2-58.** To diol **2-56** (25.3 mg, 0.0780 mmol) in benzene (0.70 mL) was added Pb(OAc)<sub>4</sub> (53.2 mg, 0.120 mmol). The reaction mixture was stirred at ambient temperature for 3.5 h, after which ethylene glycol (1.0 mL) was added and the mixture was allowed to stir for 1 h. The reaction mixture was diluted with Et<sub>2</sub>O (1.5 mL) and the layers were separated. The organic layer was washed with sat. NaHCO<sub>3</sub> (2 mL), then dried over MgSO<sub>4</sub>. The volatile materials were removed by rotary evaporation and the resulting residue was purified by flash chromatography (100% hexanes → 4:1 hexanes/EtOAc eluent), affording macrolactone **2-58** (16.3 mg, 66% yield, R<sub>f</sub> = 0.83 in 1:1 hexanes/EtOAc, stained with CAM) as a colorless oil.

**Macrolactone 2-58:**  $^1\text{H}$  NMR (400 MHz;  $\text{C}_6\text{D}_6$ ):  $\delta$  7.11-7.00 (m, 8H), 6.93-6.91 (m, 2H), 4.43 (dd,  $J = 11.7, 6.8$  Hz, 1H), 3.93-3.81 (m, 3H), 3.57 (d,  $J = 6.9$  Hz, 1H), 2.89 (ddd,  $J = 16.6, 9.2, 2.4$  Hz, 1H), 2.61 (d,  $J = 10.5$  Hz, 1H), 2.44 (ddd,  $J = 16.6, 9.2, 2.4$  Hz, 1H), 2.13-2.06 (m, 1H), 2.01-1.88 (m, 1H), 1.84-1.74 (m, 1H), 1.71 (q,  $J = 6.8$  Hz, 1H), 1.44-1.30 (m, 4H);  $^{13}\text{C}$  NMR (100 MHz;  $\text{C}_6\text{D}_6$ ):  $\delta$  205.5, 172.0, 136.9, 129.6, 128.5, 128.2, 127.9, 127.6, 126.9, 99.3, 73.1, 69.6, 62.1, 42.8, 39.8, 34.90, 34.87, 29.2, 22.93, 22.91, 13.4 IR (film) 2926, 2856, 1735, 1698, 1231, 1154  $\text{cm}^{-1}$ ; HRMS (ESI+)  $m/z$  calc'd for  $(\text{M} + \text{Na})^+$  [ $\text{C}_{24}\text{H}_{26}\text{O}_4 + \text{Na}$ ] $^+$ : 401.1729, found 401.1733.

## 2.7.6 Optimization Tables

### Catalyst Optimization (Table 2.1a)



**General procedure:** To a 2-dram vial under argon containing enyne **2-1** (14.0 mg, 0.0583 mmol) and 4,4'-di-*tert*-butylbiphenyl (internal standard, 5.3 mg, 0.0199 mmol) in toluene (0.900 mL, 0.065 M) was added the catalyst. The reaction mixture was stirred at the indicated temperature for the indicated time, and then was passed through a short plug of  $\text{Al}_2\text{O}_3$  (hexanes  $\rightarrow$  9:1 hexanes/EtOAc eluent). The volatile materials were removed by rotary evaporation. The crude residue was then diluted with  $\text{CH}_2\text{Cl}_2$  (3 mL) and the sample was analyzed by GC. The catalyst screen results are reported in Table 2.1a.

### GC Method

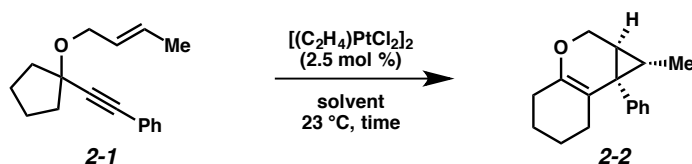
150  $^\circ\text{C}$  for 60 min

Retention times: **2-1** = 16.60 min; **2-2** = 15.98 min, internal standard = 47.40 min

## GC Column

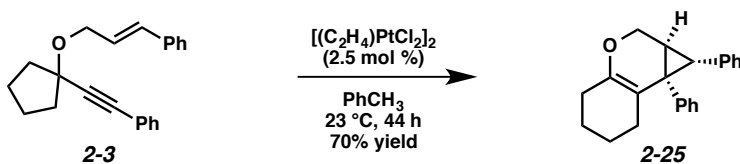
Agilent Technologies CP-Sil 8 CB (15 x 0.25)

## Solvent Optimization (Table 2.1b)



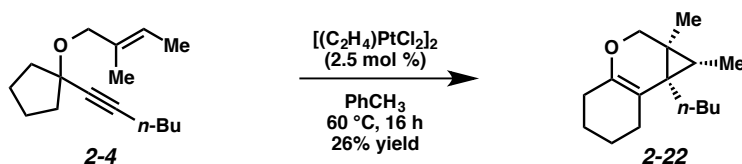
**General procedure:** To a 2-dram vial under argon containing enyne **2-1** (14.0 mg, 0.0583 mmol) and 4,4'-di-*tert*-butylbiphenyl (internal standard, 5.3 mg, 0.0199 mmol) in the indicated solvent (0.900 mL, 0.065 M) was added  $[(C_2H_4)PtCl_2]_2$  (0.9 mg, 0.00146 mmol). The reaction mixture was stirred at ambient temperature for the indicated time, and then was passed through a short plug of  $Al_2O_3$  (hexanes  $\rightarrow$  9:1 hexanes/EtOAc eluent). The volatile materials were removed by rotary evaporation. The crude residue was then diluted with  $CH_2Cl_2$  (3 mL) and the sample was analyzed by GC. The solvent screen results are reported in Table 2.1b. The same GC method and column were used as above in catalyst optimization.

## Preliminary Results with Zeise's Dimer (Table 2.2)

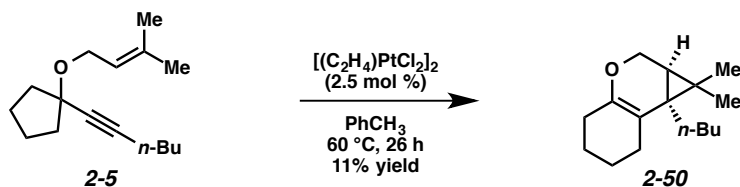


**Tricyclic 2-25.** To a solution of enyne **2-3** (15.5 mg, 50.0  $\mu$ mol) in toluene (0.77 mL) in a 2-dram vial under argon was quickly added  $[(C_2H_4)PtCl_2]_2$  (0.8 mg, 1.25  $\mu$ mol). The reaction mixture was stirred at ambient temperature for 44 h, then was diluted with an approximately equal amount of hexanes. The

mixture was stirred for 15 min, then passed through a small plug of Al<sub>2</sub>O<sub>3</sub> (hexanes → 1:1 hexanes/EtOAc eluent). The volatile materials were removed by rotary evaporation and the resulting residue was purified by flash chromatography (99:1 hexanes/CH<sub>2</sub>Cl<sub>2</sub> w/ 0.5% Et<sub>3</sub>N → 5:1 hexanes/CH<sub>2</sub>Cl<sub>2</sub> w/ 0.5% Et<sub>3</sub>N eluent) affording tricycle **2-25** (10.9 mg, 70% yield, R<sub>f</sub> = 0.61 in 1:1 CH<sub>2</sub>Cl<sub>2</sub>/hexanes, stained red with *p*-anisaldehyde) as a colorless oil.

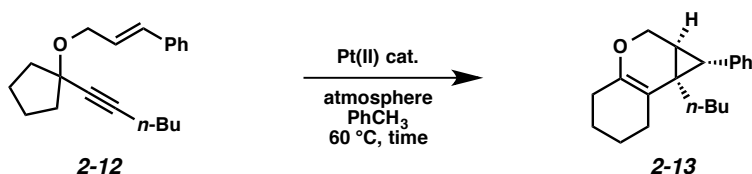


**Tricycle 2-22.** To a solution of enyne **2-4** (23.7 mg, 0.100 mmol) in toluene (1.50 mL) in a 2-dram vial under argon was quickly added  $[(C_2H_4)PtCl_2]_2$  (1.5 mg, 0.00250 mmol). The reaction mixture was stirred at 60 °C for 16 h, then was diluted with an approximately equal amount of hexanes. The mixture was stirred for 15 min, then passed through a small plug of Al<sub>2</sub>O<sub>3</sub> (hexanes → 1:1 hexanes/EtOAc eluent). The volatile materials were removed by rotary evaporation and the resulting residue was purified by flash chromatography (9:1 hexanes/CH<sub>2</sub>Cl<sub>2</sub> w/ 0.5% Et<sub>3</sub>N → 5:1 hexanes/CH<sub>2</sub>Cl<sub>2</sub> w/ 0.5% Et<sub>3</sub>N eluent) affording tricycle **2-22** (6.1 mg, 26% yield, R<sub>f</sub> = 0.81 in 1:1 CH<sub>2</sub>Cl<sub>2</sub>/hexanes, stained orange with *p*-anisaldehyde) as a colorless oil. When the same reaction was performed at ambient temperature, low conversion from enyne **2-4** was observed.



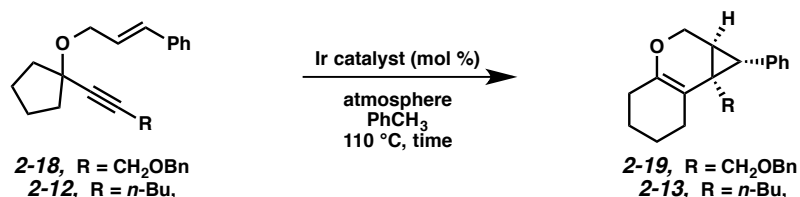
**Tricycle 2-50.** To a solution of enyne **2-5** (75.1 mg, 0.320 mmol) in toluene (4.90 mL) in a 2-dram vial under argon was quickly added  $[(C_2H_4)PtCl_2]_2$  (4.7 mg, 0.00800 mmol). The reaction mixture was stirred at 60 °C for 26 h, then was diluted with an approximately equal amount of hexanes. The mixture was stirred for 15 min, then passed through a small plug of  $Al_2O_3$  (hexanes  $\rightarrow$  1:1 hexanes/EtOAc eluent). The volatile materials were removed by rotary evaporation and the resulting residue was purified by flash chromatography (100% hexanes  $\rightarrow$  9:1 hexanes/ $CH_2Cl_2$  eluent) affording tricycle **2-50** (8.1 mg, 11% yield,  $R_f = 0.63$  in 1:1  $CH_2Cl_2$ /hexanes, stained red with *p*-anisaldehyde) as a colorless oil. When the same reaction was performed at ambient temperature, almost no reaction occurred.

### Effect of CO Atmosphere (Table 2.3)



**General Procedure:** The reaction were performed as described in *Procedure A* (for  $[(C_2H_4)PtCl_2]_2$ ) and *Procedure C* (for  $PtCl_2$ ), except the atmospheres were varied. The reactions run under argon were assembled under argon in 2 dram vials equipped with rubber septa. After the catalyst was added, the rubber septum was quickly replaced with a Teflon cap. The reactions run under CO were assembled under air in 2 dram vials equipped with screw caps with septa. After the catalyst was added, CO was bubbled through the reaction mixture using a balloon and needle outlet. The reaction mixtures were heated at 60 °C for the indicated time and then were worked up and purified according to the *General Procedures*.

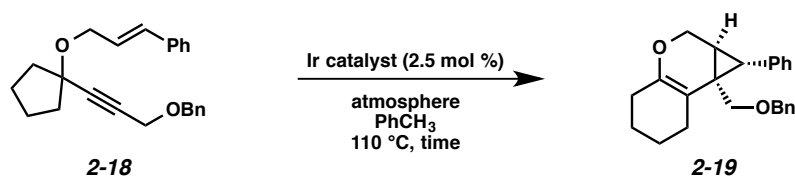
## Ir Catalyst Screen (Table 2.4)



**General procedure:** To a 2-dram vial containing either enyne **2-18** or **2-12** (0.0500 mmol) in toluene (0.065 M) was added the catalyst. The reactions performed under argon were purged by bubbling argon through the reaction mixture for 1 min. The reactions performed under CO were purged by bubbling CO through the reaction mixture for 1 min. For the “CO, then Ar” reactions, CO was bubbled through the reaction mixture for 1 min, then argon was bubbled through for 1 min. The reaction mixture was stirred at 110 °C for the indicated time, and then was passed through a short plug of Al<sub>2</sub>O<sub>3</sub> (hexanes → 9:1 hexanes/EtOAc eluent). The volatile materials were removed by rotary evaporation. The crude residue was then analyzed by <sup>1</sup>H NMR to determine conversion. Isolated yields were obtained after purification by flash chromatography. The Ir catalyst screen results are reported in Table 2.4.

Vaska’s complex, [Ir(cod)Cl]<sub>2</sub>, and [Ir(coe)<sub>2</sub>Cl]<sub>2</sub> are commercially available. Ir<sub>4</sub>(CO)<sub>12</sub>,<sup>20</sup> Ir(CO)<sub>2</sub>(acac),<sup>21</sup> and [Ir(dbcot)Cl]<sub>2</sub><sup>22</sup> were synthesized as previously reported.

## CO vs. CO, then Ar (Table 2.5)



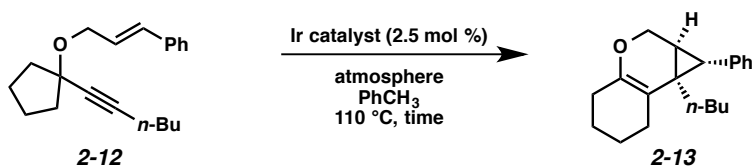
**General procedure:** Each reaction was performed on a 0.0500 mmol to 0.0750 mmol scale in toluene (0.065 M). The reactions performed under CO were purged by bubbling CO through the reaction mixture for 1 min. For the “CO, then Ar” reactions, CO was bubbled through the reaction mixture for 1 min, then argon was bubbled through for 1 min. The reaction mixture was stirred at 110 °C for the time indicated below, and then was passed through a short plug of Al<sub>2</sub>O<sub>3</sub> (hexanes → 9:1 hexanes/EtOAc eluent). The volatile materials were removed by rotary evaporation and the resulting residue was purified by flash chromatography to obtain isolated yields.

[Ir(dbcot)Cl]<sub>2</sub> : CO, 15 h; CO, then Ar; 16 h

[Ir(cod)Cl]<sub>2</sub> : CO, 22 h; CO, then Ar; 17 h

[Ir(coe)<sub>2</sub>Cl]<sub>2</sub> : CO, 15 h; CO, then Ar; 15 h

### Ir(I) Experiments where Displaced Ligand was Removed (Table 2.6)



In a representative procedure, a 16 x 125 mm glass culture tube was charged with [Ir(dbcot)Cl]<sub>2</sub> (1.3 mg, 0.00150 mmol) and toluene (0.92 mL). CO was bubbled through the solution using a balloon and needle outlet (ca. 30 s), during which time the mixture turned a dark-blue/black color. The balloon was removed and argon was bubbled through the solution in the same manner. The tube containing the catalyst mixture was then centrifuged for ~30 s to concentrate the black solid at the bottom of the tube. The toluene was carefully removed using a needle and syringe. The remaining black solid was dried under vacuum, then the tube was backfilled with argon. Fresh toluene (0.92 mL) and enyne **2-12** (17.6 mg, 0.0600 mmol) were added. The septum was quickly replaced with a Teflon cap and the solution was stirred at 110 °C for

22 h. The reaction was allowed to cool to ambient temperature and diluted with an approximately equal amount of hexanes. 1,3-Bis(diphenylphosphino)propane (dppp) (0.25 equiv) was also added to the mixture. The mixture was stirred for 15 min, then passed through a small plug of Al<sub>2</sub>O<sub>3</sub> (hexanes → 1:1 hexanes/EtOAc eluent). The volatile materials were removed by rotary evaporation and the resulting residue was purified by flash chromatography (99:1 hexanes/CH<sub>2</sub>Cl<sub>2</sub> → 9:1 hexanes/CH<sub>2</sub>Cl<sub>2</sub> eluent) affording tricycle **2-13** (11.2 mg, 64% yield) as a colorless oil.

## Chapter 2 Notes and References

---

<sup>1</sup> (a) Newcomb, E. T.; Ferreira, E. M. *Org. Lett.* **2013**, *15*, 1772-1775. (b) Newcomb, E. T.; Knutson, P. C.; Pedersen, B. A.; Ferreira, E. M. *J. Am. Chem. Soc.* **2016**, *138*, 108-111.

<sup>2</sup> (a) Allegretti, P. A.; Ferreira, E. M. *Org. Lett.* **2011**, *13*, 5924-5927. (b) Allegretti, P. A.; Ferreira, E. M. *Chem. Sci.* **2013**, *4*, 1053-1058. (c) Allegretti, P. A.; Ferreira, E. M. *J. Am. Chem. Soc.* **2013**, *135*, 17266-17269. (d) Allegretti, P. A.; Huynh, K.; Ozumerzifon, T. J.; Ferreira, E. M. *Org. Lett.* **2016**, *18*, 64-67.

<sup>3</sup> Simonneau, A.; Harrak, Y.; Jeanne-Julien, L.; Lemi re, G.; Mouri s-Mansuy, V.; Goddard, J.-P.; Malacria, M.; Fensterbank, L. *ChemCatChem* **2013**, *5*, 1096-1099.

<sup>4</sup> (a) Stevenson, S. M.; Newcomb, E. T.; Ferreira, E. M. *Chem. Commun.* **2014**, *50*, 5239-5241. (b) Stevenson, S. M.; Newcomb, E. T.; Ferreira, E. M. *Org. Chem. Front.* **2016**, DOI: 10.1039/C6QO00224B.

<sup>5</sup> Brian Newell is acknowledged for X-ray crystallography expertise.

<sup>6</sup> F rstner, A.; Davies, P. W.; Gress, T. *J. Am. Chem. Soc.* **2005**, *127*, 8244-8245.

<sup>7</sup> Gimbert, Y.; Fensterbank, L.; Gandon, V.; Goddard, J.-P.; Lesage, D. *Organometallics* **2013**, *32*, 374-376.

<sup>8</sup> Shibata, T.; Kobayashi, Y.; Maekawa, S.; Toshida, N.; Takagi, K. *Tetrahedron* **2005**, *61*, 9018-9024.

<sup>9</sup> No alkyl migrations were observed with nitrogen-tethered 1,6-enynes under our optimized conditions.

<sup>10</sup> Vaska, L.; DiLuzio, J. W. *J. Am. Chem. Soc.* **1961**, *83*, 2784-2785.

<sup>11</sup> Roberto, D.; Cariati, E.; Psaro, R.; Ugo, R. *Organometallics* **1994**, *13*, 4227-4231.

<sup>12</sup> Hartwig, J. F. *Organotransition Metal Chemistry*. University Science Books, Mill Valley, California, **2010**, p. 48.

<sup>13</sup> (a) Anton, D. R.; Crabtree, R. H. *Organometallics* **1983**, *2*, 621-627. (b) Singh, A.; Sharp, P. R. *Organometallics* **2006**, *25*, 678-683.

<sup>14</sup> (a) Luzung, M. R.; Markham, J. P.; Toste, F. D. *J. Am. Chem. Soc.* **2004**, *126*, 10858-10859. (b) Horino, Y.; Yamamoto, T.; Uedo, K.; Kuroda, S.; Toste, F. D. *J. Am. Chem. Soc.* **2009**, *131*, 2809-2811.

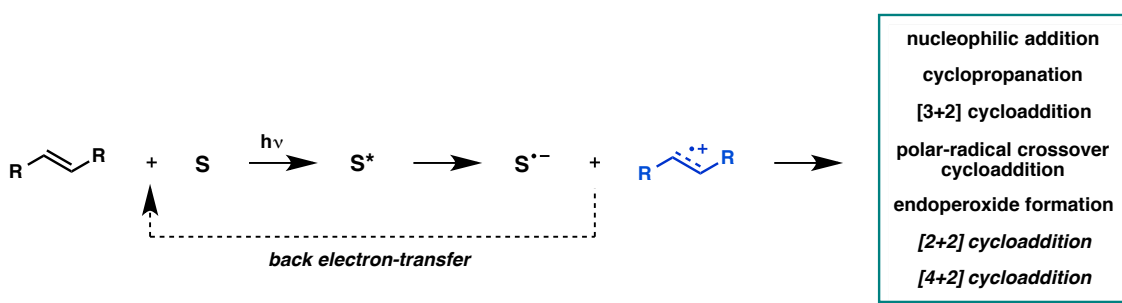
- 
- <sup>15</sup> Anslyn, E. V.; Dougherty, D. A. *Modern Physical Organic Chemistry*. University Science Books, **2006**, p. 108.
- <sup>16</sup> Fürstner, A.; Stelzer, F.; Szillat, H. *J. Am. Chem. Soc.* **2001**, *123*, 11863-11869.
- <sup>17</sup> (a) Sim, S. H.; Lee, S. I.; Park, J. H.; Chung, Y. K. *Adv. Synth. Catal.* **2010**, *352*, 317-322. (b) Benedetti, E.; Simonneau, A.; Hours, A.; Amouri, H.; Penoni, A.; Palmisano, G.; Malacria, M.; Goddard, J.-P.; Fensterbank, L. *Adv. Synth. Catal.* **2011**, *353*, 1908-1912.
- <sup>18</sup> Driggers, E. M.; Hale, S. P.; Lee, J.; Terrett, N. K. *Nat. Rev. Drug Discovery* **2008**, *7*, 608-624.
- <sup>19</sup> Yan, W.; Ye, X.; Akhmedov, N. G.; Petersen, J. L.; Shi, X. *Org. Lett.* **2012**, *14*, 2358-2361.
- <sup>20</sup> Pruchnik, F. P.; Wajda-Hermanowicz, K.; Koralewicz, M. *J. Organomet. Chem.* **1990**, *384*, 381-383.
- <sup>21</sup> Roberto, D.; Cariati, E.; Psaro, R.; Ugo, R. *Organometallics* **1994**, *13*, 4227-4231.
- <sup>22</sup> Singh, A.; Sharp, P. R. *Inorg. Chim. Acta* **2008**, *361*, 3159-3164.

## CHAPTER 3

### PHOTOSENSITIZED [2+2] AND [4+2] RADICAL CATION CYCLOADDITIONS

#### 3.1 Introduction: Radical Cation Reactions of Alkenes

In the past decade, the renaissance of photoredox catalysis has sparked a renewed interest in radical cation accelerated reactions initiated through photoinduced electron transfer (PET).<sup>1</sup> Radical cation reactions of alkenes have received particular attention, given their capacity to form a diverse range of products.<sup>2</sup>



*Scheme 3.1.* General depiction of alkene radical cation formation through PET.

A basic diagram depicting alkene radical cation formation through PET is shown in Scheme 3.1. First, a photosensitizer (S) absorbs a photon to form an excited state sensitizer complex ( $S^*$ ). This excited state has enhanced electron-accepting capabilities compared to the ground state sensitizer, so it will accept an electron from the electron-rich alkene to generate a radical cation. The radical cation can then accept an electron back from the sensitizer radical anion ( $S^{\bullet-}$ ) to regenerate the ground state species, or, in the presence of a suitable reactant, the radical cation can undergo a number of transformations, like nucleophilic addition,<sup>3</sup> cyclopropanation,<sup>4</sup> [3+2] cycloadditions,<sup>5</sup> polar-radical crossover cycloadditions,<sup>6</sup> and cycloadditions with molecular oxygen to form endoperoxides,<sup>7</sup> all of which have been the subject of



Traditionally, organic photosensitizers have dominated the area of radical cation cycloadditions, while current research is more focused on the use of transition metal photocatalysts.<sup>13</sup> Overall, each class of photosensitizers has its advantages and disadvantages. As can be seen in Figure 3.1, organic photosensitizers are generally stronger photooxidants than transition metal photocatalysts, so they are able to oxidize a wider range of substrates. On the other hand, the excitation of most organic photosensitizers requires higher energy UV light, which can result in undesired side reactions. Transition metal photocatalysis offers the opportunity of using visible light and sunlight as energy sources, which could aid in expanding the scope and selectivity of radical cation cycloadditions.

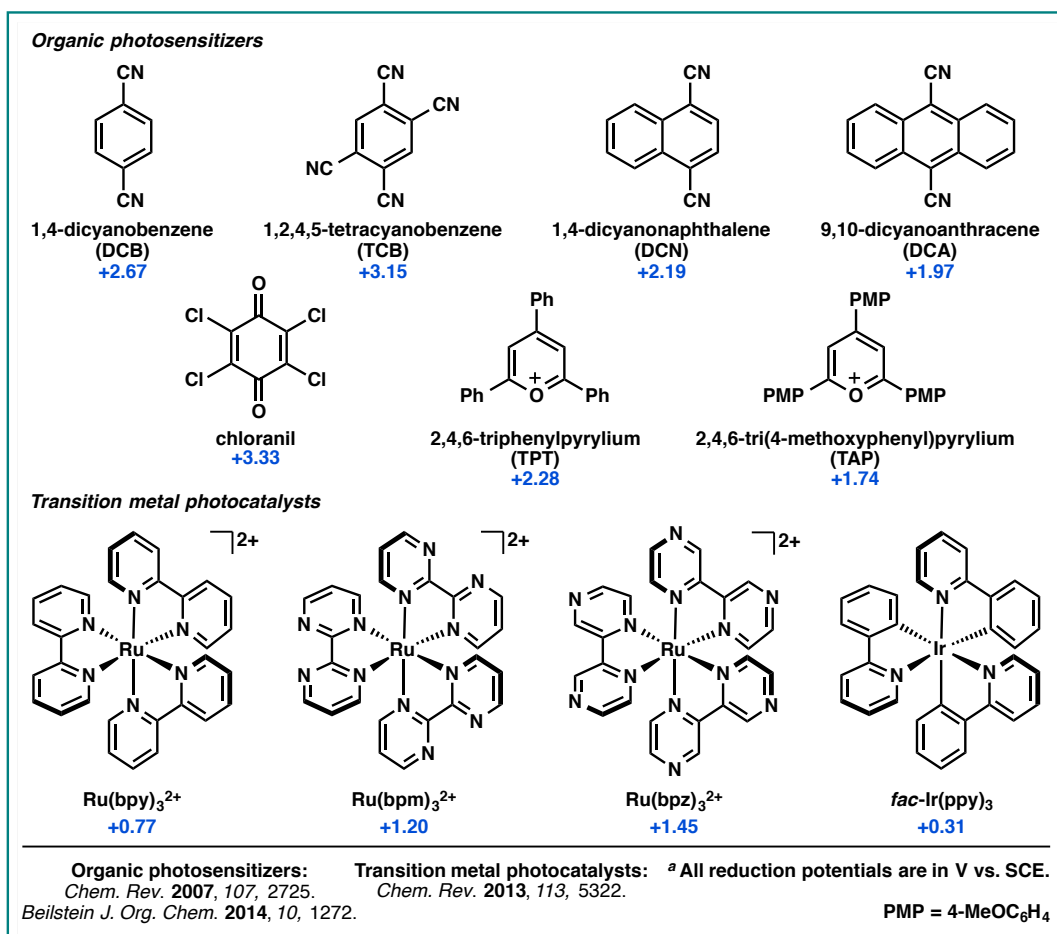
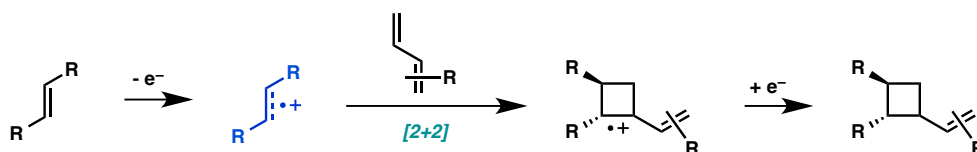


Figure 3.1. Common photosensitizers and excited state reduction potentials.<sup>a</sup>

In light of recent developments in modern PET reactions, the aim of this chapter is to provide a timeline of advancements in radical cation [2+2] and [4+2] cycloadditions from the earliest report up until the most recent. Ideally, this review will leave the reader with a fuller perspective on the various contributions that have already been made to radical cation cycloaddition chemistry and the immense potential that future investigations could hold.

### 3.2 [2+2] Radical Cation Cycloadditions



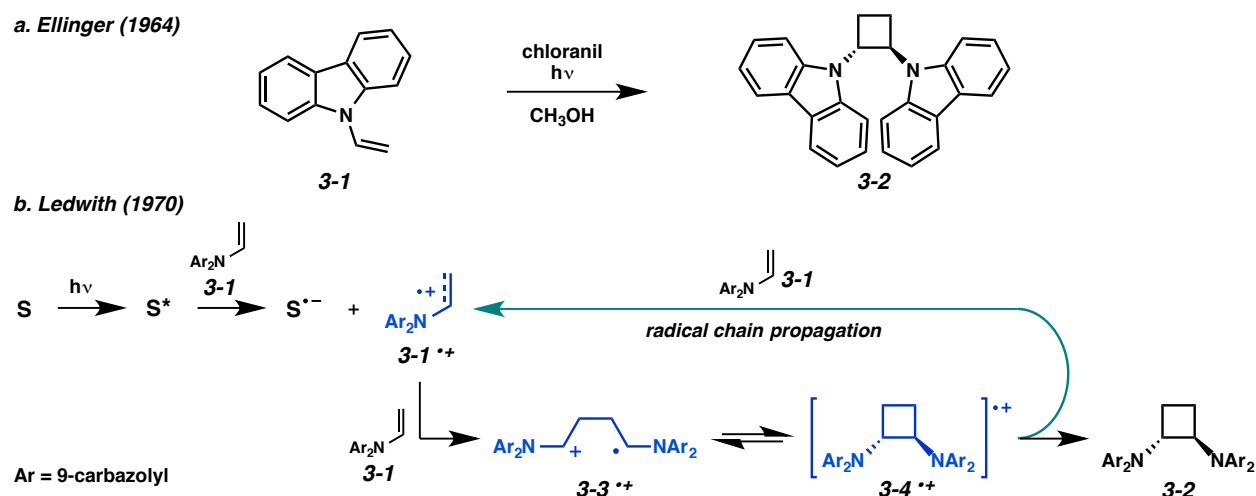
Scheme 3.3. General radical cation [2+2] cycloaddition.

The radical cation [2+2] cycloaddition has recently resurfaced as an efficient way to form cyclobutanes from electron-rich alkenes (Scheme 3.3). Though the utility of modern photoredox catalysis in accomplishing this transformation cannot be denied, the radical cation [2+2] cycloaddition has been extensively investigated since the 1960s. This section will discuss the different types of [2+2] cycloadditions that have been reported using PET techniques.

#### 3.2.1 *N*-Vinylcarbazole

The very first radical cation pericyclic reaction that was discovered was the [2+2] dimerization of *N*-vinylcarbazole (**3-1**) ( $E_{1/2} = +1.20$  V)<sup>14,15</sup> (Scheme 3.4a). This transformation was discovered by Ellinger in 1964 using chloranil as a photosensitizer.<sup>16</sup> Further studies by Ledwith and coworkers determined that the quantum yield of this reaction was 8.5, which led to the conclusion that the photocatalyzed transformation was proceeding through radical chain propagation.<sup>17</sup> The generally accepted mechanism is

shown in Scheme 3.4b. Upon single-electron oxidation by the excited photosensitizer, the radical cation of *N*-vinylcarbazole (**3-1**<sup>•+</sup>) reacts with another equivalent of *N*-vinylcarbazole (**3-1**) to form distonic radical cation (**3-3**<sup>•+</sup>). This species reversibly closes down to the cyclobutane radical cation (**3-4**<sup>•+</sup>). Then, in order to form the neutral product (**3-2**), the cyclobutane radical cation (**3-4**<sup>•+</sup>) oxidizes another equivalent of *N*-vinylcarbazole to propagate the reaction. Though a relatively simple transformation, the elucidation of the radical chain nature of this process has provided a mechanistic basis for the vast majority of radical cation [2+2] cycloadditions discovered to date.<sup>10b</sup>

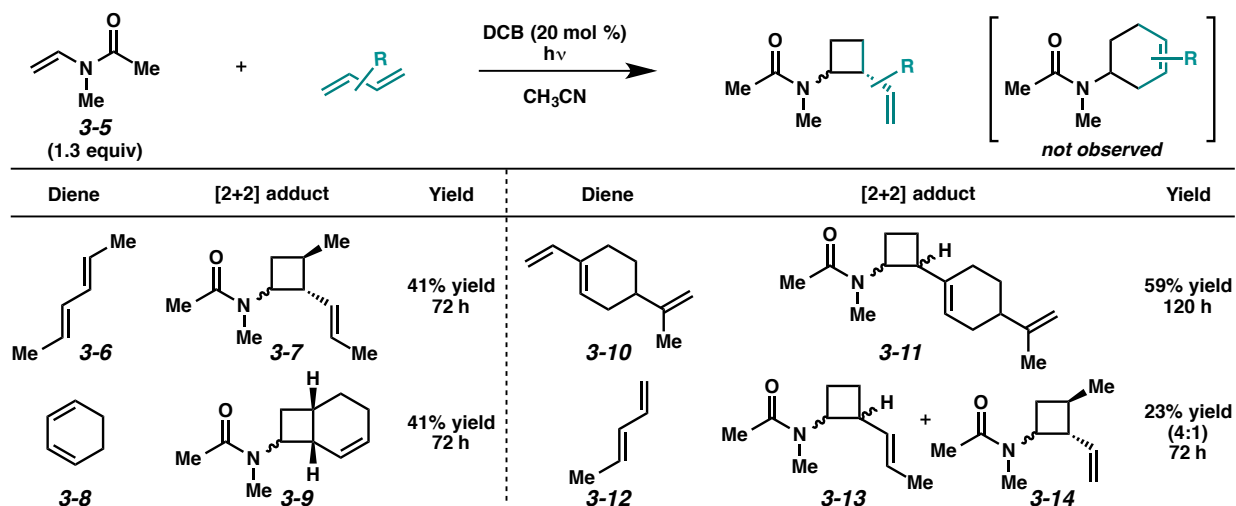


Scheme 3.4. [2+2] Dimerization of *N*-vinylcarbazole.

### 3.2.2 *N*-Methyl-*N*-vinylacetamide

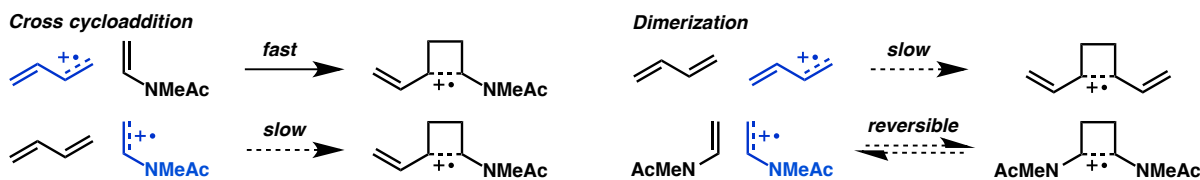
*N*-vinylamides will also undergo radical cation [2+2] cycloadditions.<sup>18</sup> Different from *N*-vinylcarbazole, however, when Bauld and coworkers exposed *N*-methyl-*N*-vinylacetamide (**3-5**) to PET conditions (DCB,  $h\nu$ ) by itself, no homodimerization occurred, even though the alkene was clearly being ionized by the photosensitizer (*vide infra*). The uncommon inability of alkene **3-5** to dimerize under PET conditions conveniently allowed for efficient cross cycloadditions with other electron-rich  $\pi$ -systems such as dienes (Scheme 3.5). In each of these reactions, high selectivity for the crossed cycloadduct was observed.

Curiously, very little diene dimerization was observed, which is not usually the case since most dienes are also oxidizable. Notably as well, *N*-methyl-*N*-vinylacetamide (**3-5**) exhibited high periselectivity for the [2+2] cycloaddition over the [4+2] cycloaddition, even with the rigidly *s*-cis cyclohexadiene (**3-8**).



Scheme 3.5. [2+2] Cycloaddition of *N*-methyl-*N*-vinylacetamide with dienes.

When considering the mechanism of this reaction, it is evident that both the diene and the vinylamide (**3-5**) are capable of being oxidized by the excited DCB\* complex ( $E_{1/2}^* = +2.67$  V). The high selectivity of this reaction for crossed [2+2] cycloadditions versus diene dimerization indicates that vinylamide **3-5** must react relatively quickly with the radical cation of the diene to prevent the diene radical cation from reacting with another equivalent of diene (Scheme 3.6). Additionally, if any dimerization of *N*-methyl-*N*-vinylacetamide (**3-5**) occurs under these conditions, the cycloaddition must be reversible, since no dimer of *N*-methyl-*N*-vinylacetamide is detected.



Scheme 3.6. All possible alkene/radical cation combinations.

The relative rates for the [2+2] cycloaddition of vinylamide **3-5** with different dienes supports this hypothesis (Table 3.1). Dienes that are easier to oxidize, or that have similar reduction potentials to vinylamide **3-5**, all react at comparable rates; dienes that are more difficult to oxidize than vinylamide **3-5**, but that should still be capable of oxidation with the chosen photosensitizer, reacted at slower rates. Thus, this data supports a mechanism where the nucleophilic vinylamide (**3-5**) is reacting with the radical cation of the diene.

Table 3.1. Relative rates of [2+2] cycloaddition of *N*-methyl-*N*-vinylacetamide with dienes.

**3-5**  
 $E_{1/2} = +1.55$  V

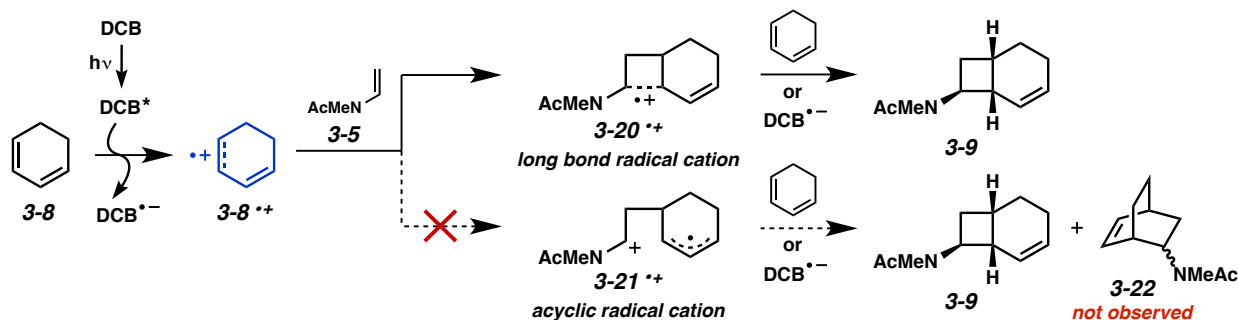
Diene	$E_{1/2}$ (V vs. SCE)	Relative rate <sup>a</sup>	Diene	$E_{1/2}$ (V vs. SCE)	Relative rate <sup>a</sup>	Diene	$E_{1/2}$ (V vs. SCE)	Relative rate <sup>a</sup>
	+1.22	6.6		+1.52	9.0		+1.73	3.0
	+1.24	7.6		+1.53	6.4		+1.95	1.0
	+1.42	6.9		+1.59	8.2		+1.98	0.7

<sup>a</sup> Relative to diene **3-18**

<sup>b</sup> Included because of its low reduction potential.

The full mechanism for this transformation is shown in Scheme 3.7 with cyclohexadiene (**3-8**) as a representative substrate. The diene is first oxidized by the excited state photosensitizer to give the cyclohexadiene radical cation (**3-8<sup>•+</sup>**). This radical cation is quickly intercepted by the vinylamide (**3-5**) before it has a chance to react with another equivalent of diene. Two possible radical cation intermediates can result: a long bond radical cation (**3-20<sup>•+</sup>**) and an acyclic radical cation (**3-21<sup>•+</sup>**), which can technically also lead to a [4+2] adduct (**3-22**). Due to the periselectivity of this transformation for the [2+2] product

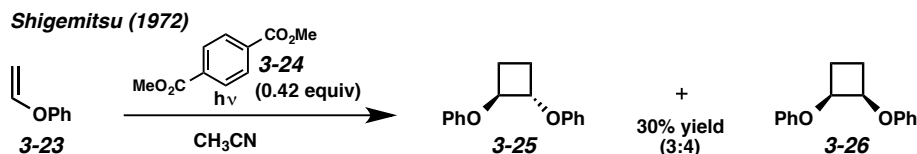
(3-9), the long bond radical cation intermediate must be preferred. After an additional electron transfer from cyclohexadiene or the reduced photosensitizer, the neutral [2+2] adduct is formed.



Scheme 3.7. Proposed mechanism for cycloaddition of a diene with *N*-methyl-*N*-vinylacetamide.

### 3.2.3 Vinyl Ethers

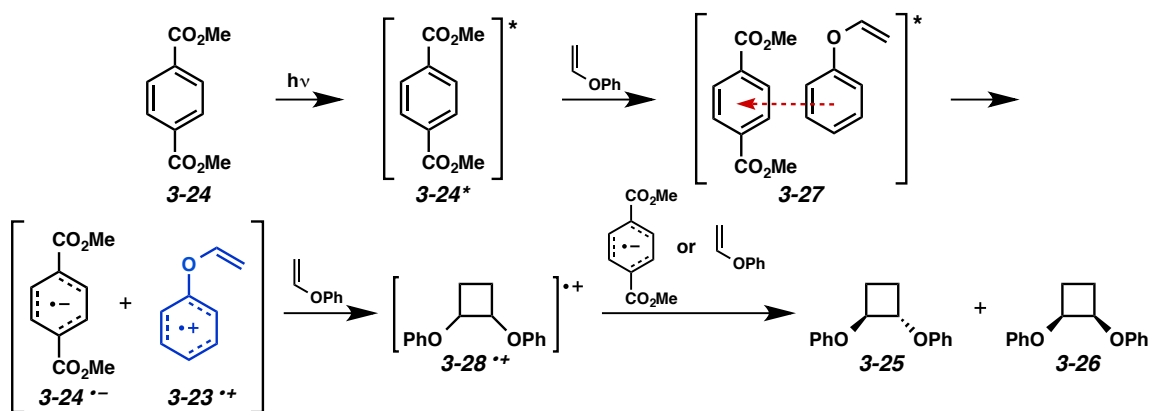
The first report of [2+2] dimerization of vinyl ethers came from the Shigemitsu group in 1972.<sup>19</sup> While exploring the photochemistry of aromatic esters, they discovered that phenyl vinyl ether (3-23) could dimerize in the presence of dimethyl terephthalate (3-24) ( $E^T = 73$  kcal/mol) and irradiation to give a mixture of syn and anti head-to-head cyclobutanes (3-25 and 3-26) (Scheme 3.8). Methyl benzoate ( $E^T = 78$  kcal/mol) and benzonitrile ( $E^T = 77$  kcal/mol) photosensitizers also effected this transformation.



Scheme 3.8. Dimerization of phenyl vinyl ether catalyzed by dimethyl terephthalate.

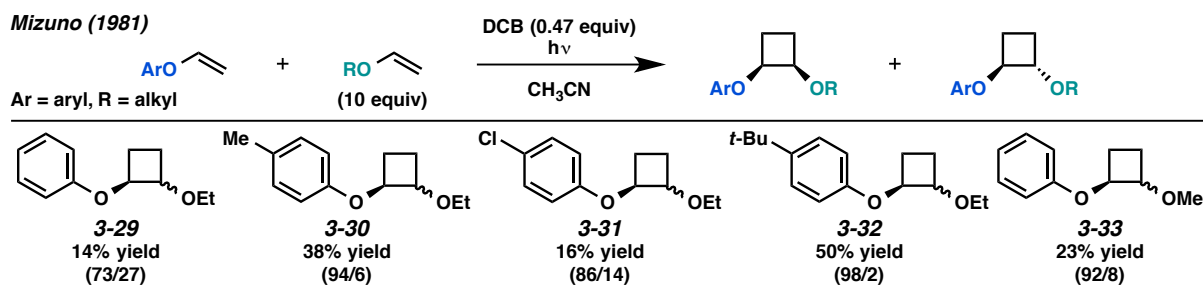
Further investigation into the mechanism indicated that the reaction was not proceeding through photosensitized energy transfer, since the triplet energies of the successful photosensitizers were lower than that of phenyl vinyl ether (3-23) ( $E^T = 80$  kcal/mol).<sup>20</sup> Instead, a donor-acceptor exciplex (3-27) was

invoked between the excited aromatic sensitizer (**3-24\***) and phenyl vinyl ether (**3-23**) (Scheme 3.9). These exciplexes are known to dissociate into ion pairs in polar solvents such as acetonitrile.<sup>21</sup> Dissociation of the exciplex affords a phenyl vinyl ether radical cation (**3-23<sup>•+</sup>**), which can be intercepted by another equivalent of phenyl vinyl ether to give cyclobutane radical cation **3-28<sup>•+</sup>**, and then the neutral cyclobutane products (**3-25** and **3-26**) upon single-electron reduction.



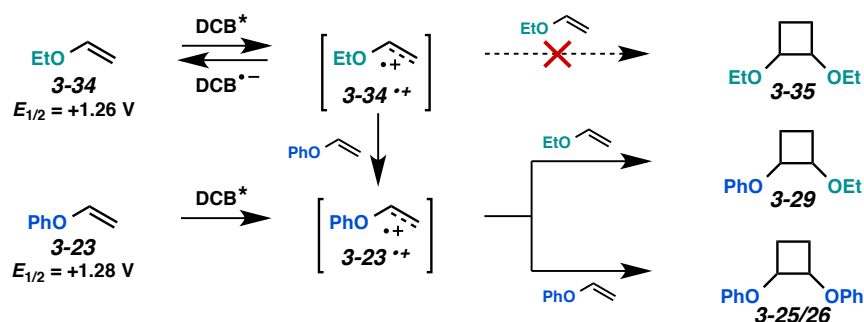
Scheme 3.9. Proposed mechanism for the dimerization of phenyl vinyl ether.

Besides dimerization, cross [2+2] cycloadditions between aryl vinyl ethers and alkyl vinyl ethers have also been accomplished. Mizuno and coworkers have reported that, in the presence of DCB and irradiation, various aryl vinyl ethers and alkyl vinyl ethers can react to form primarily syn head-to-head cyclobutanes (Scheme 3.10).<sup>22</sup>



Scheme 3.10. Cross [2+2] cycloadditions of vinyl ethers (syn/anti ratios in parentheses).

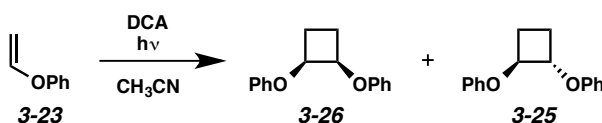
Curiously, though homodimerization of the aryl vinyl ethers was observed, no dimerization of the alkyl vinyl ether occurred. This is surprising considering DCB\* is capable of oxidizing both reactants. For example, the reduction potential of phenyl vinyl ether (**3-23**) is +1.28 V, and that of ethyl vinyl ether (**3-34**) is +1.26 V. Under the reaction conditions, however, only cross-adduct **3-29** and homodimer **3-25/26** of phenyl vinyl ether were formed; the dimer of ethyl vinyl ether (**3-35**) was not observed.<sup>23</sup> A possible explanation for why the alkyl vinyl ethers do not dimerize under radical cation conditions is that back electron transfer from the reduced photosensitizer or from another equivalent of phenyl vinyl ether is favored due to the instability of radical cation **3-34**<sup>•+</sup> compared to radical cation **3-23**<sup>•+</sup> (Scheme 3.11).



Scheme 3.11. Mechanism for the crossed [2+2] cycloaddition of vinyl ethers.

As mentioned, this process gave predominantly syn cyclobutanes. A closer look into this outcome by Mizuno and coworkers revealed the impact of concentration and temperature on stereoselectivity in the [2+2] cyclodimerization of phenyl vinyl ether.<sup>24</sup>

Mizuno (1983)

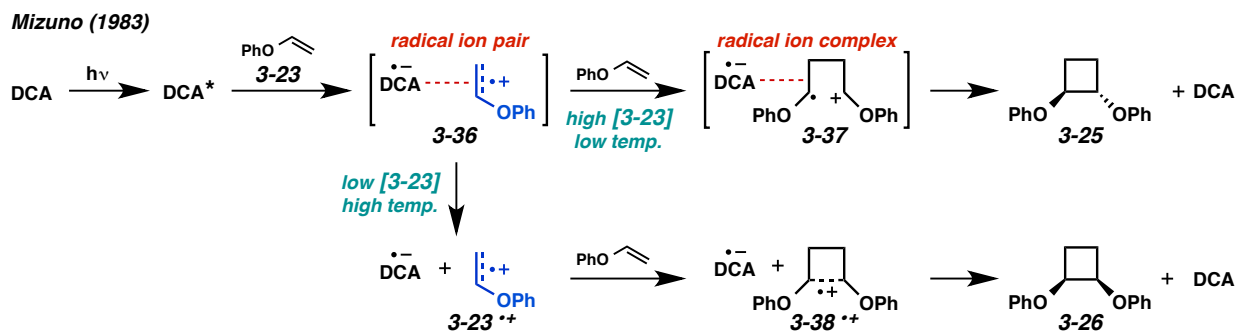


Effect of concentration			Effect of temperature <sup>a</sup>	
[ <b>3-23</b> ] (M)	syn/anti	$\phi$	temp. (K)	syn/anti
0.002	96:4	0.04	231	37:63
0.005	72:27	0.16	273	40:60
0.02	50:50	0.46	298	41:59
0.05	44:56	0.64	355	52:48
0.10	42:58	0.68	430	73:27
0.25	40:60	0.69		

<sup>a</sup> [**3-23**] = 0.20 M

Scheme 3.12. Effect of concentration and temperature on syn/anti ratio and quantum yield.

When the DCA photocatalyzed dimerization of phenyl vinyl ether was performed at low concentrations of the alkene, the syn cyclobutane (**3-26**) highly predominated (Scheme 3.12). At higher concentrations the anti isomer (**3-25**) was preferred, but a maximum syn/anti ratio of 40:60 was observed. Reaction temperature also influenced the stereochemical outcome of the dimerization. At elevated temperatures, the syn cyclobutane predominated, even at high concentrations. Additionally, the researchers found that the quantum yield of the reaction decreased with decreasing concentration of alkene **3-23**, indicating that different mechanisms were likely operative at low and high concentrations. These data led to the proposal of the mechanism in Scheme 3.13.

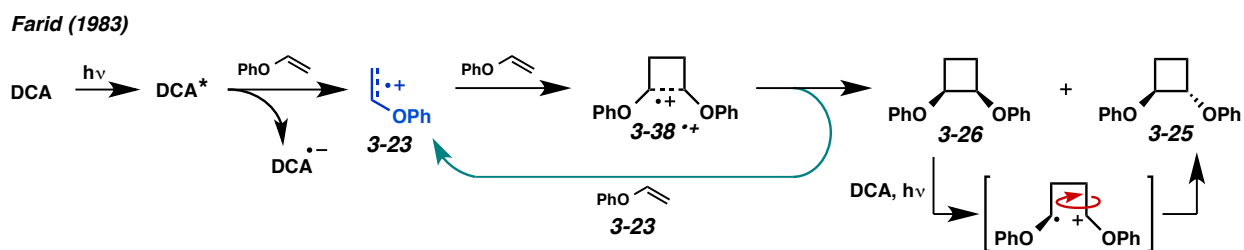


*Scheme 3.13.* Pathways to syn and anti cyclobutanes in the dimerization of phenyl vinyl ether.

When excited with light, DCA\* forms a contact radical ion pair (**3-36**) with phenyl vinyl ether (Scheme 3.13). When the concentration of phenyl vinyl ether (**3-23**) is high, this complex quickly reacts with another equivalent of phenyl vinyl ether to give the radical ion complex (**3-37**), and then the neutral cyclobutane dimer upon electron transfer. This pathway results in predominantly anti cyclobutane (**3-25**), perhaps due to the associated nature of the cyclobutane radical cation intermediate (**3-37**). Conversely, when the reaction is run at low concentrations, the contact radical ion pair is more likely to dissociate to the photosensitizer radical anion and the phenyl vinyl ether radical cation (**3-23<sup>•+</sup>**). When another equivalent of phenyl vinyl ether attacks the radical cation, a sandwich-type radical cation dimer forms (**3-38<sup>•+</sup>**), which is reduced by the DCA radical anion primarily to the syn cyclobutane (**3-26**). Increased

temperature also favors the formation of the syn product because dissociation of the contact radical ion pair is more facile.

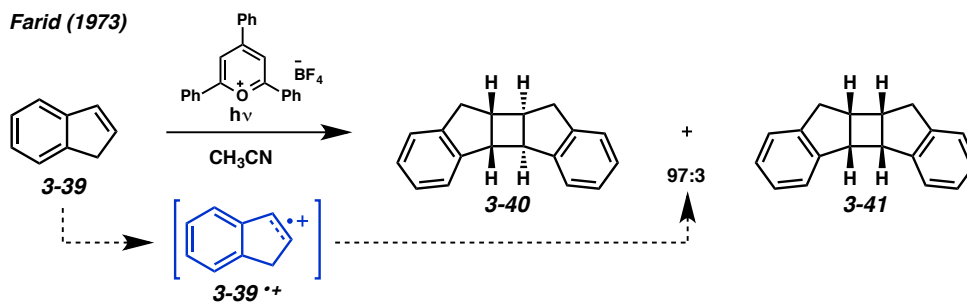
A subsequent report by Farid and coworkers disputes Mizuno's hypothesis that the anti cyclobutane (**3-25**) is a result of a radical ion pair complex (**3-37**).<sup>25</sup> Farid asserts that Mizuno's proposed mechanism does not take into account the radical chain nature of the reaction. The quantum yield of the dimerization of phenyl vinyl ether (**3-23**) has been reported as 0.84 and 1.24 at 0.1 M and 0.5 M, respectively, suggestive of chain propagation at higher concentrations where the anti product has been observed to predominate. The requirement of the radical ion pair complex (**3-37**) for the formation of the anti dimer is not consistent with a radical chain propagation mechanism, since the phenyl vinyl ether radical cation (**3-23<sup>•+</sup>**) is not generated in this process. Instead, Farid proposes that the reaction takes place through separated radical ion intermediates, and the predominance of the anti products at higher concentrations is a result of oxidative ring opening and isomerization of the syn product (**3-26**) to the anti product (**3-25**), as depicted in Scheme 3.14. Farid has shown that when the syn cyclobutane (**3-26**) is exposed to DCA and irradiation, it isomerizes to the anti cyclobutane (**3-25**). Under the same conditions, however, no isomerization of the anti cyclobutane to the syn cyclobutane occurs, likely because the anti product is more stable. In this scenario, the radical cation cycloadduct (**3-38<sup>•+</sup>**) is reduced by an equivalent of phenyl vinyl ether, generating the phenyl vinyl ether radical cation (**3-23<sup>•+</sup>**) and propagating the reaction.



*Scheme 3.14.* Farid's chain propagation mechanism for the dimerization of phenyl vinyl ether.

### 3.2.4 Styrene Derivatives

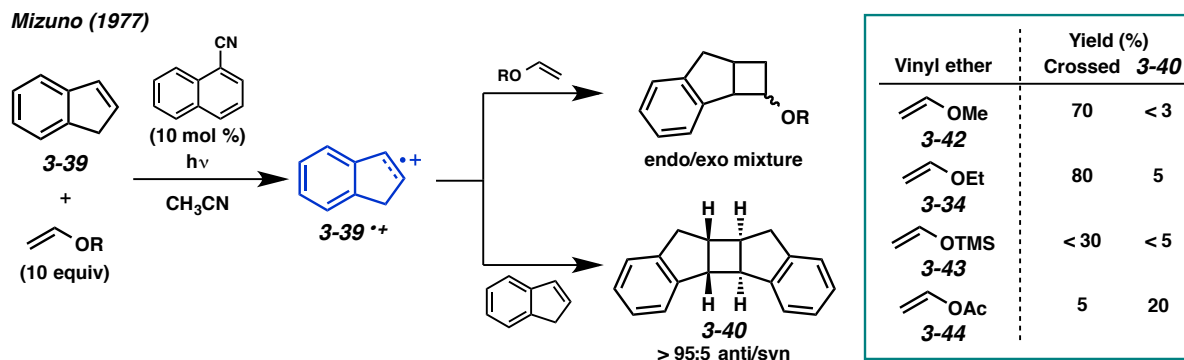
The radical cation dimerization of indene (**3-39**) ( $E_{1/2} = +1.63$  V) was first reported by Farid and Shealer in 1973.<sup>26</sup> Under photosensitization with TPT, alkene **3-39** dimerized almost exclusively to the corresponding anti head-to-head dimer (**3-40**) (Scheme 3.15). Triplet sensitization was ruled out as the cause of this reaction, since the triplet energy of TPT (53 kcal/mol) is lower than that of indene (60 kcal/mol). Additionally, the triplet sensitized dimerization of indene or dimerization through direct irradiation is known to yield all four possible adduct isomers,<sup>27</sup> but with TPT only the head-to-head isomers formed in a 97:3 anti/syn ratio. Interestingly, the authors note that the reaction was more efficient when performed under air, but degassing the reaction mixture did not affect the quantum yield. A radical chain mechanism similar to what was reported by Ledwith for the dimerization of *N*-vinylcarbazole (Scheme 3.4) was proposed.



Scheme 3.15. Dimerization of indene.

In 1977, Mizuno and coworkers developed a crossed [2+2] cycloaddition of indene with alkyl vinyl ethers.<sup>28</sup> Several alkyl vinyl ethers, as well as a trimethylsilyl (TMS) vinyl ether (**3-43**) reacted efficiently under photosensitization with 1-cyanonaphthalene to give the crossed cycloadducts and just trace amounts of the indene dimer (**3-40**) (Scheme 3.16). Only in the case of vinyl acetate (**3-44**) were considerable amounts of the indene dimer (**3-40**) formed, perhaps due to vinyl acetate's decreased nucleophilicity. Like with the crossed cycloadditions of aryl and alkyl vinyl ethers, the dimers of the alkyl

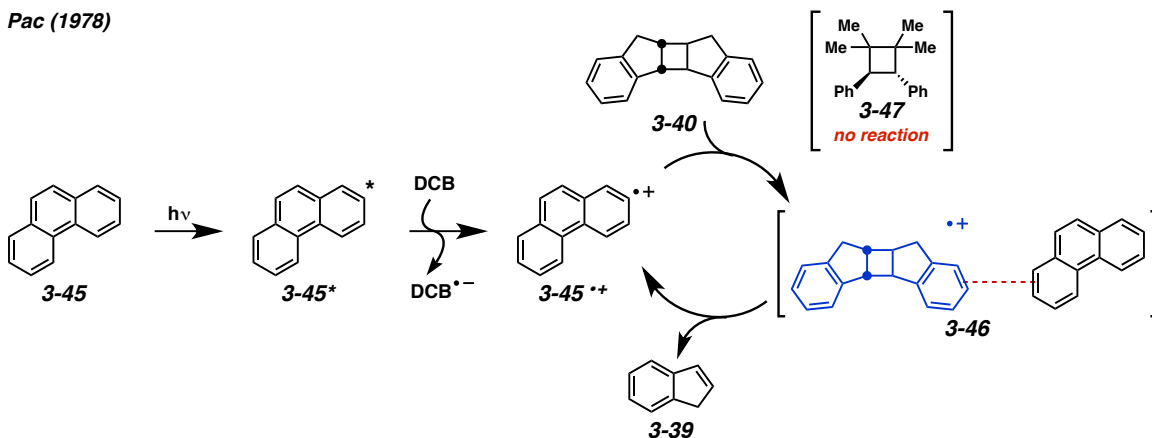
vinyl ethers were not observed. They also noted that the reaction was more efficient in acetonitrile compared to benzene, indicative of a radical cation process rather than triplet sensitization.



*Scheme 3.16.* Crossed [2+2] cycloadditions of indene and vinyl ethers.

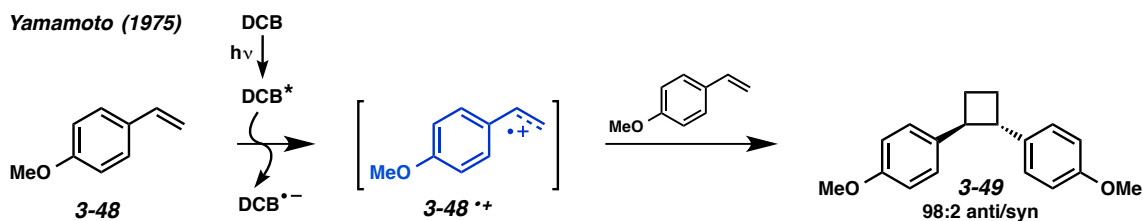
A radical chain mechanism has also been proposed for the retrocyclobutanation of the indene dimer. Pac and coworkers found that when dimer **3-40** was exposed to phenanthrene (**3-45**), DCB, and light in acetonitrile, indene (**3-39**) was formed through a retro [2+2] cycloaddition (Scheme 3.17).<sup>29</sup> The quantum yield for this process was determined to be 8.2, indicative of radical chain propagation. Though it seems as if DCB\* (+2.67 V) could oxidize the indene dimer (+1.35) and effect the retro [2+2], no reaction occurred in the absence of phenanthrene. It was noted that DCB could quench the excited state of phenanthrene, but the indene dimer could not, which led the authors to propose that the retrocyclobutanation is initiated through excitation of phenanthrene, and then electron transfer from the phenanthrene singlet (**3-45\***) to ground state DCB. The resulting phenanthrene radical cation (**3-45<sup>•+</sup>**) can then oxidize the indene dimer (**3-40**) and forms  $\pi$ -complex **3-46**; complete hole transfer from the phenanthrene radical cation to the dimer radical cation is not likely because of the lower reduction potential of phenanthrene (+1.26 V). Electron transfer results in cycloreversion to indene (**3-39**) and the phenanthrene radical cation (**3-45<sup>•+</sup>**), thus propagating the reaction. Interestingly, when cyclobutane **3-47** was exposed to the reaction conditions, no cycloreversion occurred. This lack of reactivity could be

because cyclobutane **3-47** is less strained than the indene dimer, or it could be due to the higher reduction potential of this substrate (+1.53 V).



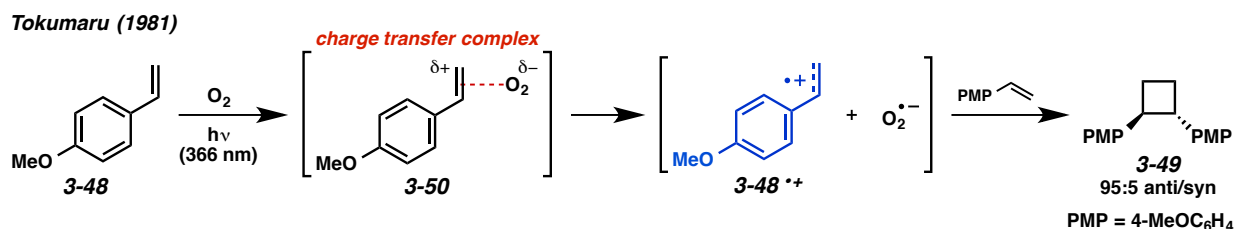
*Scheme 3.17.* Radical chain mechanism for the retrocyclobutanation of indene dimer.

The earliest report of the radical cation dimerization of 4-methoxystyrene came from Yamamoto and coworkers in 1975.<sup>30</sup> They observed that 4-methoxystyrene (**3-48**) could undergo a [2+2] cyclodimerization under DCB photosensitized conditions (Scheme 3.18). The anti dimer (**3-49**) was formed almost exclusively (98:2 anti/syn) at a rate of 13% yield per 10 h. Additionally, acetonitrile was an effective solvent for this transformation, but when the reaction was attempted in hexane or benzene, no dimer formed. A radical cation mechanism similar to what has been proposed previously also applies to this process.



*Scheme 3.18.* [2+2] dimerization of 4-methoxystyrene.

An interesting report by Tokumaru and coworkers describes the employment of molecular oxygen as a photosensitizer for the dimerization of 4-methoxystyrene (**3-48**).<sup>31</sup> Similar to Yamamoto's example with DCB, the O<sub>2</sub>-catalyzed process also preferentially provides the anti cyclobutane (**3-49**) (95:5 anti/syn). This high anti ratio is suggestive of a radical cation mechanism; dimerization through direct irradiation (254 nm) under nitrogen resulted in a 37:63 anti/syn cyclobutane ratio. Since *p*-anisaldehyde forms over the course of the reaction as well through oxidative cleavage of the alkene, the researchers considered whether *p*-anisaldehyde could be acting as a triplet sensitizer. When the dimerization was attempted under nitrogen in the presence of *p*-anisaldehyde and irradiation (313 nm), the cyclobutane (**3-49**) was formed, but in a 78:22 anti/syn ratio. This lower anti/syn ratio indicates that a different mechanism must be operative under the *p*-anisaldehyde/nitrogen atmosphere conditions compared to when the reaction was performed in the presence of O<sub>2</sub>. Thus, it is possible that the dimerization of alkene **3-48** is occurring partly through triplet sensitization with *p*-anisaldehyde, as well as excitation by direct irradiation, but a separate mechanism that involves O<sub>2</sub> is also operative, which leads to a higher anti/syn ratio. The authors propose that this radical cation pathway is proceeding through an O<sub>2</sub>-alkene charge transfer complex (**3-50**) (Scheme 3.19).

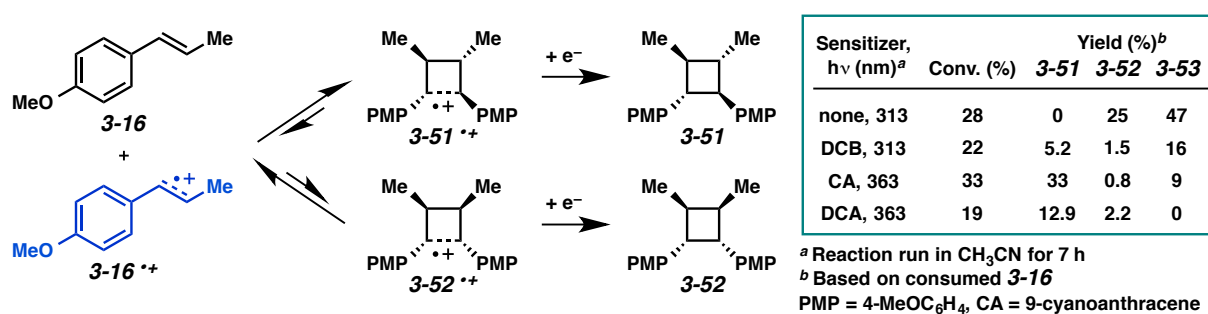


*Scheme 3.19.* Oxygen-mediated radical cation dimerization of 4-methoxystyrene.

Evidence for this O<sub>2</sub>-alkene complex (**3-50**) is provided by an absorption band at 320-370 nm that appears on the UV/Vis spectrum of 4-methoxystyrene (**3-48**) when the acetonitrile solution is saturated with O<sub>2</sub> and disappears when the system is flushed with argon. The use of 366 nm light for the dimerization thus selectively excites the O<sub>2</sub>-alkene complex, preventing direct excitation of the alkene

substrate, which would result in a lower anti/syn ratio. Essentially no reaction was observed when the dimerization was attempted with 366 nm light under nitrogen. Interestingly, in benzene, a charge-transfer band for the O<sub>2</sub>-alkene complex was also observed, but no dimerization of the styrene occurred. This result is likely due to the difficulty of generating radical ions in a nonpolar solvent.

The radical cation [2+2] dimerization of *trans*-anethole has also been reported under photosensitization with cyanoarenes by Lewis and Kojima in 1988.<sup>32</sup> *trans*-Anethole (**3-16**) dimerizes to cyclobutanes **3-51** and **3-52**, where dimer **3-51** is favored under radical cation conditions (Scheme 3.20). The researchers propose that cycloreversion of the cyclobutane radical cations and recombination is what allows the more stable all-anti cyclobutane to predominate. *cis*-Anethole (**3-53**) can also form under these conditions, but no cyclobutane products derived from cycloaddition with *cis*-anethole were detected.



Scheme 3.20. Dimerization of *trans*-anethole.

The *cis* alkene (**3-53**) also dimerizes under radical cation conditions, but in this case, five cyclobutane isomers can form: two from the cycloaddition of *cis*-anethole with the *cis*-anethole radical cation (**3-53**<sup>•+</sup>), two from the cycloaddition of *cis*-anethole with the *trans*-anethole radical cation (**3-16**<sup>•+</sup>), which forms *in situ* under the photosensitization conditions, and cyclobutane **3-51** which results from the reaction of the isomerized *trans*-anethole with its radical cation (Scheme 21a). Cyclobutane **3-55** is greatly favored over the all-syn isomer (**3-54**); however, cyclobutane **3-57** is formed over cyclobutane **3-56** with slightly less preference. Because the isomerization can occur in both polar and nonpolar solvents, the isomerization of *cis*-anethole to *trans*-anethole is thought to proceed via a triplet state (**3-58**).

Formation of the *cis*-anethole radical cation (**3-53**<sup>•+</sup>) followed by reverse electron transfer creates a triplet 1,2-diradical (**3-58**), which can rotate and recombine to form *trans*-anethole (**3-16**) (Scheme 21b).

a.

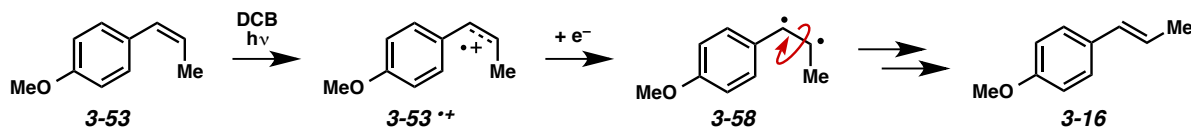
Sensitizer, hν (nm) <sup>a</sup>	Conv. (%)	Yield (%) <sup>b</sup> : 3-54	3-55	3-56	3-57	3-51	3-16
none, 313	12	0	0	17	14	0	20
DCB, 313	21	0	2.1	0.4	3.5	1.2	25
CA, 363	27	0	1.7	0.2	3.3	1.2	1
DCA, 363	21	0	0.8	N/A	1.6	0.6	0

<sup>a</sup> Reaction run in CH<sub>3</sub>CN for 7 h

PMP = 4-MeOC<sub>6</sub>H<sub>4</sub>, CA = 9-cyanoanthracene

<sup>b</sup> Based on consumed **3-53**

b. Isomerization of *cis*- to *trans*-anethole



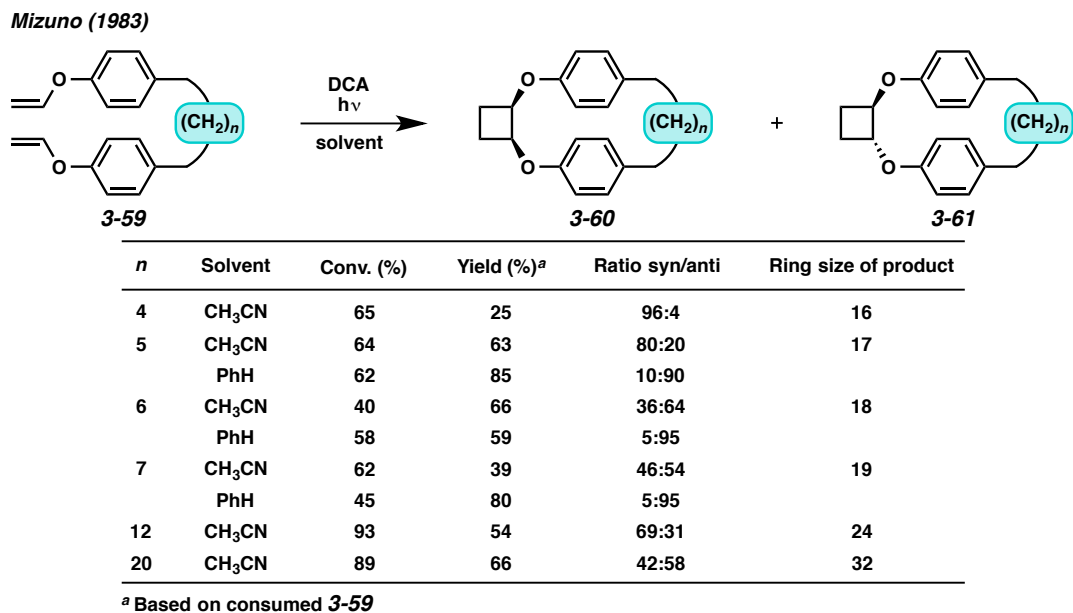
Scheme 3.21. Dimerization and isomerization of *cis*-anethole.

### 3.2.5 Intramolecular [2+2] Cycloadditions

Intramolecular variants have also been developed. The [2+2] cycloaddition of tethered aryl vinyl ethers (**3-59**) is an efficient method for the construction of macrocycles. Mizuno and coworkers have demonstrated that up to a 32-membered ring can be made through this method in respectable yield (Scheme 3.22).<sup>33</sup> Cyclobutane-containing crown ethers can also be synthesized through the intramolecular [2+2] cycloaddition of ether-linked alkenes.<sup>34</sup>

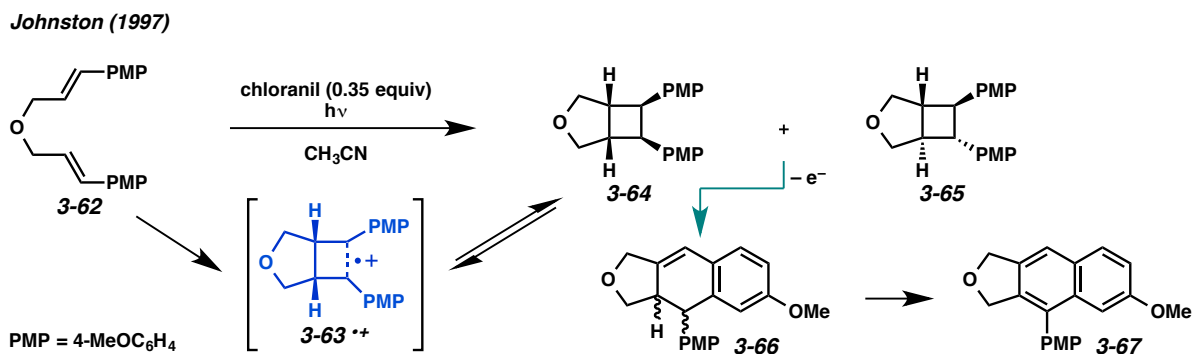
Interestingly, the syn/anti ratios of these cyclobutanes were greatly influenced by solvent. In acetonitrile, the syn isomers (**3-60**) predominated, but in benzene, the anti isomers (**3-61**) predominated. Though the source of this stereochemical preference is not clear, slightly different mechanisms are likely operative in each solvent, leading to syn products being favored in the more polar solvent (acetonitrile)

and anti products being favored in the less polar solvent (benzene). With two of the substrates ( $n = 6, 7$ ), the anti product was favored even in acetonitrile, likely due to conformational stipulations.



Scheme 3.22. Solvent effects on stereoselectivity in the [2+2] cycloaddition of tethered vinyl ethers.

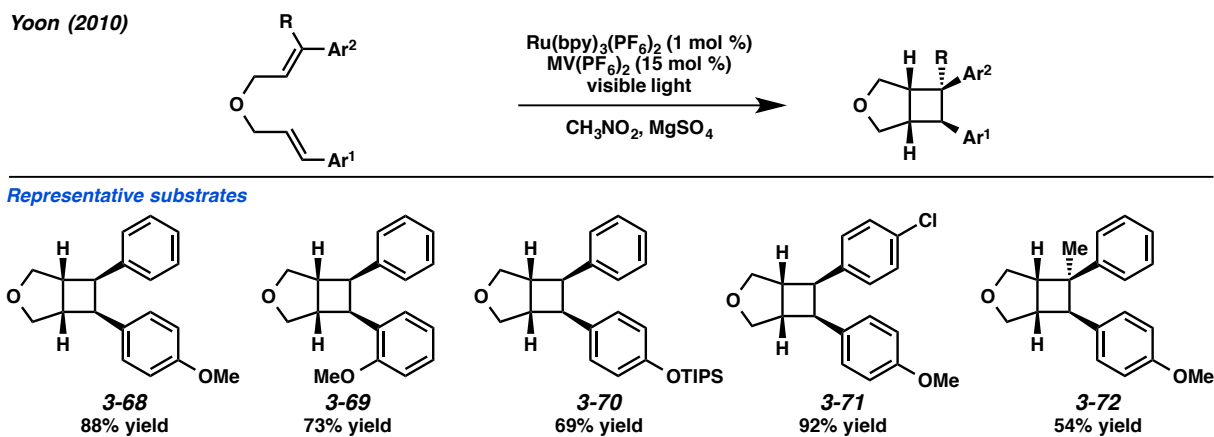
An intramolecular [2+2] cycloaddition of styrenyl alkenes has also been developed. In 1997, Johnston and coworkers reported that oxygen-tethered diene **3-62**, when exposed to chloranil and 350 nm light, cyclized mainly to cyclobutanes **3-64** and **3-65** (Scheme 3.23).<sup>35</sup> Anti isomer **3-65** was formed as a minor product, and is believed to be a result of a triplet 1,2-diradical isomerization of one of the tethered alkenes, analogous to the isomerization of *cis*- to *trans*-anethole, followed by a direct photoinduced [2+2] cycloaddition. Interestingly, at longer irradiation times, cyclohexenes **3-66** and **3-67** were also observed. The formation of these cyclohexenes occurred concurrently with the depletion of the cyclobutanes, indicating that they were forming through rearrangement of the initial formed [2+2] product. This rearrangement is a fairly common occurrence in radical cation [2+2] cycloadditions, especially with styrene-derived alkenes, and will be discussed in greater detail later.



Scheme 3.23. Intramolecular [2+2] cycloaddition and rearrangement.

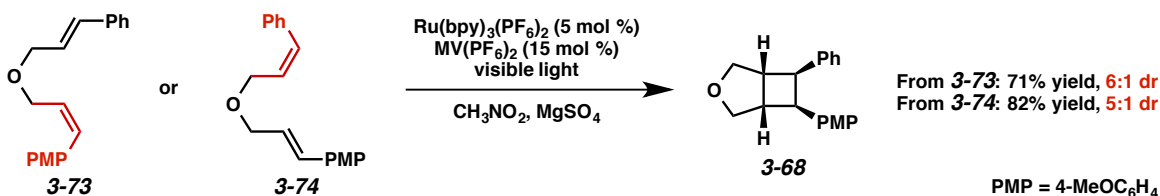
### 3.2.6 Recent Reports of Radical Cation [2+2] Cycloadditions

In 2010, Yoon and coworkers reported the intramolecular [2+2] cycloaddition of tethered styrenyl alkenes using a  $\text{Ru}(\text{bpy})_3(\text{PF}_6)_2/\text{MV}(\text{PF}_6)_2$  photocatalytic system with visible light (MV = methyl viologen).<sup>36</sup> The substrate scope of this transformation was extensively explored (Scheme 3.24). Though it was found that one of the two alkenes needed to be substituted with an aryl group containing an electron-donating group at the *ortho* or *para* position in order for radical cation formation to occur ( $\text{Ar}^1$ ), substitution at the other alkene was less restricted with both electron-rich and electron-poor aryl substitution tolerated ( $\text{Ar}^2$ ). Alkyl substituted alkenes, however, did not react in the [2+2] cycloaddition.



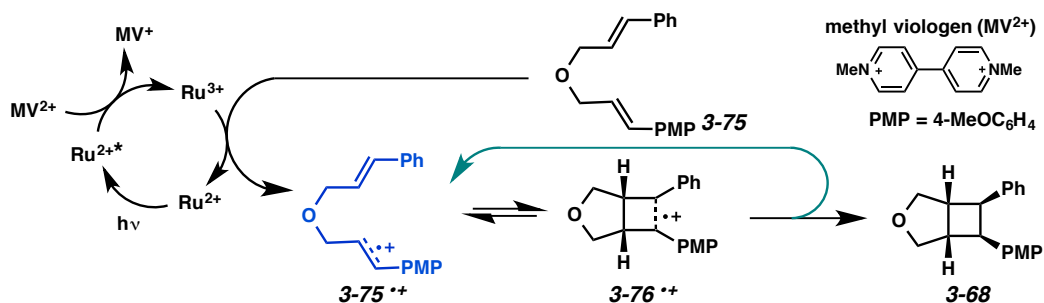
Scheme 3.24. Yoon's oxidative intramolecular [2+2] cycloaddition.

This transformation was also found to be stereoconvergent. When substrates **3-73** and **3-74**, in which one of the tethered alkenes is *cis*, were exposed to the Ru conditions, still the major product was the *syn* cyclobutane **3-68** (Scheme 3.25). The authors determined that the *cis* alkenes were likely isomerizing prior to the cycloaddition and that the cycloaddition itself is stereospecific.



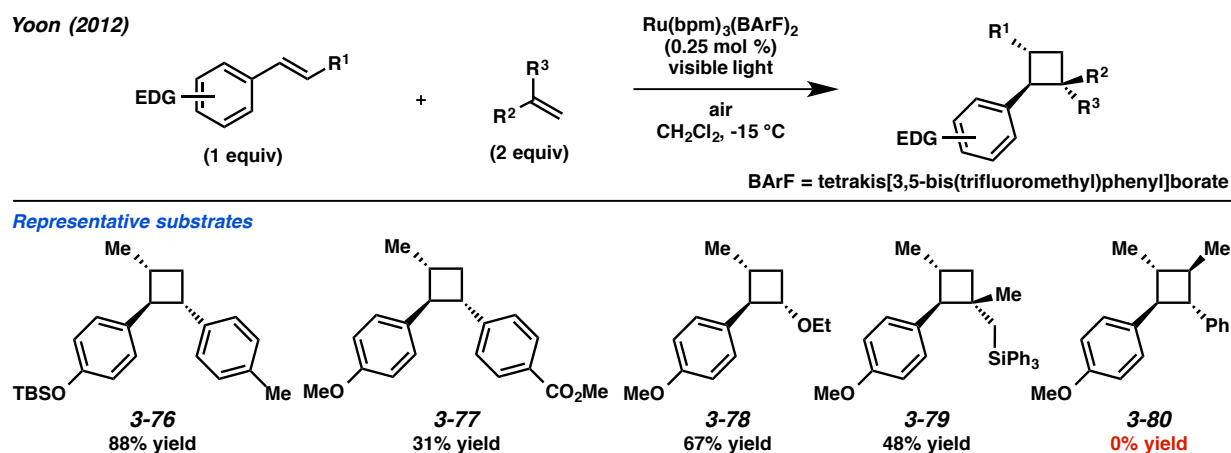
Scheme 3.25. Stereoconvergence in the intramolecular [2+2] cycloaddition.

Thus, the mechanism in Scheme 3.26 is proposed. When Ru(bpy)<sub>3</sub><sup>2+</sup> is irradiated with 450 nm light, the excited state Ru<sup>2+\*</sup> complex forms. This species can then donate an electron to methyl viologen to generate Ru<sup>3+</sup>, which abstracts an electron from the electron-rich alkene (**3-75**) to generate the radical cation (**3-75<sup>•+</sup>**) and the ground state Ru<sup>2+</sup> catalyst. Subsequent attack by the tethered alkene, then reduction with another equivalent of substrate forms the neutral cyclobutane product (**3-68**) and propagates the reaction. Notably, different from the intramolecular [2+2] cycloaddition reported by Johnston using chloranil (Scheme 3.23), with the Ru photocatalytic system, no formation of the rearranged cyclohexene products was observed.



Scheme 3.26. Proposed mechanism for intramolecular radical cation [2+2] cycloaddition.

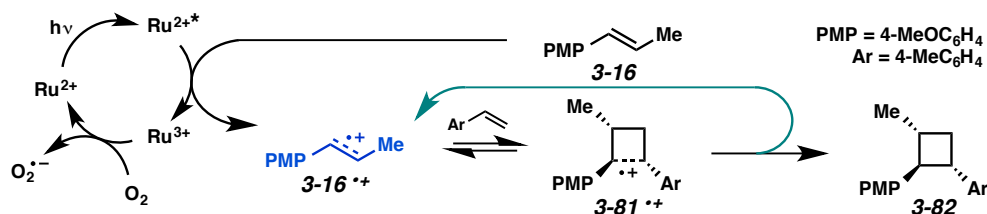
Yoon and coworkers also explored an intermolecular radical cation [2+2] cycloaddition of styrene derivatives.<sup>37</sup> Using  $\text{Ru}(\text{bpm})_3^{2+}$  under air and visible light irradiation, various [2+2] cycloadditions were achieved (Scheme 3.27). As in the intramolecular case, one of the cyclizing alkenes had to be substituted with an electron-rich aryl group in order for it to be oxidized by the catalyst. Exploring the scope of the cycloaddition partner, styrene derivatives with differential substitution on the aryl ring were successfully cyclized (**3-76**). Substrates containing electron-poor substituents (**3-77**) reacted slowly, which allowed for considerable homodimerization of *trans*-anethole to occur. This could be remedied in part by slow addition of *trans*-anethole. Non-aryl alkenes ethyl vinyl ether and an allylsilane also underwent the cycloaddition (**3-78** and **3-79**). Surprisingly, the cycloaddition between *trans*-anethole and  $\beta$ -methylstyrene was not successful (**3-80**).



Scheme 3.27. Yoon's intermolecular [2+2] cycloaddition.

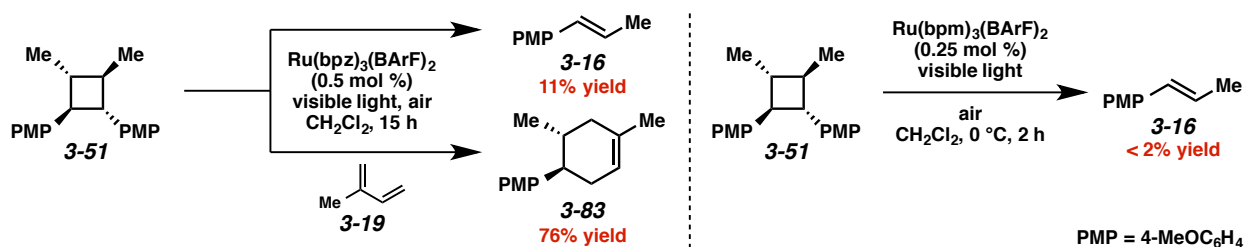
A similar reaction mechanism to its intramolecular counterpart is proposed (Scheme 3.28). With  $\text{Ru}(\text{bpm})_3^{2+}$ , however, the excited state  $\text{Ru}^{2+*}$  directly oxidizes *trans*-anethole (**3-16**) to its radical cation (**3-16<sup>•+</sup>**). Cyclization with the alkene gives cyclobutane radical cation **3-81<sup>•+</sup>**, which can abstract an electron from another *trans*-anethole equivalent to propagate the reaction and give the neutral product (**3-82**). The authors note that oxygen has an accelerating effect on the cycloaddition; in the absence of

oxygen, only 7% of cyclobutane **3-82** is observed in 1 h vs. 86% yield in 1 h in the presence of air. They propose that oxygen may be mediating catalyst turnover, as shown in Scheme 3.28.



Scheme 3.28. Proposed mechanism for intermolecular [2+2] cycloaddition.

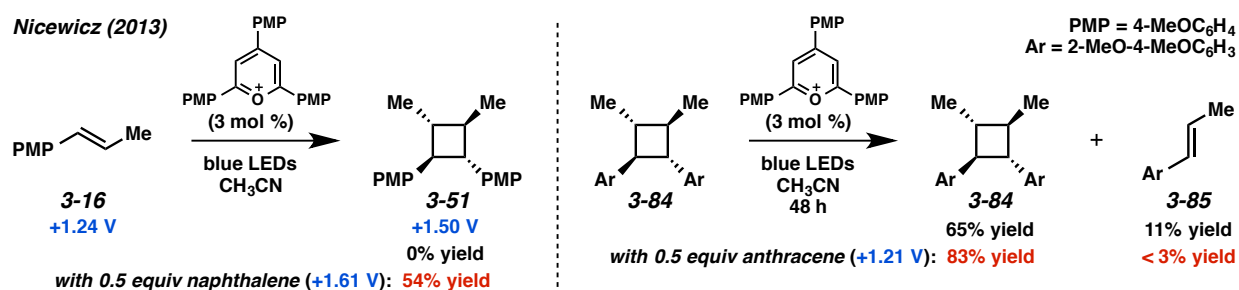
An important aspect of this transformation is the undesired propensity of the cyclobutane products to cyclorevert under the reaction conditions. When the dimerization of *trans*-anethole (**3-16**) (+1.24 V) was performed using the more strongly oxidizing  $\text{Ru}(\text{bpz})_3^{2+}$  ( $E_{1/2}^* = +1.45$  V), lower yields were observed. Exposing dimer **3-51** to the  $\text{Ru}(\text{bpz})_3^{2+}$  conditions revealed that cycloreversion was occurring; in the presence of isoprene (**3-19**), the resulting *trans*-anethole could be trapped as cyclohexene **3-83** through a radical cation [4+2] cycloaddition (Scheme 3.29). The lower reduction potential of  $\text{Ru}(\text{bpm})_3^{2+}$  ( $E_{1/2}^* = +1.20$  V) compared to  $\text{Ru}(\text{bpz})_3^{2+}$  apparently allows for selective oxidation of *trans*-anethole over the cyclobutane product (**3-51**) (+1.27 V), thereby preventing cycloreversion. To demonstrate this effect, cyclobutane **3-51** was exposed to  $\text{Ru}(\text{bpm})_3^{2+}$  at 0 °C for 2 h. Though the reduction potential of  $\text{Ru}(\text{bpm})_3^{2+}$  and cyclobutane **3-51** are still fairly close, only trace *trans*-anethole (**3-16**) was formed, confirming their hypothesis.



Scheme 3.29. Cycloreversion under Ru photocatalysis.

Nicewicz and coworkers have also emphasized the susceptibility of aryl-substituted cyclobutanes to undergo cycloreversion under oxidative conditions in their report on [2+2] dimerization of styrene derivatives and other electron-rich alkenes using 2,4,6-tris(4-methoxyphenyl)pyrylium tetrafluoroborate (TAP).<sup>38</sup> While Yoon focused on tuning the electrochemical properties of the photocatalyst in order to avoid cycloreversion, Nicewicz demonstrates that an “electron relay” reagent can be employed to prevent reoxidation and cycloreversion of the cyclobutane product.

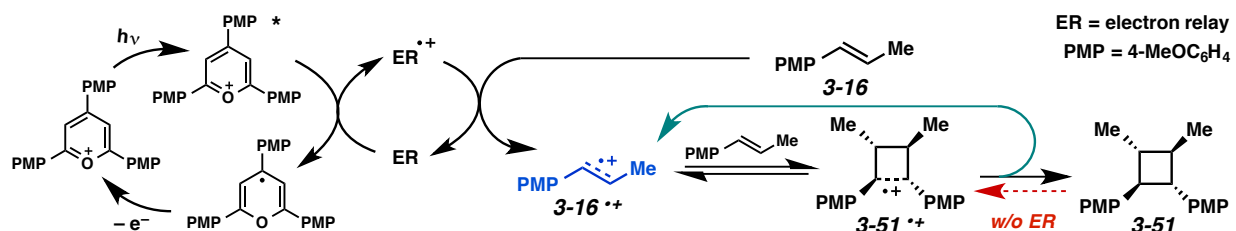
The concept behind the electron relay is that the presence of an oxidizable species with a higher reduction potential than the alkene, but a lower reduction potential than the product will allow the alkene to be oxidized and undergo the [2+2] cycloaddition, but will compete with the product for oxidation. Thus, reoxidation and cycloreversion of the cyclobutane will be less likely. For example, the reduction potentials of *trans*-anethole (**3-16**) and its dimer cyclobutane (**3-51**) are +1.24 V<sup>39</sup> and +1.50 V, respectively. The reduction potential of TAP\* is +1.74 V, so it could easily oxidize both *trans*-anethole and the dimer. When the dimerization of *trans*-anethole is performed only with the photocatalyst, 0% yield of the cyclobutane dimer is obtained, perhaps due to oxidation and cycloreversion (Scheme 3.30). When 0.5 equiv of naphthalene (+1.61 V) is added, however, the product (**3-51**) is isolated in 54% yield.



Scheme 3.30. Inhibition of cycloreversion using electron relay reagent.

Furthermore, when cyclobutane **3-84** is exposed to the photocatalyst without an electron relay reagent, 11% yield of the corresponding alkene (**3-85**) is formed, and only 65% of the cyclobutane is recovered. When the same reaction is performed, but with 0.5 equiv of anthracene (+1.21 V) added, <3%

yield of alkene **3-85** forms and 83% yield of the cyclobutane is recovered. These experiments prove that the electron relay reagents can indeed protect the cyclobutane products from cycloreversion or oxidative degradation.



Scheme 3.31. Electron relay mechanism for dimerization of *trans*-anethole.

The electron relay mechanism is depicted in Scheme 3.31. Though it would seem as if the excited photocatalyst could oxidize the alkene directly, the authors propose that the photocatalyst oxidizes the electron relay reagent (ER) instead, creating a radical cation (ER<sup>•+</sup>) that then oxidizes the electron-rich alkene (**3-16**). Cyclization of the alkene radical cation (**3-16**<sup>•+</sup>) gives the cyclobutane radical cation (**3-51**<sup>•+</sup>), which can then be reduced by either the electron relay reagent or another alkene equivalent to give the neutral cyclobutane product (**3-51**), which should not be reoxidized to a great extent in the presence of the electron relay reagent.

This electron relay strategy allowed the researchers to synthesize a number of electron-rich cyclobutanes. Notably, this methodology was exploited to access cyclobutane lignan natural products (**3-86–3-88**), which have significant bioactive properties (Figure 3.2).<sup>40</sup>

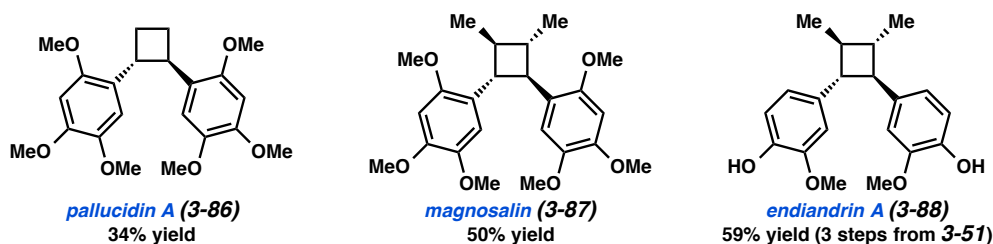
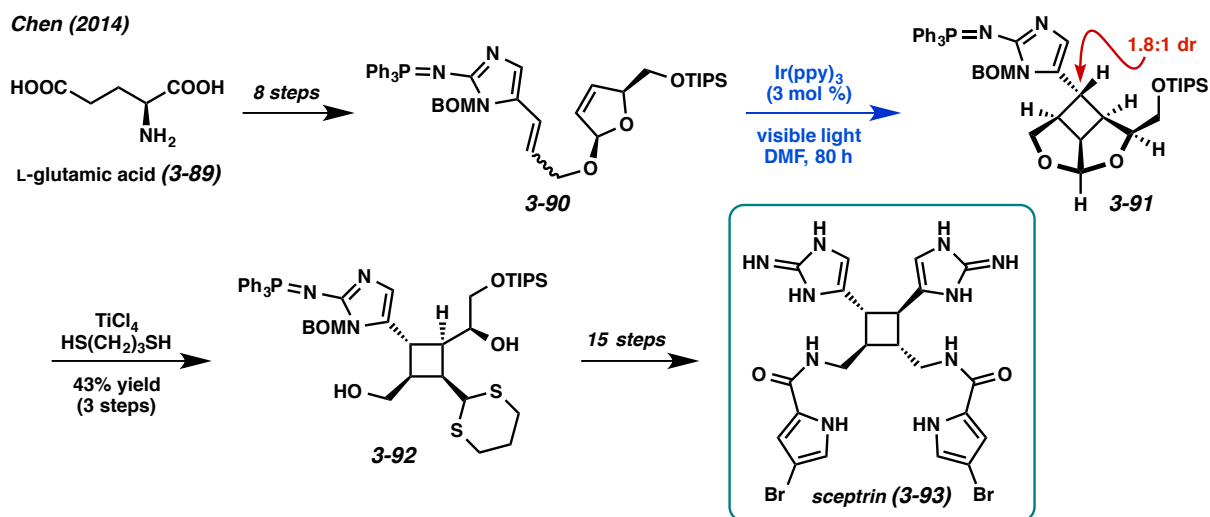


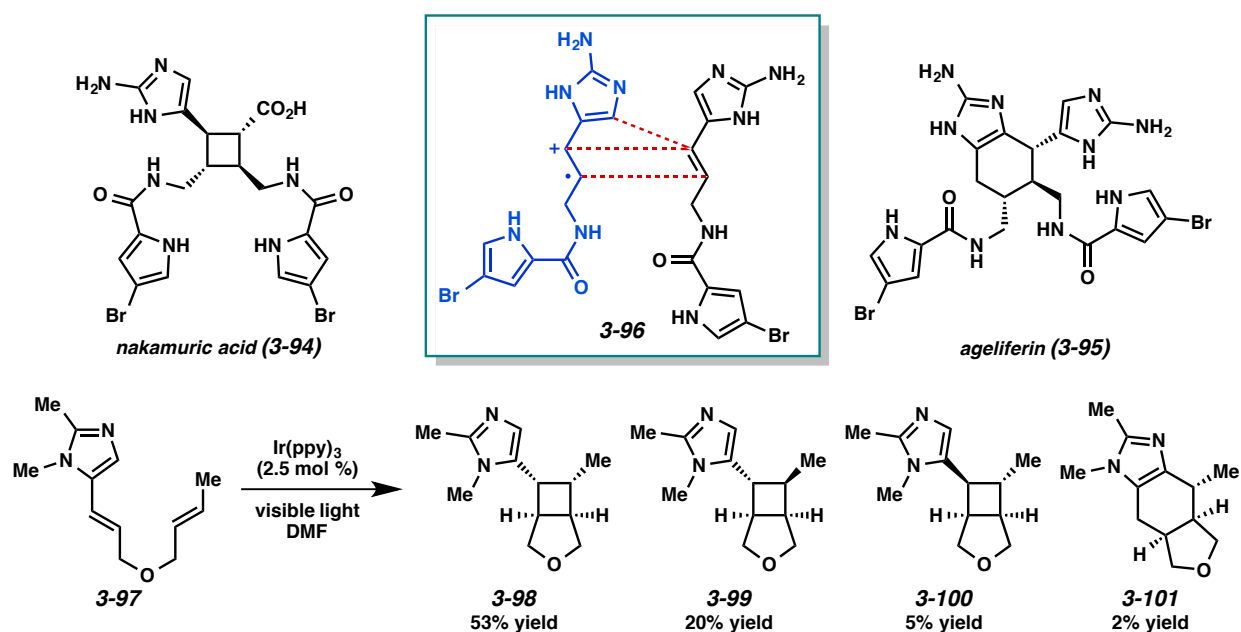
Figure 3.2. Cyclobutane lignan natural products.

In another example of natural product synthesis, Chen and workers have employed an Ir(ppy)<sub>3</sub>-catalyzed radical cation [2+2] cycloaddition in the asymmetric total synthesis of sceptrin (**3-93**).<sup>41</sup> Sceptrin belongs to a family of dimeric pyrrole-imidazole alkaloids that have been isolated from marine sponges. The biosynthesis of sceptrin is not well understood; however, since the sponges live deep under water, it is unlikely that enough light can reach them in order for the cyclobutane core of these alkaloids to be constructed through a photochemical [2+2] cycloaddition.<sup>42</sup> Instead, it has been proposed that the cyclobutane may form through an enzyme-promoted single-electron transfer mechanism.<sup>43</sup> In an effort to mimic the biosynthesis, Chen developed a synthesis of sceptrin (**3-93**) employing a radical cation [2+2] cycloaddition to construct the skeletal core. Starting from L-glutamic acid (**3-89**) as the chirality source, intermediate **3-90** was reached in 8 steps (Scheme 3.32). When this tethered alkene was exposed to Ir(ppy)<sub>3</sub> and visible light, cyclobutane **3-91** was formed in 1.8:1 dr. Other single-electron oxidants were attempted, but these resulted in substrate decomposition. Triplet sensitization was ruled out as a potential mechanistic pathway, since fluorenone, which has a similar triplet energy as the Ir catalyst ( $E^T = 55$  kcal/mol), did not succeed in catalyzing the [2+2] cycloaddition. Further synthetic manipulations provided enantiopure sceptrin (**3-93**).



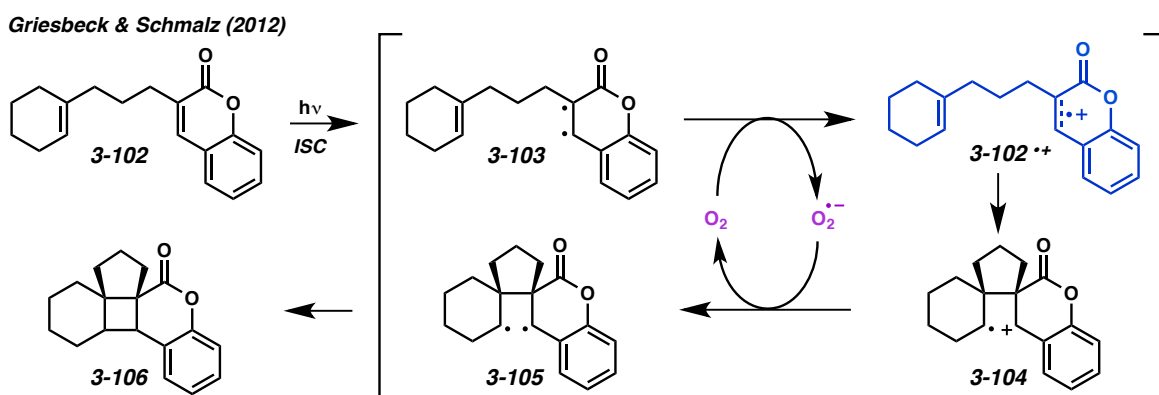
Scheme 3.32. Chen's total synthesis of sceptrin.

A further report by Chen in 2015 explored the use of this method for the synthesis of similar pyrrole-imidazole alkaloids, such as nakamuric acid (**3-94**) (Scheme 3.33).<sup>44</sup> In addition, according to the previously mentioned biosynthetic hypothesis, 6-membered ring derivatives such as ageliferin (**3-95**) could also come about from the same single-electron oxidation process (**3-96**). Alkene **3-97** was designed as a test substrate. When this tethered alkene was exposed to the Ir(ppy)<sub>3</sub> conditions, four different products formed. The major desired product (**3-98**) was formed in 53% yield, and its epimer (**3-99**) was formed in 20% yield. Another diastereomer (**3-100**), which is proposed to arise from isomerization of the vinylimidazole alkene prior to the cycloaddition, was formed in 5% yield. Lastly, cyclohexane **3-101** containing the skeleton of ageliferin (**3-95**) was formed in 2% yield. The authors note that the ratio of these four products did not change over the course of the reaction, indicating that they were formed directly from substrate **3-97** and not through subsequent reoxidation and rearrangement. The researchers also attempted various intermolecular [2+2] cycloadditions of vinylimidazole derivatives, but they were unsuccessful; the oxygen tether was required for reactivity.



Scheme 3.33. Further exploration toward the synthesis of dimeric pyrrole-imidazole alkaloids.

Lastly, in 2012, Griesbeck and Schmalz demonstrated that the intramolecular [2+2] cycloaddition of  $\alpha,\beta$ -unsaturated carbonyls and alkenes, which is traditionally accomplished through high energy UV irradiation,<sup>45</sup> could be induced using visible light in the presence of  $O_2$ .<sup>46</sup> This transformation is different from other PET reactions, however, in that the substrate is excited by light, rather than the electron-accepting reagent. Upon excitation of the  $\alpha,\beta$ -unsaturated carbonyl (**3-102**) and intersystem crossing to the triplet 1,2-diradical (**3-103**), triplet oxygen can abstract an electron from the coumarin to give a radical cation (**3-102<sup>•+</sup>**), which is intercepted by the tethered alkene, forming distonic radical cation **3-104** (Scheme 3.34). The reduced superoxide can then transfer an electron back to the substrate to afford the diradical (**3-105**), which closes to cyclobutane **3-106**. Thus,  $O_2$  acts as a redox catalyst.



*Scheme 3.34.* Proposed mechanism for the oxygen-mediated [2+2] cycloaddition of tethered alkenes.

Several different substrates were examined under Ar and  $O_2$  conditions (Table 3.2). When the reactions were performed under Ar, very slow conversion was observed. Under  $O_2$ , however, the rate of the reaction was greatly accelerated, supporting the hypothesis that  $O_2$  was acting as an electron transfer catalyst. Additionally, though it is unclear exactly why, when 5 mol % 3,5-di-*tert*-butyl-4-hydroxytoluene (BHT) was added to the  $O_2$  reaction, efficiency was further increased. An exception was substrate **3-110**, which reacted efficiently even under Ar. The authors propose that with this substrate, intramolecular electron transfer is more favorable, and  $O_2$  is not required to mediate this process. Interestingly, the

cycloaddition of enone **3-113**, which has been reported by Yoon to occur under reductive photocatalytic  $\text{Ru}(\text{bpy})_3^{2+}$  conditions,<sup>47</sup> could also be effected by this oxidative system.

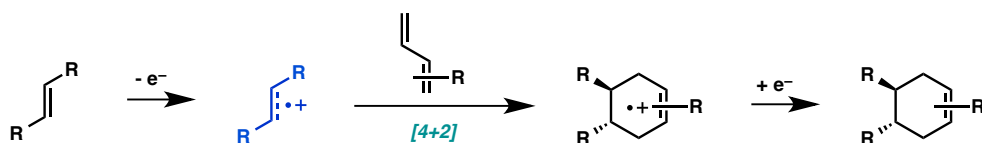
Table 3.2. Effect of different atmospheres on reaction efficiency.

Substrates					
Products					
Conditions:	$\text{CH}_2\text{Cl}_2$ , white light				
Atmosphere	Conversion <sup>a</sup> (24 h)	(96 h)	(24 h)	(4 h)	(24 h)
Ar	5	22	15	44 (85) <sup>b</sup>	21
O <sub>2</sub>	79	59	31	34	32
O <sub>2</sub> + BHT	86 (81)	84 (69)	61 (90) <sup>b</sup>	36	37 (36)

<sup>a</sup> Isolated yield in parentheses (%)

<sup>b</sup> Reaction run to completion, then isolated

### 3.3 [4+2] Radical Cation Cycloadditions



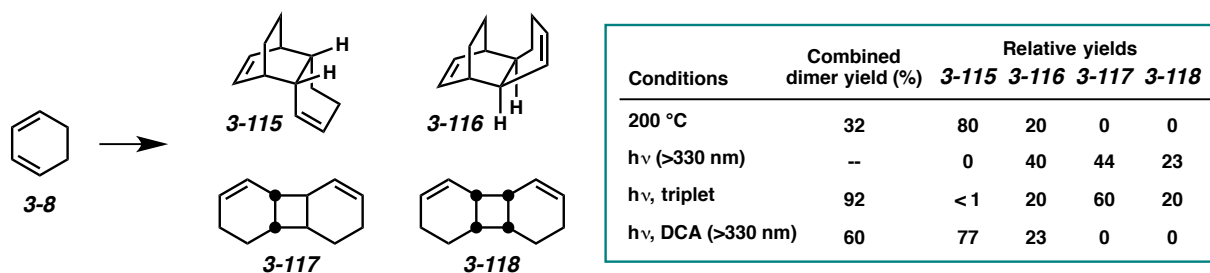
Scheme 3.35. General radical cation [4+2] cycloaddition.

Radical cation [4+2] cycloadditions with organic photosensitizers or transition metal photocatalysts can be achieved when at least one of the cycloaddition partners is a diene or styrenyl alkene (Scheme 3.35). Since the [4+2] mechanism essentially diverges from the [2+2] mechanism, [2+2] cycloadducts are sometimes observed as minor products. This section will discuss examples in which the periselectivity of the cycloaddition greatly favors the [4+2] adducts.

### 3.3.1 Dimerization of 1,3-Dienes

A commonly explored radical cation [4+2] cycloaddition is the dimerization of 1,3-dienes. In particular, the dimerization of 1,3-cyclohexadiene (**3-8**) has been extensively studied as the prototypical diene dimerization.<sup>48</sup> This transformation can be effected using a number of different single-electron oxidation methods.<sup>8a,8b,49</sup> The PET radical cation dimerization of 1,3-cyclohexadiene is especially intriguing due to the competing triplet sensitized and direct irradiation-induced dimerizations, both of which lead to different product mixtures.

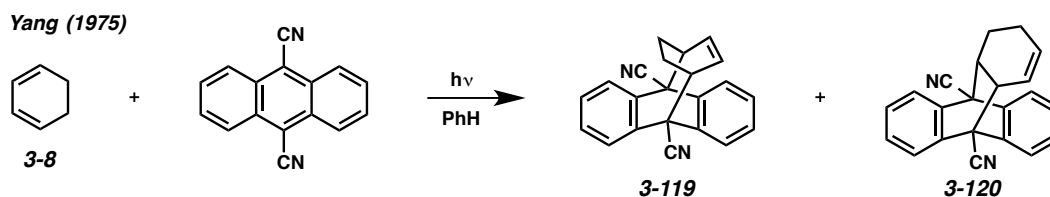
Jones and coworkers reported in 1983 that the products obtained by DCA-photosensitized dimerization of 1,3-cyclohexadiene (**3-8**) were different than those previously reported through other methods (Scheme 3.36).<sup>50</sup> Thermal conditions (200 °C), as expected, afford the [4+2] adducts (**3-115** and **3-116**) in a 4:1 endo/exo ratio.<sup>51</sup> Direct irradiation (>330 nm)<sup>52</sup> or triplet sensitization<sup>53</sup> provide a mixture of the [2+2] adducts (**3-117** and **3-118**), as well as the exo [4+2] adduct (**3-116**). Radical cation photosensitization, however, using DCA and >330 nm light in dichloromethane resulted in only the [4+2] adducts, in an 77:23 endo/exo ratio (**3-115/3-116**).



Scheme 3.36. Dimerization of cyclohexadiene product distribution under different conditions.

Jones proposed that the reaction may be proceeding through an exciplex complex between the sensitizer and the diene, which could break apart into radical ions in polar solvent to initiate the radical cation cycloaddition, similar to the non-photochemical versions. Additionally, Yang and coworkers have

previously reported that under irradiation in benzene, cyclohexadiene could react with DCA to give adducts **3-119** and **3-120**.<sup>54</sup> This supports the hypothesized exciplex formation where the radical ions can dissociate in polar solvents, but remain complexed in less polar solvents.

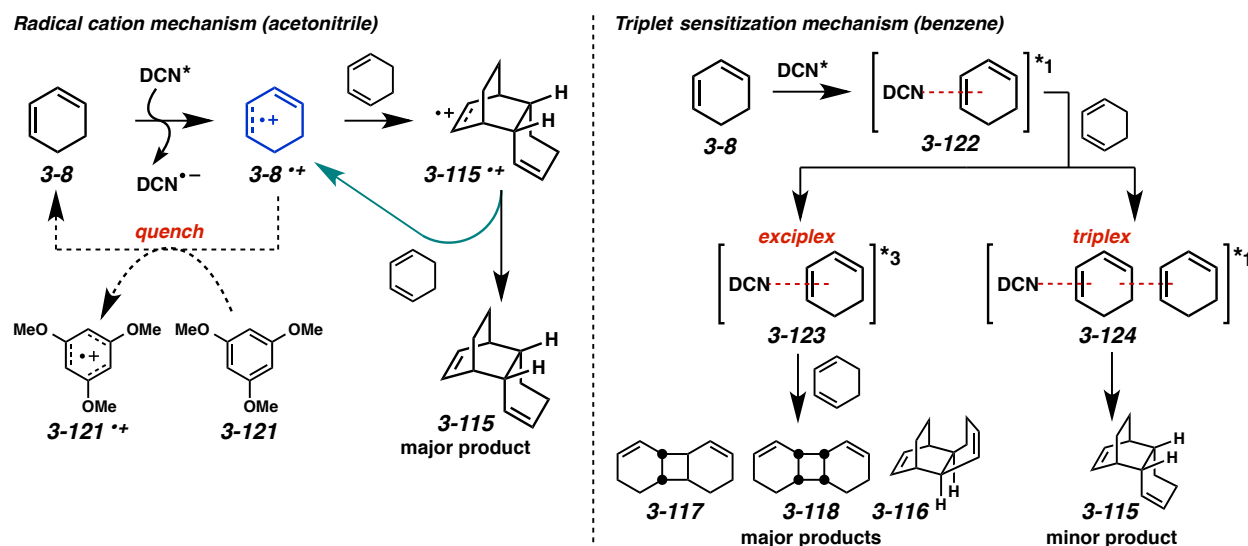


*Scheme 3.37.* Reaction of cyclohexadiene with DCA under direct irradiation in benzene.

Schuster and Calhoun further explored the mechanism of the dimerization of 1,3-cyclohexadiene under DCN photosensitized conditions (Scheme 3.38).<sup>55</sup> They found that running the reaction in either acetonitrile or benzene resulted in different product distributions, indicative of different reaction mechanisms in each solvent. When the reaction was performed in acetonitrile, a polar solvent, the [4+2] adducts predominated. Quenching experiments showed that greater than 97% of the DCN was being quenched by 1,3-cyclohexadiene (**3-8**), even at low concentrations. In addition, laser flash photolysis confirmed the presence of the radical anion of DCN in the reaction mixture. Schuster also found that the formation of the endo [4+2] product (**3-115**) could be inhibited by adding 1,3,5-trimethoxybenzene (**3-121**) (+1.36) as a radical cation quencher for cyclohexadiene ( $E_{1/2} = +1.53$  V). These experiments all point to a radical cation mechanism for the dimerization of 1,3-cyclohexadiene in acetonitrile (Scheme 3.38).

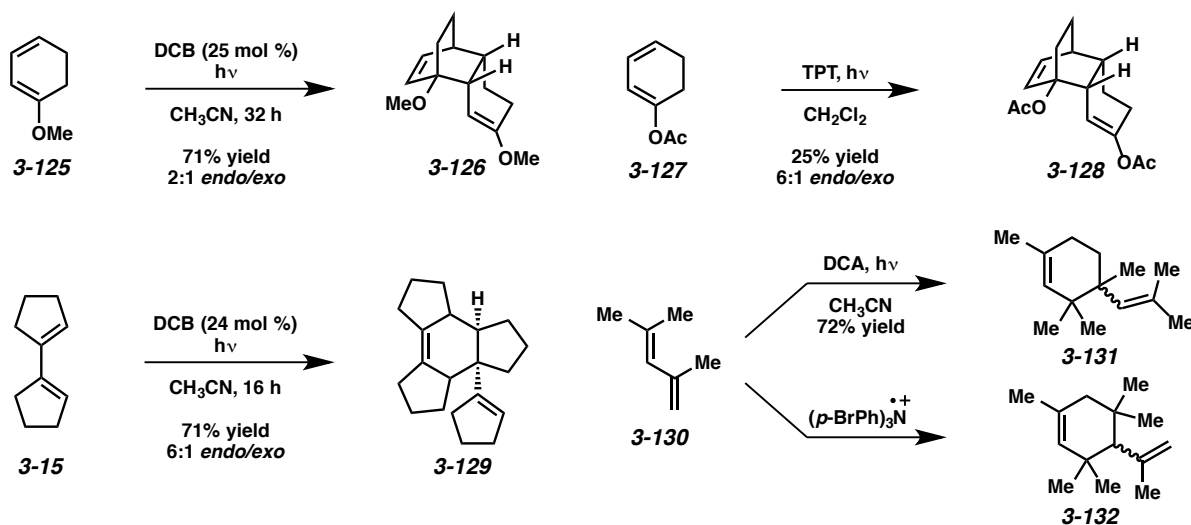
The dimerization of 1,3-cyclohexadiene (**3-8**) with DCN in benzene behaved very differently. In this case, the [2+2] adducts (**3-117** and **3-118**) and the exo [4+2] product (**3-116**) predominate. Increasing the concentration of 1,3-cyclohexadiene results in a higher ratio of the endo [4+2] product (**3-115**). The addition of 1,3,5-trimethoxybenzene (**3-121**) as a radical cation quencher did not affect the reaction. Furthermore, laser flash photolysis showed that no radical ions were forming in the reaction mixture.

These results suggest that a radical cation mechanism is not operative in benzene. Instead, the authors propose the formation of exciplex (**3-123**) and triplex (**3-124**) species between 1,3-cyclohexadiene and DCN that could lead to the formation of the different dimers (Scheme 3.38).



Scheme 3.38. Comparison of 1,3-cyclohexadiene dimerization mechanism in two different solvents.

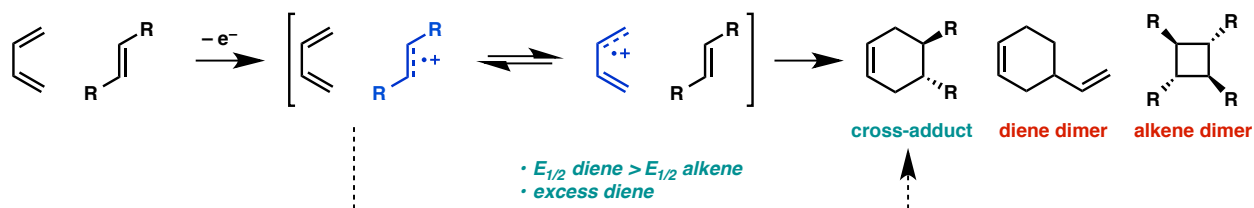
Other [4+2] dimerizations of dienes that have been reported through PET conditions include the dimerization of 1-methoxy-1,3-cyclohexadiene (**3-125**), 1-acetoxy-1,3-cyclohexadiene (**3-127**),<sup>56</sup> 1,1'-bicyclopentene (**3-15**),<sup>57</sup> and 2,4-dimethyl-1,3-pentadiene (**3-130**) (Scheme 3.39).<sup>58</sup> Interestingly, this latter dimerization under DCA photosensitized conditions results in a different constitutional isomer (**3-131**) than that which is obtained with the aminium salt catalyst (**3-132**).



Scheme 3.39. [4+2] Dimerization of other 1,3-dienes.

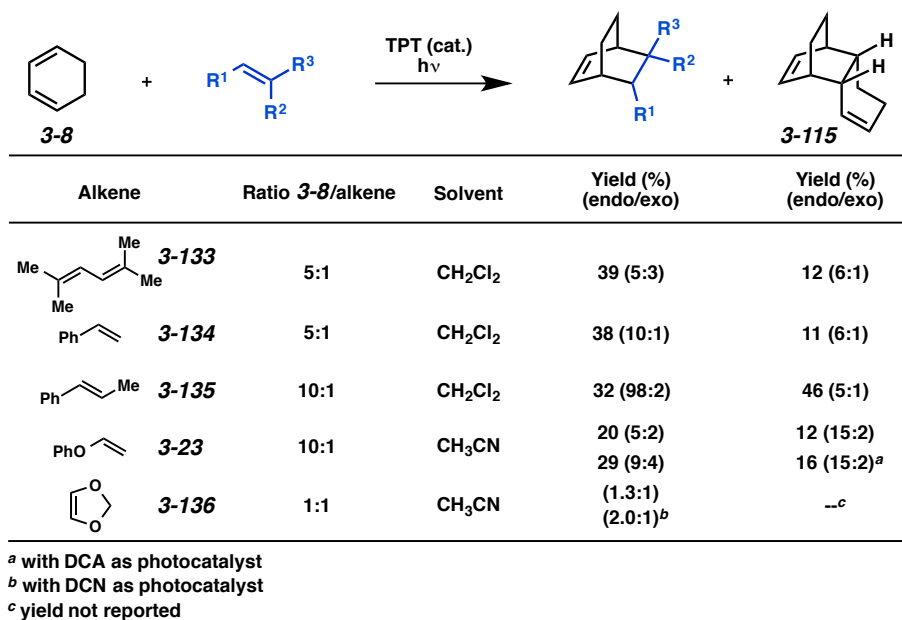
### 3.3.2 Cross [4+2] Cycloadditions

Achieving selectivity in cross [4+2] radical cation cycloadditions can be difficult due to the oxidizable nature both the diene and the alkene component; if the reaction between the diene and the alkene radical cation is too slow, then homodimerization of either species is inevitable. One possible way to ensure that the desired cross-selectivity is attained is to employ a diene that has a higher reduction potential than the alkene, thereby allowing the alkene to be selectively oxidized (Scheme 3.40). This method is not always effective, however, as the reaction rate for homodimerization can be significantly faster than the rate of the desired cross addition (see Chapter 4.4.1).



Scheme 3.40. Possible products in a cross [4+2] radical cation cycloaddition.

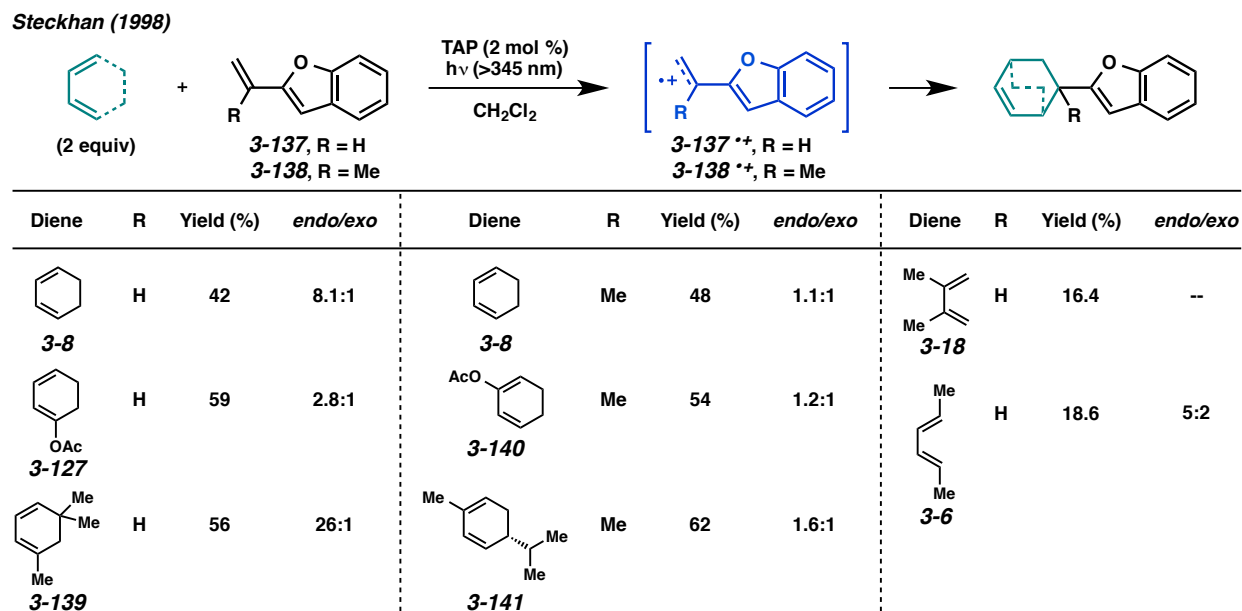
Despite these challenges, many cross [4+2] cycloadditions have seen success. For example, though the dimerization of 1,3-cyclohexadiene (**3-8**) occurs very quickly upon single-electron oxidation ( $k = 3 \times 10^8 \text{ M}^{-1}\text{s}^{-1}$ ),<sup>55</sup> a cross [4+2] cycloaddition between 1,3-cyclohexadiene and diene **3-133** can be accomplished using TPT (Scheme 3.41).<sup>59</sup> Styrene (**3-134**),  $\beta$ -methylstyrene (**3-135**), phenyl vinyl ether (**3-23**), and alkene **3-136**<sup>60</sup> also undergo cross cycloadditions with 1,3-cyclohexadiene, albeit in low yields. As expected, the cyclohexadiene dimer (**3-115**) was consistently observed as a side product.



Scheme 3.41. Cross [4+2] cycloadditions of 1,3-cyclohexadiene.

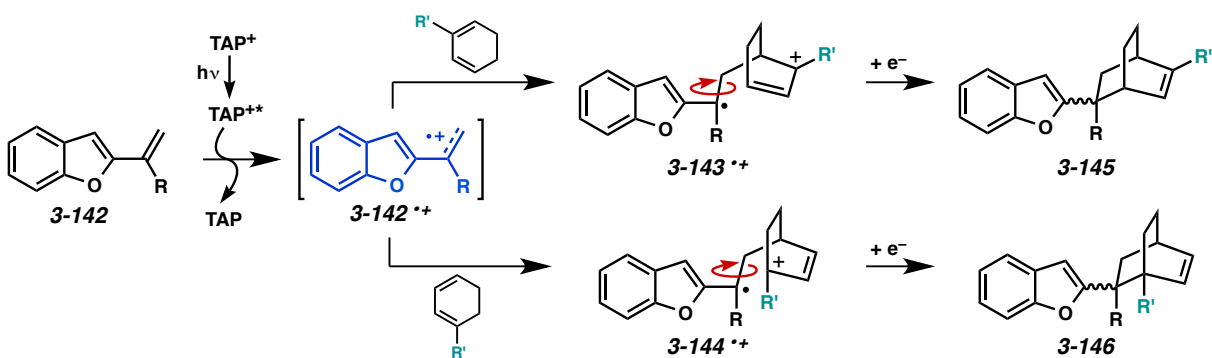
In 1998, Steckhan and coworkers explored the radical cation [4+2] cycloaddition of vinylbenzofurans with dienes (Scheme 3.42).<sup>61</sup> A variety of 1,3-cyclohexadiene derivatives and acyclic dienes underwent the cycloaddition with vinylbenzofuran (**3-137**) and isopropenylbenzofuran (**3-138**) in moderate yields. Overall, selectivity for the endo adduct ranged from low to very high. Though both the vinylbenzofuran and the diene could potentially be oxidized by TAP, in all cases, the vinyl group of the benzofuran acted as the “dienophile” component (**3-137**<sup>+</sup> and **3-138**<sup>+</sup>). The diene dimers and

vinylbenzofuran dimers were also formed in minor amounts; however, utilizing 2 equivalents of diene allowed for optimal cross-adduct formation.



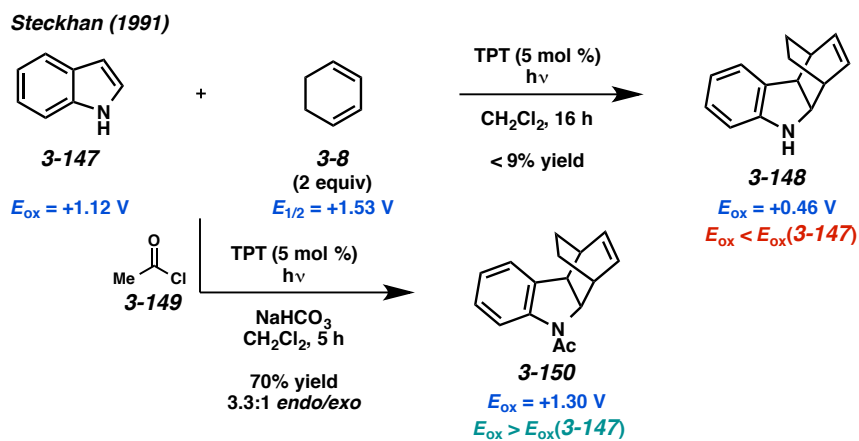
*Scheme 3.42.* Cross [4+2] cycloaddition of dienes with vinylbenzofurans.

Additionally, these reactions exhibited high regioselectivity. This is likely due to the asynchronous nature of the cycloaddition. First, the vinylbenzofuran undergoes single-electron oxidation to give the radical cation (**3-142<sup>•+</sup>**) (Scheme 3.43). This radical cation is then intercepted by the diene to yield a distonic radical cation intermediate (**3-143<sup>•+</sup>** or **3-144<sup>•+</sup>**). The regioselectivity of the cycloaddition is rationalized through the stability of the putative radical cation intermediates in which the radical is stabilized by the adjacent benzofuran and the cation is both allylic and tertiary. The formation of a distonic radical cation intermediate is also consistent with the preferential formation of the endo cycloadducts. These intermediates should be sufficiently long lived to allow rotation to the more stable endo adduct. Additionally, higher endo/exo ratios were generally observed for vinylbenzofuran (**3-137**) compared to isopropenylbenzofuran (**3-138**). This may be due to the ease of rotation in intermediate **3-143<sup>•+</sup>** or **3-144<sup>•+</sup>** when R = H compared to when R = Me.



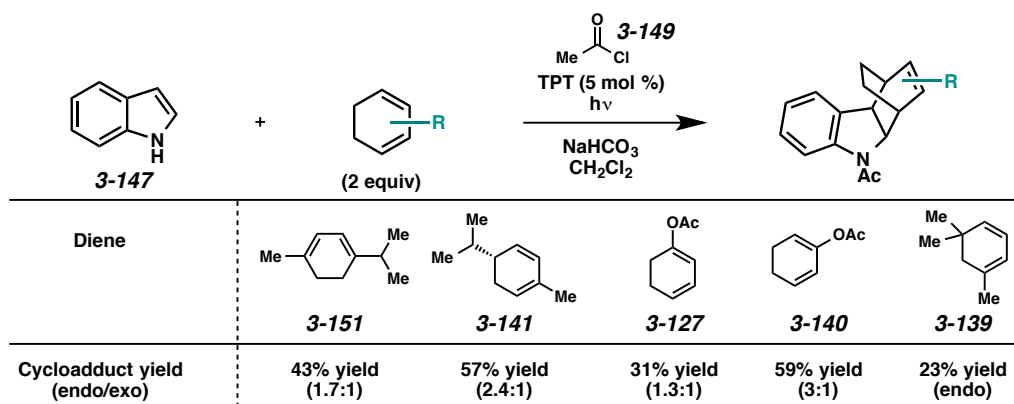
Scheme 3.43. Mechanism and origin of regioselectivity and endo selectivity.

Steckhan and coworkers have also studied the radical cation [4+2] cycloaddition between dienes and indoles.<sup>62</sup> In their preliminary experiments, when the cycloaddition of indole (**3-147**) and 1,3-cyclohexadiene (**3-8**) was attempted using TPT, <9% yield of product **3-148** was formed (Scheme 3.44). It was hypothesized that the formation of the product (**3-148**) was inhibiting the oxidation of indole (**3-147**), since the reduction potential of adduct **3-148** ( $E_{\text{ox}} = +0.46$  V) is lower than that of indole ( $E_{\text{ox}} = +1.17$  V). As a solution, the researchers proposed that adding an equivalent of acetyl chloride (**3-149**) to the reaction mixture would acylate adduct **3-150** *in situ*, creating a species with a reduction potential higher than that of indole, so indole oxidation would still be efficient. When this method was attempted, indeed, acylated product **3-150** ( $E_{\text{ox}} = +1.30$  V) was formed in 70% yield.



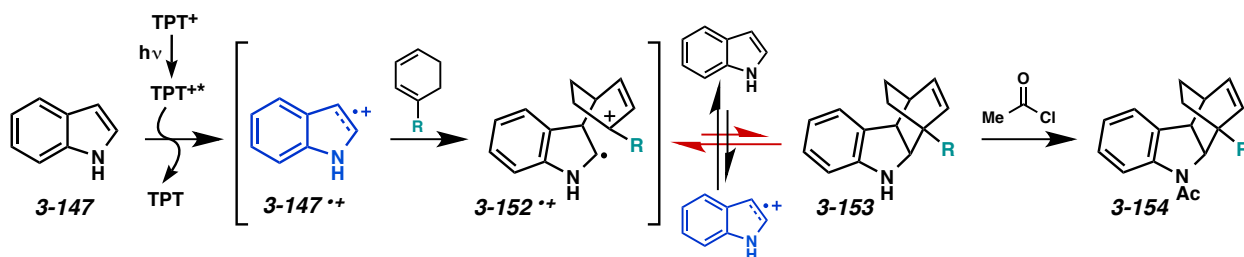
Scheme 3.44. [4+2] Cycloaddition of 1,3-cyclohexadiene and indole.

Using this approach, a variety of 1,3-cyclohexadiene derivatives successfully underwent the [4+2] cycloaddition with indole (**3-147**) in moderate yields (Scheme 3.45). The dimer of the diene was also observed in all cases, but in <10% yield.



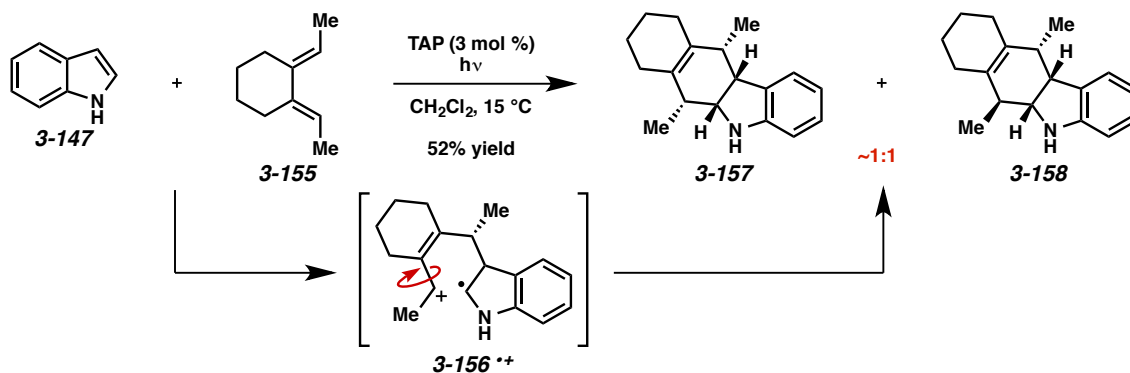
Scheme 3.45. Scope of 1,3-cyclohexadiene cycloaddition partner.

As with the vinylbenzofuran cycloadditions, the regioselectivity of this transformation was high and the endo adduct was favored. Again, this is likely derived from the stability of the distonic radical cation intermediate (**3-152<sup>•+</sup>**) upon nucleophilic attack by the diene on the indole radical cation (**3-147<sup>•+</sup>**) (Scheme 3.46).<sup>63</sup> As alluded to previously, the reduction of radical cation intermediate **3-152<sup>•+</sup>** with another equivalent of indole to give cycloadduct **3-153** is reversible due to the low reduction potential of this adduct. Trapping of this intermediate with acetyl chloride, however, provides product **3-154**, which is not oxidized in the presence of indole.



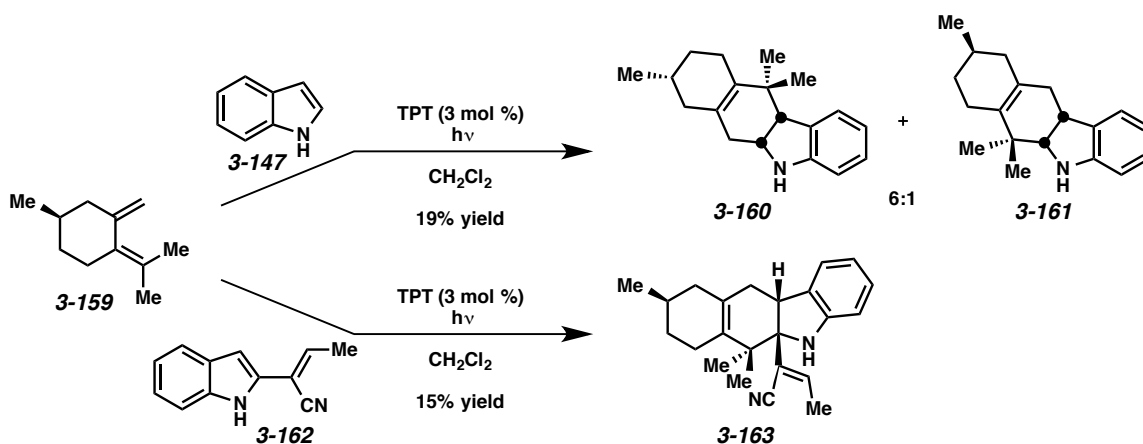
Scheme 3.46. Proposed mechanism for the cycloaddition of 1,3-cyclohexadienes with indole.

Steckhan and coworkers also explored cycloadditions of indole (**3-147**) and exocyclic dienes<sup>64</sup> to generate benzocarbazole derivative products that are attractive targets for their DNA intercalating properties and their antitumor activity.<sup>65</sup> In addition, the cycloaddition of exocyclic dienes can be used as a mechanistic probe to confirm the stepwise nature of the reaction. For example, in the cycloaddition of exocyclic diene **3-155** and indole (**3-147**), a mixture of syn and anti adducts were formed, presumably through bond rotation in the distonic radical cation intermediate (**3-156<sup>•+</sup>**) (Scheme 3.47). The formation of the anti product (**3-158**) further supports the asynchronous mechanism that is proposed for these cycloadditions.



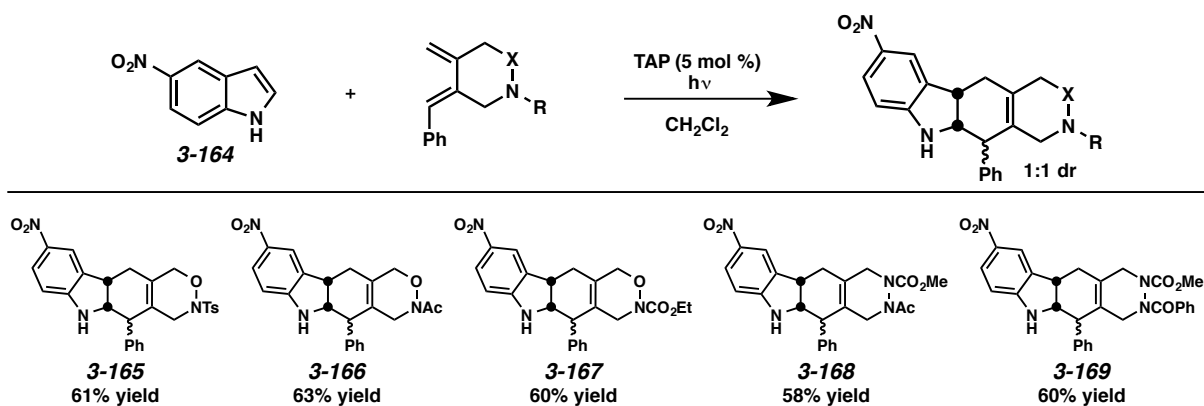
*Scheme 3.47.* Cycloaddition of an exocyclic diene with indole.

Further, a chiral exocyclic diene (**3-159**) could be employed to afford enantiopure benzocarbazoles (Scheme 3.48). Indole (**3-147**) reacted with diene **3-159** to give chiral adducts **3-160** and **3-161** in low yield, but with good regioselectivity. In the case of alkenylindole **3-162**, the diene reacted exclusively with the endocyclic alkene of the indole rather than the exocyclic alkene, although examples exist where the alkenylindole plays more of a diene role.<sup>66</sup> Interestingly, in all of these reactions, the addition of acetyl chloride was not necessary in order to allow efficient product formation.



Scheme 3.48. Cycloaddition of a chiral exocyclic diene with indoles.

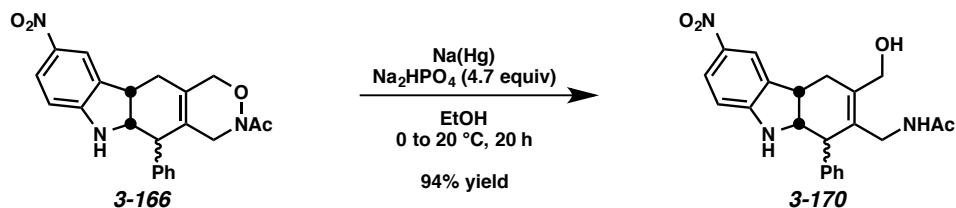
A restrictive characteristic of the described reactions of dienes with indoles is that the diene must be in a rigid *s-cis* conformation in order for the cycloaddition to occur. To circumvent this requirement, Steckhan and coworkers developed the cycloaddition of indoles with exocyclic dienes where the diene contained a functionality that could be cleaved after the cycloaddition (Scheme 3.49).<sup>67</sup>



Scheme 3.49. Cycloadditions with cleavable dienes.

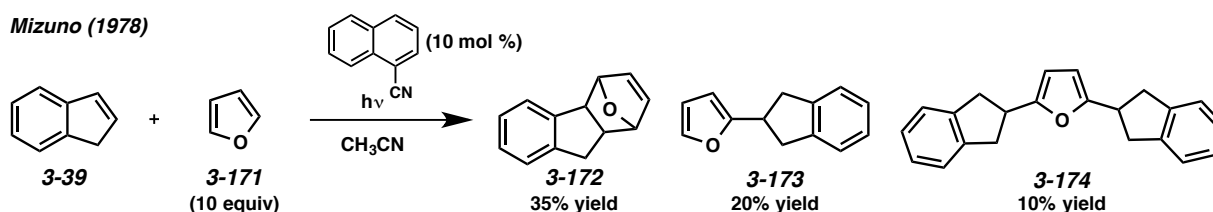
Various hydroxylamine- and hydrazide-derived exocyclic dienes were successful cycloaddition partners with indole **3-164**. The regioselectivity of these cycloadditions was high, but in each case a 1:1 mixture of diastereomers was obtained. To demonstrate the potential of these products for further

structural modification, cycloadduct **3-166** was cleaved under reductive sodium amalgam conditions,<sup>68</sup> yielding highly functionalized tetrahydrocarbazole derivative **3-170** in high yield (Scheme 3.50).



Scheme 3.50. Reductive cleavage of N–O bond.

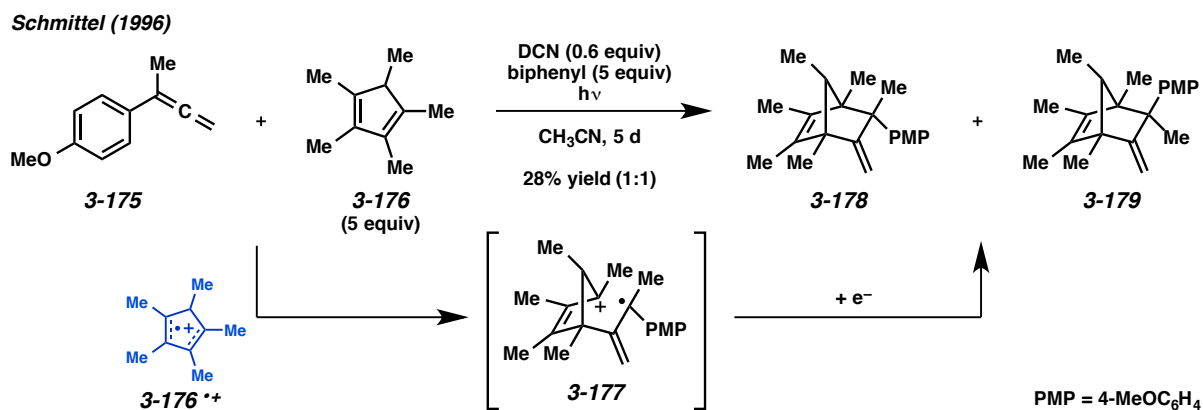
Cross [4+2] cycloadditions between furan (**3-171**) and styrenyl alkenes have also been reported by Mizuno and coworkers.<sup>69</sup> The reaction of indene (**3-39**) ( $E_{1/2} = +1.63$  V) with furan (**3-171**) ( $E_{1/2} = +1.76$  V) under 1-cyanonaphthalene photosensitized conditions gave a mixture of cycloadduct **3-172** and substituted furans **3-173** and **3-174** (Scheme 3.51). This reaction is proposed to proceed through a radical cation intermediate, since no reaction occurred in nonpolar solvents (benzene, cyclohexane). Substituted furans **3-173** and **3-174** could result from nucleophilic attack by the furan on the indene radical cation followed by H-atom abstraction.



Scheme 3.51. [4+2] cycloaddition of furan and indene.

Schmittel and coworkers have demonstrated that allenes and ketenes can also be utilized in photosensitized radical cation [4+2] cycloadditions.<sup>70</sup> Allene **3-175** reacts with cyclopentadiene **3-176** under photosensitization with DCN, yielding a mixture of products **3-178** and **3-179** after 5 days (Scheme

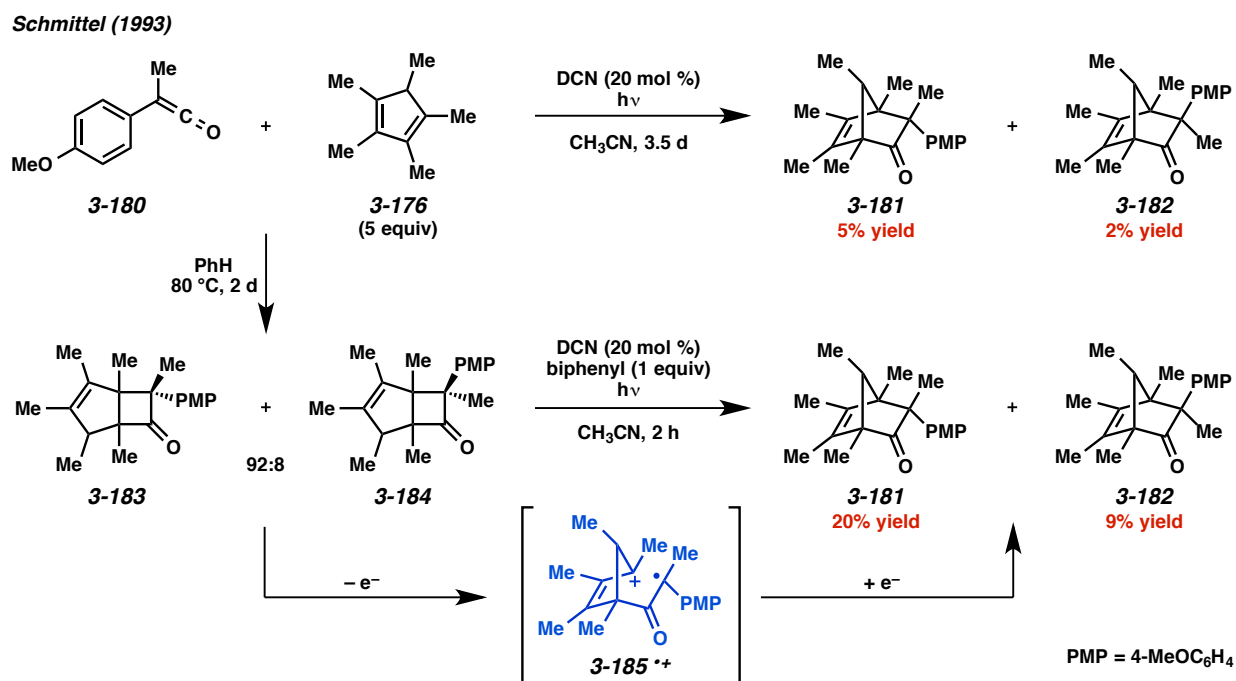
3.52). This transformation is proposed to proceed through the radical cation of the diene (**3-176<sup>•+</sup>**) ( $E_{1/2}$  (**3-176**) = +0.87 V), rather than of the allene ( $E_{1/2}$  = +1.34 V). Net [4+2] products are only achievable through this process when the diene strongly favors the *s*-cis conformation. Additionally, biphenyl was used as a cosensitizer; in the absence of biphenyl or DCN, no product formed. This could indicate that the electron transfer between the diene (**3-176**) and DCN\* is faster than the reaction of the diene radical cation (**3-176<sup>•+</sup>**) with the allene (**3-175**). Biphenyl may help to mediate the electron transfer process, allowing the diene radical cation to be longer lived.



Scheme 3.52. Radical cation cycloaddition with an allene.

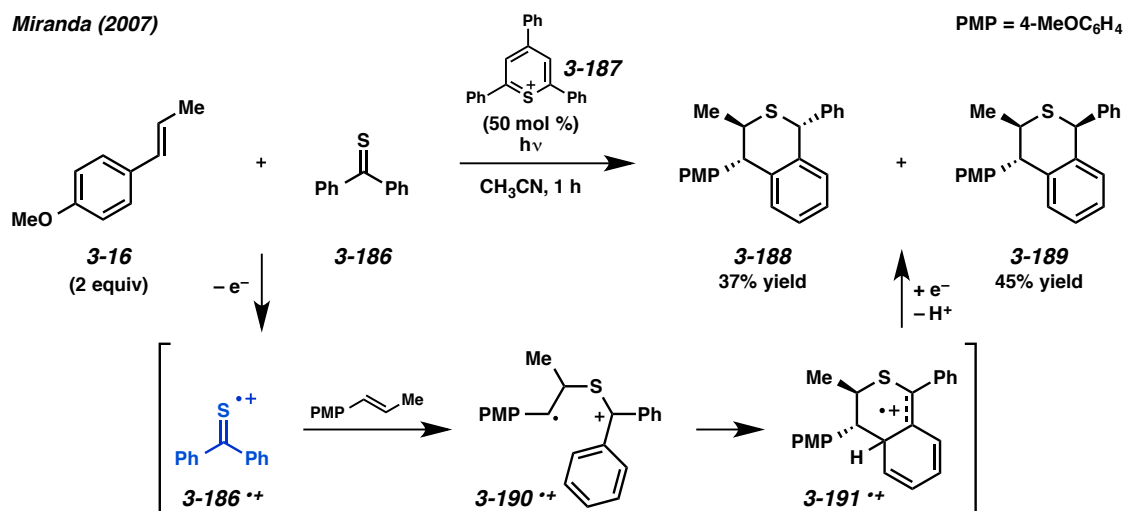
The cycloaddition of ketene **3-180** and diene **3-176** is also proposed to proceed through the intermediacy of the diene radical cation (**3-176<sup>•+</sup>**) (Scheme 3.53).<sup>71</sup> The DCN-sensitized [4+2] cycloaddition of these two components affords a mixture of cycloadducts **3-181** and **3-182** in a 5:2 ratio. Alternatively, the researchers found that thermal conditions (PhH, 80 °C) generated a mixture of the [2+2] cycloadducts **3-183** and **3-184**. When a 92:8 mixture of cyclobutanes **3-183** and **3-184** were subjected to the DCN conditions, they underwent a vinylcyclobutane rearrangement to give adducts **3-181** and **3-182** in a 20:9 ratio. Upon single-electron oxidation, the vinylcyclobutane rearrangement could proceed through two possible pathways: 1) cleavage of the bond between the vinyl group and the PMP group to give distonic radical cation intermediate **3-185<sup>•+</sup>**, or 2) complete cycloreversion to ketene **3-180** and diene

**3-176**, and recombination in a [4+2] fashion. Comparing the ratios of adducts **3-181** and **3-182** generated through the direct [4+2] cycloaddition (5:2) to the vinylcyclobutane rearrangement (20:9) indicates that complete cycloreversion and recombination likely cannot be occurring, or else a 5:2 ratio of adducts **3-181** and **3-182** would have been obtained.



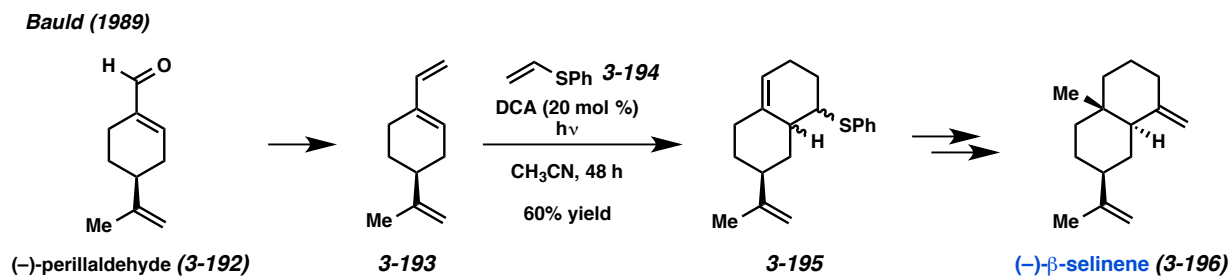
*Scheme 3.53.* Radical cation cycloaddition and rearrangement with a ketene.

An interesting report from Miranda and coworkers describes the use of a thiapyrylium salt (**3-187**) to initiate a radical cation [4+2] cycloaddition between thiobenzophenone (**3-186**) and *trans*-anethole (**3-16**).<sup>72</sup> The cycloaddition in Scheme 3.54 proceeded in 82% combined yield. Although both thiobenzophenone (**3-186**) and *trans*-anethole (**3-16**) can be oxidized by the photocatalyst, this reaction is proposed to proceed through the radical cation of thiobenzophenone (**3-186**<sup>•+</sup>). Interception of this radical cation by *trans*-anethole would give distonic radical cation **3-190**<sup>•+</sup>, which could rearrange to intermediate **3-191**<sup>•+</sup>. Reduction and loss of a proton yields the observed cycloadducts (**3-188** and **3-189**).



Scheme 3.54. [4+2] cycloaddition of thiobenzophenone.

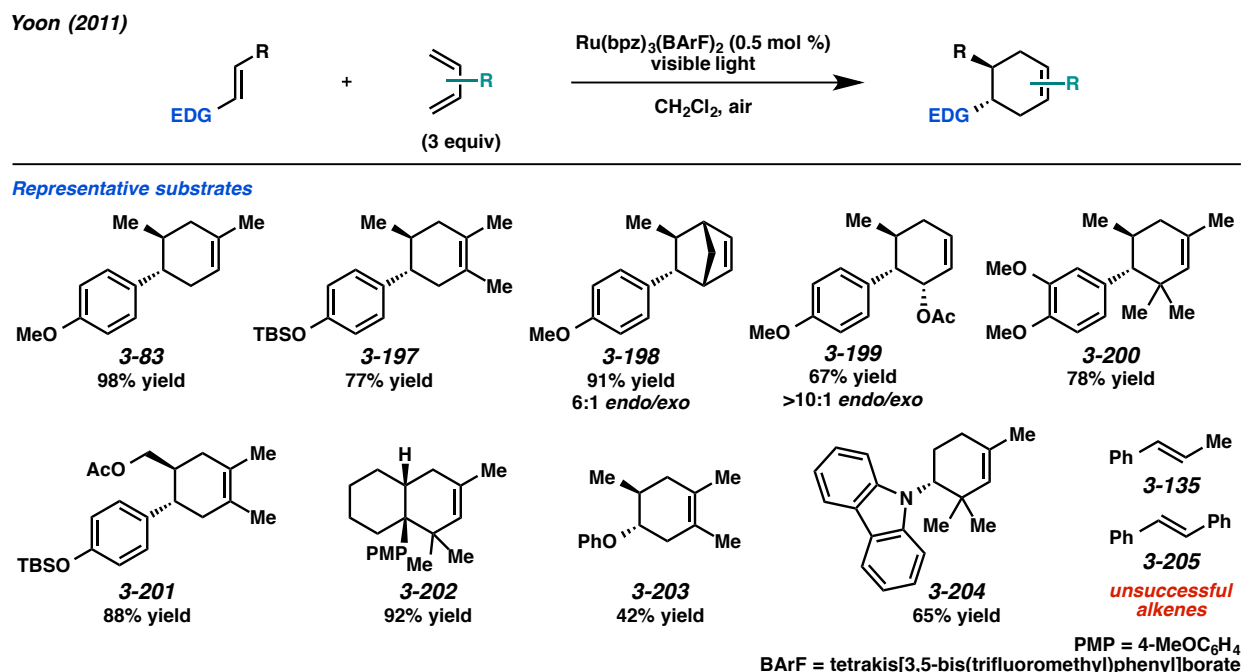
Lastly, Bauld has utilized the radical cation [4+2] cycloaddition in a concise synthesis of the eudesmane sesquiterpene (–)-β-selinene (**3-196**).<sup>73</sup> The diene (**3-193**) can be synthesized through a Wittig reaction with commercially available (–)-perillaldehyde (**3-192**) (Scheme 3.55). Then, the radical cation [4+2] cycloaddition with phenyl vinyl sulfide (**3-194**) using DCB as a photosensitizer yields adduct **3-195**, which can be further modified to give the natural product (**3-196**) in only 6 total steps.



Scheme 3.55. Total synthesis of (–)-β-selinene through a radical cation [4+2] cycloaddition.

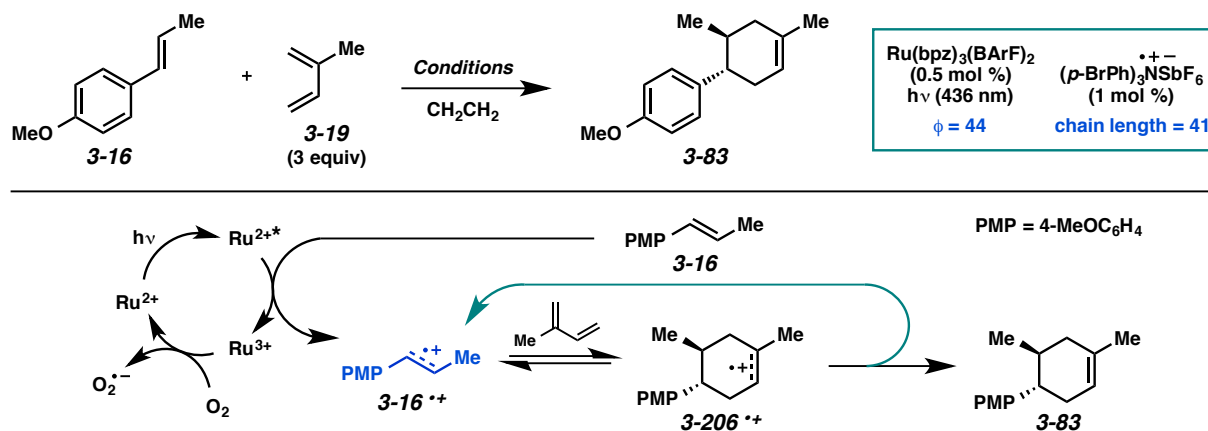
### 3.3.3 Recent Reports of Radical Cation [4+2] Cycloadditions

In 2011, Yoon and coworkers reported the radical cation Diels-Alder cycloaddition of dienes with electron-rich alkenes using a Ru photocatalyst and visible light. This study significantly expanded the substrate scope of the radical cation [4+2] cycloaddition. Representative substrates are shown in Scheme 3.56. A variety of differentially substituted dienes were found to be competent cycloaddition partners. Various “dienophiles” were also successful, including a trisubstituted alkene (**3-202**), as well as vinylcarbazole (**3-204**) and a phenyl vinyl ether (**3-203**), both of which have been known to dimerize upon single-electron oxidation. Homodimerization of the alkenes or the dienes did not seem to be a significant issue under the reaction conditions. Substrates that did not contain an electron rich aryl group, however, did not undergo the cycloaddition (**3-135** and **3-205**). Overall, high yields were obtained of the cycloadducts, which is in contrast to the yields reported with the organic photosensitizers.



Scheme 3.56. Representative substrates for the Ru-photocatalyzed radical cation Diels-Alder.

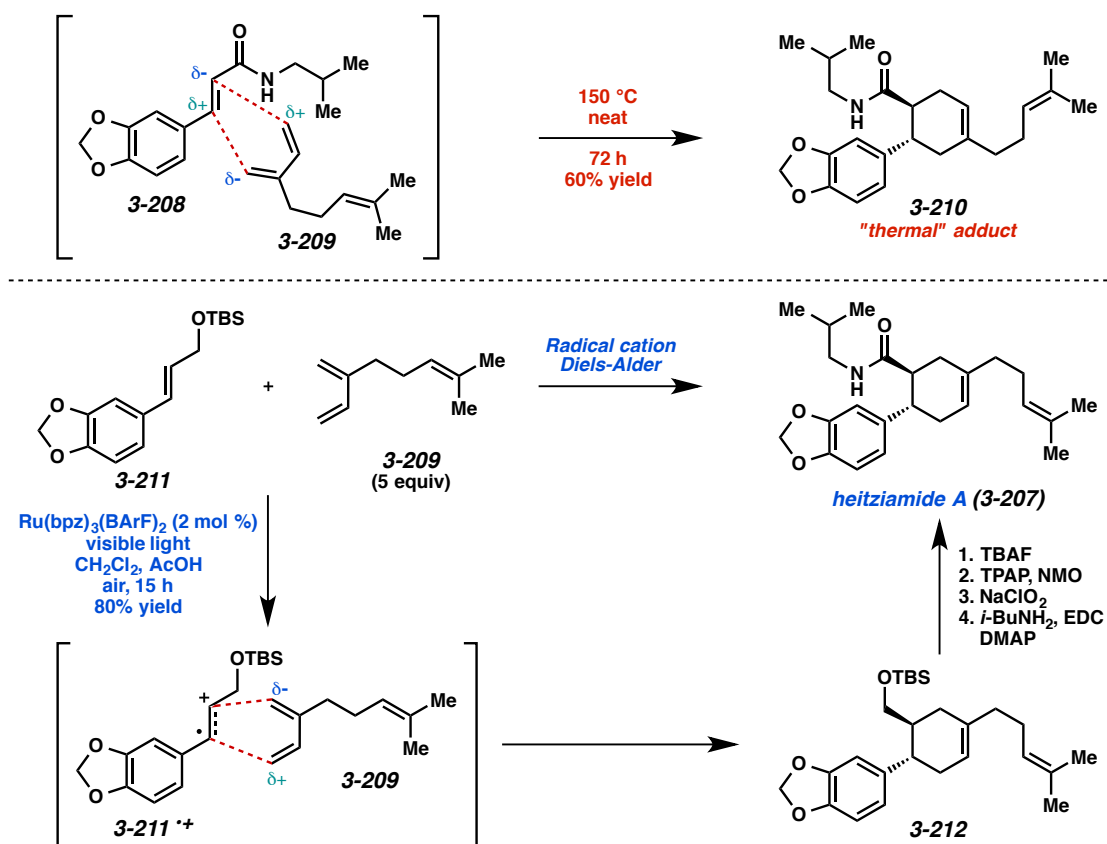
A separate report by Yoon and Cismesia determined the quantum yield of the Ru-catalyzed [4+2] cycloaddition between *trans*-anethole (**3-16**) and isoprene (**3-19**) to be 44, meaning that for every photon of light absorbed by the Ru catalyst, 44 equivalents of product **3-83** are formed.<sup>74</sup> For comparison, the researchers also determined that the chain length of the same reaction initiated by an aminium radical cation salt, was 41. The aminium salt initiated reaction is known to proceed through radical chain propagation, so the Ru-catalyzed process, which has a similar chain length, is likely also proceeding through a radical chain mechanism, as depicted in Scheme 3.57. Upon excitation with light, the excited state Ru<sup>2+\*</sup> can abstract an electron from *trans*-anethole (**3-16**), yielding radical cation **3-16<sup>•+</sup>**. Interception with isoprene affords the cyclohexene radical cation (**3-206<sup>•+</sup>**), which accepts an electron from another *trans*-anethole equivalent to give the neutral product (**3-83**) and propagate the reaction. The authors also observe that the cycloaddition was slower in the absence of air (46% conversion to **3-83** in 1 h vs. 98% yield in the presence of air). They suggest that oxygen may be assisting in catalyst turnover.



Scheme 3.57. Mechanism for the Ru-photocatalyzed radical cation Diels-Alder.

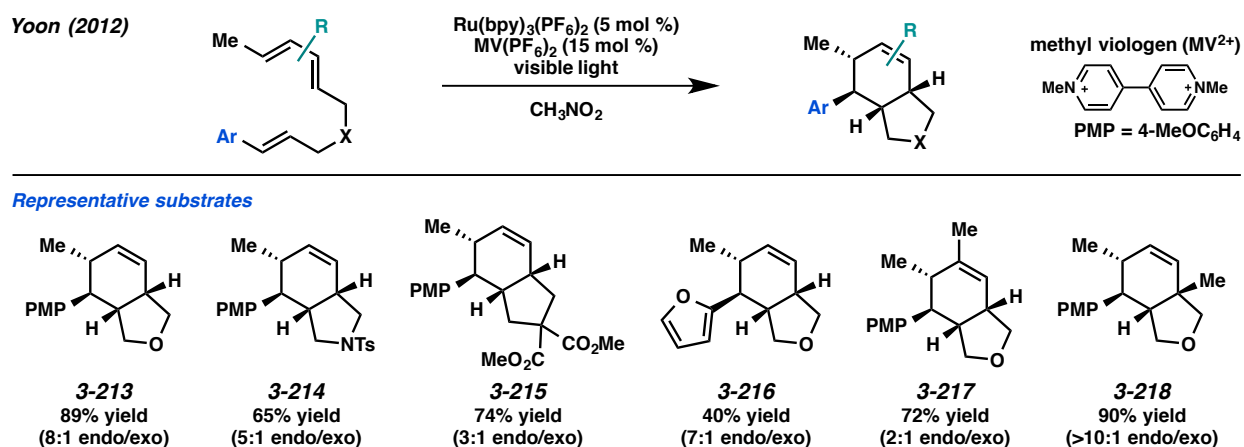
The utility of this radical cation Diels-Alder approach was demonstrated in the synthesis of natural product heitziamide A (**3-207**). A unique aspect of radical cation cycloadditions is that they are essentially an umpolung process where the polarization of the alkene is reversed upon single-electron oxidation.<sup>75</sup> This effect also results in a reversal of regioselectivity in radical cation cycloadditions. Due to

the intrinsic electronic character of the diene (**3-209**) and dienophile (**3-208**), when the synthesis of heitziamide A is attempted through thermal Diels-Alder conditions (150 °C, neat), the incorrect isomer (**3-210**) is formed in 60% yield (Scheme 3.58). Using the developed radical cation [4+2] cycloadditions with  $\text{Ru}(\text{bpz})_3^{2+}$ , however, alkene **3-211** and myrcene (**3-209**) were combined to give cycloadduct **3-212** with the desired connectivity in 80% yield. The TBS-ether was then converted to the amide in four steps to afford the natural product (**3-207**).



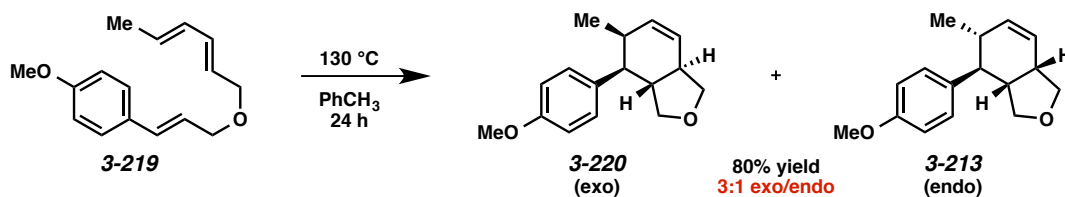
Scheme 3.58. Synthesis of heitziamide A through a radical cation Diels-Alder.

Yoon and coworkers also studied the intramolecular radical cation Diels-Alder reaction using a  $\text{Ru}(\text{bpy})_3^{2+}$ /methyl viologen photocatalytic system.<sup>76</sup> Many different tethered substrates with electron-rich alkenes and differentially substituted dienes underwent the [4+2] cycloaddition in good to high yields (Scheme 3.59).



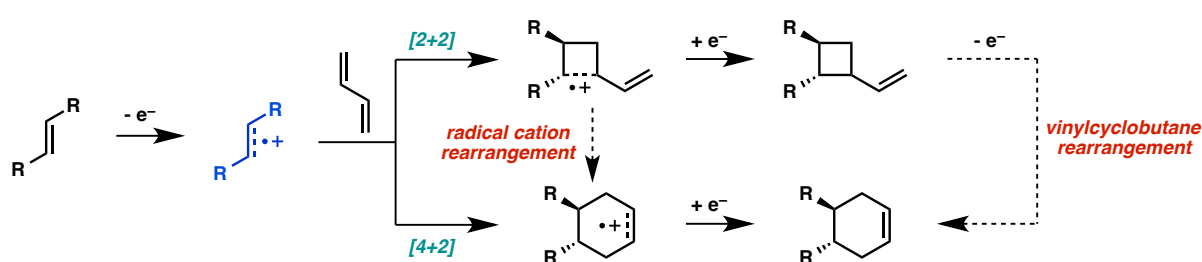
Scheme 3.59. Yoon's intramolecular radical cation Diels-Alder reaction.

It is important to note that the intramolecular Diels-Alder reaction of substrate **3-219** can also be effectively performed under thermal conditions (130 °C, toluene) (Scheme 3.60). The thermal cycloadditions, however, favor the exo adduct (**3-220**) (3:1 exo/endo), whereas the radical cation cycloaddition favors the endo adduct (**3-213**) (8:1 endo/exo).



Scheme 3.60. Thermal intramolecular Diels-Alder reaction.

### 3.4 Competing [2+2] and [4+2] Mechanistic Pathways



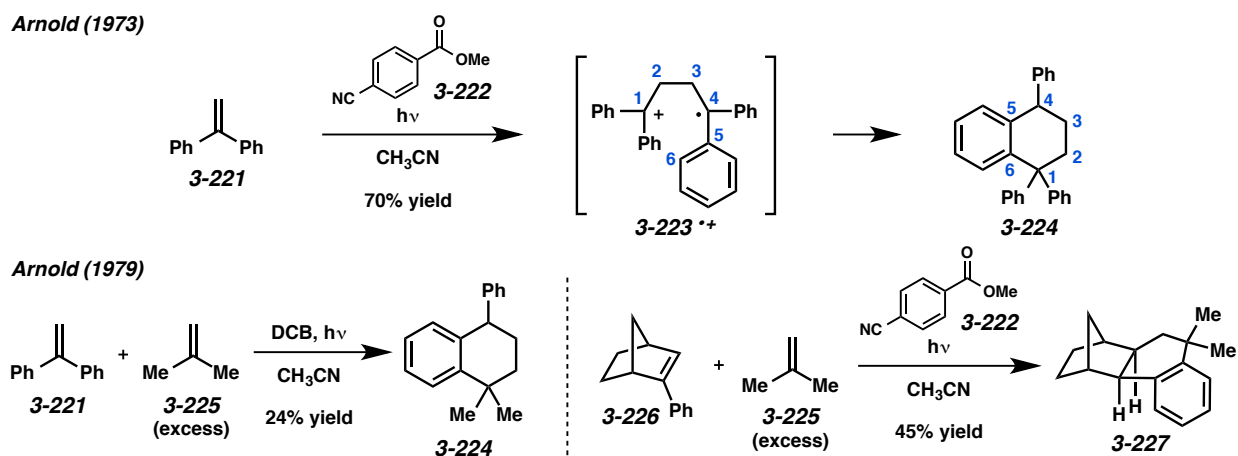
Scheme 3.61. General depiction of competitive [2+2] and [4+2] radical cation cycloadditions.

As mentioned previously, radical cation [2+2] and [4+2] cycloadditions are complementary transformations that proceed through similar intermediates. With certain substrates, these competing mechanisms can result in a mixture of [2+2] and [4+2] adducts, as was seen in Chen's synthesis of the ageliferin core (**3-101**) from the intramolecular cyclization of alkene **3-97** (Scheme 3.33). Ultimately, the formation of the [4+2] adduct can occur through two different pathways: 1) a radical cation rearrangement where the initially formed radical cation [2+2] adduct rearranges to the cyclohexene radical cation before it is reduced to the neutral cyclohexene, and 2) an indirect [4+2] cycloaddition where the neutral cyclobutane forms as usual, but is reoxidized and undergoes a vinylcyclobutane rearrangement to give the cyclohexene product (Scheme 3.61). This section will discuss these divergent mechanisms and the subtle differences in reaction conditions that can enhance periselectivity for one adduct over the other.

#### 3.4.1 Pathway 1: Radical Cation Rearrangement

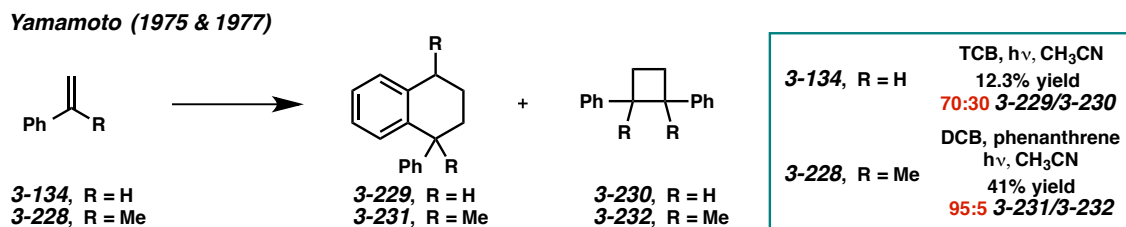
The dimerization of 1,1-diphenylethylene (**3-221**) was first reported by Arnold and Neunteufel in 1973. In the presence of methyl 4-cyanobenzoate (**3-222**) as a photosensitizer, 1,1-diphenylethylene dimerized to tetrahydronaphthalene **3-224** (Scheme 3.62).<sup>77</sup> The reaction proceeded much faster in acetonitrile than in benzene, indicating a radical cation mechanism. Product **3-224** could be thought to arise from

rearrangement of a radical cation intermediate like **3-223**<sup>+</sup>. Additionally, the quantum yield was determined to be less than 0.1, meaning that a radical chain mechanism was likely not occurring. Arnold also showed that in the presence of a different, less oxidizable alkene (**3-225**), cross cycloadditions with 1,1-diphenylethylene (**3-221**) or alkene **3-226** could be achieved (Scheme 3.62).<sup>78</sup>



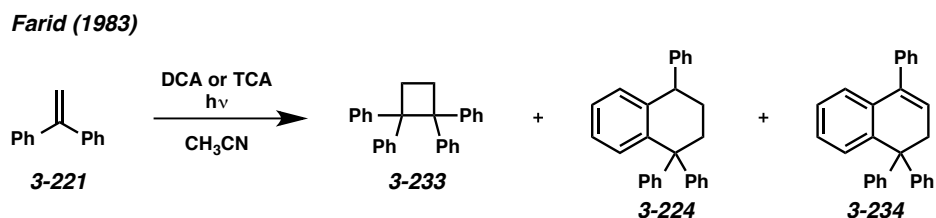
Scheme 3.62. Dimerization and cross cycloaddition of phenyl vinyl ethers.

Additional reports were provided by Yamamoto and coworkers. They found that both styrene (**3-134**) and  $\alpha$ -methylstyrene (**3-228**) could dimerize in a similar manner as 1,1-diphenylethylene; however, instead of only observing the [4+2] products, they also observed minor amounts of the [2+2] adducts. As depicted in Scheme 3.63, when styrene (**3-134**) was exposed to irradiation in the presence of TCB, a 12.3% yield of a mixture of products was obtained.<sup>79</sup> The tetrahydronaphthalene (**3-229**) was the major product, but the cyclobutane (**3-230**) was formed in a considerable amount as well.  $\alpha$ -Methylstyrene (**3-228**) dimerized in the same fashion using a DCB/phenanthrene cosensitization system.<sup>80</sup> In this case, a 95:5 ratio of the [4+2] adduct to the [2+2] adduct was obtained. The [2+2] dimerization of styrenes has been reported under triplet sensitization and direct irradiation, but the [4+2] adduct does not form under those conditions, leading the researchers to propose that a radical cation mechanism may be operative here.



Scheme 3.63. Dimerization of styrene and  $\alpha$ -methylstyrene.

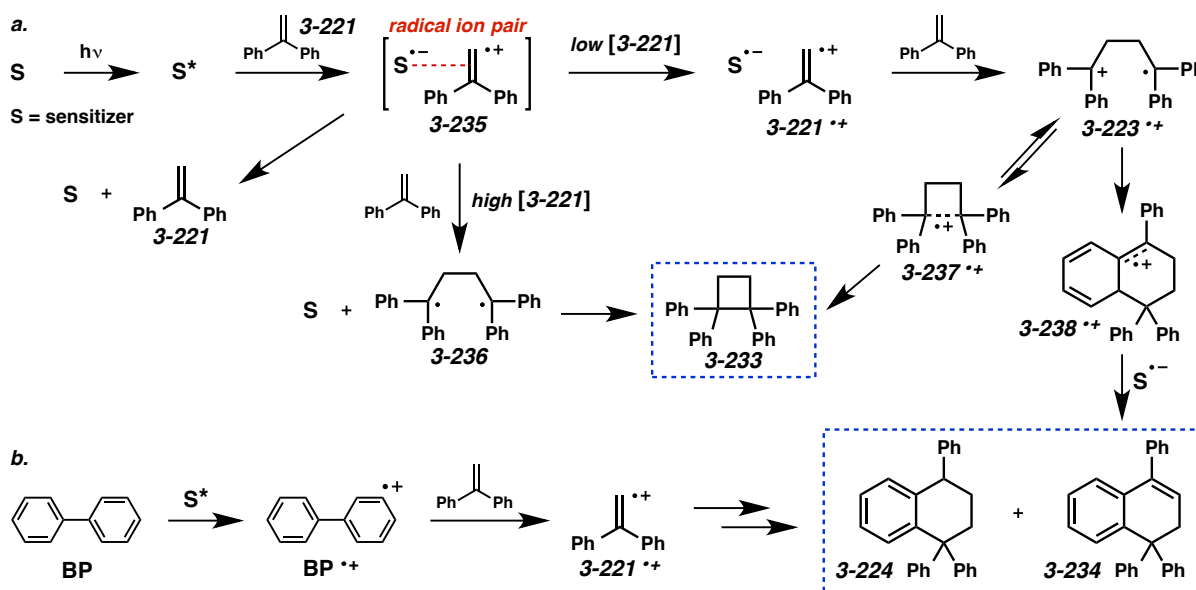
The mechanism of the dimerization of 1,1-diphenylethylene was reinvestigated by Farid and Mattes in 1983.<sup>81</sup> When 1,1-diphenylethylene (**3-221**) was exposed to irradiation with either DCA or TCA (2,6,9,10-tetracyanoanthracene), both the [2+2] dimer (**3-233**) and a mixture products arising from [4+2] processes (**3-224** and **3-234**) were formed (Scheme 3.64). The researchers found that the ratio of cyclobutane **3-233** to adducts **3-224** and **3-234** was concentration dependent; as the concentration of 1,1-diphenylethylene was decreased, the ratio of cyclobutane **3-233** compared to adducts **3-224** and **3-234** also decreased. These results indicated that formation of the [2+2] adduct was likely occurring through a different pathway than the [4+2] products.



Scheme 3.64. [2+2] and [4+2] products of 1,1-diphenylethylene dimerization.

A mechanism for the formation of the different products is shown in Scheme 3.65a. Farid proposes that upon single-electron oxidation of 1,1-diphenylethylene (**3-221**) by the excited sensitizer, an associated radical ion pair is formed (**3-235**). From here, there are three possible pathways available: 1) the radical ion path can revert back to the neutral starting materials, 2) the radical ion pair can react with another alkene equivalent to give diradical **3-236** after reverse electron transfer from the sensitizer radical

anion, or 3) the radical ion pair can dissociate to give the separate radical ions, and the alkene radical cation (**3-221<sup>•+</sup>**) can react with another alkene equivalent to give radical cation dimer **3-223<sup>•+</sup>**. Cyclobutane **3-233** is the result of pathway 2, which explains why less of this product forms at lower concentrations of 1,1-diphenylethylene (**3-221**); at lower concentrations, the associated radical ion pair (**3-235**) is less likely to be intercepted by 1,1-diphenylethylene, allowing it more time to dissociate to the separate radical ions. The separate radical ions formed in pathway 3 lead to the rearranged adducts **3-224** and **3-234**. Cyclobutane **3-233** can also result from pathway 3, but the formation of cyclobutane radical cation **3-237<sup>•+</sup>** is reversible, so the major products are the naphthalenes (**3-224** and **3-234**). In line with Arnold's results, the quantum yields of the dimerization with DCA and TCA were 0.033 and 0.15, respectively. Thus, chain propagation was likely not occurring.

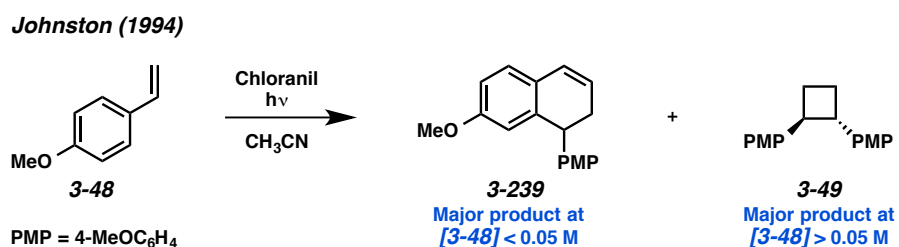


Scheme 3.65. Proposed mechanism for the dimerization of 1,1-diphenylethylene.

An additional experiment by Farid provided strong support for the proposed mechanism. When the dimerization was performed with different amounts of added biphenyl (BP), the ratio of cyclobutane **3-233** to adducts **3-224** and **3-234** decreased as the concentration of biphenyl was increased (Scheme

3.65b). Biphenyl is proposed to be oxidized by the sensitizer to its radical cation ( $\text{BP}^{\bullet+}$ ), which can in turn oxidize 1,1-diphenylethylene (**3-221**), generating the alkene radical cation (**3-221<sup>•+</sup>**) through a pathway that does not involve the formation of the associated radical ion pair (**3-235**). Since less of the radical ion pair is present in the reaction mixture, less cyclobutane **3-233** is formed, consistent with the proposed mechanism.

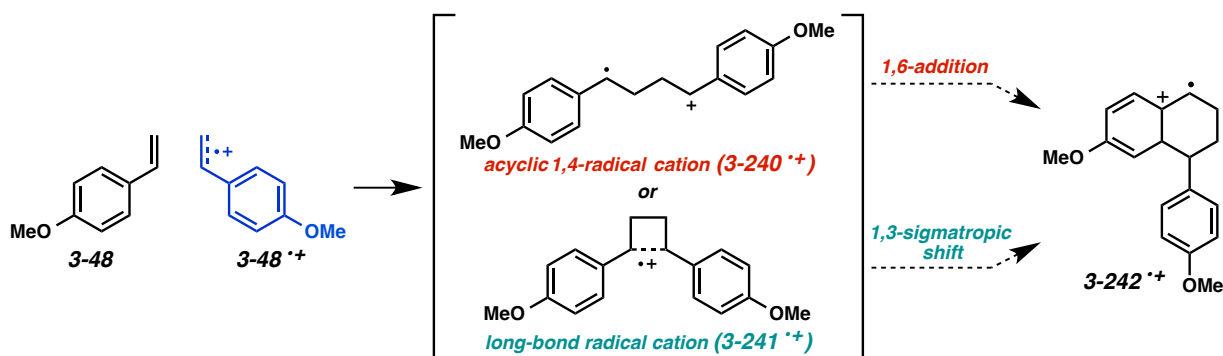
The periselectivity of the dimerization of 4-methoxystyrene (**3-48**) has also been extensively studied. Similar to what was observed in the dimerization of 1,1-diphenylethylene, the [4+2] product (**3-239**) predominates at lower concentrations and the [2+2] adduct (**3-49**) is the major product at higher concentrations (Scheme 3.66).<sup>82</sup>



Scheme 3.66. Dimerization of 4-methoxystyrene.

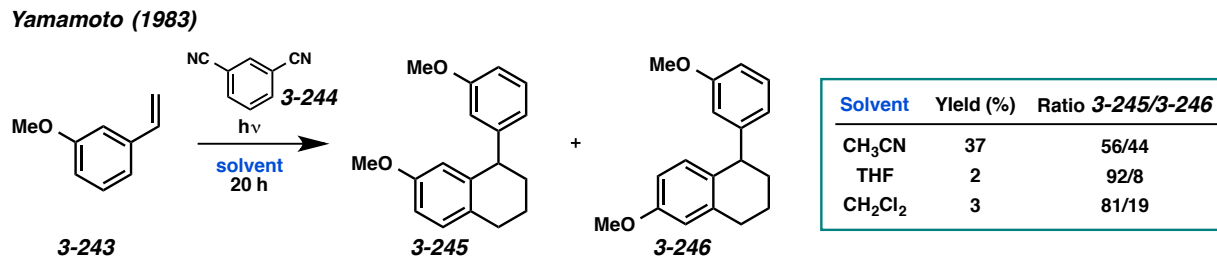
A frequently discussed question about the dimerization of 4-methoxystyrene (**3-48**), as well as the dimerization of similar styrene derivatives, concerns the mechanism of the rearrangement to the [4+2] product (**3-239**). Conceivably, dihydronaphthalene **3-239** can arise from either of two intermediates: an acyclic 1,4-radical cation (**3-240<sup>•+</sup>**), which can undergo a 1,6-addition with the arene to give radical cation **3-242<sup>•+</sup>**, or a long-bond cyclobutane radical cation (**3-241<sup>•+</sup>**), where a 1,3-sigmatropic shift can also generate intermediate **3-242<sup>•+</sup>** (Scheme 3.67). The stability of the acyclic 1,4-radical cation (**3-240<sup>•+</sup>**) has been established, and this species can be detected by pulse radiolysis.<sup>83</sup> In fact, the acyclic 1,4-radical cation of the 4-methoxystyrene dimer (**3-240<sup>•+</sup>**) was found to be significantly more stable than the analogous acyclic 1,4-radical cation of the *trans*-anethole dimer, which may explain why rearrangement to the dihydronaphthalene occurs in the dimerization of 4-methoxystyrene but not in the dimerization of

*trans*-anethole. On the other hand, long-bond intermediates have often been invoked in [2+2] cycloadditions, such as the dimerization of *trans*-anethole (**3-16**), to account for stereospecificity.<sup>49d</sup> Ultimately, computations by Wiest and O’Neil have concluded that the acyclic 1,4-radical cation (**3-240<sup>•+</sup>**) and the long-bond radical cation (**3-241<sup>•+</sup>**) are essentially isoenergetic and can be thought of as conformers in equilibrium with each other.<sup>84</sup>



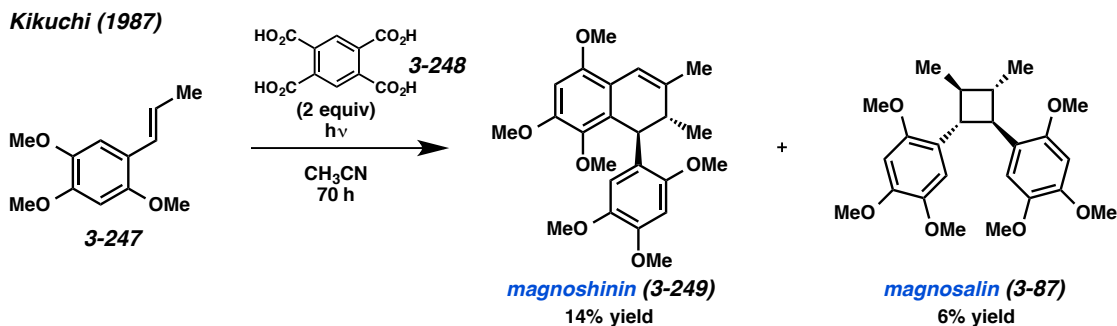
Scheme 3.67. Acyclic vs. long-bond radical cation intermediate.

In additional examples, 3-methoxystyrene (**3-243**) has also been observed to dimerize in a [4+2] fashion.<sup>85</sup> When exposed to *meta*-dicyanobenzene (**3-244**) and light, tetrahydronaphthalenes **3-245** and **3-246** are formed (Scheme 3.68). Interestingly, running the cycloaddition in different solvents resulted in different ratios of the two product isomers.



Scheme 3.68. Dimerization of 3-methoxystyrene.

The dimerization of alkene **3-247** has been exploited for the synthesis of the dihydronaphthalene neolignan natural product, magnoshinin (**3-249**).<sup>86</sup> Irradiation of alkene **3-247** in the presence of pyromellitic acid (**3-248**) gave magnoshinin (**3-249**) in 14% yield, as well as the corresponding cyclobutane, magnosalin (**3-87**), in 6% yield (Scheme 3.69). Nicewicz has also synthesized magnosalin (**3-87**) from the same starting alkene using a TAP photocatalyst (Figure 3.2), but it was not mentioned if the rearranged magnoshinin (**3-249**) formed as well.



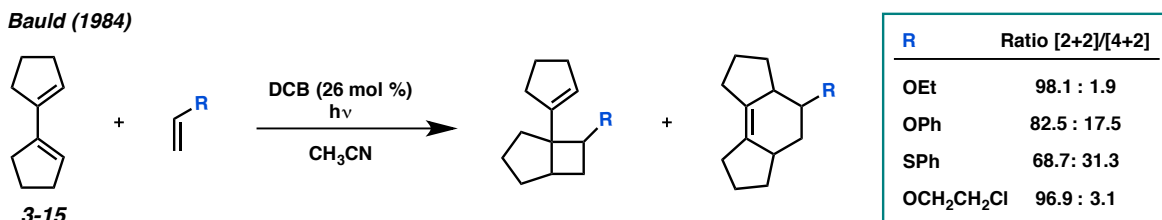
Scheme 3.69. Synthesis of natural products magnoshinin and magnosalin.

### 3.4.2 Pathway 2: Indirect [4+2] Through [2+2]/Vinylcyclobutane Rearrangement

Another pathway through which the [2+2] adducts could convert to [4+2] adducts is through vinylcyclobutane rearrangement.<sup>87</sup> In this scenario as well, both [2+2] and [4+2] adducts are formed in competition with each other. A prominent example of competition between a [2+2] cycloaddition and the indirect [4+2] cycloaddition is the reaction of 1,1'-bicyclopentenyl diene **3-15** and electron-rich alkenes.

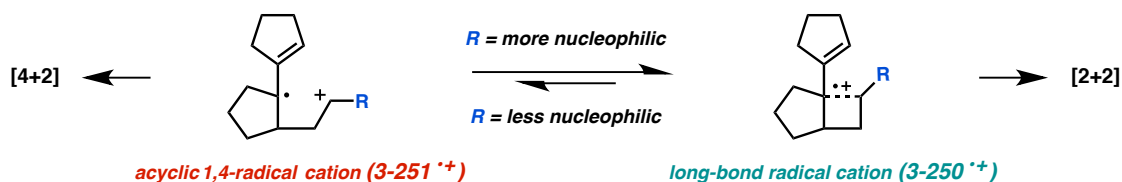
As noted by Bauld, most radical cation cycloadditions between an electron-rich alkene and a diene result in [4+2] adducts. Exceptions exist, however, of alkene/diene combinations that result in mostly [2+2] adducts. 1,1'-Bicyclopentenyl diene **3-15** is a case where the reaction of this species with an alkene under radical cation conditions results primarily the [2+2] adducts. As shown in Scheme 3.70,

when DCB was used to photosensitize the reaction of diene **3-15** with several different alkenes, a mixture of the [2+2] and [4+2] adducts was obtained, with the [2+2] adducts predominating.<sup>88</sup>



*Scheme 3.70.* Periselectivity in cycloaddition between 1,1'-bicyclopentenyl diene and alkenes.

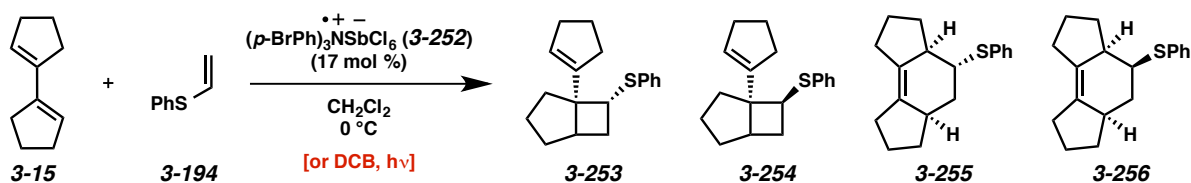
Bauld initially proposes that the nature of the radical cation intermediate between the diene and the alkene may be dependent on the nucleophilicity of the R group. When the R group is more nucleophilic, a long-bond radical cation intermediate (**3-250<sup>•+</sup>**) is favored, which results in the formation of primarily the [2+2] adducts (Scheme 3.71). When the R group is less nucleophilic, a 1,4-radical cation (**3-251<sup>•+</sup>**) can also be formed, resulting in the rearranged [4+2] product. Although a reasonable explanation, further studies by Bauld and coworkers suggested that more factors may be involved.



*Scheme 3.71.* Explanation for periselectivity of 1,1'-bicyclopentenyl diene cycloadditions.

An extensive investigation into the radical cation cycloaddition of phenyl vinyl sulfide (**3-194**) and 1,1'-bicyclopentenyl diene **3-15** revealed that two distinct mechanisms were simultaneously operative: a mechanism that proceeds through the oxidation of phenyl vinyl sulfide (**3-194**) and a mechanism that proceeds through the oxidation of the diene (**3-15**).<sup>89</sup> Four different products are formed in this reaction (Scheme 3.72).

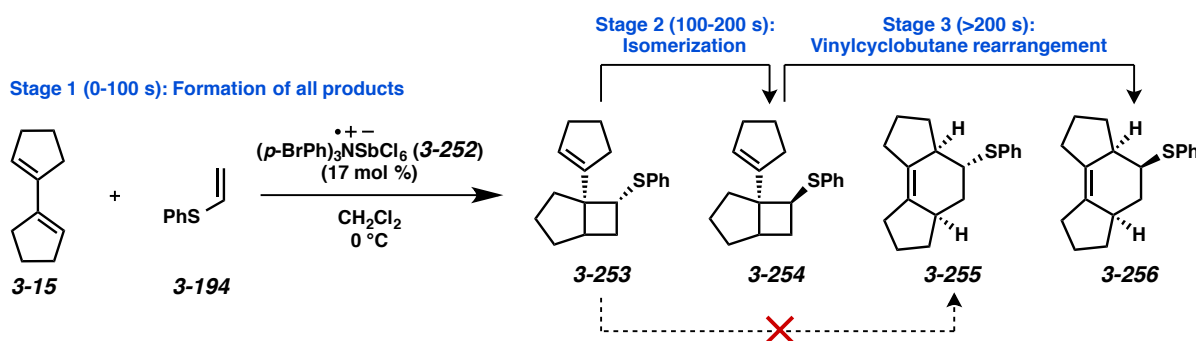
Bauld (1990)



Scheme 3.72. Cycloaddition of phenyl vinyl sulfide and 1,1'-bicyclopentenyl diene.

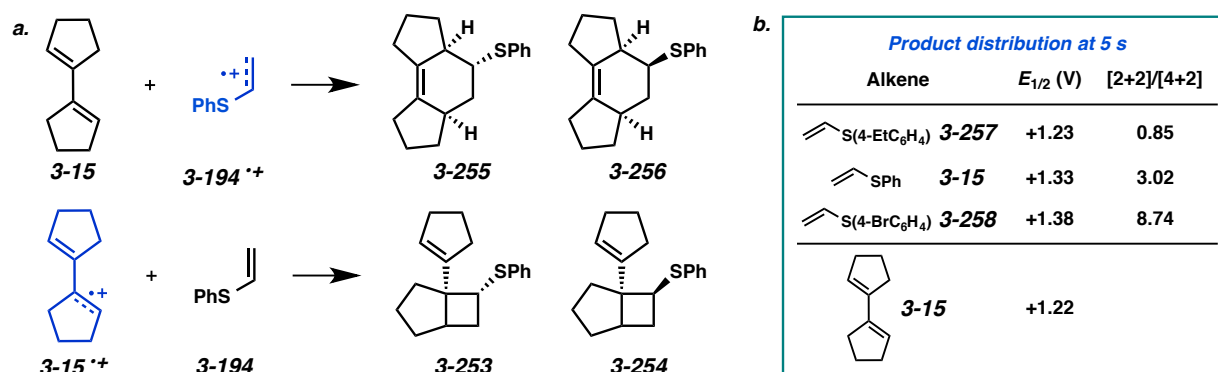
It should be noted that the majority of this study was conducted using aminium radical cation salt **3-252** as the single-electron oxidant; however, the researchers also attempted the cycloaddition under PET conditions (DCB,  $h\nu$ ) and determined that the reaction behaved the same as with the aminium salt and the product distribution and relative rates of formation of each product were comparable.

The reaction of phenyl vinyl sulfide (**3-194**) (1.1 equiv) and diene **3-15** (1 equiv) in dichloromethane at  $0^\circ\text{C}$  catalyzed by aminium salt **3-252** (17 mol %) was monitored by GC/MS. The researchers observed three major reaction stages: 1) from 0-100 seconds, all four products (**3-253–3-256**) are formed in the reaction mixture with the [2+2] products (**3-253** and **3-254**) predominating, 2) from 100-200 seconds, cyclobutane **3-253** isomerizes to cyclobutane **3-254**, and 3) at >200 seconds, cyclobutane **3-254** rearranges to cyclohexene **3-256** (Scheme 3.73). Evidently, cyclohexene **3-255** is only formed in stage 1 in a direct [4+2] cycloaddition and does not result from rearrangement of the cyclobutanes.



Scheme 3.73. Three stages of the cycloaddition.

To explain the product distribution at early reaction times, Bauld proposed that the oxidation of phenyl vinyl sulfide (**3-194<sup>+</sup>**) results primarily in the [4+2] adducts (**3-255** and **3-256**), while the oxidation of the diene (**3-15<sup>+</sup>**) preferentially affords the [2+2] adducts (**3-253** and **3-254**) (Scheme 3.74a). This conclusion can be rationalized based on the preferred conformation of the diene. Since the diene will mostly exist in its *s*-trans conformation, when diene **3-15** is oxidized and attacked by phenyl vinyl sulfide to give a distonic radical cation intermediate (**3-251<sup>+</sup>**), if the ring closing step is faster than rotation, only the [2+2] adducts should form.



Scheme 3.74. Explanation of periselectivity with reduction potentials.

The reduction potentials of the two cycloaddition components are proposed to directly influence the periselectivity of the reaction in the first 100 seconds. At the beginning of the reaction, both the diene (**3-15**) (+1.22 V) and the phenyl vinyl sulfide (**3-194**) (+1.33 V) are present in the reaction mixture in almost equal amounts, and their reduction potentials are low enough that they are both susceptible to single-electron oxidation by the aminium catalyst (**3-252**) (+1.05 V). Thus, when the catalyst is added to the reaction mixture containing the diene and alkene, they will both be oxidized by the catalyst at first, resulting in the formation of both the [4+2] and [2+2] adducts. Oxidation of the diene should be slightly favored over the alkene, so the [2+2] products will still predominate. In fact, at a reaction time of 5 seconds, a ratio of 3:1 was observed of cyclobutane to cyclohexene adducts (Scheme 3.74b). After all of the catalyst has been consumed, the reaction will continue through a radical chain propagation

mechanism, which will favor the oxidation of the diene over the alkene because of its lower reduction potential. Thus, cyclohexene **3-255** will stop forming, and cyclohexene **3-256** will only form through rearrangement of cyclobutane **3-254**.

To further demonstrate the effect of reduction potentials on the initial formation of the four cycloadducts, two other aryl vinyl sulfides were examined (Scheme 3.74b). The ratio of cyclobutane to cyclohexene products were compared at a reaction time of 5 seconds. When 4-bromophenyl vinyl sulfide (**3-258**) (+1.38 V) was reacted with diene (**3-15**), an 8.7:1 ratio of [2+2]:[4+2] adducts was formed. This is expected, since 4-bromophenyl vinyl sulfide (**3-258**) is more difficult to oxidize than phenyl vinyl sulfide, so oxidation of the diene in this case is preferred. Conversely, 4-ethylphenyl vinyl sulfide (**3-257**) (+1.23 V), which has a reduction potential almost identical to that of the diene, gave a product mixture that slightly favored the [4+2] adducts. In this case, the difference in electrochemical properties of the alkene and diene are less defined, so there is less preference for the oxidation of one over the other.

These results support Bauld's proposal of two mechanistic pathways where in the first 100 seconds of the reaction, the diene and the alkene compete for oxidation by the catalyst to give either [2+2] or [4+2] products. Thus, in the case of phenyl vinyl sulfide (**3-194**), the periselectivity of its cycloaddition with 1,1'-bicyclopentenyl diene **3-15** is less an issue of nucleophilicity, as Bauld first hypothesized, and more an issue of the comparable abilities of the diene and alkene to be oxidized and undergo cycloadditions that lead to different products. This example also demonstrates the ability of neutral cyclobutane products to undergo reoxidation and rearrangement to cyclohexenes, which is a different pathway to [4+2] products than the one proposed for the dimerization of 1,1-diphenylethylene (**3-221**) or 4-methoxystyrene (**3-48**) to naphthalene derivatives.

### 3.5 Conclusion

As described, photosensitized radical cation cycloadditions are a unique class of reactions that can be initiated by a variety of photocatalysts, both organic- and transition metal-based. In the past 6 years, transition metal photocatalyzed radical cation cycloadditions have significantly expanded the scope and efficiency of these powerful transformations. Additionally, transition metal photocatalysts are excited by visible light, which is desirable from a sustainability and green chemistry perspective;<sup>90</sup> however, the low natural abundance of Ru and Ir detracts from this benefit and is reflected in the increased cost of transition metal photocatalysts vs. organic photosensitizers.

For comparison purposes, the catalyst cost for a 1 mmol scale reaction was calculated for a variety of photocatalysts (Table 3.3). The organic photosensitizers, with the exception of TPT, are usually employed in higher catalyst loadings than the transition metal photocatalysts. Thus, a catalyst loading of 30 mol % for the organic photosensitizers and 2 mol % for the transition metal photocatalysts and TPT were chosen for calculations. It should be noted that some of these catalysts can also be prepared from starting materials that might be less expensive; however, the lowest commercial price available was used.<sup>91</sup>

Table 3.3. Cost of catalyst for a reaction run on 1 mmol scale.

Organic photosensitizer	Price, Vendor	Cost (30 mol %)	Transition metal photocatalyst	Price, Vendor	Cost (2 mol %)
DCB	25 g / \$29, Sigma-Aldrich	\$0.04	Ru(bpy) <sub>3</sub> (PF <sub>6</sub> ) <sub>2</sub>	1 g / \$120, Aspira	\$2.06
DCN	5 g / \$46, Alfa-Aesar	\$0.49	Ru(bpz) <sub>3</sub> (PF <sub>6</sub> ) <sub>2</sub>	50 mg / \$55, Aspira	\$19.03
DCA	1 g / \$54, TCI	\$3.70	Ir(ppy) <sub>3</sub>	50 mg / \$50, Aspira	\$13.10
Chloranil	10 g / \$10, Oakwood	\$0.07			
TPT(BF <sub>4</sub> )	5 g / \$31, Alfa-Aesar	\$0.05 <sup>a</sup>			

<sup>a</sup> Cost for 2 mol %

As expected, the organic photocatalysts, with the exception of DCA, are significantly less expensive than the transition metal photocatalysts, even taking into account their higher catalyst loading. Though price should not necessarily deter chemists from employing transition metal photocatalysts, it is something to keep in mind when performing reactions on larger scale. On the other hand, some UV irradiation devices that are used to excite organic photosensitizers can be fairly expensive as well. When the light source is taken into account, cost and convenience, as well as overall reaction efficiency, might favor the use of transition metal catalysts, which can be excited using common household light bulbs or sunlight.

In conclusion, though photosensitized radical cation [2+2] and [4+2] cycloadditions have been known since the 1960s, the reemergence of photoredox catalysis has brought these transformation back to the forefront of organic synthesis. Further investigation of transition metal photocatalyst systems in the coming years will likely lead to even greater advances in radical cation cycloaddition chemistry.

### Chapter 3 Notes and References

---

<sup>1</sup> (a) Teply, F. *Collect. Czech. Chem. Commun.* **2011**, *76*, 859-917. (b) Narayanam, J. M. R.; Stephenson, C. R. J. *Chem. Soc. Rev.* **2011**, *40*, 102-113. (c) Prier, C. K.; Rankic, D. A.; MacMillan, D. W. C. *Chem. Rev.* **2013**, *113*, 5322-5363. (d) Reckenthäler, M.; Griesbeck, A. G. *Adv. Synth. Catal.* **2013**, *355*, 2727-2744. (e) Nguyen, T. M.; Nicewicz, D. A. *ACS Catal.* **2014**, *4*, 355-360. (f) Fukuzumi, S.; Ohkubo, K. *Org. Biomol. Chem.* **2014**, *12*, 6059-6071. (g) Angnes, R. A.; Li, Z.; Correia, C. R. D.; Hammond, G. B. *Org. Biomol. Chem.* **2015**, *13*, 9152-9167. (h) Ravelli, D.; Protti, S.; Fagnoni, M. *Chem. Rev.* **2016**, DOI: 10.1021/acs.chemrev.5b00662.

<sup>2</sup> (a) Studer, A.; Curran, D. P. *Nature Chem.* **2014**, *6*, 765-773. (b) Luca, O. R.; Gustafson, J. L.; Maddox, S. M.; Fenwick, A. Q.; Smith, D. C. *Org. Chem. Front.* **2015**, *2*, 823-848. (c) Studer, A.; Curran, D. P. *Angew. Chem., Int. Ed.* **2016**, *55*, 58-102.

<sup>3</sup> (a) Neuteufel, R. A.; Arnold, D. R. *J. Am. Chem. Soc.* **1973**, *95*, 4080-4081. (b) Gassman, P. G.; Bottorff, K. J. *Tetrahedron Lett.* **1987**, *28*, 5449-5452. (c) Gassman, P. G.; Bottorff, K. J. *J. Am. Chem. Soc.* **1987**, *109*, 7547-7548. (d) Arnold, D. R.; Chan, M. S. W.; McManus, K. A. *Can. J. Chem.* **1996**, *74*, 2143-2166. (e) McManus, K. A.; Arnold, D. A. *Can. J. Chem.* **1995**, *73*, 2158-2169. (f) Asaoka, S.; Kitazawa, T.; Wada, T.; Inoue, Y. *J. Am. Chem. Soc.* **1999**, *121*, 8486-8498. (g) Hamilton, D. S.; Nicewicz, D. A. *J. Am. Chem. Soc.* **2012**, *134*, 18577-18580. (h) Nguyen, T. M.; Nicewicz, D. A. *J. Am. Chem. Soc.* **2013**, *135*, 9588-9591. (i) Perkowski, A. J.; Nicewicz, D. A. *J. Am. Chem. Soc.* **2013**, *135*, 10334-10337. (j) Nicewicz, D. A.; Hamilton, D. S. *Synthesis* **2014**, *25*, 1191-1196. (k) Nguyen, T. M.; Manohar, N.; Nicewicz, D. A. *Angew. Chem., Int. Ed.* **2014**, *53*, 6198-6201. (l) Wilger, D. J.; Grandjean, J. M.; Lammert, T.; Nicewicz, D. A. *Nature Chem.* **2014**, *6*, 720-726. (m) Romero, N.; Nicewicz, D. A. *J. Am. Chem. Soc.* **2014**, *136*, 17024-17035. (n) Morse, P. D.; Nicewicz, D. A. *Chem. Sci.* **2015**, *6*, 270-274.

<sup>4</sup> (a) Stufflebeme, G.; Lorenz, K. T.; Bauld, N. L. *J. Am. Chem. Soc.* **1986**, *108*, 4234-4235. (b) Bauld, N. L.; Stufflebeme, G. W.; Lorenz, K. T. *J. Phys. Org. Chem.* **1989**, *2*, 585-601. (c) Yueh, W.; Bauld, N. L. *J. Am. Chem. Soc.* **1995**, *117*, 5671-5676.

---

<sup>5</sup> For recent examples of formal [3+2] radical cation cycloadditions, see: (a) Huo, C.; Jia, X.; Zhang, W.; Yang, L.; Lu, J.; Liu, Z.-L. *Synlett* **2004**, 251-254. (b) Huo, C.; Wei, R.; Zhang, W.; Yang, L.; Liu, Z.-L. *Synlett* **2005**, 161-163. (c) Xuan, J.; Xia, X.-D.; Zeng, T.-T.; Feng, Z.-J.; Chen, J.-R.; Lu, L.-Q.; Xiao, W.-J. *Angew. Chem., Int. Ed.* **2014**, *53*, 5653-5656. (d) Nquyen, T. H.; Morris, S. A.; Zheng, N. *Adv. Synth. Catal.* **2014**, *356*, 2831-2837. (e) Nguyen, T. H.; Maity, S.; Zheng, N. *Beilstein J. Org. Chem.* **2014**, *10*, 975-980. (f) Blum, T. R.; Zhu, Y.; Nordeen, S. A.; Yoon, T. P. *Angew. Chem., Int. Ed.* **2014**, *126*, 11236-11239. (g) Lu, Z.; Parrish, J. D.; Yoon, T. P. *Tetrahedron* **2014**, *70*, 4270-4278.

<sup>6</sup> (a) Grandjean, J.; Nicewicz, D. A. *Angew. Chem., Int. Ed.* **2013**, *52*, 3967-3971. (b) Zeller, M. A.; Riener, M.; Nicewicz, D. A. *Org. Lett.* **2014**, *16*, 4810-4813. (c) Gesmundo, N. J.; Grandjean, J. M.; Nicewicz, D. A. *Org. Lett.* **2015**, *17*, 1316-1319. (d) Cavanaugh, C. L.; Nicewicz, D. A. *Org. Lett.* **2015**, *17*, 6082-6085.

<sup>7</sup> (a) Miyashi, T.; Akinori, K.; Yasutake, T. *J. Am. Chem. Soc.* **1988**, *110*, 3676-3677. (b) Takahashi, Y.; Okitsu, O.; Ando, M.; Miyashi, T. *Tetrahedron Lett.* **1994**, *35*, 3953-3956. (c) Parrish, J. D.; Ischay, M. A.; Lu, Z.; Guo, S.; Peters, N. R.; Yoon, T. P. *Org. Lett.* **2012**, *14*, 1640-1643. (d) Kamata, M.; Hagiwara, J.; Hokari, T.; Suzuki, C.; Fujino, R.; Kobayashi, S.; Kim, H.-S.; Wataya, Y. *Res. Chem. Intermed.* **2013**, *39*, 127-137. (e) Gesmundo, N. J.; Nicewicz, D. A. *Beilstein J. Org. Chem.* **2014**, *10*, 1272-1281.

<sup>8</sup> (a) Schutte, R.; Freeman, G. R. *J. Am. Chem. Soc.* **1969**, *91*, 3715-3720. (b) Penner, T. L.; Whitten, D. G.; Hammond, G. S. *J. Am. Chem. Soc.* **1970**, *92*, 2861-2867.

<sup>9</sup> (a) Wehrmann, F. *Montash. Chem.* **1964**, *95*, 1007-1009. (b) Mlcoch, J.; Steckhan, E. *Tetrahedron Lett.* **1987**, *28*, 1081-1084.

<sup>10</sup> (a) Bell, F. A.; Crellin, R. A.; Fujii, N.; Ledwith, A. *Chem. Commun.* **1969**, 251-252. (b) Ledwith, A. *Acc. Chem. Res.* **1972**, *5*, 133-139. (c) Bauld, N. L.; Gao, D. *J. Chem. Soc., Perkin. Trans. 2* **2000**, 191-192.

<sup>11</sup> (a) Reynolds, D. W.; Bauld, N. L. *Tetrahedron* **1986**, *42*, 6189-6194. (b) Bauld, N. L.; Bellville, D. J.; Harirchian, B.; Lorenz, K. T.; Pabon, R. A.; Reynolds, D. W.; Wirth, D. D.; Chiou, H.-S.; Marsh, B. K.

---

*Acc. Chem. Res.* **1987**, *20*, 371-378. (c) Reynolds, D. W.; Lorenz, K. T.; Chiou, H.-S.; Bellville, D. J.; Pabon, R. A.; Bauld, N. L. *J. Am. Chem. Soc.* **1987**, *109*, 4960-4968. (d) Bauld, N. L. *Tetrahedron* **1989**, *45*, 5307-5363. (e) Yueh, W.; Bauld, N. L. *J. Phys. Org. Chem.* **1996**, *9*, 529-538.

<sup>12</sup> For reviews of photosensitized cycloadditions of dienes and polyenes, see: (a) Dilling, W. L. *Chem. Rev.* **1969**, *69*, 845-877. (b) Liu, R. S. H.; Hammond, G. S. *Photochem. Photobiol. Sci.* **2003**, *2*, 835-844. For recent examples of [2+2] cycloadditions initiated by energy transfer, see: (c) Lu, Z.; Yoon, T. P. *Angew. Chem., Int. Ed.* **2012**, *51*, 10329-10332. (d) Hurtley, A. E.; Lu, Z.; Yoon, T. P. *Angew. Chem., Int. Ed.* **2014**, *53*, 8991-8994. (e) Alonso, R.; Bach, T. *Angew. Chem., Int. Ed.* **2014**, *53*, 4368-4371. (f) Kumarasamy, E.; Raghunathan, R.; Jockusch, S.; Ugrinov, A.; Sivaguru, J. *J. Am. Chem. Soc.* **2014**, *136*, 8729-8737. (g) Mojr, V.; Svobodová, E.; Straková, K.; Nevesely, T.; Chudoba, J.; Dvoráková, H.; Cibulka, R. *Chem. Commun.* **2015**, *51*, 12036-12039.

<sup>13</sup> (a) Müller, F.; Mattay, J. *Chem. Rev.* **1993**, *93*, 99-117. (b) Yoon, T. P. *ACS Catal.* **2013**, *3*, 895-902. (c) Liu, Y.; Song, R.; Li, J. *Sci. China Chem.* **2016**, *59*, 161-170.

<sup>14</sup> Karon, K.; Lapkowski, M. *J. Solid State Electrochem.* **2015**, *19*, 2601-2610.

<sup>15</sup> All reduction potentials are in V vs. SCE, unless otherwise noted.

<sup>16</sup> (a) Ellinger, L. P. *Polymer* **1964**, *5*, 559-578. (b) Carruthers, R. A.; Crellin, R. A.; Ledwith, A. *Chem. Commun.* **1969**, 252-253.

<sup>17</sup> (a) Carruthers, R. A.; Crellin, R. A.; Ledwith, A. *Chem. Commun.* **1969**, 252-253. (b) Crellin, R. A.; Lambert, M. C.; Ledwith, A. *J. Chem. Soc., Chem. Commun.* **1970**, 682-683.

<sup>18</sup> Bauld, N. L.; Hirirchian, B.; Reynolds, D. W.; White, J. C. *J. Am. Chem. Soc.* **1988**, *110*, 8111-8117.

<sup>19</sup> Kuwata, S.; Shigemitsu, Y.; Odaira, Y. *J. Chem. Soc., Chem. Commun.* **1972**, 2.

<sup>20</sup> Kuwata, S.; Shigemitsu, Y.; Odaira, Y. *J. Org. Chem.* **1973**, *38*, 3803-3805.

<sup>21</sup> Neunteufel, R. A.; Arnold, D. R. *J. Am. Chem. Soc.* **1973**, *95*, 4080-4081.

<sup>22</sup> Mizuno, K.; Ueda, H.; Otsuji, Y. *Chem. Lett.* **1981**, 1237-1240.

- 
- <sup>23</sup> The dimerization of alkyl vinyl ethers has been reported, but only through an energy transfer process: Mizuno, K.; Hashizume, T.; Otsuji, Y. *J. Chem. Soc., Chem. Commun.* **1983**, 772-773.
- <sup>24</sup> Mizuno, K.; Kagano, H.; Kasuga, T.; Otsuji, Y. *Chem. Lett.* **1983**, 133-136.
- <sup>25</sup> Mattes, S. L.; Luss, H. R.; Farid, S. *J. Phys. Chem.* **1983**, 87, 4779-4781.
- <sup>26</sup> Farid, S.; Shealer, S. E. *J. Chem. Soc., Chem. Commun.* **1973**, 677-678.
- <sup>27</sup> Metzner, W.; Wendisch, D. *Justus Liebigs Ann. Chem.* **1969**, 730, 111-120.
- <sup>28</sup> Mizuno, K.; Kaji, R.; Otsuji, Y. *Chem. Lett.* **1977**, 1027-1030.
- <sup>29</sup> Majima, T.; Pac, C.; Nakasone, A.; Sakurai, H. *J. Chem. Soc., Chem. Commun.* **1978**, 490-491.
- <sup>30</sup> Yamamoto, M.; Asanuma, T.; Nishijima, Y. *J. Chem. Soc., Chem. Commun.* **1975**, 53-54.
- <sup>31</sup> Kojima, M.; Sakuragi, H.; Tokumaru, K. *Tetrahedron Lett.* **1981**, 22, 2889-2892.
- <sup>32</sup> Lewis, F. D.; Kojima, M. *J. Am. Chem. Soc.* **1988**, 110, 8664-8670.
- <sup>33</sup> Mizuno, K.; Kagano, H.; Otsuji, Y. *Tetrahedron Lett.* **1983**, 24, 3849-3850.
- <sup>34</sup> Mizuno, K.; Hashizume, T.; Otsuji, Y. *J. Chem. Soc., Chem. Commun.* **1983**, 977-978.
- <sup>35</sup> Schepp, N. P.; Shukla, D.; Sarker, H.; Bauld, N. L.; Johnston, L. J. *J. Am. Chem. Soc.* **1997**, 119, 10325-10334.
- <sup>36</sup> Ischay, M. A.; Lu, Z.; Yoon, T. P. *J. Am. Chem. Soc.* **2010**, 132, 8572-8574.
- <sup>37</sup> Ischay, M. A.; Ament, M. S.; Yoon, T. P. *Chem. Sci.* **2012**, 3, 2807-2811.
- <sup>38</sup> Riener, M.; Nicewicz, D. A. *Chem. Sci.* **2013**, 4, 2625-2629.
- <sup>39</sup> Roth, H. G.; Romero, N. A.; Nicewicz, D. A. *Synlett* **2016**, 27, 714-723.
- <sup>40</sup> (a) Ruy, J.-H.; Son, H. J.; Lee, S. H.; Sohn, D. H. *Bioorg. Med. Chem. Lett.* **2002**, 12, 649-651. (b) Apers, S.; Vlietinck, A.; Pieters, L. *Phytochem. Rev.* **2003**, 2, 201-217. (c) Davis, R.; Carroll, A.; Duffy, S.; Avery, V.; Guymer, G.; Forster, P.; Quinn, R. *J. Nat. Prod.* **2007**, 70, 1118-1121. (d) Dembitsky, V. *M. J. Nat. Med.* **2008**, 62, 1-33. (e) Davis, R.; Barnes, E.; Longden, J.; Avery, V.; Healy, P. *Bioorg. Med. Chem.* **2009**, 17, 1387-1392.

- 
- <sup>41</sup> Ma, Z.; Wang, X.; Wang, X.; Rodriguez, R. A.; Moore, C. E.; Gao, S.; Tan, X.; Ma, Y.; Rheingold, A. L.; Baran, P. S.; Chen, C. *Science* **2014**, *346*, 219-224.
- <sup>42</sup> (a) Walker, R. P.; Faulkner, D. J.; van Engen, D.; Clardy, J. *J. Am. Chem. Soc.* **1981**, *103*, 6772-6773.  
(b) Baran, P. S.; Zografos, A. L.; O'Malley, D. P. *J. Am. Chem. Soc.* **2004**, *126*, 3726-3727.
- <sup>43</sup> Stout, E. P.; Wang, Y.-G.; Romo, D.; Molinski, T. F. *Angew. Chem., Int. Ed.* **2012**, *51*, 4877-4881.
- <sup>44</sup> Wang, X.; Chen, C. *Tetrahedron* **2015**, *71*, 3690-3693.
- <sup>45</sup> Corey, E. J.; Bass, J. D.; LeMahieu, R.; Mitra, R. B. *J. Am. Chem. Soc.* **1964**, *86*, 5570-5583.
- <sup>46</sup> Kranz, D. P.; Griesbeck, A. G.; Alle, R.; Perez-Ruiz, R.; Neudörfl, J. M.; Meerholz, K.; Schmalz, H.-G. *Angew. Chem., Int. Ed.* **2012**, *51*, 6000-6004.
- <sup>47</sup> Ischay, M. A.; Anzovino, M. E.; Du, J.; Yoon, T. P. *J. Am. Chem. Soc.* **2008**, *130*, 12886-12887.
- <sup>48</sup> Mella, M.; Fasani, E.; Albin, A. *Tetrahedron* **1991**, *47*, 3137-3154.
- <sup>49</sup> (a) Bellville, D. J.; Wirth, D. D.; Bauld, N. L. *J. Am. Chem. Soc.* **1981**, *103*, 718-720. (b) Bellville, D. J.; Bauld, N. L. *J. Am. Chem. Soc.* **1982**, *104*, 2665-2667. (c) Bellville, D. J.; Bauld, N. L. *J. Am. Chem. Soc.* **1982**, *104*, 5700-5702. (d) Bauld, N. L.; Pabon, R. *J. Am. Chem. Soc.* **1983**, *105*, 633-634. (e) Bauld, N. L.; Bellville, D. J.; Pabon, R.; Chelsky, R.; Green, G. *J. Am. Chem. Soc.* **1983**, *105*, 2378-2382. (f) Bellville, D. J.; Bauld, N. L.; Pabon, R.; Gardner, S. A. *J. Am. Chem. Soc.* **1983**, *105*, 3584-3588.
- <sup>50</sup> Jones, C. R.; Allman, B. J.; Mooring, A.; Spahic, B. *J. Am. Chem. Soc.* **1983**, *105*, 652-654.
- <sup>51</sup> Alder, K.; Stein, G. *Justus Liebigs Ann. Chem.* **1932**, *496*, 197-203.
- <sup>52</sup> Schenck, G. O.; Mannsfield, S.-P.; Schomburg, G.; Krauch, C. H. *Z. Naturforsch. B* **1964**, *19B*, 18-22.
- <sup>53</sup> Valentine, D.; Turro, Jr. N. J.; Hammond, G. S. *J. Am. Chem. Soc.* **1964**, *86*, 5202-5208.
- <sup>54</sup> Yang, N. C.; Srinivasachar, K.; Kim, B.; Libman, J. *J. Am. Chem. Soc.* **1975**, *97*, 5006-5008.
- <sup>55</sup> Calhoun, G. C.; Schuster, G. B. *J. Am. Chem. Soc.* **1984**, *106*, 6870-6871.
- <sup>56</sup> (a) Pabon, R. A.; Bellville, D. J.; Bauld, N. L. *J. Am. Chem. Soc.* **1983**, *105*, 5159-5160. (b) Martiny, M.; Steckhan, E.; Esch, T. *Chem. Ber.* **1993**, *126*, 1671-1682. (c) Mattay, J.; Vondenhof, M.; Denig, R. *Chem. Ber.* **1989**, *122*, 951-958.

- 
- <sup>57</sup> Reynolds, D. W.; Lorenz, K. T.; Chiou, H.-S.; Bellville, D. J.; Pabon, R. A.; Bauld, N. L. *J. Am. Chem. Soc.* **1987**, *109*, 4960-4968.
- <sup>58</sup> Gassman, P. G.; Singleton, D. A. *J. Am. Chem. Soc.* **1984**, *106*, 7994-7995.
- <sup>59</sup> Miranda, M. A.; García, H. *Chem. Rev.* **1994**, *94*, 1063-1089.
- <sup>60</sup> Mattay, J.; Gersdorf, J.; Mertes, J. *J. Chem. Soc., Chem. Commun.* **1985**, 1088-1090.
- <sup>61</sup> Botzem, J.; Haberl, U.; Steckhan, E.; Blechert, S. *Acta Chem. Scand.* **1998**, *52*, 175-193.
- <sup>62</sup> Gieseler, A.; Steckhan, E.; Wiest, O.; Knoch, F. *J. Org. Chem.* **1991**, *56*, 1405-1411.
- <sup>63</sup> Wiest, O.; Steckhan, E.; Grein, F. *J. Org. Chem.* **1992**, *57*, 4034-4037.
- <sup>64</sup> (a) Wiest, O.; Steckhan, E. *Tetrahedron Lett.* **1993**, *34*, 6391-6394. (b) Haberl, U.; Steckhan, E.; Blechert, S.; Wiest, O. *Chem. Eur. J.* **1999**, *5*, 2859-2865.
- <sup>65</sup> Pindur, U.; Haber, M.; Sattler, K. *J. Chem. Educ.* **1993**, *70*, 263-269.
- <sup>66</sup> (a) Gürtler, C. F.; Blechert, S.; Steckhan, E. *Synlett* **1994**, 141-142. (b) Gürtler, C. F.; Blechert, S.; Steckhan, E. *Chem. Eur. J.* **1997**, *3*, 447-452.
- <sup>67</sup> Peglow, T.; Blechert, S.; Steckhan, E. *Chem. Commun.* **1999**, 433-434.
- <sup>68</sup> Keck, G. E.; Fleming, S.; Nickell, D.; Weider, P. *Synth. Commun.* **1979**, *9*, 281-286.
- <sup>69</sup> Mizuno, K.; Kaji, R.; Okada, H.; Otsuji, Y. *J. Chem. Soc., Chem. Commun.* **1978**, 594-595.
- <sup>70</sup> Schmittel, M.; Wöhrle, C.; Bohn, I. *Chem. Eur. J.* **1996**, *2*, 1031-1040.
- <sup>71</sup> Schmittel, M.; von Seggern, H. *J. Am. Chem. Soc.* **1993**, *115*, 2165-2177.
- <sup>72</sup> Argüello, J. E.; Pérez-Ruiz, R.; Miranda, M. A. *Org. Lett.* **2007**, *9*, 3587-3590.
- <sup>73</sup> Harirchian, B.; Bauld, N. L. *J. Am. Chem. Soc.* **1989**, *111*, 1826-1828.
- <sup>74</sup> Cismesia, M. A.; Yoon, T. P. *Chem. Sci.* **2015**, *6*, 5426-5434.
- <sup>75</sup> Moeller, K. D. *Synlett* **2009**, 1208-1218.
- <sup>76</sup> Lin, S.; Padilla, C. E.; Ischay, M. A.; Yoon, T. P. *Tetrahedron Lett.* **2012**, *53*, 3173-3176.
- <sup>77</sup> Neunteufel, R. A.; Arnold, D. R. *J. Am. Chem. Soc.* **1973**, *95*, 4080-4081.
- <sup>78</sup> Maroulis, A. J.; Arnold, D. R. *J. Chem. Soc., Chem. Commun.* **1979**, 351-352.

- 
- <sup>79</sup> Asanuma, T.; Yamamoto, M.; Nishijima, Y. *J. Chem. Soc., Chem. Commun.* **1975**, 608-609.
- <sup>80</sup> Asanuma, T.; Gotoh, T.; Tsuchida, A.; Yamamoto, M.; Nishijima, Y. *J. Chem. Soc., Chem. Commun.* **1977**, 485-486.
- <sup>81</sup> Mattes, S. L.; Farid, S. *J. Am. Chem. Soc.* **1983**, *105*, 1386-1387.
- <sup>82</sup> Schepp, N. P.; Johnston, L. J. *J. Am. Chem. Soc.* **1994**, *116*, 6895-6903.
- <sup>83</sup> Tojo, S.; Toki, S.; Takamuku, S. *J. Org. Chem.* **1991**, *56*, 6240-6243.
- <sup>84</sup> O'Neil, L. L.; Wiest, O. *J. Org. Chem.* **2006**, *71*, 8926-8933.
- <sup>85</sup> Yamamoto, M.; Yoshikawa, H.; Gotoh, T.; Nishijima, Y. *Bull. Chem. Soc. Jpn.* **1983**, *56*, 2531-2532.
- <sup>86</sup> Kadota, S.; Tsubono, K.; Makino, K.; Takeshita, M.; Kikuchi, T. *Tetrahedron Lett.* **1987**, *28*, 2857-2860.
- <sup>87</sup> Reynolds, D. W.; Harirchian, B.; Chiou, H.-S.; Marsh, B. K.; Bauld, N. L. *J. Phys. Org. Chem.* **1989**, *2*, 57-88.
- <sup>88</sup> Pabon, R. A.; Bellville, D. J.; Bauld, N. L. *J. Am. Chem. Soc.* **1984**, *106*, 2730-2731.
- <sup>89</sup> Kim, T.; Pye, R. J.; Bauld, N. L. *J. Am. Chem. Soc.* **1990**, *112*, 6285-6290.
- <sup>90</sup> (a) Albini, A.; Fagnoni, M. *Green Chem.* **2004**, *6*, 1-6. (b) Oelgemöller, M. Jung, C.; Mattay, J. *Pure Appl. Chem.* **2007**, *79*, 1939-1947. (c) Yoon, T. P.; Ischay, M. A.; Du, J. *Nature Chem.* **2010**, *2*, 527-532.
- <sup>91</sup> The commercial price of each photocatalyst was determined on April 28, 2016.

CHAPTER 4  
 CHROMIUM-PHOTOCATALYZED RADICAL CATION DIELS-ALDER REACTIONS OF  
 ELECTRON-RICH DIENOPHILES

**4.1 Introduction: Photooxidizing Chromium Catalysts**

The past decade has seen significant advancements in the area of photoredox catalysis. Light-activated complexes of Ru and Ir, in particular, have experienced extensive investigation, uncovering new and unique reaction modes in organic synthesis.<sup>1</sup> Though these catalysts are highly effective, in a field that is predicated upon the concept of sustainable chemistry, photocatalysts based on more earth-abundant metals are desirable.<sup>2</sup> Notable achievements so far in this field have utilized Cu<sup>3</sup> and Fe<sup>4</sup> photocatalytic systems. Complexes of Cr also show potential.<sup>5</sup>

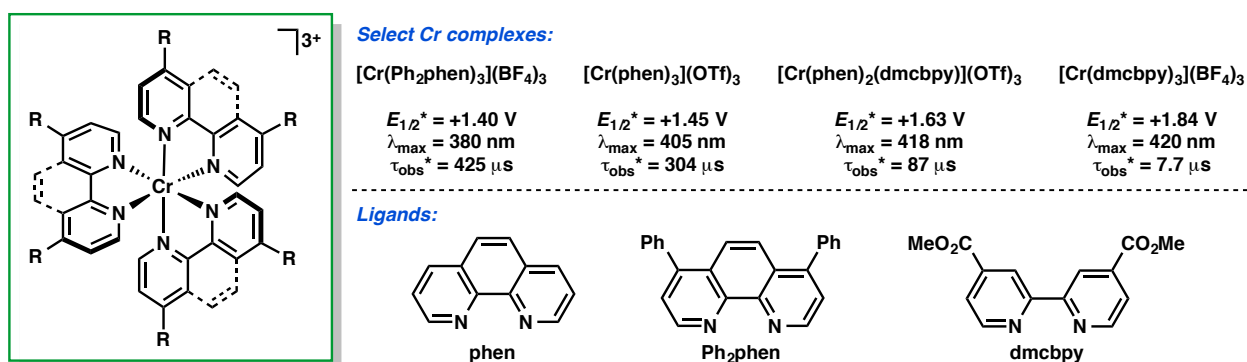


Figure 4.1. Select Cr(III) complexes utilized in this chapter.

In 2010, our collaborators in the Shores and Damrauer labs reported on poly-pyridyl and poly-phenanthrolyl Cr(III) complexes featuring promising photochemical properties (Figure 4.1).<sup>5a</sup> Notably, the Cr complexes absorb light in the near-UV/visible region, exhibit long excited state lifetimes (approx.

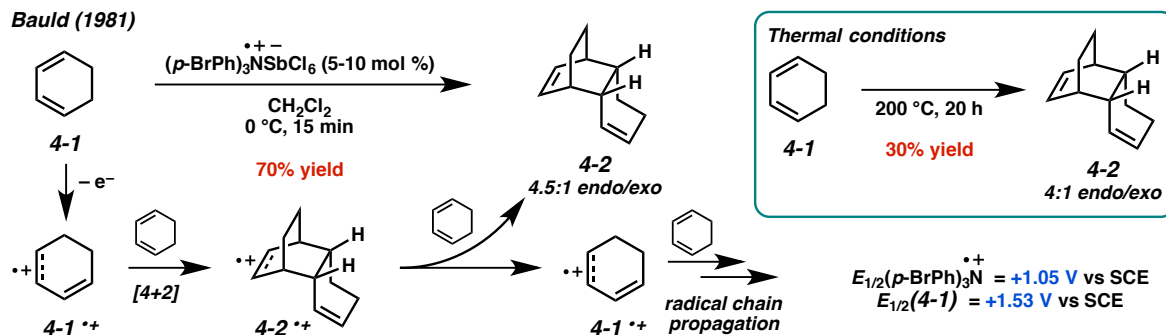
up to 0.5 ms), and possess a range of relatively high excited state reduction potentials (+1.40-1.84 V vs. SCE<sup>6</sup>). This data suggests that the Cr(III) complexes may be suitable photocatalysts for organic synthesis. In 2013, we embarked upon a collaborative effort with the Shores, Damrauer, Rappé, and Rovis groups aimed at developing photocatalysts of earth-abundant metals.<sup>7</sup> Our early endeavors toward this goal are discussed in this chapter.

## 4.2 Preliminary Experiments

We commenced our search for earth-abundant metal photocatalysts by investigating the synthetic utility of the previously described Cr complexes (Figure 4.1). Knowing that the Cr complexes had high excited state reduction potentials, we focused on photocatalytic reactions initiated by single-electron oxidation that have been previously reported in the literature. Several different reaction types were attempted, such as nucleophilic addition into oxidatively generated aminium ions of tetrahydroisoquinolines<sup>8</sup> and sulfide additions to alkenes.<sup>9</sup> The drawback to these reactions, however, was that they required additional reagents (e.g. sacrificial oxidants, hydrogen-transfer reagents, etc.) in order for product formation to occur. This extra variable was something that we initially wished to avoid, owing to our lack of complete knowledge of the Cr catalysts' reactivity. Since our first aim was to establish that the excited state Cr catalyst could be quenched by an organic substrate, we sought a reaction that would simply be initiated by the Cr catalyst and then preferably propagate itself so that catalyst regeneration or additional reagents would not be necessary.<sup>10</sup>

For this, we turned our attention to radical cation accelerated cycloadditions, namely the [4+2] dimerization of 1,3-cyclohexadiene. Discovered by Bauld and coworkers in 1981 with an aminium salt catalyst, this dimerization is initiated by single-electron oxidation of 1,3-cyclohexadiene (**4-1**) to yield diene radical cation **4-1<sup>•+</sup>** (Scheme 4.1).<sup>11</sup> This electron-poor radical cation can then react in a [4+2] fashion with another equivalent of diene **4-1** to give the cycloadduct radical cation **4-2<sup>•+</sup>**, which can

propagate the reaction by oxidizing another diene equivalent. Importantly, when this reaction was performed under thermal conditions (200 °C), only 30% yield of dimer **4-2** was obtained after 20 h.



Scheme 4.1. Radical cation catalyzed [4+2] cyclodimerization of 1,3-cyclohexadiene.

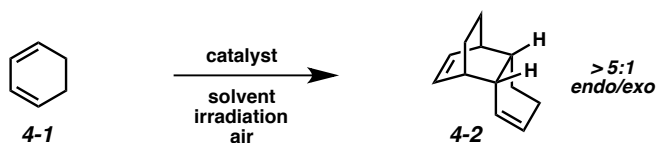
The radical cation accelerated [4+2] cycloaddition of 1,3-cyclohexadiene fit all our criteria: 1) no additional sacrificial reagents were required, 2) as a chain propagation process, the catalyst needed only to initiate the reaction, then product formation would occur rapidly and be easily detected, and 3) since 1,3-cyclohexadiene is not electron-poor, this reaction would not proceed at ambient temperature in the absence of catalyst.

#### 4.3 [4+2] Dimerization of 1,3-Cyclohexadiene

Encouragingly, when a solution of 1,3-cyclohexadiene (**4-1**) and  $\text{Cr}(\text{dmcby})_3(\text{BF}_4)_3$  ( $E_{1/2}^* = +1.84 \text{ V}$ ) in  $\text{CH}_2\text{Cl}_2$  was irradiated with a combination of 300, 350, and 419 nm lights (NUV irradiation), the desired dimer (**4-2**) formed in 19% yield (Table 4.1, entry 1). Different solvents were tested, and an increase to 39% yield was observed in acetonitrile (entry 2), but no product formation occurred in methanol or THF (entries 3 and 4). The employment of nitromethane as a solvent gave dimer **4-2** in 61% GC yield (entry 5). We attributed the increased efficiency of the dimerization in nitromethane to solubility: both 1,3-cyclohexadiene and the Cr catalyst were soluble in nitromethane, whereas the catalyst displayed low

solubility in dichloromethane and 1,3-cyclohexadiene was not very soluble in acetonitrile. Additionally, radical cation cycloadditions have often been reported to perform better in more polar solvents, an effect which could also be at play here. Next, catalyst loading was reduced to 1 mol %, affording the dimer in 66% yield (entry 6). We also attempted the reaction with different Cr photocatalysts (entries 7-9), which were all able to catalyze the cycloaddition; however, lower yields were obtained, perhaps due to these catalysts' lower excited state reduction potentials. Notably, visible light irradiation was also possible with this transformation, providing dimer **4-2** in just a slightly lower yield (entry 10).

Table 4.1. [4+2] Dimerization of 1,3-cyclohexadiene optimization.



Entry	Catalyst (mol %)	Solvent	Irradiation <sup>a</sup>	Time (h)	GC yield (%) <sup>b</sup>
1	[Cr(dmc bpy) <sub>3</sub> ](BF <sub>4</sub> ) <sub>3</sub> (2)	CH <sub>2</sub> Cl <sub>2</sub>	NUV	24	19
2	[Cr(dmc bpy) <sub>3</sub> ](BF <sub>4</sub> ) <sub>3</sub> (2)	CH <sub>3</sub> CN	NUV	24	39
3	[Cr(dmc bpy) <sub>3</sub> ](BF <sub>4</sub> ) <sub>3</sub> (2)	CH <sub>3</sub> OH	NUV	24	0
4	[Cr(dmc bpy) <sub>3</sub> ](BF <sub>4</sub> ) <sub>3</sub> (2)	THF	NUV	24	0
5	[Cr(dmc bpy) <sub>3</sub> ](BF <sub>4</sub> ) <sub>3</sub> (2)	CH <sub>3</sub> NO <sub>2</sub>	NUV	24	61
6	[Cr(dmc bpy) <sub>3</sub> ](BF <sub>4</sub> ) <sub>3</sub> (1)	CH <sub>3</sub> NO <sub>2</sub>	NUV	24	66
7	[Cr(phen) <sub>2</sub> (dmc bpy)](OTf) <sub>3</sub> (2)	CH <sub>3</sub> NO <sub>2</sub>	NUV	24	39
8	[Cr(phen) <sub>3</sub> ](OTf) <sub>3</sub> (2)	CH <sub>3</sub> NO <sub>2</sub>	NUV	24	36
9	[Cr(Ph <sub>2</sub> phen) <sub>3</sub> ](BF <sub>4</sub> ) <sub>3</sub> (2)	CH <sub>3</sub> NO <sub>2</sub>	NUV	24	40
10	[Cr(dmc bpy) <sub>3</sub> ](BF <sub>4</sub> ) <sub>3</sub> (2)	CH <sub>3</sub> NO <sub>2</sub>	23 W CFL	24	55
11	none	CH <sub>3</sub> NO <sub>2</sub>	NUV	24	< 1
12	[Cr(dmc bpy) <sub>3</sub> ](BF <sub>4</sub> ) <sub>3</sub> (2)	CH <sub>3</sub> NO <sub>2</sub>	none <sup>c</sup>	48	< 1
13	CrCl <sub>3</sub> (2)	CH <sub>3</sub> NO <sub>2</sub>	NUV	24	1
14	none, 6 mol % dmc bpy	CH <sub>3</sub> NO <sub>2</sub>	NUV	24	< 1
15	Ru(bpy) <sub>3</sub> Cl <sub>2</sub> (5)	CH <sub>2</sub> Cl <sub>2</sub>	23 W CFL	48	< 1
16	Ru(bpz) <sub>3</sub> (PF <sub>6</sub> ) <sub>2</sub> (1)	CH <sub>2</sub> Cl <sub>2</sub>	23 W CFL	24	< 1
17	Ru(bpz) <sub>3</sub> (PF <sub>6</sub> ) <sub>2</sub> (1)	CH <sub>3</sub> NO <sub>2</sub>	23 W CFL	24	21

<sup>a</sup> NUV is a combination of 300, 350, and 419 nm light bulbs

<sup>b</sup> Determined using tridecane as an internal standard

<sup>c</sup> Reaction heated at 40 °C (temperature inside photoreactor)

Several control experiments were performed to confirm the role of the Cr photocatalyst in the cycloaddition. When the reaction was performed in the absence of catalyst, only trace product was observed (entry 11). Likewise, when the reaction was performed in the absence of light, still only trace product formed (entry 12). Utilizing catalytic CrCl<sub>3</sub> instead of the photocatalyst also resulted in only trace product (entry 13), as did running the reaction without catalyst, but with 6 mol % of the dmcbpy ligand (entry 14). These experiments indicated that both the Cr photocatalyst and irradiation were required for this reaction to proceed.

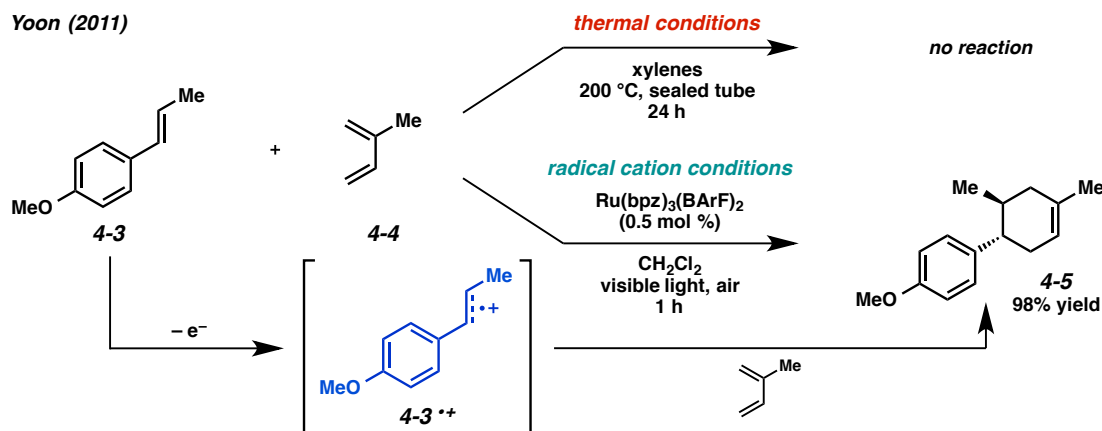
Other photooxidizing catalysts were also attempted with this transformation. Ru(bpy)<sub>3</sub>Cl<sub>2</sub> and Ru(bpz)<sub>3</sub>(PF<sub>6</sub>)<sub>2</sub> with visible light irradiation gave only trace amounts of the dimerization product in dichloromethane. In nitromethane, however, the Ru(bpz)<sub>3</sub>(PF<sub>6</sub>)<sub>2</sub> reaction gave a 21% yield of the dimer (**4-2**), highlighting the importance of solvent choice for these photoredox transformations.

Ultimately, the [4+2] dimerization of 1,3-cyclohexadiene allowed us to prove that the Cr complexes were viable photocatalysts, as well as provided us with an entry point to explore the reactivity of the Cr catalysts and determine ideal reaction conditions (solvent, irradiation, etc.)

#### 4.4 Cross [4+2] Cycloadditions

In a typical Diels-Alder reaction, the diene is electron-rich and the dienophile is electron-poor, as dictated by HOMO-raising and LUMO-lowering effects, respectively. Thus, the employment of electron-rich alkenes as dienophiles is very difficult through traditional Diels-Alder methods, but can be accomplished if the alkene is first rendered electron-poor through single-electron oxidation. In 2011, Yoon and coworkers reported the Diels-Alder reaction of electron-rich dienophiles catalyzed by Ru(bpz)<sub>3</sub><sup>2+</sup> and visible light.<sup>12</sup> When Yoon attempted the Diels-Alder reaction of electron-rich alkene **4-3** and isoprene (**4-4**) under thermal conditions (200 °C), after 24 h no cycloadduct had formed (Scheme 4.2). In contrast, when the same reaction was performed in the presence of Ru(bpz)<sub>3</sub>(BARF)<sub>2</sub> (BARF = tetrakis[3,5-bis(trifluoromethyl)phenyl]borate) and visible light, a 98% yield of cycloadduct **4-5** was obtained in just 1

h. These results demonstrate the power of single-electron oxidation in initiating Diels-Alder reactions between two electron-rich components.



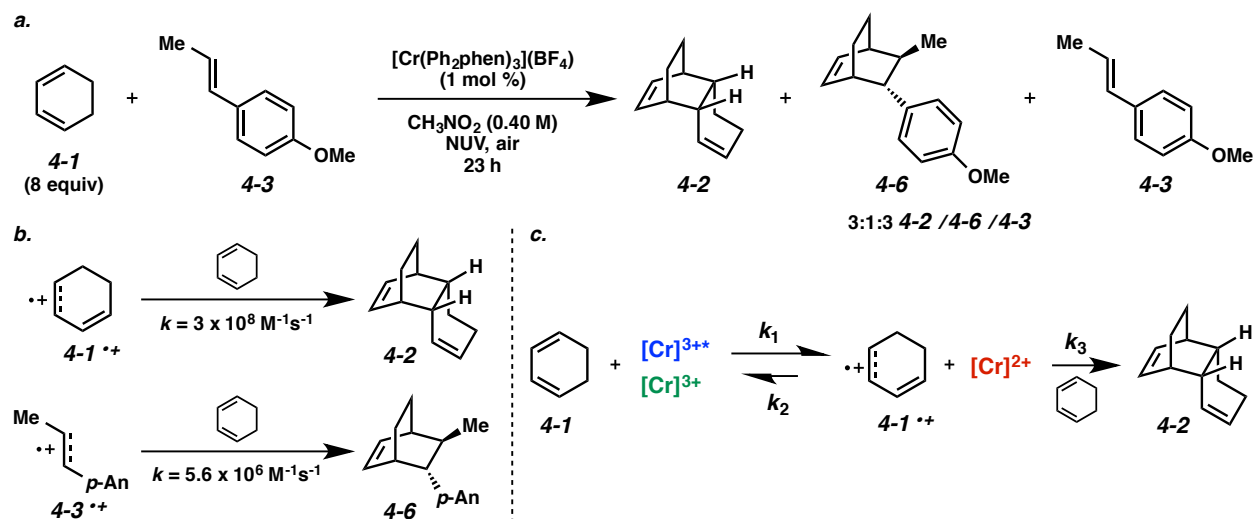
Scheme 4.2. Comparison of thermal and radical cation conditions for the Diels-Alder cycloaddition of electron-rich alkenes.

Notably, the reduction potentials of the excited state Ru(bpz)<sub>3</sub><sup>2+</sup> and Cr(Ph<sub>2</sub>phen)<sub>3</sub><sup>3+</sup> complexes are almost identical at +1.40 V. The lifetime of Cr(Ph<sub>2</sub>phen)<sub>3</sub><sup>3+\*</sup> in the presence of O<sub>2</sub> is 13 μs, while the lifetime of Ru(bpz)<sub>3</sub><sup>2+\*</sup> is 0.9 μs.<sup>1a</sup> In the interest of exploring the reactivity of the Cr complexes, we decided to investigate the radical cation Diels-Alder reaction as well, predicting that the use of a photocatalyst with different properties might allow for orthogonal reactivity to be discovered. Ultimately, we noted both similarities and differences between the Ru catalyst system described by Yoon and the Cr catalyst system developed herein.

#### 4.4.1 Cycloaddition of 1,3-Cyclohexadiene and *trans*-Anethole

To begin, we evaluated the cross cycloaddition between 1,3-cyclohexadiene (**4-1**) and *trans*-anethole (**4-3**) (Scheme 4.3a). For this transformation we elected to use the less photooxidizing Cr(Ph<sub>2</sub>phen)<sub>3</sub><sup>3+</sup> ( $E_{1/2}^* = +1.40$  V) in an effort to selectively oxidize the cycloaddition partner with the lower reduction potential.

When the cross [4+2] reaction of 1,3-cyclohexadiene (**4-1**) ( $E_{1/2} = +1.53$  V) and *trans*-anethole (**4-3**) ( $E_{1/2} = +1.24$  V)<sup>13</sup> was attempted, however, a mixture of products was obtained. We observed a 3:1:1 mixture of the 1,3-cyclohexadiene dimer (**4-2**), the desired cross-adduct (**4-6**), and recovered *trans*-anethole (**4-3**). Though unexpected, we found that this result could be explained by kinetic data: the rate of diene **4-1** reacting with the radical cation of itself (**4-1<sup>•+</sup>**)<sup>14</sup> is much faster than the rate of diene **4-1** reacting with the radical cation of *trans*-anethole (**4-3<sup>•+</sup>**)<sup>15</sup> (Scheme 4.3b). We still found it curious, however, that the diene (**4-1**) was able to be oxidized by  $\text{Cr}(\text{Ph}_2\text{phen})_3^{3+}$  ( $E_{1/2}^* = +1.40$  V), since the reduction potential of 1,3-cyclohexadiene ( $E_{1/2} = +1.53$  V) is higher than that of the excited catalyst.

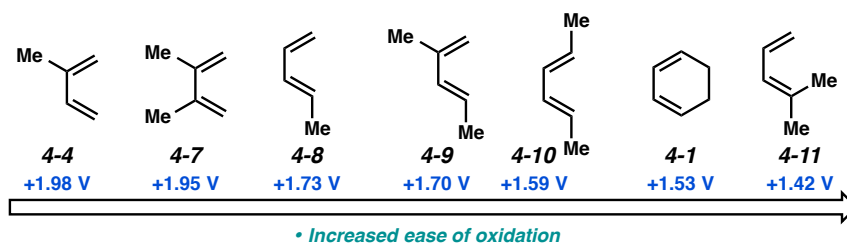


Scheme 4.3. (a) Cross cycloaddition of **4-1** with **4-3**. (b) Kinetic data. (c) Kinetic explanation for feasibility of Cr-catalyzed dimerization of 1,3-cyclohexadiene.

Conceivably, reduction potentials can be thought of as similar to  $\text{p}K_{\text{a}}$  values, but for electrons instead of protons.<sup>16</sup> When diene **4-1** and  $\text{Cr}(\text{Ph}_2\text{phen})_3^{3+}$  are in solution together, the electron being transferred will predominantly reside on one species (likely diene **4-1** because it has the higher reduction potential), but there is an equilibrium, similar to a proton being transferred in a solution of conjugate acids and bases (Scheme 4.3c). Once the electron is transferred from the diene to  $[\text{Cr}]^{3+}$  ( $k_1$ ), if the rate of the

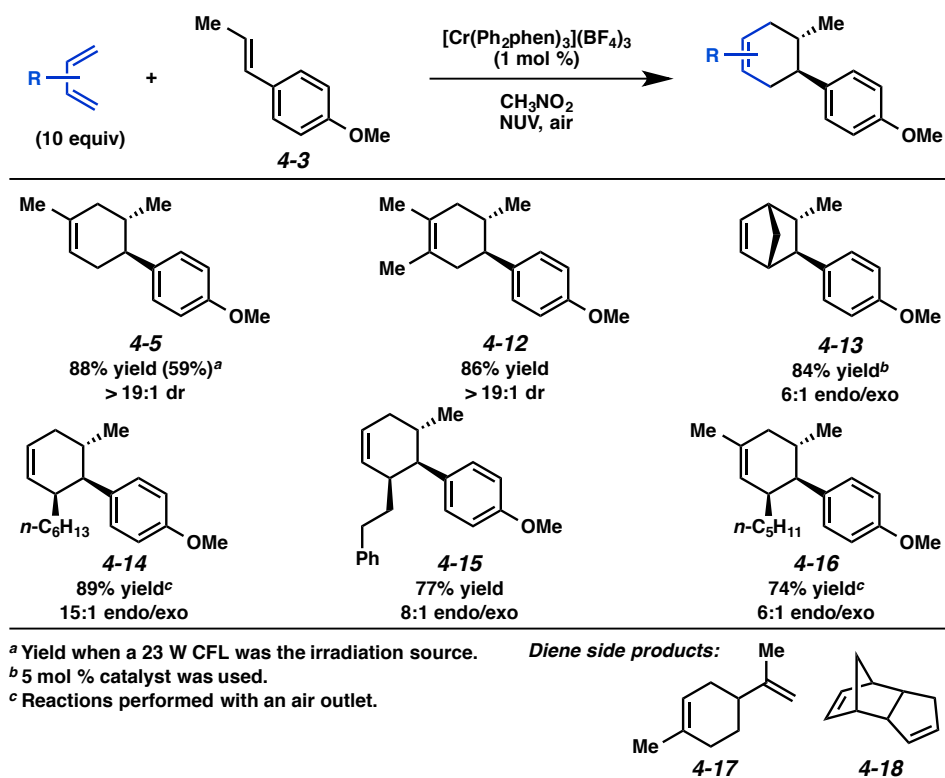
subsequent step ( $k_3$ ) is faster than the rate of electron transfer back from  $[\text{Cr}]^{2+}$  to diene radical cation **4-1<sup>+</sup>** ( $k_2$ ), then the reaction will still be successful, as we have observed. This demonstrates that reduction potentials are not the only pieces of data that should be used to determine whether a reaction initiated by single-electron transfer will work or not; kinetics are also important.

#### 4.4.2 Diene Scope



Scheme 4.4. Reduction potentials for common dienes.<sup>17</sup>

Scheme 4.4 shows a list of simple dienes in order of decreasing reduction potential. We hypothesized that a diene with a much higher reduction potential would be less likely to be oxidized by the catalyst, and, thus, also less likely to dimerize. Starting with the least oxidizable diene on the list, we attempted the cycloaddition between *trans*-anethole (**4-3**) and isoprene (**4-4**). This reaction proceeded in 88% yield of the desired cross-adduct (**4-5**) and only trace amounts of the isoprene dimer (**4-17**) were detected by <sup>1</sup>H NMR (Scheme 4.5). Moving across the list, the cycloaddition of *trans*-anethole with 2,3-dimethyl-1,3-butadiene (**4-7**) also proceeded in high yield and selectively forming the [4+2] cross-adduct (**4-12**). Cyclopentadiene was a viable diene for this transformation as well, delivering adduct **4-13** in 88% yield as a 6:1 endo/exo ratio, although considerable dicyclopentadiene (**4-18**) formation also occurred. Terminally substituted dienes were also proficient cycloaddition partners. Cyclohexenes **4-14**, **4-15**, and **4-16** were all formed in high yield and good diastereoselectivity. The reactions to form products **4-14** and **4-16** occurred more efficiently when the reaction vessel was equipped with a needle outlet, so they were essentially open to air. The impact of O<sub>2</sub> on these reactions will be discussed in detail later.

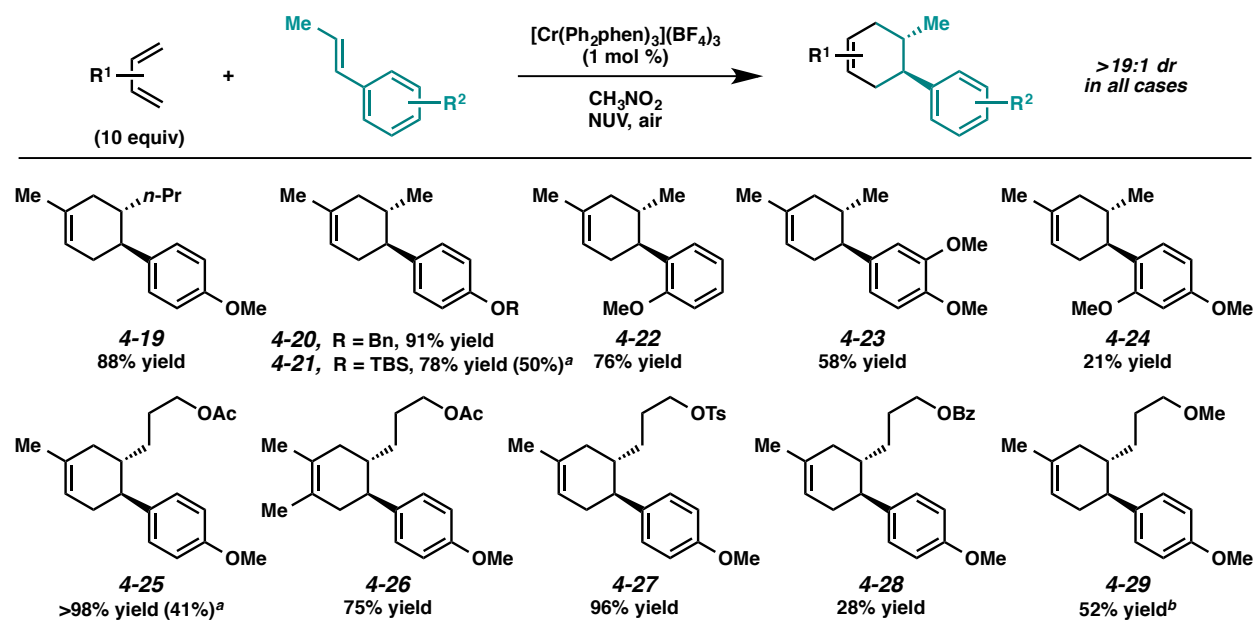


Scheme 4.5. Scope of diene component.

#### 4.4.3 Dienophile Scope

After having explored the diene component of the cycloaddition, we turned our attention to the electron-rich dienophile partner. A variety of electron-rich alkenes were viable cycloaddition counterparts for this transformation. An *n*-propyl substituted alkene underwent the cycloaddition in 88% yield (**4-19**) (Scheme 4.6). Benzyl or *tert*-butyldimethylsilyl (TBS) ethers were also viable substrates, giving products **4-20** and **4-21** in 91% and 78% yield, respectively. Differential substitution to the aryl ring was tolerated, but lower yields were obtained. *Ortho*-methoxyarene **4-22** was formed in 76% yield, while trisubstitution on the arene gave significantly lower yields (**4-23** and **4-24**). This is perhaps due to an enhanced stabilization of the radical cation intermediate that forms, rendering it less reactive. Functional group tolerance in this transformation was also evaluated using several different tethered functionalities. A tethered acetate underwent the cycloaddition with isoprene and with 2,3-dimethyl-1,3-butadiene to give products **4-25** and

**4-26** in 98% and 75% yield, respectively. Tosylate **4-27** was formed in 96% yield. A lower yield was obtained of benzoate **4-28**, perhaps due to competitive light absorption of the benzoate group with the catalyst. Methyl ether **4-29** was formed in only 52% yield. We believe this may be due to stabilization of the radical cation intermediate by the electron-rich oxygen.



<sup>a</sup> Yield when a 23 W CFL was the irradiation source.

<sup>b</sup> Reactions performed with an air outlet.

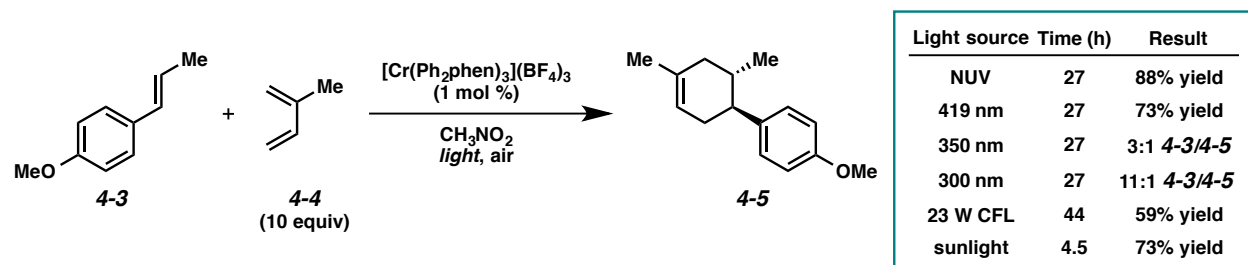
Scheme 4.6. Scope of the dienophile component.

#### 4.4.4 Evaluation of Light Sources

Since we report using a combination of three different wavelength bulbs for our irradiation source, we thought it worthwhile to evaluate each of the three bulbs individually to see which wavelength of light, or range of wavelengths, was activating the catalyst the most. When the cycloaddition of *trans*-anethole (**4-3**) and isoprene (**4-4**) was performed using only 419 nm bulbs, complete conversion to product was observed in 27 h and the product was isolated in 73% yield (Scheme 4.7). When the same experiment was performed with only the 350 nm bulbs for the same amount of time, a 3:1 *trans*-anethole/product ratio

was observed, and an 11:1 *trans*-anethole/product ratio was observed with only 300 nm bulbs. Though this indicates that the 419 nm bulbs are contributing most to exciting the catalyst, this yield was still lower than the yield we obtained under the NUV combination irradiation, thus the combination must be beneficial in some way.

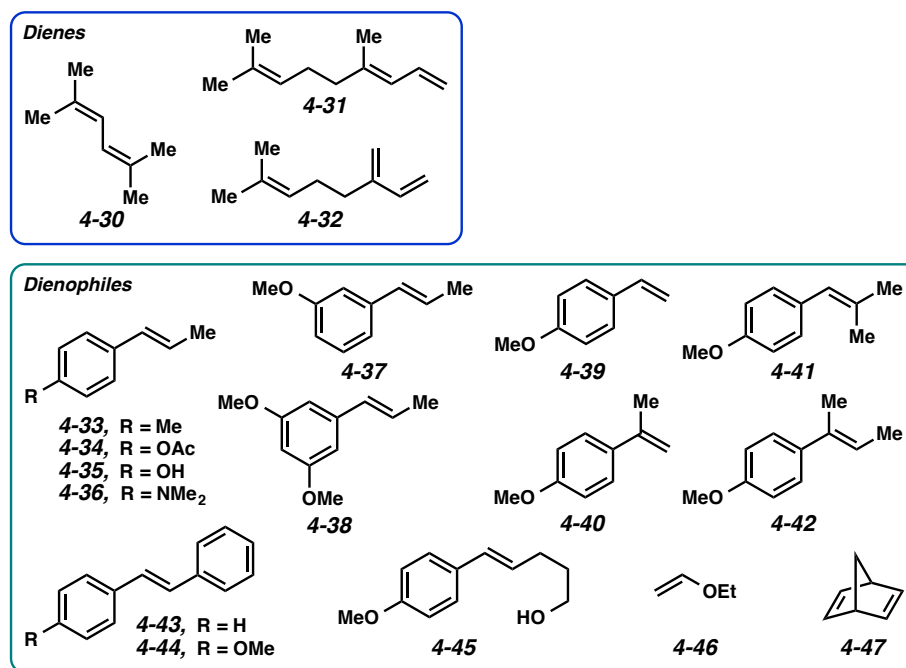
It should also be noted that it is important to take into account the absorptivity of the solvent when designing photochemical reactions. The cut-off wavelength of nitromethane is approximately 380 nm, so theoretically, only >380 nm light is able to reach the catalyst.<sup>18</sup> This may explain why the 419 nm bulbs have the greatest impact on the reaction.



Scheme 4.7. Evaluation of different irradiation sources.

We also examined visible light irradiation with this transformation. Irradiation of catalyst, *trans*-anethole (4-3), and isoprene (4-4) in nitromethane with a household 23 W compact fluorescent light gave the cycloadduct in 59% yield, compared to 88% yield with NUV irradiation. Likewise, products 4-21 and 4-25 also formed under visible light irradiation, but the yields were diminished. Additionally, sunlight, which is the model irradiation source for any photochemical reaction, was an effective energy source for this transformation, providing the product in 73% yield in just 4.5 h. Sunlight may be more suited for exciting the Cr catalyst than the 23 W CFL due to its higher emission in the NUV region. We were encouraged to see that the Cr catalyst was excited by visible light irradiation sources; however, the reaction still proceeded most efficiently under NUV irradiation.

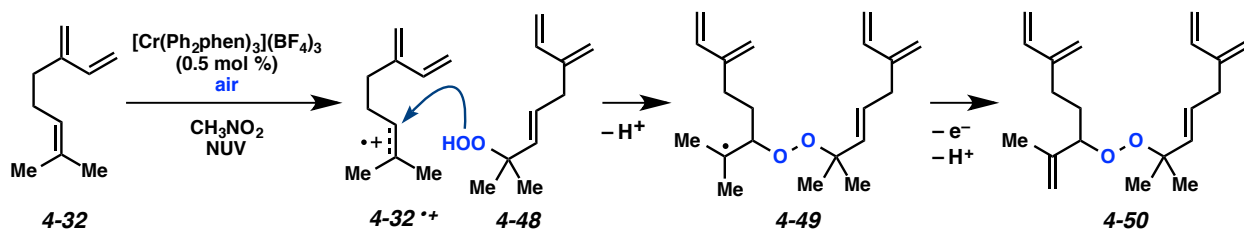
#### 4.4.5 Unsuccessful Substrates



Scheme 4.8. Dienes and dienophiles that were not successful substrates.

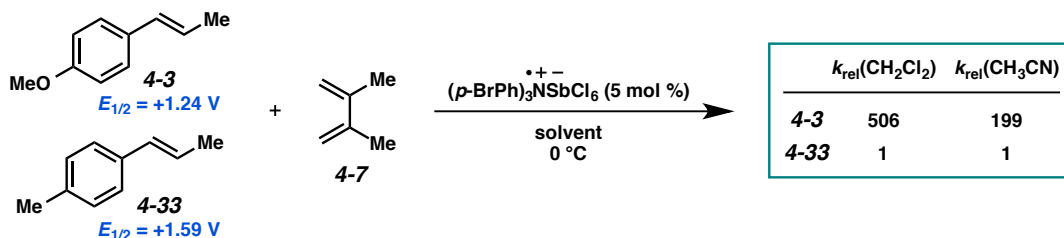
Unsuccessful substrates were also informative (Scheme 4.8). Dienes that were unsuccessful in this transformation were ones where one or both alkenes of the diene moiety were trisubstituted, such as in **4-30** and **4-31**. These dienes should have relatively low reduction potentials, and theoretically could compete with the alkene for oxidation by the catalyst. In fact, diene **4-30** has been reported to react with the radical cation of *trans*-anethole (**4-3<sup>+</sup>**) through electron-transfer, rather than cycloaddition, at a relatively fast rate ( $k = 7.2 \times 10^9 \text{ M}^{-1}\text{s}^{-1}$ ).<sup>14</sup> For comparison, the rate constant for the reaction of isoprene (**4-4**) with the radical cation of *trans*-anethole (**4-3<sup>+</sup>**) is  $1.9 \times 10^5 \text{ M}^{-1}\text{s}^{-1}$ . In addition, the steric impact of the trisubstituted alkenes in dienes **4-30** and **4-31** could be forcing them into their *s-trans* conformations, which may not be conducive to the [4+2] cycloaddition process, same as in a traditional Diels-Alder reaction.<sup>19</sup> Similarly substituted diene **4-11** has been reported to undergo a [2+2] cycloaddition with radical cation **4-3<sup>+</sup>**, but not a [4+2].<sup>20</sup>

Myrcene (**4-32**) was surprisingly also not effective, despite having a similar structure to isoprene and being a successful diene under Yoon's Ru(bpz)<sub>3</sub><sup>2+</sup> conditions.<sup>12</sup> Instead of reacting in a [4+2] fashion with *trans*-anethole (**4-3**), we observed myrcene to dimerize with incorporation of O<sub>2</sub> to give peroxide **4-50** (Scheme 4.9). The structure of dimer **4-50** was confirmed through reduction of the peroxide with lithium aluminum hydride to give the corresponding alcohols. We believe the dimerization may be occurring through a Schenck-ene reaction of <sup>1</sup>O<sub>2</sub> with the trisubstituted alkene to give hydroperoxide **4-48**, which could then add to the radical cation of myrcene (**4-32**<sup>•+</sup>) in an anti-Markovnikov fashion. Hydrogen atom abstraction from intermediate **4-49** would deliver the peroxide product (**4-50**). Interestingly, this myrcene dimerization reaction has not been reported, though the Schenck-ene reaction of myrcene with <sup>1</sup>O<sub>2</sub> has.<sup>21</sup> We suspect this side reaction is interfering with the desired cycloaddition. This was not an issue with the Ru catalyzed cycloaddition, perhaps because the Cr complex ( $\phi = 0.86$  for Cr(bpy)<sub>3</sub><sup>3+</sup>) is a more efficient <sup>1</sup>O<sub>2</sub> sensitizer than Ru(bpz)<sub>3</sub><sup>2+</sup> ( $\phi = 0.19$ ).<sup>22</sup>



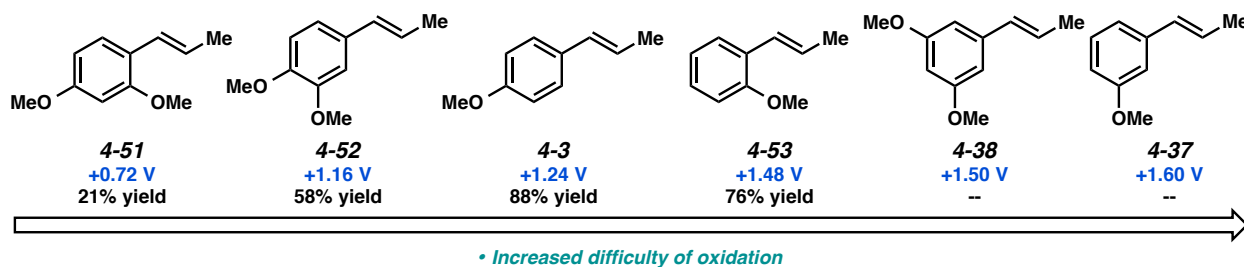
Scheme 4.9. Proposed formation of myrcene peroxide dimer.

With regard to the dienophile component, a variety of different groups on the aryl ring were not tolerated. Here, the differences in reduction potentials are probably coming into play. For instance, *p*-methyl- $\beta$ -methylstyrene (**4-33**) has a reduction potential of +1.59 V,<sup>13</sup> which is likely too high to be oxidized by the catalyst (+1.40 V). In addition, Bauld has shown that, kinetically, alkene **4-33** reacts much slower than *trans*-anethole (**4-3**): using the aminium salt conditions, the rate of the reaction of 2,3-dimethyl-1,3-butadiene (**4-7**) with *trans*-anethole (**4-3**) is 500 times faster in dichloromethane and 200 times faster in acetonitrile than the reaction of diene **4-7** with alkene **4-33** (Scheme 4.10).<sup>23</sup>



Scheme 4.10. Relative rates of **4-3** vs. **4-33** in a radical cation cycloaddition with diene **4-7**.

Acetate **4-34** was not an effective dienophile under the Cr conditions. This substrate was viable under Yoon's  $\text{Ru}(\text{bpz})_3^{2+}$  conditions, but a relatively poor yield was observed even with an increased catalyst loading. An unprotected phenol (**4-35**) was also not successful. According to Yoon, phenols can undergo competitive oxidative decomposition under the photoredox conditions.<sup>12</sup> Interestingly, dimethylaniline **4-36** was also not tolerated, though this substrate is definitely within the oxidizable range of the catalyst ( $E_{1/2}(\text{N,N-dimethylaniline}) = +0.79 \text{ V}$ ;  $E_{1/2}(\text{anisole}) = +1.81 \text{ V}$ ).<sup>13</sup> Perhaps the radical cation in this case exists more on the nitrogen than the alkene, impeding the cycloaddition.

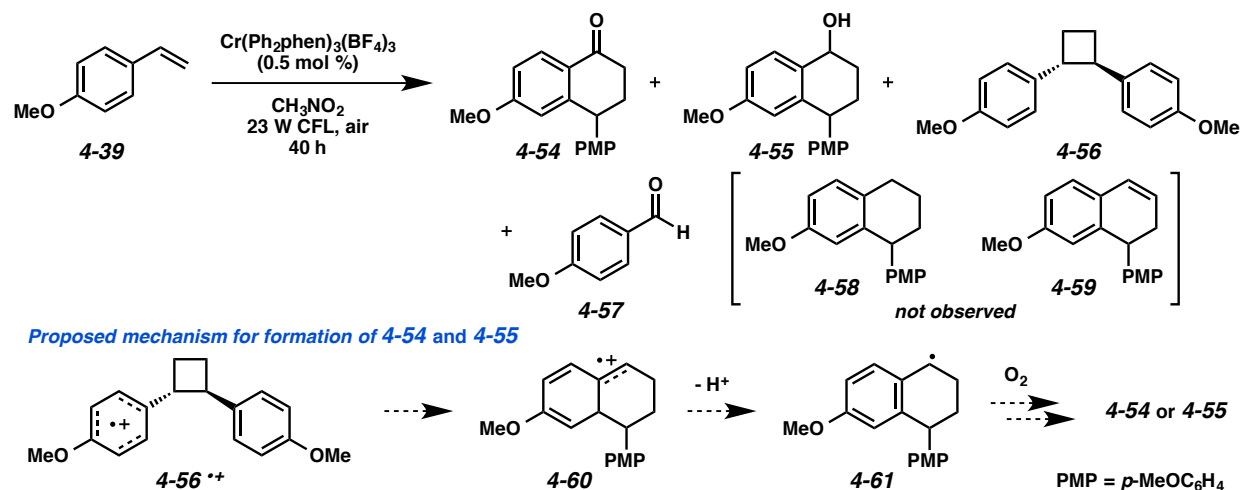


Scheme 4.11. Reduction potentials and cycloaddition yields for reaction with isoprene.<sup>13</sup>

The general trend we have observed in yields for different anethole derivatives may be based on their reduction potentials. Although it is not clear exactly why, optimal reactivity is achieved with only *para*-substitution (Scheme 4.11, **4-3**). Substrates **4-51** and **4-52** that should be more easily oxidized than *trans*-anethole reacted in lower yields, as did *ortho*-arene **4-53**. The *meta*-substituted substrates (**4-37** and

**4-38**) showed minimal conversion to product. These results indicate that there may be a “sweet spot” of reactivity for this reaction with regards to the reduction potential of the alkene.

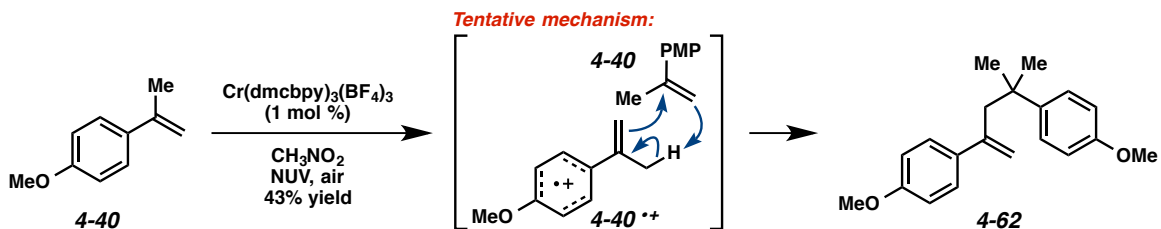
Additionally, dienophiles with varying alkene substitution were not successful in the [4+2] cycloaddition. Trisubstituted alkenes **4-41** and **4-42**, may not have been reactive due to sterics. Alkenes **4-39** and **4-40** were reactive, but not for the desired cycloaddition. When 4-methoxystyrene (**4-39**) was exposed to the reaction conditions, the desired cycloadduct was not formed; however, we did observe trace amounts of the styrene [2+2] dimer (**4-56**) (Scheme 4.12).<sup>24</sup> Interestingly, when this same reaction was run in the absence of diene, trace amounts of the [2+2] dimer (**4-56**) were detected, as was *para*-anisaldehyde (**4-57**), but the major products were ketone **4-54** and alcohol **4-55**, which would form through a rearrangement of the [2+2] adduct, followed by reaction with oxygen.<sup>25</sup> We did not observe products **4-58** or **4-59**, which have been observed under other photooxidative conditions.<sup>26</sup> Perhaps in the absence of air these products would have formed instead.



Scheme 4.12. Dimerization of 4-methoxystyrene.

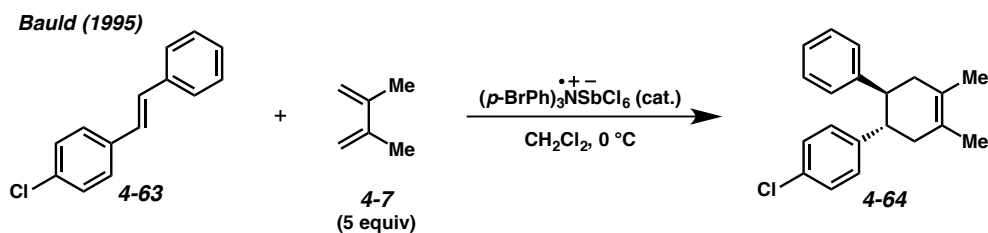
$\alpha$ -Methylstyrene **4-40** also dimerized when exposed to the Cr conditions, but not in a [2+2] fashion. Instead, we observed dimer **4-62**, which may be forming through an ene-type mechanism with radical cation **4-40**<sup>•+</sup> (Scheme 4.13).<sup>27</sup> In the absence of diene, product **4-62** was isolated in 43% yield.

Curiously, however, this dimerization only occurred with the more strongly oxidizing  $\text{Cr}(\text{dmc bpy})_3^{3+}$  catalyst, not with  $\text{Cr}(\text{Ph}_2\text{phen})_3^{3+}$ .



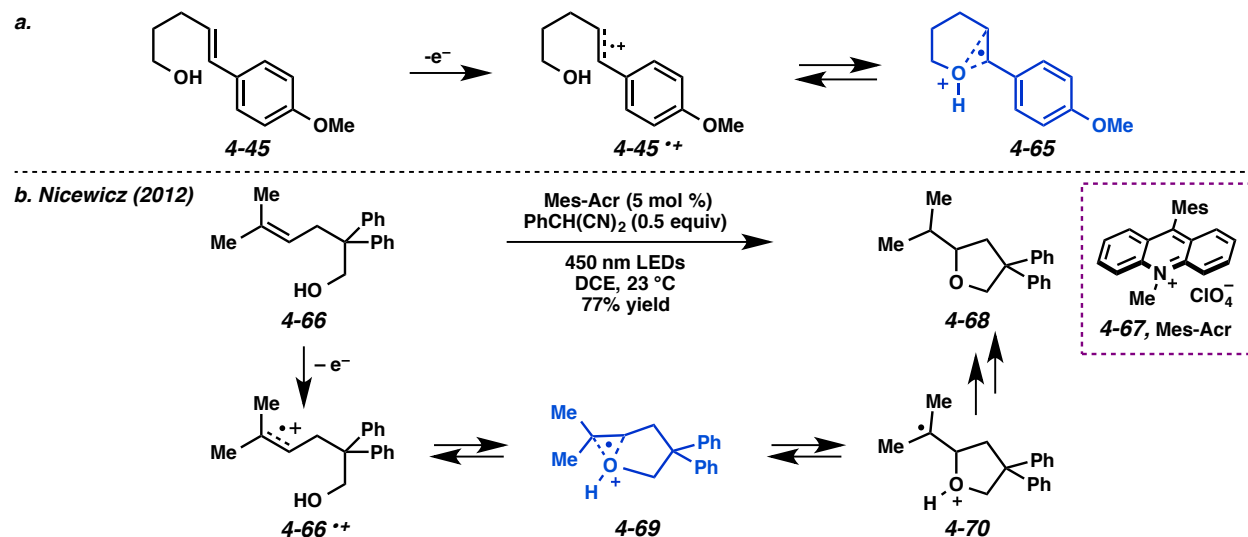
Scheme 4.13. Dimerization of  $\alpha$ -methylstyrene **4-40**.

*Trans*-stilbene (**4-43**) and 4-methoxy-*trans*-stilbene (**4-44**) did not react under the Cr conditions. The reduction potentials of *trans*-stilbene and 4-methoxy-*trans*-stilbene have been reported as +1.59 V and +0.82 V, respectively.<sup>28</sup> Though it would seem as if *trans*-stilbene is out of range of the oxidizing capabilities of the Cr catalyst, facile reactivity between *trans*-stilbene and ethyl diazoacetate has been observed in a Cr-catalyzed radical cation cyclopropanation reaction.<sup>29</sup> Interestingly as well, *trans*-stilbene derivatives have been demonstrated to undergo radical cation accelerated cycloadditions with diene **4-7** under Bauld's aminium salt conditions, including derivatives with electron-withdrawing substituents, such as 4-chloro-*trans*-stilbene (**4-63**), which would be even more difficult to oxidize than *trans*-stilbene (Scheme 4.14).<sup>30</sup>



Scheme 4.14. Bauld's cycloaddition of 4-chloro-*trans*-stilbene with diene **4-7**.

Tethered alcohol **4-45** gave none of the desired product. We believe that the alcohol group is likely able to stabilize the radical cation intermediate through a structure akin to **4-65** (Scheme 4.15). This stabilization effect may also explain why methyl ether product **4-29** was formed in lower yield (52% yield). The precedent for this proposed radical cation stabilization is based on research from the Nicewicz lab where nucleophiles such as alcohols have been observed to add across radical cations generated from the single-electron oxidation of electron-rich alkenes with a strongly oxidizing acridinium photocatalyst (**4-67**) ( $E_{1/2}^* = +2.06$  V).<sup>31</sup> Notably, the product of this reaction is exclusively the anti-Markovnikov adduct (**4-68**) due to the inherent reversal in polarity of the alkene upon radical cation formation.

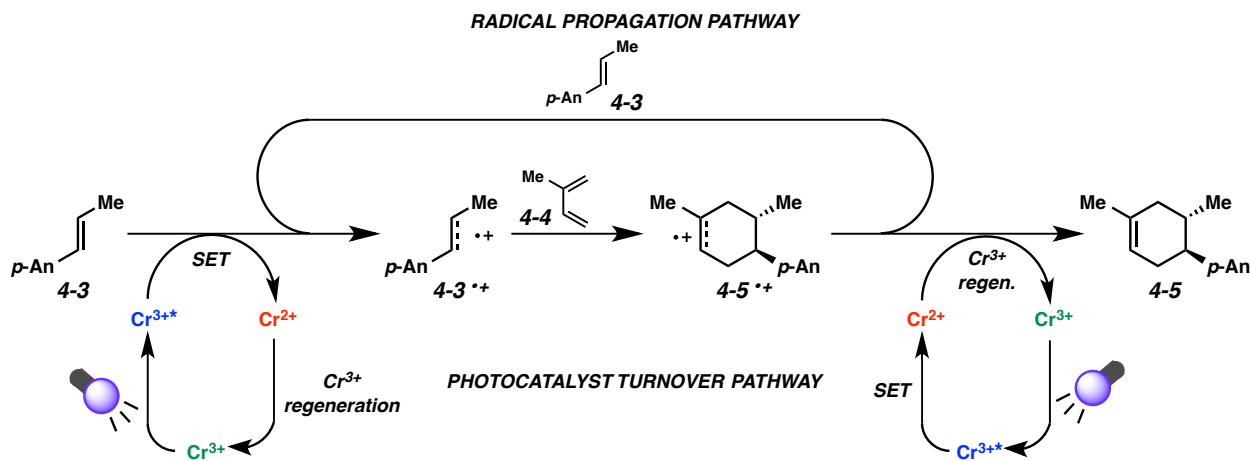


*Scheme 4.15.* (a) Proposed stabilization of radical cation with alcohol. (b) Nicewicz's anti-Markovnikov addition of alcohols to alkenes.

Lastly, non-aryl alkenes with relatively low reduction potentials, ethyl vinyl ether (**4-46**) ( $E_{1/2} = 1.60$  V)<sup>17</sup> and norbornadiene (**4-47**) ( $E_{1/2} = +1.54$  V)<sup>32</sup>, showed no reaction under the Cr conditions, once again reinforcing the necessity of the electron-rich arene for effective reactivity. This demonstrates as well that the success of these reactions are not predicated on reduction potentials alone; there are many factors that can have an impact on the reaction outcome.

## 4.5 Mechanistic Studies

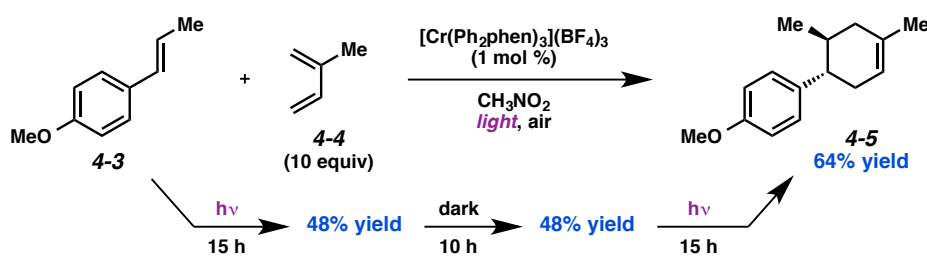
Our initial understanding of the mechanism for the Cr-catalyzed cycloaddition of *trans*-anethole (**4-3**) with isoprene (**4-4**) was similar to what was proposed by Yoon and coworkers for their Ru-catalyzed variant (Scheme 4.16). Upon irradiation with light, ground state  $[\text{Cr}]^{3+}$  is excited to  $[\text{Cr}]^{3+*}$ . Single-electron transfer (SET) from *trans*-anethole to  $[\text{Cr}]^{3+*}$  then forms the reduced  $[\text{Cr}]^{2+}$  species and radical cation **4-3<sup>•+</sup>**. Next, cyclization of the diene (**4-4**) with radical cation **4-3<sup>•+</sup>** occurs to give cycloadduct-radical cation **4-5<sup>•+</sup>**. The last step, however, where the  $[\text{Cr}]^{3+}$  is potentially regenerated and an electron is transferred to radical cation cycloadduct **4-5<sup>•+</sup>**, was less clear. We tentatively proposed that the final product (**4-5**) could be formed by either oxidation of the  $[\text{Cr}]^{2+}$  species with adduct **4-5<sup>•+</sup>** to regenerate ground state  $[\text{Cr}]^{3+}$  (*photocatalyst turnover pathway*), or by adduct **4-5<sup>•+</sup>** abstracting an electron from another *trans*-anethole (**4-3**) equivalent to propagate the reaction (*radical propagation pathway*).



Scheme 4.16. Initial proposed mechanism for Cr-photocatalyzed radical cation Diels-Alder.

### 4.5.1 Discontinuous Irradiation Experiment

In order to gain insight into whether catalyst regeneration or radical propagation was occurring, we performed a discontinuous irradiation experiment where the reaction of *trans*-anethole (**4-3**) and isoprene (**4-4**) was irradiated with light until ~50% conversion to product was observed, then was placed in the dark for a similar amount of time (Scheme 4.17). During the time the reaction was in the dark, we observed no considerable product formation, leading us to infer that radical chain propagation was not occurring to a great extent. This experiment also confirmed that continuous irradiation was necessary for reactivity, suggesting that  $\text{Cr}^{3+}$  regeneration was a viable mechanistic pathway. A recent publication by Yoon and coworkers, however, discusses the radical chain-nature of photoredox reactions, and demonstrates that, because of the relatively short propagation chain lengths of these processes, the discontinuous irradiation experiment is not valid assessment of whether or not chain propagation is occurring.<sup>33</sup> This indicated that further experiments were necessary to understand how adduct **4-5**<sup>++</sup> was being reduced to the product (**4-5**).

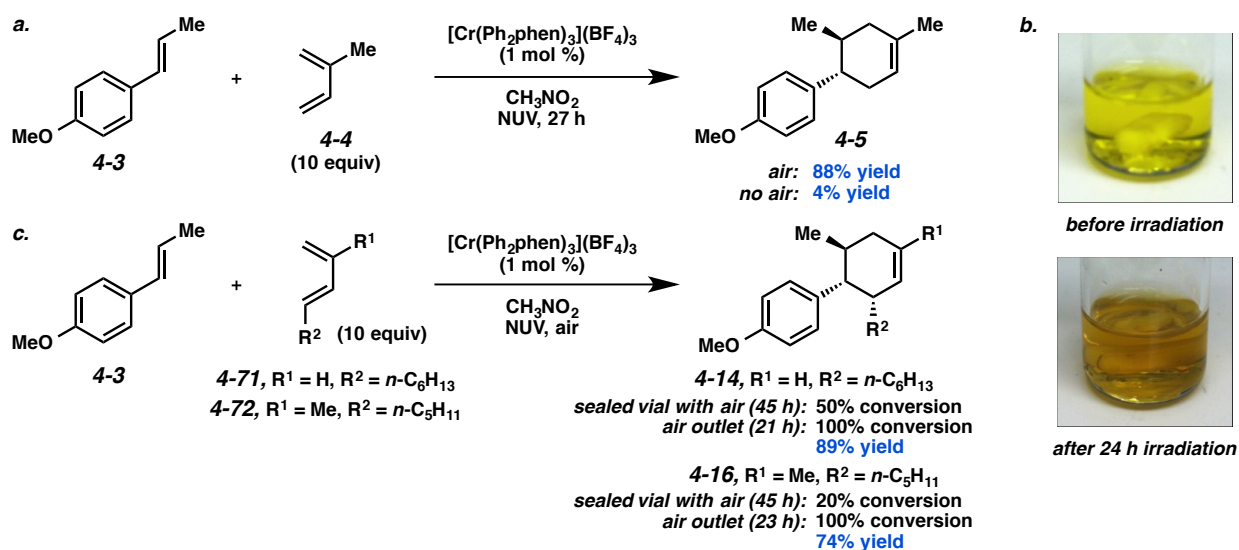


Scheme 4.17. Discontinuous irradiation experiment.

### 4.5.2 Roles of Oxygen in the Cr-Photocatalyzed Cycloaddition Mechanism

An additional observation we had made was that  $\text{O}_2$  was necessary for reactivity; when the reaction was degassed and run under Ar, only 4% yield of product **4-5** was formed (Scheme 4.18a). In most cases, the

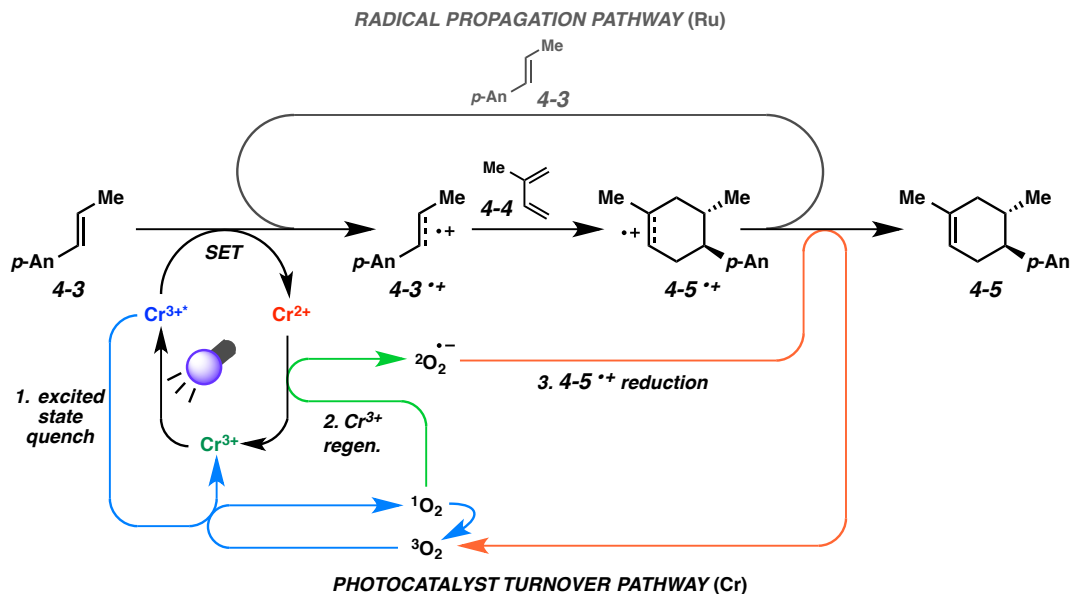
reaction was simply assembled open to air and capped, and this seemingly provided sufficient O<sub>2</sub> for effective reactivity. We also observed a change in color of the reaction mixture over time from bright yellow (the color of the catalyst) to a darker tan when no additional air was allowed to enter the reaction vessel during the course of the reaction (Scheme 4.18b). Additionally, the cycloadditions of certain substrates performed better when they were run open to air, as opposed to in a sealed vial with air. For example, dienes **4-71** and **4-72** with substitution at the terminal position reacted slowly in a capped vial with air, but when they were performed open to air with a needle outlet, they reacted efficiently and in high yields to give cyclohexenes **4-14** and **4-16** (Scheme 4.18c). These observations implied that O<sub>2</sub> may be necessary for catalyst regeneration and/or product formation in some way.



Scheme 4.18. Preliminary experiments exploring the effect of air on reactivity.

Efforts by our collaborators have elucidated the crucial roles of O<sub>2</sub> in this Cr-photocatalyzed cycloaddition.<sup>34</sup> Through a combination of catalysis, electrochemical, spectroscopic, and computational studies, O<sub>2</sub> was determined to play three subsequent roles in the photocatalytic cycle (Scheme 4.19). First, <sup>3</sup>O<sub>2</sub> can quench the [Cr]<sup>3+\*</sup> complex, preventing decomposition of the catalyst, as well as forming <sup>1</sup>O<sub>2</sub>.

Second,  $^1\text{O}_2$  can oxidize the  $[\text{Cr}]^{2+}$  species to regenerate the ground state  $[\text{Cr}]^{3+}$  complex. And third, the resulting  $^2\text{O}_2^{\bullet -}$  (superoxide) can reduce the radical cation cycloadduct (**4-5<sup>•+</sup>**) to generate the product.



Scheme 4.19. Proposed mechanism showing roles of  $\text{O}_2$ .

#### 4.5.3 $^3\text{O}_2$ Quenches $[\text{Cr}]^{3+*}$

The presence of  $\text{O}_2$  greatly reduces the excited state lifetime of the  $[\text{Cr}]^{3+*}$  complex from 441 to 13  $\mu\text{s}$ . This is a result of  $^3\text{O}_2$  quenching the  $[\text{Cr}]^{3+*}$  excited state to form  $^1\text{O}_2$  and the ground state  $[\text{Cr}]^{3+}$  complex. Through Stern-Volmer plots, our collaborators in the Damrauer lab showed that the quenching rate of  $[\text{Cr}]^{3+*}$  by *trans*-anethole (**4-3**) was essentially the same both in the presence of ambient  $\text{O}_2$  ( $k_q = 9.5 \times 10^8 \text{ M}^{-1}\text{s}^{-1}$ ) and degassed ( $k_q = 9.4 \times 10^8 \text{ M}^{-1}\text{s}^{-1}$ ) (Figure 4.2). Thus, though the presence of  $\text{O}_2$  decreases the lifetime of the  $[\text{Cr}]^{3+*}$ , which would not seem to be conducive to reactivity, overall, the rate of *trans*-anethole (**4-3**) oxidation is not decreased. This process must occur independently of  $\text{O}_2$ .

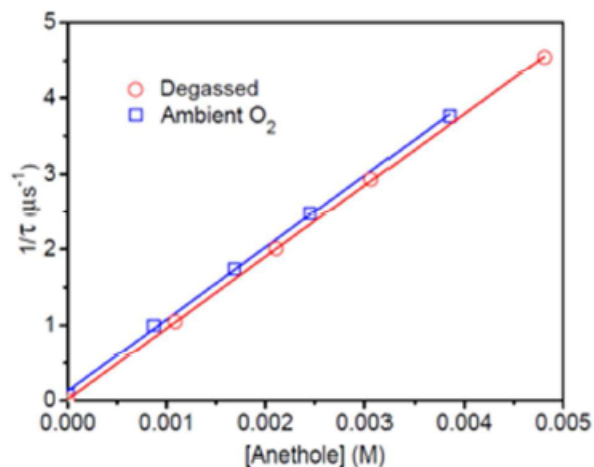
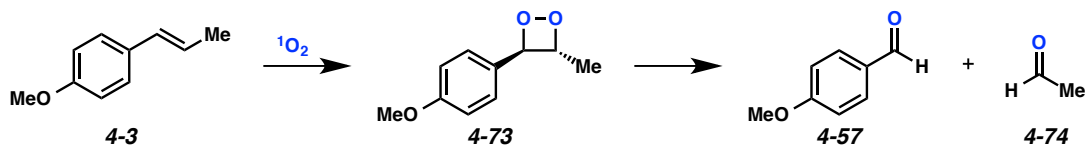


Figure 4.2. Stern-Volmer plot showing the rate of *trans*-anethole oxidation with and without O<sub>2</sub>.

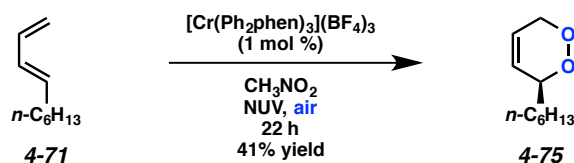
By quenching the excited state [Cr]<sup>3+\*</sup>, O<sub>2</sub> is also protecting [Cr]<sup>3+\*</sup> from degradation, which can occur through ligand loss or solvent incorporation if an equivalent of *trans*-anethole is not readily available.<sup>35</sup> Oftentimes, photocatalytic reactions are performed under Ar because the <sup>1</sup>O<sub>2</sub> formed from this type of quenching can lead to unwanted oxidation side-products. It should be noted that we sometimes observed the formation of *para*-anisaldehyde (**4-57**) when the cycloaddition proceeded slowly. This side product likely was the result of a [2+2] reaction between <sup>1</sup>O<sub>2</sub> and *trans*-anethole (**4-3**) to form a dioxetane (**4-73**), followed by a retro-[2+2] cycloaddition to give *para*-anisaldehyde (**4-57**) and acetaldehyde (**4-74**) (Scheme 4.20). Since our Cr system required O<sub>2</sub> to preserve the catalyst, it was fortunate that the formation of O<sub>2</sub>-related side-products in this transformation was minimal.



Scheme 4.20. Proposed formation of *para*-anisaldehyde from *trans*-anethole.

#### 4.5.4 $^1\text{O}_2$ Oxidizes $[\text{Cr}]^{2+}$

The lack of undesired side reactions observed between our substrates and  $^1\text{O}_2$  could be due to the further involvement of  $^1\text{O}_2$  in the catalytic cycle. Interestingly, in the absence of *trans*-anethole, when just terminally substituted diene **4-71** was exposed to the reaction conditions, endoperoxide **4-75** formed (Scheme 4.21). This endoperoxide was not observed in the reaction mixture when *trans*-anethole was present. Given what we have proposed about the role of *trans*-anethole in the catalytic cycle (it reduces  $[\text{Cr}]^{3+*}$  to  $[\text{Cr}]^{2+}$ , which in turn reacts with  $^1\text{O}_2$  to give  $[\text{Cr}]^{3+}$  and superoxide) it would be fair to postulate that, in the absence of *trans*-anethole, there is a build up of  $^1\text{O}_2$ , which can be trapped by the diene to deliver endoperoxide **4-75**. This notable observation provides further experimental evidence for the proposed oxidation of  $[\text{Cr}]^{2+}$  with  $^1\text{O}_2$ .



Scheme 4.21. Formation of endoperoxide through [4+2] with  $^1\text{O}_2$ .

Just as there is a buildup of  $^1\text{O}_2$  in the absence of  $[\text{Cr}]^{2+}$ , we also observed a buildup of  $[\text{Cr}]^{2+}$  in the absence of  $\text{O}_2$ . Physically, a brown precipitate forms in the reaction mixture when  $\text{O}_2$  is not present, which is likely a  $[\text{Cr}]^{2+}$  degradation product (Scheme 4.18c). When  $\text{O}_2$  is present, however, this brown precipitate does not form. When the reaction of *trans*-anethole (**4-3**) with isoprene (**4-4**) is monitored by electronic absorption spectroscopy, in the absence of  $\text{O}_2$ , a feature at  $\sim 450$  nm grows in on the spectrum at a rate of 1 for the loss of every 5 equivalents of  $[\text{Cr}]^{3+}$  (Figure 4.3, left). We believe this feature is related to a  $[\text{Cr}]^{2+}$  degradation product. In contrast, when the same experiment is monitored in the presence of  $\text{O}_2$ , the loss of  $[\text{Cr}]^{3+}$  is still observed ( $\sim 400$  nm), but no feature related to  $[\text{Cr}]^{2+}$  forms (Figure 4.3, right). This demonstrates that the  $^1\text{O}_2$  generated by quenching  $[\text{Cr}]^{3+*}$  is able to convert the  $[\text{Cr}]^{2+}$  back to  $[\text{Cr}]^{3+}$ .

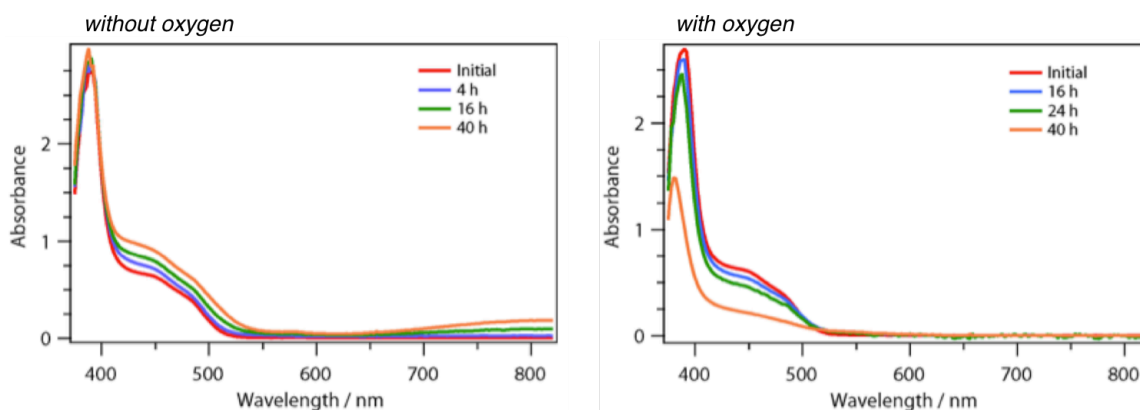


Figure 4.3. Electronic absorption spectra showing a  $[\text{Cr}]^{2+}$  degradation product in the absence of  $\text{O}_2$ .

Additionally, computations by our collaborator Prof. Anthony Rappé suggest that the oxidation of  $[\text{Cr}]^{2+}$  by  $^1\text{O}_2$  is exothermic by 15 kcal/mol. The same oxidation of  $[\text{Cr}]^{2+}$  by  $^3\text{O}_2$  was also considered, but this process would be endothermic by 6 kcal/mol, so the former pathway is favored. Based on computations, adduct  $4\text{-}5^{++}$  should also be able to oxidize  $[\text{Cr}]^{2+}$  (exoergic by 39 kcal/mol); however, as we observed, no product is formed without  $\text{O}_2$ , so this process must be kinetically slow. All of these data strongly suggest that  $^1\text{O}_2$  is responsible for regenerating the ground state  $[\text{Cr}]^{3+}$  catalyst by oxidizing  $[\text{Cr}]^{2+}$  and being converted to superoxide.

#### 4.5.5 Superoxide Reduces $4\text{-}5^{++}$

The last question is, then: how is radical cation adduct  $4\text{-}5^{++}$  converted to product  $4\text{-}5$ ? Though both  $[\text{Cr}]^{2+}$  and *trans*-anethole ( $4\text{-}3$ ) are thermodynamically capable of reducing adduct  $4\text{-}5^{++}$ , evidently, neither of them actually perform this reduction, since without  $\text{O}_2$ , no product forms. Instead, the radical cation adduct ( $4\text{-}5^{++}$ ) is likely being reduced by superoxide formed through the oxidation of  $[\text{Cr}]^{2+}$  with  $^1\text{O}_2$ . Electrochemical analysis by our collaborators in the Shores lab established the reduction potential of  $\text{O}_2$  to  $\text{O}_2^-$  to be +1.82 V, and the reduction potential of  $4\text{-}5^{++}$  to  $4\text{-}5$  to be +1.69 V, indicating that the reduction of adduct  $4\text{-}5^{++}$  by superoxide is allowed. A control experiment where 10 mol % of

benzoquinone, a superoxide scavenger, was added to the cycloaddition demonstrated impeded reactivity, with only 34% yield of **4-5** being formed in 27 h (27% **4-3** remaining), consistent with superoxide inhibition.

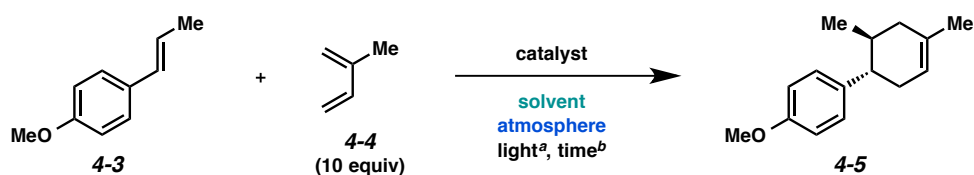
Additionally, calculations show that the reduction of adduct **4-5**<sup>•+</sup> by *trans*-anethole (**4-3**) to initiate propagation is 7 kcal exoergic. Comparatively, the proposed reduction of adduct **4-5**<sup>•+</sup> by superoxide is 48 kcal exoergic, so it is more energetically favorable. This data, combined with the knowledge that product formation does not occur in the absence of O<sub>2</sub>, suggests radical propagation is not occurring in this case, but an oxygen-mediated photocatalytic cycle is.

#### 4.5.6 Cr vs. Ru

As stated previously, the mechanism proposed for the reaction of *trans*-anethole (**4-3**) with isoprene (**4-4**) catalyzed by Ru(bpz)<sub>3</sub><sup>2+</sup> in dichloromethane with visible light was determined to be radical chain propagation.<sup>33</sup> Air was found to be advantageous for this reaction (Table 4.2, entry 7); however, when the reaction was attempted in the absence of O<sub>2</sub>, 46% yield of product **4-5** still formed (entry 8). In contrast, <5% yield of product **4-5** formed under the Cr conditions in the absence of air (entry 2).

Considering the importance of solvent to catalyst behavior, we attempted the Cr-catalyzed cycloaddition of *trans*-anethole (**4-3**) with isoprene (**4-4**) in dichloromethane, both with and without air. In the presence of air in dichloromethane, product **4-5** was formed in 50% yield (entry 3); without air, a 12% yield of cyclohexene **4-5** was formed (entry 4). This indicates that solvent is somewhat important to the overall mechanism. In contrast, when the Ru-catalyzed cycloaddition was performed in nitromethane without air, 88% yield of product **4-5** was obtained (entry 6), which was almost identical to the yield when the reaction was run with air (entry 5). This indicates that the Ru-catalytic cycle is not inhibited without air in the same way as the Cr cycle. These experiments demonstrate that there is likely a difference between the reactivity of the catalysts and that the reaction pathway (radical chain propagation or O<sub>2</sub>-mediated photocatalysis) is not simply solvent-dependent.

Table 4.2. Impact of solvent and atmosphere on Cr and Ru catalyzed cycloadditions.



Entry	Catalyst (mol %)	Solvent	Atmosphere	Yield (%)
1	[Cr(Ph <sub>2</sub> phen) <sub>3</sub> ](BF <sub>4</sub> ) <sub>3</sub> (1)	CH <sub>3</sub> NO <sub>2</sub>	air	88
2	[Cr(Ph <sub>2</sub> phen) <sub>3</sub> ](BF <sub>4</sub> ) <sub>3</sub> (1)	CH <sub>3</sub> NO <sub>2</sub>	degas, Ar	4 <sup>c,d</sup>
3	[Cr(Ph <sub>2</sub> phen) <sub>3</sub> ](BF <sub>4</sub> ) <sub>3</sub> (1)	CH <sub>2</sub> Cl <sub>2</sub>	air	50 <sup>d</sup>
4	[Cr(Ph <sub>2</sub> phen) <sub>3</sub> ](BF <sub>4</sub> ) <sub>3</sub> (1)	CH <sub>2</sub> Cl <sub>2</sub>	degas, Ar	12 <sup>c,d</sup>
5	[Ru(bpz) <sub>3</sub> ](PF <sub>6</sub> ) <sub>2</sub> (1)	CH <sub>3</sub> NO <sub>2</sub>	air	87 <sup>c</sup>
6	[Ru(bpz) <sub>3</sub> ](PF <sub>6</sub> ) <sub>2</sub> (1)	CH <sub>3</sub> NO <sub>2</sub>	degas, Ar	88 <sup>c</sup>
7	[Ru(bpz) <sub>3</sub> ](BARF) <sub>2</sub> (0.5)	CH <sub>2</sub> Cl <sub>2</sub>	air	98 <sup>e</sup>
8	[Ru(bpz) <sub>3</sub> ](BARF) <sub>2</sub> (0.5)	CH <sub>2</sub> Cl <sub>2</sub>	degas, Ar	46 <sup>e</sup>

<sup>a</sup> Cr reactions were performed with NUV light; Ru reactions were performed with a 23 W CFL.

<sup>b</sup> Cr reactions were run for 27 h; Ru reactions were run for 1 h.

<sup>c</sup> Yields determined by <sup>1</sup>H NMR with dodecyl acetate as an internal standard.

<sup>d</sup> Starting material was not consumed.

<sup>e</sup> Yoon's results, 3 equiv diene.

BARF = tetrakis[3,5-bis(trifluoromethyl)phenyl]borate

This conclusion is further supported by the quantum yields of each catalyst for the reaction of *trans*-anethole (4-3) with isoprene (4-4). With Ru(bpz)<sub>3</sub><sup>2+</sup>, the quantum yield was reported to be 44,<sup>33</sup> while the quantum yield of the Cr-catalyzed reaction was determined by our collaborators to be 0.35. This means that, in the Ru case, for every photon that is absorbed by the catalyst, 44 equivalents of product are formed, which is indicative of a radical chain propagation mechanism. In contrast, less than one equivalent of product forms for every photon absorbed by the Cr catalyst, strongly ruling out a radical chain process. For comparison, the quantum yield of the same transformation under Bauld's aminium salt conditions was calculated to be 41.<sup>33</sup> Since the aminium salt catalyzed reaction must proceed through a radical chain propagation mechanism, the similarity between this value and Ru quantum yield, as well as the disparity between this value and the Cr quantum yield reaffirms our assessment that the Cr reaction does not proceed through chain propagation, while the Ru reaction does. It should be noted that, though we assert that the Cr-catalyzed catalyst regeneration mechanism requires oxygen to proceed so it must not occur through radical chain propagation, this is not always the case. Oxygen can sometimes be an

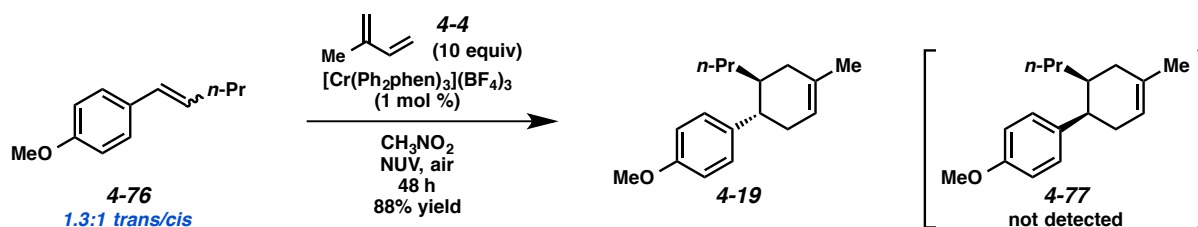
accelerant, and even a requirement, for photocatalyzed transformations proceeding through radical chain propagation.<sup>36</sup>

In conclusion, experiments by our collaborators have highlighted the key roles of O<sub>2</sub> as an energy and electron shuttle in the Cr-photocatalyzed cycloaddition of electron-rich dienophiles and dienes. Their insights complete our mechanistic picture of this transformation.

## 4.6 Stereoconvergence

### 4.6.1 Initial Observations

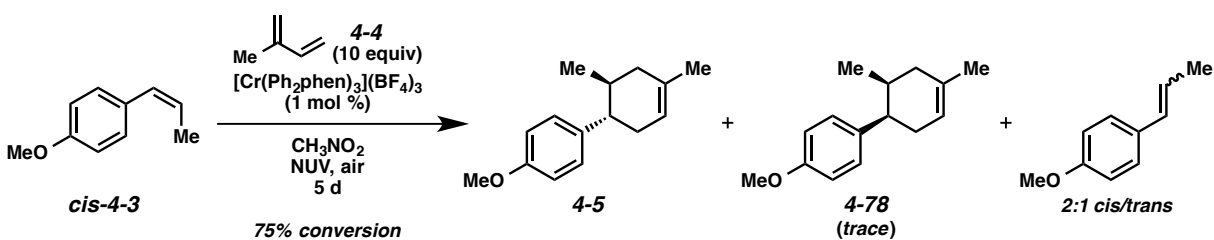
An observation we made while exploring the substrate scope of the radical cation Diels-Alder of electron-rich dienophiles was that no matter the isomeric ratio of the alkene, anti cyclohexenes were formed exclusively, with seemingly none of the syn product detectable by <sup>1</sup>H NMR. For instance, a 1.3:1 mixture of trans and cis isomers of alkene **4-76**, when reacted with isoprene under the standard conditions, gave anti adduct **4-19** in 88% yield, with no syn adduct **4-77** detected (Scheme 4.22). In addition, some isomeric mixtures of alkenes reacted in very high yields, indicating that whatever process that was occurring to convert the cis alkene to the anti product was not impeding the reaction to a great extent.



Scheme 4.22. Cycloaddition of isomeric mixture of alkene **4-76**.

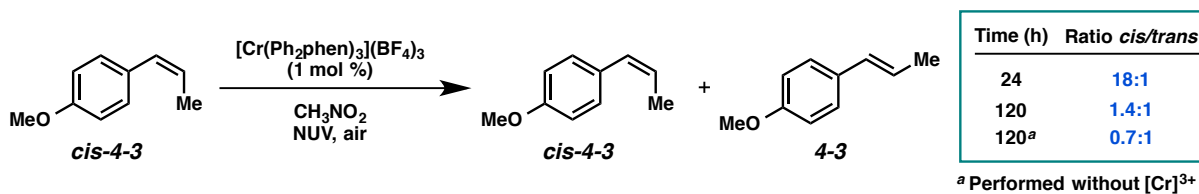
When pure *cis*-anethole (*cis*-**4-3**) was exposed to the reaction conditions with isoprene, however, the reaction proceeded rather slowly, giving about 75% conversion to the anti product (**4-5**) after 5 d, with

only very trace syn product **4-78** detected by  $^1\text{H}$  NMR (Scheme 4.23). The remaining anethole in this case was a 2:1 mixture of *cis*- and *trans*-anethole isomers. The presence of *trans*-anethole (**4-3**) in the reaction mixture made us think that perhaps the reaction is so sluggish is because *cis*-anethole must first isomerize to *trans*-anethole before it can be oxidized by the catalyst; this would explain why the anti adducts were being formed almost exclusively.



Scheme 4.23. Cr-catalyzed cycloaddition of *cis*-anethole.

Indeed, isomerization of *cis*-anethole (*cis*-**4-3**) to *trans*-anethole (**4-3**) in the presence of  $\text{Cr}(\text{Ph}_2\text{phen})_3^{3+}$  was observed, but it was very slow; after 24 h, only trace *trans*-anethole was observed by  $^1\text{H}$  NMR, and after 5 d, not even 50% conversion to *trans*-anethole had occurred (Scheme 4.24). In the absence of catalyst, the photoinduced isomerization was still slow ( $\lambda_{\text{max}}(\mathbf{4-3}) = 258 \text{ nm}$ ,  $\lambda_{\text{max}}(\mathbf{cis-4-3}) = 254 \text{ nm}$ ),<sup>37</sup> but a slightly greater ratio of *trans*-anethole was formed.

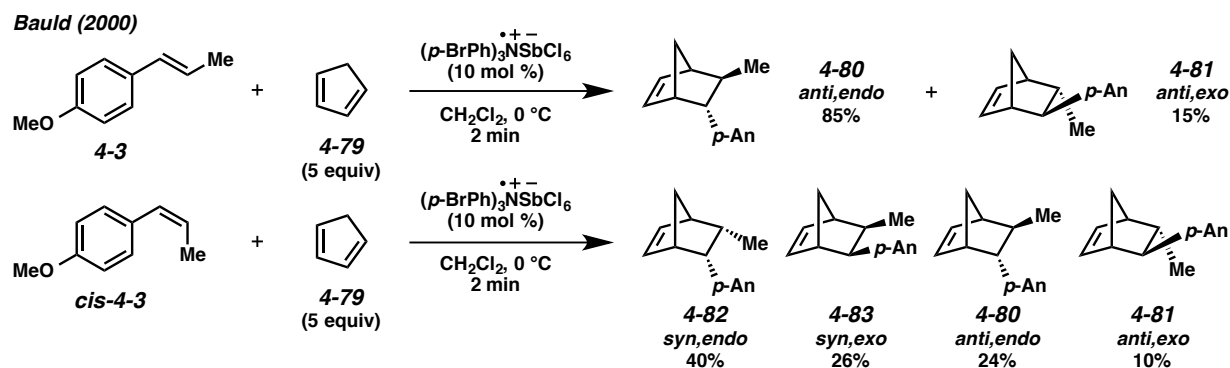


Scheme 4.24. Isomerization of *cis*-anethole to *trans*-anethole.

Under the same conditions, *trans*-anethole (**4-3**) was not observed to isomerize to *cis*-anethole (*cis*-**4-3**), although this isomerization has been reported with high energy UV light.<sup>38</sup> While these results

favor our hypothesis that *cis*-anethole might first need to isomerize to *trans*-anethole before it can react with the catalyst,<sup>39</sup> and product formation in this reaction is slow because the isomerization is slow, on the other hand, the reduction potential of *cis*-anethole (*cis*-**4-3**) is +1.24 V<sup>40</sup> (in nitromethane), which is well within range of oxidation by the catalyst. It would be surprising if the isomerization of *cis*-anethole was faster than oxidation by the catalyst followed by trapping of the radical cation with the diene. Additionally, in the presence of catalyst, isomerization occurred more slowly than when just irradiation was used, suggesting that the formation of radical cations impedes the isomerization. In any case, these experiments alone do not provide us with enough information to conclusively establish the mechanism for the anti product's formation; further studies were required.

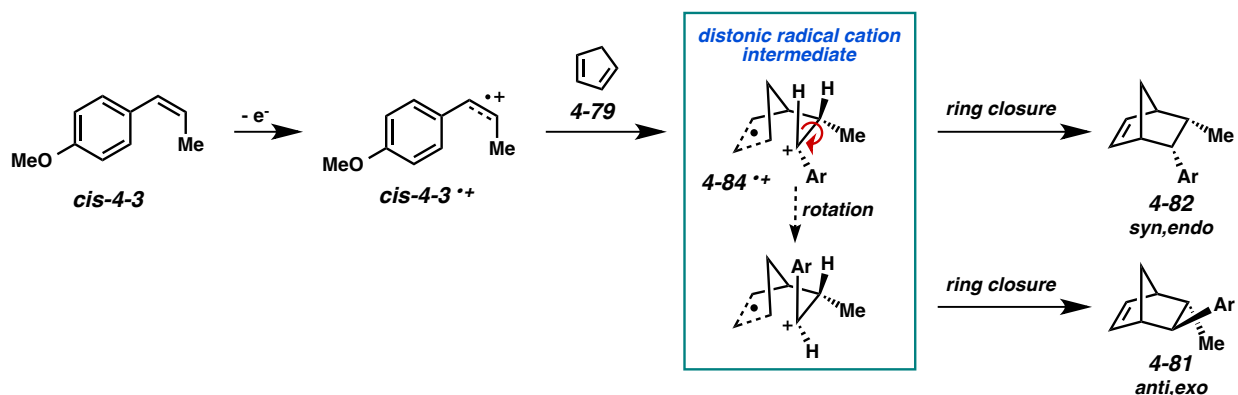
#### 4.6.2 Bauld's Report



Scheme 4.25. Aminium salt-catalyzed cycloaddition of cyclopentadiene with *trans*- and *cis*-anethole.

In 2000, Bauld and coworkers investigated the cycloaddition of both *cis*- and *trans*-anethole with cyclopentadiene (**4-79**) using their aminium radical cation salt conditions.<sup>41</sup> In the cycloaddition of *trans*-anethole (**4-3**), they observed a 6:1 ratio of the *anti,endo* adduct **4-80** to *anti,exo* adduct **4-81** (Scheme 4.25). With *cis*-anethole (*cis*-**4-3**), however, they observed the *syn,endo* (**4-82**) and *syn,exo* (**4-83**) diastereomers, as well as the *anti,endo* (**4-80**) and *anti,exo* (**4-81**) isomers.

Like us, they wondered how the anti products might be forming from *cis*-anethole. They also entertained the idea that the *cis*-anethole might be isomerizing to *trans*-anethole prior to reacting with cyclopentadiene. Several pieces of evidence, however, indicated that this was not the case: 1) when they analyzed the reaction mixture prior to complete consumption of *cis*-anethole, no *trans*-anethole was detected,<sup>42</sup> 2) the product ratio was always the same no matter at what time they analyzed the reaction mixture, 3) different equivalents of diene had no effect on relative ratios of the 4 diastereomers; if isomerization was occurring, then the higher concentration of diene would trap the *cis*-anethole radical cation sooner and less anti products would be expected, and 4) photosensitized electron transfer conditions using 1,4-dicyanobenzene as a photosensitizer also produced a similar mixture of the 4 diastereomers and no *trans*-anethole, indicating that there is nothing special about the aminium conditions that would cause *trans*-anethole to form.

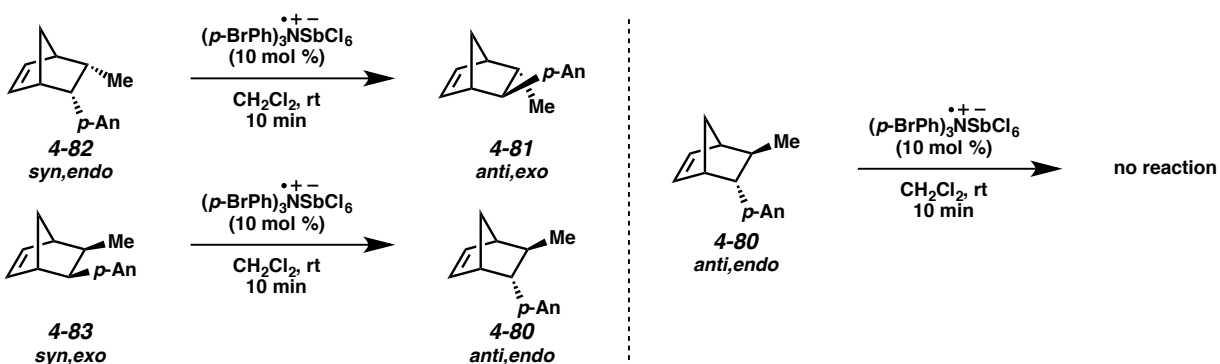


Scheme 4.26. Proposed mechanism for formation of anti products from *cis*-anethole.

Another explanation for the formation of the anti products from *cis*-anethole, then, is that an intermediate in the reaction mechanism is able to rotate to create an anti relationship between the methyl and aryl groups. Bauld proposes the following mechanistic explanation: reaction of cyclopentadiene (4-79) with the radical cation of *cis*-anethole (*cis*-4-3 $^{\bullet+}$ ) generates distonic radical cation intermediate 4-84 $^{\bullet+}$ ,

which allows for rotation about the original anethole bond before ring closure to give anti product **4-81** (Scheme 4.26).

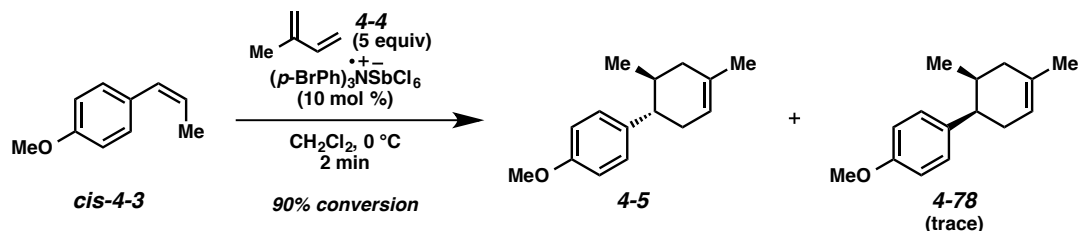
Bauld asserts that the products were stable at 0 °C, but interestingly, when the individual diastereomers were exposed to the aminium salt at ambient temperature, syn,endo adduct **4-82** isomerized to anti,exo adduct **4-81**, and syn,exo adduct **4-83** isomerized to anti,endo adduct **4-80** (Scheme 4.27). No isomerization of anti adduct **4-80** occurred. Because the 4 diastereomers did not isomerize at 0 °C, they still believed that the anti products were a result of bond rotation in the distonic radical cation intermediate, as opposed to forming from the syn adducts, but these experiments validate the prospect of bond rotation in the distonic radical cation intermediate.



Scheme 4.27. Isomerization of syn cycloadducts to anti cycloadducts.

For comparison, we attempted the cycloaddition of *cis*-anethole (*cis*-**4-3**) and isoprene (**4-4**) under Bauld's aminium salt conditions, where *cis*- to *trans*-anethole isomerization is presumably less prominent (Scheme 4.28). As was observed with the Cr-photocatalytic conditions, the anti product (**4-5**) was formed almost exclusively. Comparing Bauld's aminium salt conditions to the Cr-photocatalyzed conditions, the main experimental difference between the two systems is reaction time. As mentioned previously, in the reaction of *cis*-anethole and isoprene under the Cr conditions, only 75% conversion to product was achieved in 5 d. The same reaction, but with the aminium salt conditions, resulted in 90% conversion to product in just 2 min. This disparity in reaction times is likely due to the aminium salt-

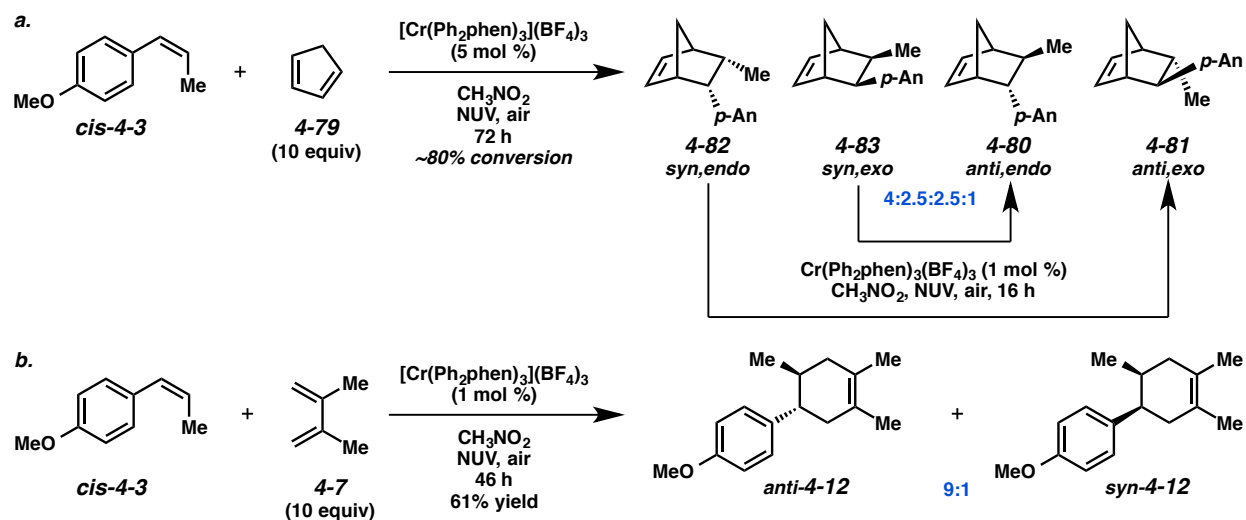
catalyzed cycloaddition occurring through radical chain propagation, while we have determined that the Cr-catalyzed reaction is proceeding through an O<sub>2</sub>-mediated photocatalytic cycle. The Cr conditions also rely on photons to excite the [Cr]<sup>3+</sup> complex, whereas the aminium salt is already very active as is. Reducing the catalyst loading of the aminium salt to 1 mol % did slow the reaction; however, overall it was still significantly faster than Cr-catalyzed version. Despite the differences between these catalyst systems, the fact that both the aminium salt and Cr conditions gave us primarily the anti adduct in the cycloaddition of *cis*-anethole and isoprene led us to believe that there may be similarities in the reaction mechanisms.



Scheme 4.28. Cycloaddition of *cis*-anethole with isoprene under the aminium salt conditions.

#### 4.6.3 Cr-catalyzed Cycloaddition of *cis*-Anethole with Other Dienes

In accordance with this theory, when the cycloaddition of *cis*-anethole (*cis*-4-3) with cyclopentadiene (4-79) was attempted under the Cr conditions, we obtained approximately the same ratio of the 4 diastereomeric products as Bauld reported with the aminium salt (Scheme 4.29a). Furthermore, in the cycloaddition of *cis*-anethole with 2,3-dimethyl-1,3-butadiene (4-7), cycloadduct 4-12 was formed as a 9:1 mixture of anti and syn products (Scheme 4.29b). These results, combined with Bauld's report, indicated that perhaps our initial hypothesis that the *cis*-anethole must isomerize to the *trans*-anethole before reacting, giving rise to only the anti products, was incorrect, and the same pathway proposed by Bauld was likely also occurring for the Cr-catalyzed cycloaddition. Indeed, when enriched samples of syn isomers 4-82 and 4-83 were exposed the Cr conditions, they both isomerized to their anti counterparts.



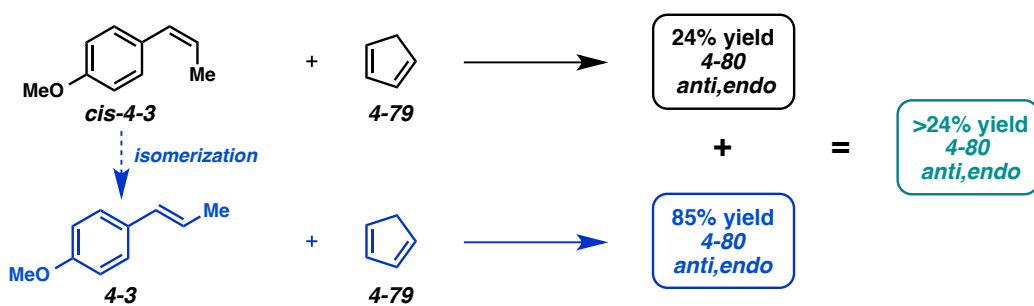
Scheme 4.29. Cr-catalyzed cycloaddition of *cis*-anethole with other dienes.

Ultimately, it seems as if the reactivity of *cis*-anethole (*cis*-4-3) and the diastereomeric ratio of products produced is not related to the specific catalyst, but to the nucleophilicity of the diene. Cyclopentadiene (4-79), which is the most reactive, gave the highest overall ratio of *syn* products (2:1 *syn*/*anti*). 2,3-Dimethyl-1,3-butadiene (4-79), which is less reactive than cyclopentadiene, but more nucleophilic than isoprene (4-4), gave a 9:1 mixture of *anti* and *syn* products. Lastly, isoprene gave nearly all *anti* product. The lesser nucleophilicity of isoprene likely increases the lifetime of the distonic radical cation intermediate, allowing more time for rotation about the anethole bond to occur to deliver the more stable *anti* cyclohexene. Dienes 4-79 and 4-7 close down faster, conserving the original *cis* character of the alkene to a greater extent.<sup>43</sup>

#### 4.6.4 Isomerization Detection Experiment

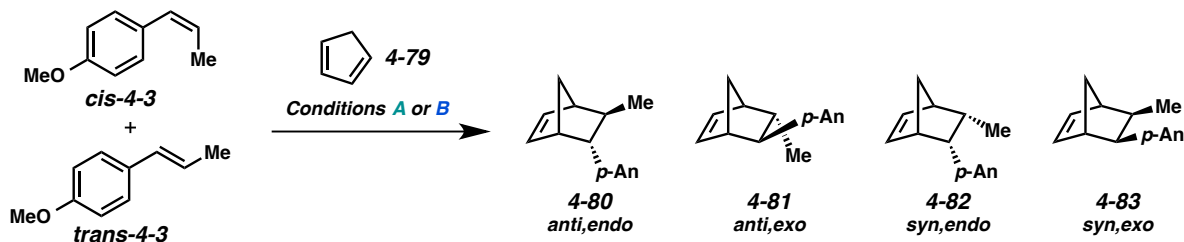
Still, from our control experiments, we knew that *cis*- to *trans*-anethole isomerization was also possible and could not be ruled out as contributing to the formation of *anti* product. In order to determine exactly how much *anti* product was a result of *cis*-anethole isomerization, we devised an experiment based on the

reactions of *cis*-anethole (*cis*-**4-3**) and *trans*-anethole (**4-3**) with cyclopentadiene (**4-79**). In the cycloadditions with cyclopentadiene, we could take advantage of the different ratios of anti,endo/anti,exo (**4-80/4-81**) products that formed when starting from the different anethole isomers. For example, in the cycloaddition of pure *cis*-anethole (*cis*-**4-3**) with diene **4-79** in Bauld's report, 24% yield of the anti,endo (**4-80**) isomer was formed (Scheme 4.30). In the cycloaddition of *trans*-anethole (**4-3**) with diene **4-79**, 85% yield of the anti,endo isomer was formed. Using these yields as a baseline, if we were performing the cycloaddition of *cis*-anethole (*cis*-**4-3**) and diene **4-79** and some of the *cis*-anethole were to isomerize to *trans*-anethole, that *trans*-anethole would go on to react with diene **4-79**, and we would theoretically obtain a >24% yield of the anti,endo product (**4-80**) (Scheme 4.30).



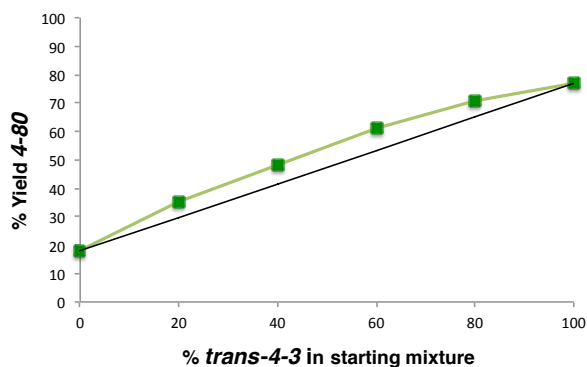
Scheme 4.30. Proposed experiment to detect *cis*- to *trans*-anethole isomerization.

In order to quantitatively display this, we set up reactions containing different ratios of *cis*- and *trans*-anethole, as shown in Scheme 4.31. We then allowed these mixtures to react under both the Cr-photocatalyzed and aminium salt conditions, and we analyzed the product mixtures to determine the percent yield of the anti,endo product (**4-80**), as well as other pertinent data.



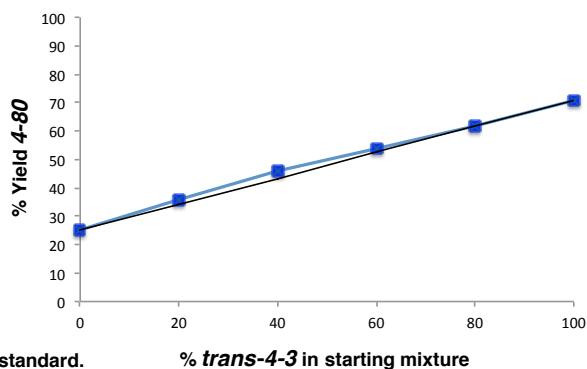
**Conditions A:** [Cr(Ph<sub>2</sub>phen)<sub>3</sub>](BF<sub>4</sub>)<sub>3</sub> (5 mol %)  
10 equiv 4-79, CH<sub>3</sub>NO<sub>2</sub>, air, NUV, 24 h

Starting 4-3 mix. cis/trans	Yield (%) <sup>a</sup>			
	<i>anti,endo</i> (4-80)	<i>anti,exo</i> (4-81)	<i>syn</i> (4-82 + 4-83)	anethole ( <i>cis + trans</i> )
100:0	18	6	32	26
80:20	35	9	31	11
60:40	48	10	22	12
40:60	61	11	15	5
20:80	71	12	6	2
0:100	77	12	0	<1



**Conditions B:** (p-BrPh)<sub>3</sub>N<sup>+</sup>Sb<sup>-</sup>Cl<sub>6</sub> (10 mol %)  
5 equiv 4-79, CH<sub>2</sub>Cl<sub>2</sub>, 0 °C, 10 min

Starting 4-3 mix. cis/trans	Yield (%) <sup>a</sup>			
	<i>anti,endo</i> (4-80)	<i>anti,exo</i> (4-81)	<i>syn</i> (4-82 + 4-83)	anethole ( <i>cis + trans</i> )
100:0	25	11	47	<1
80:20	36	11	37	<1
60:40	46	12	27	<1
40:60	54	12	18	<1
20:80	62	12	9	<1
0:100	71	12	0	<1



<sup>a</sup> Yields determined by <sup>1</sup>H NMR with dodecyl acetate as an internal standard.

Scheme 4.31. Detection of *cis*-anethole isomerization before cycloaddition.

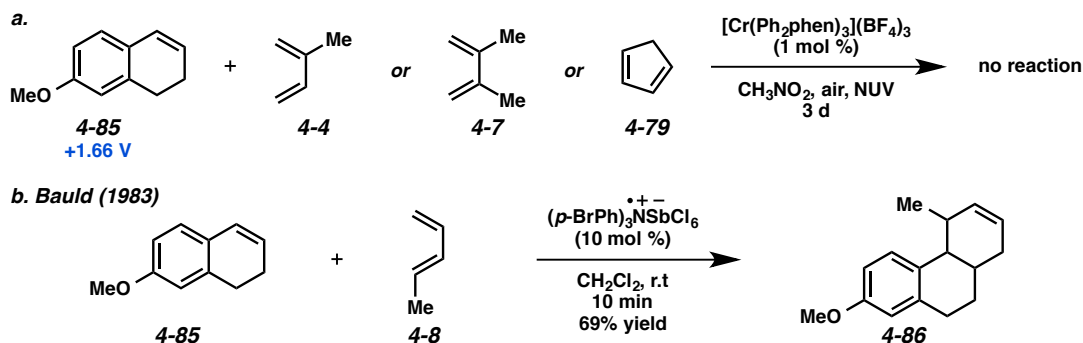
In the reaction with 100% *cis*-anethole (*cis*-4-3), we see similar ratios of the *anti*/*syn* products for both the Cr and aminium conditions. A more substantial amount of unreacted starting material is observed for the Cr case, as we would expect. As the ratio of *trans*-anethole (4-3) in the starting mixture is increased, less starting material is recovered, reinforcing the difference in rates between *cis*-anethole and *trans*-anethole. This disparity could be attributed to the higher reduction potential of *cis*-anethole (+1.24 V vs. SCE in nitromethane) versus *trans*-anethole (+1.13 V vs. SCE in nitromethane).<sup>40</sup> The difference in reactivity of *cis*- and *trans*-anethole is less defined in the aminium salt-catalyzed cycloadditions, since they are much faster.

The percent yield of the anti,endo product (**4-80**) was plotted versus the percent of *trans*-anethole (**4-3**) in the starting mixture. Also shown on each graph is the line for the expected yields of isomer **4-80** that would be obtained from each starting mixture if no isomerization of *cis*- to *trans*-anethole occurred (straight black line). In both the Cr- and aminium-catalyzed cycloadditions, the experimental line was deviated above the expected line, and to a much greater extent in the Cr case. This deviation from the expected line is a result of *cis*- to *trans*-anethole isomerization. The curve is more pronounced in the Cr reaction, likely because of the longer reaction time required for this reaction (24 h) versus the aminium-catalyzed reaction (10 min), allowing *cis*-anethole more time to isomerize before the cycloaddition. In addition, the photochemical conditions in the Cr case might aid in *cis* to *trans* isomerization of *cis*-anethole simply through irradiation ( $\lambda_{\text{max}}(\textit{cis}\text{-4-3}) = 254 \text{ nm}$ ).<sup>37</sup>

Ultimately, this experiment demonstrates that bond rotation in the distonic radical cation intermediate is likely the dominant pathway to anti product formation. Additionally, it confirms that *cis*- to *trans*-anethole isomerization is contributing to the formation of the anti products as well, particularly under the slower Cr-photocatalyzed conditions.

#### 4.6.5 Cyclic Alkene

Lastly, though all results thus far indicated that both *cis*- and *trans*-alkenes are viable substrates for this cycloaddition, cyclic alkene **4-85**, locked in the *cis* position, gave no desired product when the cycloaddition was attempted with isoprene (**4-4**), 2,3-dimethyl-1,3-butadiene (**4-7**), or cyclopentadiene (**4-79**) (Scheme 4.32a). This is surprising, considering calculations predict this substrate to be 1.7 kcal/mol easier to oxidize than *trans*-anethole (**4-3**).<sup>44</sup> For comparison, calculations predict that *cis*-anethole (*cis*-**4-3**) should be 2.0 kcal/mol more difficult to oxidize than *trans*-anethole. The reduction potential of cyclohexene **4-85** was determined to be +1.66 V<sup>40</sup>, which could indicate why these reactions were not successful. Interestingly, though, Bauld was able to utilize this substrate in a radical cation cycloaddition under the aminium salt conditions (Scheme 4.32b).<sup>45</sup>



Scheme 4.32. Cycloaddition of cyclohexene **4-85**.

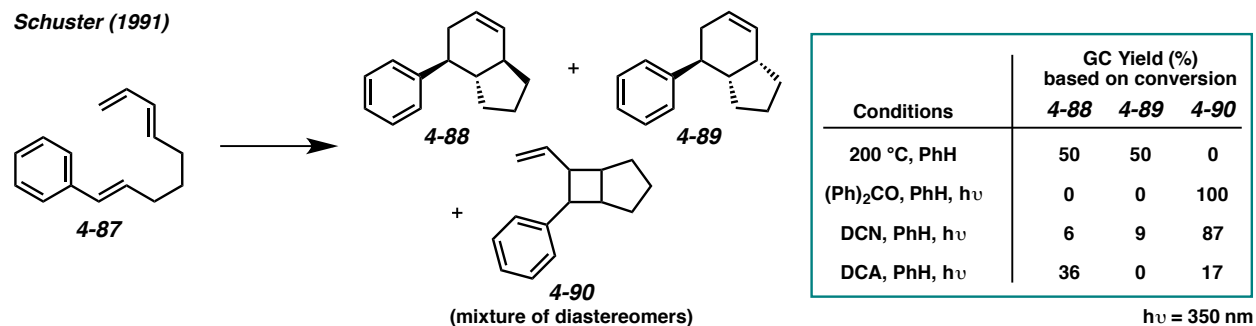
## 4.7 Differential Reactivity in Intramolecular Cycloadditions

In addition to demonstrating the synthetic utility of the Cr photocatalysts, we also wanted to show that the reactivity of the Cr complexes was somehow different from that of other catalyst systems. This was accomplished through a study of intramolecular Diels-Alder reactions, which can be catalyzed by either radical cation formation or energy transfer photosensitization.

### 4.7.1 Photosensitized Cycloadditions of Alkenes

In 1991, Schuster and coworkers reported the intramolecular triplex Diels-Alder of tethered triene **4-87**.<sup>46</sup> They evaluated this transformation thermally and with photosensitizers benzophenone, DCN (1,4-dicyanonaphthalene), and DCA (9,10-dicyanoanthracene) using UV irradiation (350 nm) (Scheme 4.33). Thermal conditions (200 °C, PhH) gave a 1:1 mixture of the syn and anti [4+2] adducts (**4-88** and **4-89**). Photosensitization with benzophenone (PhH, hv) gave none of the [4+2] adducts, but instead gave the [2+2] product **4-90** as a 3:2 mixture of two diastereomers. Photosensitization with DCN or DCA (PhH, hv) gave a mixture of [4+2] and [2+2] products. The [2+2] adduct isomers (**4-90**) predominated with the DCN conditions, and with DCA the [4+2] isomer **4-88** was formed in an approximately 2:1 ratio with the [2+2] adduct mixture. The trend in these results is partly logical. With thermal conditions, only the [4+2]

products should form, since [2+2] cycloadditions are not thermally allowed. The divergent reactivity observed between the different photosensitizers, however, is less straightforward.

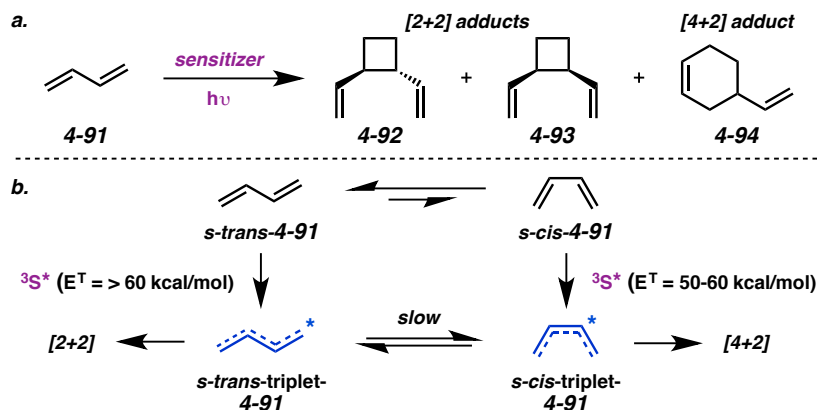


Scheme 4.33. [4+2] vs. [2+2] cycloadditions in the triplex Diels-Alder reaction.

#### 4.7.2 Photodimerization of 1,3-Butadiene

In order to understand the product distributions obtained with the different photosensitizers, it is beneficial to first look at a simpler case: the photosensitized dimerization of 1,3-butadiene (**4-91**). This transformation was explored by Hammond and coworkers in 1965.<sup>47</sup> In the photosensitized dimerization of 1,3-butadiene ( $E^T = 60$  kcal/mol),<sup>48</sup> either a [2+2] or [4+2] cycloaddition is possible (Scheme 4.34a). With higher energy photosensitizers ( $E^T = >60$  kcal/mol), the [2+2] predominates (**4-92** and **4-93**), but with lower energy photosensitizers ( $E^T = 50$ -60 kcal/mol) the [4+2] predominates (**4-94**). This is likely due to selective activation of the *s-trans* or the *s-cis* conformer of 1,3-butadiene (**4-91**). Although the energy required to excite *s-trans*-**4-91** is higher than the energy required to excite *s-cis*-**4-91**, 1,3-butadiene should contain >95% of the *s-trans* conformer at room temperature (Scheme 4.34b). Thus, when a higher energy triplet photosensitizer is employed, the result will be a much greater ratio of *s-trans*-triplet-**4-91** than *s-cis*-triplet-**4-91**, simply due to the conformational composition of 1,3-butadiene. In contrast, the lower energy sensitizers are unable to excite *s-trans*-**4-91**, so they will more selectively excite *s-cis*-**4-91**. Isomerization is possible between the triplet *s-trans* and triplet *s-cis* conformers, but it is

very slow. As a result, the two stereoisomeric triplets undergo characteristic reactions: *s-trans*-triplet-**4-91** reacts with 1,3-butadiene in a [2+2] fashion, while *s-cis*-triplet-**4-91** will undergo [4+2] cycloadditions.



Scheme 4.34. Photosensitized dimerization of 1,3-cyclobutadiene.

#### 4.7.3 Application to Schuster's Experiment

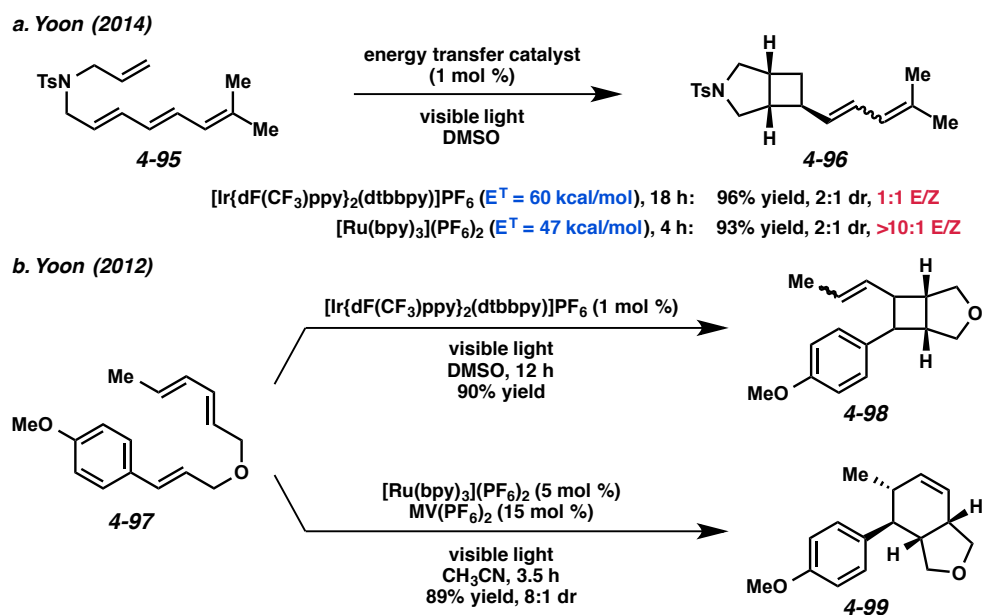
These results can be used to rationalize the outcome of the triplex cycloaddition of tethered diene **4-87**. The three sensitizers used in Schuster's report were benzophenone, DCN, and DCA, which have triplet energies of 68, 63, and 42 kcal/mol, respectively.<sup>49</sup> Based on the above 1,3-butadiene example, both benzophenone and DCN should be able to mediate the formation of the *s-trans*-triplet of diene **4-87**, while DCA should only be able to sensitize *s-cis*-triplet formation. Sensitization of the *s-trans* conformer would lead primarily to the intramolecular [2+2] products (**4-90**), while *s-cis*-diene excitation would lead to the [4+2] products (**4-88 and 4-89**). Consistent with their triplet energies, benzophenone (68 kcal/mol) gives only the [2+2] adducts, DCN (63 kcal/mol) gives a mixture favoring the [2+2] adducts, and DCA (42 kcal/mol) gives a mixture favoring the [4+2] adducts (Scheme 4.33).

This explanation overlooks, however, the potential formation of the styrenyl alkene triplet ( $E^T(\text{styrene}) = 65 \text{ kcal/mol}$ )<sup>50</sup> that could react with the diene in either a [2+2] or [4+2] fashion. Theoretically, benzophenone and DCN would be better suited than DCA to excite the styrenyl alkene, but

the selectivity of this excitation versus diene excitation, and how that selectivity would affect product distribution, is still in question. In either case, it is evident that lower energy triplet sensitizers favor the formation of the [4+2] product over the [2+2].

#### 4.7.4 Selectivity in Photosensitized Cycloadditions

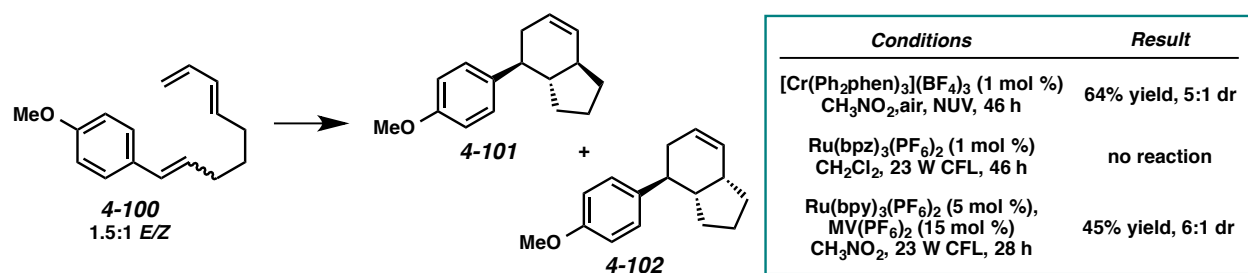
Another example of utilizing a lower energy sensitizer to more selectively induce photoexcitation was provided by Yoon and coworkers in 2014.<sup>51</sup> When the intramolecular [2+2] cycloaddition of nitrogen-tethered triene **4-95** was attempted with  $[\text{Ir}\{\text{dF}(\text{CF}_3)\text{ppy}\}_2(\text{dtbbpy})]\text{PF}_6$  ( $E^T = 60$  kcal/mol), the desired cyclobutane (**4-96**) formed in 96% yield; however, the Ir-sensitizer also incited isomerization of the diene, delivering a 1:1 E/Z ratio of diene isomers (Scheme 4.35a). Using  $\text{Ru}(\text{bpy})_3(\text{PF}_6)_2$  with a lower triplet energy ( $E^T = 47$  kcal/mol) increased the selectivity of the reaction, sensitizing the formation of cyclobutane **4-96** in 93% yield, while preserving the stereochemistry of the diene (>10:1 E/Z).



Scheme 4.35. Examples from Yoon of selective photosensitization of alkenes.

Yoon and coworkers also demonstrated the differential reactivity between energy transfer and photooxidizing catalyst conditions with the cycloaddition of substrate **4-97** (Scheme 4.35b).<sup>52</sup> Utilizing energy transfer catalyst  $[\text{Ir}\{\text{dF}(\text{CF}_3)\text{ppy}\}_2(\text{dtbbpy})]\text{PF}_6$ , cyclobutane **4-98** was formed in 90% yield. Switching to photooxidizing conditions ( $[\text{Ru}(\text{bpy})_3(\text{PF}_6)_2$  + methyl viologen), however, yielded the [4+2] adduct (**4-99**) in 89% yield.

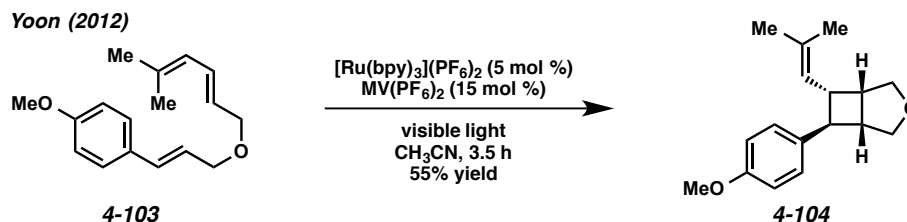
In order to increase selectivity for the intramolecular Diels-Alder over the [2+2], we thought it would be helpful to invoke a radical cation mechanism as well, employing a Cr photocatalyst with a relatively high reduction potential and excited state energy. When tethered diene **4-100** was exposed to  $\text{Cr}(\text{Ph}_2\text{phen})_3^{3+}$  ( $E_{1/2} = +1.40$  V,  $E^* = 38$  kcal/mol)<sup>5</sup> in nitromethane with NUV irradiation, the desired [4+2] product was formed in 64% yield (5:1 **4-101/4-102**) with no detection of the [2+2] cycloadduct (Scheme 4.36). Interestingly, when this reaction was attempted with  $\text{Ru}(\text{bpz})_3^{2+}$ , no reaction occurred.  $\text{Ru}(\text{bpy})_3^{2+}$  conditions, however, gave the [4+2] product in 45% yield (6:1 **4-101/4-102**). This diminished yield is perhaps due to the higher triplet energy of  $\text{Ru}(\text{bpy})_3^{2+}$  ( $E^T = 47$  kcal/mol), which could be causing other side reactions like the [2+2] cycloaddition; the crude  $^1\text{H}$  NMR of this reaction showed trace alkene protons which could be related to a [2+2] cycloadduct.



Scheme 4.36. Radical cation intramolecular Diels-Alder reaction.

It should be noted that [2+2] cycloadditions can occur under photooxidizing radical cation conditions, not just through photosensitization.<sup>53</sup> For instance, while attempting the intramolecular Diels-

Alder reaction of tethered triene **4-103** with photooxidizing Ru-conditions, Yoon observed only [2+2] adduct **4-104** in 55% yield, perhaps because of the sterically hindered diene (Scheme 4.37).<sup>54</sup>



Scheme 4.37. Intramolecular [2+2] cycloaddition under photooxidizing conditions.

In summary, the investigation of intramolecular cycloadditions has revealed orthogonal reactivity and an additional advantage of the Cr photocatalysts. Because  $\text{Cr}(\text{Ph}_2\text{phen})_3^{3+}$  has a lower excited state energy, it more selectively catalyzes radical cation processes, and, thus, is a more beneficial catalyst for cycloadditions in which competing energy transfer would lead to undesired side products.

## 4.8 Conclusion

In conclusion, through the radical cation accelerated Diels-Alder reaction of electron-rich dienophiles, we have begun to explore the catalytic capabilities of photooxidizing Cr(III) complexes. Our early results indicate that the Cr photocatalysts display differential behavior from their Ru counterparts, both mechanistically and in terms of reactivity. Further synthetic applications and investigations of the  $\text{Cr}(\text{Ph}_2\text{phen})_3^{3+}$  photocatalyst system will be discussed in Chapter 5.

## 4.9 Experimental Section

### 4.9.1 Materials and Methods

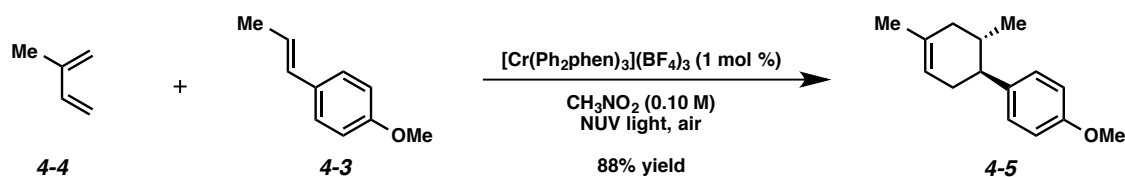
Cr catalysts were synthesized as previously described.<sup>5,34</sup> The preparation of  $[\text{Cr}(\text{Ph}_2\text{phen})_3](\text{BF}_4)_3$  is also provided in Chapter 4.9.17.  $\text{Ru}(\text{bpz})_3(\text{PF}_6)_2$  and  $\text{Ru}(\text{bpy})_3\text{Cl}_2$  were purchased from Sigma-Aldrich.  $\text{Ru}(\text{bpy})_3(\text{PF}_6)_2$  and methyl viologen bis(hexafluorophosphate) were prepared according to the procedures by Yoon and coworkers.<sup>55</sup> All solvents, excluding nitromethane, were purified by passing through activated alumina columns. All reagents were used as received unless otherwise noted. Commercially available chemicals were purchased from Alfa Aesar (Ward Hill, MA), Sigma-Aldrich (St. Louis, MO), Oakwood Products, (West Columbia, SC), Strem (Newburyport, MA) and TCI America (Portland, OR). Qualitative TLC analysis was performed on 250 mm thick, 60 Å, glass backed, F254 silica (Silicycle, Quebec City, Canada). Visualization was accomplished with UV light and exposure to *p*-anisaldehyde or  $\text{KMnO}_4$  solution followed by heating. Flash chromatography was performed using Silicycle silica gel (230-400 mesh). Reactions under near-UV irradiation (NUV) were performed in either a Rayonet chamber reactor equipped with 16 lamps of wavelengths 419, 350, and 300 nm or a Luzchem photoreactor equipped with 10 lamps of the same wavelengths. Irradiation with visible light was performed in a sealed box using a 23 W compact fluorescent light bulb (EcoSmart 23 W bright white CFL spiral light bulb, 1600 lumens). NMR spectra were acquired at both the Colorado State University Central Instrument Facility on an Agilent (Varian) 400-MR and at the University of Georgia Chemical Sciences Magnetic Resonance Facility on a Varian Mercury Plus 400 MHz NMR.  $^1\text{H}$  NMR spectra were acquired at 400 MHz and are reported relative to  $\text{SiMe}_4$  ( $\delta$  0.00).  $^{13}\text{C}$  NMR spectra were at 100 MHz and are reported relative to  $\text{SiMe}_4$  ( $\delta$  0.0). IR spectra were obtained on a Nicolet 380 FT-IR. High resolution mass spectrometry data were acquired by the Colorado State University Central Instrument Facility on an Agilent 6210 TOF LC/MS and by the Proteomics and Mass Spectrometry

Facility at the University of Georgia on a Thermo Orbitrap Elite. GC yields were obtained on a Shimadzu GC-2010 (fused silica column, Shimadzu cat. # 220-94536-01).

#### 4.9.2 Radical Cation Accelerated Diels-Alder Reactions

**General Notes:** Nitromethane was purchased from Alfa Aesar (98+%, A11806) and used without further purification. Diastereomeric ratios were determined by  $^1\text{H}$  NMR. NMR spectral data reported are those of the major diastereomer.

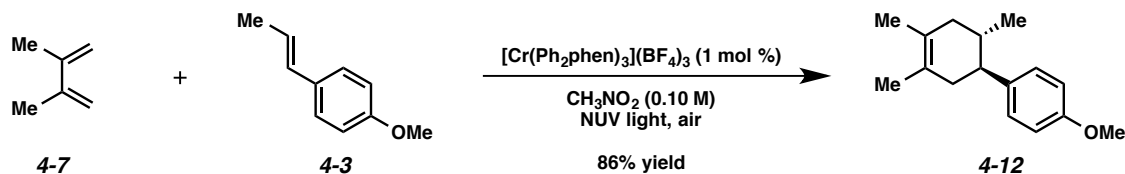
**General Procedure for the radical cation accelerated [4+2] cycloaddition.** To a flame-dried vial open to air was added the alkene (1 equiv), diene (10 equiv),  $[\text{Cr}(\text{Ph}_2\text{phen})_3](\text{BF}_4)_3$  (1 mol %), and nitromethane (0.10 M). The vial was then capped and placed in the photoreactor equipped with 419, 350, and 300 nm light bulbs (NUV light). The reaction was irradiated with stirring until consumption of the alkene was complete, as determined by TLC. The reaction was then diluted to twice the volume with  $\text{H}_2\text{O}$  and transferred to a separatory funnel. The aqueous layer was extracted with  $\text{Et}_2\text{O}$  (3x). The combined organic layers were washed with brine and dried over  $\text{Na}_2\text{SO}_4$ . The solvent was removed by rotary evaporation and the resulting residue was purified by flash chromatography.



**Cycloadduct 4-5.** Prepared according to the *General Procedure* using *trans*-anethole (4-3) (17.7 mg, 0.120 mmol), isoprene (4-4) (0.120 mL, 1.20 mmol),  $[\text{Cr}(\text{Ph}_2\text{phen})_3](\text{BF}_4)_3$  (1.6 mg, 0.00120 mmol), and nitromethane (1.20 mL). The reaction was irradiated for 27 h. The crude product was purified by flash chromatography (100% hexanes→9:1 hexanes/EtOAc eluent) to afford cycloadduct 4-5 (22.7 mg, 88% yield) as a colorless oil.

**TLC:**  $R_f = 0.56$  in 9:1 hexanes/EtOAc, stained blue with *p*-anisaldehyde.

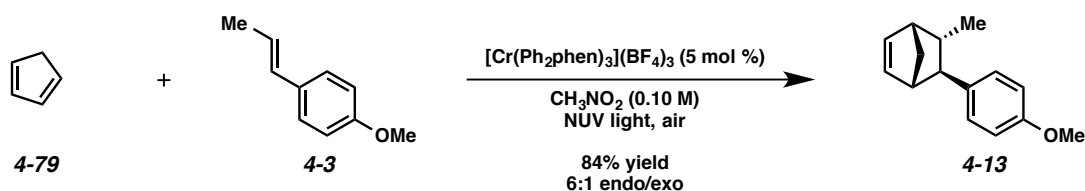
All spectroscopic data were consistent with previously reported values.<sup>12</sup>



**Cycloadduct 4-12.** Prepared according to the *General Procedure* using *trans*-anethole (**4-3**) (17.7 mg, 0.120 mmol), 2,3-dimethyl-1,3-butadiene (**4-7**) (0.135 mL, 1.20 mmol),  $[\text{Cr}(\text{Ph}_2\text{phen})_3](\text{BF}_4)_3$  (1.6 mg, 0.00120 mmol), and nitromethane (1.20 mL). The reaction was irradiated for 24 h. The crude product was purified by flash chromatography (100% hexanes→9:1 hexanes/EtOAc eluent) to afford cycloadduct **4-12** (23.8 mg, 86% yield) as a colorless oil.

**TLC:**  $R_f = 0.53$  in 9:1 hexanes/EtOAc, stained blue with *p*-anisaldehyde.

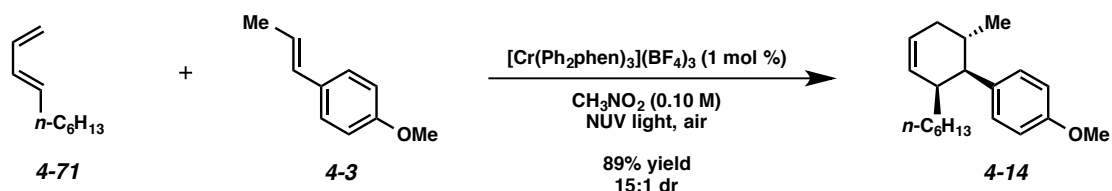
All spectroscopic data were consistent with previously reported values.<sup>12</sup>



**Cycloadduct 4-13.** Prepared according to the *General Procedure* using *trans*-anethole (**4-3**) (8.9 mg, 60.0  $\mu\text{mol}$ ), cyclopentadiene (**4-79**) (50.0  $\mu\text{L}$ , 600  $\mu\text{mol}$ ),  $[\text{Cr}(\text{Ph}_2\text{phen})_3](\text{BF}_4)_3$  (3.9 mg, 3.00  $\mu\text{mol}$ ), and nitromethane (0.600 mL). The reaction was irradiated for 48 h. The crude product was purified by flash chromatography (100% hexanes→9:1 hexanes/EtOAc eluent) to afford cycloadduct **4-13** (10.8 mg, 84% yield, 6:1 endo/exo) as a colorless oil.

**TLC:**  $R_f = 0.80$  in 4:1 hexanes/EtOAc, stained blue with *p*-anisaldehyde.

All spectroscopic data were consistent with previously reported values.<sup>41</sup>



**Cycloadduct 4-14.** Prepared according to the *General Procedure* using *trans*-anethole (**4-3**) (17.8 mg, 0.120 mmol), *trans*-1,3-decadiene (**4-71**) (0.166 g, 1.20 mmol),  $[\text{Cr}(\text{Ph}_2\text{phen})_3](\text{BF}_4)_3$  (1.6 mg, 0.00120 mmol), and nitromethane (1.20 mL). The reaction was irradiated for 21 h in a *septum-capped vial with needle outlet*. The crude product was purified by flash chromatography (100% hexanes $\rightarrow$ 9:1 hexanes/EtOAc eluent) to afford cycloadduct **4-14** (30.7 mg, 89% yield, 15:1 dr) as a colorless oil.

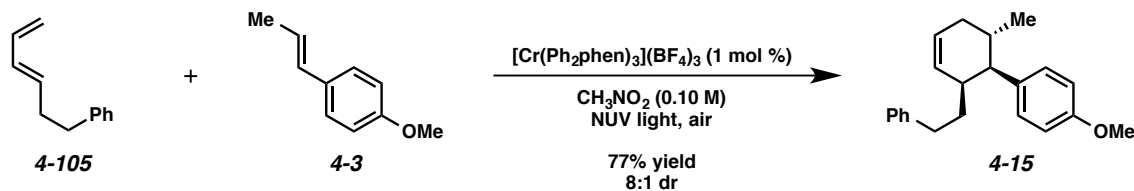
**TLC:**  $R_f = 0.56$  in 9:1 hexanes/EtOAc, stained blue with *p*-anisaldehyde.

**<sup>1</sup>H NMR** (400 MHz;  $\text{CDCl}_3$ ):  $\delta$  7.09 (d,  $J = 8.7$  Hz, 2H), 6.82 (d,  $J = 8.7$  Hz, 2H), 5.84-5.80 (m, 1H), 5.70-5.66 (m, 1H), 3.80 (s, 3H), 2.68 (dd,  $J = 9.1, 5.4$  Hz, 1H), 2.29-2.22 (m, 1H), 2.20-2.16 (m, 1H), 2.12-2.04 (m, 1H), 1.80-1.72 (m, 1H), 1.30-1.12 (comp. m, 10H), 0.90 (d,  $J = 6.6$  Hz, 3H), 0.82 (t,  $J = 7.1$  Hz, 3H).

**<sup>13</sup>C NMR** (100 MHz;  $\text{CDCl}_3$ ):  $\delta$  157.5, 135.5, 131.5, 130.2, 125.6, 113.1, 55.1, 50.0, 38.8, 33.3, 31.8, 31.5, 29.5, 28.5, 27.5, 22.6, 20.9, 14.0.

**IR** (ATR, neat): 2924, 2855, 1611, 1511, 1462, 1245, 1040  $\text{cm}^{-1}$ .

**HRMS** (ESI+):  $m/z$  calc'd for  $(\text{M} + \text{H})^+$   $[\text{C}_{20}\text{H}_{30}\text{O} + \text{H}]^+$ : 287.2369, found 287.2378.



**Cycloadduct 4-15.** Prepared according to the *General Procedure* using *trans*-anethole (**4-3**) (7.4 mg, 50.0  $\mu\text{mol}$ ), diene (**4-105**) (65.1 mg, 500  $\mu\text{mol}$ ),  $[\text{Cr}(\text{Ph}_2\text{phen})_3](\text{BF}_4)_3$  (0.7 mg, 0.500  $\mu\text{mol}$ ), and nitromethane (0.500 mL). The reaction was irradiated for 66 h. The crude product was purified by flash chromatography (100% hexanes $\rightarrow$ 9:1 hexanes/EtOAc eluent) to afford cycloadduct **4-15** (10.7 mg, 77% yield, 8:1 dr) as a colorless oil.

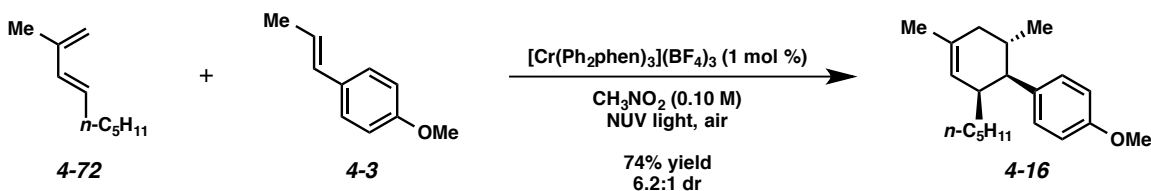
**TLC:**  $R_f = 0.65$  in 9:1 hexanes/EtOAc, stained blue with *p*-anisaldehyde.

**$^1\text{H}$  NMR** (400 MHz;  $\text{CDCl}_3$ ):  $^1\text{H}$  NMR (400 MHz;  $\text{CDCl}_3$ ):  $\delta$  7.30-7.27 (m, 2H), 7.22-7.18 (m, 1H), 7.11 (t,  $J = 8.8$  Hz, 2H), 7.00 (d,  $J = 7.3$  Hz, 2H), 6.82 (d,  $J = 8.8$  Hz, 2H), 5.88-5.71 (m, 2H), 3.79 (s, 3H), 2.75-2.55 (m, 3H), 2.32-2.26 (m, 2H), 2.13-2.05 (m, 1H), 1.81-1.74 (m, 1H), 1.54-1.50 (m, 2H), 0.91 (d,  $J = 6.6$  Hz, 3H).

**$^{13}\text{C}$  NMR** (100 MHz;  $\text{CDCl}_3$ ):  $^{13}\text{C}$  NMR (100 MHz;  $\text{CDCl}_3$ ):  $\delta$  157.6, 142.8, 135.2, 131.0, 130.2, 128.3, 128.1, 126.2, 125.5, 113.2, 55.2, 49.6, 38.4, 33.8, 33.4, 33.1, 28.7, 20.8.

**IR** (ATR, neat): 2928, 2853, 1611, 1508, 1462, 1242, 1038  $\text{cm}^{-1}$ .

**LRMS** (EI):  $m/z$  calc'd for M  $[\text{C}_{22}\text{H}_{26}\text{O}]$ : 306.45, found 306.3.



**Cycloadduct 4-16.** Prepared according to the *General Procedure* using *trans*-anethole (**4-3**) (17.8 mg, 0.120 mmol), *trans*-2-methyl-1,3-nonadiene (**4-72**) (0.166 g, 1.20 mmol),  $[\text{Cr}(\text{Ph}_2\text{phen})_3](\text{BF}_4)_3$  (1.6 mg, 0.00120 mmol), and nitromethane (1.20 mL). The reaction was irradiated for 23 h in a *septum-capped vial with needle outlet*. The crude product was purified by flash chromatography (100% hexanes $\rightarrow$ 9:1 hexanes/EtOAc eluent) to afford cycloadduct **4-16** (25.4 mg, 74% yield, 6.2:1 dr) as a colorless oil.

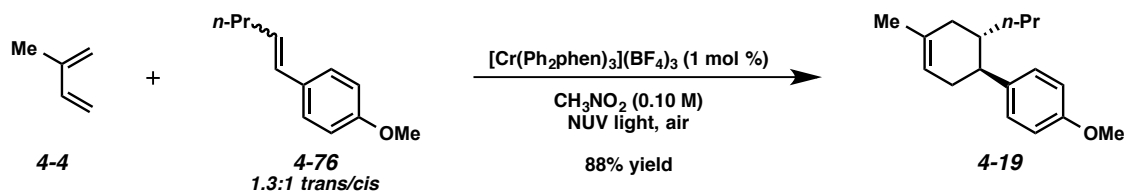
**TLC:**  $R_f = 0.61$  in 9:1 hexanes/EtOAc, stained blue with *p*-anisaldehyde.

**<sup>1</sup>H NMR** (400 MHz; CDCl<sub>3</sub>): δ 7.06 (d, *J* = 8.7 Hz, 2H), 6.81 (d, *J* = 8.7 Hz, 2H), 5.53 (br s, 1H), 3.79 (s, 3H), 2.61 (dd, *J* = 8.7, 5.4 Hz, 1H), 2.17-2.04 (comp. m, 4H), 1.70 (s, 3H), 1.32-1.24 (m, 2H), 1.21-1.00 (comp. m, 6H), 0.89 (d, *J* = 6.4 Hz, 3H), 0.80 (t, *J* = 7.1 Hz, 3H).

**<sup>13</sup>C NMR** (100 MHz; CDCl<sub>3</sub>): δ 156.2, 135.7, 132.5, 130.2, 125.6, 113.1, 55.1, 49.9, 39.0, 38.2, 32.1, 31.6, 28.8, 27.3, 23.7, 22.6, 20.9, 14.0.

**IR** (ATR, neat): 2925, 2856, 1611, 1511, 1454, 1244, 1178, 1039 cm<sup>-1</sup>.

**HRMS** (ESI+): *m/z* calc'd for (M + H)<sup>+</sup> [C<sub>20</sub>H<sub>30</sub>O + H]<sup>+</sup>: 287.2369, found 287.2371.



**Cycloadduct 4-19.** Prepared according to the *General Procedure* using alkene **4-76** (10.7 mg, 60.0 μmol), isoprene (**4-4**) (60.1 μL, 0.600 mmol),  $[\text{Cr}(\text{Ph}_2\text{phen})_3](\text{BF}_4)_3$  (0.8 mg, 0.600 μmol), and nitromethane (0.600 mL). The reaction was irradiated for 48 h. The crude product was purified by flash chromatography (100% hexanes→10:1 hexanes/EtOAc eluent) to afford cycloadduct **4-19** (13.1 mg, 88% yield) as a colorless oil.

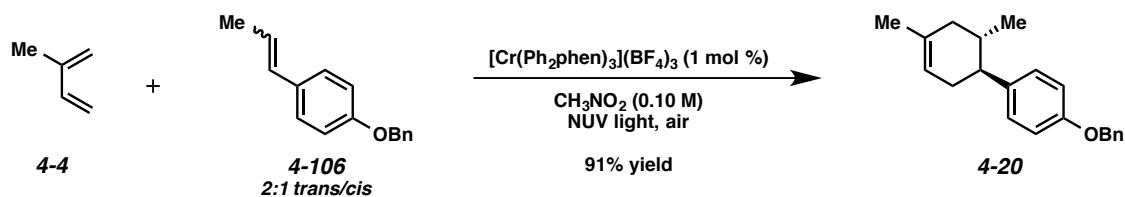
**TLC:** *R<sub>f</sub>* = 0.78 in 4:1 hexanes/EtOAc, stained blue with *p*-anisaldehyde.

**<sup>1</sup>H NMR** (400 MHz; CDCl<sub>3</sub>): δ 7.07 (d, *J* = 8.6 Hz, 2H), 6.83 (d, *J* = 8.6 Hz, 2H), 5.44 (br s, 1H), 3.80 (s, 3H), 2.42-2.36 (m, 1H), 2.20-2.10 (m, 2H), 1.82-1.72 (m, 2H), 1.69 (s, 3H), 1.36-1.26 (m, 2H), 1.19-1.08 (m, 2H), 0.94-0.84 (m, 1H), 0.76 (t, *J* = 7.1 Hz, 3H).

**<sup>13</sup>C NMR** (100 MHz; CDCl<sub>3</sub>): δ 157.7, 138.3, 133.6, 128.5, 120.7, 113.6, 55.2, 45.4, 38.2, 36.4, 36.3, 35.2, 23.5, 19.5, 14.2.

**IR** (ATR, neat): 2958, 2930, 2873, 1611, 1512, 1465, 1265, 1246, 1178, 1037 cm<sup>-1</sup>.

**HRMS** (ESI+): *m/z* calc'd for (M + H)<sup>+</sup> [C<sub>17</sub>H<sub>24</sub>O + H]<sup>+</sup>: 245.1900, found 245.1909.



**Cycloadduct 4-20.** Prepared according to the *General Procedure* using alkene **4-106** (13.0 mg, 60.0  $\mu\text{mol}$ ), isoprene (**4-4**) (60.1  $\mu\text{L}$ , 600  $\mu\text{mol}$ ),  $[\text{Cr}(\text{Ph}_2\text{phen})_3](\text{BF}_4)_3$  (0.8 mg, 0.600  $\mu\text{mol}$ ), and nitromethane (0.600 mL). The reaction was irradiated for 21 h. The crude product was purified by flash chromatography (100% hexanes  $\rightarrow$  10:1 hexanes/EtOAc eluent) to afford cycloadduct **4-20** (15.4 mg, 91% yield) as a white solid.

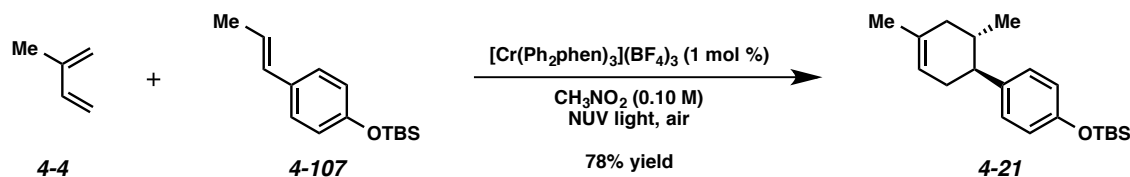
**TLC:**  $R_f = 0.75$  in 4:1 hexanes/EtOAc, stained blue with *p*-anisaldehyde.

**$^1\text{H}$  NMR** (400 MHz;  $\text{CDCl}_3$ ):  $\delta$  7.45-7.43 (m, 2H), 7.40-7.36 (m, 2H), 7.34-7.30 (m, 1H), 7.08 (d,  $J = 8.7$  Hz, 2H), 6.91 (d,  $J = 8.7$  Hz, 2H), 5.44 (br s, 1H), 5.04 (s, 2H), 2.30 (td,  $J = 10.6, 5.3$  Hz, 1H), 2.20-2.13 (m, 2H), 2.11-2.06 (m, 1H), 1.93-1.75 (m, 2H), 1.69 (s, 3H), 0.71 (d,  $J = 6.4$  Hz, 3H).

**$^{13}\text{C}$  NMR** (100 MHz;  $\text{CDCl}_3$ ):  $\delta$  157.0, 138.5, 137.3, 133.8, 128.51, 128.49, 127.8, 127.5, 120.9, 114.6, 70.0, 46.9, 39.8, 35.2, 33.9, 23.4, 20.2.

**IR** (ATR, neat): 2997, 1610, 1509, 1437, 1386, 1238, 1177, 1017  $\text{cm}^{-1}$ .

**HRMS** (ESI<sup>+</sup>):  $m/z$  calc'd for  $(\text{M} + \text{H})^+$   $[\text{C}_{21}\text{H}_{24}\text{O} + \text{H}]^+$ : 293.1900, found 293.1896.



**Cycloadduct 4-21.** Prepared according to the *General Procedure* using alkene **4-107** (14.6 mg, 60.0  $\mu\text{mol}$ ), isoprene (**4-4**) (60.1  $\mu\text{L}$ , 600  $\mu\text{mol}$ ),  $[\text{Cr}(\text{Ph}_2\text{phen})_3](\text{BF}_4)_3$  (0.8 mg, 0.600  $\mu\text{mol}$ ), and nitromethane (0.600 mL). The reaction was irradiated for 30 h. The crude product was purified by flash

chromatography (100% hexanes→20:1 hexanes/EtOAc eluent) to afford cycloadduct **4-21** (14.5 mg, 78% yield) as a colorless oil.

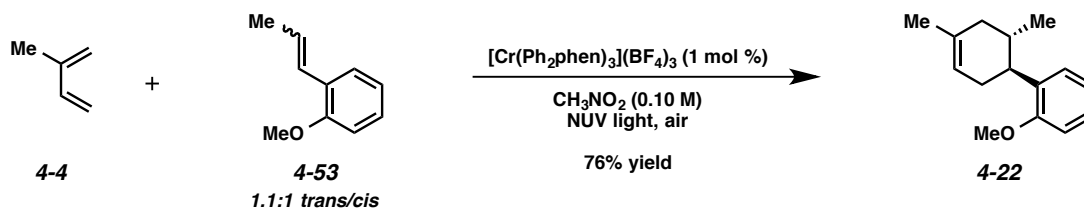
**TLC:**  $R_f$  = 0.92 in 4:1 hexanes/EtOAc, stained blue with *p*-anisaldehyde.

**$^1\text{H NMR}$**  (400 MHz;  $\text{CDCl}_3$ ):  $\delta$  7.00 (d,  $J$  = 8.4 Hz, 2H), 6.75 (d,  $J$  = 8.4 Hz, 2H), 5.44 (br s, 1H), 2.27 (td,  $J$  = 10.4, 5.2 Hz, 1H), 2.19-2.13 (m, 2H), 2.10-2.05 (m, 1H), 1.90-1.75 (m, 2H), 1.69 (s, 3H), 0.98 (s, 9H), 0.69 (d,  $J$  = 6.2 Hz, 3H), 0.19 (s, 6H).

**$^{13}\text{C NMR}$**  (100 MHz;  $\text{CDCl}_3$ ):  $\delta$  153.6, 138.7, 133.7, 128.4, 120.9, 119.7, 47.0, 39.8, 35.1, 34.0, 25.7, 23.4, 20.2, 18.2, -4.4.

**IR** (ATR, neat): 2887, 1609, 1509, 1453, 1238, 1017  $\text{cm}^{-1}$ .

**HRMS** (ESI+):  $m/z$  calc'd for  $(\text{M} + \text{NH}_4)^+ [\text{C}_{20}\text{H}_{32}\text{OSi} + \text{NH}_4]^+$ : 334.2561, found 334.2563.



**Cycloadduct 4-22.** Prepared according to the *General Procedure* using alkene **4-53** (8.0 mg, 54.0  $\mu\text{mol}$ ), isoprene (**4-4**) (60.1  $\mu\text{L}$ , 600  $\mu\text{mol}$ ),  $[\text{Cr}(\text{Ph}_2\text{phen})_3](\text{BF}_4)_3$  (0.8 mg, 0.600  $\mu\text{mol}$ ), and nitromethane (0.600 mL). The reaction was irradiated for 21 h. The crude product was purified by flash chromatography (100% hexanes→10:1 hexanes/EtOAc eluent) to afford cycloadduct **4-22** (8.9 mg, 76% yield) as a colorless oil.

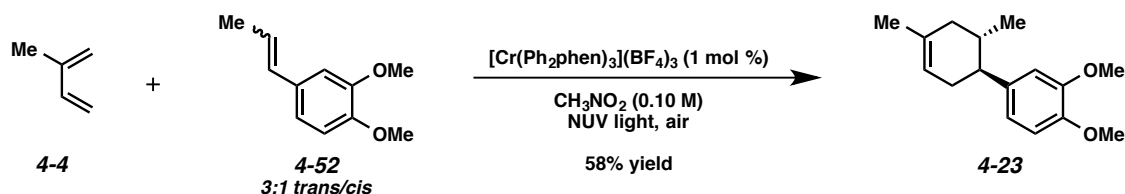
**TLC:**  $R_f$  = 0.69 in 4:1 hexanes/EtOAc, stained blue with *p*-anisaldehyde.

**$^1\text{H NMR}$**  (400 MHz;  $\text{CDCl}_3$ ):  $\delta$  7.16 (t,  $J$  = 8.0 Hz, 2H), 6.92 (t,  $J$  = 7.4 Hz, 1H), 6.86 (d,  $J$  = 8.0 Hz, 1H), 5.45 (br s, 1H), 3.80 (s, 3H), 2.95-2.88 (m, 1H), 2.17-2.16 (m, 2H), 2.10-2.01 (m, 2H), 1.86-1.78 (m, 1H), 1.70 (s, 3H), 0.74 (d,  $J$  = 6.2 Hz, 3H).

<sup>13</sup>C NMR (100 MHz; CDCl<sub>3</sub>): δ 157.5, 134.1, 133.7, 127.8, 126.5, 121.1, 120.6, 110.6, 55.4, 39.8, 33.5, 32.7, 23.4, 19.8.

IR (ATR, neat): 2886, 1609, 1509, 1438, 1376, 1237, 1017 cm<sup>-1</sup>.

HRMS (ESI+): *m/z* calc'd for (M + H)<sup>+</sup> [C<sub>15</sub>H<sub>20</sub>O + H]<sup>+</sup>: 217.1587, found 217.1591.



**Cycloadduct 4-23.** Prepared according to the *General Procedure* using alkene **4-52** (13.9 mg, 78.0 μmol), isoprene (**4-4**) (75.1 μL, 750 μmol), [Cr(Ph<sub>2</sub>phen)<sub>3</sub>](BF<sub>4</sub>)<sub>3</sub> (1.0 mg, 0.750 μmol), and nitromethane (0.750 mL). Prior to irradiation, O<sub>2</sub> was bubbled through the reaction mixture for 30 s with a balloon and needle outlet. The reaction vessel was then sealed and the reaction was irradiated for 30 h. The crude product was purified by flash chromatography (100% hexanes→10:1 hexanes/EtOAc eluent) to afford cycloadduct **4-23** (11.2 mg, 58% yield) as a colorless oil.

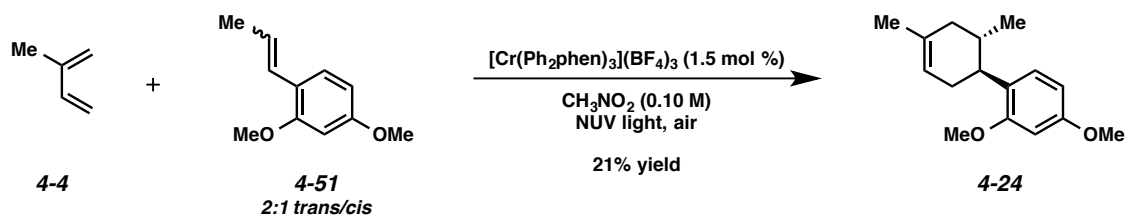
**TLC:** R<sub>f</sub> = 0.48 in 4:1 hexanes/EtOAc, visualized by UV.

<sup>1</sup>H NMR (400 MHz; CDCl<sub>3</sub>): δ 6.80 (d, *J* = 8.0 Hz, 1H), 6.72 (s, 1H), 6.70 (t, *J* = 2.5 Hz, 1H), 5.44 (br s, 1H), 3.864 (s, 3H), 3.859 (s, 3H), 2.29 (td, *J* = 10.5, 5.2 Hz, 1H), 2.19 (m, 2H), 2.11-2.06 (m, 1H), 1.89 (ddd, *J* = 17.4, 6.9, 1.8 Hz, 2H), 1.69 (s, 3H), 0.72 (d, *J* = 6.3 Hz, 3H).

<sup>13</sup>C NMR (100 MHz; CDCl<sub>3</sub>): δ 148.8, 147.1, 138.8, 133.8, 120.7, 119.6, 111.1, 110.7, 55.84, 55.80, 47.4, 39.8, 35.2, 34.0, 23.3, 20.2.

IR (ATR, neat): 2903, 2833, 1590, 1515, 1451, 1255, 1237, 1139, 1028 cm<sup>-1</sup>.

HRMS (ESI+): *m/z* calc'd for (M + NH<sub>4</sub>)<sup>+</sup> [C<sub>16</sub>H<sub>22</sub>O<sub>2</sub> + NH<sub>4</sub>]<sup>+</sup>: 264.1961, found 264.1958.



**Cycloadduct 4-24.** Prepared according to the *General Procedure* using alkene **4-51** (10.5 mg, 58.9  $\mu\text{mol}$ ), isoprene (**4-4**) (60.1  $\mu\text{L}$ , 600  $\mu\text{mol}$ ),  $[\text{Cr}(\text{Ph}_2\text{phen})_3](\text{BF}_4)_3$  (0.8 mg, 0.600  $\mu\text{mol}$ ), and nitromethane (0.600 mL). Prior to irradiation,  $\text{O}_2$  was bubbled through the reaction mixture for 30 s with a balloon and needle outlet. The reaction vessel was then sealed and the reaction was irradiated for 24 h, at which time, 0.4 mg  $[\text{Cr}(\text{Ph}_2\text{phen})_3](\text{BF}_4)_3$  (0.300  $\mu\text{mol}$ ) were added,  $\text{O}_2$  was bubbled through again, and the reaction vessel was sealed and irradiated 24 h more. The crude product was purified by flash chromatography (100% hexanes  $\rightarrow$  9:1 hexanes/EtOAc eluent) to afford cycloadduct **4-24** (3.1 mg, 21% yield) as a colorless oil.

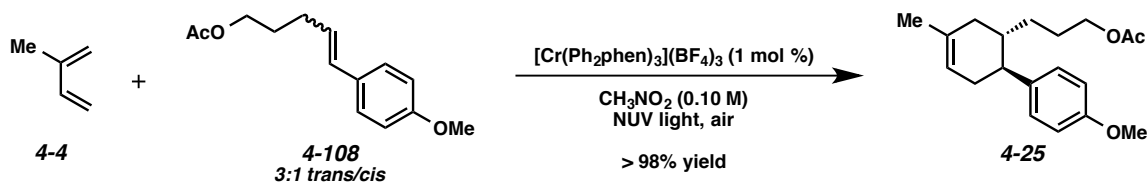
**TLC:**  $R_f = 0.70$  in 4:1 hexanes/EtOAc, stained red with *p*-anisaldehyde.

**$^1\text{H}$  NMR** (400 MHz;  $\text{CDCl}_3$ ):  $\delta$  7.02 (d,  $J = 8.0$  Hz, 1H), 6.47 (d,  $J = 2.5$  Hz, 1H), 6.45 (t,  $J = 2.5$  Hz, 1H), 5.44 (br s, 1H), 3.79 (s, 3H), 3.77 (s, 3H), 2.80 (dt,  $J = 10.7, 8.0$  Hz, 1H), 2.14 (ddt,  $J = 6.5, 3.3, 1.6$  Hz, 2H), 2.09-2.03 (m, 1H), 2.02-1.95 (m, 1H), 1.84-1.80 (m, 1H), 1.68 (s, 3H), 0.73 (d,  $J = 6.4$  Hz, 3H).

**$^{13}\text{C}$  NMR** (100 MHz;  $\text{CDCl}_3$ ):  $\delta$  158.4, 137.6, 133.7, 128.2, 126.5, 121.2, 104.3, 98.5, 55.4, 55.2, 44.0, 39.9, 33.6, 32.9, 23.4, 19.8.

**IR** (ATR, neat): 2951, 2922, 2834, 1610, 1586, 1504, 1454, 1292, 1259, 1206, 1155, 1117, 1037  $\text{cm}^{-1}$ .

**HRMS** (ESI<sup>+</sup>):  $m/z$  calc'd for  $(\text{M} + \text{H})^+$   $[\text{C}_{16}\text{H}_{22}\text{O}_2 + \text{H}]^+$ : 247.1693, found 247.1689.



**Cycloadduct 4-25.** Prepared according to the *General Procedure* using alkene **4-108** (14.7 mg, 62.7  $\mu\text{mol}$ ), isoprene (**4-4**) (60.1  $\mu\text{L}$ , 600  $\mu\text{mol}$ ),  $[\text{Cr}(\text{Ph}_2\text{phen})_3](\text{BF}_4)_3$  (0.8 mg, 0.600  $\mu\text{mol}$ ), and nitromethane (0.600 mL). The reaction was irradiated for 22 h. The crude product was purified by flash chromatography (100% hexanes $\rightarrow$ 9:1 hexanes/EtOAc eluent) to afford cycloadduct **4-25** (19.0 mg, >98% yield) as a colorless oil.

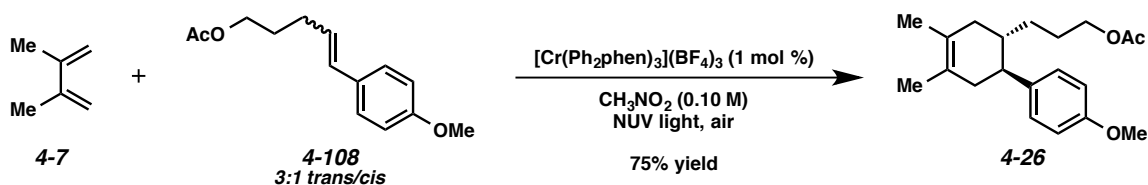
**TLC:**  $R_f = 0.54$  in 4:1 hexanes/EtOAc, visualized by UV.

**$^1\text{H}$  NMR** (400 MHz;  $\text{CDCl}_3$ ):  $\delta$  7.06 (d,  $J = 8.7$  Hz, 2H), 6.83 (d,  $J = 8.7$  Hz, 2H), 5.44 (br s, 1H), 3.97-3.84 (m, 2H), 3.79 (s, 3H), 2.43-2.36 (m, 1H), 2.20-2.10 (m, 2H), 1.97 (s, 3H), 1.85-1.73 (m, 2H), 1.69 (s, 3H), 1.67-1.59 (m, 2H), 1.49-1.38 (m, 1H), 1.28-1.19 (m, 1H), 1.00-0.91 (m, 1H).

**$^{13}\text{C}$  NMR** (100 MHz;  $\text{CDCl}_3$ ):  $\delta$  171.1, 157.8, 137.7, 133.3, 128.5, 120.8, 113.8, 64.6, 55.2, 45.3, 38.1, 36.3, 35.1, 30.0, 25.4, 23.5, 20.9.

**IR** (ATR, neat): 2960, 2906, 2836, 1731, 1611, 1512, 1243, 1036  $\text{cm}^{-1}$ .

**HRMS** (ESI+):  $m/z$  calc'd for  $(\text{M} + \text{NH}_4)^+ [\text{C}_{19}\text{H}_{26}\text{O}_3 + \text{NH}_4]^+$ : 320.2220, found 320.2224.



**Cycloadduct 4-26.** Prepared according to the *General Procedure* using alkene **4-108** (58.4 mg, 0.250 mmol), 2,3-dimethyl-1,3-butadiene (**4-7**) (0.281 mL, 2.50 mmol),  $[\text{Cr}(\text{Ph}_2\text{phen})_3](\text{BF}_4)_3$  (3.3 mg, 0.00250 mmol), and 2.50 mL nitromethane. The reaction was irradiated for 40 h in a capped 2-dram vial. The crude product was purified by flash chromatography (100% hexanes $\rightarrow$ 9:1 hexanes/EtOAc eluent) to afford cycloadduct **4-26** (58.7 mg, 75% yield) as a colorless oil.

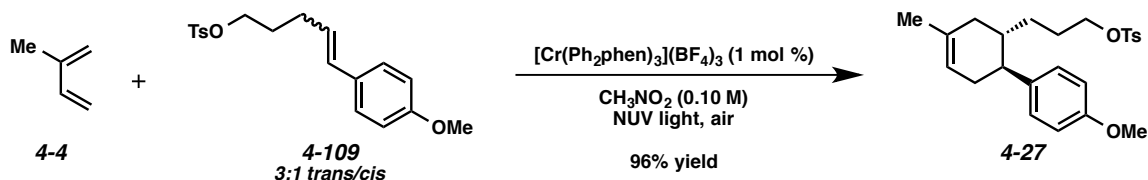
**TLC:**  $R_f = 0.52$  in 4:1 hexanes/EtOAc, visualized by UV.

**<sup>1</sup>H NMR** (400 MHz; CDCl<sub>3</sub>): δ 7.06 (d, *J* = 8.7 Hz, 2H), 6.83 (d, *J* = 8.7 Hz, 2H), 3.93 (ddd, *J* = 11.0, 7.5, 6.4 Hz, 2H), 3.79 (s, 3H), 2.46-2.40 (m, 1H), 2.15-2.12 (m, 2H), 1.96 (s, 3H), 1.80-1.76 (m, 2H), 1.63 (comp. m, 8H), 1.49-1.38 (m, 1H), 1.28-1.19 (m, 1H), 0.98-0.88 (m, 1H).

**<sup>13</sup>C NMR** (100 MHz; CDCl<sub>3</sub>): δ 171.1, 157.8, 137.7, 128.4, 125.4, 124.8, 113.8, 64.6, 55.2, 46.2, 41.7, 38.4, 38.1, 29.9, 25.6, 20.9, 18.8, 18.6.

**IR** (ATR, neat): 2908, 2833, 1736, 1611, 1512, 1453, 1365, 1242, 1177, 1035 cm<sup>-1</sup>.

**HRMS** (ESI<sup>+</sup>): *m/z* calc'd for (M + H)<sup>+</sup> [C<sub>20</sub>H<sub>28</sub>O<sub>3</sub> + H]<sup>+</sup>: 317.2111, found 317.2123.



**Cycloadduct 4-27.** Prepared according to the *General Procedure* using alkene **4-109** (20.5 mg, 60.0 μmol), isoprene (**4-4**) (60.1 μL, 600 μmol), [Cr(Ph<sub>2</sub>phen)<sub>3</sub>](BF<sub>4</sub>)<sub>3</sub> (0.8 mg, 0.600 μmol), and nitromethane (0.600 mL). The reaction was irradiated for 40 h. The crude product was purified by flash chromatography (100% hexanes→9:1 hexanes/EtOAc eluent) to afford cycloadduct **4-27** (19.0 mg, 96% yield) as a colorless oil.

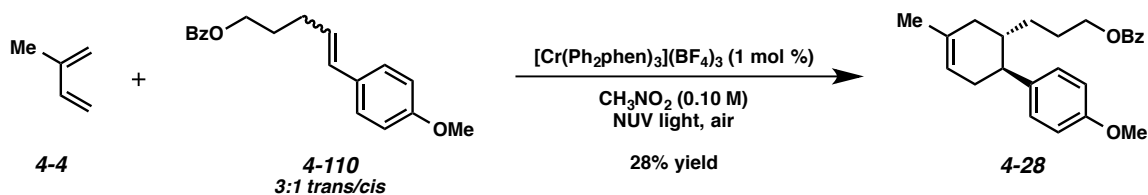
**TLC:** R<sub>f</sub> = 0.44 in 4:1 hexanes/EtOAc, stained blue with *p*-anisaldehyde.

**<sup>1</sup>H NMR** (400 MHz; CDCl<sub>3</sub>): δ 7.70 (d, *J* = 8.5 Hz, 2H), 7.30 (d, *J* = 8.5 Hz, 2H), 7.01 (d, *J* = 8.7 Hz, 2H), 6.82 (d, *J* = 8.7 Hz, 2H), 5.43 (br s, 1H), 3.86 (ddt, *J* = 10.1, 6.7, 3.4 Hz, 2H), 3.79 (s, 3H), 2.44 (s, 3H), 2.37-2.31 (m, 1H), 2.21-2.11 (comp. m, 3H), 1.76-1.62 (comp. m, 5H), 1.49-1.38 (m, 1H), 1.24-1.28 (m, 1H), 1.21-1.12 (m, 1H), 0.95-0.85 (m, 1H).

**<sup>13</sup>C NMR** (100 MHz; CDCl<sub>3</sub>): δ 157.8, 144.5, 137.5, 133.2, 133.1, 129.7, 128.4, 127.8, 120.8, 113.8, 70.8, 55.2, 45.2, 38.0, 36.3, 35.0, 29.7, 25.9, 23.4, 21.6.

**IR** (ATR, neat): 2957, 2908, 2836, 1611, 1512, 1442, 1357, 1265, 1246, 1176, 1035 cm<sup>-1</sup>.

**HRMS** (ESI+):  $m/z$  calc'd for  $(M + H)^+$   $[C_{24}H_{30}O_4S + H]^+$ : 415.1938, found 415.1936.



**Cycloadduct 4-28.** Prepared according to the *General Procedure* using alkene **4-110** (17.3 mg, 58.4  $\mu$ mol), isoprene (**4-4**) (60.1  $\mu$ L, 600  $\mu$ mol),  $[Cr(Ph_2phen)_3](BF_4)_3$  (0.8 mg, 0.600  $\mu$ mol), and nitromethane (0.600 mL). The reaction was irradiated for 48 h. The crude product was purified by flash chromatography (100% hexanes $\rightarrow$ 9:1 hexanes/EtOAc eluent) to afford cycloadduct **4-28** (5.9 mg, 28% yield) as a colorless oil.

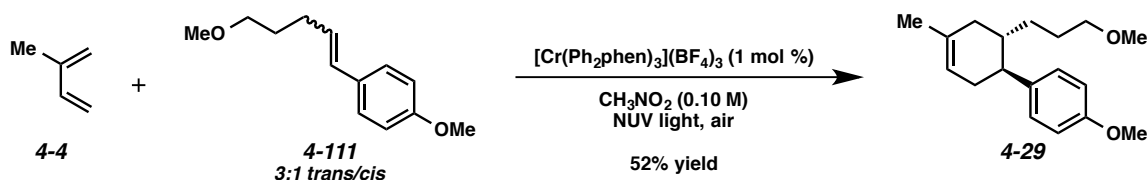
**TLC:**  $R_f$  = 0.65 in 4:1 hexanes/EtOAc, stained blue with *p*-anisaldehyde.

**$^1H$  NMR** (400 MHz;  $CDCl_3$ ):  $\delta$  7.90 (d,  $J$  = 8.4 Hz, 2H), 7.55-7.52 (m, 1H), 7.43-7.39 (m, 2H), 7.07 (d,  $J$  = 8.7 Hz, 2H), 6.80 (d,  $J$  = 8.7 Hz, 2H), 5.45 (br s, 1H), 4.17 (t,  $J$  = 6.6 Hz, 2H), 3.76 (s, 3H), 2.43 (td,  $J$  = 10.3, 5.6 Hz, 1H), 2.20-2.15 (comp. m, 3H), 1.89-1.76 (comp. m, 3H), 1.70 (s, 3H), 1.62-1.56 (m, 1H), 1.43-1.35 (m, 1H), 1.10-1.03 (m, 1H).

**$^{13}C$  NMR** (100 MHz;  $CDCl_3$ ):  $\delta$  202.5, 157.8, 137.7, 133.3, 132.7, 130.5, 129.5, 128.5, 128.2, 120.8, 113.8, 64.9, 55.1, 45.3, 38.1, 36.4, 35.2, 30.1, 25.5, 23.5.

**IR** (ATR, neat): 2958, 2908, 2836, 1790, 1715, 1610, 1512, 1451, 1273, 1246, 1176, 1111, 1036  $cm^{-1}$ .

**HRMS** (ESI+):  $m/z$  calc'd for  $(M + H)^+$   $[C_{24}H_{28}O_3 + H]^+$ : 365.2111, found 365.2099.



**Cycloadduct 4-29.** Prepared according to the *General Procedure* using alkene **4-111** (12.5 mg, 60.0  $\mu\text{mol}$ ), isoprene (**4-4**) (60.1  $\mu\text{L}$ , 600  $\mu\text{mol}$ ),  $[\text{Cr}(\text{Ph}_2\text{phen})_3](\text{BF}_4)_3$  (0.8 mg, 0.600  $\mu\text{mol}$ ), and nitromethane (0.600 mL). Prior to irradiation,  $\text{O}_2$  was bubbled through the reaction mixture for 30 s with a balloon and needle outlet. The reaction vessel was then sealed and the reaction was irradiated for 42 h. The crude product was purified by flash chromatography (100% hexanes $\rightarrow$ 9:1 hexanes/EtOAc eluent) to afford cycloadduct **4-29** (8.6 mg, 52% yield) as a colorless oil.

**TLC:**  $R_f = 0.61$  in 4:1 hexanes/EtOAc, stained blue with *p*-anisaldehyde.

**$^1\text{H}$  NMR** (400 MHz;  $\text{CDCl}_3$ ):  $\delta$  7.07 (d,  $J = 8.7$  Hz, 2H), 6.83 (d,  $J = 8.7$  Hz, 2H), 5.43 (s, 1H), 3.79 (s, 3H), 3.25 (s, 3H), 3.23-3.17 (m, 2H), 2.44-2.37 (m, 1H), 2.21-2.11 (comp. m, 3H), 1.83-1.74 (m, 2H), 1.69 (s, 3H), 1.64-1.56 (m, 1H), 1.43-1.33 (m, 1H), 1.27-1.18 (m, 1H), 1.00-0.91 (m, 1H).

**$^{13}\text{C}$  NMR** (100 MHz;  $\text{CDCl}_3$ ):  $\delta$  157.7, 138.0, 133.5, 128.5, 120.7, 113.7, 113.5, 73.1, 58.4, 55.2, 45.3, 38.4, 36.4, 35.1, 30.4, 26.5, 23.5.

**IR** (ATR, neat): 2919, 2853, 1610, 1511, 1452, 1245, 1176, 1116, 1036  $\text{cm}^{-1}$ .

**HRMS** (ESI+):  $m/z$  calc'd for  $(\text{M} + \text{NH}_4)^+ [\text{C}_{18}\text{H}_{26}\text{O}_2 + \text{NH}_4]^+$ : 292.2271, found 292.2267.

### 4.9.3 Evaluation of Light Sources

Reactions were prepared according to the *General Procedure for the radical cation accelerated [4+2] cycloadditions* using *trans*-anethole (**4-3**) (14.8 mg, 0.100 mmol), isoprene (**4-4**) (0.100 mL, 1.00 mmol),  $[\text{Cr}(\text{Ph}_2\text{phen})_3](\text{BF}_4)_3$  (1.3 mg, 0.00100 mmol), and nitromethane (1.00 mL). The reaction was irradiated for the indicated time with the specified light source (Scheme 4.7). The crude product was analyzed by  $^1\text{H}$  NMR to determine the starting material/product ratio. The reaction irradiated with sunlight was performed by stirring the reaction mixture next to a window on a sunny day. Window glass has an effective transmittance of  $>310$  nm, which is similar to that of Pyrex glass ( $>280$  nm).<sup>56</sup>

## Other Cycloadditions with Visible Light

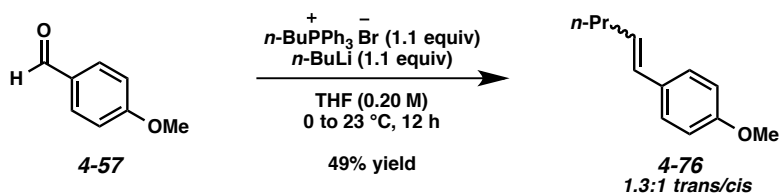
Reactions were prepared according to the *General Procedure for the radical cation accelerated [4+2] cycloaddition* was followed, except the reaction was irradiated with a 23 W compact fluorescent light bulb in a closed cardboard box completely lined with aluminum foil. Reaction times and yields are shown below.

**4-21:** 44 h, 50% yield

**4-25:** 44 h, 41% yield

### 4.9.4 Synthesis of Alkenes

**General Notes:** All reactions were performed in flame-dried glassware under argon. Aldehydes were used directly from commercial sources with no further purification. Ethyltriphenylphosphonium bromide was dried under vacuum for several hours prior to use. Alkene isomer ratios were determined by <sup>1</sup>H NMR. Unless otherwise noted, the reported NMR values are those of the major alkene isomer.



**Alkene 4-76.** To a suspension of *n*-butyltriphenylphosphonium bromide (2.20 g, 5.50 mmol) in THF (25.0 mL) at 0 °C in a flame-dried flask under argon was added *n*-BuLi (2.36 mL, 2.33 M in hexanes, 5.50 mmol). The mixture was allowed to warm to ambient temperature. After 1 h, *p*-anisaldehyde (**4-57**) (0.608 mL, 5.00 mmol) was added and the mixture was stirred an additional 14 h. The reaction mixture was then quenched with sat. aq. NH<sub>4</sub>Cl (25 mL) and extracted with Et<sub>2</sub>O (3 x 20 mL). The combined

organic layers were washed with brine (50 mL) and dried over MgSO<sub>4</sub>. The solvent was removed by rotary evaporation and the crude product was purified by flash chromatography (100% hexanes→9:1 hexanes/EtOAc eluent) to afford alkene **4-76** (0.431 g, 49% yield, 1.3:1 trans/cis) as a colorless oil.

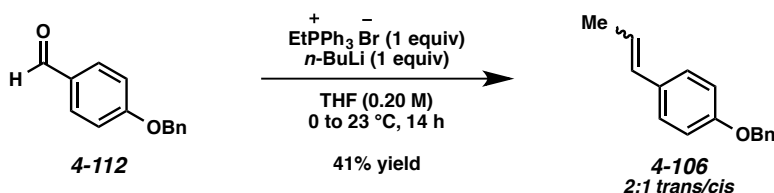
**TLC:** R<sub>f</sub> = 0.72 in 4:1 hexanes/EtOAc.

**<sup>1</sup>H NMR** (400 MHz; CDCl<sub>3</sub>): **trans isomer:** δ 7.28 (d, *J* = 8.7 Hz, 2H), 6.83 (d, *J* = 8.7 Hz, 2H), 6.34 (dd, *J* = 13.7, 9.4 Hz, 1H), 6.08 (dt, *J* = 15.8, 6.9 Hz, 1H), 3.80 (s, 3H), 2.19-2.13 (m, 2H), 1.47 (dtq, *J* = 11.1, 7.4, 3.7 Hz, 2H), 0.94 (td, *J* = 7.4, 2.3 Hz, 3H). **cis isomer:** δ 7.22 (d, *J* = 8.7 Hz, 2H), 6.87 (d, *J* = 8.7 Hz, 2H), 6.34 (dd, *J* = 13.7, 9.4 Hz, 1H), 5.57 (dt, *J* = 11.6, 7.2 Hz, 1H), 3.81 (s, 3H), 2.30 (qd, *J* = 7.4, 1.8 Hz, 2H), 1.47 (dtd, *J* = 14.8, 7.4, 2.6 Hz, 2H), 0.94 (td, *J* = 7.4, 2.3 Hz, 3H).

**<sup>13</sup>C NMR** (100 MHz; CDCl<sub>3</sub>): δ 131.4, 129.9, 129.2, 128.8, 128.2, 126.9, 113.9, 113.5, 55.3, 55.2, 35.1, 30.7, 23.2, 22.7, 13.9, 13.7.

**IR** (ATR, neat): 2958, 2931, 2836, 1608, 1510, 1464, 1244, 1174, 1035, 965 cm<sup>-1</sup>.

**HRMS** (ESI+): *m/z* calc'd for (M + H)<sup>+</sup> [C<sub>12</sub>H<sub>16</sub>O + H]<sup>+</sup>: 177.1274, found 177.1278.

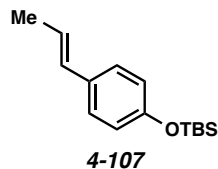


**Alkene 4-106.** To a suspension of ethyltriphenylphosphonium bromide (0.371 g, 1.00 mmol) in THF (5.00 mL) at 0 °C in a flame-dried flask under argon was added *n*-BuLi (0.630 mL, 1.6 M in hexanes, 1.00 mmol). The mixture was allowed to warm to ambient temperature. After 1 h, 4-benzyloxybenzaldehyde (**4-112**) (0.212 g, 1.00 mmol) was added and the mixture was stirred for an additional 14 h. The reaction mixture was then quenched with sat. aq. NH<sub>4</sub>Cl (10 mL) and extracted with Et<sub>2</sub>O (3 x 10 mL). The combined organic layers were washed with brine (20 mL) and dried over MgSO<sub>4</sub>. The solvent was removed by rotary evaporation and the crude product was purified by flash

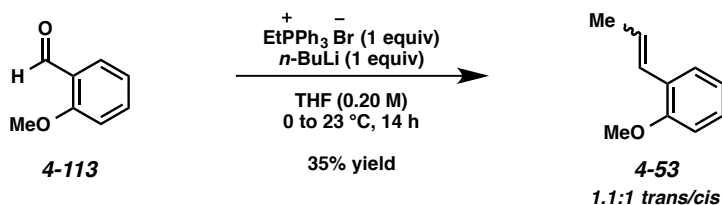
chromatography (100% hexanes→15:1 hexanes/EtOAc eluent) to afford alkene **4-106** (92.4 mg, 41% yield, 2:1 trans/cis) as a white solid.

**TLC:**  $R_f = 0.69$  in 4:1 hexanes/EtOAc, stained with  $\text{KMnO}_4$ .

All spectroscopic data were consistent with previously reported values.<sup>53a</sup>



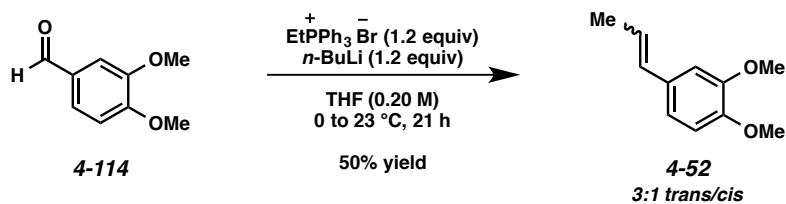
**Alkene 4-107.** Prepared according to the procedure by Yoon and coworkers.<sup>12</sup>



**Alkene 4-53.** To a suspension of ethyltriphenylphosphonium bromide (0.371 g, 1.00 mmol) in THF (5.00 mL) at 0 °C in a flame-dried flask under argon was added *n*-BuLi (0.630 mL, 1.6 M in hexanes, 1.00 mmol). The mixture was allowed to warm to ambient temperature. After 1 h, *ortho*-anisaldehyde (**4-113**) (120  $\mu\text{L}$ , 1.00 mmol) was added and the mixture was stirred an additional 14 h. The reaction mixture was then quenched with sat. aq.  $\text{NH}_4\text{Cl}$  (10 mL) and extracted with  $\text{Et}_2\text{O}$  (3 x 10 mL). The combined organic layers were washed with brine (20 mL) and dried over  $\text{MgSO}_4$ . The solvent was removed by rotary evaporation and the crude product was purified by flash chromatography (100% hexanes→15:1 hexanes/EtOAc eluent) to afford alkene **4-53** (37.5 mg, 25% yield, 1.1:1 trans/cis) as a colorless oil.

**TLC:**  $R_f = 0.64$  in 4:1 hexanes/EtOAc, stained with  $\text{KMnO}_4$ .

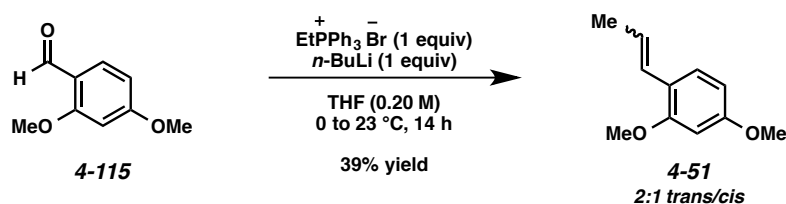
All spectroscopic data were consistent with previously reported values.<sup>12</sup>



**Alkene 4-52.** To a suspension of ethyltriphenylphosphonium bromide (0.891 g, 2.40 mmol) in THF (10.0 mL) at 0 °C in a flame-dried flask under argon was added  $n\text{-BuLi}$  (1.78 mL, 1.35 M in hexanes, 2.40 mmol). The mixture was allowed to warm to ambient temperature. After 1 h, 3,4-dimethoxybenzaldehyde (**4-114**) (0.332 g, 2.00 mmol) was added and the mixture was stirred an additional 21 h. The reaction mixture was then quenched with sat. aq.  $\text{NH}_4\text{Cl}$  (15 mL) and extracted with  $\text{Et}_2\text{O}$  (3 x 15 mL). The combined organic layers were washed with brine (30 mL) and dried over  $\text{MgSO}_4$ . The solvent was removed by rotary evaporation and the crude product was purified by flash chromatography (100% hexanes→9:1 hexanes/ $\text{EtOAc}$  eluent) to afford alkene **4-52** (0.178 g, 50% yield, 3:1 trans/cis) as a colorless oil.

**TLC:**  $R_f = 0.50$  in 4:1 hexanes/ $\text{EtOAc}$ , stained red with  $p$ -anisaldehyde.

All spectroscopic data were consistent with previously reported values.<sup>57</sup>



**Alkene 4-51.** To a suspension of ethyltriphenylphosphonium bromide (0.371 g, 1.00 mmol) in THF (5.00 mL) at 0 °C in a flame-dried flask under argon was added  $n\text{-BuLi}$  (0.630 mL, 1.6 M in hexanes, 1.00 mmol). The mixture was allowed to warm to ambient temperature. After 1 h, 2,4-dimethoxybenzaldehyde (**4-115**) (0.166 g, 1.00 mmol) was added and the mixture was stirred an additional 14 h. The reaction mixture was then quenched with sat. aq.  $\text{NH}_4\text{Cl}$  (10 mL) and extracted with  $\text{Et}_2\text{O}$  (3 x 10 mL). The

combined organic layers were washed with brine (20 mL) and dried over MgSO<sub>4</sub>. The solvent was removed by rotary evaporation and the crude product was purified by flash chromatography (100% hexanes→15:1 hexanes/EtOAc eluent) to afford alkene **4-51** (70.2 mg, 39% yield, 2:1 trans/cis) as a colorless oil.

**TLC:** R<sub>f</sub> = 0.64 in 4:1 hexanes/EtOAc, stained red/purple with *p*-anisaldehyde.

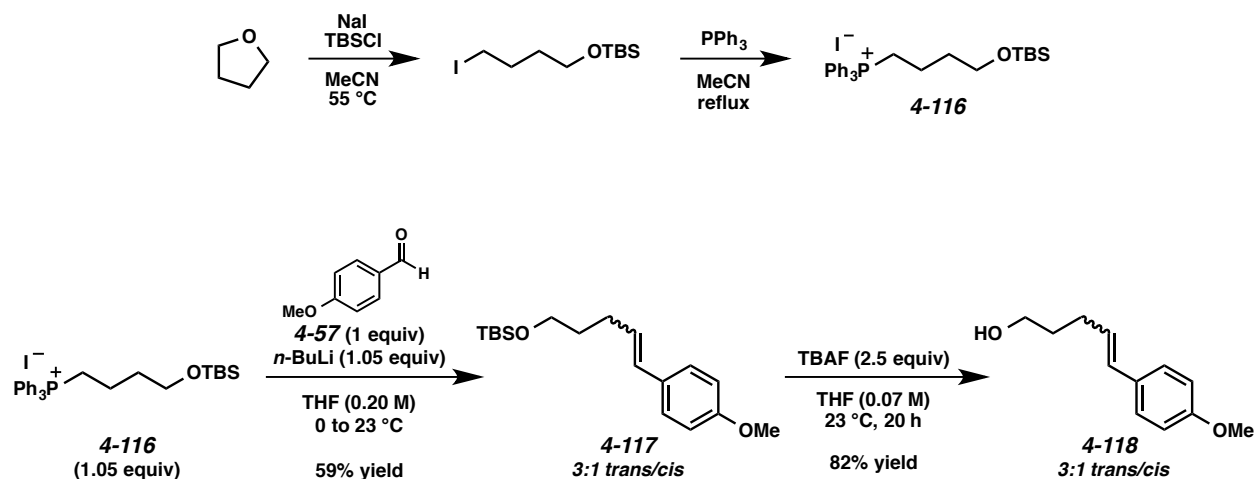
**<sup>1</sup>H NMR** (400 MHz; CDCl<sub>3</sub>): δ 7.29 (d, *J* = 8.3 Hz, 1H), 6.61 (dd, *J* = 15.9, 1.7 Hz, 1H), 6.48-6.43 (m, 2H), 6.10 (dq, *J* = 15.8, 6.6 Hz, 1H), 3.82 (s, 6H), 1.87 (dd, *J* = 6.6, 1.7 Hz, 3H).

**<sup>13</sup>C NMR** (100 MHz; CDCl<sub>3</sub>): δ 159.7, 130.4, 127.0, 125.6, 125.2, 124.7, 124.4, 120.2, 104.7, 103.7, 98.4, 98.3, 55.4, 55.3, 18.8 (*trans*), 14.6 (*cis*).

**IR** (ATR, neat): 3053, 2838, 1608, 1503, 1465, 1264, 1208, 1158, 1034 cm<sup>-1</sup>.

**HRMS** (ESI<sup>+</sup>): *m/z* calc'd for (M + H)<sup>+</sup> [C<sub>11</sub>H<sub>14</sub>O<sub>2</sub> + H]<sup>+</sup>: 179.1067, found 179.1066.

Alkenes **4-108–4-111** were synthesized from alcohol **4-118**. The synthesis of alcohol **4-118** was accomplished according to the following scheme. The synthesis of phosphonium salt **4-116** was carried out according to literature procedures.<sup>58,59</sup>



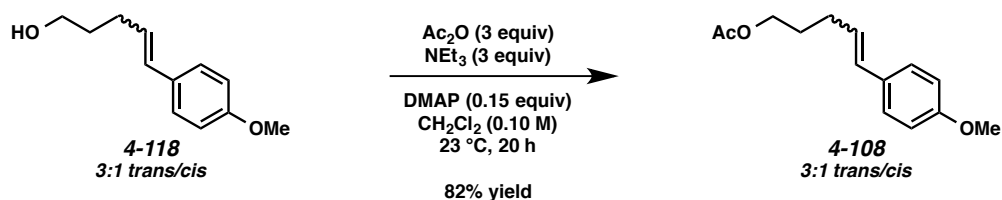
**TBS-ether 4-117.** To a suspension of phosphonium salt **4-116** (4.39 g, 7.61 mmol) in THF (36.0 mL) at 0 °C in a flame-dried flask under argon was added *n*-BuLi (3.27 mL, 2.33 M in hexanes, 7.61 mmol). The mixture was allowed to warm to ambient temperature. After 1 h, *p*-anisaldehyde (**4-57**) (0.880 mL, 7.25 mmol) was added and the mixture was stirred an additional 14 h. The reaction mixture was then quenched with sat. aq. NH<sub>4</sub>Cl (25 mL) and extracted with Et<sub>2</sub>O (3 x 20 mL). The combined organic layers were washed with brine (50 mL) and dried over MgSO<sub>4</sub>. The solvent was removed by rotary evaporation and the crude product was purified by flash chromatography (100% hexanes→9:1 hexanes/EtOAc eluent) to afford TBS-ether **4-117** (1.31 g, 59% yield, 3:1 trans/cis) as a colorless oil.

**TLC:** R<sub>f</sub> = 0.69 in 4:1 hexanes/EtOAc, stained yellow with *p*-anisaldehyde.

**Alcohol 4-118.** To a solution of TBS-ether **4-117** (1.31 g, 4.27 mmol) in THF (61.0 mL) was added TBAF (10.7 mL, 1.0 M in THF, 10.7 mmol). The reaction was stirred for 20 h at ambient temperature, then quenched with sat. aq. NH<sub>4</sub>Cl (50 mL) and extracted with EtOAc (3 x 50 mL). The combined organic layers were washed with brine (100 mL) and dried over MgSO<sub>4</sub>. The solvent was removed by rotary evaporation and the crude product was purified by flash chromatography (100% hexanes→1:1 hexanes/EtOAc eluent) to afford alcohol **4-118** (0.672 g, 82% yield, 3:1 trans/cis) as a white solid.

**TLC:** R<sub>f</sub> = 0.53 in 1:1 hexanes/EtOAc.

All spectroscopic data were consistent with previously reported values.<sup>31</sup>



**Acetate 4-108.** To a solution of alcohol **4-118** (96.5 mg, 0.502 mmol), Et<sub>3</sub>N (0.210 mL, 1.51 mmol), and DMAP (9.2 mg, 75.3 μmol) in CH<sub>2</sub>Cl<sub>2</sub> (5.00 mL) was added Ac<sub>2</sub>O (0.140 mL, 1.48 mmol). The reaction was stirred at ambient temperature for 20 h then quenched with sat. aq. NH<sub>4</sub>Cl (10 mL) and extracted with

CH<sub>2</sub>Cl<sub>2</sub> (3 x 10 mL). The combined organic layers were washed with brine (30 mL) and dried over MgSO<sub>4</sub>. The solvent was removed by rotary evaporation and the crude product was purified by flash chromatography (100% hexanes→9:1 hexanes/EtOAc eluent) to afford acetate **4-108** (95.7 mg, 82% yield, 3:1 trans/cis) as a colorless oil.

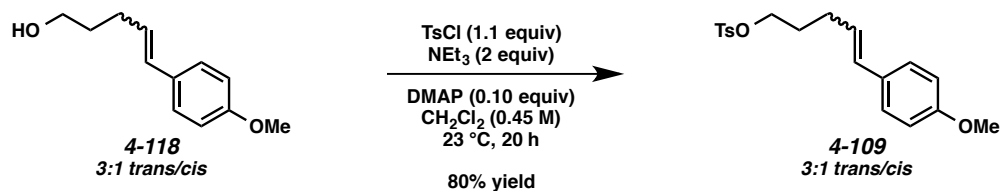
**TLC:** R<sub>f</sub> = 0.42 in 4:1 hexanes/EtOAc, stained with KMnO<sub>4</sub>.

**<sup>1</sup>H NMR** (400 MHz; CDCl<sub>3</sub>): δ 7.27 (d, *J* = 8.7 Hz, 2H), 6.84 (d, *J* = 8.7 Hz, 2H), 6.35 (d, *J* = 15.8 Hz, 1H), 6.05 (dt, *J* = 15.8, 6.9 Hz, 1H), 4.10 (dt, *J* = 13.1, 6.6 Hz, 2H), 3.80 (s, 3H), 2.29-2.23 (m, 2H), 2.05 (s, 3H), 1.79 (dq, *J* = 14.4, 7.2 Hz, 2H).

**<sup>13</sup>C NMR** (100 MHz; CDCl<sub>3</sub>): δ 171.2, 130.4, 130.0, 129.9, 129.2, 127.0, 113.9, 64.0, 55.3, 29.3, 28.4, 21.0.

**IR** (ATR, neat): 3055, 2957, 2838, 1733, 1607, 1511, 1465, 1366, 1243, 1175, 1035 cm<sup>-1</sup>.

**HRMS** (ESI<sup>+</sup>): *m/z* calc'd for (M + H)<sup>+</sup> [C<sub>14</sub>H<sub>18</sub>O<sub>3</sub> + H]<sup>+</sup>: 235.1329, found 235.1334.



**Tosylate 4-109.** To a solution of alcohol **4-118** (96.0 mg, 0.499 mmol), Et<sub>3</sub>N (0.140 mL, 0.997 mmol), and DMAP (6.1 mg, 49.9 μmol) in CH<sub>2</sub>Cl<sub>2</sub> (1.1 mL) was added TsCl (0.105 g, 0.551 mmol). The reaction was stirred at ambient temperature for 20 h then quenched with sat. aq. NH<sub>4</sub>Cl (3 mL) and extracted with CH<sub>2</sub>Cl<sub>2</sub> (3 x 5 mL). The combined organic layers were washed with brine (20 mL) and dried over MgSO<sub>4</sub>. The solvent was removed by rotary evaporation and the crude product was purified by flash chromatography (100% hexanes→9:1 hexanes/EtOAc eluent) to afford tosylate **4-109** (0.139 g, 80% yield, 3:1 trans/cis) as a colorless oil.

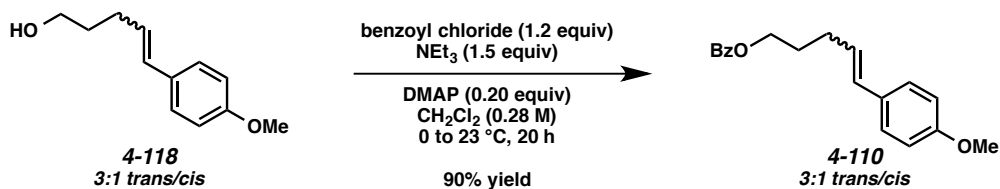
**TLC:** R<sub>f</sub> = 0.30 in 4:1 hexanes/EtOAc, stained with KMnO<sub>4</sub>.

**<sup>1</sup>H NMR** (400 MHz; CDCl<sub>3</sub>): δ 7.79 (d, *J* = 8.3 Hz, 2H), 7.32 (d, *J* = 8.3 Hz, 2H), 7.20 (d, *J* = 8.7 Hz, 2H), 6.82 (d, *J* = 8.7 Hz, 2H), 6.25 (d, *J* = 15.8 Hz, 1H), 5.90 (dt, *J* = 15.8, 7.0 Hz, 1H), 4.09-4.05 (m, 2H), 3.80 (s, 3H), 2.43 (s, 3H), 2.25-2.19 (m, 2H), 1.81 (dt, *J* = 13.9, 6.9 Hz, 2H).

**<sup>13</sup>C NMR** (100 MHz; CDCl<sub>3</sub>): δ 158.8, 144.6, 130.6, 130.1, 129.9, 129.8, 127.9, 127.8, 127.1, 126.1, 113.9, 113.6, 69.7, 55.3, 29.1, 28.6, 21.6.

**IR** (ATR, neat): 3055, 2957, 2838, 1607, 1511, 1357, 1247, 1174, 1034, 965, 925 cm<sup>-1</sup>.

**HRMS** (ESI<sup>+</sup>): *m/z* calc'd for (M + NH<sub>4</sub>)<sup>+</sup> [C<sub>19</sub>H<sub>22</sub>O<sub>4</sub>S + NH<sub>4</sub>]<sup>+</sup>: 364.1577, found 364.1574.



**Benzoate 4-110.** To a suspension of alcohol **4-118** (96.9 mg, 0.504 mmol), Et<sub>3</sub>N (104 μL, 0.750 mmol), and DMAP (12.2 mg, 99.9 μmol) in CH<sub>2</sub>Cl<sub>2</sub> (1.80 mL) was added benzoyl chloride (69.7 μL, 0.600 mmol). The reaction was stirred at ambient temperature for 20 h, then quenched with brine (5 mL) and extracted with CH<sub>2</sub>Cl<sub>2</sub> (3 x 5 mL). The combined organic layers were washed with brine (20 mL) and dried over Na<sub>2</sub>SO<sub>4</sub>. The solvent was removed by rotary evaporation and the crude product was purified by flash chromatography (100% hexanes→9:1 hexanes/EtOAc eluent) to afford benzoate **4-110** (0.133 g, 90% yield, 3:1 *trans/cis*) as a colorless oil.

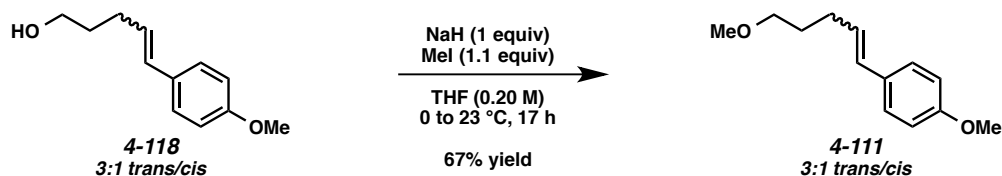
**TLC:** R<sub>f</sub> = 0.56 in 4:1 hexanes/EtOAc, visualized by UV.

**<sup>1</sup>H NMR** (400 MHz; CDCl<sub>3</sub>): δ 8.05 (dd, *J* = 8.1, 1.0 Hz, 2H), 7.45-7.40 (comp. m, 3H), 7.28 (d, *J* = 8.7 Hz, 2H), 6.83 (d, *J* = 8.7 Hz, 2H), 6.39 (d, *J* = 15.8 Hz, 1H), 6.10 (dt, *J* = 15.8, 6.9 Hz, 1H), 4.36 (dt, *J* = 14.8, 6.5 Hz, 2H), 3.80 (s, 3H), 2.40-2.34 (m, 2H), 1.97-1.89 (m, 2H).

**<sup>13</sup>C NMR** (100 MHz; CDCl<sub>3</sub>): δ 201.6, 132.8, 130.6, 130.1, 129.9, 129.5, 128.3, 127.2, 127.1, 113.9, 113.6, 64.5, 29.5, 28.6, 25.0.

**IR** (ATR, neat): 2954, 2836, 1788, 1715, 1606, 1510, 1451, 1271, 1245, 1174, 1112, 1027  $\text{cm}^{-1}$ .

**HRMS** (ESI+):  $m/z$  calc'd for  $(M + H)^+$  [ $\text{C}_{19}\text{H}_{20}\text{O}_3 + \text{H}$ ] $^+$ : 297.1485, found 297.1491.



**Methyl ether 4-111.** To a solution of alcohol **4-118** (96.3 mg, 0.500 mmol) in THF (2.50 mL) at 0 °C was added NaH (20.0 mg, 60% dispersion in mineral oil, 0.500 mmol). The reaction was allowed to warm to ambient temperature and stirred for 2 h. MeI (34.0  $\mu\text{L}$ , 0.550 mmol) was then added dropwise and the reaction was stirred for an additional 17 h. The reaction was quenched with sat. aq.  $\text{NH}_4\text{Cl}$  (5 mL) and extracted with  $\text{Et}_2\text{O}$  (3 x 5 mL). The combined organic layers were washed with brine (20 mL) and dried over  $\text{MgSO}_4$ . The solvent was removed by rotary evaporation and the crude product was purified by flash chromatography (100% hexanes  $\rightarrow$  20:1 hexanes/ $\text{EtOAc}$  eluent) to afford ether **4-111** (68.7 mg, 67% yield, 3:1 *trans/cis*) as a colorless oil.

**TLC:**  $R_f$  = 0.54 in 4:1 hexanes/ $\text{EtOAc}$ , visualized by UV.

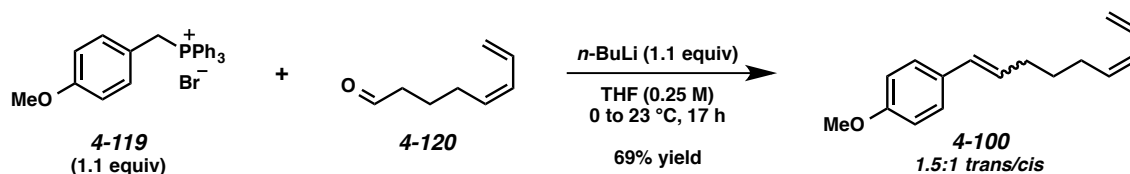
**$^1\text{H}$  NMR** (400 MHz;  $\text{CDCl}_3$ ):  $\delta$  7.28 (d,  $J$  = 8.7 Hz, 2H), 6.84 (d,  $J$  = 8.7 Hz, 2H), 6.34 (d,  $J$  = 15.8 Hz, 1H), 6.07 (dt,  $J$  = 15.8, 7.0 Hz, 1H), 3.80 (s, 3H), 3.42 (t,  $J$  = 6.6 Hz, 2H), 3.34 (s, 3H), 2.28-2.23 (m, 2H), 1.73 (dtd,  $J$  = 14.4, 7.0, 4.3 Hz, 2H).

**$^{13}\text{C}$  NMR** (100 MHz;  $\text{CDCl}_3$ ):  $\delta$  158.7, 130.6, 129.9, 128.0, 127.0, 113.9, 72.1, 58.6, 55.3, 29.4, 25.2.

**IR** (ATR, neat): 2933, 2835, 1607, 1510, 1463, 1245, 1175, 1116, 1034, 965  $\text{cm}^{-1}$ .

**HRMS** (ESI+):  $m/z$  calc'd for  $(M + H)^+$  [ $\text{C}_{13}\text{H}_{18}\text{O}_2 + \text{H}$ ] $^+$ : 207.1380, found 207.1383.

To synthesize triene **4-100**, Roush's procedure was followed to synthesize aldehyde **4-120**.<sup>60</sup> 4-Methoxybenzyltriphenylphosphonium bromide (**4-119**) was synthesized according to the procedure by Hierso and coworkers.<sup>61</sup>



**Triene 4-100.** To a suspension of 4-methoxybenzyltriphenylphosphonium bromide (**4-119**) (0.277 g, 0.598 mmol) in THF (2.20 mL) at 0 °C in a flame-dried flask under argon was added  $n\text{-BuLi}$  (0.260 mL, 2.33 M in hexanes, 0.598 mmol). The mixture was allowed to warm to ambient temperature. After 1 h, aldehyde **4-120** (67.0 mg, 0.540 mmol) was added and the mixture was stirred an additional 17 h. The reaction mixture was then quenched with sat. aq.  $\text{NH}_4\text{Cl}$  (5 mL) and extracted with  $\text{Et}_2\text{O}$  (3 x 5 mL). The combined organic layers were washed with brine (20 mL) and dried over  $\text{MgSO}_4$ . The solvent was removed by rotary evaporation and the crude product was purified by flash chromatography (100% hexanes→20:1 hexanes/EtOAc eluent) to afford triene **4-100** (86.1 mg, 69% yield, 1.5:1 *trans/cis*) as a colorless oil.

**TLC:**  $R_f$  = 0.70 in 4:1 hexanes/EtOAc, visualized by UV.

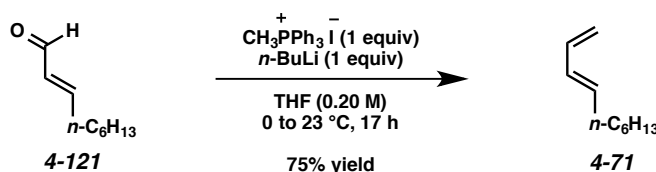
**$^1\text{H}$  NMR** (400 MHz;  $\text{CDCl}_3$ ): **trans isomer:**  $\delta$  7.27 (d,  $J$  = 8.7 Hz, 2H), 6.83 (d,  $J$  = 8.7 Hz, 2H), 6.37-6.24 (m, 2H), 6.10-5.99 (m, 1H), 5.76-5.65 (m, 1H), 5.56 (dt,  $J$  = 11.6, 7.3 Hz, 1H), 5.11-5.04 (m, 1H), 4.98-4.93 (m, 1H), 3.80 (s, 3H), 2.23-2.09 (comp. m, 4H), 1.58 (d,  $J$  = 7.4 Hz, 2H). **cis isomer:**  $\delta$  7.21 (*cis*, d,  $J$  = 8.7 Hz, 2H), 6.86 (*cis*, d,  $J$  = 8.7 Hz, 2H), 6.37-6.24 (m, 2H), 6.10-5.99 (m, 1H), 5.76-5.65 (m, 1H), 5.56 (dt,  $J$  = 11.6, 7.3 Hz, 1H), 5.11-5.04 (m, 1H), 4.98-4.93 (m, 1H), 3.81 (s, 3H), 2.33 (*cis*, qd,  $J$  = 7.4, 1.6 Hz, 2H), 2.23-2.09 (m, 2H), 1.58 (d,  $J$  = 7.4 Hz, 2H).

**$^{13}\text{C}$  NMR** (100 MHz;  $\text{CDCl}_3$ ):  $\delta$  135.0, 131.2, 130.7, 129.9, 129.4, 128.4, 127.0, 114.8, 113.9, 113.5, 55.3, 32.4, 32.0, 28.9.

**IR** (ATR, neat): 2930, 2837, 1688, 1607, 1511, 1463, 1246, 1175, 1033, 1005, 976  $\text{cm}^{-1}$ .

**HRMS** (ESI+):  $m/z$  calc'd for  $(M + H)^+$  [ $\text{C}_{16}\text{H}_{20}\text{O} + \text{H}$ ] $^+$ : 229.1587, found 229.1591.

#### 4.9.5 Synthesis of Dienes



**Diene 4-71.** To a suspension of methyltriphenylphosphonium iodide (1.62 g, 4.00 mmol) in THF (20.0 mL) at 0 °C in a flame-dried flask under argon was added  $n\text{-BuLi}$  (1.58 mL, 2.53 M in hexanes, 4.00 mmol). The yellow/orange mixture was allowed to warm to ambient temperature. After 1 h, *trans*-2-nonenal (**4-121**) (0.660 mL, 4.00 mmol) was added dropwise and the mixture was stirred an additional 17 h. The reaction mixture was then quenched with sat. aq.  $\text{NH}_4\text{Cl}$  (20 mL) and extracted with pentane (3 x 20 mL). The combined organic layers were washed with brine (50 mL) and dried over  $\text{MgSO}_4$ . The solvent was removed by rotary evaporation and the crude product was purified by flash chromatography (100% pentane eluent) to afford diene **4-71** (0.415 g, 75% yield) as a colorless oil.

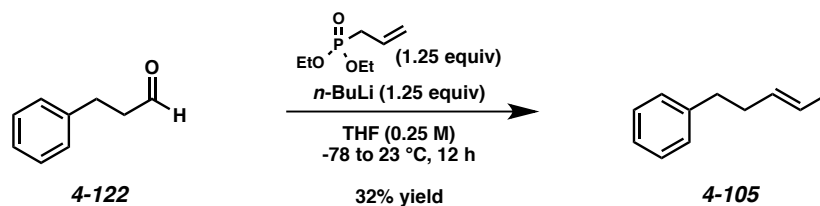
**TLC:**  $R_f$  = 0.85 in pentane, stained blue with *p*-anisaldehyde.

**$^1\text{H}$  NMR** (400 MHz;  $\text{CDCl}_3$ ):  $\delta$  6.31 (dt,  $J$  = 17.0, 10.3 Hz, 1H), 6.05 (dd,  $J$  = 15.2, 10.3 Hz, 1H), 5.71 (dt,  $J$  = 14.9, 7.3 Hz, 1H), 5.10 (d,  $J$  = 17.0 Hz, 1H), 4.95 (d,  $J$  = 10.1 Hz, 1H), 2.08 (q,  $J$  = 7.1 Hz, 2H), 1.40-1.37 (m, 2H), 1.29 (dq,  $J$  = 7.5, 2.4 Hz, 6H), 0.88 (t,  $J$  = 6.8 Hz, 3H).

**$^{13}\text{C}$  NMR** (100 MHz;  $\text{CDCl}_3$ ):  $\delta$  137.3, 135.6, 130.8, 114.5, 32.5, 31.7, 29.1, 28.9, 22.6, 14.1.

**IR** (ATR, neat): 2925, 2855, 1001, 949, 895  $\text{cm}^{-1}$ .

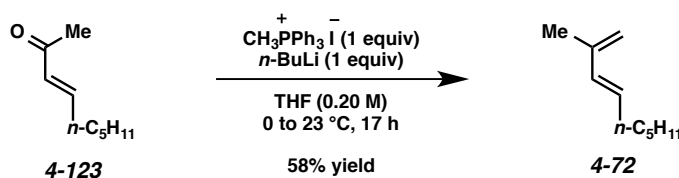
**HRMS** (ESI+):  $m/z$  calc'd for  $(M + \text{NH}_4)^+$  [ $\text{C}_{10}\text{H}_{18} + \text{NH}_4$ ] $^+$ : 156.1747, found 156.1752.



**Diene 4-105.** To a suspension of diethyl allylphosphonate (0.891 g, 5.00 mmol) in THF (16.0 mL) at -78 °C in a flame-dried flask under argon was added *n*-BuLi (2.23 mL, 2.24 M in hexanes, 5.00 mmol). The yellow/orange mixture was stirred at -78 °C for 1 h, at which time hydrocinnamaldehyde (**4-122**) (0.530 mL, 4.00 mmol) was added dropwise. The mixture was allowed to warm to ambient temperature and was stirred an additional 12 h. The reaction mixture was then quenched with sat. aq.  $\text{NH}_4\text{Cl}$  (20 mL) and extracted with diethyl ether (3 x 20 mL). The combined organic layers were washed with brine (50 mL) and dried over  $\text{MgSO}_4$ . The solvent was removed by rotary evaporation and the crude product was purified by flash chromatography (100% hexanes eluent) to afford diene **4-105** (0.165 g, 32% yield) as a colorless oil.

**TLC:**  $R_f = 0.31$  in hexanes, stained with  $\text{KMnO}_4$ .

All spectroscopic data were consistent with previously reported values.<sup>62</sup>



**Diene 4-72.** To a suspension of methyltriphenylphosphonium iodide (1.62 g, 4.00 mmol) in THF (20.0 mL) at 0 °C in a flame-dried flask under argon was added *n*-BuLi (1.58 mL, 2.53 M in hexanes, 4.00 mmol). The yellow/orange mixture was allowed to warm to ambient temperature. After 1 h, *trans*-3-nonen-2-one (**4-123**) (0.660 mL, 4.00 mmol) was added dropwise and the mixture was stirred an additional 17 h. The reaction mixture was then quenched with sat. aq.  $\text{NH}_4\text{Cl}$  (20 mL) and extracted with

pentane (3 x 20 mL). The combined organic layers were washed with brine (50 mL) and dried over MgSO<sub>4</sub>. The solvent was removed by rotary evaporation and the crude product was purified by flash chromatography (100% pentane eluent) to afford diene **4-72** (0.321 g, 58% yield) as a colorless oil.

**TLC:** R<sub>f</sub> = 0.81 in pentane, stained blue with *p*-anisaldehyde.

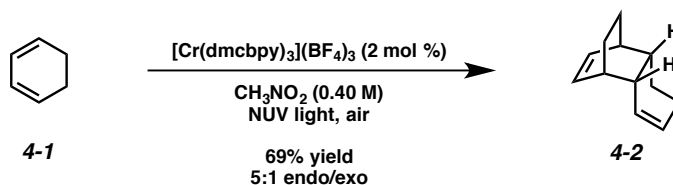
**<sup>1</sup>H NMR** (400 MHz; CDCl<sub>3</sub>): δ 6.13 (d, *J* = 15.6 Hz, 1H), 5.66 (dt, *J* = 15.6, 7.0 Hz, 1H), 4.86 (s, 2H), 2.13-2.07 (m, 2H), 1.83 (s, 3H), 1.40 (dt, *J* = 14.5, 7.2 Hz, 2H), 1.33-1.26 (comp. m, 4H), 0.89 (t, *J* = 6.9 Hz, 3H).

**<sup>13</sup>C NMR** (100 MHz; CDCl<sub>3</sub>): δ 142.2, 132.6, 131.1, 114.0, 32.7, 31.4, 29.1, 22.5, 18.7, 14.0.

**IR** (ATR, neat): 2957, 2924, 2856, 1609, 1455, 1378, 963, 880 cm<sup>-1</sup>.

**HRMS** (ESI+): *m/z* calc'd for (M + NH<sub>4</sub>)<sup>+</sup> [C<sub>10</sub>H<sub>18</sub> + NH<sub>4</sub>]<sup>+</sup>: 156.1747, found 156.1752.

#### 4.9.6 Dimerization of 1,3-Cyclohexadiene



**Dimer 4-2.** To 1,3-cyclohexadiene (**4-1**) (47.6 μL, 0.500 mmol) in nitromethane (1.25 mL) was added [Cr(dmcbpy)<sub>3</sub>](BF<sub>4</sub>)<sub>3</sub> (11.3 mg, 10.0 μmol). The vial was then capped and placed in the photoreactor equipped with 419, 350, and 300 nm light bulbs. The reaction was irradiated for 26 h, then diluted with H<sub>2</sub>O (5 mL) and transferred to a separatory funnel. The aqueous layer was extracted with pentane (3 x 5 mL) and the combined organic layers were washed with brine (15 mL), dried over Na<sub>2</sub>SO<sub>4</sub>, and filtered. The solvent was removed by rotary evaporation to afford dimer **4-2** (27.7 mg, 69% yield, 5:1 endo/exo) as a colorless oil.

**TLC:** R<sub>f</sub> = 0.88 in 9:1 hexanes/EtOAc, stained blue in *p*-anisaldehyde.

All spectroscopic data were consistent with previously reported values.<sup>63</sup>

### **GC yield determination for the [4+2] dimerization of cyclohexadiene**

In general, for the reactions in Table 4.1, 1,3-cyclohexadiene (31.8  $\mu\text{L}$ , 0.300 mmol, 1 equiv) was added to a solution of Cr complex (6.00  $\mu\text{mol}$ , 2 mol %) and tridecane (36.6  $\mu\text{L}$ , 0.150 mmol, 0.5 equiv) in nitromethane (750  $\mu\text{L}$ , 0.40 M) in a flame-dried 1-dram vial. The reaction was capped and irradiated with the reported light source for 24 or 48 h with stirring. The reaction was then diluted to approximately 10 times its volume with  $\text{CH}_2\text{Cl}_2$  and this sample was directly analyzed by GC. Any modifications to this procedure are described in Table 4.1.

#### **GC Method**

40  $^\circ\text{C}$  for 4 min, increase to 120  $^\circ\text{C}$  (40  $^\circ\text{C}$  per min) for 9 min (15 min total).

#### **GC Column**

Fused silica column, cat. # 220-94536-01, phase SHR5XLB, dimensions L 30 m, ID 0.25 micron, DF 0.25 micron

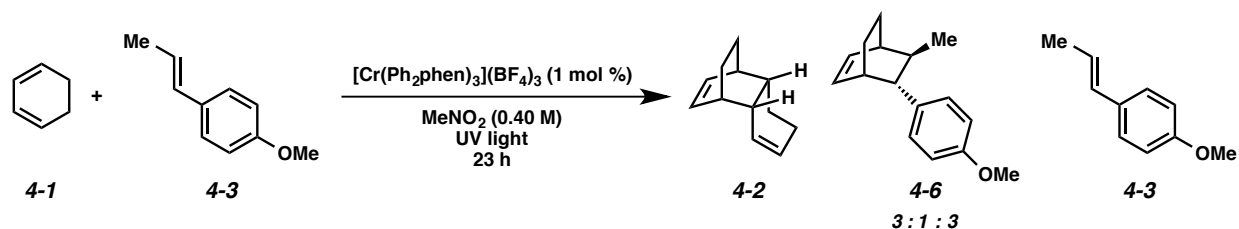
#### **Light sources**

Irradiation with NUV light was performed by running the reactions in a Rayonet photoreactor equipped with light bulbs of wavelengths 300, 350, and 419 nm.

Reactions in the dark were performed by wrapping the reaction vessel in aluminum foil.

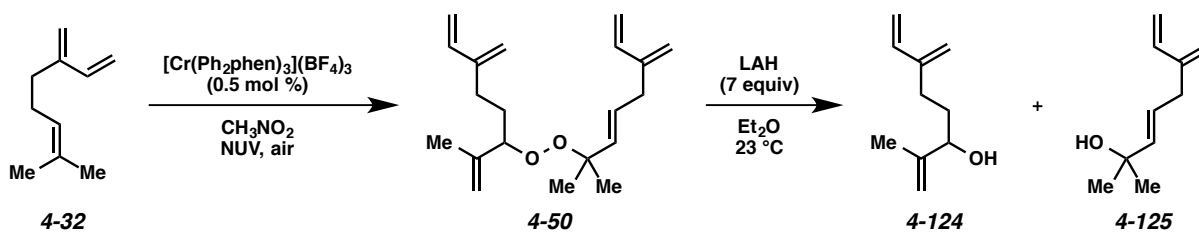
Reactions with visible light were performed by running the reactions in front of a 23 W CFL in a sealed box.

#### 4.9.7 Cycloaddition of 1,3-Cyclohexadiene and *trans*-Anethole



To a flame-dried vial open to air was added *trans*-anethole (**8a**) (17.8 mg, 0.120 mmol, 1 equiv), 1,3-cyclohexadiene (**5**) (91.6  $\mu\text{L}$ , 0.960 mmol, 8 equiv),  $[\text{Cr}(\text{Ph}_2\text{phen})_3](\text{BF}_4)_3$  (1.6 mg, 0.00120 mmol, 1 mol %), and nitromethane (300  $\mu\text{L}$ , 0.40 M). The vial was capped and placed in the photoreactor equipped with 419, 350, and 300 nm light bulbs. The reaction was irradiated with stirring for 23 h. The reaction was then diluted to twice the volume with  $\text{H}_2\text{O}$  and transferred to a separatory funnel. The aqueous layer was extracted with pentane (3x). The combined organic layers were washed with brine and dried over  $\text{Na}_2\text{SO}_4$ . The solvent was removed by rotary evaporation and the crude reaction mixture was analyzed by  $^1\text{H}$  NMR. Through  $^1\text{H}$  NMR analysis, it was determined that a 3:1:3 ratio was obtained of **4-2**:**4-6**:**4-3**.

#### 4.9.8 Dimerization of Myrcene



**Endoperoxide 4-50.** To a flame-dried vial open to air was added myrcene (**4-32**) (27.2 mg, 0.200 mmol),  $[\text{Cr}(\text{Ph}_2\text{phen})_3](\text{BF}_4)_3$  (1.3 mg, 0.00100 mmol), and nitromethane (0.800 mL). The vial was then capped and placed in the photoreactor equipped with 419, 350, and 300 nm light bulbs. The reaction was

irradiated with for 54 h. The reaction mixture was then passed through a short plug of silica (2.5 cm high  $\times$  1 cm wide, Et<sub>2</sub>O eluent). The volatile materials were removed by rotary evaporation and the resulting residue was purified by flash chromatography (100% hexanes $\rightarrow$ 15:1 hexanes/EtOAc eluent) to afford endoperoxide **4-50** as a colorless oil (yield not obtained).

**TLC:** R<sub>f</sub> = 0.60 in 3:1 hexanes/EtOAc, stained blue with *p*-anisaldehyde.

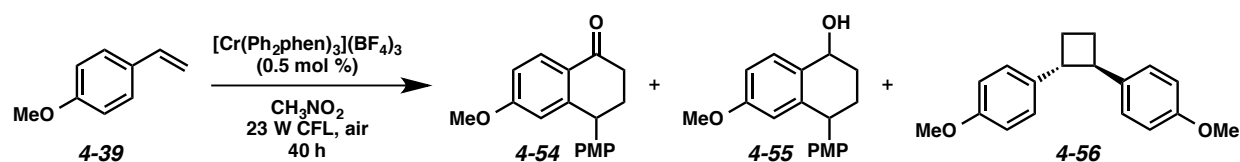
**<sup>1</sup>H NMR** (400 MHz; CDCl<sub>3</sub>):  $\delta$  6.38 (td, *J* = 16.5, 11.2 Hz, 2H), 5.78 (dt, *J* = 15.9, 6.5 Hz, 1H), 5.61 (d, *J* = 15.9 Hz, 1H), 5.23 (dd, *J* = 17.7, 4.9 Hz, 2H), 5.09-5.01 (comp. m, 8H), 4.36 (t, *J* = 6.8 Hz, 1H), 2.98 (d, *J* = 6.5 Hz, 2H), 2.36-2.18 (m, 2H), 1.78-1.63 (m, 2H), 1.75 (s, 3H), 1.34 (s, 6H).

**Alcohols 4-124 and 4-125.** The same procedure was followed as described for the synthesis of endoperoxide **4-50**; however, after the reaction mixture was passed through silica and concentrated, the crude reaction mixture was taken up in dry Et<sub>2</sub>O (2.00 mL) under argon and LAH (53.0 mg, 1.40 mmol) was added at room temperature. The reaction mixture was stirred for 5 h, then was diluted (slowly) with H<sub>2</sub>O (5 mL) and transferred to a separatory funnel. The aqueous layer was extracted with Et<sub>2</sub>O (3  $\times$  5 mL). The combined organic layers were washed with brine (15 mL) and dried over MgSO<sub>4</sub>. The solvent was removed by rotary evaporation and the resulting residue was purified by flash chromatography (100% hexanes $\rightarrow$ 6:1 hexanes/EtOAc eluent) to afford alcohol **4-124** and alcohol **4-125** as a colorless oils (yields not obtained).

**TLC:** [**4-124**] R<sub>f</sub> = 0.59 in 3:1 hexanes/EtOAc, stained yellow with *p*-anisaldehyde. [**4-125**] R<sub>f</sub> = 0.49 in 3:1 hexanes/EtOAc, stained blue with *p*-anisaldehyde.

All spectroscopic data were consistent with previously reported values: **4-124**<sup>64</sup> and **4-125**.<sup>65</sup>

#### 4.9.9 Dimerization of 4-Methoxystyrene

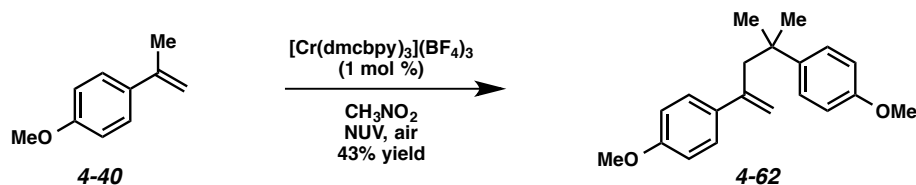


To a vial open to air was added 4-methoxystyrene (**4-39**) (13.4 mg, 0.100 mmol),  $[\text{Cr}(\text{Ph}_2\text{phen})_3](\text{BF}_4)_3$  (0.7 mg, 0.000500 mmol), and nitromethane (1.00 mL). The vial was then capped and irradiated with a 23 W CFL in a sealed box lined with aluminum foil. The reaction was irradiated with for 40 h. The reaction mixture was then passed through a short plug of silica (2.5 cm high  $\times$  1 cm wide,  $\text{Et}_2\text{O}$  eluent). The volatile materials were removed by rotary evaporation and the resulting residue was purified by flash chromatography (100% hexanes $\rightarrow$ 9:1 hexanes/ $\text{EtOAc}$  eluent) to afford samples of **4-54**, **4-55**, and **4-56** (yields not obtained).

**TLC:** [**4-54**]  $R_f = 0.40$  in 3:1 hexanes/ $\text{EtOAc}$ . [**4-55**]  $R_f = 0.25$  in 3:1 hexanes/ $\text{EtOAc}$ . [**4-56**]  $R_f = 0.78$  in 3:1 hexanes/ $\text{EtOAc}$ , visualized by UV.

All spectroscopic data were consistent with previously reported values: **4-54**,<sup>66</sup> **4-55**,<sup>67</sup> **4-56**.<sup>53b</sup>

#### 4.9.10 Dimerization of $\alpha$ -Methyl-4-methoxystyrene

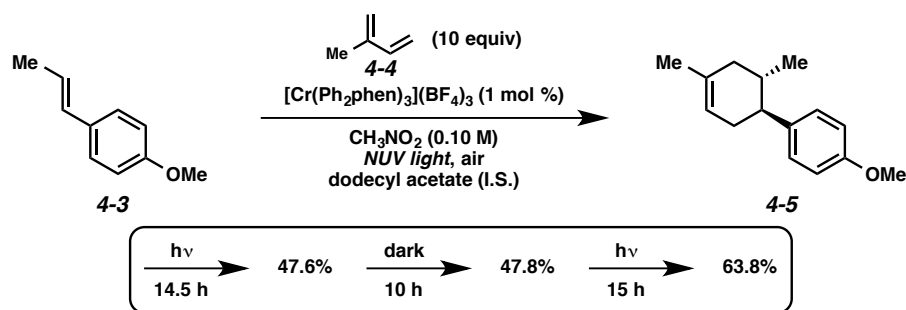


**Dimer 4-62.** To a vial open to air was added  $\alpha$ -methyl-4-methoxystyrene (**4-40**) (14.4 mg, 0.100 mmol),  $[\text{Cr}(\text{dmc bpy})_3](\text{BF}_4)_3$  (1.1 mg, 0.00100 mmol), and nitromethane (1.00 mL). The vial was then capped and placed in the photoreactor equipped with 419, 350, and 300 nm light bulbs. The reaction was irradiated with for 40 h. The reaction was then diluted to twice the volume with  $\text{H}_2\text{O}$  and transferred to a separatory funnel. The aqueous layer was extracted with  $\text{Et}_2\text{O}$  (3x). The combined organic layers were washed with brine and dried over  $\text{Na}_2\text{SO}_4$ . The volatile materials were removed by rotary evaporation and the resulting residue was purified by flash chromatography (100% hexanes $\rightarrow$ 9:1 hexanes/ $\text{EtOAc}$  eluent) to afford dimer **4-62** (6.4 mg, 43% yield) as a colorless oil.

TLC:  $R_f = 0.63$  in 4:1 hexanes/EtOAc, stained pink with *p*-anisaldehyde.

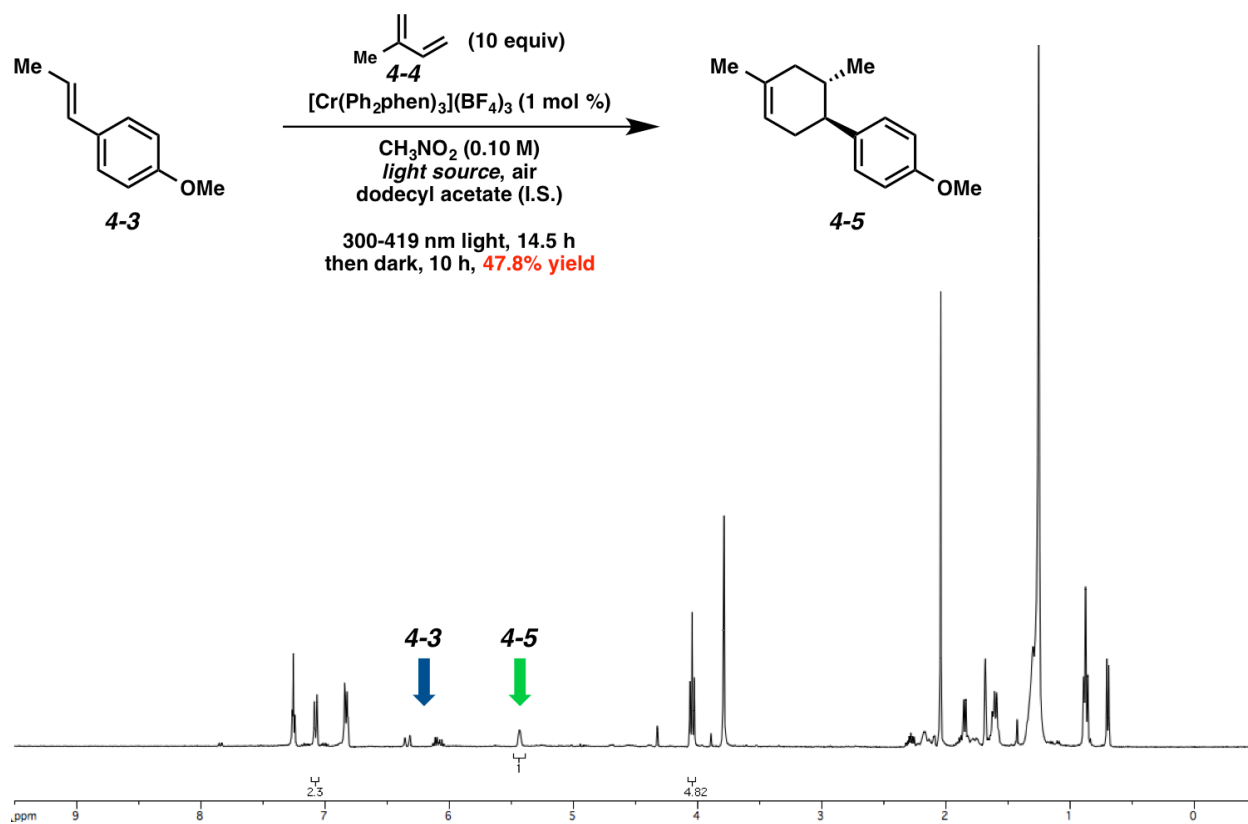
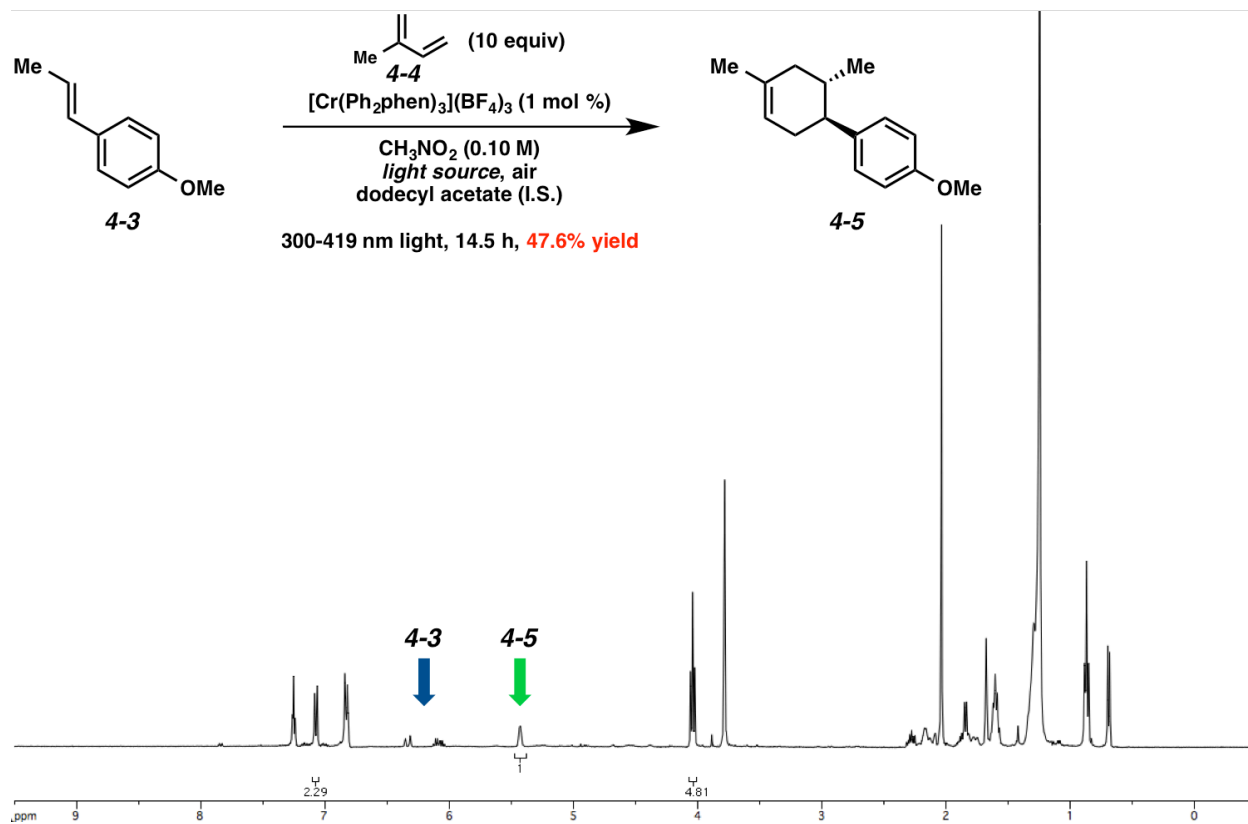
All spectroscopic data were consistent with previously reported values.<sup>68</sup>

#### 4.9.11 Lights On/Off Experiment



Isoprene (**4-4**) (150  $\mu\text{L}$ , 1.50 mmol) was added to a solution of  $[\text{Cr}(\text{Ph}_2\text{phen})_3](\text{BF}_4)_3$  (2.0 mg, 0.00150 mmol), *trans*-anethole (**4-3**) (22.2 mg, 0.150 mmol), and dodecyl acetate (39.6  $\mu\text{L}$ , 0.150 mmol) in nitromethane (1.50 mL) in a flame-dried 2-dram vial. The reaction was capped and irradiated with 300, 350, and 419 nm light for 14.5 h. At this time, an aliquot of approximately one third of the reaction mixture was removed by pipette. The reaction vial was then wrapped in aluminum foil (dark) and allowed to stir for 10 h. A second aliquot was then taken. Lastly, the reaction was irradiated with 300, 350, and 419 nm light again for 15 h, and then the last aliquot was taken.

Each aliquot was immediately worked up as described above in the *General Procedure for the radical cation accelerated [4+2] cycloaddition*. The crude samples were analyzed by  $^1\text{H}$  NMR to determine the % yield of product **4-5** using dodecyl acetate as the internal standard.



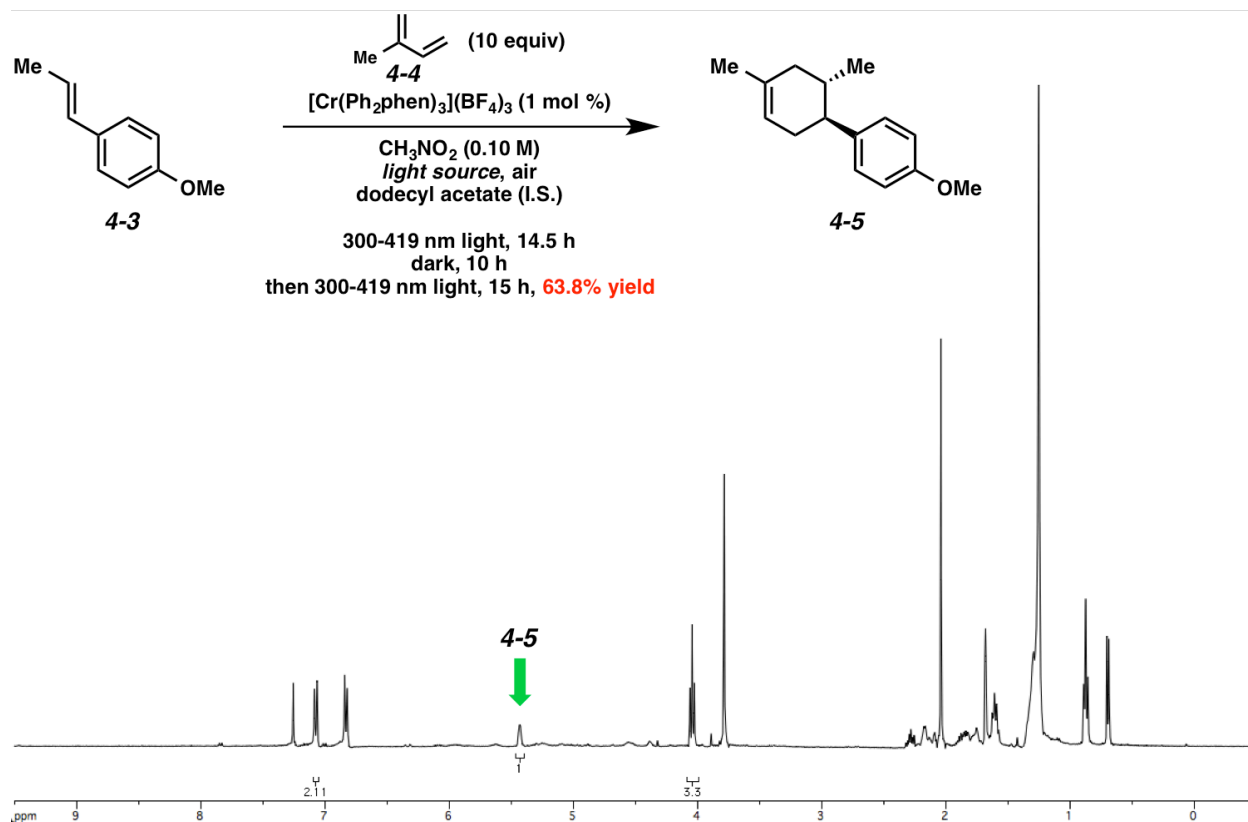
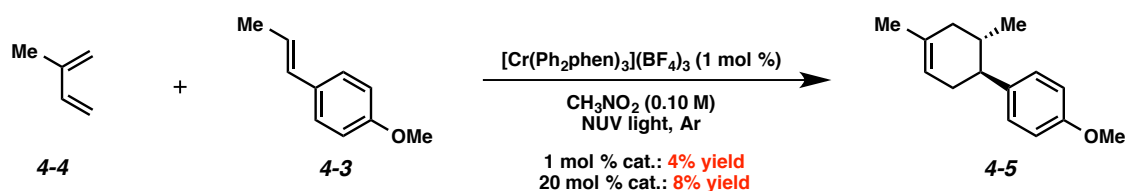


Figure 4.4.  $^1\text{H}$  NMR spectra of reaction mixture during lights on/off experiment.

#### 4.9.12 Degassed Cycloaddition Experiment

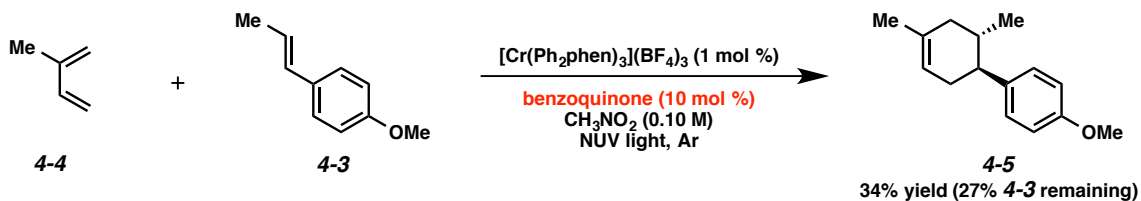


**1 mol % catalyst:** To a 25-mL Schlenk flask was added *trans*-anethole (**4-3**) (14.8 mg, 0.100 mmol), isoprene (**4-4**) (0.100 mL, 1.00 mmol),  $[\text{Cr}(\text{Ph}_2\text{phen})_3](\text{BF}_4)_3$  (1.3 mg, 0.00100 mmol), nitromethane (1.00 mL), and dodecyl acetate (22.8 mg, 0.100 mmol) as an internal standard. The flask was sealed, and the reaction mixture was degassed by 3 freeze-pump-thaw cycles and put under Ar. The reaction was then placed in a Luzchem photoreactor equipped with 419, 350, and 300 nm light bulbs. The reaction mixture

was irradiated with stirring for 27 h. The reaction mixture was then passed through a short plug of silica (2.5 cm high  $\times$  1 cm wide, Et<sub>2</sub>O eluent). The volatile materials were removed by rotary evaporation, and the resulting residue was analyzed by <sup>1</sup>H NMR. Based on the integrations of the product alkene peak at 5.44 ppm and the internal standard triplet at 4.05 ppm, product **4-5** was formed in 4% yield.

**20 mol % catalyst:** To a 25-mL Schlenk flask was added *trans*-anethole (**4-3**) (7.4 mg, 0.0500 mmol), isoprene (**4-4**) (0.0500 mL, 0.500 mmol), [Cr(Ph<sub>2</sub>phen)<sub>3</sub>](BF<sub>4</sub>)<sub>3</sub> (13.1 mg, 0.0100 mmol), nitromethane (0.500 mL), and dodecyl acetate (11.4 mg, 0.0500 mmol) as an internal standard. The flask was sealed, and the reaction mixture was degassed by 3 freeze-pump-thaw cycles and put under Ar. The reaction was then placed in a Luzchem photoreactor equipped with 419, 350, and 300 nm light bulbs. The reaction mixture was irradiated with stirring for 27 h. The reaction mixture was then passed through a short plug of silica (2.5 cm high  $\times$  1 cm wide, Et<sub>2</sub>O eluent). The volatile materials were removed by rotary evaporation, and the resulting residue was analyzed by <sup>1</sup>H NMR. Based on the integrations of the product alkene peak at 5.44 ppm and the internal standard triplet at 4.05 ppm, product **4-5** was formed in 8% yield.

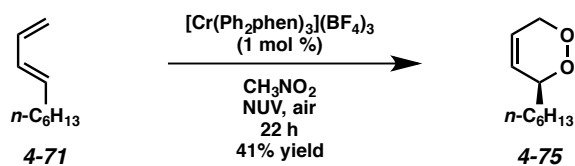
#### 4.9.13 Cycloaddition with Added Benzoquinone



To a 2-dr vial open to air was added *trans*-anethole (**4-3**) (14.8 mg, 0.100 mmol), isoprene (**4-4**) (0.100 mL, 1.00 mmol), [Cr(Ph<sub>2</sub>phen)<sub>3</sub>](BF<sub>4</sub>)<sub>3</sub> (1.3 mg, 0.00100 mmol), nitromethane (1.00 mL), benzoquinone (1.1 mg, 0.0100 mmol), and dodecyl acetate (22.8 mg, 0.100 mmol) as an internal standard. The vial was capped, and the reaction mixture was placed in a Luzchem photoreactor equipped with 419, 350, and 300

nm light bulbs. The reaction mixture was irradiated with stirring for 27 h. The reaction mixture was then passed through a short plug of silica (2.5 cm high  $\times$  1 cm wide, Et<sub>2</sub>O eluent). The volatile materials were removed by rotary evaporation, and the resulting residue was analyzed by <sup>1</sup>H NMR. Based on the integrations of the product alkene peak at 5.44 ppm and the internal standard triplet at 4.05 ppm, product **4-5** was formed in 34% yield (27% remaining **4-3**).

#### 4.9.14 [4+2] Cycloaddition with Singlet Oxygen



**Endoperoxide 4-75.** To a flame-dried vial open to air was added diene **4-71** (13.8 mg, 0.100 mmol), [Cr(Ph<sub>2</sub>phen)<sub>3</sub>](BF<sub>4</sub>)<sub>3</sub> (1.3 mg, 0.00100 mmol), and nitromethane (1.00 mL). The vial was then capped and placed in the photoreactor equipped with 419, 350, and 300 nm light bulbs. The reaction was irradiated with for 22 h. The reaction was then diluted to twice the volume with H<sub>2</sub>O and transferred to a separatory funnel. The aqueous layer was extracted with pentane (3x). The combined organic layers were washed with water and dried over Na<sub>2</sub>SO<sub>4</sub>. The solvent was removed by rotary evaporation and the resulting residue was purified by flash chromatography (100% hexanes  $\rightarrow$  9:1 hexanes/EtOAc eluent) to afford endoperoxide **4-75** (7.0 mg, 41% yield) as a colorless oil.

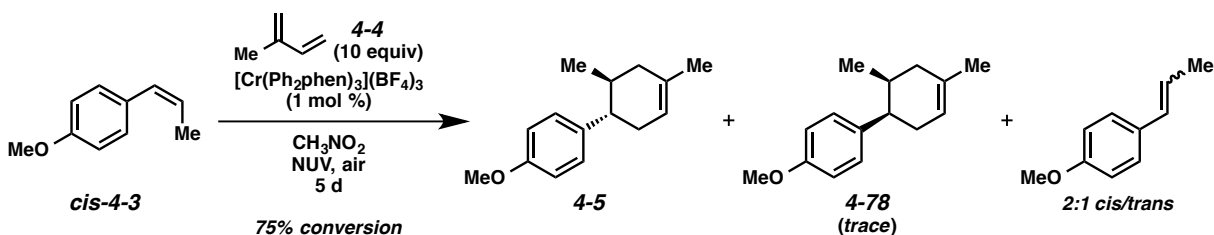
**TLC:** R<sub>f</sub> = 0.60 in 9:1 hexanes/EtOAc, stained blue with *p*-anisaldehyde.

**<sup>1</sup>H NMR** (400 MHz; CDCl<sub>3</sub>): δ 5.97-5.88 (comp. m, 2H), 4.65-4.42 (comp. m, 3H), 1.62-1.43 (comp. m, 2H), 1.35-1.22 (comp. m, 8H), 0.88 (t, *J* = 6.4 Hz, 3H).

**LRMS** (EI): *m/z* calc'd for (M + H)<sup>+</sup> [C<sub>10</sub>H<sub>18</sub>O<sub>2</sub> + H]<sup>+</sup>: 171.1, found 171.2.

#### 4.9.15 Reactions of *cis*-Anethole

Alkene *cis*-4-3 was synthesized according to the procedure by Yoon and coworkers.<sup>69</sup>



**Cycloaddition of *cis*-anethole and isoprene.** To a vial open to air was added alkene *cis*-4-3 (14.8 mg, 0.100 mmol), diene 4-4 (0.100 mL, 1.00 mmol),  $[\text{Cr}(\text{Ph}_2\text{phen})_3](\text{BF}_4)_3$  (1.3 mg, 0.00100 mmol), and nitromethane (1.00 mL). The vial was then capped and placed in the photoreactor equipped with 419, 350, and 300 nm light bulbs. The reaction was irradiated for 5 d. The reaction mixture was then passed through a short plug of silica (2.5 cm high  $\times$  1 cm wide,  $\text{Et}_2\text{O}$  eluent). The volatile materials were removed by rotary evaporation, and the resulting residue was analyzed by  $^1\text{H}$  NMR. The crude reaction mixture showed  $\sim$ 75% conversion to product 4-5 and trace product 4-78 (benzylic proton at  $\sim$ 2.89 ppm). The remaining anethole was a 2:1 mixture of *cis*-4-3 and 4-3.

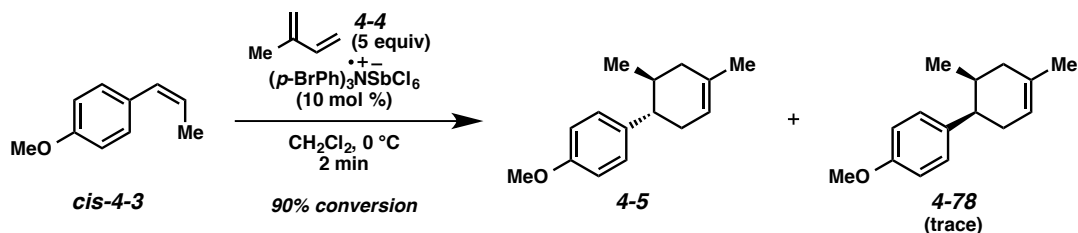


**Isomerization of *cis*-Anethole (with catalyst, 24 h).** To a vial open to air was added alkene *cis*-4-3 (7.4 mg, 0.0500 mmol),  $[\text{Cr}(\text{Ph}_2\text{phen})_3](\text{BF}_4)_3$  (0.7 mg, 0.000500 mmol), nitromethane (0.500 mL), and dodecyl acetate (11.4 mg, 0.0500 mmol) as an internal standard. The vial was then capped and placed in the photoreactor equipped with 419, 350, and 300 nm light bulbs. The reaction was irradiated for 24 h.

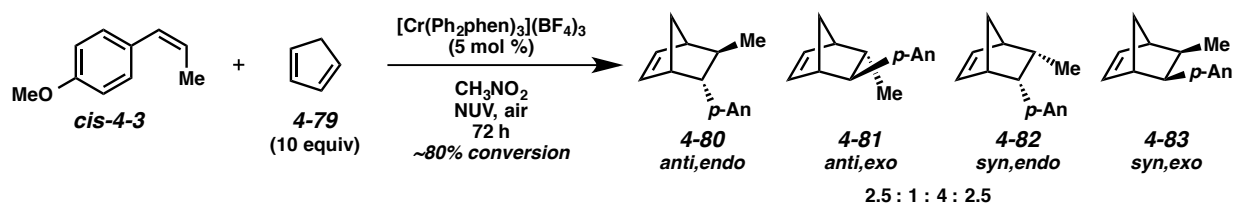
The reaction mixture was then passed through a short plug of silica (2.5 cm high  $\times$  1 cm wide, Et<sub>2</sub>O eluent). The volatile materials were removed by rotary evaporation, and the resulting residue was analyzed by <sup>1</sup>H NMR. The crude reaction mixture was an 18:1 ratio of *cis*-4-3/4-3.

**Isomerization of *cis*-Anethole (with catalyst, 5 d).** To a vial open to air was added alkene *cis*-4-3 (14.8 mg, 0.100 mmol), [Cr(Ph<sub>2</sub>phen)<sub>3</sub>](BF<sub>4</sub>)<sub>3</sub> (1.3 mg, 0.00100 mmol), and nitromethane (1.00 mL). The vial was then capped and placed in the photoreactor equipped with 419, 350, and 300 nm light bulbs. The reaction was irradiated for 5 d. The reaction mixture was then passed through a short plug of silica (2.5 cm high  $\times$  1 cm wide, Et<sub>2</sub>O eluent). The volatile materials were removed by rotary evaporation, and the resulting residue was analyzed by <sup>1</sup>H NMR. The crude reaction mixture was a 1.4:1 ratio of *cis*-4-3/4-3.

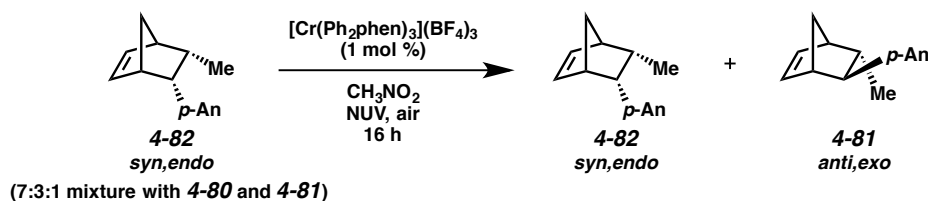
**Isomerization of *cis*-Anethole (without catalyst, 5 d).** The same procedure was followed as with catalyst, but no [Cr(Ph<sub>2</sub>phen)<sub>3</sub>](BF<sub>4</sub>)<sub>3</sub> was added. The crude reaction mixture was a 0.7:1 ratio of *cis*-4-3/4-3.



**Cycloaddition of *cis*-anethole and isoprene under aminium salt conditions.** To alkene *cis*-4-3 (14.8 mg, 0.100 mmol) and diene 4-4 (0.0500 mL, 0.500 mmol) in CH<sub>2</sub>Cl<sub>2</sub> (1.3 mL) under argon at 0 °C was added (p-BrPh)<sub>3</sub>NSbCl<sub>6</sub> (8.2 mg, 0.0100 mmol). The reaction was stirred at 0 °C for 2 min. The reaction was then diluted with H<sub>2</sub>O (5 mL) and transferred to a separatory funnel. The layers were separated and the aqueous layer was extracted with dichloromethane (3 x 5 mL). The combined organic layers were washed with brine and dried over Na<sub>2</sub>SO<sub>4</sub>. The volatile materials were removed by rotary evaporation, and the resulting residue was analyzed by <sup>1</sup>H NMR. The crude reaction mixture showed ~90% conversion to product 4-5 and trace product 4-78.

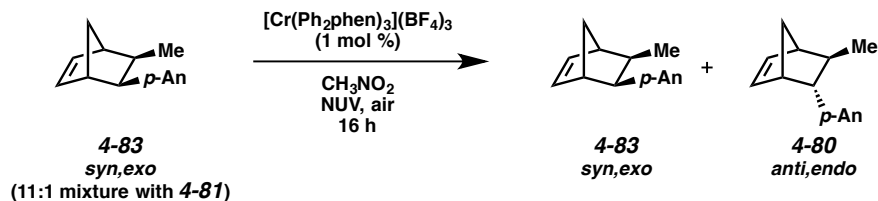


**Cycloaddition of *cis*-anethole and cyclopentadiene.** To a vial open to air was added alkene *cis*-4-3 (14.8 mg, 0.100 mmol), diene 4-4 (0.084 mL, 1.00 mmol),  $[\text{Cr}(\text{Ph}_2\text{phen})_3](\text{BF}_4)_3$  (6.5 mg, 0.00500 mmol), and nitromethane (1.00 mL). The vial was then capped and placed in the photoreactor equipped with 419, 350, and 300 nm light bulbs. The reaction was irradiated for 72 h. The reaction mixture was then passed through a short plug of silica (2.5 cm high  $\times$  1 cm wide,  $\text{Et}_2\text{O}$  eluent). The volatile materials were removed by rotary evaporation, and the resulting residue was analyzed by  $^1\text{H}$  NMR. The crude reaction mixture showed ~80% conversion from alkene *cis*-4-3. A 4:2.5:2.5:1 4-82/4-83/4-80/4-81 mixture of the four diastereomers was obtained. These products could be partially separated by flash chromatography (100% hexanes  $\rightarrow$  10:1 hexanes/ $\text{CH}_2\text{Cl}_2$  eluent). The spectroscopic data for the four diastereomeric adducts was reported by Bauld.<sup>41</sup>



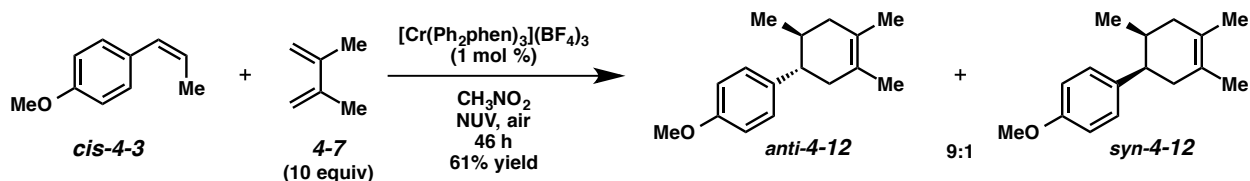
**Isomerization of *syn,endo* adduct 4-82.** To a vial open to air was added an enriched sample of adduct 4-82 (7:3:1 4-82/4-80/4-81) (3.5 mg, 0.0163 mmol),  $[\text{Cr}(\text{Ph}_2\text{phen})_3](\text{BF}_4)_3$  (0.2 mg, 0.000163 mmol) and nitromethane (0.16 mL). The vial was then capped and placed in the photoreactor equipped with 419, 350, and 300 nm light bulbs. The reaction was irradiated for 16 h. The reaction mixture was then passed through a short plug of silica (2.5 cm high  $\times$  1 cm wide,  $\text{Et}_2\text{O}$  eluent). The volatile materials were

removed by rotary evaporation, and the resulting residue was analyzed by  $^1\text{H}$  NMR. A 1:2.5 ratio of **4-82/4-81** was observed, showing that adduct **4-82** had isomerized adduct **4-81**.



**Isomerization of syn,exo adduct 4-83.** To a vial open to air was added an enriched sample of adduct **4-83** (11:1 **4-83/4-81**) (2.7 mg, 0.0126 mmol),  $[\text{Cr}(\text{Ph}_2\text{phen})_3](\text{BF}_4)_3$  (0.2 mg, 0.000126 mmol) and nitromethane (0.13 mL). The vial was then capped and placed in the photoreactor equipped with 419, 350, and 300 nm light bulbs. The reaction was irradiated for 16 h. The reaction mixture was then passed through a short plug of silica (2.5 cm high  $\times$  1 cm wide,  $\text{Et}_2\text{O}$  eluent). The volatile materials were removed by rotary evaporation, and the resulting residue was analyzed by  $^1\text{H}$  NMR. A 1.5:1 ratio of **4-83/4-80** was observed, showing that adduct **4-83** had isomerized to adduct **4-80**.

In an analogous experiment, a 6:1 mixture of anti adducts **4-80/4-81** was exposed to the Cr conditions; no isomerization to the syn adducts occurred.



**Cycloaddition of cis-anethole and 2,3-dimethyl-1,3-butadiene.** To a vial open to air was added alkene **cis-4-3** (10.4 mg, 0.0700 mmol), diene **4-7** (0.079 mL, 0.700 mmol),  $[\text{Cr}(\text{Ph}_2\text{phen})_3](\text{BF}_4)_3$  (0.9 mg, 0.000700 mmol), and nitromethane (0.700 mL). The vial was then capped and placed in the photoreactor equipped with 419, 350, and 300 nm light bulbs. The reaction was irradiated for 46 h. The reaction

mixture was then passed through a short plug of silica (2.5 cm high  $\times$  1 cm wide, Et<sub>2</sub>O eluent). The volatile materials were removed by rotary evaporation, and the resulting residue was purified by flash chromatography (100% hexanes  $\rightarrow$  10:1 hexanes/EtOAc eluent) to afford cycloadduct **4-12** (9.9 mg, 61% yield, 9:1 anti/syn) as a colorless oil. The anti/syn ratio was determined by comparing the integrations of the peak at 2.34 ppm (anti) and the peak at 2.91 ppm (syn) in the crude <sup>1</sup>H NMR (Figure 4.5). When this reaction was performed for 24 h or 72 h, the product anti/syn ratio was the same

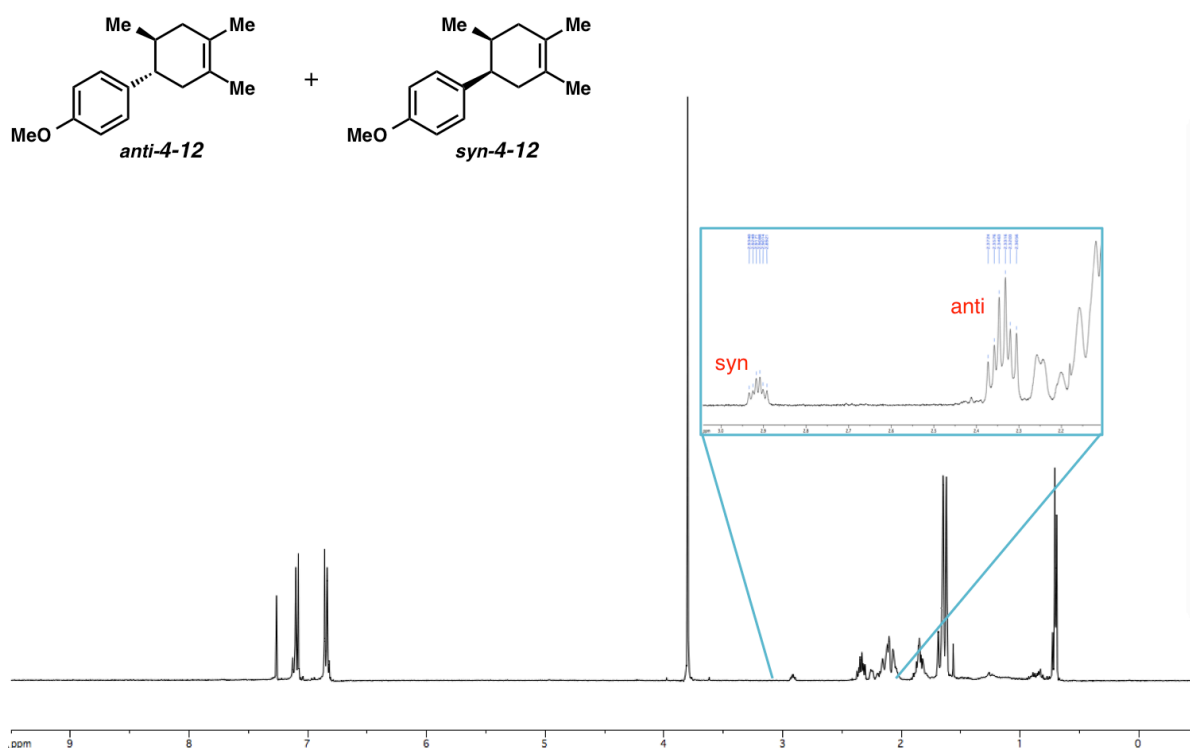
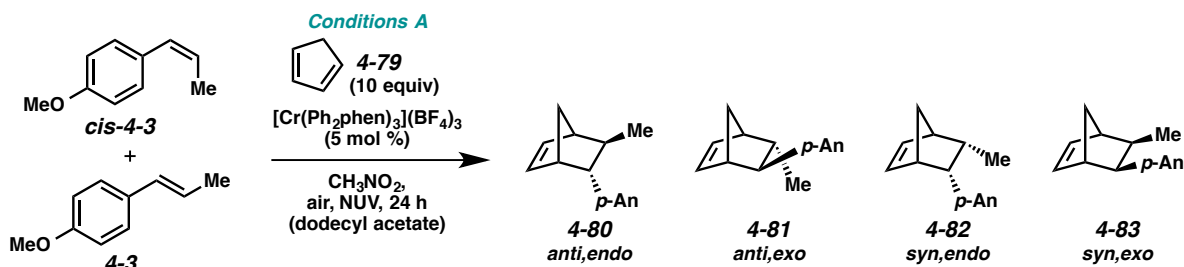


Figure 4.5. <sup>1</sup>H NMR spectrum of anti/syn-**4-12** mixture.

## Isomerization Detection Experiment



**Conditions A:** A stock solution of the internal standard was made to contain 79.8 mg of dodecyl acetate in 0.350 mL dichloromethane. To each of six 1-dram vials was added 0.0500 mL of this stock solution (11.4 mg, 0.0500 mmol per vial). The contents of each vial were concentrated by rotary evaporation. Two more stock solutions, one containing 37.1 mg of alkene **4-3** (0.250 mmol) in 2.50 mL nitromethane, and another containing 37.1 mg of alkene *cis*-**4-3** (0.250 mmol) in 2.50 mL nitromethane, were also made. Open to air, the contents of these two stock solutions were distributed between the six vials (already containing the dodecyl acetate) as follows:

*Vial 1:* 0.500 mL *cis*-**4-3** solution (0.0500 mmol *cis*-**4-3**)

*Vial 2:* 0.400 mL *cis*-**4-3** solution (0.0400 mmol *cis*-**4-3**), 0.100 mL **4-3** solution (0.0100 mmol **4-3**)

*Vial 3:* 0.300 mL *cis*-**4-3** solution (0.0300 mmol *cis*-**4-3**), 0.200 mL **4-3** solution (0.0200 mmol **4-3**)

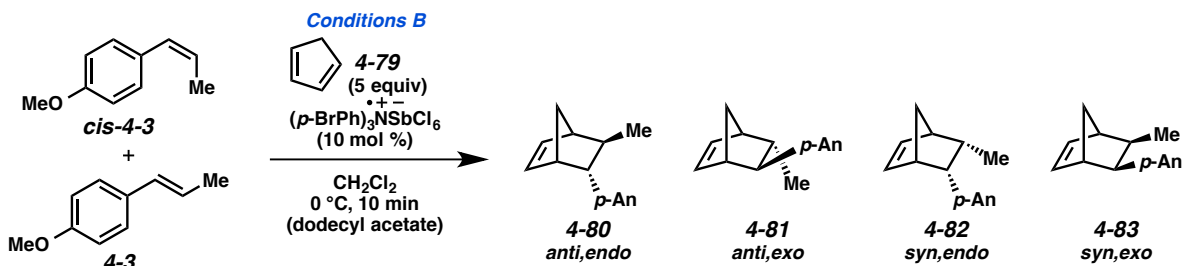
*Vial 4:* 0.200 mL *cis*-**4-3** solution (0.0200 mmol *cis*-**4-3**), 0.300 mL **4-3** solution (0.0300 mmol **4-3**)

*Vial 5:* 0.100 mL *cis*-**4-3** solution (0.0100 mmol *cis*-**4-3**), 0.400 mL **4-3** solution (0.0400 mmol **4-3**)

*Vial 6:* 0.500 mL **4-3** solution (0.0500 mmol **4-3**)

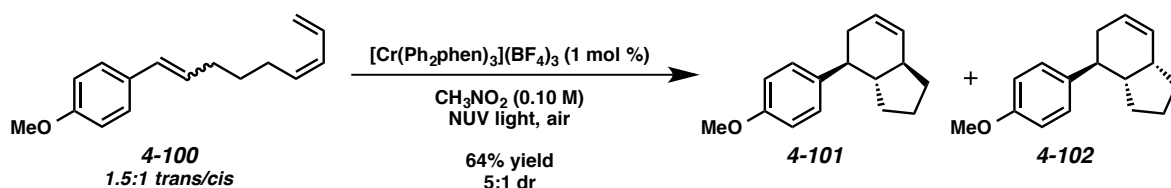
To each vial was then added  $[\text{Cr}(\text{Ph}_2\text{phen})_3](\text{BF}_4)_3$  (3.3 mg, 0.00250 mmol, 5 mol %) and diene **4-79** (0.0420 mL, 0.500 mmol, 10 equiv). The vials were capped and placed in the photoreactor equipped with 419, 350, and 300 nm light bulbs. The vials were irradiated with stirring for 24 h. Each reaction mixture was then passed through a short plug of silica (2.5 cm high  $\times$  1 cm wide,  $\text{Et}_2\text{O}$  eluent). The volatile

materials were removed by rotary evaporation, and the resulting residues was analyzed by  $^1\text{H}$  NMR. The results of this experiment are reported in Scheme 4-31.



**Conditions B:** For the reaction with the aminium salt catalyst, the same set-up procedure as above was followed, except for the following changes: 1) the solutions of 4-3 and *cis*-4-3 were made in  $\text{CH}_2\text{Cl}_2$  instead of nitromethane, 2)  $(p\text{-BrPh})_3\text{NSbCl}_6$  (10 mol %) was used instead of the Cr catalyst, and 3) 5 equiv of diene 4-79 were used instead of 10 equiv. To each vial containing dodecyl acetate and the mixture of *cis*-4-3 and 4-3 (open to air) was added diene 4-79 (0.0210 mL, 0.250 mmol, 5 equiv). The vials were cooled to 0 °C, then  $(p\text{-BrPh})_3\text{NSbCl}_6$  (4.1 mg, 0.00500 mmol, 10 mol %) was added to each. The vials were capped and the reactions were stirred at 0 °C for 10 min. Each reaction mixture was then diluted with sat. aq.  $\text{K}_2\text{CO}_3$  solution (1 mL). The layers were separated and the aqueous layer was extracted with  $\text{CH}_2\text{Cl}_2$  (3 x 3 mL). The combined organic layers were washed with brine (10 mL) and dried over  $\text{Na}_2\text{SO}_4$ . The volatile materials were removed by rotary evaporation, and the resulting residues was analyzed by  $^1\text{H}$  NMR. The results of this experiment are reported in Scheme 4-31.

#### 4.9.16 Intramolecular Cycloadditions



**Cycloadducts 4-101/4-102.** Prepared according to the *General Procedure* using triene **4-100** (15.9 mg, 70.0  $\mu\text{mol}$ ),  $[\text{Cr}(\text{Ph}_2\text{phen})_3](\text{BF}_4)_3$  (0.9 mg, 0.700  $\mu\text{mol}$ ), and nitromethane (0.700 mL). The reaction was irradiated for 46 h. The crude product was purified by flash chromatography (100% hexanes $\rightarrow$ 20:1 hexanes/EtOAc eluent) to afford a 5:1 mixture of diastereomers **4-101** and **4-102** (10.2 mg, 64% yield) as a colorless oil. The diastereomeric ratio was determined by comparing the  $^1\text{H}$  NMR to that of the similar molecules reported by Schuster (Figure 4.6).<sup>46</sup> The reported NMR data is for the *trans* isomer (**4-101**).

**TLC:**  $R_f = 0.76$  in 4:1 hexanes/EtOAc, stained blue with *p*-anisaldehyde.

**$^1\text{H}$  NMR** (400 MHz;  $\text{CDCl}_3$ ):  $\delta$  7.12 (d,  $J = 8.7$  Hz, 2H), 6.84 (d,  $J = 8.7$  Hz, 3H), 5.89 (dd,  $J = 9.8, 1.8$  Hz, 1H), 5.65 (ddt,  $J = 9.8, 4.2, 2.7$  Hz, 1H), 3.79 (s, 3H), 2.68 (td,  $J = 11.1, 6.1$  Hz, 1H), 2.45-2.37 (m, 1H), 2.20-2.10 (m, 1H), 2.06-1.97 (m, 1H), 1.93-1.85 (m, 1H), 1.68-1.60 (comp. m, 3H), 1.52-1.43 (m, 1H), 1.30-1.21 (m, 1H), 1.08-0.97 (m, 1H).

**$^{13}\text{C}$  NMR** (100 MHz;  $\text{CDCl}_3$ ):  $\delta$  157.8, 138.3, 130.0, 128.0, 127.2, 113.7, 55.2, 49.2, 45.8, 45.5, 36.8, 29.6, 28.4, 21.8.

**IR** (ATR, neat): 2957, 2869, 1611, 1513, 1442, 1264, 1178, 1036  $\text{cm}^{-1}$ .

**HRMS** (ESI+):  $m/z$  calc'd for  $(\text{M} + \text{NH}_4)^+ [\text{C}_{16}\text{H}_{20}\text{O} + \text{NH}_4]^+$ : 246.1852, found 246.1845.

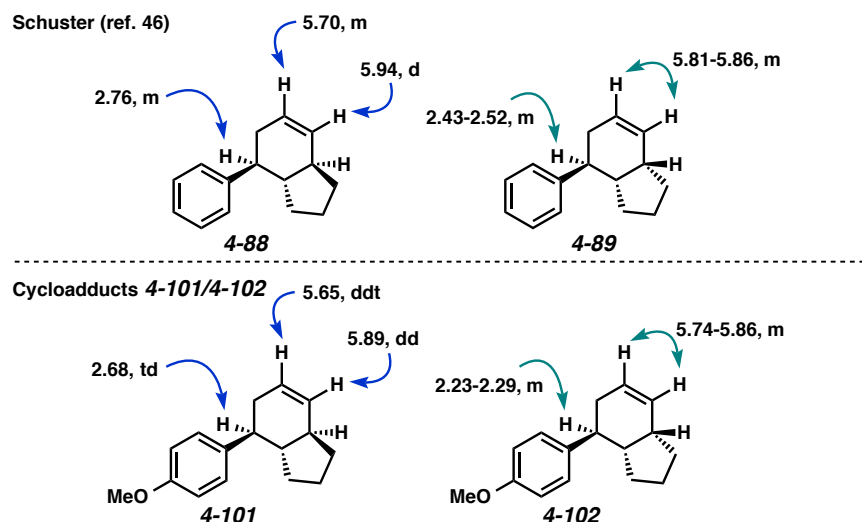
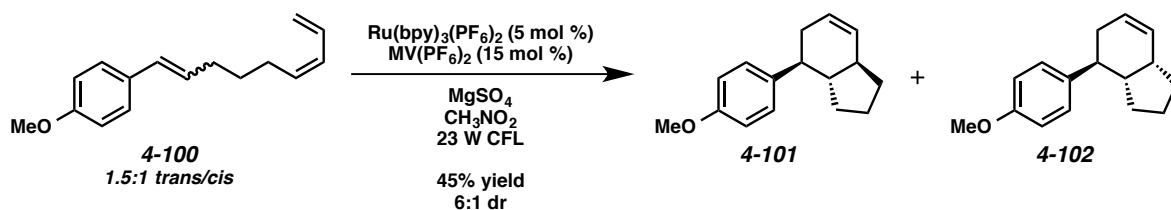
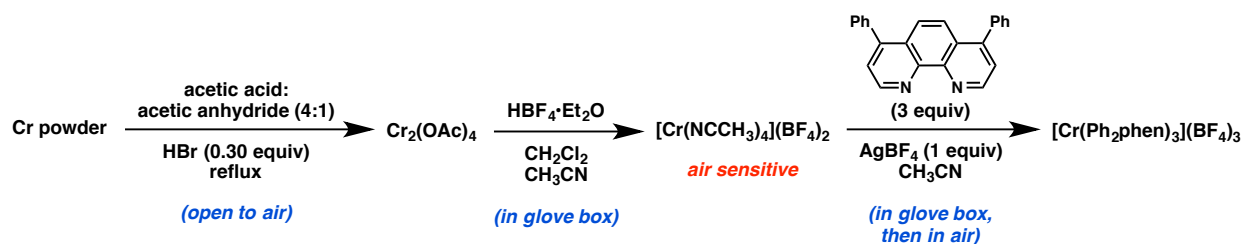


Figure 4.6. Comparison of  $^1\text{H}$  NMR chemical shifts of cycloadducts **4-101** and **4-102** to reported NMR data of similar cycloadducts **4-88** and **4-89** in order to determine the diastereomeric ratio.



**Cycloaddition under Ru conditions.** To a vial open to air was added triene **4-100** (8.5 mg, 0.0370 mmol),  $\text{Ru}(\text{bpy})_3(\text{PF}_6)_2$  (1.6 mg, 0.00190 mmol), methyl viologen (2.7 mg, 0.00560 mmol),  $\text{MgSO}_4$  (17.0 mg, 2 wt. equiv), and nitromethane (0.740 mL). The vial was then capped and irradiated with a 23 W CFL in a sealed box lined with aluminum foil. The reaction was irradiated for 28 h. The reaction mixture was then passed through a short plug of silica (2.5 cm high  $\times$  1 cm wide,  $\text{Et}_2\text{O}$  eluent). The volatile materials were removed by rotary evaporation, and the resulting residue was purified by flash chromatography (100% hexanes  $\rightarrow$  10:1 hexanes/ $\text{Et}_2\text{O}$  eluent) to afford a 6:1 mixture of diastereomers **4-101** and **4-102** (3.8 mg, 45% yield) as a white solid.

#### 4.9.17 Synthesis of $[\text{Cr}(\text{Ph}_2\text{phen})_3](\text{BF}_4)_3$



$\text{Cr}_2(\text{OAc})_4$  was prepared according to the literature procedure.<sup>70</sup> To a mixture of Cr powder (325 mesh, 1.51 g, 29.0 mmol) in glacial acetic acid (40 mL) and acetic anhydride (10 mL) in a 250 mL round bottom flask open to air was slowly added 48% aq. HBr (1.00 mL, 8.70 mmol). The flask was equipped with a reflux condenser and the reaction mixture was refluxed (115 °C) open to air with stirring. Over the course of the reaction, the mixture turned from gray to dark brown. After refluxing for 1.5 h, the reaction mixture was allowed to cool to ambient temperature. The reflux condenser was then replaced with a plastic yellow cap and the reaction mixture was cooled in an ice bath for 30 min. The resulting precipitate was collected by vacuum filtration. The solid was washed with acetone and then dried under vacuum overnight to yield  $\text{Cr}_2(\text{OAc})_4$  as a red-brown powder (2.44 g, 50% yield), which was stored under argon.

$[\text{Cr}(\text{NCCH}_3)_4](\text{BF}_4)_2$  was prepared according to the literature procedure using Schlenk/air-free techniques.<sup>71</sup> All solvents were degassed by three freeze-pump-thaw cycles prior to being brought into the glove box. A solution of  $\text{Cr}_2(\text{OAc})_4$  (2.44 g, 7.18 mmol) in  $\text{CH}_2\text{Cl}_2$  (20 mL) and  $\text{CH}_3\text{CN}$  (10 mL) in a 100 mL Schlenk flask was degassed by three freeze-pump-thaw cycles, and then was also transferred into the glove box. Inside the glove box,  $\text{HBF}_4 \cdot \text{Et}_2\text{O}$  (50-55 wt. %, 4.88 mL) was added dropwise to the solution of  $\text{Cr}_2(\text{OAc})_4$  in  $\text{CH}_2\text{Cl}_2$  and  $\text{CH}_3\text{CN}$ . The reaction mixture was stirred for 2 h, during which time the color of the reaction mixture changed from maroon to deep blue. The Schlenk flask was sealed and brought out of the glove box. The solvent was removed by vacuum overnight, after which a blue solid lined the walls of the flask. The flask was then backfilled with argon and brought back into the glove box. The solid was washed sequentially with  $\text{Et}_2\text{O}$  (10 mL) and pentane (10 mL). The flask containing the

solid was then brought out of the box again and the solid was dried under vacuum for 1-2 h yielding  $[\text{Cr}(\text{NCCH}_3)_4](\text{BF}_4)_2$  (~5.73 g) as a deep blue solid.  $[\text{Cr}(\text{NCCH}_3)_4](\text{BF}_4)_2$  is very air sensitive and should be stored in the glove box.

$[\text{Cr}(\text{Ph}_2\text{phen})_3](\text{BF}_4)_3$  was synthesized according to the literature procedure.<sup>34</sup> In the glove box, a solution of  $[\text{Cr}(\text{NCCH}_3)_4](\text{BF}_4)_2$  (0.500 g, 1.28 mmol) in  $\text{CH}_3\text{CN}$  (10.5 mL) was added to a mixture of bathophenanthroline (1.28 g, 3.84 mmol) in  $\text{CH}_3\text{CN}$  (10.5 mL). The reaction mixture was stirred for 10 min, then  $\text{AgBF}_4$  (0.249 g, 1.28 mmol) was added. The reaction mixture was stirred for an additional 10 min, resulting in a brownish-colored mixture. The reaction vessel was then sealed and removed from the glove box and the reaction mixture was stirred in the hood for 1 h. The mixture was then filtered by vacuum filtration, washing with  $\text{CH}_3\text{CN}$ . To the filtrate, which contained the desired product, was added  $\text{Et}_2\text{O}$  (100 mL), causing a bright yellow solid to precipitate out. The solid was collected by vacuum filtration, washed with  $\text{Et}_2\text{O}$ , and then dried under vacuum, yielding  $[\text{Cr}(\text{Ph}_2\text{phen})_3](\text{BF}_4)_3$  as a bright yellow solid (1.07 g, 64% yield).  $[\text{Cr}(\text{Ph}_2\text{phen})_3](\text{BF}_4)_3$  is air stable and was stored in a desiccator.

*Note:* The color of the solid should be bright yellow, not tan or orange-yellow. If this is the case, the catalyst should be recrystallized. In a general recrystallization procedure, ~500 mg of the crude catalyst was completely dissolved in  $\text{CH}_3\text{CN}$  (~100 mL).  $\text{Et}_2\text{O}$  was then slowly added to the  $\text{CH}_3\text{CN}$  solution by pipetting the  $\text{Et}_2\text{O}$  down the sides of the flask so that two layers were formed. The bottom layer ( $\text{CH}_3\text{CN}$ ) was clear and a tannish yellow color and appeared to contain the impurities, and the top layer ( $\text{Et}_2\text{O}$ ) contained the pure catalyst. After a certain amount of  $\text{Et}_2\text{O}$  was added, the top layer started to become yellow and cloudy, which seemed to be the result of the pure catalyst accumulating in the  $\text{Et}_2\text{O}$  layer. In total, ~300 mL  $\text{Et}_2\text{O}$  were added. The flask was left to rest for 30 min and was not shaken or swirled, so as to not combine the layers. The yellow top layer was then removed by pipette and filtered by vacuum filtration, washing with  $\text{Et}_2\text{O}$ . The bright yellow solid was dried under vacuum. More  $\text{Et}_2\text{O}$  could be added to the remaining  $\text{CH}_3\text{CN}$  solution to precipitate out more of the pure catalyst.

## Chapter 4 Notes and References

---

<sup>1</sup> (a) Prier, C. K.; Rankic, D. A. MacMillan, D. W. C. *Chem. Rev.* **2013**, *113*, 5322-5363. (b) Narayanam, J. M. R.; Stephenson, C. R. J. *Chem. Soc. Rev.* **2011**, *40*, 102-113. (c) Tucker, J. W.; Stephenson, C. R. J. *J. Org. Chem.* **2012**, *77*, 1617-1622. (d) Angnes, R. A.; Li, Z.; Correia, C. R. D.; Hammond, G. B. *Org. Biomol. Chem.* **2015**, *13*, 9152-9167. (e) Yoon, T. P.; Ischay, M. A.; Du, J. *Nat. Chem.* **2010**, *2*, 527-532. (f) Schultz, D. M.; Yoon, T. P. *Science* **2014**, *343*, 985-993.

<sup>2</sup> Non-metal photocatalysts also exist: (a) Fukuzumi, S.; Ohkubo, K. *Org. Biomol. Chem.* **2014**, *12*, 6059-6071. (b) Nicewicz, D. A.; Nguyen, T. M. *ACS Catal.* **2014**, *4*, 355-360.

<sup>3</sup> (a) Kern, J.-M.; Sauvage, J.-P. *J. Chem. Soc., Chem. Commun.* **1987**, 546-548. (b) Pirtsch, M.; Paria, S.; Matsuno, T.; Isobe, H.; Reiser, O. *Chem. Eur. J.* **2012**, *18*, 7336-7340. (c) Paria, S.; Pirtsch, M.; Kais, V.; Reiser, O. *Synthesis* **2013**, *45*, 2689-2698. (d) Paria, S.; Reiser, O. *ChemCatChem* **2014**, *6*, 2477-2483. (e) Knorn, M.; Rawner, T.; Czerwieniec, R.; Reiser, O. *ACS Catal.* **2015**, *5*, 5186-5193. (f) Hernandez-Perez, A. C.; Vlassova, A.; Collins, S. K. *Org. Lett.* **2012**, *14*, 2988-2991. (g) Hernandez-Perez, A. C.; Collins, S. K. *Angew. Chem., Int. Ed.* **2013**, *52*, 12696-12700. (h) Caron, A.; Hernandez-Perez, A. C.; Collins, S. K. *Org. Process Res. Dev.* **2014**, *18*, 1571-1574. (i) Baralle, A.; Fensterbank, L.; Goddard, J.-P.; Ollivier, C. *Chem. Eur. J.* **2013**, *19*, 10809-10813. (j) Majek, M.; Jacobi von Wangelin, A. *Angew. Chem., Int. Ed.* **2013**, *52*, 5919-5921. (k) Tang, X.-J.; Dolbier, Jr., W. R. *Angew. Chem., Int. Ed.* **2015**, *127*, 4320-4323. (l) Creutz, S. E.; Lotito, K. J.; Fu, G. C.; Peters, J. C. *Science* **2012**, *338*, 647-651. (m) Ziegler, D. T.; Choi, J.; Muñoz-Molina, J. M.; Bissember, A. C.; Peters, J. C.; Fu, G. C. *J. Am. Chem. Soc.* **2013**, *135*, 13107-13112. (n) Bissember, A. C.; Lundgren, R. L.; Creutz, S. E.; Peters, J. C.; Fu, G. C. *Angew. Chem., Int. Ed.* **2013**, *52*, 5129-5133. (o) Uyeda, C.; Tan, Y.; Fu, G. C.; Peters, J. C. *J. Am. Chem. Soc.* **2013**, *135*, 9548-9552. (p) Tan, Y.; Muñoz-Molina, J. M.; Fu, G. C.; Peters, J. C. *Chem. Sci.*, **2014**, *5*, 2831-2835. (q) Do, H.-Q.; Bachman, S.; Bissember, A. C.; Peters, J. C.; Fu, G. C. *J. Am. Chem. Soc.* **2014**, *136*, 2162-2167. (r) Ratani, T. S.; Bachman, S.; Fu, G. C.; Peters, J. C. *J. Am. Chem. Soc.* **2015**, *137*, 13902-13907. (s) Kainz, Q. M.; Matier, C. D.; Bartoszewicz, A.; Zultanski, S. L.; Peters, J. C.; Fu, G. C. *Science*

---

**2016**, 351, 681-684. (t) Johnson, M. W.; Hannoun, K. I.; Tan, Y.; Fu, G. C.; Peters, J. C. *Chem Sci.* **2016**, 7, 4091-4100.

<sup>4</sup> Gualandi, A.; Marchini, M.; Mengozzi, L.; Natali, M.; Lucarini, M.; Cernoni, P. Cozzi, P. G. *ACS Catal.* **2015**, 5, 5927-5931.

<sup>5</sup> (a) McDaniel, A. M.; Tseng, H.-W.; Damrauer, N. H.; Shores, M. P. *Inorg. Chem.* **2010**, 49, 7981-7991.

(b) Stevenson, S. M.; Shores, M. P.; Ferreira, E. M. *Angew. Chem., Int. Ed.* **2015**, 54, 6506-6510.

<sup>6</sup> Unless otherwise noted, all reduction potentials are in V vs. SCE, taken in acetonitrile.

<sup>7</sup> The Shores, Rappé, and Rovis groups are at Colorado State University. The Damrauer group is at the University of Colorado–Boulder.

<sup>8</sup> Freeman, D. B.; Furst, L.; Condie, A. G.; Stephenson, C. R. *J. Org. Lett.* **2012**, 14, 94-97.

<sup>9</sup> Tyson, E. L.; Ament, M. S.; Yoon, T. P. *J. Org. Chem.* **2013**, 78, 2046–2050.

<sup>10</sup> Hopkins, M. N.; Gómez-Suárez, A.; Teders, M.; Sahoo, B.; Glorius, F. *Angew. Chem., Int. Ed.* **2016**, 55, 4361-4366.

<sup>11</sup> Bellville, D. J.; Wirth, D. W.; Bauld, N. L. *J. Am. Chem. Soc.* **1981**, 103, 718-720.

<sup>12</sup> Lin, S.; Ischay, M. A.; Fry, C. G.; Yoon, T. P. *J. Am. Chem. Soc.* **2011**, 133, 19350-19353.

<sup>13</sup> Roth, H. G.; Romero, N. A.; Nicewicz, D. A. *Synlett* **2016**, 27, 714-723.

<sup>14</sup> Calhoun, G. C.; Schuster, G. B. *J. Am. Chem. Soc.* **1984**, 106, 6870-6871.

<sup>15</sup> Schepp, N. P.; Johnston, L. J. *J. Am. Chem. Soc.* **1994**, 116, 10330-10331.

<sup>16</sup> Studer, A.; Curran, D. P. *Nat. Chem.* **2014**, 6, 765-773.

<sup>17</sup> Bauld, N. L.; Bellville, D. J.; Harirchian, B.; Lorenz, K. T.; Pabon, R. A.; Reynolds, D. W.; Wirth, D. D.; Chiou, H.-S.; Marsh, B. K. *Acc. Chem. Res.* **1987**, 20, 371-378.

<sup>18</sup> <https://www.chem.fsu.edu/~shatruck/docs/Solvent-UV-cutoffs.pdf>

<sup>19</sup> Bellville, D. J.; Bauld, N. L.; Pabon, R.; Gardner, S. A. *J. Am. Chem. Soc.* **1983**, 105, 3584-3588.

<sup>20</sup> Reynolds, D. W.; Bauld, N. L. *Tetrahedron* **1986**, 42, 6189-6194.

<sup>21</sup> Matsumoto, M.; Kondo, K. *J. Org. Chem.* **1975**, 40, 2259-2260.

- 
- <sup>22</sup> DeRosa, M. C.; Crutchley, R. J. *Coord. Chem. Rev.* **2002**, *233-234*, 351-371.
- <sup>23</sup> Yueh, W.; Bauld, N. L. *J. Phys. Org. Chem.* **1996**, *9*, 529-538.
- <sup>24</sup> Schepp, N. P.; Johnston, L. J. *J. Am. Chem. Soc.* **1994**, *116*, 6895-6903.
- <sup>25</sup> (a) Kojima, M.; Sakuragi, H.; Tokumaru, K. *Tetrahedron Lett.* **1981**, *22*, 2889-2892. (b) Nair, V.; Sheeba, V.; Panicker, S. B.; George, T. G.; Rajan, R.; Balagopal, L.; Vairamani, M.; Prabhakar, S. *Tetrahedron* **2000**, *56*, 2461-2467. (c) Wang, K.; Meng, L.-G.; Zhang, Q.; Wang, L. *Green Chem.* **2016**, *18*, 2864-2870.
- <sup>26</sup> (a) Kadota, S.; Tsubono, K.; Makino, K.; Takeshita, M.; Kikuchi, T. *Tetrahedron Lett.* **1987**, *28*, 2857-2860. (b) O'Neil, L.; Wiest, O. *J. Org. Chem.* **2006**, *71*, 8926-8933.
- <sup>27</sup> (a) Giacco, T. D.; Faltoni, A.; Elisei, F. *Phys. Chem. Chem. Phys.* **2008**, *10*, 200-210. (b) Miyake, Y.; Moriyama, T.; Tanabe, Y.; Onodera, G.; Nishibayashi, Y. *Organometallics* **2011**, *30*, 5972-5977.
- <sup>28</sup> Yueh, W.; Bauld, N. L. *J. Am. Chem. Soc.* **1995**, *117*, 5671-5676.
- <sup>29</sup> Sarabia, F. J.; Ferreira, E. M. *manuscript in preparation*.
- <sup>30</sup> Yueh, W.; Bauld, N. L. *J. Chem. Soc., Perkin Trans. 2* **1995**, 871-873.
- <sup>31</sup> Hamilton, D. S.; Nicewicz, D. A. *J. Am. Chem. Soc.* **2012**, *134*, 18577-18580.
- <sup>32</sup> Shono, T.; Hayashi, A. I.; Hakozaiki, S. *J. Am. Chem. Soc.* **1975**, *97*, 4261-4264.
- <sup>33</sup> Cismesia, M. A.; Yoon, T. P. *Chem. Sci.* **2015**, *6*, 5426-5434.
- <sup>34</sup> Higgins, R. F.; Fatur, S. M.; Shepard, S. G.; Stevenson, S. M.; Boston, D. J.; Ferreira, E. M.; Damrauer, N. H.; Rappé, A. K.; Shores, M. P. *J. Am. Chem. Soc.* **2016**, *138*, 5451-5464.
- <sup>35</sup> Serpone, N.; Jamieson, M. A.; Henry, M. S.; Hoffman, M. Z.; Bolletta, F.; Maestri, M. *J. Am. Chem. Soc.* **1979**, *101*, 2907-2916.
- <sup>36</sup> (a) Crellin, R. A.; Lambert, M. C.; Ledwith, A. *J. Chem. Soc., Chem. Commun.* **1970**, 682-683. (b) Ledwith, A. *Acc. Chem. Res.* **1972**, *5*, 133-139.
- <sup>37</sup> Lewis, F. D.; Kojima, M. *J. Am. Chem. Soc.* **1988**, *110*, 8660-8664.

- 
- <sup>38</sup> (a) Castro, H. T.; Martínez, J. R.; Stashenko, E. *Molecules* **2010**, *15*, 5012-5030. (b) Lewis, F. D.; Bassani, D. M.; Caldwell, R. A.; Unett, D. J. *J. Am. Chem. Soc.* **1994**, *116*, 10477-10485.
- <sup>39</sup> Prof. Anthony Rappé: *cis*-anethole 0.08 V more difficult to oxidize than *trans*-anethole.
- <sup>40</sup> Robert Higgins is acknowledged for reduction potential data.
- <sup>41</sup> Bauld, N. L.; Gao, D. *J. Chem. Soc., Perkin Trans. 2* **2000**, 931-934.
- <sup>42</sup> In our own experiments, we observed that the isomerization of *cis*- to *trans*-anethole was possible under the aminium conditions; however, it was slower than the cycloaddition (20% conversion to *trans*-anethole in 5 min, but the cycloaddition was complete in 2 min).
- <sup>43</sup> According to reference 15, the reaction of 2,3-dimethyl-1,3-butadiene with the *trans*-anethole radical cation is slower than the reaction of isoprene with the *trans*-anethole radical cation. The distonic radical cation intermediate in the 2-3-dimethyl-1,3-butadiene case must still close down faster, though, in order to give more of the syn product.
- <sup>44</sup> Anthony Rappé is acknowledged for calculations.
- <sup>45</sup> Pabon, R. A.; Bellville, D. J.; Bauld, N. L. *J. Am. Chem. Soc.* **1983**, *105*, 5158-5159.
- <sup>46</sup> Wölfle, I.; Chan, S.; Schuster, G. B. *J. Org. Chem.* **1991**, *56*, 7313-7319.
- <sup>47</sup> Liu, R. S. H.; Turro Jr., N. J.; Hammond, G. S. *J. Am. Chem. Soc.* **1965**, *87*, 3406-3412.
- <sup>48</sup> Evans, D. F. *J. Chem. Soc.* **1960**, 1735-1745.
- <sup>49</sup> Benzophenone: Lin, Z.-P.; Aue, W. A. *Spectrochimica Acta Part A* **2000**, *56*, 111-117.; DCN: Davis, H. F.; Das, P. K.; Griffin, G. W.; Timpa, J. D. *J. Org. Chem.* **1983**, *48*, 5256-5259.; DCA: Darmany, A. *P. Chem. Phys. Lett.* **1984**, *110*, 89-94.
- <sup>50</sup> Ni, T.; Caldwell, R. A.; Melton, L. A. *J. Am. Chem. Soc.* **1989**, *111*, 457-464.
- <sup>51</sup> Hurlley, A. E.; Lu, Z.; Yoon, T. P. *Angew. Chem., Int. Ed.* **2014**, *53*, 8991-8994.
- <sup>52</sup> Lu, Z.; Yoon, T. P. *Angew. Chem., Int. Ed.* **2012**, *51*, 10329-10332.
- <sup>53</sup> (a) Ischay, M. A.; Ament, M. S.; Yoon, T. P. *Chem. Sci.* **2012**, *3*, 2807-2811. (b) Reiner, M.; Nicewicz, D. A. *Chem. Sci.* **2013**, *4*, 2625-2629.

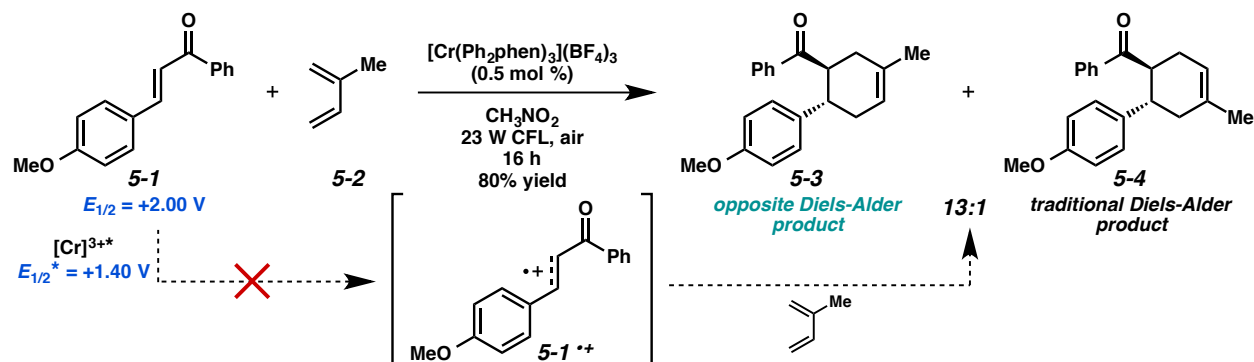
- 
- <sup>54</sup> Lin, S.; Padilla, C. E.; Ischay, M. A.; Yoon, T. P. *Tetrahedron Lett.* **2012**, *53*, 3073-3076.
- <sup>55</sup> Ischay, M. A.; Lu, Z.; Yoon, T. P. *J. Am. Chem. Soc.* **2010**, *132*, 8572-8574.
- <sup>56</sup> Smith, M. B. *Organic Synthesis, Third Edition*. Academic Press, **2011**, p.1086.
- <sup>57</sup> Falk, A.; Göderz, A.-L.; Schmalz, H.-G. *Angew. Chem. Int. Ed.* **2013**, *52*, 1576-1580.
- <sup>58</sup> Nortcliffe, A.; Ekstrom, A. G.; Black, J. R.; Ross, J. A.; Habib, F. K.; Botting, N. P.; O'Hagan, D. *Bioorg. Med. Chem.* **2014**, *22*, 756-761.
- <sup>59</sup> Crane, S. N.; Bateman, K.; Gagne, S.; Levesque, J.-F. *J. Label Compd. Radiopharm* **2006**, *49*, 1273-1285.
- <sup>60</sup> Roush, W. R.; Gillis, H. R.; Ko, A. I. *J. Am. Chem. Soc.* **1982**, *104*, 2269-2283.
- <sup>61</sup> Chalal, M.; Vervandier-Fasseur, D.; Meunier, P.; Cattey, H.; Hierso, J.-C. *Tetrahedron* **2012**, *68*, 3899-3907.
- <sup>62</sup> Liu, B.; Liu, T.; Luo, S.; Gong, L. *Org. Lett.* **2014**, *16*, 6164-6167.
- <sup>63</sup> Lorenz, K. T.; Bauld, N. L. *J. Am. Chem. Soc.* **1987**, *109*, 1157-1160.
- <sup>64</sup> Gally, C.; Nestl, B. M.; Hauer, B. *Angew. Chem., Int. Ed.* **2015**, *54*, 12952-12956.
- <sup>65</sup> Tueting, D. R.; Echavarren, A. M.; Stille, J. K. *Tetrahedron* **1989**, *45*, 979-992.
- <sup>66</sup> Nair, V.; Sheeba, V.; Panicker, S. B.; George, T. G.; Rajan, R.; Balagopal, L.; Vairamani, M.; Prabhakar, S. *Tetrahedron* **2000**, *56*, 2461-2467.
- <sup>67</sup> Assignment of the structure of alcohol **4-55** was made by comparison to similar molecules in: Bégué, J.-P.; Cerceau, C.; Dogbeavou, A.; Mathé, K.; Sicsic, S. *J. Chem. Soc. Perkin Trans. I* **1992**, 3141-3144.
- <sup>68</sup> Giacco, T. D.; Faltoni, A.; Elisei, F. *Phys. Chem. Chem. Phys.* **2008**, *10*, 200-210.
- <sup>69</sup> Blum, T. R.; Zhu, Y.; Nordeen, S. A.; Yoon, T. P. *Angew. Chem., Int. Ed.* **2014**, *126*, 11236-11239.
- <sup>70</sup> Levy, O.; Bogoslavsky, B.; Bino, A. *Inorg. Chim. Acta.* **2012**, *391*, 179-181.
- <sup>71</sup> Henriques, R. T.; Herdtweck, E.; Kühn, F. E.; Lopes, A. D.; Mink, J.; Romão, C. C. *J. Chem. Soc., Dalton Trans.* **1998**, 1293-1297.

## CHAPTER 5

### A CHROMIUM-PHOTOCATALYZED APPROACH TO DIELS-ALDER ADDUCTS OF REVERSED REGIOSELECTIVITY

#### 5.1 Introduction: An Unlikely Result

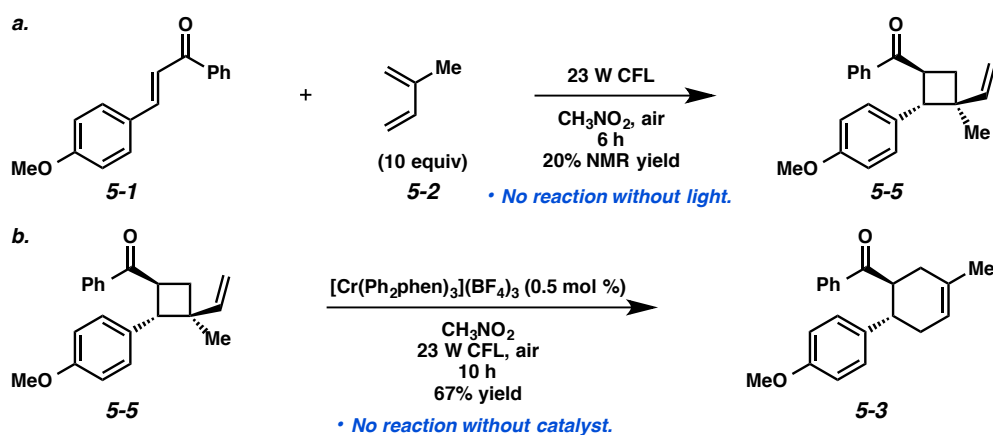
While exploring the radical cation Diels-Alder cycloaddition of electron-rich dienophiles, we obtained an unexpected result: 4-methoxychalcone (**5-1**) reacted with isoprene (**5-2**) under Cr-photocatalysis to yield cyclohexene **5-3** in 80% yield (Scheme 5.1). The success of this electron-poor substrate was a surprise, since we expected that the cycloaddition would go through a radical cation mechanism and the reduction potential of alkene **5-1** ( $E_{1/2} = +2.00$  V,  $\text{CH}_3\text{NO}_2$ , under  $\text{O}_2$ )<sup>1,2</sup> was significantly higher than that of  $\text{Cr}(\text{Ph}_2\text{phen})_3^{3+*}$  ( $E_{1/2}^* = +1.40$  V).<sup>3</sup> These values imply that the direct oxidation of alkene **5-1** by the catalyst should not be possible, but a different mechanism might be operative. Also intriguing about this result was that, though alkene **5-1** resembles the type of electron-poor dienophile one would expect to see in a traditional Diels-Alder reaction, the structural connectivity of the major cyclohexene product (**5-3**) was the opposite of what would be obtained through traditional Diels-Alder conditions (**5-4**).



Scheme 5.1. Unexpected cycloaddition result with electron-poor alkene.

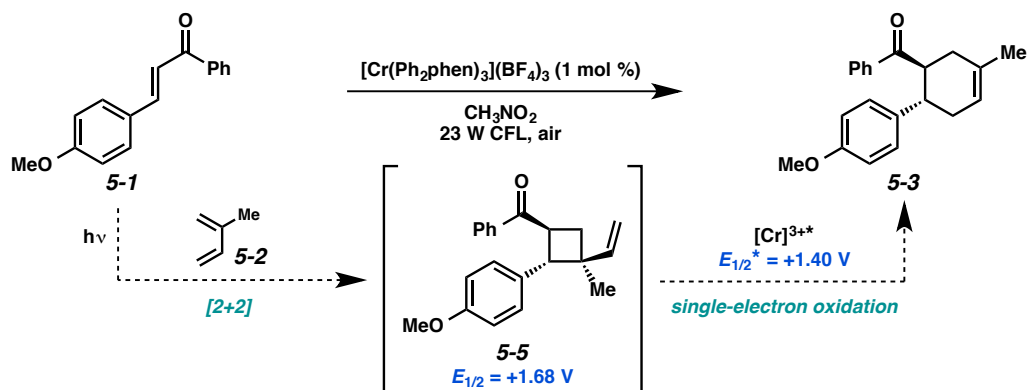
## 5.2 Preliminary Results and Optimization

Excited by the prospect of this transformation, we investigated further. Early on in our preliminary studies, vinylcyclobutane **5-5** ( $E_{1/2} = +1.68$  V,  $\text{CH}_3\text{NO}_2$ , under  $\text{O}_2$ ) was identified as a side product. Control experiments revealed that the vinylcyclobutane (**5-5**) still formed in the absence of catalyst (Scheme 5.2a), but not in the absence of light. Additionally, when vinylcyclobutane **5-5** was exposed to the Cr photocatalysis conditions, rearrangement to cyclohexene **5-3** occurred, implicating the vinylcyclobutane as a possible reaction intermediate; no rearrangement occurred in the absence of the Cr catalyst (Scheme 5.2b).



Scheme 5.2. Preliminary experiments implicating vinylcyclobutane **5-5** as a reaction intermediate.

These early results suggest that the reaction might be proceeding through a light-induced [2+2] cycloaddition of the electron-poor alkene (**5-1**) and diene (**5-2**) to form vinylcyclobutane **5-5**, followed by a Cr-catalyzed vinylcyclobutane rearrangement to form cyclohexene **5-3** (Scheme 5.3). This possible mechanistic pathway would account for the fact that the catalyst should not be able to oxidize enone **5-1**. Though the reduction potential of the vinylcyclobutane (**5-5**) is still higher than that of the excited state Cr complex, it is seemingly low enough that as long as the vinylcyclobutane rearrangement occurs quickly upon single-electron oxidation, cyclohexene **5-3** will be formed efficiently, as we have observed.



Scheme 5.3. Early mechanistic hypothesis.

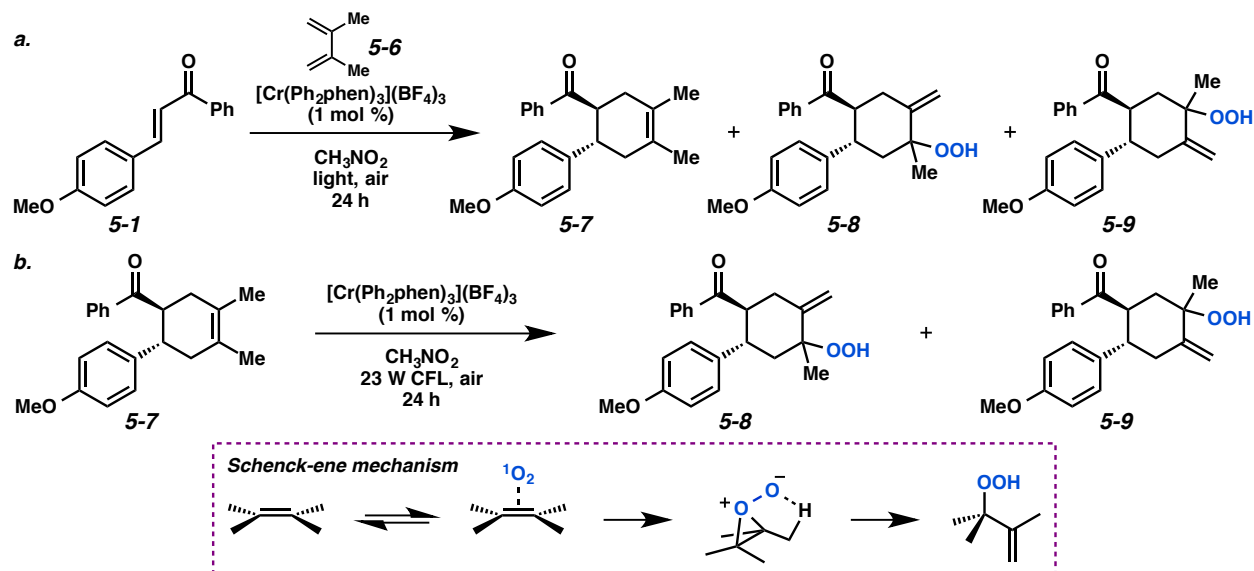
Though this vinylcyclobutane pathway fit with our initial observations, we were still hesitant to conclude that we had uncovered the complete mechanistic picture. Many of the experiments described herein were performed under the assumption that the reaction was proceeding through a [2+2] cycloaddition/vinylcyclobutane rearrangement; however, other mechanistic pathways are also likely operative. See Chapter 5.6 for a more in depth discussion of the mechanism.

### 5.2.1 Singlet Oxygen Side Products

After obtaining these preliminary results, we set out to optimize the Cr-photocatalyzed cycloaddition. We initially chose the cycloaddition of alkene **5-1** and symmetrical diene **5-6** for our optimization studies, since only one isomer of the product would be formed (Scheme 5.4a). We quickly discovered, though, that the product of this cycloaddition (**5-7**) was susceptible to oxidation to afford hydroperoxides **5-8** and/or **5-9**, which was drastically lowering the yield of cyclohexene **5-7**.

Control experiments revealed that these side products (**5-8** and **5-9**) only formed when both air and catalyst were present, implicating  $^1\text{O}_2$  as the cause of the undesired reaction. Additionally, we confirmed that the side products were resulting from  $^1\text{O}_2$  reacting with cyclohexene **5-7**: when cyclohexene **5-7** was exposed to the  $\text{Cr}(\text{Ph}_2\text{phen})_3^{3+}$ , air, and light, the starting material was completely

consumed and the oxidized product mixture formed (Scheme 5.4b). The hydroperoxides are likely forming through a Schenck-ene reaction between  $^1\text{O}_2$  and cyclohexene **5-7**.<sup>4</sup>



Scheme 5.4. Schenck-ene reaction of singlet oxygen with cycloadduct **5-7**.

Unfortunately, when we attempted the cycloaddition under argon, the reaction was very sluggish and full conversion to product was not achieved. As we had seen in the electron-rich alkene cycloadditions, reactions run without air turned from bright yellow to dark tan, indicating that oxygen was likely necessary to protect the catalyst from degradation.

Because air was essential to the efficiency of the reaction, instead of trying to find a way to accomplish the reaction without air, we wondered if adding a small amount of a  $^1\text{O}_2$  quencher might prevent the  $^1\text{O}_2$  from reacting with the product. The cycloaddition of alkene **5-1** and diene **5-6** was attempted with several different  $^1\text{O}_2$  quenchers ( $\text{PPh}_3$ ,  $\text{P}(\text{OEt})_3$ ,  $\text{SMe}_2$ , DABCO,  $\text{Et}_3\text{N}$ , etc.), but in all cases no product formation occurred, likely due to quenching of the catalyst.

Kinetic data show that the rate constant for the reaction of  $^1\text{O}_2$  with tetrasubstituted alkene 2,3-dimethyl-2-butene ( $25 \times 10^6 \text{ M}^{-1}\text{s}^{-1}$ ) is significantly faster than the rate of  $^1\text{O}_2$  reacting with a trisubstituted olefin like 1-methylcyclohexene ( $0.16 \times 10^6 \text{ M}^{-1}\text{s}^{-1}$ ) (Figure 5.1).<sup>5</sup> This implies that product oxidation

might be inevitable specifically for cycloadduct **5-7**, which contains a tetrasubstituted olefin. We decided to continue optimization with isoprene (**5-2**) as the diene instead, anticipating that undesired oxidation would be less of an issue with cyclohexene **5-3**.

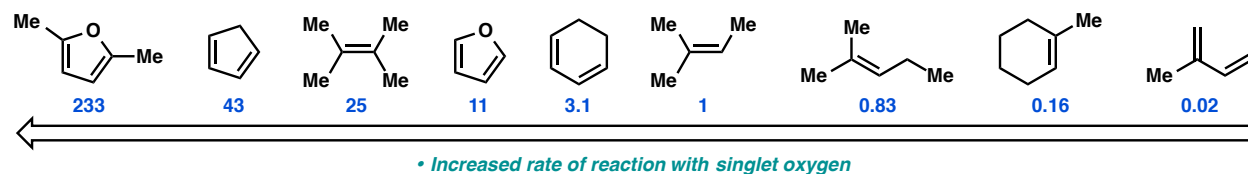


Figure 5.1. Reaction rate constants in  $\text{CHCl}_3$  for reaction with singlet oxygen (rate  $\times 10^6 \text{ M}^{-1}\text{s}^{-1}$ ).

### 5.2.2 Optimization with Isoprene

An abbreviated optimization for the reaction of alkene **5-1** with isoprene (**5-2**) is shown in Table 5.1. Using the same conditions that were developed for the electron-rich dienophile cycloadditions, 70% yield of cyclohexene **5-3** was formed in 6 h (entry 1). In acetonitrile, the reaction was much slower, giving only 26% yield of the product in the same amount of time, and 29% yield of the intermediate vinylcyclobutane **5-5** (entry 2). Increasing or decreasing the concentration of the reaction had very little effect on yield (entries 3 and 4).

Gratifyingly, we found that visible light was a more effective irradiation source for this reaction. The employment of blue LEDs resulted in a 75% yield of cyclohexene **5-3** (entry 5). Also in this reaction, however, we observed a 10% yield of the oxidized product **5-10**, indicating that  $^1\text{O}_2$  might still be an issue. Running the reaction under argon significantly decelerated product formation: only 26% yield of product **5-3** was observed after 6 h (entry 6). Increasing the catalyst loading to 2 mol % and increasing the time to 21 h under argon still only resulted in 57% yield (entry 7). We thought that if catalyst degradation were occurring in the absence of oxygen, then maybe adding a second portion of catalyst after a certain amount a time might allow the reaction to go to completion. This method, however, was not effective, as only 37% yield of product **5-3** was formed (entry 8). We also considered that the size of the reaction

vessel might be influential in limiting the formation of the  $^1\text{O}_2$  side product because of variations in head space. This theory proved to be true. When the reaction was run in a 2-dram vial, 77% yield of product **5-3** was obtained, with 12% yield of the side product (**5-10**) (entry 9). When a 1/2-dram vial was used instead, 71% yield of cyclohexene **5-3** was formed, and only trace amounts of the oxidized product were detected (entry 10). The reaction performed in the 2-dram vial with more head space proceeded faster than the reaction run in the 1/2-dram vial, likely because more air was present. At the same time, however, more of side product **5-10** also formed, likely for the same reason. This suggested that the careful selection of reaction vessel might allow us to optimize yield and minimize oxidation. Also, we anticipated that reactions run on a larger scale would not be as affected by  $^1\text{O}_2$ .

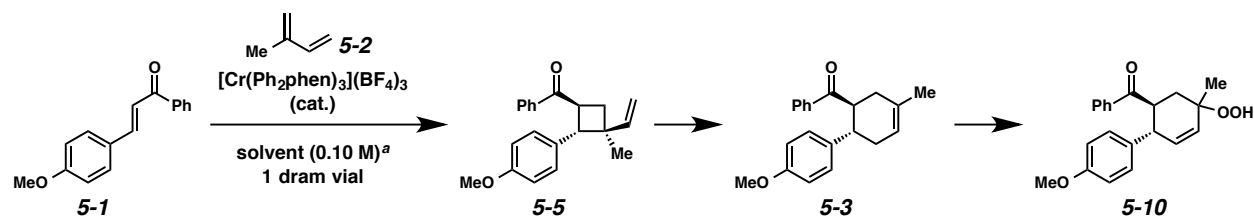
Continuing optimization, we attempted the reaction with a common 23 W compact fluorescent light (CFL) bulb. This reaction proceeded in 81% yield (entry 11). Consistent with previous results, lack of oxygen significantly slowed the cycloaddition (entry 12). Satisfyingly, we found that the catalyst loading could be decreased to 0.5 mol % without decreasing the yield (entry 13). When 2 mol% catalyst was used, however, the yield decreased, perhaps due to an increase in  $^1\text{O}_2$  formation (entry 14). Diene equivalents could also be reduced to 3, providing product **5-3** in 85% NMR yield and 80% isolated yield (entry 15); this set of conditions was concluded to be optimal. Surprisingly, just 1 equiv of diene was also effective, but a lower yield of product **5-3** was obtained (entry 16).

Different light sources were also evaluated. Amazingly, the simplest, least expensive light sources seemed to work the best (entries 17-22). Sunlight was also effective in activating the catalyst; 54% yield of product **5-3** was detected, as well as 21% yield of the oxidized product (**5-10**) (entry 22).

Control experiments confirmed that running the reaction in the absence of light gave no product (**5-3**) or vinylcyclobutane **5-5** (entry 23). Running the reaction with light, but without catalyst, however, resulted in a 20% yield of the vinylcyclobutane (**5-5**) (entry 24), which could form through a purely photochemical [2+2] cycloaddition. These early observations led us to hypothesize that, if the reaction were truly occurring through a [2+2] cycloaddition/rearrangement cascade, then the catalyst must be involved in the [2+2] step in some way. This is based on the fact that only 20% of cyclobutane **5-5** was

formed in the absence of catalyst, but, under Cr catalysis, full conversion to product was achieved in the same amount of time.

Table 5.1. Reaction optimization.



Entry	mol % cat.	Solvent (M)	Diene equiv	Light Source <sup>b</sup>	Atmosphere <sup>c</sup>	NMR Yield (%) <sup>d</sup>		
						5-5	5-3	5-10
1	1	CH <sub>3</sub> NO <sub>2</sub>	10	NUV	air	0	70	< 5
2	1	CH <sub>3</sub> CN	10	NUV	air	29	26	--
3	1	CH <sub>3</sub> NO <sub>2</sub> (0.05)	10	NUV	air	0	71	< 5
4	1	CH <sub>3</sub> NO <sub>2</sub> (0.20)	10	NUV	air	0	69	< 5
5	1	CH <sub>3</sub> NO <sub>2</sub>	10	blue LEDs	air	0	75	10
6	1	CH <sub>3</sub> NO <sub>2</sub>	10	blue LEDs	Ar	3	26	--
7	2	CH <sub>3</sub> NO <sub>2</sub>	10	blue LEDs	Ar (21 h)	4	57	--
8	2 (1+1)	CH <sub>3</sub> NO <sub>2</sub>	10	blue LEDs	Ar (45 h)	3	37	--
9	0.5	CH <sub>3</sub> NO <sub>2</sub>	10	blue LEDs	air (2 dram vial)	0	77	12
10	0.5	CH <sub>3</sub> NO <sub>2</sub>	10	blue LEDs	air (1/2 dram vial)	0	71	< 5%
11	1	CH <sub>3</sub> NO <sub>2</sub>	10	23 W CFL	air	0	81	< 5%
12	0.5	CH <sub>3</sub> NO <sub>2</sub>	10	23 W CFL	Ar (19 h)	26	31	--
13	0.5	CH <sub>3</sub> NO <sub>2</sub>	10	23 W CFL	air	0	82	< 5%
14	2	CH <sub>3</sub> NO <sub>2</sub>	10	23 W CFL	air	0	73	6
15	0.5	CH <sub>3</sub> NO <sub>2</sub>	3	23 W CFL	air	0	85 (80) <sup>e</sup>	< 5%
16	0.5	CH <sub>3</sub> NO <sub>2</sub>	1	23 W CFL	air	0	71	< 5%
17	2	CH <sub>3</sub> NO <sub>2</sub>	10	420 nm light	air	0	68	10
18	1	CH <sub>3</sub> NO <sub>2</sub>	10	350 nm light	air	41	51	--
19	0.5	CH <sub>3</sub> NO <sub>2</sub>	10	white LEDs	air	0	72	< 5%
20	0.5	CH <sub>3</sub> NO <sub>2</sub>	10	daylight LED	air	0	82	5
21	1	CH <sub>3</sub> NO <sub>2</sub>	10	daylight CFL	air	0	69	9
22	1	CH <sub>3</sub> NO <sub>2</sub>	10	sun	air	0	54	21
23	1	CH <sub>3</sub> NO <sub>2</sub>	10	dark	air	0	0	0
24	no cat.	CH <sub>3</sub> NO <sub>2</sub>	10	23 W CFL	air	20	0	0

<sup>a</sup> All reactions were run at a concentration of 0.10 M unless noted.

<sup>b</sup> NUV = 300, 350, and 419 nm light.

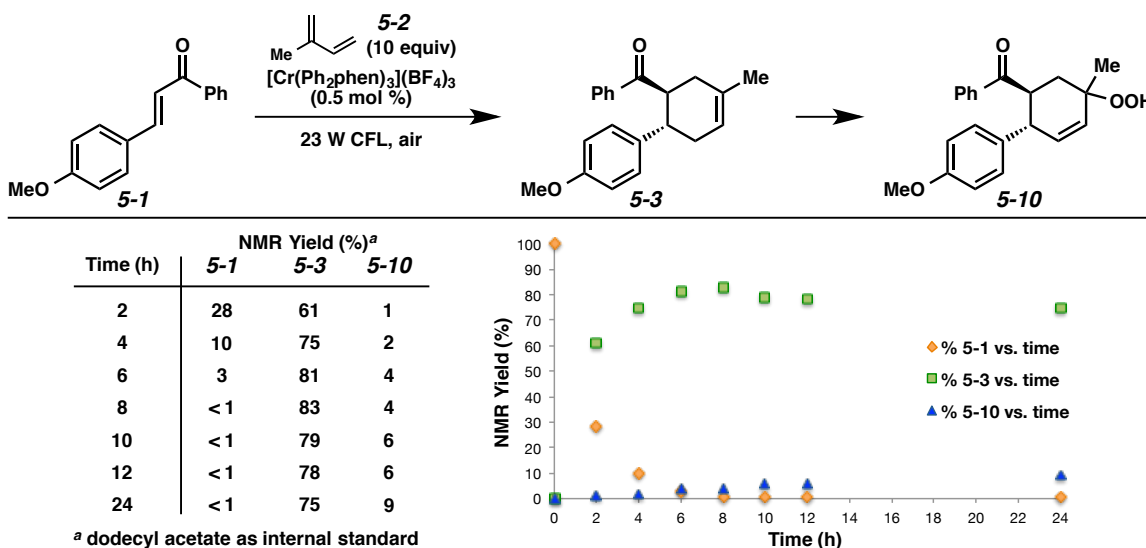
<sup>c</sup> An air atmosphere means the reaction was assembled in air, then capped.

<sup>d</sup> NMR yield with dodecyl acetate as internal standard, the rest of the material is alkene 5-1.

<sup>e</sup> Isolated yield in parentheses.

### 5.2.3 Analysis of Singlet Oxygen Side Reaction

Since it seemed as if  $^1\text{O}_2$  oxidation of our cyclohexene products was going to be unavoidable, we designed an experiment to determine the extent of oxidation that was occurring (Scheme 5.5). Seven vials were filled with an equal portion of a stock solution containing the reaction components. Each reaction was assembled open to air, and then the vial was capped. The reaction mixtures were irradiated with a 23 W CFL, and at each time point a vial was removed from the light and analyzed by  $^1\text{H}$  NMR. This allowed us to detect the amount of oxidized product over time.

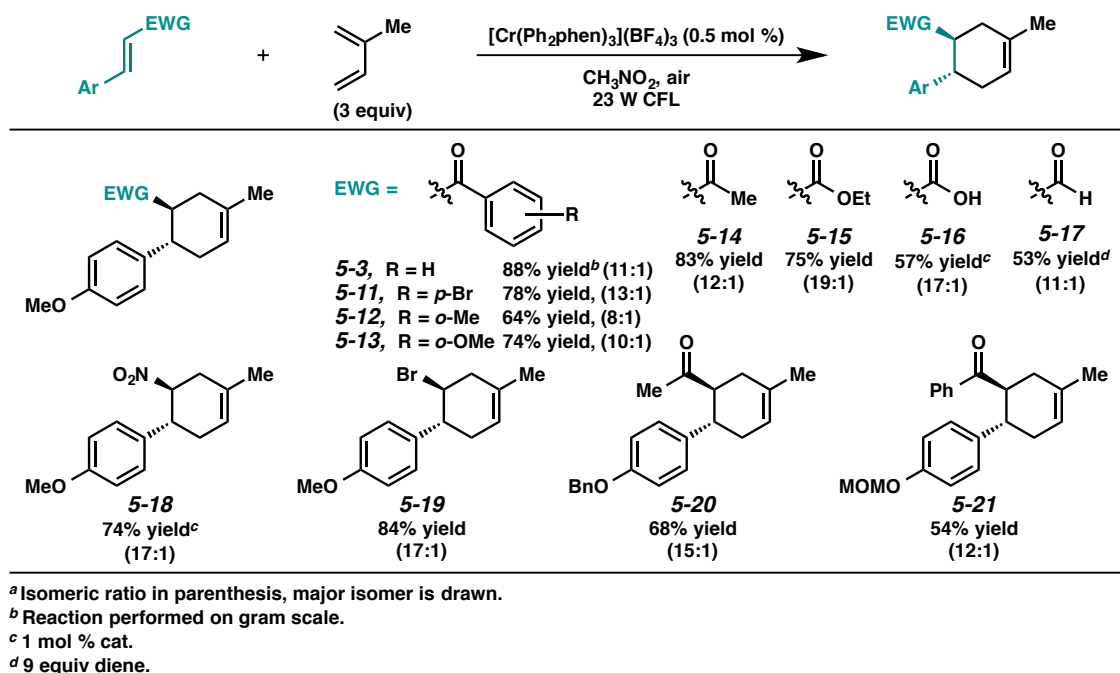


Scheme 5.5. Formation of oxidized product over time.

From this data, we observed that product formation seemed to reach a maximum at around 8 h. The oxidation side product (**5-10**) was also forming during this time, but minimally. After product formation was complete, the  $^1\text{O}_2$  oxidation continued occurring, but the formation of side product **5-10** leveled out at about 9% yield, even 16 h after the starting material was consumed. This effect could be due to catalyst degradation once all of the oxygen in the vial was consumed, ceasing the further

generation of  $^1\text{O}_2$ . Overall, these results indicated that product oxidation by  $^1\text{O}_2$  was unlikely to be a major problem as long as the reactions were monitored carefully.

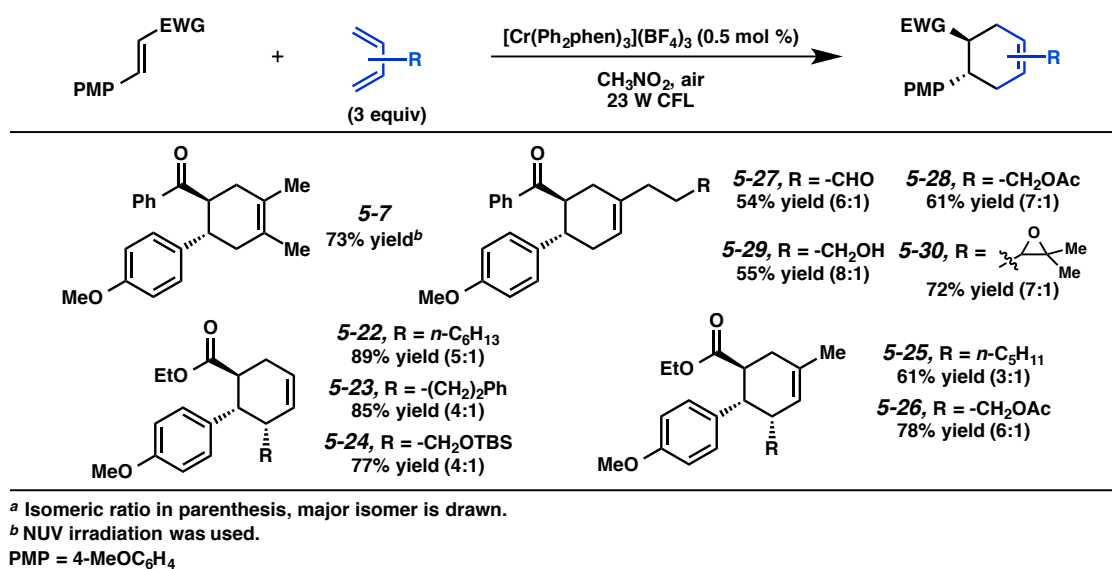
### 5.3 Substrate Scope



Scheme 5.6. Scope of electron-poor alkenes.<sup>a</sup>

A variety of alkenes substituted with electron-poor functional groups were proficient dienophiles in this transformation (Scheme 5.6). Differentially substituted chalcones reacted in good yields (**5-11–5-13**). Gratifyingly, the cycloaddition of phenyl ketone **5-1** and isoprene (**5-2**) could be performed on gram scale, resulting in 88% yield of cyclohexene **5-3**. A methyl ketone and an ester were also suitable substrates, providing cyclohexenes **5-14** and **5-15** in 83% and 75% yield, respectively. Carboxylic acid and aldehyde functionalities were tolerated, but these reactions were more difficult. Good yields of products **5-16** and **5-17** were obtained, even with modifications to the standard conditions. Nitrocyclohexene **5-18** also required an increase in catalyst loading; however, a 74% yield was obtained.

In this case, the crude NMR spectra of incomplete reaction mixtures revealed a large amount of the corresponding unreacted vinylcyclobutane. Experiments by our collaborators in the Shores Lab (CSU) suggest that the rearrangement of the nitro-substituted vinylcyclobutane is slower than its formation, which perhaps indicates why increasing the catalyst loading allowed this reaction to go to completion. A vinyl bromide reacted smoothly to afford cyclohexene **5-19**. The mechanism of this cycloaddition, however, is likely the same mechanism as we proposed for the electron-rich dienophile cycloadditions, since the reduction potential of  $\beta$ -bromo-4-methoxystyrene ( $E_{1/2} = +1.45 \text{ V}$ )<sup>2</sup> is much closer to that of the catalyst ( $E_{1/2}^* = +1.40 \text{ V}$ ). Lastly, substrates with aryl groups other than *para*-methoxyphenyl (PMP) were found to be proficient for the reaction, albeit forming cyclohexenes **5-20** and **5-21** in lower yields. Overall, high regioselectivities favoring the reversed Diels-Alder products were obtained (>10:1).



Scheme 5.7. Scope of diene.<sup>a</sup>

Dienes other than isoprene also reacted efficiently (Scheme 5.7). Symmetrical 2,3-dimethyl-1,3-butadiene (**5-6**) reacted with alkene **5-1** to give the corresponding cyclohexene (**5-7**) in 73% yield, along with small amounts of peroxides **5-8** and **5-9**. Curiously, NUV irradiation provided adduct **5-7** in higher yield than irradiation with the 23 W CFL. Dienes substituted at the terminal position reacted in high

yields (5-22–5-24); however, the regioselectivity of these processes was considerably lower than with isoprene. Terminal dienes also substituted at the 3-position gave cyclohexenes 5-25 and 5-26 in lower regioselectivities as well, indicating that, even with internal substitution, substitution at the terminal position has a significant impact on the selectivity of the cycloaddition. General functional group tolerance was also tested with different dienes derived from myrcene. Dienes containing a tethered aldehyde (5-27), acetate (5-28), alcohol (5-29), and epoxide (5-30) were all competent cycloaddition partners; however, lower yields were obtained compared to isoprene.

### 5.3.1 Unsuccessful Substrates

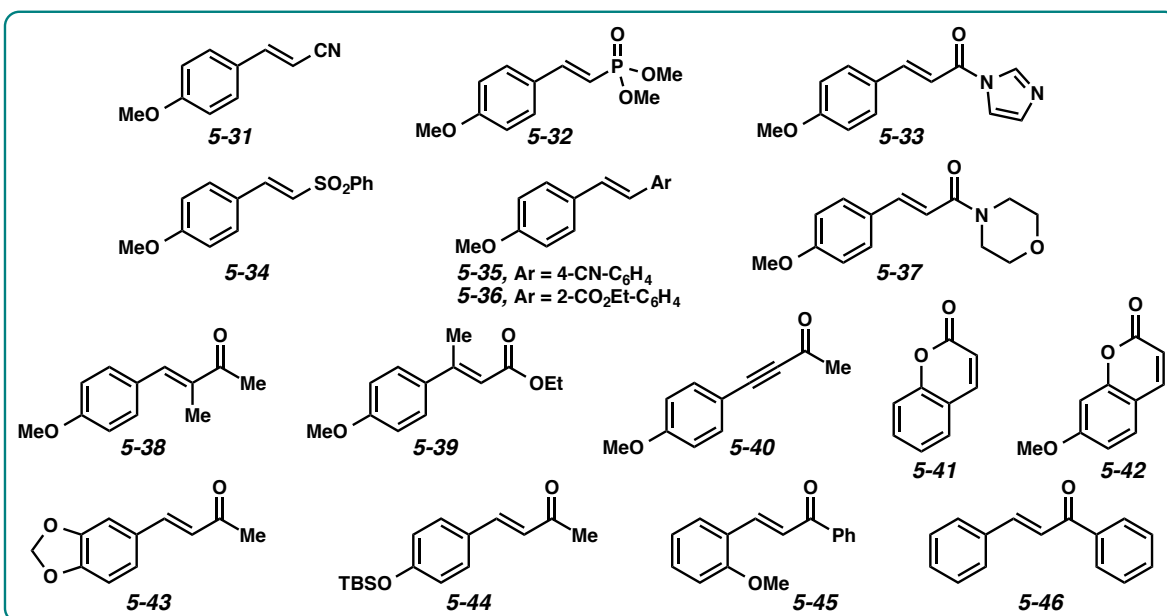


Figure 5.2. Unsuccessful dienophiles.

Substrates that were not successful in this transformation are shown in Figure 5.2. Because we do not yet have a complete understanding of the reaction mechanism, it is difficult to deduce exactly why some of these substrates did not work. Most of the electron-poor alkenes showed minimal reactivity under the photocatalytic conditions (5-31–5-34, 5-37), but some were completely unreactive (5-35 and 5-36).

Additionally, trisubstituted alkenes **5-38** and **5-39** formed only trace product, perhaps due to sterics, and alkyne **5-40** was not reactive. Coumarins **5-41** and **5-42** also gave essentially no reaction under the cycloaddition conditions. This result is surprising, considering that the majority of enone/alkene [2+2] cycloadditions are reported with cyclic enones; acyclic enones are prone to *E/Z*-isomerization, and thus are typically unproductive toward cycloadditions.<sup>6</sup>

Electron-rich aryl groups other than *para*-methoxyphenyl (PMP), such as in substrates **5-43–5-45**, were overall much less effective for this transformation. Nucleophilic groups at the *ortho* position could potentially add into the radical cation of the alkene, perhaps inhibiting the cycloaddition in the case of 2-methoxychalcone (**5-45**).<sup>7</sup> In addition, Bauld has suggested that the PMP group seems to be especially proficient at accelerating vinylcyclobutane rearrangements.<sup>8</sup> Along these lines, when chalcone (**5-46**) was exposed to the Cr conditions, only a trace amount of the corresponding vinylcyclobutane was formed.

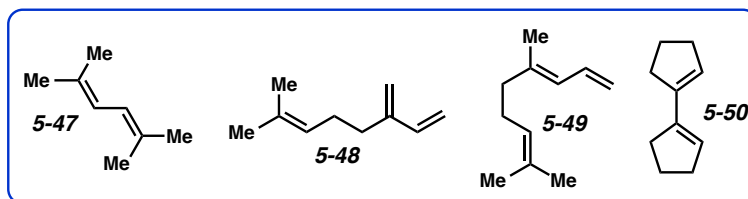
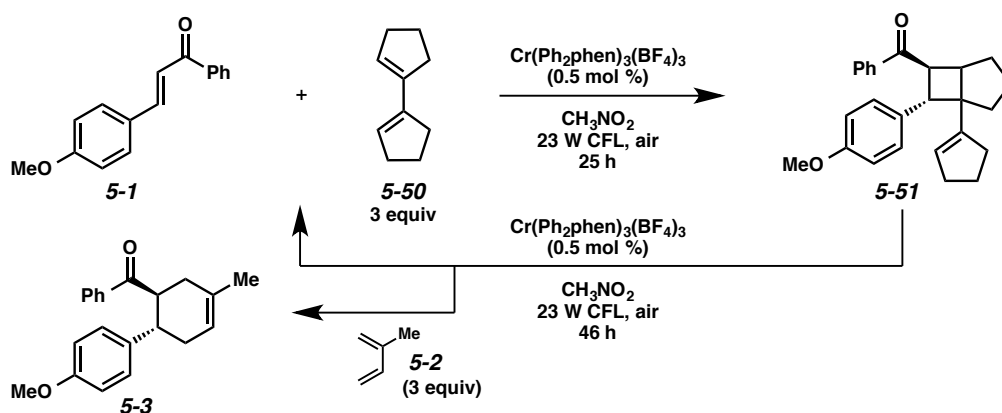


Figure 5.3. Unsuccessful dienes.

In terms of diene scope, the same dienes that were unsuccessful in the radical cation Diels-Alder reaction (Chapter 4.4.5) were also unsuccessful here (**5-47–5-49**), likely for similar reasons (Figure 5.3). Additionally, bicyclopentenyldiene **5-50**, which has a relatively low reduction potential ( $E_{1/2} = +1.22$  V)<sup>9</sup> reacted with enone **5-1** to give vinylcyclobutane **5-51**, but not the cyclohexene (Scheme 5.8). Radical cation cycloadditions between alkenes and diene **5-50**, where the diene is the more oxidizable component, generally result in [2+2] rather than [4+2] cycloadditions.<sup>10</sup> This does not explain, though, why vinylcyclobutane **5-51** did not rearrange at all, since rearrangement is observed in similar examples.<sup>9,11</sup> In fact, when vinylcyclobutane **5-51** was exposed to the Cr conditions, a retro [2+2] occurred to give the

starting enone (**5-1**) and, in the presence of isoprene (**5-2**), cyclohexene **5-3**. Retro [2+2] cycloadditions of oxidizable cyclobutanes are known;<sup>12</sup> however, vinylcyclobutane **5-5**, which results from enone **5-1** and isoprene (**5-2**), does not revert (Chapter 5.6.1.2). This lack of cycloreversion could be because the reduction potentials of both enone **5-1** and isoprene (**5-2**) are high ( $E_{1/2} = +2.00$  V and  $+1.98$  V, respectively) compared to the reduction potential of the bicyclopentenyl diene (**5-50**), so the formation of the corresponding radical cation of either species would be unfavorable. Overall these results may indicate that vinylcyclobutanes where the corresponding diene has a lower reduction potential than the vinylcyclobutane itself might be more prone to cycloreversion than rearrangement.

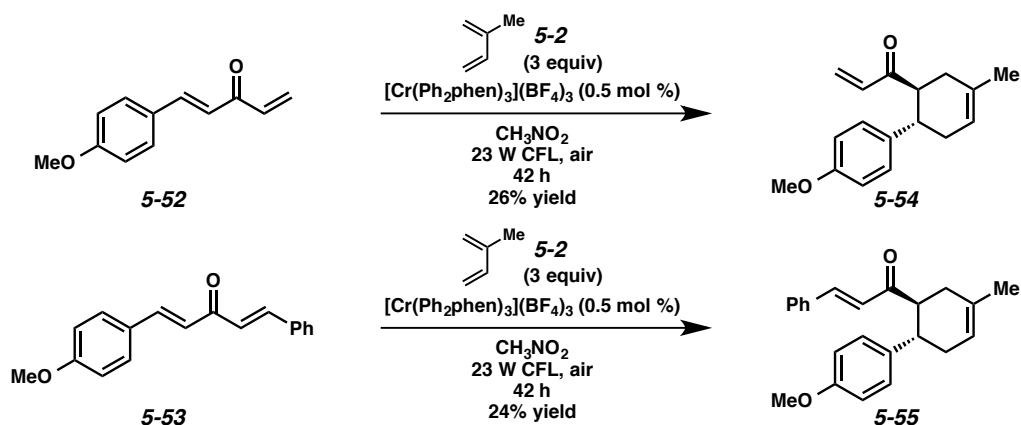


Scheme 5.8. Cycloaddition of bicyclopentenyl diene **5-50**.

### 5.3.2 Alkene Selectivity of [2+2] Cycloaddition

Vinylketones **5-52** and **5-53** were designed to test the effect of the PMP group on the selectivity of the putative [2+2] cycloaddition (Scheme 5.9). In each of these substrates, a [2+2] reaction between either of the  $\alpha,\beta$ -unsaturated alkenes of the enone is possible, but we wondered if the cycloaddition between the diene and the PMP substituted alkene would be preferred. When these vinylketones were exposed to the standard Cr conditions, the starting material was consumed and the desired cyclohexenes (**5-54** and **5-55**) were formed, albeit in low yields. A variety of unidentified cycloadducts were also formed. Additionally,

the undesired cycloadducts seemed to predominate more in the reaction of the styrenyl ketone (**5-53**), likely due to the lower energy of the styrenyl alkene compared to the vinyl one (**5-52**). Ultimately, these experiments show that even if the Cr catalyzed [2+2]/rearrangement process were selective for PMP-substituted alkenes, the presence of other alkenes in the molecule may not be tolerated because of the abundance of possible [2+2] cycloadditions that can occur under photochemical conditions.



Scheme 5.9. Cycloaddition of vinyl enones.

### 5.3.3 Attempts to Replace PMP in [2+2]/ Rearrangement Cascade

We also wished to see if groups other than PMP could incite the vinylcyclobutane rearrangement through single electron oxidation. Ideally, this process would yield cycloadducts containing additional functional group handles for further synthetic modification. Figure 5.4 shows the reduction potentials of different oxidizable moieties. Though the actual reduction potentials of these vinylcyclobutanes have not been reported, it seems as if the reduction potentials of the specific groups on their own may be comparable to the reduction potentials of the corresponding substituted vinylcyclobutanes. For instance, the reduction potential of 4-methylanisole is +1.72 V, and the reduction potential of the corresponding vinylcyclobutane (**5-5**) is +1.68 V. Based on the values shown in Figure 5.4, we hypothesized that vinylcyclobutanes substituted with some of these groups might also be able to rearrange.

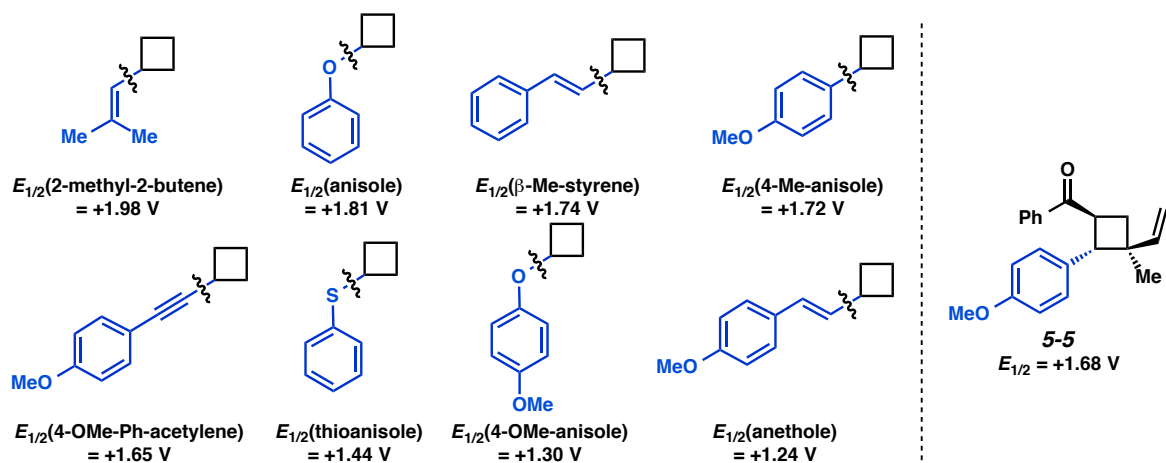
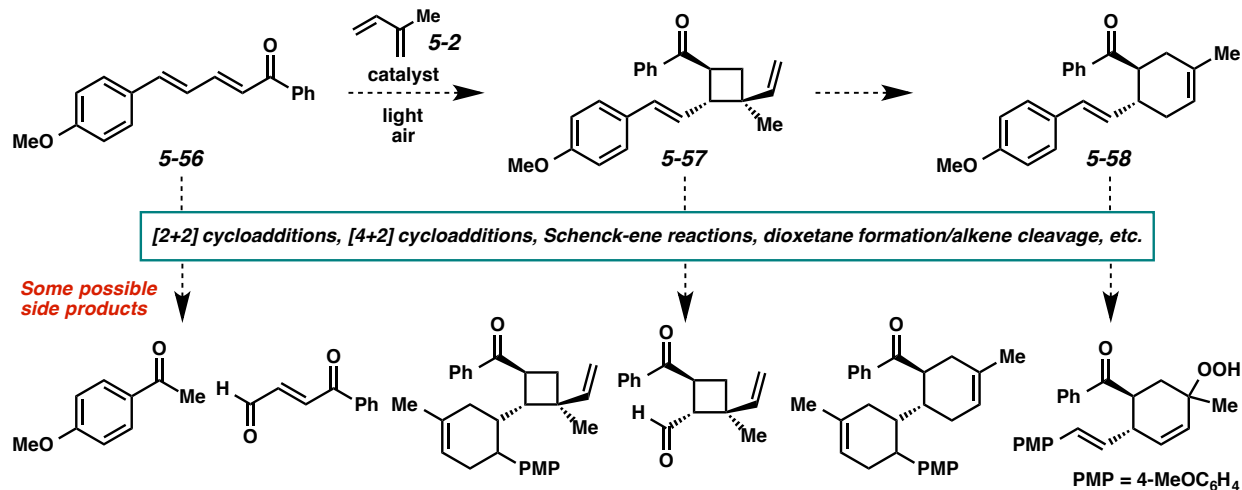


Figure 5.4. Reduction potentials of different functionalities.<sup>13</sup>

We began by looking at the cycloaddition of enone **5-56** and isoprene (**5-2**) (Scheme 5.10). The putative vinylcyclobutane (**5-57**) that would form in this reaction would be substituted with a highly oxidizable anethole group, which could initiate a vinylcyclobutane rearrangement to cyclohexene **5-58**.



Scheme 5.10. Possible side products that could form under photooxidative conditions.

Like with vinylenones **5-52** and **5-53**, the success of this process would be dependent on the selectivity of the [2+2] cycloaddition between the diene and the  $\alpha,\beta$ -unsaturated alkene. Additionally, radical cation cycloadditions between isoprene and the anethole moiety at any step of the reaction could

also occur, as well as reactions with  $^1\text{O}_2$  (Scheme 5.10). When all of the possible side reactions are taken into account, it seems unlikely that cyclohexene **5-58** would be formed at all.

Ultimately, we did achieve some success with this transformation, but the reaction was not efficient. A variety of catalyst conditions were attempted for the cycloaddition of enone **5-56** and isoprene (**5-2**) (Table 5.2).  $\text{Cr}(\text{Ph}_2\text{phen})_3^{3+}$  conditions under air provided the product (**5-58**) in 13% yield (entry 1), and running this reaction under Ar slowed it considerably (entry 2). Of the other Cr catalysts,  $\text{Cr}(\text{phen})_3^{3+}$  ( $E_{1/2}^* = +1.45 \text{ V}$ ,  $E^{\text{T}} = 39 \text{ kcal/mol}$ )<sup>3</sup> provided the product in the highest yield (20% yield, entry 3). Running the  $\text{Cr}(\text{phen})_3^{3+}$  reactions in  $\text{CH}_2\text{Cl}_2$  or  $\text{CH}_3\text{CN}$  increased the yield to 28% and 22% yield, respectively (entries 6 and 7). NUV light was also attempted, but did not significantly increase the yield (entry 8).

The reaction was also attempted with  $\text{Ru}(\text{bpz})_3^{2+}$ , which has a similar reduction potential to  $\text{Cr}(\text{phen})_3^{3+}$ , but a higher excited state energy ( $E_{1/2}^* = +1.45 \text{ V}$ ,  $E^* = 48 \text{ kcal/mol}$ )<sup>14</sup>, but similar results were obtained (22% yield, entry 9). Next we attempted the cycloaddition with the strongly photooxidizing triphenylpyrilium tetrafluoroborate (TPT) ( $E_{1/2}^* = +2.28 \text{ V}$ ,  $E^{\text{T}} = 53 \text{ kcal/mol}$ )<sup>15</sup>. Under air, the starting enone (**5-56**) was completely consumed and a 33% yield of product **5-58** was formed (entry 10). Another strong photooxidant, 9-mesityl-10-methylacridinium tetrafluoroborate (Mes-Acr) ( $E_{1/2}^* = +2.06 \text{ V}$ ,  $E^{\text{T}} = 45 \text{ kcal/mol}$ )<sup>16</sup> gave us 42% yield of product **5-58** when run in DCE (entry 11). This yield was the highest we were able to obtain, though, as modifications to atmosphere or solvent gave lower yields (entry 12-15), and even doubling the catalyst loading did not improve the outcome (entry 16). In all of these reactions, the remaining composition of the mass balance was a complex mixture of cycloadducts.

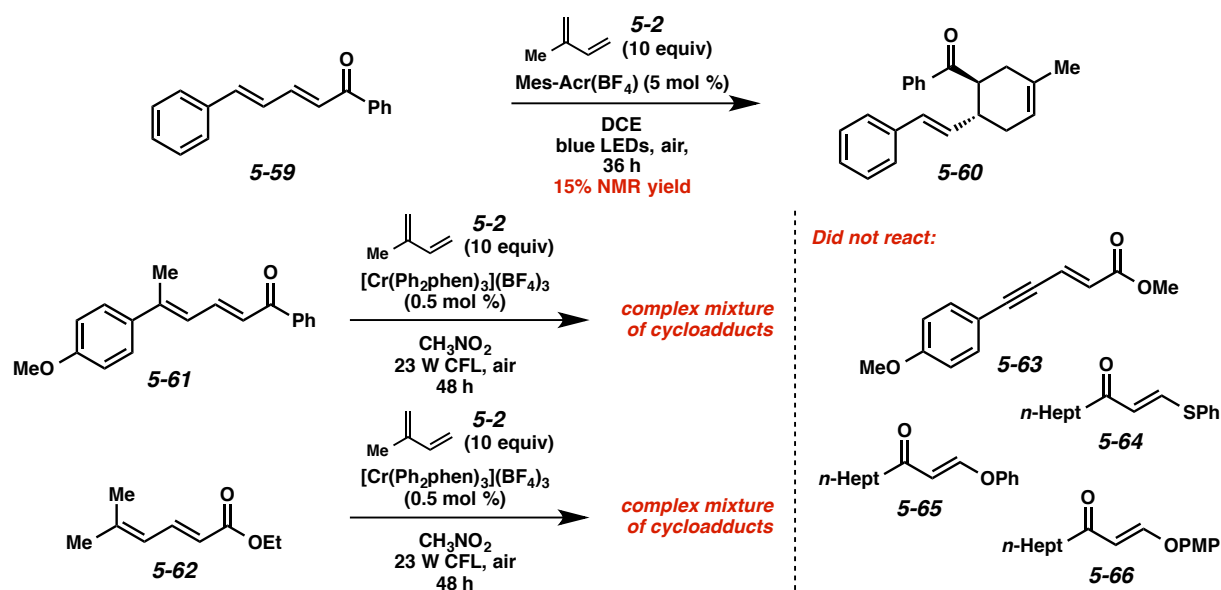
Table 5.2. Cycloaddition of enone **5-56**.

Entry	Catalyst (mol %)	Solvent	Light source	Atmosphere	Time (h)	Yield <b>5-58</b> (%) <sup>a</sup>	<b>5-56</b> (%) <sup>b</sup>
1	[Cr(Ph <sub>2</sub> phen) <sub>3</sub> ](BF <sub>4</sub> ) <sub>3</sub> (5)	CH <sub>3</sub> NO <sub>2</sub>	23 W CFL	air	46	13	20
2	[Cr(Ph <sub>2</sub> phen) <sub>3</sub> ](BF <sub>4</sub> ) <sub>3</sub> (5)	CH <sub>3</sub> NO <sub>2</sub>	23 W CFL	Ar	68	8	50
3	[Cr(phen) <sub>3</sub> ](OTf) <sub>3</sub> (5)	CH <sub>3</sub> NO <sub>2</sub>	23 W CFL	air	46	20	15
4	[(phen) <sub>2</sub> Cr(dmcbpy)](OTf) <sub>3</sub> (5)	CH <sub>3</sub> NO <sub>2</sub>	23 W CFL	air	46	17	19
5	[Cr(dmcbpy)](BF <sub>4</sub> ) <sub>3</sub> (5)	CH <sub>3</sub> NO <sub>2</sub>	23 W CFL	air	46	13	32
6	[Cr(phen) <sub>3</sub> ](OTf) <sub>3</sub> (5)	CH <sub>2</sub> Cl <sub>2</sub>	23 W CFL	air	46	28	9
7	[Cr(phen) <sub>3</sub> ](OTf) <sub>3</sub> (5)	CH <sub>3</sub> CN	23 W CFL	air	46	22	17
8	[Cr(phen) <sub>3</sub> ](OTf) <sub>3</sub> (5)	CH <sub>3</sub> NO <sub>2</sub>	NUV	air	46	22	8
9	Ru(bpz) <sub>3</sub> (PF <sub>6</sub> ) <sub>2</sub> (5)	CH <sub>3</sub> NO <sub>2</sub>	23 W CFL	air	46	22	7
10	TPT (5)	CH <sub>3</sub> CN	blue LEDs	air	36	33	0
11	Mes-Acr(BF <sub>4</sub> ) (5)	DCE	blue LEDs	air	36	42	11
12	Mes-Acr(BF <sub>4</sub> ) (5)	DCE	blue LEDs	Ar	36	21	21
13	Mes-Acr(BF <sub>4</sub> ) (5)	CH <sub>3</sub> NO <sub>2</sub>	blue LEDs	air	36	30	18
14	Mes-Acr(BF <sub>4</sub> ) (5)	CH <sub>3</sub> CN	blue LEDs	air	36	8	21
15	Mes-Acr(BF <sub>4</sub> ) (5)	CH <sub>2</sub> Cl <sub>2</sub>	blue LEDs	air	36	22	12
16	Mes-Acr(BF <sub>4</sub> ) (10)	DCE	blue LEDs	air	36	28	21

<sup>a</sup> Yield determined by <sup>1</sup>H NMR with dodecyl acetate as an internal standard.

<sup>b</sup> Yield for recovered **5-56**; the rest of mass balance is a complex mixture of cycloadducts.

Anticipating that the *para*-methoxy group might not be necessary for the rearrangement to occur, we also attempted this transformation with enone **5-59** (Scheme 5.11). Cyclohexene **5-60** does not have an anethole moiety like cyclohexene **5-58**, so any additional undesired radical cation cycloadditions would be prevented. Under the Mes-Acr conditions, however, product **5-60** was formed in only 15% NMR yield, accompanied by a complex mixture of cycloadducts. We also attempted the cycloaddition of substrate **5-61** with an extra methyl group on the alkene. We thought that this methyl group might inhibit the reactivity of this alkene toward undesired cycloadditions, since radical cation cycloadditions of trisubstituted electron-rich alkenes were not successful in our previous studies. Still, a complex mixture of cycloadducts was obtained.



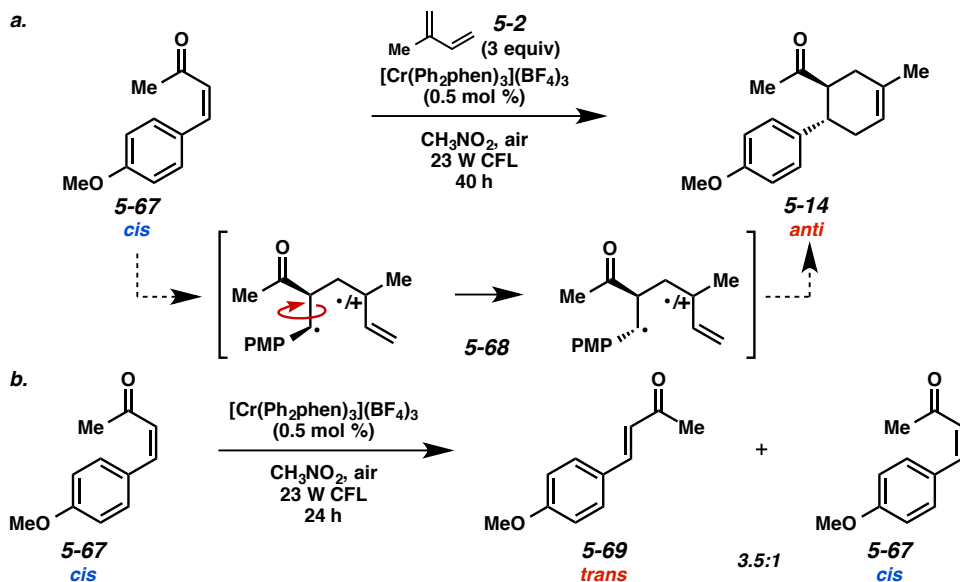
Scheme 5.11. Other attempted substrates.

Lastly, we attempted several other substrates with different oxidizable groups. Ester **5-62** also resulted in a complex mixture of cycloadducts, and enyne **5-63**, interestingly, did not react at all (Scheme 5.11). We also explored enones with a vinyl sulfide (**5-64**) and vinyl ethers (**5-65** and **5-66**). The oxidation of these groups have been demonstrated in the literature to incite vinylcyclobutane rearrangements,<sup>8,9</sup> but no reaction occurred under our conditions, indicating that perhaps these alkenes were not reactive toward the [2+2] cycloaddition. Ultimately, we did not have much success with the cycloaddition employing groups other than PMP; additional oxidizable alkenes led to side products, and the non-alkene groups were unreactive.

#### 5.4 Stereoconvergence

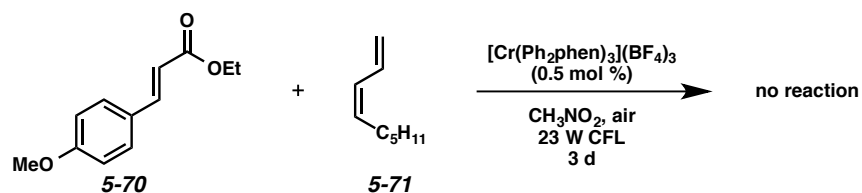
The cycloadditions resulted in exclusively the anti cyclohexene products. Interestingly, when *cis*-enone **5-67** was exposed to the reaction conditions, still just the anti product formed (**5-14**). Since these [2+2] cycloadditions are stepwise and proceed through radical intermediates (**5-68**), it is possible that rotation

can occur after the first bond forming step to give the lower energy anti product (Scheme 5.12a). If the reaction were proceeding through a radical cation mechanism, rotation would also be allowed. Conversely, isomerization of *cis*-enone **5-67** to *trans*-enone **5-69** may be occurring under the reaction conditions prior to any interaction with the diene; when the *cis*-enone was exposed to the reaction conditions minus diene, considerable isomerization to the *trans*-enone occurred (Scheme 5.12b). The fact that coumarins **5-41** and **5-42**, which are not able to isomerize to their *trans* isomers, were not reactive under the Cr conditions may indicate that latter hypothesis is correct, and only *trans* alkenes are suitable substrates for this transformation.



Scheme 5.12. (a) Formation of *anti*-cyclohexene from *cis*-enone. (b) Isomerization of *cis*-enone.

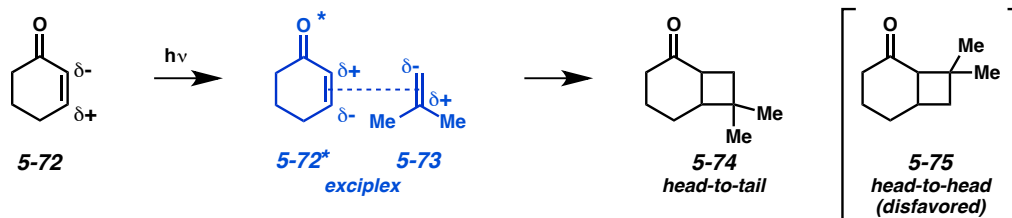
We also attempted the cycloaddition of ester **5-70** with terminally substituted (*Z*)-diene (**5-71**) (Scheme 5.13). Diene **5-71**, however, was completely unreactive; not even the [2+2] product formed. A better understanding of the reaction mechanism may be necessary to understand this result.



Scheme 5.13. Unsuccessful (Z)-diene.

## 5.5 Regioselectivity

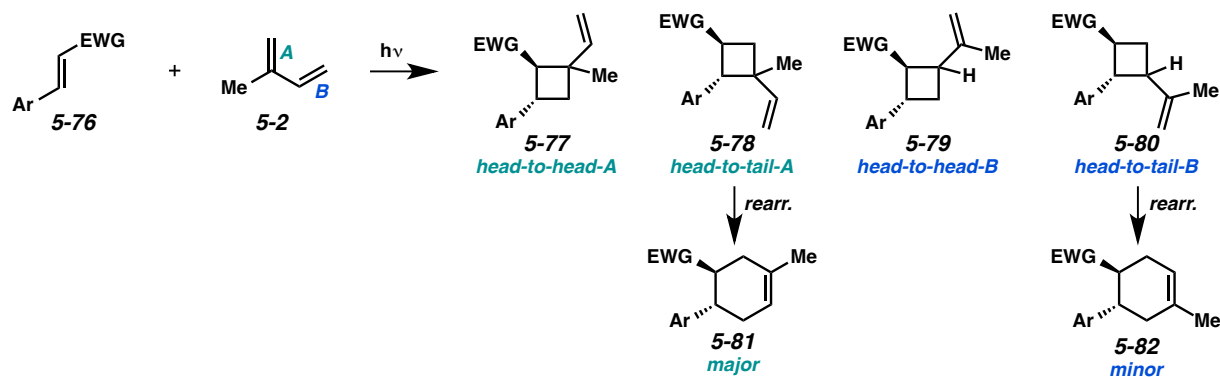
As mentioned previously, the regioselectivity of this net [4+2] cycloaddition is the opposite of the regioselectivity that is observed under normal Diels-Alder conditions. If the reaction is actually occurring through a [2+2]/rearrangement, then the regiochemical outcome is likely established during the photochemical [2+2] cycloaddition.<sup>17</sup> The regioselectivity of enone/alkene [2+2] cycloadditions was explored by Corey and coworkers over 50 years ago.<sup>18</sup> The irradiation of an enone (5-72) with light of the appropriate wavelength will cause an excited state enone (5-72\*) to form (Scheme 5.14). In the excited state, the polarity of the alkene is reversed, so the enone is now electrophilic at the  $\alpha$ -position and nucleophilic at the  $\beta$ -position. Thus, alkenes that are electron-rich (5-73) will add to the enone in a head-to-tail fashion (5-74).



Scheme 5.14. General explanation of enone/alkene [2+2] regioselectivity.

In the reaction of isoprene (5-2) with an electron-poor alkene, four possible cyclobutanes can form: the head-to-head and head-to-tail cyclobutanes between the dienophile and alkene A of the diene,

and the head-to-head and head-to-tail cyclobutanes between the dienophile and alkene *B* of the diene. As shown in Scheme 5.15, in only the head-to-tail isomers (**5-78** and **5-80**) are the vinyl group and the electron-rich aryl group on adjacent carbons, so only these two cyclobutanes are able to rearrange to cyclohexenes. The major cyclohexene isomer (**5-81**) that we observe with the reversed Diels-Alder regioselectivity results from the rearrangement of cyclobutane **5-78**, and the minor cyclohexene isomer (**5-82**) results from rearrangement of the other head-to-tail cyclobutane (**5-80**). The formation of cyclobutane **5-78** is likely favored over cyclobutane **5-80** because alkene *A* is more electron rich than alkene *B*.



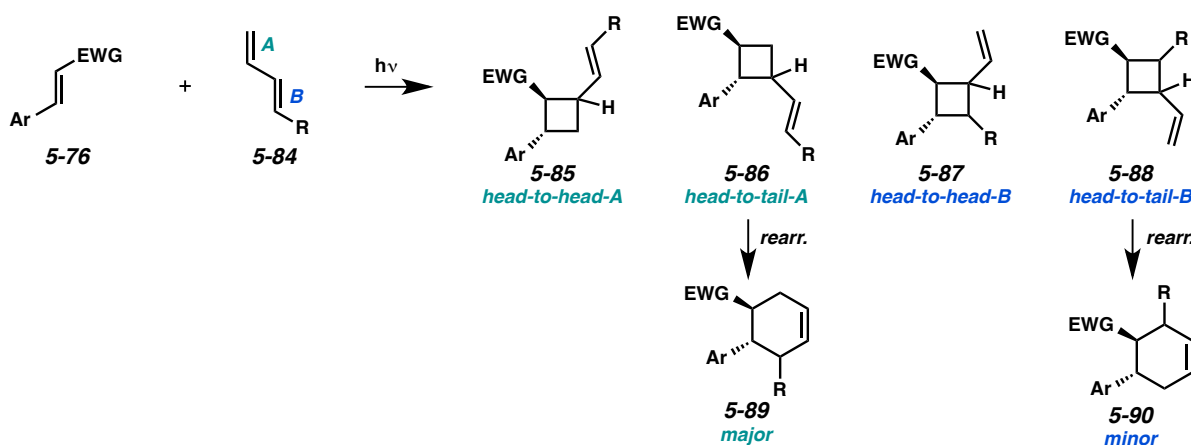
Scheme 5.15. Possible regiochemical explanation.

In the chance that this reaction is proceeding through the radical cation of the electron-poor alkene, this reversed selectivity will prevail because putative distonic radical cation intermediate **5-83** would place the radical at the stable benzylic position and the cation at the tertiary allylic position (Scheme 5.16).



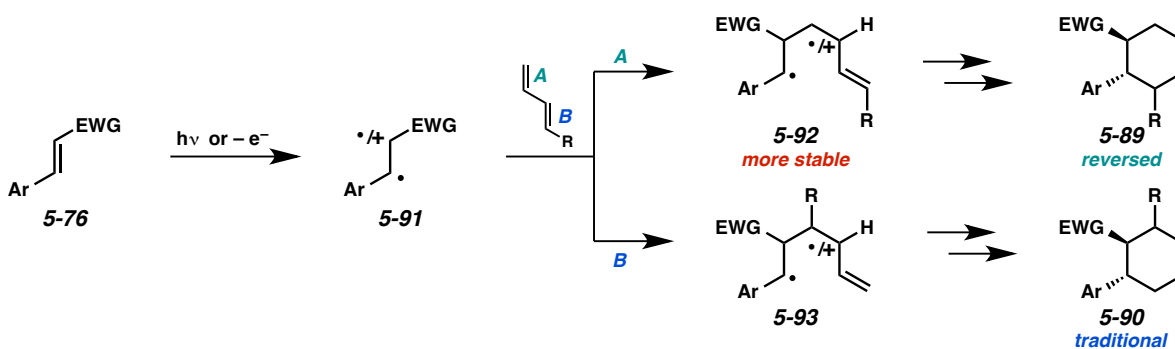
Scheme 5.16. Reversed regioselectivity through radical cation mechanism.

With the 1-substituted dienes, lower regioselectivities were observed. Again, there are four possible adducts that can form in a [2+2] cycloaddition between the electron-poor alkene (**5-76**) and the terminal diene (**5-84**), and only two of these (head-to-tail isomers **5-86** and **5-88**) are able to rearrange to the corresponding cyclohexenes (**5-89** and **5-90**) (Scheme 5.17).



Scheme 5.17. Proposed regiochemical explanation for 1-substituted dienes.

In this case, the difference in reactivity between the two alkenes of the diene is less defined. Whether the cycloaddition is proceeding through a photoinduced [2+2] mechanism or a radical cation process, alkene *A* is ultimately favored to react with the dienophile (**5-91**) because a more stable allylic diradical or distonic radical cation intermediate (**5-92**) is formed (Scheme 5.18).



Scheme 5.18. Possible regiochemical explanation for 1-substituted dienes.

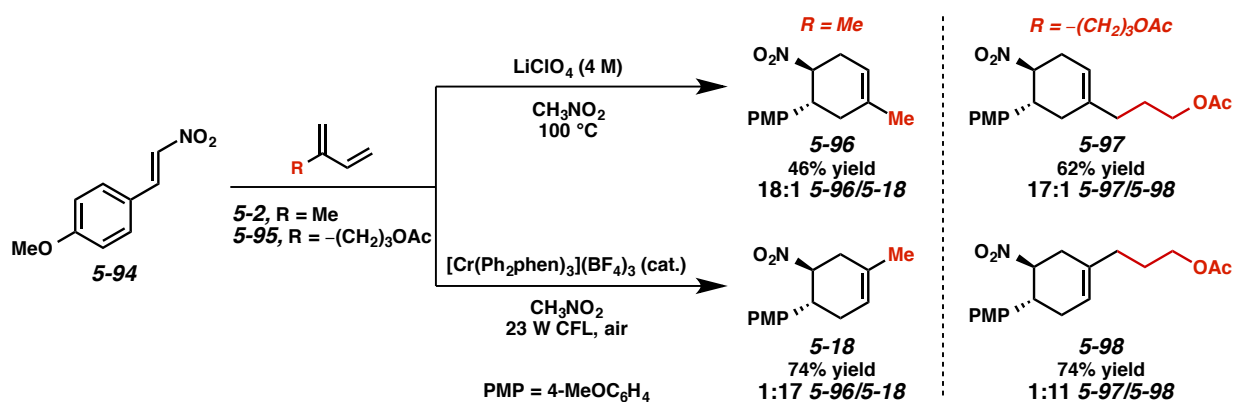
Interestingly, however, some [2+2] cycloadditions of 1-substituted dienes under direct irradiation can give elevated ratios of cycloadditions with internal alkenes of dienes (*B*).<sup>19</sup> This side reaction may be a minor source of vinylcyclobutane **5-88**, which would rearrange to the traditional Diels-Alder adduct (**5-90**).

Overall, the internally substituted dienes like isoprene (**5-2**) displayed higher regioselectivities than the terminally substituted dienes. This may be due to the formation of a tertiary (**5-83**) versus a secondary (**5-92**) allylic radical cation intermediate. In the case of products **5-25** and **5-26**, however, which result from dienes that are both internally and terminally substituted, relatively low regioselectivities were still observed, indicating that other factors may be operative.

### 5.5.1 Regioselectivity Comparison to Normal Diels-Alder Conditions

The expected regiochemical outcome of a normal electron-demand Diels-Alder reaction can be determined by comparing molecular orbital coefficients of the frontier molecular orbitals for the diene and dienophile, or by simply drawing resonance structures. Efforts to reverse the natural regioselectivity of Diels-Alder cycloadditions have been reported, but only a handful of strategies have seen success.<sup>20</sup> These include either the incorporation of electronically steering substituents that can be subsequently removed,<sup>21</sup> or catalyzed vs. thermal/noncatalyzed cycloadditions that adjust the molecular orbital coefficients of the reactants (e.g., selective coordination of a sterically unhindered carbonyl).<sup>22</sup> So far there has been no report of a purely conditions-based approach to generate Diels-Alder adducts of reversed regioselectivity.

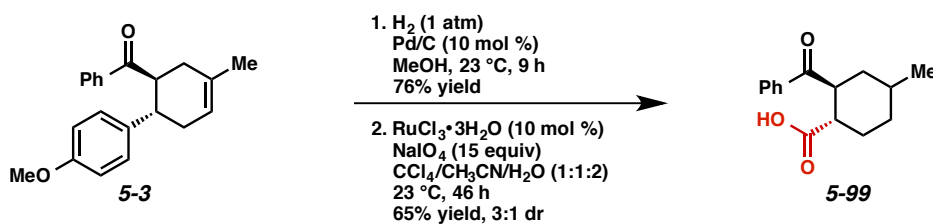
To exhibit the regiodivergency of this Cr-photocatalyzed method, we compared the regioselectivity of the cycloaddition between nitroolefin **5-94** and dienes **5-2** and **5-95** using both Lewis acid-catalyzed Diels-Alder conditions (LiClO<sub>4</sub> in nitromethane, 100 °C)<sup>23</sup> and our Cr conditions (Scheme 5.19). These complementary reaction conditions provided the cycloadducts in nearly complete opposite regioselectivity, demonstrating the singularity of this Cr-photocatalyzed cascade approach.



Scheme 5.19. Regiochemical comparison to traditional Diels-Alder conditions.

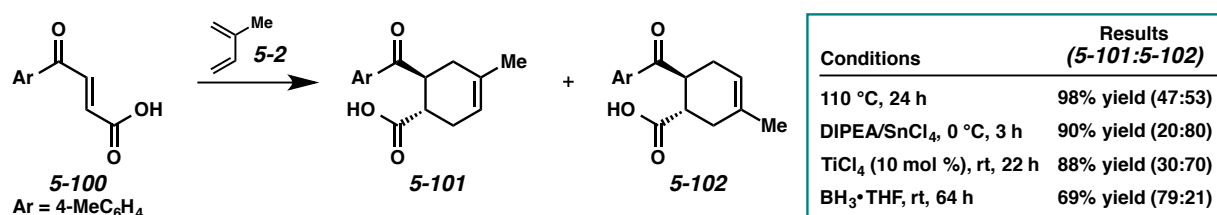
### 5.5.2 Oxidative Aryl Cleavage

Clearly, one of the limitations of this reaction is the necessity of the PMP or other select electron-rich aryl group. In an effort to demonstrate that further synthetic manipulations of the product aryl group were still possible, we proposed that the PMP group of the cyclohexene products could be oxidatively cleaved to give the corresponding carboxylic acids. Using conditions developed by Sharpless<sup>24</sup> and modified by Aggarwal,<sup>25</sup> we attempted the oxidative aryl cleavage of cyclohexene **5-3**. To avoid cleavage of the alkene, cyclohexene **5-3** was first hydrogenated, and then exposed to the oxidative conditions (Scheme 5.20). This furnished the carboxylic acid product (**5-99**) in 65% yield after 46 h. The hydrogenation of the alkene also resulted in reduction of the phenyl ketone to the alcohol, but this was oxidized to the ketone under the cleavage conditions.



Scheme 5.20. Oxidative cleavage of PMP group.

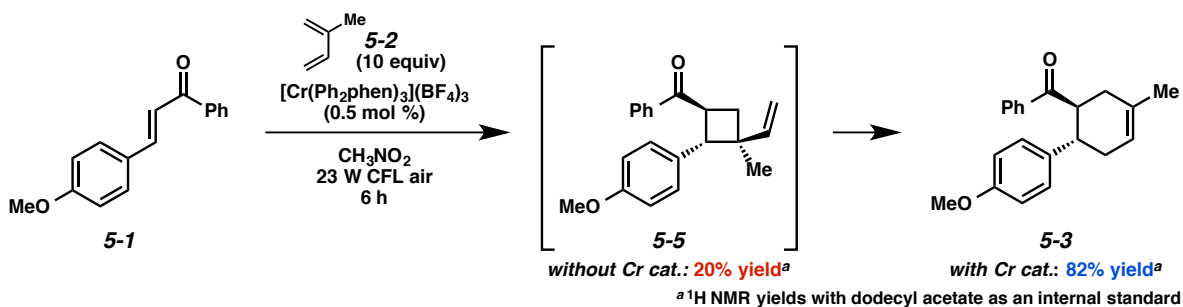
The use of the PMP group as a surrogate for a carboxylic acid provides unique access to cyclohexane rings with substitution patterns that might be difficult to obtain through the traditional Diels-Alder reaction of acrylic acid **5-100** and isoprene (**5-2**) (Scheme 5.21). Under purely thermal conditions (110 °C, 24 h), a high yield of cyclohexenes **5-101** and **5-102** can be obtained, but as an almost 1:1 mixture.<sup>26</sup> The employment of Lewis acids can aid in increasing the regioselectivity of the cycloaddition, however, SnCl<sub>4</sub> and TiCl<sub>4</sub> still favor the formation of isomer **5-102**.<sup>27</sup> The opposite isomer (**5-101**) can be more preferentially obtained with BH<sub>3</sub>•THF, but selectivity is not high (~4:1 **5-101**/**5-102**). The oxidative cleavage of the PMP group of our Cr-photocatalyzed cycloaddition products provides a different and potentially useful approach to constructing cyclohexanes of this substitution pattern.



Scheme 5.21. Regioselectivity in the Diels-Alder reaction of acrylic acid **5-100**.

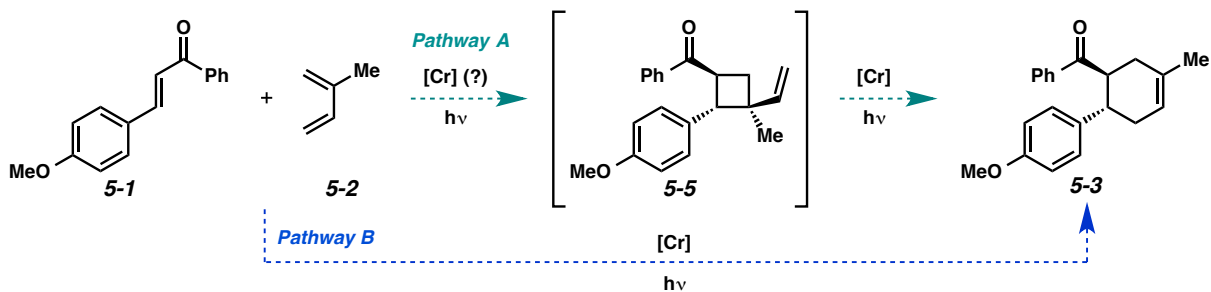
## 5.6 Mechanistic Discussion

As mentioned previously, it seems unlikely that the Cr catalyst ( $E_{1/2}^* = +1.40$ ) could be directly oxidizing 4-methoxychalcone (**5-1**) ( $E_{1/2} = +2.00$  V) or isoprene (**5-2**) ( $E_{1/2} = +1.98$  V) to initiate the cycloaddition. Because this transformation is evidently not a standard radical cation cycloaddition, a complete mechanistic framework has been difficult to construct. An observation that was made during our initial optimization experiments was that, in the presence of the Cr catalyst, cyclohexene **5-3** was formed in 82% yield (Table 5.1, entry 13), but in the absence of catalyst, vinylcyclobutane **5-5** was formed in only 20% yield (Table 5.1, entry 24) (Scheme 5.22).



Scheme 5.22. Reaction progress with and without catalyst.

This result implies that, if the [2+2] cycloaddition/vinylcyclobutane rearrangement cascade is the major mechanistic pathway (*Pathway A*, Scheme 5.23), then the presence of the Cr catalyst must be accelerating the [2+2] cycloaddition in some way. On the other hand, this result could also suggest that the Cr catalyst is involved in a completely different mechanistic pathway than the [2+2]/rearrangement that coincidentally leads to the same cycloaddition product (*Pathway B*).



Scheme 5.23. Two possible mechanistic pathways.

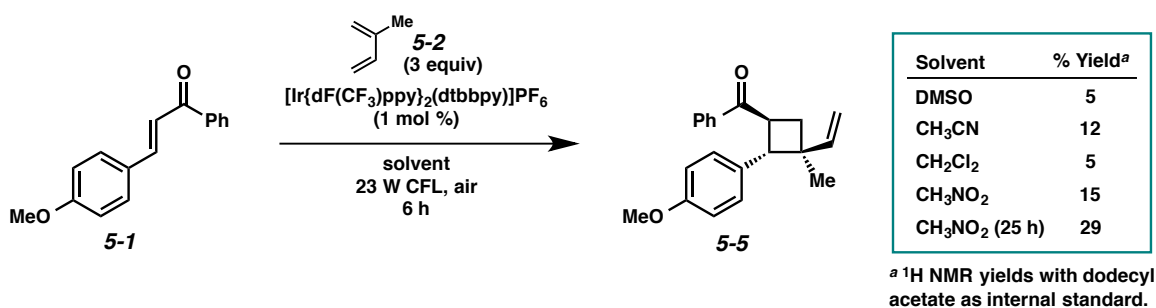
### 5.6.1 Pathway A

Based on our control experiments, we know that *Pathway A* is viable mechanistic pathway and that it is definitely occurring to a certain extent. In terms of the involvement of the catalyst in *Pathway A*, it is evident that  $\text{Cr}(\text{Ph}_2\text{phen})_3^{3+}$  is initiating the vinylcyclobutane rearrangement through single-electron oxidation of the vinylcyclobutane. The potential role of the catalyst in the [2+2] cycloaddition, however,

is less defined. If *Pathway A* is the dominant reaction pathway, there are several possible explanations for how the presence of the Cr catalyst could be accelerating the [2+2] process, including: 1) the Cr catalyst could act as a sensitizer for the [2+2] cycloaddition, 2) a competitive retro [2+2] cycloaddition is occurring, or 3) the vinylcyclobutane is inhibiting the [2+2] cycloaddition through competitive light absorption.

### 5.6.1.1 Photosensitization through Energy Transfer

Yoon and coworkers have demonstrated that Ir and Ru photocatalysts can act as triplet sensitizers for intramolecular [2+2] cycloadditions.<sup>28</sup> If the triplet energy of the excited state photocatalyst is greater than or equal to that of the substrate, then an energy transfer from the excited state catalyst to the alkene can occur to initiate the cycloaddition. The excited state energy of  $\text{Cr}(\text{Ph}_2\text{phen})_3^{3+*}$  is 38 kcal/mol,<sup>3</sup> which is considerably lower than the triplet energies of 4-methoxychalcone (**5-1**) or isoprene (**5-2**) (both ~60 kcal/mol),<sup>29</sup> so the Cr catalyst is likely not acting as a sensitizer for the [2+2] cycloaddition. We wondered, however, if the Ir photocatalyst,  $\text{Ir}[\text{dF}(\text{CF}_3)\text{ppy}]_2(\text{dtbbpy})^+$ , could sensitize the [2+2] cycloaddition of enone **5-1** and isoprene (**5-2**) because of its similar triplet energy ( $E^T = 60$  kcal/mol).<sup>28</sup>

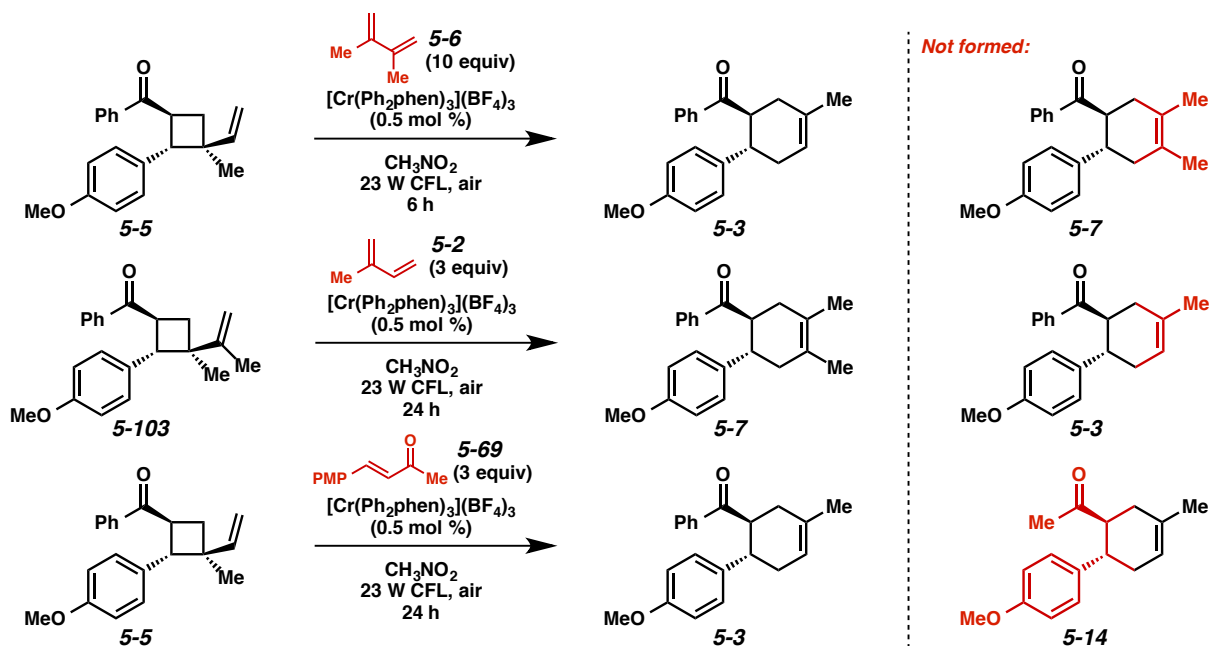


Scheme 5.24. Attempts at triplet sensitized [2+2] cycloaddition.

We attempted the Ir-sensitized [2+2] cycloadditions in several different solvents, but yields of the vinylcyclobutane (**5-5**) were approximately the same as the yield without catalyst (20% yield) (Scheme

5.24). Even after 25 h in nitromethane, only 29% yield of cycloadduct **5-5** was observed. Though the triplet energies of the reactants and catalyst suggested that this reaction might have worked, the intermolecularity of the proposed cycloaddition may have been why the sensitized [2+2] was not successful; the two cycloadditions reported by Yoon were intramolecular. In any case, all evidence points to the Cr catalyst not being involved in the [2+2] cycloaddition as an energy transfer catalyst.

### 5.6.1.2 Retro [2+2] Cycloaddition



Scheme 5.25. Trapping experiments.

Another possibility we considered to explain how 82% yield of cyclohexene **5-3** could be formed with catalyst, compared to only 20% yield of vinylcyclobutane **5-5** without catalyst, was that perhaps without catalyst to initiate the rearrangement of the vinylcyclobutane (**5-5**), it could cyclorevert to the starting materials. To test whether a retro [2+2] cycloaddition of the intermediate vinylcyclobutanes was happening, we performed several trapping experiments where the vinylcyclobutane rearrangements were performed in the presence of either a different diene or a different dienophile than the diene or dienophile

that was represented in the vinylcyclobutane (Scheme 5.25). If a cyclohexene formed that was not a result of the direct rearrangement of the given vinylcyclobutane, then we would know that a retro [2+2] cycloaddition of the vinylcyclobutane had occurred. The product that we observed in each experiment, however, was only the product of the vinylcyclobutane rearrangement, not the cross adduct between a component of the vinylcyclobutane and the added trapping reagent, indicating that cycloreversion was not occurring. Thus, this rules out that the role of the Cr catalyst is to drive the reaction forward so that retrocyclobutanation does not occur.

### 5.6.1.3 Vinylcyclobutane Inhibition

Another possible explanation is that the build up of the vinylcyclobutane inhibits further [2+2] cycloadditions through competitive light absorption. Since UV-Vis data shows that vinylcyclobutane **5-5** absorbs light more weakly than enone **5-1**, and at lower wavelengths, it is likely not acting as an inhibitor for the [2+2] cycloaddition (Figure 5.5).<sup>2</sup>

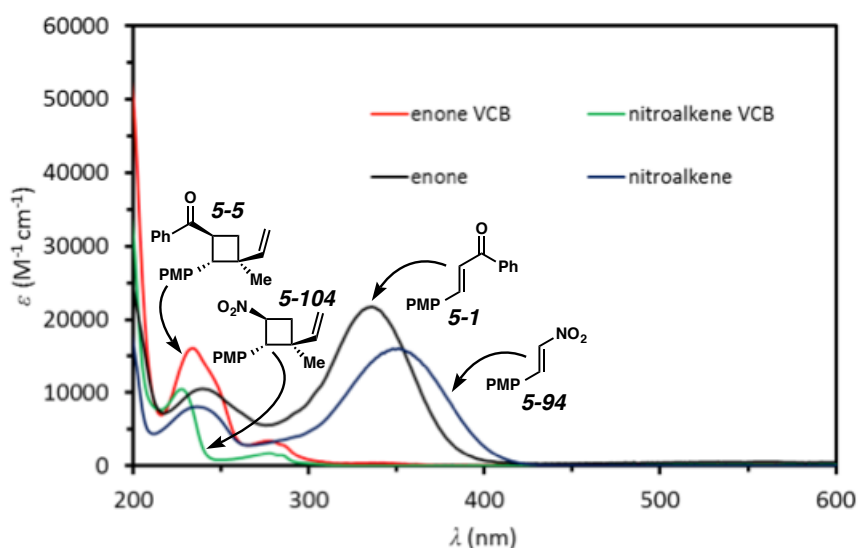
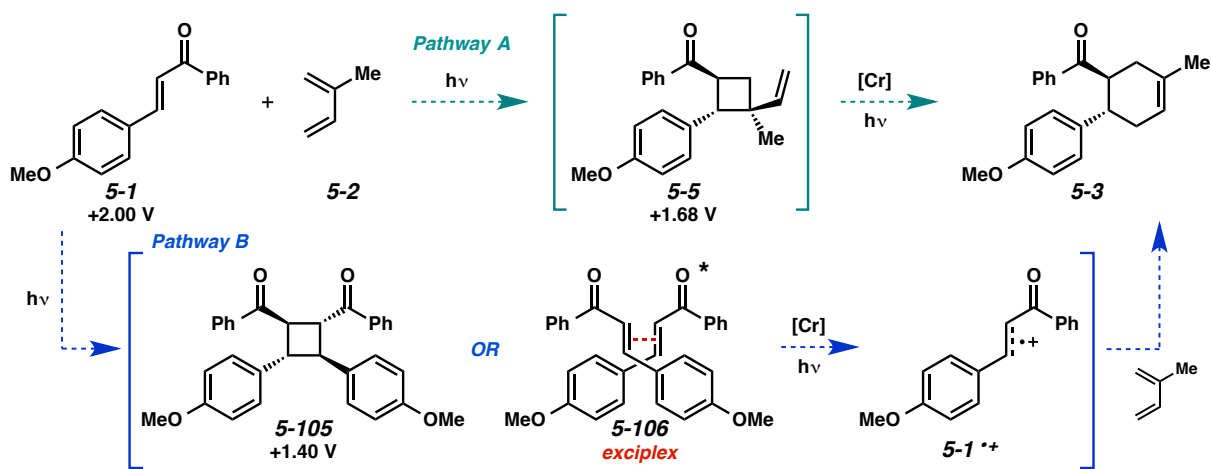


Figure 5.5. UV/Vis spectrum of electron-poor alkenes and their corresponding vinylcyclobutanes.

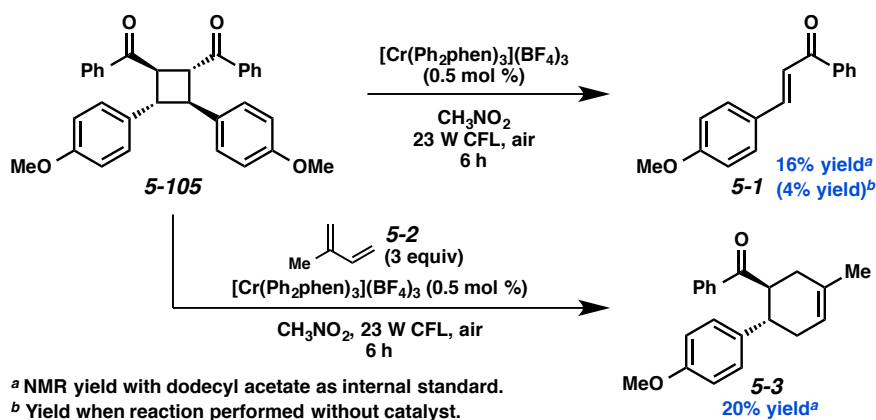
### 5.6.2 Pathway B

Evidently, the reasonable mechanisms through which the Cr catalyst could be accelerating the [2+2] cycloaddition of *Pathway A* are likely not operative. This strongly suggests that the Cr catalyst is involved in a completely different mechanistic pathway that is seemingly more efficient than the [2+2]/rearrangement cascade. Though mechanistic investigations by our collaborators are still in progress, kinetic studies by Robert Higgins in the Shores groups show that the Cr-photocatalyzed cycloaddition of enone **5-1** and isoprene (**5-2**) is second order in enone **5-1**, perhaps implying enone dimerization of some kind. We currently believe that *Pathway B* could involve enone dimer **5-105** or enone exciplex **5-106**<sup>30</sup> (Scheme 5.26). Firstly, the reduction potential of the enone dimer (**5-105**) is +1.40 V (CH<sub>3</sub>NO<sub>2</sub>, under O<sub>2</sub>), which is sufficiently low to be oxidized by the Cr catalyst. Thus, enone radical cation **5-1**<sup>•+</sup> could potentially be forming from oxidation and cycloreversion of the enone dimer (**5-105**) formed *in situ*. Subsequent reaction with isoprene in a radical cation [4+2] cycloaddition or [2+2]/rearrangement could afford the cyclohexene (**5-3**). Though this putative enone radical cation (**5-1**<sup>•+</sup>) seems an unlikely intermediate due to its electron-poor nature, radical cations of  $\alpha,\beta$ -unsaturated carbonyl compounds have been invoked in photoredox mechanisms (see Chapter 3.2.6).<sup>31</sup>



Scheme 5.26. Working mechanistic hypothesis involving an enone dimer or exciplex.

Control experiments revealed that enone dimer **5-105** underwent a retro [2+2] cycloaddition in the presence of the Cr catalyst, forming 4-methoxychalcone (**5-1**) in 16% yield in 6 h (Scheme 5.27). In the absence of the Cr catalyst, a 4% yield of the enone was obtained. Thus, the enone dimer cycloreverted more quickly under Cr photocatalysis conditions, perhaps due to single-electron oxidation. A trapping experiment with enone dimer **5-105** further supports its proposed role in the mechanism. When dimer **5-105** was exposed to the typical isoprene cycloaddition conditions in place of enone **5-1**, cyclohexene **5-3** formed in 20% yield, indicating that the dimer is a possible reaction intermediate. Still, with only 20% yield of cyclohexene **5-3** forming from isoprene and dimer **5-105** compared to >80% yield forming from isoprene and enone **5-1**, our mechanistic explanation is not yet complete.

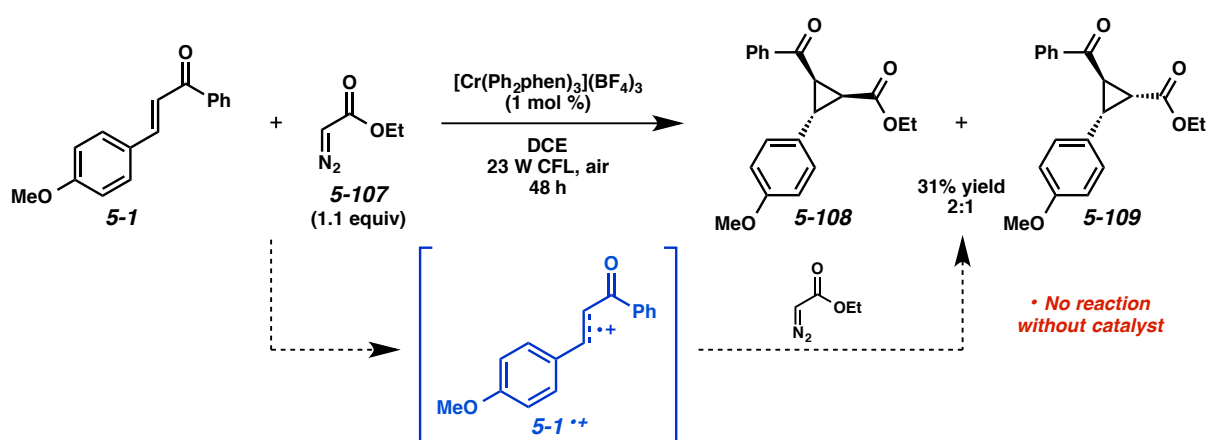


Scheme 5.27. Validation of dimer **5-105** as a reaction intermediate.

From a practicality standpoint, enone dimer **5-105** is actually quite difficult to synthesize;<sup>32</sup> direct irradiation (350 nm) of a concentrated solution of enone **5-1** affords low conversion to dimer **5-105**, even after prolonged reaction times (6 d). Since the cycloaddition of enone **5-1** and isoprene (**5-2**) is complete in 6 h, the slow dimerization of enone **5-1** renders dimer **5-105** a relatively improbable intermediate. An alternate explanation that accounts for the cycloaddition being second order in enone is that two enone equivalents could be forming an exciplex (Scheme 5.26, **5-106**),<sup>33</sup> rather than a covalently bonded

cyclobutane (**5-105**), which might lower the reduction potential of the enone enough to be oxidized by the catalyst. Preliminary results by our collaborators are in support of this hypothesis.

Lastly, we proposed to trap the putative enone radical cation (**5-1<sup>•+</sup>**) with a nucleophile other than a diene in order to confirm its formation. Diazo species are known to add into radical cations to form cyclopropanes,<sup>34</sup> and Francisco Sarabia in our lab has demonstrated that radical cation cyclopropanation can be accomplished under Cr-photocatalysis.<sup>35</sup> When enone **5-1** was exposed to ethyl diazoacetate in the presence of the Cr catalyst, cyclopropanes **5-108** and **5-109** formed in 31% combined yield; these cyclopropanes did not form without the Cr catalyst, indicative of a radical cation cyclopropanation mechanism (Scheme 5.28).<sup>36</sup> The reaction of enone **5-1** under the Cr conditions with a non-diene species highly implicates the intermediacy of enone radical cation **5-1<sup>•+</sup>**.

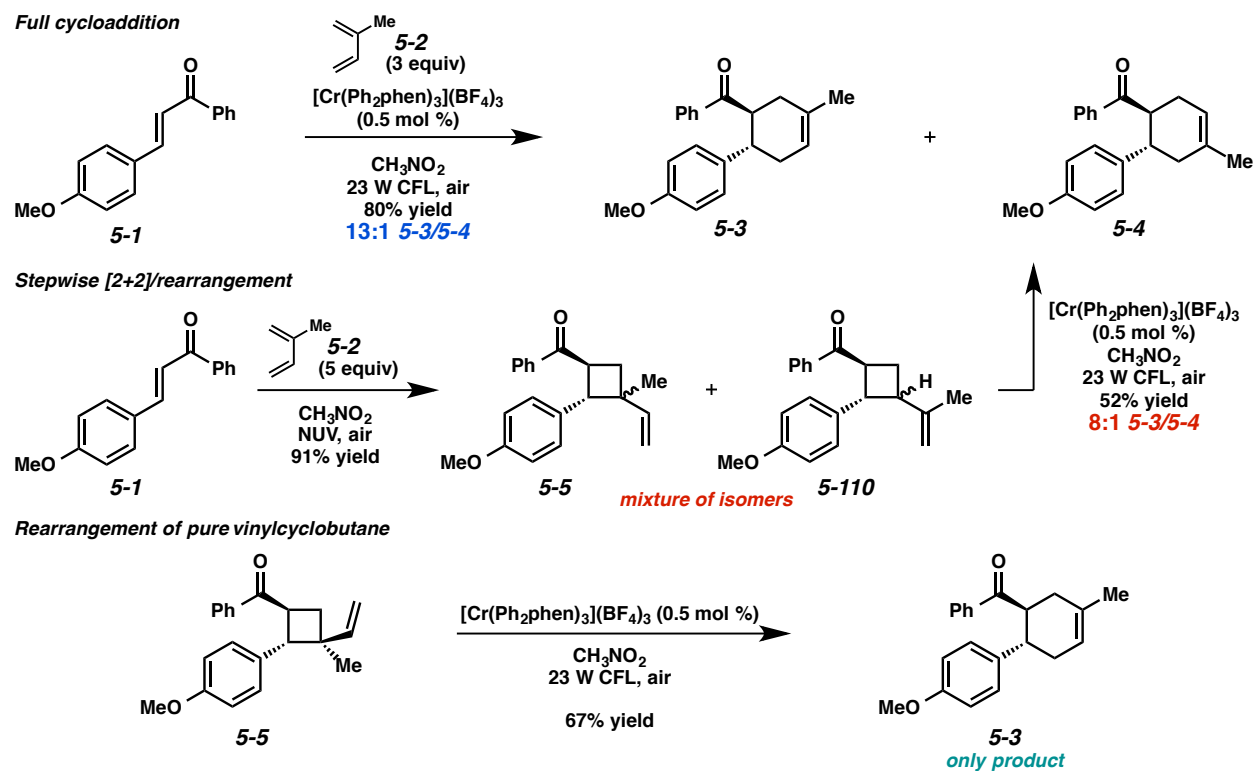


Scheme 5.28. Radical cation cyclopropanation of 4-methoxychalcone.

Ultimately, the Cr-photocatalyzed cycloaddition of dienes with electron-poor alkenes seems to proceed through a combination of multiple reaction pathways that all contribute to formation of the cyclohexene products. Further investigation by our collaborators will aid in unraveling this complex mechanistic puzzle.

### 5.6.3 Regioselectivity Difference Between Mechanistic Pathways

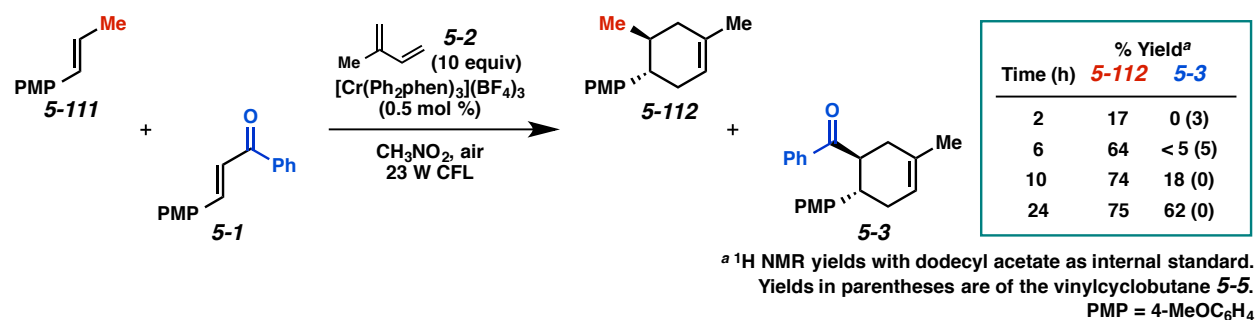
In addition to the increased efficiency of proposed *Pathway B*, this pathway also appears to be more regioselective than the [2+2]/rearrangement process (*Pathway A*). While the regioselectivity of the cycloaddition between enone **5-1** and isoprene (**5-2**) is 13:1 favoring the unnatural Diels-Alder adduct (**5-3**), the regioselectivity of the cycloadduct that is formed through a sequential photoinduced [2+2] cycloaddition, then Cr-catalyzed vinylcyclobutane rearrangement is lower (8:1) (Scheme 5.29). This outcome may be a result of the [2+2] cycloaddition with direct irradiation yielding a mixture of vinylcyclobutane isomers, some of which could rearrange to the minor cyclohexene adduct (**5-4**). When a pure isomer of vinylcyclobutane **5-5** is exposed to the Cr conditions, only one isomer of the product is formed. These results lead us to believe that either the Cr catalyst is improving the selectivity of the [2+2] step of *Pathway A*, or the regioselectivity preference in putative *Pathway B* is inherently higher.



Scheme 5.29. Regioselectivity of full cycloaddition vs. stepwise [2+2]/rearrangement.

### 5.6.4 Competition Experiment

A competition experiment using a 1:1 mixture of *trans*-anethole (**5-111**) and enone **5-1** with excess isoprene (**5-2**) was also conducted (Scheme 5.30). Here, the cycloaddition with the electron-rich dienophile (**5-111**) occurred first, with the formation of cyclohexene **5-3** proceeding only after the majority of the *trans*-anethole (**5-111**) was consumed. This result indicates that the radical cation-mediated cycloaddition of *trans*-anethole (**5-111**) predominates over the cycloaddition of the electron-poor enone (**5-1**). Further, this experiment may also implicate an enone radical cation intermediate (**5-1<sup>+</sup>**) for the cycloaddition of the electron-poor alkene, since this reaction was almost completely inhibited by the presence of the more oxidizable alkene ( $E_{1/2}(\textit{trans}\text{-anethole}) = +1.24 \text{ V}$ ).



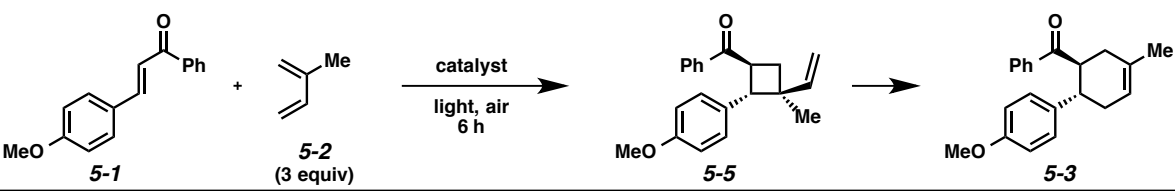
Scheme 5.30. Competition experiment between *trans*-anethole and 4-methoxychalcone.

### 5.6.5 Catalyst Evaluation

The cycloaddition of 4-methoxychalcone (**5-1**) and isoprene (**5-2**), as well as the rearrangement of vinylcyclobutane **5-5** were examined using a variety of different photocatalysts (Table 5.3). Overall, our original Cr conditions with Cr(Ph<sub>2</sub>phen)<sub>3</sub><sup>3+</sup> afforded the highest yield of cyclohexene **5-3** for the full cycloaddition (85% yield, entry 1), but gave a slightly lower yield than the other metal photocatalysts for just the vinylcyclobutane rearrangement step (67% yield); this is due in part to the formation of oxidation

product **5-10**, as already discussed. Essentially all of the metal photocatalysts were proficient for the vinylcyclobutane rearrangement, but were less effective for the full cycloaddition (entries 1-5).

Table 5.3. Evaluation of photocatalysts.



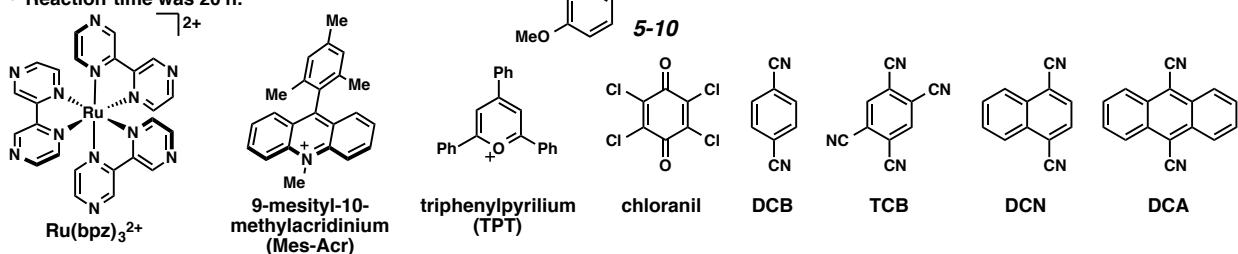
Entry	Catalyst (mol %)	$E_{1/2}^*$ (V vs. SCE)	ET (kcal/mol)	Solvent	Light source	Yield (%) <sup>a</sup> 5-5	Yield (%) <sup>a</sup> 5-3	Yield (%) <sup>a</sup> 5-5 → 5-3
1	[Cr(Ph <sub>2</sub> phen) <sub>3</sub> ](BF <sub>4</sub> ) <sub>3</sub> (0.5)	+1.40	38	CH <sub>3</sub> NO <sub>2</sub>	23 W CFL	0	85	67 <sup>b</sup>
2	[Cr(phen) <sub>3</sub> ](OTf) <sub>3</sub> (0.5)	+1.45	39	CH <sub>3</sub> NO <sub>2</sub>	23 W CFL	6	52 <sup>c</sup>	79
3	[(phen) <sub>2</sub> Cr(dmcbpy)](OTf) <sub>3</sub> (0.5)	+1.68	39	CH <sub>3</sub> NO <sub>2</sub>	23 W CFL	12	26 <sup>c</sup>	82
4	[Cr(dmcbpy) <sub>3</sub> ](BF <sub>4</sub> ) <sub>3</sub> (0.5)	+1.84	39	CH <sub>3</sub> NO <sub>2</sub>	23 W CFL	9	14 <sup>c</sup>	75
5	Ru(bpz) <sub>3</sub> (PF <sub>6</sub> ) <sub>2</sub> (1.0)	+1.45	48	CH <sub>3</sub> NO <sub>2</sub>	23 W CFL	8	55 <sup>c</sup>	77
6	Mes-Acr(BF <sub>4</sub> ) (5)	+2.06	45	DCE	blue LEDs	0	53 <sup>c</sup>	23 <sup>c</sup>
7	TPT(BF <sub>4</sub> ) (3)	+2.53	53	CH <sub>3</sub> CN	blue LEDs	0	3 <sup>c</sup>	84
8	chloranil (10)	+3.33	49	CH <sub>3</sub> CN	NUV	7	36 <sup>c,d</sup>	
9	DCB (10)	+2.67	73	CH <sub>3</sub> CN	NUV	42	10 <sup>c,d</sup>	
10	TCB (10)	+3.15		CH <sub>3</sub> CN	NUV	8	50 <sup>c,d</sup>	41
11	DCN (10)	+2.19	63	CH <sub>3</sub> CN	NUV	14	39 <sup>c,d</sup>	
12	DCA (10)	+1.97	42	CH <sub>3</sub> CN	NUV	4	43 <sup>c,d</sup>	41

<sup>a</sup> <sup>1</sup>H NMR yields with dodecyl acetate as internal standard

<sup>b</sup> Yield diminished because of oxidation to **5-10**.

<sup>c</sup> Majority of mass balance is recovered starting material.

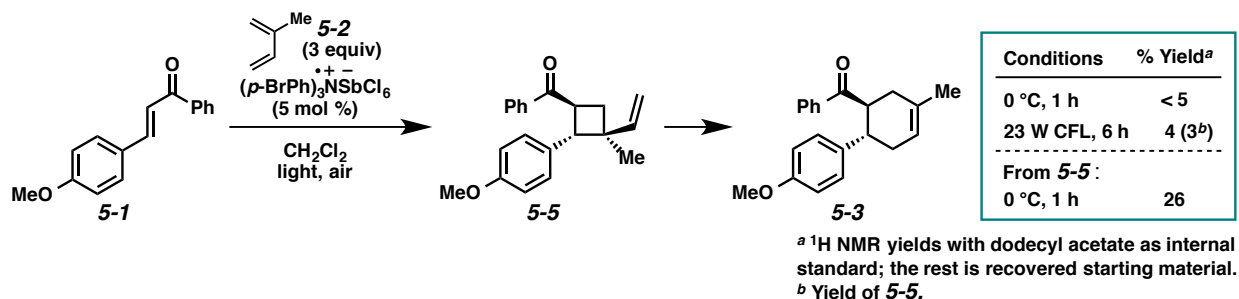
<sup>d</sup> Reaction time was 20 h.



Organic photocatalysts were also examined. The Mes-Acr photocatalyst gave a 53% yield of cyclohexene **5-3** in the full cycloaddition, but only 23% yield for the vinylcyclobutane rearrangement step (entry 6). The higher yield observed with Mes-Acr for the full cycloaddition compared to the rearrangement may suggest that this catalyst favors an enone radical cation mechanism over a

vinylcyclobutane rearrangement pathway; the high reduction potential of the Mes-Acr catalyst ( $E_{1/2}^* = +2.06$  V) could allow it to oxidize the enone (**5-1**) directly. Conversely, the TPT salt, which has an even higher reduction potential ( $E_{1/2}^* = +2.28$  V), afforded only a trace amount of the cycloadduct for the full cycloaddition, but was very efficient at catalyzing the vinylcyclobutane rearrangement, providing cyclohexene **5-3** in 84% yield (entry 7). Some of the more classical organic photosensitizers were shown to catalyze the cycloaddition as well, but these reactions were considerably slower and conversion to product was less clean (entries 8-12).

We also attempted the cycloaddition with Bauld's aminium radical cation salt, which does not require light. Under Bauld's standard aminium salt conditions ( $\text{CH}_2\text{Cl}_2$ ,  $0^\circ\text{C}$ ) we saw trace cyclohexene **5-3** in 1 h (Scheme 5.31). Hypothesizing that light could enable the formation of the enone dimer or exciplex (**5-105** or **5-106**), which could be then oxidized by the aminium salt as in *Pathway B*, we performed the reaction with irradiation (23 W CFL), but still only trace product **5-3** was formed, along with trace vinylcyclobutane **5-5**. This result implies that if the Cr-catalyzed process is going through an enone dimer or exciplex intermediate, then the Cr catalyst specifically might be playing a role in the formation of the intermediate dimer species. We also noted that the aminium salt was able to catalyze the vinylcyclobutane rearrangement, but not as efficiently as some of the photocatalysts, possibly because of its lower reduction potential ( $E_{1/2} = +1.05$  V). Evidently, the small amount of product that formed in the first two reactions from enone **5-1** was likely a result of a light-induced [2+2] cycloaddition, then an aminium salt catalyzed rearrangement; *Pathway B* is seemingly not occurring with this catalyst.



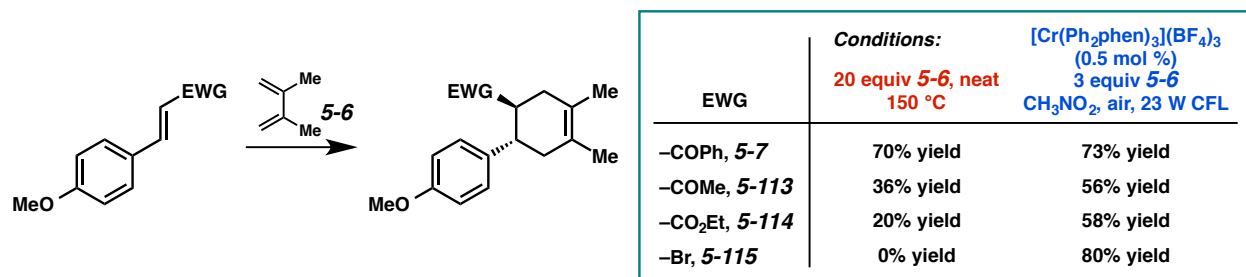
Scheme 5.31. Cycloaddition with an aminium radical cation salt.

Ultimately, all the photooxidants we attempted were able to catalyze the rearrangement of vinylcyclobutane **5-5** to a certain extent. This demonstrates that *Pathway A*, a light-induced [2+2] cycloaddition, followed by single-electron oxidation and vinylcyclobutane rearrangement, is a feasible mechanistic pathway for most photocatalysts to accomplish this transformation. As can be seen, however, this pathway is not particularly efficient, since the photochemical [2+2] cycloaddition is relatively slow. The particular proficiency of  $\text{Cr}(\text{Ph}_2\text{phen})_3^{3+}$  for catalyzing the overall cycloaddition could imply that this catalyst is remarkably equipped to mediate a process like *Pathway B*.

### 5.7 Diels-Alder Conditions vs. Cr Conditions

Though the electron-poor alkenes utilized in our substrate scope would appear to be typical dienophiles for Diels-Alder cycloadditions, chalcone derivatives and other cinnamyl carbonyl species are in fact rather stubborn dienophiles. Only a handful of reports exist that utilize this class of electron-poor alkenes as dienophiles, and typically the reaction conditions are harsh, employing high heat,<sup>37</sup> pressure,<sup>38</sup> microwaves,<sup>39</sup> or other less common reagents.<sup>40</sup> Further, the majority of reported reactions employ 1,3-cyclopentadiene as the diene, likely because it is more reactive.

An attribute of the Cr-photocatalyzed process is that it appears to circumvent some intrinsic limitations of the traditional [4+2] cycloaddition. As shown in Scheme 5.32 the cycloaddition of 2,3-dimethyl-1,3-butadiene (**5-6**) with a range of dienophiles under thermal conditions (neat, 150 °C) provided varying reactivity. The phenyl ketone was sufficiently reactive, but the methyl ketone, ethyl ester, and bromide all dropped off considerably in reactivity. Other traditional Diels-Alder conditions (e.g., Lewis acid catalyzed) were even less successful. Using the photocatalyzed cascade, however, all four dienophiles were effective reactants. Thus, the Cr conditions provide a mild means of accomplishing net-[4+2] cycloadditions with these types of difficult dienophiles.



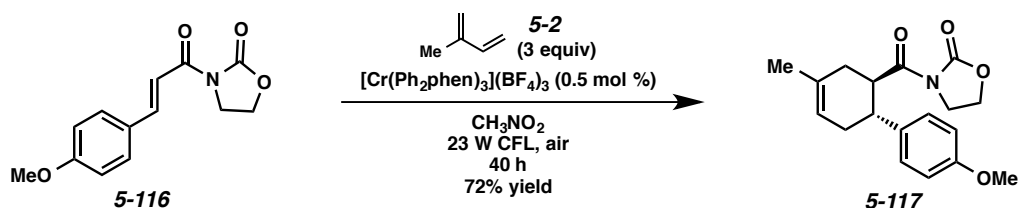
Scheme 5.32. Cr-photocatalyzed vs. thermal Diels-Alder conditions.

## 5.8 Efforts Toward an Enantioselective Cycloaddition

Photochemical transformations are notoriously difficult to render enantioselective.<sup>41</sup> Unlike most enantioselective transformations in organic synthesis that can utilize a chiral catalyst to both activate the substrate and induce enantioselectivity, in a photochemical reaction, light is the catalyst. Thus, in order for a photochemical transformation to be enantioselective, the substrate must already be in a chiral environment when excitation occurs. Despite this obstacle, several enantioselective photocatalyzed reactions have been developed. Recent examples include Yoon's enantioselective reductive [2+2] cycloaddition with Ru(bpy)<sub>3</sub><sup>2+</sup> and a chiral Lewis acid,<sup>42</sup> Meggers's enantioselective alkylation of acyl imidazoles with a chiral iridium photocatalyst,<sup>43</sup> Miranda and Bach's enantioselective [2+2] cycloaddition of quinolones catalyzed by an H-bonding chiral photosensitizer,<sup>44</sup> and Fu and MacMillan's enantioselective decarboxylative arylation of  $\alpha$ -amino acids using an iridium/nickel dual catalyst system.<sup>45</sup> Notably, all of these transformations proceed through energy transfer or reductive photocatalytic cycles; an enantioselective photooxidative transformation has yet to be developed.

### 5.8.1 Chiral Oxazolidinones

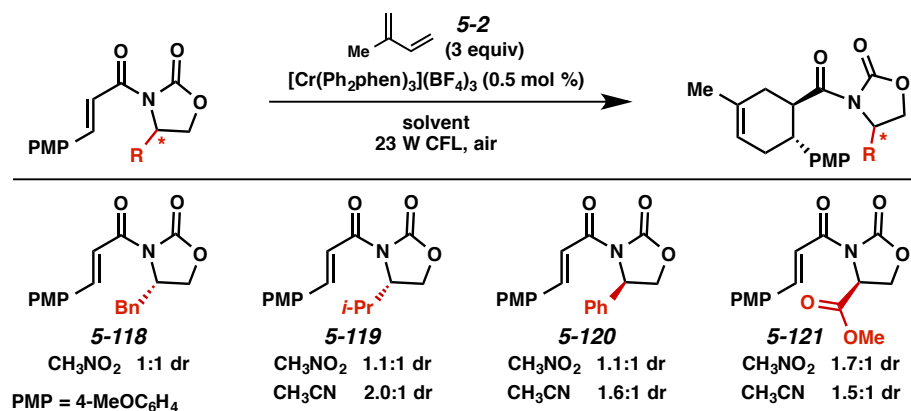
While exploring the substrate scope of the Cr-catalyzed cycloaddition, we found that oxazolidinone **5-116** reacted smoothly to give product **5-117** in 72% yield (Scheme 5.33). We saw this substrate as an opportunity to develop an enantioselective cascade reaction using oxazolidinones as chiral auxiliaries.



Scheme 5.33. Cycloaddition of oxazolidinone substrate.

Since we originally believed that the cycloadditions was proceeding through a [2+2]/rearrangement cascade, we hypothesized that any enantioselectivity obtained would result from the enantioselectivity of the [2+2] cycloaddition. Enantioselective cycloadditions with chiral oxazolidinones have been reported, but mainly for Diels-Alder reactions.<sup>46</sup> The only reports of stereoselective [2+2] cycloadditions utilizing chiral oxazolidinones are of  $\alpha,\beta$ -unsaturated oxazolidinones with  $^1\text{O}_2$  as the cycloaddition partner,<sup>47</sup> and the [2+2] reaction of chiral amino ketene equivalents with imines to generate chiral  $\beta$ -lactams.<sup>48</sup> Despite the lack of literature precedents, we wondered if the Cr-photocatalyzed cascade could be rendered enantioselective by employing a chiral oxazolidinone.

Several chiral oxazolidinone substrates were synthesized and exposed to the standard Cr conditions with isoprene (**5-2**) in both nitromethane and acetonitrile, but low diastereomeric ratios of the corresponding cyclohexenes were observed (Scheme 5.34).



Scheme 5.34. Cycloaddition of chiral oxazolidinones.

A fairly extensive Lewis acid screen was performed to determine if the coordination of the two carbonyls by a metal species might enhance the stereoselectivity of the [2+2] cycloaddition (Table 5.4). None of the Lewis acid additives provided an improvement in enantioselectivity compared to the Lewis acid-free conditions (entries 1 and 2). In many cases, the presence of the Lewis acid actually inhibited the cycloaddition and no reaction occurred (Table 5.4). The highest dr we achieved was 2:1.

Table 5.4. Chiral oxazolidinone cycloaddition Lewis acid screen.

Entry	Lewis acid	Solvent	Result	dr <sup>b</sup>	Entry	Lewis acid	Solvent	Result	dr <sup>b</sup>
1	none	CH <sub>3</sub> NO <sub>2</sub>	complete	1.1:1	8	Cu(OAc) <sub>2</sub>	CH <sub>3</sub> CN	trace product	--
2	none	CH <sub>3</sub> CN	not complete	2.0:1	9	Eu(OTf) <sub>3</sub>	CH <sub>3</sub> CN	trace product	--
3	NaBF <sub>4</sub>	CH <sub>3</sub> NO <sub>2</sub>	complete	1.4:1	10	La(OTf) <sub>3</sub>	CH <sub>3</sub> CN	not complete	2.0:1
4	NaBF <sub>4</sub>	CH <sub>3</sub> CN	complete	1.8:1	11	Sc(OTf) <sub>3</sub>	CH <sub>3</sub> CN	trace product	--
5	AgBF <sub>4</sub>	CH <sub>3</sub> NO <sub>2</sub>	not complete	2.0:1	12	Et <sub>2</sub> AlCl <sup>a</sup>	CH <sub>3</sub> CN	trace product	--
6	AgBF <sub>4</sub>	CH <sub>3</sub> CN	no reaction	--	13	ZrCl <sub>4</sub> <sup>a</sup>	CH <sub>3</sub> CN	no reaction	--
7	Zn(OTf) <sub>2</sub>	CH <sub>3</sub> CN	complete	2.0:1	14	Ti(O <i>i</i> -Pr) <sub>4</sub> <sup>a</sup>	CH <sub>3</sub> CN	no reaction	--

<sup>a</sup> Run under Ar.

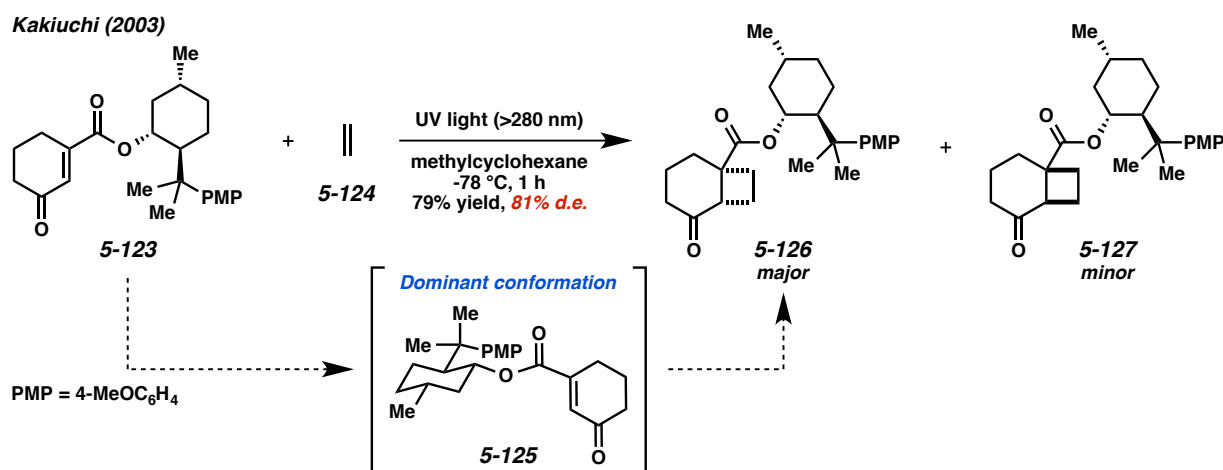
<sup>b</sup> Determined by analysis of the crude <sup>1</sup>H NMR spectra.

PMP = 4-MeOC<sub>6</sub>H<sub>4</sub>

Overall, the reactions performed in acetonitrile were slower, but seemed to result in slightly higher diastereoselectivities than the reactions run in nitromethane. Since nonpolar solvents typically enable higher diastereomeric ratios, we also attempted the cycloaddition in dichloromethane, but the reaction was prohibitively slower. Based on these results and the shortage of enantioselective [2+2] cycloadditions with chiral oxazolidinones in the literature, we decided to try a different chiral auxiliary.

### 5.8.2 Chiral Menthyl Esters

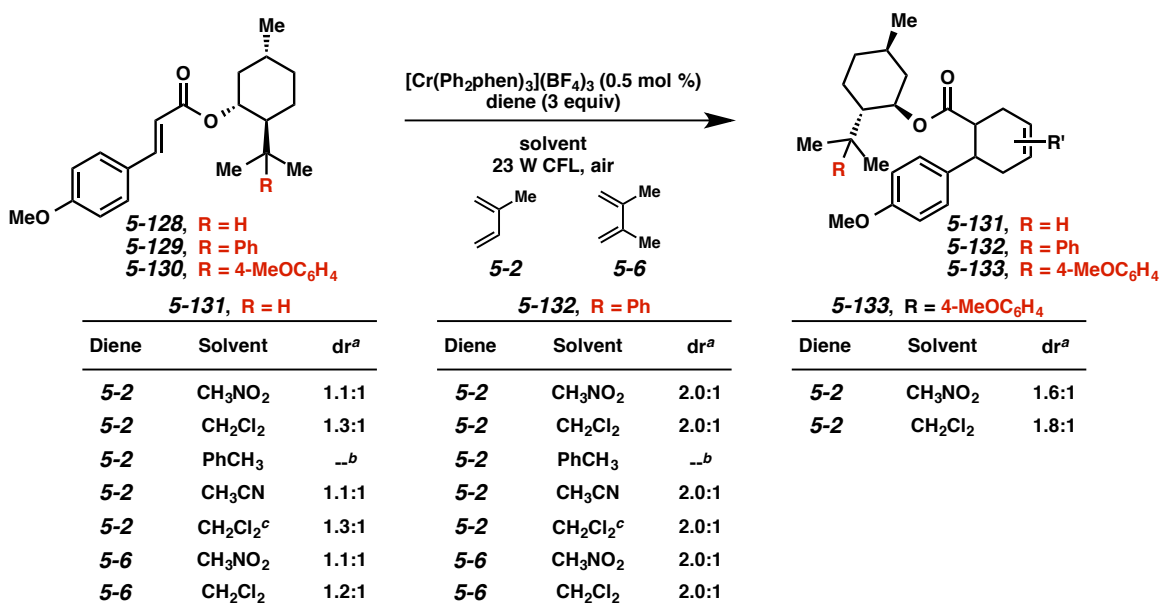
The literature precedent for enantioselective [2+2] cycloadditions of menthyl esters showed slightly more promise. The vast majority of reports, however, utilize cyclohexene carboxylates such as enone **5-123**, which could indicate a narrow substrate scope in terms of the enantioinduction abilities of menthyl esters (Scheme 5.35).<sup>49</sup> Additionally, the best diastereoselectivities were obtained in nonpolar solvents at low temperatures. Since radical cation processes favor polar solvents and we have observed inhibited reactivity at lower temperatures, these two procedural aspects would be difficult to overcome.



Scheme 5.35. Enantioselective [2+2] cycloadditions with menthyl cyclohexene carboxylates.

Nevertheless, we explored the Cr-catalyzed cycloadditions of menthyl ester **5-128**, 8-phenyl menthyl ester **5-129**, and 8-(4-methoxy)phenyl menthyl ester **5-130** (Table 5.5). We attempted the cycloadditions in both polar and nonpolar solvents, with different dienes, and at 0 °C, but none of these factors seemed to have a significant impact on the dr. The ability of the menthyl ester to induce enantioselectivity must be fairly substrate dependent. It is also possible that high diastereoselectivities in these reactions were not achieved because the predominant mechanistic pathway does not begin with a photoinduced [2+2] cycloaddition.

Table 5.5. Cycloadditions with menthyl esters.



<sup>a</sup> Determined by analysis of the crude <sup>1</sup>H NMR spectra.

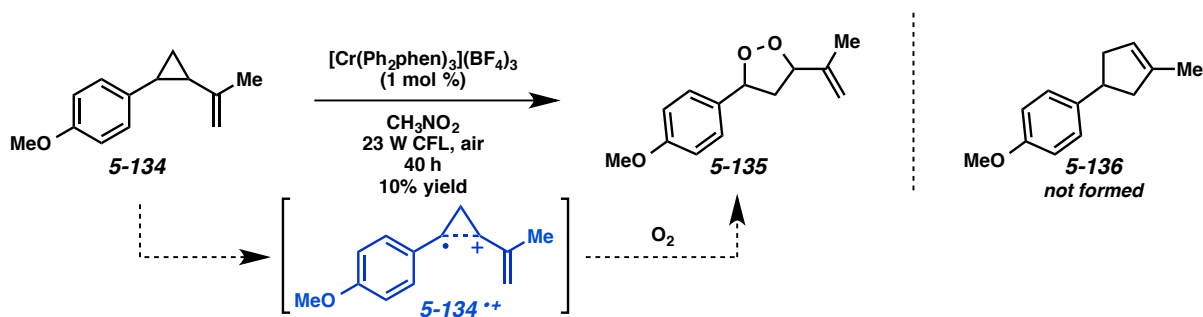
<sup>b</sup> No reaction; catalyst not soluble in PhCH<sub>3</sub>.

<sup>c</sup> Run at 0 °C; starting material not consumed.

## 5.9 Attempted Vinylcyclopropane Rearrangement

Lastly, since the Cr catalyst could induce a vinylcyclobutane rearrangement, we wondered if a vinylcyclopropane rearrangement could be accomplished as well. According to literature reports, when the radical cation of the vinylcyclopropane forms, the breaking of the cyclopropane bond is calculated to

be barrierless and the rearrangement should occur quickly.<sup>50</sup> Curiously, however, when we attempted the rearrangement of cyclopropane **5-134** under our standard Cr conditions, cyclopentene **5-136** was not formed (Scheme 5.36). Instead, a [3+2] cycloaddition occurred between the distonic radical cation (**5-134**<sup>•+</sup>) and oxygen to afford endoperoxide **5-135**. This general transformation has been reported by Yoon and coworkers, but they did not employ a vinylcyclopropane substrate.<sup>51</sup> It is strange that the rearrangement, which is supposed to be energetically favorable, was outcompeted by a cycloaddition with oxygen. In addition, when the reaction was attempted under Ar, only trace conversion was observed.<sup>52</sup>



Scheme 5.36. [3+2] cycloaddition of cyclopropane vinylcyclopropane and oxygen.

## 5.10 Conclusion

In conclusion, we have developed a Cr-photocatalyzed cycloaddition of electron-poor alkenes and dienes that yields Diels-Alder adducts of reversed regioselectivity.<sup>53</sup> Though the exact mechanism of this reaction is not entirely known, the collective results point to a predominant pathway involving an enone radical cation intermediate. The employment of electron-poor alkenes in intermolecular radical cation cycloadditions, combined with the unique proficiency of a first-row transition metal complex in catalyzing this transformation, sets this methodology apart from previously reported radical cation cycloadditions described in the literature. Experiments are underway by us and our collaborators to further uncover the singularity of this Cr-photocatalyzed cycloaddition approach.

## 5.11 Experimental Section

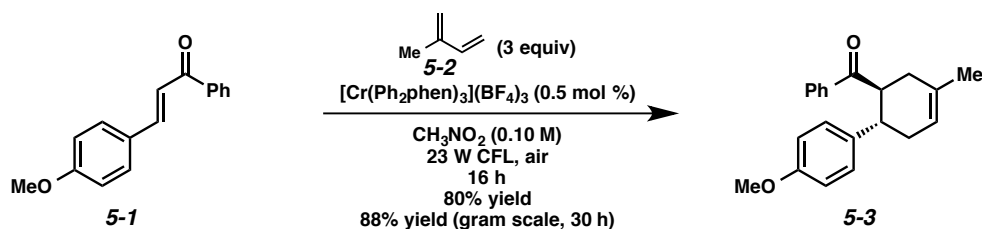
### 5.11.1 Materials and Methods

Cr catalysts were synthesized as previously described.<sup>3,54</sup> The preparation of  $[\text{Cr}(\text{Ph}_2\text{phen})_3](\text{BF}_4)_3$  is also provided in Chapter 4.9.17.  $\text{Ru}(\text{bpz})_3(\text{PF}_6)_2$ , 9-mesityl-10-methylacridinium tetrafluoroborate, and 2,4,6-triphenylpyrilium tetrafluoroborate were purchased from Sigma-Aldrich. Chloranil, 1,4-dicyanobenzene, 1,2,4,5-tetracyanobenzene, 1,4-dicyanonaphthalene, and 9,10-dicyanoanthracene are commercially available. All solvents, excluding acetonitrile and nitromethane, were purified by passing through activated alumina columns; acetonitrile was distilled over  $\text{CaH}_2$ , and nitromethane was purchased from Alfa Aesar (98+%, A11806) and used without further purification. All reagents were used as received unless otherwise noted. Commercially available chemicals were purchased from Alfa Aesar (Ward Hill, MA), Sigma-Aldrich (St. Louis, MO), Oakwood Products, (West Columbia, SC), Strem (Newburyport, MA) and TCI America (Portland, OR). Qualitative TLC analysis was performed on 250 mm thick, 60 Å, glass backed, F254 silica (Silicycle, Quebec City, Canada). Visualization was accomplished with UV light and exposure to *p*-anisaldehyde or  $\text{KMnO}_4$  solution followed by heating. Flash chromatography was performed using Silicycle silica gel (230-400 mesh). Reactions under NUV irradiation were performed in a Luzchem chamber reactor equipped with 10 lamps of wavelengths 419, 350, and 300 nm. Irradiation with visible light was performed in a sealed box using a 23 W compact fluorescent light bulb (EcoSmart 23 W bright white CFL spiral light bulb, 1600 lumens). NMR spectra were acquired at the University of Georgia Chemical Sciences Magnetic Resonance Facility on a Varian Mercury Plus 400 MHz NMR.  $^1\text{H}$  NMR spectra were acquired at 400 MHz and are reported relative to  $\text{SiMe}_4$  ( $\delta$  0.00).  $^{13}\text{C}$  NMR spectra were at 100 MHz and are reported relative to  $\text{SiMe}_4$  ( $\delta$  0.0). IR spectra were obtained on a Shimadzu IRPrestige-21 FT-IR. High resolution mass spectrometry data were acquired by the Proteomics and Mass Spectrometry Facility at the University of Georgia on a Thermo Orbitrap Elite.

### 5.11.2 Cr-Photocatalyzed Cycloaddition

**General Notes:** Irradiation was performed in a sealed box using a 23 W compact fluorescent light bulb; the temperature inside the box was recorded at ~45 °C. Reported NMR data are of the major isomer. Ratios of “opposite”/“normal” Diels-Alder isomers were determined through analysis of crude <sup>1</sup>H NMR spectra. Reported yields are for the mixture of isomers.

**General Procedure for the Cr-Photocatalyzed Cycloaddition:** A flame-dried 2-dram borosilicate vial open to air was charged with the alkene (1 equiv), diene (3 equiv), [Cr(Ph<sub>2</sub>phen)<sub>3</sub>](BF<sub>4</sub>)<sub>3</sub> (0.5 mol %), and nitromethane (0.10 M). The vial was then capped and placed in front of a bright white 23 W compact fluorescent light bulb in a closed box lined with aluminum foil. The solution was irradiated with stirring until consumption of the alkene was complete, as determined by TLC, and then it was passed through a short plug of silica (2.0-2.5 cm high x 1 cm wide, Et<sub>2</sub>O eluent). The volatile materials were removed by rotary evaporation, and the resulting residue was purified by flash chromatography.



**Cyclohexene 5-3.** Prepared according to the *General Procedure* using alkene **5-1** (23.8 mg, 0.100 mmol), diene **5-2** (30.1 μL, 0.300 mmol), [Cr(Ph<sub>2</sub>phen)<sub>3</sub>](BF<sub>4</sub>)<sub>3</sub> (0.7 mg, 0.000500 mmol), and nitromethane (1.00 mL). The reaction mixture was irradiated for 16 h. The crude product was purified by flash chromatography (100% hexanes → 9:1 hexanes/EtOAc eluent) to afford cyclohexene **5-3** (24.5 mg, 80% yield, 13:1 isomeric ratio) as a white solid.

**Gram-scale procedure:** Prepared according to a modified *General Procedure* (modification: the reaction was run in a 250-mL round-bottom flask and stoppered with a plastic cap) using alkene **5-1** (1.00 g, 4.20

mmol), diene **5-2** (1.26 mL, 12.6 mmol),  $[\text{Cr}(\text{Ph}_2\text{phen})_3](\text{BF}_4)_3$  (27.5 mg, 0.0210 mmol), and nitromethane (42.0 mL). The reaction mixture was irradiated for 30 h. The crude product was purified by flash chromatography (100% hexanes  $\rightarrow$  9:1 hexanes/EtOAc eluent) to afford cyclohexene **5-3** (1.13 g, 88% yield, 11:1 isomeric ratio) as a white solid.

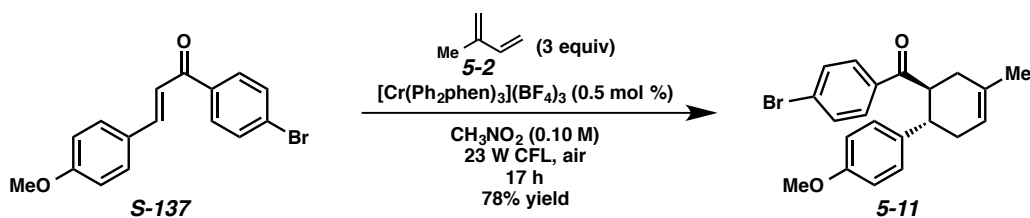
**TLC:**  $R_f$  = 0.68 in 3:1 hexanes/EtOAc, visualized by UV.

**$^1\text{H}$  NMR** (400 MHz;  $\text{CDCl}_3$ ):  $\delta$  7.79 (d,  $J$  = 7.2 Hz, 2H), 7.47 (t,  $J$  = 7.2 Hz, 1H), 7.36 (t,  $J$  = 7.6 Hz, 2H), 7.09 (d,  $J$  = 8.7 Hz, 2H), 6.68 (d,  $J$  = 8.7 Hz, 2H), 5.54 (br s, 1H), 3.97 (td,  $J$  = 10.7, 5.5 Hz, 1H), 3.68 (s, 3H), 3.18 (td,  $J$  = 10.7, 5.5 Hz, 1H), 2.35-2.24 (comp. m, 4H), 1.72 (s, 3H).

**$^{13}\text{C}$  NMR** (100 MHz;  $\text{CDCl}_3$ ):  $\delta$  203.8, 157.8, 137.4, 135.7, 132.7, 128.39, 128.36, 128.0, 122.0, 120.9, 113.7, 55.1, 47.3, 41.5, 35.2, 34.2, 23.2.

**IR** (ATR, neat): 3055, 2909, 2839, 1682, 1512, 1242, 1034, 734, 702  $\text{cm}^{-1}$ .

**HRMS** (ESI+):  $m/z$  calc'd for  $(\text{M} + \text{H})^+$   $[\text{C}_{21}\text{H}_{22}\text{O}_2 + \text{H}]^+$ : 307.1693, found 307.1699.



**Cyclohexene 5-11.** Prepared according to the *General Procedure* using alkene **5-137** (31.7 mg, 0.100 mmol), diene **5-2** (30.1  $\mu\text{L}$ , 0.300 mmol),  $[\text{Cr}(\text{Ph}_2\text{phen})_3](\text{BF}_4)_3$  (0.7 mg, 0.000500 mmol), and nitromethane (1.00 mL). The reaction mixture was irradiated for 17 h. The crude product was purified by flash chromatography (100% hexanes  $\rightarrow$  6:1 hexanes/EtOAc eluent) to afford cyclohexene **5-11** (29.9 mg, 78% yield, 13:1 isomeric ratio) as a colorless oil.

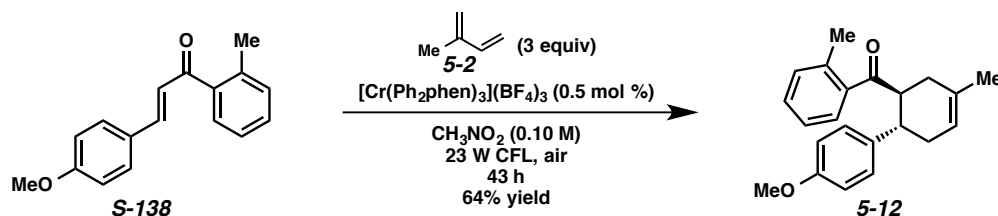
**TLC:**  $R_f$  = 0.71 in 3:1 hexanes/EtOAc, stained blue with *p*-anisaldehyde.

**<sup>1</sup>H NMR** (400 MHz; CDCl<sub>3</sub>): δ 7.64 (d, *J* = 8.4 Hz, 2H), 7.49 (d, *J* = 8.4 Hz, 2H), 7.06 (d, *J* = 8.6 Hz, 2H), 6.68 (d, *J* = 8.6 Hz, 2H), 5.53 (br s, 1H), 3.89 (td, *J* = 10.7, 5.3 Hz, 1H), 3.68 (s, 3H), 3.14 (td, *J* = 10.7, 5.5 Hz, 1H), 2.32-2.15 (comp. m, 4H), 1.71 (s, 3H).

**<sup>13</sup>C NMR** (100 MHz; CDCl<sub>3</sub>): δ 202.9, 157.9, 136.2, 136.1, 132.3, 131.7, 129.5, 128.3, 127.8, 121.0, 113.7, 55.1, 47.4, 41.7, 35.1, 34.1, 23.2.

**IR** (ATR, neat): 2963, 2901, 2832, 1682, 1582, 1512, 1242, 1003, 826, 733 cm<sup>-1</sup>.

**HRMS** (ESI+): *m/z* calc'd for (M + H)<sup>+</sup> [C<sub>21</sub>H<sub>21</sub>BrO<sub>2</sub> + H]<sup>+</sup>: 385.0798, found 385.0805.



**Cyclohexene 5-12.** Prepared according to the *General Procedure* using alkene **5-138** (25.2 mg, 0.100 mmol), diene **5-2** (30.1 μL, 0.300 mmol), [Cr(Ph<sub>2</sub>phen)<sub>3</sub>](BF<sub>4</sub>)<sub>3</sub> (0.7 mg, 0.000500 mmol), and nitromethane (1.00 mL). The reaction mixture was irradiated for 43 h. The crude product was purified by flash chromatography (100% hexanes → 6:1 hexanes/EtOAc eluent) to afford cyclohexene **5-12** (20.6 mg, 64% yield, 8:1 isomeric ratio) as a colorless oil.

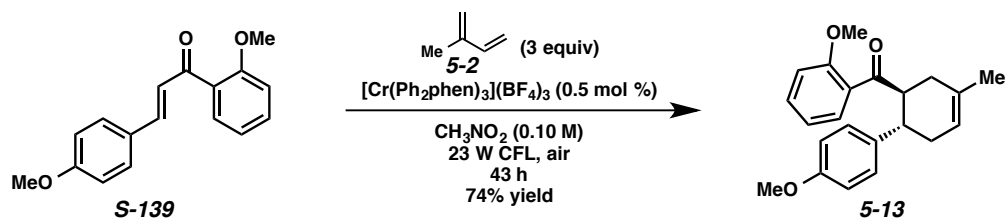
**TLC:** R<sub>f</sub> = 0.82 in 3:1 hexanes/EtOAc, visualized by UV.

**<sup>1</sup>H NMR** (400 MHz; CDCl<sub>3</sub>): δ 7.41 (d, *J* = 7.7 Hz, 1H), 7.26 (t, *J* = 7.5 Hz, 1H), 7.16 (t, *J* = 7.5 Hz, 1H), 7.08 (comp. m, 3H), 6.70 (d, *J* = 8.4 Hz, 2H), 5.51 (br s, 1H), 3.78-3.73 (m, 1H), 3.72 (s, 3H), 3.11 (td, *J* = 10.8, 5.7 Hz, 1H), 2.42-2.29 (comp. m, 2H), 2.25-2.18 (comp. m, 2H), 2.05 (s, 3H), 1.73 (s, 3H).

**<sup>13</sup>C NMR** (100 MHz; CDCl<sub>3</sub>): δ 208.2, 158.0, 139.6, 137.6, 136.3, 132.5, 131.4, 130.7, 128.6, 127.4, 125.3, 120.9, 113.7, 55.2, 50.9, 42.2, 34.8, 34.4, 23.3, 20.2.

**IR** (ATR, neat): 2963, 2909, 2839, 1682, 1512, 1242, 1034, 734 cm<sup>-1</sup>.

**HRMS** (ESI+): *m/z* calc'd for (M + H)<sup>+</sup> [C<sub>22</sub>H<sub>24</sub>O<sub>2</sub> + H]<sup>+</sup>: 321.1849, found 321.1849.



**Cyclohexene 5-13.** Prepared according to the *General Procedure* using alkene **5-139** (26.8 mg, 0.100 mmol), diene **5-2** (30.1  $\mu\text{L}$ , 0.300 mmol),  $[\text{Cr}(\text{Ph}_2\text{phen})_3](\text{BF}_4)_3$  (0.7 mg, 0.000500 mmol), and nitromethane (1.00 mL). The reaction mixture was irradiated for 43 h. The crude product was purified by flash chromatography (100% hexanes  $\rightarrow$  6:1 hexanes/EtOAc eluent) to afford cyclohexene **5-13** (24.8 mg, 74% yield, 10:1 isomeric ratio) as a colorless oil.

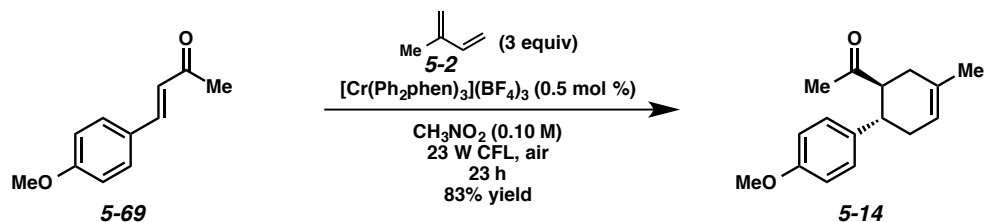
**TLC:**  $R_f = 0.52$  in 3:1 hexanes/EtOAc, visualized by UV.

**$^1\text{H NMR}$**  (400 MHz;  $\text{CDCl}_3$ ):  $\delta$  7.29 (td,  $J = 7.8, 0.8$  Hz, 1H), 7.03 (d,  $J = 8.6$  Hz, 2H), 6.82 (t,  $J = 7.5$  Hz, 2H), 6.74 (t,  $J = 7.5$  Hz, 1H), 6.67 (d,  $J = 8.6$  Hz, 2H), 5.48 (br s, 1H), 3.84 (s, 3H), 3.84-3.80 (m, 1H), 3.71 (s, 3H), 3.04 (td,  $J = 10.5, 5.7$  Hz, 1H), 2.39-2.16 (comp. m, 4H), 1.73 (s, 3H).

**$^{13}\text{C NMR}$**  (100 MHz;  $\text{CDCl}_3$ ):  $\delta$  208.0, 157.8, 157.2, 136.5, 133.1, 132.2, 130.7, 129.3, 128.7, 120.43, 120.40, 113.4, 110.8, 55.5, 55.2, 52.4, 42.5, 34.0, 33.7, 23.4.

**IR** (ATR, neat): 2963, 2901, 2832, 1682, 1598, 1512, 1242, 1018, 756  $\text{cm}^{-1}$ .

**HRMS** (ESI<sup>+</sup>):  $m/z$  calc'd for  $(\text{M} + \text{H})^+ [\text{C}_{22}\text{H}_{24}\text{O}_3 + \text{H}]^+$ : 337.1798, found 337.1801.



**Cyclohexene 5-14.** Prepared according to the *General Procedure* using alkene **5-69** (17.6 mg, 0.100 mmol), diene **5-2** (30.1  $\mu\text{L}$ , 0.300 mmol),  $[\text{Cr}(\text{Ph}_2\text{phen})_3](\text{BF}_4)_3$  (0.7 mg, 0.000500 mmol), and

nitromethane (1.00 mL). The reaction mixture was irradiated for 23 h. The crude product was purified by flash chromatography (100% hexanes → 9:1 hexanes/EtOAc eluent) to afford cyclohexene **5-14** (20.3 mg, 83% yield, 12:1 isomeric ratio) as a colorless oil.

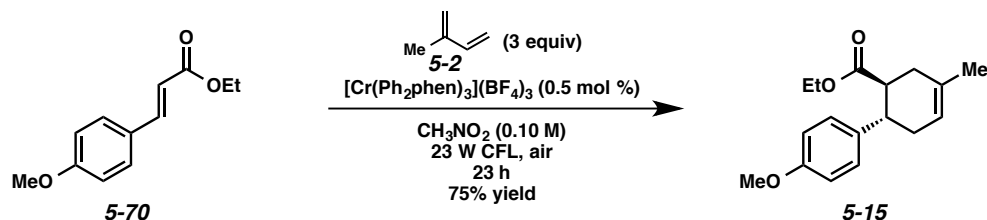
**TLC:**  $R_f$  = 0.61 in 3:1 hexanes/EtOAc, stained yellow with *p*-anisaldehyde.

**$^1\text{H NMR}$**  (400 MHz;  $\text{CDCl}_3$ ):  $\delta$  7.09 (d,  $J$  = 8.6 Hz, 2H), 6.81 (d,  $J$  = 8.6 Hz, 2H), 5.46 (br s, 1H), 3.76 (s, 3H), 3.00 (td,  $J$  = 10.9, 5.2 Hz, 1H), 2.87 (td,  $J$  = 10.9, 5.4 Hz, 1H), 2.29-2.04 (comp. m, 4H), 1.82 (s, 3H), 1.71 (s, 3H).

**$^{13}\text{C NMR}$**  (100 MHz;  $\text{CDCl}_3$ ):  $\delta$  212.4, 158.1, 136.0, 132.1, 128.4, 120.7, 113.9, 55.2, 53.8, 41.9, 34.1, 33.3, 29.8, 23.2.

**IR** (ATR, neat): 2963, 2909, 2832, 1705, 1612, 1512, 1435, 1242, 1173, 1034, 826  $\text{cm}^{-1}$ .

**HRMS** (ESI+):  $m/z$  calc'd for  $(\text{M} + \text{H})^+$  [ $\text{C}_{16}\text{H}_{20}\text{O}_2 + \text{H}$ ] $^+$ : 245.1536, found 245.1538.



**Cyclohexene 5-15.** Prepared according to the *General Procedure* using alkene **5-70** (20.6 mg, 0.100 mmol), diene **5-2** (30.1  $\mu\text{L}$ , 0.300 mmol),  $[\text{Cr}(\text{Ph}_2\text{phen})_3](\text{BF}_4)_3$  (0.7 mg, 0.000500 mmol), and nitromethane (1.00 mL). The reaction mixture was irradiated for 23 h. The crude product was purified by flash chromatography (100% hexanes → 6:1 hexanes/EtOAc eluent) to afford cyclohexene **5-15** (20.6 mg, 75% yield, 19:1 isomeric ratio) as a colorless oil.

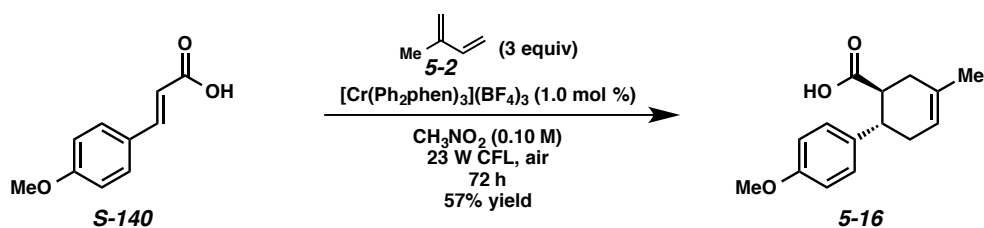
**TLC:**  $R_f$  = 0.67 in 3:1 hexanes/EtOAc, visualized by UV.

**$^1\text{H NMR}$**  (400 MHz;  $\text{CDCl}_3$ ):  $\delta$  7.12 (d,  $J$  = 8.5 Hz, 2H), 6.80 (d,  $J$  = 8.5 Hz, 2H), 5.46 (br s, 1H), 3.85 (qd,  $J$  = 7.1, 1.5 Hz, 2H), 3.76 (s, 3H), 2.90 (td,  $J$  = 10.9, 5.4 Hz, 1H), 2.80 (td,  $J$  = 10.9, 5.1 Hz, 1H), 2.42-2.16 (comp. m, 4H), 1.71 (s, 3H), 0.93 (t,  $J$  = 7.1 Hz, 3H).

$^{13}\text{C}$  NMR (100 MHz;  $\text{CDCl}_3$ ):  $\delta$  175.2, 158.1, 136.0, 132.1, 128.5, 120.6, 113.6, 59.9, 55.21, 55.19, 46.9, 42.1, 33.9, 23.2, 13.9.

IR (ATR, neat): 2963, 2901, 2839, 1782, 1512, 1242, 1172, 1034, 826  $\text{cm}^{-1}$ .

HRMS (ESI+):  $m/z$  calc'd for  $(\text{M} + \text{H})^+$  [ $\text{C}_{17}\text{H}_{22}\text{O}_3 + \text{H}$ ] $^+$ : 275.1642, found 275.1640.



**Cyclohexene 5-16.** Prepared according to a modified *General Procedure* (modification: 1 mol % catalyst was used) using alkene **5-140** (17.8 mg, 0.100 mmol), diene **5-2** (30.1  $\mu\text{L}$ , 0.300 mmol),  $[\text{Cr}(\text{Ph}_2\text{phen})_3](\text{BF}_4)_3$  (1.3 mg, 0.00100 mmol), and nitromethane (1.00 mL). The reaction mixture was irradiated for 72 h. The crude product was purified by flash chromatography (100% hexanes  $\rightarrow$  2:1 hexanes/EtOAc eluent) to afford cyclohexene **5-16** (14.0 mg, 57% yield, 17:1 isomeric ratio) as a white solid.

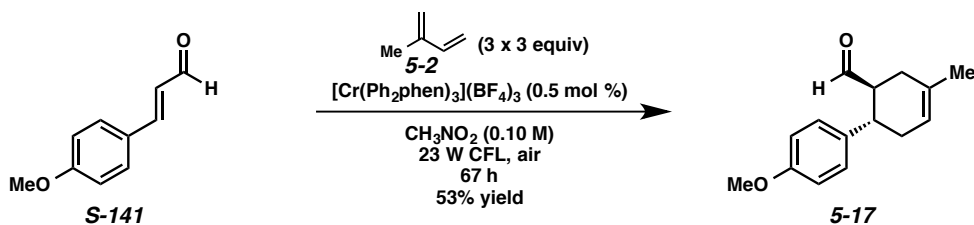
TLC:  $R_f = 0.64$  in 1:1 hexanes/EtOAc, stained with  $\text{KMnO}_4$ .

$^1\text{H}$  NMR (400 MHz;  $\text{CDCl}_3$ ):  $\delta$  7.11 (d,  $J = 8.6$  Hz, 2H), 6.80 (d,  $J = 8.6$  Hz, 2H), 5.45 (br s, 1H), 3.77 (s, 3H), 2.91 (td,  $J = 10.6, 5.4$  Hz, 1H), 2.81 (td,  $J = 10.6, 5.4$  Hz, 1H), 2.37-2.08 (comp. m, 4H), 1.70 (s, 3H).

$^{13}\text{C}$  NMR (100 MHz;  $\text{CDCl}_3$ ):  $\delta$  180.0, 158.1, 135.8, 131.8, 128.3, 120.6, 113.8, 55.2, 46.3, 41.3, 33.64, 33.61, 23.1.

IR (ATR, neat): 3364, 2970, 2909, 2839, 1713, 1512, 1242, 949, 826  $\text{cm}^{-1}$ .

HRMS (ESI+):  $m/z$  calc'd for  $(\text{M} + \text{H})^+$  [ $\text{C}_{15}\text{H}_{18}\text{O}_3 + \text{H}$ ] $^+$ : 247.1329, found 247.1326.



**Cyclohexene 5-17.** Prepared according to a modified *General Procedure* (modification: 9 equivalents of diene were used, and it was added in 3 portions) using alkene **5-141** (8.1 mg, 50.0  $\mu\text{mol}$ ), diene **5-2** (15.0  $\mu\text{L}$ , 150  $\mu\text{mol}$ ),  $[\text{Cr}(\text{Ph}_2\text{phen})_3](\text{BF}_4)_3$  (0.3 mg, 0.250  $\mu\text{mol}$ ), and nitromethane (0.500 mL). After 24 and 48 h, additional portions of diene **5-2** (15.0  $\mu\text{L}$  each) were added. The reaction mixture was irradiated for 67 h total. The crude product was purified by flash chromatography (100% hexanes  $\rightarrow$  9:1 hexanes/EtOAc eluent) to afford cyclohexene **5-17** (6.1 mg, 53% yield, 11:1 isomeric ratio) as a colorless oil.

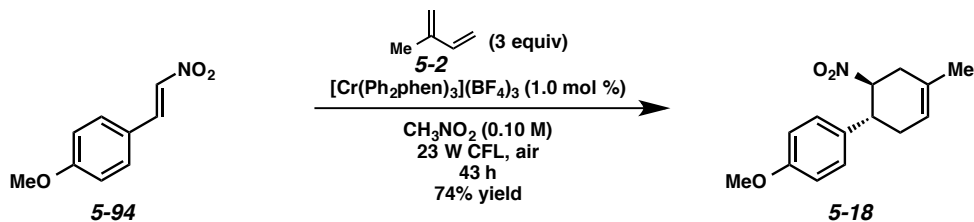
**TLC:**  $R_f = 0.63$  in 3:1 hexanes/EtOAc, stained blue with *p*-anisaldehyde.

**$^1\text{H NMR}$**  (400 MHz;  $\text{CDCl}_3$ ):  $\delta$  9.45 (s, 1H), 7.13 (d,  $J = 8.6$  Hz, 2H), 6.84 (d,  $J = 8.6$  Hz, 2H), 5.49 (br s, 1H), 3.78 (s, 3H), 2.98 (td,  $J = 9.8, 5.6$  Hz, 1H), 2.82-2.75 (m, 1H), 2.34-2.02 (comp. m, 4H), 1.73 (s, 3H).

**$^{13}\text{C NMR}$**  (100 MHz;  $\text{CDCl}_3$ ):  $\delta$  204.5, 158.3, 135.3, 131.8, 128.4, 120.9, 114.1, 55.2, 51.9, 39.9, 33.4, 29.5, 23.3.

**IR** (ATR, neat): 2970, 2909, 2839, 1721, 1512, 1250, 826  $\text{cm}^{-1}$ .

**HRMS** (ESI<sup>+</sup>):  $m/z$  calc'd for  $(\text{M} + \text{H})^+ [\text{C}_{15}\text{H}_{18}\text{O}_2 + \text{H}]^+$ : 231.1380, found 231.1379.



**Cyclohexene 5-18.** Prepared according to a modified *General Procedure* (modification: 1 mol % catalyst was used) using alkene **5-94** (17.9 mg, 0.100 mmol), diene **5-2** (30.1  $\mu$ L, 0.300 mmol),  $[\text{Cr}(\text{Ph}_2\text{phen})_3](\text{BF}_4)_3$  (1.3 mg, 0.00100 mmol), and nitromethane (1.00 mL). The reaction mixture was irradiated for 43 h. The crude product was purified by flash chromatography (100% hexanes  $\rightarrow$  6:1 hexanes/EtOAc eluent) to afford cyclohexene **5-18** (18.2 mg, 74% yield, 17:1 isomeric ratio) as a pale yellow oil.

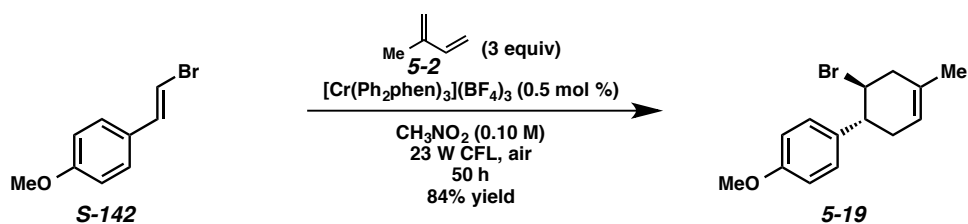
**TLC:**  $R_f$  = 0.65 in 3:1 hexanes/EtOAc, visualized by UV.

**$^1\text{H}$  NMR** (400 MHz;  $\text{CDCl}_3$ ):  $\delta$  7.13 (d,  $J$  = 8.4 Hz, 2H), 6.83 (d,  $J$  = 8.4 Hz, 2H), 5.49 (br s, 1H), 4.91 (td,  $J$  = 10.8, 5.6 Hz, 1H), 3.76 (s, 3H), 3.29 (td,  $J$  = 10.8, 5.8 Hz, 1H), 2.79-2.72 (m, 1H), 2.59-2.52 (m, 1H), 2.44-2.37 (m, 1H), 2.34-2.24 (m, 1H), 1.75 (s, 3H).

**$^{13}\text{C}$  NMR** (100 MHz;  $\text{CDCl}_3$ ):  $\delta$  158.8, 131.9, 130.3, 128.3, 120.7, 114.2, 88.1, 55.2, 43.4, 35.6, 33.1, 22.8.

**IR** (ATR, neat): 2963, 2909, 2839, 1551, 1512, 1373, 1242, 1033, 826, 733  $\text{cm}^{-1}$ .

**HRMS** (ESI+):  $m/z$  calc'd for  $(\text{M} + \text{H})^+ [\text{C}_{14}\text{H}_{17}\text{NO}_3 + \text{H}]^+$ : 248.1281, found 248.1286.



**Cyclohexene 5-19.** Prepared according to the *General Procedure* using alkene **5-142** (21.3 mg, 0.100 mmol), diene **5-2** (30.1  $\mu$ L, 0.300 mmol),  $[\text{Cr}(\text{Ph}_2\text{phen})_3](\text{BF}_4)_3$  (0.7 mg, 0.000500 mmol), and nitromethane (1.00 mL). The reaction mixture was irradiated for 50 h. The crude product was purified by flash chromatography (100% hexanes  $\rightarrow$  9:1 hexanes/EtOAc eluent) to afford cyclohexene **5-19** (23.5 mg, 84% yield, 17:1 isomeric ratio) as a colorless oil.

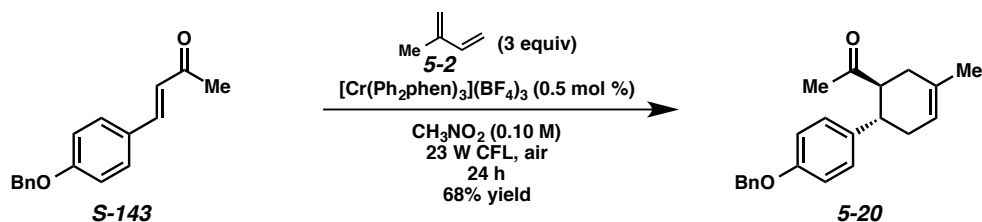
**TLC:**  $R_f$  = 0.79 in 3:1 hexanes/EtOAc, stained blue with *p*-anisaldehyde.

**<sup>1</sup>H NMR** (400 MHz; CDCl<sub>3</sub>): δ 7.13 (d, *J* = 8.4 Hz, 2H), 6.86 (d, *J* = 8.4 Hz, 2H), 5.50 (br s, 1H), 4.43 (dt, *J* = 9.6, 7.3 Hz, 1H), 3.80 (s, 3H), 3.06 (td, *J* = 9.6, 5.9 Hz, 1H), 2.66 (d, *J* = 6.3 Hz, 2H), 2.51-2.45 (m, 1H), 2.31-2.23 (m, 1H), 1.70 (s, 3H).

**<sup>13</sup>C NMR** (100 MHz; CDCl<sub>3</sub>): δ 158.3, 136.2, 132.4, 128.3, 120.5, 113.8, 55.2, 54.4, 47.3, 41.3, 33.7, 22.8.

**IR** (ATR, neat): 2963, 2909, 2839, 1512, 1250, 1180, 1034, 810 cm<sup>-1</sup>.

**LRMS** (ESI+): *m/z* calc'd for (M - Br) [C<sub>14</sub>H<sub>17</sub>BrO - Br]: 201.1, found 201.2.



**Cyclohexene 5-20.** Prepared according to the *General Procedure* using alkene **5-143** (25.2 mg, 0.100 mmol), diene **5-2** (30.1 μL, 0.300 mmol), **[Cr(Ph<sub>2</sub>phen)<sub>3</sub>](BF<sub>4</sub>)<sub>3</sub>** (0.7 mg, 0.000500 mmol), and nitromethane (1.00 mL). The reaction mixture was irradiated for 24 h. The crude product was purified by flash chromatography (100% hexanes → 6:1 hexanes/EtOAc eluent) to afford cyclohexene **5-20** (21.9 mg, 68% yield, 15:1 isomeric ratio) as a white solid.

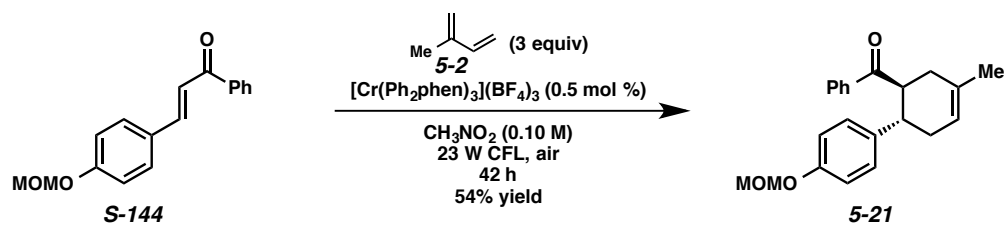
**TLC:** R<sub>f</sub> = 0.68 in 3:1 hexanes/EtOAc, stained yellow with *p*-anisaldehyde.

**<sup>1</sup>H NMR** (400 MHz; CDCl<sub>3</sub>): δ 7.42-7.29 (comp. m, 5H), 7.10 (d, *J* = 8.6 Hz, 2H), 6.89 (d, *J* = 8.6 Hz, 2H), 5.46 (br s, 1H), 5.01 (s, 2H), 3.00 (td, *J* = 10.9, 5.3 Hz, 1H), 2.88 (td, *J* = 10.9, 5.4 Hz, 1H), 2.29-2.05 (comp. m, 4H), 1.83 (s, 3H), 1.71 (s, 3H).

**<sup>13</sup>C NMR** (100 MHz; CDCl<sub>3</sub>): δ 212.4, 157.4, 137.0, 136.3, 132.2, 128.6, 128.4, 127.9, 127.5, 120.71, 120.70, 114.9, 70.0, 53.8, 42.0, 34.1, 33.3, 23.2.

**IR** (ATR, neat): 2970, 2909, 2839, 1705, 1512, 1242, 903, 725 cm<sup>-1</sup>.

**HRMS** (ESI+): *m/z* calc'd for (M + H)<sup>+</sup> [C<sub>22</sub>H<sub>24</sub>O<sub>2</sub> + H]<sup>+</sup>: 321.1849, found 321.1853.



**Cyclohexene 5-21.** Prepared according to the *General Procedure* using alkene **5-144** (26.8 mg, 0.100 mmol), diene **5-2** (30.1  $\mu\text{L}$ , 0.300 mmol),  $[\text{Cr}(\text{Ph}_2\text{phen})_3](\text{BF}_4)_3$  (0.7 mg, 0.000500 mmol), and nitromethane (1.00 mL). The reaction mixture was irradiated for 42 h. The crude product was purified by flash chromatography (100% hexanes  $\rightarrow$  6:1 hexanes/EtOAc eluent) to afford cyclohexene **5-21** (18.1 mg, 54% yield, 12:1 isomeric ratio) as a colorless oil.

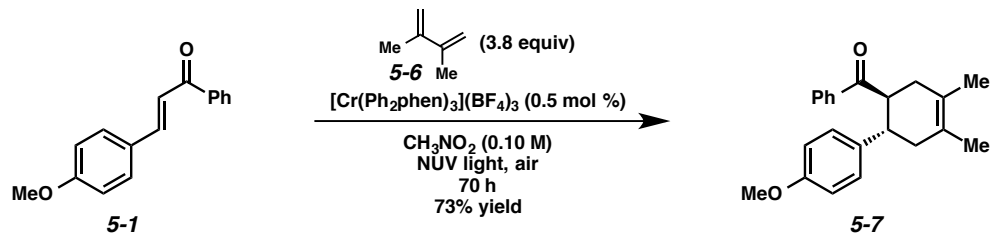
**TLC:**  $R_f = 0.63$  in 3:1 hexanes/EtOAc, stained blue with *p*-anisaldehyde.

**$^1\text{H NMR}$**  (400 MHz;  $\text{CDCl}_3$ ):  $\delta$  7.80 (d,  $J = 7.6$  Hz, 2H), 7.47 (t,  $J = 7.6$  Hz, 1H), 7.37 (t,  $J = 7.6$  Hz, 2H), 7.09 (d,  $J = 8.5$  Hz, 2H), 6.81 (d,  $J = 8.5$  Hz, 2H), 5.52 (br s, 1H), 5.07-5.02 (comp. m, 2H), 3.97 (td,  $J = 10.5, 5.4$  Hz, 1H), 3.39 (s, 3H), 3.18 (td,  $J = 10.5, 5.7$  Hz, 1H), 2.38-2.19 (comp. m, 4H), 1.71 (s, 3H).

**$^{13}\text{C NMR}$**  (100 MHz;  $\text{CDCl}_3$ ):  $\delta$  203.7, 155.5, 137.9, 137.3, 132.7, 132.4, 128.42, 128.38, 128.0, 120.9, 116.1, 94.4, 55.9, 47.2, 41.5, 35.2, 34.2, 23.2.

**IR** (ATR, neat): 2970, 2901, 2839, 1682, 1512, 1234, 1150, 1003, 903, 725  $\text{cm}^{-1}$ .

**HRMS** (ESI<sup>+</sup>):  $m/z$  calc'd for  $(\text{M} + \text{H})^+ [\text{C}_{22}\text{H}_{24}\text{O}_3 + \text{H}]^+$ : 337.1798, found 337.1799.



**Cyclohexene 5-7.** Prepared according to a modified *General Procedure* (modification: 300-420 nm irradiation was used) using alkene **5-1** (23.8 mg, 0.100 mmol), diene **5-6** (43.0  $\mu\text{L}$ , 0.380 mmol),

[Cr(Ph<sub>2</sub>phen)<sub>3</sub>](BF<sub>4</sub>)<sub>3</sub> (0.7 mg, 0.000500 mmol), and nitromethane (1.00 mL). The reaction mixture was irradiated with 300-420 nm light for 70 h. The crude product was purified by flash chromatography (100% hexanes → 9:1 hexanes/EtOAc eluent) to afford cyclohexene **5-7** (23.4 mg, 73% yield) as a colorless oil.

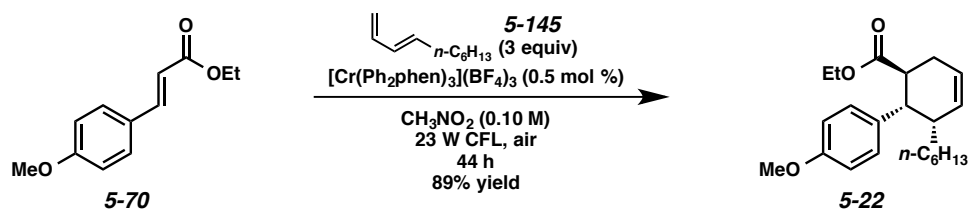
**TLC:** R<sub>f</sub> = 0.63 in 3:1 hexanes/EtOAc, stained with KMnO<sub>4</sub>.

**<sup>1</sup>H NMR** (400 MHz; CDCl<sub>3</sub>): δ 7.81 (d, *J* = 7.4 Hz, 2H), 7.48 (t, *J* = 7.4 Hz, 1H), 7.37 (t, *J* = 7.7 Hz, 2H), 7.10 (d, *J* = 8.6 Hz, 2H), 6.69 (d, *J* = 8.6 Hz, 2H), 3.95 (td, *J* = 10.8, 5.4 Hz, 1H), 3.68 (s, 3H), 3.25-3.22 (m, 1H), 2.31-2.21 (comp. m, 4H), 1.67 (app. s, 6H).

**<sup>13</sup>C NMR** (100 MHz; CDCl<sub>3</sub>): δ 203.7, 157.8, 137.4, 136.7, 132.6, 128.4, 128.3, 128.0, 125.7, 124.1, 113.7, 55.1, 47.7, 42.2, 40.7, 37.0, 18.7, 18.6.

**IR** (ATR, neat): 2901, 2832, 1674, 1512, 1242, 1034, 825, 733, 694 cm<sup>-1</sup>.

**HRMS** (ESI<sup>+</sup>): *m/z* calc'd for (M + H)<sup>+</sup> [C<sub>22</sub>H<sub>24</sub>O<sub>2</sub> + H]<sup>+</sup>: 321.1849, found 321.1855.



**Cyclohexene 5-22** Prepared according to the *General Procedure* using alkene **5-70** (15.5 mg, 75.0 μmol), diene **5-145**<sup>55</sup> (31.1 mg, 225 μmol), [Cr(Ph<sub>2</sub>phen)<sub>3</sub>](BF<sub>4</sub>)<sub>3</sub> (0.5 mg, 0.375 μmol), and nitromethane (0.750 mL). The reaction mixture was irradiated for 44 h. The crude product was purified by flash chromatography (100% hexanes → 9:1 hexanes/EtOAc eluent) to afford cyclohexene **5-22** (22.9 mg, 89% yield, 5:1 isomeric ratio) as a colorless oil.

**TLC:** R<sub>f</sub> = 0.76 in 3:1 hexanes/EtOAc, stained blue with *p*-anisaldehyde.

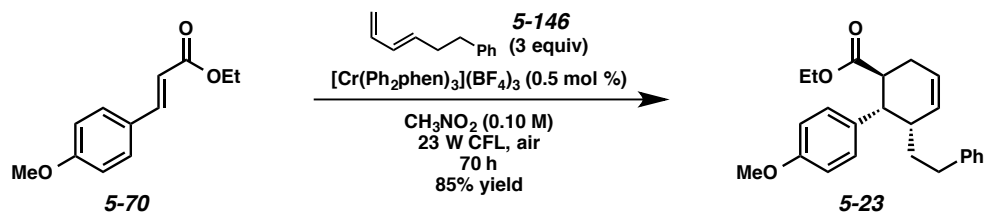
**<sup>1</sup>H NMR** (400 MHz; CDCl<sub>3</sub>): δ 7.11 (d, *J* = 8.5 Hz, 2H), 6.80 (d, *J* = 8.5 Hz, 2H), 5.89-5.86 (m, 1H), 5.72-5.69 (m, 1H), 3.96 (q, *J* = 7.1 Hz, 2H), 3.77 (s, 3H), 3.29 (dd, *J* = 10.4, 5.4 Hz, 1H), 3.00 (dt, *J* =

10.4, 7.6 Hz, 1H), 2.38-2.36 (comp. m, 2H), 2.24-2.21 (m, 1H), 1.27-1.09 (comp. m, 10H), 1.04 (t,  $J = 7.1$  Hz, 3H), 0.81 (t,  $J = 7.1$  Hz, 3H).

$^{13}\text{C}$  NMR (100 MHz;  $\text{CDCl}_3$ ):  $\delta$  175.5, 157.8, 134.2, 131.5, 129.4, 124.1, 113.3, 60.1, 55.1, 44.9, 41.2, 39.0, 31.7, 31.4, 29.4, 28.9, 27.3, 22.5, 14.04, 14.01.

IR (ATR, neat): 2955, 2924, 2855, 1728, 1512, 1242, 1242, 1173, 1034, 833  $\text{cm}^{-1}$ .

HRMS (ESI+):  $m/z$  calc'd for  $(\text{M} + \text{H})^+$  [ $\text{C}_{22}\text{H}_{32}\text{O}_3 + \text{H}$ ] $^+$ : 345.2424, found 345.2426.



**Cyclohexene 5-23.** Prepared according to the *General Procedure* using alkene **5-70** (15.5 mg, 75.0  $\mu\text{mol}$ ), diene **5-146**<sup>55</sup> (35.6 mg, 225  $\mu\text{mol}$ ),  $[\text{Cr}(\text{Ph}_2\text{phen})_3](\text{BF}_4)_3$  (0.5 mg, 0.375  $\mu\text{mol}$ ), and nitromethane (0.750 mL). The reaction mixture was irradiated for 70 h. The crude product was purified by flash chromatography (100% hexanes  $\rightarrow$  15:1 hexanes/EtOAc eluent) to afford cyclohexene **5-23** (23.1 mg, 85% yield, 4:1 isomeric ratio) as a colorless oil.

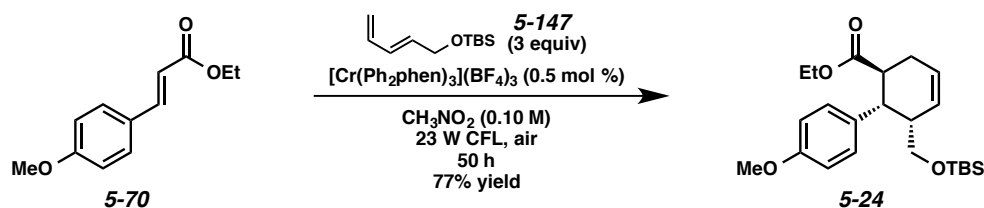
TLC:  $R_f = 0.74$  in 3:1 hexanes/EtOAc, stained red with *p*-anisaldehyde.

$^1\text{H}$  NMR (400 MHz;  $\text{CDCl}_3$ ):  $\delta$  7.20 (t,  $J = 7.2$  Hz, 3H), 7.13 (d,  $J = 8.4$  Hz, 2H), 6.99 (d,  $J = 7.6$  Hz, 2H), 6.81 (d,  $J = 8.4$  Hz, 2H), 5.94-5.90 (m, 1H), 5.81-5.75 (m, 1H), 3.97 (q,  $J = 7.1$  Hz, 2H), 3.78 (s, 3H), 3.35 (dd,  $J = 10.2, 5.4$  Hz, 1H), 3.01 (dt,  $J = 10.2, 7.5$  Hz, 1H), 2.42-2.39 (comp. m, 3H), 2.35-2.27 (comp. m, 2H), 1.54-1.41 (comp. m, 2H), 1.04 (t,  $J = 7.1$  Hz, 3H).

$^{13}\text{C}$  NMR (100 MHz;  $\text{CDCl}_3$ ):  $\delta$  175.4, 157.9, 142.3, 133.9, 131.0, 129.4, 128.24, 128.19, 125.6, 124.7, 113.5, 60.2, 55.2, 44.7, 41.3, 38.5, 33.6, 33.2, 28.6, 14.0.

IR (ATR, neat): 3024, 2932, 2839, 1728, 1512, 1242, 1157, 1034, 833, 733, 702  $\text{cm}^{-1}$ .

HRMS (ESI+):  $m/z$  calc'd for  $(\text{M} + \text{H})^+$  [ $\text{C}_{24}\text{H}_{28}\text{O}_3 + \text{H}$ ] $^+$ : 365.2111, found 365.2109.



**Cyclohexene 5-24.** Prepared according to the *General Procedure* using alkene **5-70** (24.7 mg, 0.120 mmol), diene **5-147** (71.4 mg, 0.360 mmol),  $[\text{Cr}(\text{Ph}_2\text{phen})_3](\text{BF}_4)_3$  (0.8 mg, 0.000600 mmol), and nitromethane (1.20 mL). The reaction mixture was irradiated for 50 h. The crude product was purified by flash chromatography (100% hexanes  $\rightarrow$  15:1 hexanes/EtOAc eluent) to afford cyclohexene **5-24** (37.6 mg, 77% yield, 4:1 isomeric ratio) as a colorless oil.

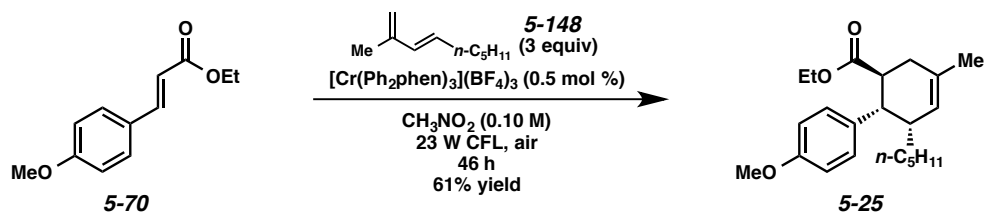
**TLC:**  $R_f = 0.76$  in 3:1 hexanes/EtOAc, stained red with *p*-anisaldehyde.

**$^1\text{H NMR}$**  (400 MHz;  $\text{CDCl}_3$ ):  $\delta$  7.18 (d,  $J = 8.5$  Hz, 2H), 6.80 (d,  $J = 8.5$  Hz, 2H), 5.86-5.75 (comp. m, 2H), 3.93 (q,  $J = 7.1$  Hz, 2H), 3.78 (s, 3H), 3.35 (d,  $J = 4.4$  Hz, 2H), 3.32-3.26 (m, 1H), 2.36-2.32 (comp. m, 3H), 1.01 (t,  $J = 7.1$  Hz, 3H), 0.86 (s, 9H), -0.05 (s, 3H), -0.08 (s, 3H).

**$^{13}\text{C NMR}$**  (100 MHz;  $\text{CDCl}_3$ ):  $\delta$  175.8, 158.0, 133.7, 129.4, 129.0, 126.0, 113.3, 63.3, 60.0, 55.2, 44.0, 41.82, 41.77, 28.9, 25.8, 18.2, 14.0, -5.6.

**IR** (ATR, neat): 2932, 2901, 2855, 1728, 1512, 1250, 1042, 833, 772  $\text{cm}^{-1}$ .

**HRMS** (ESI+):  $m/z$  calc'd for  $(\text{M} + \text{H})^+ [\text{C}_{23}\text{H}_{36}\text{O}_4\text{Si} + \text{H}]^+$ : 405.2456, found 405.2455.



**Cyclohexene 5-25.** Prepared according to the *General Procedure* using alkene **5-70** (15.5 mg, 75.0  $\mu\text{mol}$ ), diene **5-148**<sup>55</sup> (31.1 mg, 225  $\mu\text{mol}$ ),  $[\text{Cr}(\text{Ph}_2\text{phen})_3](\text{BF}_4)_3$  (0.5 mg, 0.375  $\mu\text{mol}$ ), and nitromethane (0.750 mL). The reaction mixture was irradiated for 46 h. The crude product was purified by flash chromatography (100% hexanes  $\rightarrow$  9:1 hexanes/EtOAc eluent) to afford cyclohexene **5-25** (15.8 mg, 61% yield, 3:1 isomeric ratio) as a colorless oil.

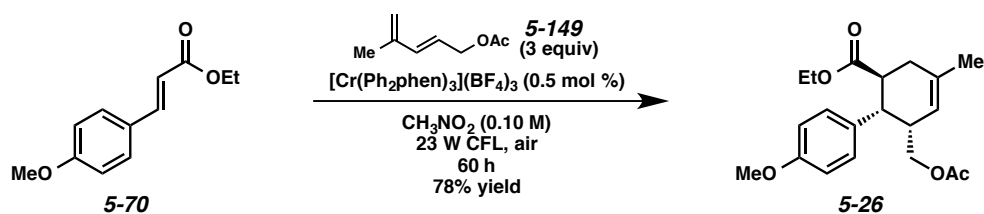
**TLC:**  $R_f = 0.78$  in 3:1 hexanes/EtOAc, stained blue with *p*-anisaldehyde.

**$^1\text{H NMR}$**  (400 MHz;  $\text{CDCl}_3$ ):  $\delta$  7.09 (d,  $J = 8.5$  Hz, 2H), 6.79 (d,  $J = 8.5$  Hz, 2H), 5.57 (br s, 1H), 3.97 (q,  $J = 7.1$  Hz, 2H), 3.77 (s, 3H), 3.24 (dd,  $J = 10.3, 5.4$  Hz, 1H), 3.04-2.98 (m, 1H), 2.29-2.16 (comp. m, 3H), 1.72 (s, 3H), 1.36-1.14 (comp. m, 8H), 1.05 (t,  $J = 7.1$  Hz, 3H), 0.79 (t,  $J = 7.0$  Hz, 3H).

**$^{13}\text{C NMR}$**  (100 MHz;  $\text{CDCl}_3$ ):  $\delta$  175.6, 157.8, 134.2, 131.3, 129.4, 125.7, 113.3, 60.1, 55.1, 47.7, 44.9, 41.7, 39.1, 33.3, 32.0, 31.4, 27.1, 23.4, 22.6, 14.0.

**IR** (ATR, neat): 2955, 2924, 2855, 1736, 1512, 1466, 1250, 1180, 1034, 833  $\text{cm}^{-1}$ .

**HRMS** (ESI+):  $m/z$  calc'd for  $(\text{M} + \text{H})^+ [\text{C}_{22}\text{H}_{32}\text{O}_3 + \text{H}]^+$ : 345.2424, found 345.2423.



**Cyclohexene 5-26.** Prepared according to the *General Procedure* using alkene **5-70** (15.5 mg, 75.0  $\mu\text{mol}$ ), diene **5-149** (31.5 mg, 225  $\mu\text{mol}$ ),  $[\text{Cr}(\text{Ph}_2\text{phen})_3](\text{BF}_4)_3$  (0.5 mg, 0.375  $\mu\text{mol}$ ), and nitromethane (0.750 mL). The reaction mixture was irradiated for 60 h. The crude product was purified by flash chromatography (100% hexanes  $\rightarrow$  10:1 hexanes/EtOAc eluent) to afford cyclohexene **5-26** (20.2 mg, 78% yield, 6:1 isomeric ratio) as a colorless oil.

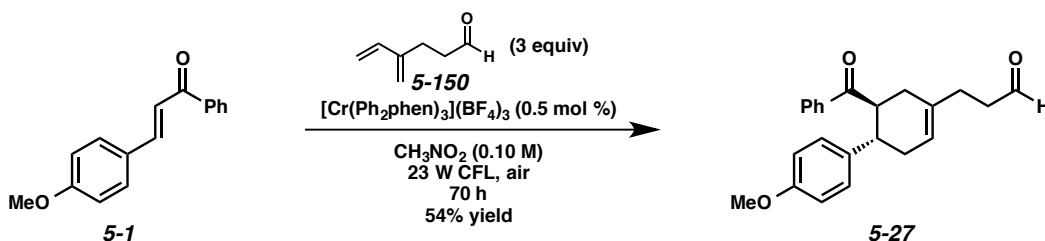
**TLC:**  $R_f = 0.55$  in 3:1 hexanes/EtOAc, visualized by UV.

**<sup>1</sup>H NMR** (400 MHz; CDCl<sub>3</sub>): δ 7.10 (d, *J* = 8.6 Hz, 2H), 6.80 (d, *J* = 8.6 Hz, 2H), 5.45 (br s, 1H), 3.97 (q, *J* = 7.1 Hz, 2H), 3.90 (dd, *J* = 11.0, 5.3 Hz, 1H), 3.76 (s, 3H), 3.67 (dd, *J* = 11.0, 6.4 Hz, 1H), 3.31 (dd, *J* = 10.8, 6.0 Hz, 1H), 3.12 (ddd, *J* = 10.8, 8.8, 6.3 Hz, 1H), 2.63-2.57 (m, 1H), 2.32-2.28 (comp. m, 2H), 1.91 (s, 3H), 1.74 (s, 3H), 1.04 (t, *J* = 7.1 Hz, 3H).

**<sup>13</sup>C NMR** (100 MHz; CDCl<sub>3</sub>): δ 175.2, 169.6, 158.2, 134.2, 132.9, 129.0, 121.6, 113.7, 65.1, 60.3, 55.1, 43.1, 41.8, 39.0, 33.3, 23.3, 20.9, 14.0.

**IR** (ATR, neat): 2963, 2901, 2839, 1728, 1512, 1247, 1172, 1034, 833 cm<sup>-1</sup>.

**HRMS** (ESI<sup>+</sup>): *m/z* calc'd for (M + H)<sup>+</sup> [C<sub>20</sub>H<sub>26</sub>O<sub>5</sub> + H]<sup>+</sup>: 347.1853, found 347.1853.



**Cyclohexene 5-27.** Prepared according to the *General Procedure* using alkene **5-1** (17.9 mg, 75.0 μmol), diene **5-150** (24.8 mg, 225 μmol), [Cr(Ph<sub>2</sub>phen)<sub>3</sub>](BF<sub>4</sub>)<sub>3</sub> (0.5 mg, 0.375 μmol), and nitromethane (0.750 mL). The reaction mixture was irradiated for 70 h. The crude product was purified by flash chromatography (100% hexanes → 3:1 hexanes/EtOAc eluent) to afford cyclohexene **5-27** (14.1 mg, 54% yield, 6:1 isomeric ratio) as a colorless oil.

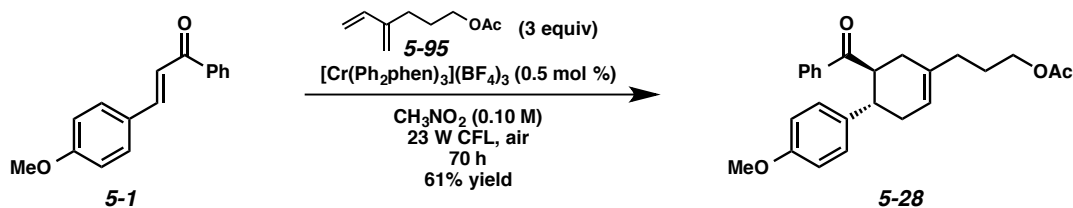
**TLC:** R<sub>f</sub> = 0.35 in 3:1 hexanes/EtOAc, stained blue with *p*-anisaldehyde.

**<sup>1</sup>H NMR** (400 MHz; CDCl<sub>3</sub>): δ 9.79 (s, 1H), 7.79 (d, *J* = 7.3 Hz, 2H), 7.48 (t, *J* = 7.3 Hz, 1H), 7.37 (t, *J* = 7.7 Hz, 2H), 7.09 (d, *J* = 8.6 Hz, 2H), 6.68 (d, *J* = 8.6 Hz, 2H), 5.57 (br s, 1H), 3.95 (td, *J* = 10.5, 5.2 Hz, 1H), 3.68 (s, 3H), 3.21-3.15 (m, 1H), 2.60-2.56 (comp. m, 2H), 2.37-2.19 (comp. m, 6H).

**<sup>13</sup>C NMR** (100 MHz; CDCl<sub>3</sub>): δ 203.6, 202.1, 157.9, 137.2, 136.1, 134.3, 132.8, 128.5, 128.4, 128.0, 121.5, 113.7, 55.1, 47.0, 41.7, 41.6, 33.9, 33.5, 29.4.

**IR** (ATR, neat): 2901, 2832, 2723, 1721, 1674, 1512, 1242, 1034, 826, 733 cm<sup>-1</sup>.

**HRMS** (ESI+):  $m/z$  calc'd for  $(M + H)^+$   $[C_{23}H_{24}O_3 + H]^+$ : 349.1798, found 349.1796.



**Cyclohexene 5-28**. Prepared according to the *General Procedure* using alkene **5-1** (17.9 mg, 75.0  $\mu$ mol), diene **5-95** (34.7 mg, 225  $\mu$ mol),  $[Cr(Ph_2phen)_3](BF_4)_3$  (0.5 mg, 0.375  $\mu$ mol), and nitromethane (0.750 mL). The reaction mixture was irradiated for 70 h. The crude product was purified by flash chromatography (100% hexanes  $\rightarrow$  3:1 hexanes/EtOAc eluent) to afford cyclohexene **5-28** (18.0 mg, 61% yield, 7:1 isomeric ratio) as a colorless oil.

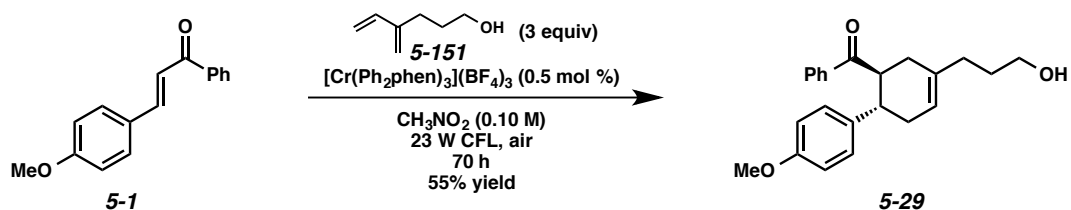
**TLC**:  $R_f = 0.50$  in 3:1 hexanes/EtOAc, visualized by UV.

**$^1H$  NMR** (400 MHz;  $CDCl_3$ ):  $\delta$  7.79 (d,  $J = 7.3$  Hz, 2H), 7.48 (t,  $J = 7.3$  Hz, 1H), 7.37 (t,  $J = 7.7$  Hz, 2H), 7.09 (d,  $J = 8.6$  Hz, 2H), 6.69 (d,  $J = 8.6$  Hz, 2H), 5.57 (br s, 1H), 4.07 (t, 2H,  $J = 6.4$  Hz), 3.98-3.92 (m, 1H), 3.68 (s, 3H), 3.18 (td,  $J = 10.8, 5.7$  Hz, 1H), 2.41-2.20 (comp. m, 4H), 2.09-2.05 (comp. m, 2H), 2.05 (s, 3H), 1.82-1.74 (comp. m, 2H).

**$^{13}C$  NMR** (100 MHz;  $CDCl_3$ ):  $\delta$  203.7, 171.2, 157.8, 137.2, 136.3, 135.0, 132.8, 128.5, 128.34, 128.28, 128.0, 121.3, 113.7, 64.1, 55.1, 47.2, 41.6, 34.1, 33.5, 26.4, 21.0.

**IR** (ATR, neat): 2955, 2901, 2832, 1728, 1674, 1512, 1234, 1034, 826, 702  $cm^{-1}$ .

**HRMS** (ESI+):  $m/z$  calc'd for  $(M + H)^+$   $[C_{25}H_{28}O_4 + H]^+$ : 393.2060, found 393.2065.



**Cyclohexene 5-29.** Prepared according to the *General Procedure* using alkene **5-1** (17.9 mg, 75.0  $\mu\text{mol}$ ), diene **5-151** (25.2 mg, 225  $\mu\text{mol}$ ),  $[\text{Cr}(\text{Ph}_2\text{phen})_3](\text{BF}_4)_3$  (0.5 mg, 0.375  $\mu\text{mol}$ ), and nitromethane (0.750 mL). The reaction mixture was irradiated for 70 h. The crude product was purified by flash chromatography (100% hexanes  $\rightarrow$  4:1 hexanes/EtOAc eluent) to afford cyclohexene **5-29** (14.5 mg, 55% yield, 8:1 isomeric ratio) as a colorless oil.

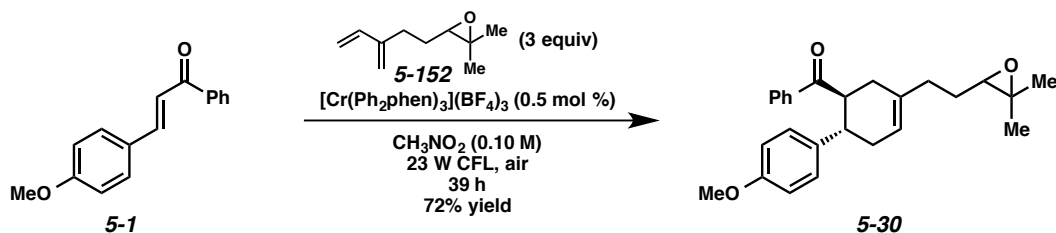
**TLC:**  $R_f$  = 0.62 in 1:1 hexanes/EtOAc, stained blue with *p*-anisaldehyde.

**$^1\text{H}$  NMR** (400 MHz;  $\text{CDCl}_3$ ):  $\delta$  7.79 (d,  $J$  = 8.0 Hz, 2H), 7.48 (t,  $J$  = 7.4 Hz, 1H), 7.37 (t,  $J$  = 7.6 Hz, 2H), 7.09 (d,  $J$  = 8.4 Hz, 2H), 6.69 (d,  $J$  = 8.4 Hz, 2H), 5.59 (br s, 1H), 3.95 (td,  $J$  = 10.4, 5.1 Hz, 1H), 3.68 (s, 3H), 3.22-3.15 (m, 1H), 2.41-2.21 (comp. m, 4H), 2.12-2.08 (comp. m, 2H), 1.75-1.65 (comp. m, 4H).

**$^{13}\text{C}$  NMR** (100 MHz;  $\text{CDCl}_3$ ):  $\delta$  203.8, 157.8, 136.4, 135.7, 132.8, 128.5, 128.3, 128.0, 121.0, 113.7, 62.6, 55.1, 47.2, 41.6, 34.1, 33.6, 33.5, 30.5.

**IR** (ATR, neat): 3387, 2931, 2909, 2839, 1674, 1512, 1265, 1242, 1034, 732, 702  $\text{cm}^{-1}$ .

**HRMS** (ESI+):  $m/z$  calc'd for  $(\text{M} + \text{H})^+$   $[\text{C}_{23}\text{H}_{26}\text{O}_3 + \text{H}]^+$ : 351.1955, found 351.1955.



**Cyclohexene 5-30.** Prepared according to the *General Procedure* using alkene **5-1** (23.8 mg, 0.100 mmol), diene **5-152** (45.7 mg, 0.300 mmol),  $[\text{Cr}(\text{Ph}_2\text{phen})_3](\text{BF}_4)_3$  (0.7 mg, 0.000500 mmol), and nitromethane (1.00 mL). The reaction mixture was irradiated for 39 h. The crude product was purified by flash chromatography (100% hexanes  $\rightarrow$  9:1 hexanes/EtOAc eluent) to afford cyclohexene **5-30** (28.2 mg, 72% yield, 7:1 isomeric ratio) as a colorless oil.

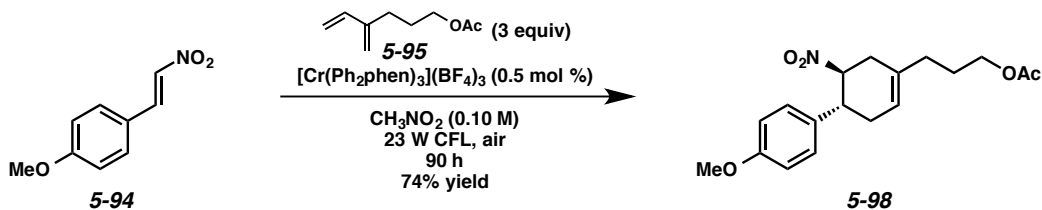
**TLC:**  $R_f$  = 0.52 in 3:1 hexanes/EtOAc, stained yellow with *p*-anisaldehyde.

**<sup>1</sup>H NMR** (400 MHz; CDCl<sub>3</sub>): δ 7.81-7.78 (comp. m, 2H), 7.48 (t, *J* = 7.3 Hz, 1H), 7.37 (t, *J* = 7.6 Hz, 2H), 7.09 (d, *J* = 8.5 Hz, 2H), 6.69 (d, *J* = 8.5 Hz, 2H), 5.61 (br s, 1H), 3.99-3.92 (m, 1H), 3.68 (s, 3H), 3.23-3.16 (m, 1H), 2.73 (q, *J* = 5.4 Hz, 1H), 2.44-2.10 (comp. m, 6H), 1.68-1.63 (comp. m, 2H), 1.32 (s, 3H), 1.27 (d, *J* = 1.4 Hz, 3H).

**<sup>13</sup>C NMR** (100 MHz; CDCl<sub>3</sub>): δ 203.7, 157.8, 137.2, 136.3, 135.3, 132.8, 128.4, 128.0, 121.0, 113.7, 64.0, 58.4, 55.1, 47.1, 41.6, 34.2, 34.0, 27.3, 24.9, 18.8.

**IR** (ATR, neat): 3055, 2963, 2909, 2839, 1682, 1512, 1250, 734, 702 cm<sup>-1</sup>.

**HRMS** (ESI<sup>+</sup>): *m/z* calc'd for (M + H)<sup>+</sup> [C<sub>26</sub>H<sub>30</sub>O<sub>3</sub> + H]<sup>+</sup>: 391.2268, found 391.2267.



**Cyclohexene 5-98.** Prepared according to the *General Procedure* using alkene **5-94** (9.0 mg, 50.0 μmol), diene **5-95** (23.1 mg, 150 μmol), [Cr(Ph<sub>2</sub>phen)<sub>3</sub>](BF<sub>4</sub>)<sub>3</sub> (0.5 mg, 0.250 μmol), and nitromethane (0.500 mL). The reaction mixture was irradiated for 90 h. The crude product was purified by flash chromatography (100% hexanes → 4:1 hexanes/EtOAc eluent) to afford cyclohexene **5-98** (12.4 mg, 74% yield, 11:1 isomeric ratio) as a yellow oil.

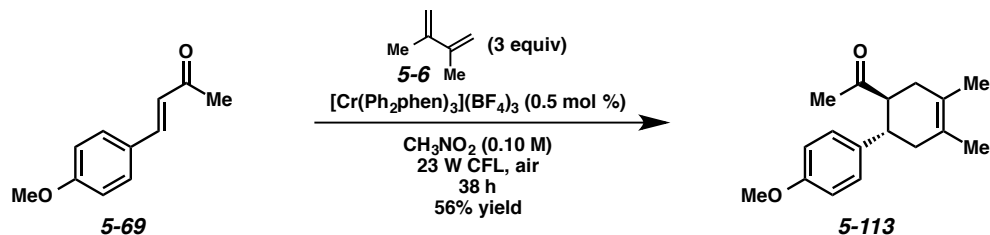
**TLC:** R<sub>f</sub> = 0.57 in 3:1 hexanes/EtOAc, stained with KMnO<sub>4</sub>.

**<sup>1</sup>H NMR** (500 MHz; CDCl<sub>3</sub>): δ 7.16 (d, *J* = 8.6 Hz, 2H), 6.87 (d, *J* = 8.6 Hz, 2H), 5.56 (br s, 1H), 4.93 (td, *J* = 10.6, 5.7 Hz, 1H), 4.11 (t, *J* = 13.2, 6.6 Hz, 2H), 3.80 (s, 3H), 3.34 (td, *J* = 10.6, 5.9 Hz, 1H), 2.83-2.78 (comp. m, 2H), 2.61 (dd, *J* = 16.6, 5.2 Hz, 1H), 2.52-2.46 (m, 1H), 2.37-2.31 (m, 1H), 2.15 (t, *J* = 7.5 Hz, 2H), 2.10 (s, 3H), 2.08-2.07 (m, 1H), 1.84-1.78 (comp. m, 2H).

**<sup>13</sup>C NMR** (100 MHz; CDCl<sub>3</sub>): δ 171.2, 158.9, 132.9, 128.4, 127.9, 121.0, 114.2, 88.0, 63.81, 63.79, 55.2, 43.5, 34.0, 33.1, 32.9, 26.3, 21.0.

**IR** (ATR, neat): 2918, 2839, 1732, 1548, 1514, 1375, 1244, 1032, 829, 733  $\text{cm}^{-1}$ .

**HRMS** (ESI+):  $m/z$  calc'd for  $(M + \text{Na})^+$  [ $\text{C}_{18}\text{H}_{23}\text{NO}_5 + \text{Na}$ ] $^+$ : 356.1468, found 356.1468.



**Cyclohexene 5-113.** Prepared according to the *General Procedure* using alkene **5-69** (15.4 mg, 0.0873 mmol), diene **5-6** (29.0  $\mu\text{L}$ , 0.262 mmol),  $[\text{Cr}(\text{Ph}_2\text{phen})_3](\text{BF}_4)_3$  (0.6 mg, 0.000437 mmol), and nitromethane (0.870 mL). The reaction mixture was irradiated for 38 h. The crude product was purified by flash chromatography (100% hexanes  $\rightarrow$  10:1 hexanes/EtOAc eluent) to afford cyclohexene **5-113** (12.6 mg, 56% yield) as a colorless oil.

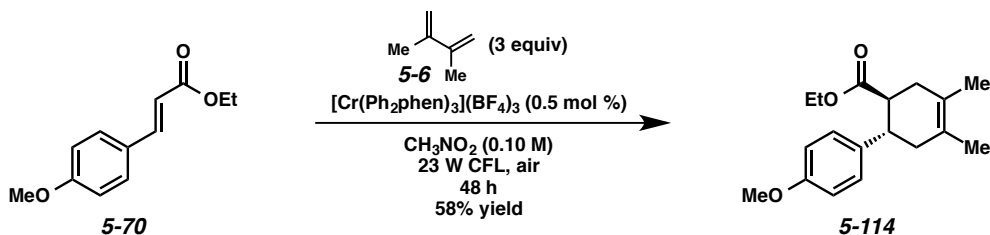
**TLC:**  $R_f = 0.65$  in 3:1 hexanes/EtOAc, stained with  $\text{KMnO}_4$ .

**$^1\text{H}$  NMR** (400 MHz;  $\text{CDCl}_3$ ):  $\delta$  7.10 (d,  $J = 8.7$  Hz, 2H), 6.82 (d,  $J = 8.7$  Hz, 2H), 3.77 (s, 3H), 3.01-2.89 (comp. m, 2H), 2.32-2.03 (comp. m, 4H), 1.84 (s, 3H), 1.67 (s, 3H), 1.63 (s, 3H).

**$^{13}\text{C}$  NMR** (100 MHz;  $\text{CDCl}_3$ ):  $\delta$  212.3, 158.1, 136.1, 128.3, 125.4, 123.7, 113.9, 55.2, 54.2, 42.7, 40.6, 35.0, 29.6, 18.7, 18.6.

**IR** (ATR, neat): 2991, 2911, 1705, 1512, 1244, 1176, 1033, 827  $\text{cm}^{-1}$ .

**HRMS** (ESI+):  $m/z$  calc'd for  $(M + \text{H})^+$  [ $\text{C}_{17}\text{H}_{22}\text{O}_2 + \text{H}$ ] $^+$ : 259.1693, found 259.1689.



**Cyclohexene 5-114.** Prepared according the *General Procedure* using alkene **5-70** (20.6 mg, 0.100 mmol), diene **5-6** (33.8  $\mu$ L, 0.300 mmol),  $[\text{Cr}(\text{Ph}_2\text{phen})_3](\text{BF}_4)_3$  (0.7 mg, 0.000500 mmol), and nitromethane (1.00 mL). The reaction mixture was irradiated for 48 h. The crude product was purified by flash chromatography (100% hexanes  $\rightarrow$  9:1 hexanes/EtOAc eluent) to afford cyclohexene **5-114** (16.6 mg, 58% yield) as a colorless oil.

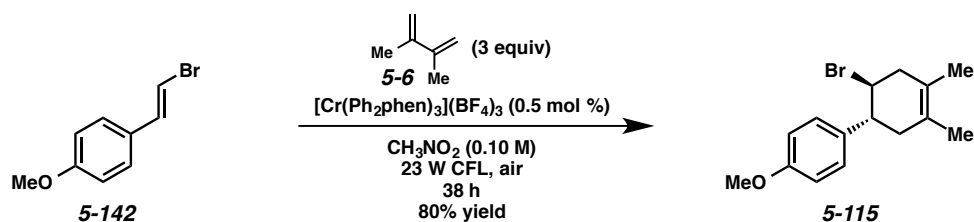
**TLC:**  $R_f$  = 0.73 in 3:1 hexanes/EtOAc, stained with  $\text{KMnO}_4$ .

**$^1\text{H}$  NMR** (400 MHz;  $\text{CDCl}_3$ ):  $\delta$  7.13 (d,  $J$  = 8.7 Hz, 2H), 6.81 (d,  $J$  = 8.7 Hz, 2H), 3.86 (qd,  $J$  = 7.1, 2.5 Hz, 2H), 3.77 (s, 3H), 2.99-2.92 (m, 1H), 2.78 (td,  $J$  = 11.2, 5.3 Hz, 1H), 2.45-2.38 (m, 1H), 2.23-2.15 (comp. m, 3H), 1.66 (s, 3H), 1.63 (s, 3H), 0.94 (t,  $J$  = 7.1 Hz, 3H).

**$^{13}\text{C}$  NMR** (100 MHz;  $\text{CDCl}_3$ ):  $\delta$  175.2, 158.1, 136.1, 128.4, 125.3, 123.7, 113.6, 59.9, 55.2, 47.2, 42.9, 40.3, 35.5, 18.7, 18.6, 13.9.

**IR** (ATR, neat): 2980, 2904, 1728, 1512, 1244, 1176, 1153, 1033, 829  $\text{cm}^{-1}$ .

**HRMS** (ESI+):  $m/z$  calc'd for  $(\text{M} + \text{H})^+ [\text{C}_{18}\text{H}_{24}\text{O}_3 + \text{H}]^+$ : 289.1798, found 289.1799.



**Cyclohexene 5-115.** Prepared according the *General Procedure* using alkene **5-142** (18.6 mg, 0.0873 mmol), diene **5-6** (29.0  $\mu$ L, 0.262 mmol),  $[\text{Cr}(\text{Ph}_2\text{phen})_3](\text{BF}_4)_3$  (0.6 mg, 0.000437 mmol), and nitromethane (0.870 mL). The reaction mixture was irradiated for 38 h. The crude product was purified by flash chromatography (100% hexanes  $\rightarrow$  10:1 hexanes/EtOAc eluent) to afford cyclohexene **5-115** (20.5 mg, 80% yield) as a colorless oil.

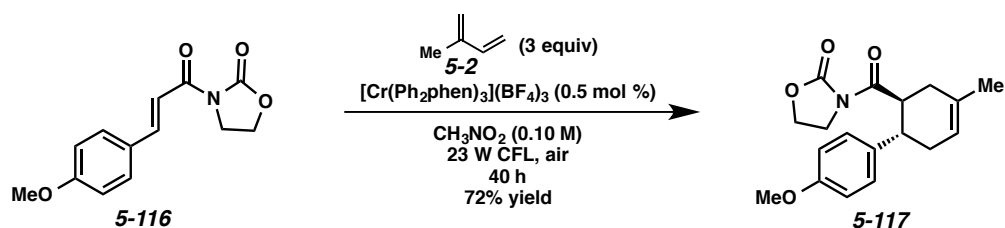
**TLC:**  $R_f$  = 0.78 in 3:1 hexanes/EtOAc, stained with  $\text{KMnO}_4$ .

**<sup>1</sup>H NMR** (400 MHz; CDCl<sub>3</sub>): δ 7.13 (d, *J* = 8.7 Hz, 2H), 6.87 (d, *J* = 8.7 Hz, 2H), 4.41 (ddd, *J* = 10.0, 8.1, 6.5 Hz, 1H), 3.80 (s, 3H), 3.10 (td, *J* = 10.0, 6.0 Hz, 1H), 2.69 (d, *J* = 6.5 Hz, 2H), 2.41-2.22 (m, 2H), 1.66 (s, 3H), 1.63 (s, 3H).

**<sup>13</sup>C NMR** (100 MHz; CDCl<sub>3</sub>): δ 158.3, 136.3, 128.2, 125.4, 124.4, 113.8, 55.2, 54.8, 48.6, 43.0, 40.5, 18.5, 18.4.

**IR** (ATR, neat): 2980, 2909, 1611, 1512, 1246, 1176, 1035, 827, 773, 687 cm<sup>-1</sup>.

**HRMS** (ESI<sup>+</sup>): *m/z* calc'd for (M + Na)<sup>+</sup> [C<sub>15</sub>H<sub>19</sub>BrO + Na]<sup>+</sup>: 317.0511, found 317.0510.



**Cyclohexene 5-117.** Prepared according the *General Procedure* using alkene **5-116** (12.4 mg, 0.0500 mmol), diene **5-2** (15.0 μL, 0.150 mmol),  $[\text{Cr}(\text{Ph}_2\text{phen})_3](\text{BF}_4)_3$  (0.3 mg, 0.000250 mmol), and nitromethane (0.500 mL). The reaction mixture was irradiated for 40 h. The crude product was purified by flash chromatography (100% hexanes → 2:1 hexanes/EtOAc eluent) to afford cyclohexene **5-117** (11.3 mg, 72% yield, 19:1 isomeric ratio) as a colorless oil.

**TLC:** *R<sub>f</sub>* = 0.64 in 1:1 hexanes/EtOAc, stained with KMnO<sub>4</sub>.

**<sup>1</sup>H NMR** (400 MHz; CDCl<sub>3</sub>): δ 7.14 (d, *J* = 8.6 Hz, 2H), 6.80 (d, *J* = 8.6 Hz, 2H), 5.48 (br s, 1H), 4.37 (td, *J* = 10.9, 5.2 Hz, 1H), 4.22 (td, *J* = 8.5, 5.2 Hz, 1H), 3.98 (q, *J* = 8.5 Hz, 1H), 3.84-3.78 (m, 1H), 3.76 (s, 3H), 3.52 (ddd, *J* = 10.6, 9.7, 5.7 Hz, 1H), 2.97 (q, *J* = 9.7 Hz, 1H), 2.40-2.16 (comp. m, 4H), 1.71 (s, 3H).

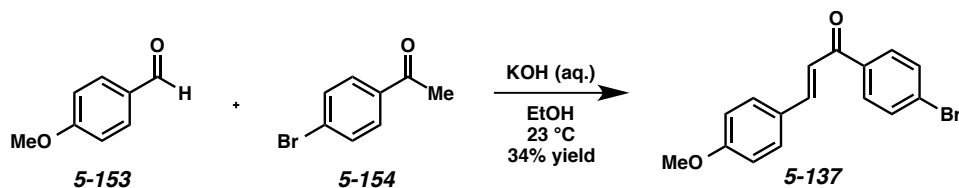
**<sup>13</sup>C NMR** (100 MHz; CDCl<sub>3</sub>): δ 176.2, 158.1, 153.1, 135.9, 132.0, 128.5, 120.6, 113.6, 61.7, 55.2, 43.6, 42.9, 42.6, 33.7, 23.2.

**HRMS** (ESI<sup>+</sup>): *m/z* calc'd for (M + H)<sup>+</sup> [C<sub>18</sub>H<sub>21</sub>NO<sub>4</sub> + H]<sup>+</sup>: 316.1543, found 316.1528.

### 5.11.3 Synthesis of Electron-Poor Alkenes

**General Notes:** Reactions were performed in flame-dried glassware under Ar, unless otherwise noted.

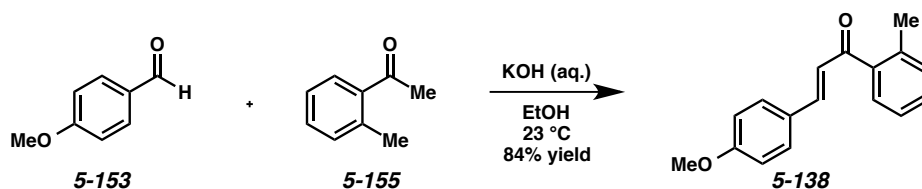
Aldol condensation reactions did not require flame-dried glassware and could be run in a stoppered flask.



**Ketone 5-137.** To a solution of aldehyde **5-153** (0.120 mL, 1.00 mmol) and ketone **5-154** (0.199 g, 1.00 mmol) in EtOH (10.0 mL) at 23 °C was added aq. KOH (0.500 g in 1.00 mL H<sub>2</sub>O). The reaction mixture was capped and stirred at ambient temperature for 16 h. EtOH was removed by rotary evaporation, and the crude mixture was partitioned between H<sub>2</sub>O (15 mL) and EtOAc (15 mL). The aqueous layer was extracted with EtOAc (3 x 15 mL). The organic layers were combined, washed with brine (40 mL), and dried over MgSO<sub>4</sub>. The solvent was removed by rotary evaporation, and the crude residue was purified by flash chromatography (100% hexanes → 6:1 hexanes/EtOAc eluent) to afford ketone **5-137** (0.108 g, 34% yield) as an off-white solid.

**TLC:** R<sub>f</sub> = 0.46 in 4:1 hexanes/EtOAc, stained with KMnO<sub>4</sub>.

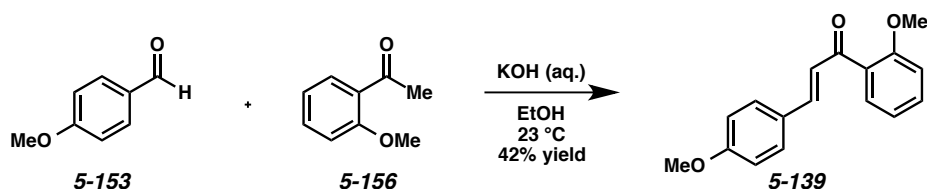
All spectroscopic data were consistent with previously reported values.<sup>56</sup>



**Ketone 5-138.** To a solution of aldehyde **5-153** (0.120 mL, 1.00 mmol) and ketone **5-155** (0.130 mL, 1.00 mmol) in EtOH (10.0 mL) at 23 °C was added aq. KOH (0.500 g in 1.00 mL H<sub>2</sub>O). The reaction mixture was capped and stirred at ambient temperature for 16 h. EtOH was removed by rotary evaporation, and the crude mixture was partitioned between H<sub>2</sub>O (15 mL) and EtOAc (15 mL). The aqueous layer was extracted with EtOAc (3 x 15 mL). The organic layers were combined, washed with brine (40 mL), and dried over MgSO<sub>4</sub>. The solvent was removed by rotary evaporation, and the crude residue was purified by flash chromatography (100% hexanes → 6:1 hexanes/EtOAc eluent) to afford ketone **5-138** (0.212 g, 84% yield) as a yellow oil.

**TLC:** R<sub>f</sub> = 0.42 in 4:1 hexanes/EtOAc, stained with KMnO<sub>4</sub>.

All spectroscopic data were consistent with previously reported values.<sup>57</sup>



**Ketone 5-139.** To a solution of aldehyde **5-153** (0.120 mL, 1.00 mmol) and ketone **5-156** (0.14 mL, 1.00 mmol) in EtOH (10.0 mL) at 23 °C was added aq. KOH (0.500 g in 1.00 mL H<sub>2</sub>O). The reaction mixture was capped and stirred at ambient temperature for 16 h. EtOH was removed by rotary evaporation, and the crude mixture was partitioned between H<sub>2</sub>O (15 mL) and EtOAc (15 mL). The aqueous layer was extracted with EtOAc (3 x 15 mL). The organic layers were combined, washed with brine (40 mL), and dried over MgSO<sub>4</sub>. The solvent was removed by rotary evaporation, and the crude residue was purified by flash chromatography (100% hexanes → 6:1 hexanes/EtOAc eluent) to afford ketone **5-139** (0.114 g, 42% yield) as a yellow oil.

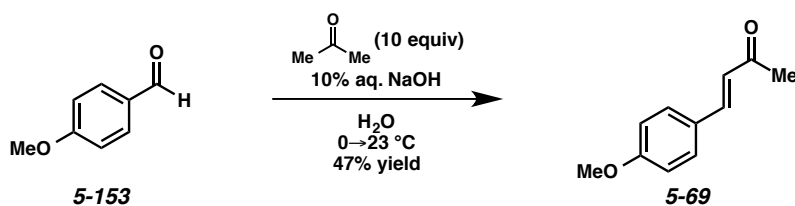
**TLC:** R<sub>f</sub> = 0.22 in 4:1 hexanes/EtOAc, stained with KMnO<sub>4</sub>.

**<sup>1</sup>H NMR** (400 MHz; CDCl<sub>3</sub>): δ 7.59-7.52 (comp. m, 3H), 7.46 (t, *J* = 7.9 Hz, 1H), 7.05-6.98 (comp. m, 2H), 6.91 (d, *J* = 8.4 Hz, 2H), 3.89 (s, 3H), 3.84 (s, 3H).

**<sup>13</sup>C NMR** (100 MHz; CDCl<sub>3</sub>): δ 193.2, 161.4, 157.9, 143.4, 132.5, 130.2, 130.1, 129.5, 127.8, 124.9, 120.7, 114.3, 111.6, 55.7, 55.4.

**IR** (ATR, neat): 2970, 2839, 1651, 1589, 1172, 1026, 825, 756 cm<sup>-1</sup>.

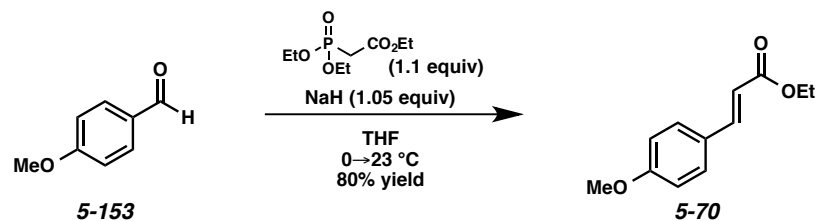
**HRMS** (ESI<sup>+</sup>): *m/z* calc'd for (M + H)<sup>+</sup> [C<sub>17</sub>H<sub>16</sub>O<sub>3</sub> + H]<sup>+</sup>: 269.1172, found 269.1176.



**Ketone 5-69.** To a solution of aldehyde **5-153** (1.22 mL, 10.0 mmol) and acetone (7.35 mL, 100 mmol) in H<sub>2</sub>O (2.00 mL) at 0 °C was added 10% aq. NaOH (5.00 mL) dropwise over 30 min. The mixture was allowed to warm to ambient temperature. After stirring for 20 h, 1 M aq. HCl was added slowly until a white precipitate formed (ca. 15 mL). After stirring for 30 min, the precipitate was collected by vacuum filtration through a Büchner funnel. The solid was washed sequentially with ice cold H<sub>2</sub>O and EtOH, then dried under vacuum. The crude yellow solid was purified by flash chromatography (8:1 → 1:1 hexanes/EtOAc eluent) to afford ketone **5-69** (0.834 g, 47% yield) as a yellow solid.

**TLC:** R<sub>f</sub> = 0.33 in 4:1 hexanes/EtOAc, stained red with *p*-anisaldehyde.

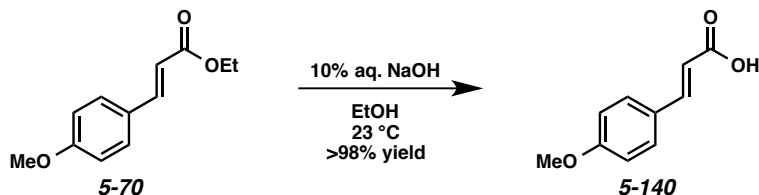
All spectroscopic data were consistent with previously reported values.<sup>58</sup>



**Ester 5-70.** To a solution of triethyl phosphonoacetate (5.46 mL, 27.5 mmol) in THF (31.0 mL) at 0 °C was added NaH (1.06 g, 60% dispersion in mineral oil, 26.5 mmol). The reaction mixture was stirred at 0 °C for 45 min, then aldehyde **5-153** (3.04 mL, 25.0 mmol) was added dropwise. The mixture was allowed to warm to ambient temperature and maintained for 15 h. The reaction mixture was then diluted with brine (30 mL), and the THF was removed by rotary evaporation. The mixture was extracted with CH<sub>2</sub>Cl<sub>2</sub> (3 x 20 mL), and the combined organic layers were washed with brine (50 mL), then dried over MgSO<sub>4</sub>. The solvent was removed by rotary evaporation, and the crude residue was purified by flash chromatography (100% hexanes → 4:1 hexanes/EtOAc) to afford ester **5-70** (4.14 g, 80% yield) as a white solid.

**TLC:** R<sub>f</sub> = 0.48 in 4:1 hexanes/EtOAc, visualized by UV.

All spectroscopic data were consistent with previously reported values.<sup>59</sup>

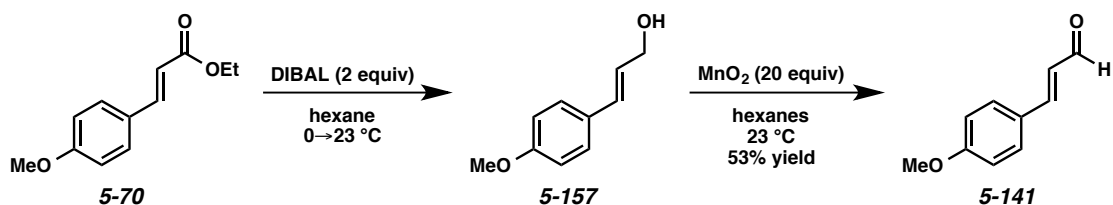


**Carboxylic acid 5-140.** To a solution of ester **5-70** (1.00 g, 4.85 mmol) in EtOH (9.70 mL) at 23 °C was added 10% aq. NaOH (19.0 mL). The flask was stoppered, and the reaction mixture was stirred at ambient temperature for 45 h. The reaction mixture was diluted with 1 M aq. HCl (25 mL). EtOAc was added until the white solid was completely dissolved (ca. 75 mL). The layers were separated, and the

aqueous layer was extracted with EtOAc (3 x 25 mL). The combined organic layers were washed with brine (60 mL) and dried over MgSO<sub>4</sub>. The solvent was removed by rotary evaporation to afford carboxylic acid **5-140** (0.864 g, quantitative) as a white solid. The crude residue was sufficiently pure by <sup>1</sup>H NMR and therefore was used without further purification.

**TLC:** R<sub>f</sub> = 0.60 in 1:1 hexanes/EtOAc, visualized by UV.

All spectroscopic data were consistent with previously reported values.<sup>60</sup>

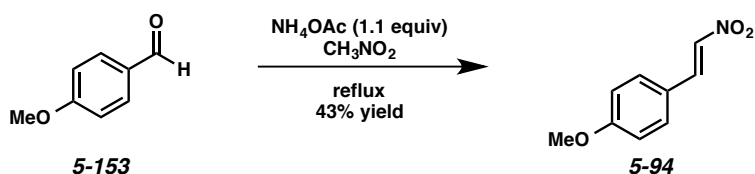


**Alcohol 5-157.** To a solution of ester **5-70** (1.50 g, 7.27 mmol) in hexane (58.0 mL) at 0 °C was added DIBAL (14.6 mL, 1.0 M in hexane) dropwise with an addition funnel. The reaction mixture was stirred at 0 °C for 2 h, then was allowed to warm to ambient temperature and stirred an additional 20 min. The reaction mixture was then diluted with sat. aq. Rochelle salt (75.0 mL) and stirred overnight. The layers were separated, and the aqueous layer was extracted with CH<sub>2</sub>Cl<sub>2</sub> (3 x 50 mL). The combined organic layers were washed with brine (50 mL), then dried over MgSO<sub>4</sub>. The volatile materials were removed by rotary evaporation to afford alcohol **5-157** as a white solid, which was used in subsequent reactions without further purification. All spectroscopic data were consistent with previously reported values.<sup>61</sup>

**Aldehyde 5-141.** To a solution of alcohol **5-157** (0.739 g, 4.50 mmol) in hexanes (22.5 mL) was added MnO<sub>2</sub> (7.82 g, 90.0 mmol). The reaction mixture was stirred for 3 h, and then was filtered through a short plug of silica (5 cm high x 3 cm wide EtOAc eluent). The filtrate was concentrated by rotary evaporation, and the crude residue was purified by flash chromatography (100% hexanes → 3:1 hexanes/EtOAc eluent) to afford aldehyde **5-141** (0.387 g, 53% yield) as a white solid.

**TLC:** R<sub>f</sub> = 0.56 in 3:1 hexanes/EtOAc, stained with KMnO<sub>4</sub>.

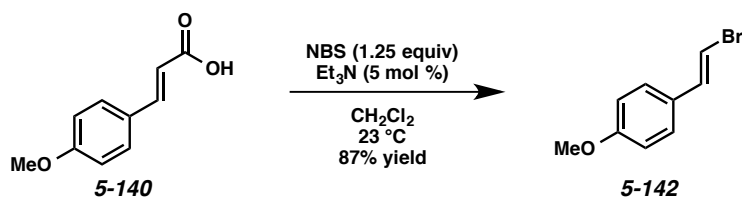
All spectroscopic data were consistent with previously reported values.<sup>6</sup>



**Nitroalkene 5-94.** To a solution of  $\text{NH}_4\text{OAc}$  (0.848 g, 11.0 mmol) in nitromethane (14.0 mL, 0.71 M with respect to **5-153**) at 23 °C was added aldehyde **5-153** (1.22 mL, 10.0 mmol). The reaction flask was equipped with a reflux condenser (open to air) and the mixture was heated at 100 °C for 4 h. The reaction was allowed to cool to ambient temperature, and the nitromethane was removed by rotary evaporation. The resulting residue was dissolved in  $\text{CH}_2\text{Cl}_2$  (20 mL), and the organic layer was washed sequentially with  $\text{H}_2\text{O}$  (20 mL) and brine (20 mL), then dried over  $\text{Na}_2\text{SO}_4$ . The volatile materials were removed by rotary evaporation, and the crude residue was purified by flash chromatography (20:1 → 5:1 hexanes/EtOAc eluent) to afford nitroalkene **5-94** (0.764 g, 43% yield) as a yellow solid.

**TLC:**  $R_f = 0.81$  in 1:1 hexanes/EtOAc, stained with  $\text{KMnO}_4$ .

All spectroscopic data were consistent with previously reported values.<sup>62</sup>

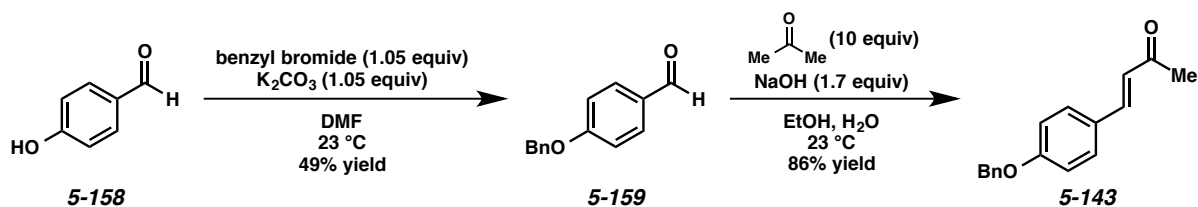


**Bromoalkene 5-142.** To a solution of carboxylic acid **5-140** (0.500 g, 2.80 mmol) in  $\text{CH}_2\text{Cl}_2$  (28.0 mL) at 23 °C was added triethylamine (20.0  $\mu\text{L}$ , 0.140 mmol). After stirring for 5 min,  $\text{NBS}$  (0.623 g, 3.50 mmol) was added. The reaction mixture was stirred for 13 h, and then concentrated by rotary evaporation.

The crude residue was purified by flash chromatography (100% hexanes → 10:1 hexanes/EtOAc eluent) to afford bromoalkene **5-142** (0.522 g, 87% yield) as a white solid.

**TLC:**  $R_f = 0.77$  in 3:1 hexanes/EtOAc, stained with  $\text{KMnO}_4$ .

All spectroscopic data were consistent with previously reported values.<sup>63</sup>



**Aldehyde 5-159.** To a solution of aldehyde **5-158** (1.83 g, 15.0 mmol) and  $\text{K}_2\text{CO}_3$  (2.18 g, 15.8 mmol) in DMF (15.0 mL) at 23 °C was added benzyl bromide (1.87 mL, 15.8 mmol). The reaction mixture was stirred for 24 h, and then was diluted with  $\text{H}_2\text{O}$  (20 mL) and EtOAc (20 mL). The layers were separated, and the aqueous layer was extracted with EtOAc (3 x 20 mL). The combined organic layers were washed with brine (50 mL), then dried over  $\text{Na}_2\text{SO}_4$ . The volatile materials were removed by rotary evaporation, and the crude residue was purified by flash chromatography (10:1 → 2:1 hexanes/EtOAc eluent) to afford aldehyde **5-159** (1.572 g, 49% yield) as a white solid.

**TLC:**  $R_f = 0.42$  in 4:1 hexanes/EtOAc, stained with  $\text{KMnO}_4$ .

**$^1\text{H}$  NMR** (400 MHz;  $\text{CDCl}_3$ ):  $\delta$  9.88 (s, 1H), 7.84 (d,  $J = 8.7$  Hz, 2H), 7.44-7.35 (comp. m, 5H), 7.08 (d,  $J = 8.7$  Hz, 2H), 5.15 (s, 2H).

**Ketone 5-143.** To a solution of aldehyde **5-159** (0.424 g, 2.00 mmol) and acetone (1.47 mL, 20.0 mmol) in EtOH (3.30 mL) at 23 °C was added a solution of NaOH (0.136 g, 3.40 mmol) in  $\text{H}_2\text{O}$  (3.30 mL). The reaction mixture was stirred at ambient temperature for 20 h, and it was then diluted with  $\text{H}_2\text{O}$  (10 mL) and EtOAc (10 mL). The layers were separated, and the aqueous layer was extracted with EtOAc (3 x 10 mL). The combined organic layers were washed with brine (30 mL), then dried over  $\text{MgSO}_4$ . The volatile materials were removed by rotary evaporation, and the crude residue was purified by flash

chromatography (10:1 → 4:1 hexanes/EtOAc eluent) to afford ketone **5-143** (0.433 g, 86% yield) as an off-white solid.

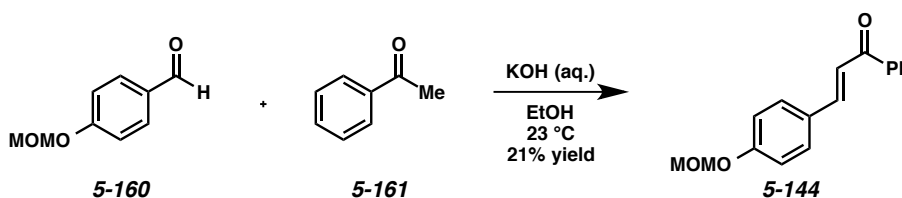
**TLC:**  $R_f$  = 0.24 in 4:1 hexanes/EtOAc, stained with  $\text{KMnO}_4$ .

**$^1\text{H NMR}$**  (400 MHz;  $\text{CDCl}_3$ ):  $\delta$  7.51-7.48 (comp. m, 2H), 7.45-7.34 (comp. m, 6H), 6.99 (d,  $J$  = 8.6 Hz, 2H), 6.60 (d,  $J$  = 16.1 Hz, 1H), 5.10 (s, 2H), 2.36 (s, 3H).

**$^{13}\text{C NMR}$**  (100 MHz;  $\text{CDCl}_3$ ):  $\delta$  198.4, 160.7, 143.2, 136.3, 130.0, 128.7, 128.2, 127.5, 127.3, 125.1, 115.3, 70.1, 27.4.

**IR** (ATR, neat): 2978, 2886, 1667, 1597, 1242, 1172, 910, 732  $\text{cm}^{-1}$ .

**HRMS** (ESI<sup>+</sup>):  $m/z$  calc'd for  $(\text{M} + \text{H})^+$  [ $\text{C}_{17}\text{H}_{16}\text{O}_2 + \text{H}$ ]<sup>+</sup>: 253.1223, found 253.1224.



**Ketone 5-144.** To aldehyde **5-160**<sup>64</sup> (0.341 g, 2.05 mmol) in EtOH (20.0 mL) and aq. KOH (1.00 g in 2.00 mL  $\text{H}_2\text{O}$ ) at 23 °C was added ketone **5-161** (0.230 mL, 2.00 mmol). The reaction mixture was capped and stirred at ambient temperature for 24 h. Then EtOH was removed by rotary evaporation, and the crude mixture was partitioned between  $\text{H}_2\text{O}$  (25 mL) and EtOAc (25 mL). The aqueous layer was extracted with EtOAc (3 x 20 mL). The organic layers were combined, washed with brine (50 mL), and dried over  $\text{MgSO}_4$ . The solvent was removed by rotary evaporation, and the crude residue was purified by flash chromatography (100% hexanes → 6:1 hexanes/EtOAc eluent) to afford ketone **5-144** (0.172 g, 21% yield) as a yellow oil.

**TLC:**  $R_f$  = 0.35 in 4:1 hexanes/EtOAc, visualized by UV.

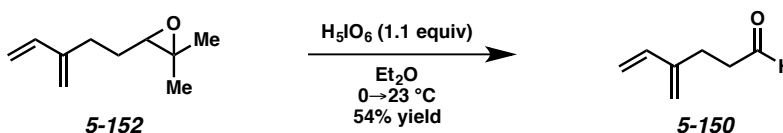
**<sup>1</sup>H NMR** (400 MHz; CDCl<sub>3</sub>): δ 8.01 (d, *J* = 8.6 Hz, 2H), 7.83 (d, *J* = 8.7 Hz, 1H), 7.61-7.56 (comp. m, 3H), 7.50 (t, *J* = 7.4 Hz, 2H), 7.43 (d, *J* = 15.7 Hz, 1H), 7.07 (d, *J* = 8.6 Hz, 2H), 5.22 (s, 2H), 3.49 (s, 3H).

**<sup>13</sup>C NMR** (100 MHz; CDCl<sub>3</sub>): δ 190.5, 159.2, 144.5, 138.4, 132.6, 131.9, 130.1, 128.6, 128.4, 120.2, 116.5, 94.1, 56.2.

**IR** (ATR, neat): 2978, 2901, 2824, 1659, 1589, 1504, 1149, 980, 833, 694 cm<sup>-1</sup>.

**HRMS** (ESI<sup>+</sup>): *m/z* calc'd for (M + H)<sup>+</sup> [C<sub>17</sub>H<sub>16</sub>O<sub>3</sub> + H]<sup>+</sup>: 269.1172, found 269.1172.

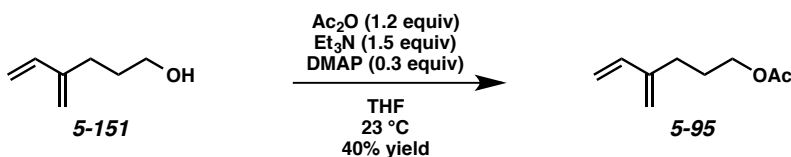
#### 5.11.4 Synthesis of Dienes



**Diene 5-150.** To a solution of epoxide **5-152** (0.581 g, 3.81 mmol) in Et<sub>2</sub>O (15.2 mL) at 0 °C was added periodic acid (0.955 g, 4.19 mmol). The reaction mixture was allowed to warm to ambient temperature, and was stirred for 20 h. The reaction mixture was passed through a short plug of celite (3 cm high x 2 cm wide, Et<sub>2</sub>O eluent), and then the filtrate was washed sequentially with sat. aq. NaHCO<sub>3</sub> (20 mL) and 10% aq. Na<sub>2</sub>S<sub>2</sub>O<sub>3</sub> (20 mL). The combined aqueous washes were extracted with Et<sub>2</sub>O (50 mL), and the combined organic layers were washed with brine (50 mL), then dried over MgSO<sub>4</sub>. The solvent was removed by rotary evaporation, and the crude residue was purified by flash chromatography (100% hexanes → 15:1 hexanes/EtOAc eluent) to afford diene **5-150** (0.228 g, 54% yield) as a colorless oil.

**TLC:** R<sub>f</sub> = 0.67 in 3:1 hexanes/EtOAc, stained with KMnO<sub>4</sub>.

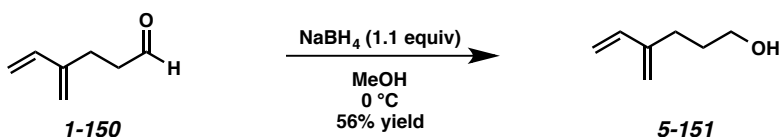
All spectroscopic data were consistent with previously reported values.<sup>65</sup>



**Diene 5-95.** To a solution of alcohol **5-151** (0.168 g, 1.50 mmol) and acetic anhydride (0.170 mL, 1.80 mmol) in THF (15.0 mL) at 23 °C were added triethylamine (0.310 mL, 2.25 mmol) and DMAP (55.0 mg, 0.450 mmol). The reaction mixture was stirred at ambient temperature for 22 h. The solvent was removed by rotary evaporation, and the crude residue was purified by flash chromatography (100% hexanes → 9:1 hexanes/EtOAc eluent) to afford diene **5-95** (93.3 mg, 40% yield) as a colorless oil.

**TLC:**  $R_f = 0.76$  in 3:1 hexanes/EtOAc, stained with  $\text{KMnO}_4$ .

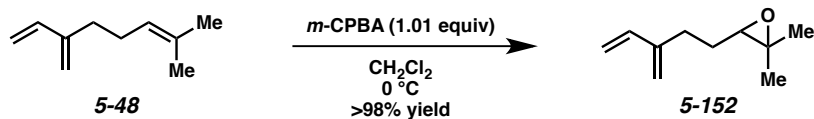
All spectroscopic data were consistent with previously reported values.<sup>66</sup>



**Diene 5-151.** To a solution of aldehyde **5-150** (2.64 g, 24.0 mmol) in MeOH (20.0 mL) at 0 °C was added  $\text{NaBH}_4$  (0.999 g, 26.4 mmol). The reaction mixture was stirred at 0 °C for 20 min, then diluted with  $\text{H}_2\text{O}$  (20 mL) and  $\text{Et}_2\text{O}$  (20 mL), and was allowed to warm to ambient temperature. The layers were separated, and the aqueous layer was washed with  $\text{Et}_2\text{O}$  (3 x 30 mL). The combined organic layers were washed with brine (50 mL) and dried over  $\text{MgSO}_4$ . The solvent was removed by rotary evaporation, and the crude residue was purified by flash chromatography (100% hexanes → 3:1 hexanes/EtOAc eluent) to afford diene **5-151** (1.57 g, 56% yield) as a colorless oil.

**TLC:**  $R_f = 0.27$  in 3:1 hexanes/EtOAc, stained with  $\text{KMnO}_4$ .

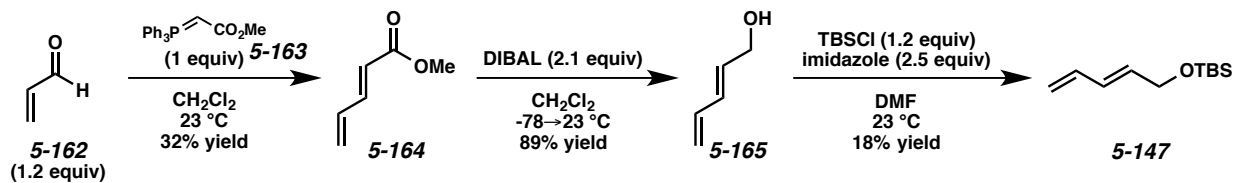
All spectroscopic data were consistent with previously reported values.<sup>67</sup>



**Diene 5-152.** To a solution of myrcene (**5-48**) (0.860 mL, 5.00 mmol) in  $\text{CH}_2\text{Cl}_2$  (6.90 mL) at 0 °C was added *m*-CPBA (1.25 g, 5.05 mmol). The reaction mixture was stirred at 0 °C for 10 min, and then was diluted with 10% aq. NaOH (10 mL). The reaction mixture was allowed to warm to ambient temperature. The layers were separated, and the aqueous layer was extracted with  $\text{CH}_2\text{Cl}_2$  (3 x 10 mL). The combined organic layers were washed sequentially with  $\text{H}_2\text{O}$  (20 mL) and brine (20 mL), then dried over  $\text{MgSO}_4$ . The solvent was removed by rotary evaporation to afford diene **5-152** (0.767 g, quantitative) as a colorless oil which was used without further purification.

**TLC:**  $R_f = 0.76$  in 3:1 hexanes/EtOAc, stained blue with *p*-anisaldehyde.

All spectroscopic data were consistent with previously reported values.<sup>65</sup>



**Ester 5-164.** To a solution of ylide **5-163** (8.36 g, 25.0 mmol) in  $\text{CH}_2\text{Cl}_2$  (62.5 mL) at 23 °C was added aldehyde **5-162** (2.00 mL, 30.0 mmol). The reaction mixture was stirred for 45 h, and then was filtered through a plug of silica (5 cm high x 3 cm wide,  $\text{CH}_2\text{Cl}_2$  eluent). The filtrate was concentrated by rotary evaporation, and the crude residue was purified by flash chromatography (100% hexanes  $\rightarrow$  9:1 hexanes/EtOAc eluent) to afford ester **5-164** (0.891 g, 32% yield) as a colorless oil.

**TLC:**  $R_f = 0.72$  in 3:1 hexanes/EtOAc, stained with  $\text{KMnO}_4$ .

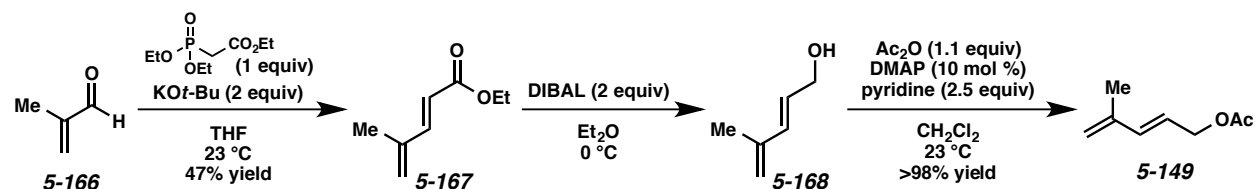
$^1\text{H NMR}$  (400 MHz;  $\text{CDCl}_3$ ):  $\delta$  7.27 (dd,  $J = 15.4, 10.7$  Hz, 1H), 6.45 (dt,  $J = 16.9, 10.7$  Hz, 1H), 5.91 (d,  $J = 15.4$  Hz, 1H), 5.61 (d,  $J = 16.9$  Hz, 1H), 5.50 (d,  $J = 10.1$  Hz, 1H), 3.75 (s, 3H).

**Alcohol 5-165.** To a solution of ester **5-164** (0.516 g, 4.60 mmol) in  $\text{CH}_2\text{Cl}_2$  (7.70 mL) at  $-78$  °C was added DIBAL (9.70 mL, 1.0 M in hexanes, 9.70 mmol). The reaction mixture was allowed to warm to 23 °C, and was stirred for 3.5 h. The reaction mixture was diluted with  $\text{Et}_2\text{O}$  (15 mL), then  $\text{H}_2\text{O}$  (0.330 mL) was added, followed by 1.0 M aq. NaOH (0.660 mL), then  $\text{H}_2\text{O}$  (0.330 mL) again, causing a white precipitate to form. The mixture was stirred for 1 h, then  $\text{MgSO}_4$  was added. After stirring for an additional 10 min, the mixture was filtered through celite ( $\text{CH}_2\text{Cl}_2$  eluent). The solvent was removed by rotary evaporation to afford alcohol **5-165** (0.345 g, 89% yield), which was used without further purification. All spectroscopic data were consistent with previously reported values.<sup>68</sup>

**Diene 5-147.** To a solution of alcohol **5-165** (0.505 g, 6.00 mmol) in DMF (8.80 mL) at 23 °C was added TBSCl (1.09 g, 7.20 mmol) and imidazole (1.02 g, 15.0 mmol). The reaction mixture was stirred at ambient temperature for 16 h, and then was diluted with sat. aq.  $\text{NH}_4\text{Cl}$  (10 mL) and  $\text{Et}_2\text{O}$  (10 mL). The layers were separated, and the aqueous layer was extracted with  $\text{Et}_2\text{O}$  (3 x 15 mL). The combined organic layers were washed with brine (30 mL) and dried over  $\text{MgSO}_4$ . The solvent was removed by rotary evaporation, and the crude residue was purified by flash chromatography (100% hexanes  $\rightarrow$  20:1 hexanes/ $\text{EtOAc}$  eluent) to afford diene **5-147** (0.220 g, 18% yield) as a colorless oil.

**TLC:**  $R_f = 0.86$  in 3:1 hexanes/ $\text{EtOAc}$ , stained with  $\text{KMnO}_4$ .

All spectroscopic data were consistent with previously reported values.<sup>69</sup>



**Ester 5-167.** To a solution of triethyl phosphonoacetate (3.97 mL, 20.0 mmol) in THF (40.0 mL) at 23 °C was added KO<sup>t</sup>-Bu (4.49 g, 40.0 mmol). The reaction mixture was stirred for 35 min, then aldehyde **5-166** (1.65 mL, 20.0 mmol) was added. The reaction mixture was stirred for 3 h, and then was diluted with H<sub>2</sub>O (40 mL) and Et<sub>2</sub>O (40 mL). The layers were separated, and the aqueous layer was extracted with Et<sub>2</sub>O (3 x 30 mL). The combined organic layers were washed with brine (50 mL), then dried over MgSO<sub>4</sub>. The solvent was removed by rotary evaporation, and the crude residue was purified by flash chromatography (100% hexanes → 4:1 hexanes/EtOAc) to afford ester **5-167** (1.32 g, 47% yield) as a colorless oil.

**TLC:** R<sub>f</sub> = 0.71 in 4:1 hexanes/EtOAc, stained with KMnO<sub>4</sub>.

All spectroscopic data were consistent with previously reported values.<sup>70</sup>

**Alcohol 5-168.** To a solution of ester **5-167** (1.32 g, 9.42 mmol) in Et<sub>2</sub>O (23.6 mL) at 0 °C was added DIBAL (18.8 mL, 1.0 M in hexanes, 18.8 mmol). The reaction mixture stirred at 0 °C for 2 h, and then was diluted with MeOH (5.00 mL), then 1.0 M aq. HCl (5.00 mL) was added, followed by Et<sub>2</sub>O (10.0 mL). The layers were separated, and the aqueous layer was extracted with Et<sub>2</sub>O (3 x 15 mL). The combined organic layers were washed with brine (20 mL), then dried over MgSO<sub>4</sub>. The solvent was removed by rotary evaporation to afford alcohol **5-168**, which was used without further purification. All spectroscopic data were consistent with previously reported values.<sup>71</sup>

**Diene 5-149.** To a solution of alcohol **5-168** (0.196 g, 2.00 mmol) in CH<sub>2</sub>Cl<sub>2</sub> (8.00 mL) at 23 °C was added DMAP (24.4 mg, 0.200 mmol) and pyridine (0.400 mL, 5.00 mmol). The solution was stirred at ambient temperature for 15 min, and then acetic anhydride (0.210 mL, 2.20 mmol) was added. After 16 h, the reaction mixture was diluted with H<sub>2</sub>O (10 mL). The layers were separated, and the organic layer was washed sequentially with 1 M aq. HCl (10 mL), H<sub>2</sub>O (10 mL), sat. aq. NaHCO<sub>3</sub> (10 mL), and brine (10 mL). The organic layer was dried over MgSO<sub>4</sub>, and the solvent was removed by rotary evaporation. The crude residue was purified by flash chromatography (100% pentane → 9:1 pentane/Et<sub>2</sub>O) to afford diene **5-149** (0.279 g, quantitative) as a colorless oil.

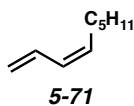
**TLC:** R<sub>f</sub> = 0.69 in 4:1 hexanes/EtOAc, stained with KMnO<sub>4</sub>.

**<sup>1</sup>H NMR** (400 MHz; CDCl<sub>3</sub>): δ 6.37 (d, *J* = 15.7 Hz, 1H), 5.75-5.68 (m, 1H), 5.02 (d, *J* = 4.4 Hz, 1H), 4.63 (s, 1H), 4.61 (s, 1H), 2.07 (s, 3H), 1.84 (s, 3H).

**<sup>13</sup>C NMR** (100 MHz; CDCl<sub>3</sub>): δ 170.8, 141.0, 137.0, 123.0, 117.9, 65.0, 21.0, 18.4.

**IR** (ATR, neat): 2978, 2886, 1736, 1227, 964, 733 cm<sup>-1</sup>.

**HRMS** (ESI+): *m/z* calc'd for (M + H)<sup>+</sup> [C<sub>8</sub>H<sub>12</sub>O<sub>2</sub> + H]<sup>+</sup>: 141.0910, found 141.0908.



(*Z*)-diene **5-71** was synthesized according to the procedure by Morken and coworkers.<sup>72</sup>

### 5.11.5 Structural and Stereochemical Determination of 1-Substituted Diene Products

The major constitutional isomer of cyclohexene **5-22** was determined through COSY and HMQC NMR. The COSY NMR (Figure 5.6) revealed that protons  $H_a$  and  $H_b$  are coupled to each other, as are  $H_c$  and  $H_d$ .

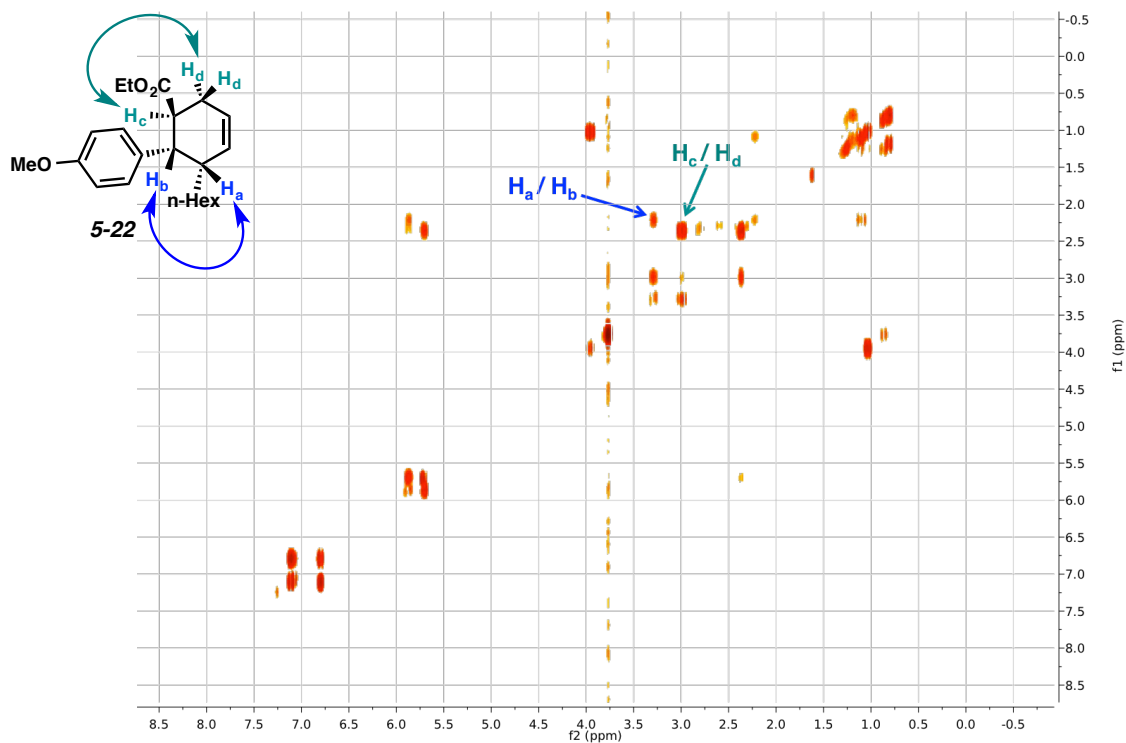


Figure 5.6. COSY NMR of cyclohexene **5-22**.

HMQC NMR was used to confirm that the proton peak at 2.37 ppm with an integration of 2 was a result of just the  $H_d$  protons and not a mix of  $H_d$  and  $H_c$ . The HMQC spectrum (Figure 5.7) indicated that the protons represented by that peak were both bonded to the same carbon atom, thus further solidifying our structural assignment of cyclohexene **5-22**.

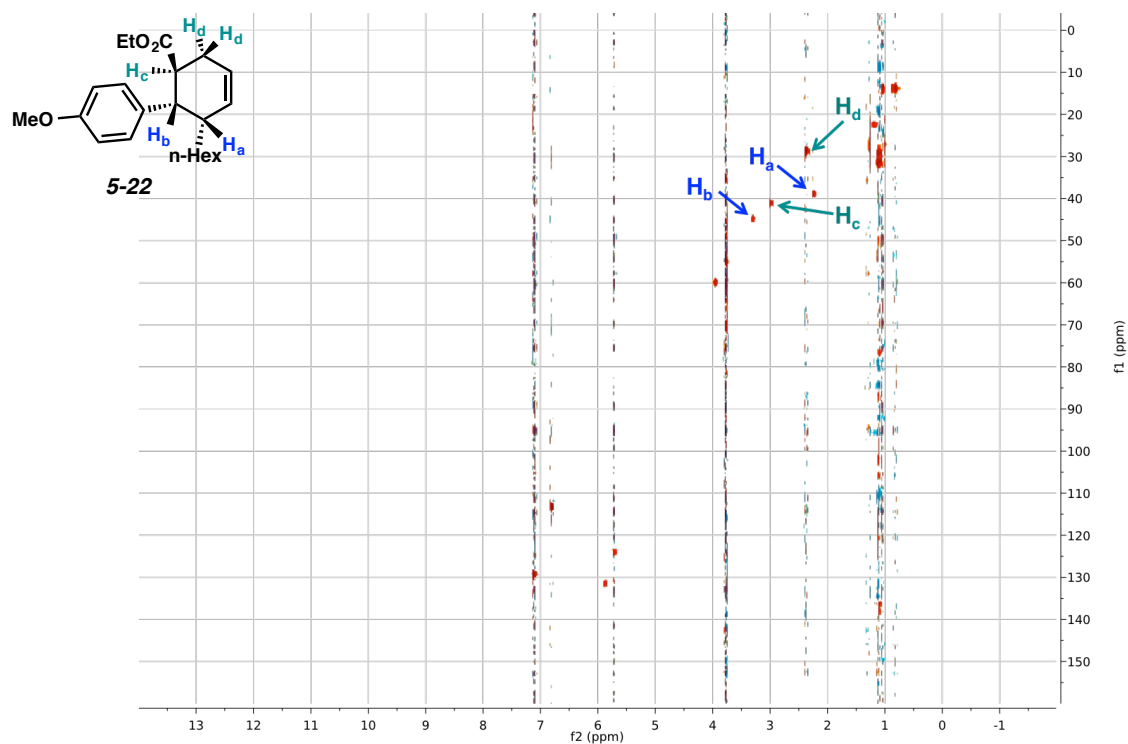
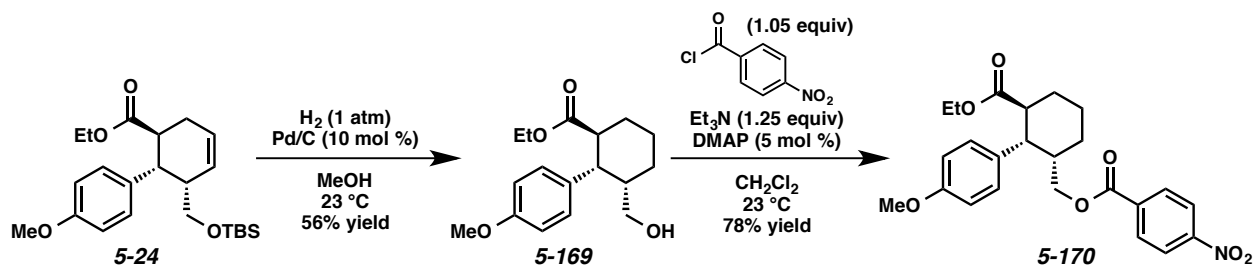


Figure 5.7. HMQC NMR of cyclohexene **5-22**.

## Decoupling Experiment

The stereochemistry of the 1-substituted diene products was determined through structural modification of cyclohexene **5-24** and a  $^1\text{H}$  NMR decoupling experiment.



**Cyclohexane 5-169.** To a solution of cyclohexene **5-24** (37.6 mg, 93.0  $\mu\text{mol}$ ) in MeOH (0.900 mL) at 23  $^{\circ}\text{C}$  was added 10% Pd/C (dry powder, 9.9 mg, 9.30  $\mu\text{mol}$ ). The flask was sealed with a rubber septum, and  $\text{H}_2$  was bubbled through the solution for 1 min using a balloon and needle outlet. The needle outlet was removed, and the reaction mixture was left under positive pressure of  $\text{H}_2$  and stirred for 9 h. The crude reaction mixture was passed through a short plug of celite ( $\text{Et}_2\text{O}$  eluent), and the solvent was removed by rotary evaporation. The resulting residue was purified by flash chromatography (100% hexanes  $\rightarrow$  2:1 hexanes/EtOAc eluent) to afford cyclohexane **5-169** (15.3 mg, 56% yield) as a colorless oil.

**TLC:**  $R_f = 0.16$  in 3:1 hexanes/EtOAc, stained with  $\text{KMnO}_4$ .

**$^1\text{H}$  NMR** (400 MHz;  $\text{CDCl}_3$ ):  $\delta$  7.09 (d,  $J = 8.4$  Hz, 2H), 6.81 (d,  $J = 8.4$  Hz, 2H), 3.93 (q,  $J = 7.1$  Hz, 2H), 3.76 (s, 3H), 3.54-3.47 (comp. m, 2H), 3.17 (dd,  $J = 11.7, 4.2$  Hz, 1H), 2.90 (td,  $J = 11.7, 2.8$  Hz, 1H), 2.07-1.99 (comp. m, 2H), 1.65-1.53 (comp. m, 4H), 1.01 (t,  $J = 7.1$  Hz, 3H).

**Nitrobenzoate 5-170.** To a solution of cyclohexane **5-169** (15.3 mg, 52.3  $\mu\text{mol}$ ) and 4-nitrobenzoyl chloride (10.2 mg, 55.0  $\mu\text{mol}$ ) in  $\text{CH}_2\text{Cl}_2$  (0.500 mL) at 23  $^{\circ}\text{C}$  was added triethylamine (9.0  $\mu\text{L}$ , 65.0  $\mu\text{mol}$ ), then DMAP (0.3 mg, 2.60  $\mu\text{mol}$ ). The reaction mixture was stirred at ambient temperature for 16 h, then was diluted with  $\text{CH}_2\text{Cl}_2$  (3.00 mL), and the solution was washed with  $\text{H}_2\text{O}$  (2 x 3.00 mL) and dried over  $\text{Na}_2\text{SO}_4$ . The solvent was removed by rotary evaporation, and the crude residue was purified by flash chromatography (100% hexanes  $\rightarrow$  9:1 hexanes/EtOAc eluent) to afford nitrobenzoate **5-170** (16.6 mg, 78% yield) as a colorless oil.

**TLC:**  $R_f = 0.50$  in 9:1 hexanes/EtOAc, visualized by UV.

**$^1\text{H}$  NMR** (400 MHz;  $\text{CDCl}_3$ ):  $\delta$  8.21 (d,  $J = 8.5$  Hz, 2H), 7.97 (d,  $J = 8.5$  Hz, 2H), 7.11 (d,  $J = 8.5$  Hz, 2H), 6.78 (d,  $J = 8.5$  Hz, 2H), 4.41 (t,  $J = 11.0$  Hz, 1H), 4.12 (dd,  $J = 11.0, 5.3$  Hz, 1H), 3.95 (q,  $J = 7.1$  Hz, 2H), 3.71 (s, 3H), 3.27 (dd,  $J = 11.5, 4.6$  Hz, 1H), 2.99 (td,  $J = 11.5, 3.3$  Hz, 1H), 2.45-2.41 (m, 1H), 2.15-1.96 (comp. m, 2H), 1.75-1.49 (comp. m, 4H), 1.03 (t,  $J = 7.1$  Hz, 3H).

Decoupling of proton  $H_c$  (2.45 ppm) of cyclohexane **5-170** resulted in peak  $H_b$  changing from a doublet of doublets ( $J = 11.5, 4.6$  Hz) to just a doublet ( $J = 11.5$  Hz) (Figure 5.8). From this data, we can conclude that the coupling constant between  $H_a$  and  $H_b$  is 11.5 Hz, corresponding to an anti relationship, and the coupling constant between  $H_b$  and  $H_c$  is 4.6 Hz, corresponding to a syn relationship.

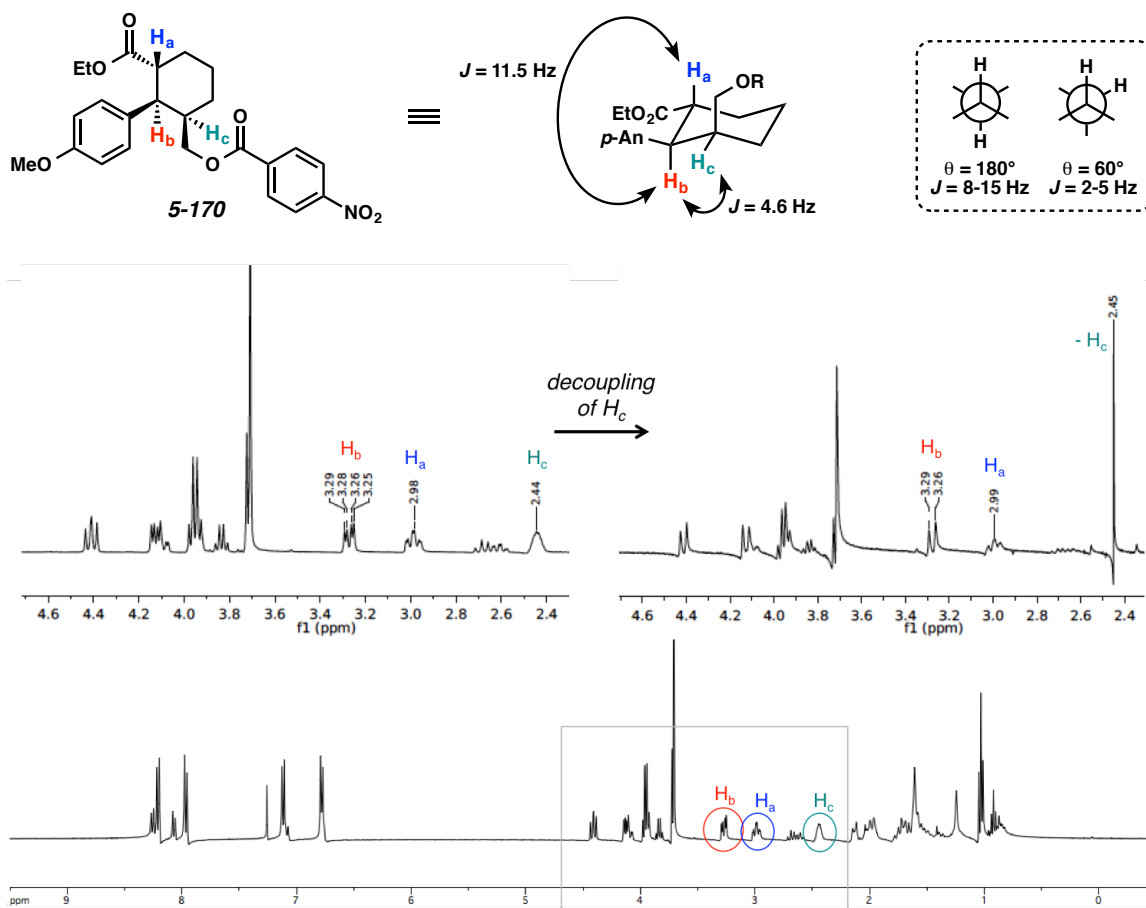


Figure 5.8.  $^1\text{H}$  NMR decoupling experiment on cyclohexane **5-170**.

## Identification of Minor Isomer

In all cases, the minor isomer was assigned as the constitutional isomer, shown below (Figure 5.9). For the 2-substituted diene products, this was determined by comparing the  $^1\text{H}$  NMR spectra of several of the products obtained with the Cr conditions to those obtained through traditional Diels-Alder conditions (i.e., **5-18** vs. **5-96**); the remaining cyclohexene products were assigned by analogy.

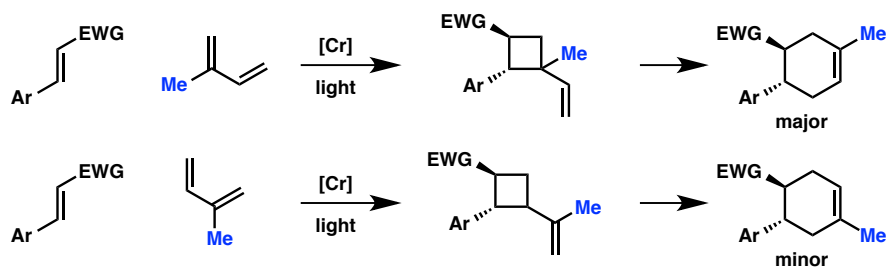


Figure 5.9. Major and minor isomers from cycloaddition with isoprene.

In the cases of the 1-substituted diene products, the minor isomer was assigned based on the splitting pattern and coupling constants of the peaks for the benzylic proton ( $\text{H}_a$ ) and the proton alpha to the ester ( $\text{H}_b$ ) in the  $^1\text{H}$  NMR spectrum of cyclohexene **5-22** (Figure 5.10).

The peaks of the major and minor isomer were assigned with the benzylic proton ( $\text{H}_a$ ) being the farther downfield peak and the proton alpha to the ester ( $\text{H}_b$ ) being the more upfield peak. This trend is observed in all of the ester cyclohexene products. These two protons are presumed anti to each other because of their large coupling constant ( $J = 10.4$  Hz). Throughout this research, we have only ever observed an anti relationship in the products between the two substituents of the starting alkene of the dienophile.

The peak of the benzylic proton ( $\text{H}_a$ ) of the minor isomer is a triplet of doublets, indicating that  $\text{H}_a$  is being split by 3 other protons; the peak of the proton alpha to the ester ( $\text{H}_b$ ) of the minor isomer is a triplet, indicating that  $\text{H}_b$  is being split by 2 other protons. This assessment is aligned with the minor

product being the constitutional isomer (**5-171**). This minor isomer was formed in too small of an amount for its stereochemistry to be determined.

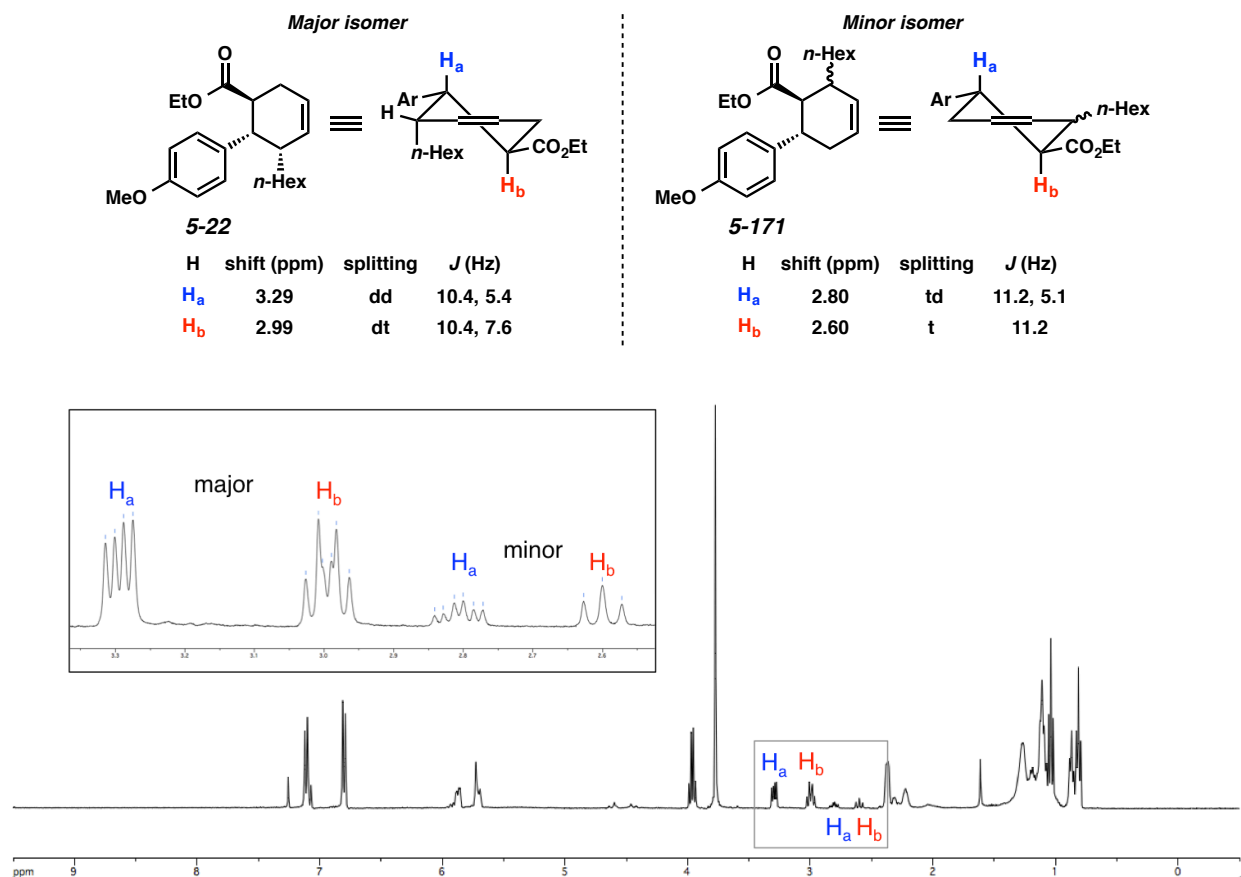


Figure 5.10. Identification of minor isomer **5-171**.

The other possible minor product, if not a constitutional isomer, would be the diastereomer, cyclohexene **5-172** (Figure 5.11). This diastereomer is likely not the minor product, since the coupling constant between H<sub>a</sub> and H<sub>c</sub> is 5.1 Hz, which is small and not indicative of an anti relationship, as would be required in the exo diastereomer.

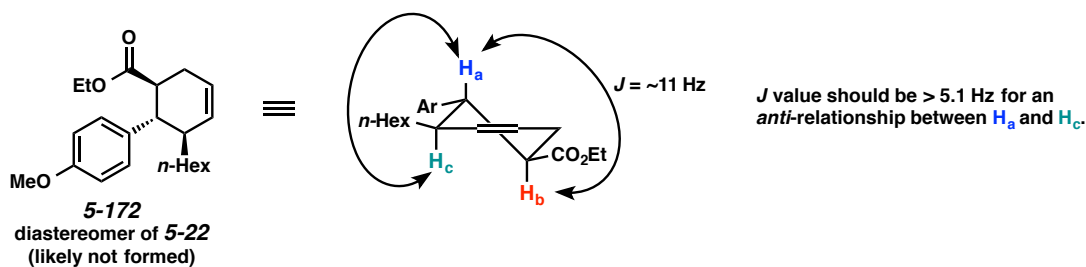
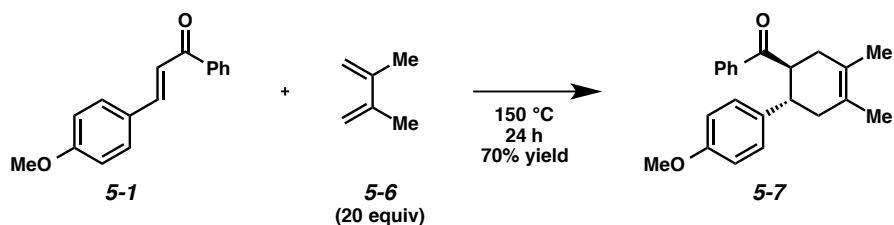


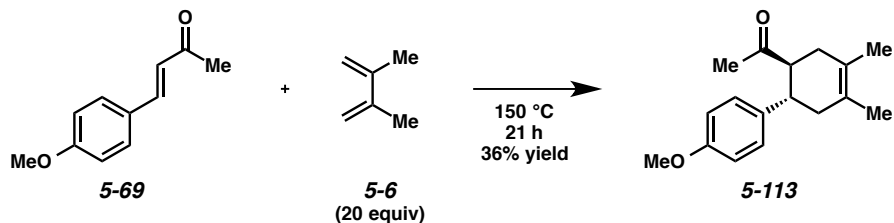
Figure 5.11. Evaluation of the diastereomer **5-172** as possible minor isomer.

## 5.11.6 Additional Experiments

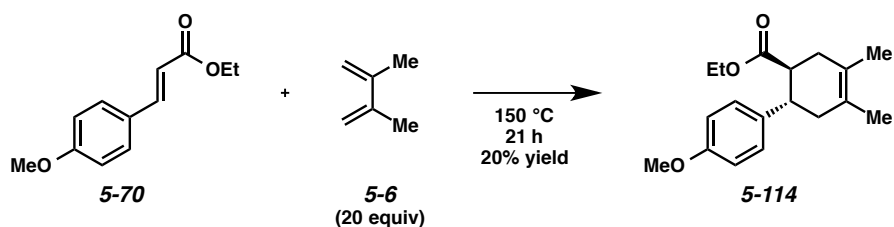
### 5.11.6.1 Cycloadditions Under Traditional Diels-Alder Conditions



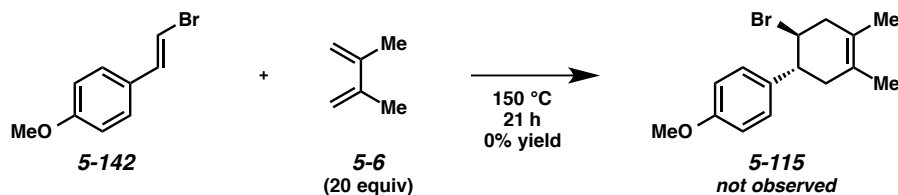
**Cyclohexene 5-7.** A 16 x 125 mm glass culture tube was charged with alkene **5-1** (95.3 mg, 0.400 mmol) and diene **5-6** (0.900 mL, 8.00 mmol). The tube was sealed with a Teflon cap and heated at 150 °C for 24 h. The reaction mixture was allowed to cool to ambient temperature, and the unreacted diene was removed by rotary evaporation. The resulting residue was purified by flash chromatography (100% hexanes  $\rightarrow$  20:1 hexanes/EtOAc eluent) to afford cyclohexene **5-7** (90.0 mg, 70% yield) as a colorless oil.



**Cyclohexene 5-113.** A 2-dr vial was charged with alkene **5-69** (15.4 mg, 0.0873 mmol) and diene **5-6** (0.200 mL, 1.75 mmol). The vial was sealed with a Teflon cap and heated at 150 °C for 21 h. The reaction mixture was allowed to cool to ambient temperature, and the unreacted diene was removed by rotary evaporation. The resulting residue was purified by flash chromatography (100% hexanes → 9:1 hexanes/EtOAc eluent) to afford cyclohexene **5-113** (8.1 mg, 36% yield) as a colorless oil.

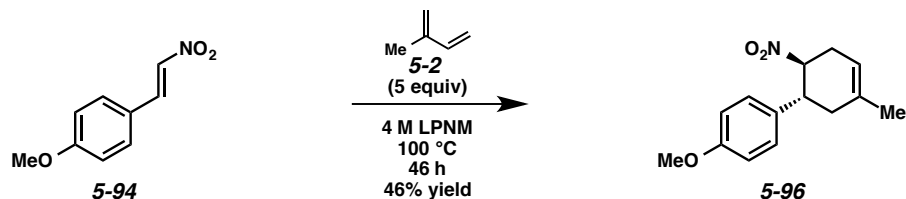


**Cyclohexene 5-114.** A 2-dr vial was charged with alkene **5-70** (18.0 mg, 0.0873 mmol) and diene **5-6** (0.200 mL, 1.75 mmol). The vial was sealed with a Teflon cap and heated at 150 °C for 21 h. The reaction mixture was allowed to cool to ambient temperature, and the unreacted diene was removed by rotary evaporation. The resulting residue was purified by flash chromatography (100% hexanes → 9:1 hexanes/EtOAc eluent) to afford cyclohexene **5-114** (5.0 mg, 20% yield) as a colorless oil.



**Cyclohexene 5-115.** A 2-dr vial was charged with alkene **5-142** (18.6 mg, 0.0873 mmol) and diene **5-6** (0.200 mL, 1.75 mmol). The vial was sealed with a Teflon cap and heated at 150 °C for 21 h. The reaction mixture was allowed to cool to ambient temperature, and the unreacted diene was removed by

rotary evaporation. The resulting residue was analyzed by  $^1\text{H}$  NMR. Cyclohexene **5-115** was not observed.



**Cyclohexene 5-96.** The 4 M LPNM solution was prepared by adding anhydrous  $\text{LiClO}_4$  (0.145 g, 1.36 mmol) to nitromethane (0.340 mL, 0.50 M with respect to alkene **5-94**) in a flame-dried 1-dram vial, open to air. The vial was capped and the mixture was stirred until complete dissolution of the  $\text{LiClO}_4$  was achieved (ca. 2 h). To the solution was added alkene **5-94** (30.0 mg, 0.167 mmol) and diene **5-2** (85.2  $\mu\text{L}$ , 0.850 mmol). The vial was capped, and the reaction mixture was stirred at 100 °C. After 46 h, the reaction mixture was allowed to cool to ambient temperature, and then was diluted with  $\text{H}_2\text{O}$  (1 mL) and  $\text{Et}_2\text{O}$  (1 mL). The layers were separated, and the aqueous layer was extracted with  $\text{Et}_2\text{O}$  (2 x 1 mL). The combined organic layers were washed with brine, then dried over  $\text{MgSO}_4$ . The solvent was removed by rotary evaporation, and the crude residue was purified by flash chromatography (100% hexanes  $\rightarrow$  9:1 hexanes/ $\text{EtOAc}$  eluent) to afford cyclohexene **5-96** (19.4 mg, 46% yield, 18:1) as an off-white solid.

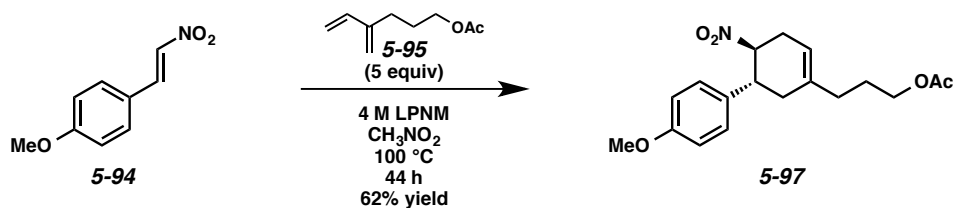
**TLC:**  $R_f = 0.74$  in 3:1 hexanes/ $\text{EtOAc}$ , stained blue with *p*-anisaldehyde.

**$^1\text{H}$  NMR** (400 MHz;  $\text{CDCl}_3$ ):  $\delta$  7.14 (d,  $J = 8.4$  Hz, 2H), 6.84 (d,  $J = 8.4$  Hz, 2H), 5.40 (br s, 1H), 4.85 (td,  $J = 10.6, 5.7$  Hz, 1H), 3.77 (s, 3H), 3.39 (td,  $J = 10.6, 6.7$  Hz, 1H), 2.81-2.64 (comp. m, 2H), 2.35-2.23 (comp. m, 2H), 1.71 (s, 3H).

**$^{13}\text{C}$  NMR** (100 MHz;  $\text{CDCl}_3$ ):  $\delta$  158.8, 134.1, 132.0, 128.3, 116.7, 114.2, 87.7, 55.2, 43.8, 37.9, 31.3, 22.8.

**IR** (ATR, neat): 2963, 2909, 2839, 1551, 1512, 1250, 1034, 833, 733  $\text{cm}^{-1}$ .

**HRMS** (ESI+):  $m/z$  calc'd for  $(\text{M} + \text{Na})^+$  [ $\text{C}_{14}\text{H}_{17}\text{NO}_3 + \text{Na}$ ] $^+$ : 270.1101, found 270.1105.



**Cyclohexene 5-97.** The 4 M LPNM solution was prepared by adding anhydrous LiClO<sub>4</sub> (85.1 mg, 0.800 mmol) to nitromethane (0.200 mL, 0.25 M with respect to alkene **5-94**) in a flame-dried 1-dram vial, open to air. The vial was capped and the reaction mixture was stirred until complete dissolution of the LiClO<sub>4</sub> was achieved (ca. 2 h). To the solution was added alkene **5-94** (9.0 mg, 0.0500 mmol) and diene **5-95** (38.6 mg, 0.250 mmol). The vial was capped, and the reaction mixture was stirred at 100 °C. After 44 h, the reaction mixture was allowed to cool to ambient temperature, and then was diluted with H<sub>2</sub>O (0.5 mL) and Et<sub>2</sub>O (0.5 mL). The layers were separated, and the aqueous layer was extracted with Et<sub>2</sub>O (2 x 1 mL). The combined organic layers were washed with brine, then dried over MgSO<sub>4</sub>. The solvent was removed by rotary evaporation, and the crude residue was purified by flash chromatography (100% hexanes → 9:1 hexanes/EtOAc eluent) to afford cyclohexene **5-97** (10.3 mg, 62% yield, 17:1) as a colorless oil.

**TLC:** R<sub>f</sub> = 0.36 in 3:1 hexanes/EtOAc, visualized by UV.

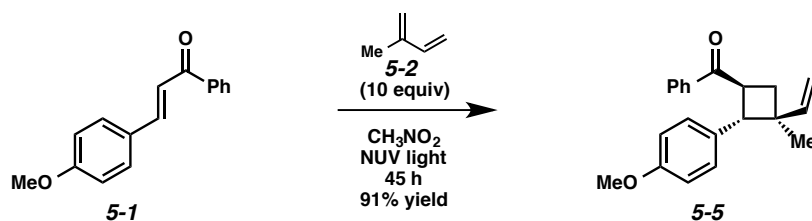
**<sup>1</sup>H NMR** (500 MHz; CDCl<sub>3</sub>): δ 7.17 (d, *J* = 8.7 Hz, 2H), 6.87 (d, *J* = 8.7 Hz, 2H), 5.47 (br s, 1H), 4.89 (ddd, *J* = 11.0, 10.1, 5.8 Hz, 1H), 4.08 (t, *J* = 13.0, 6.5 Hz, 3H), 3.80 (s, 3H), 3.41 (td, *J* = 11.0, 6.1 Hz, 1H), 2.82-2.72 (comp. m, 2H), 2.41-2.28 (comp. m, 2H), 2.12-2.05 (comp. m, 7H), 1.80-1.77 (comp. m, 2H).

**<sup>13</sup>C NMR** (100 MHz; CDCl<sub>3</sub>): δ 171.1, 158.9, 136.8, 131.9, 128.3, 117.0, 114.2, 87.7, 63.9, 55.3, 43.7, 36.3, 33.0, 31.2, 26.4, 21.0.

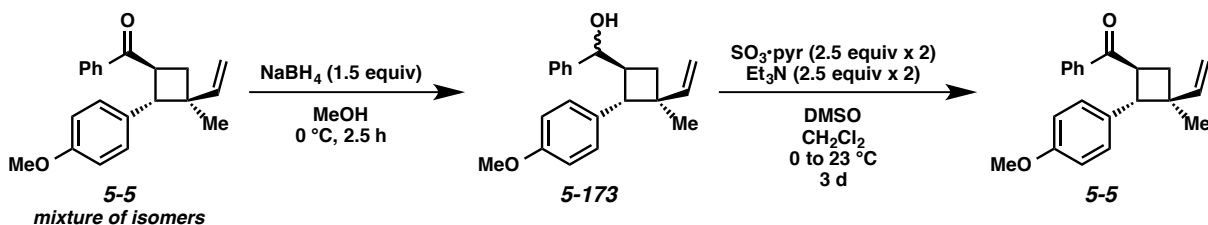
**IR** (ATR, neat): 2956, 2855, 1732, 1548, 1514, 1366, 1238, 1033, 831 cm<sup>-1</sup>.

**HRMS** (ESI<sup>+</sup>): *m/z* calc'd for (M + Na)<sup>+</sup> [C<sub>18</sub>H<sub>23</sub>NO<sub>5</sub> + Na]<sup>+</sup>: 356.1468, found 356.1467.

### 5.11.6.2 Photochemical [2+2] Cycloaddition



**Vinylcyclobutane 5-5.** A flame-dried 2-dram borosilicate vial open to air was charged with alkene **5-1** (0.238 g, 1.00 mmol), diene **5-2** (1.00 mL, 10.0 mmol), and nitromethane (2.50 mL). The vial was capped, and the reaction mixture was irradiated with 300, 350, and 419 nm light, with stirring, for 45 h. The volatile materials were then removed by rotary evaporation, and the residue was purified by flash chromatography (100% hexanes  $\rightarrow$  15:1 hexanes/EtOAc eluent) to afford cyclobutane **5-5** as the major product of a mixture of isomers (0.278 g, 91% combined yield) as a pale yellow oil.



The vinylcyclobutane isomers were difficult to separate by flash chromatography. The phenyl ketone was reduced to the alcohol (**5-173**) to make purification easier, and then was oxidized to the ketone again.

**Vinylcyclobutane 5-173.** To the vinylcyclobutane mixture (148.0 mg, 0.483 mmol) in MeOH (3.22 mL) at 0 °C under argon was added  $\text{NaBH}_4$  (27.4 mg, 0.725 mmol). The reaction mixture was stirred at 0 °C for 2.5 h, then the volatile materials were removed by rotary evaporation. The crude residue was taken up in  $\text{Et}_2\text{O}$  (10 mL) and sat. aq.  $\text{NH}_4\text{Cl}$  (10 mL). The layers were separated and the aqueous layer was

extracted with Et<sub>2</sub>O (2 x 10 mL). The combined organic layers were washed with brine (30 mL) and dried over MgSO<sub>4</sub>. The volatile materials were then removed by rotary evaporation, and the residue was purified by flash chromatography (100% hexanes → 10:1 hexanes/EtOAc eluent) to afford a pure sample of alcohol **5-173** (21.3 mg, ~1:1 mixture of diastereomers at the alcohol carbon) as a colorless oil. The remaining desired alcohol product coeluted with the undesired isomers.

**TLC:** R<sub>f</sub> = 0.52 in 3:1 hexanes/EtOAc, stained blue with *p*-anisaldehyde.

**<sup>1</sup>H NMR** (400 MHz; CDCl<sub>3</sub>): δ 7.39-7.27 (m, 10H), 7.14 (d, *J* = 8.4 Hz, 2H), 6.90 (d, *J* = 8.4 Hz, 2H), 6.83 (d, *J* = 8.7 Hz, 2H), 6.74 (d, *J* = 8.7 Hz, 2H), 6.05 (ddd, *J* = 17.2, 12.4, 10.7 Hz, 2H), 4.99-4.95 (comp. m, 3H), 4.93 (dd, *J* = 9.4, 1.3 Hz, 1H), 4.74 (d, *J* = 5.1 Hz, 1H), 4.69 (d, *J* = 8.3 Hz, 1H), 3.79 (s, 3H), 3.76 (s, 3H), 3.40 (d, *J* = 10.3 Hz, 1H), 3.35 (d, *J* = 9.8 Hz, 1H), 3.01-2.88 (comp. m, 2H), 2.16 (t, *J* = 10.2 Hz, 1H), 1.82 (t, *J* = 10.2 Hz, 2H), 1.71 (dd, *J* = 10.6, 8.4 Hz, 1H), 1.55 (dd, *J* = 10.6, 8.4 Hz, 2H), 0.80 (app. s, 6H). (reported for 1:1 mixture of diastereomers)

**Pure vinylcyclobutane 5-5.** To DMSO (0.28 mL) and CH<sub>2</sub>Cl<sub>2</sub> (0.07 mL) at 0 °C under argon was added sulfur trioxide pyridine complex (27.5 mg, 0.173 mmol). The mixture was stirred for 10 min at 0 °C, then vinylcyclobutane **5-173** (21.3 mg, 0.0691 mmol) and Et<sub>3</sub>N (0.024 mL, 0.173 mmol) were added as a solution in CH<sub>2</sub>Cl<sub>2</sub>. The reaction mixture was stirred at 0 °C for 1.5 h, then was allowed to warm to ambient temperature and stirred for 10 h. At this time, the vinylcyclobutane (**5-173**) was not yet consumed, so additional sulfur trioxide pyridine complex (27.5 mg, 0.173 mmol) and Et<sub>3</sub>N (0.024 mL, 0.173 mmol) were added. The reaction was stirred for 3 d total. The reaction mixture was then diluted with H<sub>2</sub>O (2 mL) and CH<sub>2</sub>Cl<sub>2</sub> (2 mL). The layers were separated and the aqueous layer was extracted with CH<sub>2</sub>Cl<sub>2</sub> (2 x 5 mL). The combined organic layers were washed with brine (10 mL) and dried over Na<sub>2</sub>SO<sub>4</sub>. The volatile materials were then removed by rotary evaporation, and the residue was purified by flash chromatography (100% hexanes → 9:1 hexanes/EtOAc eluent) to afford pure vinylcyclobutane **5-5** (16.4 mg, 77% yield) as a colorless oil.

**TLC:** R<sub>f</sub> = 0.66 in 3:1 hexanes/EtOAc, visualized by UV.

**$^1\text{H}$  NMR** (400 MHz;  $\text{CDCl}_3$ ):  $\delta$  7.96 (d,  $J = 7.6$  Hz, 2H), 7.56 (t,  $J = 7.6$  Hz, 1H), 7.45 ( $J = 7.6$  Hz, 1H), 7.05 (d,  $J = 8.7$  Hz, 2H), 6.82 (d,  $J = 8.7$  Hz, 2H), 6.09 (dd,  $J = 17.6, 10.4$  Hz, 1H), 5.04 (d,  $J = 1.9$  Hz, 1H), 5.00 (dd,  $J = 4.0, 1.9$  Hz, 1H), 4.24 (q,  $J = 9.7$  Hz, 1H), 3.95 (d,  $J = 9.7$  Hz, 1H), 3.78 (s, 3H), 2.30 (t,  $J = 10.0$  Hz, 1H), 2.17 (t,  $J = 10.0$  Hz, 1H), 1.03 (s, 3H).

**$^{13}\text{C}$  NMR** (100 MHz;  $\text{CDCl}_3$ ):  $\delta$  200.4, 158.1, 147.1, 136.1, 133.0, 131.4, 128.6, 128.4, 128.3, 113.5, 111.4, 55.2, 48.3, 41.8, 40.9, 36.7, 20.5.

**IR** (ATR, neat): 2963, 2832, 1674, 1512, 1242, 1033, 732, 694  $\text{cm}^{-1}$ .

**HRMS** (ESI+):  $m/z$  calc'd for  $(\text{M} + \text{H})^+$  [ $\text{C}_{21}\text{H}_{22}\text{O}_2 + \text{H}$ ] $^+$ : 307.1693, found 307.1693.

The stereochemistry of vinylcyclobutane **5-5** was confirmed through 1D NOESY NMR (Figure 5.12).

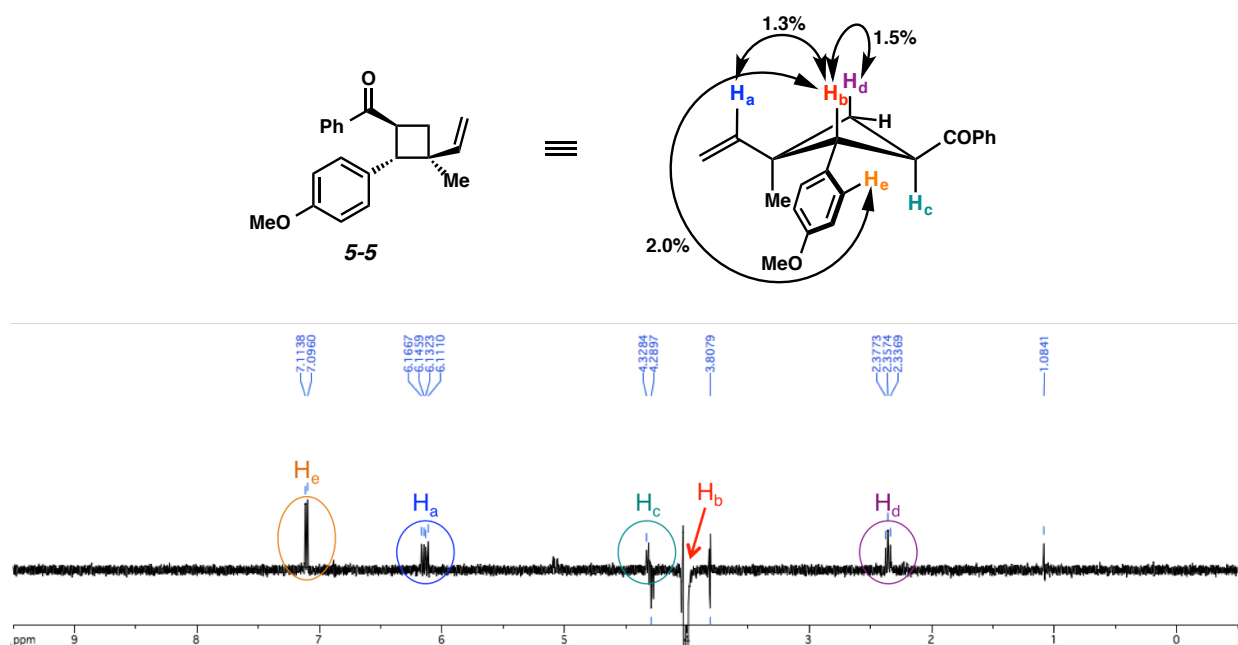
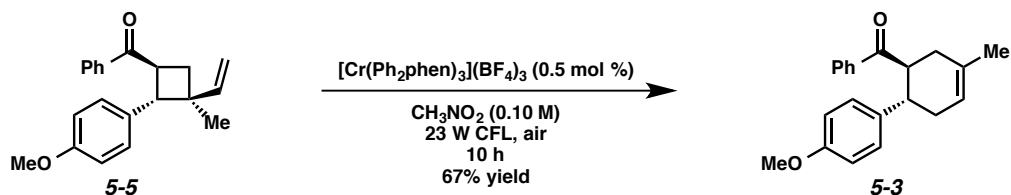


Figure 5.12. 1D NOESY of vinylcyclobutane **5-5**.

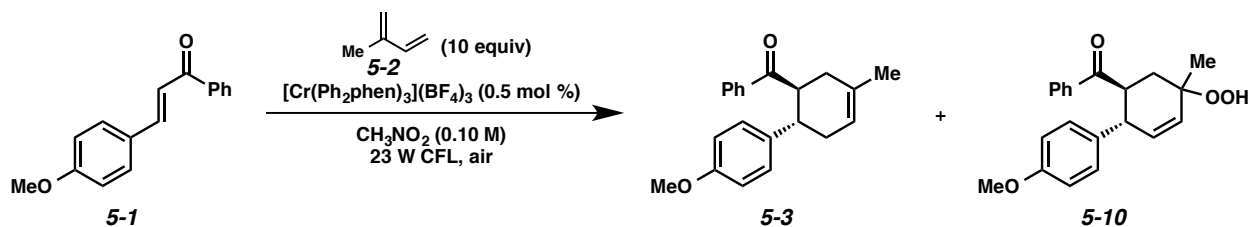
### 5.11.6.3 Vinylcyclobutane Rearrangement



A 1/2-dram borosilicate vial open to air was charged with vinylcyclobutane **5-5** (15.3 mg, 0.0500 mmol),  $[\text{Cr}(\text{Ph}_2\text{phen})_3](\text{BF}_4)_3$  (0.3 mg, 0.000250 mmol) and nitromethane (0.500 mL). The vial was capped and irradiated with a 23 W CFL in a closed box lined with aluminum foil for 10 h with stirring. The reaction mixture was then passed through a short plug of silica (2.0-2.5 x 1 cm,  $\text{Et}_2\text{O}$  eluent). The solvent was removed by rotary evaporation, and the crude product was purified by flash chromatography (100% hexanes  $\rightarrow$  9:1 hexanes/ $\text{EtOAc}$  eluent) to afford cyclohexene **5-3** (10.2 mg, 67% yield) as a colorless oil.

When this same reaction was performed under Ar (degassed by three freeze-pump-thaw cycles) in a 50-mL Schlenk flask, the product was formed in 64% yield.

#### 5.11.6.4 Monitoring of Singlet Oxygen Side Reaction



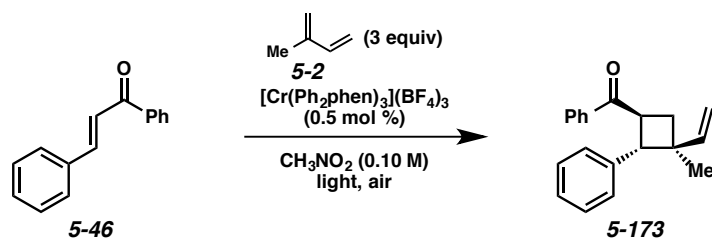
A stock solution was prepared containing alkene **5-1** (47.7 mg, 0.200 mmol), diene **5-2** (0.200 mL, 2.00 mmol),  $[\text{Cr}(\text{Ph}_2\text{phen})_3](\text{BF}_4)_3$  (1.3 mg, 0.00100 mmol), and dodecyl acetate (internal standard, 45.7 mg, 0.200 mmol) in nitromethane (2.00 mL). Into seven 1-dr borosilicate vials was added 0.28 mL of the stock solution. The vials were capped and placed in front of a bright white 23 W compact fluorescent light bulb in a closed box lined with aluminum foil. At each indicated time, a vial was removed from the box, and the reaction mixture was passed through a short plug of silica (2.0-2.5 x 1 cm,  $\text{Et}_2\text{O}$  eluent). The volatile materials were removed by rotary evaporation, and the resulting crude product mixture was analyzed by  $^1\text{H}$  NMR. The results of this experiment are displayed in Scheme 5.5.

A fairly pure sample of oxidized product **5-10** was obtained from the gram-scale cycloaddition of **5-1** and **5-2**. In this reaction, product **5-10** was formed in 2% yield (32.2 mg).

**TLC:**  $R_f = 0.33$  in 3:1 hexanes/ $\text{EtOAc}$ , stained red with *p*-anisaldehyde.

**$^1\text{H}$  NMR** (400 MHz;  $\text{CDCl}_3$ ):  $\delta$  7.86 (d,  $J = 7.3$  Hz, 2H), 7.47 (t,  $J = 7.1$  Hz, 1H), 7.35 (t,  $J = 7.3$  Hz, 3H), 7.14 (d,  $J = 8.5$  Hz, 2H), 6.73 (d,  $J = 8.5$  Hz, 2H), 5.99 (dd,  $J = 10.2, 1.4$  Hz, 1H), 5.72 (dd,  $J = 10.2, 1.4$  Hz, 1H), 4.10-4.04 (m, 1H), 3.93 (dd,  $J = 9.5, 0.6$  Hz, 1H), 3.70 (s, 3H), 2.46-2.43 (m, 2H), 1.41 (s, 3H).

#### 5.11.6.5 Chalcone [2+2] Cycloaddition

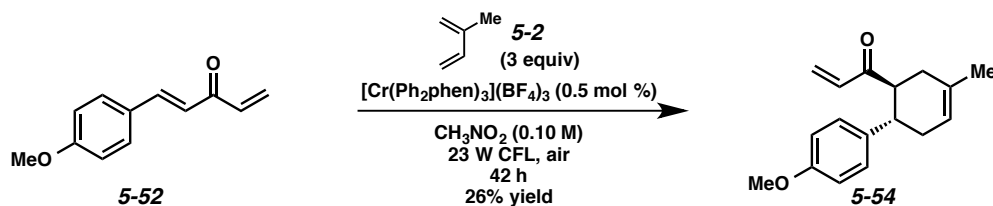


Time (h)	Light source	Catalyst?	Yield <b>5-173</b> (%) <sup>a</sup>
72 h	23 W CFL	with cat.	11
72 h	23 W CFL	no cat.	15
64 h	NUV	with cat.	33
64 h	NUV	no cat.	40

<sup>a</sup> NMR yields with dodecyl acetate as the internal standard  
[*cis*-chalcone was also observed in all cases.]

A 2-dr borosilicate vial open to air was charged with alkene **5-46** (15.6 mg, 0.0750 mmol), diene **5-2** (22.5  $\mu\text{L}$ , 0.225 mmol),  $[\text{Cr}(\text{Ph}_2\text{phen})_3](\text{BF}_4)_3$  (0.5 mg, 0.000375 mmol) (if catalyst was being used), nitromethane (0.750 mL), and dodecyl acetate (internal standard, 17.1 mg, 0.0750 mmol). The vial was then capped and placed in front of the indicated light source. The solution was irradiated with stirring for the indicated time, then passed through a short plug of silica (2.0-2.5 x 1 cm,  $\text{Et}_2\text{O}$  eluent). The volatile materials were removed by rotary evaporation, and the resulting crude product mixture was analyzed by  $^1\text{H}$  NMR.

#### 5.11.6.6 Cycloadditions of Divinyl Ketones

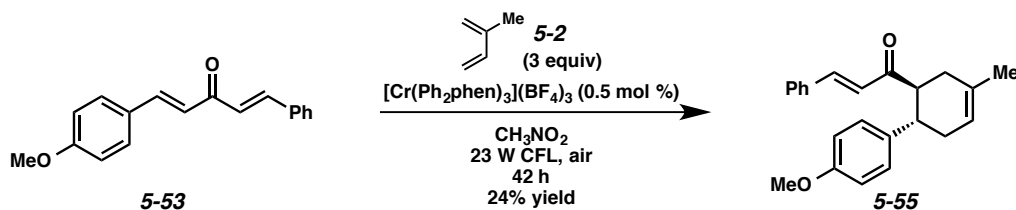


Vinyl ketone **5-52** was prepared in two steps by addition of vinyl magnesium chloride into aldehyde **5-141**, followed by oxidation of the resulting alcohol with MnO<sub>2</sub>. All spectroscopic data were consistent with previously reported values.<sup>73</sup>

**Cyclohexene 5-54.** Prepared according to the *General Procedure* using alkene **5-52** (10.0 mg, 0.0531 mmol), diene **5-2** (15.9 μL, 0.159 mmol), [Cr(Ph<sub>2</sub>phen)<sub>3</sub>](BF<sub>4</sub>)<sub>3</sub> (0.3 mg, 0.000266 mmol), and nitromethane (0.531 mL). The reaction mixture was irradiated for 42 h. The crude product was purified by flash chromatography (100% hexanes → 10:1 hexanes/EtOAc eluent) to afford cyclohexene **5-54** (3.6 mg, 26% yield, 9:1 isomeric ratio) as a colorless oil.

**TLC:** R<sub>f</sub> = 0.67 in 3:1 hexanes/EtOAc, stained yellow with *p*-anisaldehyde.

**<sup>1</sup>H NMR** (400 MHz; CDCl<sub>3</sub>): δ 7.08 (d, *J* = 8.7 Hz, 2H), 6.78 (d, *J* = 8.7 Hz, 2H), 6.22-6.05 (m, 2H), 5.62-5.59 (m, 1H), 5.50 (br s, 1H), 3.75 (s, 3H), 3.32 (td, *J* = 10.9, 5.5 Hz, 1H), 2.99 (td, *J* = 10.9, 5.5 Hz, 1H), 2.32-2.07 (comp. m, 4H), 1.72 (s, 3H).



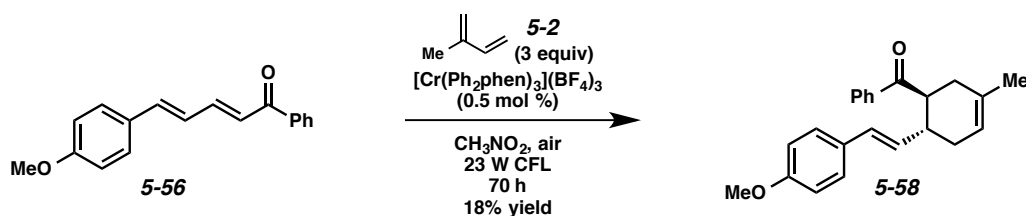
Styrenyl ketone **5-55** was prepared through the Aldol condensation of ketone **5-69** with benzaldehyde. All spectroscopic data were consistent with previously reported values.<sup>74</sup>

**Cyclohexene 5-55.** Prepared according to the *General Procedure* using alkene **5-53** (19.8 mg, 0.0750 mmol), diene **5-2** (22.5 μL, 0.225 mmol), [Cr(Ph<sub>2</sub>phen)<sub>3</sub>](BF<sub>4</sub>)<sub>3</sub> (0.5 mg, 0.000375 mmol), and nitromethane (0.750 mL). The reaction mixture was irradiated for 45 h. The crude product was purified by flash chromatography (100% hexanes → 15:1 hexanes/EtOAc eluent) to afford cyclohexene **5-55** (6.0 mg, 24% yield, 10:1 isomeric ratio) as a colorless oil.

**TLC:** R<sub>f</sub> = 0.63 in 3:1 hexanes/EtOAc, stained yellow with *p*-anisaldehyde.

$^1\text{H NMR}$  (400 MHz;  $\text{CDCl}_3$ ):  $\delta$  7.44-7.42 (comp. m, 3H), 7.38-7.35 (comp. m, 3H), 7.13 (d,  $J = 8.7$  Hz, 2H), 6.76 (d,  $J = 8.7$  Hz, 2H), 6.56 (d,  $J = 16.0$  Hz, 1H), 5.52 (br s, 1H), 3.70 (s, 3H), 3.35 (td,  $J = 10.9$ , 5.5 Hz, 1H), 3.05 (td,  $J = 10.9$ , 5.5 Hz, 1H), 2.39-2.14 (comp. m, 4H), 1.74 (s, 3H).

#### 5.11.6.7 Cycloaddition of $\alpha,\beta,\gamma,\delta$ -Unsaturated Carbonyls



**Cycloadduct 5-58.** An isolated yield was obtained under the Cr conditions. Prepared according to the *General Procedure* using alkene **5-56** (26.4 mg, 0.100 mmol), diene **5-2** (30.1  $\mu\text{L}$ , 0.300 mmol),  $[\text{Cr}(\text{Ph}_2\text{phen})_3](\text{BF}_4)_3$  (0.7 mg, 0.000500 mmol), and nitromethane (1.00 mL). The reaction mixture was irradiated for 70 h. The crude product was purified by flash chromatography (100% hexanes  $\rightarrow$  10:1 hexanes/EtOAc eluent) to afford cyclohexene **5-58** (6.0 mg, 18% yield,) as a yellow oil.

**TLC:**  $R_f = 0.68$  in 3:1 hexanes/EtOAc, stained blue with *p*-anisaldehyde.

$^1\text{H NMR}$  (400 MHz;  $\text{CDCl}_3$ ):  $\delta$  7.91 (d,  $J = 7.7$  Hz, 2H), 7.52-7.49 (m, 1H), 7.43 (d,  $J = 7.7$  Hz, 2H), 7.03 (d,  $J = 8.5$  Hz, 2H), 6.71 (d,  $J = 8.5$  Hz, 2H), 6.31 (d,  $J = 15.7$  Hz, 1H), 5.82 (dd,  $J = 15.7$ , 8.4 Hz, 1H), 5.46 (br s, 1H), 3.74 (s, 3H), 3.65 (td,  $J = 10.3$ , 5.1 Hz, 1H), 2.81-2.72 (m, 1H), 2.38-2.04 (m, 4H), 1.70 (s, 3H).

**General Procedure for Cycloaddition of 5-56 with Other Catalysts:** A flame-dried 2-dram borosilicate vial open to air was charged with alkene **5-56** (13.2 mg, 0.0500 mmol), diene **5-2** (50.0  $\mu\text{L}$ , 0.500 mmol), catalyst, solvent (0.500 mL), and dodecyl acetate (internal standard, 11.4 mg, 0.0500 mmol). The vial was then capped and placed in front of the indicated light source. The solution was irradiated with stirring for the indicated time, then passed through a short plug of silica (2.0-2.5  $\times$  1 cm,  $\text{Et}_2\text{O}$  eluent). The volatile

materials were removed by rotary evaporation, and the resulting crude product mixture was analyzed by  $^1\text{H}$  NMR. See Table 5.2 for results.

Analogous procedures were followed for the cycloaddition attempts of alkenes **5-59**, **5-61–5-66**.

Alkenes **5-56** and **5-59**<sup>74</sup> and **5-61** were prepared through Aldol condensation reactions according to the literature procedure.<sup>75</sup>

**5-61:**  $^1\text{H}$  NMR (400 MHz;  $\text{CDCl}_3$ ):  $\delta$  8.03-8.01 (m, 2H), 7.99-7.95 (m, 1H), 7.58-7.47 (m, 4H), 7.25 (d,  $J$  = 8.8 Hz, 1H), 7.11 (d,  $J$  = 14.7 Hz, 1H), 6.94 (d,  $J$  = 8.9 Hz, 2H), 6.76 (d,  $J$  = 11.8 Hz, 1H), 3.87 (s, 3H), 2.37 (s, 3H).

Alkene **5-62**<sup>76</sup> were prepared through an HWE reaction with the corresponding aldehyde in an analogous procedure as was used to synthesize ester **5-70**. Alkyne **5-63**<sup>77</sup> was also synthesized from the corresponding aldehyde by reaction with methyl (triphenylphosphoranylidene)acetate.

Alkenes **5-64**, **5-65**, **5-66** were prepared according to the literature procedure.<sup>78</sup>

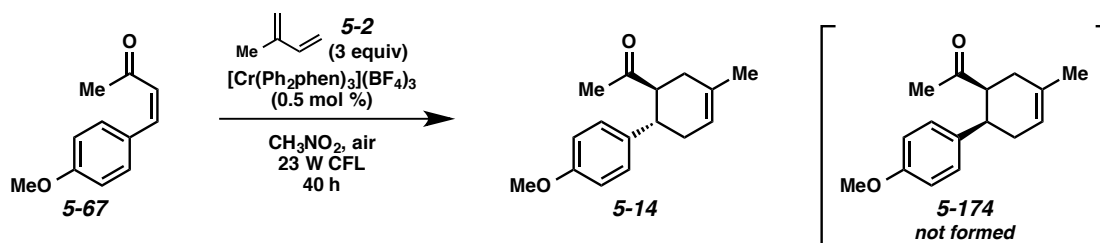
**5-64:**  $^1\text{H}$  NMR (400 MHz;  $\text{CDCl}_3$ ):  $\delta$  7.49-7.47 (m, 2H), 7.40 (ddd,  $J$  = 7.1, 4.5, 2.9 Hz, 1H), 7.37-7.34 (m, 1H), 7.25-7.22 (m, 2H), 6.37 (d,  $J$  = 9.6 Hz, 1H), 2.52 (t,  $J$  = 7.4 Hz, 2H), 1.64 (dq,  $J$  = 12.4, 5.9 Hz, 2H), 1.31-1.24 (m, 8H), 0.89-0.84 (m, 3H).

**5-65:**  $^1\text{H}$  NMR (400 MHz;  $\text{CDCl}_3$ ):  $\delta$  7.76 (d,  $J$  = 12.2 Hz, 1H), 7.38 (t,  $J$  = 7.8 Hz, 2H), 7.21-7.17 (m, 1H), 7.06 (d,  $J$  = 7.8 Hz, 2H), 5.93 (d,  $J$  = 12.2 Hz, 1H), 2.46 (t,  $J$  = 7.5 Hz, 2H), 1.65-1.59 (m, 2H), 1.29-1.26 (m, 8H), 0.87 (t,  $J$  = 6.7 Hz, 3H).

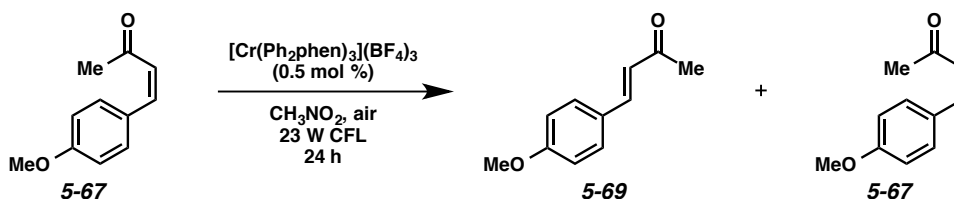
**5-66:**  $^1\text{H}$  NMR (400 MHz;  $\text{CDCl}_3$ ):  $\delta$  7.71 (d,  $J$  = 12.3 Hz, 1H), 7.01-6.98 (m, 1H), 6.91 (dd,  $J$  = 17.5, 9.0 Hz, 2H), 6.78 (d,  $J$  = 9.0 Hz, 1H), 5.84 (d,  $J$  = 12.3 Hz, 1H), 3.78 (s, 3H), 2.45 (t,  $J$  = 7.4 Hz, 2H), 1.62-1.57 (m, 2H), 1.29-1.26 (m, 8H), 0.87 (dd,  $J$  = 6.4, 2.9 Hz, 3H).

#### 5.11.6.8 Stereoconvergence Experiments

*cis*-Enone **5-67** was synthesized by reduction of the corresponding alkyne with H<sub>2</sub>/Lindlar's catalyst. Considerable over-reduction to the alkane was also observed. All spectroscopic data were consistent with previously reported values.<sup>79</sup>



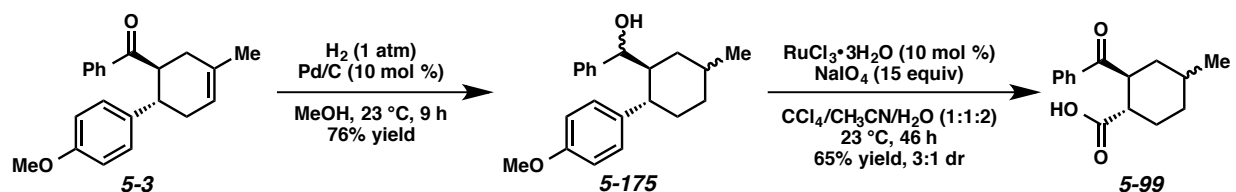
**Cycloaddition of *cis*-Enone.** Performed according to the *General Procedure* using alkene **5-67** (5.9 mg, 0.0325 mmol), diene **5-2** (10.0 μL, 0.101 mmol), [Cr(Ph<sub>2</sub>phen)<sub>3</sub>](BF<sub>4</sub>)<sub>3</sub> (0.2 mg, 0.000168 mmol), and nitromethane (0.340 mL). The reaction mixture was irradiated for 40 h, then was passed through a short plug of silica (2.0-2.5 x 1 cm, Et<sub>2</sub>O eluent). The volatile materials were removed by rotary evaporation and the crude reaction mixture was analyzed by <sup>1</sup>H NMR to reveal only the formation of *anti*-cyclohexene **5-14**, and no *cis* adduct (**5-174**).



**Isomerization of *cis*-Enone.** Performed in a 1/2-dram vial on 1.0 mg of *cis*-enone **5-67** (0.00570 mmol) in the presence of [Cr(Ph<sub>2</sub>phen)<sub>3</sub>](BF<sub>4</sub>)<sub>3</sub> (0.1 mg, 0.000028 mmol) in nitromethane (0.0600 mL). The reaction was irradiated with a 23 W CFL for 24 h, then was passed through a short plug of silica (2.0-2.5 x 1 cm, Et<sub>2</sub>O eluent). The volatile materials were removed by rotary evaporation, and the resulting crude

product mixture was analyzed by  $^1\text{H}$  NMR. A 3.5:1 ratio of **5-69**/**5-67** was observed. When this same experiment was performed without catalyst, a 5:1 ratio of **5-69**/**5-67** was observed.

### 5.11.6.9 Oxidative Cleavage of PMP Group



**Cyclohexane 5-175.**  $\text{H}_2$  gas was bubbled through a mixture of cyclohexene **5-3** (60.0 mg, 0.200 mmol) and Pd/C (10%, 21.3 mg, 0.0200 mmol) in MeOH (2.00 mL) for 30 s using a balloon of  $\text{H}_2$  and needle outlet. The needle outlet was removed and the reaction mixture was left under positive pressure of  $\text{H}_2$  and stirred for 9 h. The reaction mixture was then passed through a short plug of celite (2.0-2.5 x 1 cm, EtOAc eluent). The volatile materials were removed by rotary evaporation and the crude product was purified by flash chromatography (100% hexanes  $\rightarrow$  15:1 hexanes/EtOAc eluent) to afford cyclohexane **5-175** (47.0 mg, 76% yield) as a colorless oil. The NMR spectrum of the major diastereomer is reported.

**TLC:**  $R_f$  = 0.48 in 3:1 hexanes/EtOAc, stained blue with *p*-anisaldehyde.

**$^1\text{H}$  NMR** (400 MHz;  $\text{CDCl}_3$ ):  $\delta$  7.31-7.15 (m, 7H), 6.92 (d,  $J$  = 8.7 Hz, 2H), 4.61 (d,  $J$  = 4.1 Hz, 1H), 3.82 (s, 3H), 2.24 (tt,  $J$  = 11.7, 3.8 Hz, 1H), 2.03 (td,  $J$  = 11.7, 3.8 Hz, 1H), 1.94 (dq,  $J$  = 12.9, 2.5 Hz, 1H), 1.78-1.65 (comp. m, 2H), 1.56-1.24 (comp. m, 3H), 1.06 (d,  $J$  = 7.1 Hz, 1H), 0.88 (d,  $J$  = 6.5 Hz, 3H), 0.86-0.81 (m, 1H).

**$^{13}\text{C}$  NMR** (100 MHz;  $\text{CDCl}_3$ ):  $\delta$  157.9, 138.0, 128.5, 127.71, 127.65, 127.20, 127.17, 114.2, 75.3, 55.2, 48.3, 46.1, 37.7, 35.2, 35.0, 32.2, 22.7.

**IR** (film): 3386, 3031, 2920, 1611, 1512, 1249, 1036, 704  $\text{cm}^{-1}$ .

**HRMS** (ESI+):  $m/z$  calc'd for  $(\text{M} + \text{Na})^+$  [ $\text{C}_{21}\text{H}_{26}\text{O}_2 + \text{Na}$ ] $^+$ : 333.1825, found 333.1824.

**Carboxylic acid 5-99.** To cyclohexane **5-175** (10.4 mg, 0.0335 mmol) in CCl<sub>4</sub> (0.170 mL), acetonitrile (0.170 mL), and H<sub>2</sub>O (0.340 mL) under argon was added RuCl<sub>3</sub>•H<sub>2</sub>O (0.9 mg, 0.00337 mmol), then NaIO<sub>4</sub> (108.2 mg, 0.506 mmol). The reaction mixture was stirred for 46 h, then was diluted with H<sub>2</sub>O (2 mL) and CH<sub>2</sub>Cl<sub>2</sub> (2 mL). The layers were separated and the aqueous layer was extracted with CH<sub>2</sub>Cl<sub>2</sub> (2 x 5 mL). The combined CH<sub>2</sub>Cl<sub>2</sub> layers were passed through a short plug of silica (EtOAc eluent). The volatile materials were removed by rotary evaporation and the crude product was purified by flash chromatography (4:1 → 2:1 hexanes/EtOAc eluent) to afford carboxylic acid **5-99** (5.4 mg, 65% yield) as a colorless oil. The NMR spectrum of the major diastereomer is reported.

**TLC:** R<sub>f</sub> = 0.23 in 3:1 hexanes/EtOAc, visualized by UV.

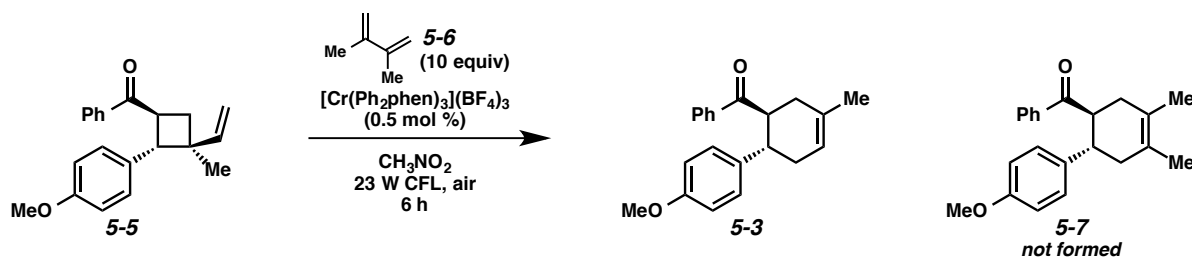
**<sup>1</sup>H NMR** (400 MHz; CDCl<sub>3</sub>): δ 7.96-7.91 (m, 2H), 7.57-7.54 (m, 1H), 7.46 (t, *J* = 7.6 Hz, 2H), 3.63-3.56 (m, 1H), 2.92-2.85 (m, 1H), 2.22 (dd, *J* = 13.2, 3.5 Hz, 1H), 1.98-1.92 (m, 1H), 1.86-1.72 (comp. m, 2H), 1.62-1.46 (comp. m, 3H), 0.90 (d, *J* = 6.5 Hz, 3H).

**<sup>13</sup>C NMR** (100 MHz; CDCl<sub>3</sub>): δ 211.8, 202.6, 136.0, 132.9, 128.6, 128.4, 46.8, 43.8, 37.9, 34.1, 32.3, 29.1, 22.0.

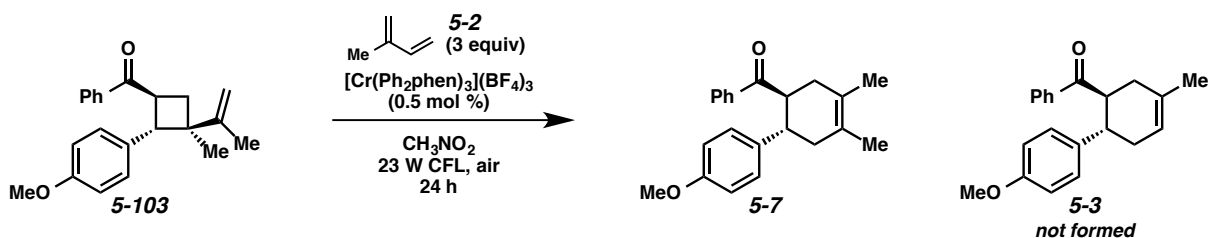
**IR** (film): 3060, 2255, 1703, 1448, 1286, 700 cm<sup>-1</sup>.

**HRMS** (ESI<sup>+</sup>): *m/z* calc'd for (M + Na)<sup>+</sup> [C<sub>15</sub>H<sub>18</sub>O<sub>3</sub> + Na]<sup>+</sup>: 269.1148, found 269.1149.

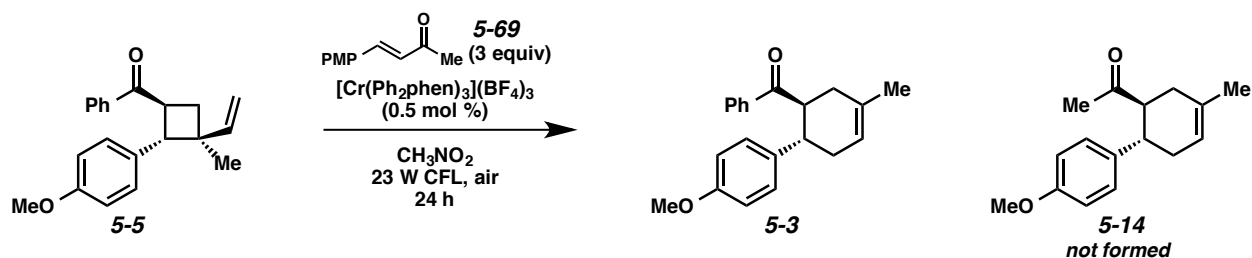
### 5.11.6.10 Vinylcyclobutane Trapping Experiments



Performed according to the *General Procedure* using vinylcyclobutane **5-5** (9.5 mg, 0.0310 mmol), diene **5-6** (34.0  $\mu$ L, 0.310 mmol),  $[\text{Cr}(\text{Ph}_2\text{phen})_3](\text{BF}_4)_3$  (0.2 mg, 0.000155 mmol), and nitromethane (0.310 mL). The reaction mixture was irradiated for 6 h, then was passed through a short plug of silica (2.0-2.5 x 1 cm,  $\text{Et}_2\text{O}$  eluent). The volatile materials were removed by rotary evaporation and the crude reaction mixture was analyzed by  $^1\text{H}$  NMR to reveal only the formation of cyclohexene **5-3**. Cyclohexene **5-7** was not formed.



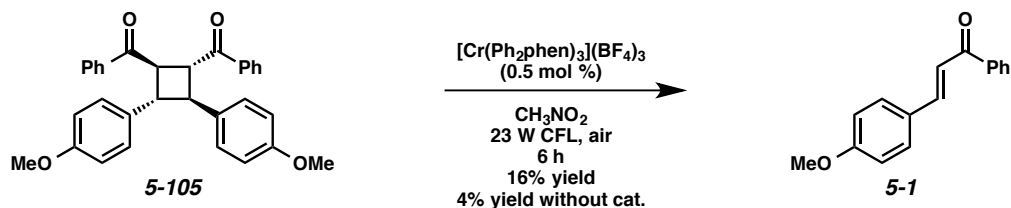
Performed according to the *General Procedure* using vinylcyclobutane **5-103**<sup>80</sup> (16.0 mg, 0.0500 mmol), diene **5-2** (15.0  $\mu$ L, 0.150 mmol),  $[\text{Cr}(\text{Ph}_2\text{phen})_3](\text{BF}_4)_3$  (0.3 mg, 0.000250 mmol), nitromethane (0.500 mL), and dodecyl acetate (internal standard, 11.4 mg, 0.0500 mmol). The reaction mixture was irradiated for 24 h, then was passed through a short plug of silica (2.0-2.5 x 1 cm,  $\text{Et}_2\text{O}$  eluent). The volatile materials were removed by rotary evaporation and the crude reaction mixture was analyzed by  $^1\text{H}$  NMR to reveal only the formation of cyclohexene **5-7**. Cyclohexene **5-3** was not formed.



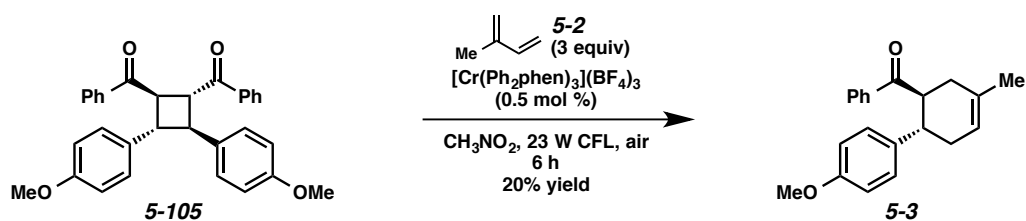
Performed according to the *General Procedure* using vinylcyclobutane **5-5** (15.3 mg, 0.0500 mmol), alkene **5-69** (26.4 mg, 0.150 mmol),  $[\text{Cr}(\text{Ph}_2\text{phen})_3](\text{BF}_4)_3$  (0.3 mg, 0.000250 mmol), nitromethane (0.500 mL), and dodecyl acetate (internal standard, 11.4 mg, 0.0500 mmol). The reaction mixture was irradiated for 24 h, then was passed through a short plug of silica (2.0-2.5 x 1 cm, Et<sub>2</sub>O eluent). The volatile materials were removed by rotary evaporation and the crude reaction mixture was analyzed by <sup>1</sup>H NMR to reveal only the formation of cyclohexene **5-3**. Cyclohexene **5-14** was not formed.

### 5.11.6.11 Enone Dimer Experiments

Enone dimer **5-105** was synthesized by Robert Higgins through irradiation (350 nm) of a concentrated solution of 4-methoxychalcone (**5-1**) in nitromethane in the presence of benzophenone (0.5 equiv). All spectroscopic data were consistent with previously reported values.<sup>32</sup>

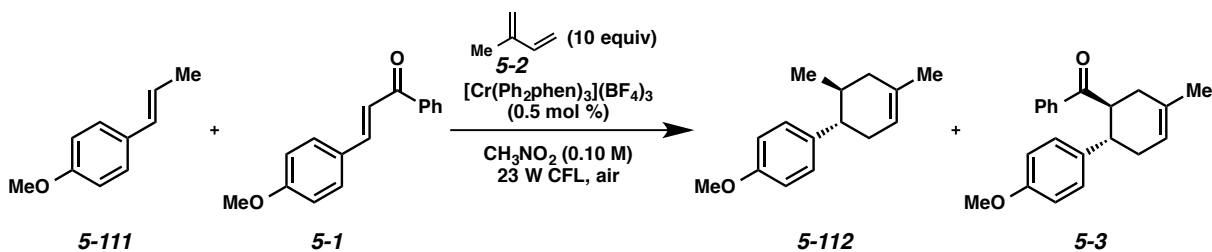


**Cycloreversion of Enone Dimer.** To a 1/2-dram vial upon to air was added dimer **5-105** (8.0 mg, 0.0168 mmol),  $[\text{Cr}(\text{Ph}_2\text{phen})_3](\text{BF}_4)_3$  (0.1 mg, 0.0000840 mmol), nitromethane (0.170 mL), and dodecyl acetate (internal standard, 3.8 mg, 0.0168 mmol). The vial was capped and stirred in front of a 23 W CFL in a closed box lined with aluminum foil. The reaction mixture was irradiated for 6 h, then was passed through a short plug of silica (2.0-2.5 x 1 cm, Et<sub>2</sub>O eluent). The volatile materials were removed by rotary evaporation and the crude reaction mixture was analyzed by <sup>1</sup>H NMR. In the presence of catalyst, enone **5-1** was obtained in 16% NMR yield. In the absence of catalyst, 4% NMR yield of enone **5-1** was observed.



**Trapping Experiment with Enone Dimer.** To a 1/2-dram vial upon to air was added dimer **5-105** (8.0 mg, 0.0168 mmol), diene **5-2** (5.00  $\mu$ L, 0.0504 mmol),  $[\text{Cr}(\text{Ph}_2\text{phen})_3](\text{BF}_4)_3$  (0.1 mg, 0.0000840 mmol), nitromethane (0.170 mL), and dodecyl acetate (internal standard, 3.8 mg, 0.0168 mmol). The vial was capped and stirred in front of a 23 W CFL in a closed box lined with aluminum foil. The reaction mixture was irradiated for 6 h, then was passed through a short plug of silica (2.0-2.5 x 1 cm, Et<sub>2</sub>O eluent). The volatile materials were removed by rotary evaporation and the crude reaction mixture was analyzed by <sup>1</sup>H NMR. Cyclohexene **5-3** was obtained in 20% NMR yield.

### 5.11.6.12 Competition Experiment



Time (h)	% Remaining <sup>a</sup>		% Formed <sup>a,b</sup>	
	<b>5-111</b>	<b>5-1</b>	<b>5-112</b>	<b>5-3</b>
2	45	97	17	0 (3)
4	22	94	29	0 (4)
6	>5	94	64	<5 (5)
10	0	60	74	18 (0)
24	0	25	75	62 (0)

<sup>a</sup> NMR yields with dodecyl acetate as the internal standard.

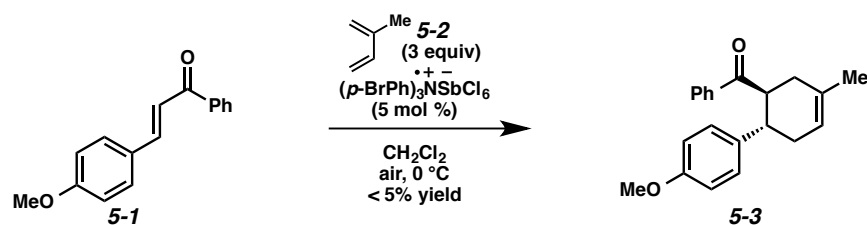
<sup>b</sup> Numbers in parentheses are yields of vinylcyclobutane **5-5**.

A stock solution was prepared containing alkene **5-111** (36.8 mg, 0.248 mmol), alkene **5-1** (59.1 mg, 0.248 mmol), diene **5-2** (0.250 mL, 2.48 mmol), [Cr(Ph<sub>2</sub>phen)<sub>3</sub>](BF<sub>4</sub>)<sub>3</sub> (1.6 mg, 0.00124 mmol), and dodecyl acetate (internal standard, 56.6 mg, 0.248 mmol) in nitromethane (2.48 mL). Into five 1-dram borosilicate vials was added 0.400 mL of the stock solution. The vials were capped and placed in front of a bright white 23 W compact fluorescent light bulb in a closed box lined with aluminum foil. At each indicated time, a vial was removed from the box, and the reaction mixture was passed through a short plug of silica (2.0-2.5 x 1 cm, Et<sub>2</sub>O eluent). The volatile materials were removed by rotary evaporation, and the resulting crude product mixture was analyzed by <sup>1</sup>H NMR.

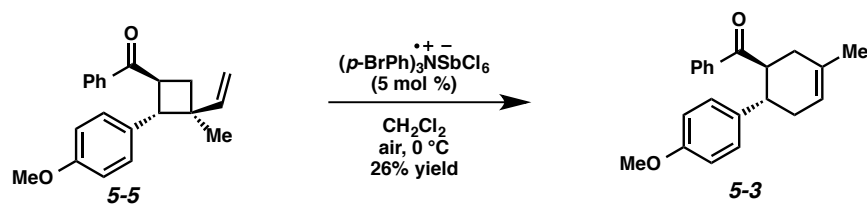
#### **5.11.6.13 Catalyst Evaluation (Table 5.3)**

**General Procedure for Cycloaddition:** A flame-dried 2-dram borosilicate vial open to air was charged with alkene **5-1** (11.9 mg, 0.0500 mmol), diene **5-2** (15.0 μL, 0.150 mmol), catalyst, solvent (0.500 mL), and dodecyl acetate (internal standard, 11.4 mg, 0.0500 mmol). The vial was then capped and placed in front of the indicated light source. The solution was irradiated with stirring for 6 h, then passed through a short plug of silica (2.0-2.5 x 1 cm, Et<sub>2</sub>O eluent). The volatile materials were removed by rotary evaporation, and the resulting crude product mixture was analyzed by <sup>1</sup>H NMR. See Table 5.3 for results.

**General Procedure for Vinylcyclobutane Rearrangement:** A flame-dried 2-dram borosilicate vial open to air was charged with vinylcyclobutane **5-5** (9.2 mg, 0.0300 mmol), catalyst, solvent (0.300 mL), and dodecyl acetate (internal standard, 6.9 mg, 0.0300 mmol). The vial was then capped and placed in front of the indicated light source. The solution was irradiated with stirring for 6 h, then passed through a short plug of silica (2.0-2.5 x 1 cm, Et<sub>2</sub>O eluent). The solvent was removed by rotary evaporation, and the resulting crude product mixture was analyzed by <sup>1</sup>H NMR. See Table 5.3 for results.

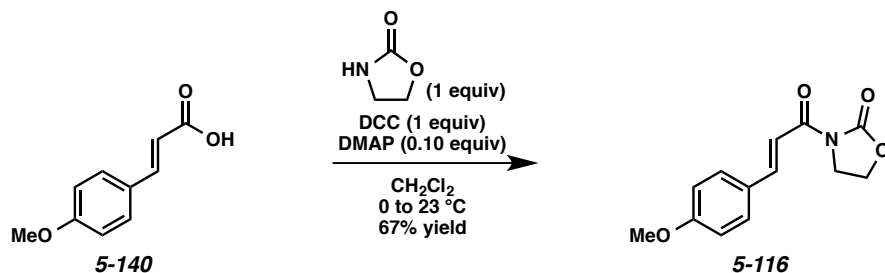


**Cycloaddition with Aminium Salt:** A flame-dried 2-dram borosilicate vial open to air was charged with alkene **5-1** (9.5 mg, 0.0400 mmol), diene **5-2** (12.0  $\mu$ L, 0.120 mmol),  $\text{CH}_2\text{Cl}_2$  (0.400 mL), and dodecyl acetate (internal standard, 9.1 mg, 0.0400 mmol). The vial was then capped and cooled to 0  $^\circ\text{C}$ , then  $(p\text{-BrPh})_3\text{NSbCl}_6$  (1.6 mg, 0.00200 mmol) was added. The reaction mixture was stirred at 0  $^\circ\text{C}$  for 1 h, then was passed through a short plug of silica (2.0-2.5 x 1 cm,  $\text{CH}_2\text{Cl}_2$  eluent). The volatile materials were removed by rotary evaporation, and the resulting crude product mixture was analyzed by  $^1\text{H}$  NMR. <5% yield of cyclohexene **5-3** had formed. An analogous experiment was performed where the vial was irradiated with a 23 W CFL ( $\sim 45$   $^\circ\text{C}$ ) for 6 h. Again, <5% yield of cyclohexene **5-3** was formed.



**Vinylcyclobutane Rearrangement with Aminium Salt:** A flame-dried 2-dram borosilicate vial open to air was charged with vinylcyclobutane **5-5** (12.3 mg, 0.0400 mmol),  $\text{CH}_2\text{Cl}_2$  (0.400 mL), and dodecyl acetate (internal standard, 9.1 mg, 0.0400 mmol). The vial was then capped and cooled to 0  $^\circ\text{C}$ , then  $(p\text{-BrPh})_3\text{NSbCl}_6$  (1.6 mg, 0.00200 mmol) was added. The reaction mixture was stirred at 0  $^\circ\text{C}$  for 1 h, then was passed through a short plug of silica (2.0-2.5 x 1 cm,  $\text{CH}_2\text{Cl}_2$  eluent). The volatile materials were removed by rotary evaporation, and the resulting crude product mixture was analyzed by  $^1\text{H}$  NMR. 26% yield of cyclohexene **5-3** had formed.

#### 5.11.6.14 Oxazolidinone Synthesis



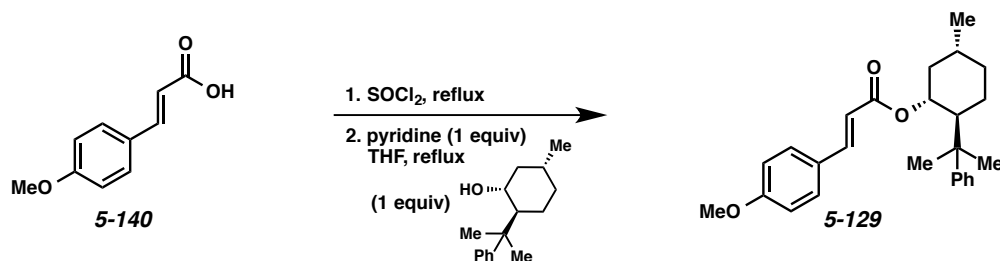
**Oxazolidinone 5-116.** (*representative procedure*) To carboxylic acid **5-140** (53.5 mg, 0.300 mmol), DMAP (3.7 mg, 0.0300), and 2-oxazolidinone (26.1 mg, 0.300 mmol) in CH<sub>2</sub>Cl<sub>2</sub> (0.400 mL) in a flame-dried vial at 0 °C was added DCC (61.9 mg, 0.300 mmol). The vial was capped and allowed to warm to ambient temperature. The reaction mixture was stirred for 20 h, then was filtered, washing with CH<sub>2</sub>Cl<sub>2</sub>. The filtrate was washed sequentially with sat. aq. NaHCO<sub>3</sub> (5 mL) and brine (5 mL), and then was dried over MgSO<sub>4</sub>. The solvent was removed by rotary evaporation, and the crude residue was purified by flash chromatography (20:1 → 1:1 hexanes/EtOAc eluent) to afford oxazolidinone **5-116** (49.5 mg, 67% yield) as a white solid.

**TLC:** R<sub>f</sub> = 0.42 in 1:1 hexanes/EtOAc, stained with KMnO<sub>4</sub>.

All spectroscopic data were consistent with previously reported values.<sup>81</sup>

The other oxazolidinone substrates discussed in Scheme 5.34 (**5-118–5-121**) were synthesized through an analogous method using the corresponding chiral oxazolidinones.

### 5.11.6.15 Menthyl Ester Synthesis



**Menthyl ester 5-129.** (*representative procedure*) To a flame-dried 2-dram vial was added carboxylic acid **5-140** (0.134 g, 0.750 mmol) and  $\text{SOCl}_2$  (0.44 mL, 6.00 mmol). The vial was capped and heated at 76 °C for 3 h. The reaction mixture was allowed to cool to ambient temperature, then the volatile materials were removed by rotary evaporation. The crude residue was azeotroped with  $\text{CH}_2\text{Cl}_2$  (3 x 1 mL). To the crude residue was added pyridine (0.0610 mL, 0.750 mmol), 8-phenylmenthol (0.174 g, 0.750 mmol), and THF (0.300 mL). The vial was capped and stirred at 66 °C for 6 h. The reaction mixture was allowed to cool to ambient temperature, then was diluted with EtOAc (5 mL) and transferred to a separatory funnel. The organic layer was washed sequentially with sat. aq.  $\text{NaHCO}_3$  (5 mL), brine (5 mL), and  $\text{H}_2\text{O}$  (5 mL), and then was dried over  $\text{MgSO}_4$ . The solvent was removed by rotary evaporation, and the crude residue was purified by flash chromatography (100% hexanes  $\rightarrow$  10:1 hexanes/EtOAc eluent) to afford ester **5-129** (0.256 g, 87% yield) as a pale yellow oil.

**TLC:**  $R_f = 0.68$  in 3:1 hexanes/EtOAc, visualized by UV.

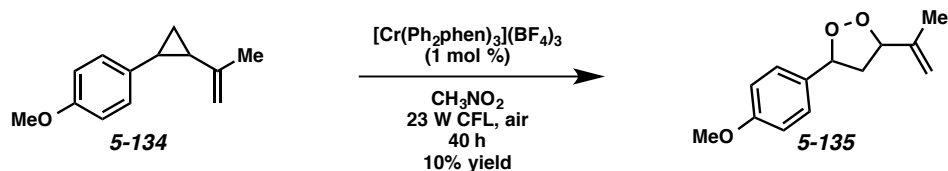
All spectroscopic data were consistent with previously reported values.<sup>82</sup>

The other menthyl ester substrates discussed in Table 5.5 (**5-128** and **5-130**) were synthesized through an analogous method using the corresponding menthol derivatives.

**Cycloadditions with Chiral Substrates.** Performed according to *General Procedure* with dodecyl acetate as an internal standard. The crude product mixtures were analyzed by  $^1\text{H}$  NMR to determine their

diastereomeric ratios. These results are reported in Section 5.8. The alcohol 8-(4-methoxy)phenyl menthol was synthesized according to the literature procedure.<sup>83</sup>

#### 5.11.6.16 Vinylcyclopropane [3+2] with Oxygen



**Endoperoxide 5-135.** To a vial open to air was added cyclopropane **5-134** (14.1 mg, 0.0750 mmol),  $[\text{Cr}(\text{Ph}_2\text{phen})_3](\text{BF}_4)_3$  (1.0 mg, 0.00075 mmol), and nitromethane (0.750 mL). The vial was capped and irradiated with a 23 W CFL with stirring for 40 h. The reaction mixture was then passed through a short plug of silica (2.0-2.5 x 1 cm,  $\text{Et}_2\text{O}$  eluent). The volatile materials were removed by rotary evaporation, and the crude residue was purified by flash chromatography (100% hexanes  $\rightarrow$  15:1 hexanes/ $\text{EtOAc}$  eluent) to afford endoperoxide **5-135** (1.6 mg, 10% yield) as a colorless oil. The rest of the material was mostly cyclopropane **5-134** and *p*-anisaldehyde.

**TLC:**  $R_f$  = 0.66 in 3:1 hexanes/ $\text{EtOAc}$ , stained purple with *p*-anisaldehyde.

**$^1\text{H}$  NMR** (400 MHz;  $\text{CDCl}_3$ ):  $\delta$  7.33 (d,  $J$  = 8.7 Hz, 2H), 6.89 (d,  $J$  = 8.7 Hz, 2H), 5.26 (t,  $J$  = 7.5 Hz, 1H), 5.11 (s, 1H), 4.96 (s, 1H), 4.86 (t,  $J$  = 7.5 Hz, 1H), 3.81 (s, 3H), 3.10 (dt,  $J$  = 12.2, 7.9 Hz, 1H), 2.52 (dt,  $J$  = 12.2, 7.9 Hz, 1H), 1.81 (s, 3H).

## Chapter 5 Notes and References

- <sup>1</sup> All reduction potentials are in V vs. SCE, unless otherwise noted.
- <sup>2</sup> Robert Higgins is acknowledged for collecting this data.
- <sup>3</sup> McDaniel, A. M.; Tseng, H.-W.; Damrauer, N. H.; Shores, M. P. *Inorg. Chem.* **2010**, *49*, 7981-7991.
- <sup>4</sup> Clennan, E. L. *Tetrahedron* **2000**, *56*, 9151-9179.
- <sup>5</sup> Frimer, A. A. *Singlet O<sub>2</sub>*. CRC: Boca Raton, FL, **1985**.
- <sup>6</sup> (a) Crimmins, M. T.; Reinhold, T. L. *Enone Olefin [2 + 2] Photochemical Cycloadditions*. Organic Reactions. **2004**. 44:2:297-588. (b) Poplata, S.; Tröster, A.; Zou, Y.-Q.; Bach, T. *Chem. Rev.* **2016**, DOI: 10.1021/acs.chemrev.5b00723.
- <sup>7</sup> (a) Pandey, G.; Krishna, A.; Kumaraswamy, G. *Tetrahedron Lett.* **1987**, *28*, 4615-4616. (b) Climent, M. J.; García, H.; Iborra, S.; Miranda, M. A.; Primo, J. *Heterocycles* **1989**, *29*, 115-121. (c) Kar, S.; Lahiri, S. *J. Chem. Soc. Chem. Commun.* **1995**, 957-958. (d) Kar, S.; Lahiri, S. *Ind. J. Chem.* **2001**, *40B*, 1121-1124.
- <sup>8</sup> Reynolds, D. W.; Harirchian, B.; Chiou, H.-S.; Marsh, B. K.; Bauld, N. L. *J. Phys. Org. Chem.* **1989**, *2*, 57-88.
- <sup>9</sup> Kim, T.; Pye, R. J.; Bauld, N. L. *J. Am. Chem. Soc.* **1990**, *112*, 6285-6290.
- <sup>10</sup> Bauld, N. L.; Bellville, D. J.; Harirchian, B.; Lorenz, K. T.; Pabon, Jr. R. A.; Reynolds, D. W.; Wirth, D. D.; Chiou, H.-S.; Marsh, B. K. *Acc. Chem. Res.* **1987**, *20*, 371-378.
- <sup>11</sup> (a) Pabon, R. A.; Bellville, D. J.; Bauld, N. L. *J. Am. Chem. Soc.* **1984**, *106*, 2730-2731.
- <sup>12</sup> (a) Ischay, M. A.; Ament, M. S.; Yoon, T. P. *Chem. Sci.* **2012**, *3*, 2807-2811. (b) Riener, M.; Nicewicz, D. A. *Chem. Sci.* **2013**, *4*, 2625-2629.
- <sup>13</sup> Reduction potentials were found in: (a) Roth, H. G.; Romero, N. A.; Nicewicz, D. A. *Synlett* **2016**, *27*, 714-723. (b) Tajima, T.; Fuchigama, T. *Chem. Eur. J.* **2005**, *11*, 6192-6196.
- <sup>14</sup> Prier, C. K.; Rankic, D. A.; MacMillan, D. W. C. *Chem. Rev.* **2013**, *113*, 5322-5363.

- 
- <sup>15</sup> (a) Gesmundo, N. J.; Nicewicz, D. A. *Beilstein J. Org. Chem.* **2014**, *10*, 1272-1281. (b) Miranda, M. A.; García, H. *Chem. Rev.* **1994**, *94*, 1063-1089.
- <sup>16</sup> (a) Nicewicz, D. A.; Nguyen, T. M. *ACS Catal.* **2014**, *4*, 355-360. (b) Benniston, A. C.; Harriman, A.; Li, P.; Rostron, J. P.; van Ramesdonk, H. J.; Groeneveld, M. M.; Zhang, H.; Verhoeven, J. W. *J. Am. Chem. Soc.* **2005**, *127*, 16054-16064.
- <sup>17</sup> (a) Crimmins, M. T. *Chem. Rev.* **1988**, *88*, 1453-1473. (b) Schuster, D. I.; Lem, G.; Kaprinidis, N. A. *Chem. Rev.* **1993**, *93*, 3-22.
- <sup>18</sup> Corey, E. J.; Bass, J. D.; LeMahieu, R.; Mitra, R. B. *J. Am. Chem. Soc.* **1964**, *86*, 5570-5583.
- <sup>19</sup> Lewis, F. D.; Hirsch, R. H. *J. Am. Chem. Soc.* **1976**, *98*, 5914-5924.
- <sup>20</sup> Peng, F.; Grote, R. E.; Wilson, R. M.; Danishefsky, S. J. *Proc. Natl. Acad. Sci.* **2013**, *110*, 10904-10909.
- <sup>21</sup> (a) Danishefsky, S.; Prisbylla, M. P.; Hiner, S. *J. Am. Chem. Soc.* **1978**, *100*, 2918-2920. (b) Ono, N.; Miyake, H.; Kaji, A. *J. Chem. Soc., Chem. Commun.* **1982**, 33-34.
- <sup>22</sup> (a) Trost, B. M.; Ippen, J.; Vladuchick, W. C. *J. Am. Chem. Soc.* **1977**, *99*, 8116-8118. (b) Stojanac, Z.; Dickinson, R. A.; Stojanac, N.; Woznow, R. J.; Valenta, Z. *Can. J. Chem.* **1975**, *53*, 616-618. (c) Tou, J. S.; Reusch, W. *J. Org. Chem.* **1980**, *45*, 5012-5014. (d) Alston, P. V.; Gordon, M. D.; Ottenbrite, R. M.; Cohen, T. *J. Org. Chem.* **1983**, *48*, 5051-5054.
- <sup>23</sup> Ayerbe, M.; Cossio, F. P. *Tetrahedron Lett.* **1995**, *36*, 4447-4450.
- <sup>24</sup> Carlson, P. H. J.; Katsuki, T.; Martin, V. S. Sharpless, K. B. *J. Org. Chem.* **1981**, *46*, 3936-3938.
- <sup>25</sup> Balieu, S.; Hallet, G. E.; Burns, M.; Bootwicha, T.; Studley, J.; Aggarwal, V. K. *J. Am. Chem. Soc.* **2015**, *137*, 4398-4403.
- <sup>26</sup> Miles, W. H.; Cohen, E. M.; Naimoli, B. J. *Synth. Commun.* **2013**, *43*, 1980-1991.
- <sup>27</sup> Miller, K. K.; Zhang, P.; Nishizawa-Brennen, Y.; Frost, J. W. *ACS Sustainable Chem. Eng.* **2014**, *2*, 2053-2056.

- 
- <sup>28</sup> (a) Lu, Z.; Yoon, T. P. *Angew. Chem., Int. Ed.* **2012**, *51*, 10329-10332. (b) Hurtley, A. E.; Lu, Z.; Yoon, T. P. *Angew. Chem., Int. Ed.* **2014**, *53*, 8991-8994.
- <sup>29</sup> (a) Caldwell, R. A.; Singh, M. *J. Am. Chem. Soc.* **1983**, *105*, 5139-5140. (b) Caldwell, R. A. *J. Am. Chem. Soc.* **1970**, *92*, 3229-3230.
- <sup>30</sup> The orientation of the two enones as drawn may not be correct.
- <sup>31</sup> Kranz, P. D.; Griesbeck, A. G.; Alle, R.; Perez-Ruiz, R.; Neudörfl, J. M.; Meerholz, K.; Schmalz, H.-G. *Angew. Chem., Int. Ed.* **2012**, *51*, 6000-6004.
- <sup>32</sup> Toda, F.; Tanaka, K.; Kato, M. *J. Chem. Soc., Perkin Trans. 1* **1998**, 1315-1318.
- <sup>33</sup> Chatterjee, S.; Kar, S.; Lahiri, S.; Basu, S. *Spectrochimica Acta Part A* **2004**, *60*, 1713-1718.
- <sup>34</sup> (a) Stufflebeme, G.; Lorenz, K. T.; Bauld, N. L. *J. Am. Chem. Soc.* **1986**, *108*, 4234-4235. (b) Bauld, N. L.; Stufflebeme, G. W.; Lorenz, K. T. *J. Phys. Org. Chem.* **1989**, *2*, 585-601. (c) Yueh, W.; Bauld, N. L. *J. Am. Chem. Soc.* **1995**, *117*, 5671-5676.
- <sup>35</sup> Sarabia, F. J.; Ferreira, E. M. *manuscript in preparation*.
- <sup>36</sup> Francisco Sarabia is acknowledged for the cyclopropanation results.
- <sup>37</sup> (a) Nomura, T.; Pukai, T.; Narita, T.; Terada, S.; Uzawa, J.; Iitaka, Y. *Tetrahedron Lett.* **1981**, *22*, 2195-2198. (b) Brito, C. M.; Pinto, D. C. G. A.; Silva, A. M. S.; Silva, A. M. G.; Tomé, A. C.; Cavaleiro, J. A. S. *Eur. J. Org. Chem.* **2006**, 2558-2569. (c) Chee, C. F.; Abdullah, I.; Buckle, M. J. C.; Rahman, N. A. *Tetrahedron Lett.* **2010**, *51*, 495-495.
- <sup>38</sup> (a) Kinsman, A. C.; Kerr, M. A. *Org. Lett.* **2000**, *2*, 3517-3520. (b) Ballerini, E.; Minuti, L.; Piermatti, O. *J. Org. Chem.* **2010**, *75*, 4251-4260.
- <sup>39</sup> (a) Karthikeyan, M.; Kamakshi, R.; Sridar, V.; Reddy, B. S. R. *Synth. Commun.* **2003**, *33*, 4199-4204. (b) Kamakshi, R.; Reddy, B. S. R. *J. Polym. Sci. A Polym. Chem.* **2008**, *46*, 1521-1531.
- <sup>40</sup> (a) Reetz, M. F.; Jiao, N. *Angew. Chem., Int. Ed.* **2006**, *45*, 2416-2419. (b) Corbett, J. L.; Weaver, R. T. *Synth. Commun.* **2008**, *38*, 489-498. (c) Cong, H.; Ledbetter, D.; Rowe, G. T.; Caradonna, J. P.; Porco, J. A. *J. Am. Chem. Soc.* **2008**, *130*, 9214-9215. (d) Cong, H.; Becker, C. F.; Elliott, S. J.; Grinstaff, M. W.;

---

Porco, J. A. *J. Am. Chem. Soc.* **2010**, *132*, 7514-7518. (e) Bah, J.; Franzén, J. *Chem. Eur. J.* **2014**, *20*, 1066-1072.

<sup>41</sup> Brimioulle, R.; Lenhart, D.; Maturi, M. M.; Bach, T. *Angew. Chem., Int. Ed.* **2015**, *54*, 3872-3890.

<sup>42</sup> Du, J.; Skubi, K. L.; Schultz, D. M.; Yoon, T. P. *Science* **2014**, *344*, 392-396.

<sup>43</sup> Huo, H.; Shen, X.; Wang, C.; Zhang, L.; Röse, P.; Chen, L.-A.; Harms, K.; Marsch, M.; Hilt, G.; Meggers, E. *Nature* **2014**, *515*, 100-103.

<sup>44</sup> Müller, C.; Bauer, A.; Maturi, M. M.; Consuelo Cuquerella, M.; Miranda, M. A.; Bach, T. *J. Am. Chem. Soc.* **2011**, *133*, 16689-16697.

<sup>45</sup> Zuo, Z.; Cong, H.; Li, W.; Choi, J.; Fu, G. C.; MacMillan, D. W. C. *J. Am. Chem. Soc.* **2016**, *138*, 1832-1835.

<sup>46</sup> Evans, D. A.; Chapman, K. T.; Bisaha, J. *J. Am. Chem. Soc.* **1988**, *110*, 1238-1256.

<sup>47</sup> (a) Adam, W.; Bosio, S. G.; Turro, N. J. *J. Am. Chem. Soc.* **2002**, *124*, 8814-8815. (b) Adam, W.; Bosio, S. G.; Turro, N. J.; Wolff, B. T. *J. Org. Chem.* **2004**, *69*, 1704-1715.

<sup>48</sup> (a) Palomo, C.; Aizpurua, J. M.; Legido, M.; Galarza, R.; Deya, P. M.; Dunogues, J.; Picard, J. P.; Ricci, A.; Seconi, G. *Angew. Chem., Int. Ed.* **1996**, *35*, 1239-1241. (b) Palomo, C.; Aizpurua, J. M.; Legido, M.; Mielgo, A.; Galarza, R. *Chem. Eur. J.* **1997**, *3*, 1432-1441. (c) Palomo, C.; Aizpurua, J. M.; Galarza, R.; Benito, A.; Khamrai, U. K.; Eikeseth, U.; Linden, A. *Tetrahedron* **2000**, *56*, 5563-5570.

<sup>49</sup> (a) Lange, G. L.; Decicco, C.; Tan, S. L.; Chamberlain, G. *Tetrahedron Lett.* **1985**, *26*, 4707-4710. (b) Lange, G. L.; Decicco, C.; Lee, M. *Tetrahedron Lett.* **1987**, *28*, 2833-2836. (c) Herzog, H.; Koch, H.; Scharf, H.-D.; Runsink, J. *Tetrahedron* **1986**, *42*, 3547-3558. (d) Tsutsumi, K.; Endou, K.; Furutani, A.; Ikki, T.; Nakano, H.; Shintani, T.; Morimoto, T.; Kakiuchi, K. *Chirality* **2003**, *15*, 504-509. (e) Furutani, A.; Tsutsumi, K.; Nakano, H.; Morimoto, T.; Kakiuchi, K. *Tetrahedron Lett.* **2004**, *45*, 7621-7624. (f) Inhülsen, I.; Akiyama, N.; Tsutsumi, K.; Nishiyama, Y.; Kakiuchi, K. *Tetrahedron* **2013**, *69*, 782-790. (g) Nishiyama, Y.; Nakatani, K.; Tanimoto, H.; Morimoto, T.; Kakiuchi, K. *J. Org. Chem.* **2013**, *78*, 7186-

---

7193. (h) Nishiyama, Y.; Shibata, M.; Ishii, T.; Morimoto, T.; Tanimoto, H.; Tsutsumi, K.; Kakiuchi, K. *Molecules* **2013**, *18*, 1626-1637.

<sup>50</sup> (a) Dinnocenzo, J. P.; Conlon, D. A. *J. Am. Chem. Soc.* **1988**, *110*, 2324-2326. (b) Oxgaard, J.; Wiest, O. *Eur. J. Org. Chem.* **2003**, 1454-1462.

<sup>51</sup> Lu, Z.; Parrish, J. D.; Yoon, T. P. *Tetrahedron* **2014**, *70*, 4270-4278.

<sup>52</sup> Sang Lee is acknowledged for this result.

<sup>53</sup> Stevenson, S. M.; Higgins, R. F.; Shores, M. P.; Ferreira, E. M. *manuscript submitted*.

<sup>54</sup> Higgins, R. F.; Fatur, S. M.; Shepard, S. G.; Stevenson, S. M.; Boston, D. J.; Ferreira, E. M.; Damrauer, N. H.; Rappé, A. K.; Shores, M. P. *J. Am. Chem. Soc.* **2016**, *138*, 5451-5464.

<sup>55</sup> The synthesis of this substrate is described in Chapter 4.9.5.

<sup>56</sup> Vaidya, S. S.; Vinaya, H.; Mahajan, S. S. *Med. Chem. Res.* **2012**, *21*, 4311-4323.

<sup>57</sup> Gao, F.; Feng, H.; Sun, Z. *Tetrahedron Lett.* **2014**, *55*, 6451-6454.

<sup>58</sup> Chen, X.; Zhou, H.; Zhang, K.; Li, J.; Huang, H. *Org. Lett.* **2014**, *16*, 3912-3915.

<sup>59</sup> Kelly, C. B.; Ovian, J. M.; Cywar, R. M.; Gosselin, T. R.; Wiles, R. J.; Leadbeater, N. E. *Org. Biomol. Chem.* **2015**, *13*, 4255-4259.

<sup>60</sup> Salabert, J.; Sebastian, R. M.; Vallribera, A.; Cívicos, J. F.; Najera, C. *Tetrahedron* **2013**, *69*, 2655-2659.

<sup>61</sup> Morales-Serna, J. A.; García-Ríos, E.; Bernal, J.; Paleo, E.; Gaviño, R.; Cárdenas, J. *Synthesis* **2011**, *9*, 1375-1382.

<sup>62</sup> Yang, H.; Fu, L.; Wei, L.; Liang, J.; Binks, B. P. *J. Am. Chem. Soc.* **2015**, *137*, 1362-1371.

<sup>63</sup> Chang, D.; Gu, Y.; Shen, Q. *Chem. Eur. J.* **2015**, *21*, 6074-6078.

<sup>64</sup> Patil, C. B.; Mahajan, S. K.; Katti, S. A. *J. Pharm. Sci. & Res.* **2009**, *1*, 11-22.

<sup>65</sup> Wu, J. Y.; Stanzl, B. N.; Ritter, T. *J. Am. Chem. Soc.* **2010**, *132*, 13214-13216.

<sup>66</sup> Lautens, M.; Tam, W.; Sood, C. *J. Org. Chem.* **1993**, *58*, 4513-4515.

<sup>67</sup> Wu, J. Y.; Moreau, B.; Ritter, T. *J. Am. Chem. Soc.* **2009**, *131*, 12915-12917.

- 
- <sup>68</sup> Llaveria, J.; Beltrán, Á.; Díaz-Requejo, M. M.; Matheu, M. I.; Castellón, S.; Pérez, P. J. *Angew. Chem., Int. Ed.* **2010**, *49*, 7092-7095.
- <sup>69</sup> Pullin, R. D. C.; Sellars, J. D.; Steel, P. G. *Org. Biomol. Chem.* **2007**, *5*, 3201-3206.
- <sup>70</sup> Hirner, J. J.; Blum, S. A. *Organometallics* **2011**, *30*, 1299-1302.
- <sup>71</sup> Laird, T.; Ollis, W. D.; Sutherland, I. O. *J. Chem. Soc., Perkin Trans. 1* **1980**, 2033-2048.
- <sup>72</sup> Kliman, L. T.; Mlynarski, S. N.; Ferris, G. E. Morken, J. P. *Angew. Chem., Int. Ed.* **2012**, *51*, 521-524.
- <sup>73</sup> Hu, F.-L.; Wei, Y.; Shi, M. *Adv. Synth. Catal.* **2014**, *356*, 736-742.
- <sup>74</sup> Roman, B. I.; De Ryck, T.; Verhasselt, S.; Bracke, M. E.; Stevens, C. V. *Bioorg. Med. Chem. Lett.* **2015**, *25*, 1021-1025.
- <sup>75</sup> Santos, C. M. M.; Silva, A. M. S.; Cavaleiro, J. A. S.; Lévai, A.; Patonay, T. *Eur. J. Org. Chem.* **2007**, 2877-2887.
- <sup>76</sup> Curti, C.; Sartori, A.; Battistini, L.; Brindani, N.; Rassu, G.; Pelosi, G.; Lodola, A.; Mor, M.; Casiraghi, G.; Zanardi, F. *Chem. Eur. J.* **2015**, *21*, 6433-6442.
- <sup>77</sup> Tseng, P.-Y.; Chuang, S.-C. *Adv. Synth. Catal.* **2013**, *355*, 2165-2171.
- <sup>78</sup> Zhou, Q.-F.; Yang, F.; Guo, Q.-X.; Xue, S. *Synlett* **2007**, *2*, 215-218.
- <sup>79</sup> Bellassoued, M.; Aatar, J.; Bouzid, M.; Damak, M. *Phosphorus Sulfer Silicon Relat. Elem.* **2010**, *185*, 1886-1895.
- <sup>80</sup> Vinylcyclobutane **5-103** was prepared analogously to vinylcyclobutane **5-5**.
- <sup>81</sup> Soloshonok, V. A.; Cai, C.; Hruby, V.; Van Meervelt, L.; Yamazaki, T. *J. Org. Chem.* **2000**, *65*, 6688-6696.
- <sup>82</sup> Ye, S.; Tang, Y.; Dai, L.-X. *J. Org. Chem.* **2001**, *66*, 5717-5722.
- <sup>83</sup> Yang, D.; Xu, M.; Bian, M.-Y. *Org. Lett.* **2001**, *3*, 111-114.

## APPENDIX A

## CRYSTALLOGRAPHIC DATA FOR PRODUCT 2-2

**Table 1. Crystal data and structure refinement for 2-2**

Identification code	<b>2-2</b>
Empirical formula	C <sub>17</sub> H <sub>20</sub> O
Formula weight	240.33
Temperature/K	100(2)
Crystal system	monoclinic
Space group	Cc
a/Å	16.9694(6)
b/Å	10.1758(6)
c/Å	7.7382(3)
α/°	90.00
β/°	92.801(3)
γ/°	90.00
Volume/Å <sup>3</sup>	1334.61(11)
Z	4
ρ <sub>calc</sub> /mg/mm <sup>3</sup>	1.196
m/mm <sup>-1</sup>	0.072
F(000)	520.0
Crystal size/mm <sup>3</sup>	0.57 × 0.47 × 0.37
2θ range for data collection	4.66 to 78.76°
Index ranges	-30 ≤ h ≤ 30, -18 ≤ k ≤ 17, -13 ≤ l ≤ 13
Reflections collected	28192
Independent reflections	7745[R(int) = 0.0359]
Data/restraints/parameters	7745/2/164
Goodness-of-fit on F <sup>2</sup>	1.064
Final R indexes [I ≥ 2σ (I)]	R <sub>1</sub> = 0.0323, wR <sub>2</sub> = 0.0884
Final R indexes [all data]	R <sub>1</sub> = 0.0344, wR <sub>2</sub> = 0.0898
Largest diff. peak/hole / e Å <sup>-3</sup>	0.44/-0.21
Flack parameter	0.3(5)

**Table 2. Fractional Atomic Coordinates ( $\times 10^4$ ) and Equivalent Isotropic Displacement Parameters ( $\text{\AA}^2 \times 10^3$ ) for 2-2.  $U_{\text{eq}}$  is defined as 1/3 of the trace of the orthogonalised  $U_{\text{IJ}}$  tensor.**

Atom	x	y	z	U(eq)
O1	2433.8(3)	3952.5(5)	7948.6(6)	17.52(8)
C1	2547.6(3)	2872.7(5)	6904.3(7)	14.09(8)
C2	1791.7(3)	2460.5(6)	5986.7(8)	19.35(9)
C3	1850.2(4)	1084.4(7)	5229.4(9)	22.48(11)
C4	2626.8(4)	936.6(7)	4327.2(9)	23.85(11)
C5	3338.8(3)	1121.1(6)	5597.0(7)	16.95(9)
C6	3249.0(3)	2268.5(5)	6809.1(6)	12.15(7)
C7	3942.0(3)	2700.0(5)	7954.2(6)	11.92(7)
C8	3837.1(3)	4030.3(5)	8789.1(7)	14.49(8)
C9	3109.2(4)	4787.4(5)	8212.4(7)	16.49(9)
C10	3797.7(3)	2817.6(5)	9894.9(7)	14.76(8)
C11	4442.3(4)	2563.0(7)	11270.5(8)	20.96(10)
C12	4740.9(3)	2293.9(5)	7406.4(6)	12.97(8)
C13	5046.6(3)	1060.0(5)	7863.3(7)	15.81(8)
C14	5767.5(3)	641.1(6)	7284.9(8)	19.55(10)
C15	6195.8(3)	1450.8(7)	6225.0(8)	21.97(11)
C16	5901.4(4)	2685.1(7)	5771.5(9)	22.63(11)
C17	5180.1(3)	3107.7(6)	6366.3(7)	18.19(9)

**Table 3. Anisotropic Displacement Parameters ( $\text{\AA}^2 \times 10^3$ ) for 2-2. The Anisotropic displacement factor exponent takes the form:  $-2\pi^2[h^2a^{*2}U_{11}+\dots+2hka \times b \times U_{12}]$**

Atom	$U_{11}$	$U_{22}$	$U_{33}$	$U_{23}$	$U_{13}$	$U_{12}$
O1	14.84(16)	18.22(18)	19.61(17)	-2.34(13)	1.96(13)	5.73(13)
C1	12.34(17)	16.17(19)	13.70(18)	0.70(15)	0.04(14)	2.79(15)
C2	12.57(18)	24.7(2)	20.3(2)	1.57(19)	-3.27(16)	2.21(18)
C3	17.8(2)	25.2(3)	23.7(2)	-1.1(2)	-7.12(19)	-1.9(2)
C4	23.1(2)	29.3(3)	18.6(2)	-7.7(2)	-5.11(19)	1.3(2)
C5	16.23(19)	18.1(2)	16.3(2)	-5.30(16)	-0.91(16)	1.76(16)
C6	11.37(16)	13.34(17)	11.73(17)	-0.35(14)	0.27(13)	1.77(13)
C7	11.48(16)	12.08(17)	12.16(16)	-0.98(13)	0.32(13)	2.06(13)
C8	16.38(19)	12.38(18)	14.58(18)	-2.00(14)	-0.54(15)	2.79(15)
C9	20.1(2)	13.96(18)	15.4(2)	-0.88(15)	0.22(16)	5.40(16)
C10	15.80(18)	16.97(19)	11.42(17)	-0.03(15)	-0.25(14)	3.90(15)
C11	23.2(2)	23.6(2)	15.4(2)	-0.89(18)	-5.02(18)	6.3(2)
C12	11.34(16)	13.65(18)	13.90(18)	-1.38(14)	0.53(13)	0.99(14)
C13	13.53(18)	14.78(19)	19.1(2)	-0.92(16)	1.10(15)	2.91(15)
C14	15.02(19)	21.1(2)	22.5(2)	-5.00(19)	0.28(17)	5.70(17)
C15	13.24(19)	31.1(3)	21.9(2)	-7.8(2)	3.17(17)	1.79(19)
C16	19.0(2)	28.2(3)	21.3(3)	-2.0(2)	7.13(19)	-3.2(2)
C17	18.1(2)	18.3(2)	18.5(2)	1.32(17)	3.85(17)	0.02(17)

**Table 4. Bond Lengths for 2-2.**

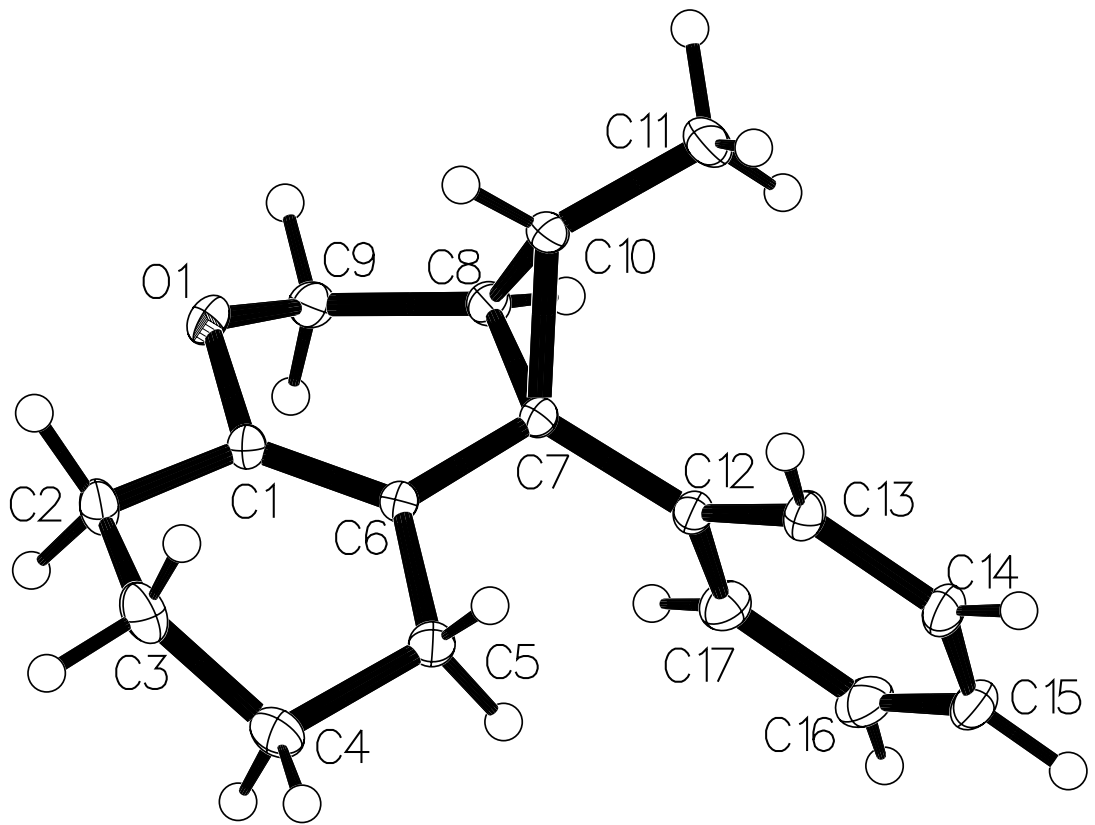
<b>Atom</b>	<b>Atom</b>	<b>Length/Å</b>	<b>Atom</b>	<b>Atom</b>	<b>Length/Å</b>
O1	C1	1.3830(7)	C7	C12	1.4982(7)
O1	C9	1.4332(8)	C8	C9	1.5048(8)
C1	C2	1.4955(8)	C8	C10	1.5051(8)
C1	C6	1.3449(7)	C10	C11	1.5109(8)
C2	C3	1.5230(10)	C12	C13	1.3974(7)
C3	C4	1.5285(10)	C12	C17	1.3956(8)
C4	C5	1.5313(8)	C13	C14	1.3899(7)
C5	C6	1.5100(7)	C14	C15	1.3922(10)
C6	C7	1.5030(7)	C15	C16	1.3903(10)
C7	C8	1.5142(7)	C16	C17	1.3965(8)
C7	C10	1.5380(7)			

**Table 5. Bond Angles for 2-2.**

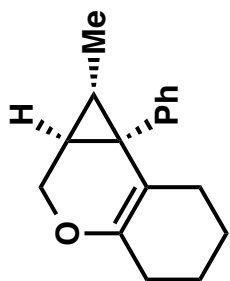
<b>Atom Atom Atom</b>	<b>Angle/°</b>	<b>Atom Atom Atom</b>	<b>Angle/°</b>
C1 O1 C9	114.88(4)	C12 C7 C10	119.15(4)
O1 C1 C2	111.06(4)	C9 C8 C7	116.30(4)
C6 C1 O1	122.98(5)	C9 C8 C10	121.98(5)
C6 C1 C2	125.92(5)	C10 C8 C7	61.25(3)
C1 C2 C3	111.72(5)	O1 C9 C8	112.20(4)
C2 C3 C4	109.88(5)	C8 C10 C7	59.67(3)
C3 C4 C5	111.45(5)	C8 C10 C11	119.36(5)
C6 C5 C4	113.14(5)	C11 C10 C7	122.02(5)
C1 C6 C5	120.26(5)	C13 C12 C7	120.41(5)
C1 C6 C7	120.21(4)	C17 C12 C7	121.04(5)
C7 C6 C5	119.49(4)	C17 C12 C13	118.49(5)
C6 C7 C8	114.07(4)	C14 C13 C12	121.05(5)
C6 C7 C10	116.18(4)	C13 C14 C15	120.08(6)
C8 C7 C10	59.08(3)	C16 C15 C14	119.46(5)
C12 C7 C6	116.44(4)	C15 C16 C17	120.32(6)
C12 C7 C8	119.61(4)	C12 C17 C16	120.58(6)

**Table 6. Hydrogen Atom Coordinates ( $\text{\AA}\times 10^4$ ) and Isotropic Displacement Parameters ( $\text{\AA}^2\times 10^3$ ) for 2-2.**

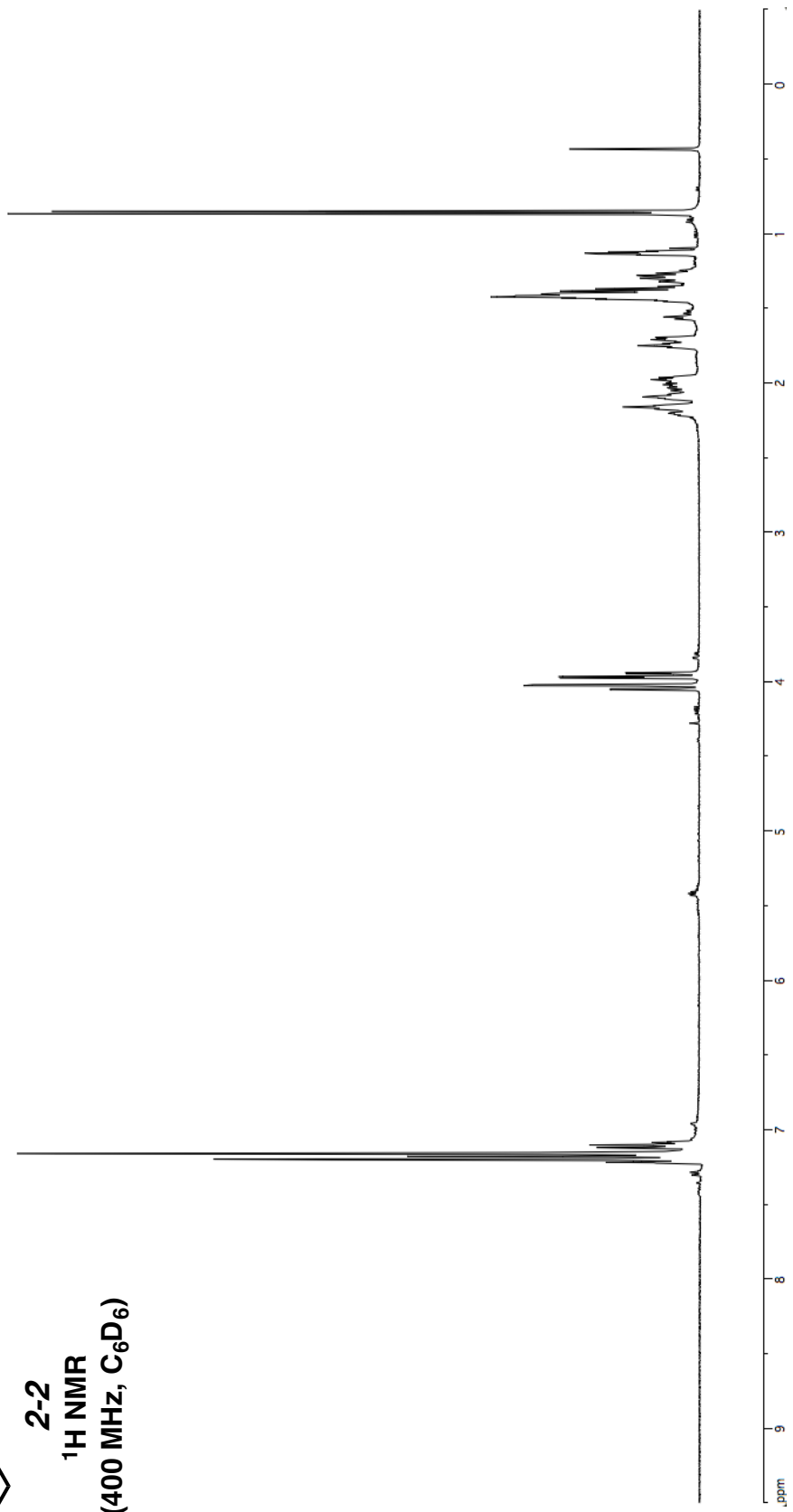
<b>Atom</b>	<b>x</b>	<b>y</b>	<b>z</b>	<b>U(eq)</b>
H2A	1657	3092	5045	23
H2B	1362	2481	6808	23
H3A	1401	929	4388	27
H3B	1824	424	6164	27
H4A	2648	1596	3390	29
H4B	2650	53	3797	29
H5A	3417	309	6288	20
H5B	3817	1256	4934	20
H8	4329	4565	8964	17
H9A	2998	5456	9097	20
H9B	3207	5253	7120	20
H10	3255	2567	10223	18
H11A	4946	2888	10872	31
H11B	4482	1617	11493	31
H11C	4317	3020	12338	31
H13	4757	499	8581	19
H14	5968	-199	7613	23
H15	6685	1162	5815	26
H16	6192	3244	5054	27
H17	4987	3957	6060	22

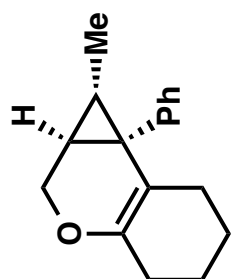


APPENDIX B  
NMR SPECTRA RELEVANT TO CHAPTER 2



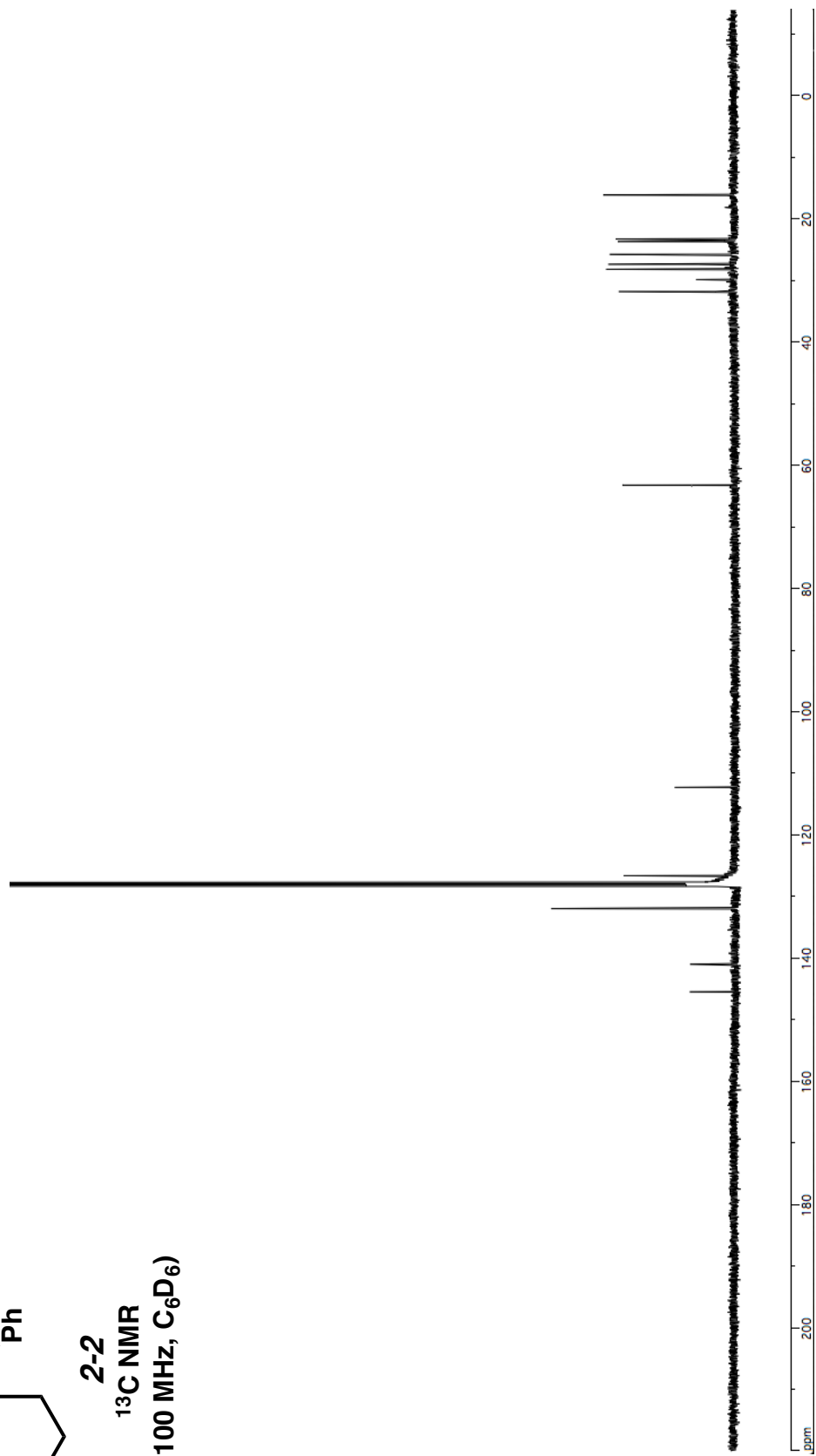
**2-2**  
**<sup>1</sup>H NMR**  
**(400 MHz, C<sub>6</sub>D<sub>6</sub>)**

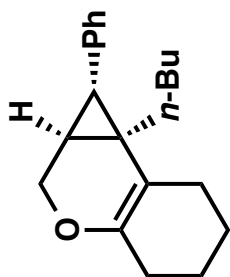




2-2

<sup>13</sup>C NMR  
(100 MHz, C<sub>6</sub>D<sub>6</sub>)

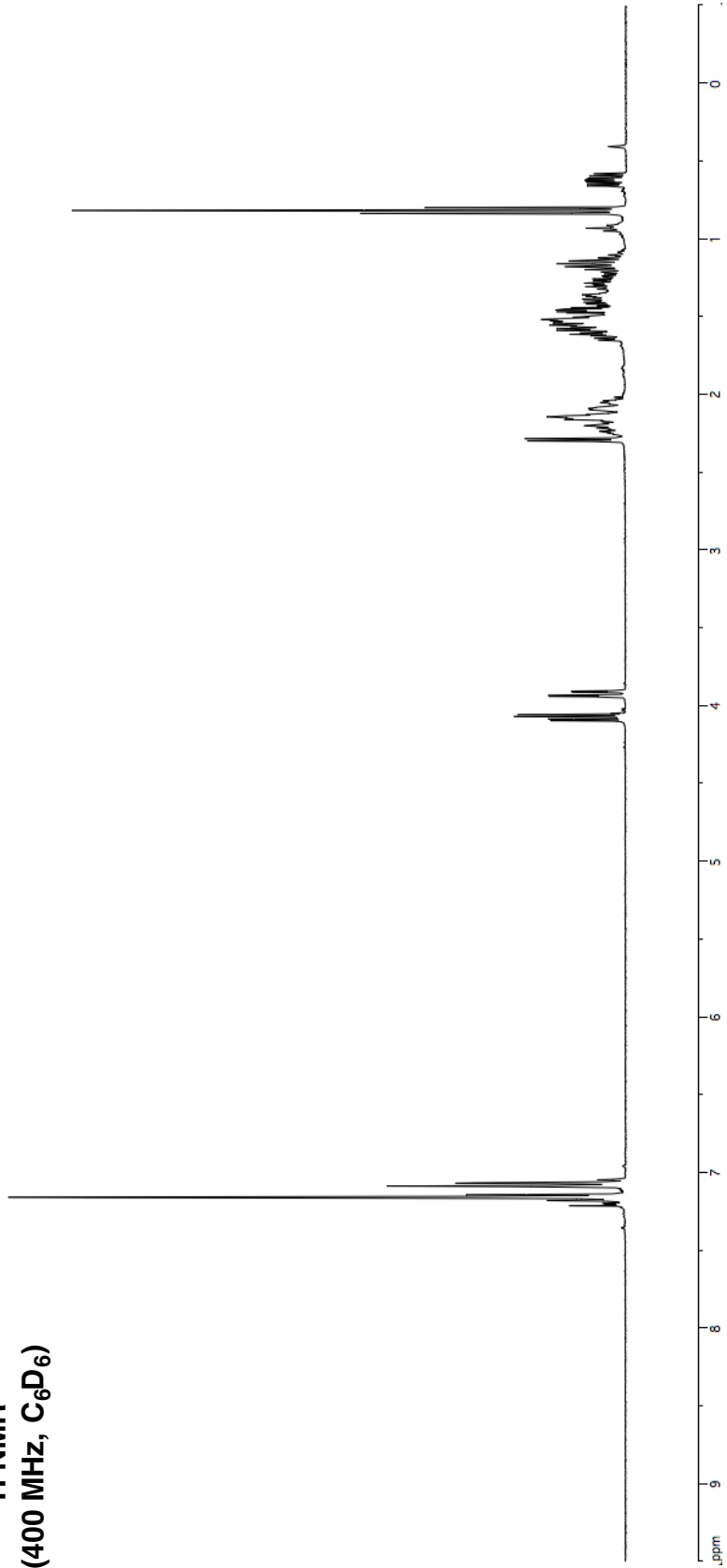


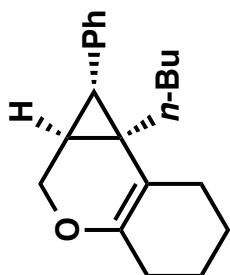


2-13

<sup>1</sup>H NMR

(400 MHz, C<sub>6</sub>D<sub>6</sub>)

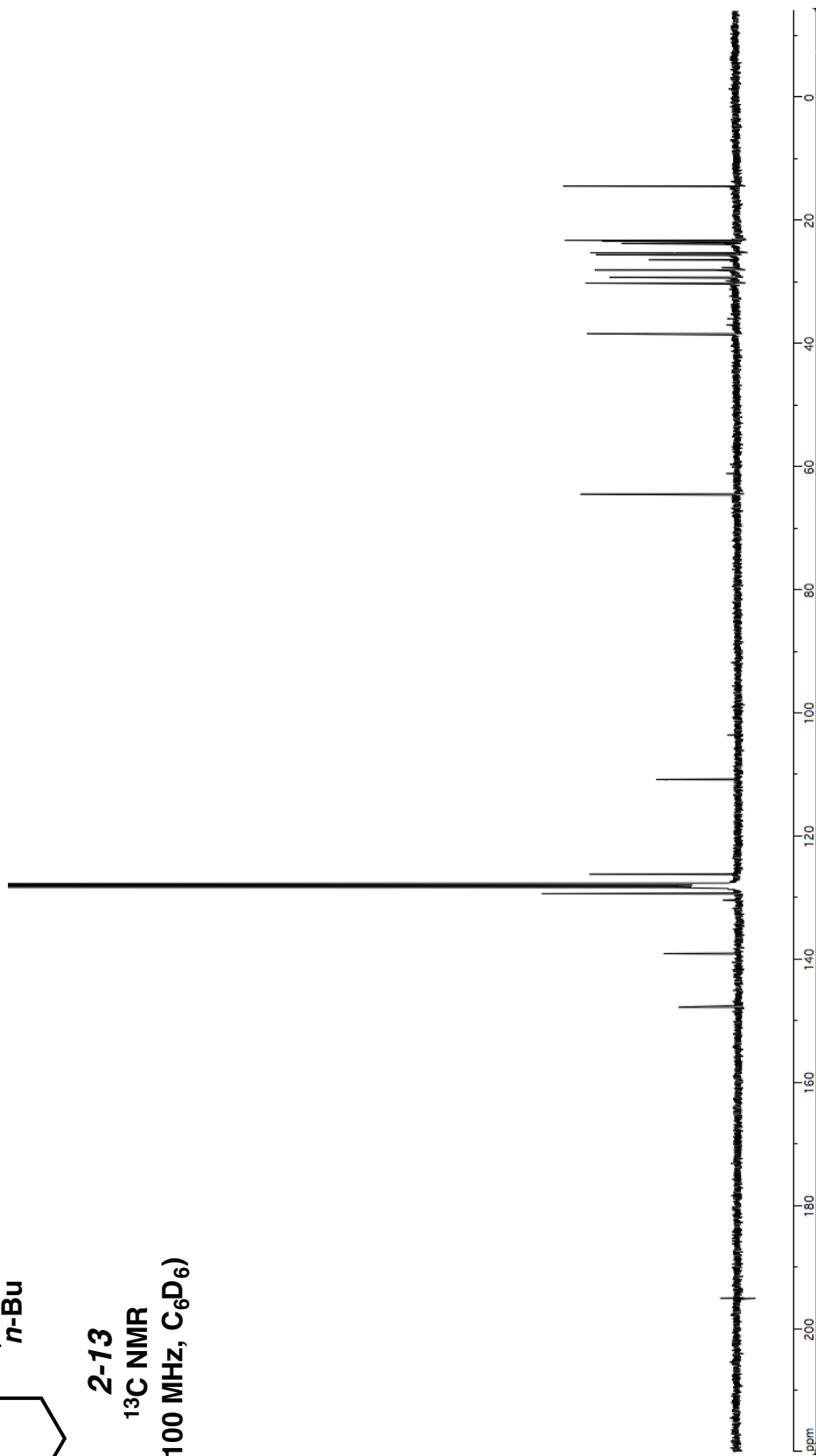


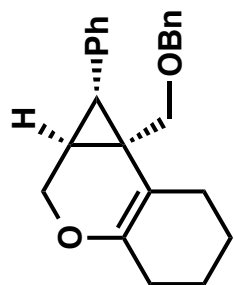


**2-13**

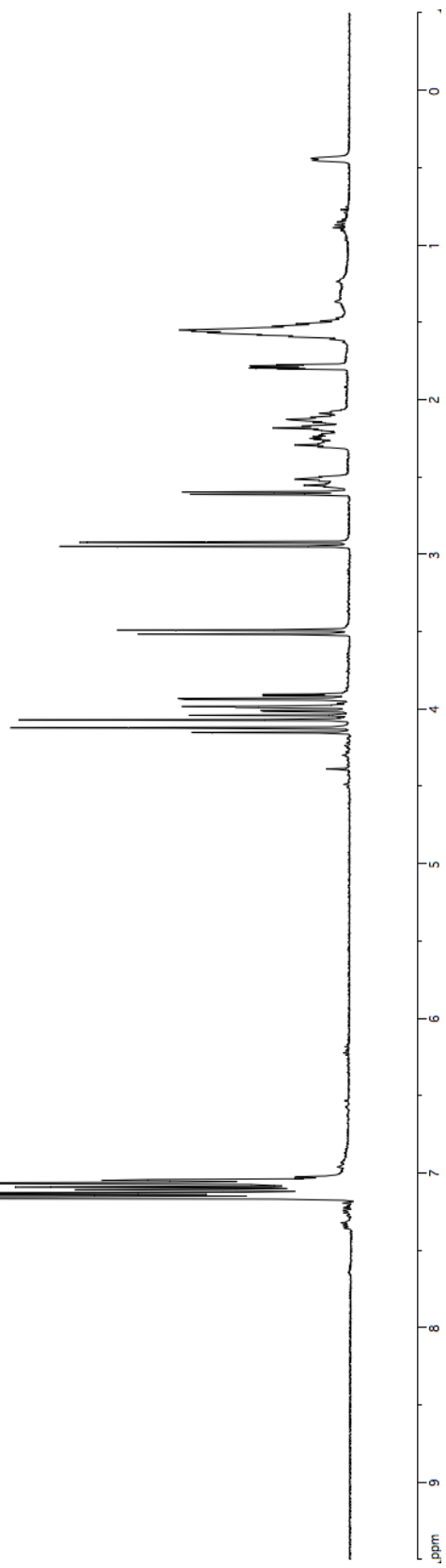
<sup>13</sup>C NMR

(100 MHz, C<sub>6</sub>D<sub>6</sub>)

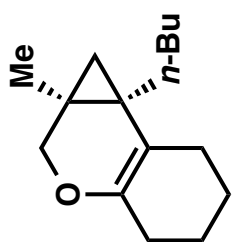




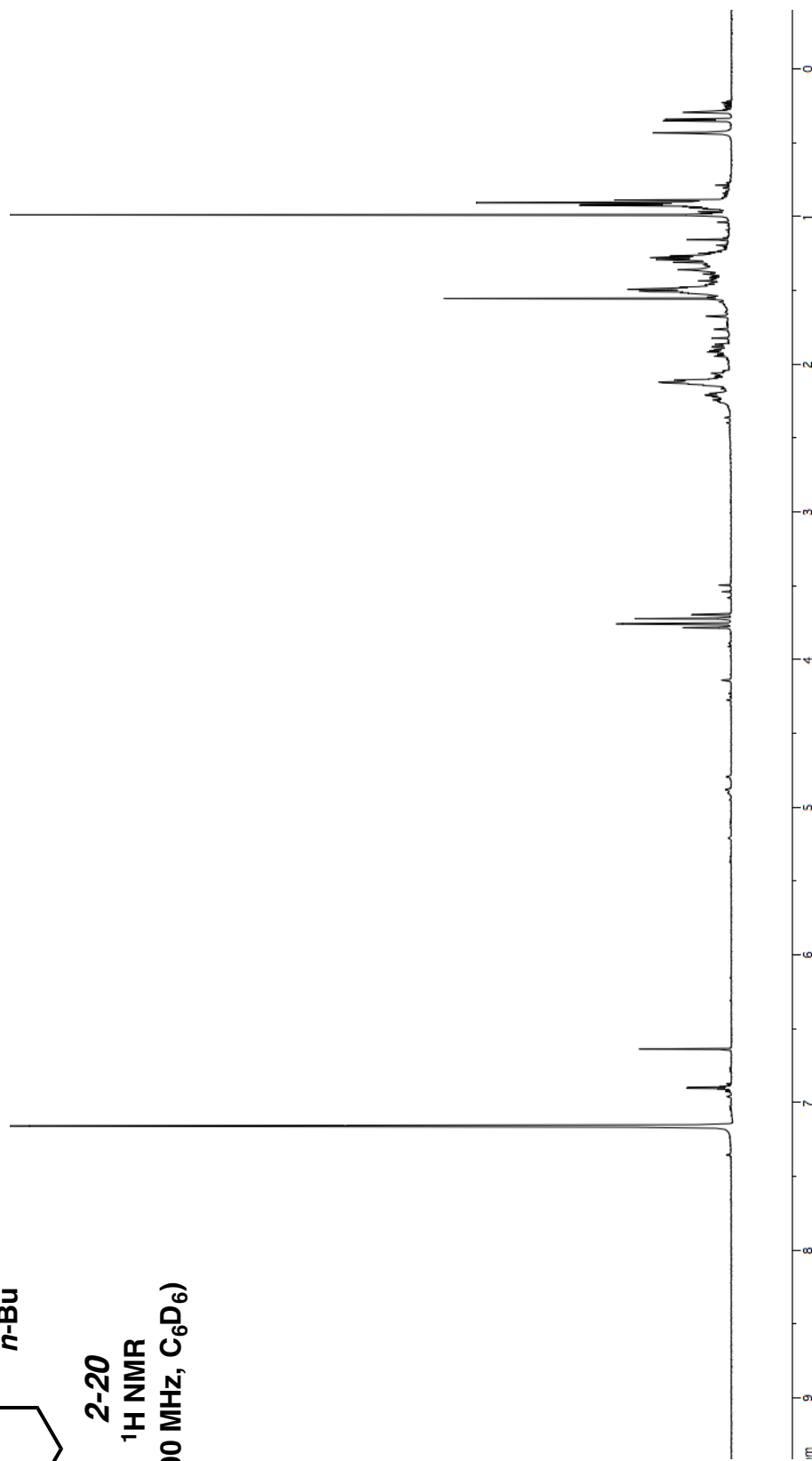
**2-19**  
**<sup>1</sup>H NMR**  
**(400 MHz, C<sub>6</sub>D<sub>6</sub>)**

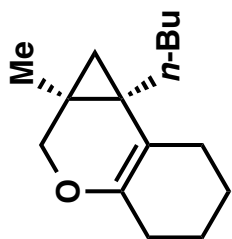






**2-20**  
**<sup>1</sup>H NMR**  
**(400 MHz, C<sub>6</sub>D<sub>6</sub>)**

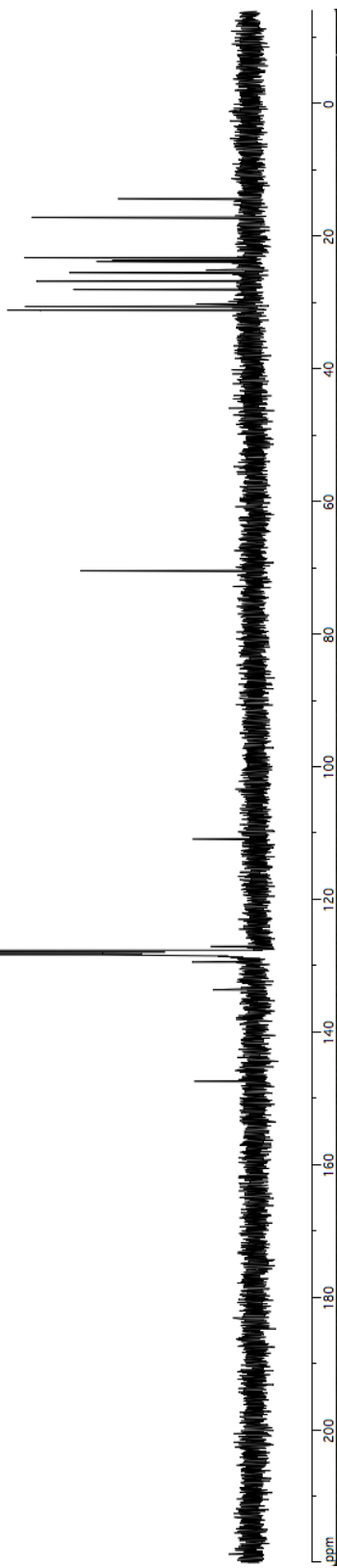


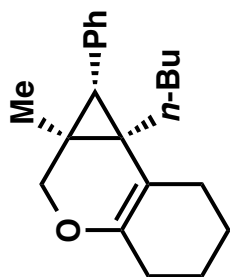


2-20

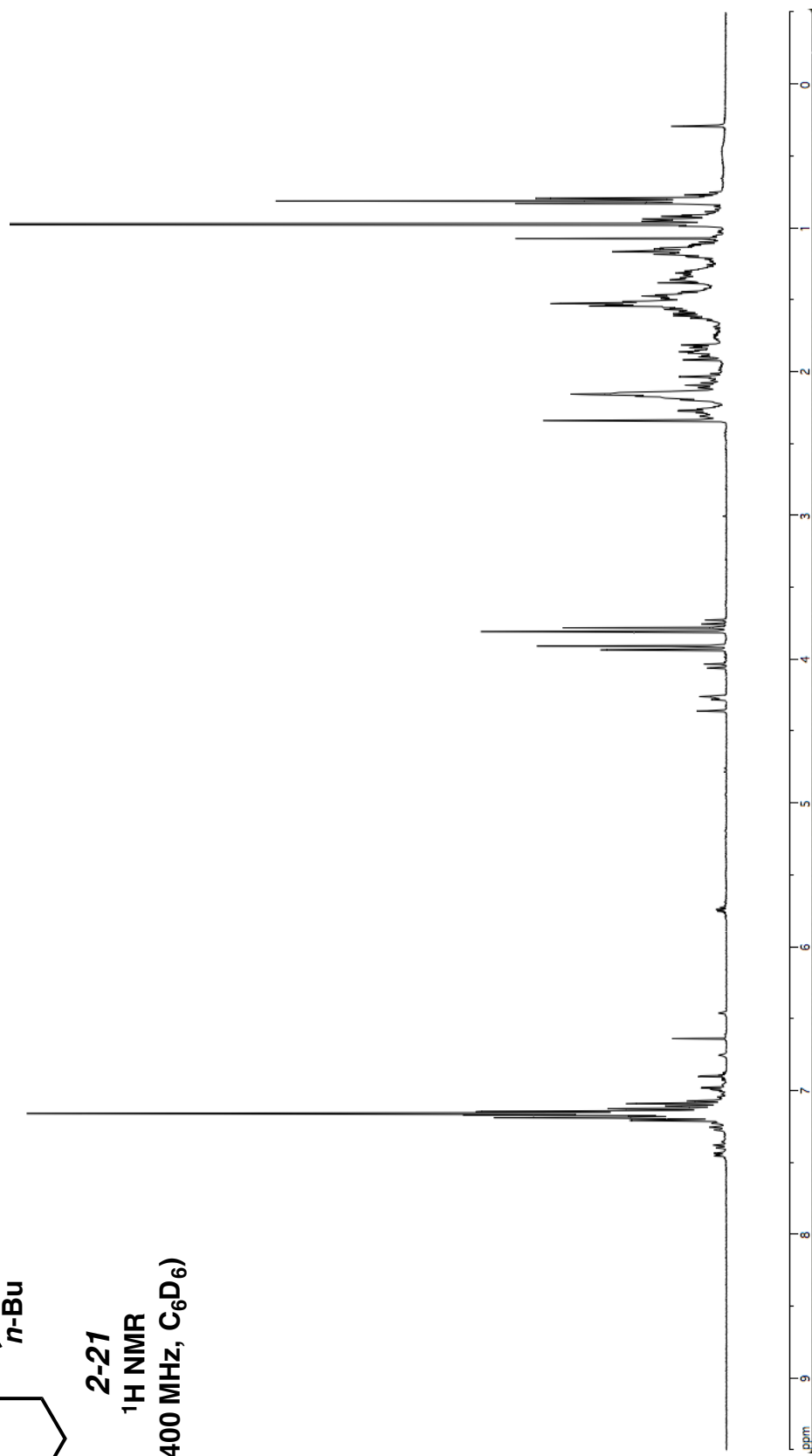
<sup>13</sup>C NMR

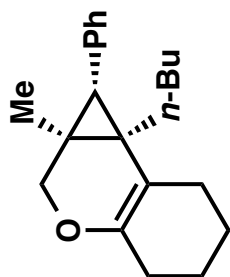
(100 MHz, C<sub>6</sub>D<sub>6</sub>)





**2-21**  
**<sup>1</sup>H NMR**  
**(400 MHz, C<sub>6</sub>D<sub>6</sub>)**

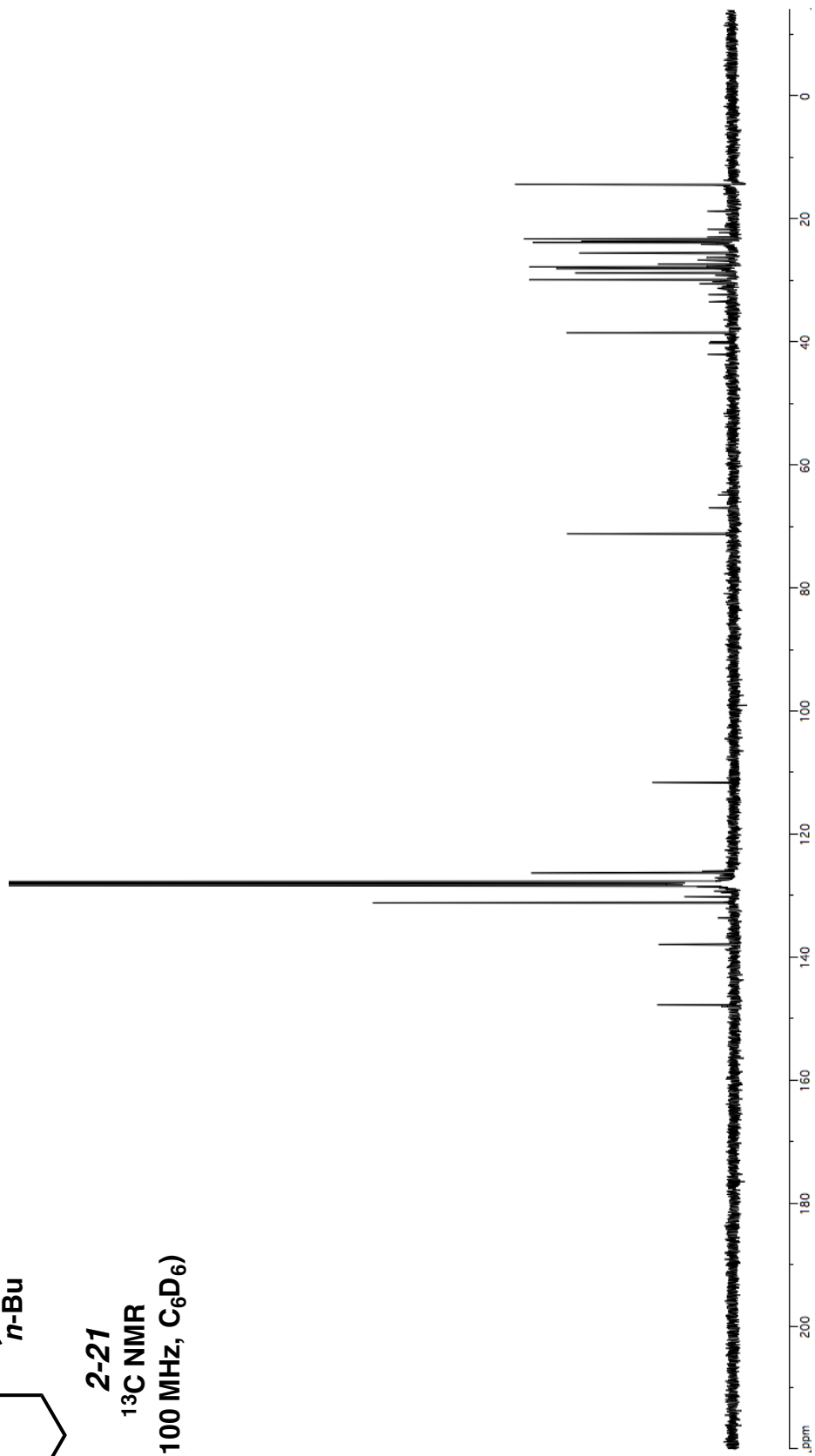




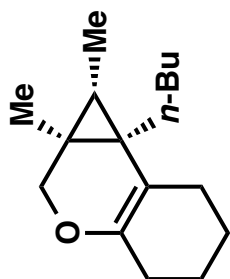
**2-21**

<sup>13</sup>C NMR

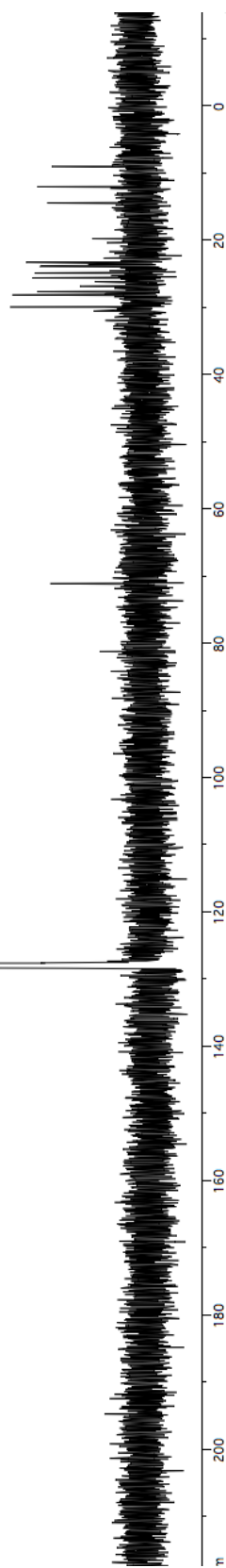
(100 MHz, C<sub>6</sub>D<sub>6</sub>)

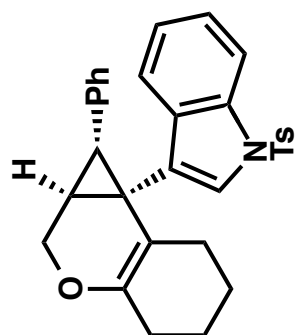




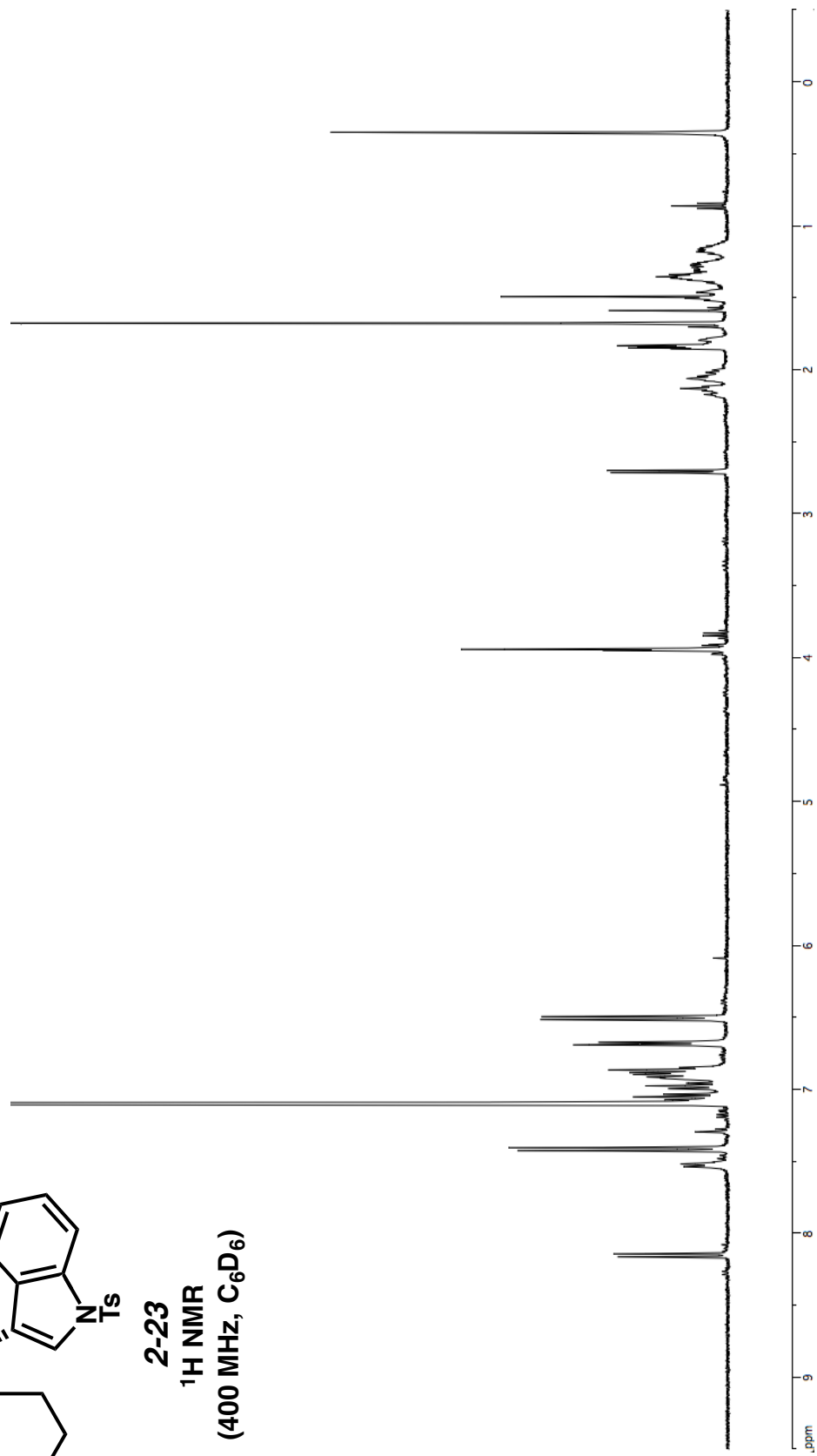


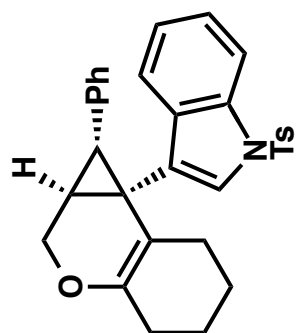
**2-22**  
**<sup>13</sup>C NMR**  
**(100 MHz, C<sub>6</sub>D<sub>6</sub>)**



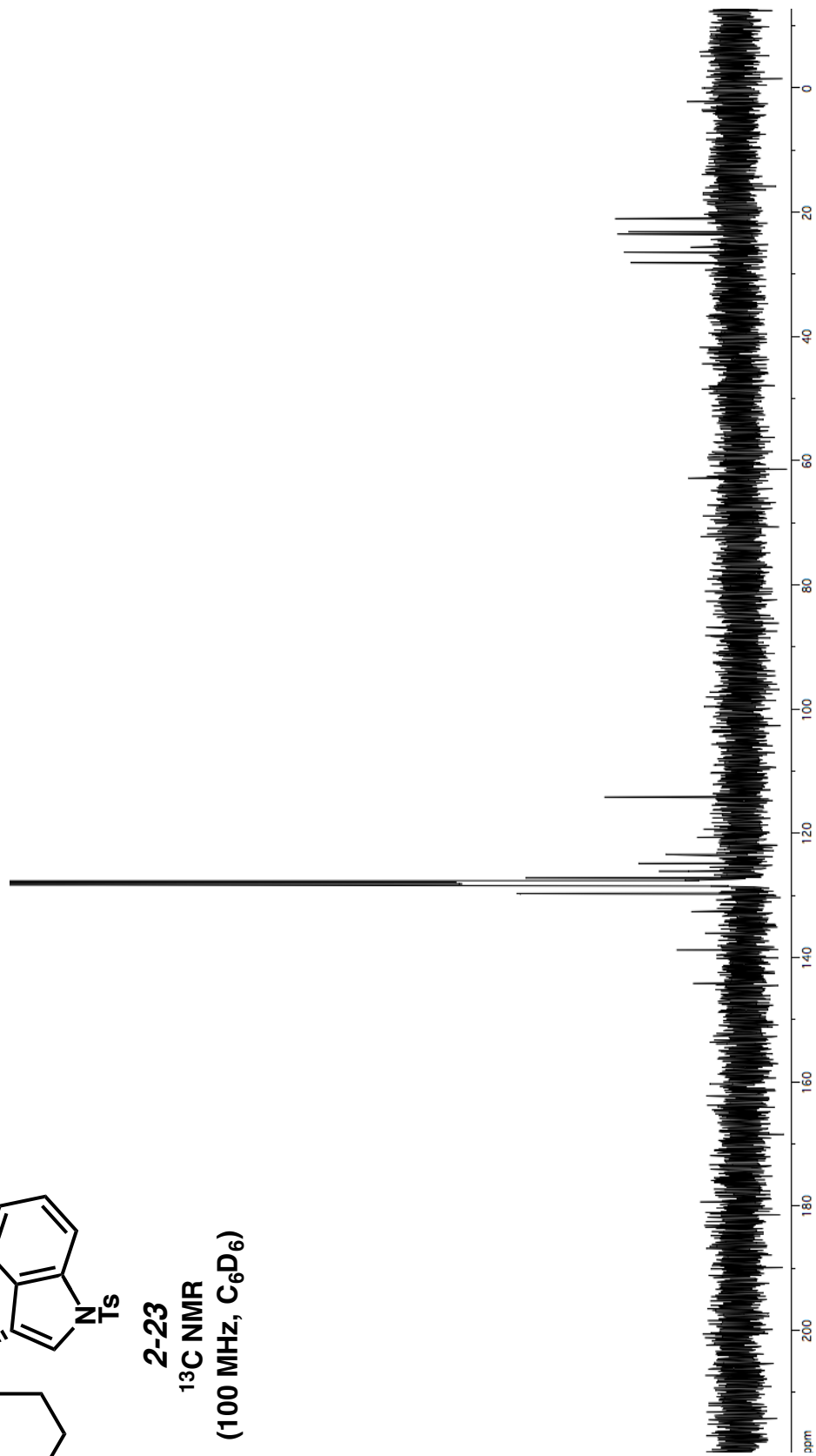


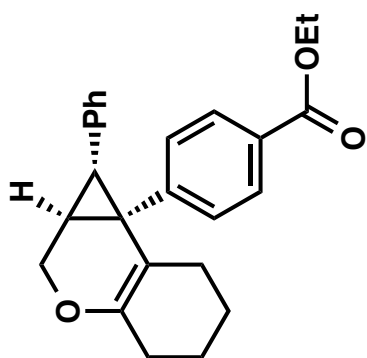
**2-23**  
**<sup>1</sup>H NMR**  
**(400 MHz, C<sub>6</sub>D<sub>6</sub>)**



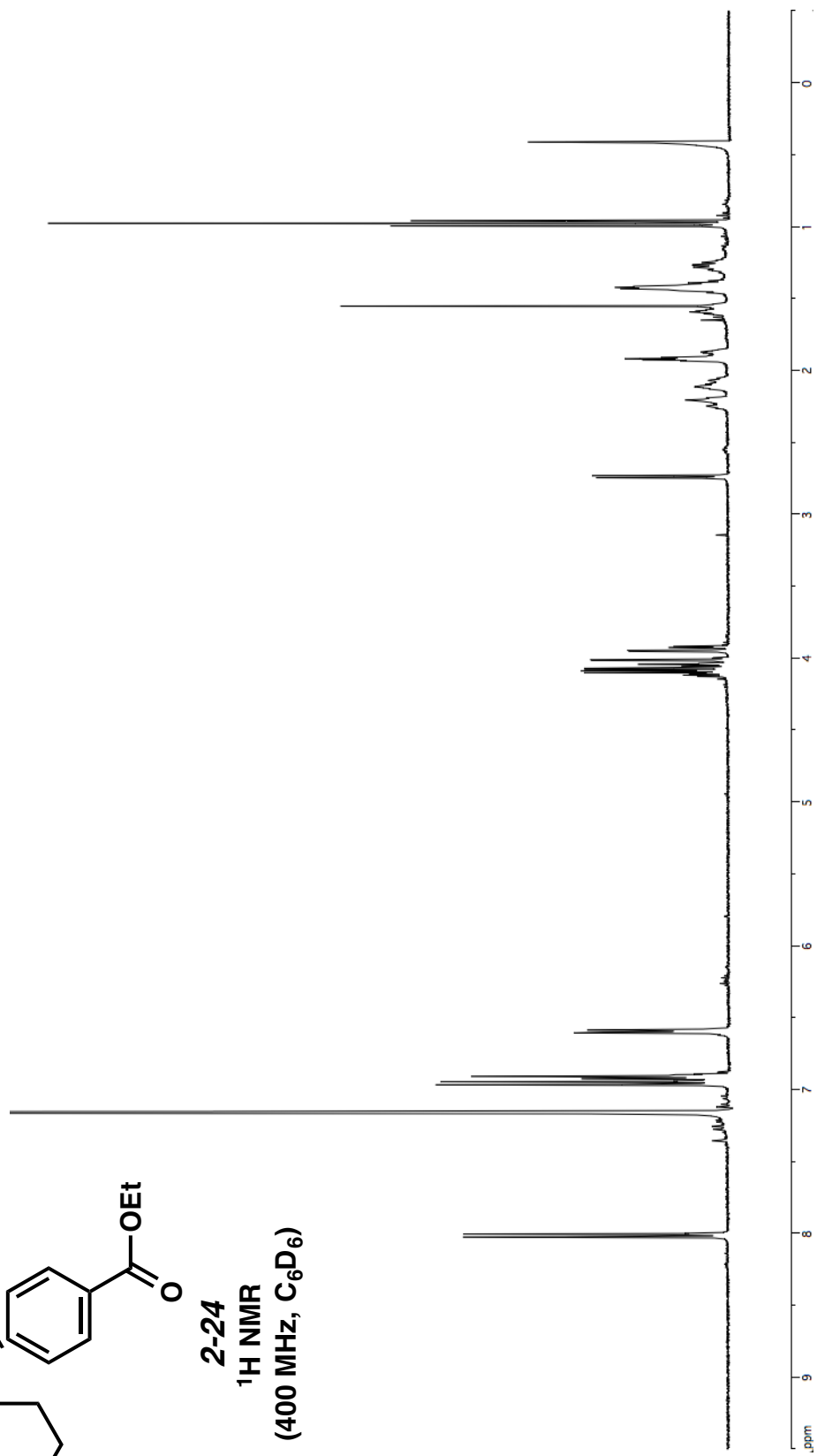


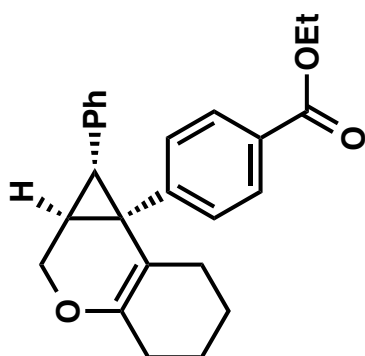
**2-23**  
**<sup>13</sup>C NMR**  
**(100 MHz, C<sub>6</sub>D<sub>6</sub>)**



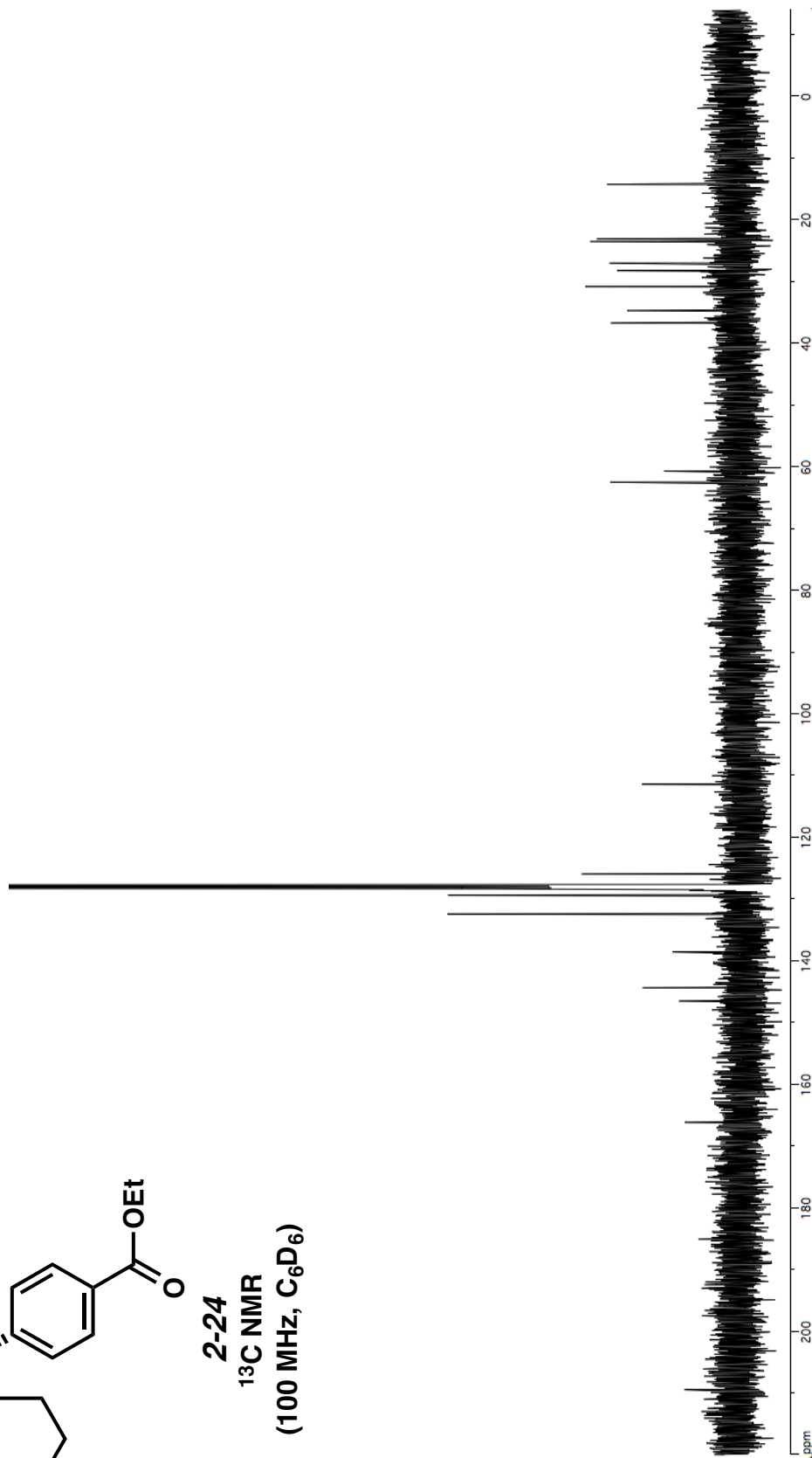


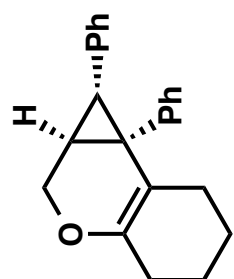
**2-24**  
**<sup>1</sup>H NMR**  
**(400 MHz, C<sub>6</sub>D<sub>6</sub>)**



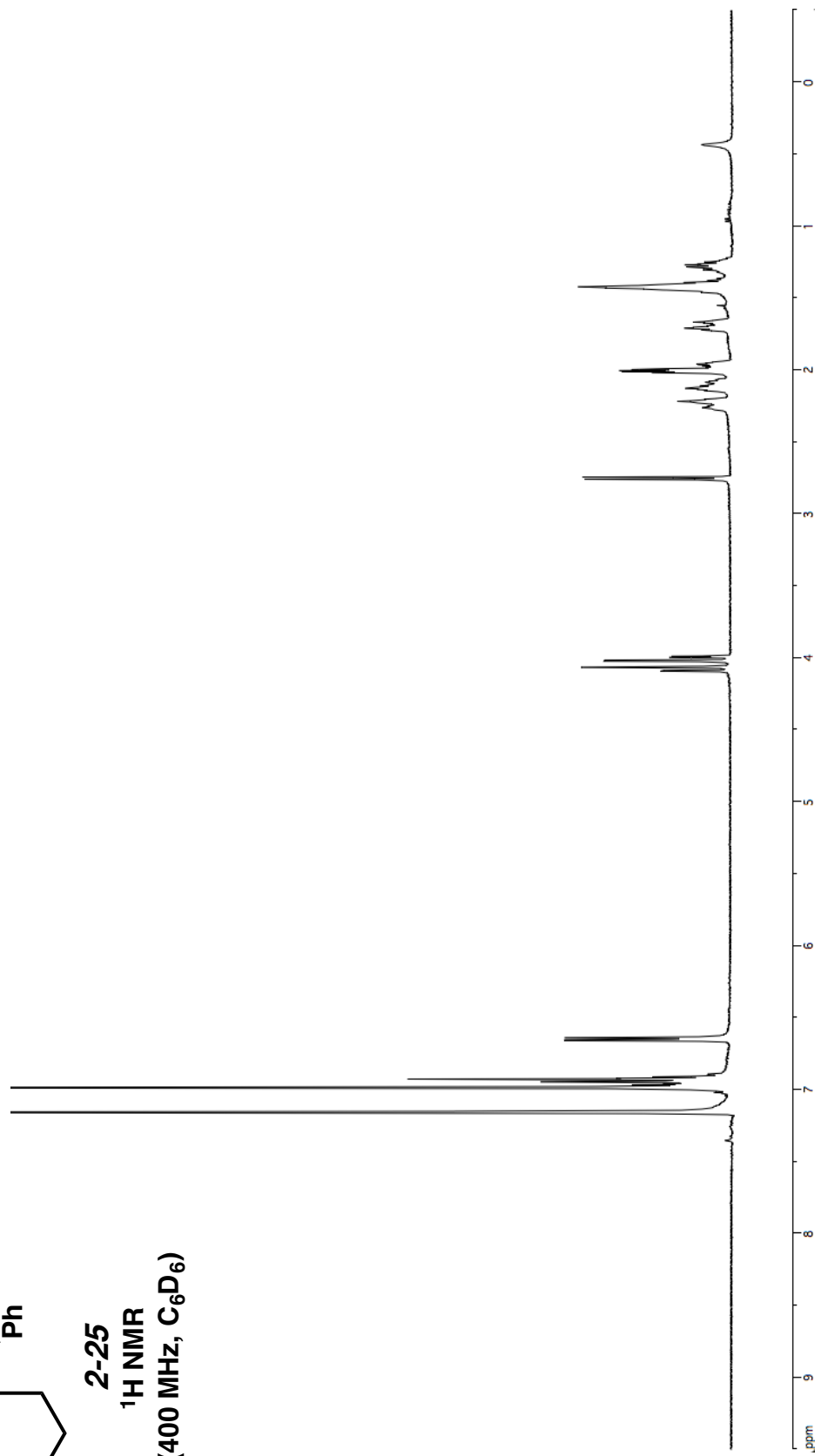


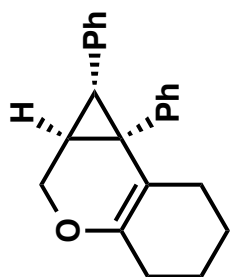
**2-24**  
**<sup>13</sup>C NMR**  
**(100 MHz, C<sub>6</sub>D<sub>6</sub>)**





2-25  
<sup>1</sup>H NMR  
(400 MHz, C<sub>6</sub>D<sub>6</sub>)

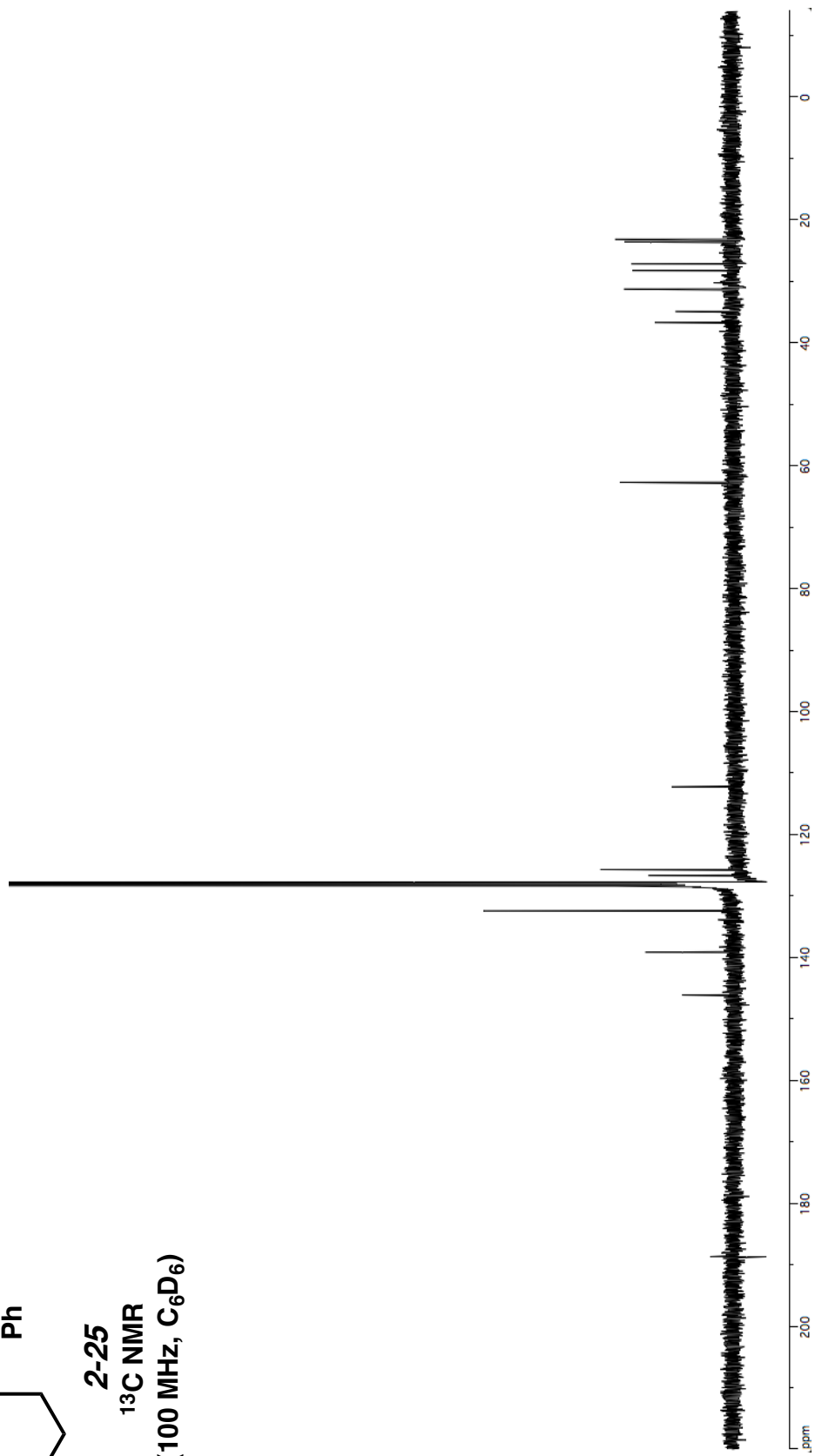


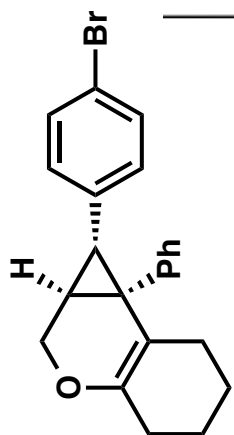


2-25

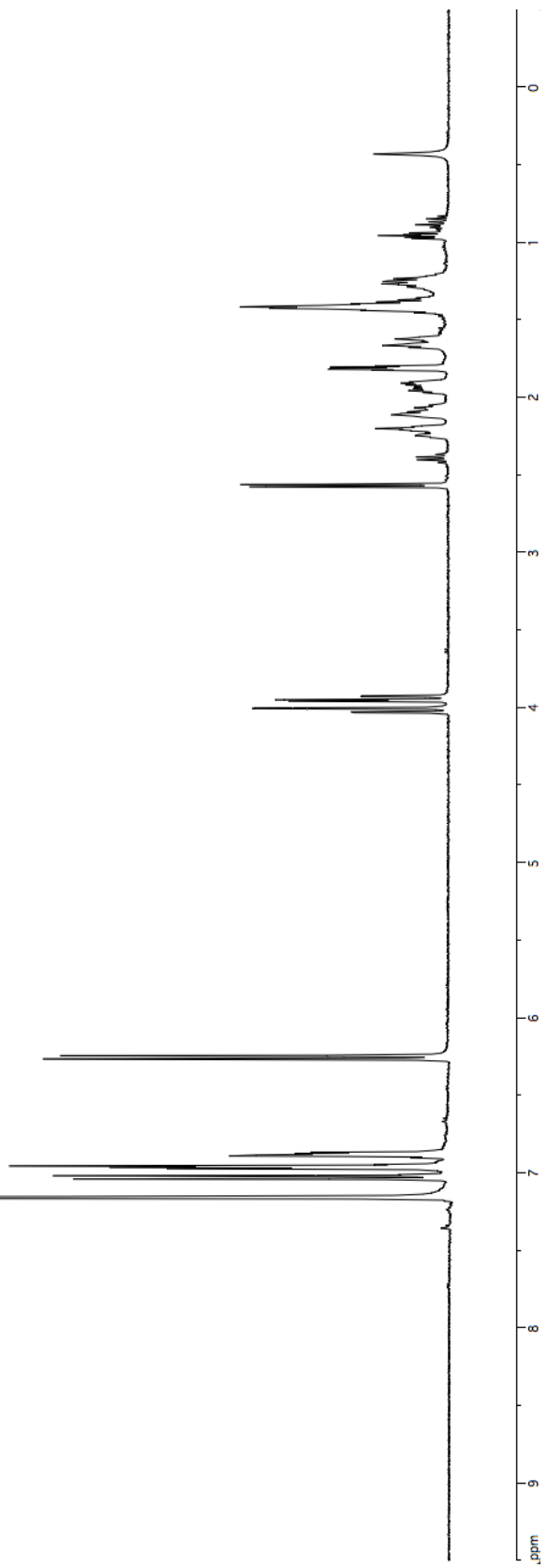
<sup>13</sup>C NMR

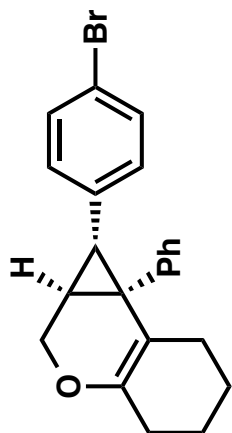
(100 MHz, C<sub>6</sub>D<sub>6</sub>)



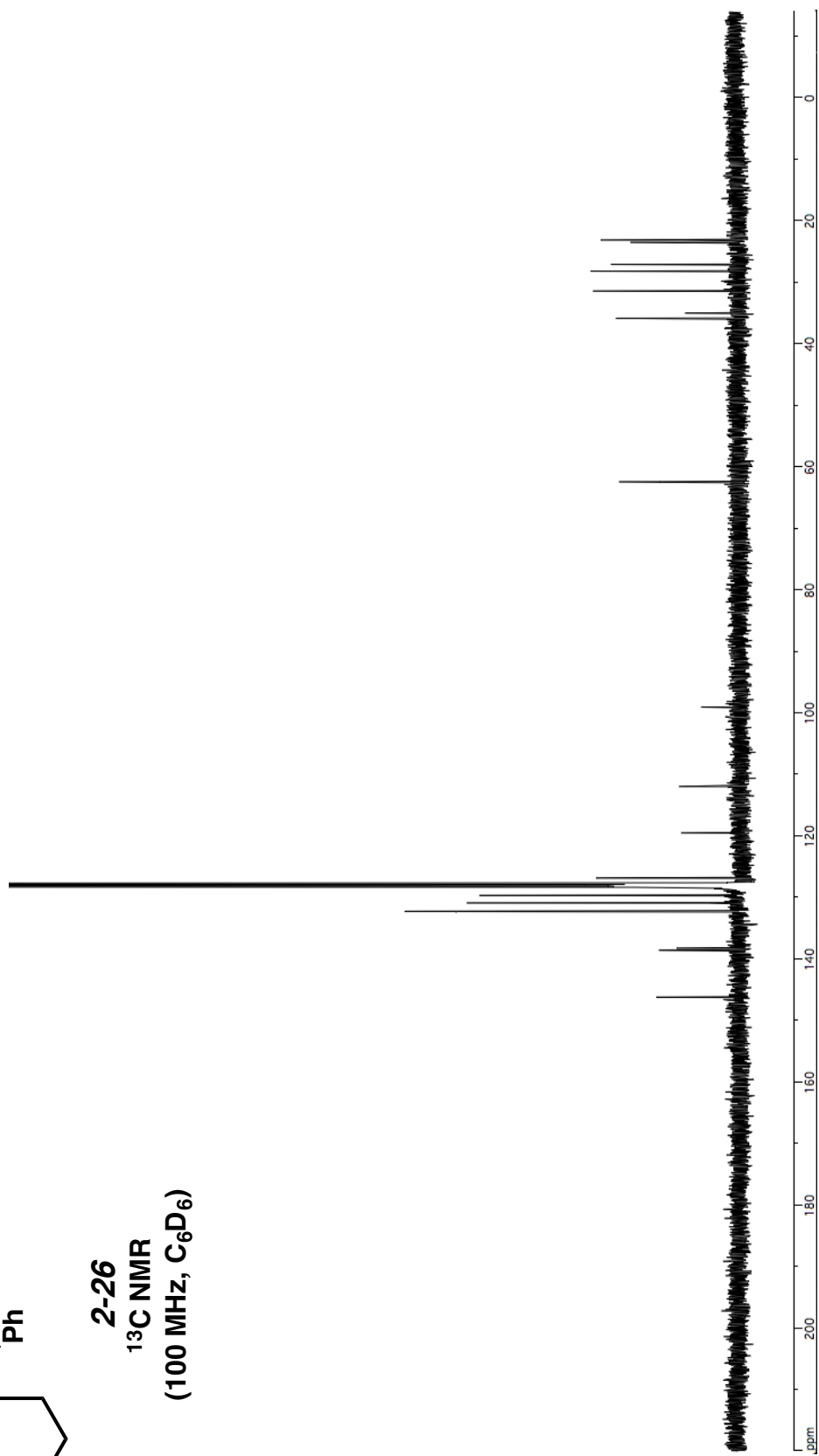


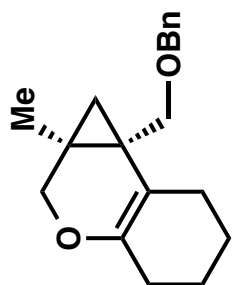
**2-26**  
**<sup>1</sup>H NMR**  
**(400 MHz, C<sub>6</sub>D<sub>6</sub>)**





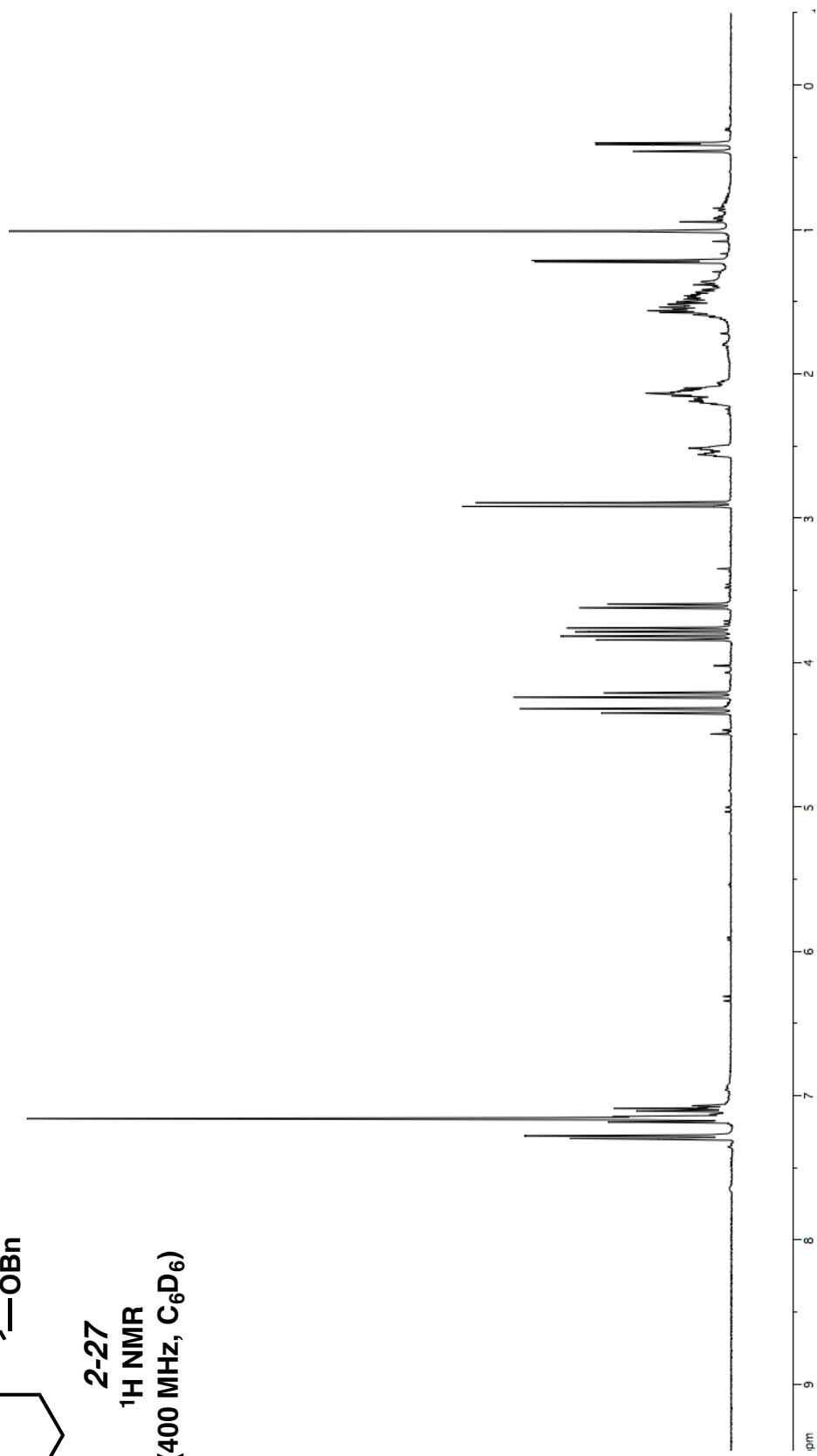
**2-26**  
**<sup>13</sup>C NMR**  
**(100 MHz, C<sub>6</sub>D<sub>6</sub>)**

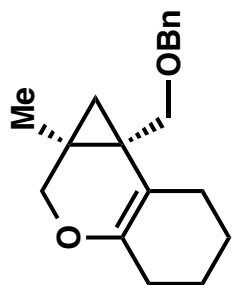




2-27

<sup>1</sup>H NMR  
(400 MHz, C<sub>6</sub>D<sub>6</sub>)

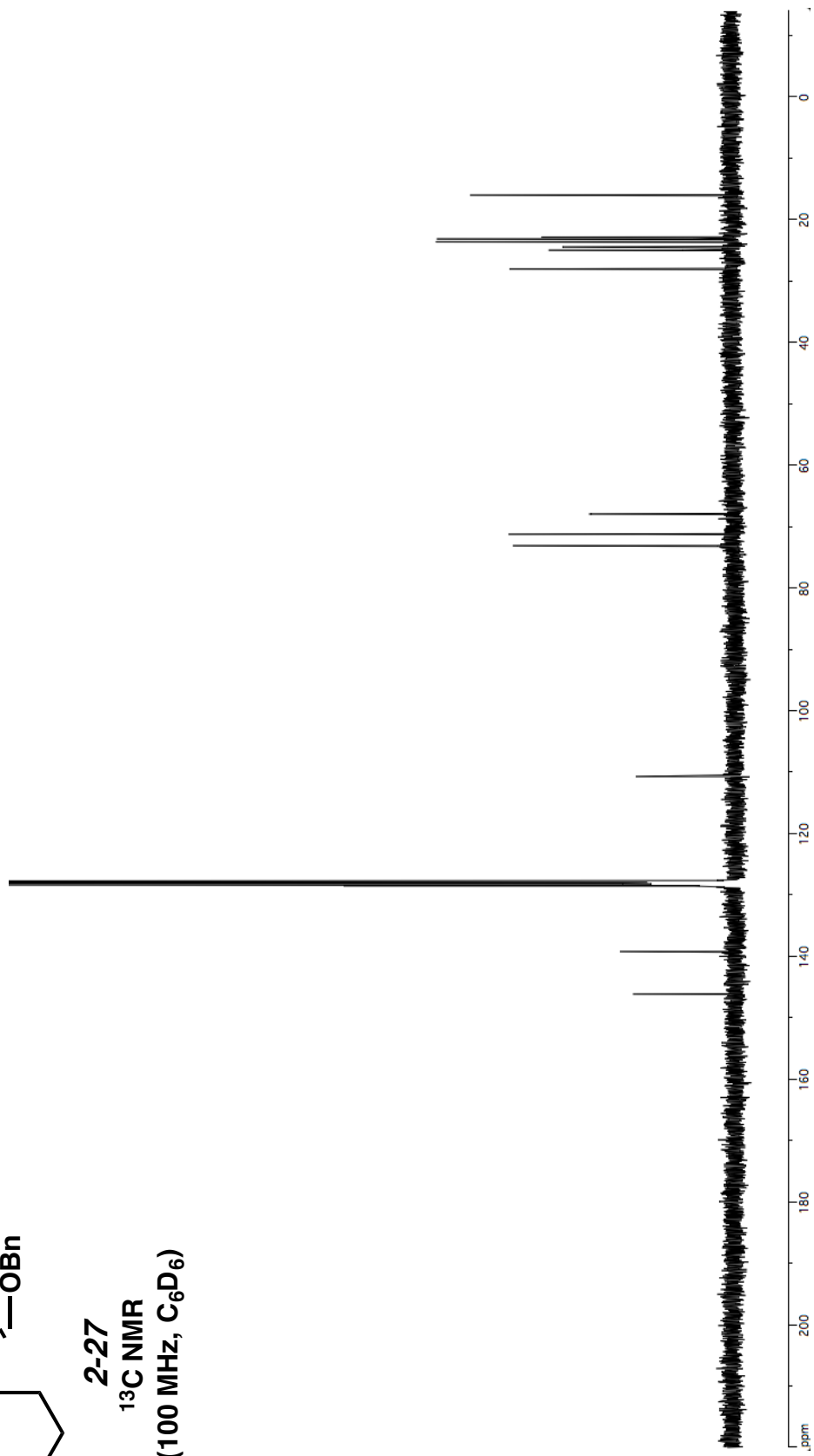


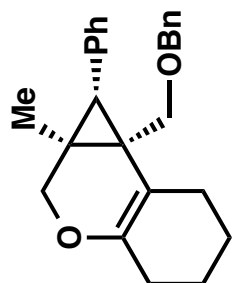


2-27

$^{13}\text{C}$  NMR

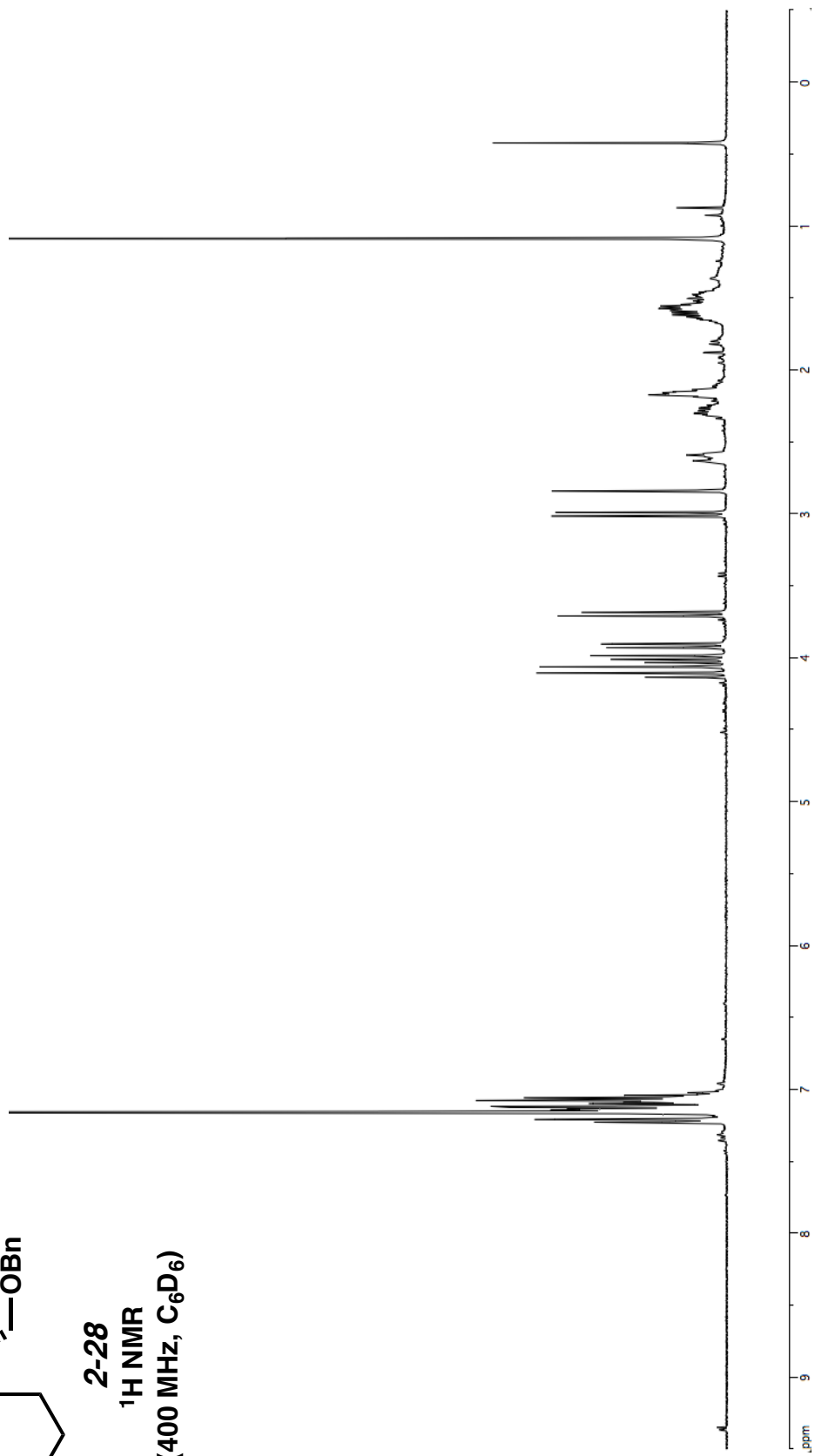
(100 MHz,  $\text{C}_6\text{D}_6$ )

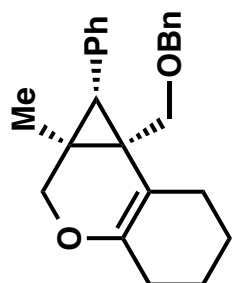




2-28

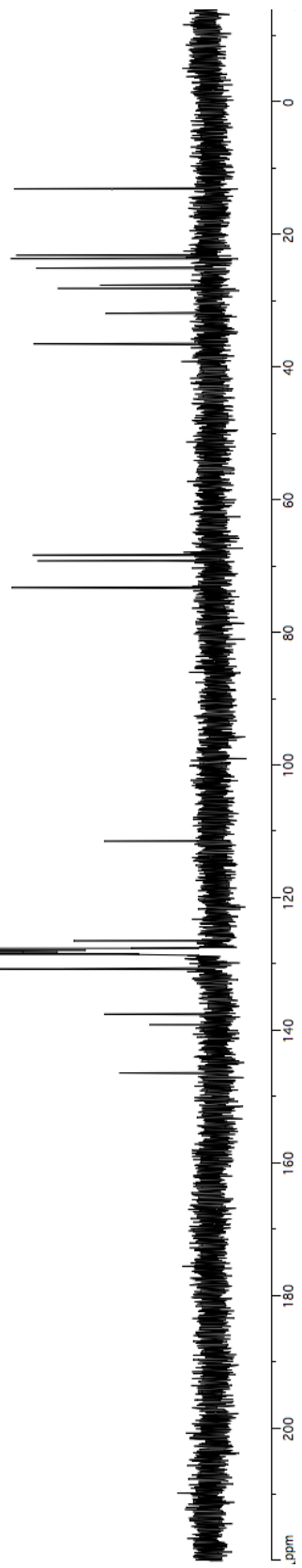
$^1\text{H NMR}$   
(400 MHz,  $\text{C}_6\text{D}_6$ )

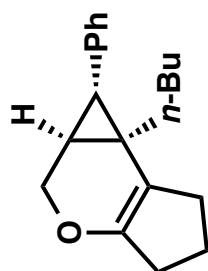




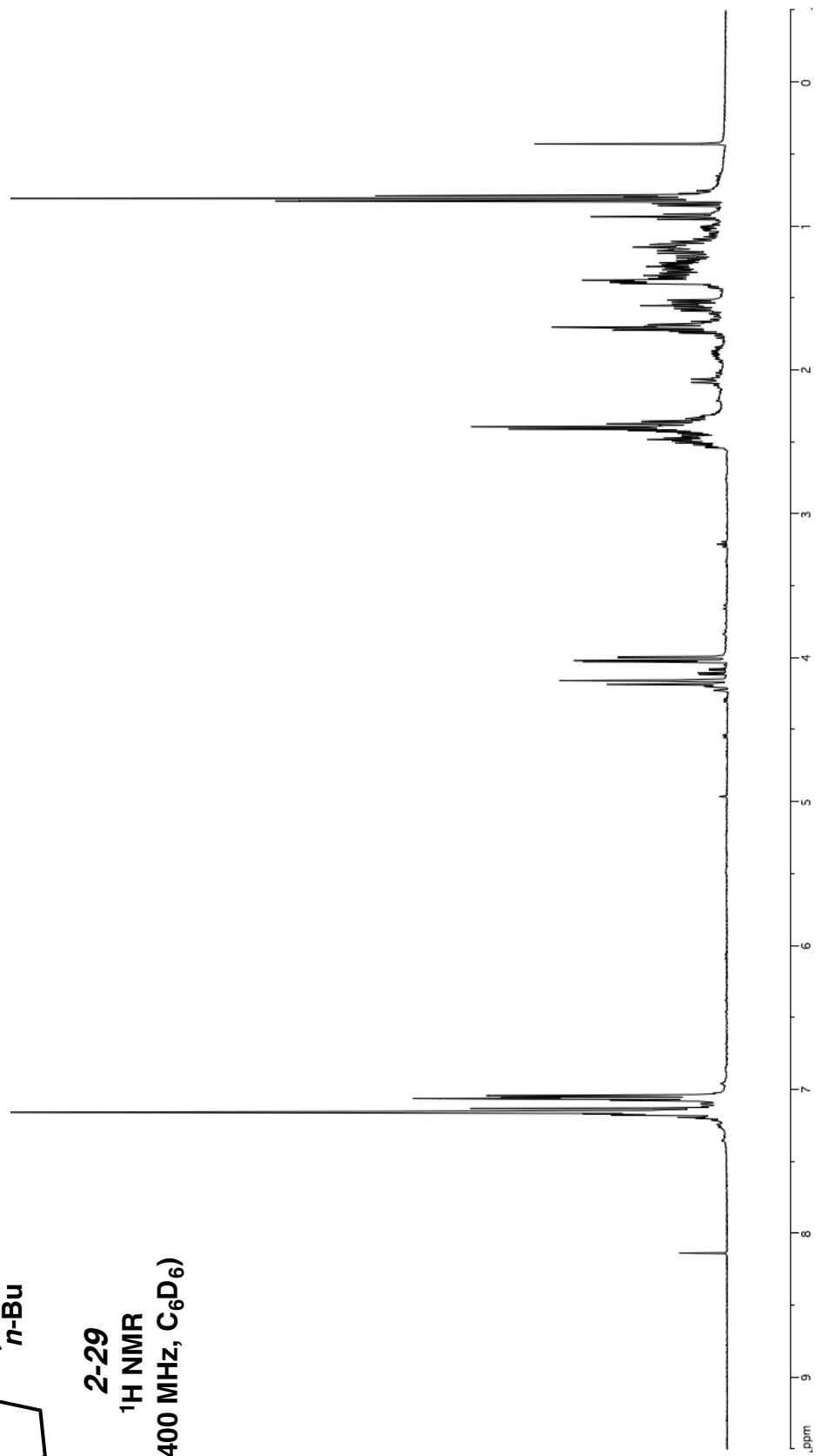
**2-28**

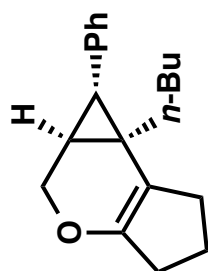
**$^{13}\text{C}$  NMR  
(100 MHz,  $\text{C}_6\text{D}_6$ )**



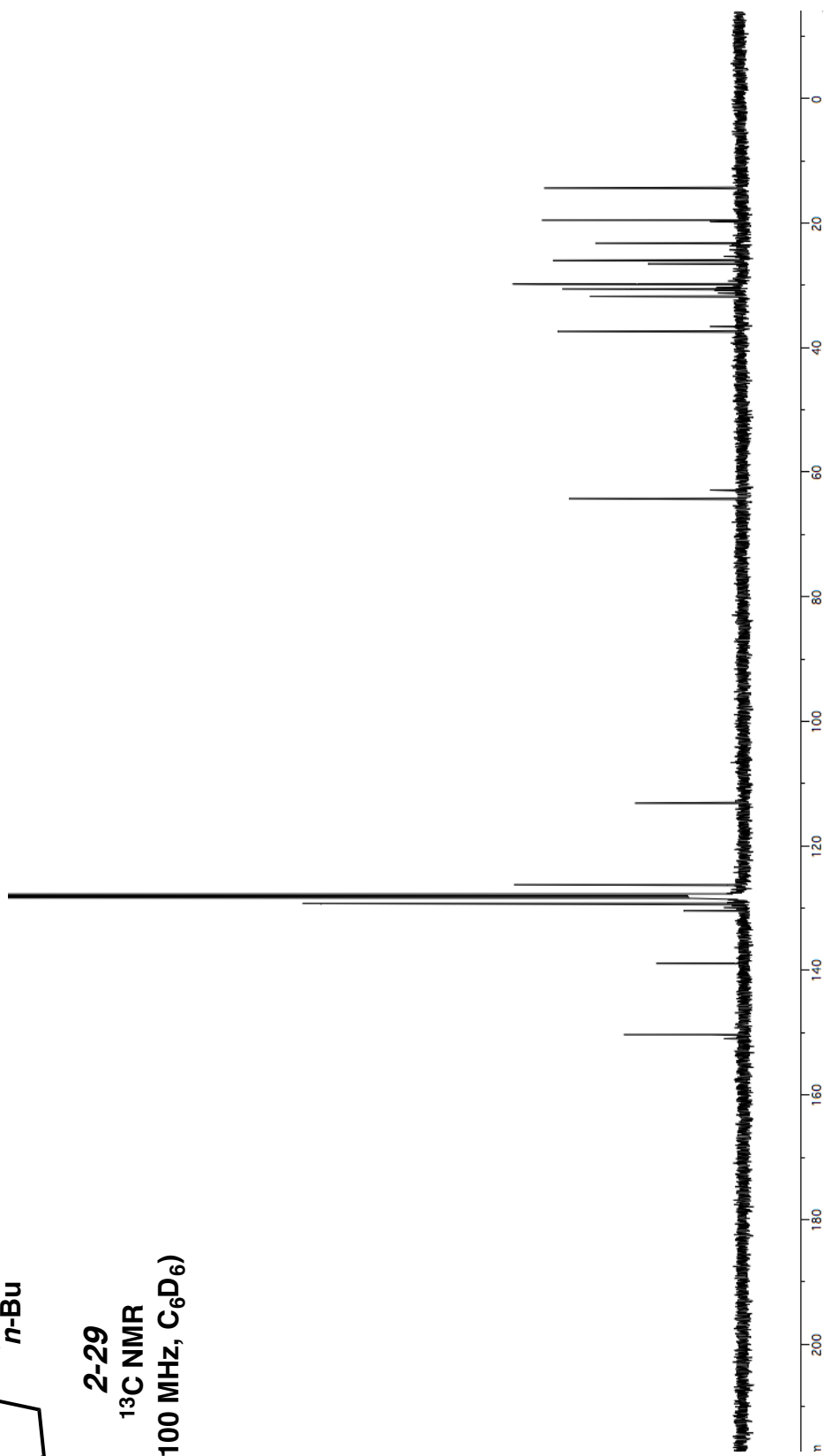


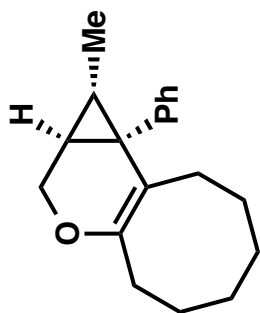
**2-29**  
**<sup>1</sup>H NMR**  
**(400 MHz, C<sub>6</sub>D<sub>6</sub>)**





**2-29**  
**<sup>13</sup>C NMR**  
**(100 MHz, C<sub>6</sub>D<sub>6</sub>)**

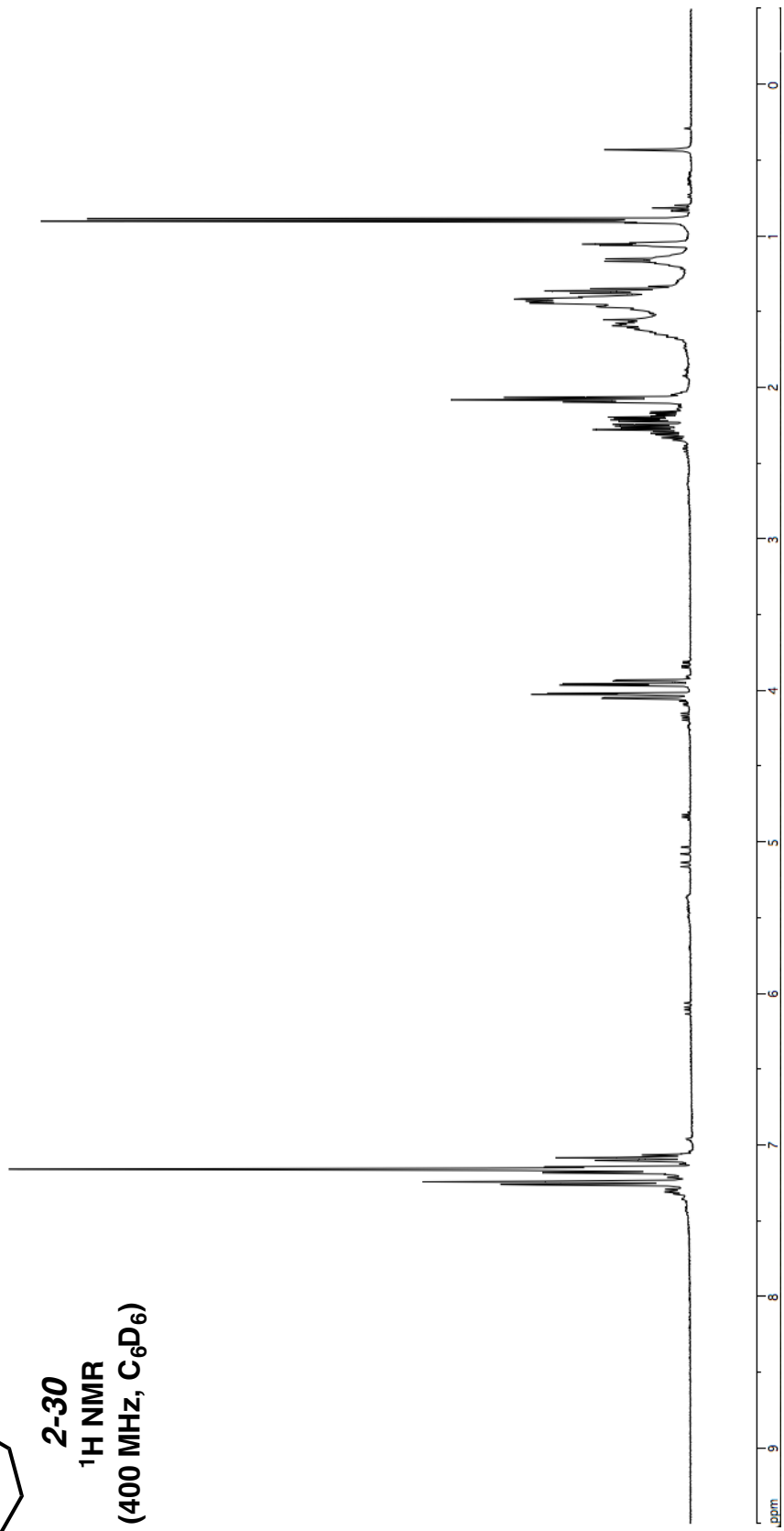


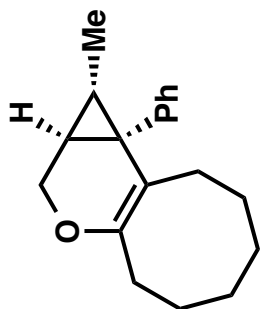


2-30

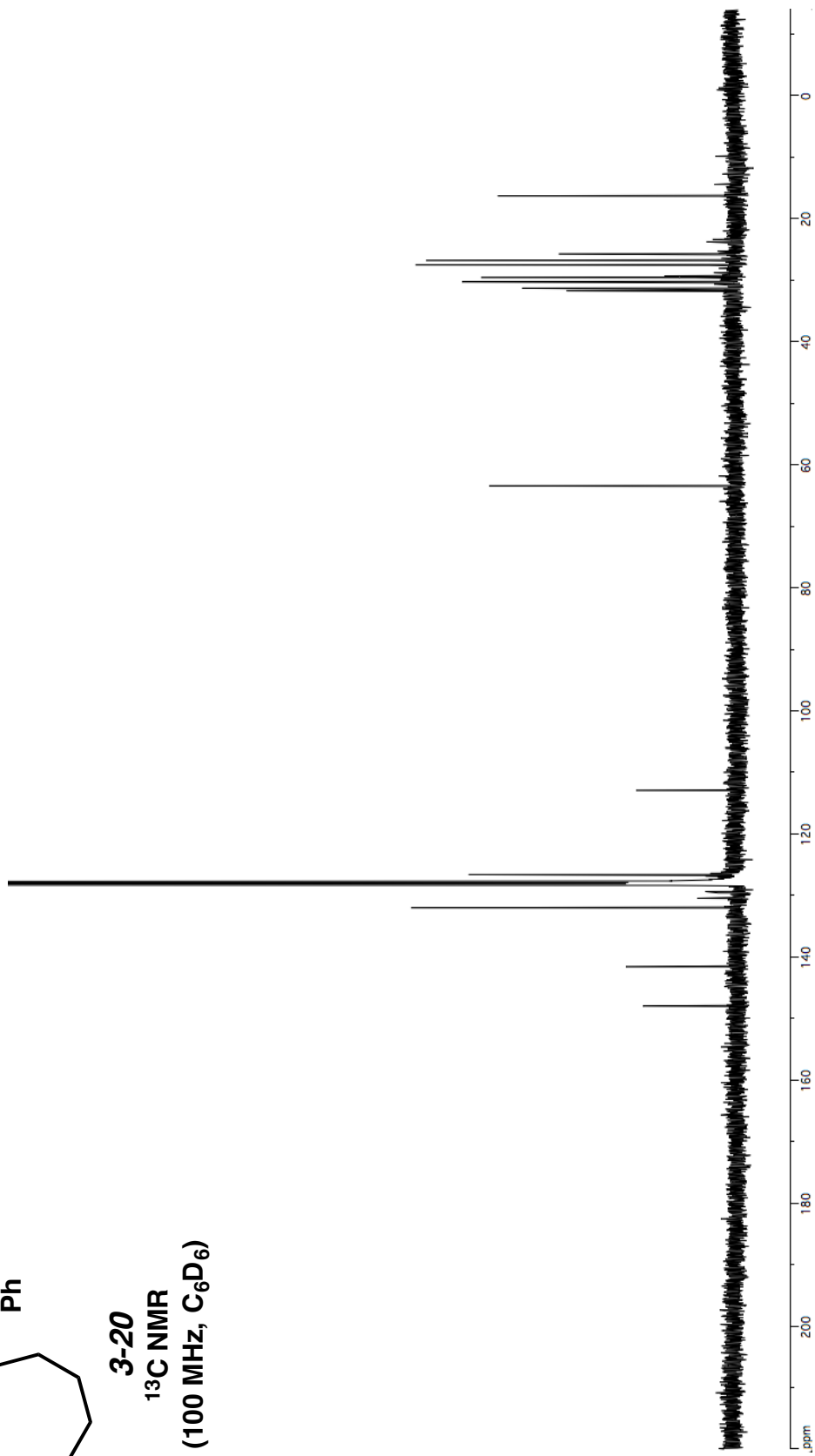
<sup>1</sup>H NMR

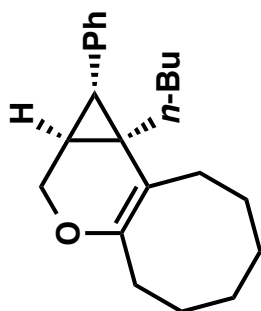
(400 MHz, C<sub>6</sub>D<sub>6</sub>)



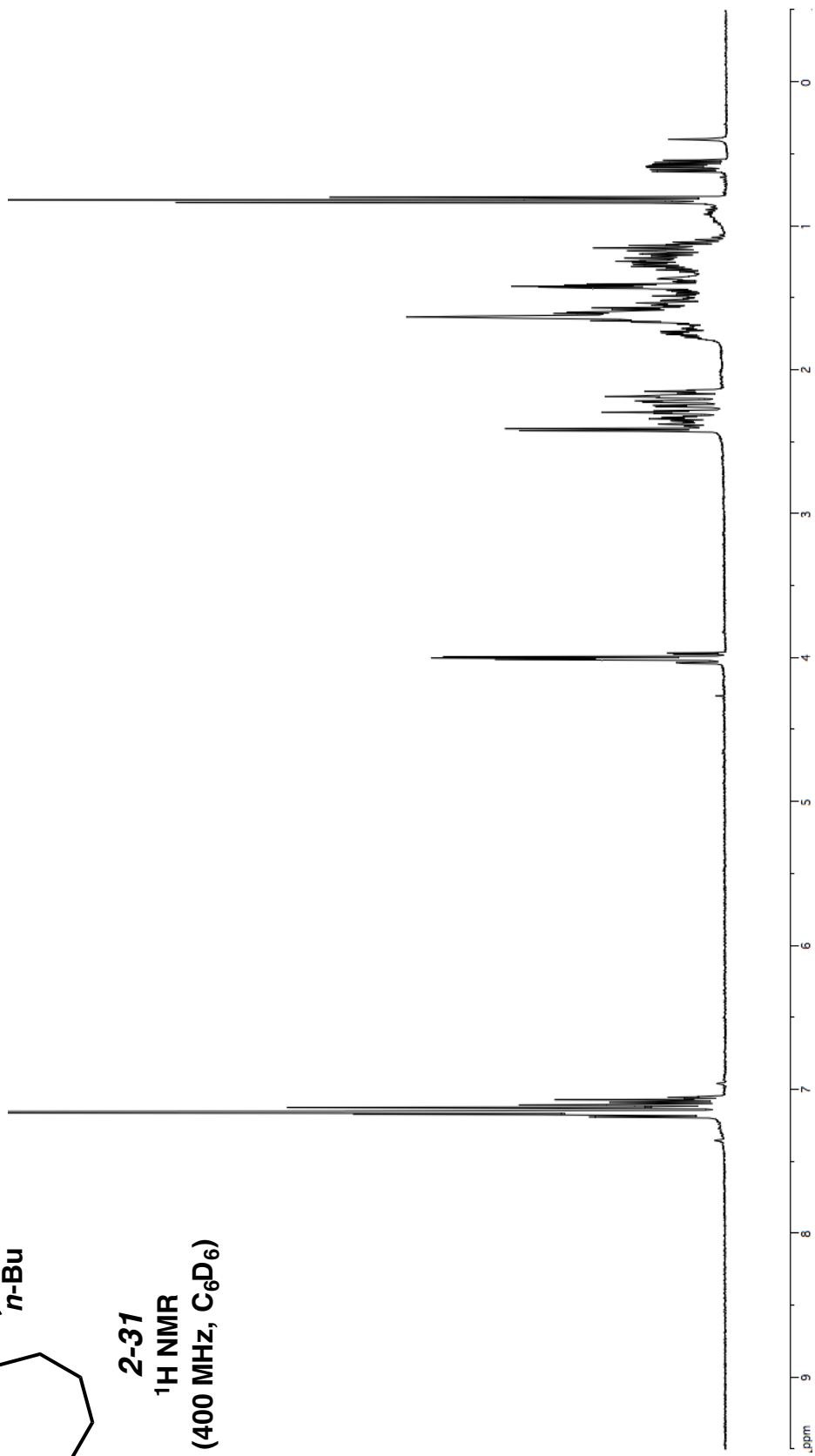


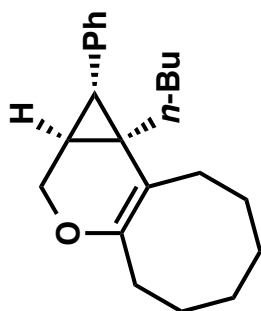
**3-20**  
**<sup>13</sup>C NMR**  
**(100 MHz, C<sub>6</sub>D<sub>6</sub>)**



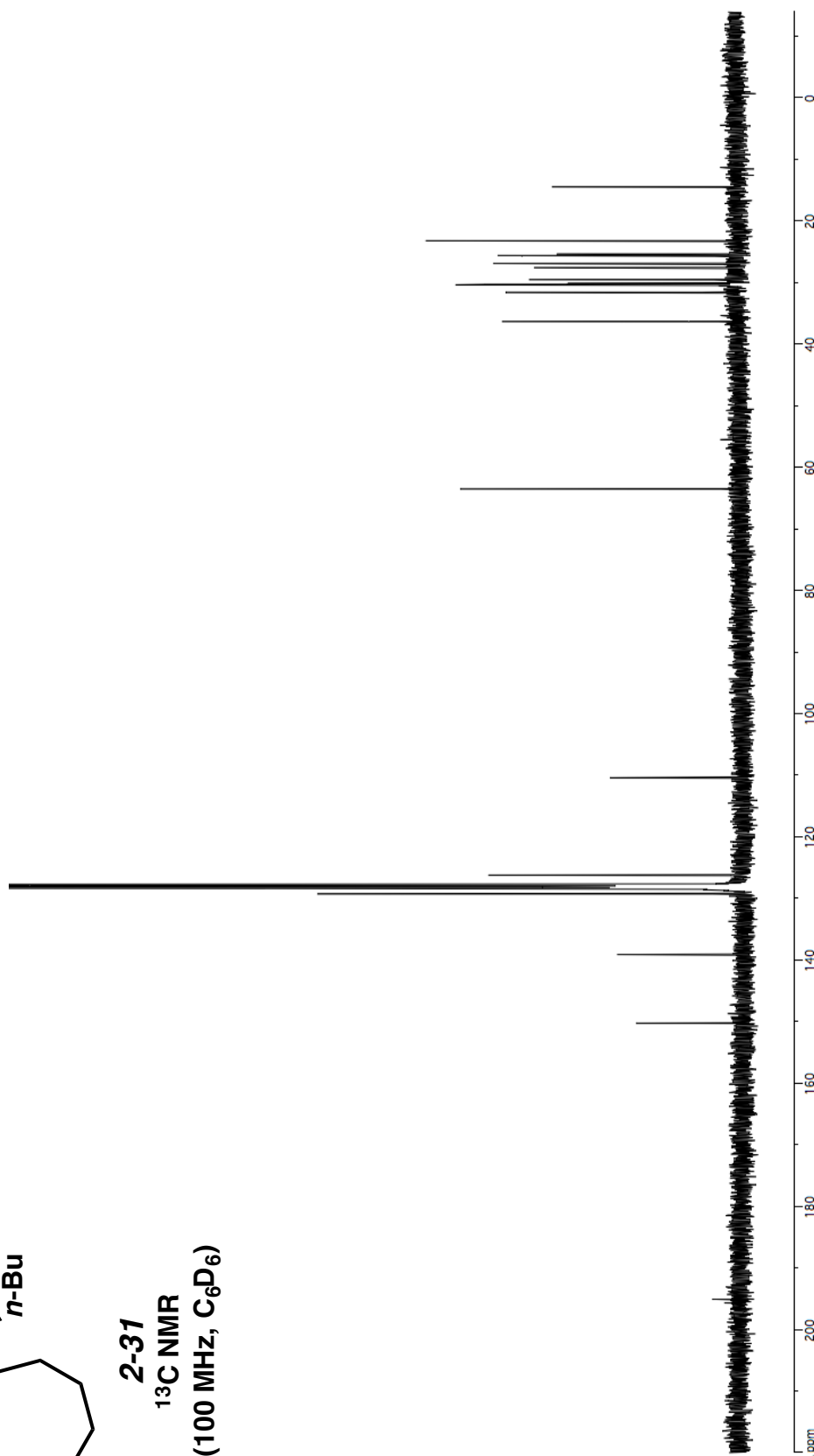


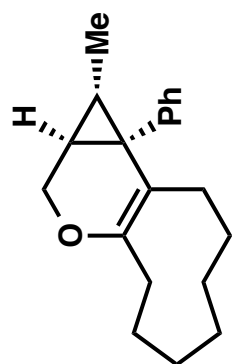
**2-31**  
**<sup>1</sup>H NMR**  
**(400 MHz, C<sub>6</sub>D<sub>6</sub>)**



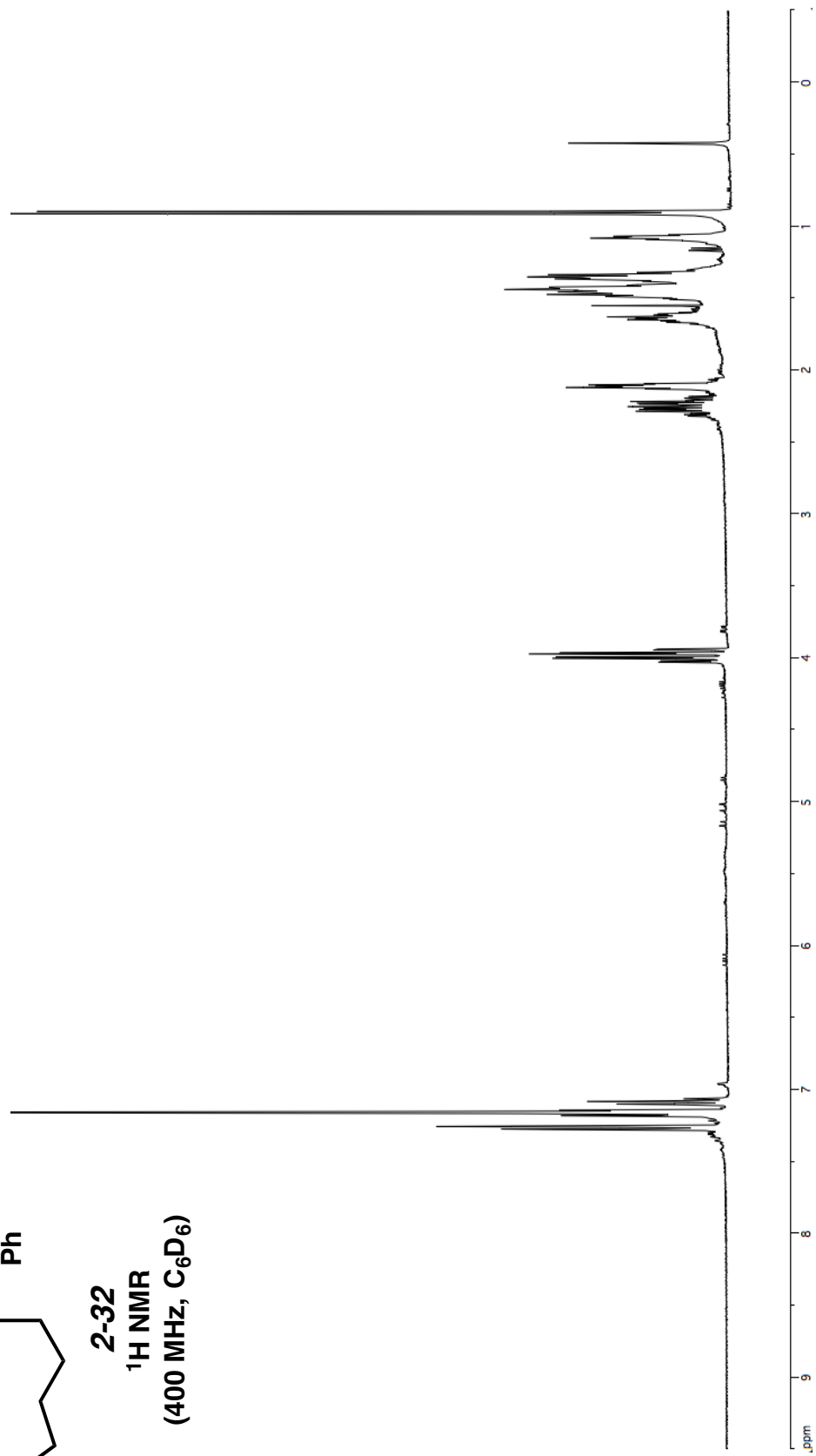


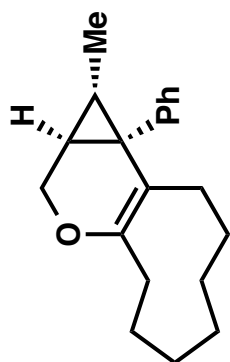
**2-31**  
**<sup>13</sup>C NMR**  
**(100 MHz, C<sub>6</sub>D<sub>6</sub>)**



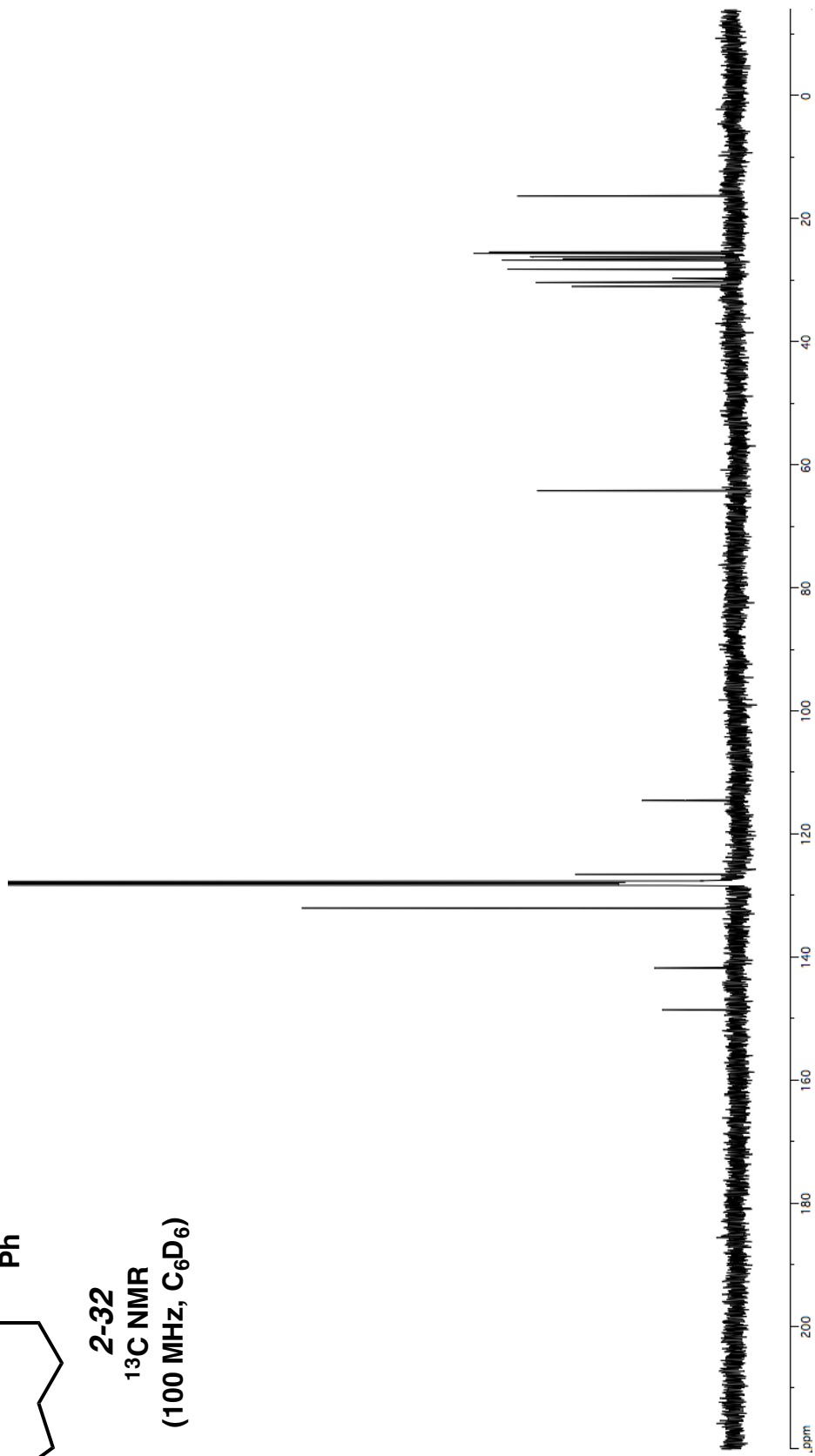


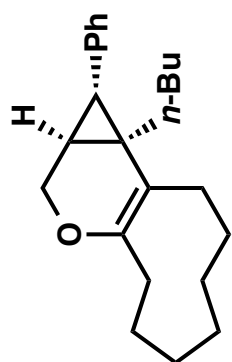
**2-32**  
**<sup>1</sup>H NMR**  
**(400 MHz, C<sub>6</sub>D<sub>6</sub>)**



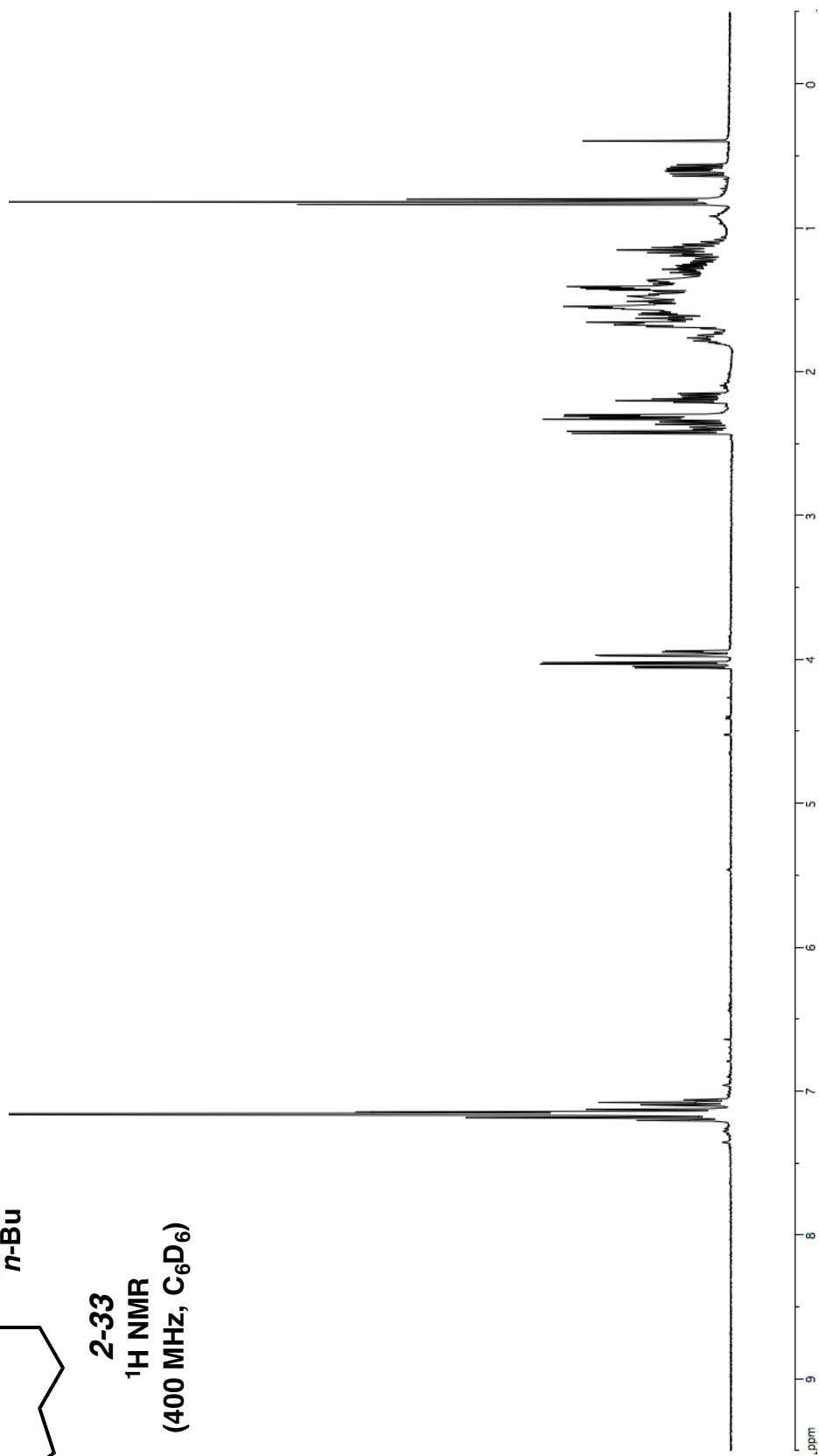


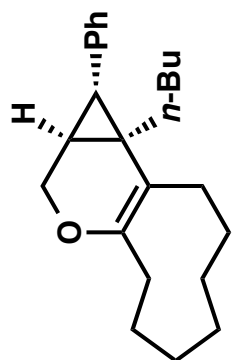
**2-32**  
**<sup>13</sup>C NMR**  
**(100 MHz, C<sub>6</sub>D<sub>6</sub>)**



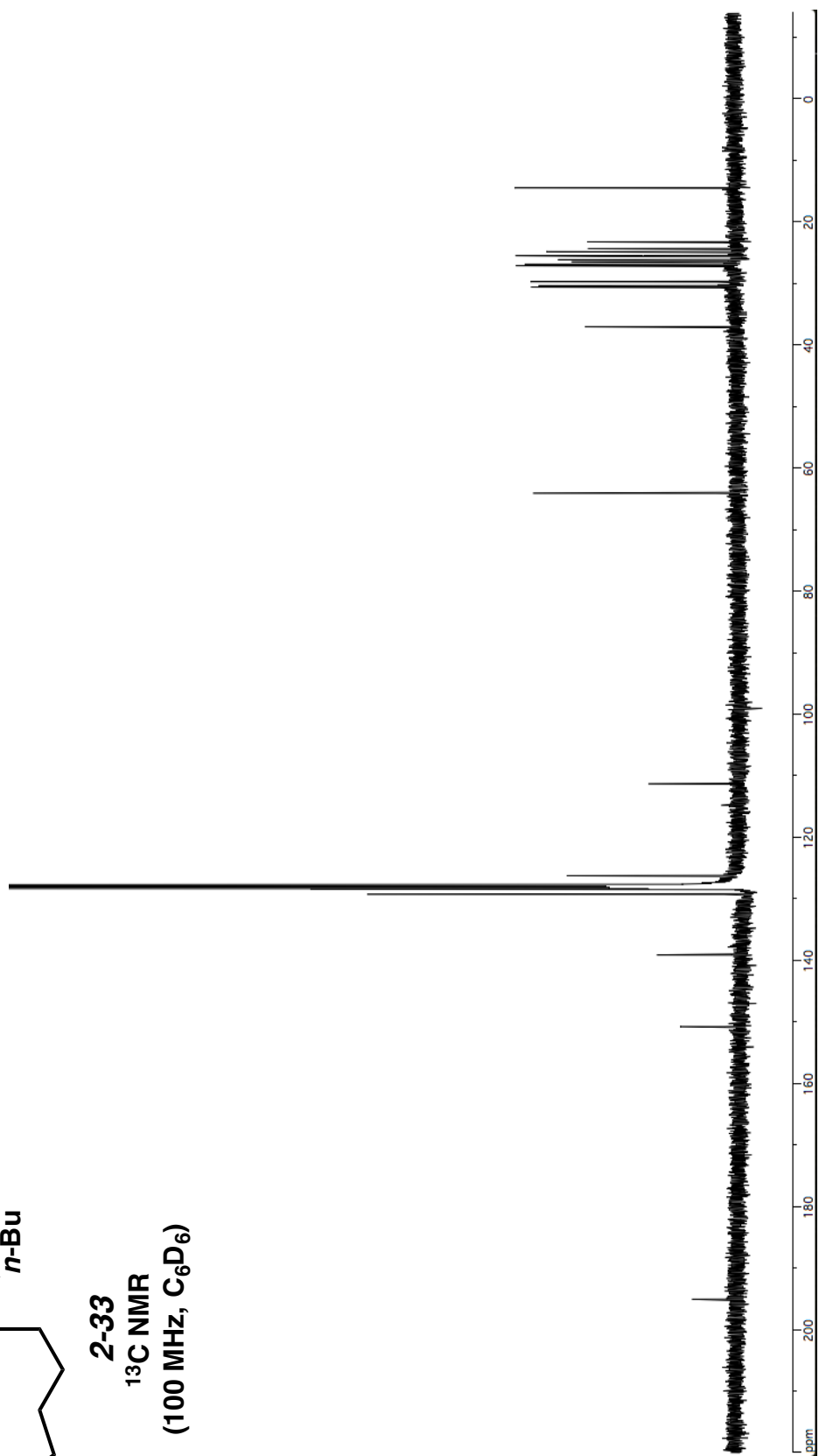


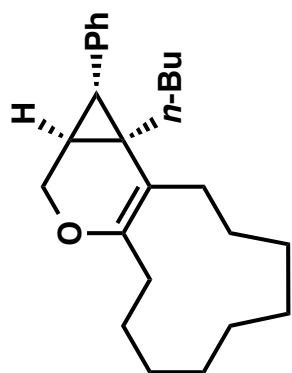
**2-33**  
**<sup>1</sup>H NMR**  
**(400 MHz, C<sub>6</sub>D<sub>6</sub>)**



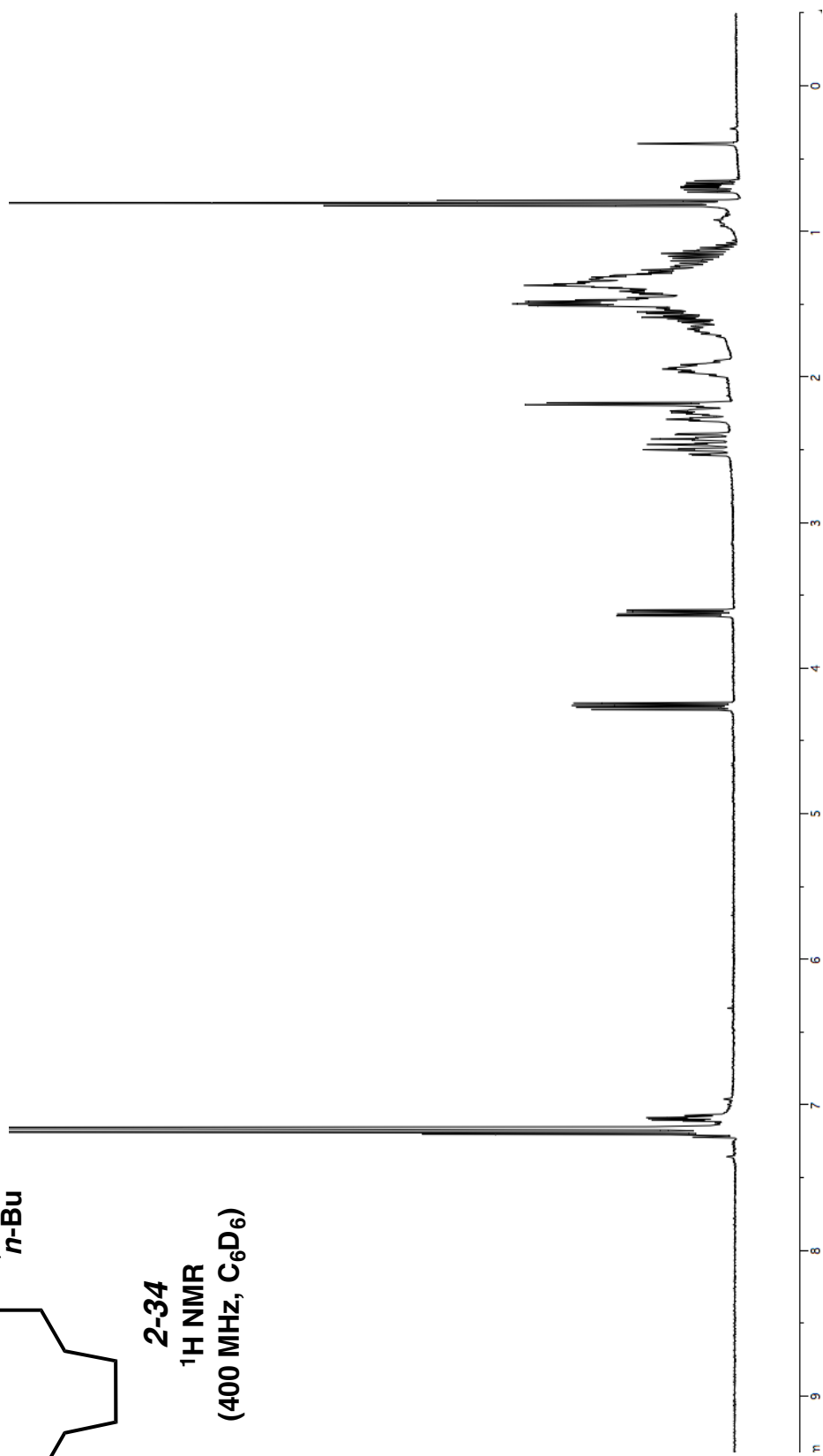


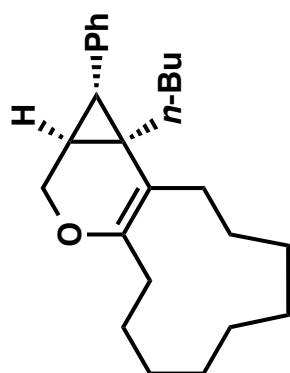
**2-33**  
**<sup>13</sup>C NMR**  
**(100 MHz, C<sub>6</sub>D<sub>6</sub>)**



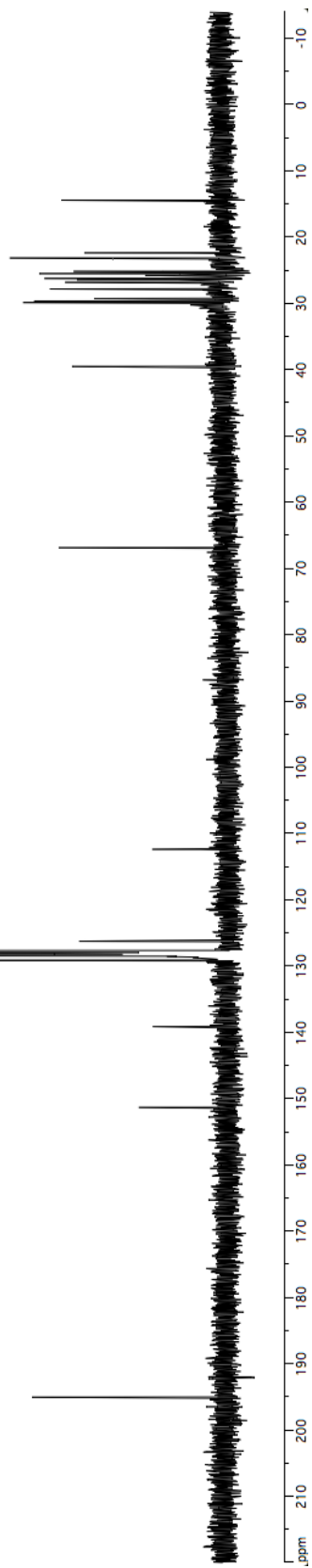


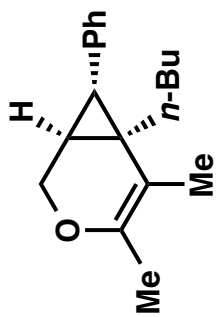
**2-34**  
**<sup>1</sup>H NMR**  
**(400 MHz, C<sub>6</sub>D<sub>6</sub>)**





**2-34**  
**<sup>13</sup>C NMR**  
**(100 MHz, C<sub>6</sub>D<sub>6</sub>)**

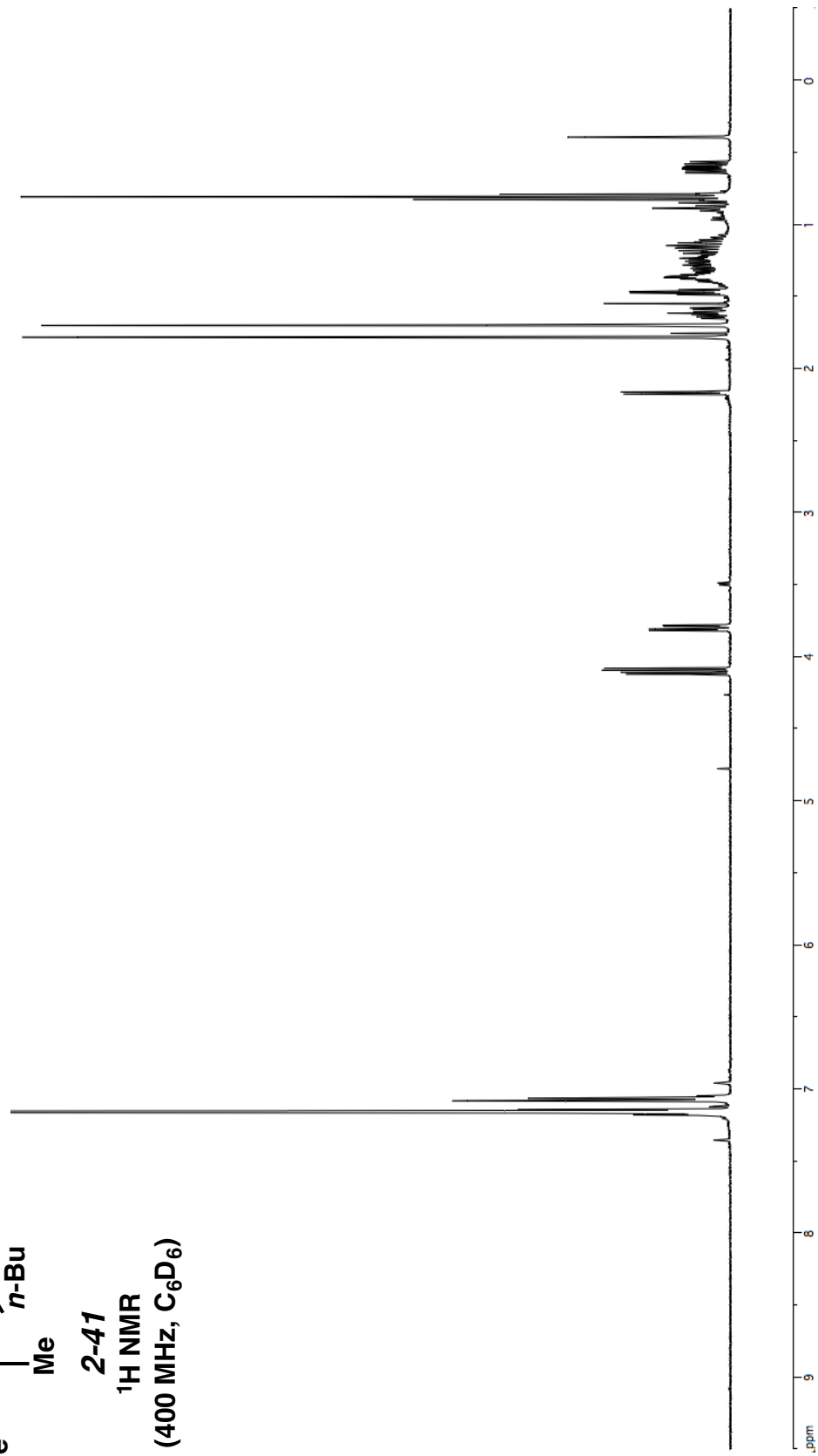




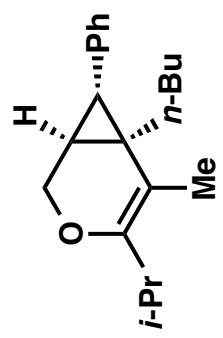
**2-41**

**<sup>1</sup>H NMR**

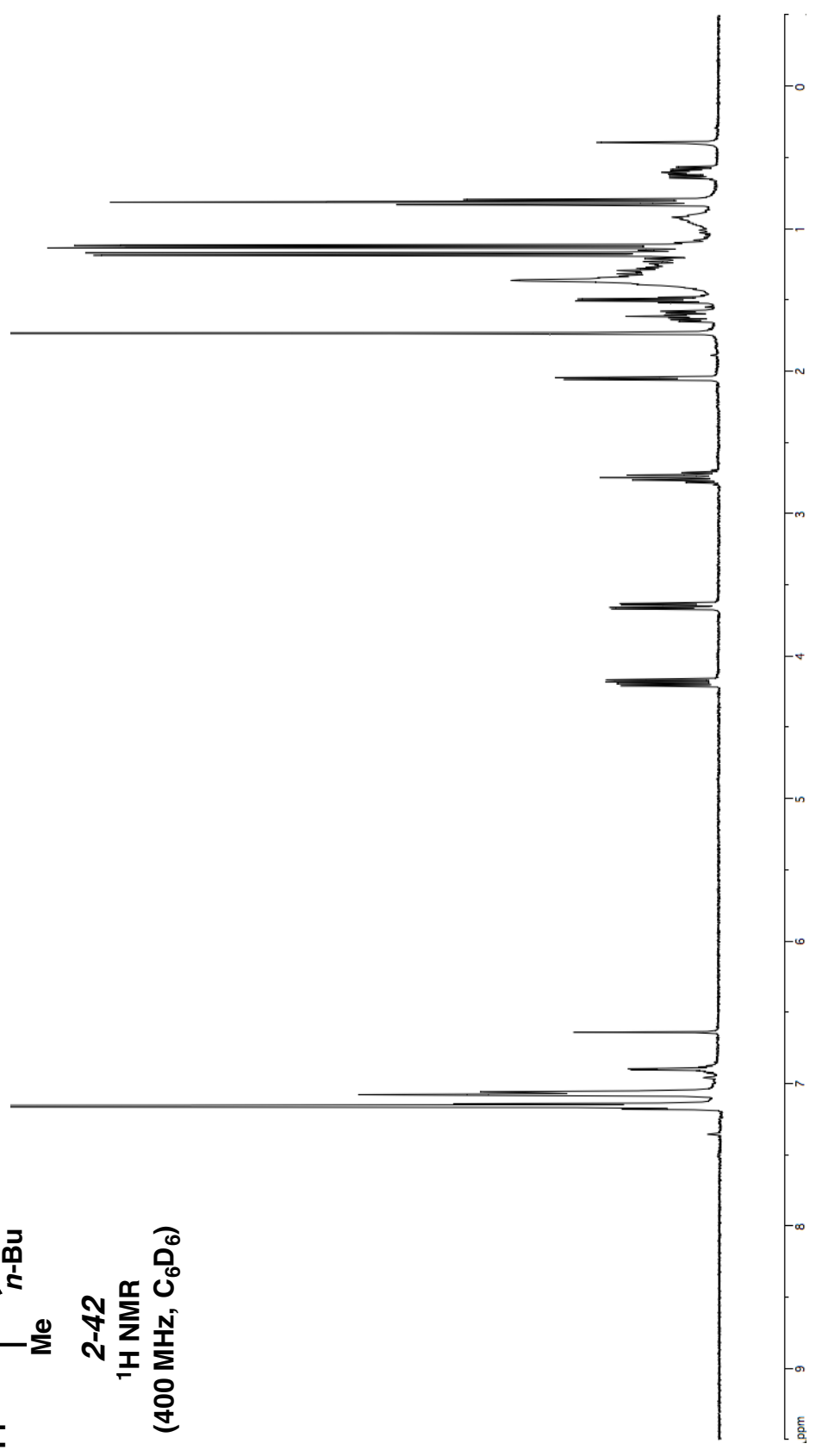
**(400 MHz, C<sub>6</sub>D<sub>6</sub>)**

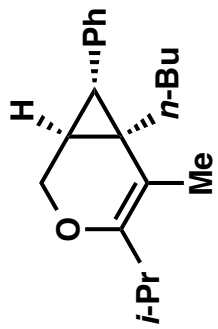




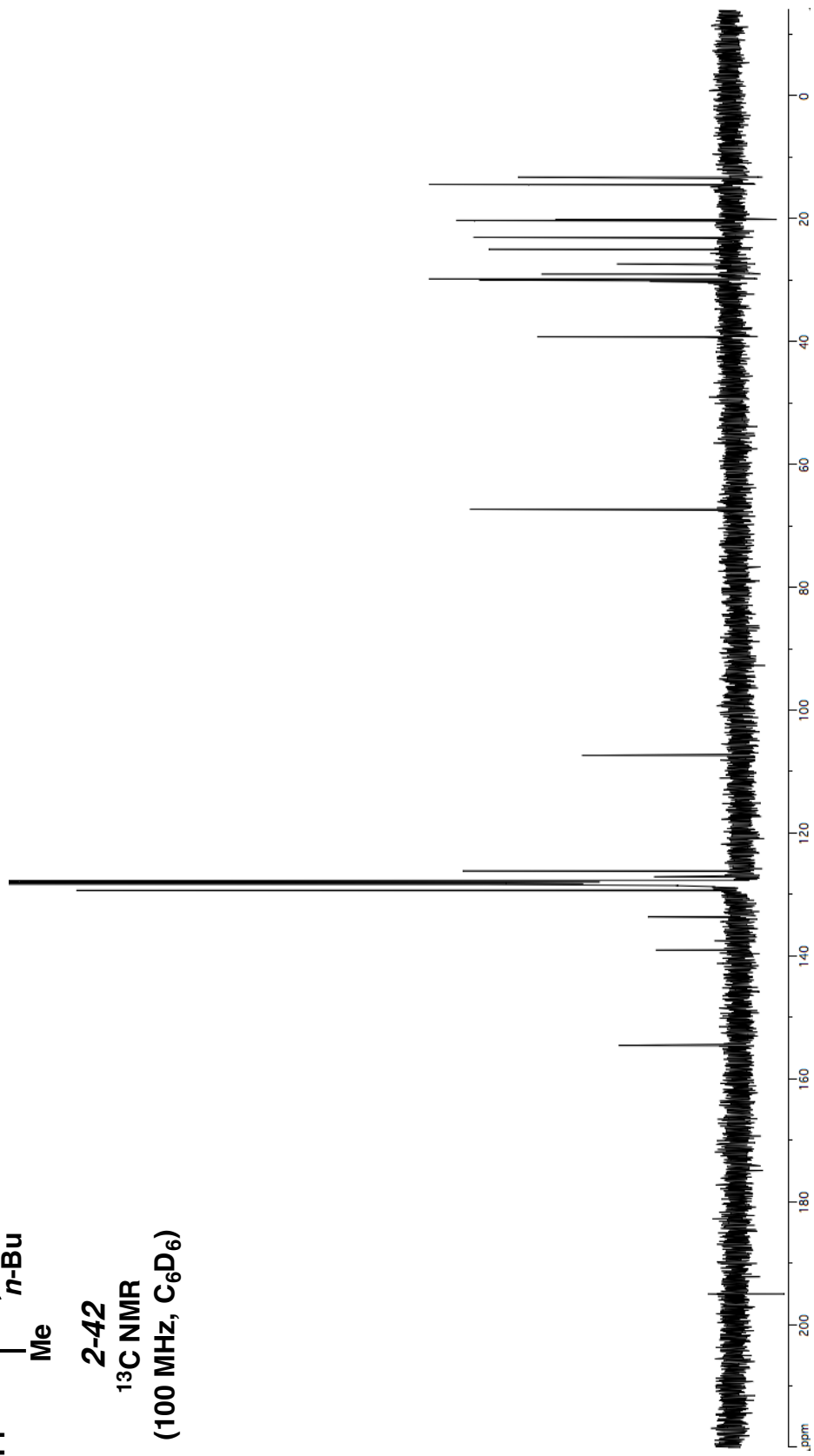


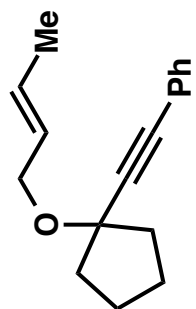
**2-42**  
**<sup>1</sup>H NMR**  
**(400 MHz, C<sub>6</sub>D<sub>6</sub>)**



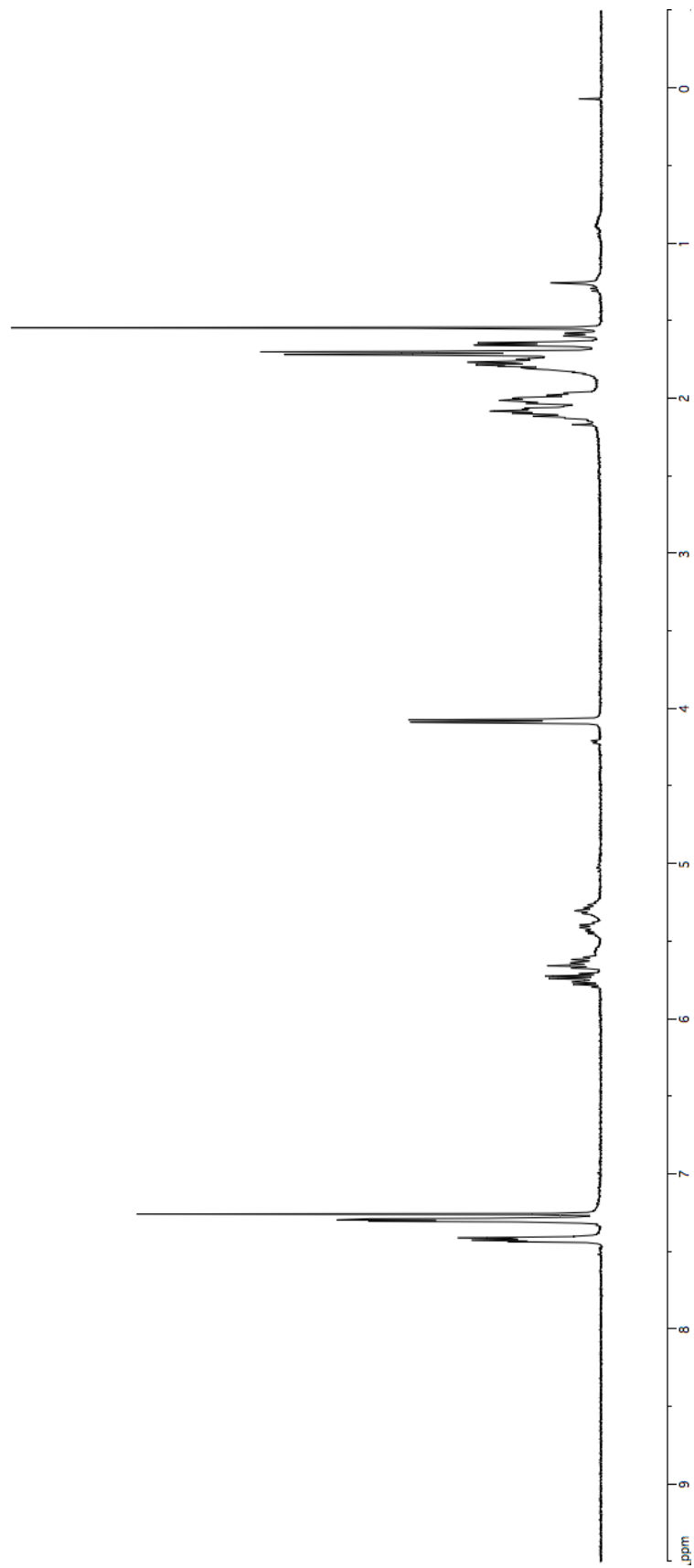


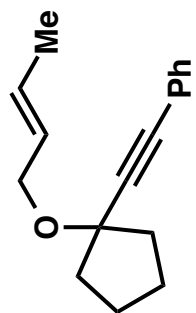
**2-42**  
<sup>13</sup>C NMR  
(100 MHz, C<sub>6</sub>D<sub>6</sub>)





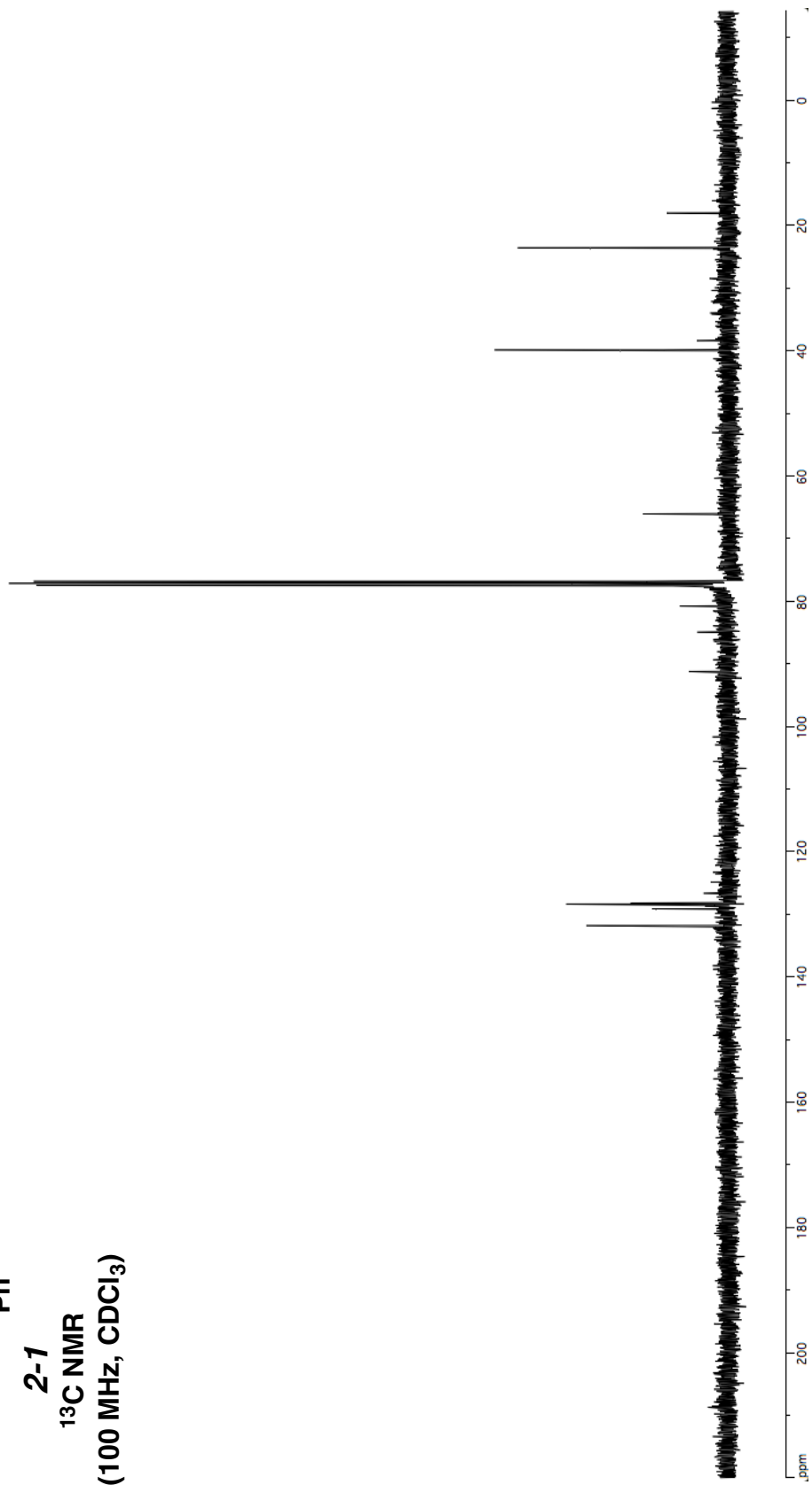
**2-1**  
**<sup>1</sup>H NMR**  
**(400 MHz, CDCl<sub>3</sub>)**



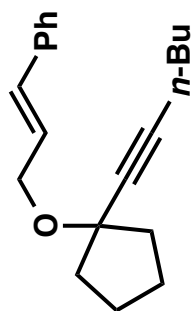


2-1

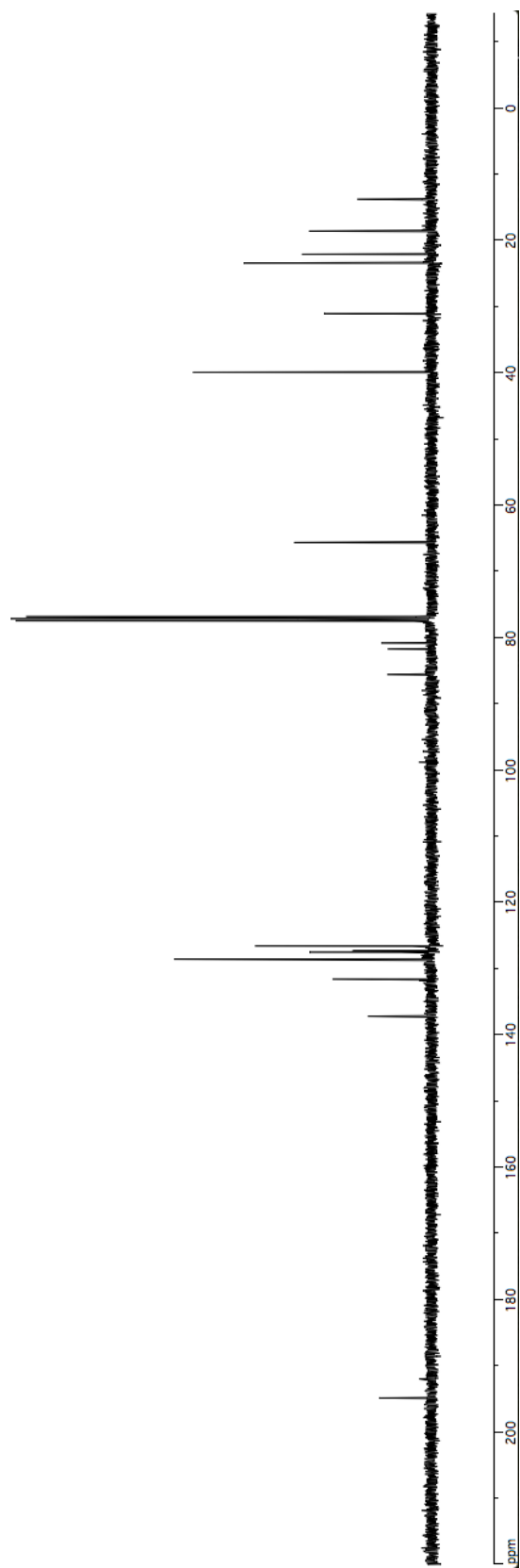
<sup>13</sup>C NMR  
(100 MHz, CDCl<sub>3</sub>)

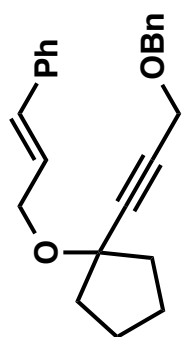




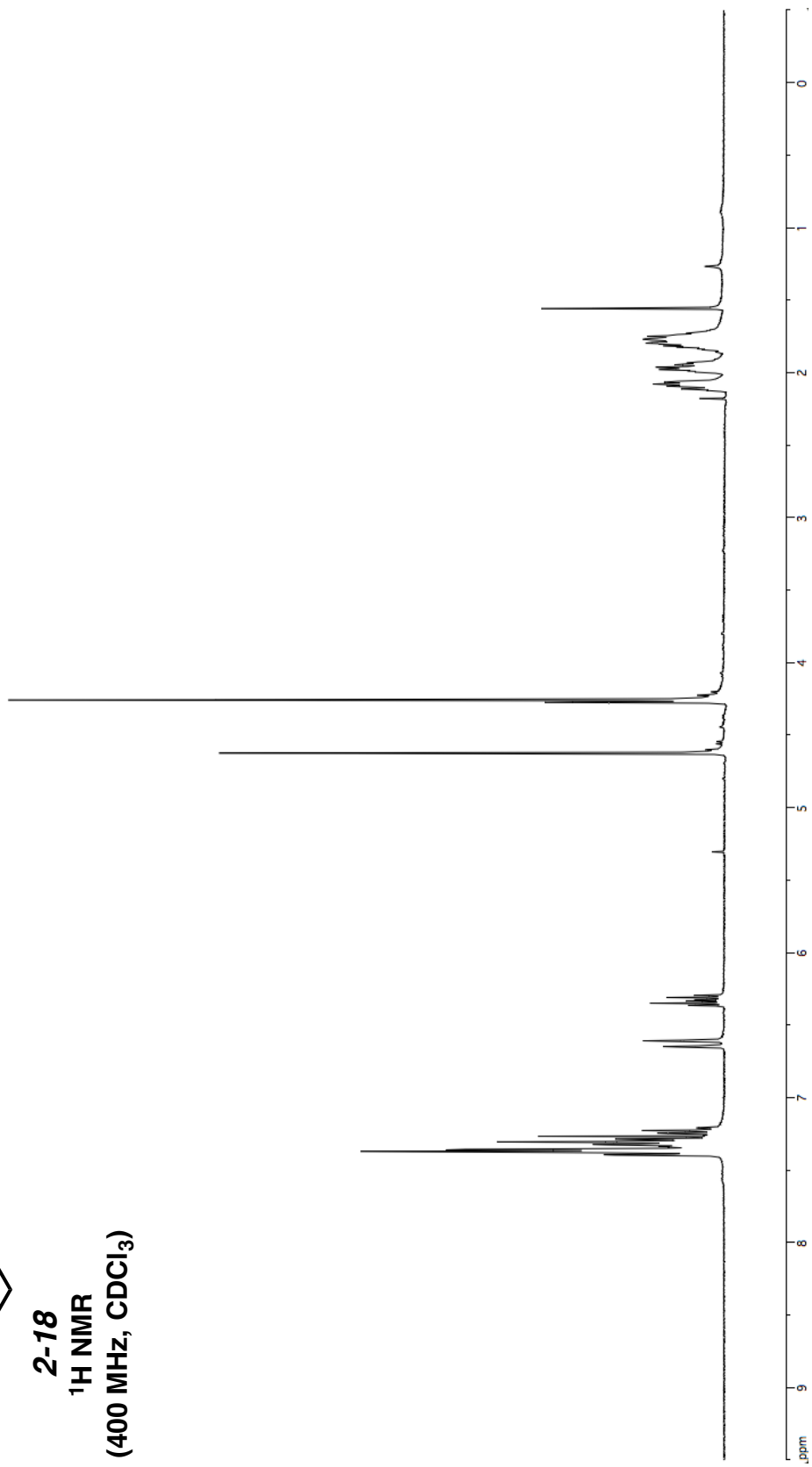


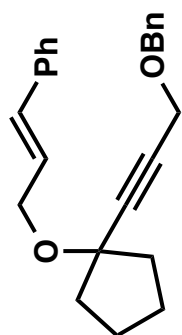
**2-12**  
**<sup>13</sup>C NMR**  
**(100 MHz, CDCl<sub>3</sub>)**



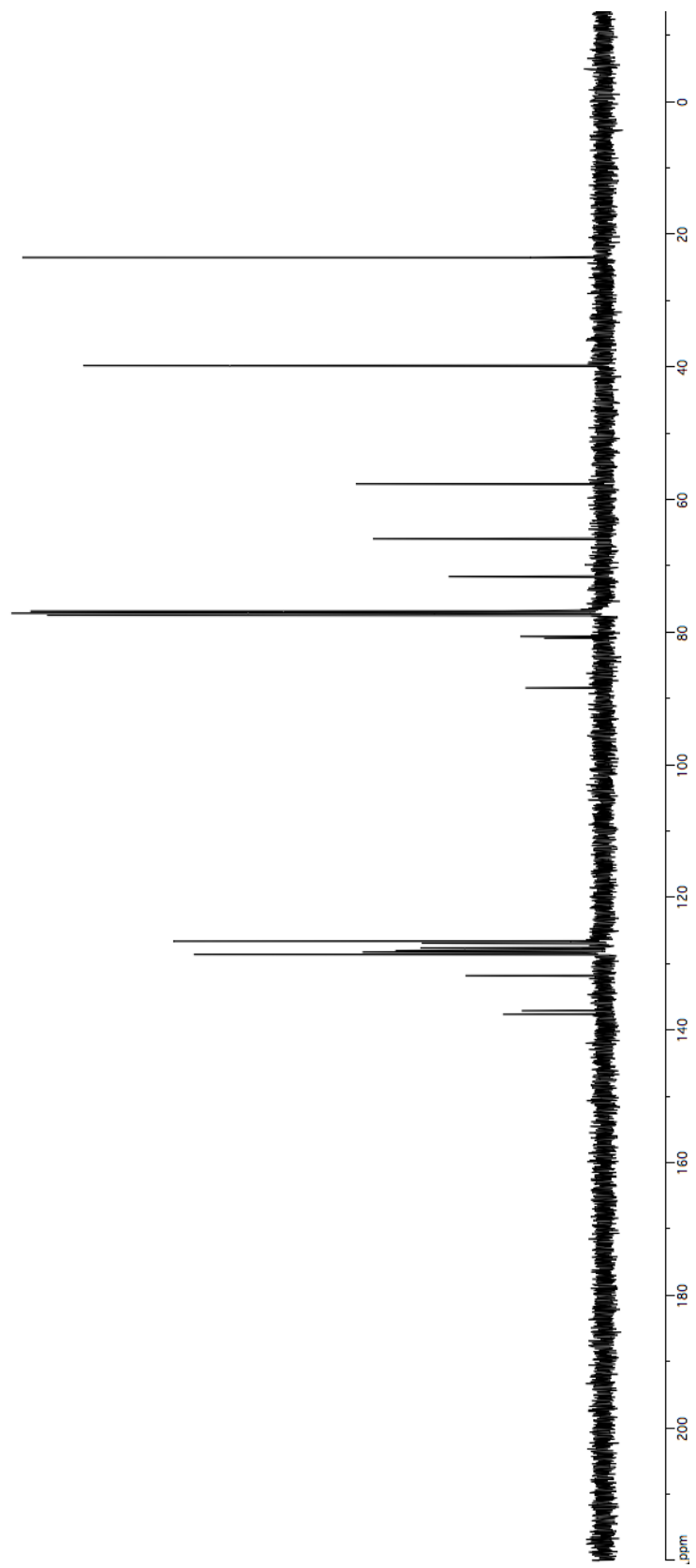


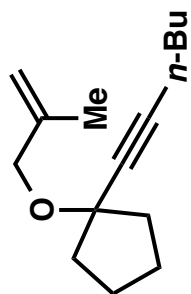
**2-18**  
**<sup>1</sup>H NMR**  
**(400 MHz, CDCl<sub>3</sub>)**





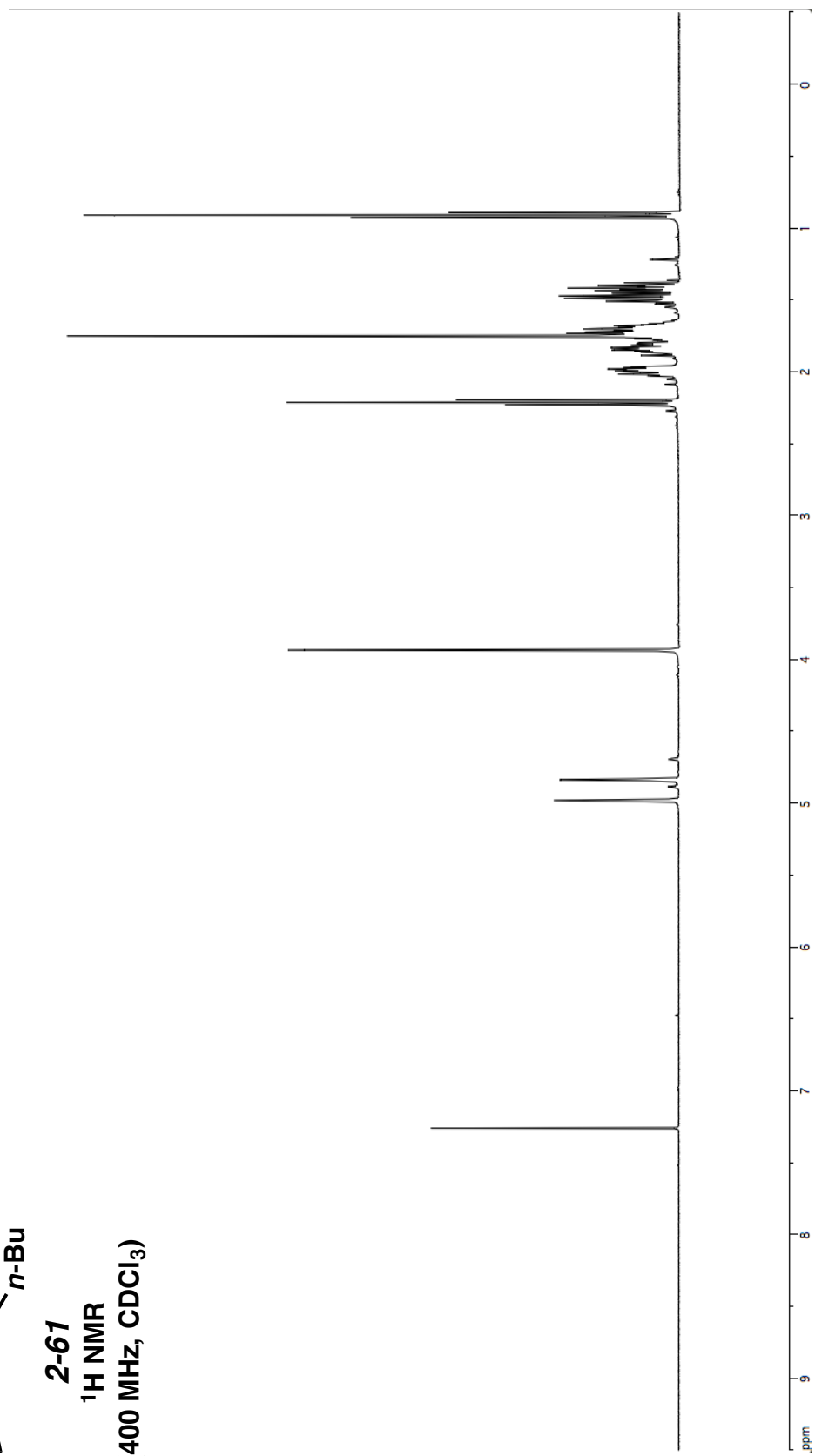
**2-18**  
<sup>13</sup>C NMR  
(100 MHz, CDCl<sub>3</sub>)

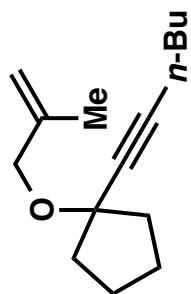




2-61

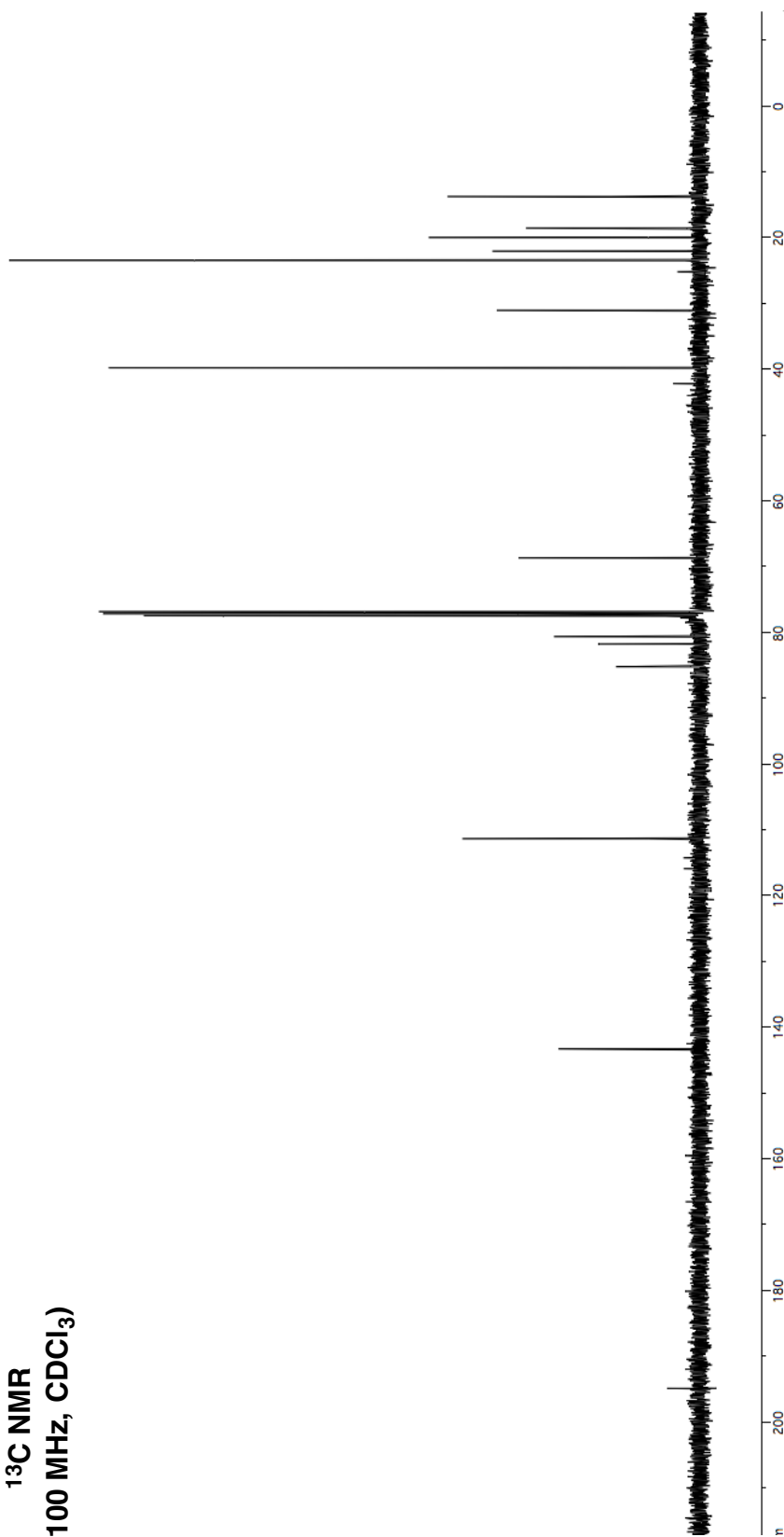
<sup>1</sup>H NMR  
(400 MHz, CDCl<sub>3</sub>)

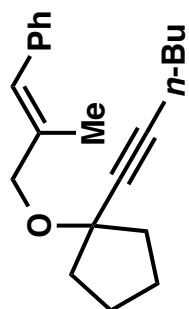




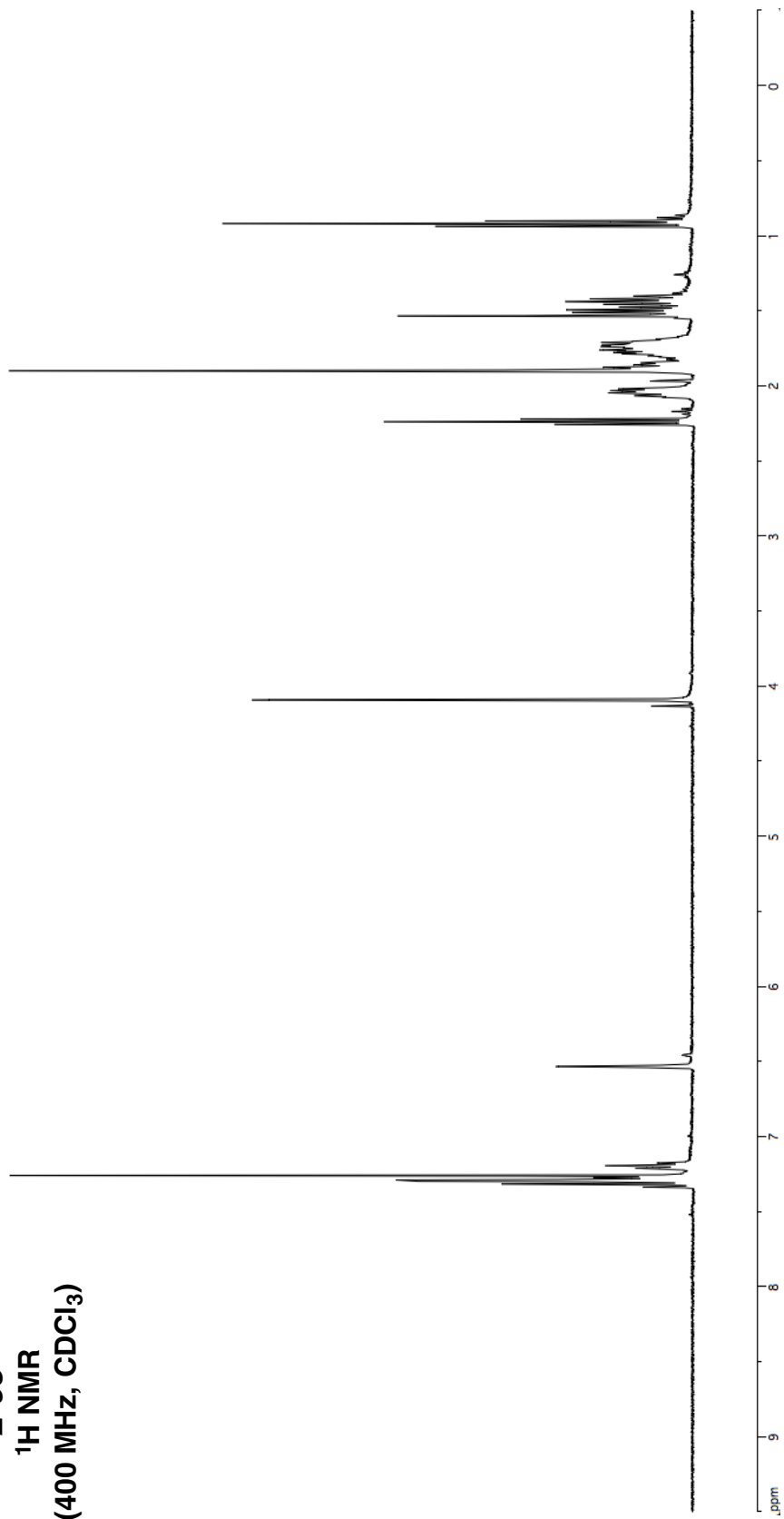
**2-61**

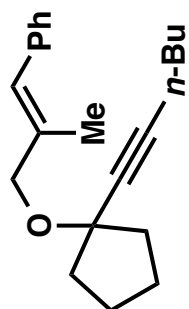
**<sup>13</sup>C NMR  
(100 MHz, CDCl<sub>3</sub>)**





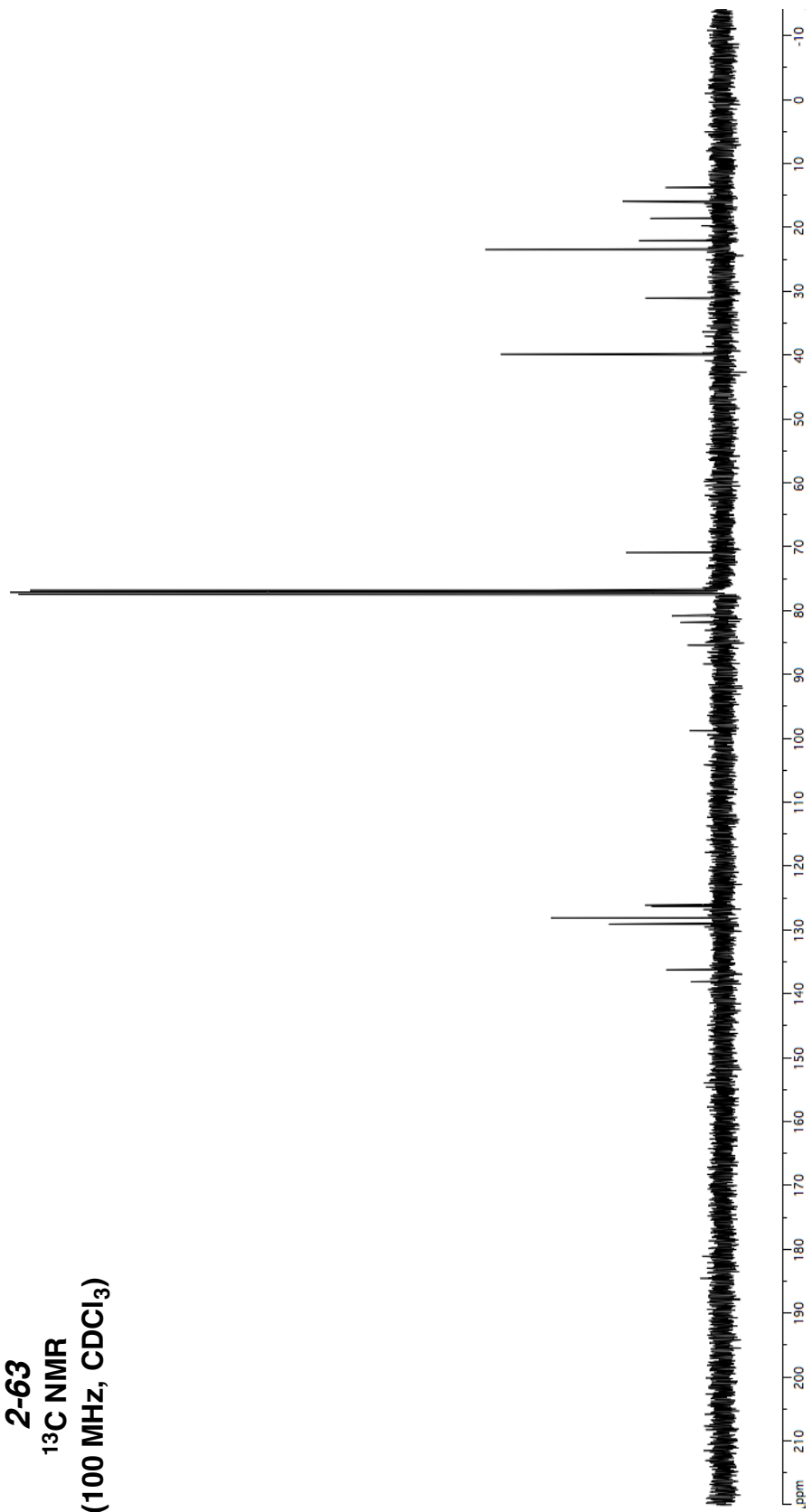
**2-63**  
**<sup>1</sup>H NMR**  
**(400 MHz, CDCl<sub>3</sub>)**

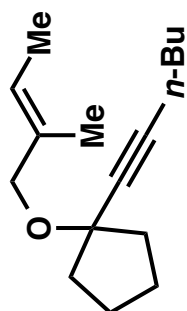




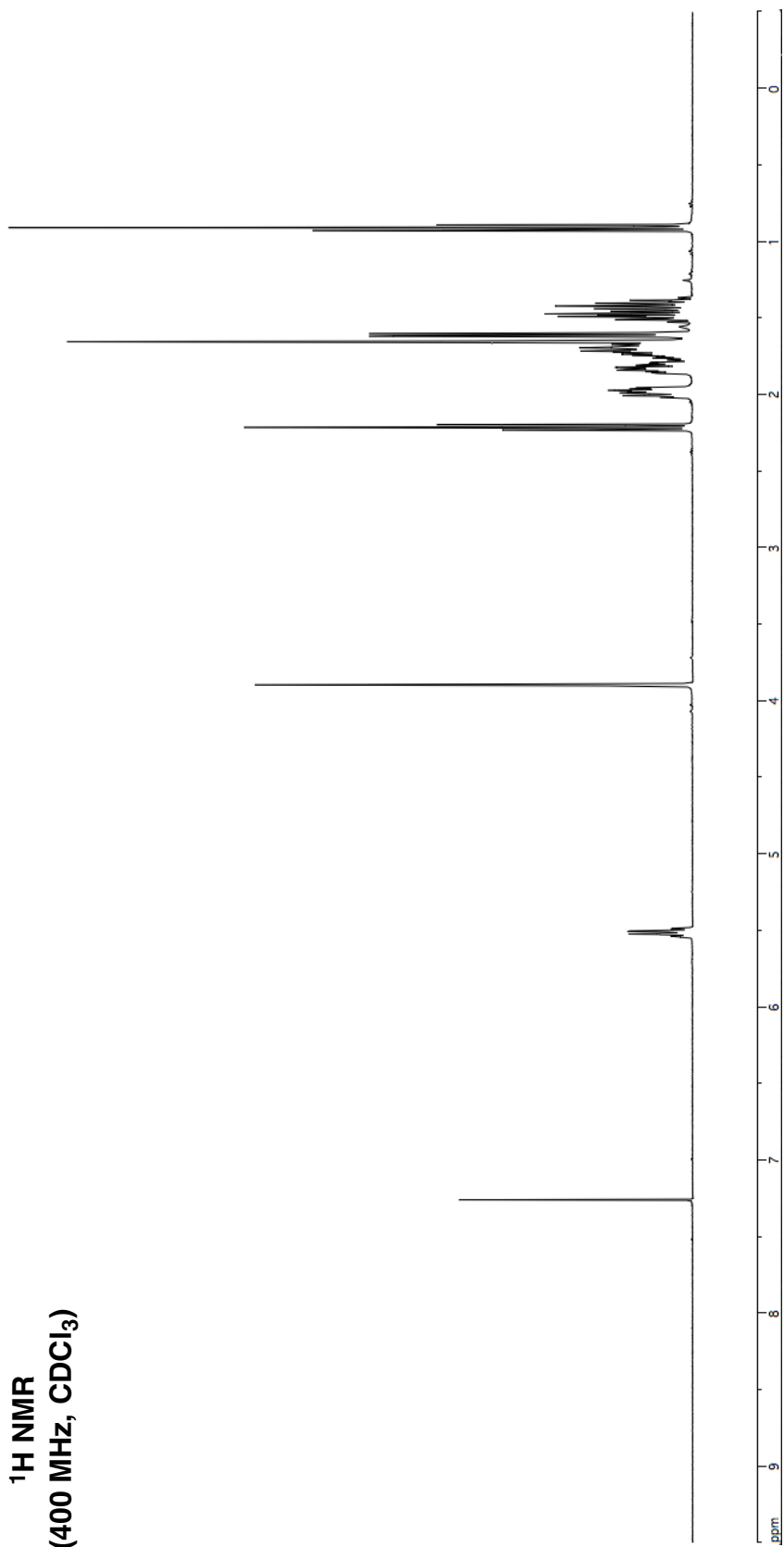
2-63

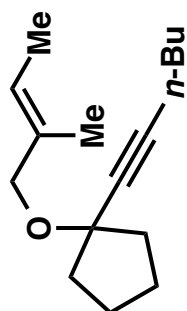
<sup>13</sup>C NMR  
(100 MHz, CDCl<sub>3</sub>)



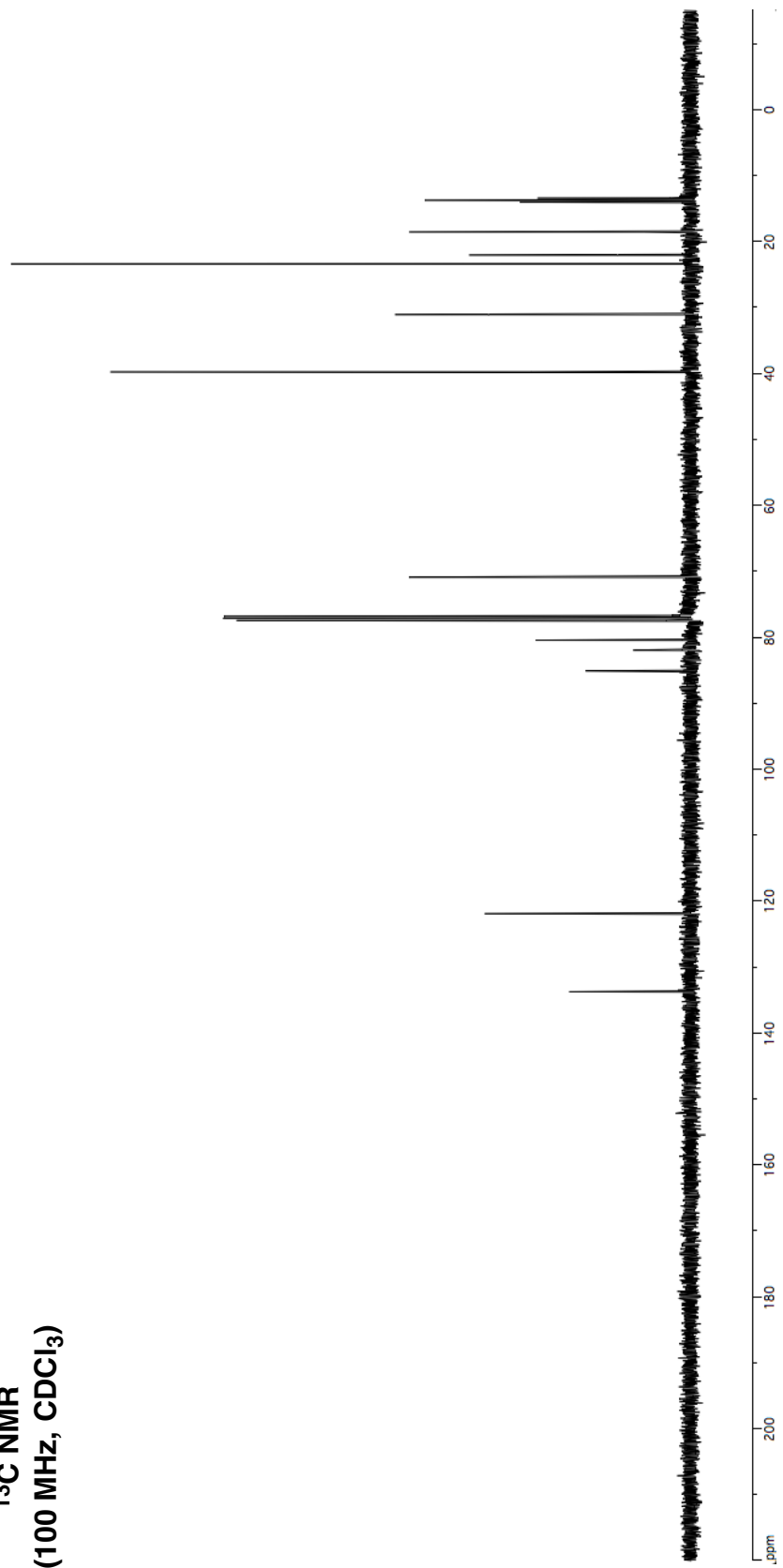


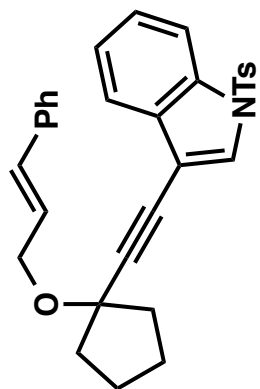
**2-4**  
**<sup>1</sup>H NMR**  
**(400 MHz, CDCl<sub>3</sub>)**



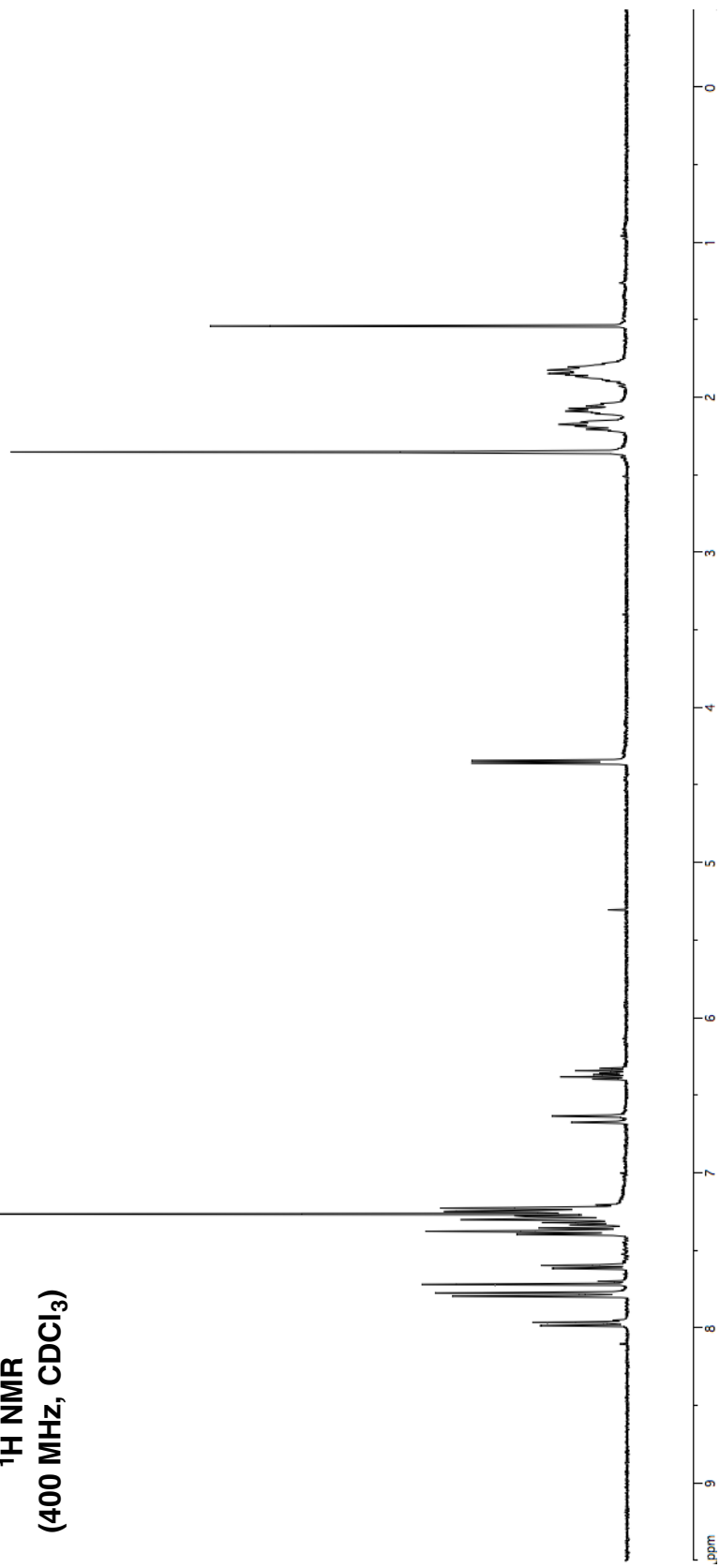


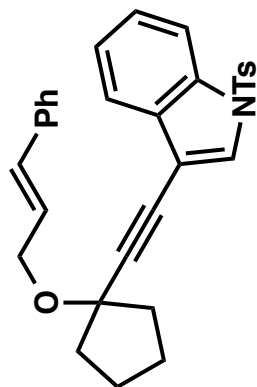
**2-4**  
**<sup>13</sup>C NMR**  
**(100 MHz, CDCl<sub>3</sub>)**



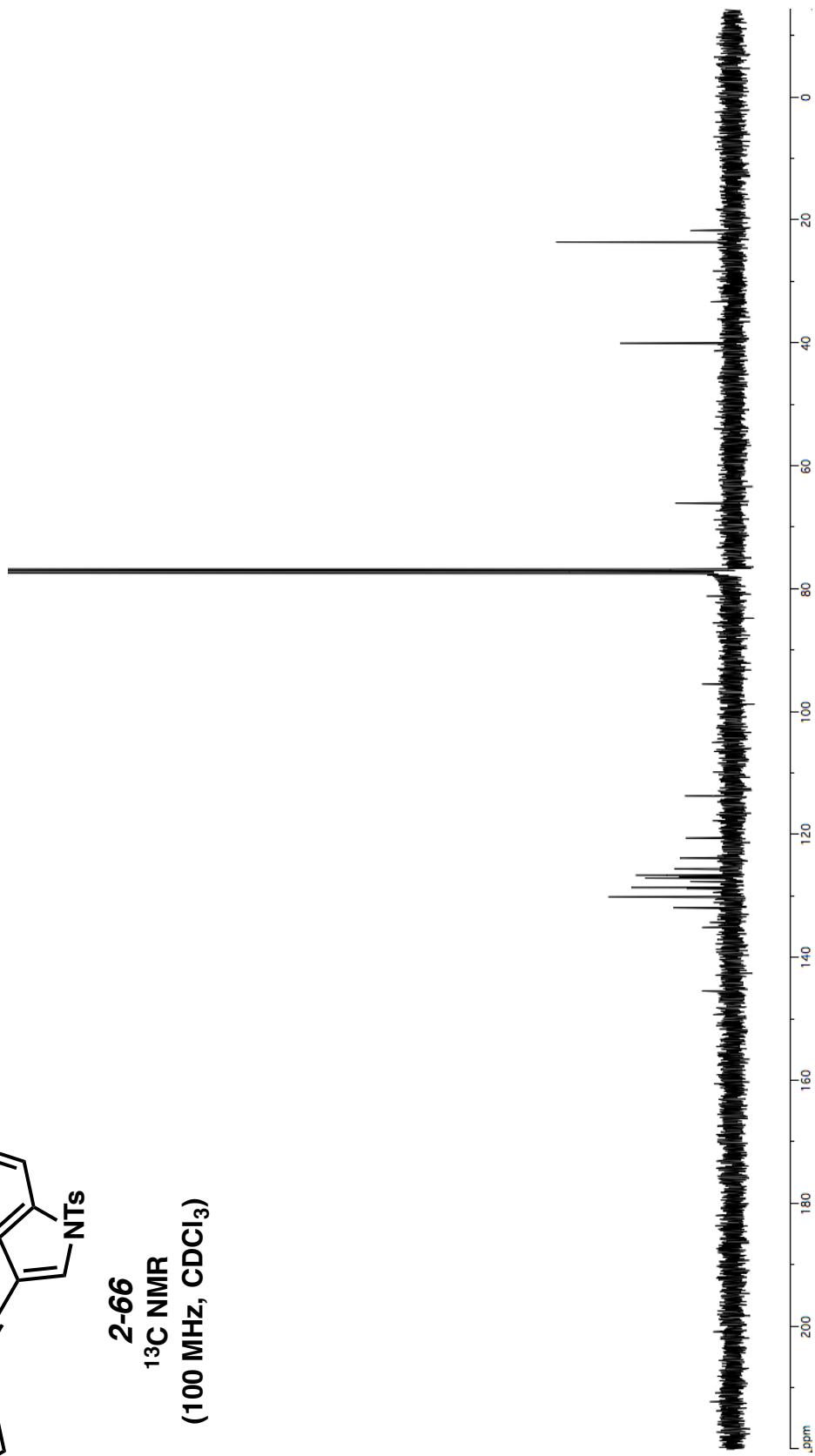


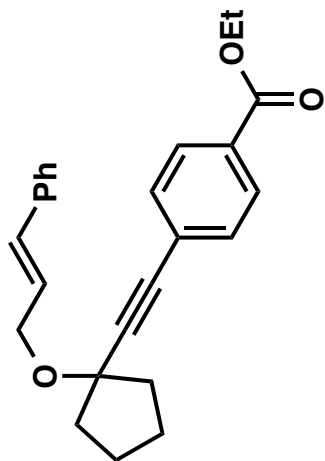
**2-66**  
**<sup>1</sup>H NMR**  
**(400 MHz, CDCl<sub>3</sub>)**



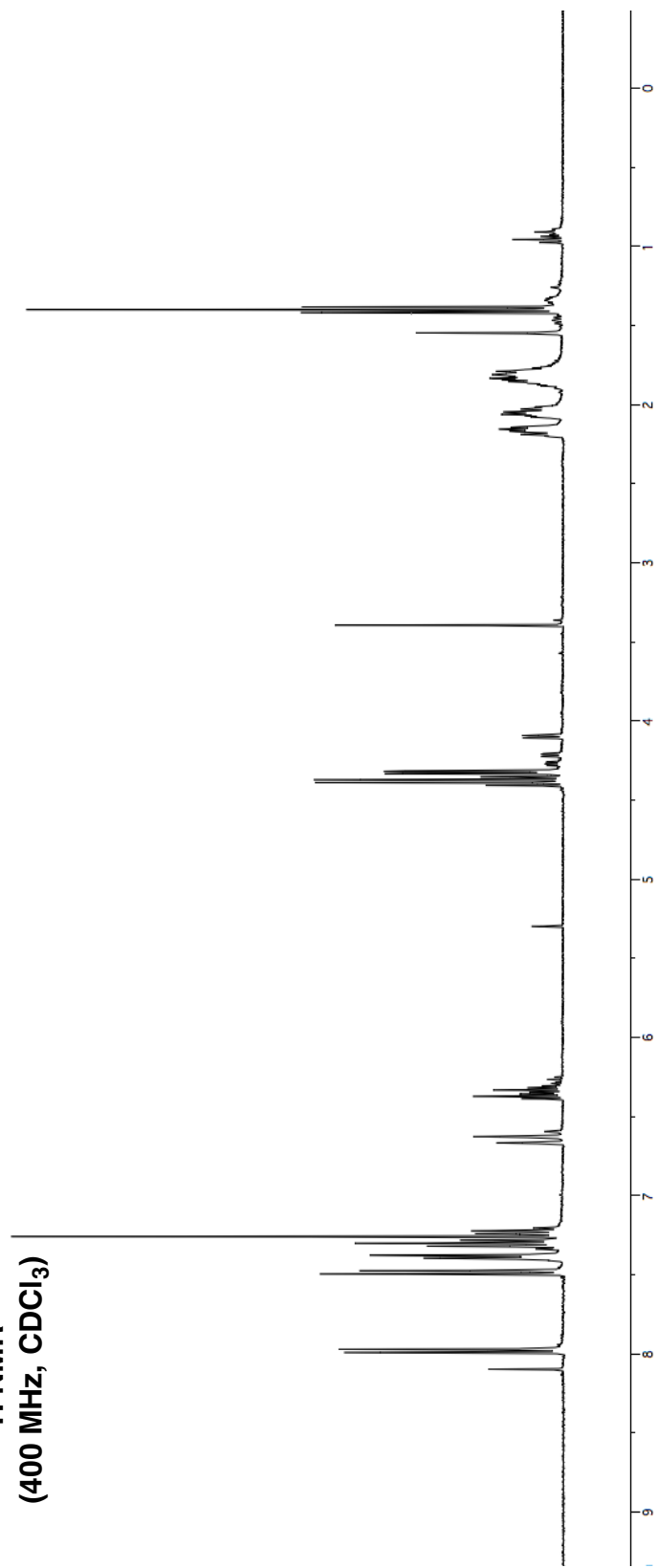


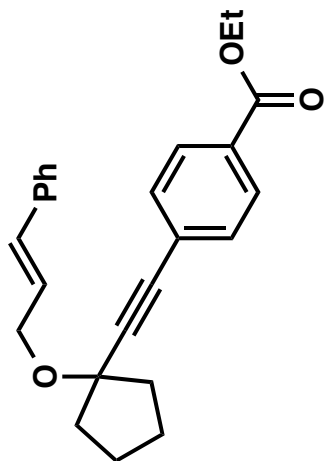
**2-66**  
**<sup>13</sup>C NMR**  
**(100 MHz, CDCl<sub>3</sub>)**



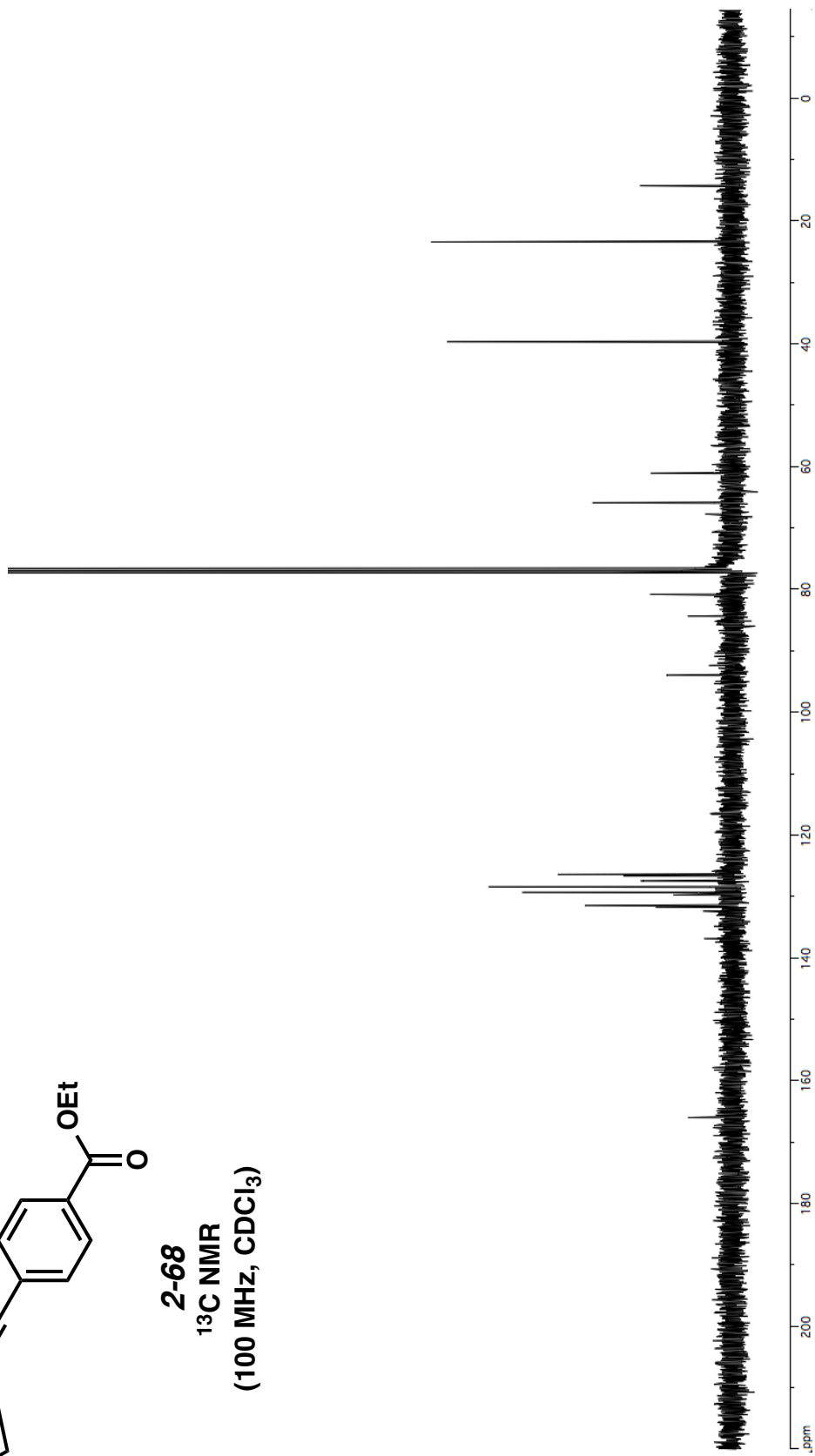


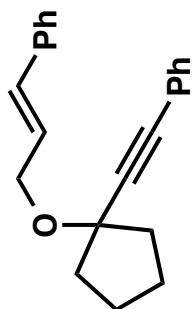
**2-68**  
**<sup>1</sup>H NMR**  
**(400 MHz, CDCl<sub>3</sub>)**



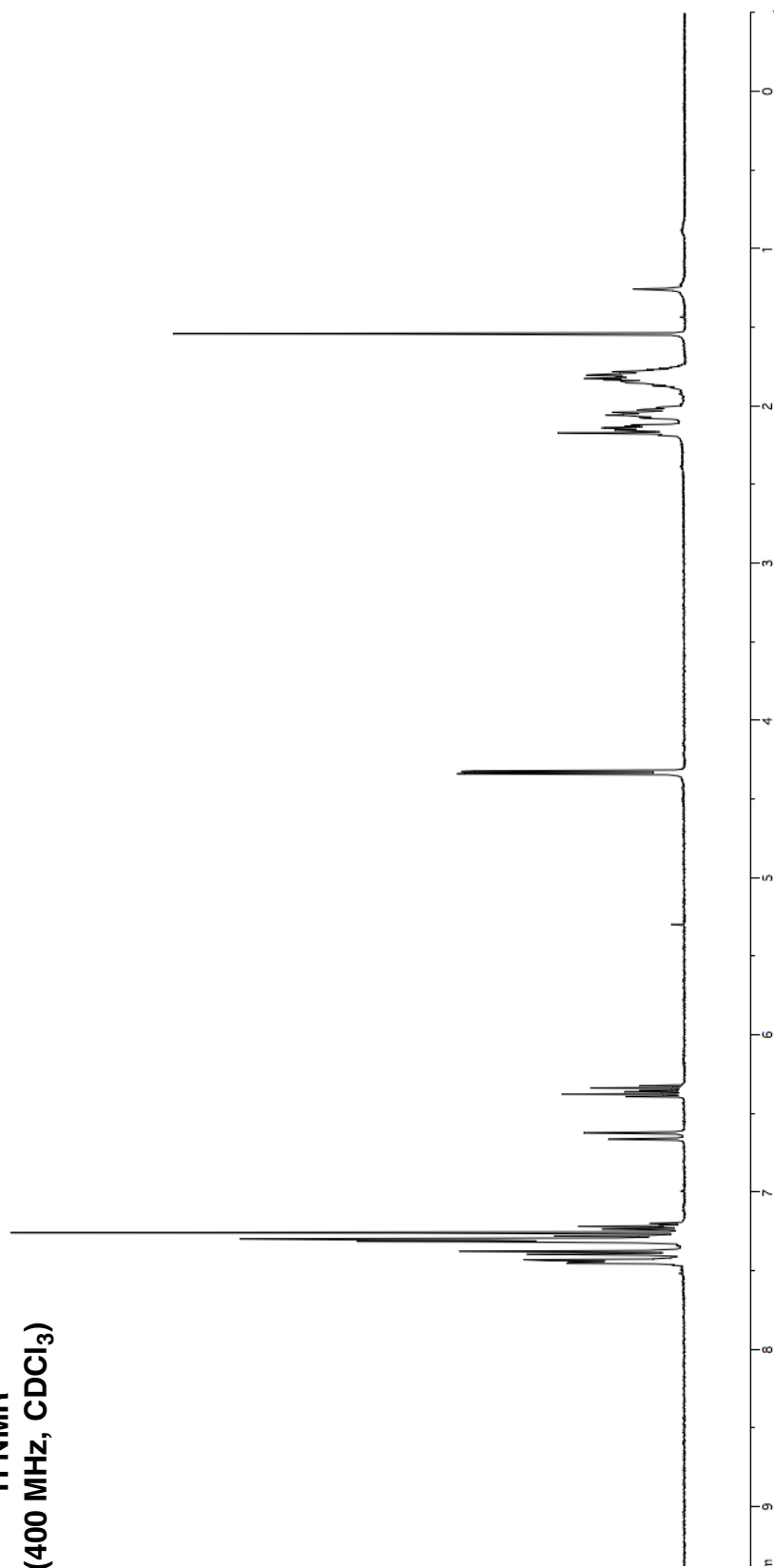


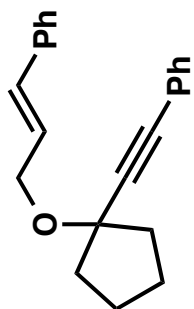
**2-68**  
**<sup>13</sup>C NMR**  
**(100 MHz, CDCl<sub>3</sub>)**





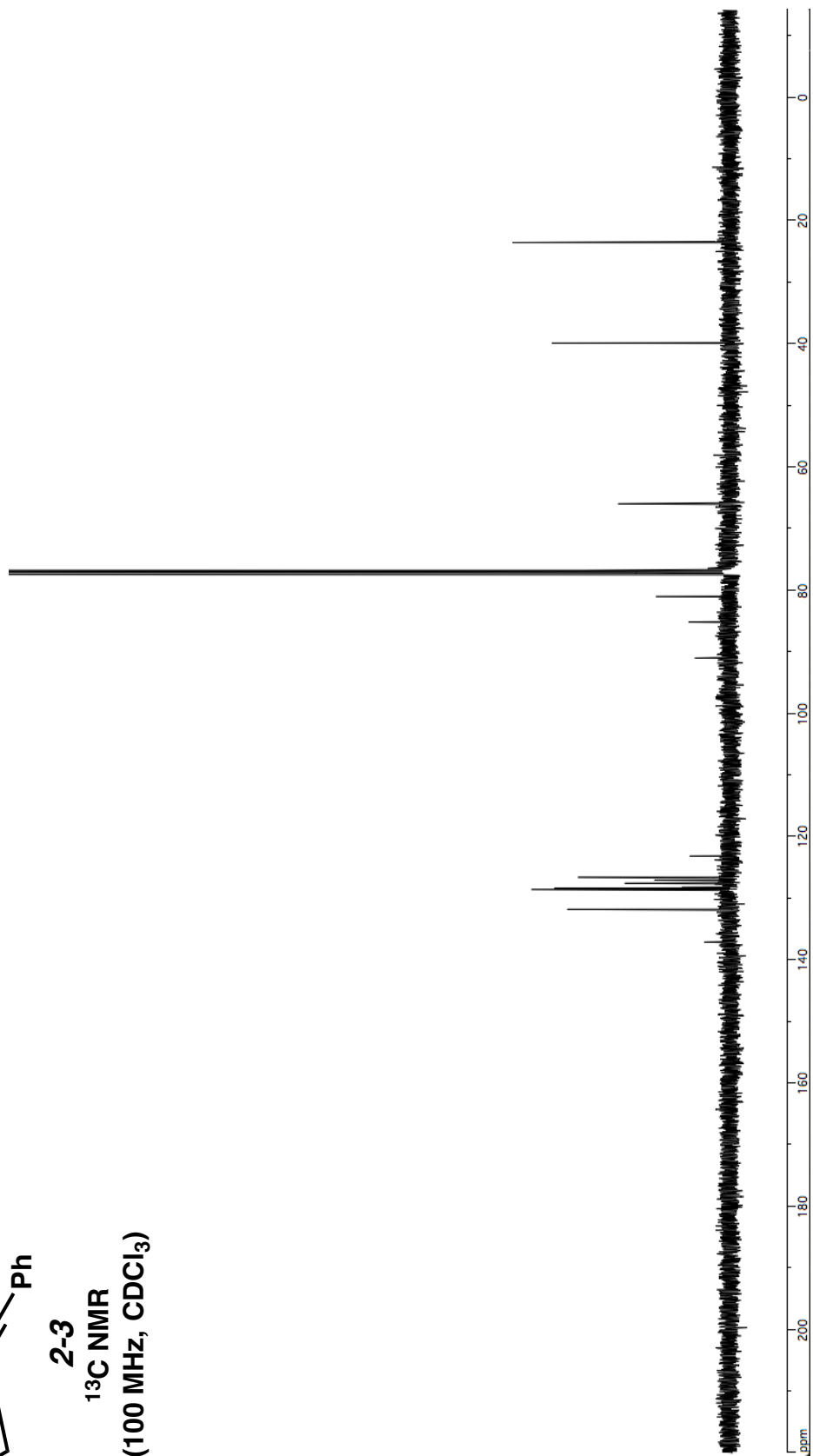
2-3  
<sup>1</sup>H NMR  
(400 MHz, CDCl<sub>3</sub>)

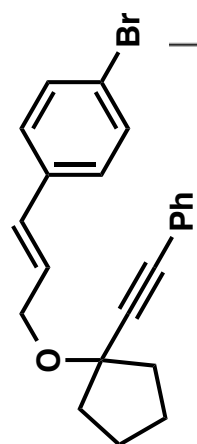




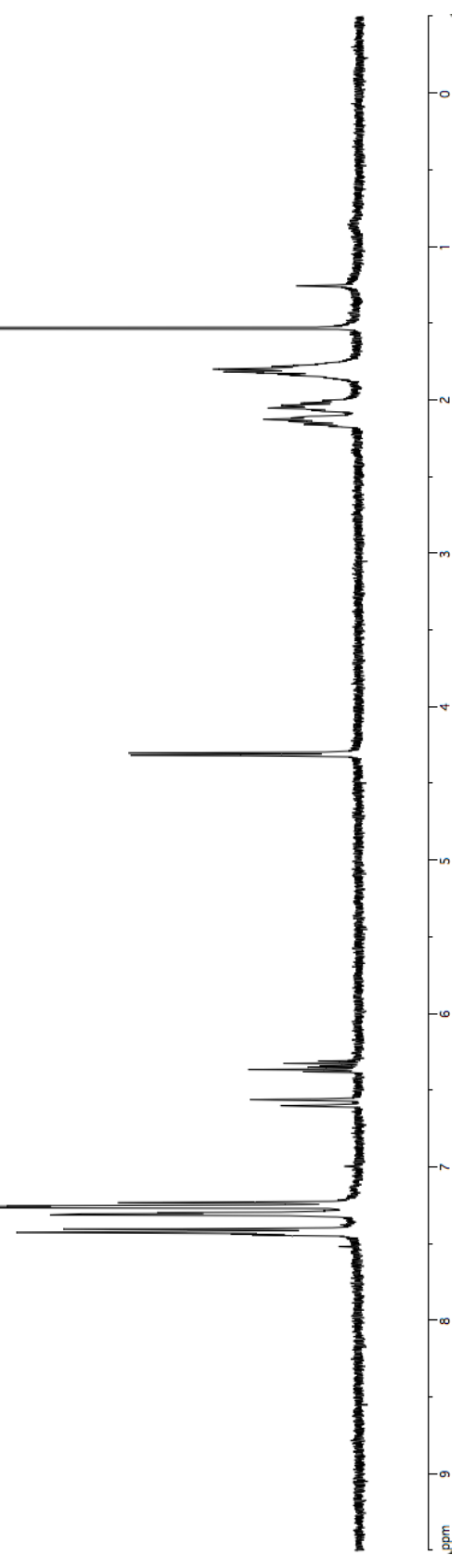
2-3

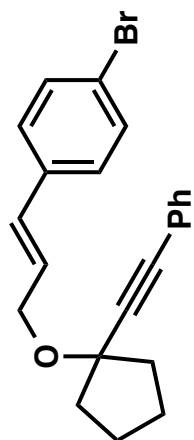
<sup>13</sup>C NMR  
(100 MHz, CDCl<sub>3</sub>)



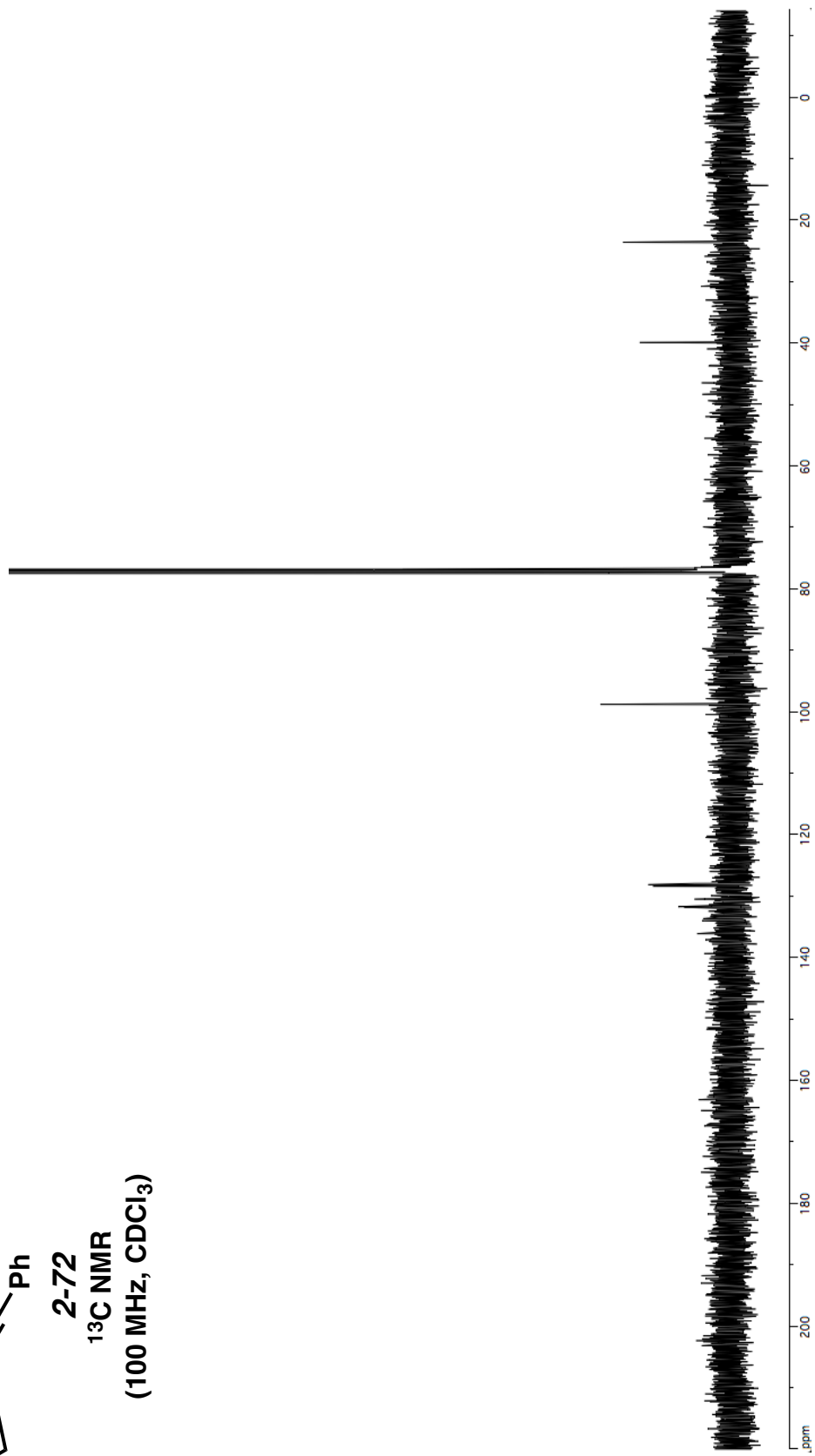


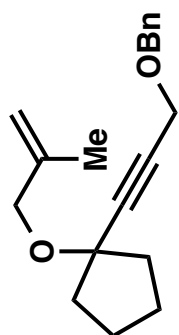
2-72  
<sup>1</sup>H NMR  
(400 MHz, CDCl<sub>3</sub>)



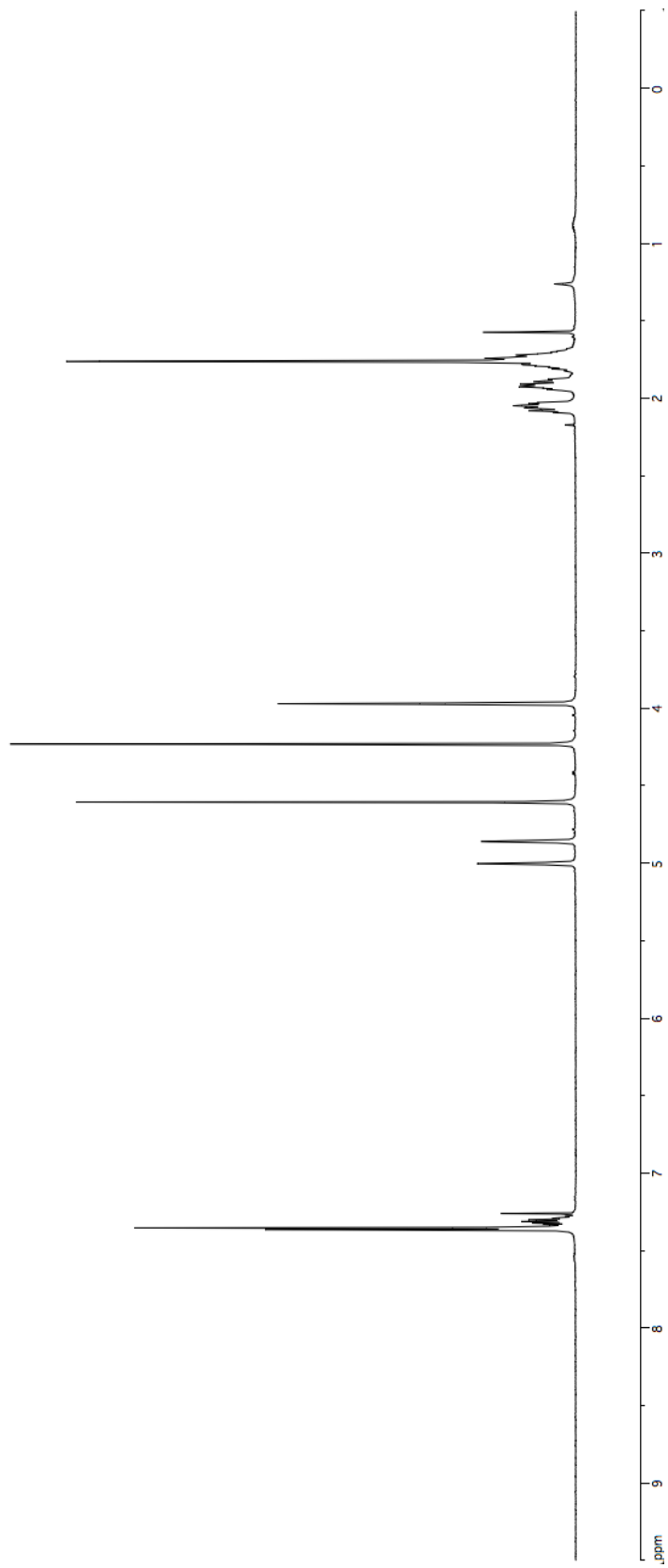


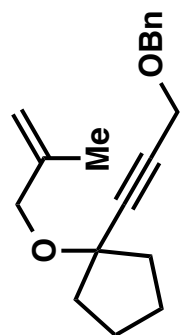
**2-72**  
**<sup>13</sup>C NMR**  
**(100 MHz, CDCl<sub>3</sub>)**



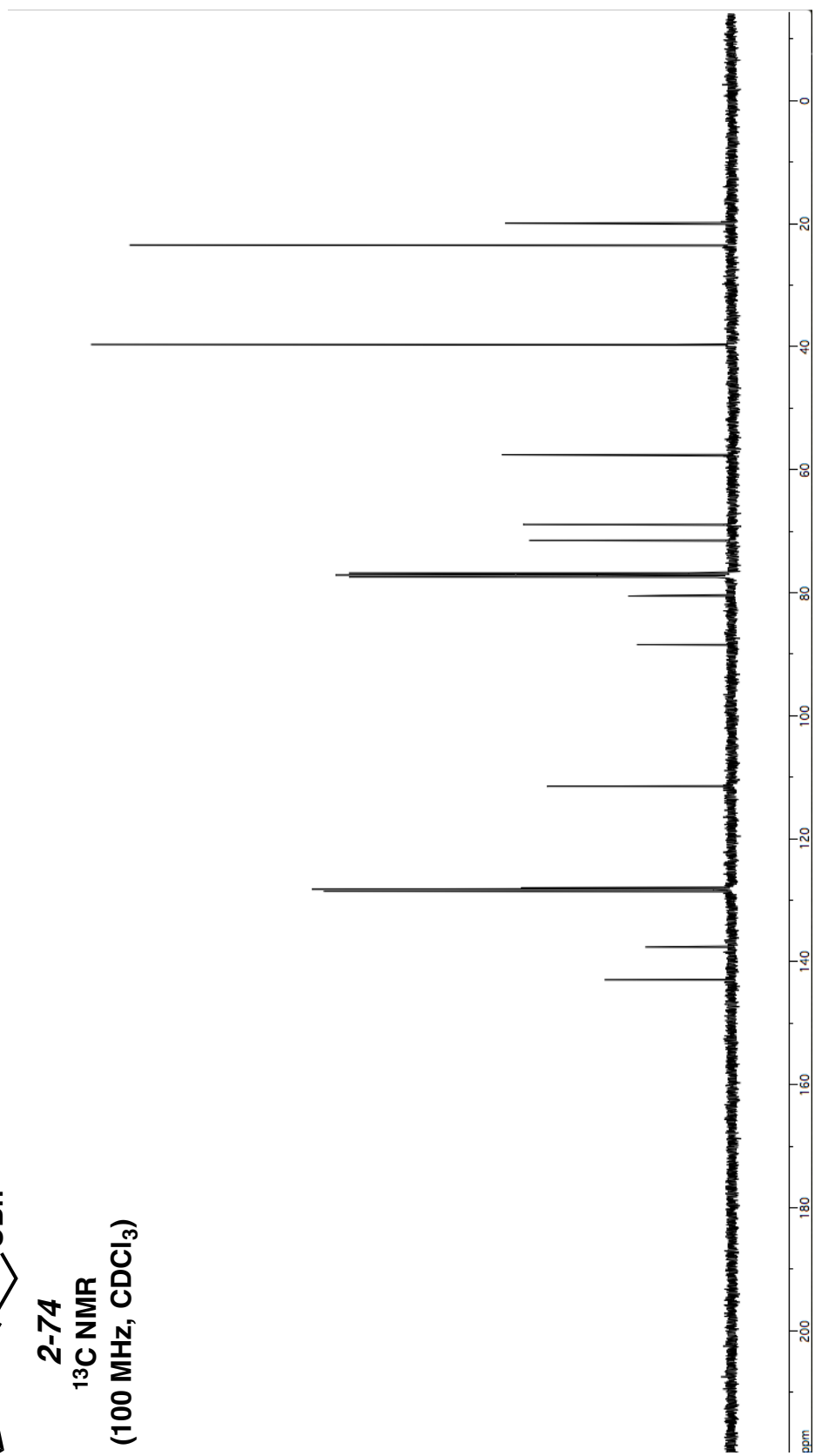


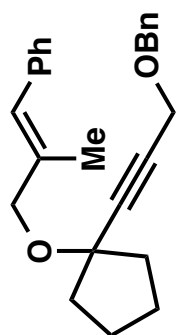
**2-74**  
**<sup>1</sup>H NMR**  
**(400 MHz, CDCl<sub>3</sub>)**



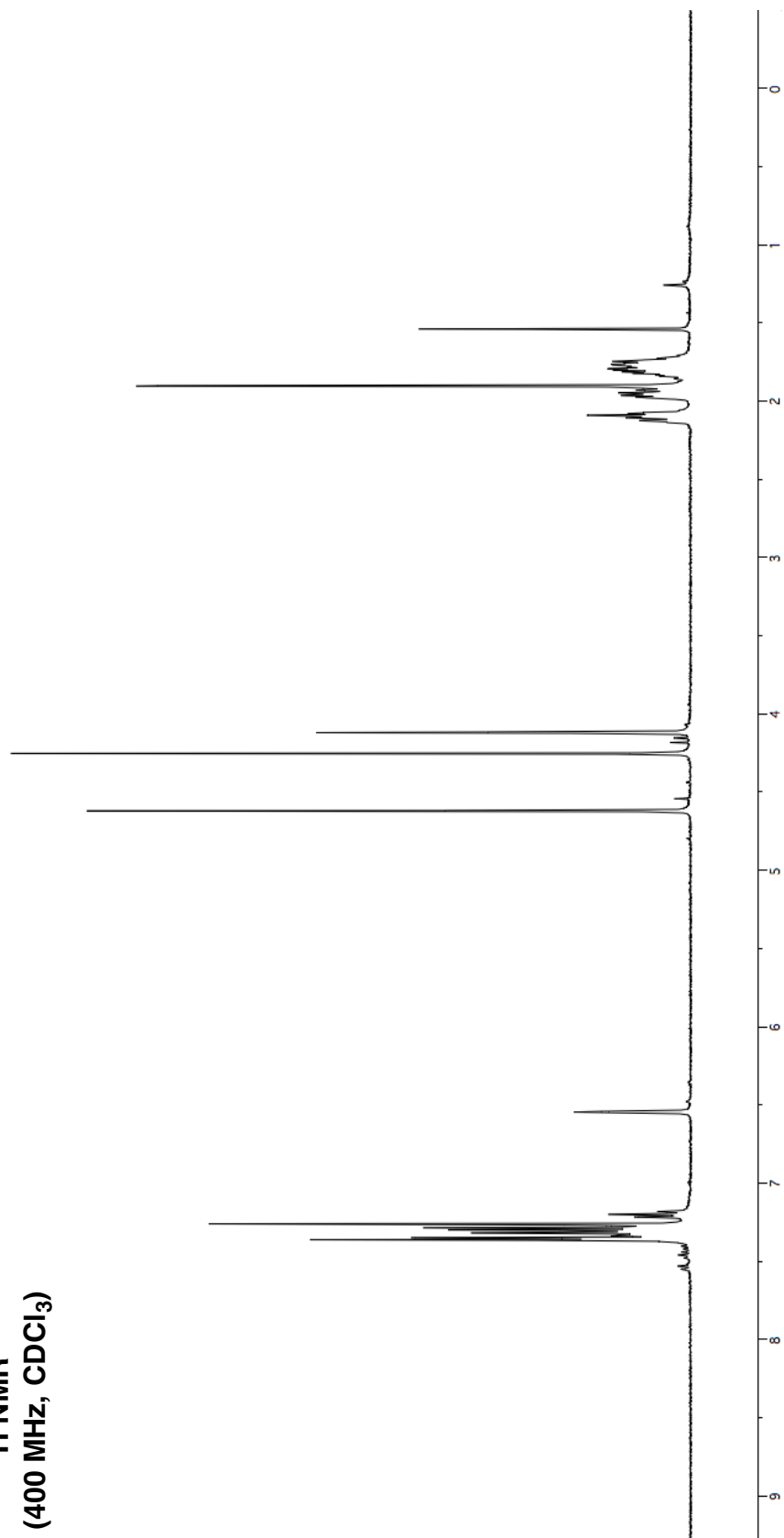


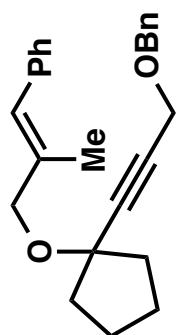
**2-74**  
**<sup>13</sup>C NMR**  
**(100 MHz, CDCl<sub>3</sub>)**



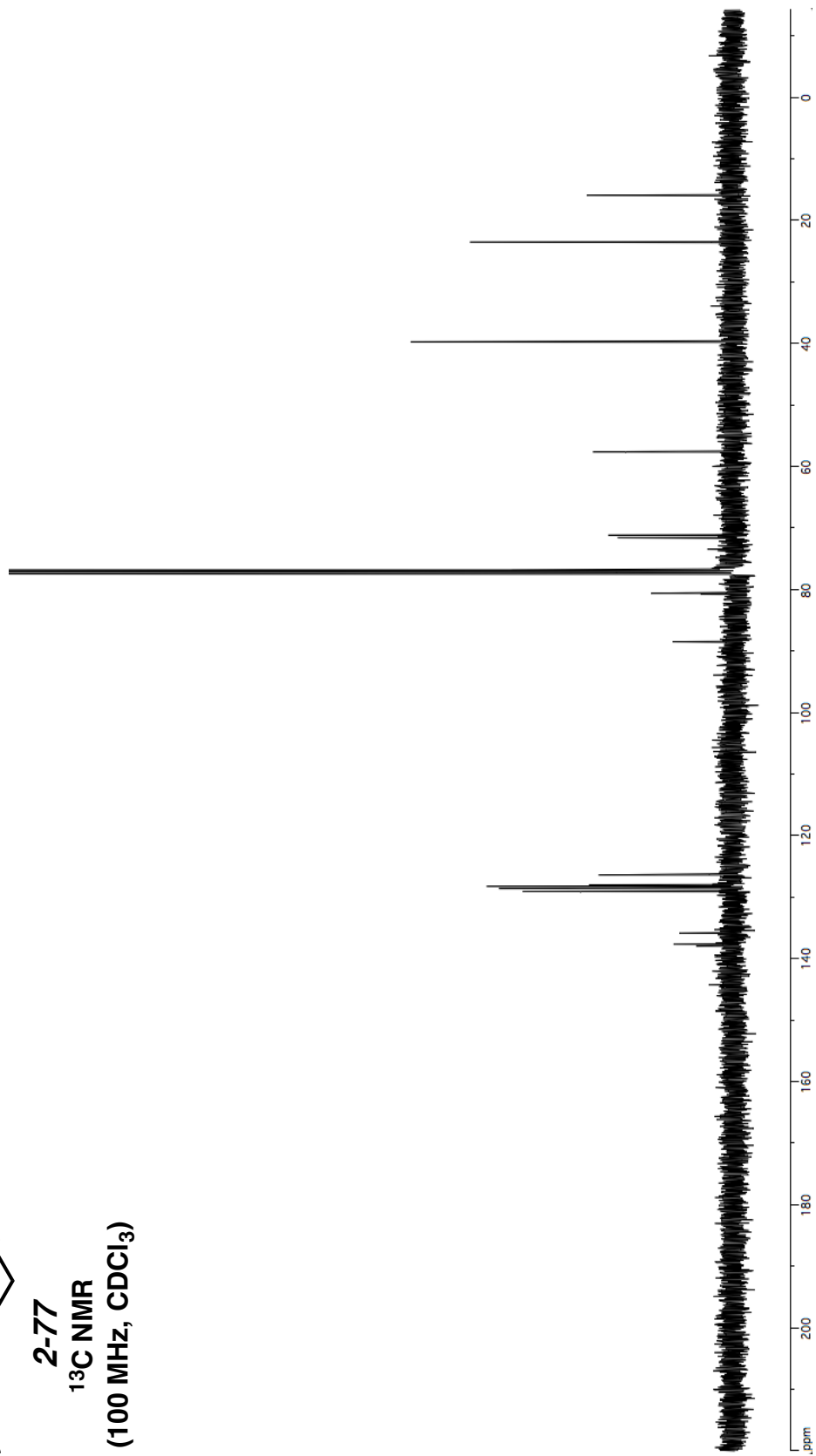


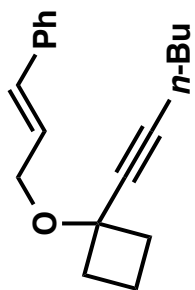
2-77  
<sup>1</sup>H NMR  
(400 MHz, CDCl<sub>3</sub>)





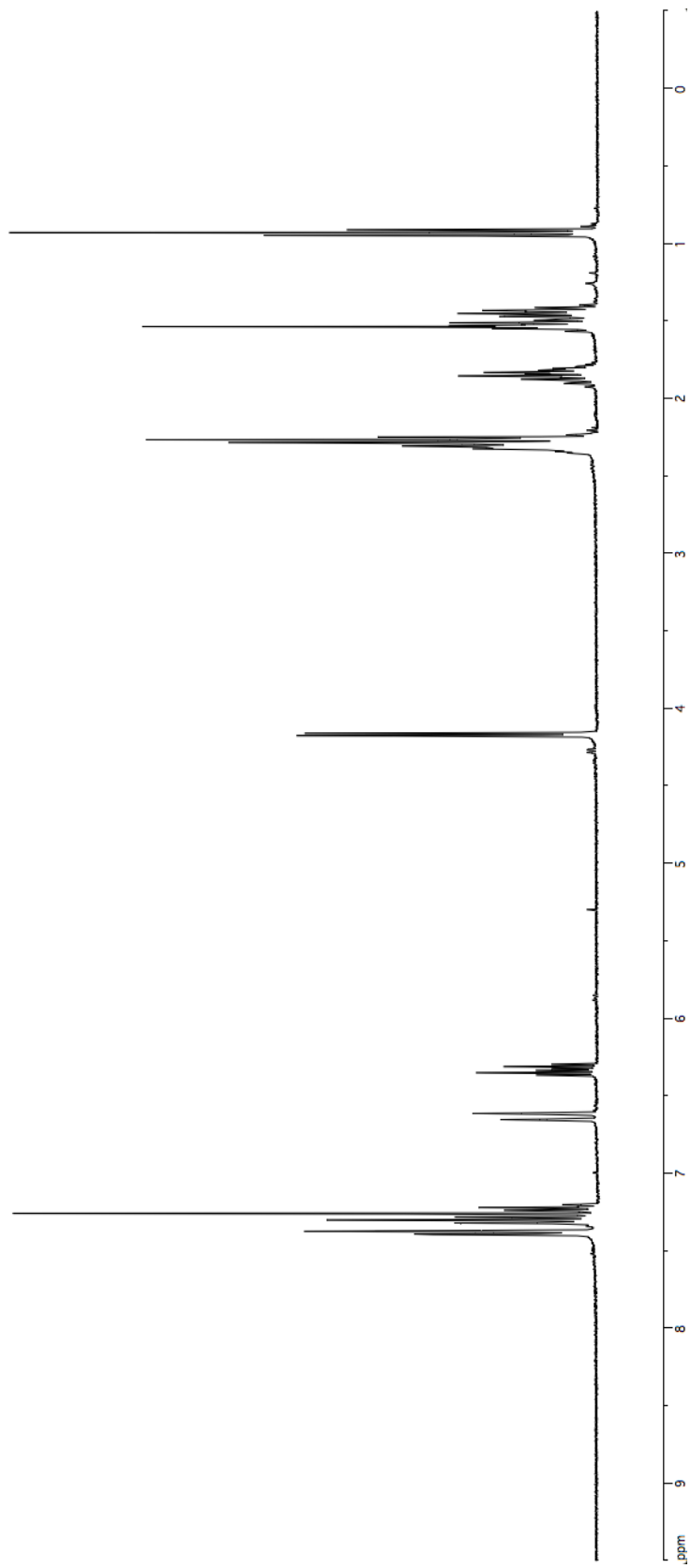
**2-77**  
**<sup>13</sup>C NMR**  
**(100 MHz, CDCl<sub>3</sub>)**

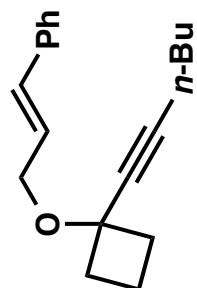




2-79

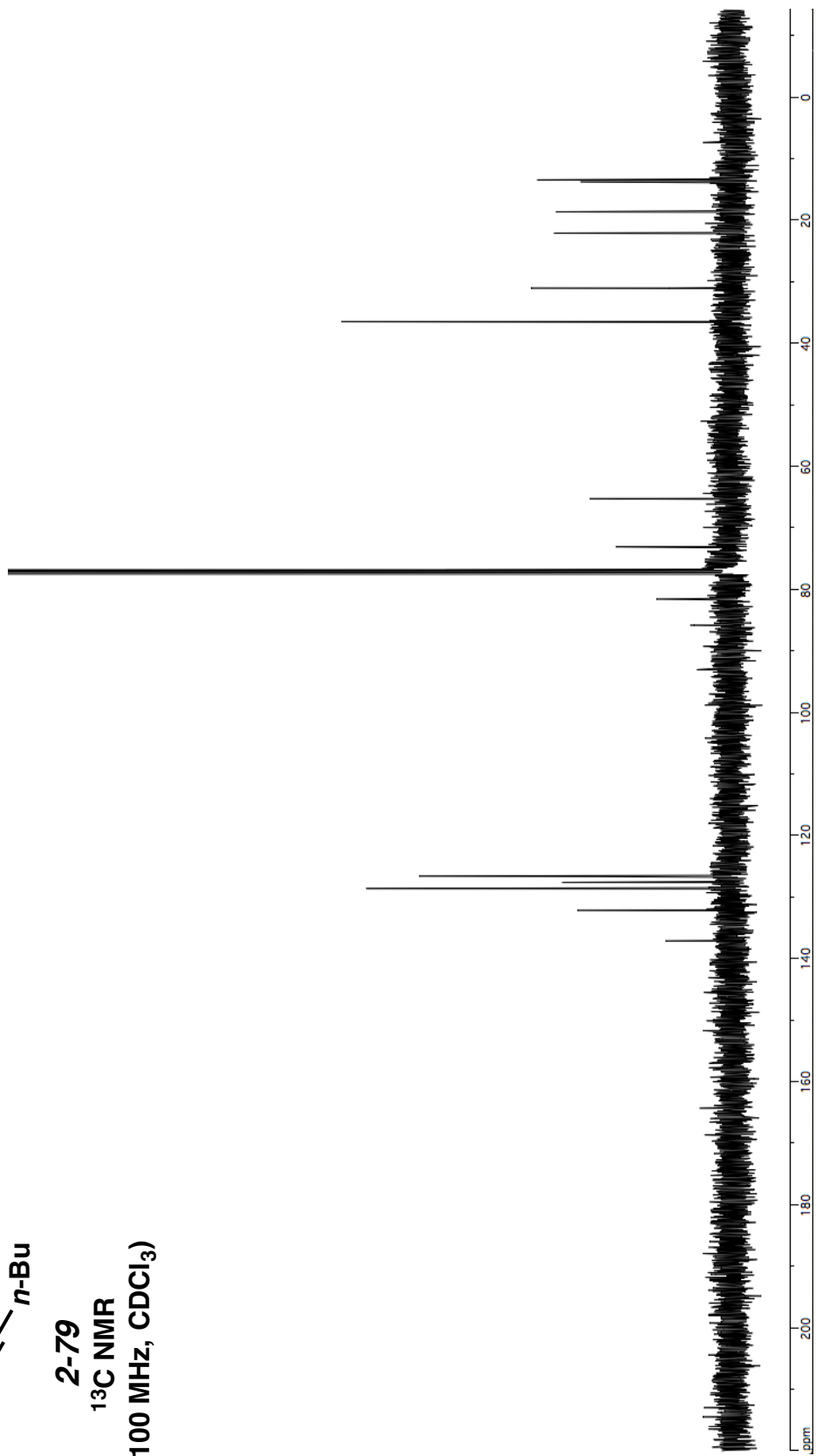
<sup>1</sup>H NMR  
(400 MHz, CDCl<sub>3</sub>)

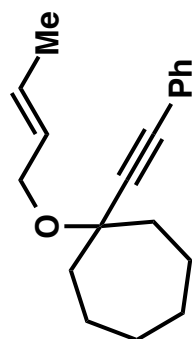




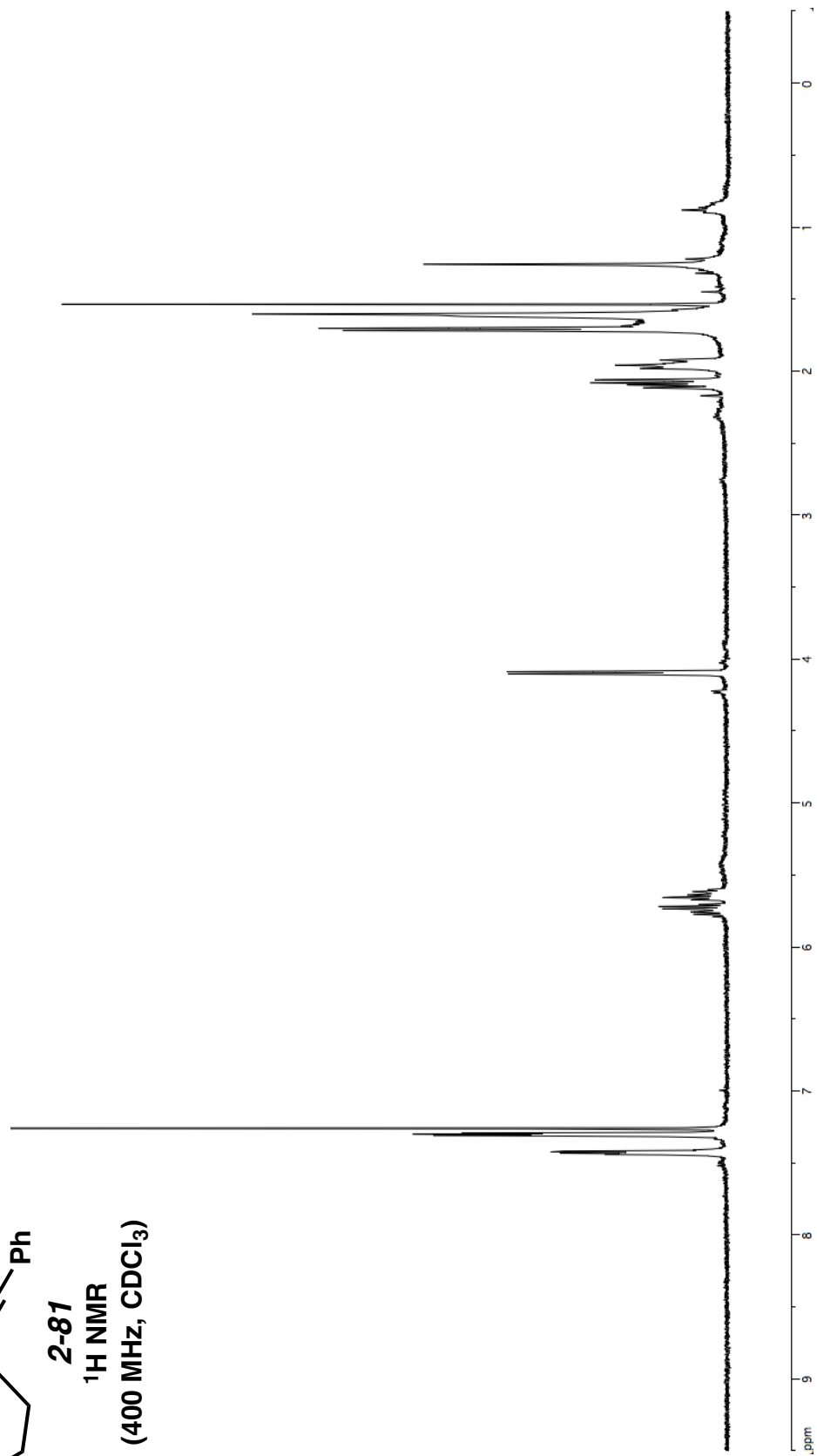
2-79

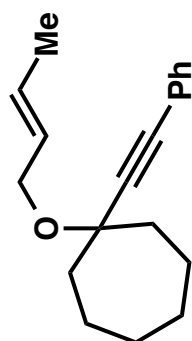
<sup>13</sup>C NMR  
(100 MHz, CDCl<sub>3</sub>)



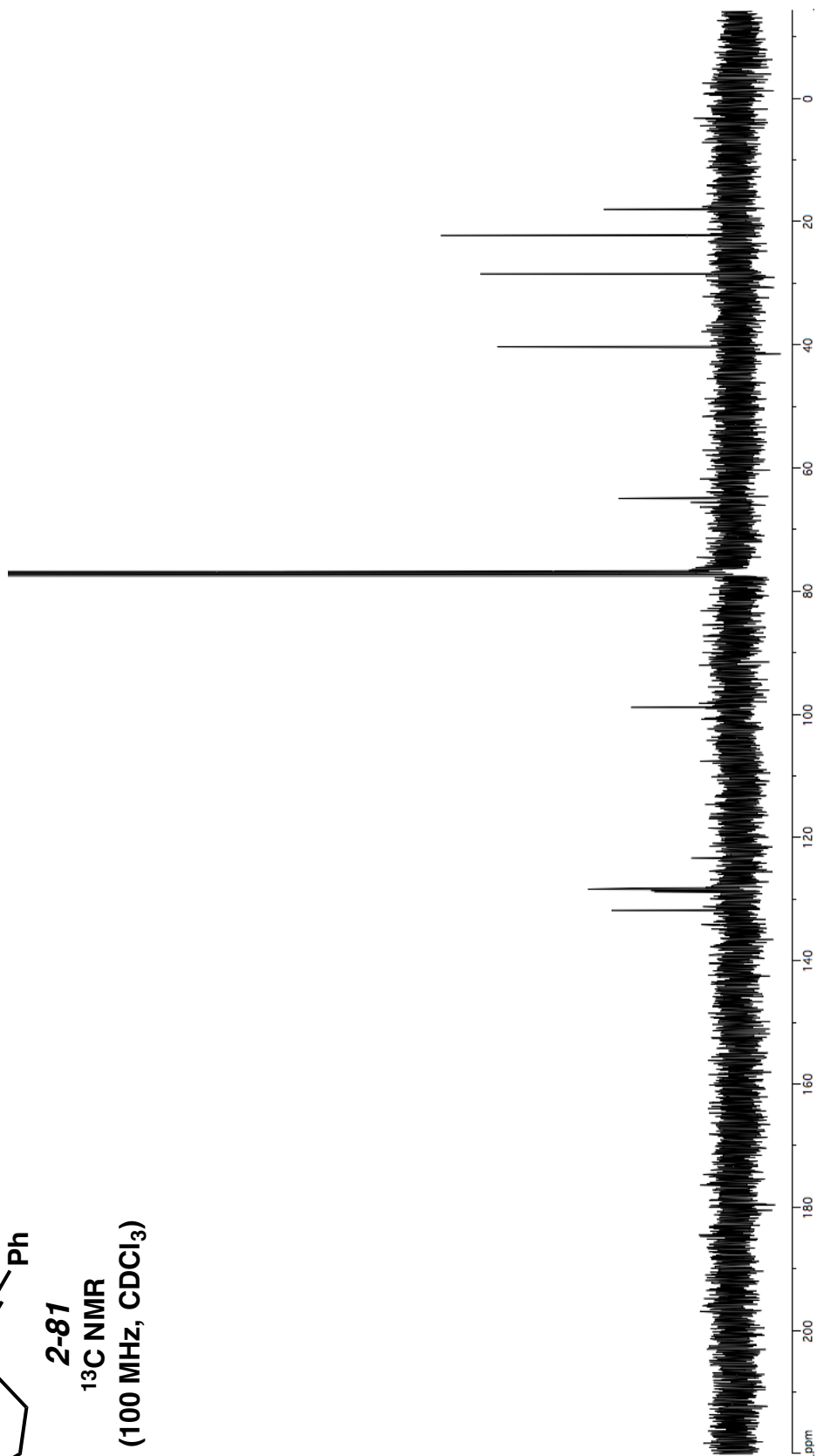


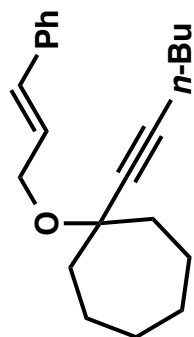
**2-81**  
<sup>1</sup>H NMR  
(400 MHz, CDCl<sub>3</sub>)



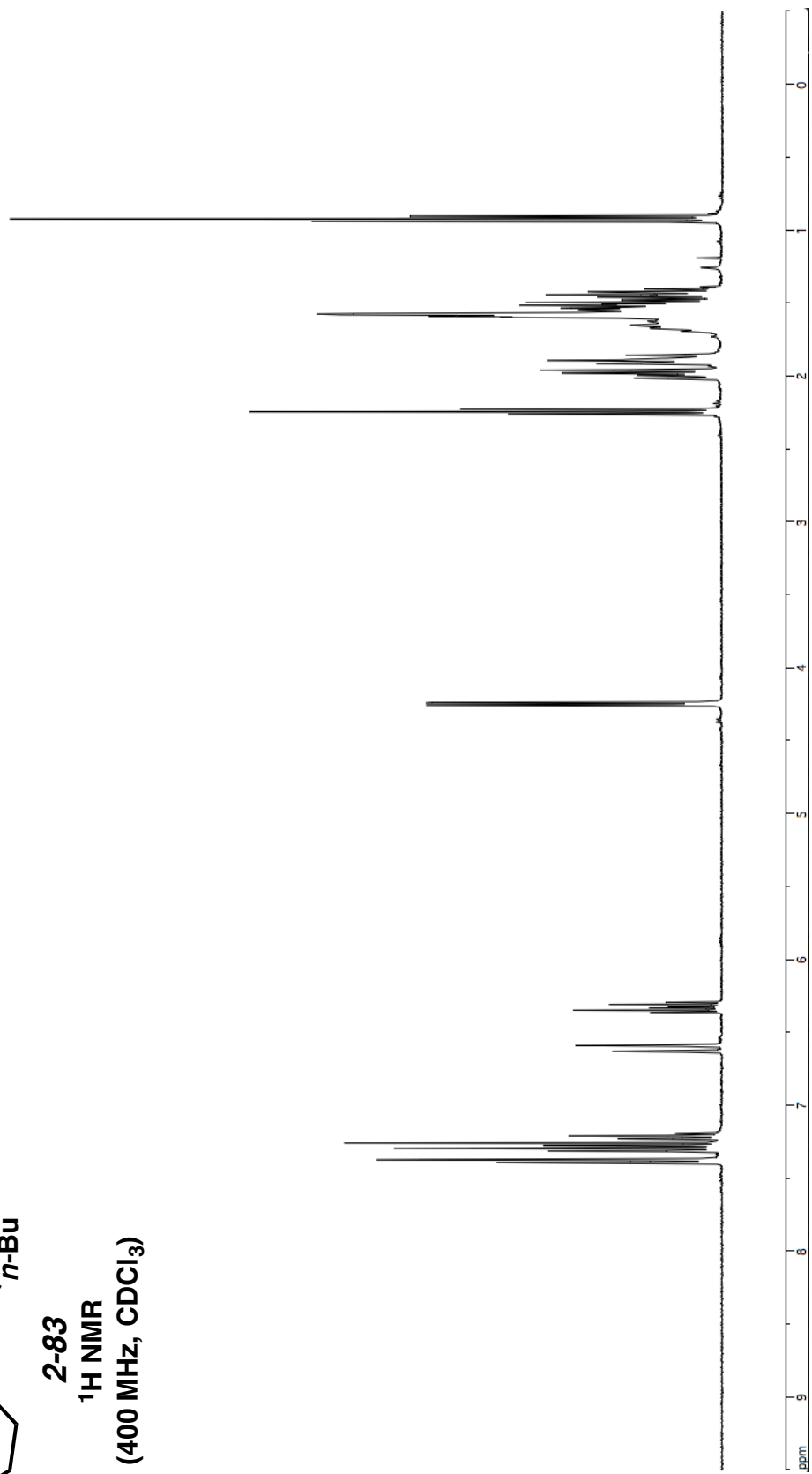


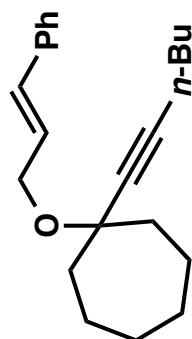
**2-81**  
**<sup>13</sup>C NMR**  
**(100 MHz, CDCl<sub>3</sub>)**





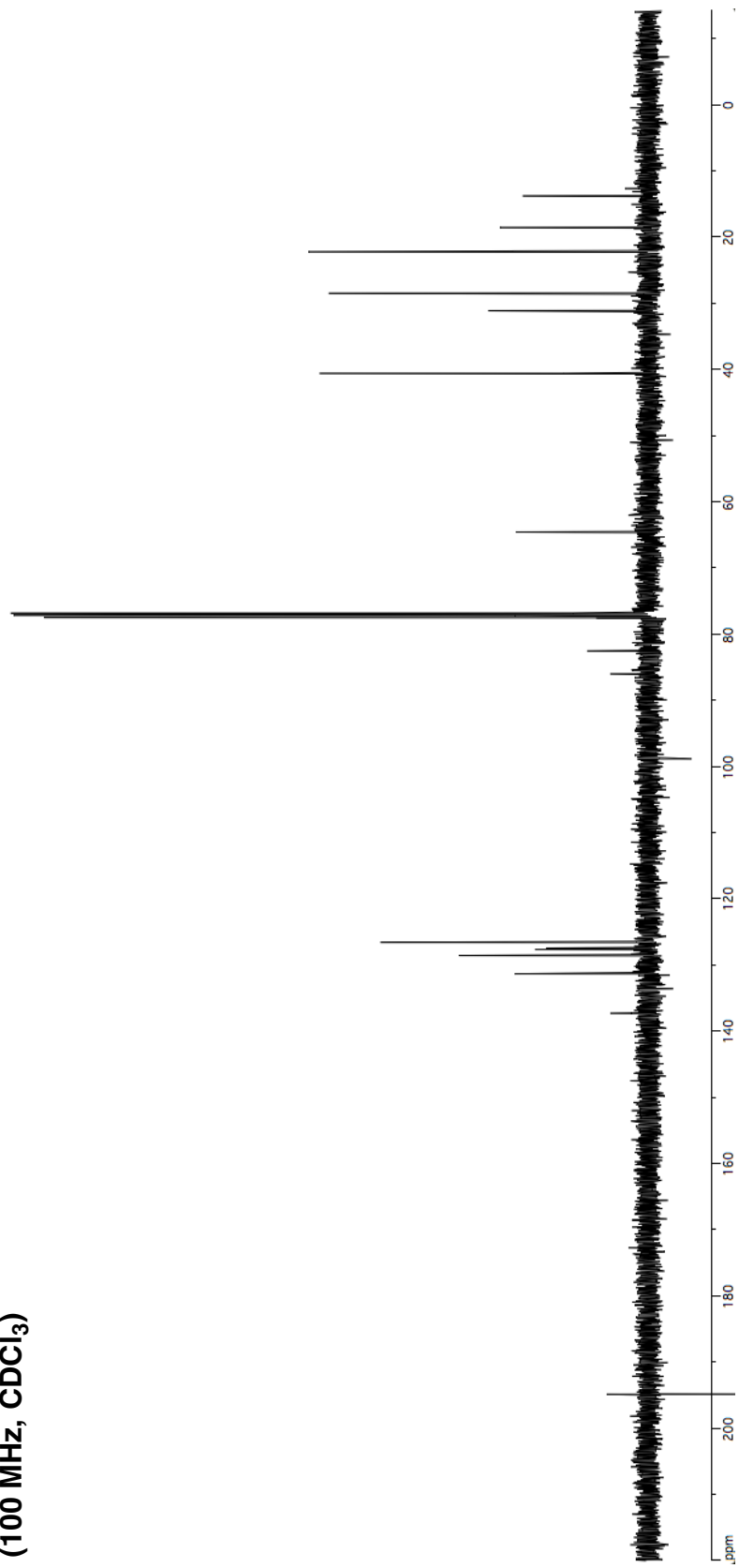
**2-83**  
**<sup>1</sup>H NMR**  
**(400 MHz, CDCl<sub>3</sub>)**

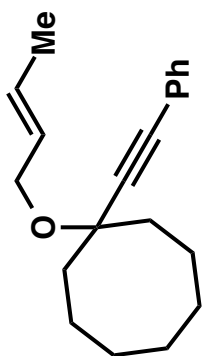




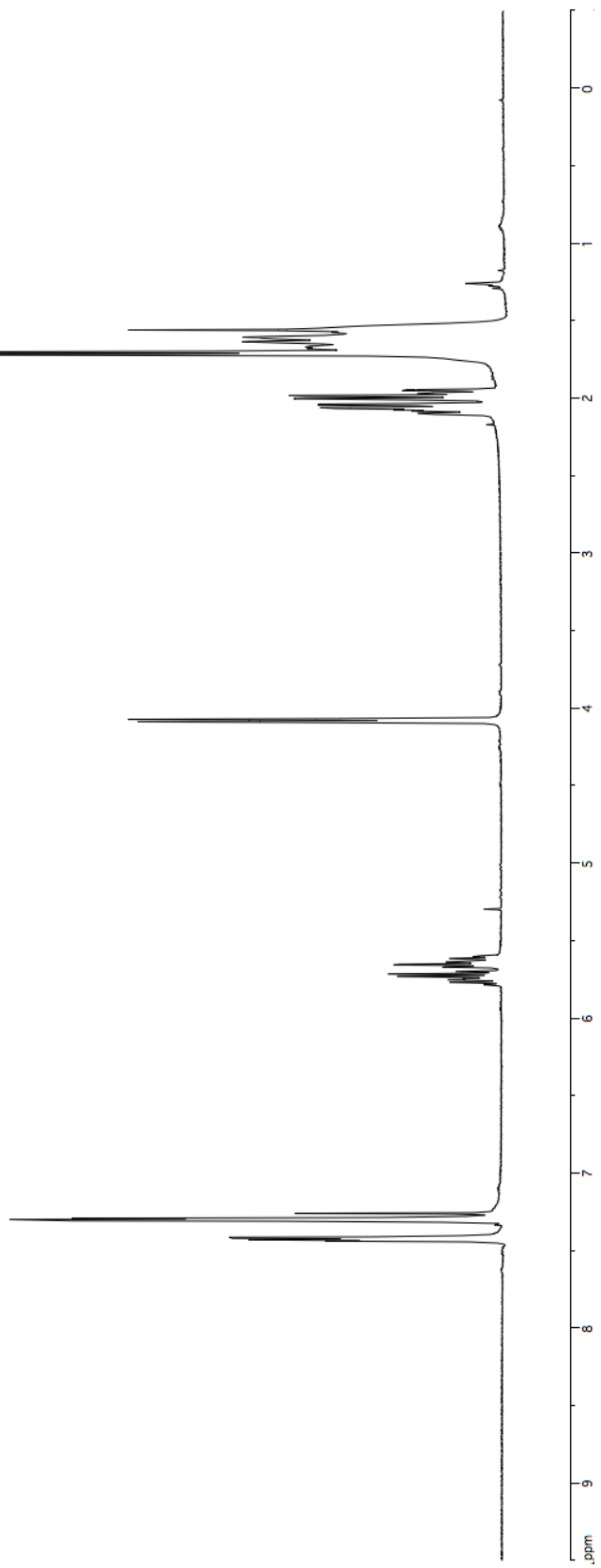
**2-83**

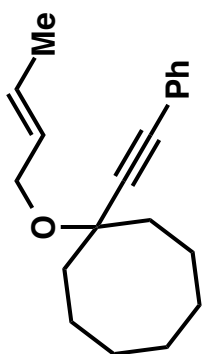
<sup>13</sup>C NMR  
(100 MHz, CDCl<sub>3</sub>)



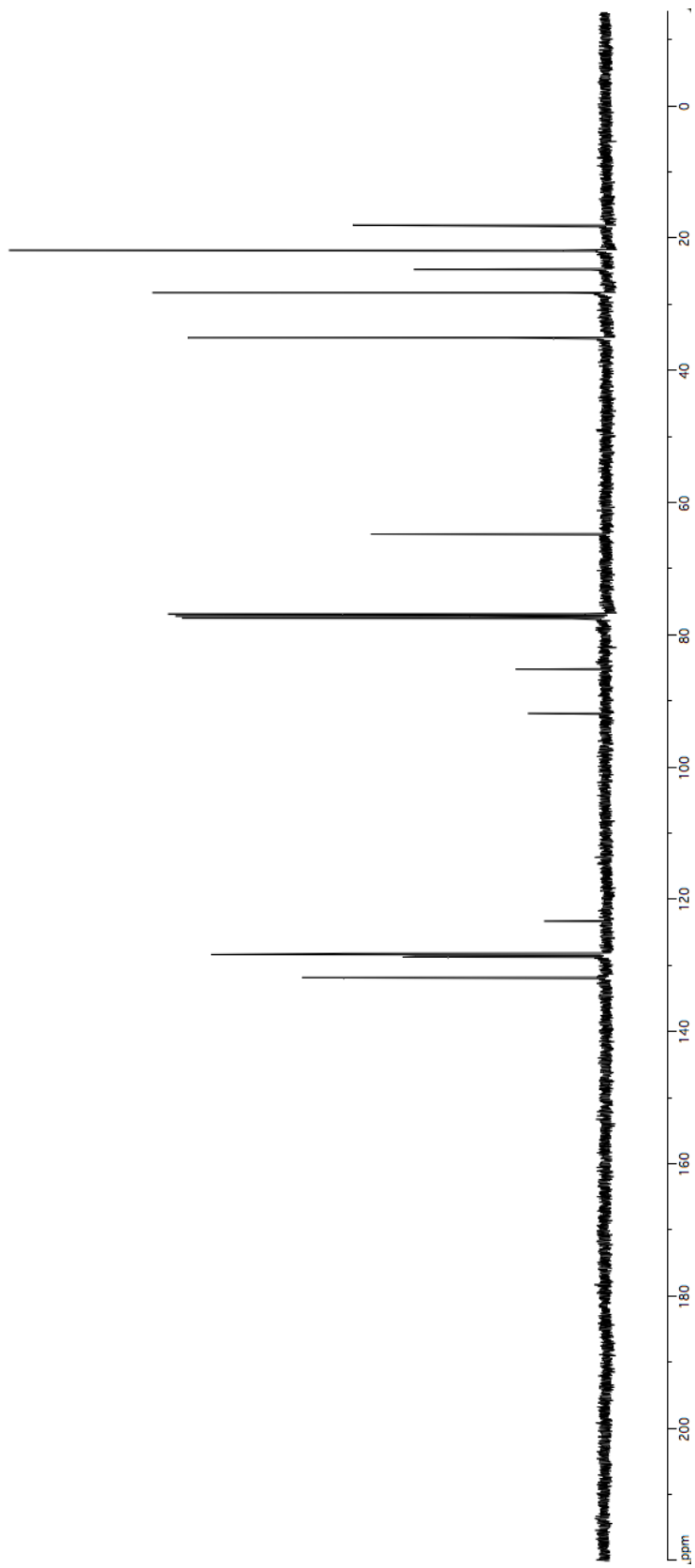


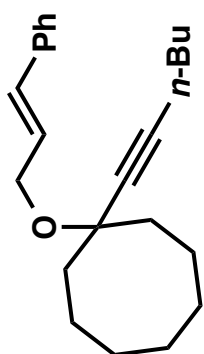
**2-85**  
**<sup>1</sup>H NMR**  
**(400 MHz, CDCl<sub>3</sub>)**



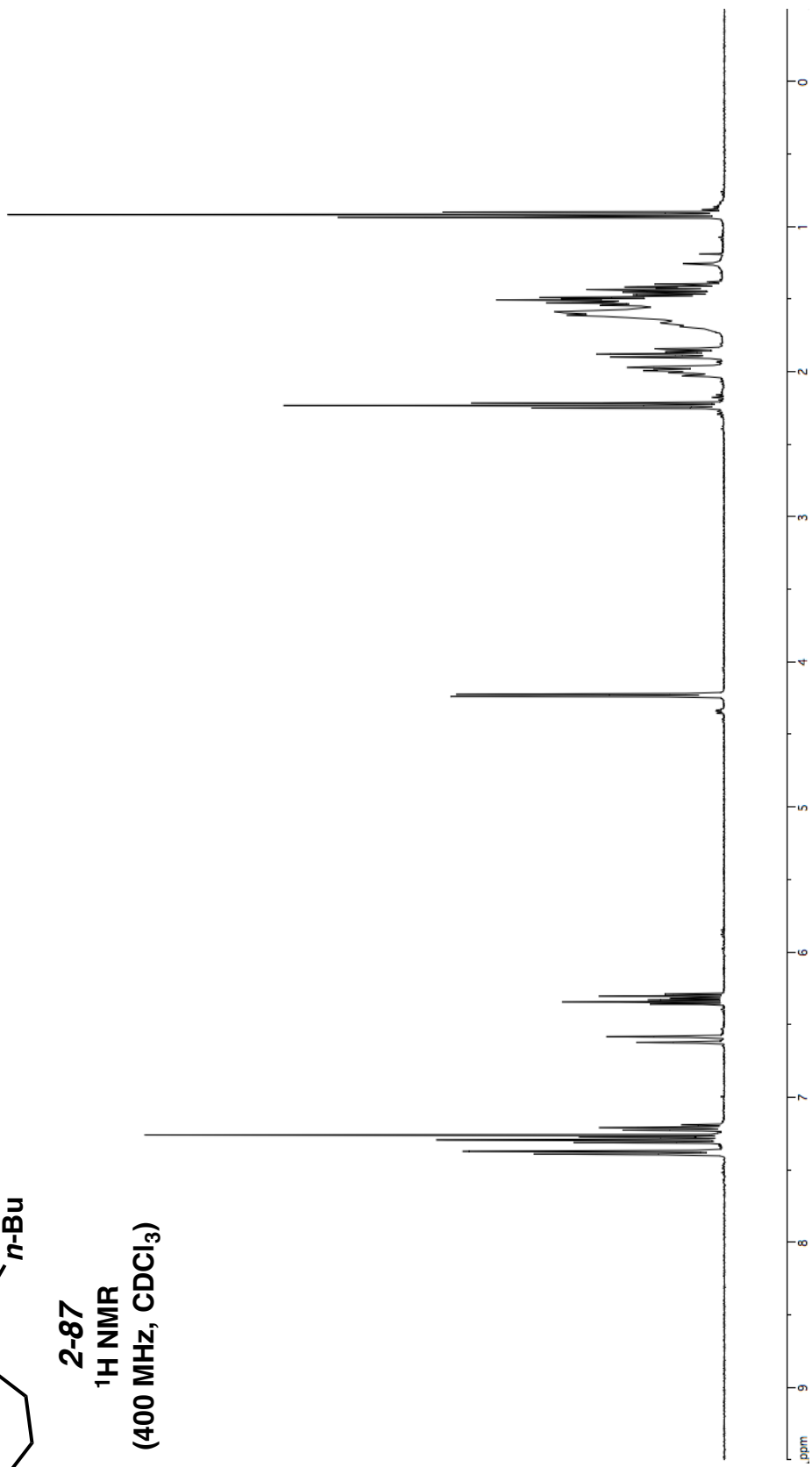


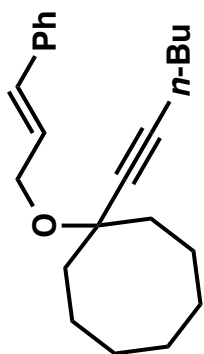
**2-85**  
**<sup>13</sup>C NMR**  
**(100 MHz, CDCl<sub>3</sub>)**



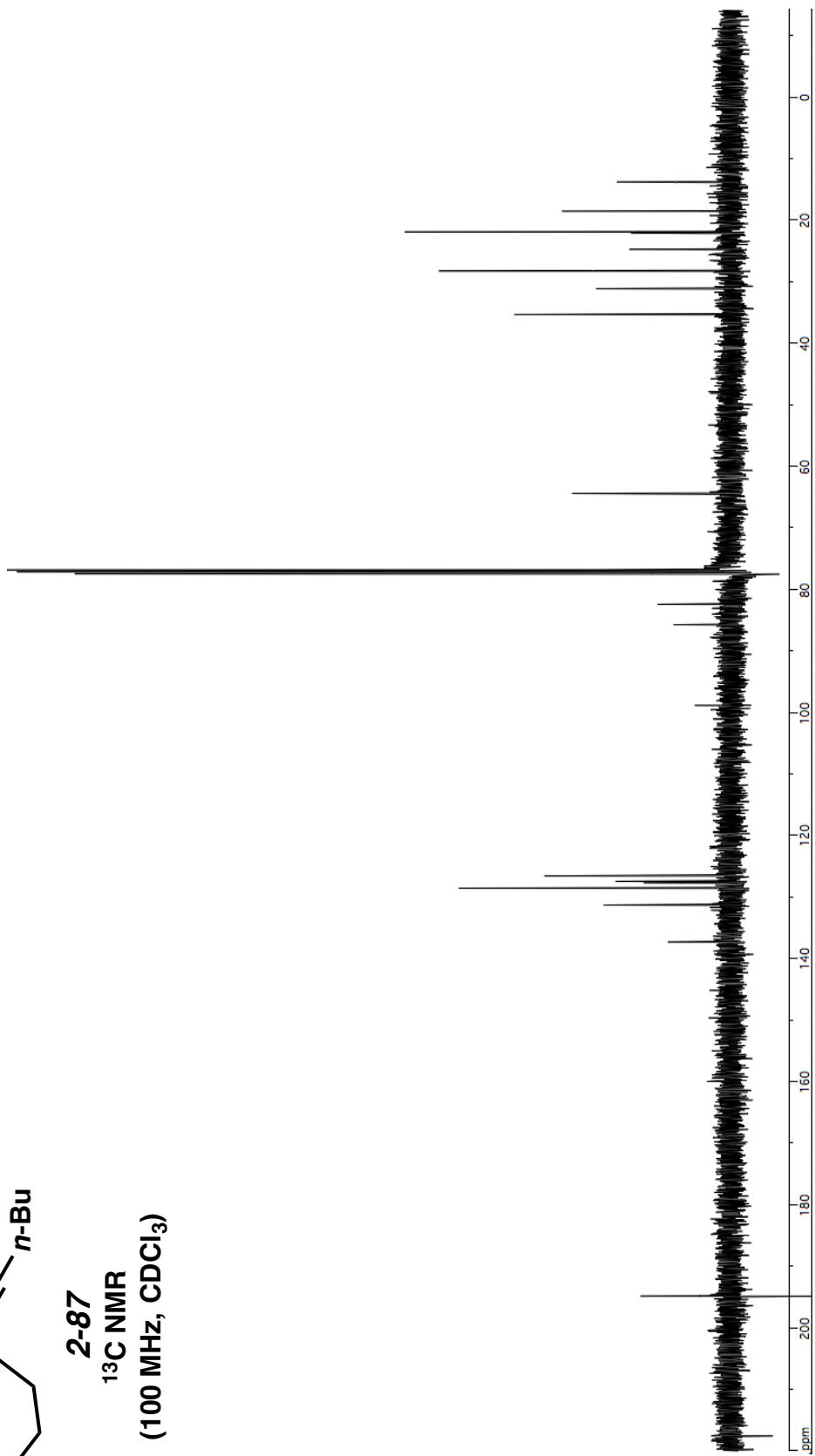


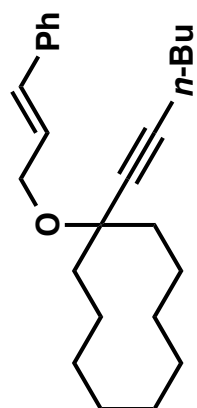
**2-87**  
**<sup>1</sup>H NMR**  
**(400 MHz, CDCl<sub>3</sub>)**



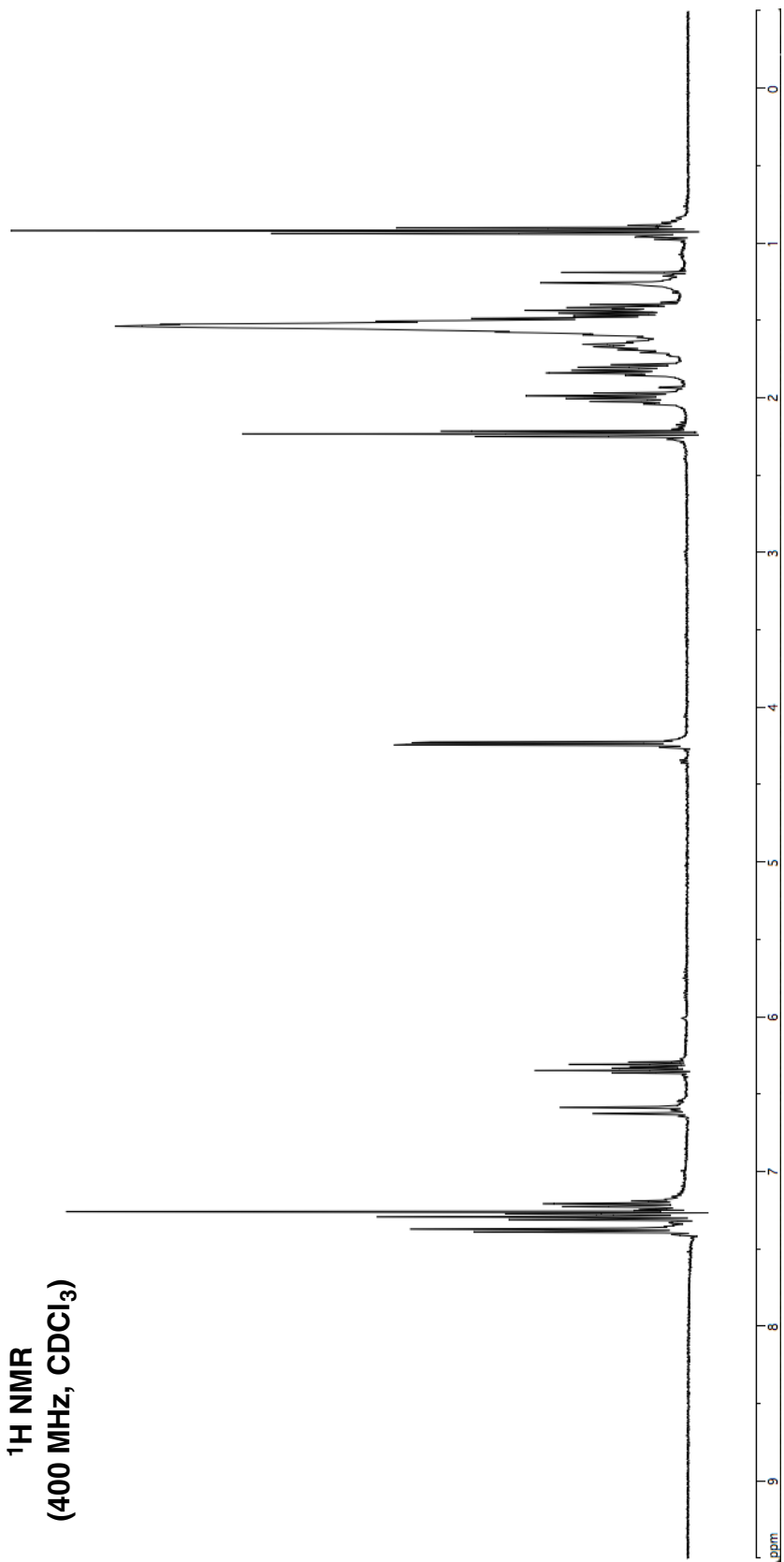


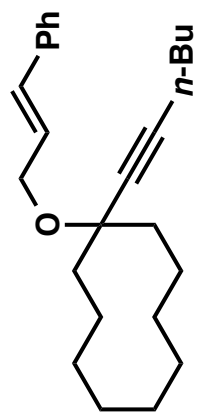
**2-87**  
<sup>13</sup>C NMR  
(100 MHz, CDCl<sub>3</sub>)





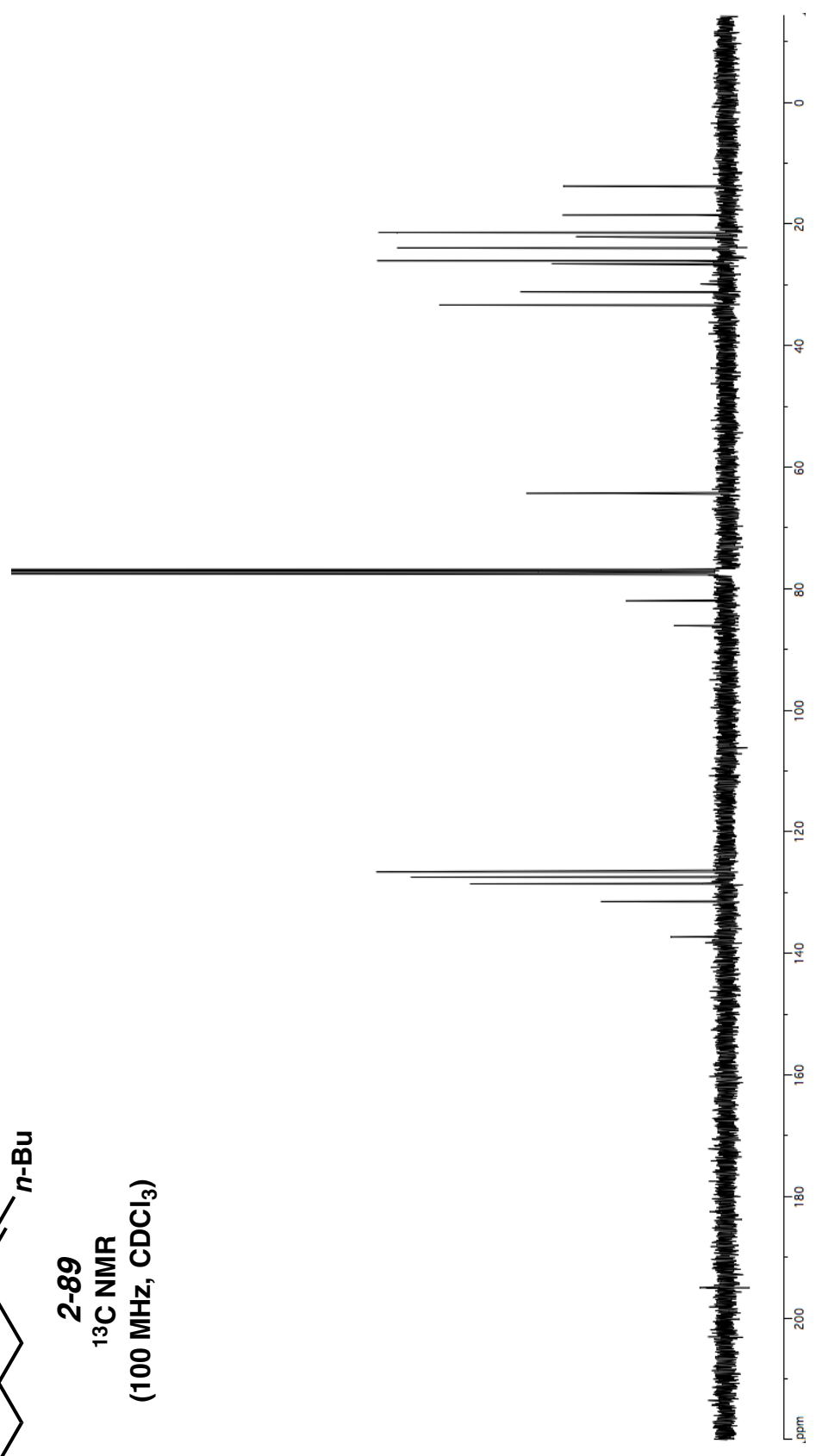
**2-89**  
**<sup>1</sup>H NMR**  
**(400 MHz, CDCl<sub>3</sub>)**

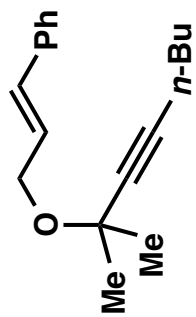




2-89

<sup>13</sup>C NMR  
(100 MHz, CDCl<sub>3</sub>)

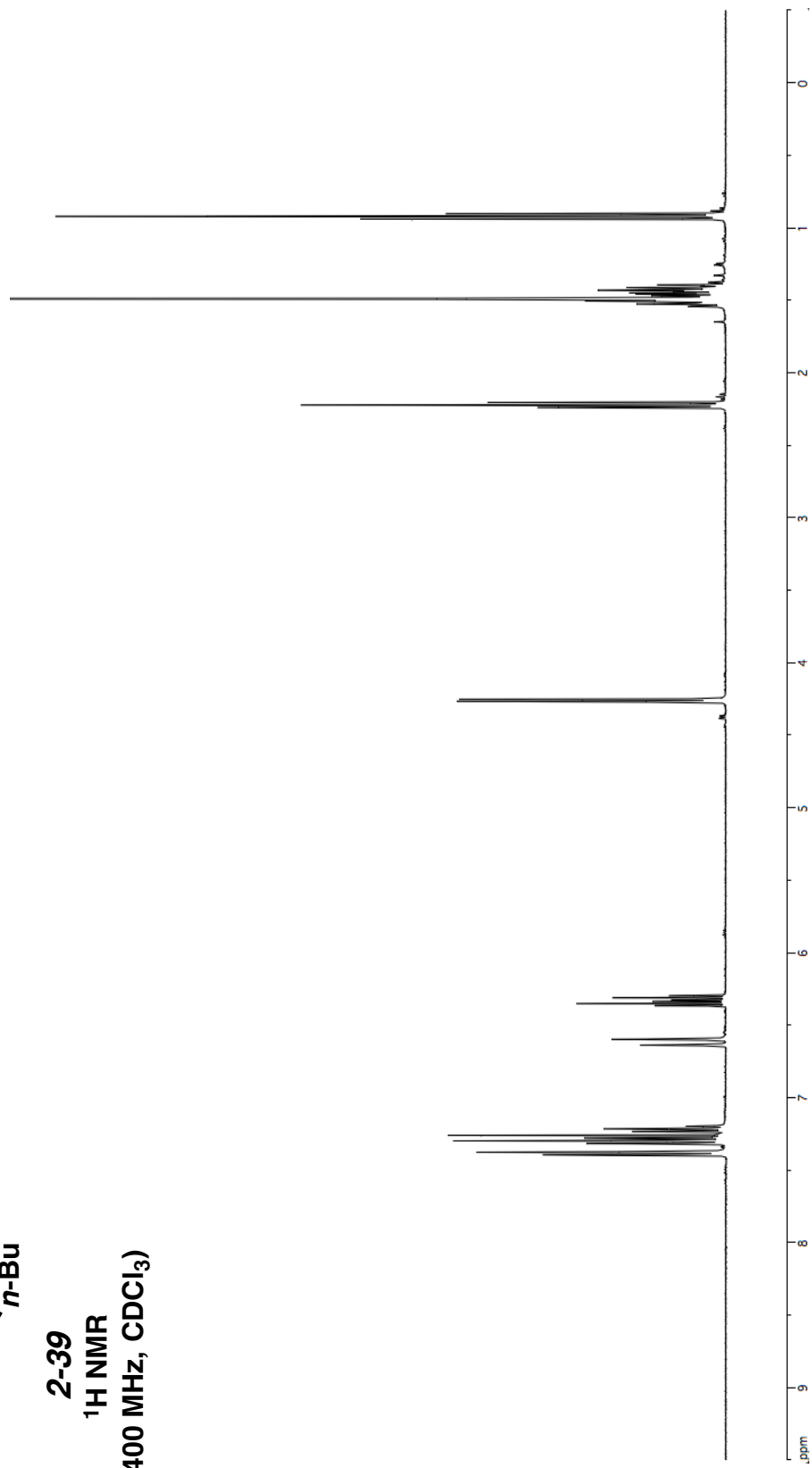


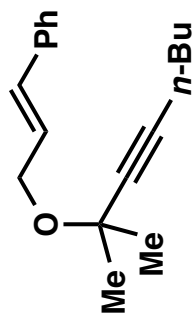


2-39

<sup>1</sup>H NMR

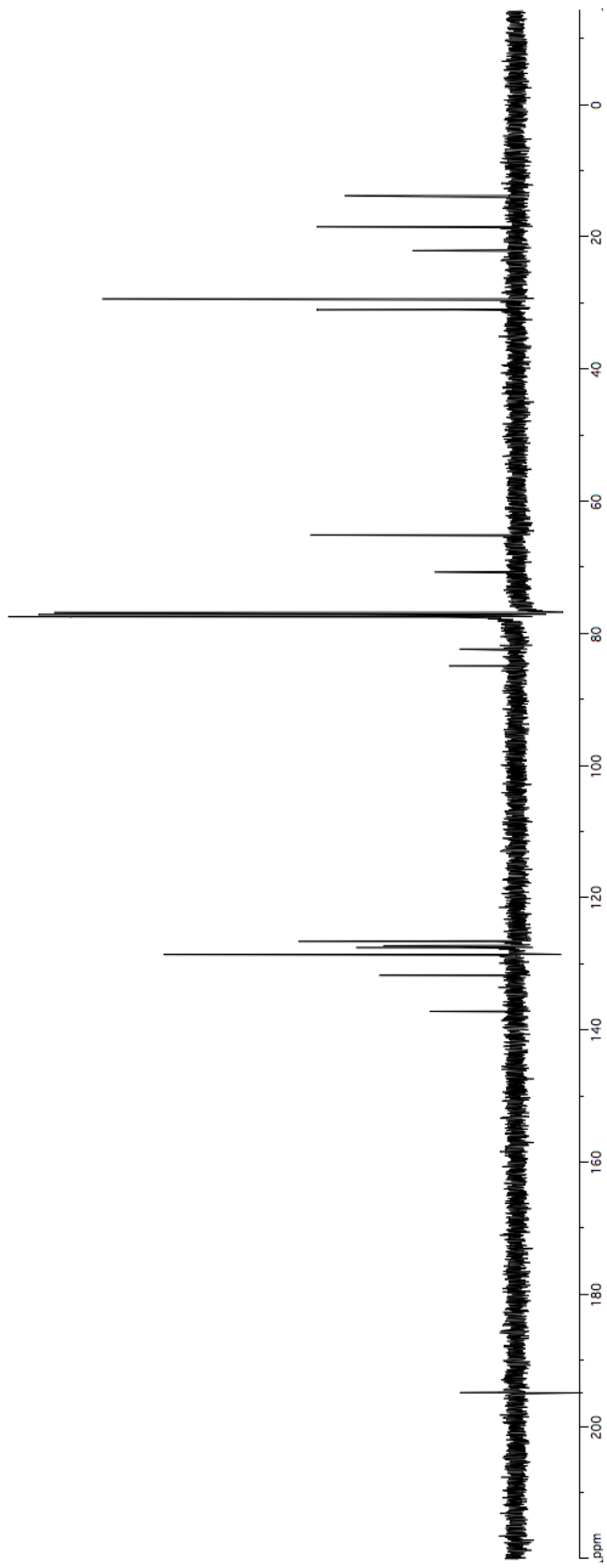
(400 MHz, CDCl<sub>3</sub>)

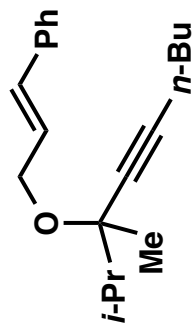




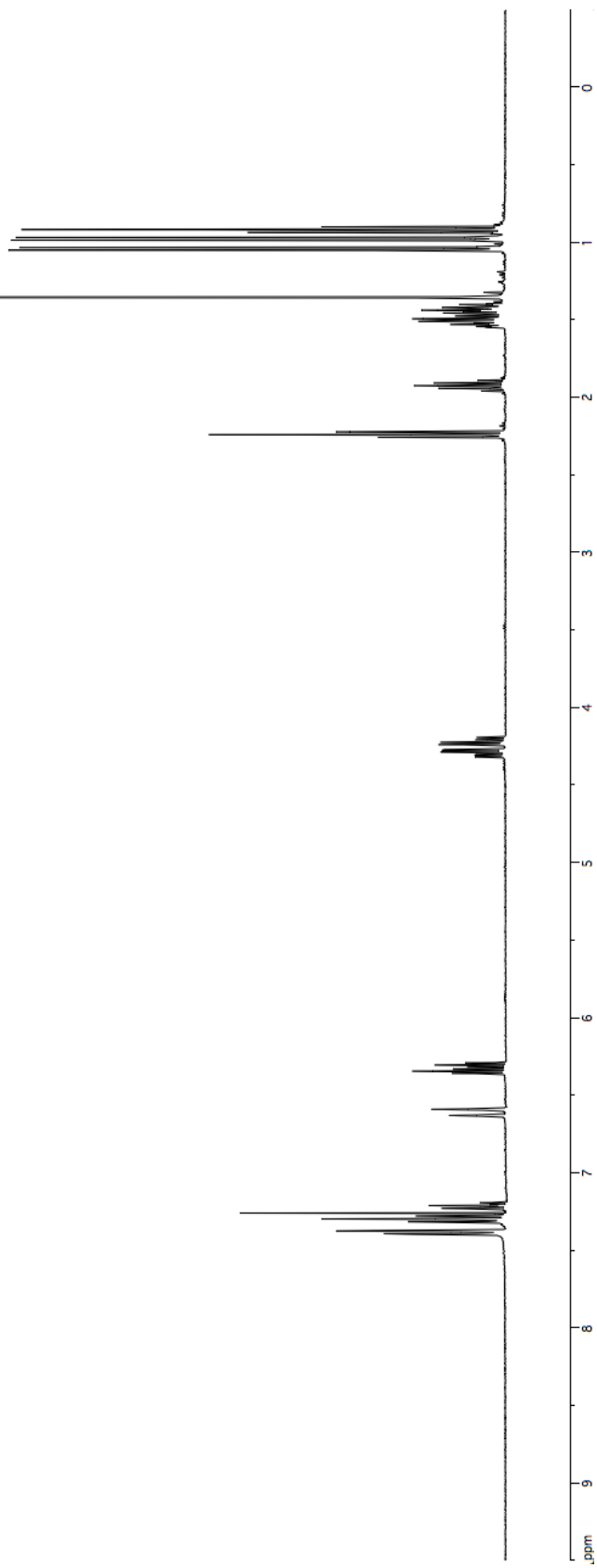
2-39

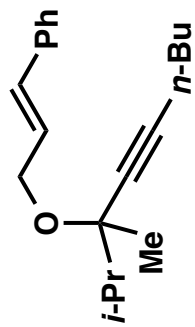
<sup>13</sup>C NMR  
(100 MHz, CDCl<sub>3</sub>)





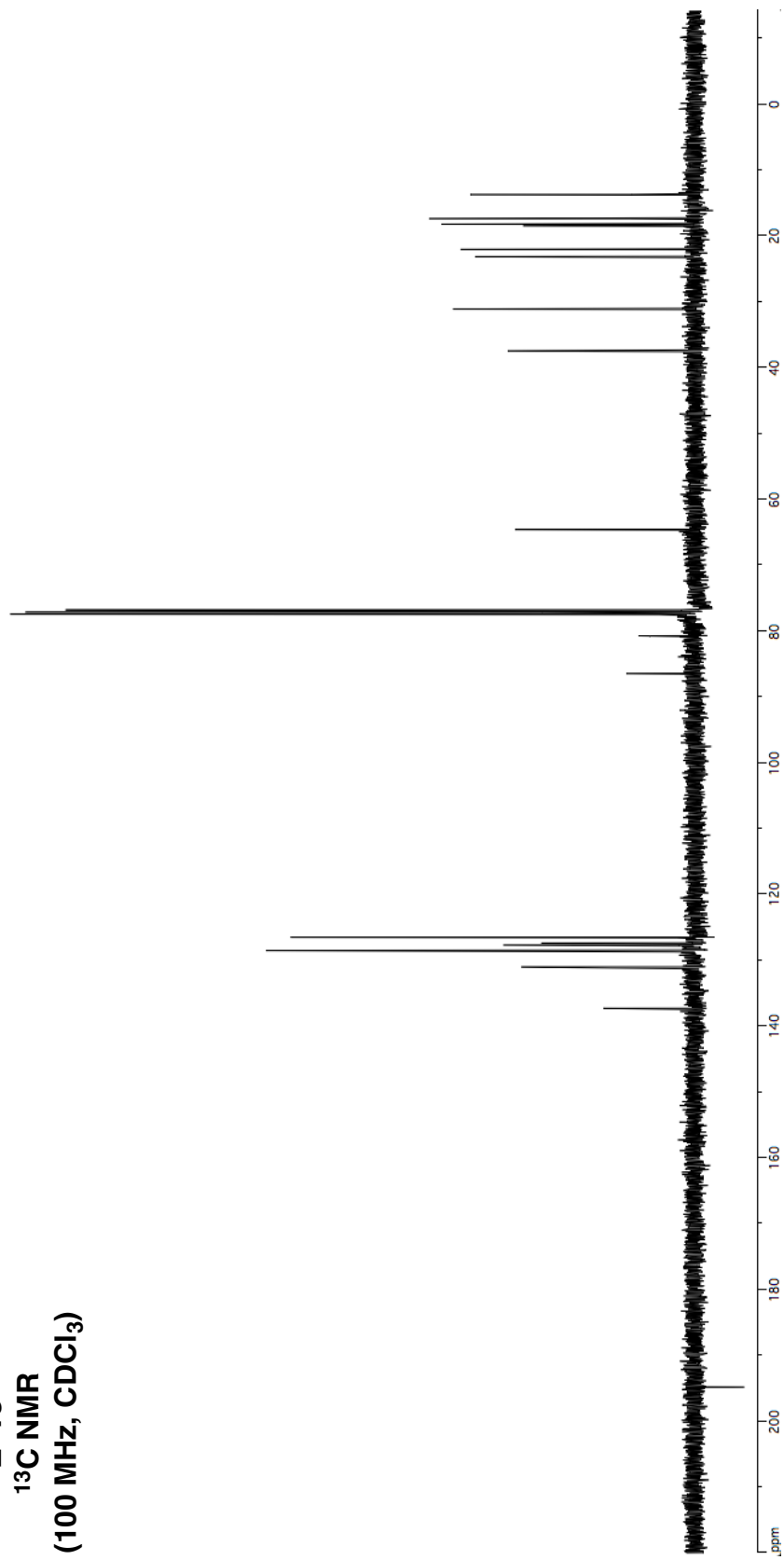
2-40  
<sup>1</sup>H NMR  
(400 MHz, CDCl<sub>3</sub>)

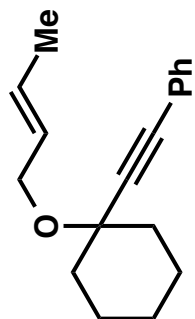




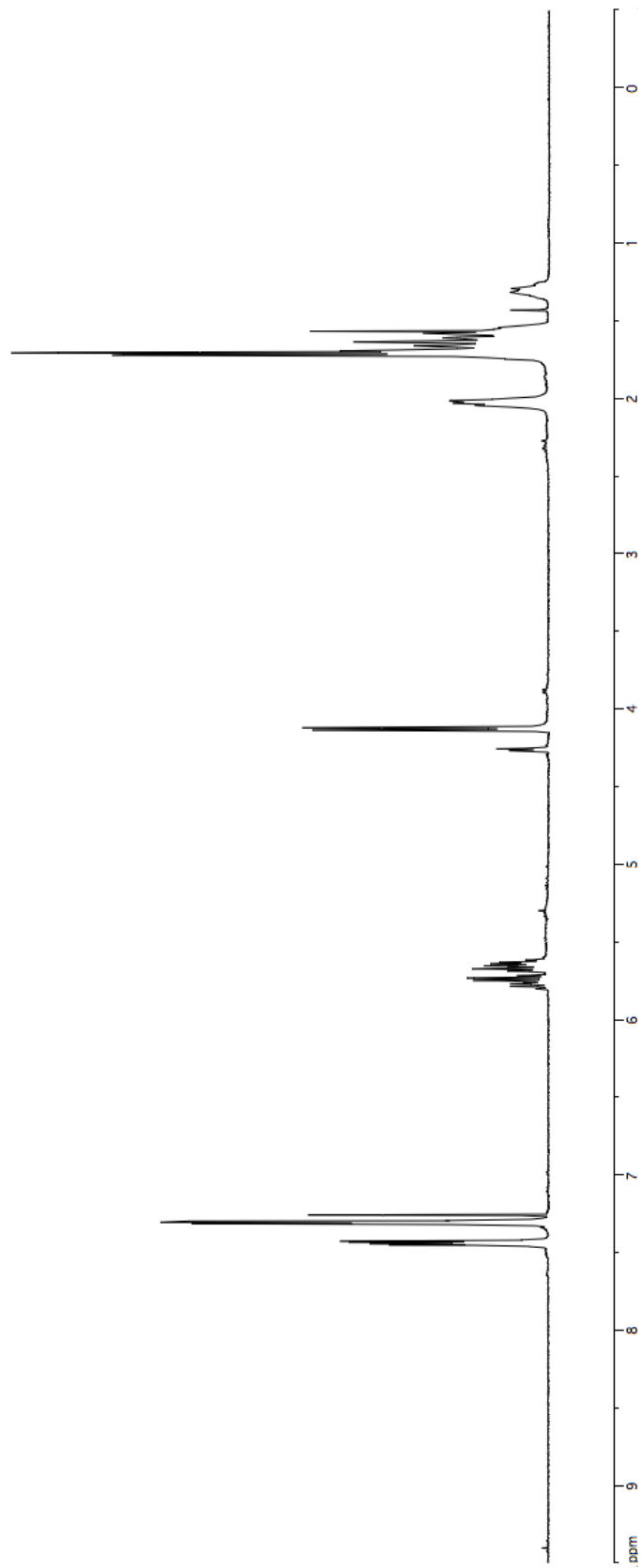
2-40

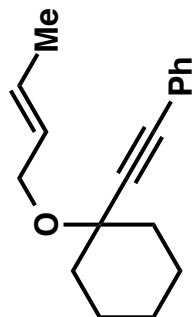
<sup>13</sup>C NMR  
(100 MHz, CDCl<sub>3</sub>)





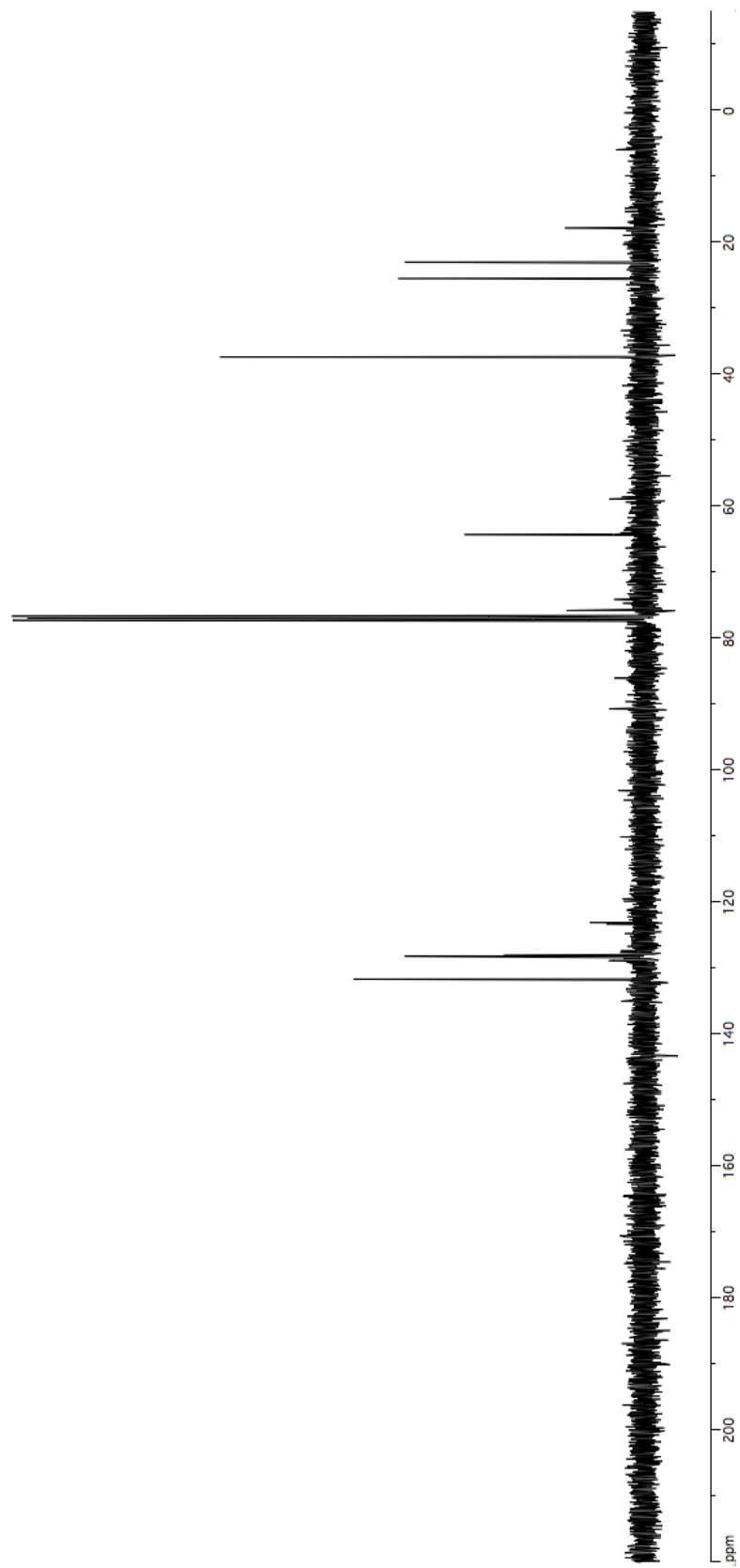
**2-47**  
**<sup>1</sup>H NMR**  
**(400 MHz, CDCl<sub>3</sub>)**

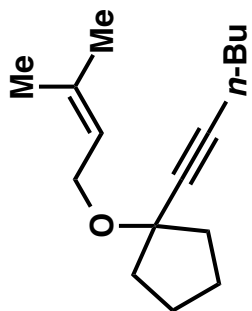




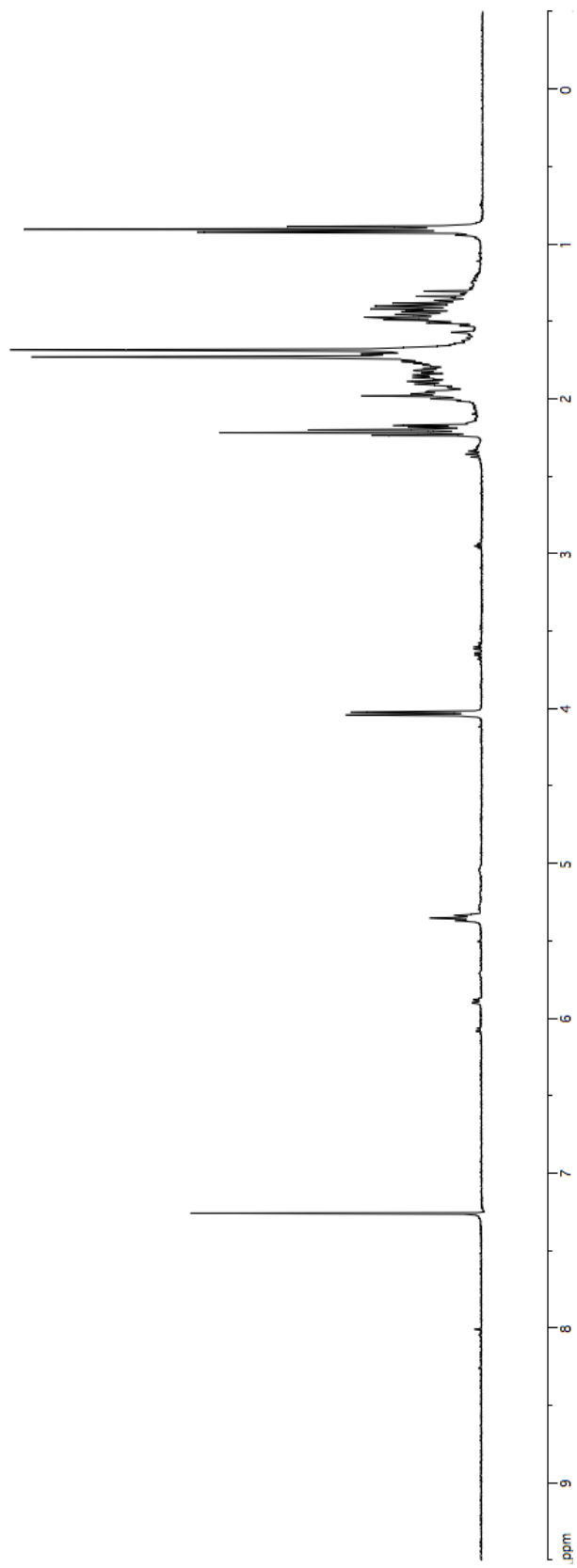
2-47

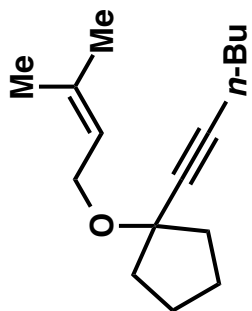
<sup>13</sup>C NMR  
(100 MHz, CDCl<sub>3</sub>)



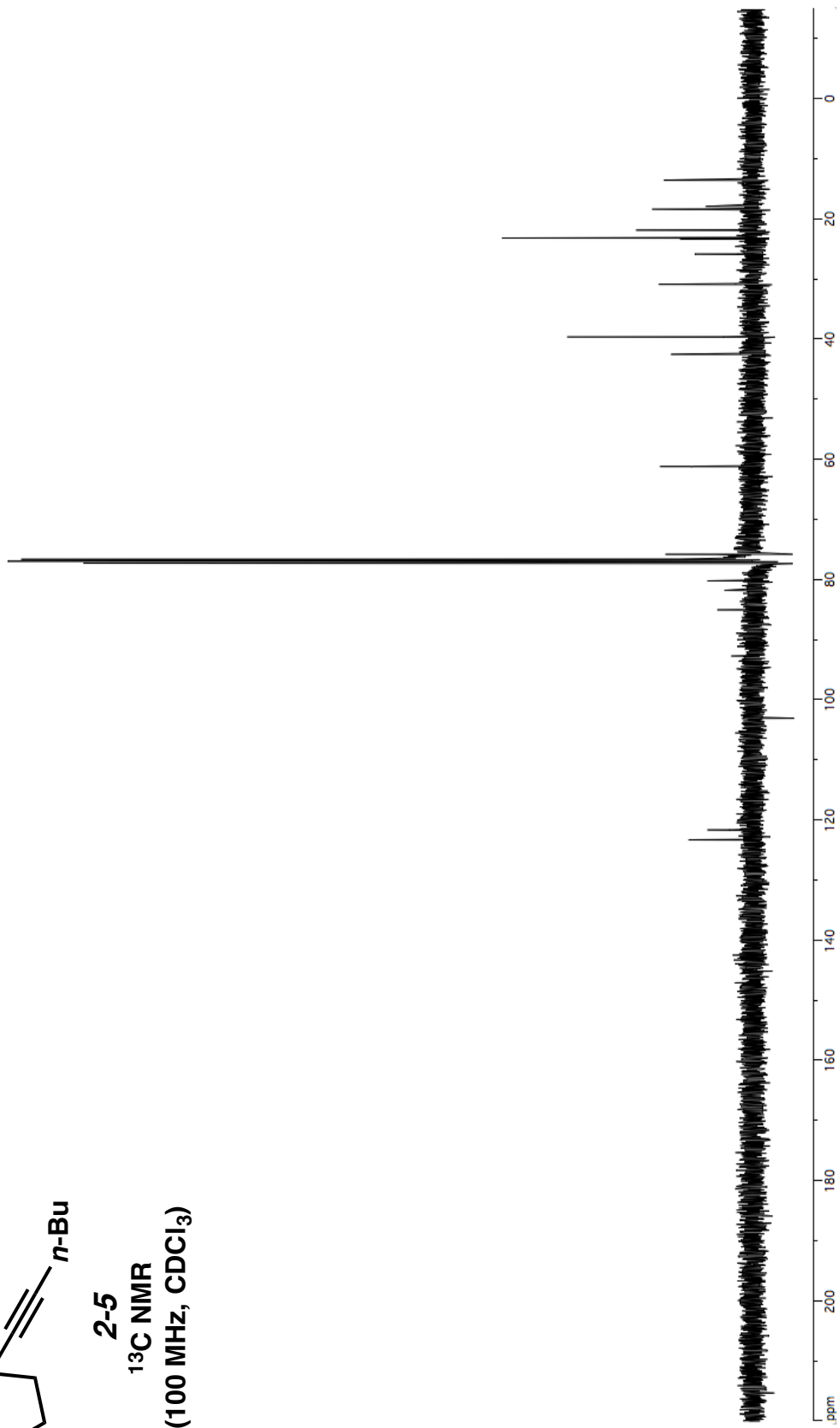


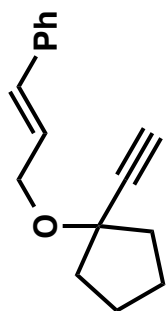
**2-5**  
**<sup>1</sup>H NMR**  
**(400 MHz, CDCl<sub>3</sub>)**



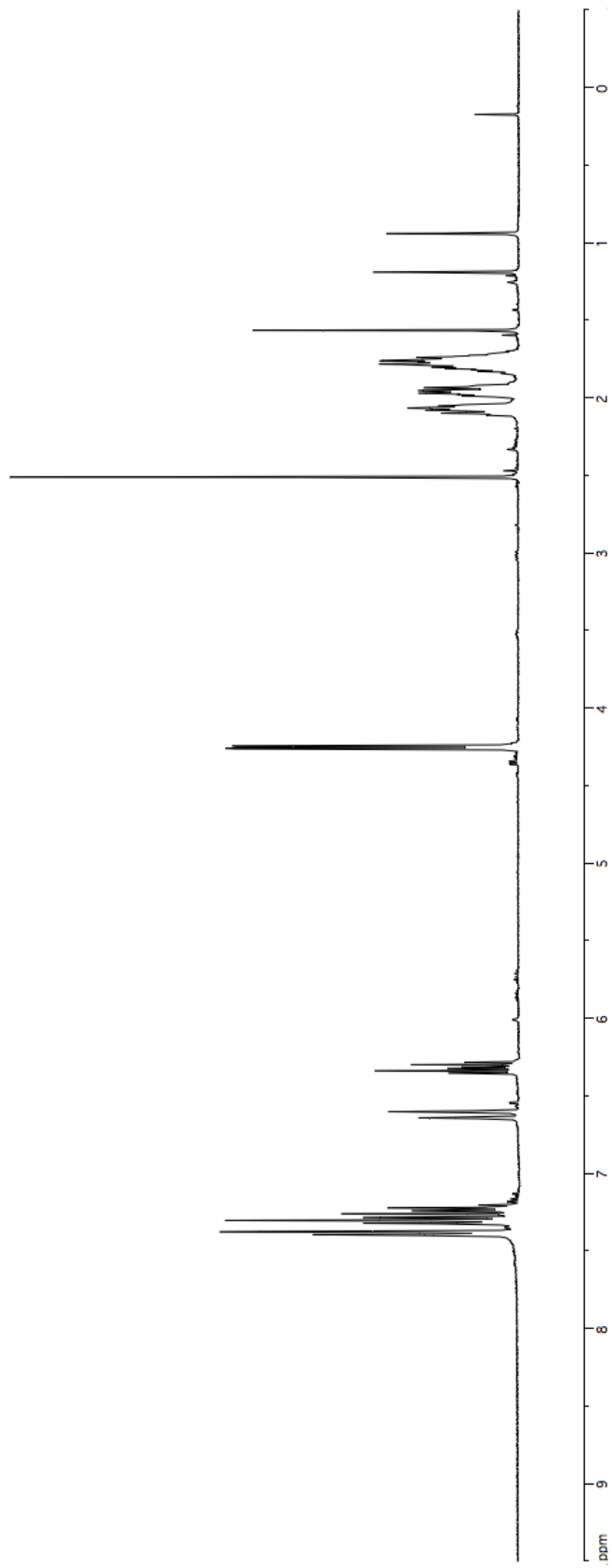


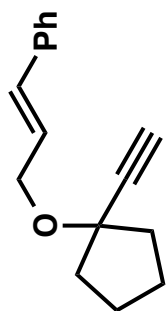
**2-5**  
**<sup>13</sup>C NMR**  
**(100 MHz, CDCl<sub>3</sub>)**



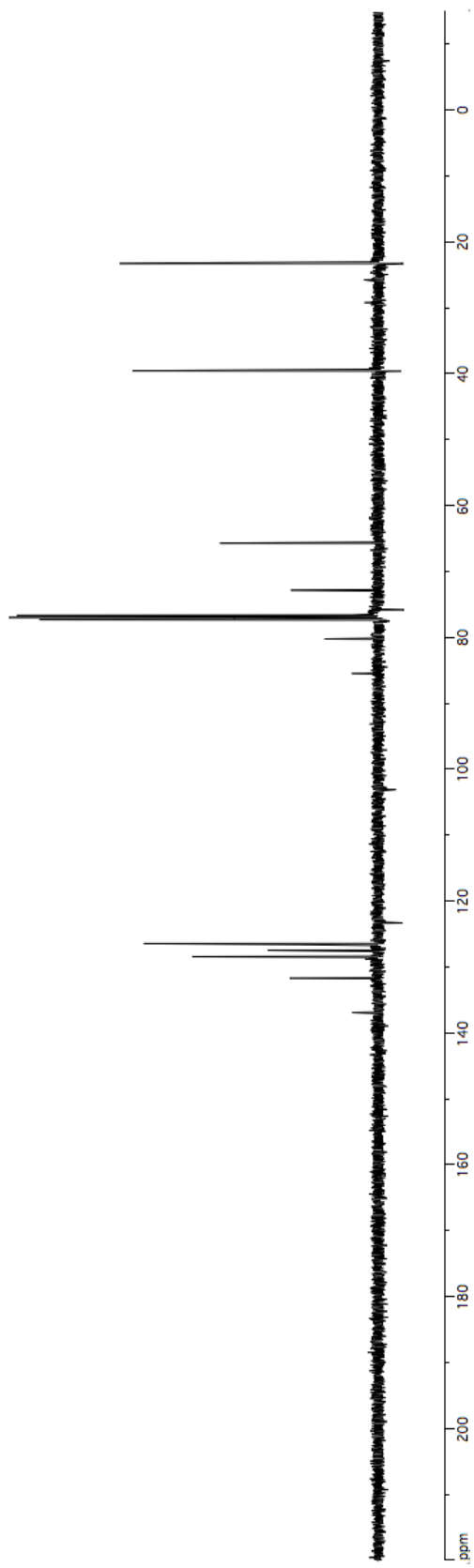


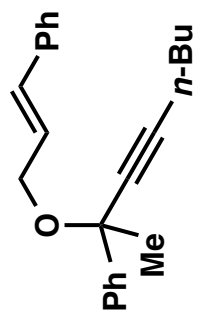
**2-48**  
**<sup>1</sup>H NMR**  
**(400 MHz, CDCl<sub>3</sub>)**





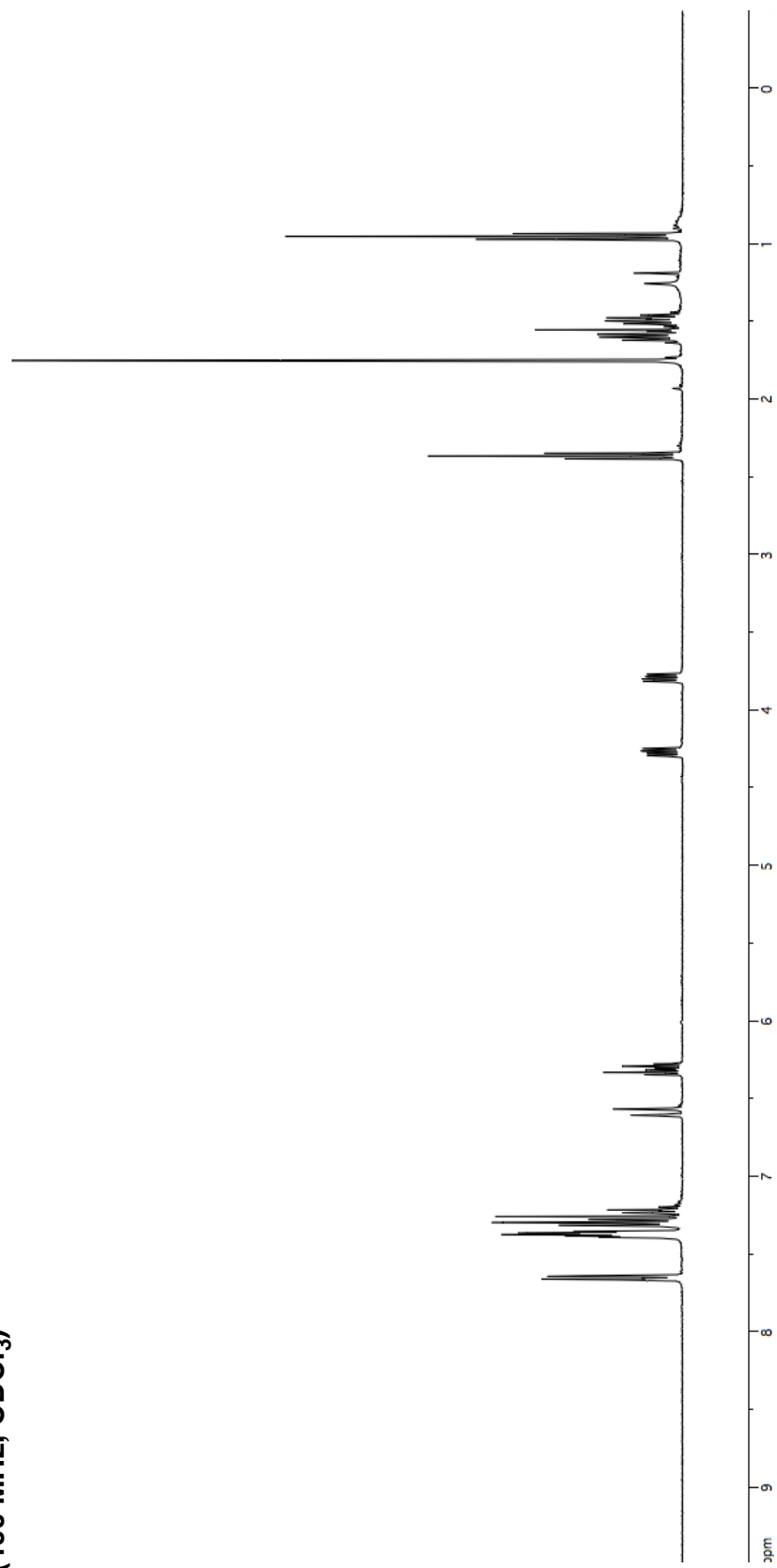
**2-48**  
**<sup>13</sup>C NMR**  
**(100 MHz, CDCl<sub>3</sub>)**

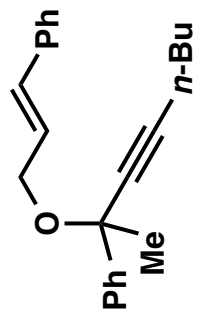




2-49

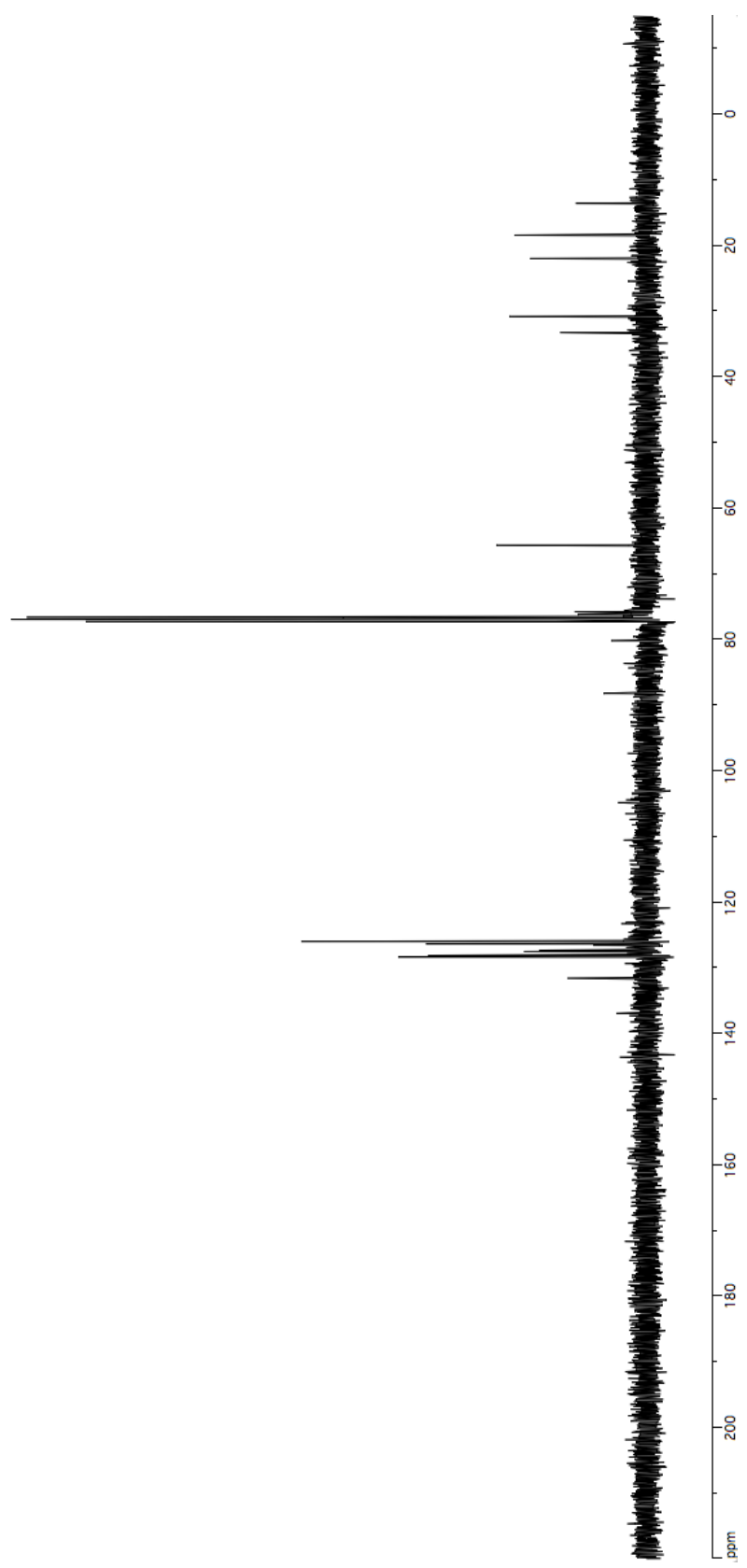
<sup>1</sup>H NMR  
(400 MHz, CDCl<sub>3</sub>)

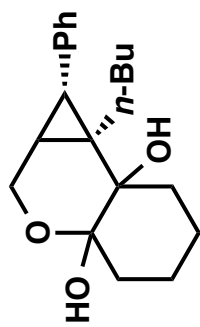




**2-49**

**<sup>13</sup>C NMR  
(100 MHz, CDCl<sub>3</sub>)**

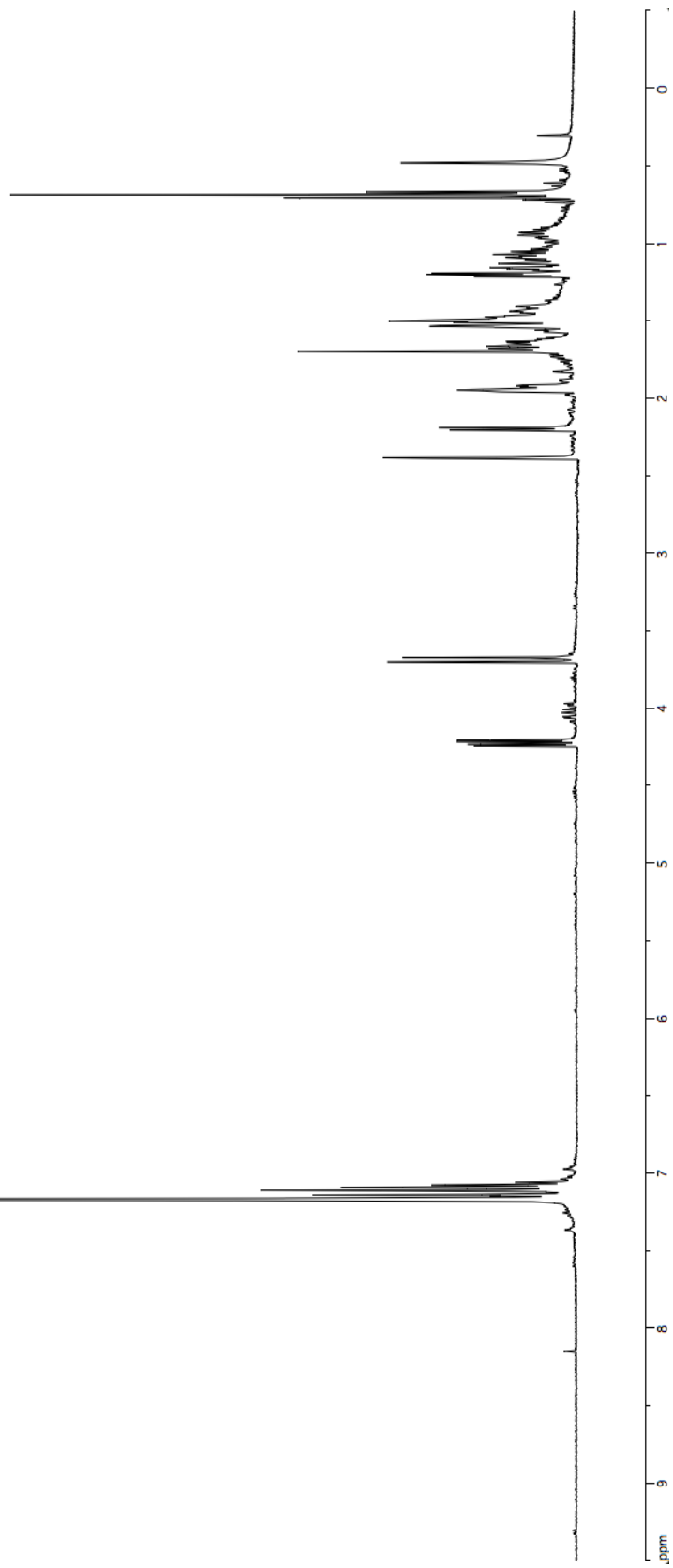


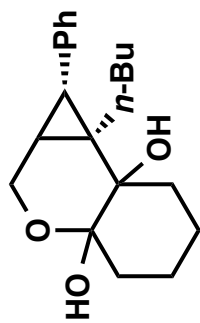


2-55

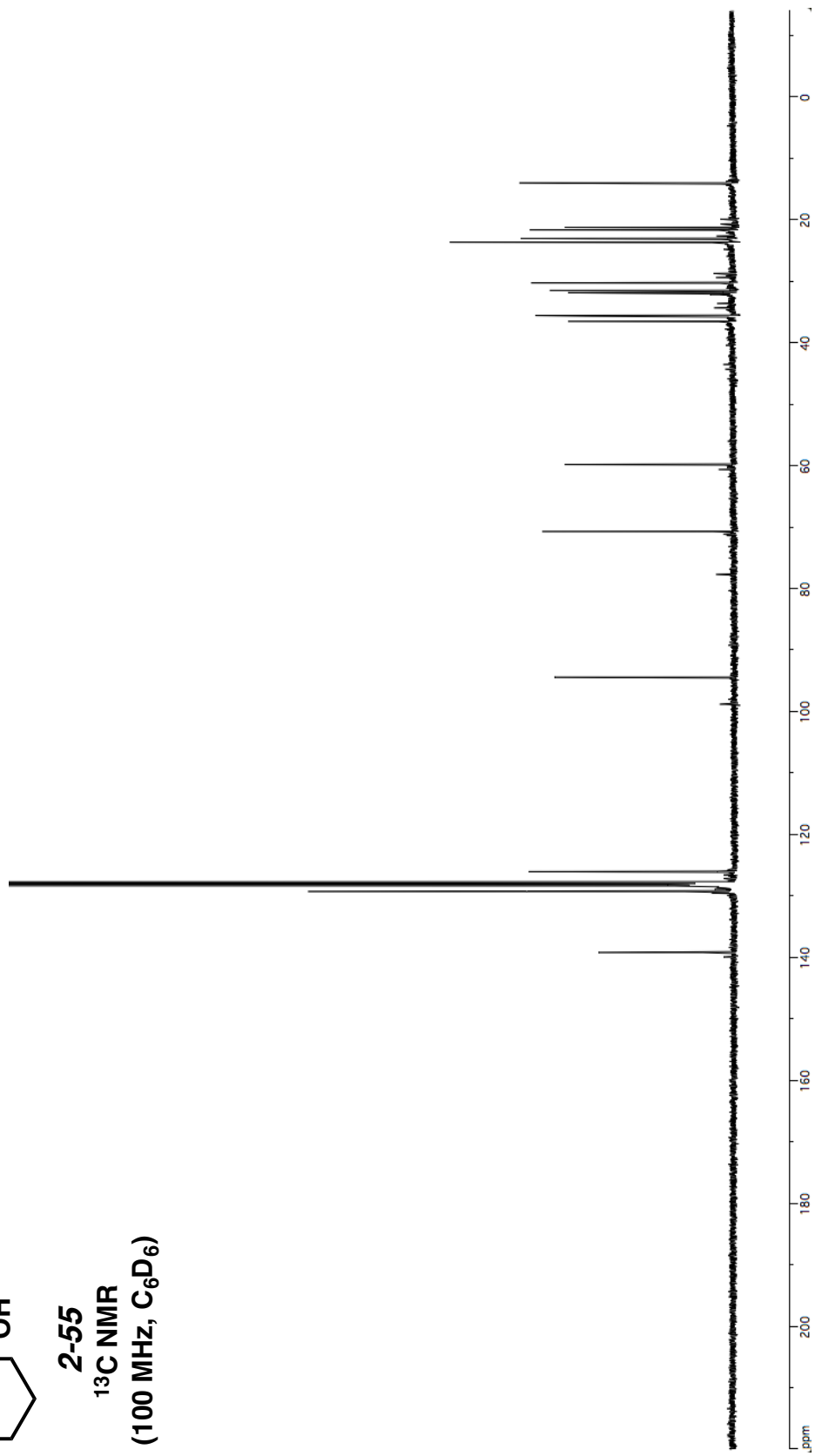
<sup>1</sup>H NMR

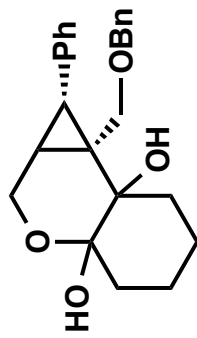
(400 MHz, C<sub>6</sub>D<sub>6</sub>)



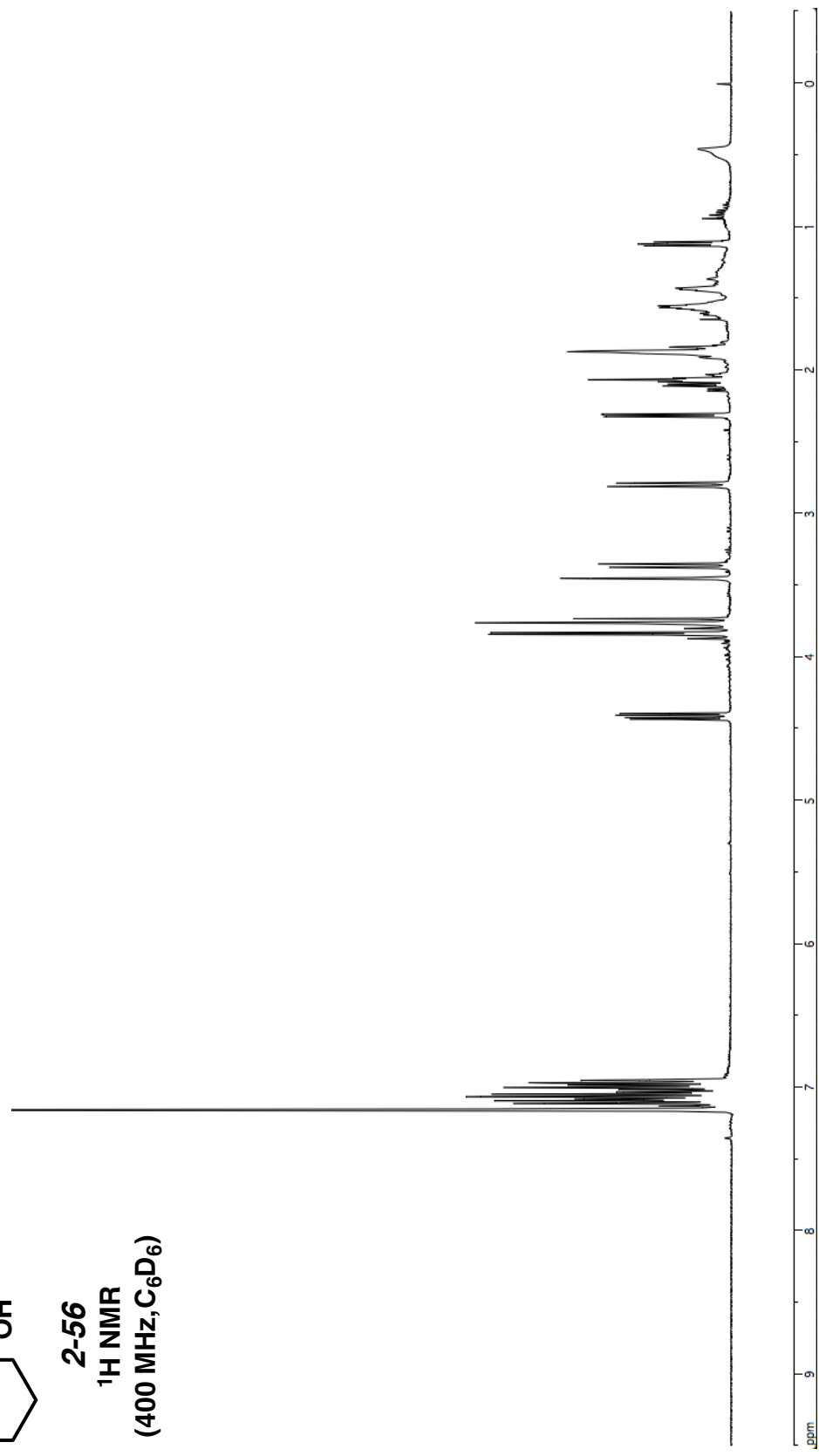


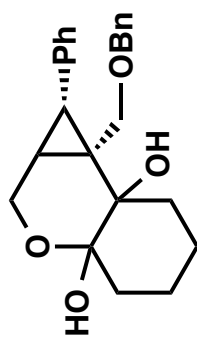
**2-55**  
**<sup>13</sup>C NMR**  
**(100 MHz, C<sub>6</sub>D<sub>6</sub>)**



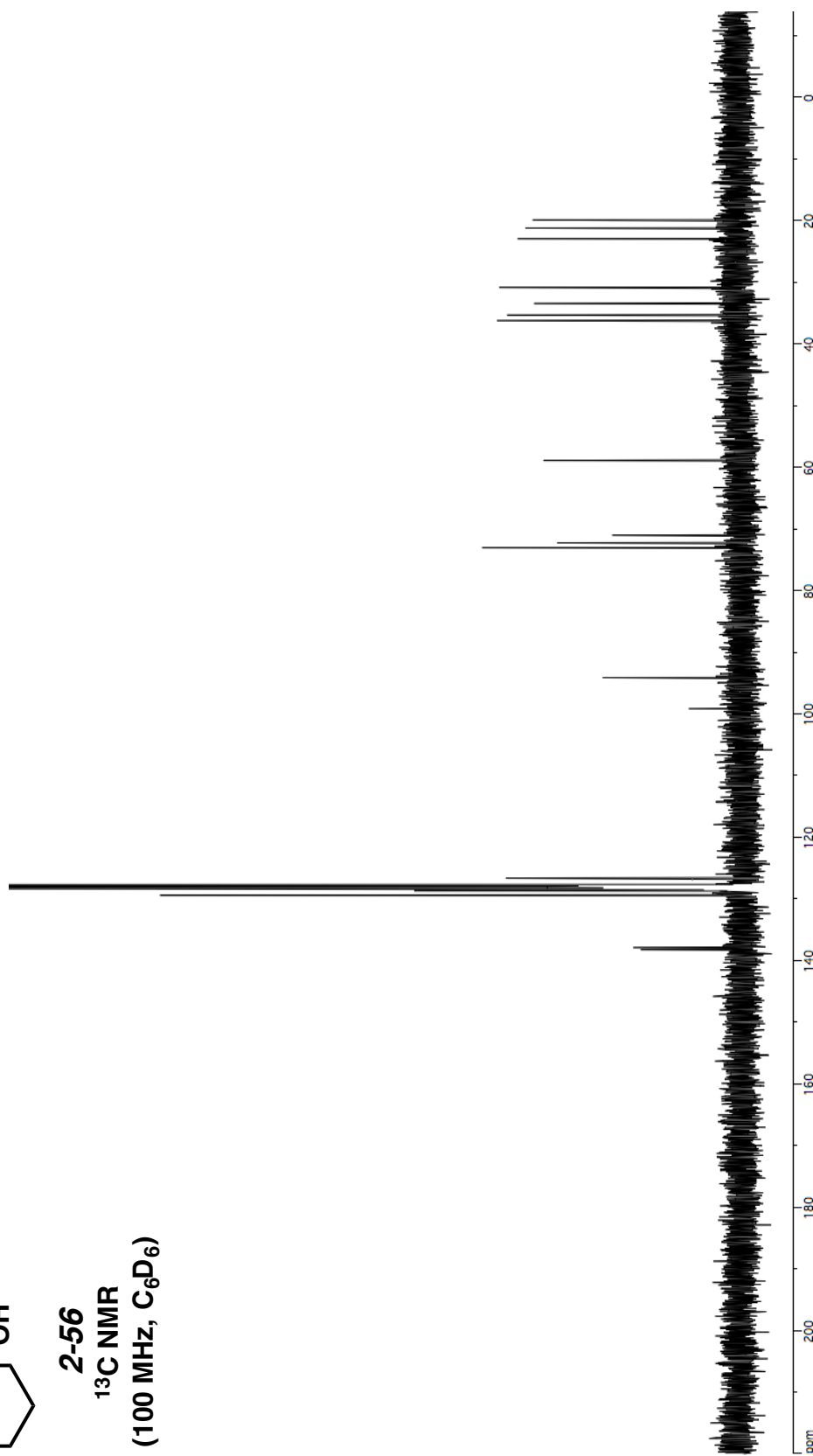


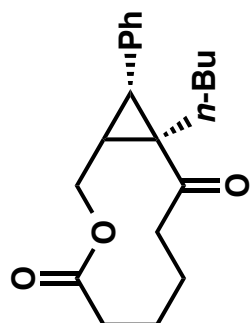
**2-56**  
**<sup>1</sup>H NMR**  
**(400 MHz, C<sub>6</sub>D<sub>6</sub>)**



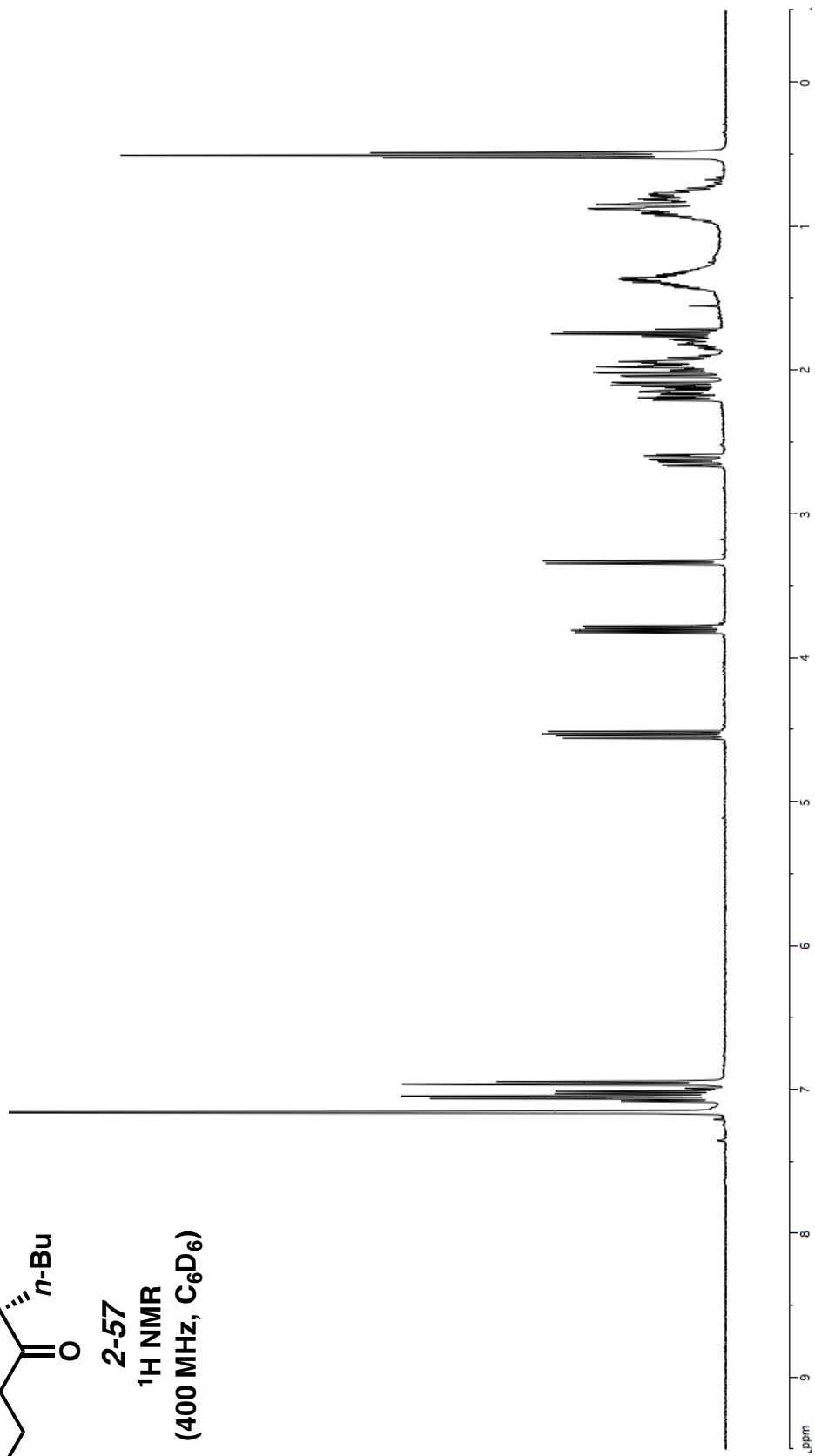


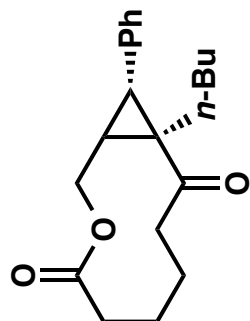
**2-56**  
**<sup>13</sup>C NMR**  
**(100 MHz, C<sub>6</sub>D<sub>6</sub>)**



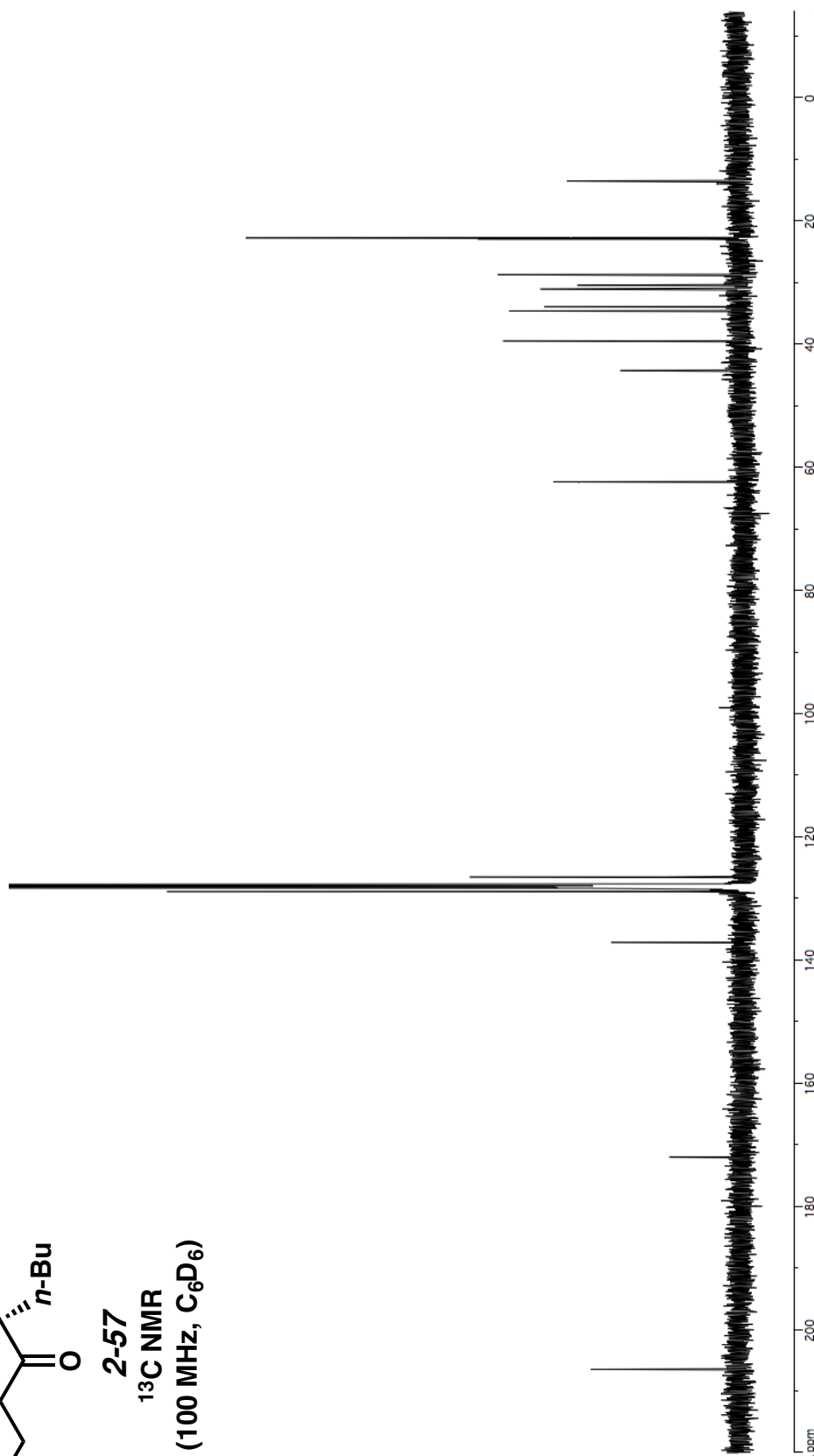


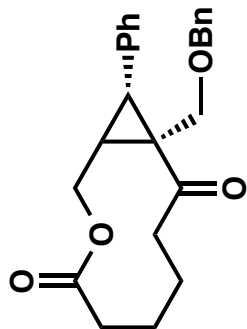
2-57  
<sup>1</sup>H NMR  
(400 MHz, C<sub>6</sub>D<sub>6</sub>)



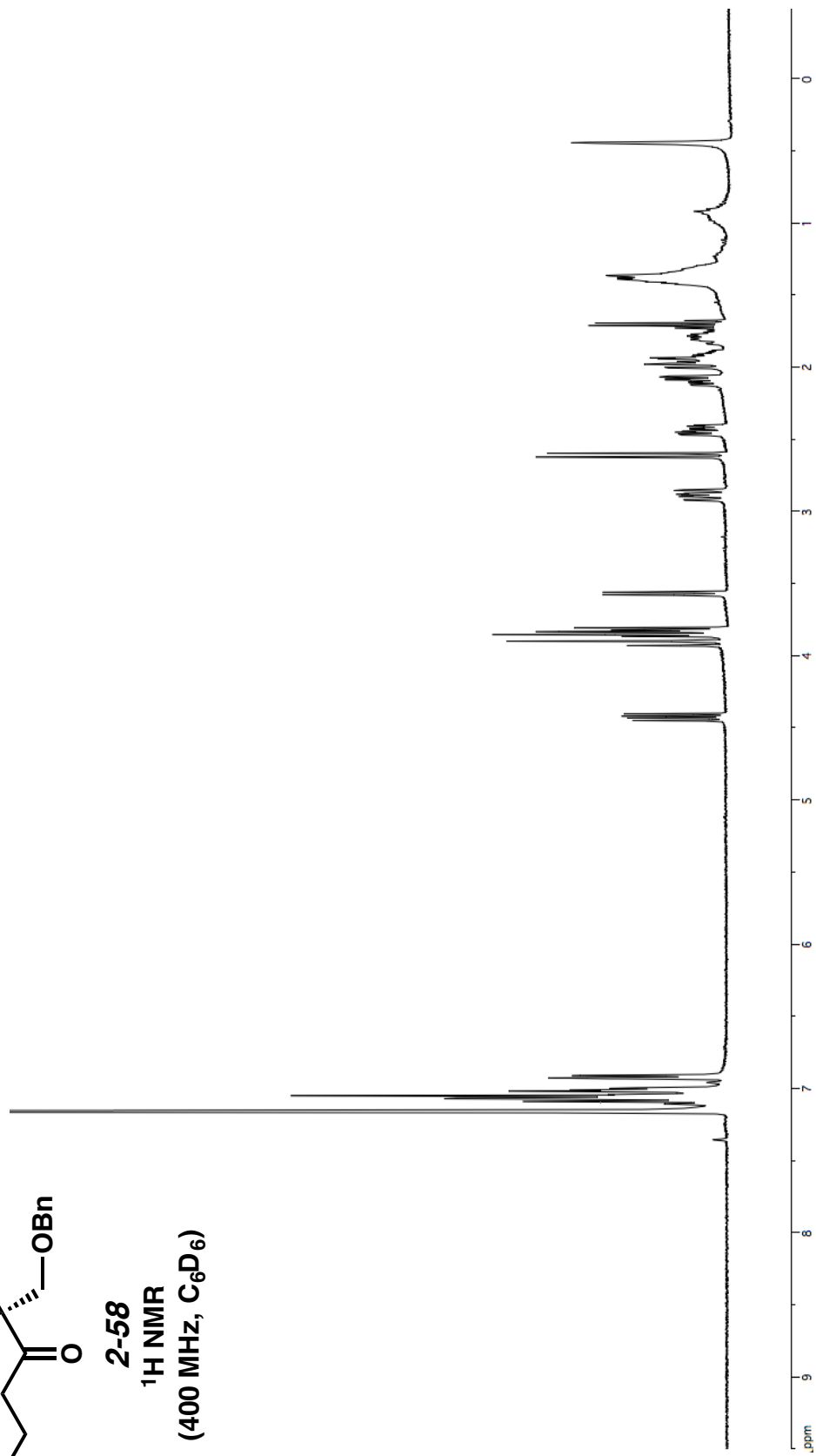


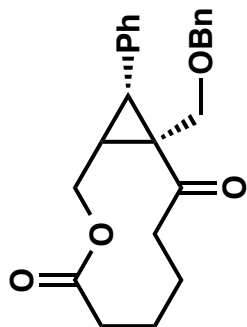
**2-57**  
<sup>13</sup>C NMR  
(100 MHz, C<sub>6</sub>D<sub>6</sub>)



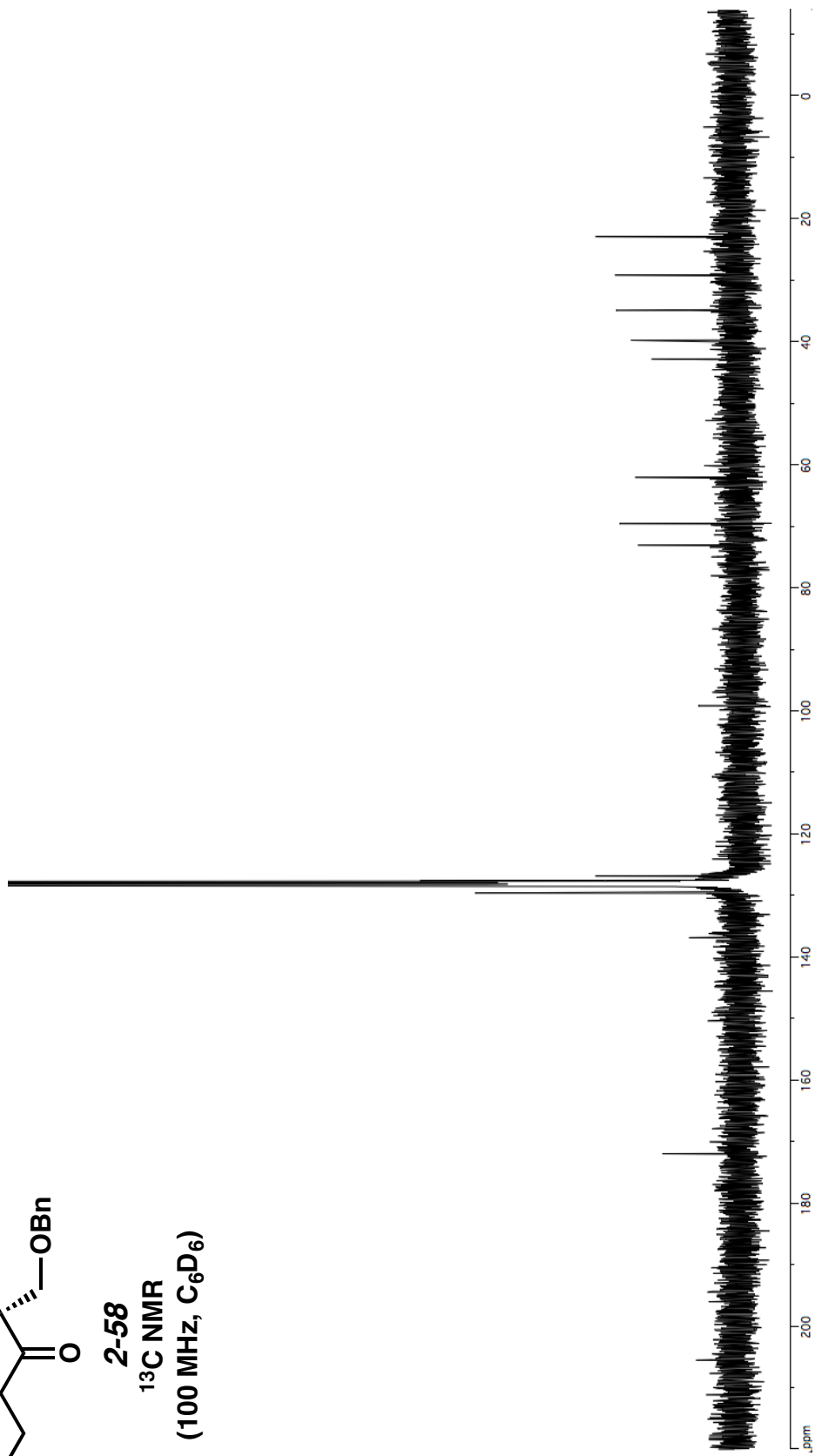


**2-58**  
**<sup>1</sup>H NMR**  
**(400 MHz, C<sub>6</sub>D<sub>6</sub>)**

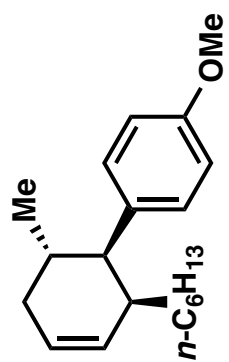




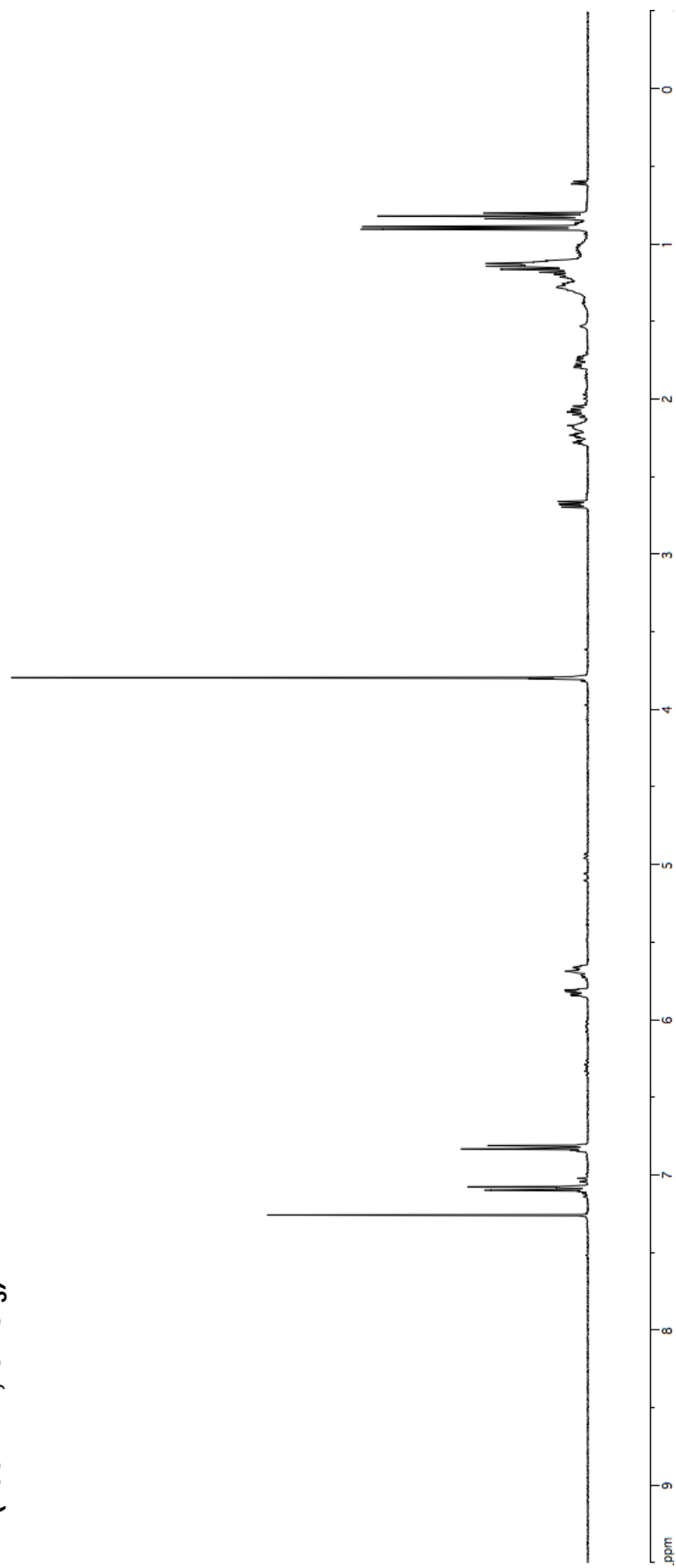
**2-58**  
<sup>13</sup>C NMR  
(100 MHz, C<sub>6</sub>D<sub>6</sub>)

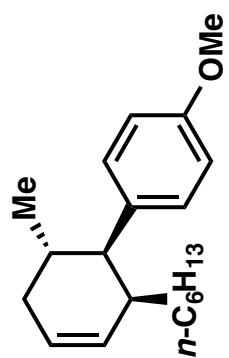


APPENDIX C  
NMR SPECTRA RELEVANT TO CHAPTER 4

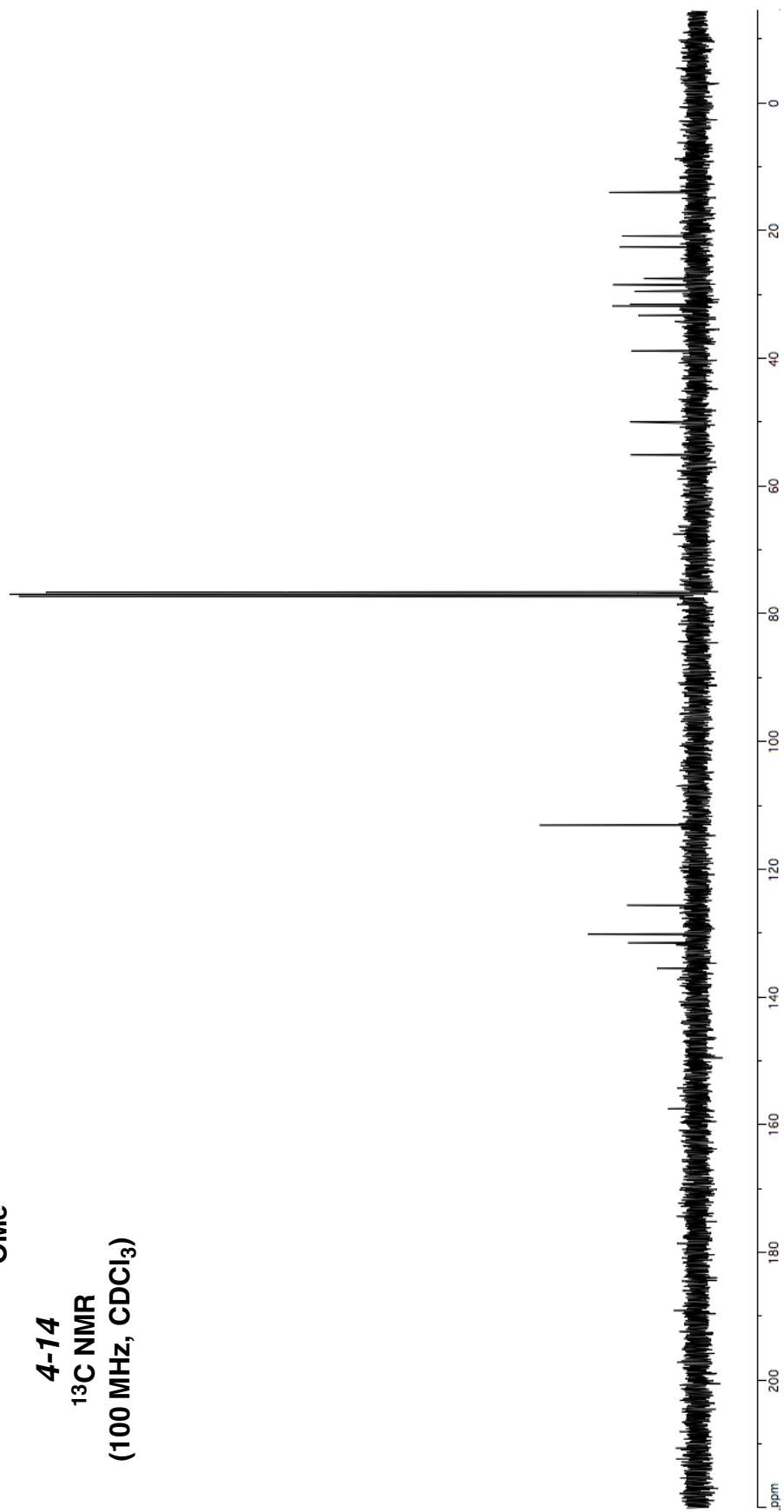


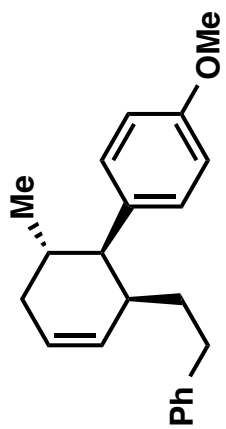
**4-14**  
**<sup>1</sup>H NMR**  
**(400 MHz, CDCl<sub>3</sub>)**



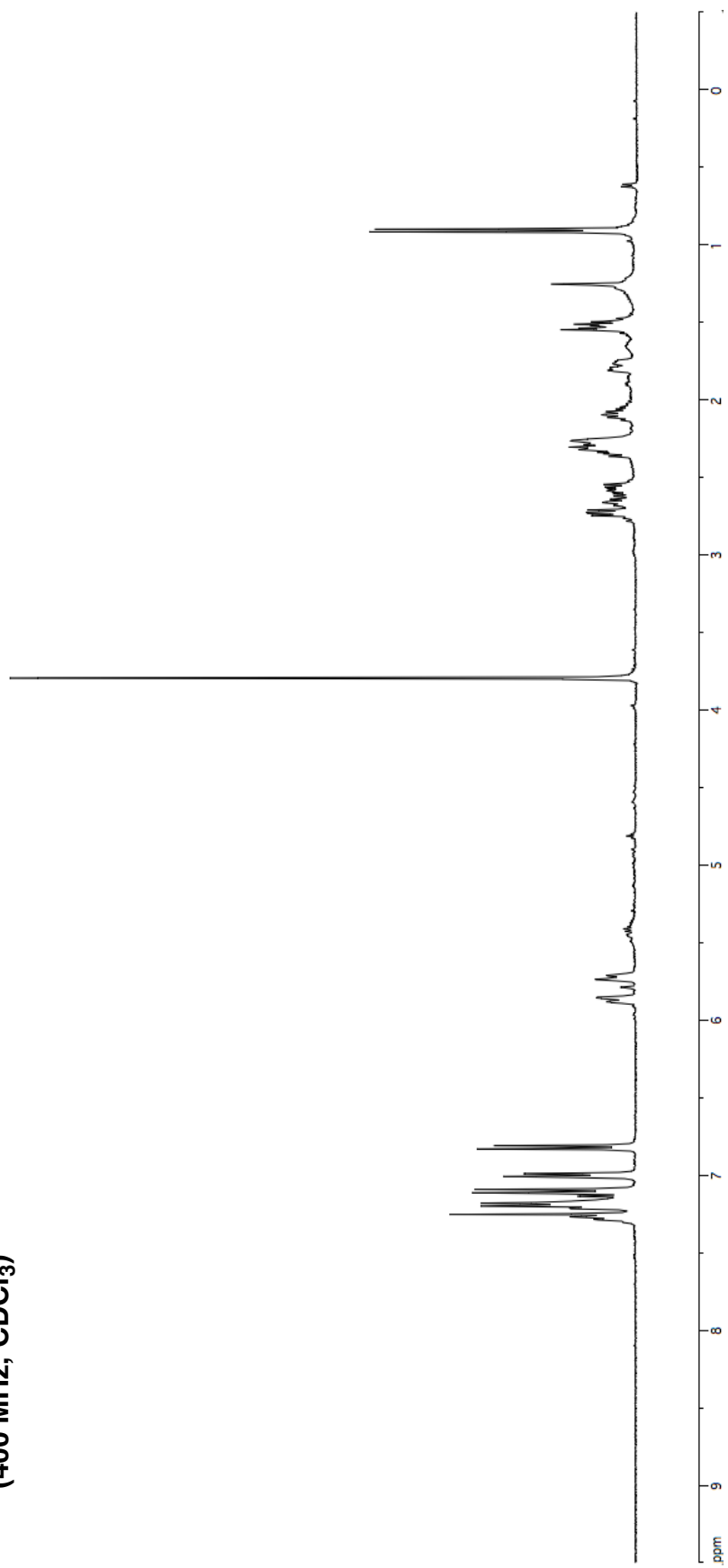


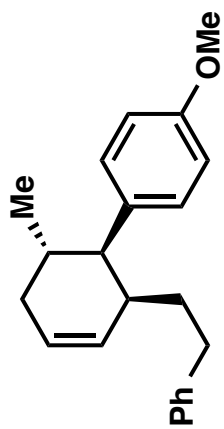
**4-14**  
 **$^{13}\text{C}$  NMR**  
**(100 MHz,  $\text{CDCl}_3$ )**



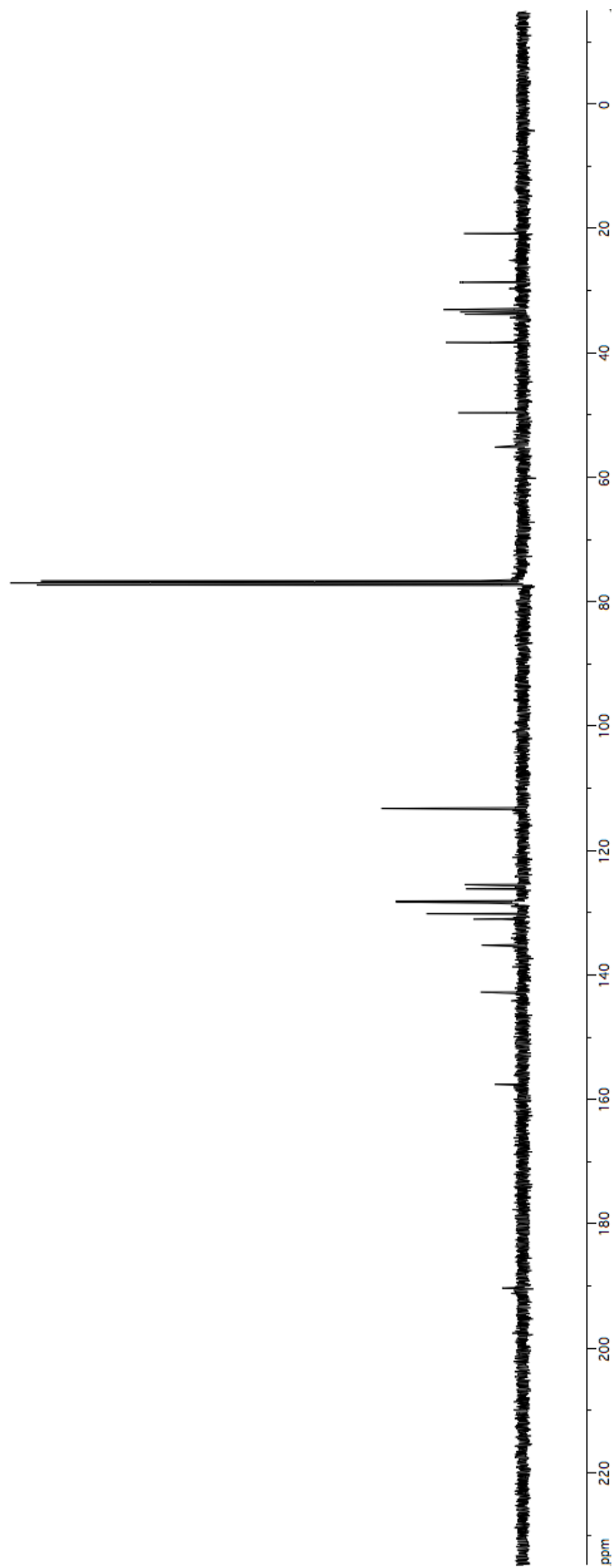


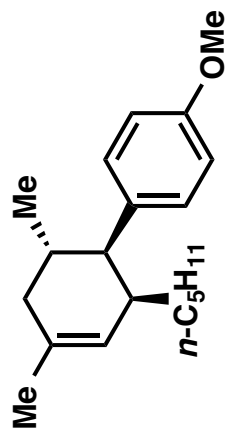
4-15  
<sup>1</sup>H NMR  
(400 MHz, CDCl<sub>3</sub>)



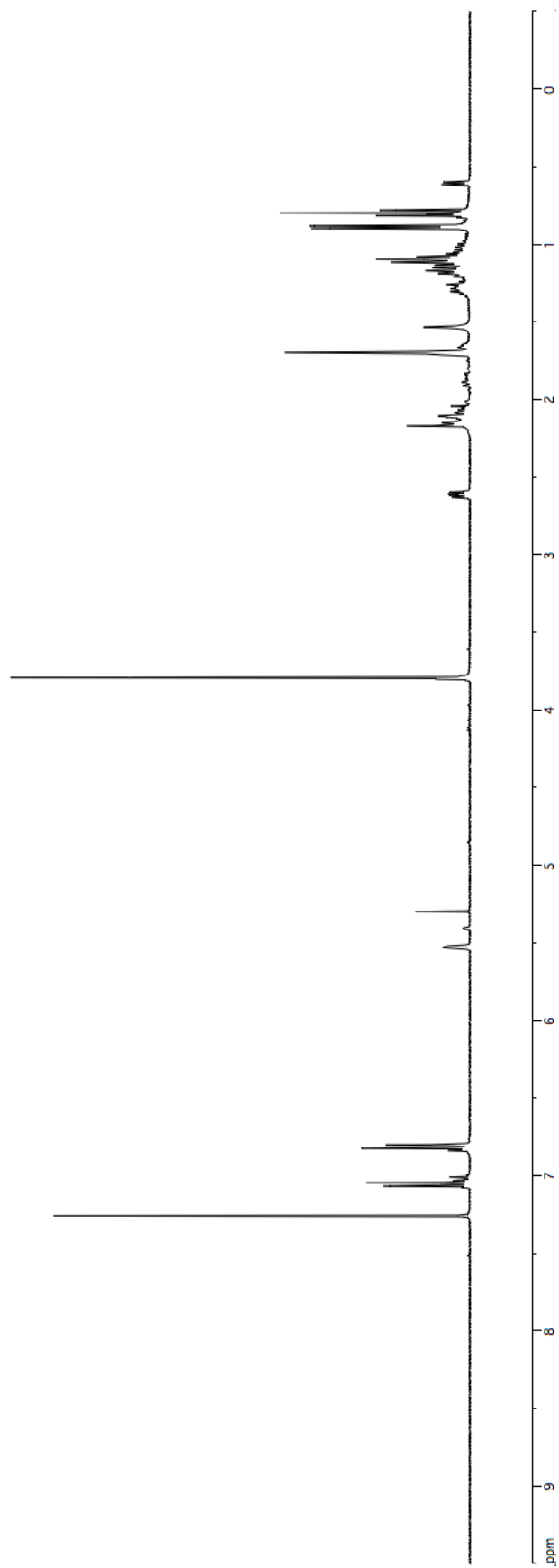


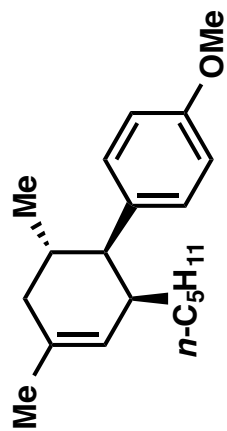
**4-15**  
**<sup>13</sup>C NMR**  
**(100 MHz, CDCl<sub>3</sub>)**



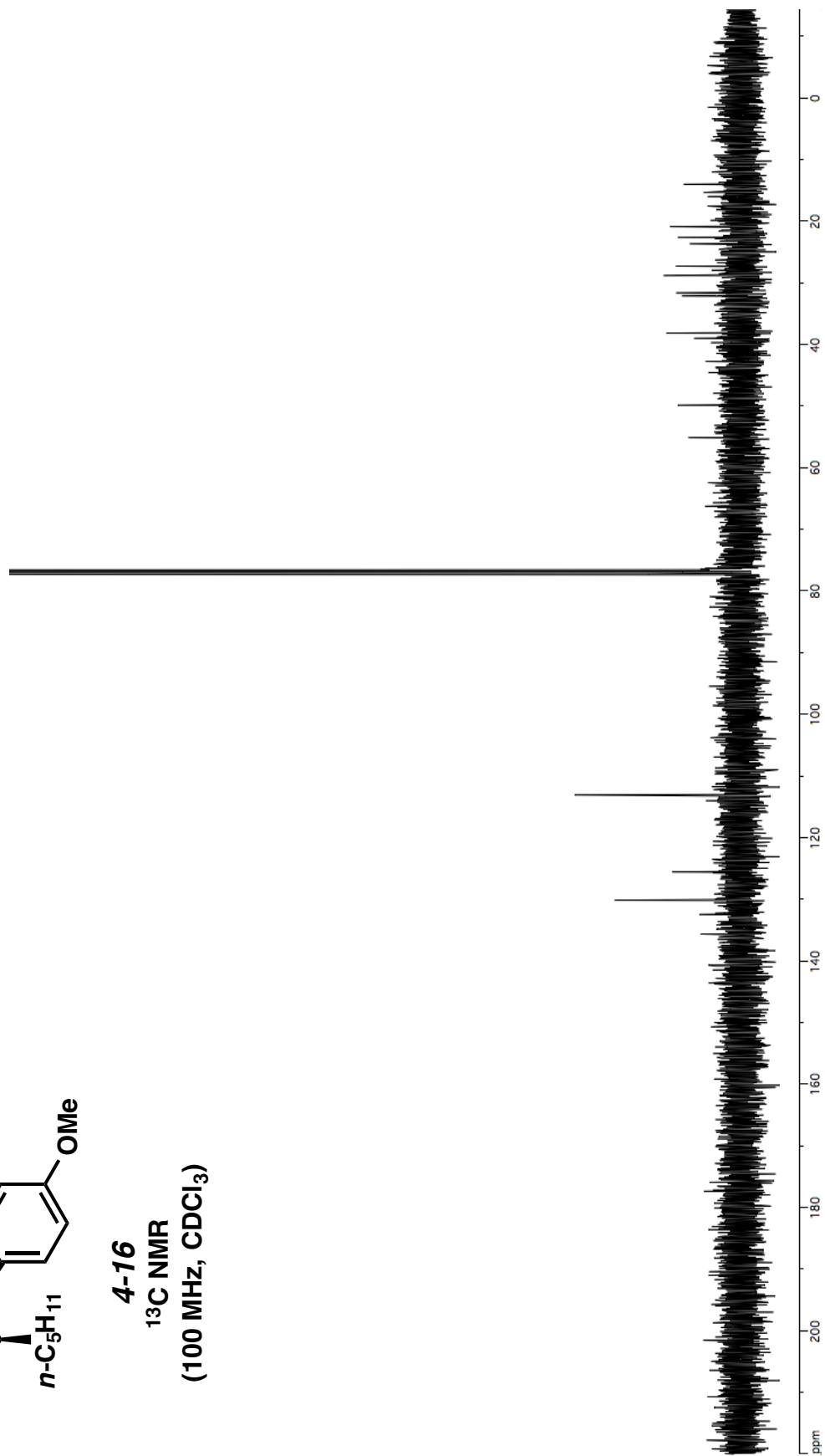


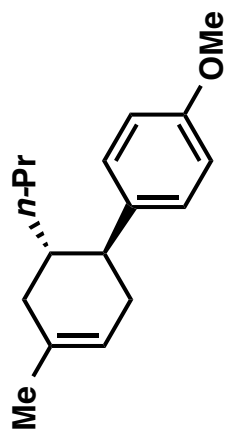
**4-16**  
 $^1\text{H}$  NMR  
(400 MHz,  $\text{CDCl}_3$ )



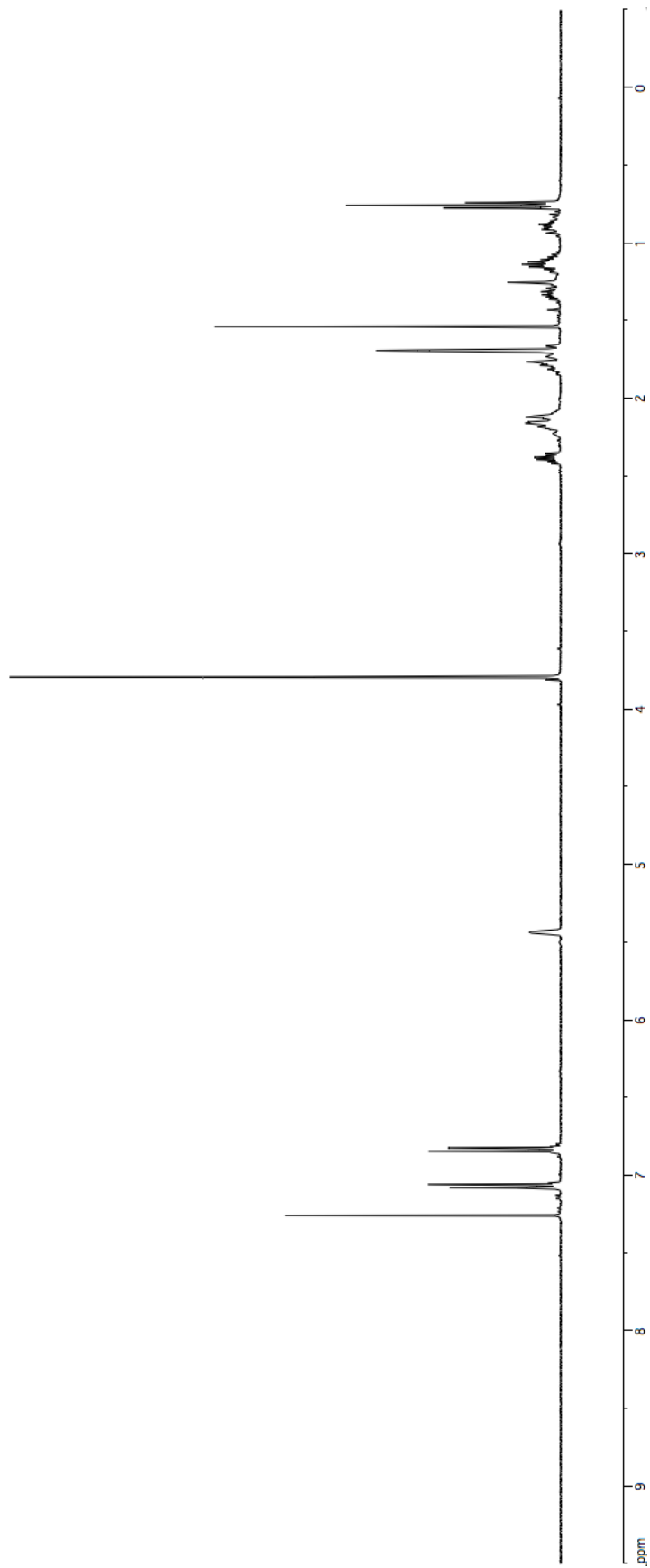


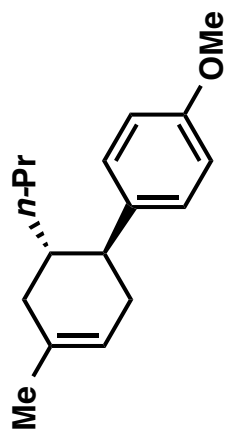
**4-16**  
 $^{13}\text{C}$  NMR  
(100 MHz,  $\text{CDCl}_3$ )



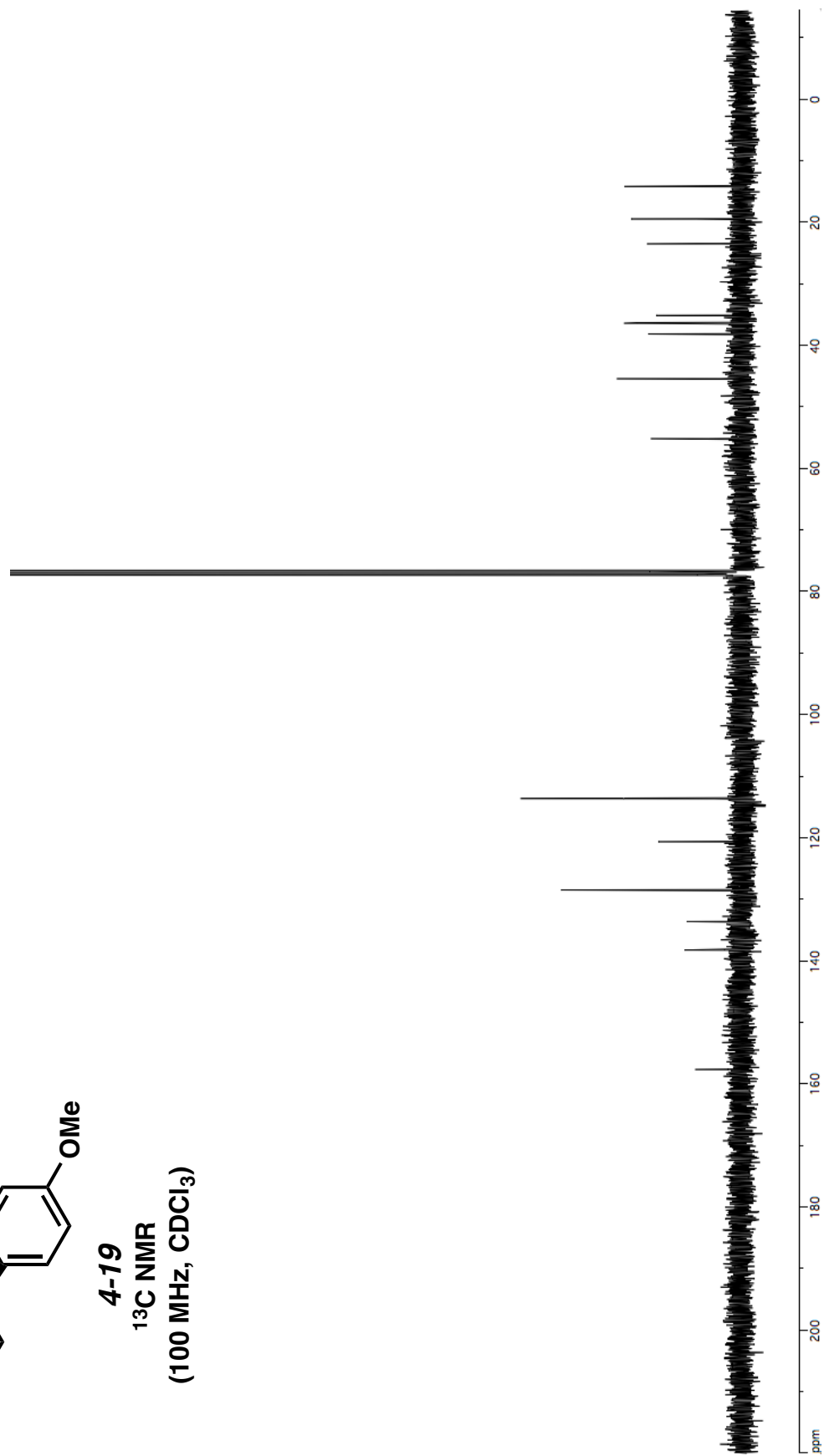


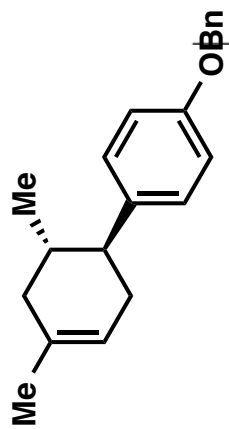
**4-19**  
**<sup>1</sup>H NMR**  
**(400 MHz, CDCl<sub>3</sub>)**



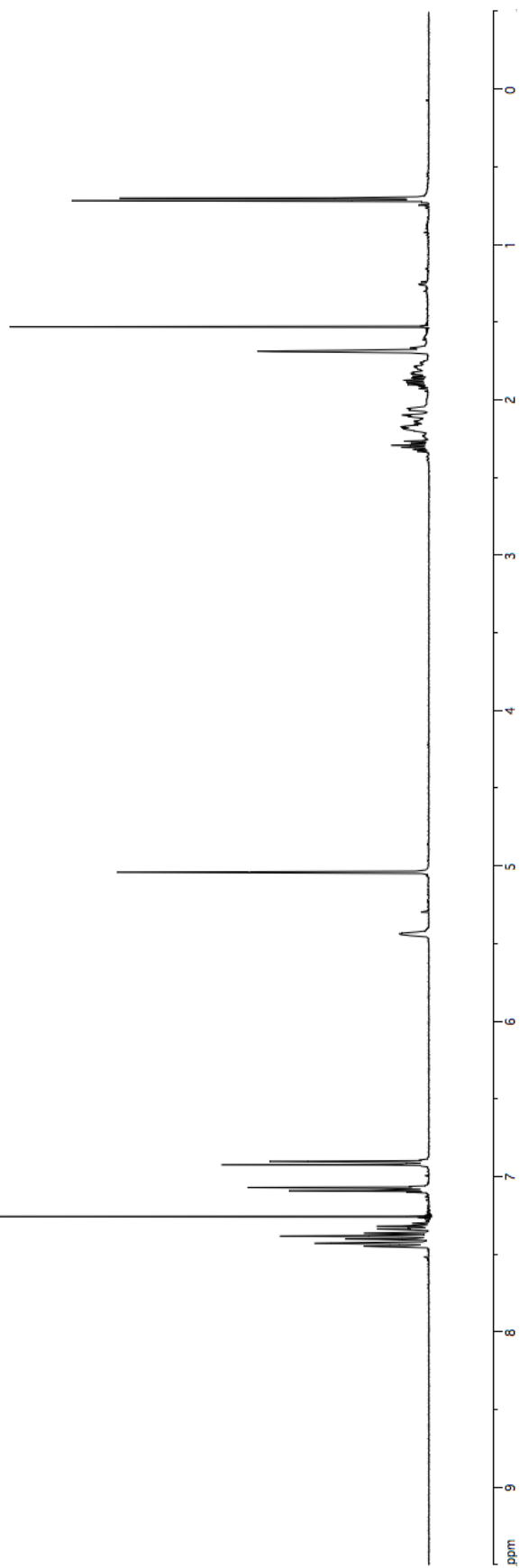


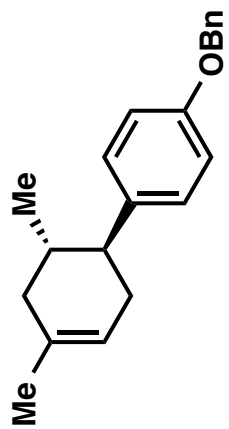
**4-19**  
**<sup>13</sup>C NMR**  
**(100 MHz, CDCl<sub>3</sub>)**



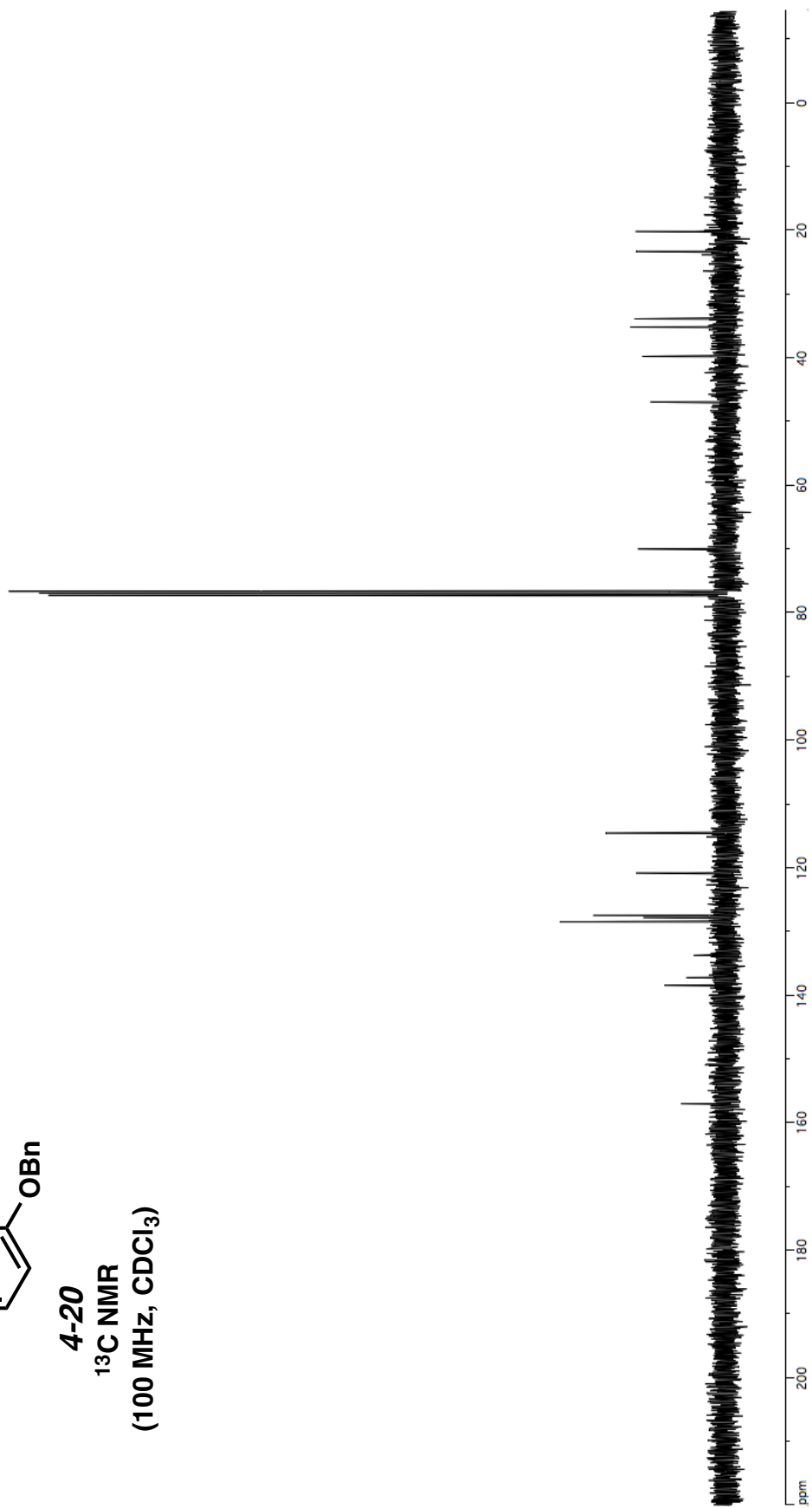


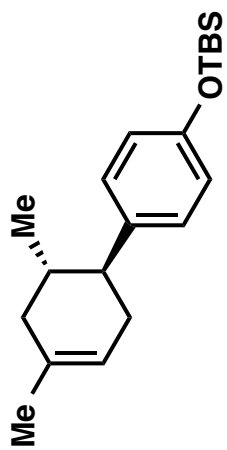
4-20  
<sup>1</sup>H NMR  
(400 MHz, CDCl<sub>3</sub>)



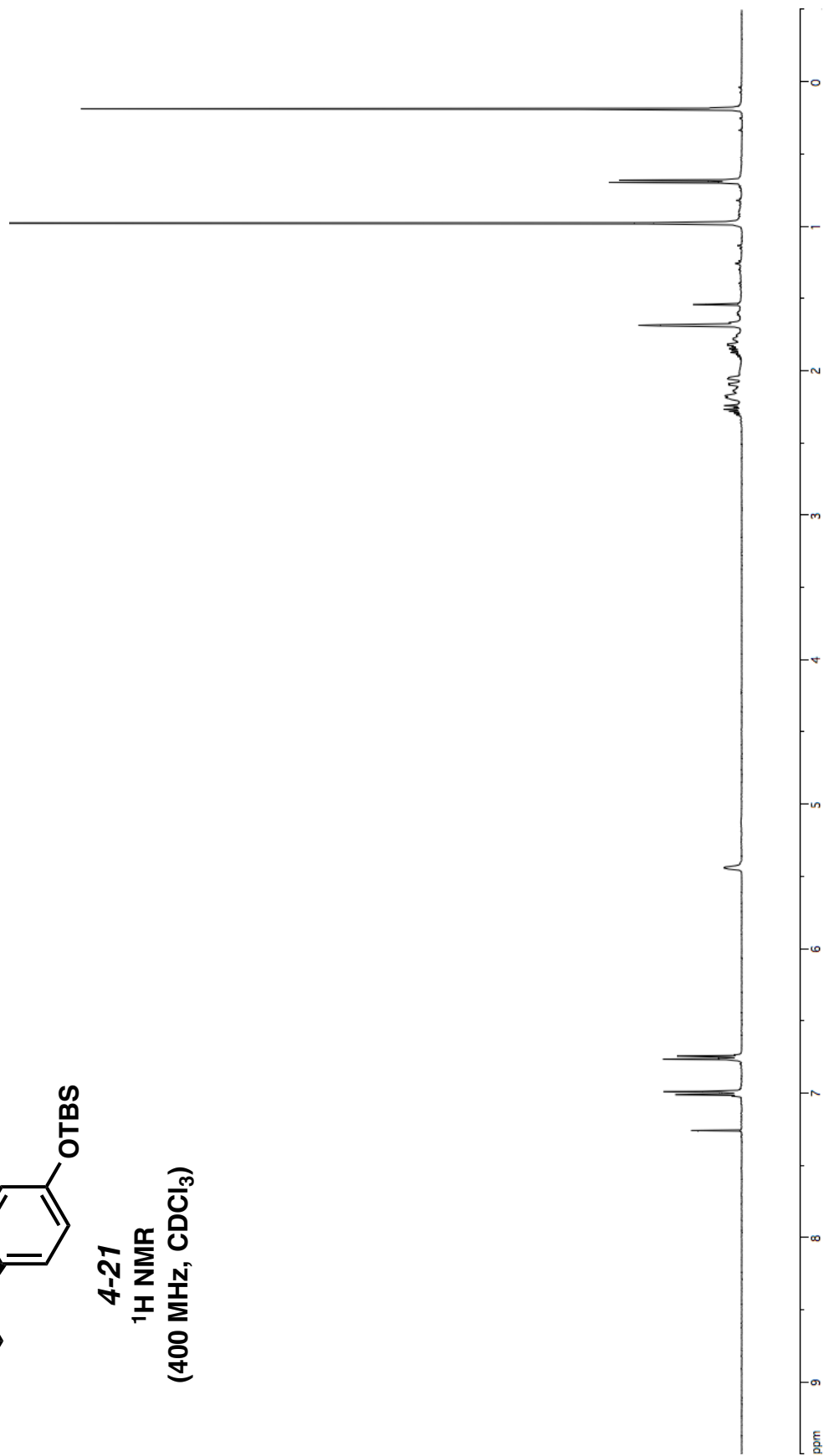


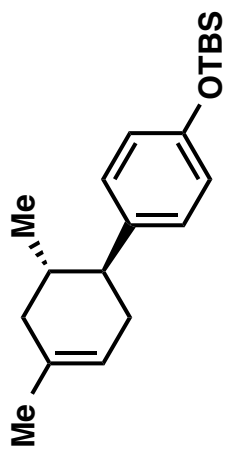
4-20  
<sup>13</sup>C NMR  
(100 MHz, CDCl<sub>3</sub>)



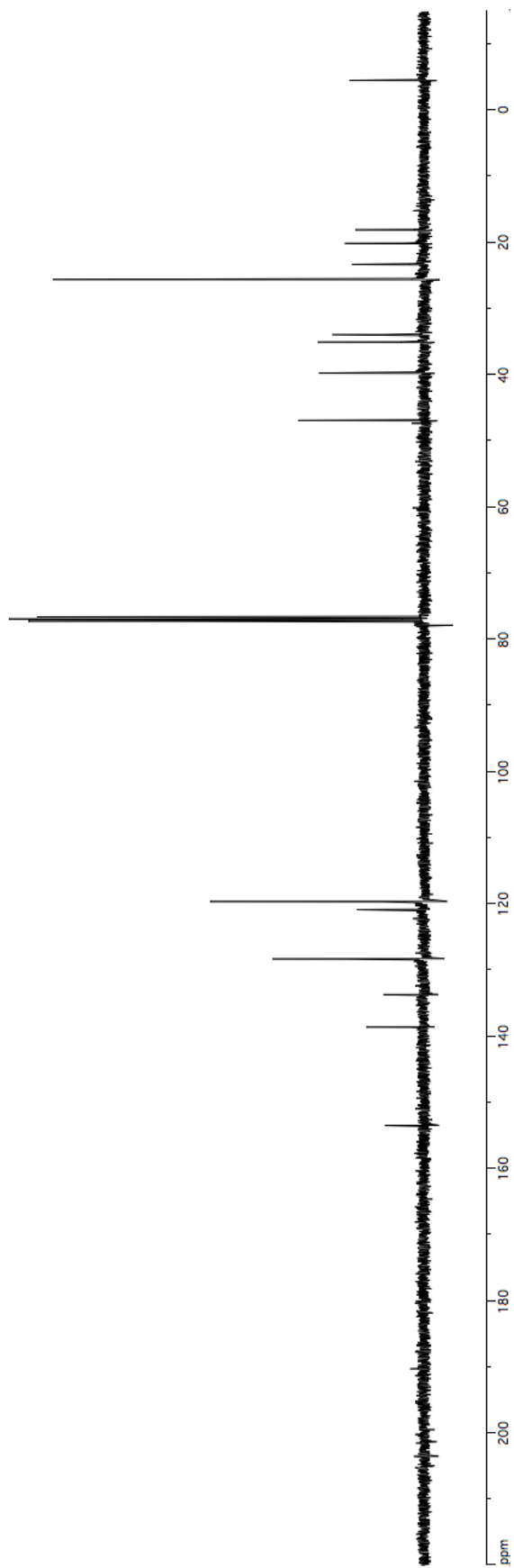


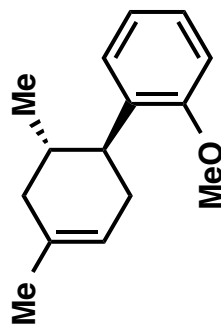
4-21  
<sup>1</sup>H NMR  
(400 MHz, CDCl<sub>3</sub>)





**4-21**  
**<sup>13</sup>C NMR**  
**(100 MHz, CDCl<sub>3</sub>)**

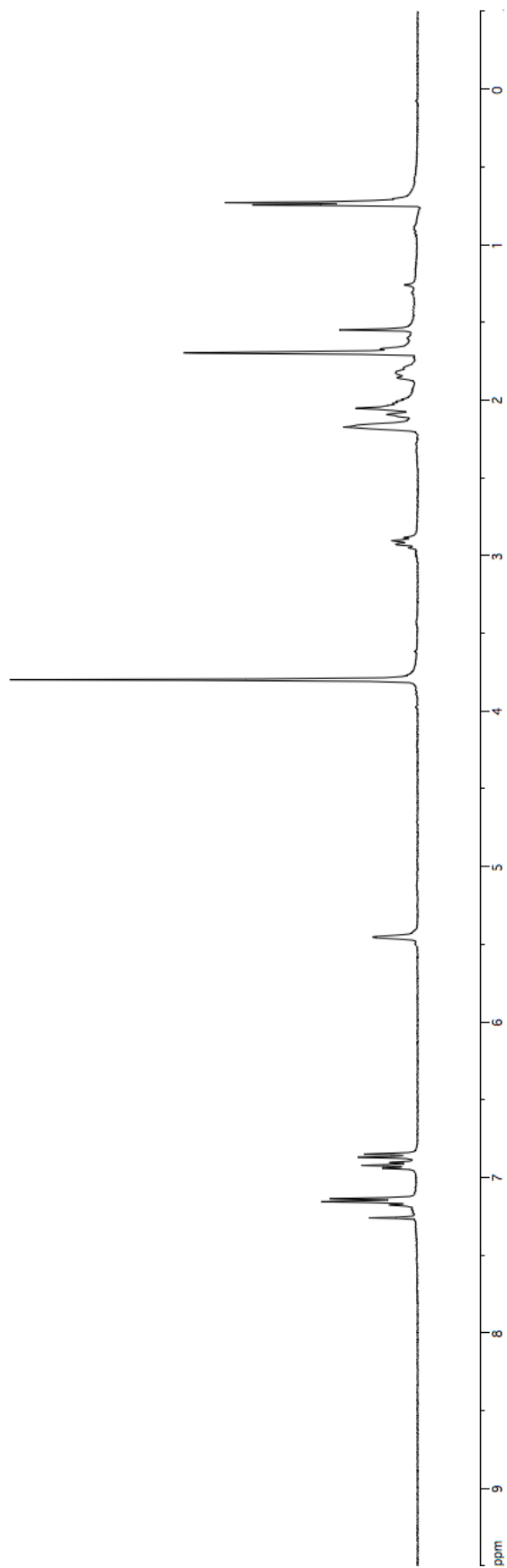


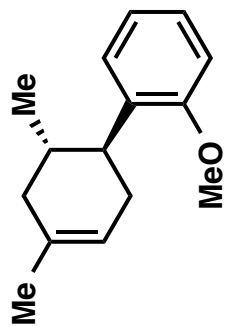


4-22

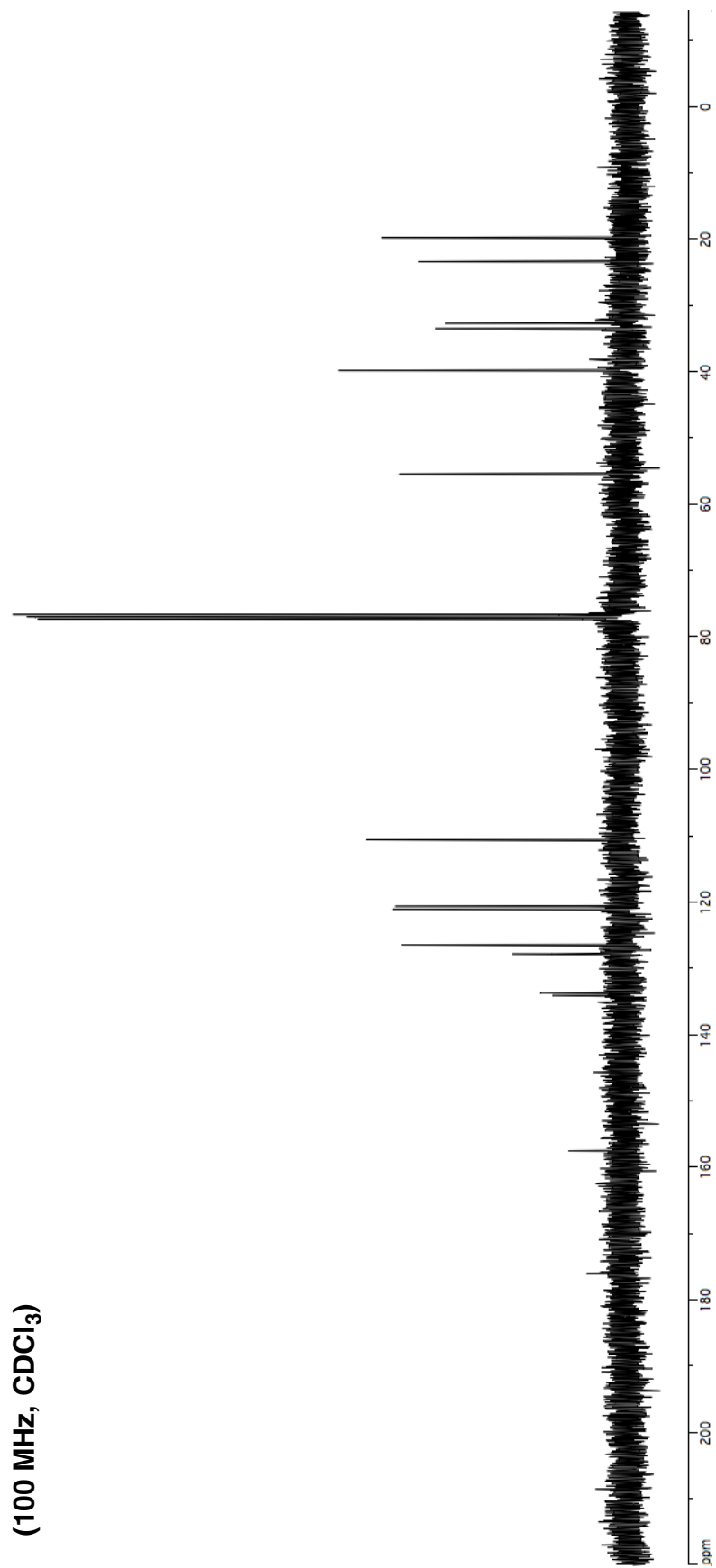
<sup>1</sup>H NMR

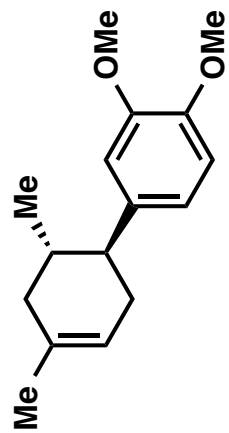
(400 MHz, CDCl<sub>3</sub>)



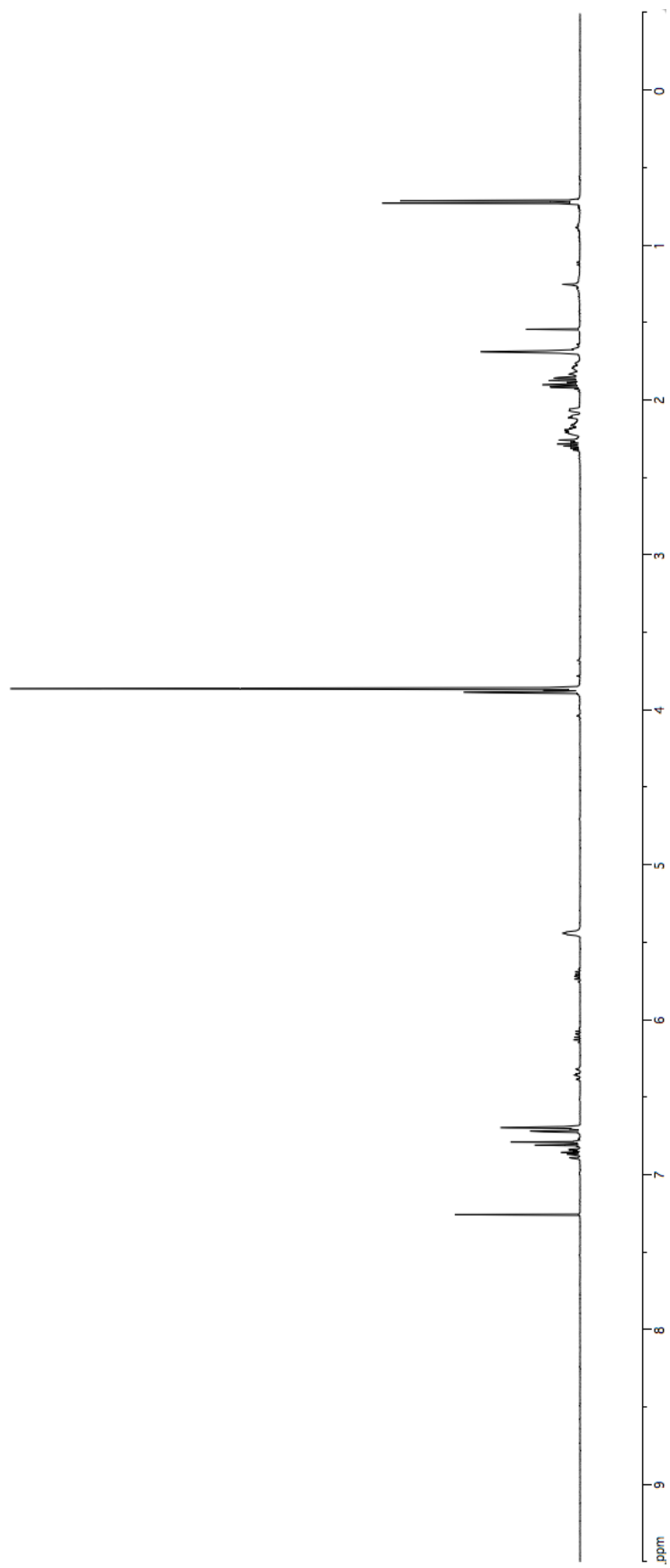


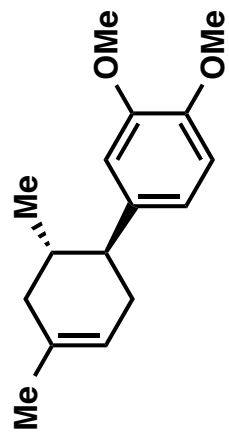
**4-22**  
**<sup>13</sup>C NMR**  
**(100 MHz, CDCl<sub>3</sub>)**



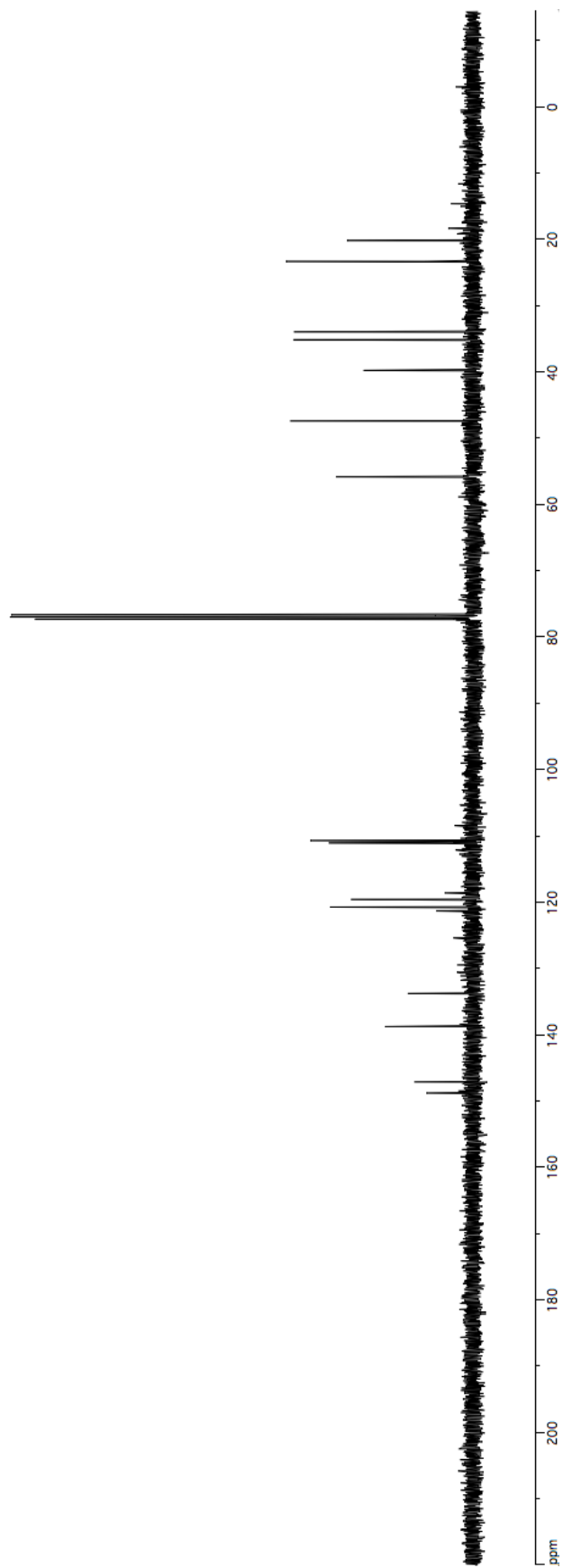


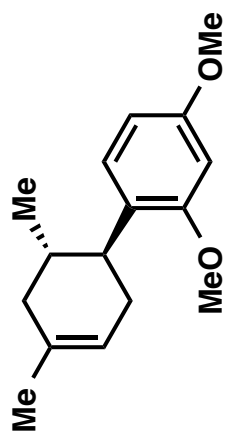
**4-23**  
**<sup>1</sup>H NMR**  
**(400 MHz, CDCl<sub>3</sub>)**



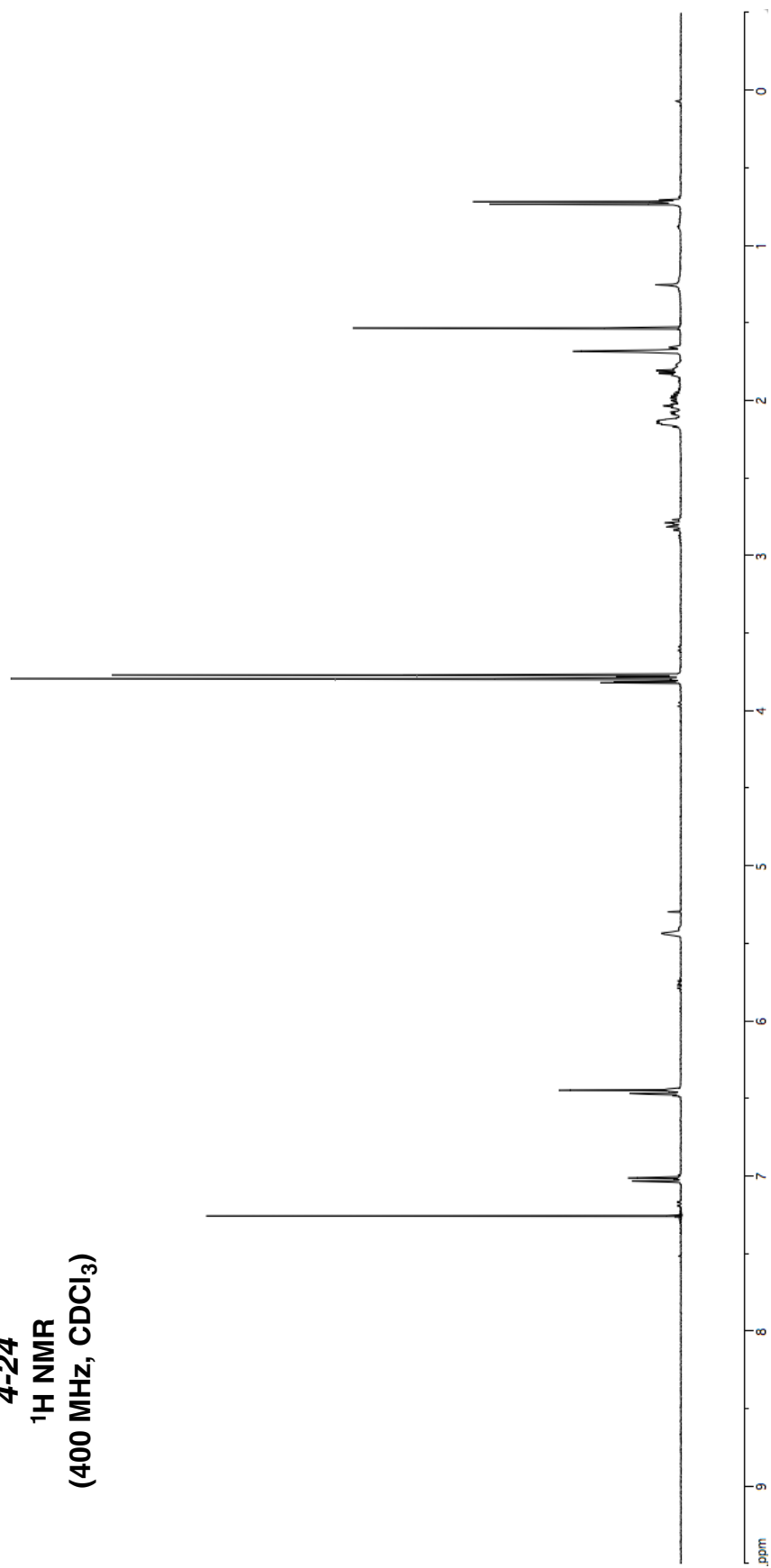


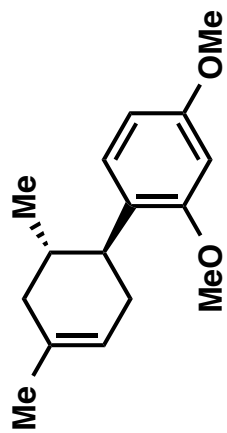
**4-23**  
**<sup>13</sup>C NMR**  
**(100 MHz, CDCl<sub>3</sub>)**





4-24  
<sup>1</sup>H NMR  
(400 MHz, CDCl<sub>3</sub>)

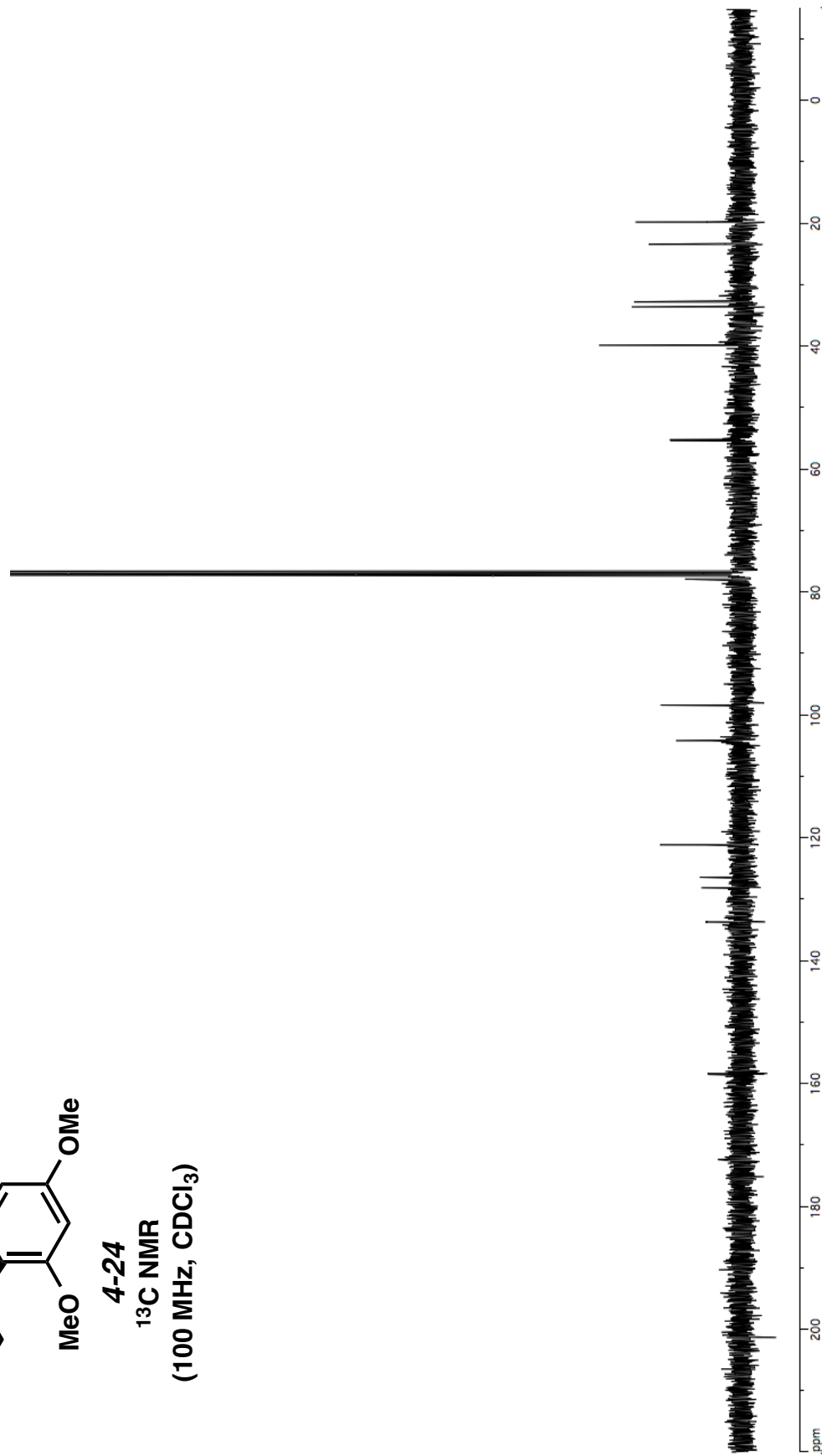


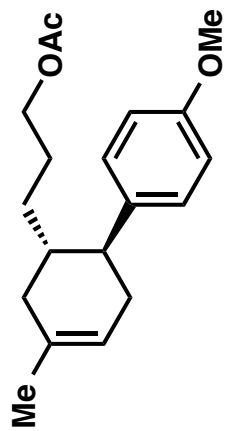


4-24

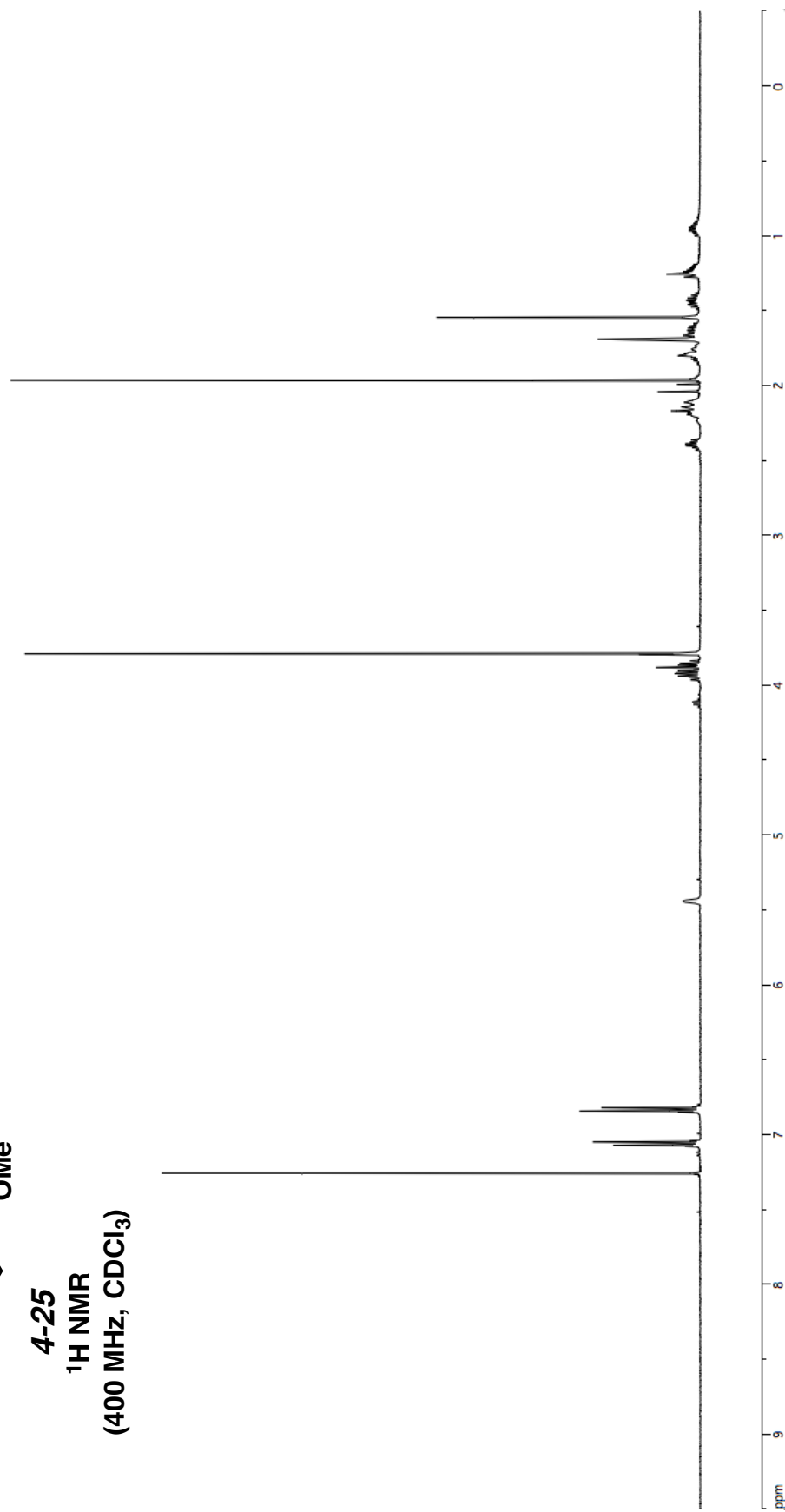
<sup>13</sup>C NMR

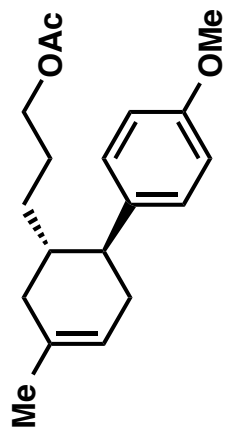
(100 MHz, CDCl<sub>3</sub>)



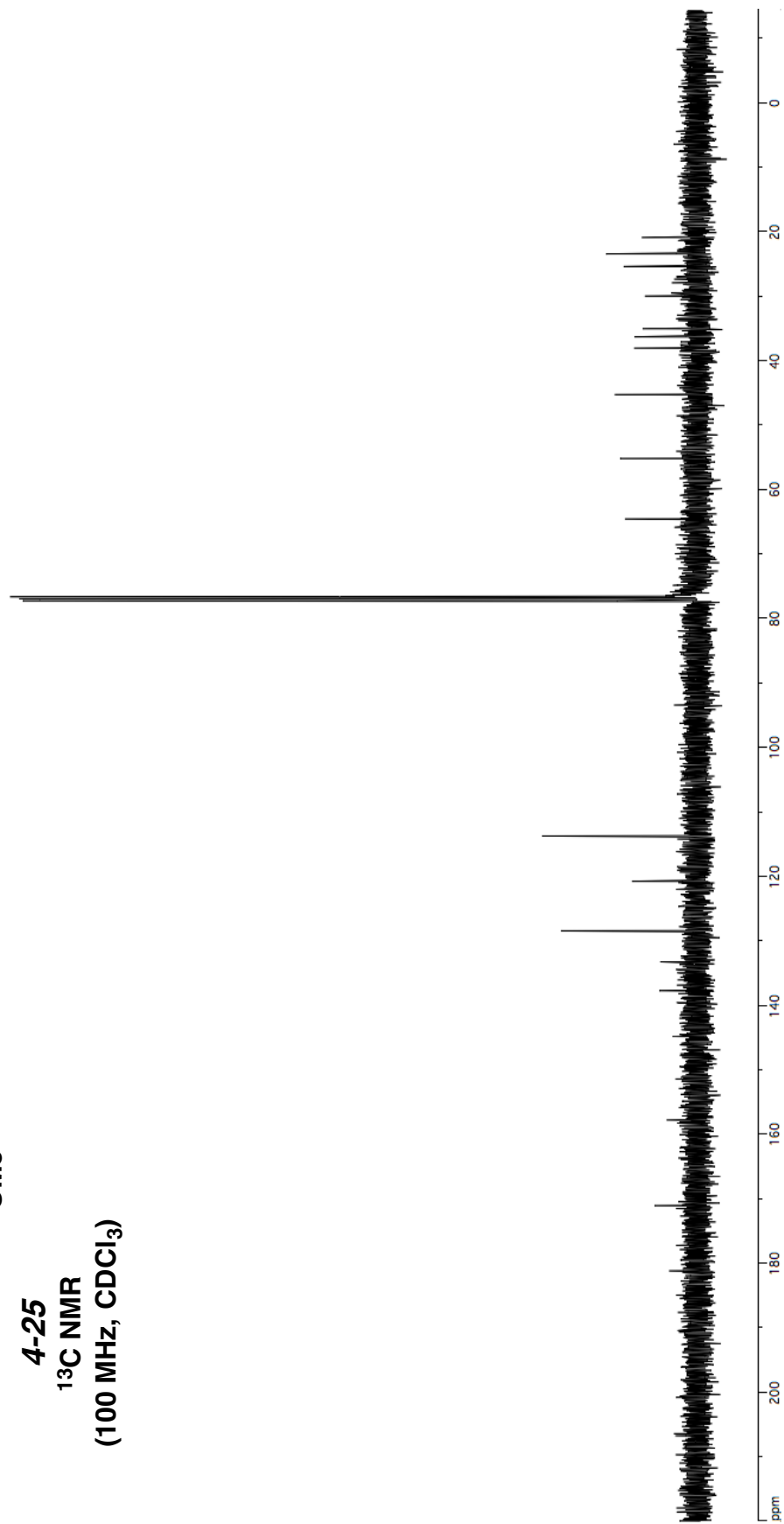


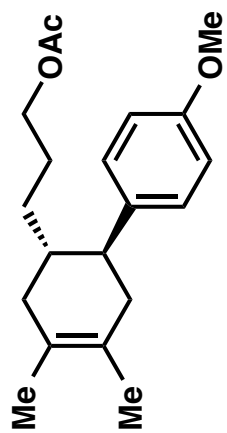
4-25  
<sup>1</sup>H NMR  
(400 MHz, CDCl<sub>3</sub>)



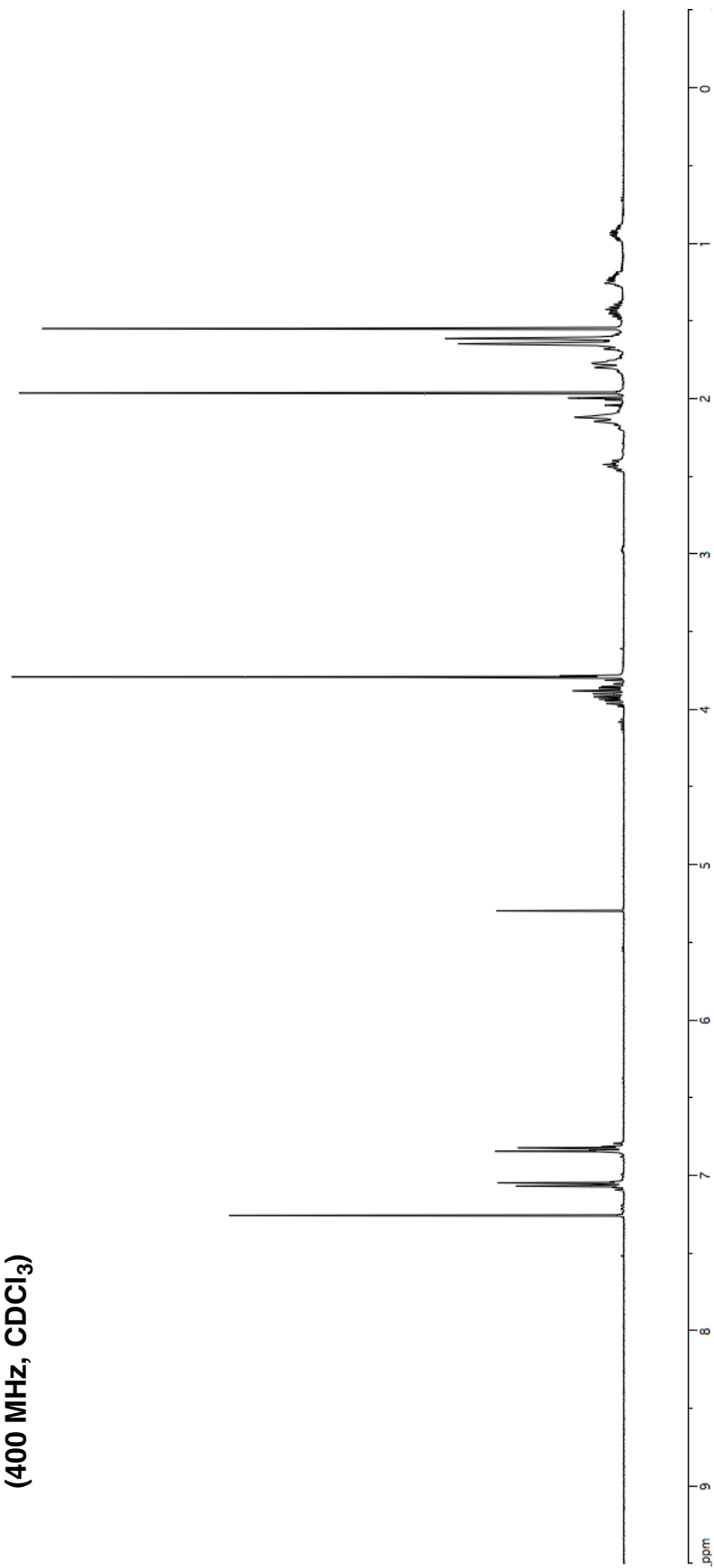


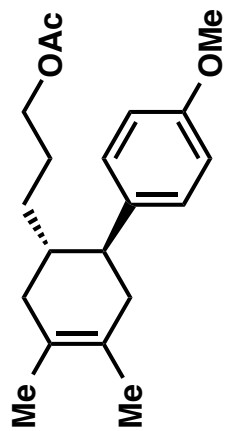
**4-25**  
**<sup>13</sup>C NMR**  
**(100 MHz, CDCl<sub>3</sub>)**



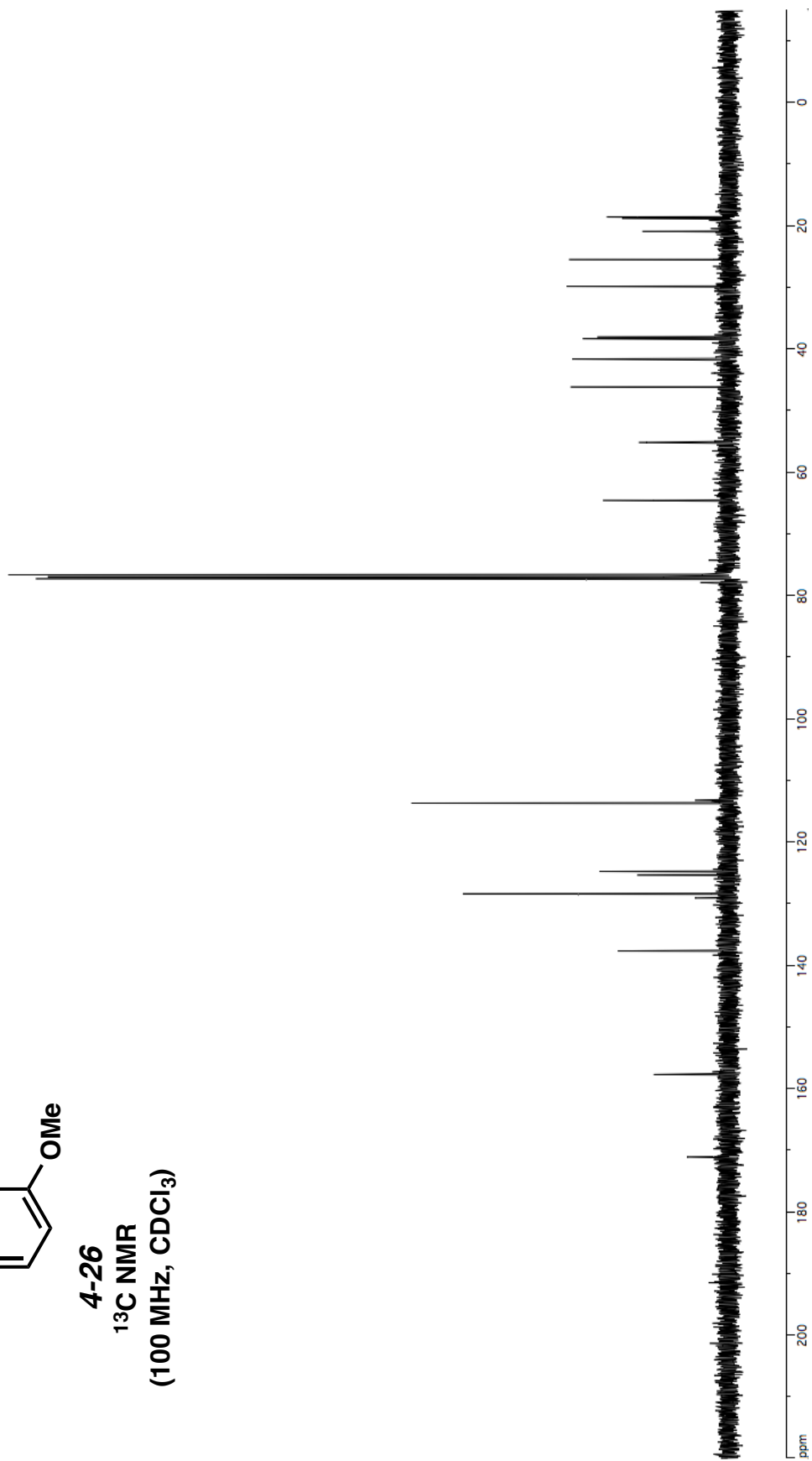


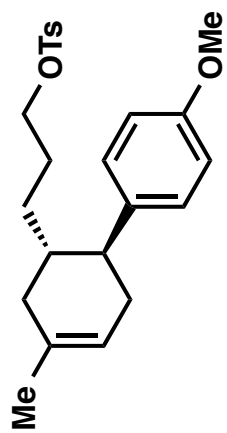
**4-26**  
**<sup>1</sup>H NMR**  
**(400 MHz, CDCl<sub>3</sub>)**



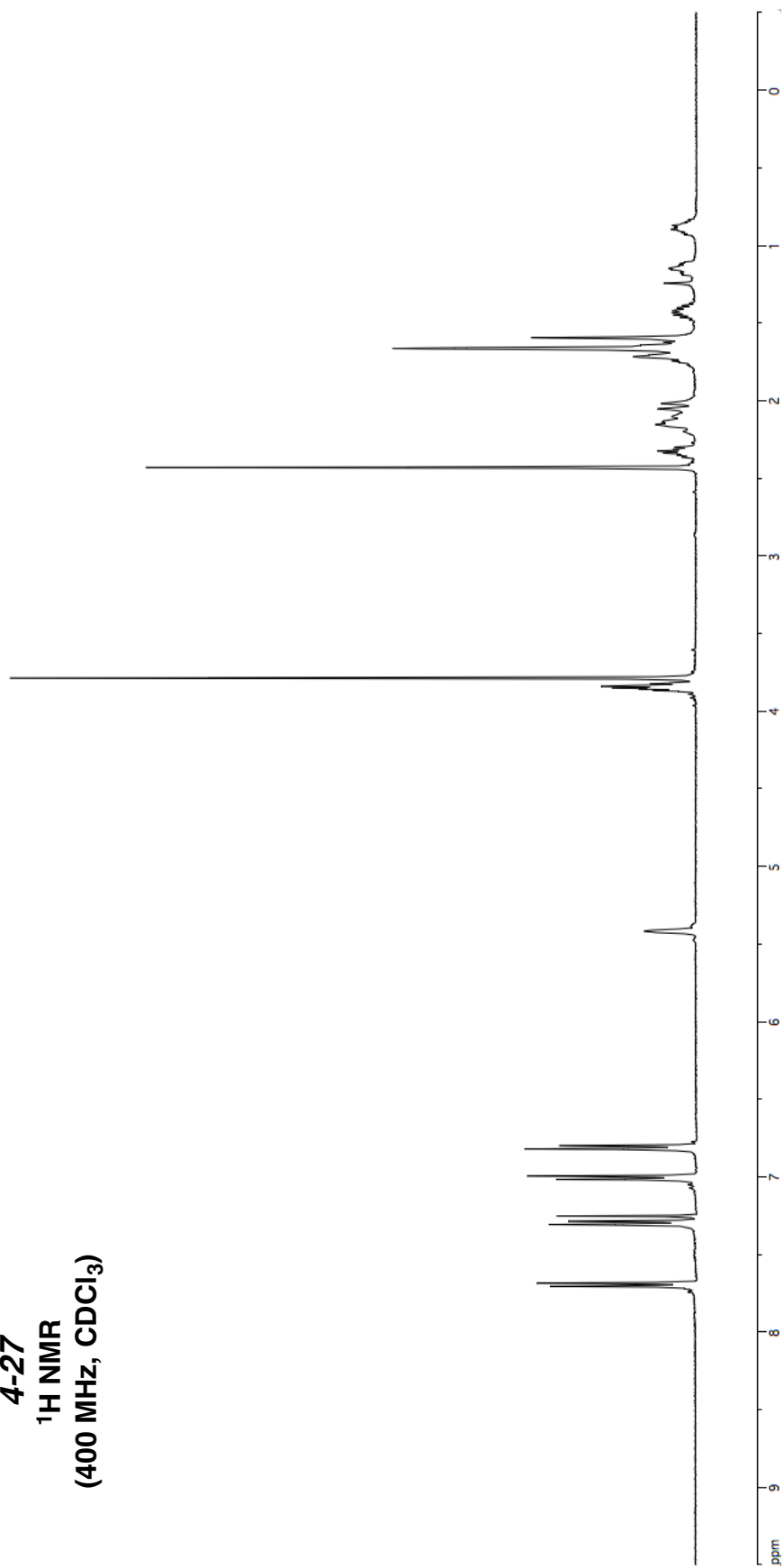


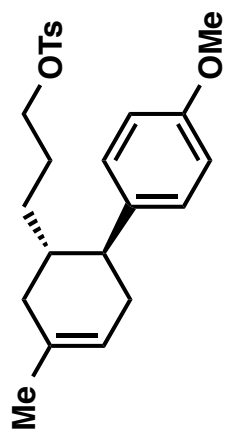
**4-26**  
**<sup>13</sup>C NMR**  
**(100 MHz, CDCl<sub>3</sub>)**



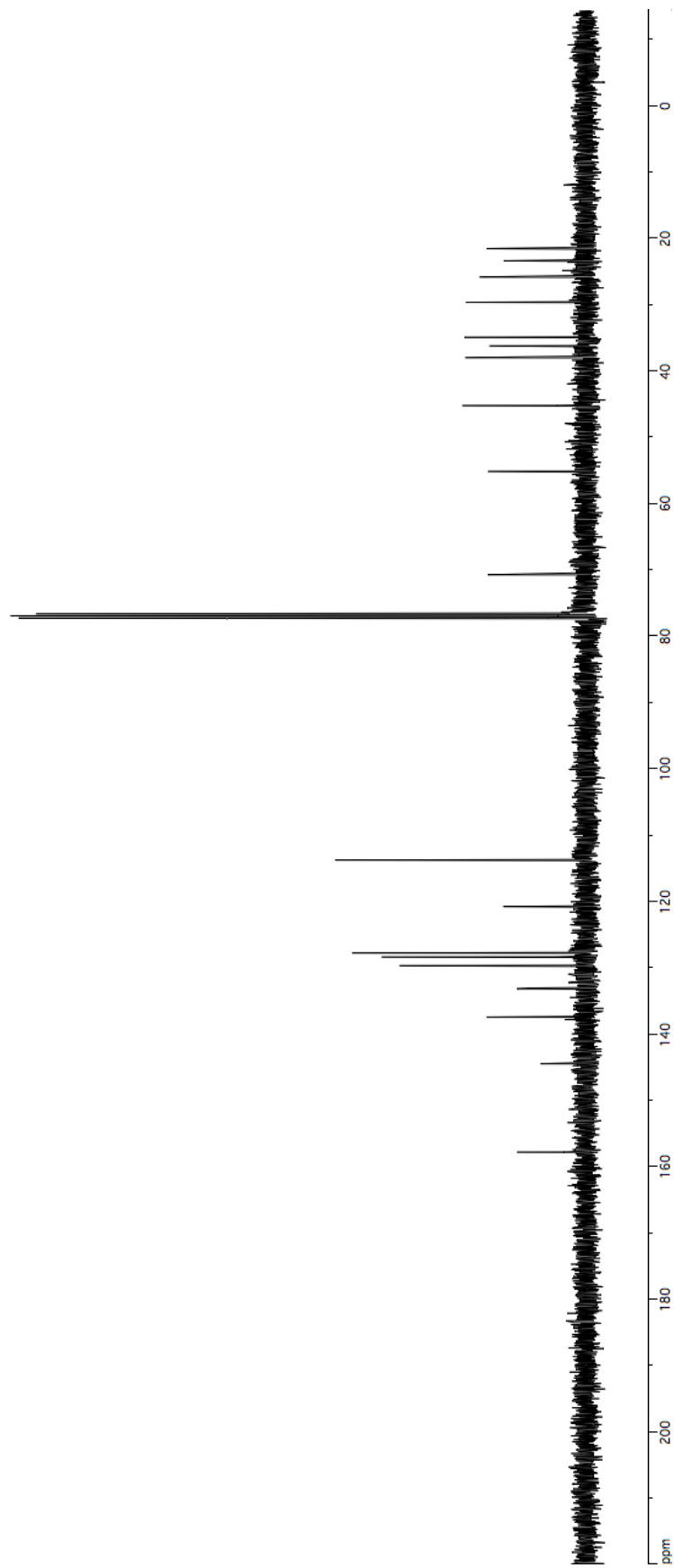


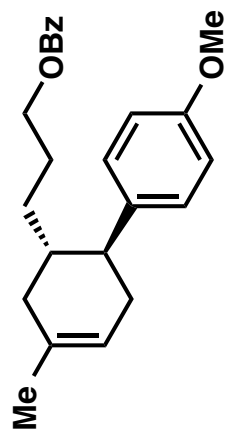
4-27  
<sup>1</sup>H NMR  
(400 MHz, CDCl<sub>3</sub>)



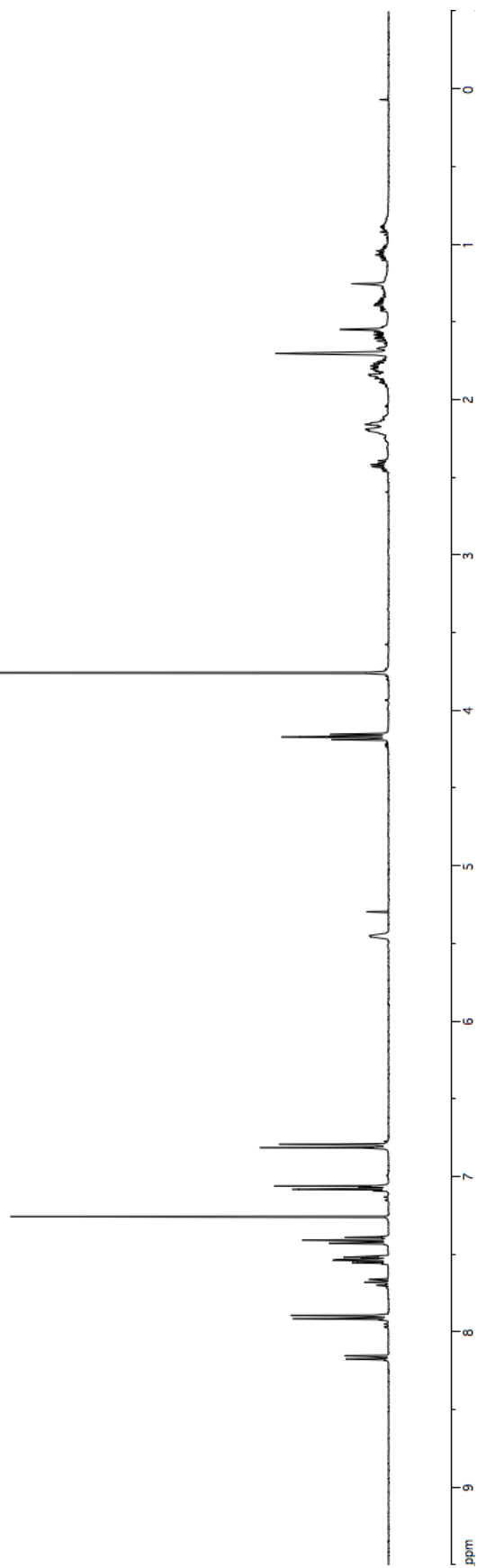


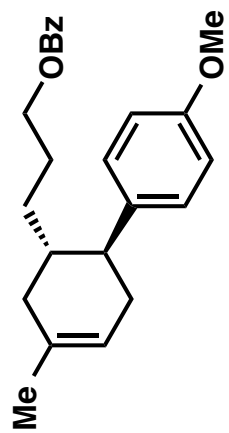
**4-27**  
**<sup>13</sup>C NMR**  
**(100 MHz, CDCl<sub>3</sub>)**



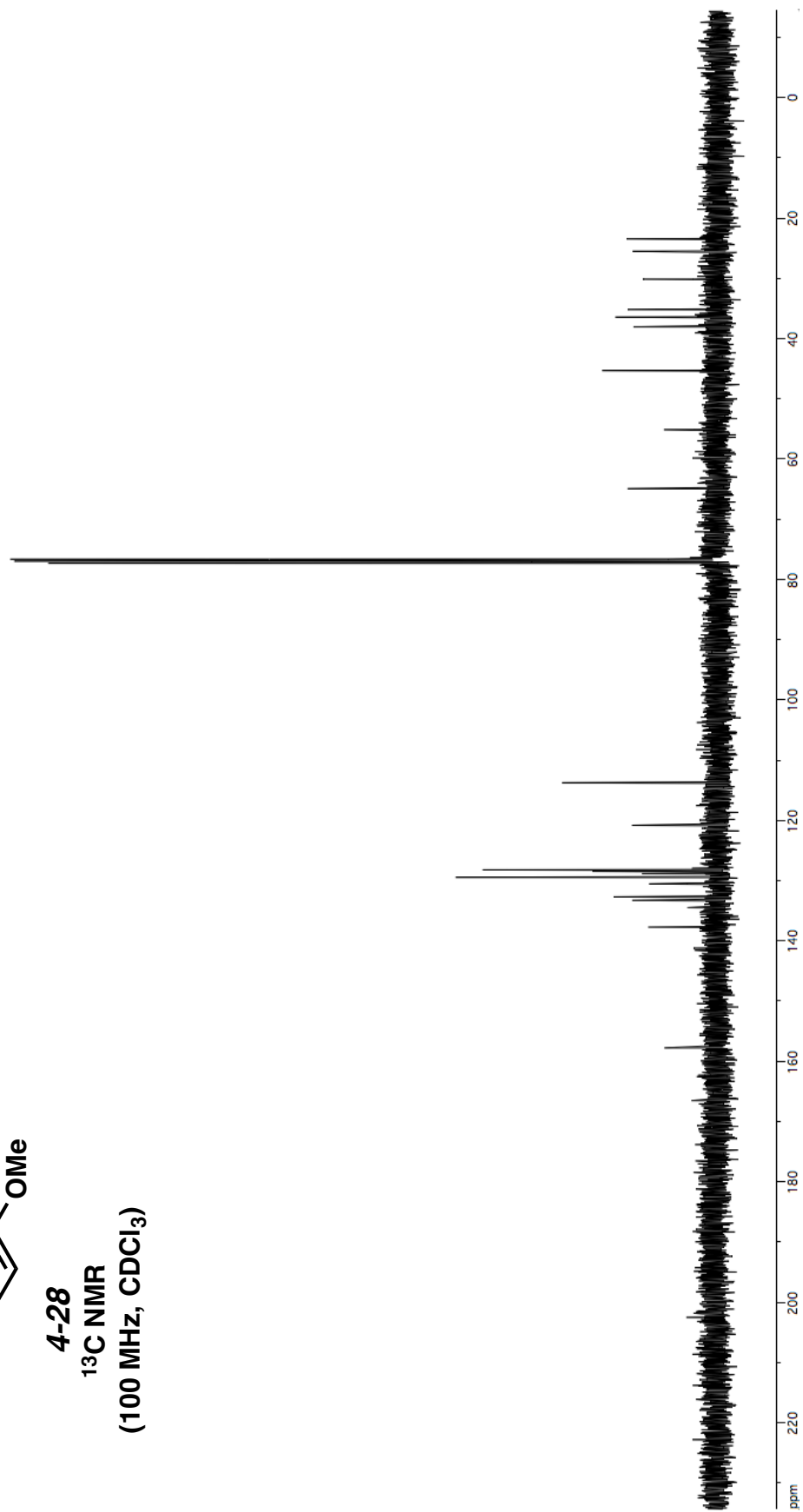


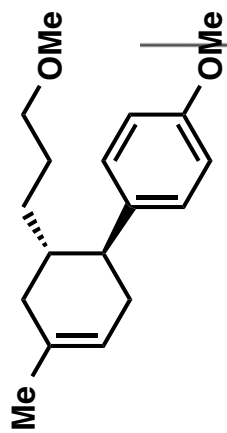
**4-28**  
**<sup>1</sup>H NMR**  
**(400 MHz, CDCl<sub>3</sub>)**



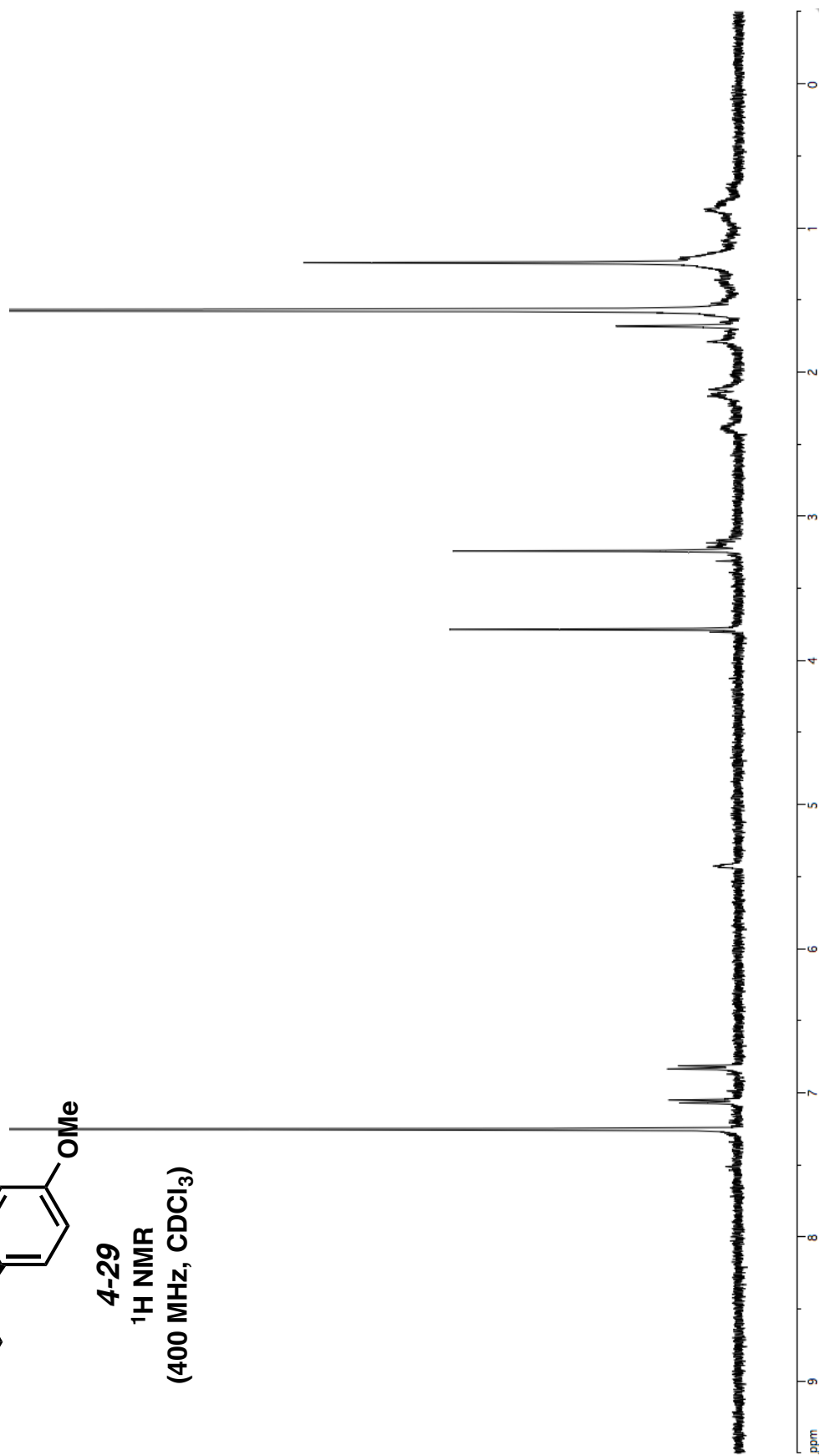


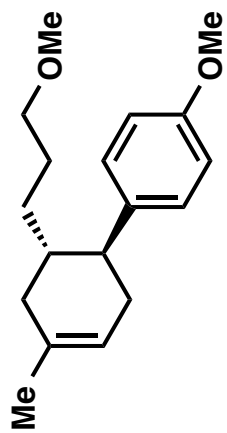
**4-28**  
**<sup>13</sup>C NMR**  
**(100 MHz, CDCl<sub>3</sub>)**



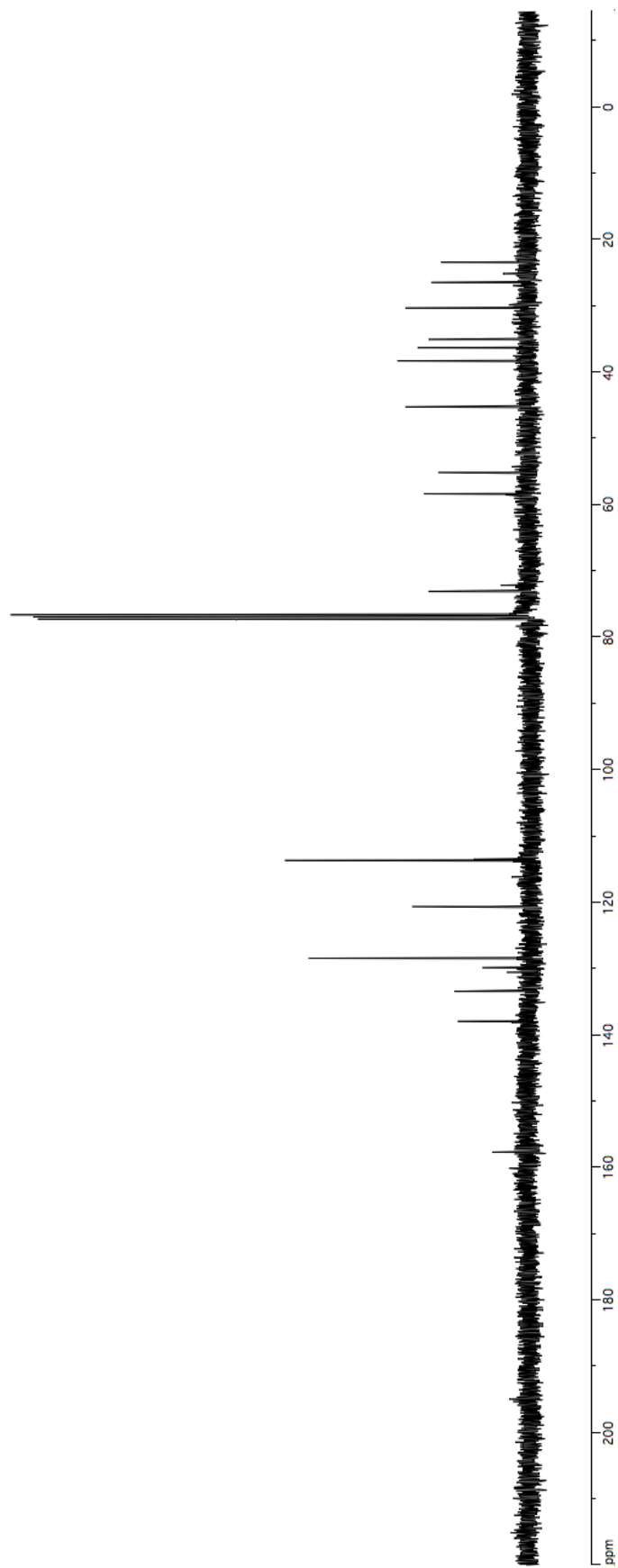


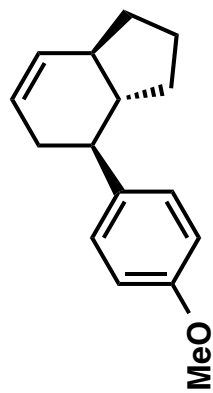
4-29  
<sup>1</sup>H NMR  
(400 MHz, CDCl<sub>3</sub>)



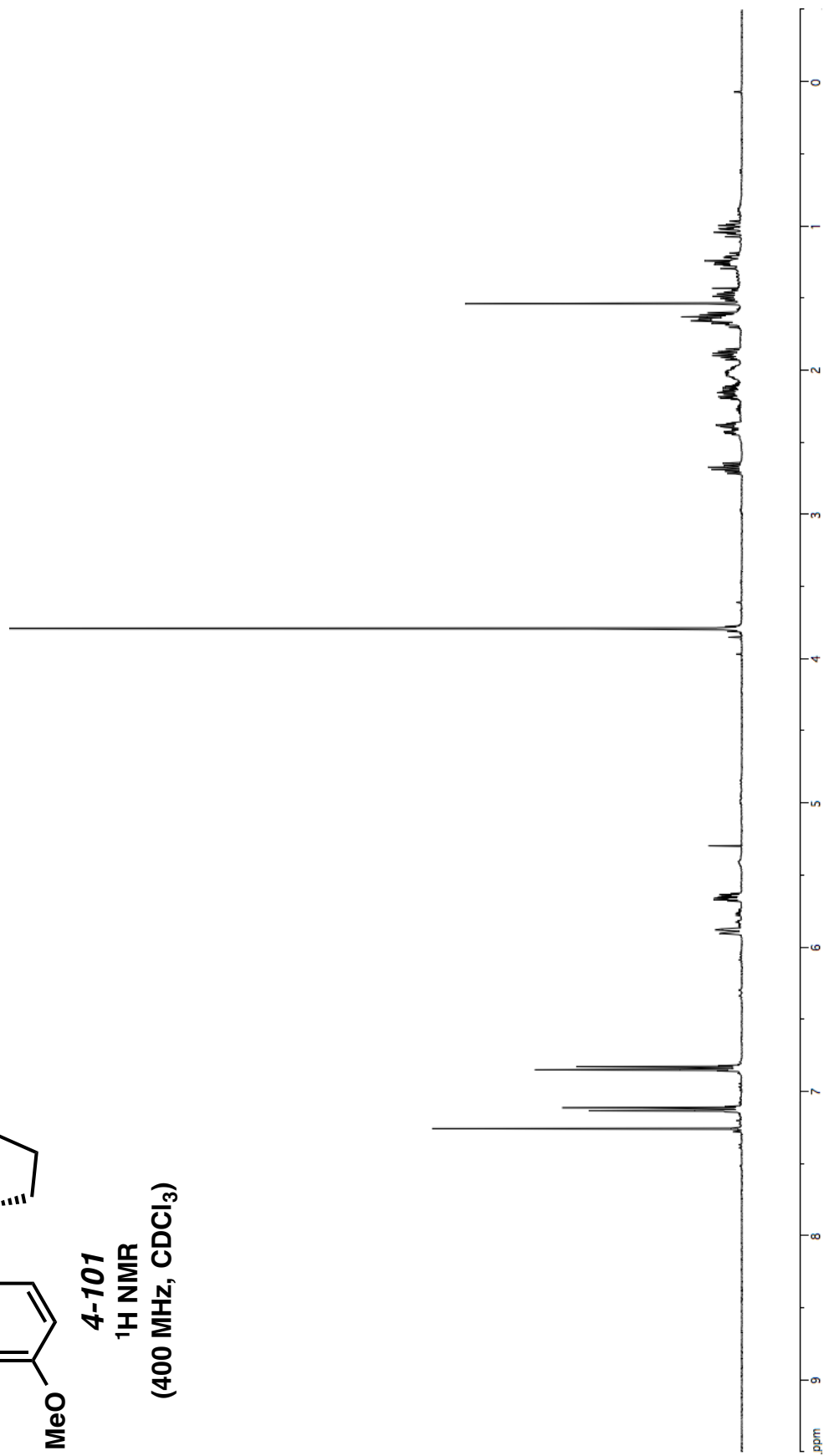


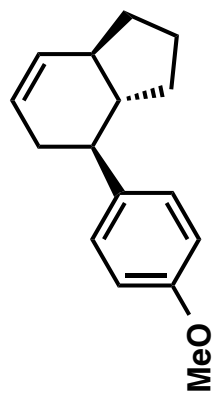
**4-29**  
**<sup>13</sup>C NMR**  
**(100 MHz, CDCl<sub>3</sub>)**



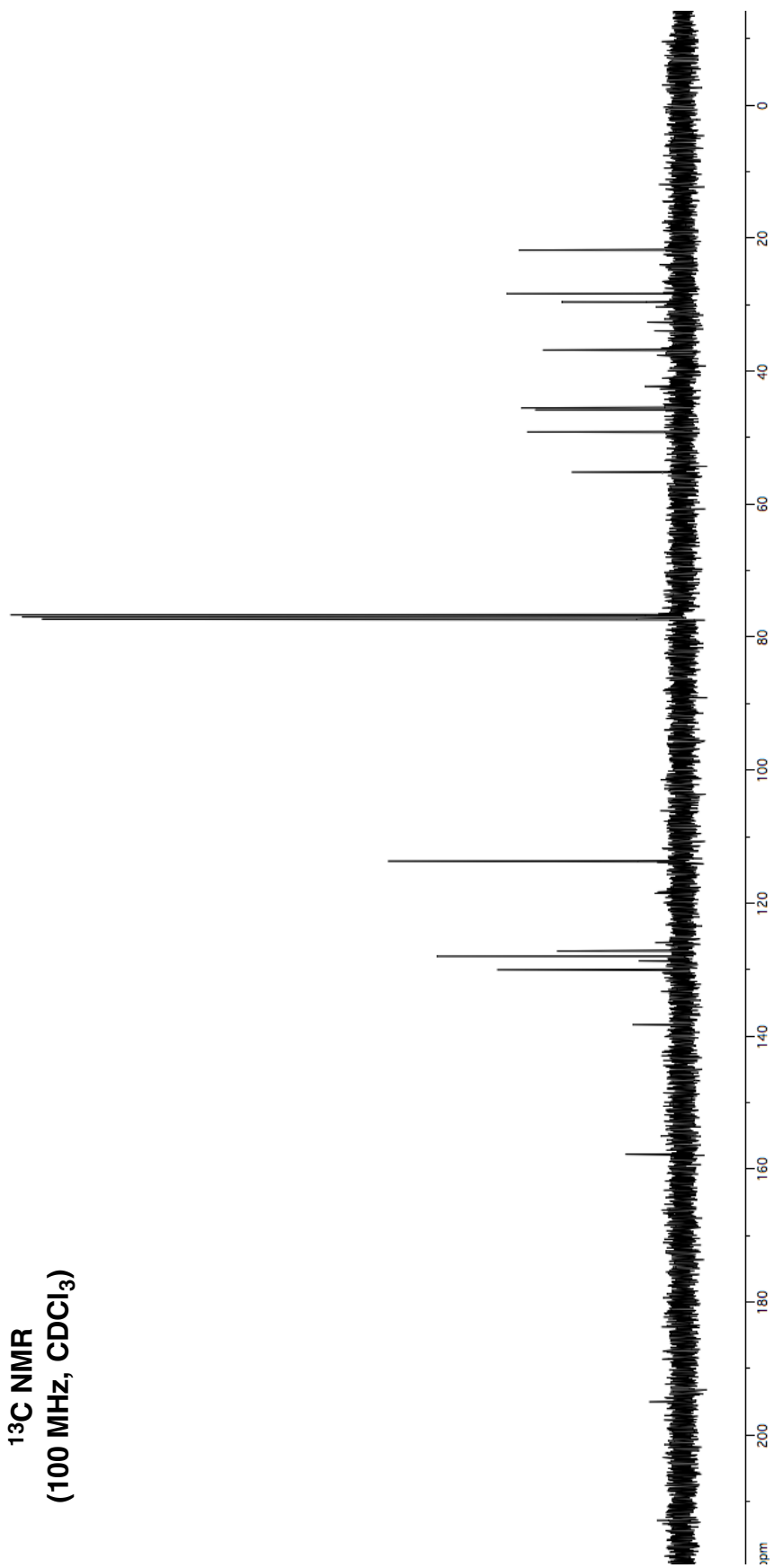


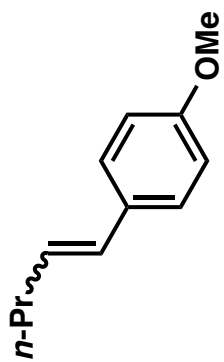
**4-101**  
**<sup>1</sup>H NMR**  
**(400 MHz, CDCl<sub>3</sub>)**



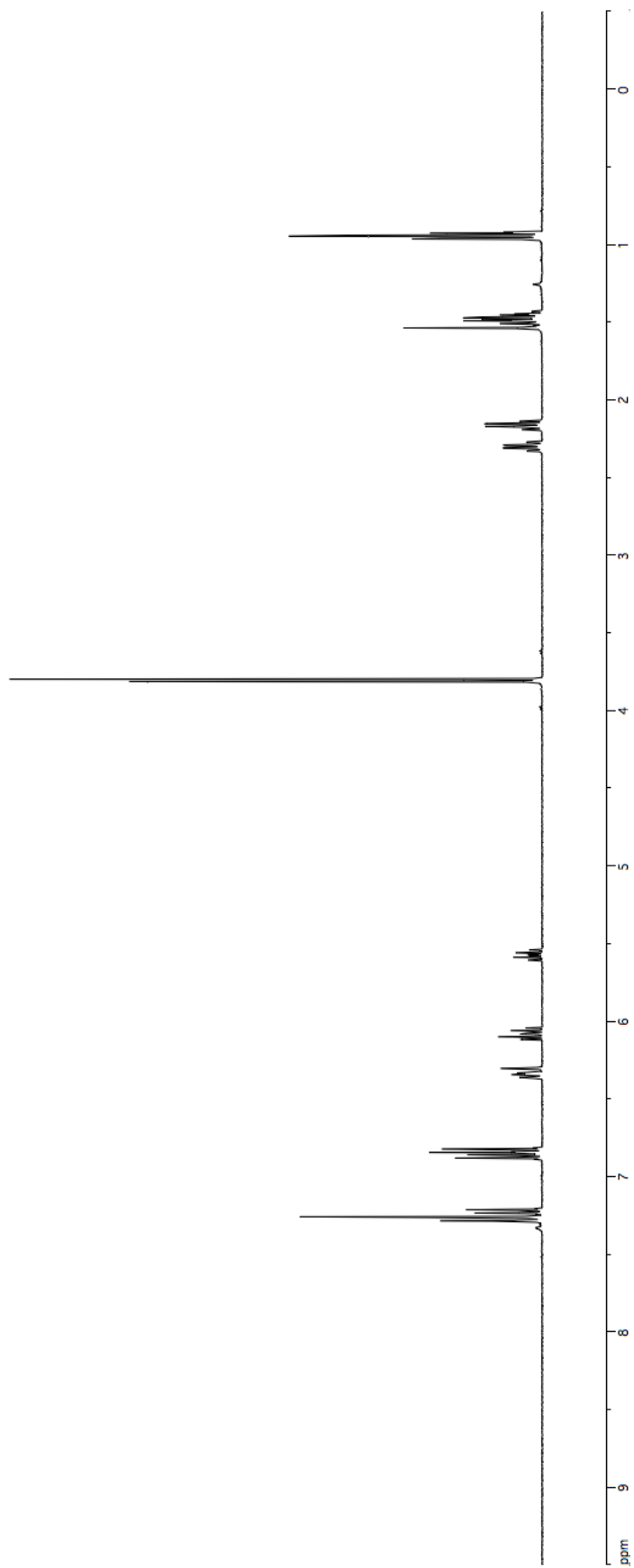


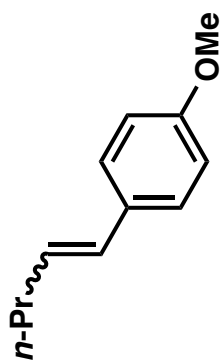
**4-101**  
**<sup>13</sup>C NMR**  
**(100 MHz, CDCl<sub>3</sub>)**



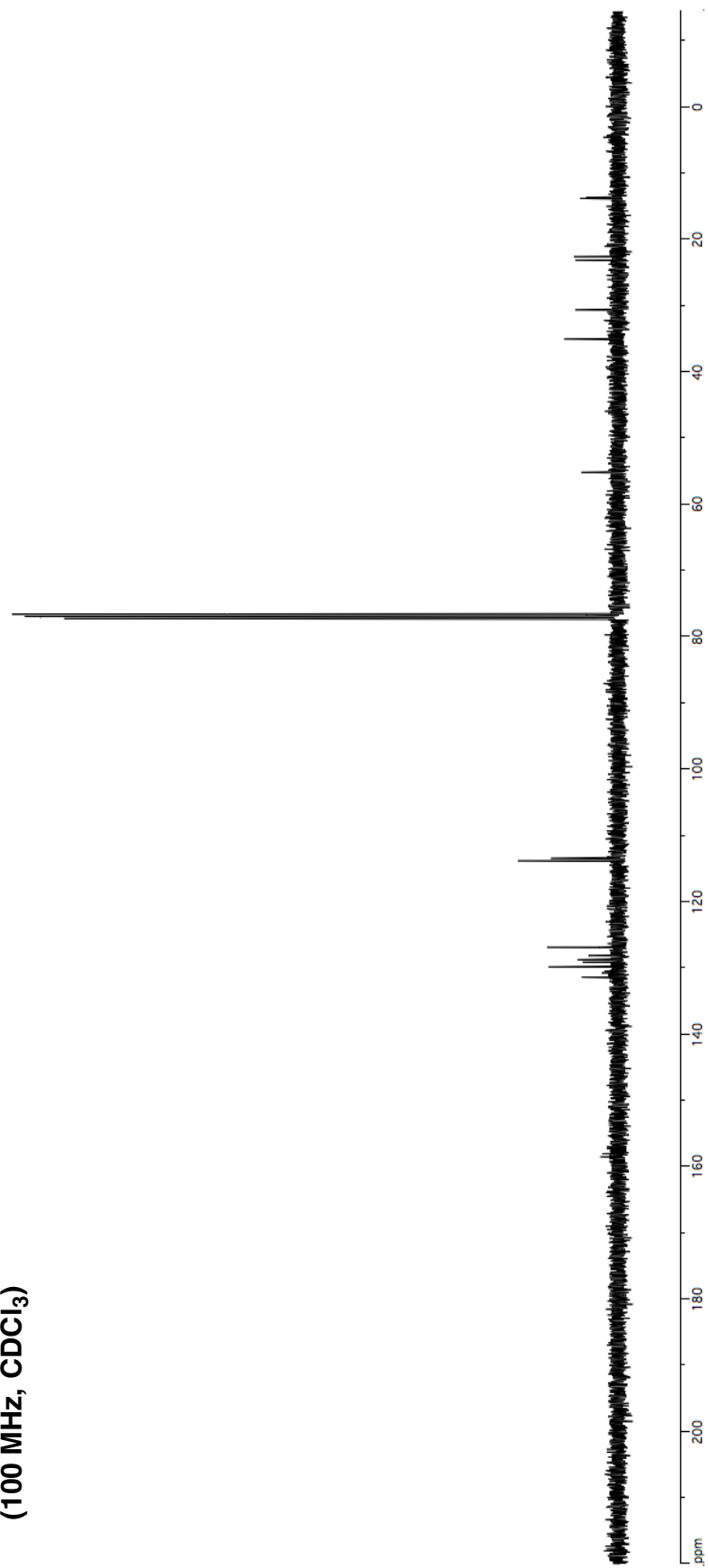


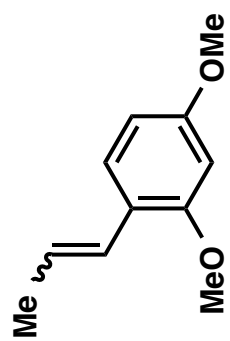
4-76  
<sup>1</sup>H NMR  
(400 MHz, CDCl<sub>3</sub>)





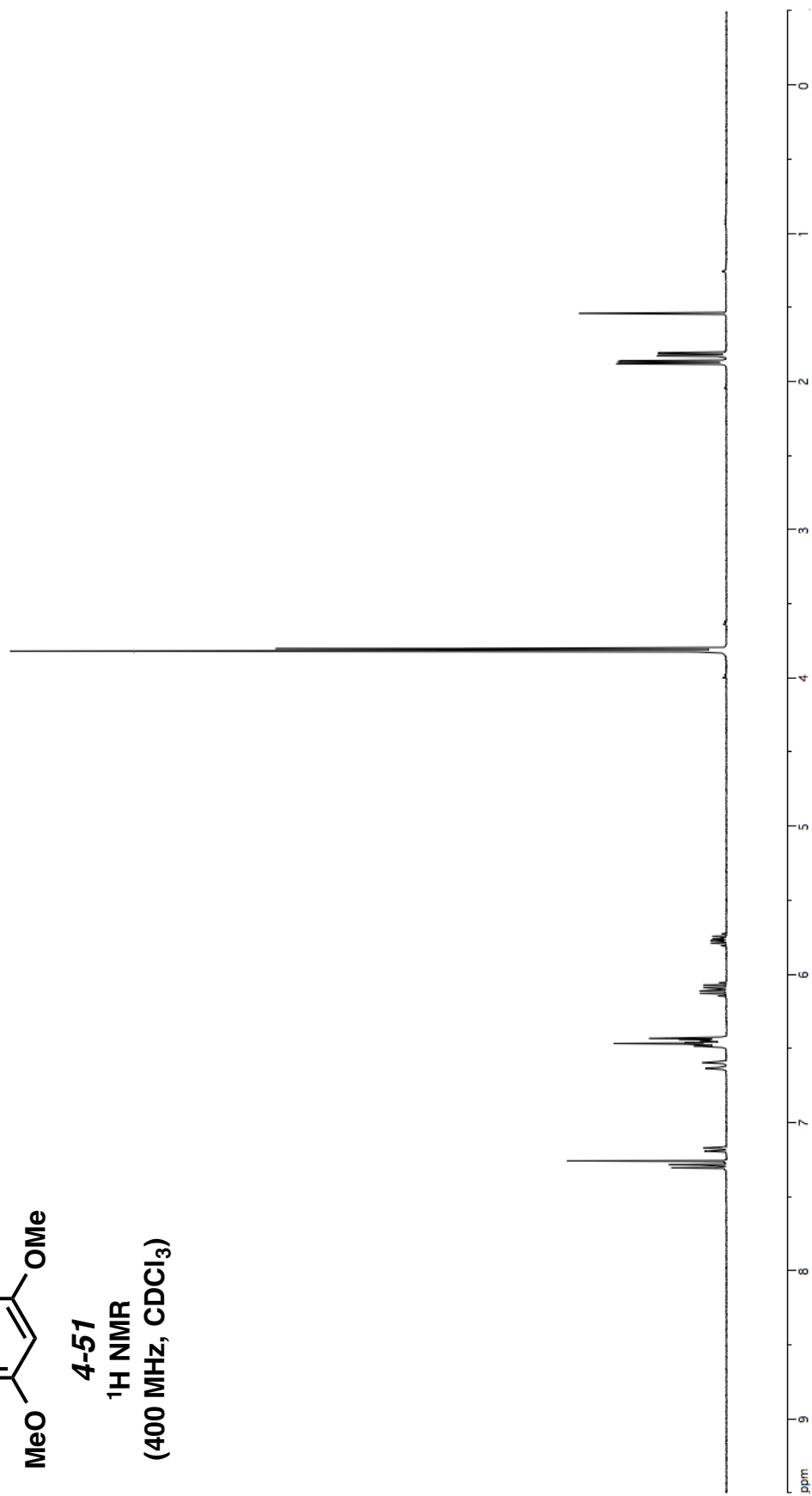
**4-76**  
**<sup>13</sup>C NMR**  
**(100 MHz, CDCl<sub>3</sub>)**

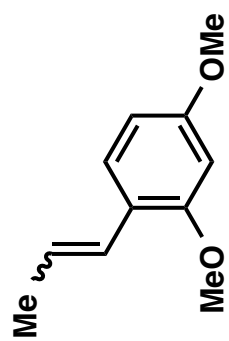




4-51

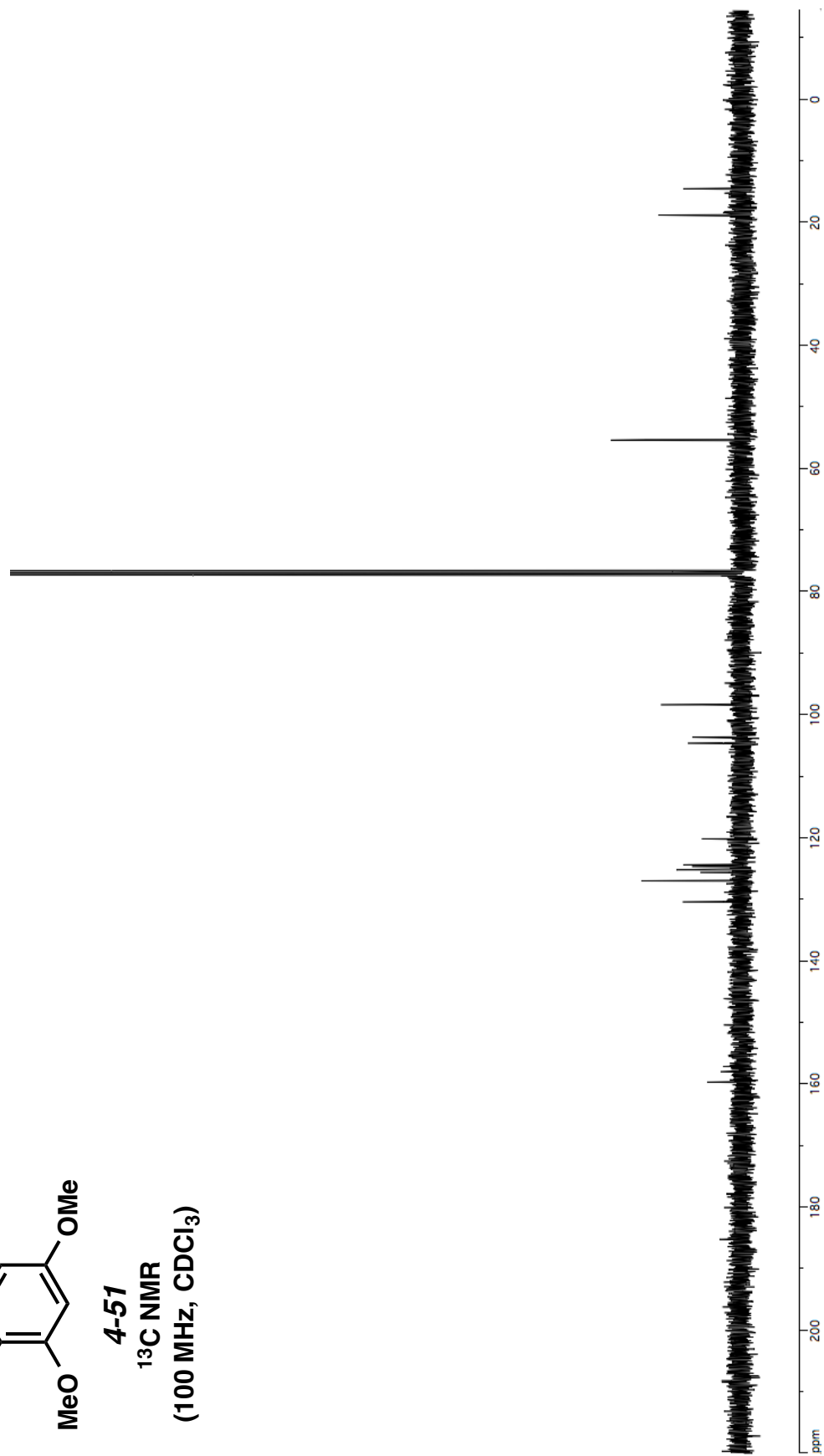
<sup>1</sup>H NMR  
(400 MHz, CDCl<sub>3</sub>)



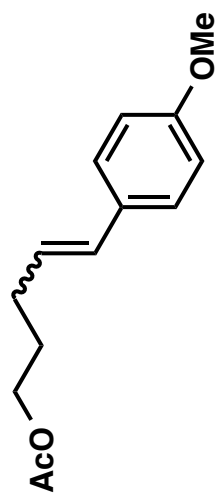


4-51

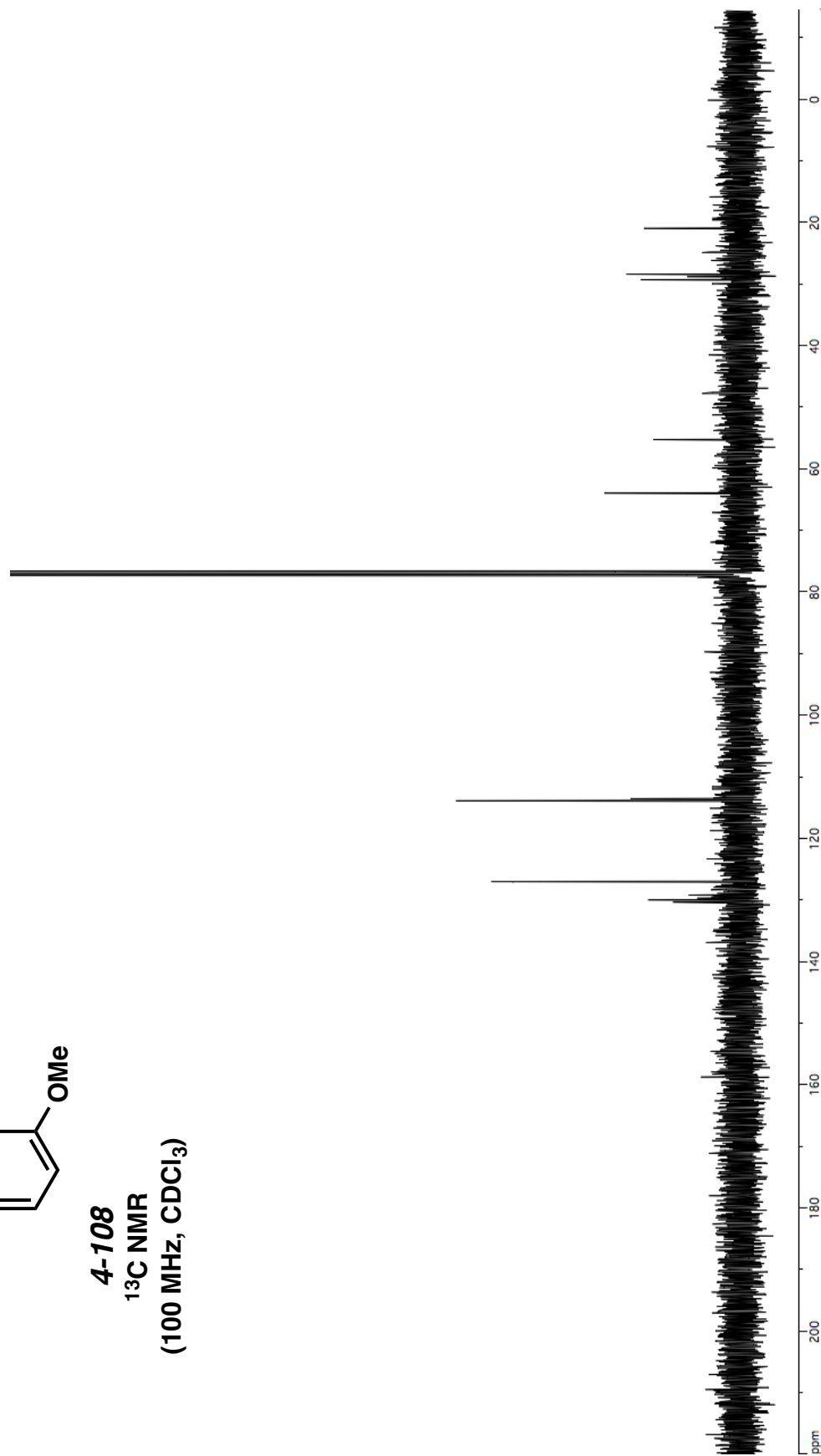
<sup>13</sup>C NMR  
(100 MHz, CDCl<sub>3</sub>)



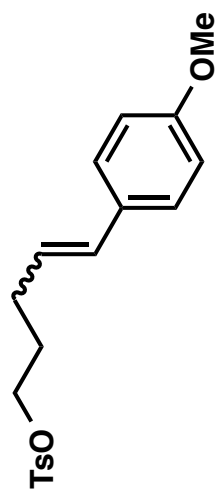




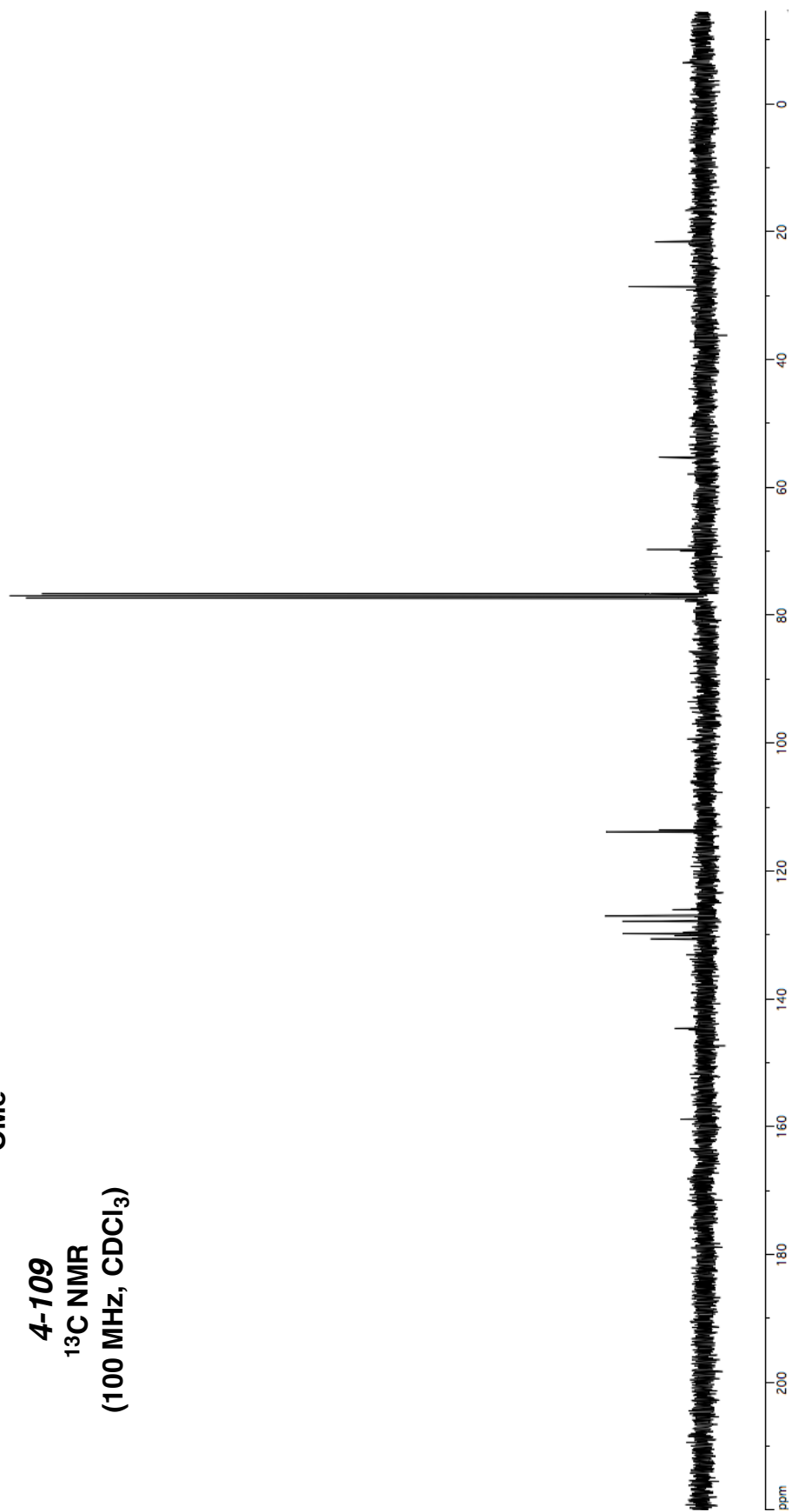
**4-108**  
**<sup>13</sup>C NMR**  
**(100 MHz, CDCl<sub>3</sub>)**

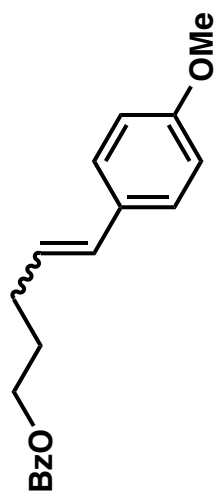




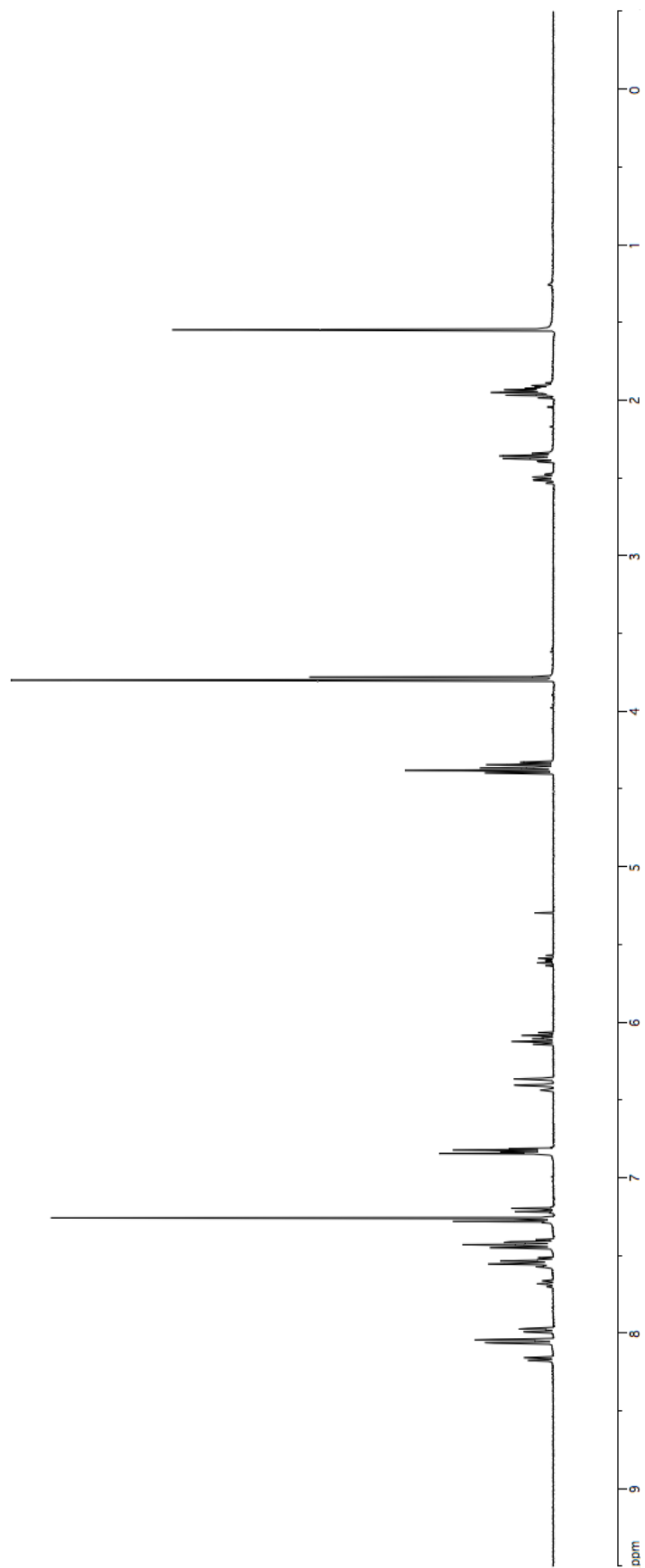


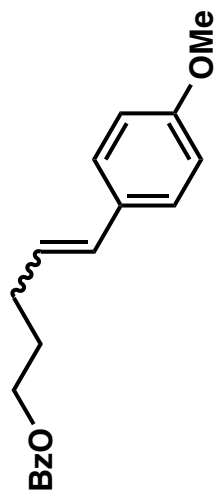
**4-109**  
**<sup>13</sup>C NMR**  
**(100 MHz, CDCl<sub>3</sub>)**



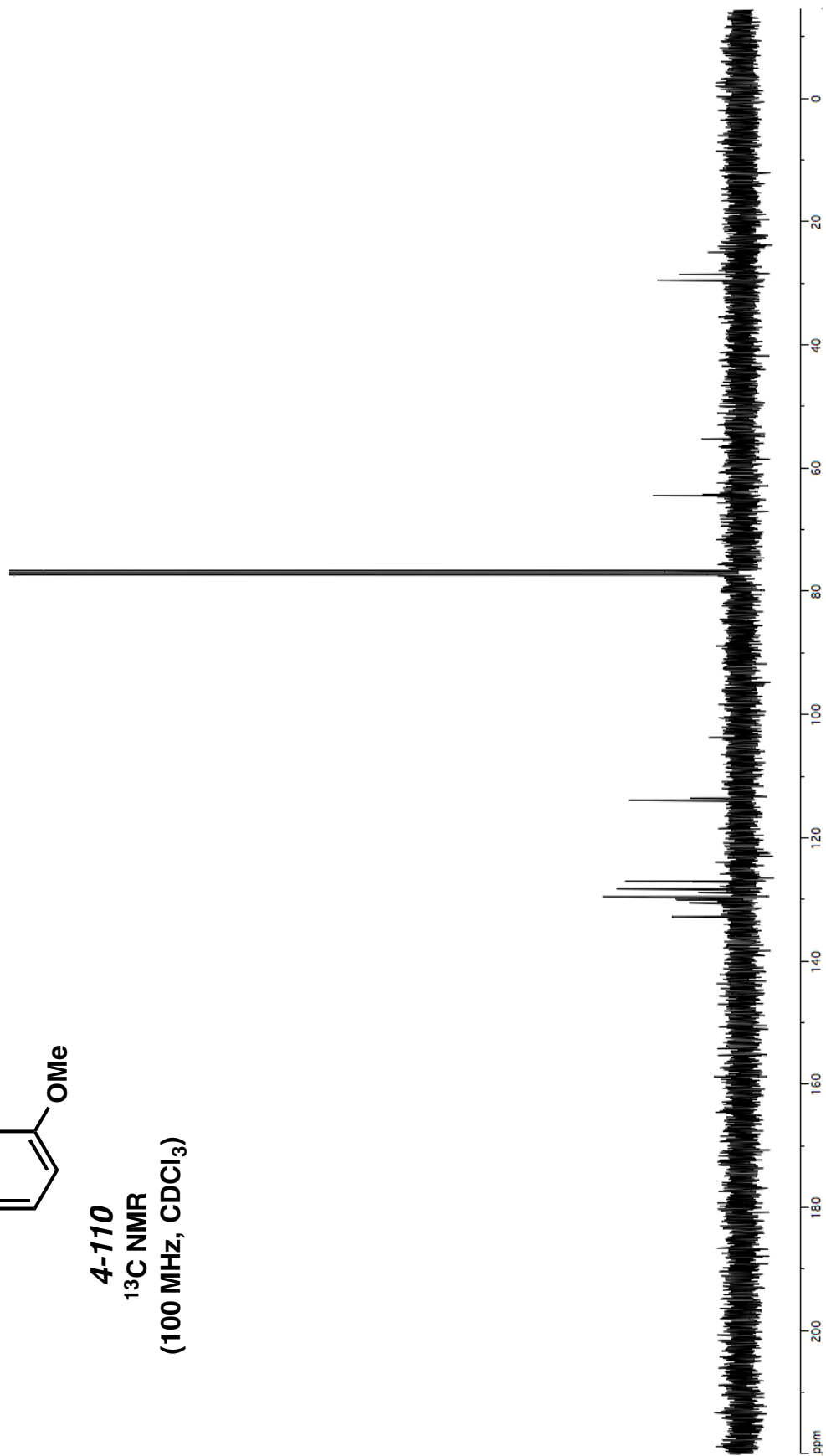


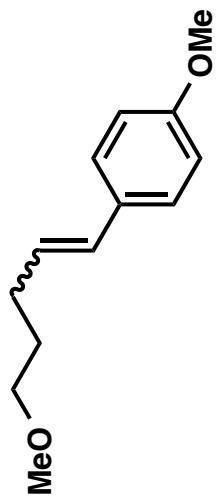
**4-110**  
**<sup>1</sup>H NMR**  
**(400 MHz, CDCl<sub>3</sub>)**



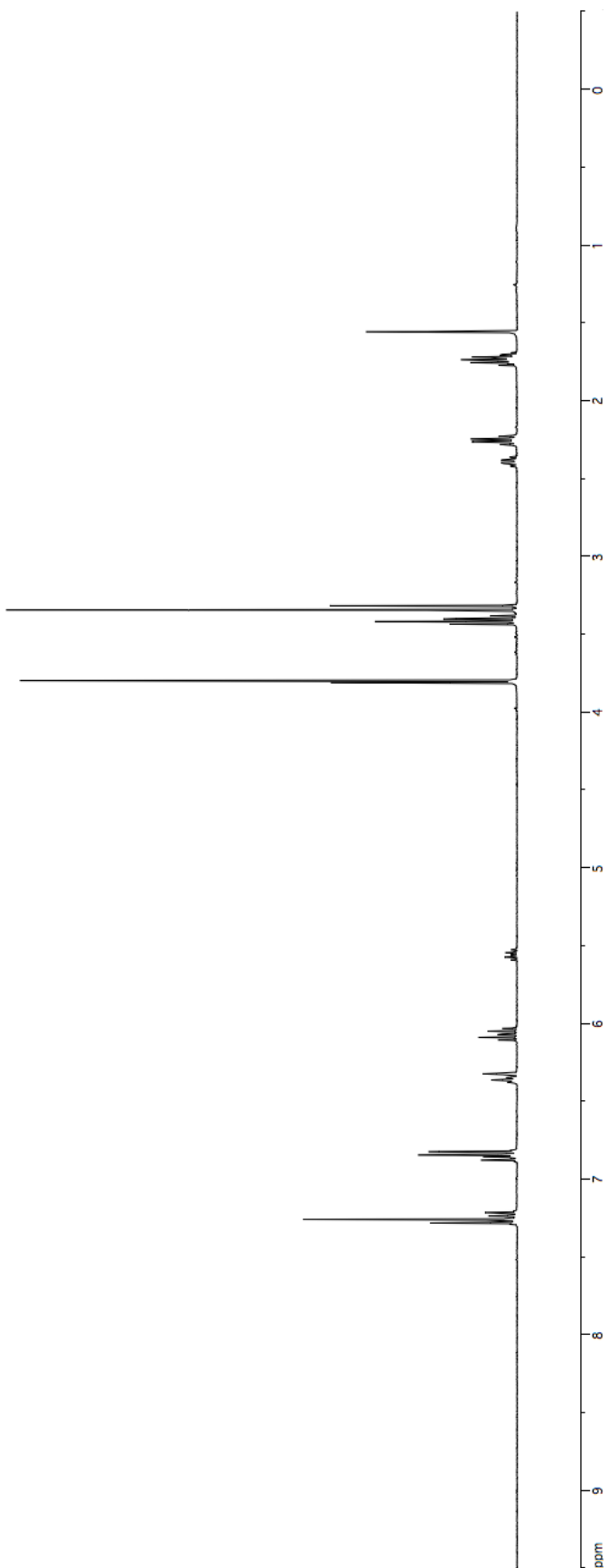


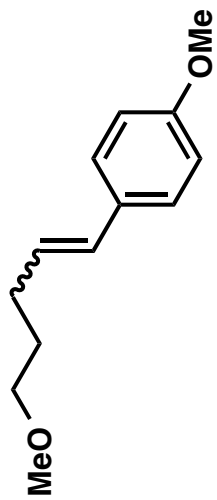
**4-110**  
**<sup>13</sup>C NMR**  
**(100 MHz, CDCl<sub>3</sub>)**



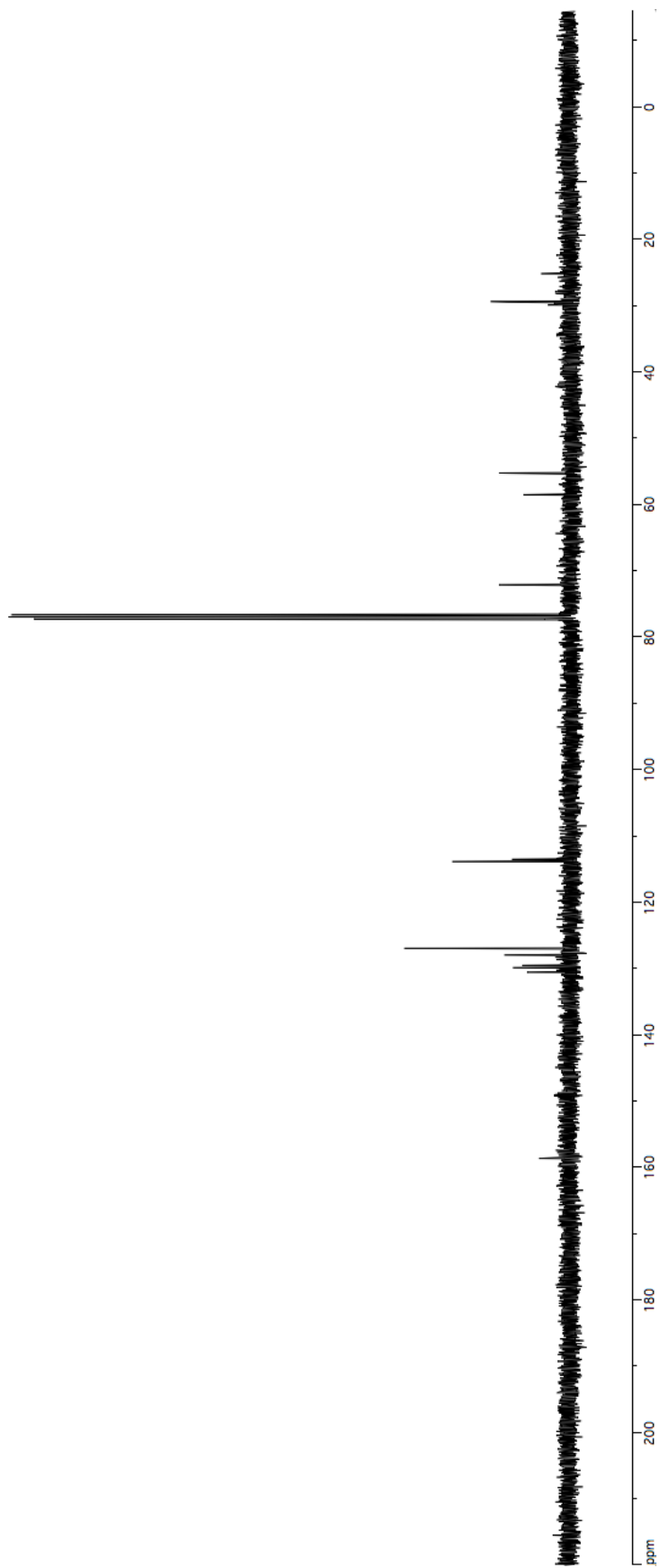


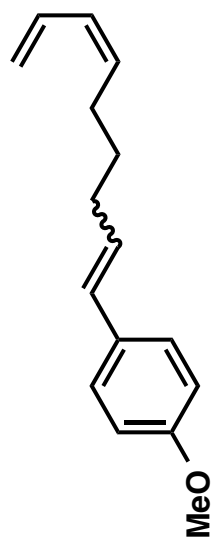
**4-111**  
**<sup>1</sup>H NMR**  
**(400 MHz, CDCl<sub>3</sub>)**



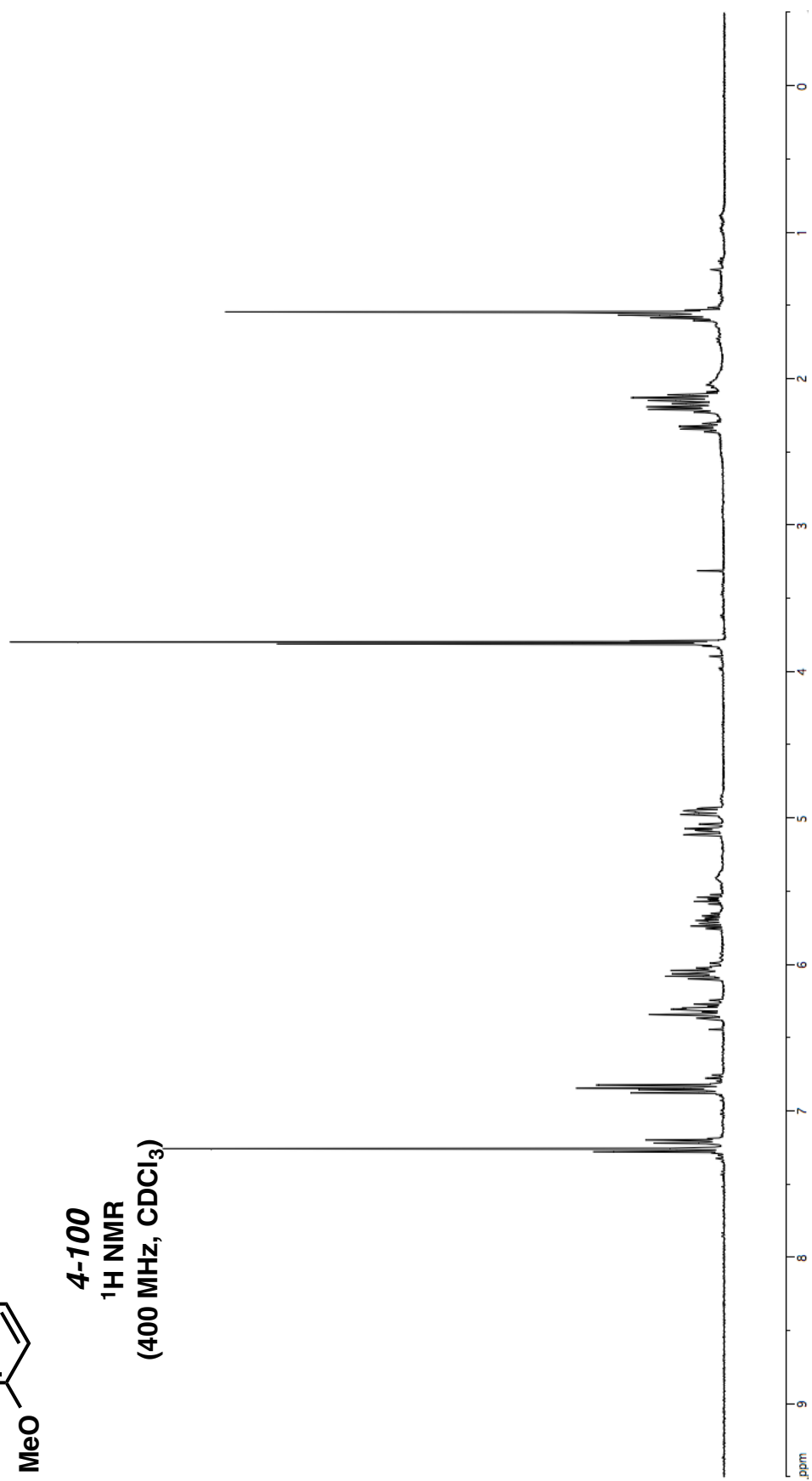


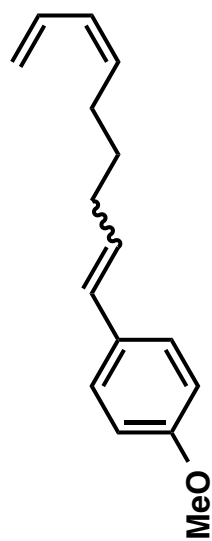
**4-111**  
**<sup>13</sup>C NMR**  
**(100 MHz, CDCl<sub>3</sub>)**



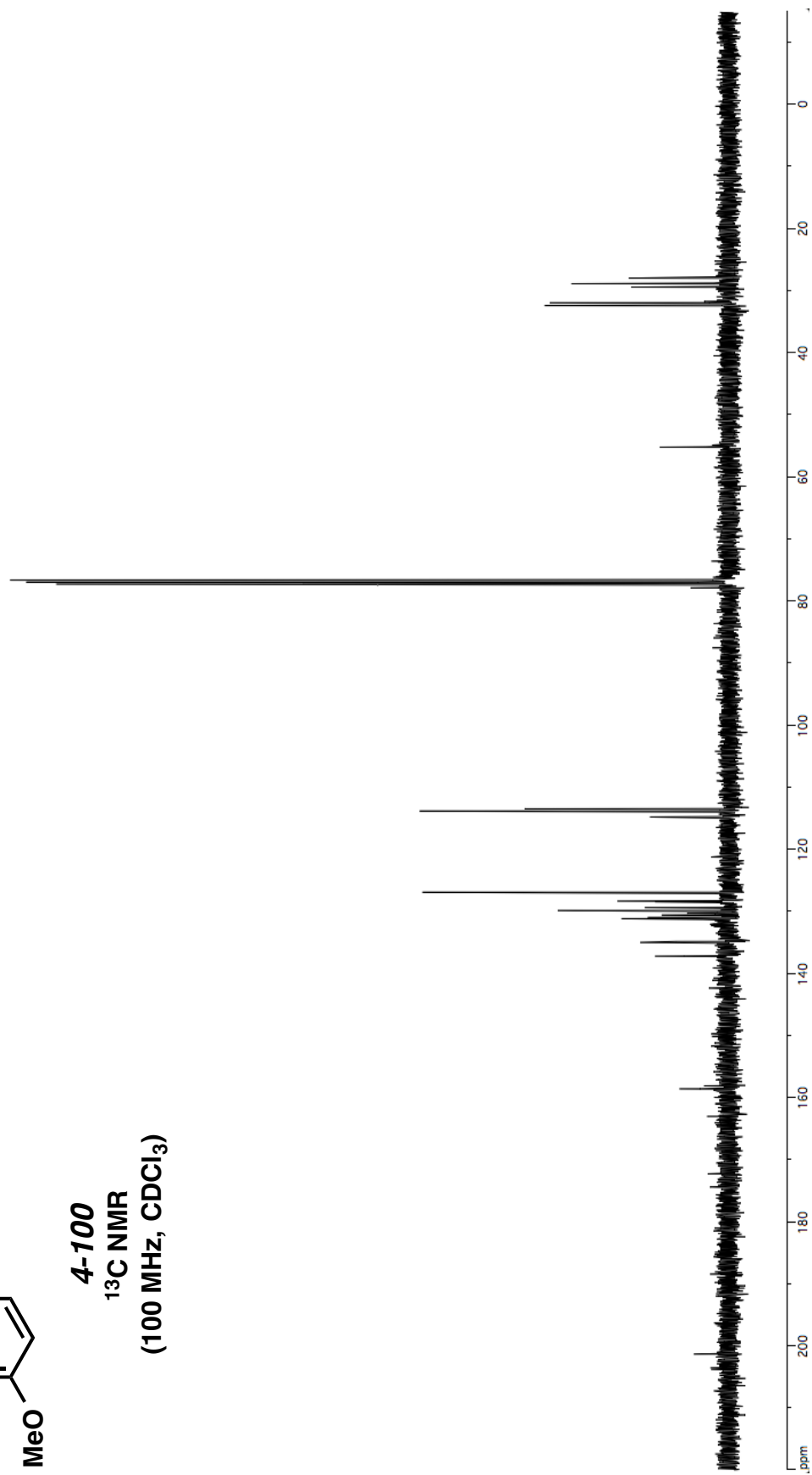


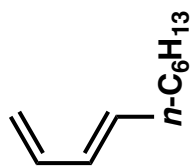
**4-100**  
**<sup>1</sup>H NMR**  
**(400 MHz, CDCl<sub>3</sub>)**





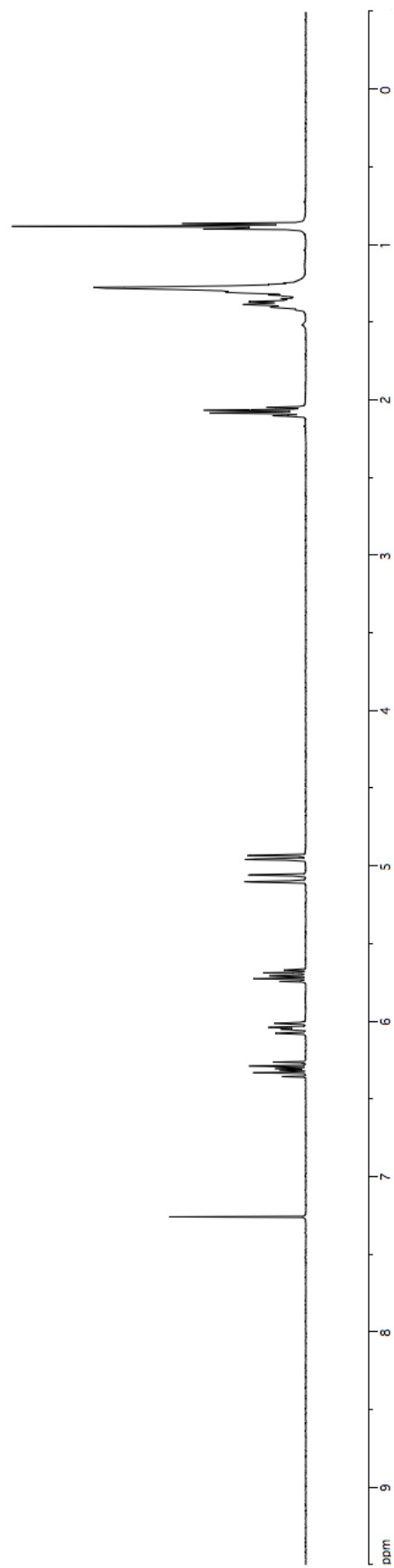
**4-100**  
**<sup>13</sup>C NMR**  
**(100 MHz, CDCl<sub>3</sub>)**

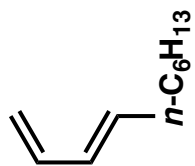




4-71

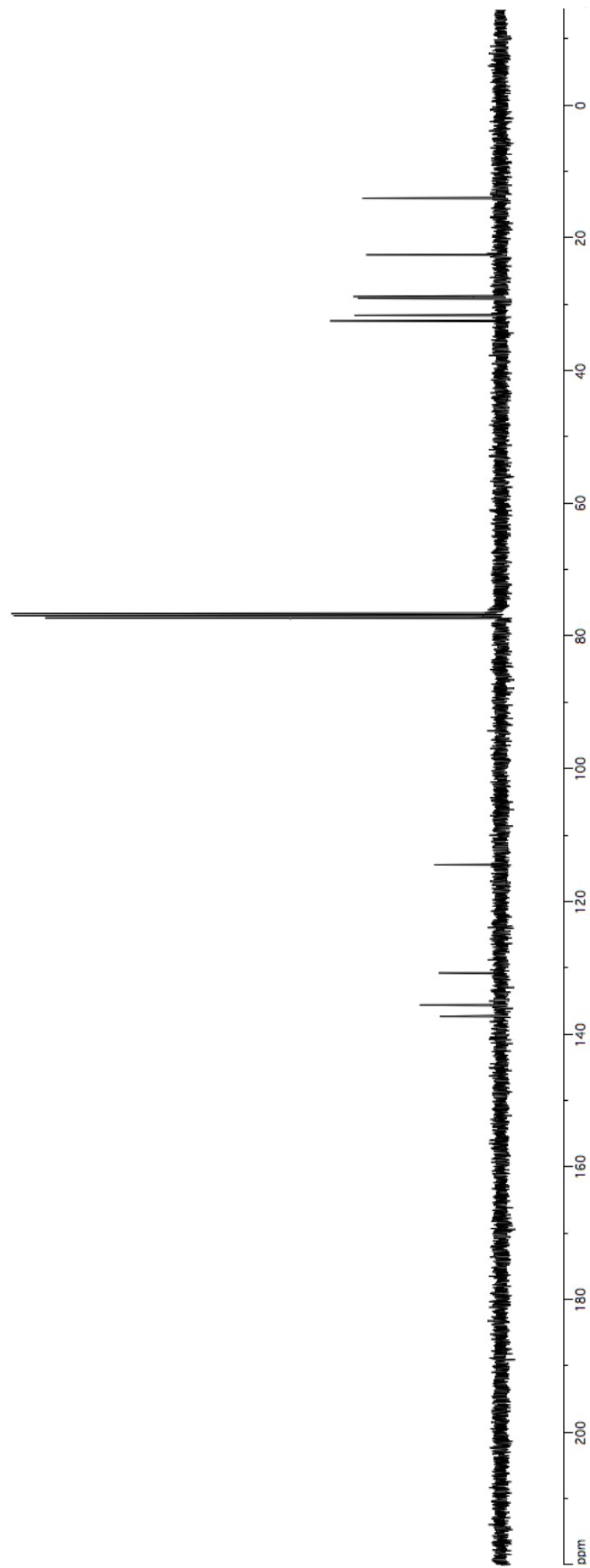
<sup>1</sup>H NMR  
(400 MHz, CDCl<sub>3</sub>)

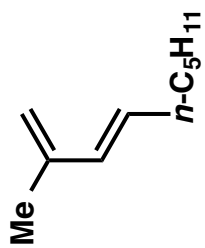




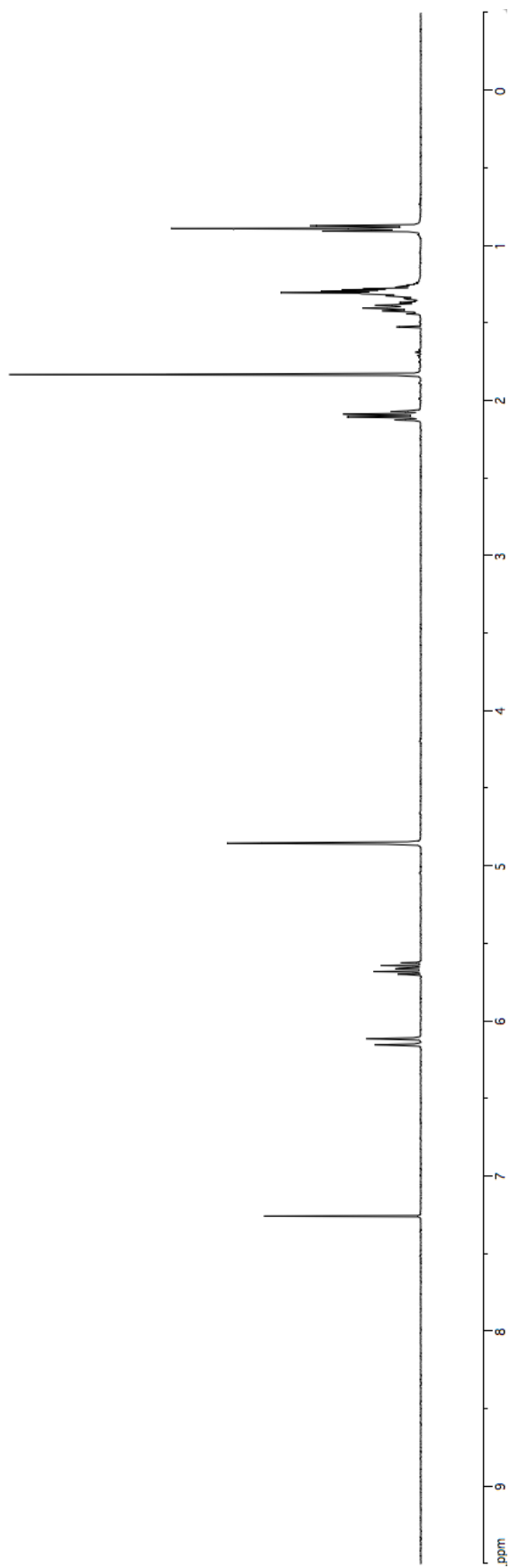
4-71

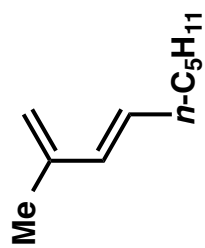
$^{13}\text{C}$  NMR  
(100 MHz,  $\text{CDCl}_3$ )



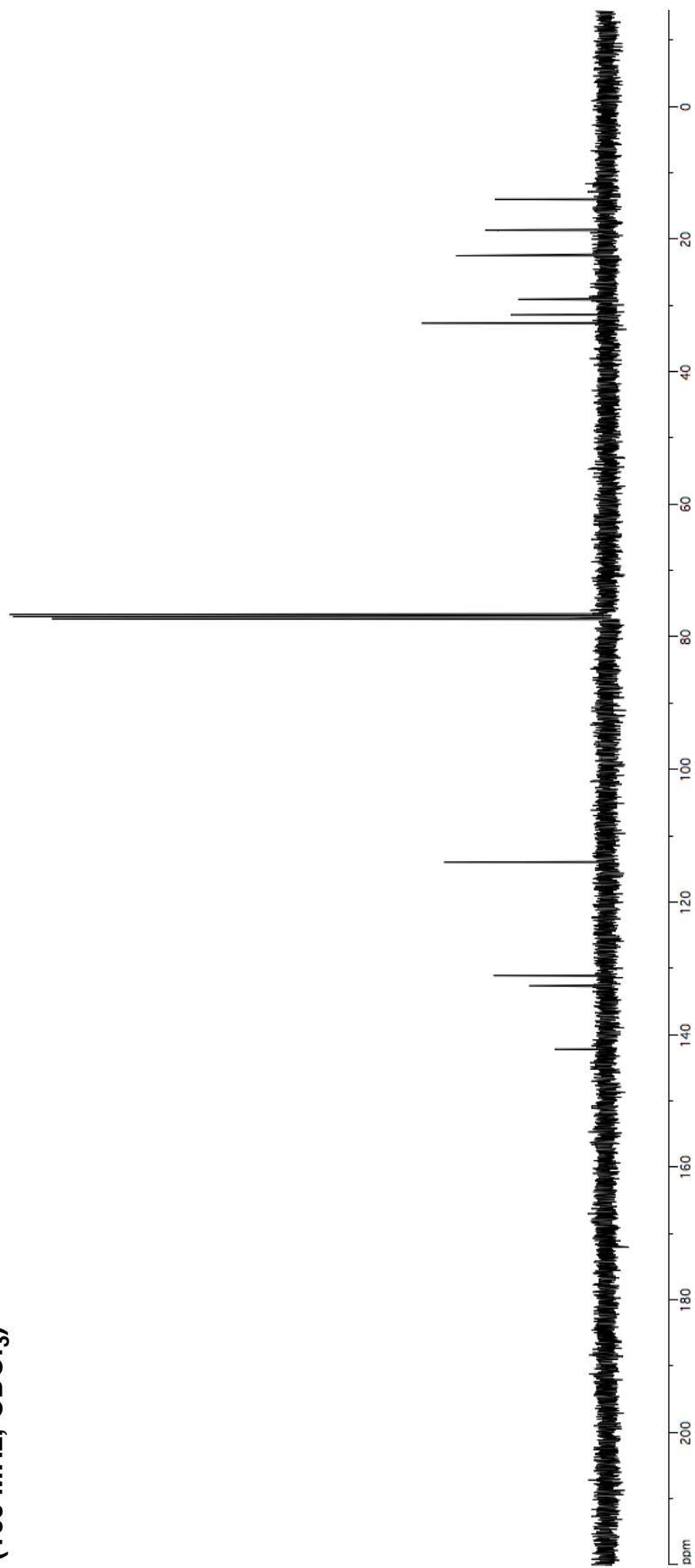


4-72  
 $^1\text{H NMR}$   
(400 MHz,  $\text{CDCl}_3$ )

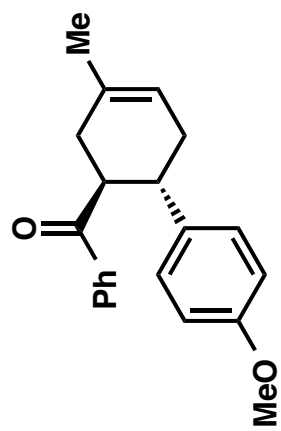




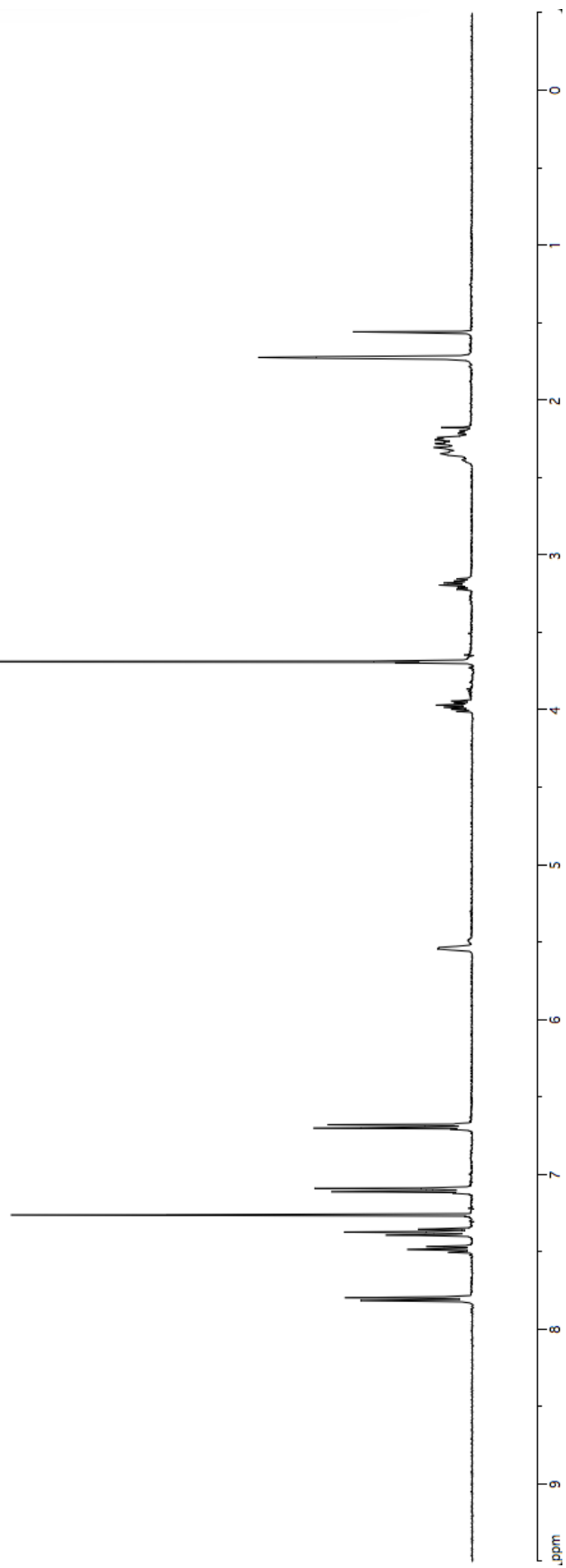
4-72  
<sup>13</sup>C NMR  
(100 MHz, CDCl<sub>3</sub>)

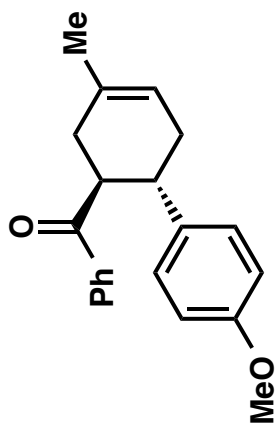


APPENDIX D  
NMR SPECTRA RELEVANT TO CHAPTER 5

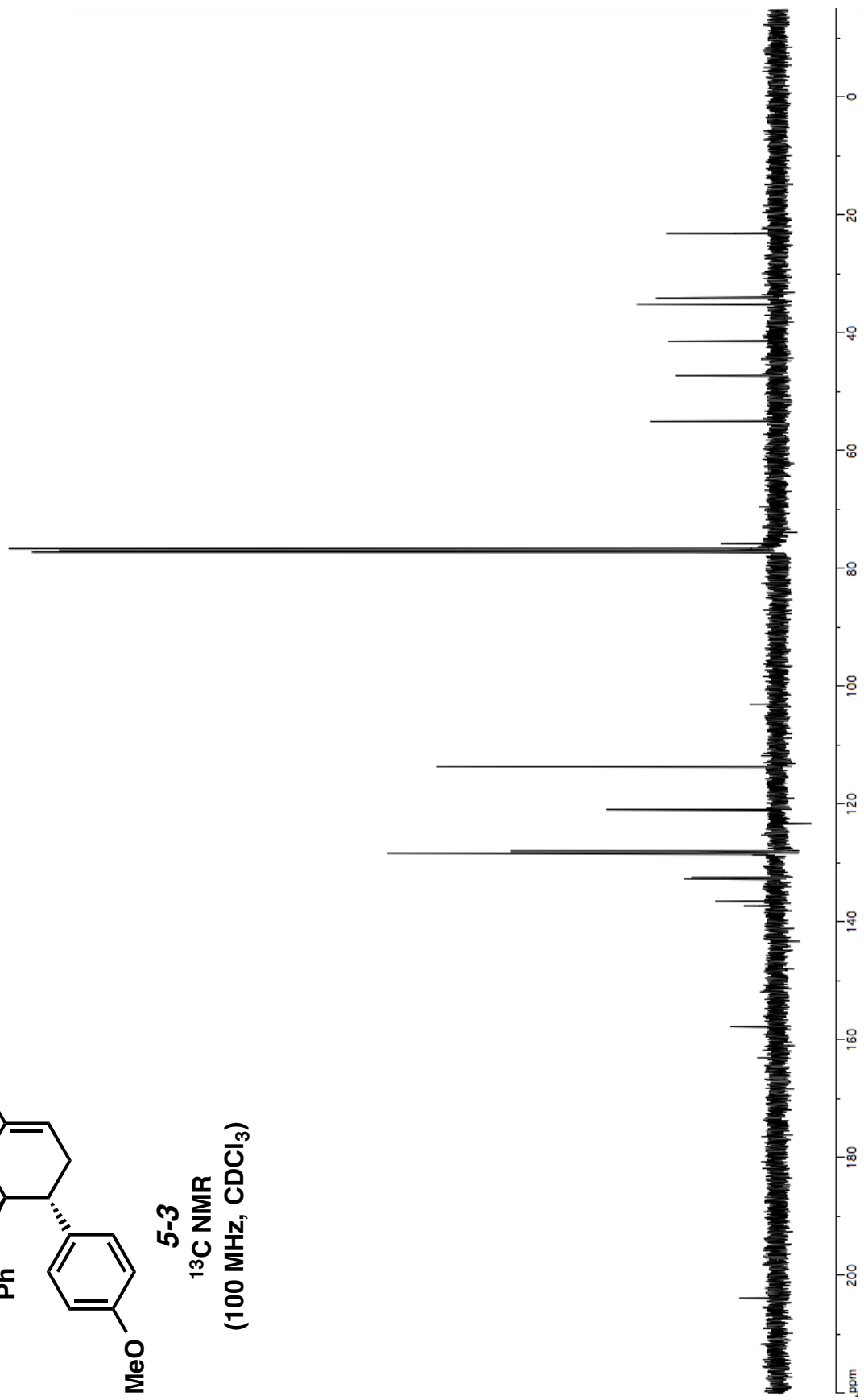


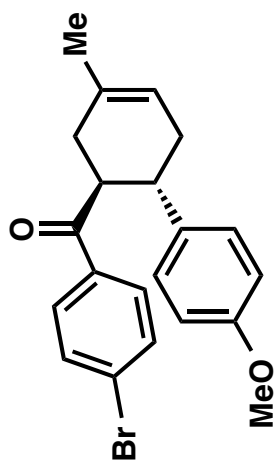
5-3  
<sup>1</sup>H NMR  
(400 MHz, CDCl<sub>3</sub>)



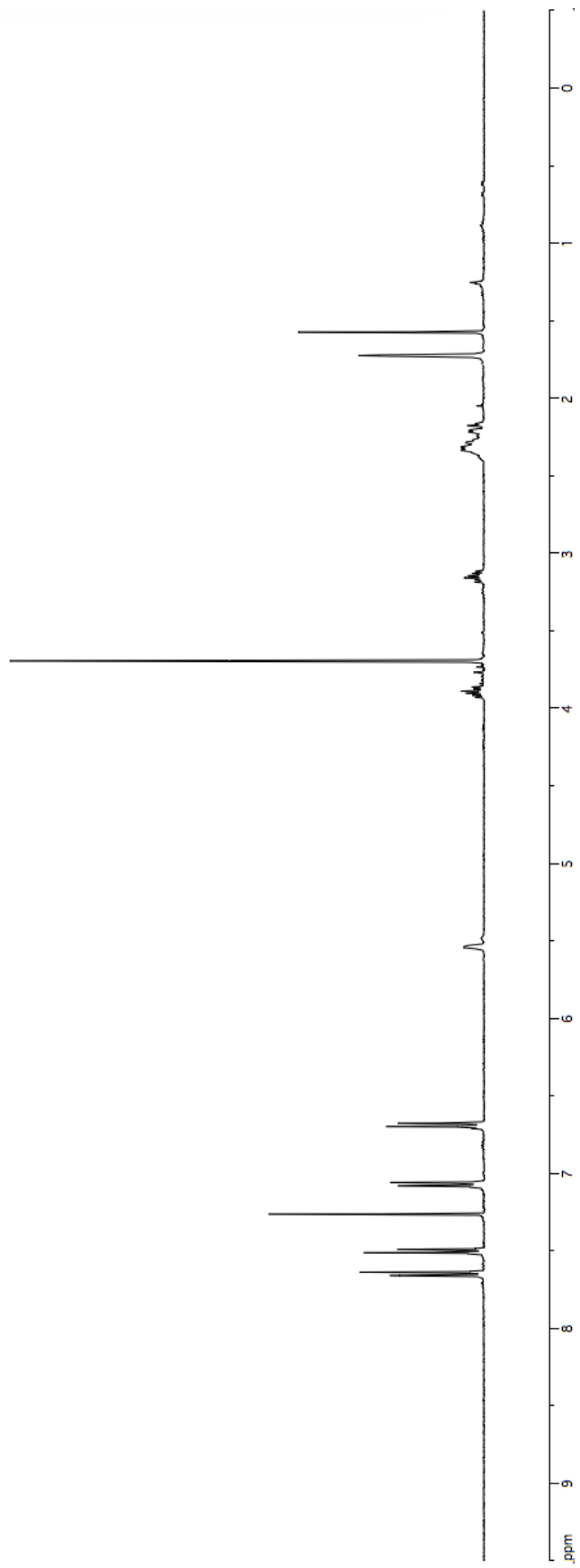


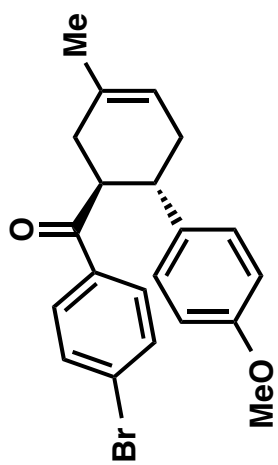
**5-3**  
**<sup>13</sup>C NMR**  
**(100 MHz, CDCl<sub>3</sub>)**



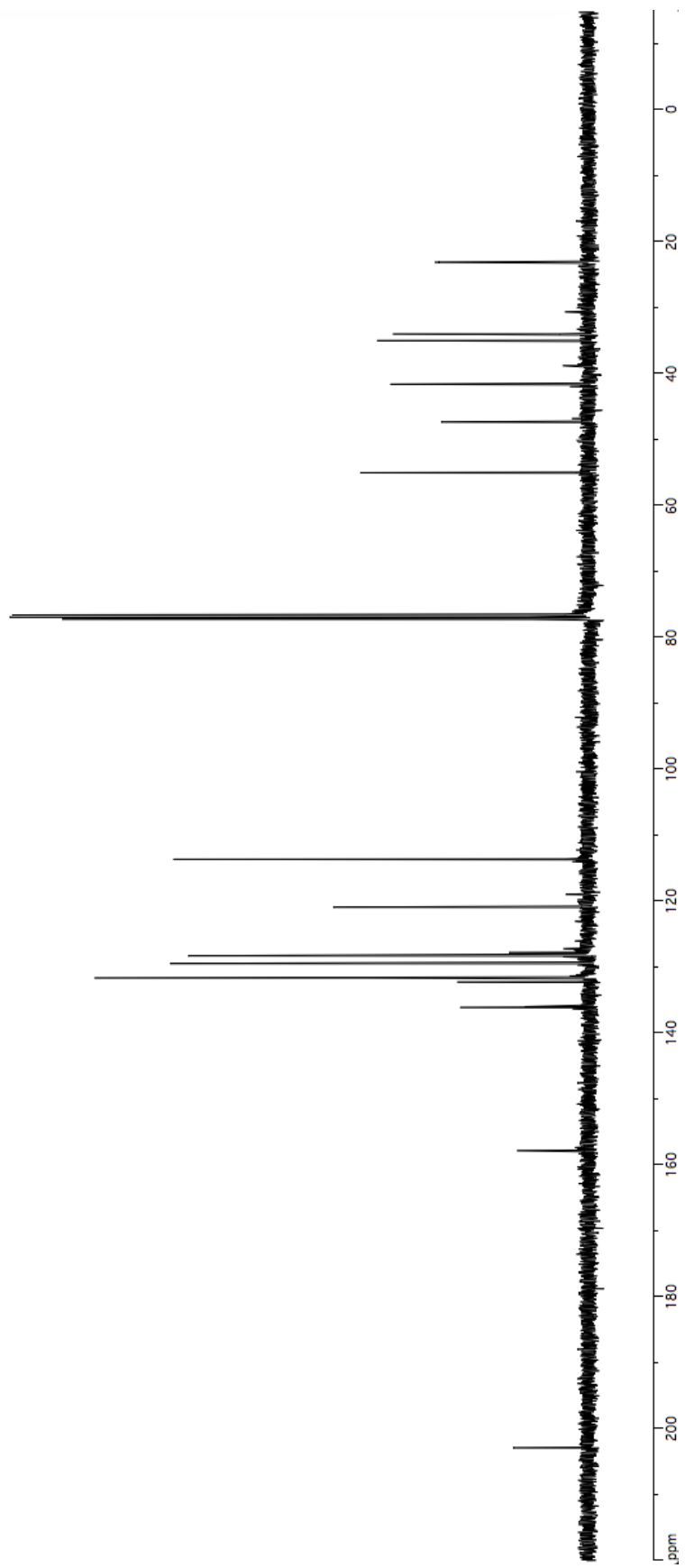


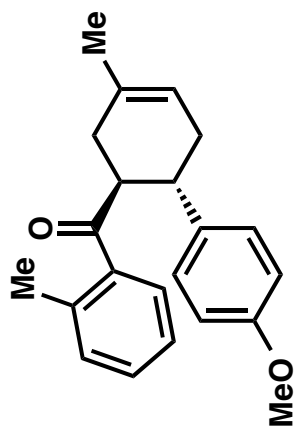
**5-11**  
**<sup>1</sup>H NMR**  
**(400 MHz, CDCl<sub>3</sub>)**



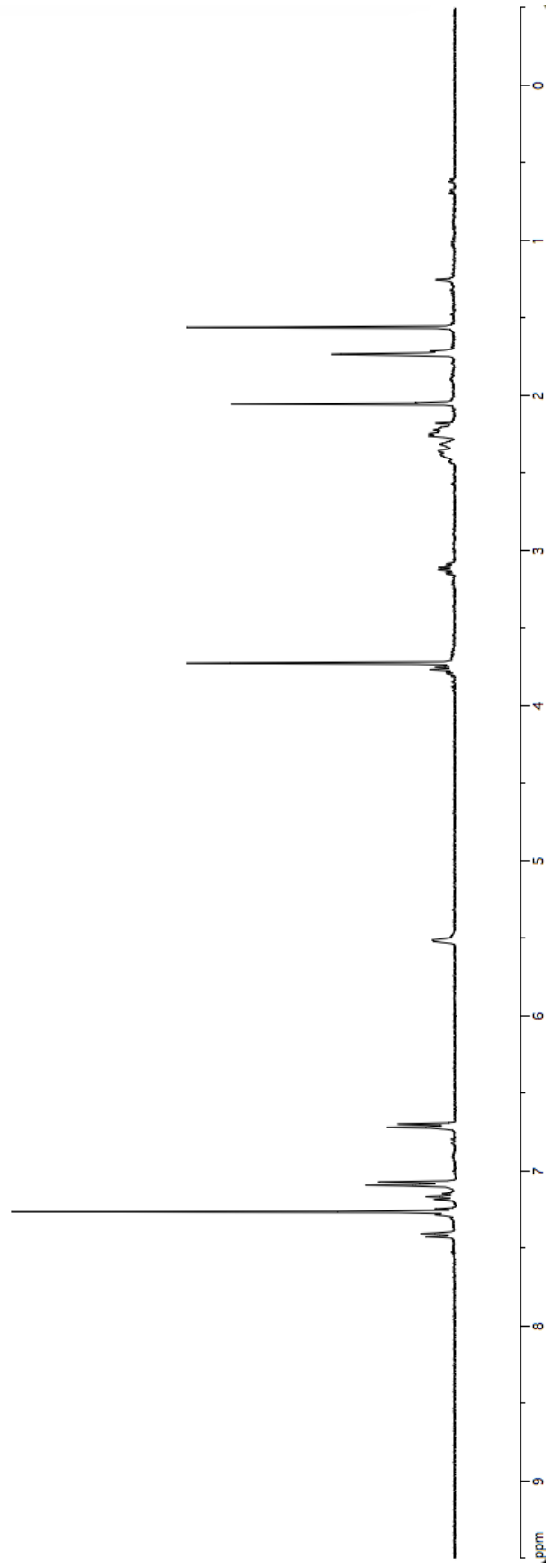


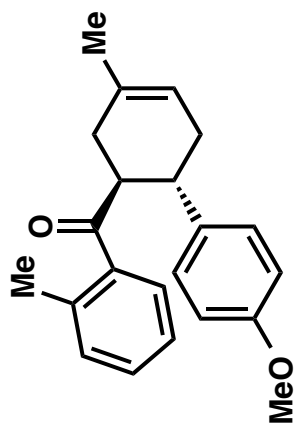
**5-11**  
**<sup>13</sup>C NMR**  
**(100 MHz, CDCl<sub>3</sub>)**



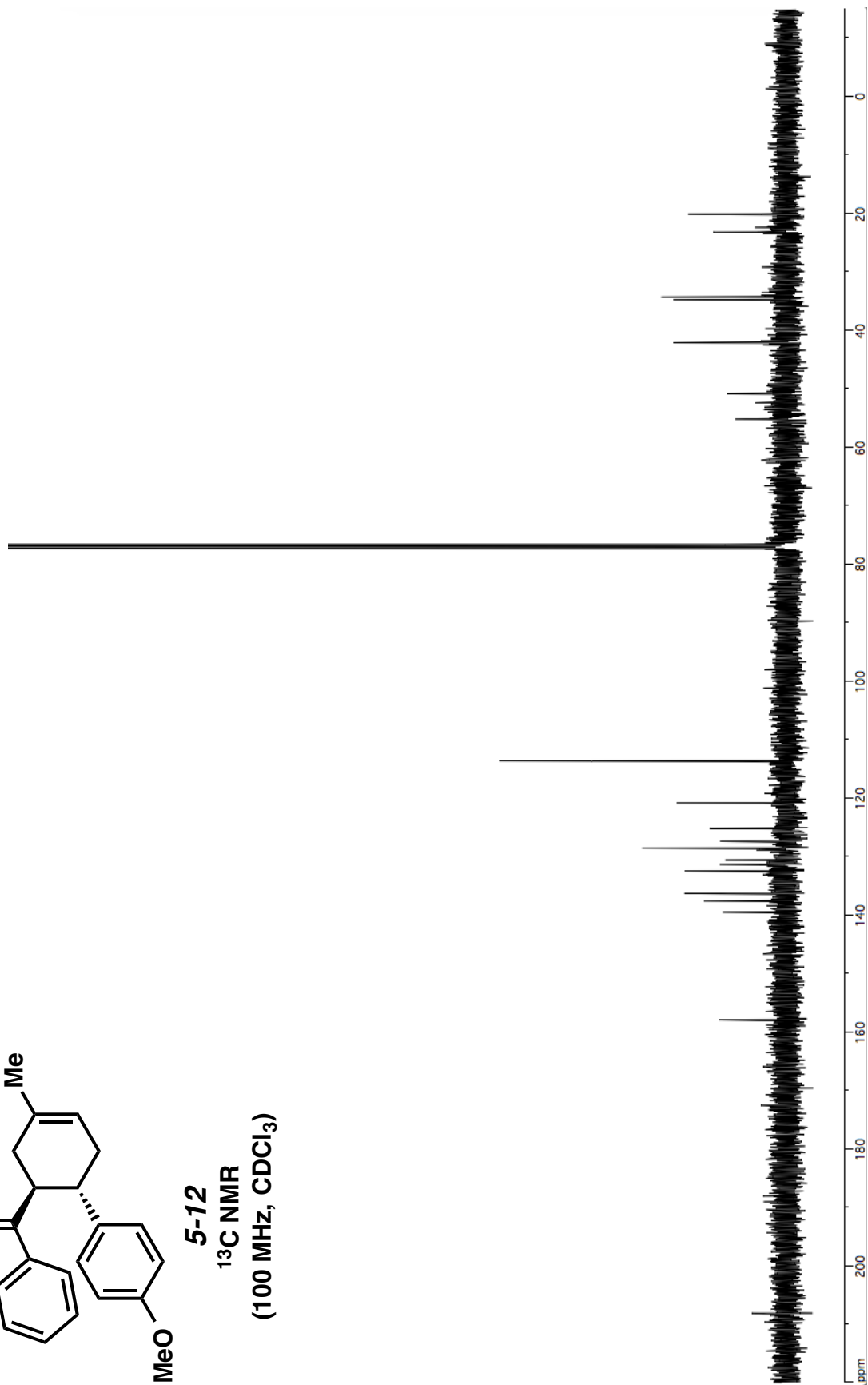


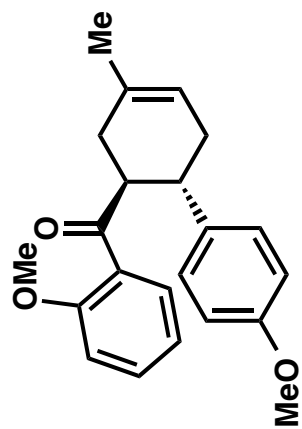
**5-12**  
**<sup>1</sup>H NMR**  
**(400 MHz, CDCl<sub>3</sub>)**





**5-12**  
**<sup>13</sup>C NMR**  
**(100 MHz, CDCl<sub>3</sub>)**

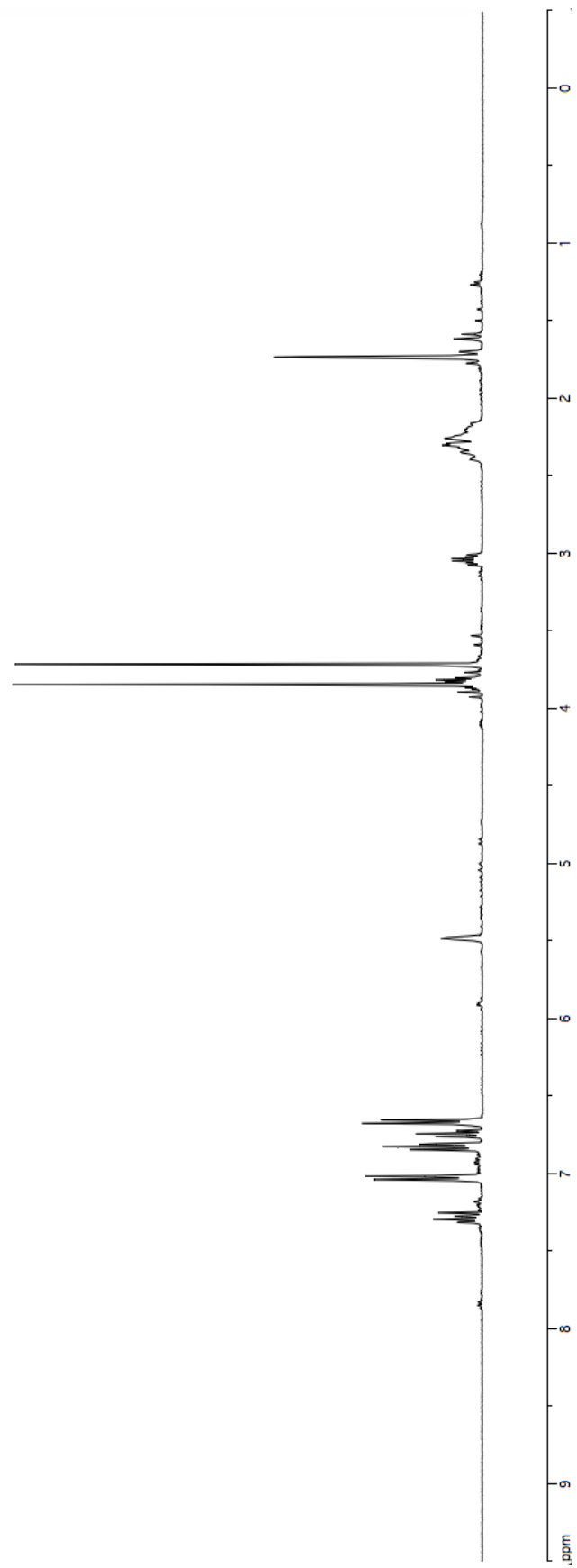


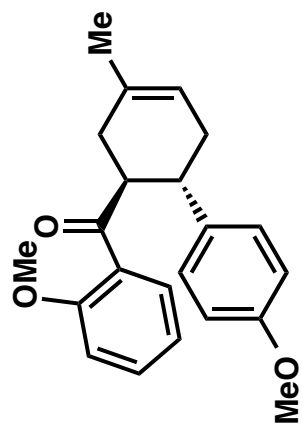


5-13

<sup>1</sup>H NMR

(400 MHz, CDCl<sub>3</sub>)

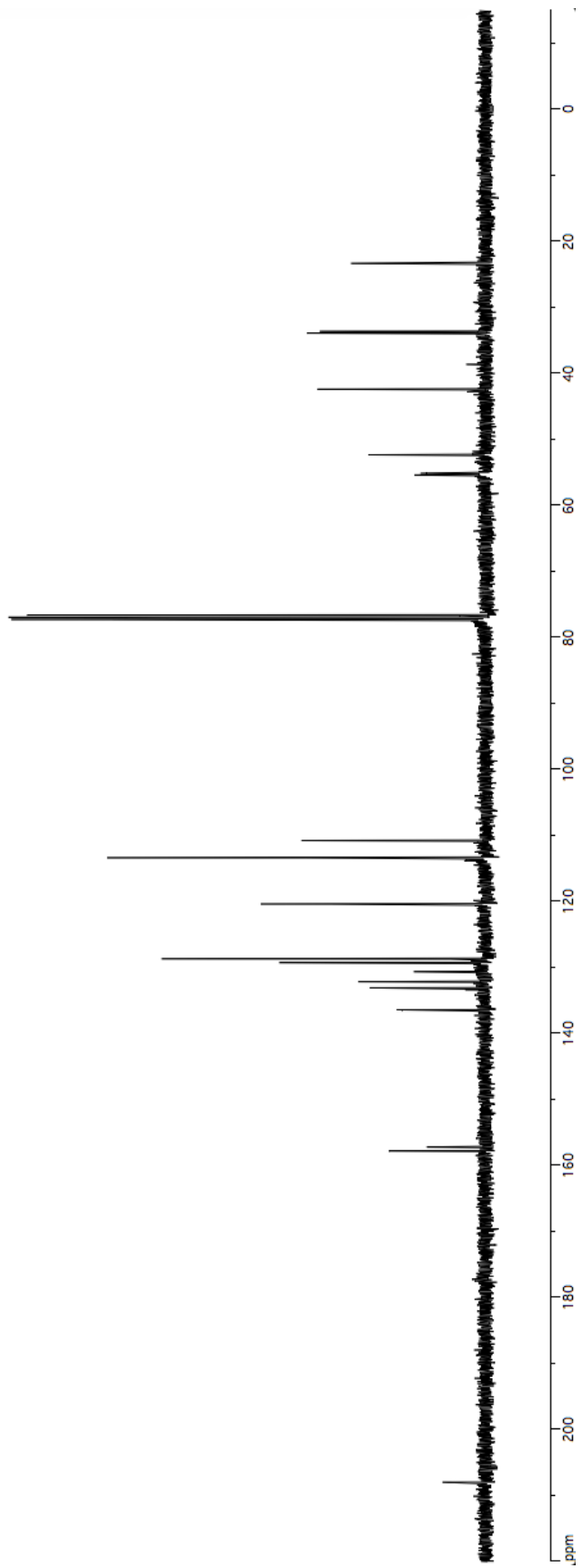


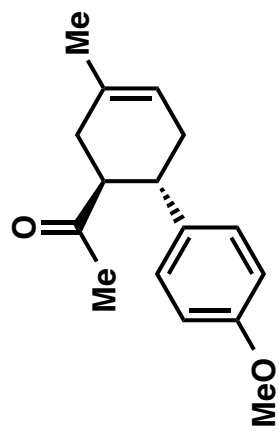


5-13

<sup>13</sup>C NMR

(100 MHz, CDCl<sub>3</sub>)

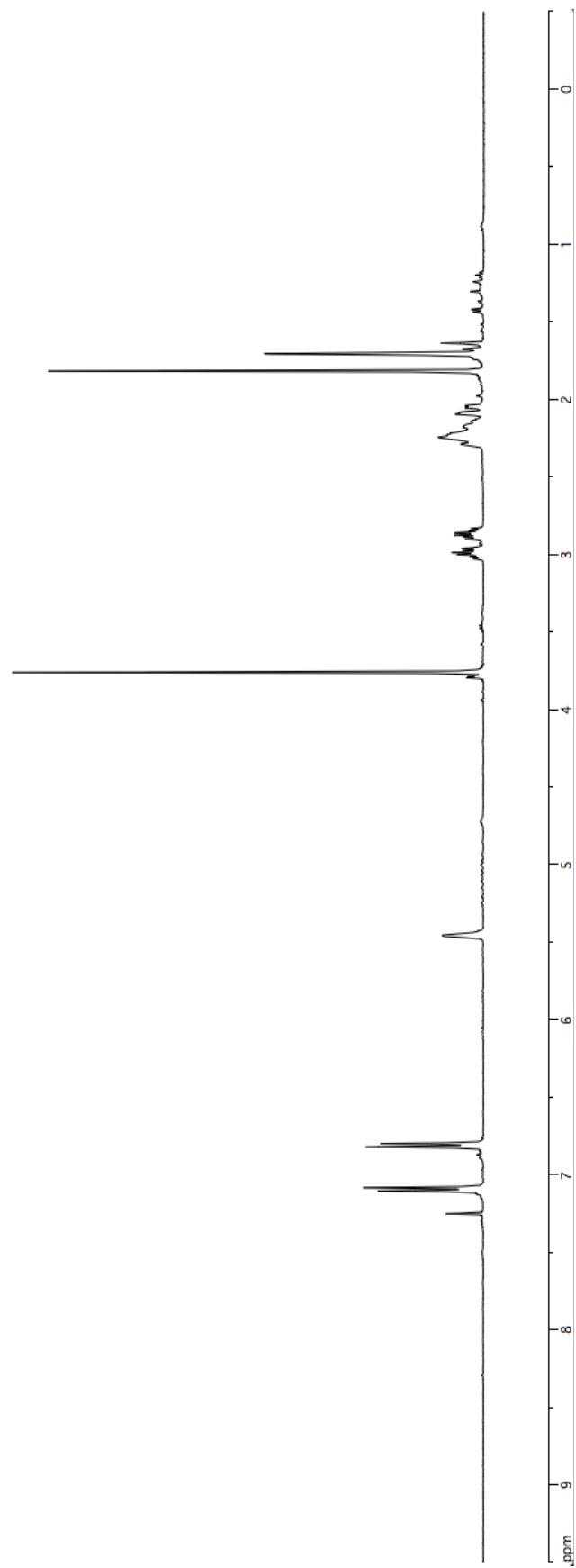


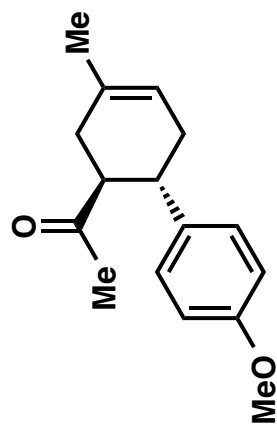


5-14

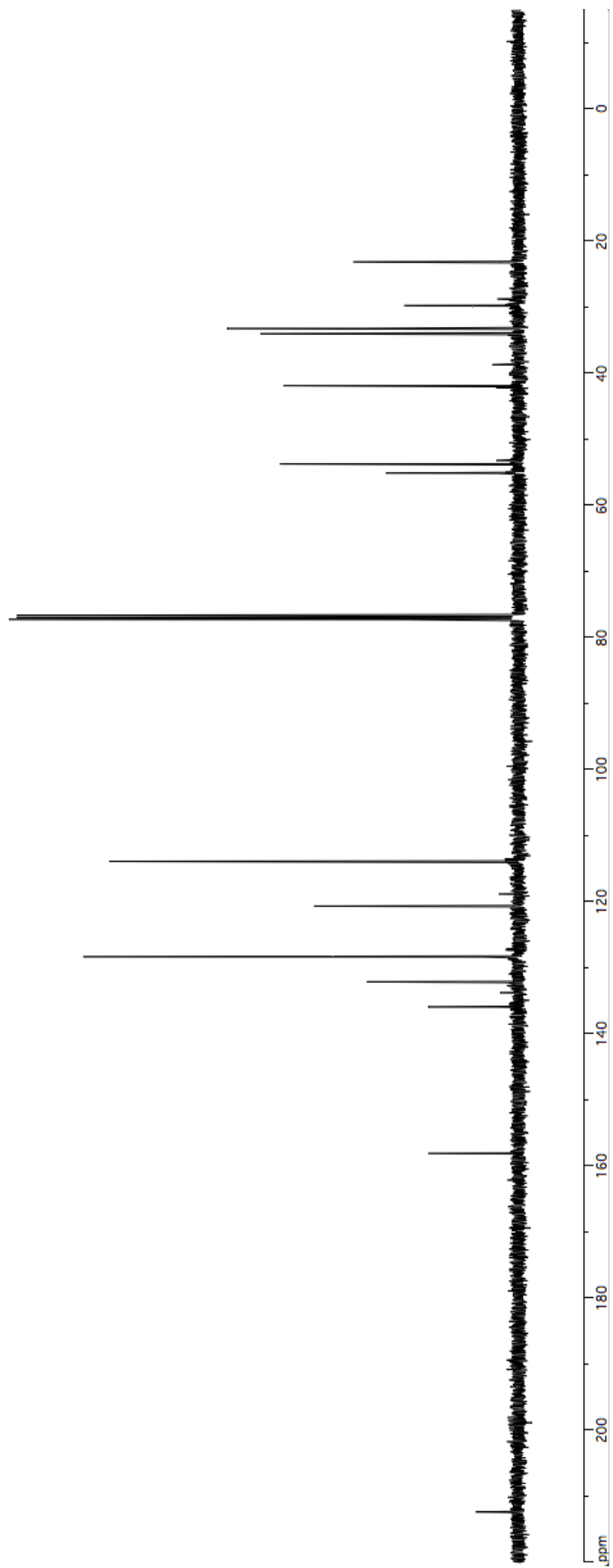
<sup>1</sup>H NMR

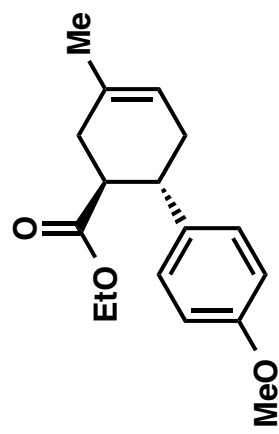
(400 MHz, CDCl<sub>3</sub>)



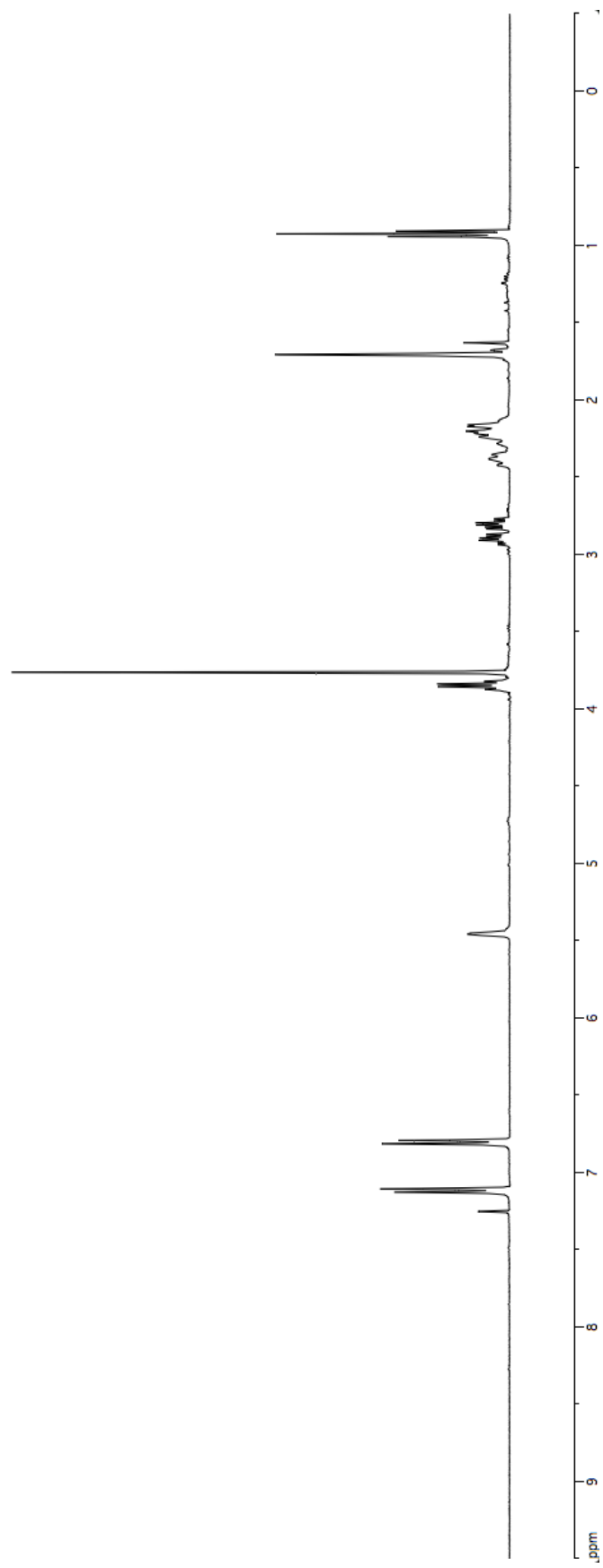


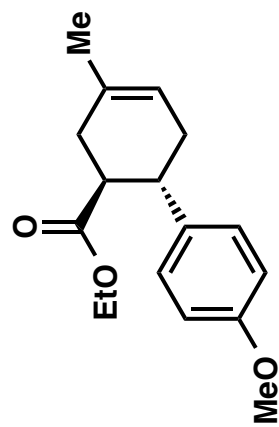
**5-14**  
**<sup>13</sup>C NMR**  
**(100 MHz, CDCl<sub>3</sub>)**



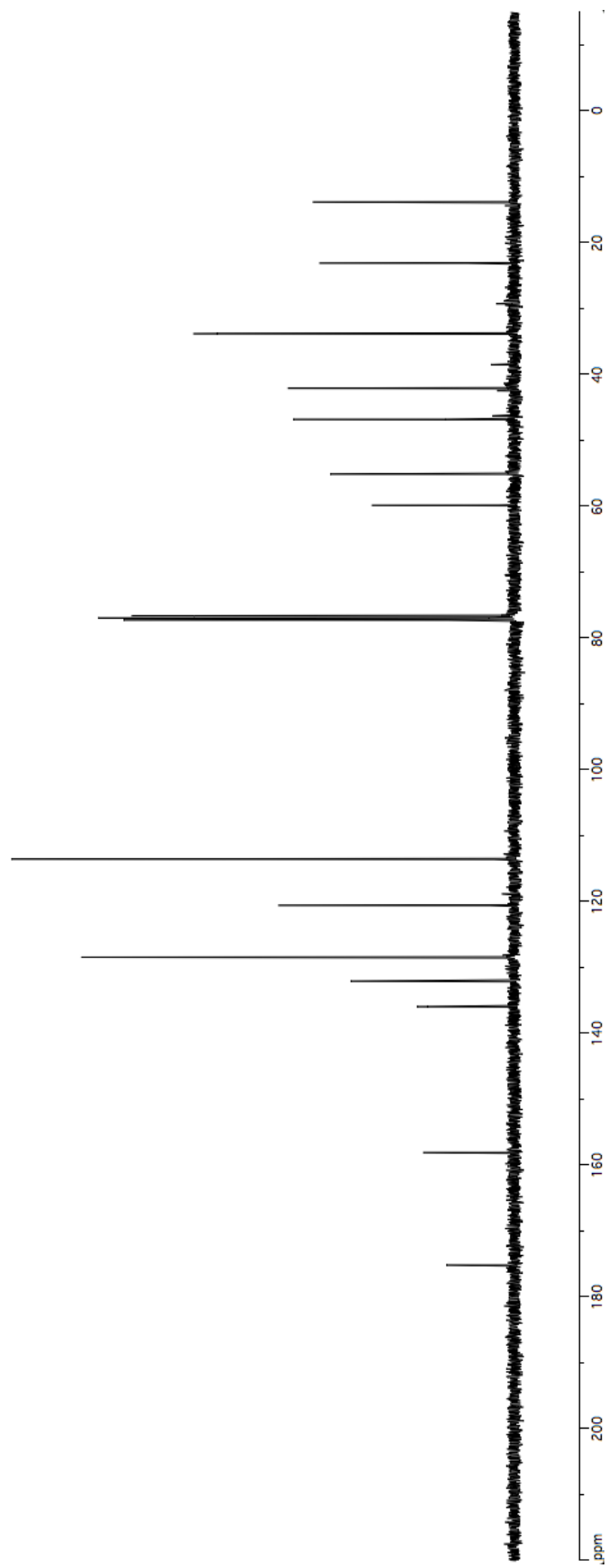


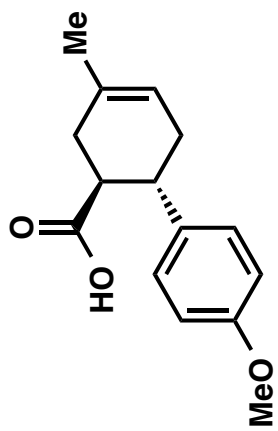
**5-15**  
**<sup>1</sup>H NMR**  
**(400 MHz, CDCl<sub>3</sub>)**





**5-15**  
**<sup>13</sup>C NMR**  
**(100 MHz, CDCl<sub>3</sub>)**

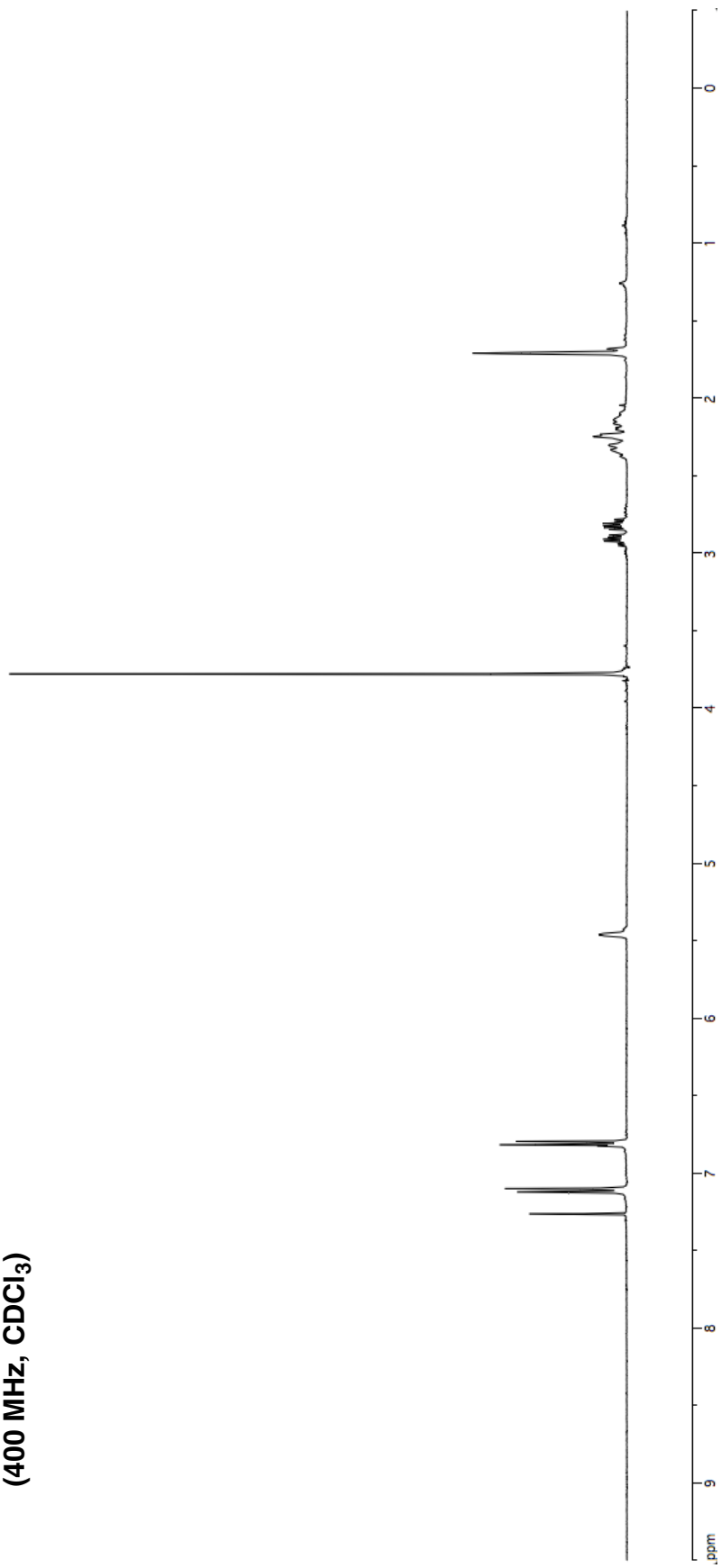


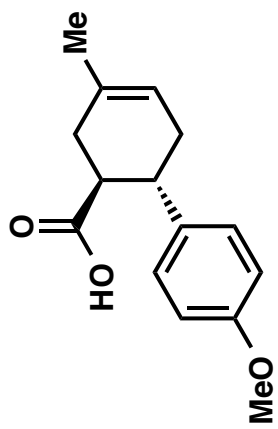


5-16

<sup>1</sup>H NMR

(400 MHz, CDCl<sub>3</sub>)

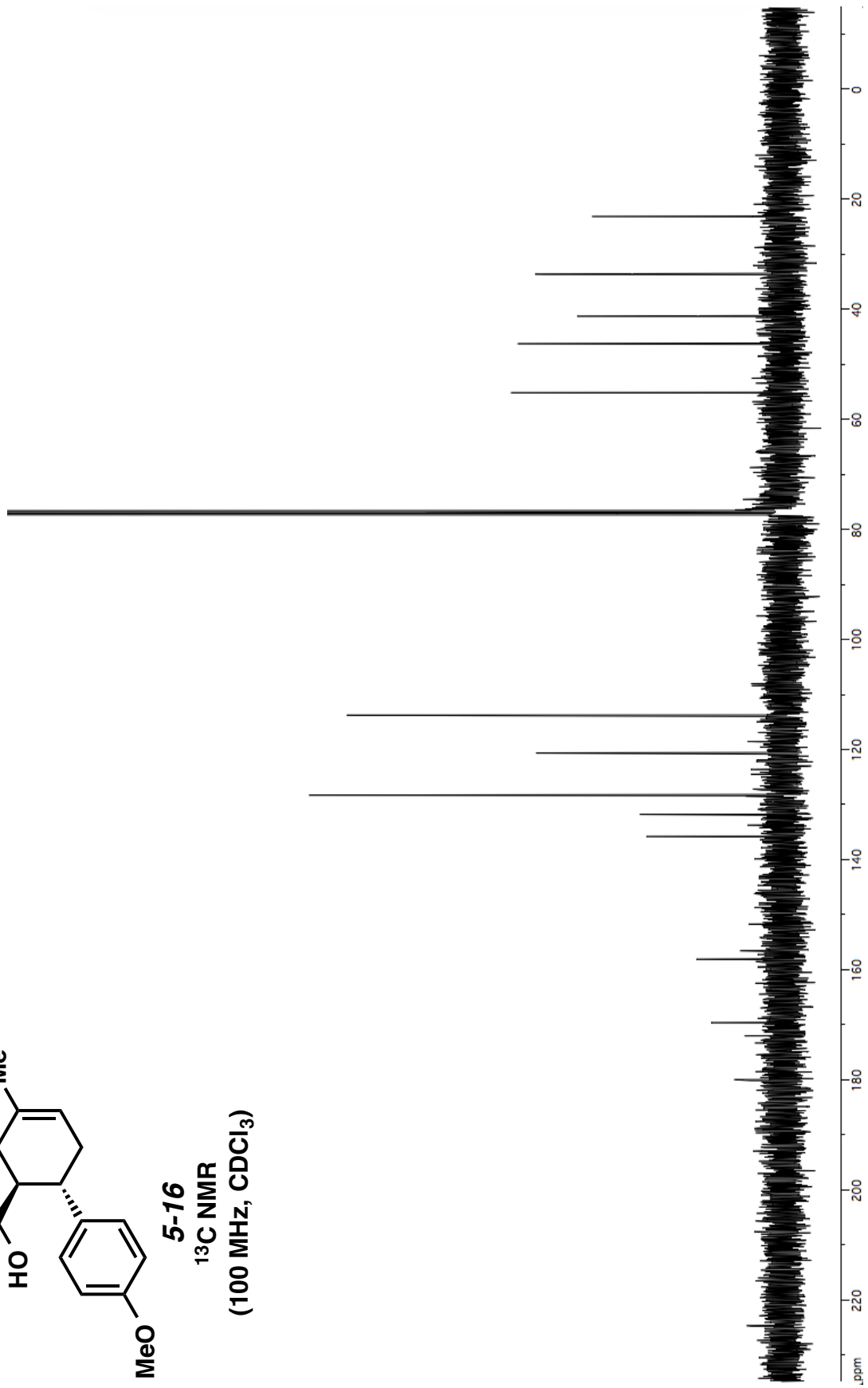


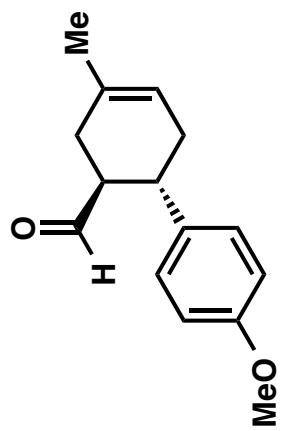


5-16

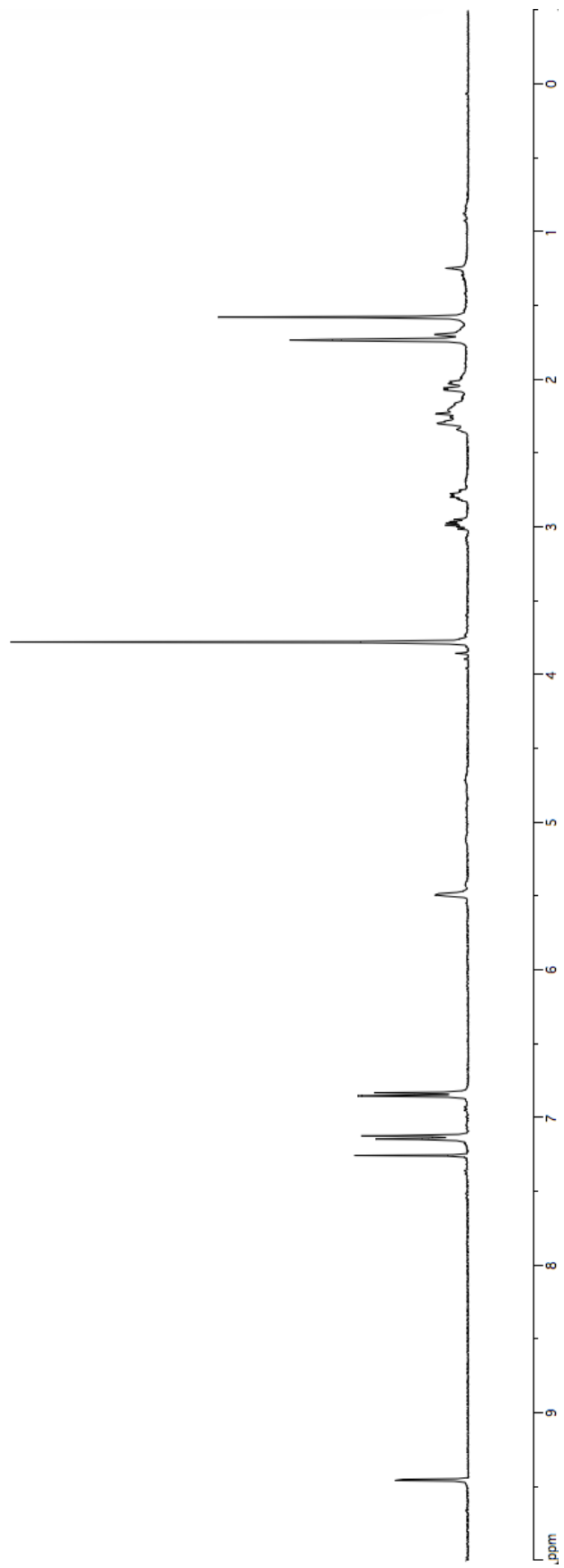
$^{13}\text{C}$  NMR

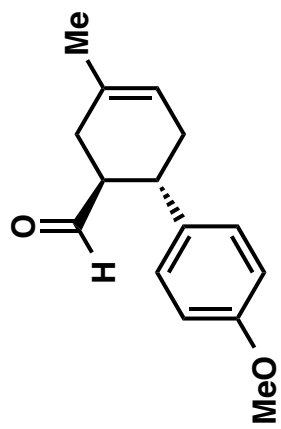
(100 MHz,  $\text{CDCl}_3$ )



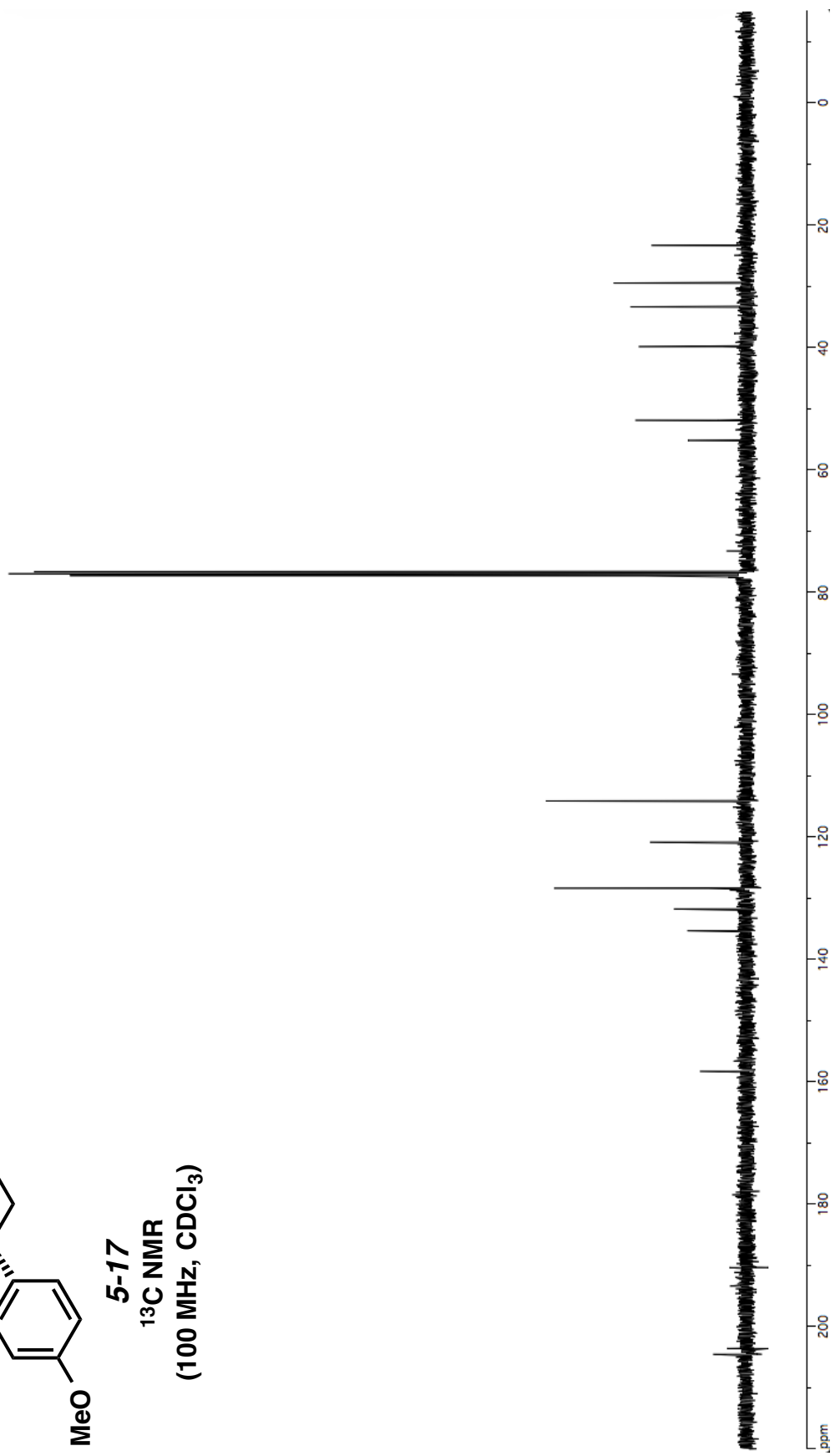


5-17  
<sup>1</sup>H NMR  
(400 MHz, CDCl<sub>3</sub>)

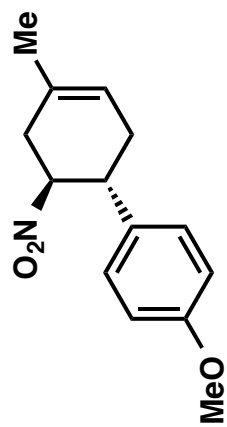




**5-17**  
**<sup>13</sup>C NMR**  
**(100 MHz, CDCl<sub>3</sub>)**



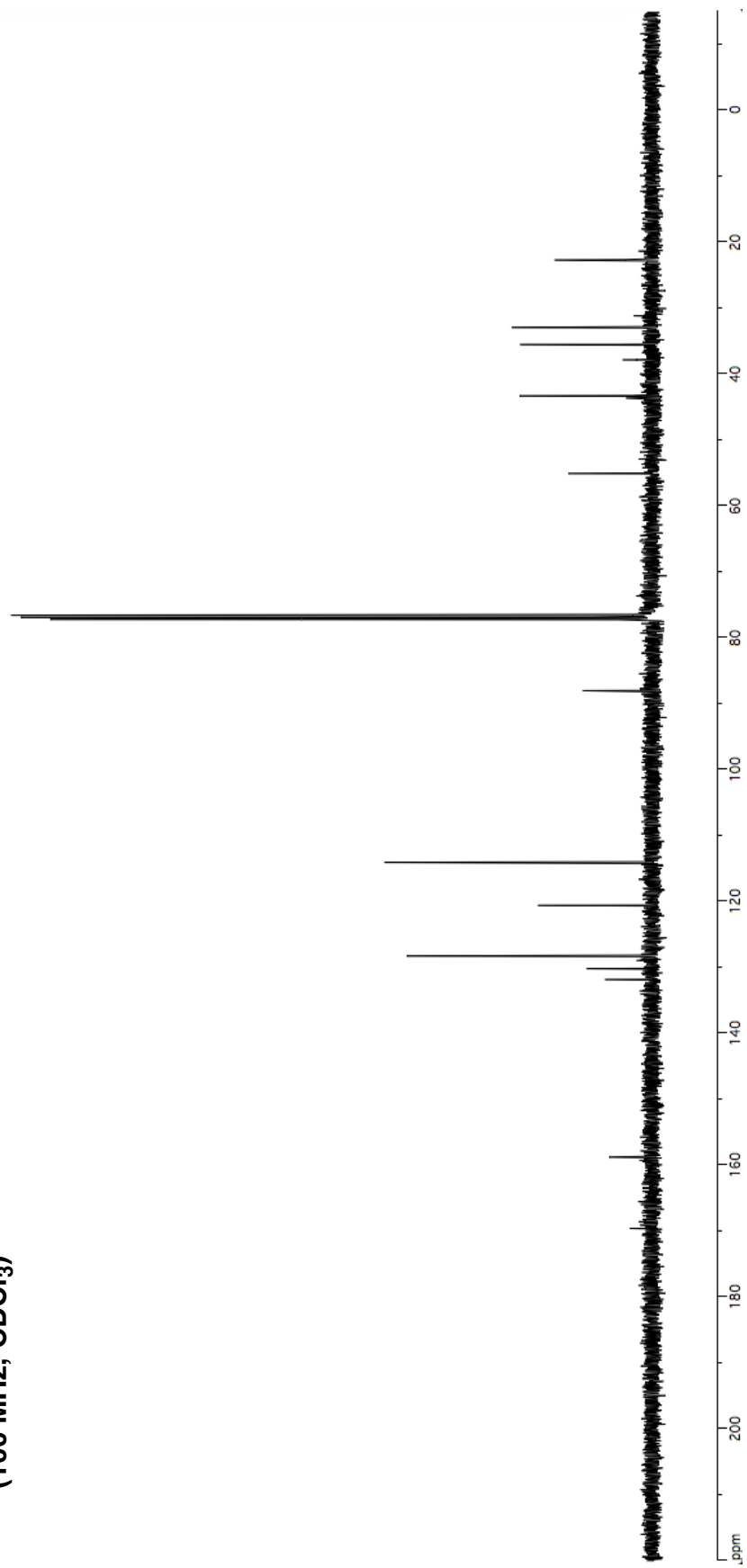


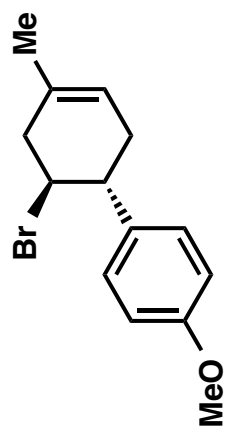


5-18

<sup>13</sup>C NMR

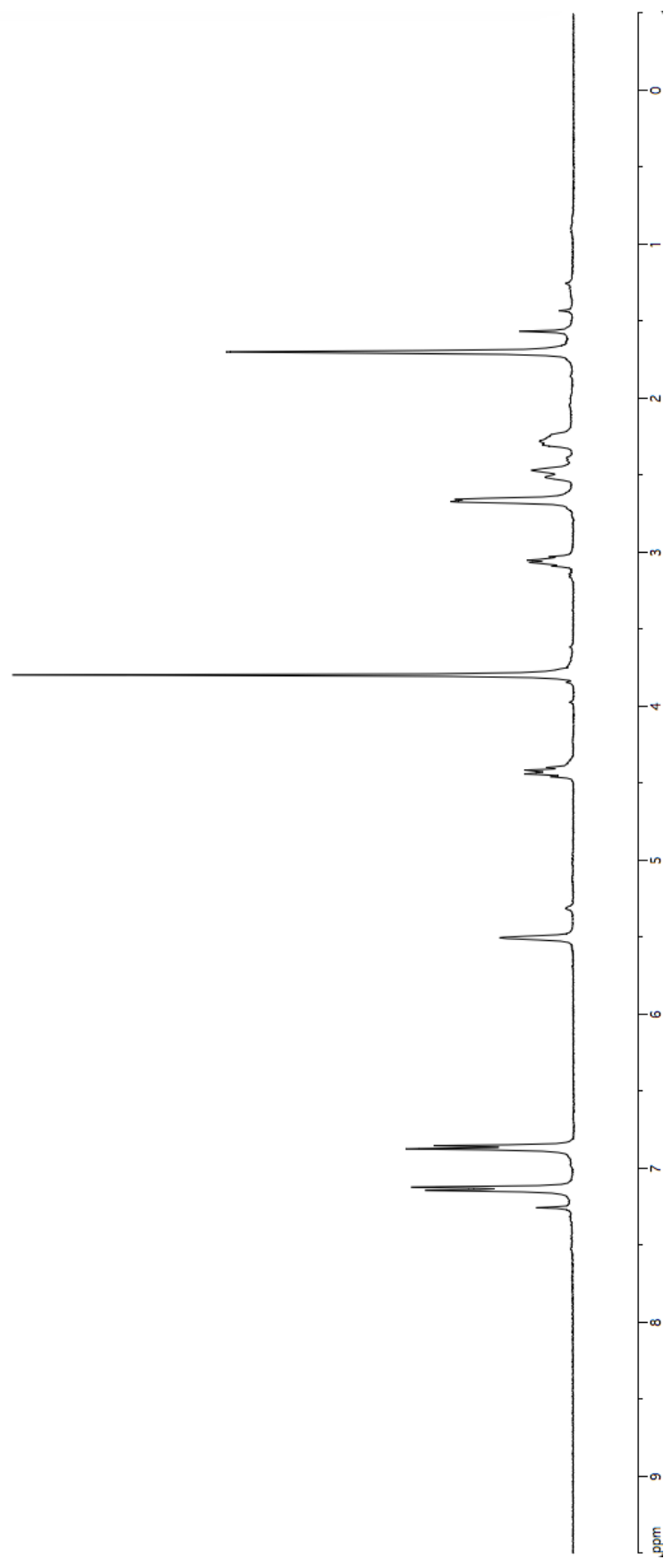
(100 MHz, CDCl<sub>3</sub>)

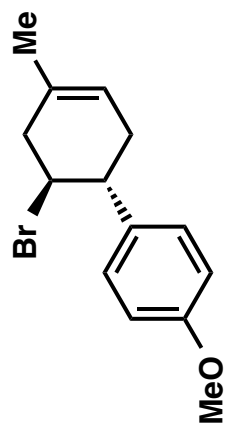




5-19

<sup>1</sup>H NMR  
(400 MHz, CDCl<sub>3</sub>)

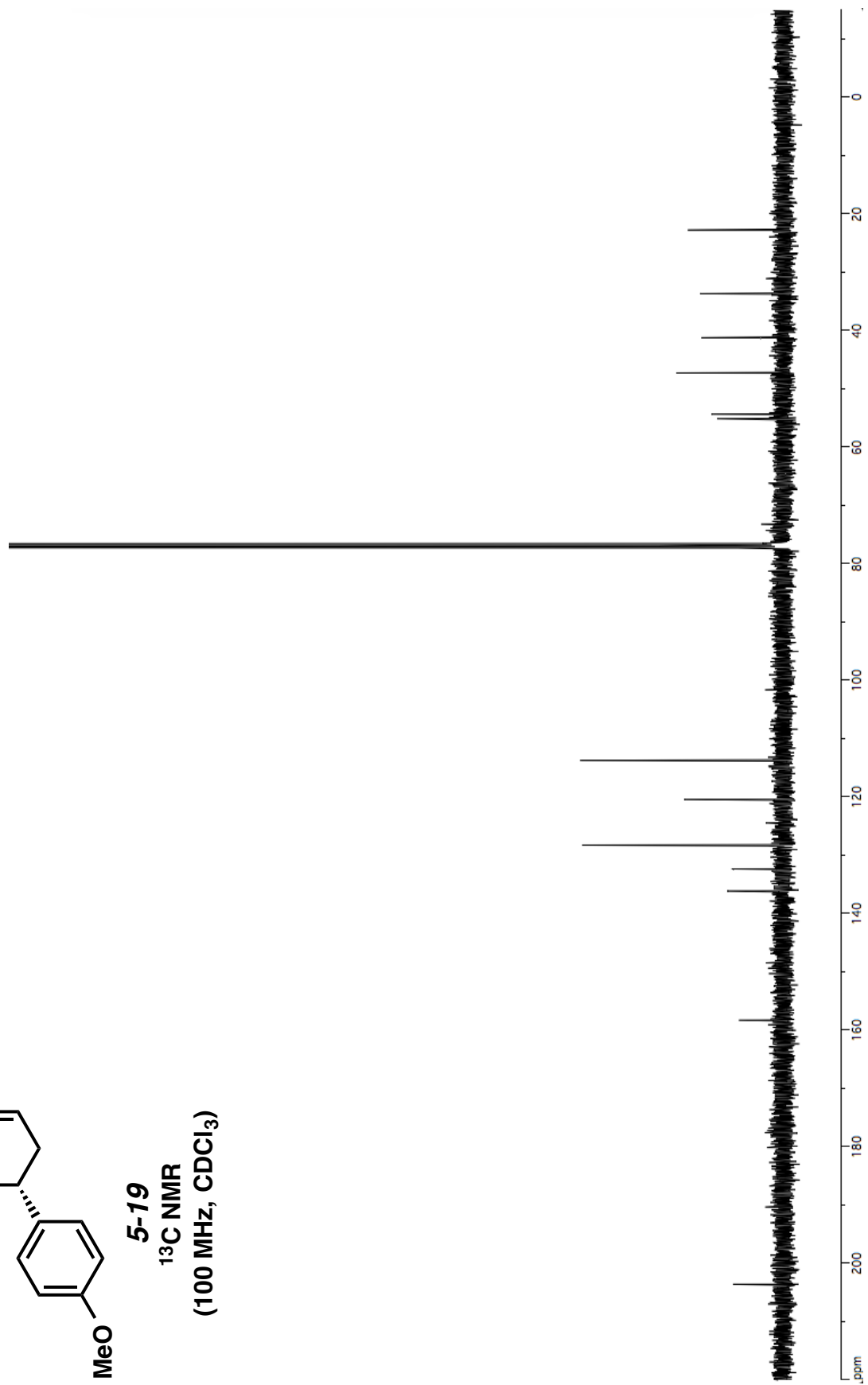


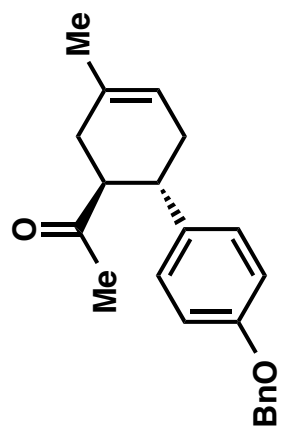


5-19

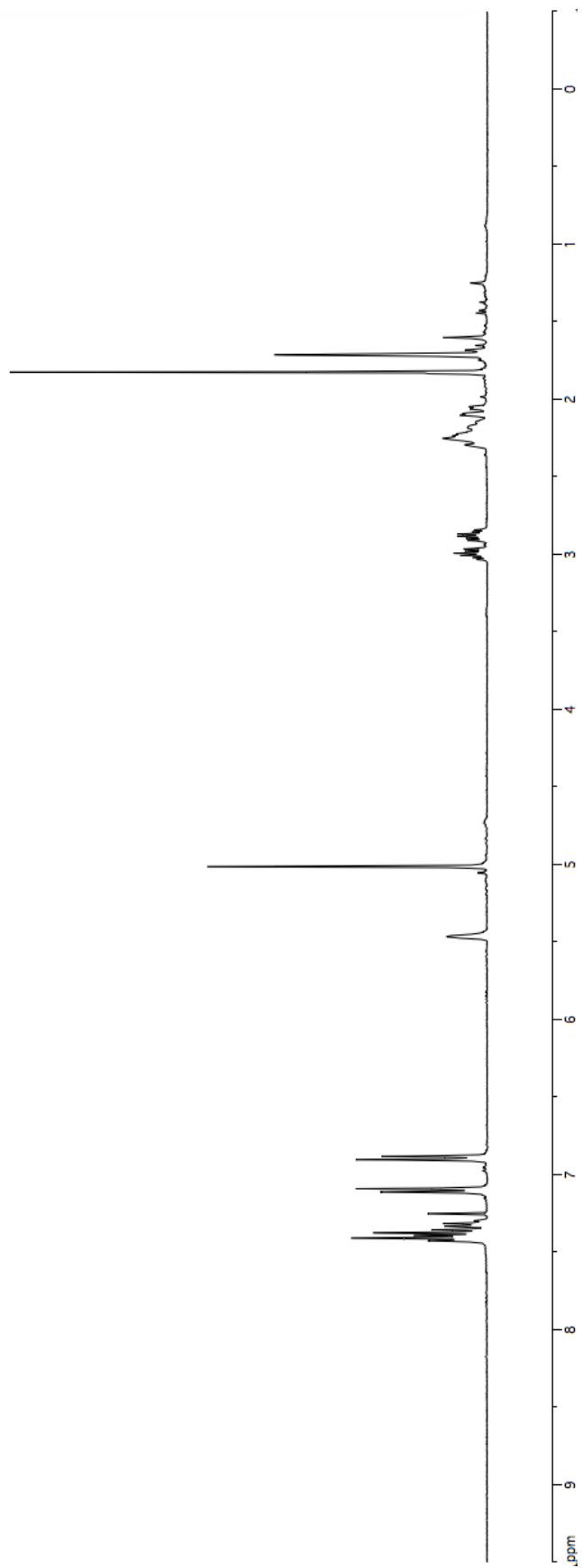
<sup>13</sup>C NMR

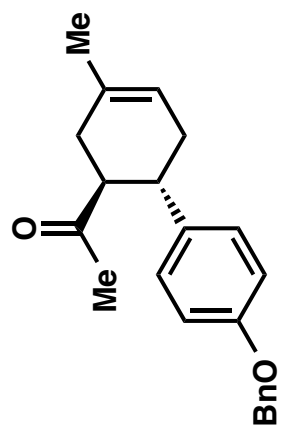
(100 MHz, CDCl<sub>3</sub>)



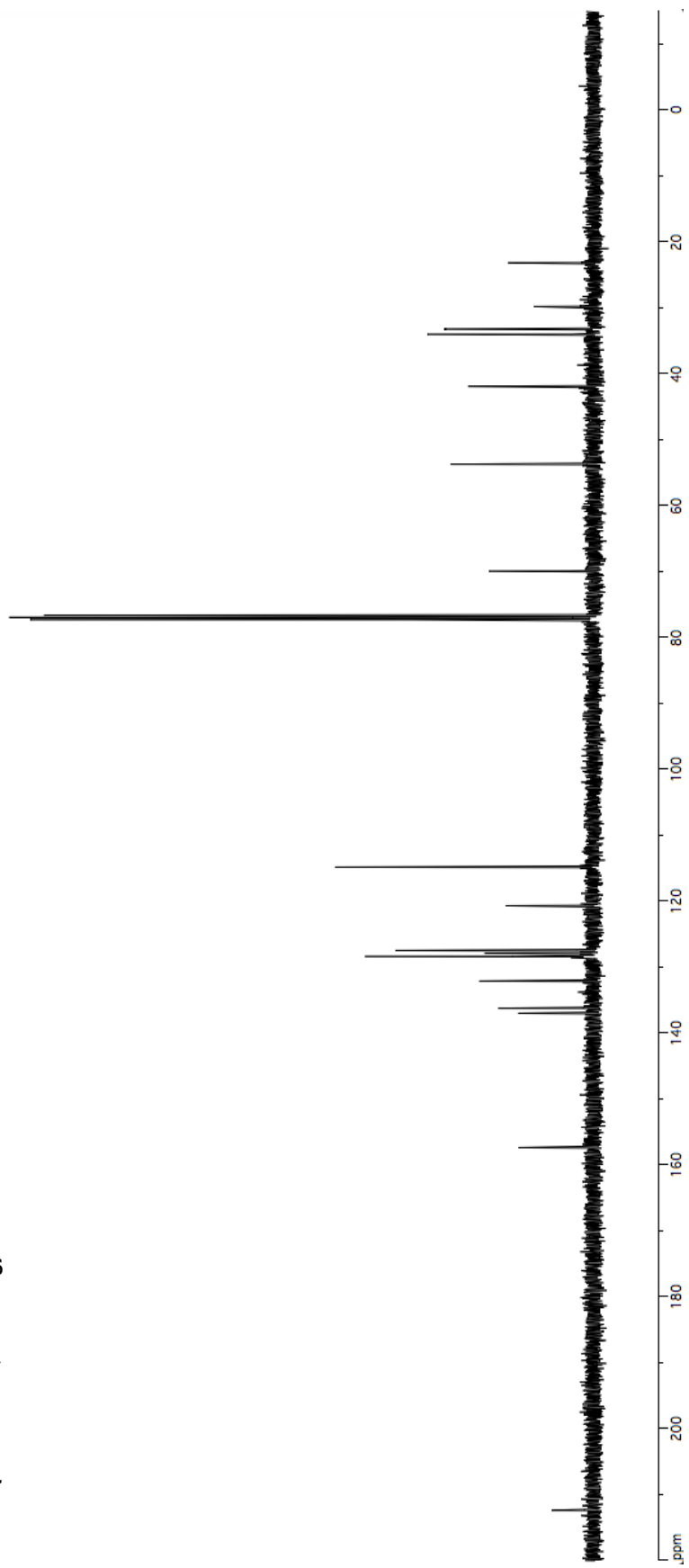


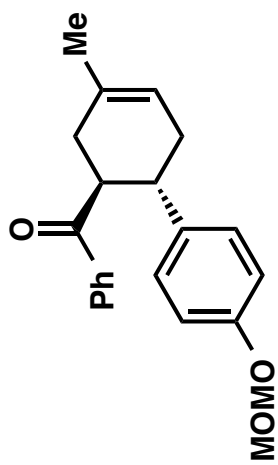
**5-20**  
**<sup>1</sup>H NMR**  
**(400 MHz, CDCl<sub>3</sub>)**



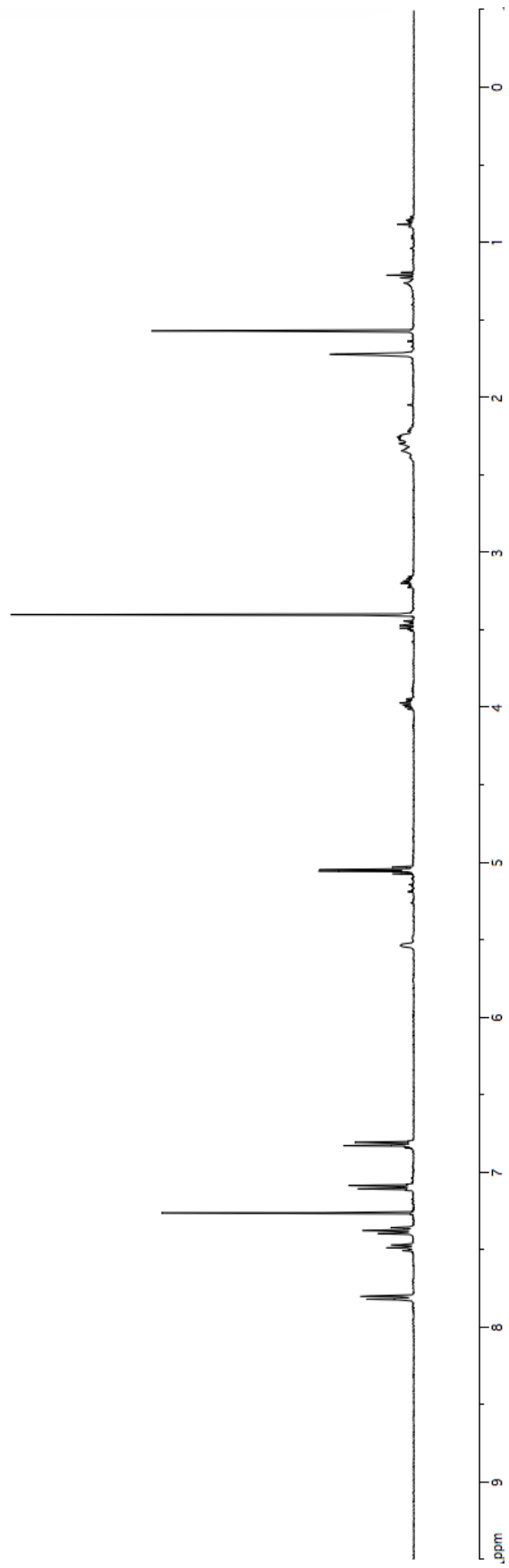


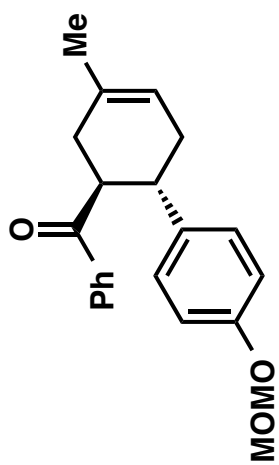
**5-20**  
**<sup>13</sup>C NMR**  
**(100 MHz, CDCl<sub>3</sub>)**



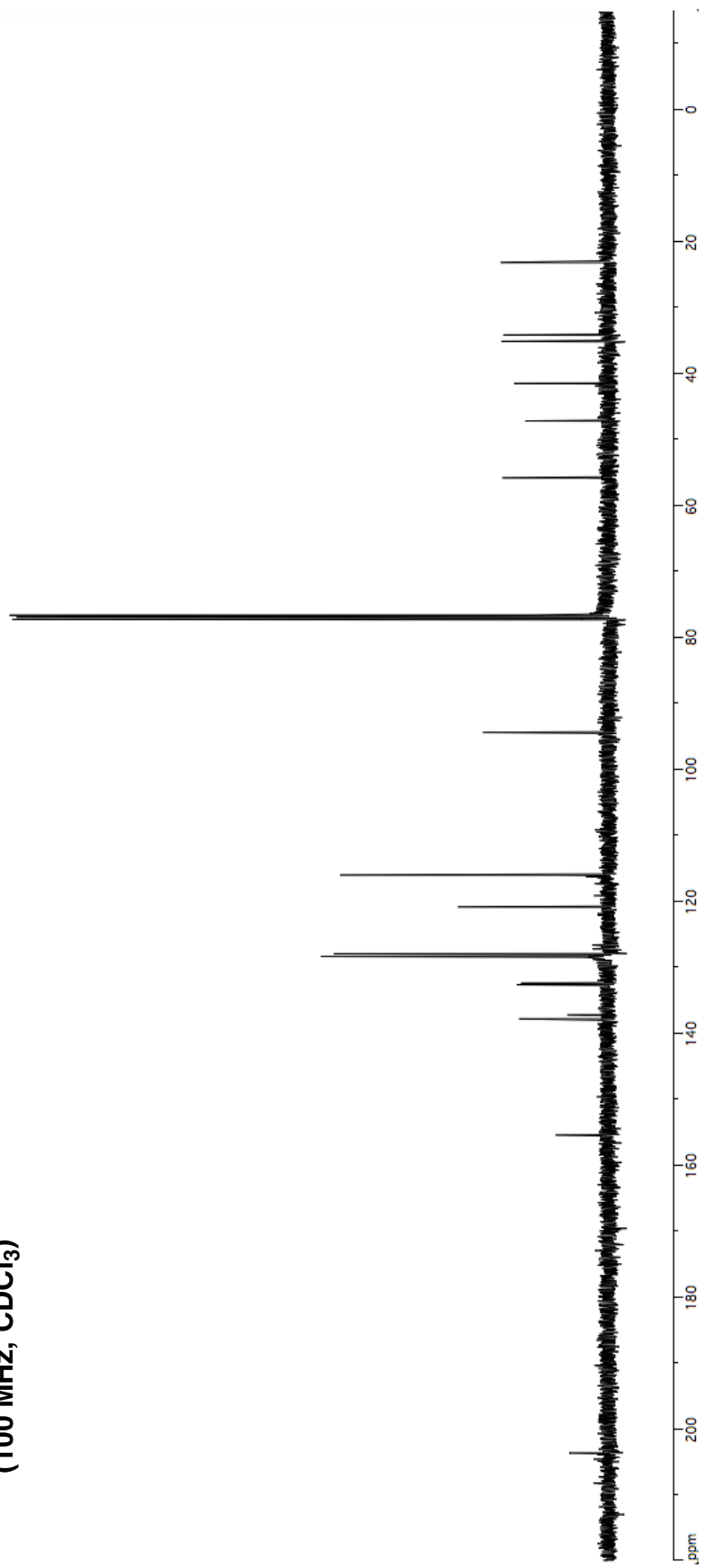


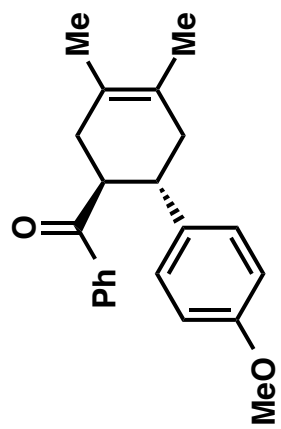
5-21  
<sup>1</sup>H NMR  
(400 MHz, CDCl<sub>3</sub>)





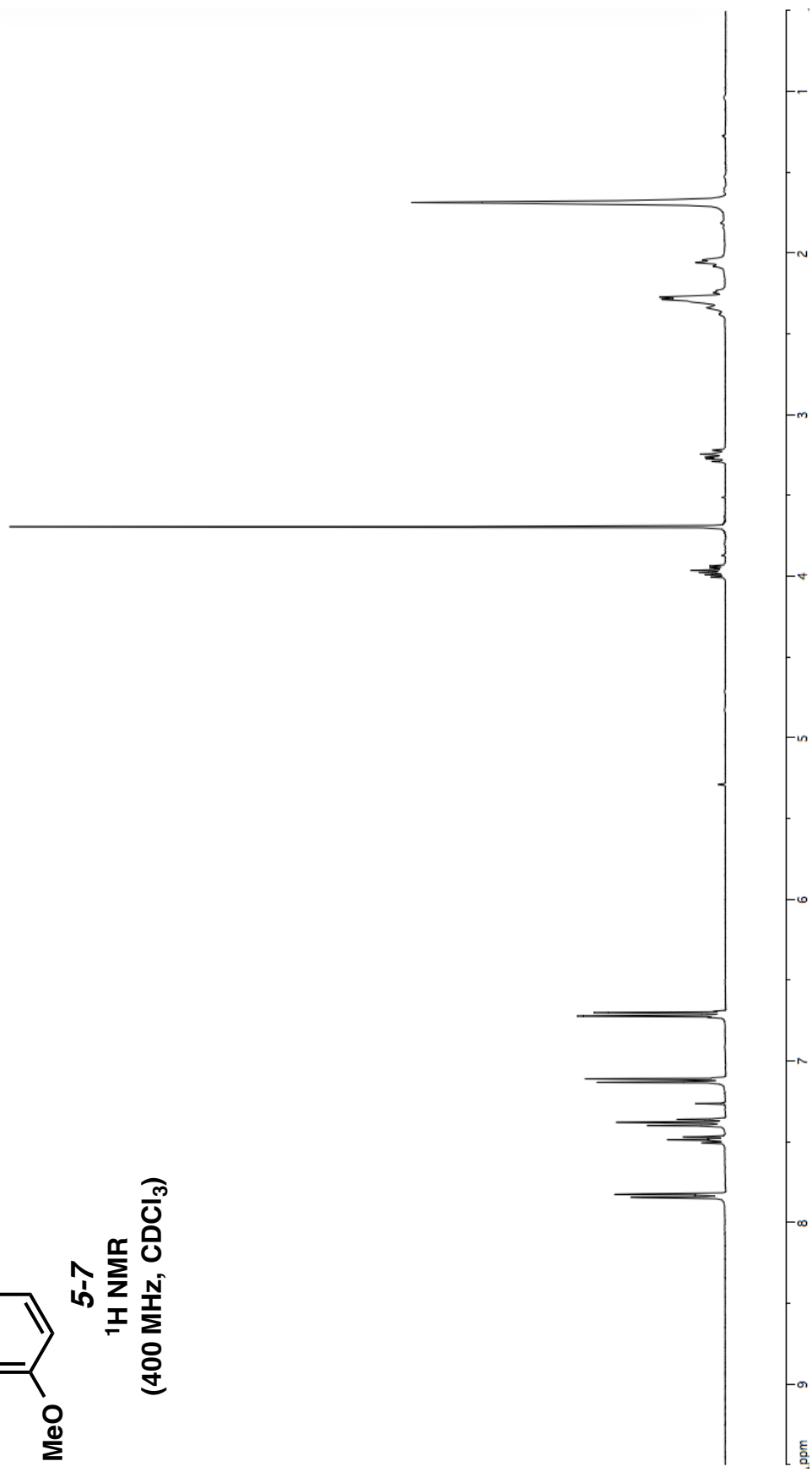
**5-21**  
**<sup>13</sup>C NMR**  
**(100 MHz, CDCl<sub>3</sub>)**

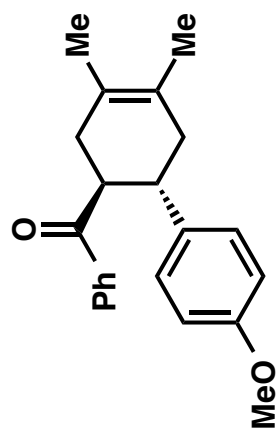




5-7

<sup>1</sup>H NMR  
(400 MHz, CDCl<sub>3</sub>)

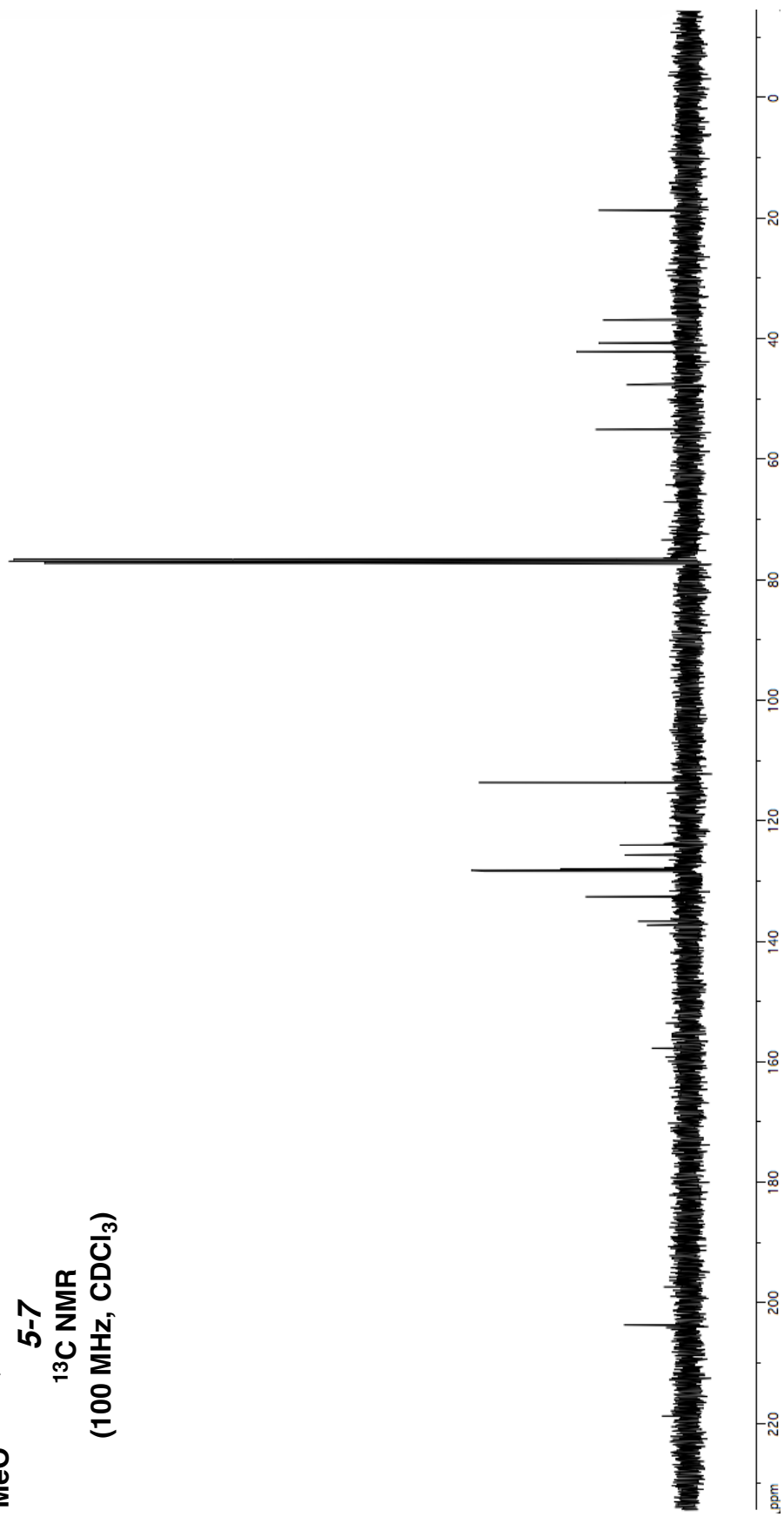


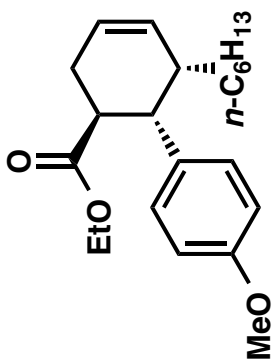


5-7

<sup>13</sup>C NMR

(100 MHz, CDCl<sub>3</sub>)

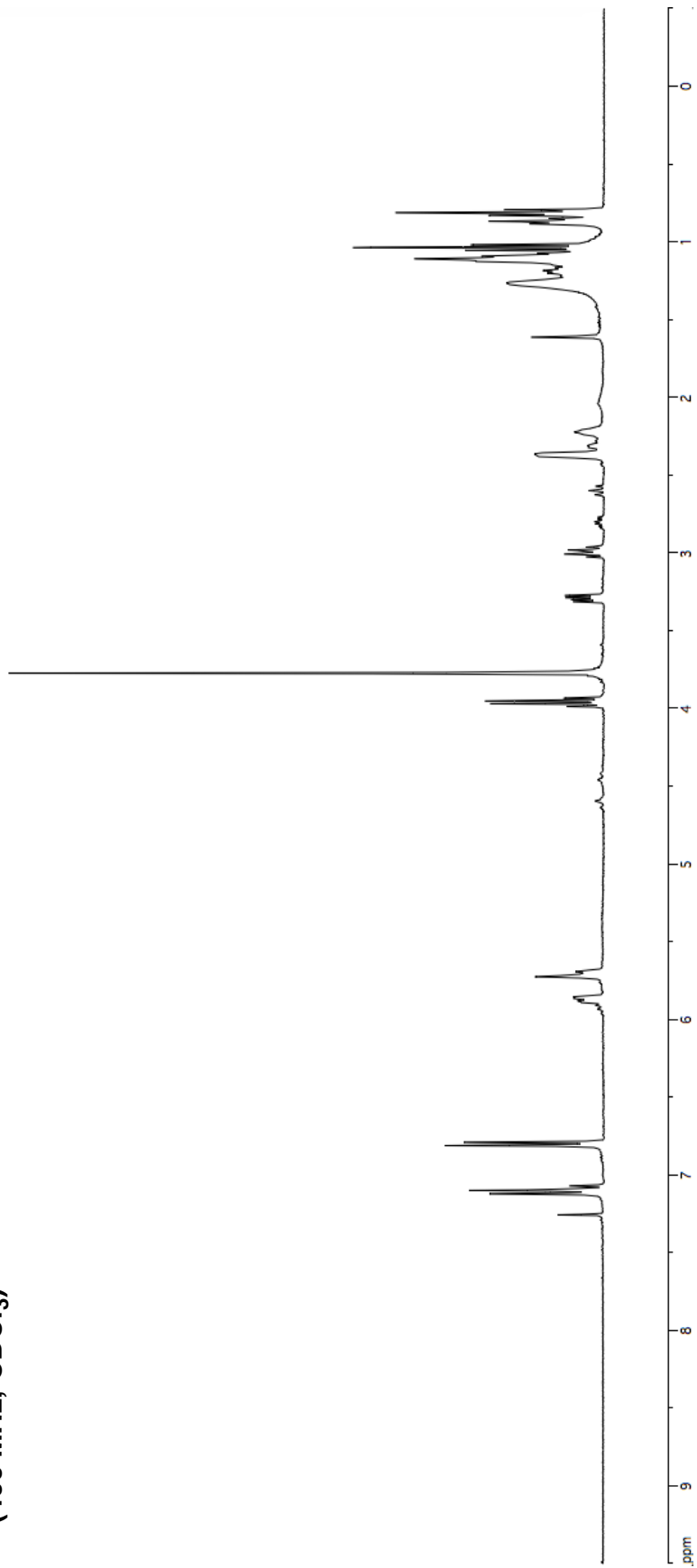


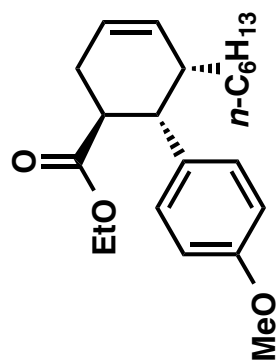


5-22

<sup>1</sup>H NMR

(400 MHz, CDCl<sub>3</sub>)

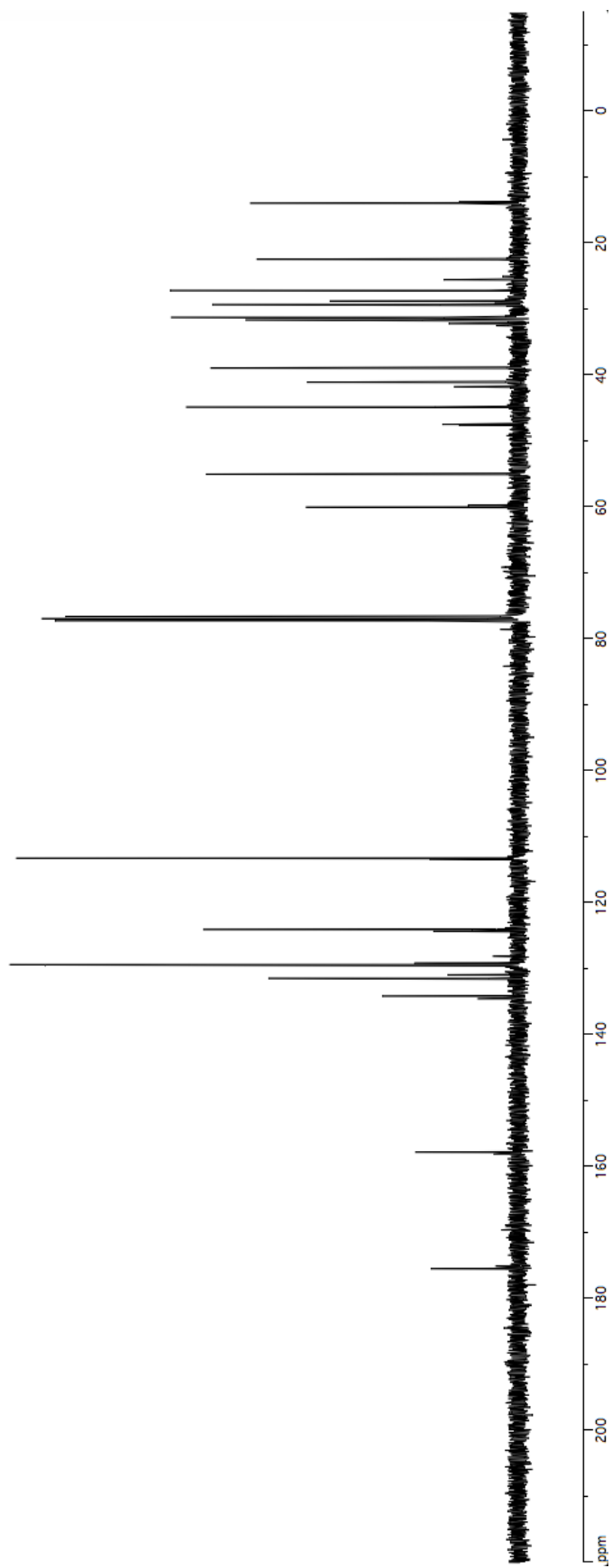


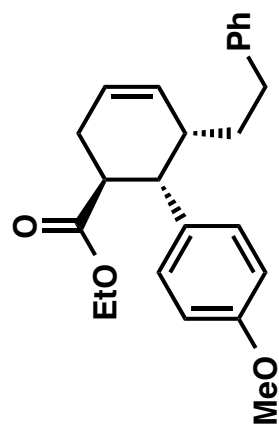


5-22

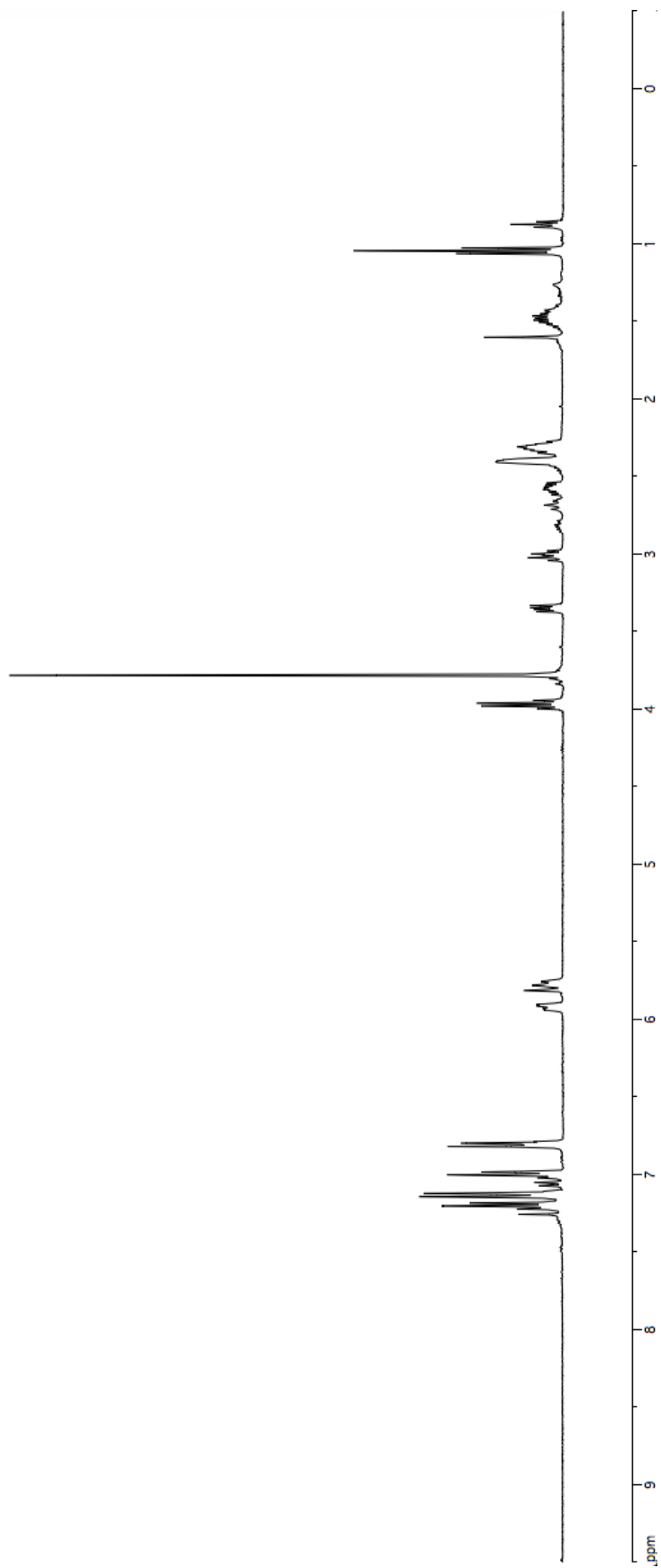
<sup>13</sup>C NMR

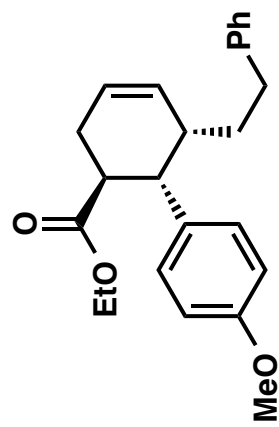
(100 MHz, CDCl<sub>3</sub>)



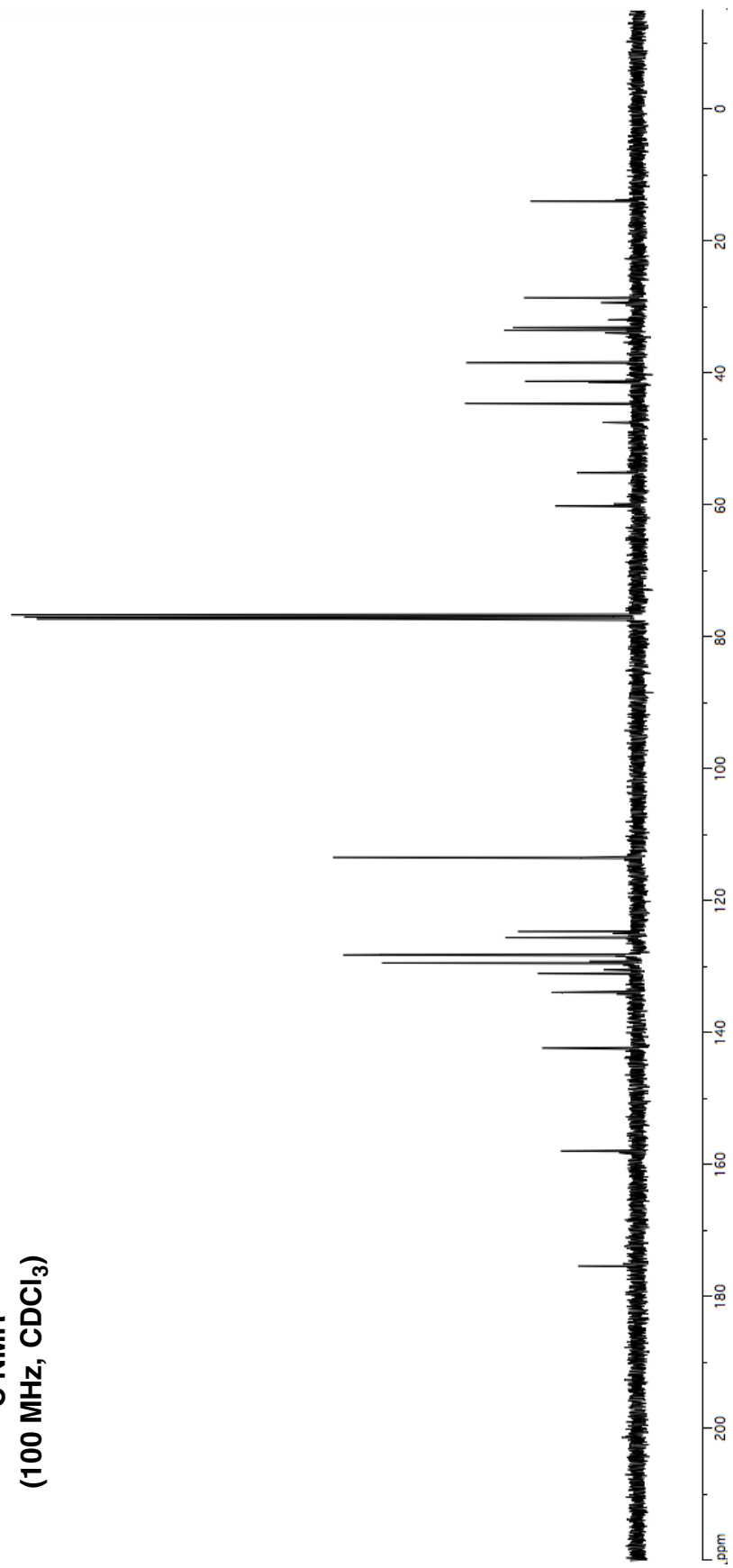


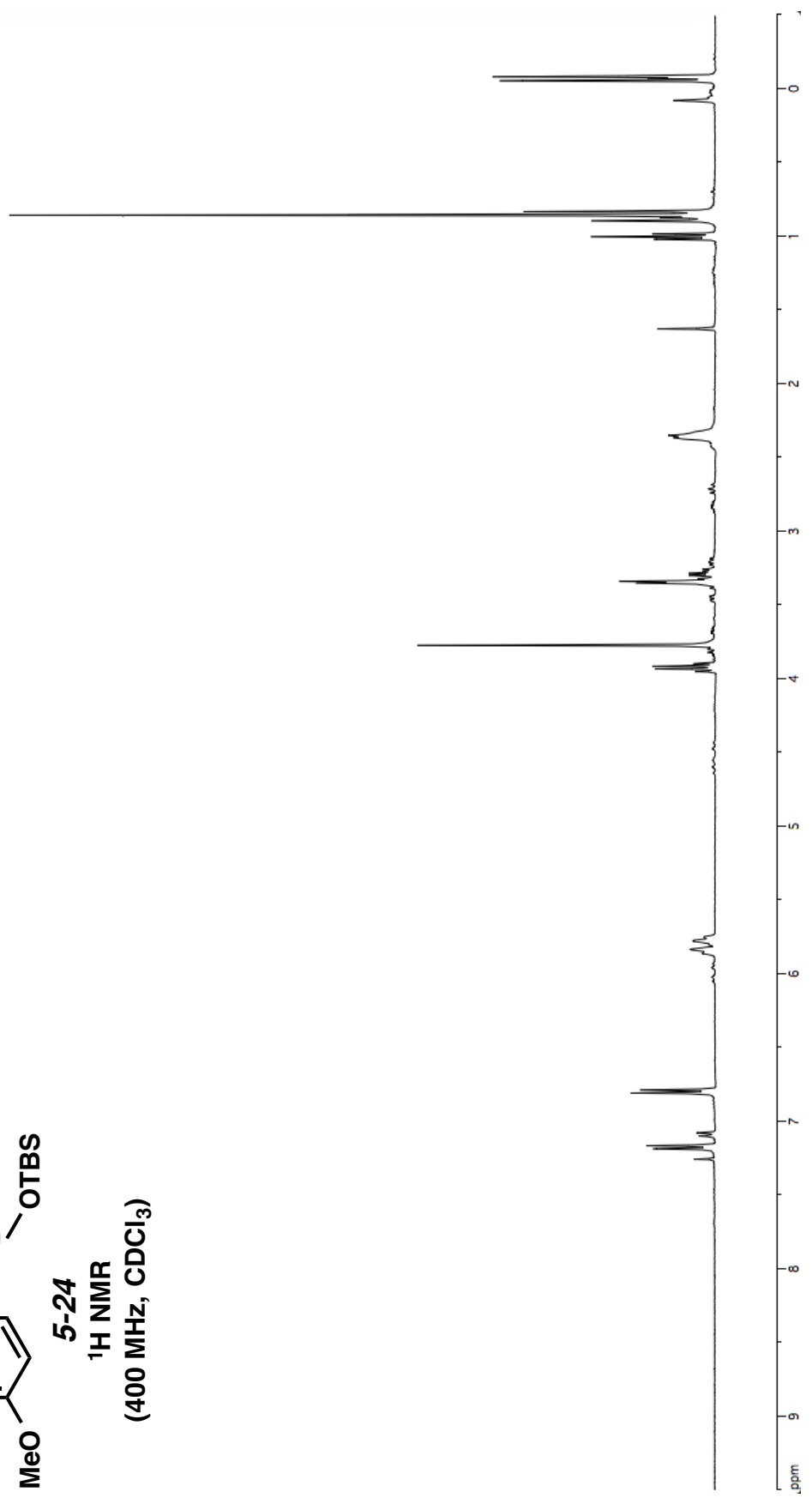
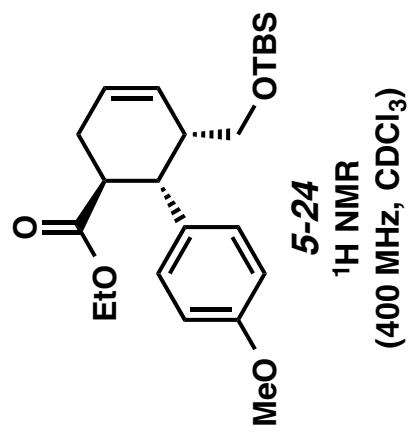
5-23  
<sup>1</sup>H NMR  
(400 MHz, CDCl<sub>3</sub>)

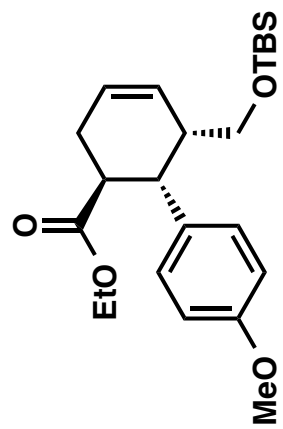




**5-23**  
**<sup>13</sup>C NMR**  
**(100 MHz, CDCl<sub>3</sub>)**



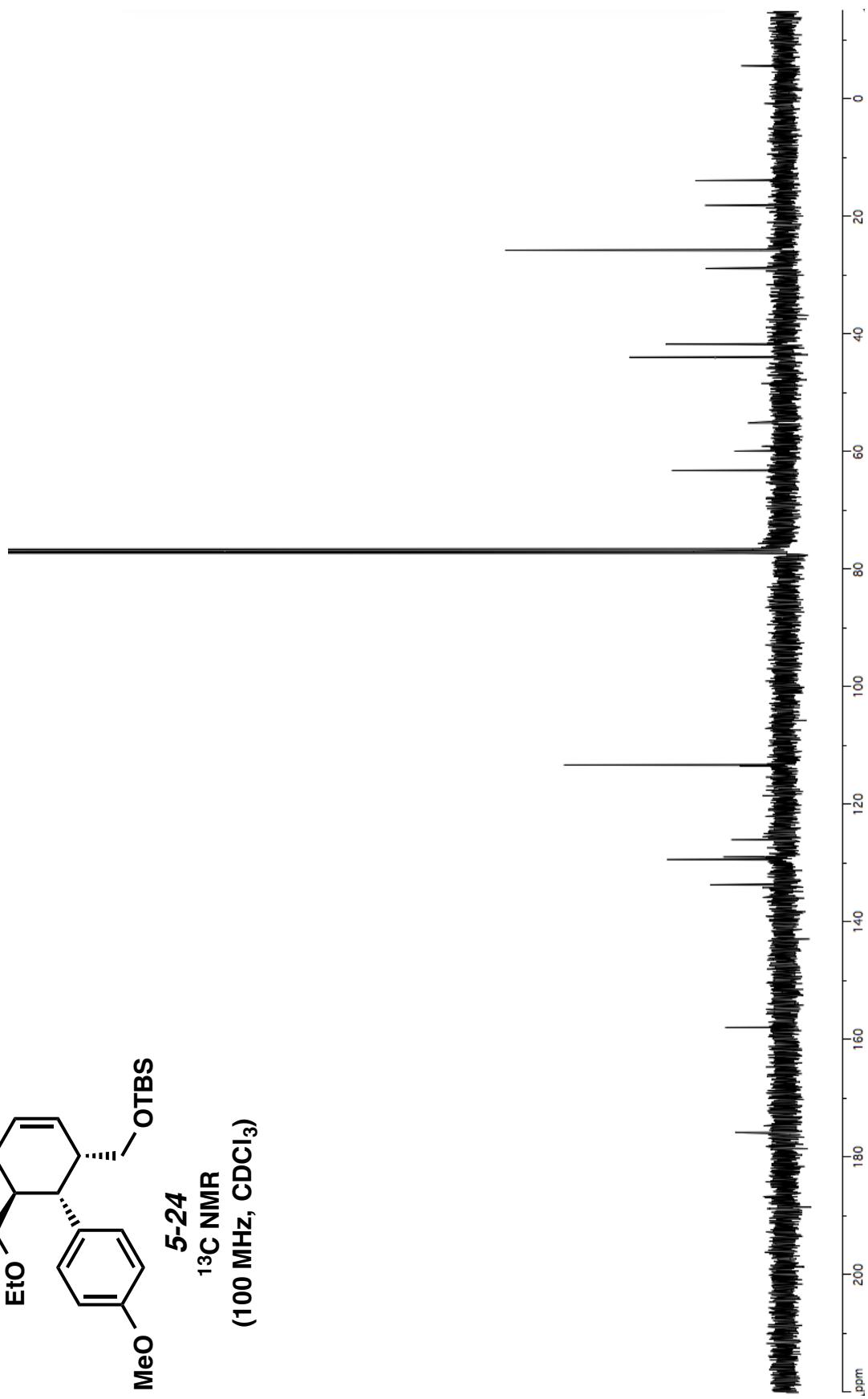


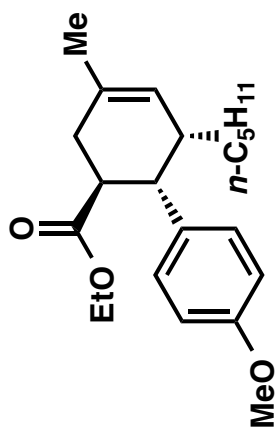


5-24

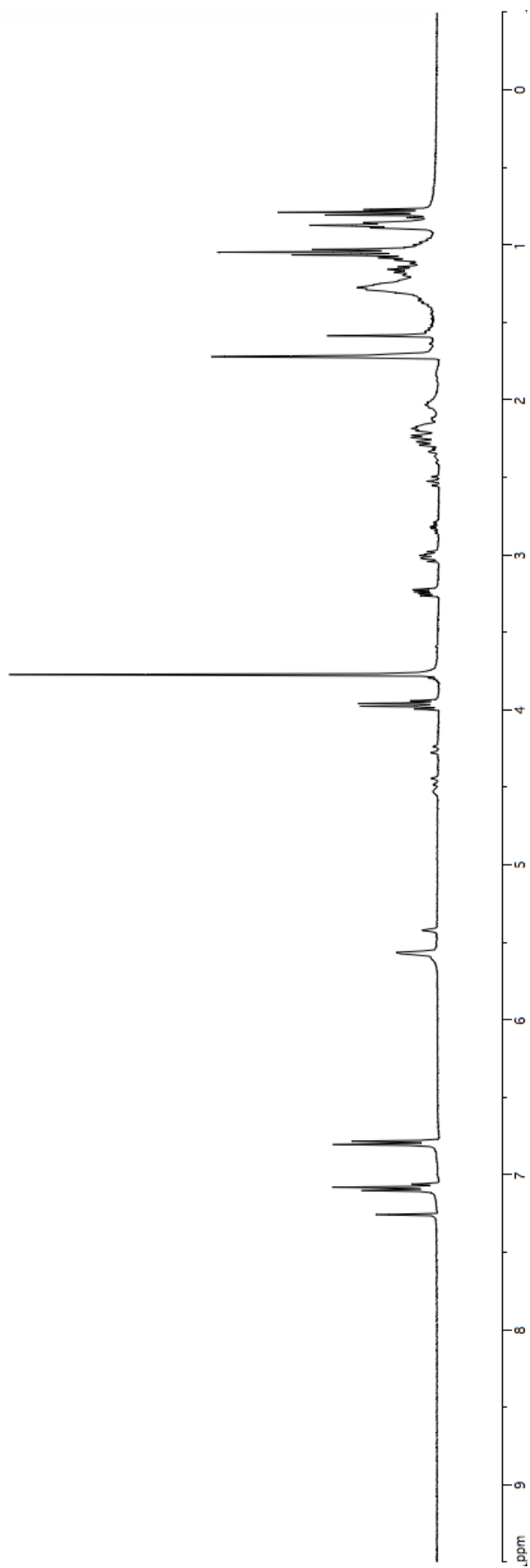
$^{13}\text{C}$  NMR

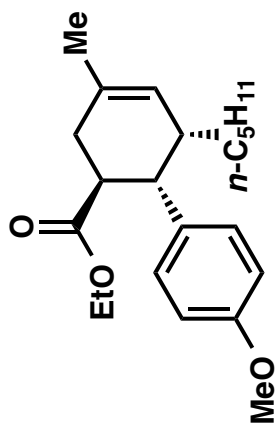
(100 MHz,  $\text{CDCl}_3$ )



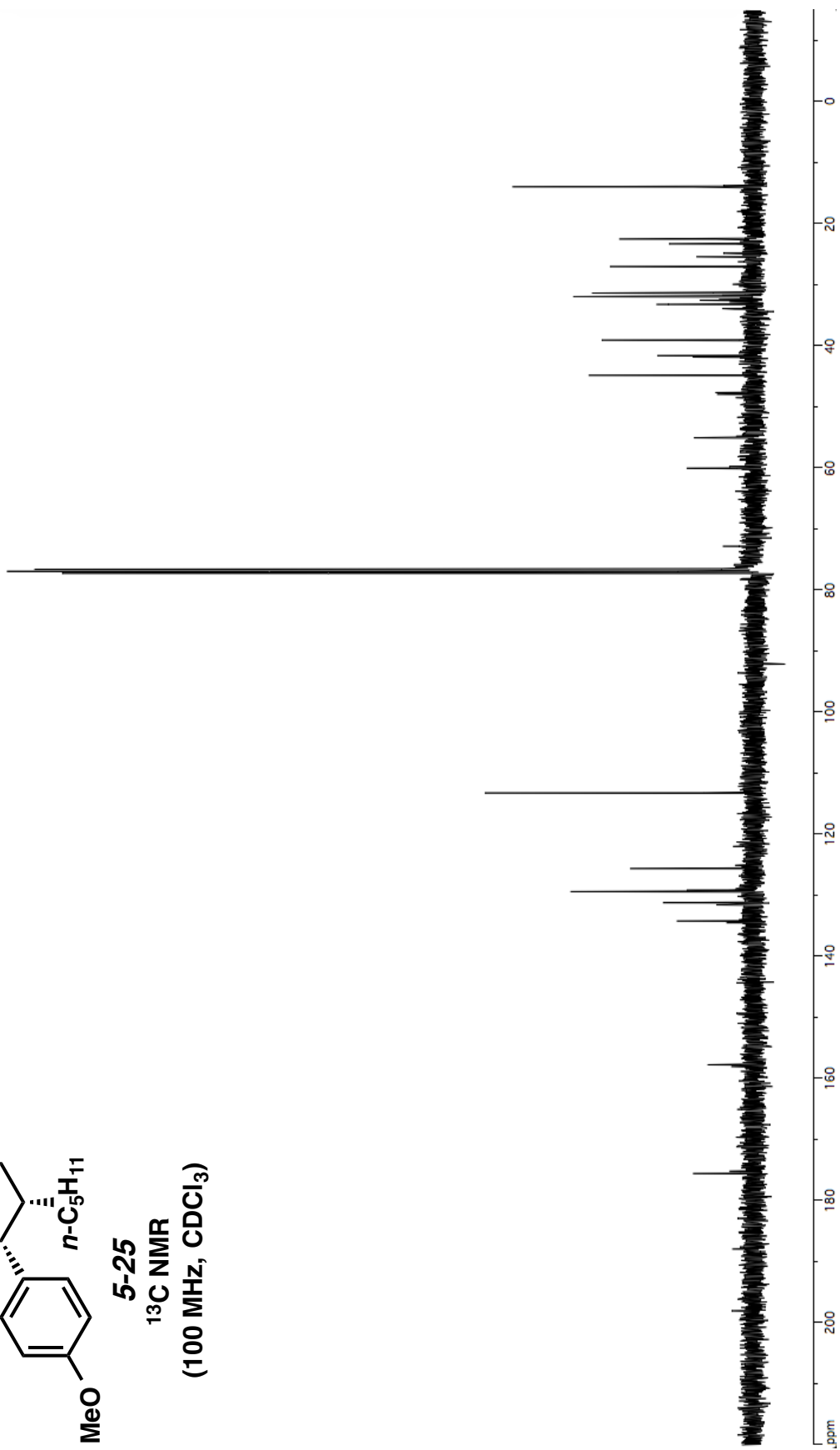


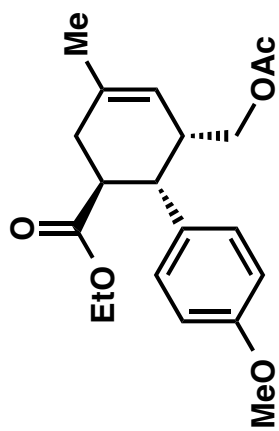
5-25  
<sup>1</sup>H NMR  
(400 MHz, CDCl<sub>3</sub>)



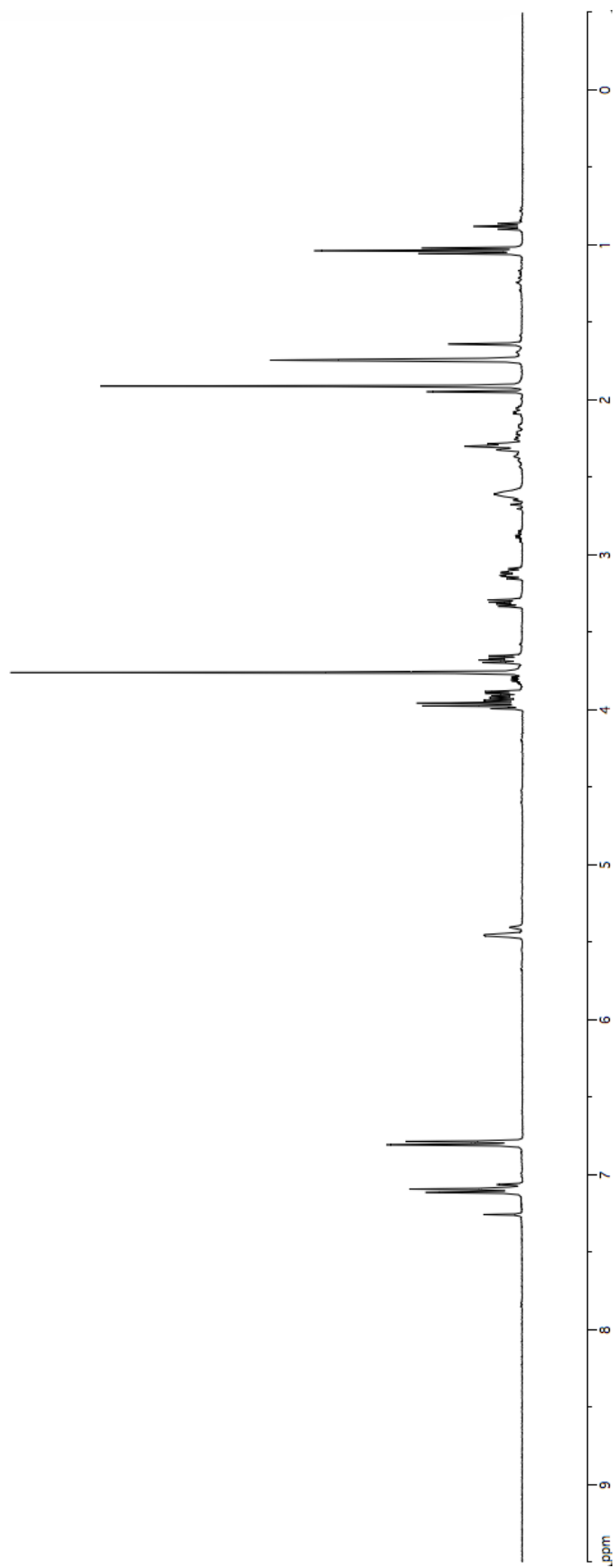


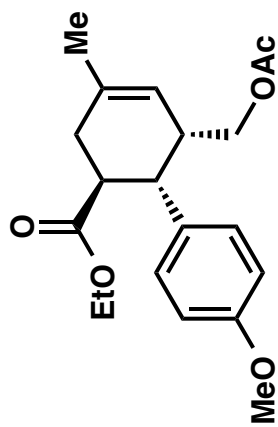
5-25  
<sup>13</sup>C NMR  
(100 MHz, CDCl<sub>3</sub>)



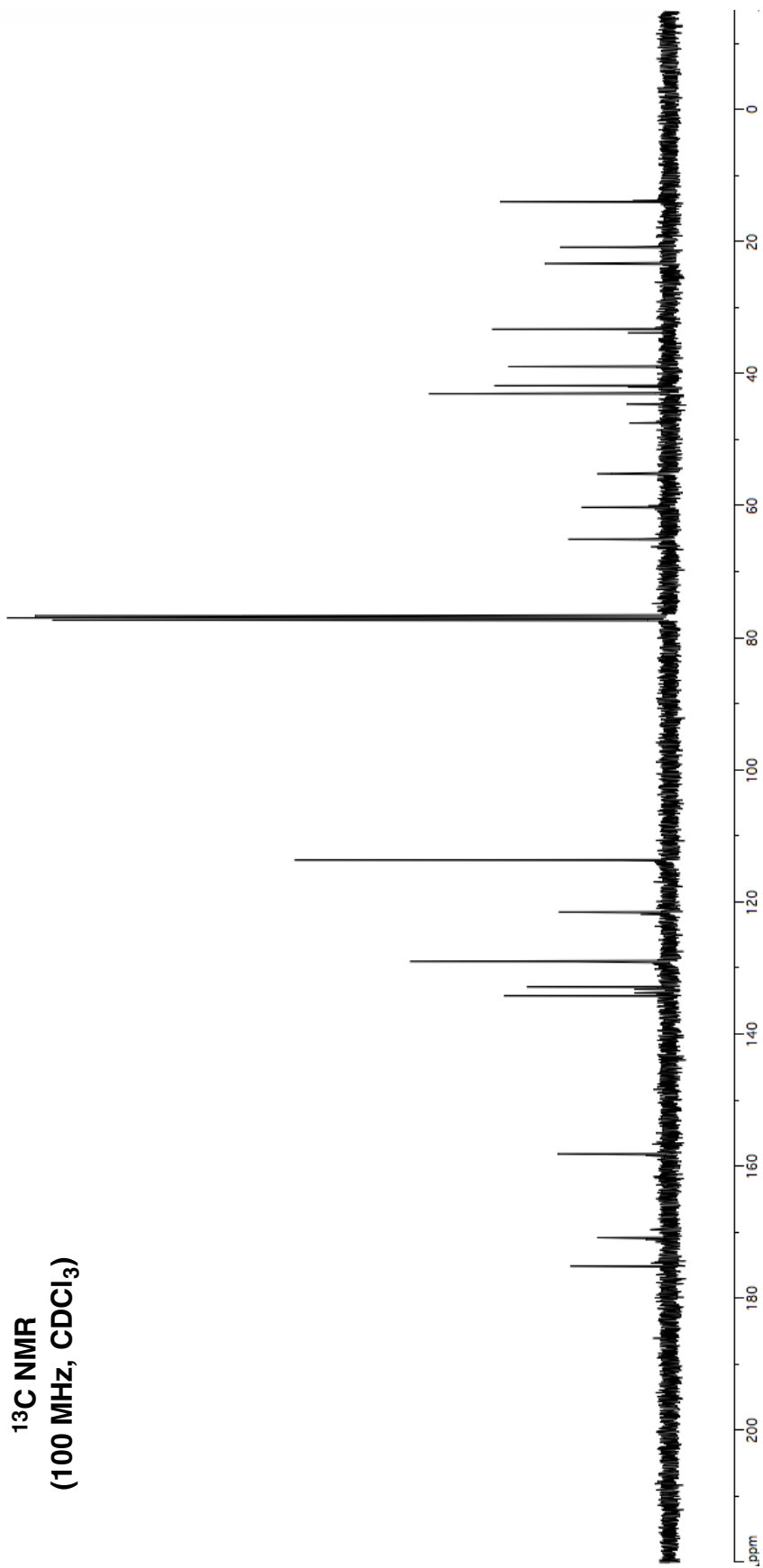


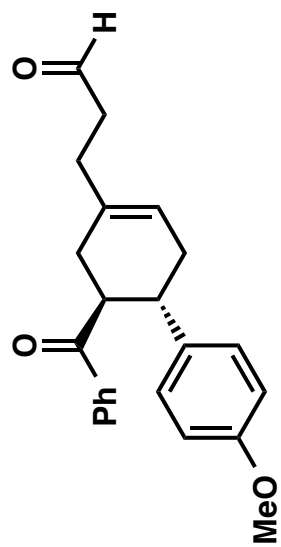
5-26  
 $^1\text{H}$  NMR  
(400 MHz,  $\text{CDCl}_3$ )



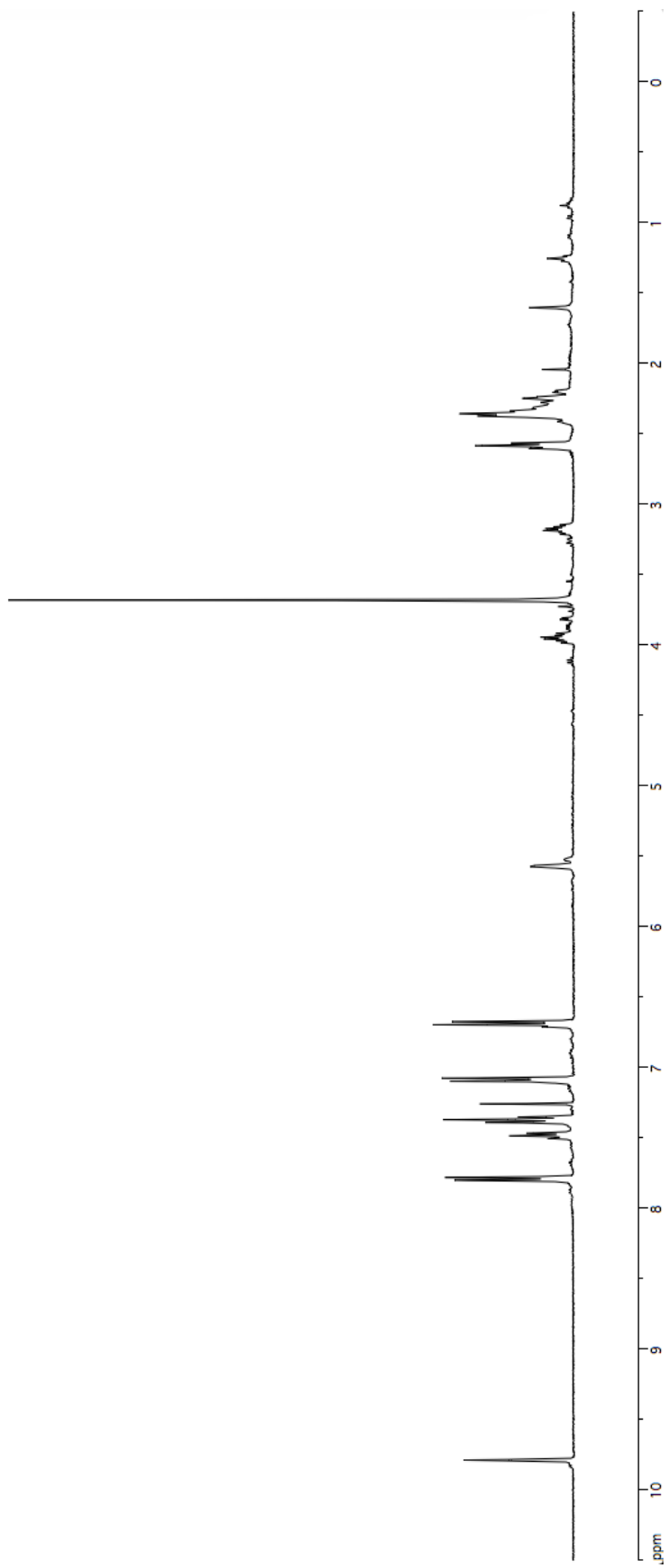


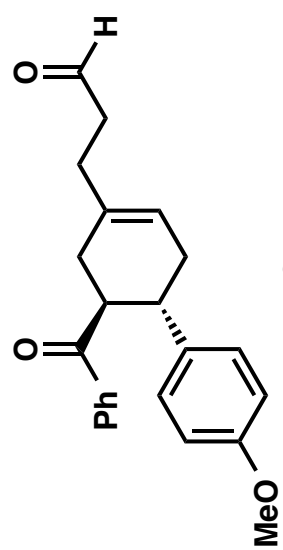
**5-26**  
**<sup>13</sup>C NMR**  
**(100 MHz, CDCl<sub>3</sub>)**



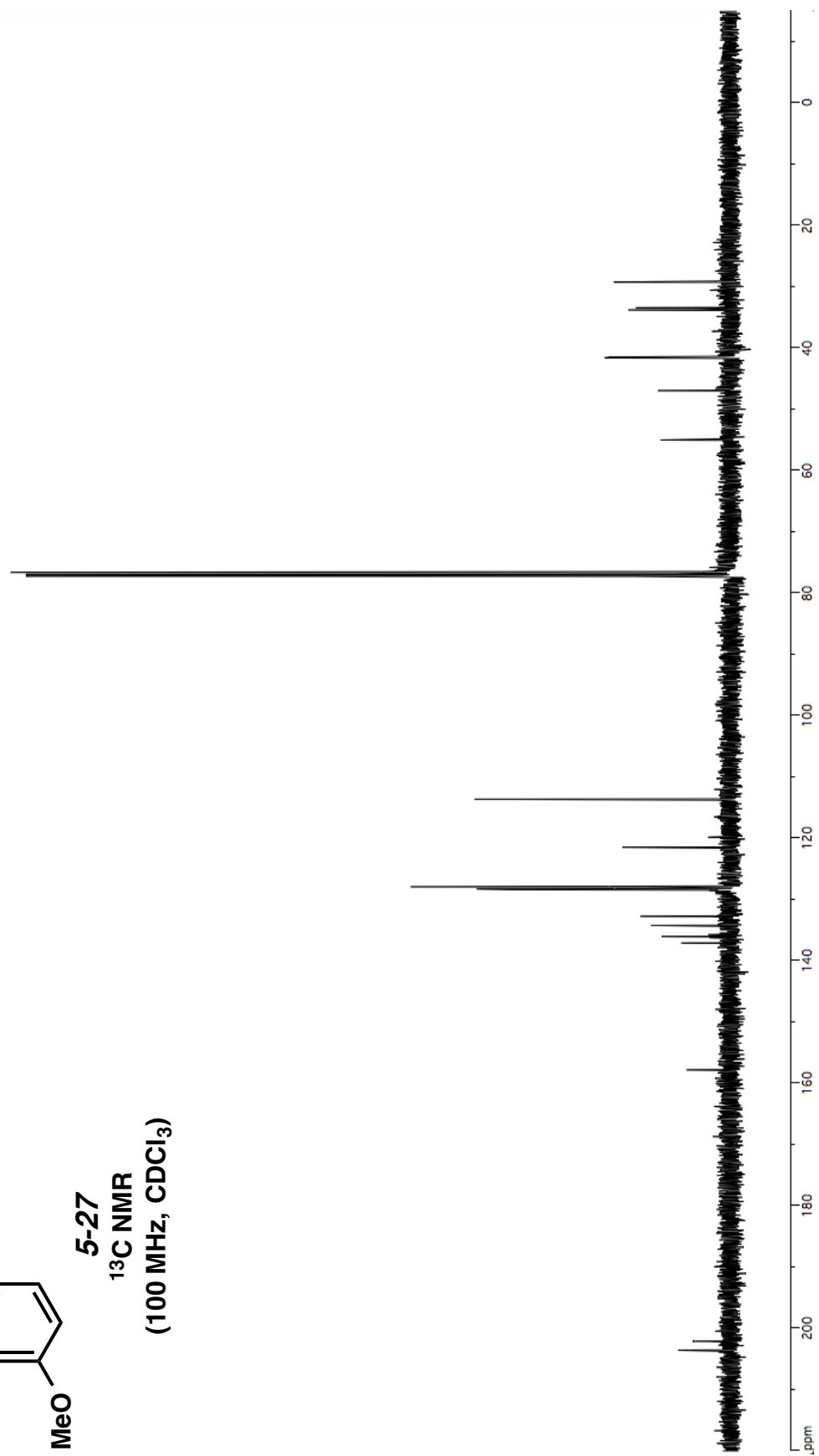


5-27  
<sup>1</sup>H NMR  
(400 MHz, CDCl<sub>3</sub>)

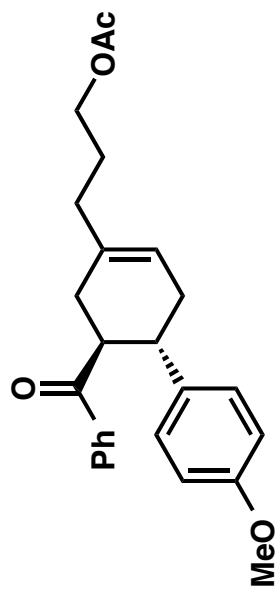




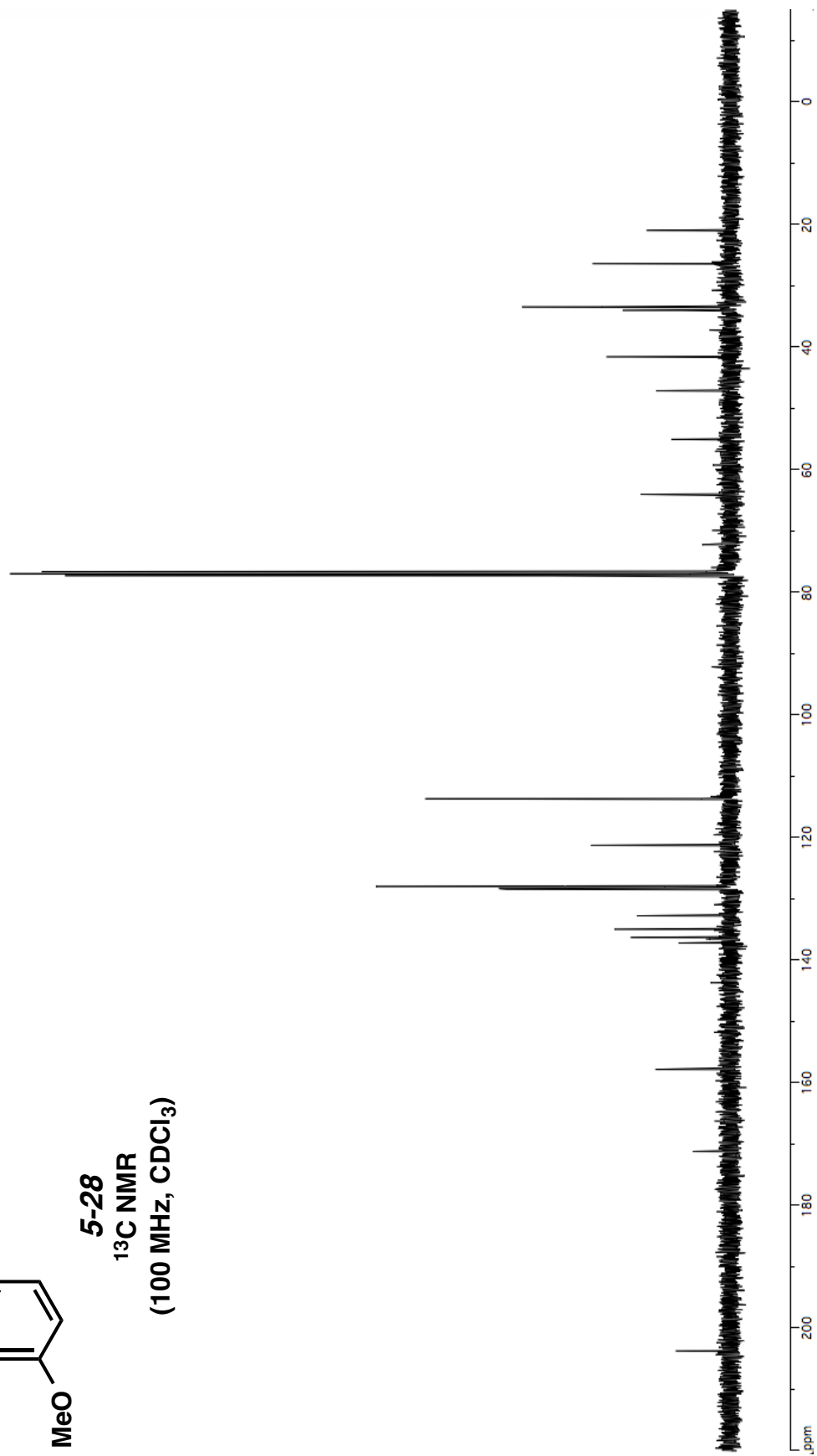
**5-27**  
**<sup>13</sup>C NMR**  
**(100 MHz, CDCl<sub>3</sub>)**

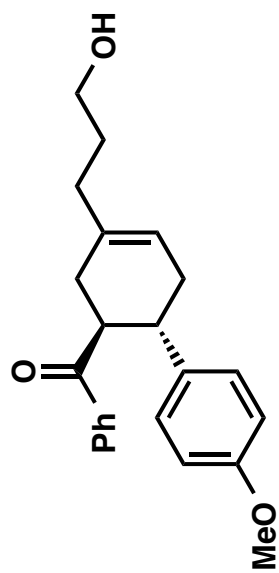




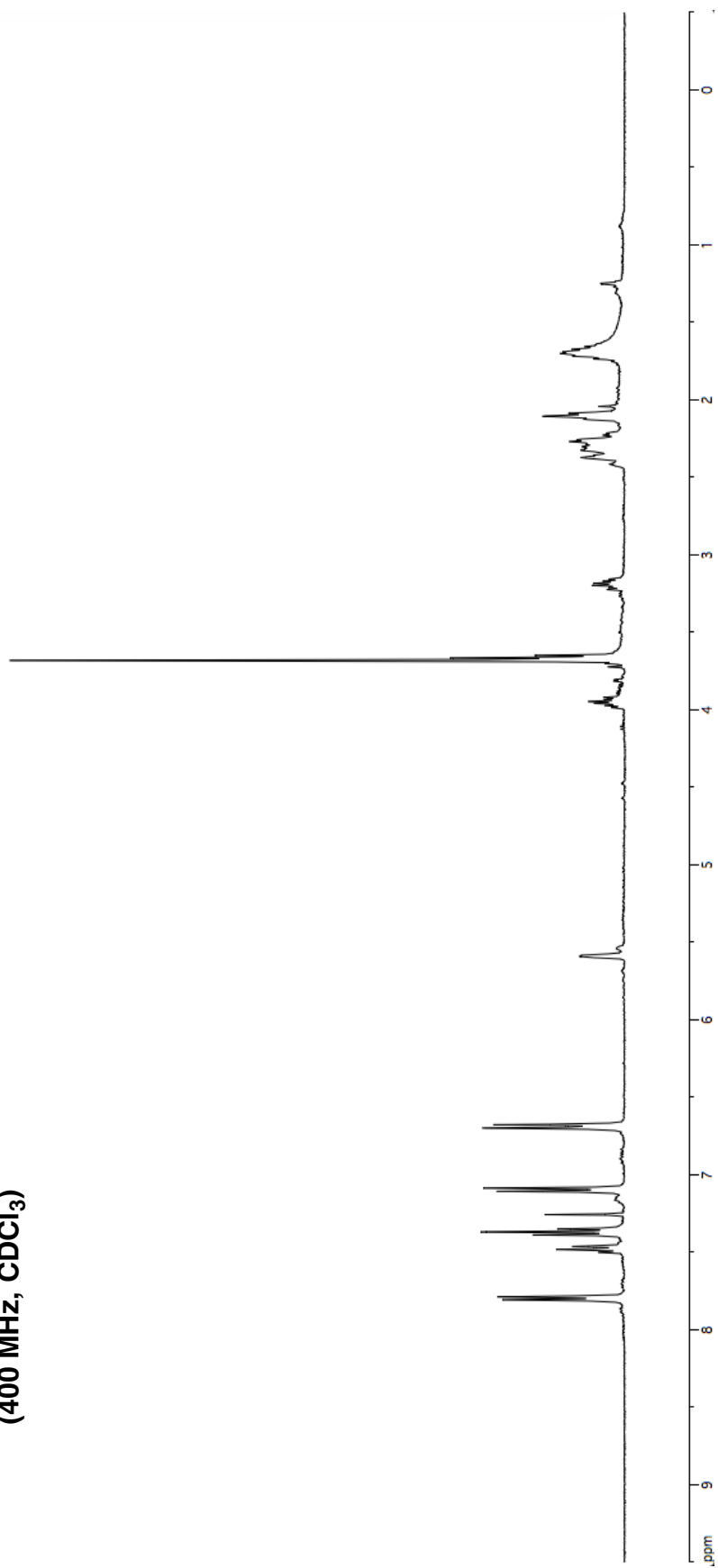


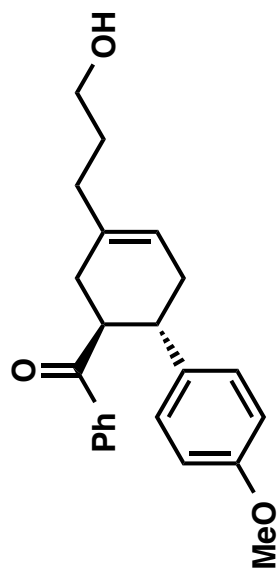
**5-28**  
**<sup>13</sup>C NMR**  
**(100 MHz, CDCl<sub>3</sub>)**



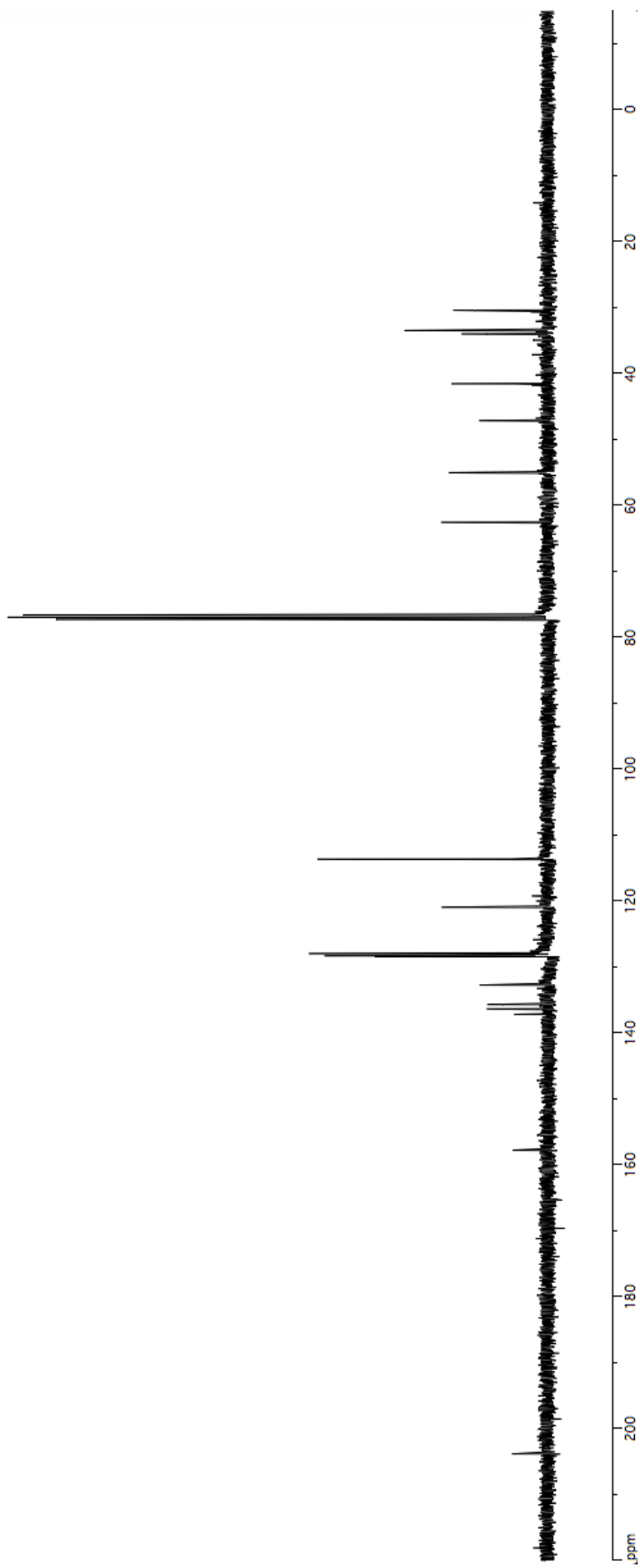


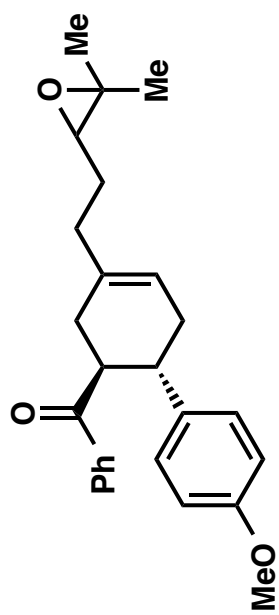
**5-29**  
**<sup>1</sup>H NMR**  
**(400 MHz, CDCl<sub>3</sub>)**





**5-29**  
**<sup>13</sup>C NMR**  
**(100 MHz, CDCl<sub>3</sub>)**

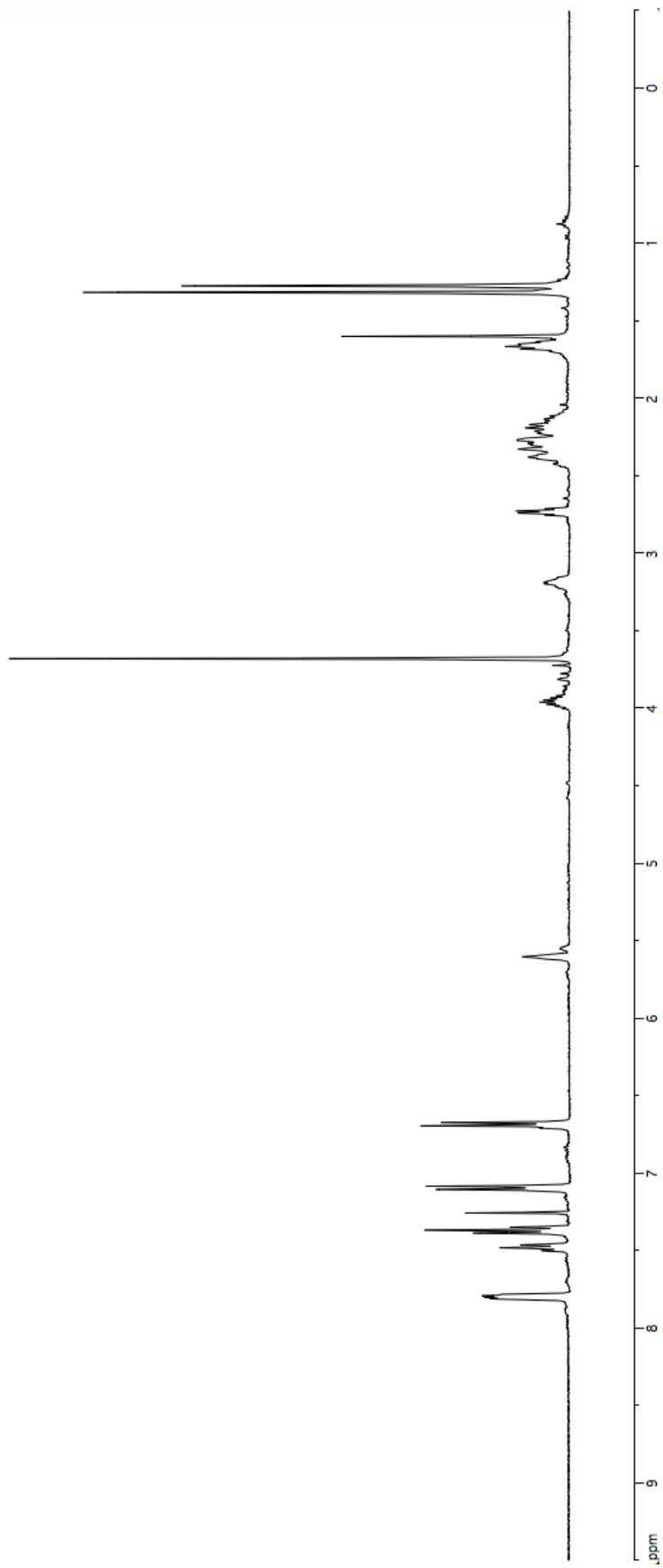


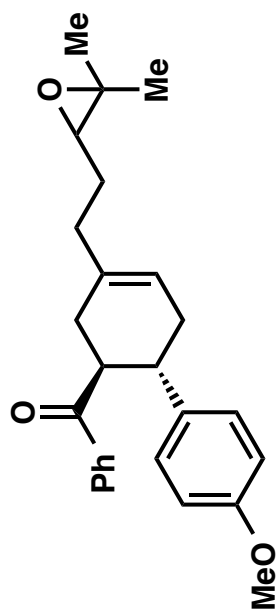


5-30

<sup>1</sup>H NMR

(400 MHz, CDCl<sub>3</sub>)

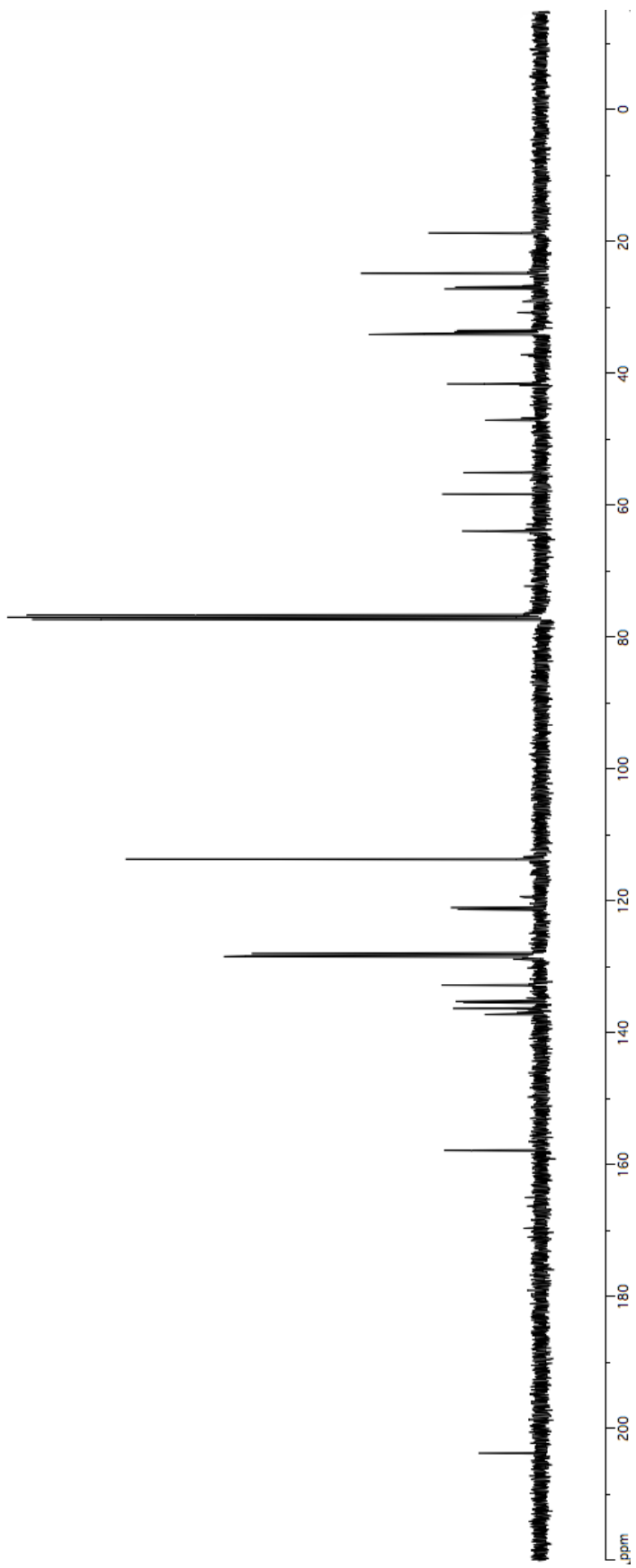


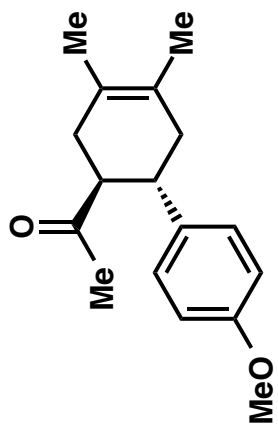


5-30

<sup>13</sup>C NMR

(100 MHz, CDCl<sub>3</sub>)

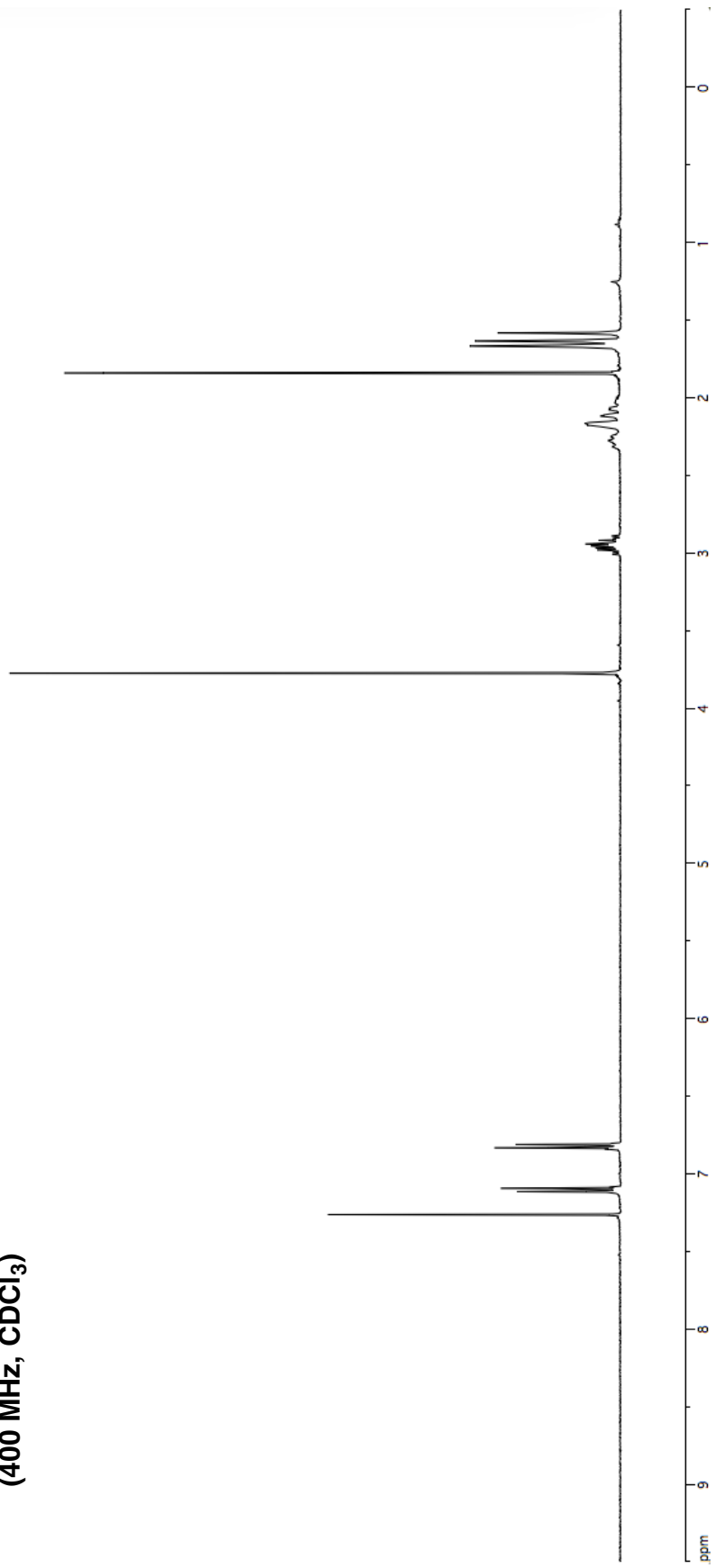


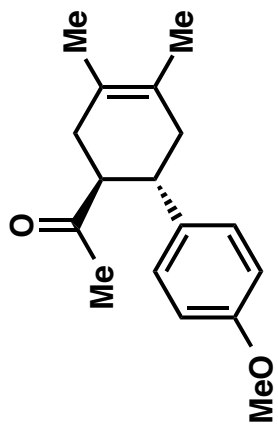


5-113

<sup>1</sup>H NMR

(400 MHz, CDCl<sub>3</sub>)

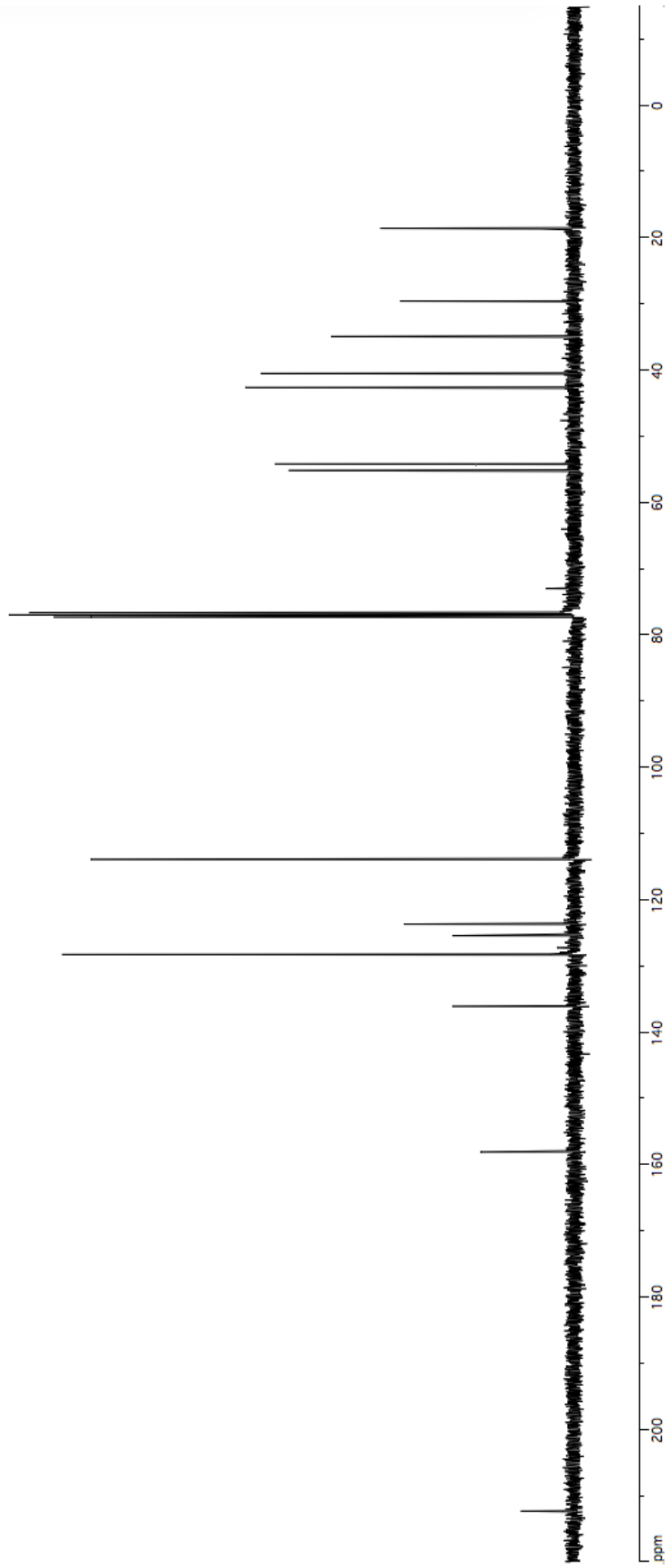


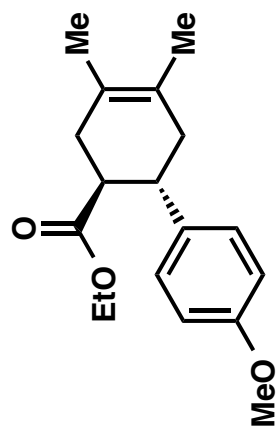


5-113

<sup>13</sup>C NMR

(100 MHz, CDCl<sub>3</sub>)

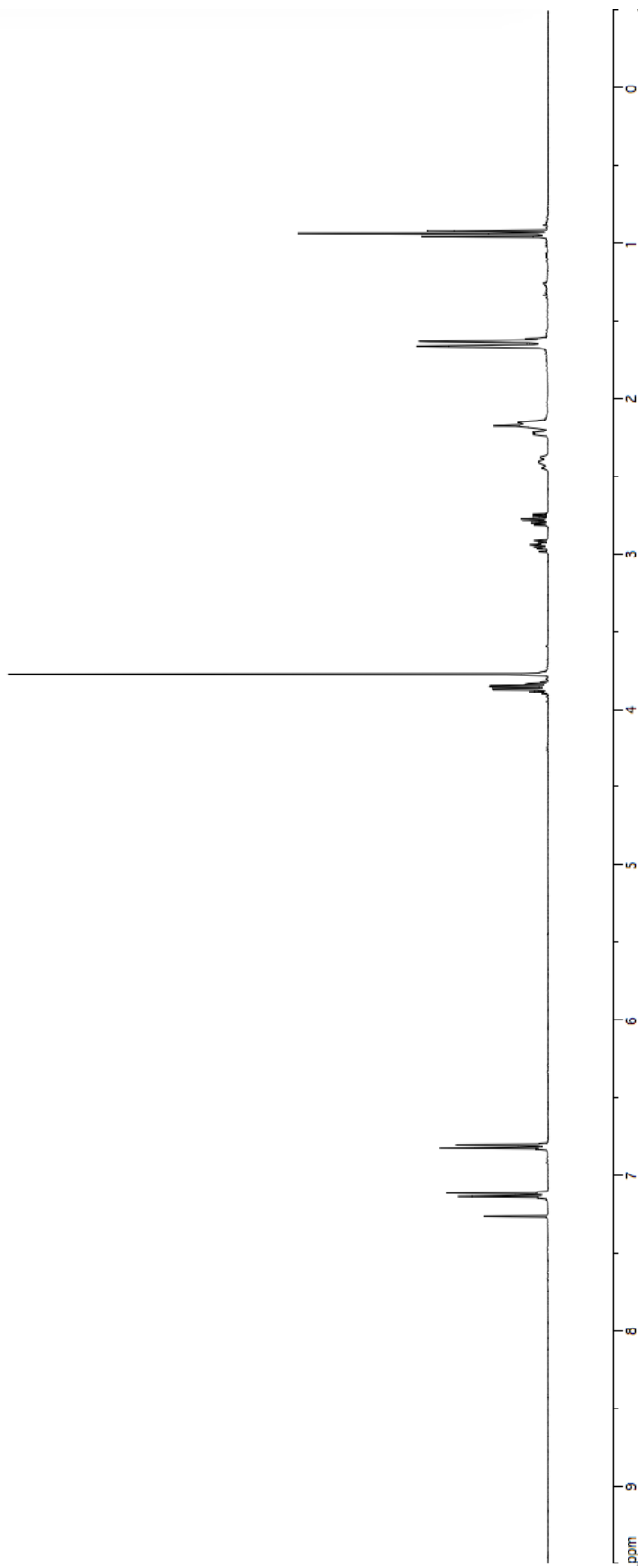


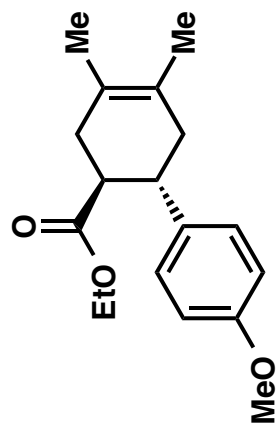


5-114

<sup>1</sup>H NMR

(400 MHz, CDCl<sub>3</sub>)

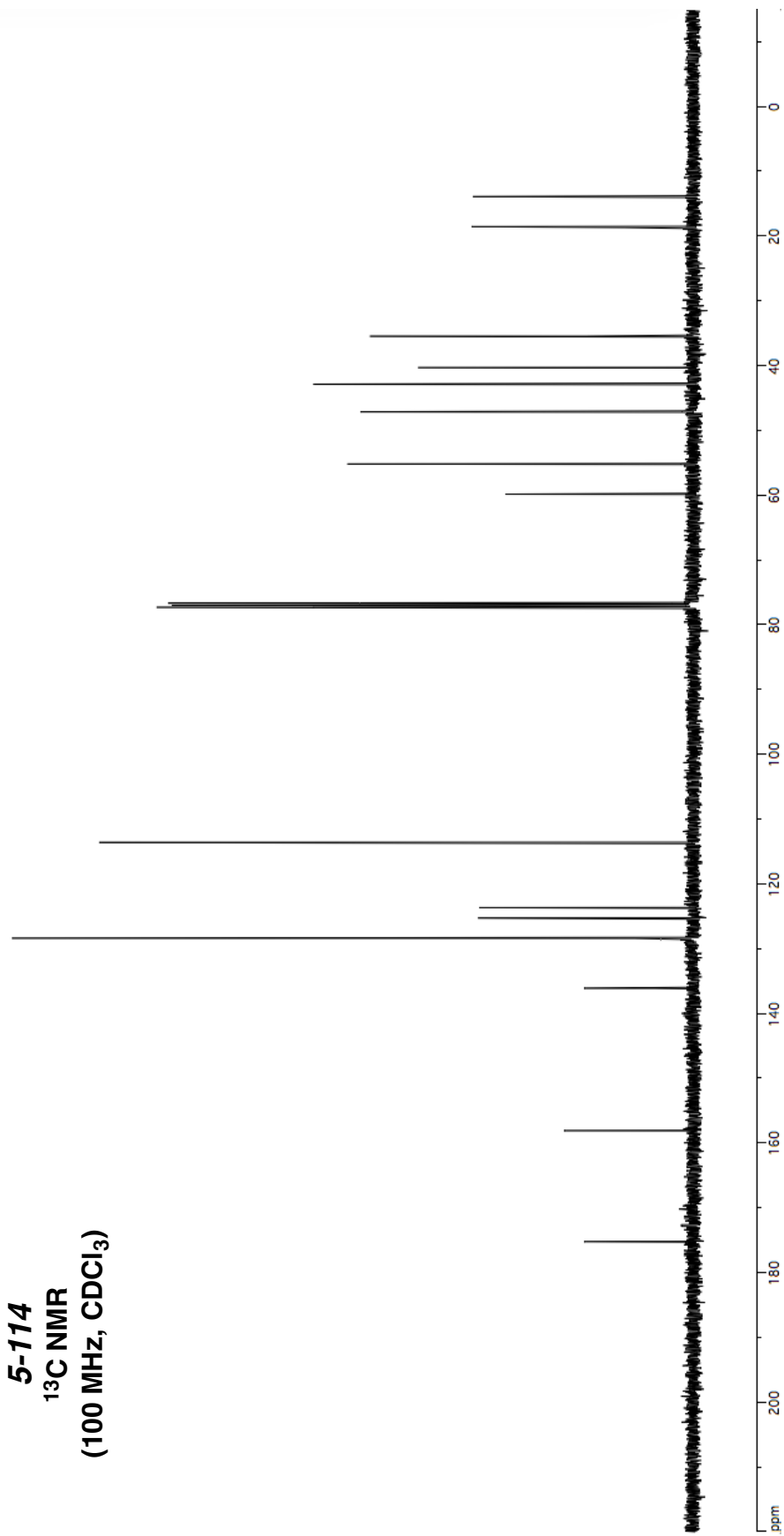


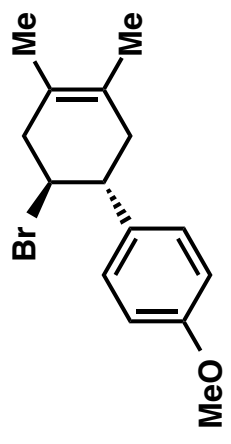


5-114

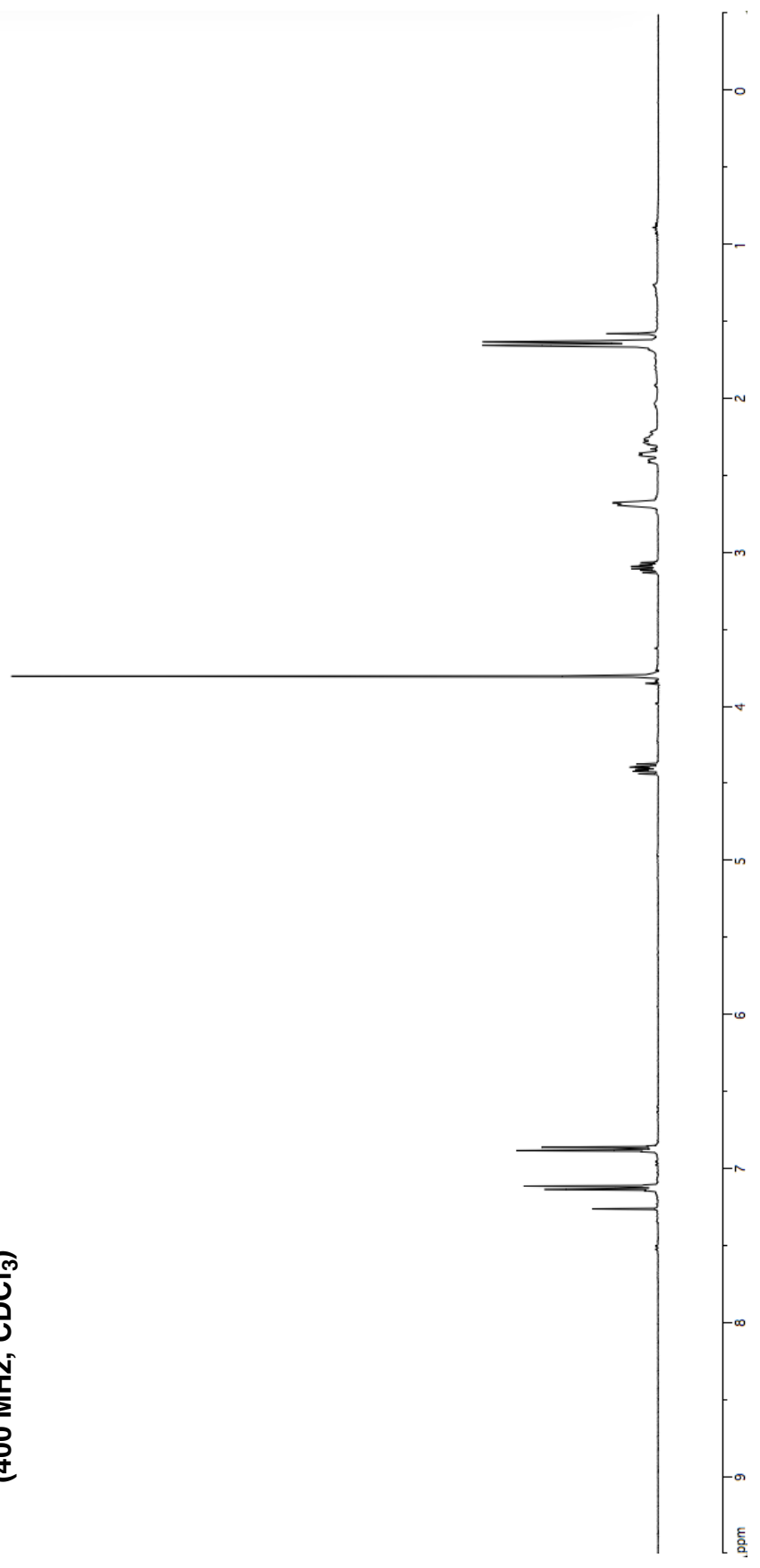
<sup>13</sup>C NMR

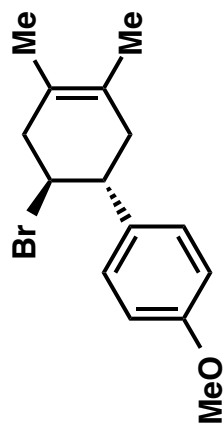
(100 MHz, CDCl<sub>3</sub>)



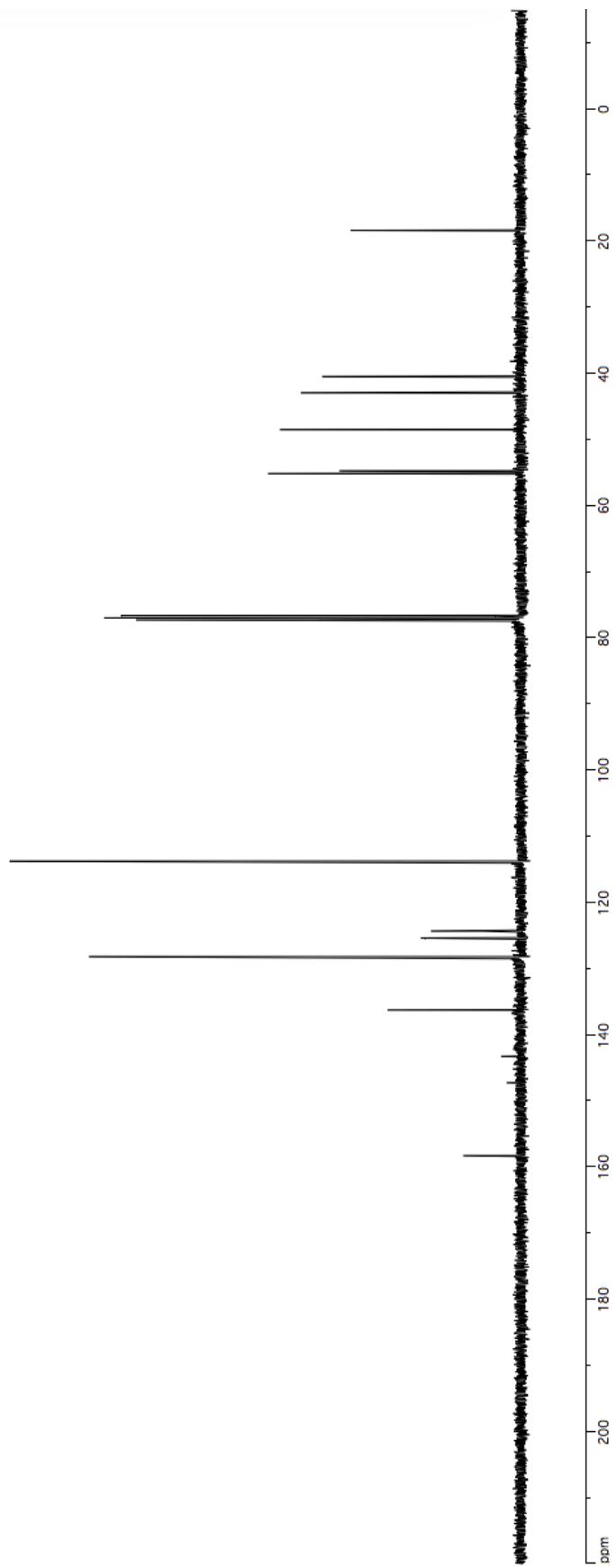


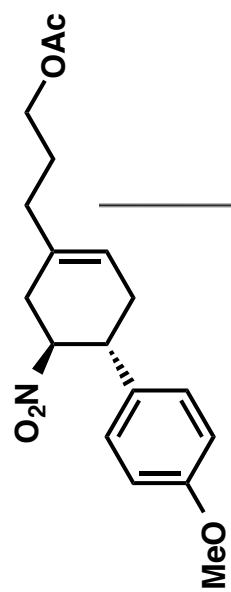
5-115  
<sup>1</sup>H NMR  
(400 MHz, CDCl<sub>3</sub>)



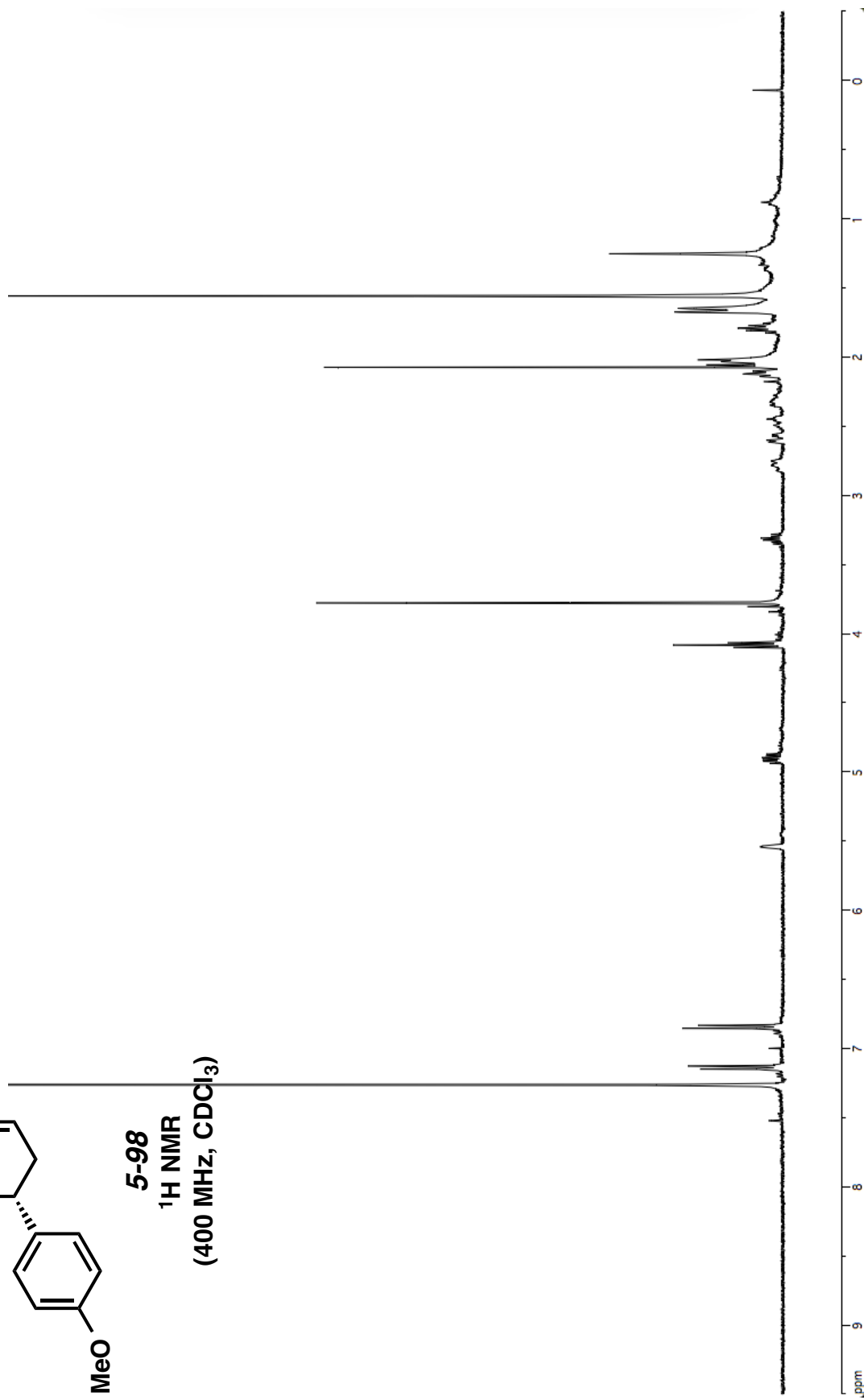


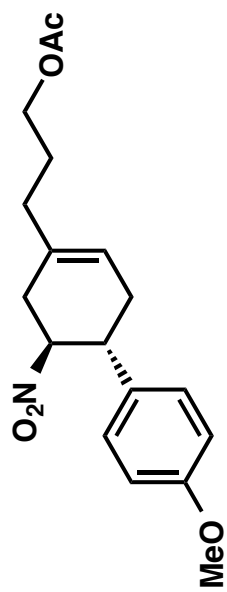
**5-115**  
**<sup>13</sup>C NMR**  
**(100 MHz, CDCl<sub>3</sub>)**



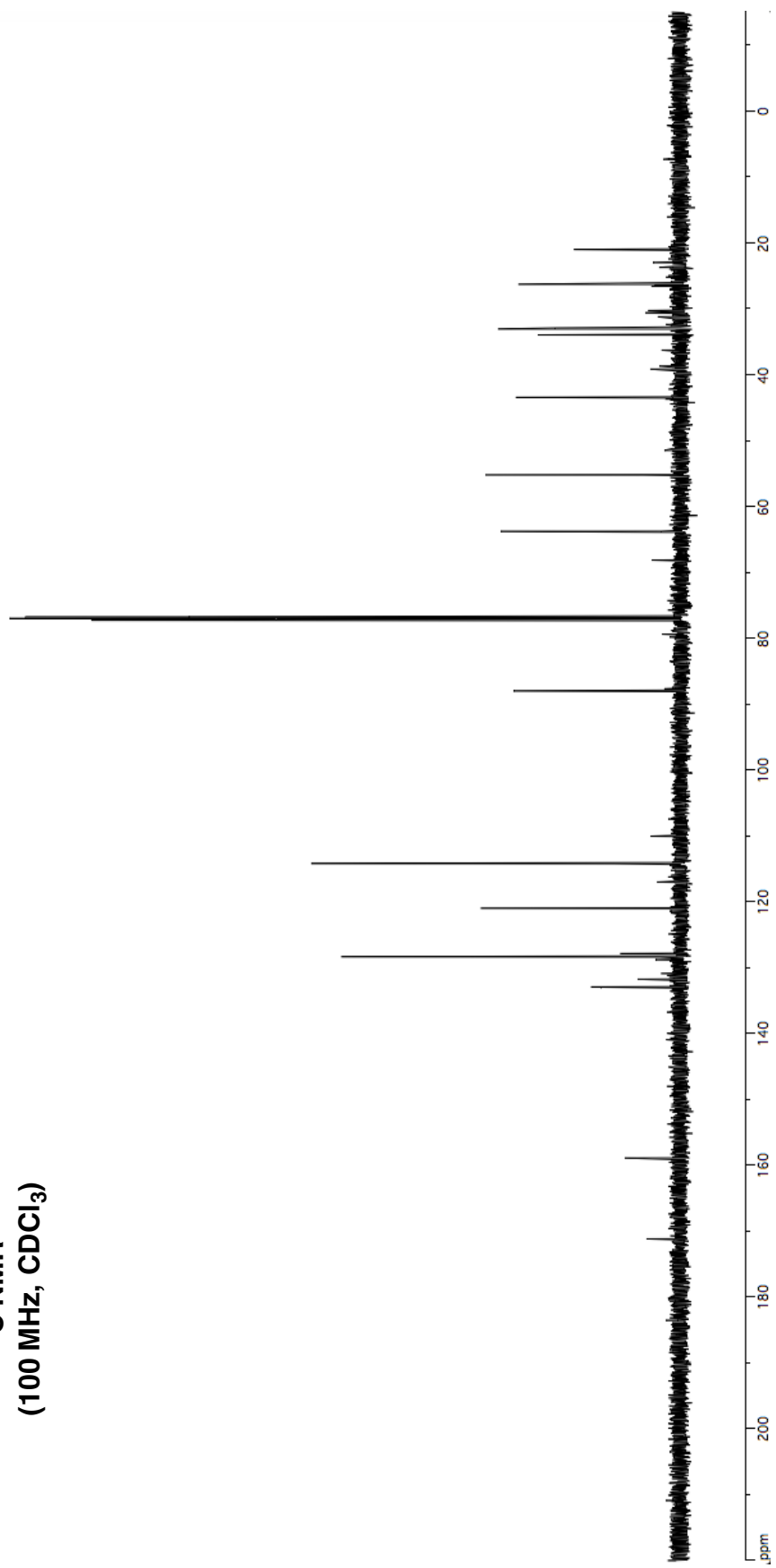


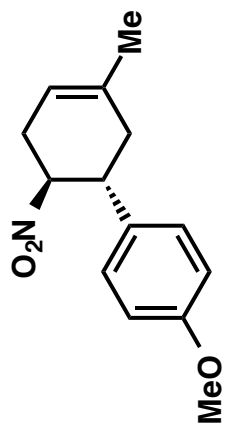
5-98  
<sup>1</sup>H NMR  
(400 MHz, CDCl<sub>3</sub>)





**5-98**  
**<sup>13</sup>C NMR**  
**(100 MHz, CDCl<sub>3</sub>)**

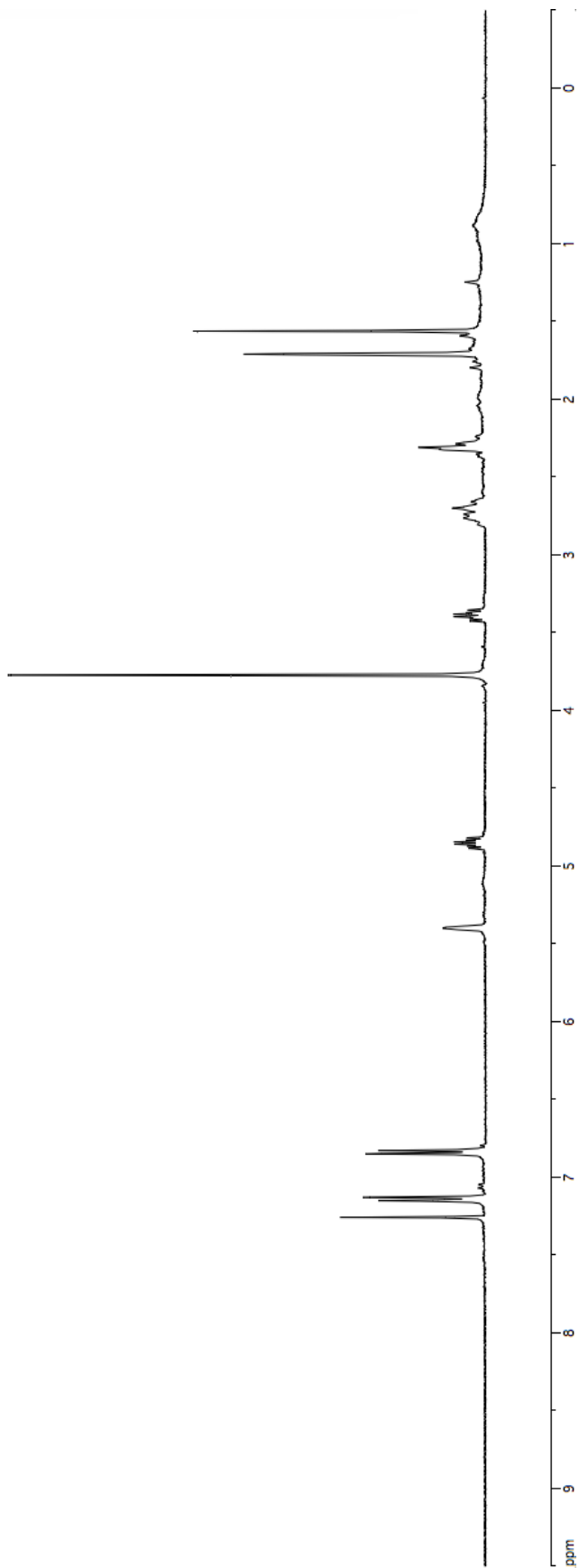


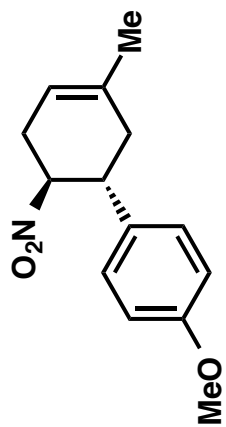


5-96

<sup>1</sup>H NMR

(400 MHz, CDCl<sub>3</sub>)

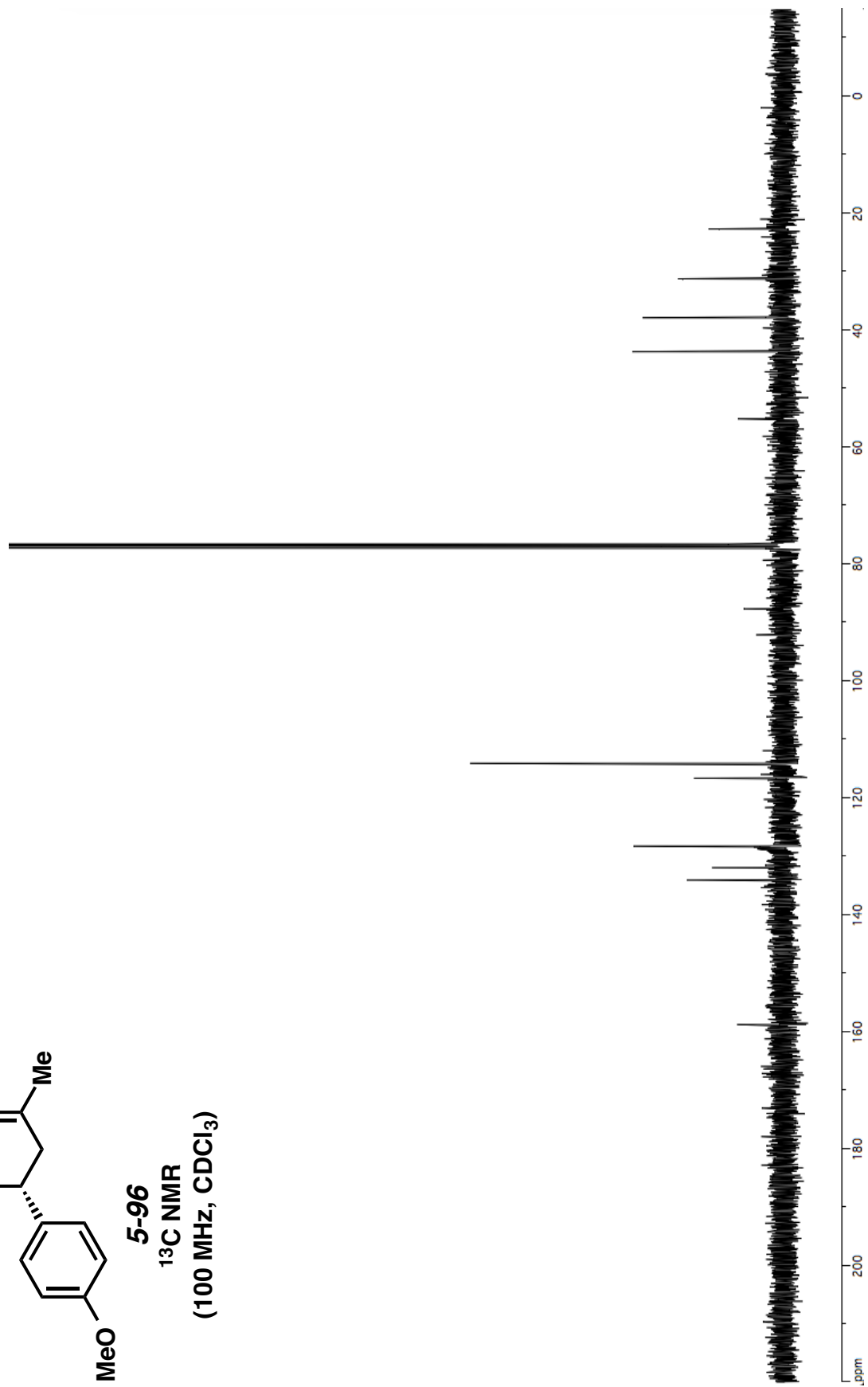


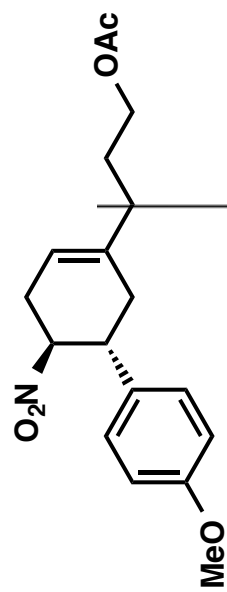


5-96

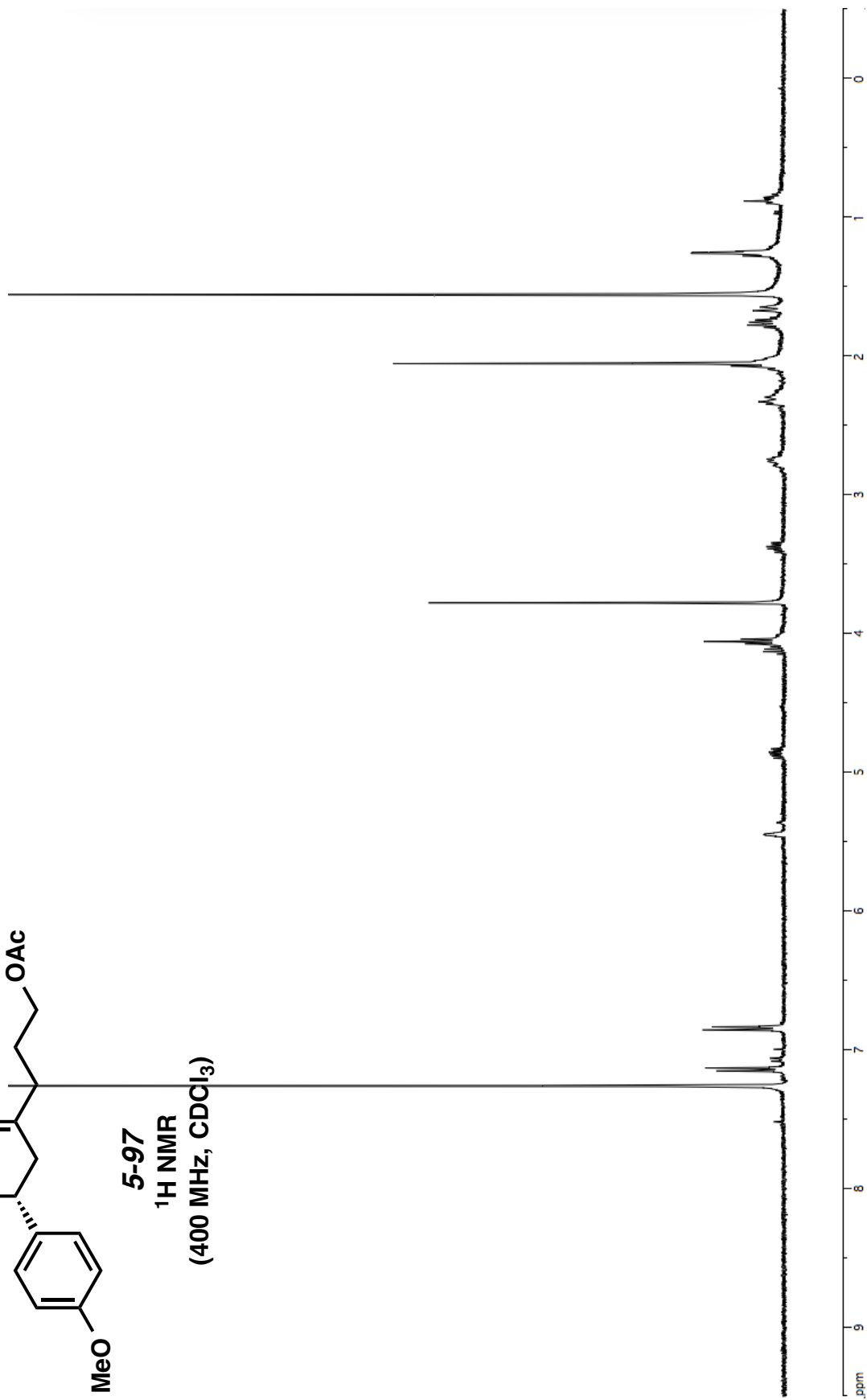
<sup>13</sup>C NMR

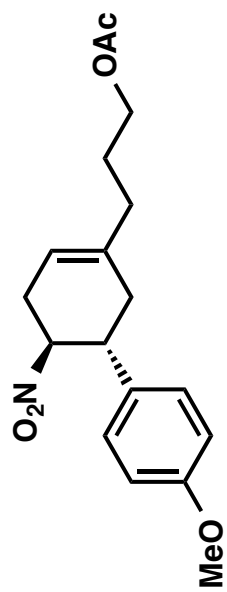
(100 MHz, CDCl<sub>3</sub>)



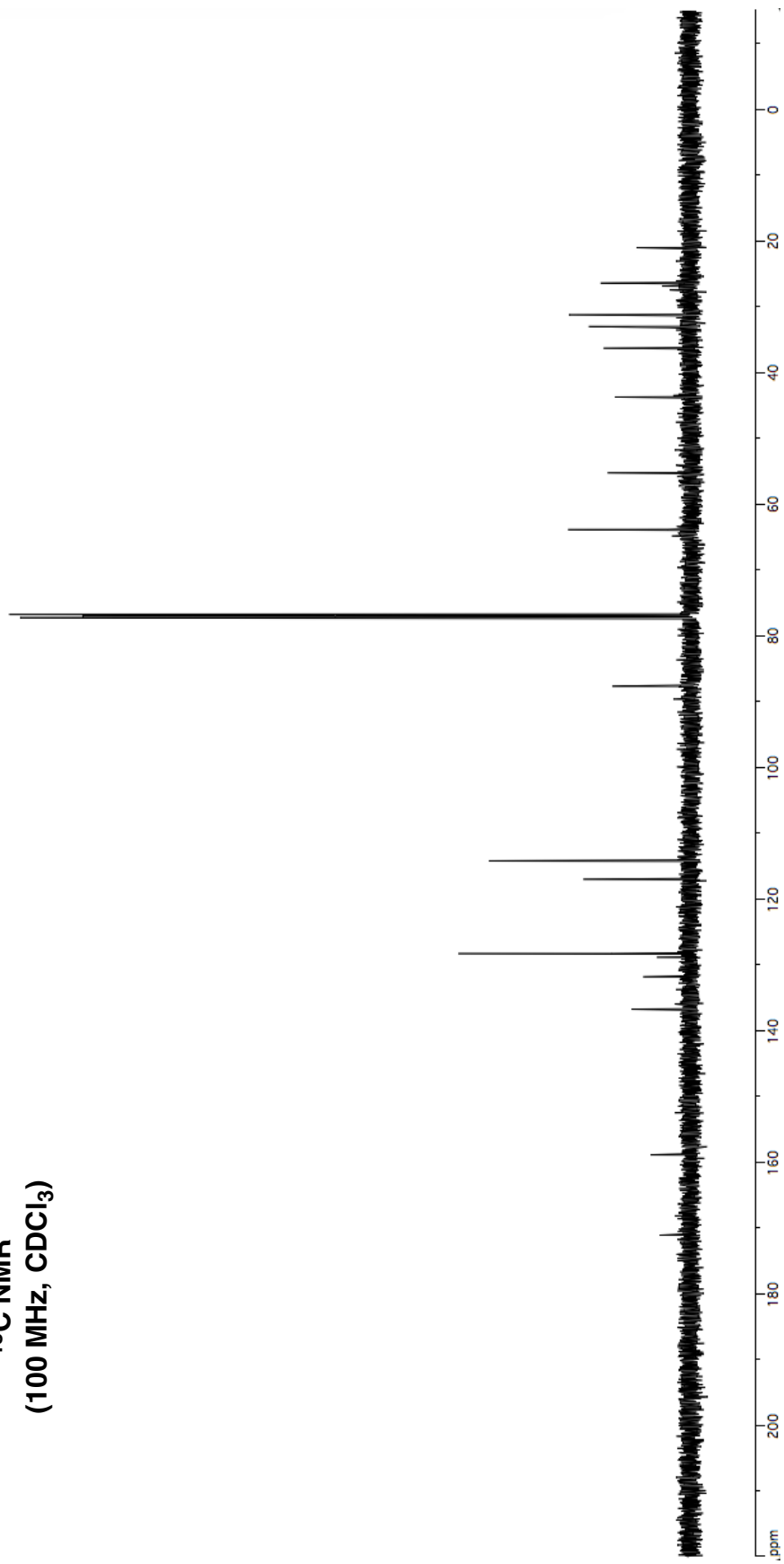


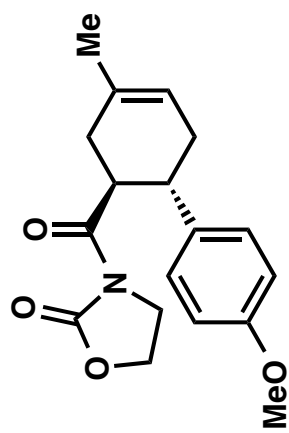
5-97  
<sup>1</sup>H NMR  
(400 MHz, CDCl<sub>3</sub>)



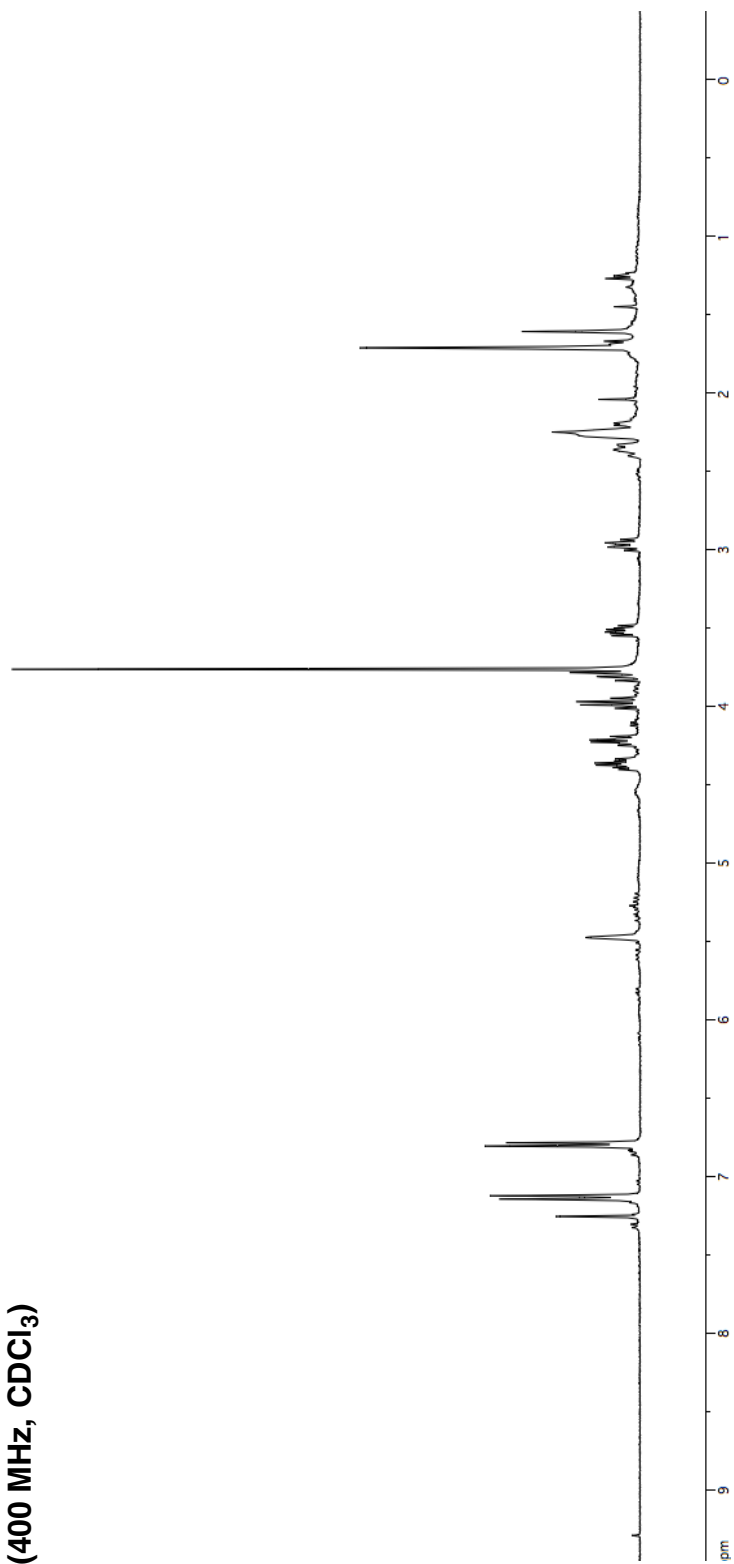


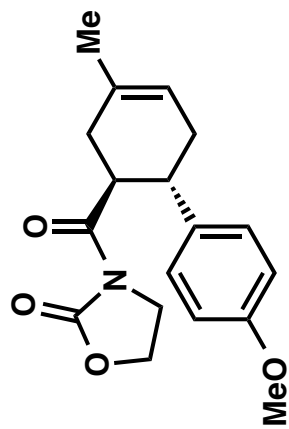
**5-97**  
<sup>13</sup>C NMR  
(100 MHz, CDCl<sub>3</sub>)



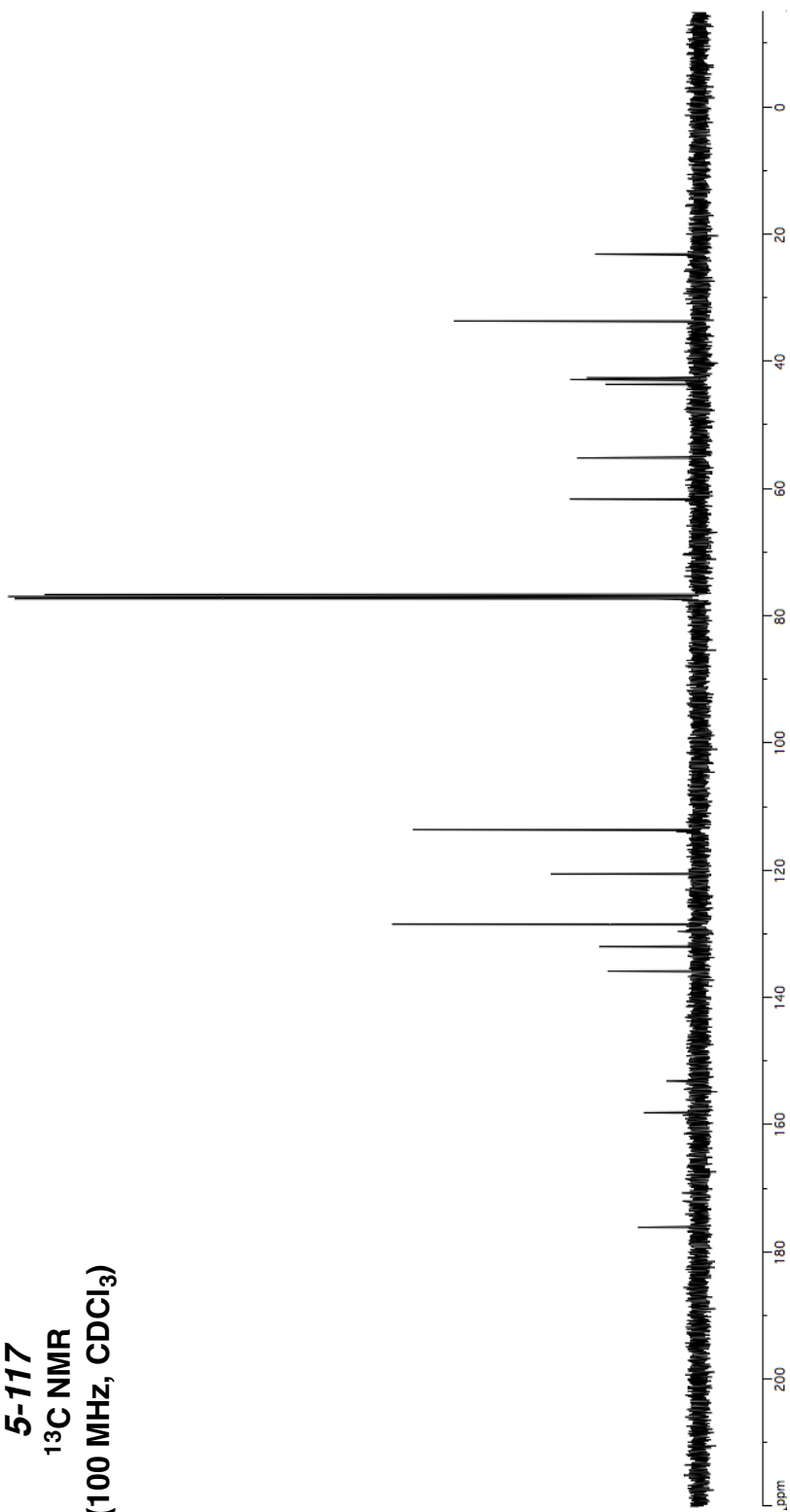


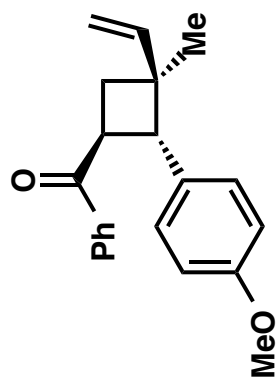
5-117  
<sup>1</sup>H NMR  
(400 MHz, CDCl<sub>3</sub>)



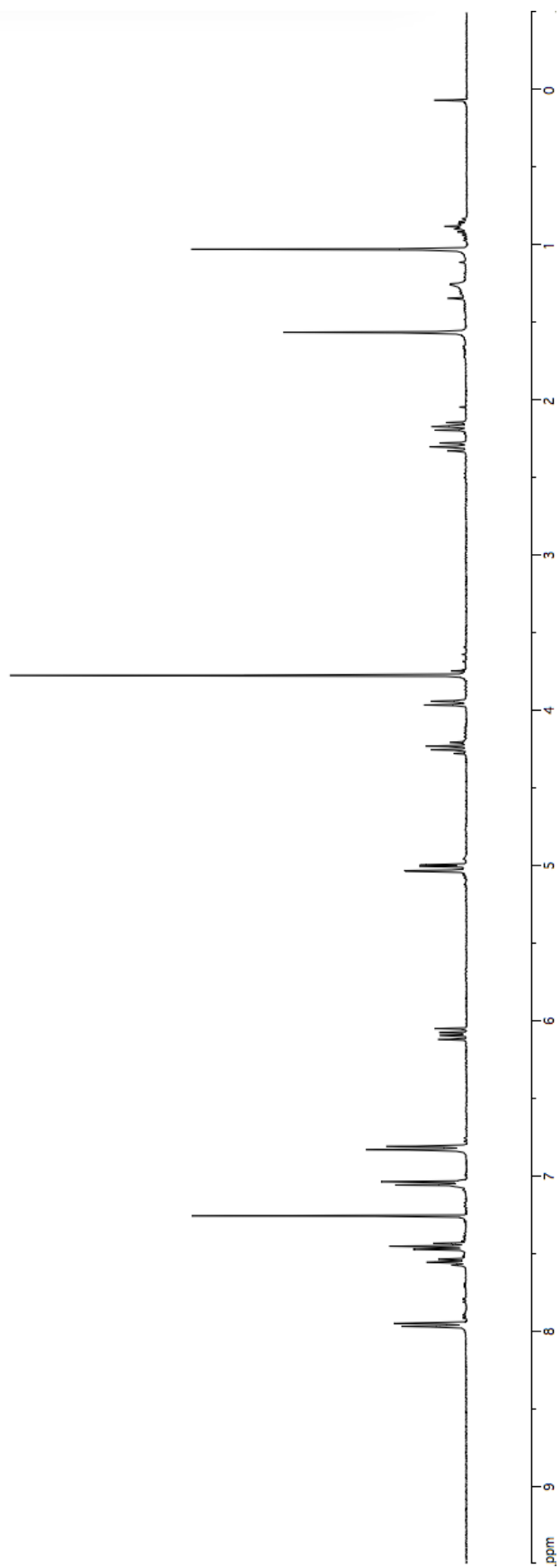


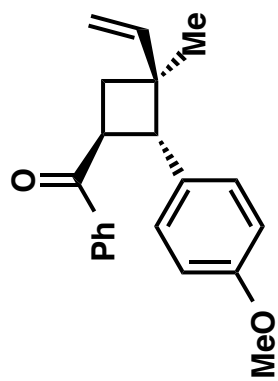
**5-117**  
**<sup>13</sup>C NMR**  
**(100 MHz, CDCl<sub>3</sub>)**



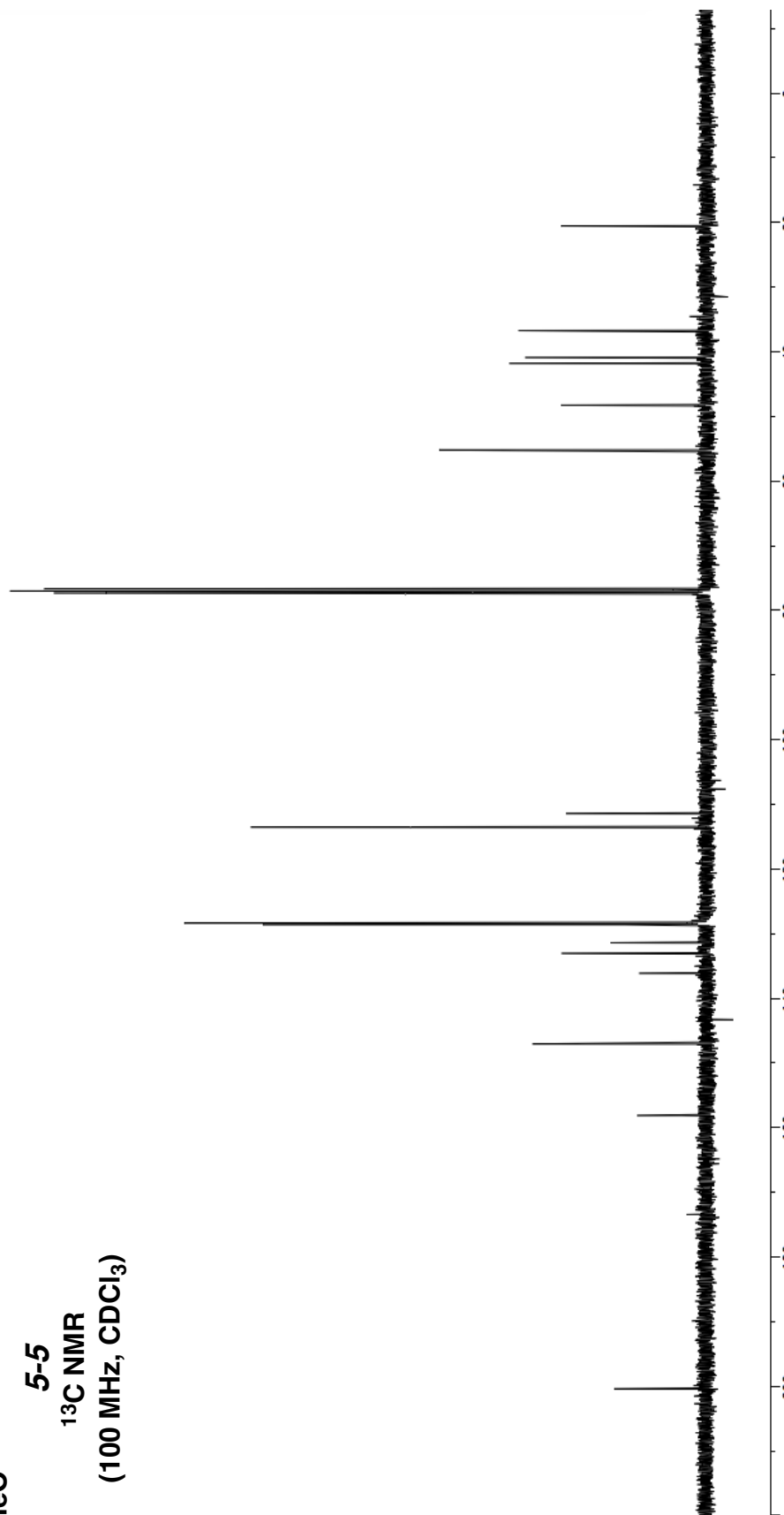


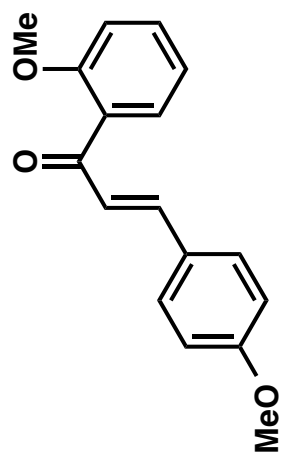
5-5  
<sup>1</sup>H NMR  
(400 MHz, CDCl<sub>3</sub>)



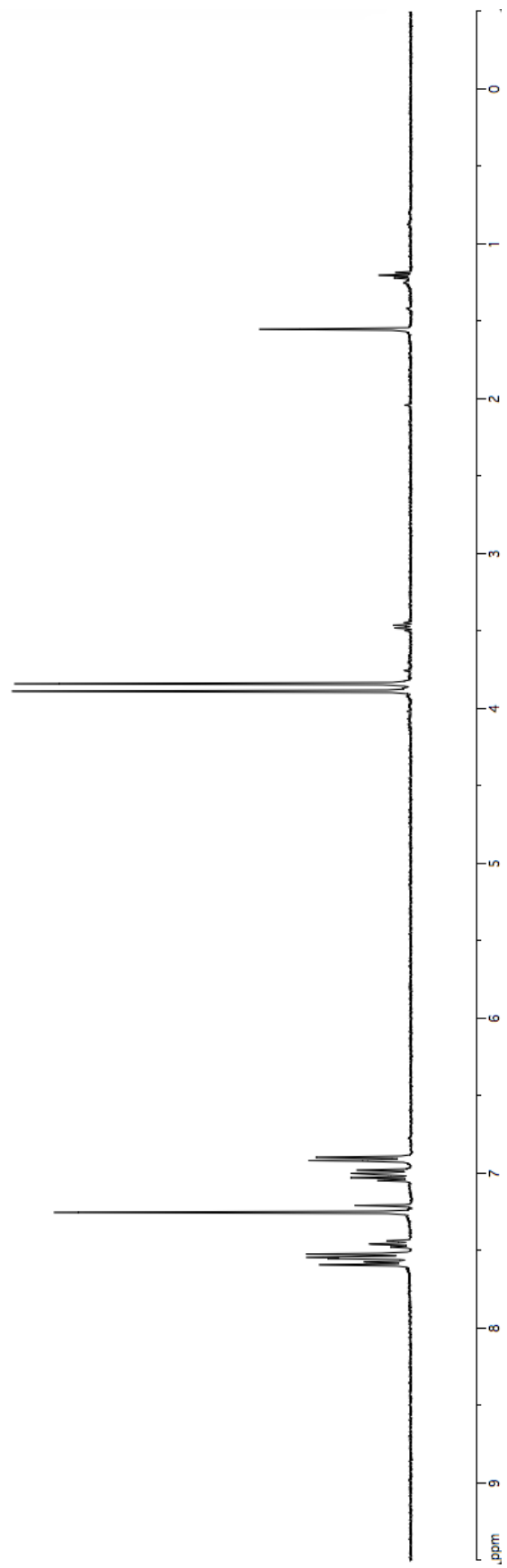


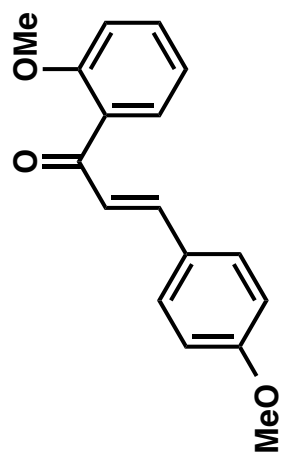
5-5  
<sup>13</sup>C NMR  
(100 MHz, CDCl<sub>3</sub>)



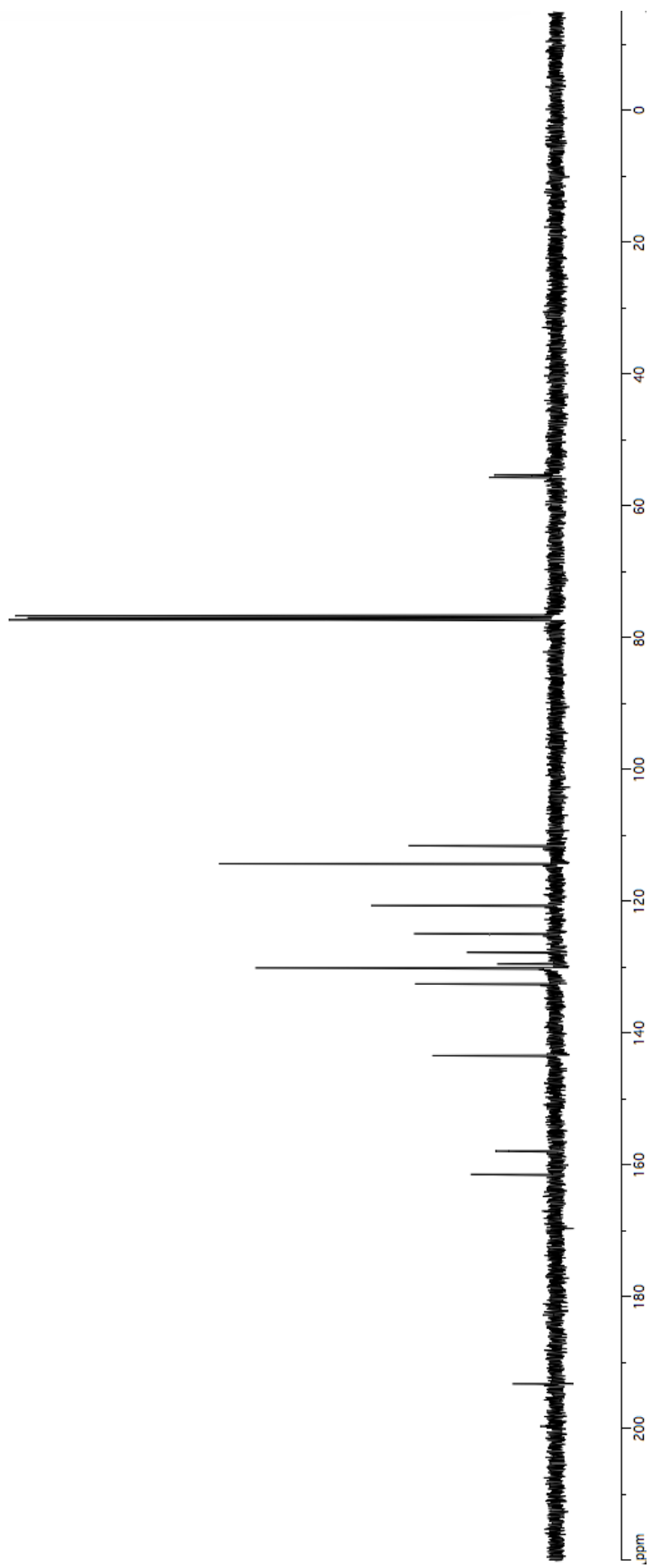


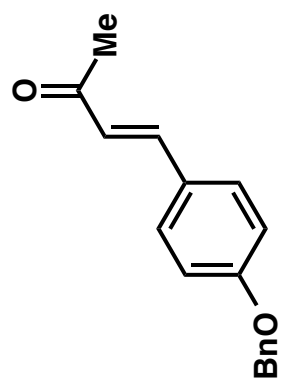
**5-139**  
**<sup>1</sup>H NMR**  
**(400 MHz, CDCl<sub>3</sub>)**



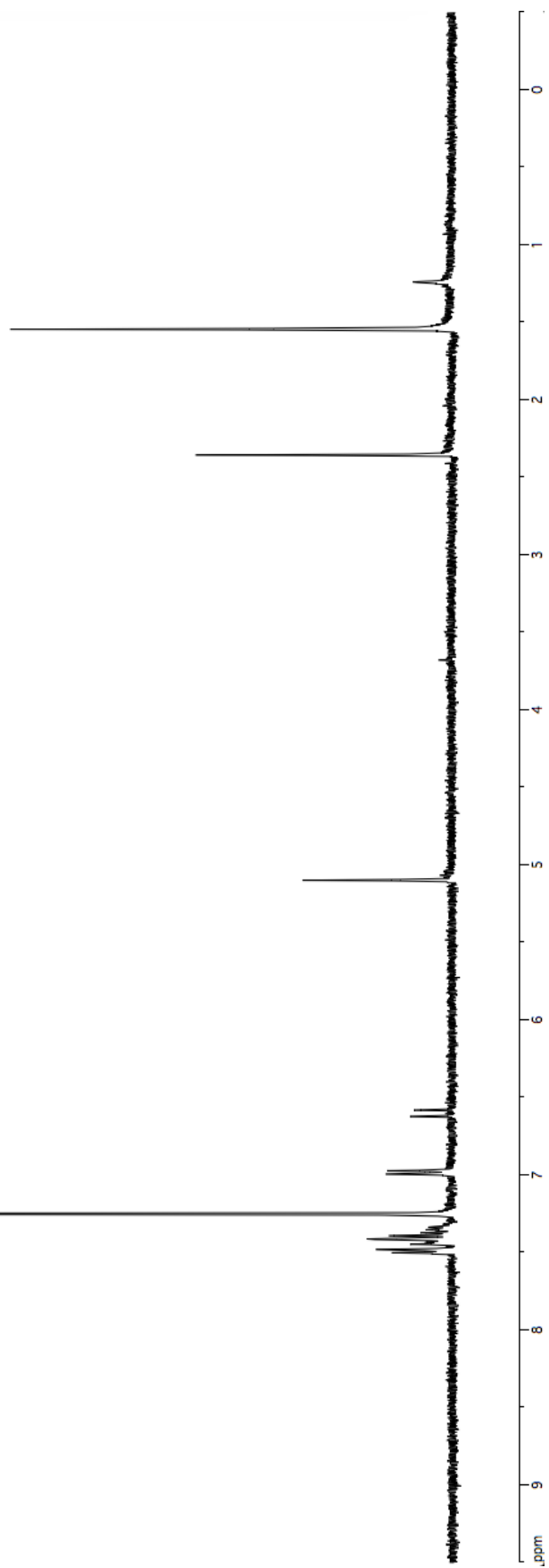


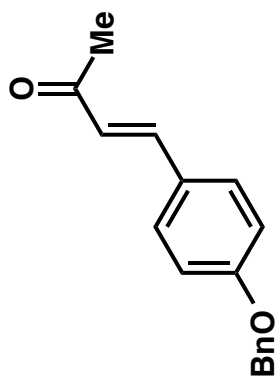
**5-139**  
**<sup>13</sup>C NMR**  
**(100 MHz, CDCl<sub>3</sub>)**



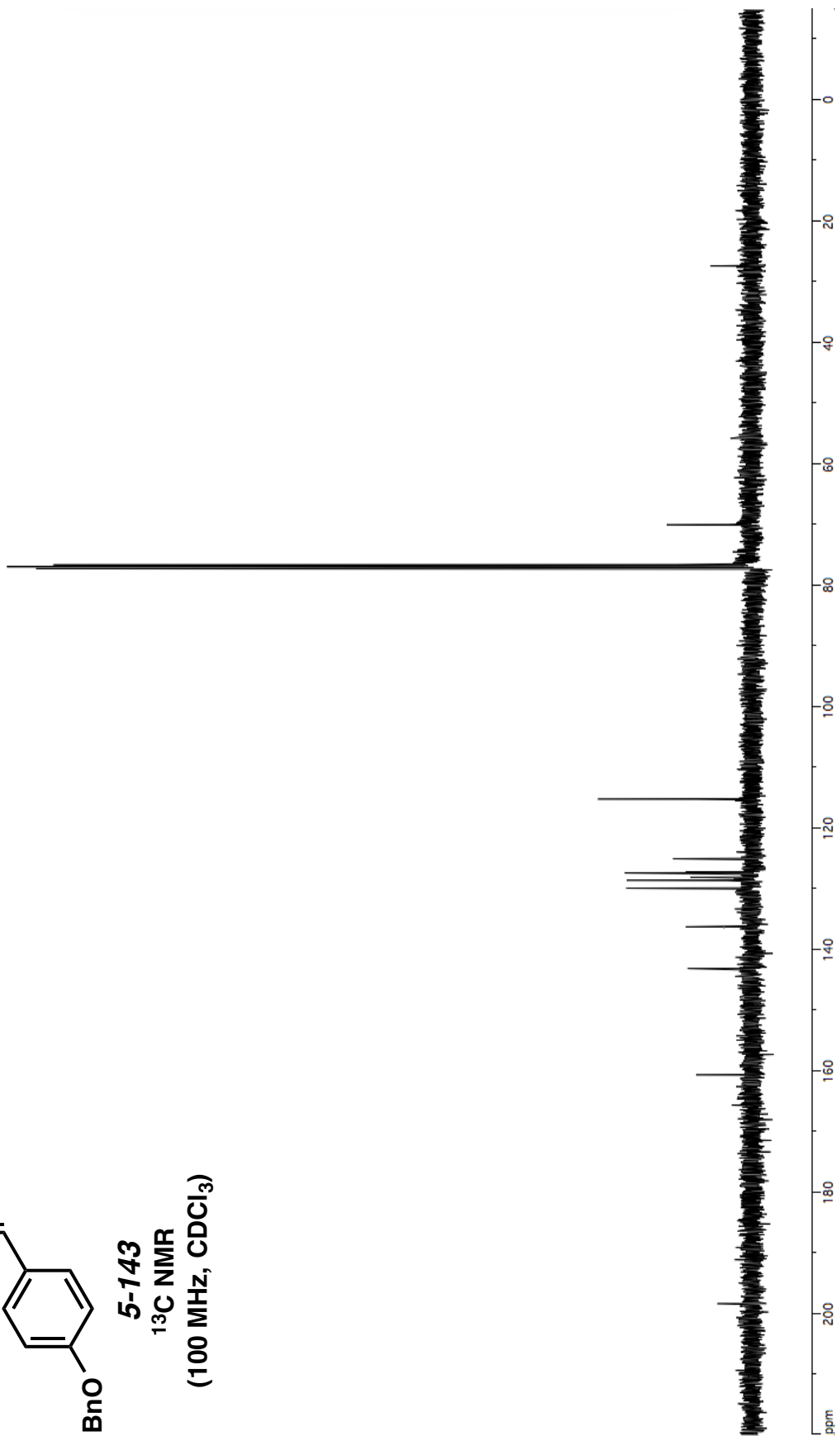


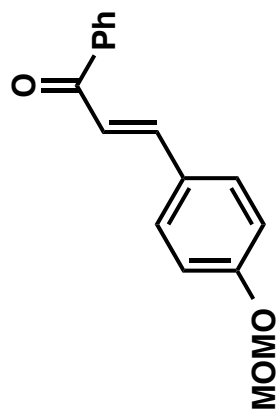
**5-143**  
**<sup>1</sup>H NMR**  
**(400 MHz, CDCl<sub>3</sub>)**



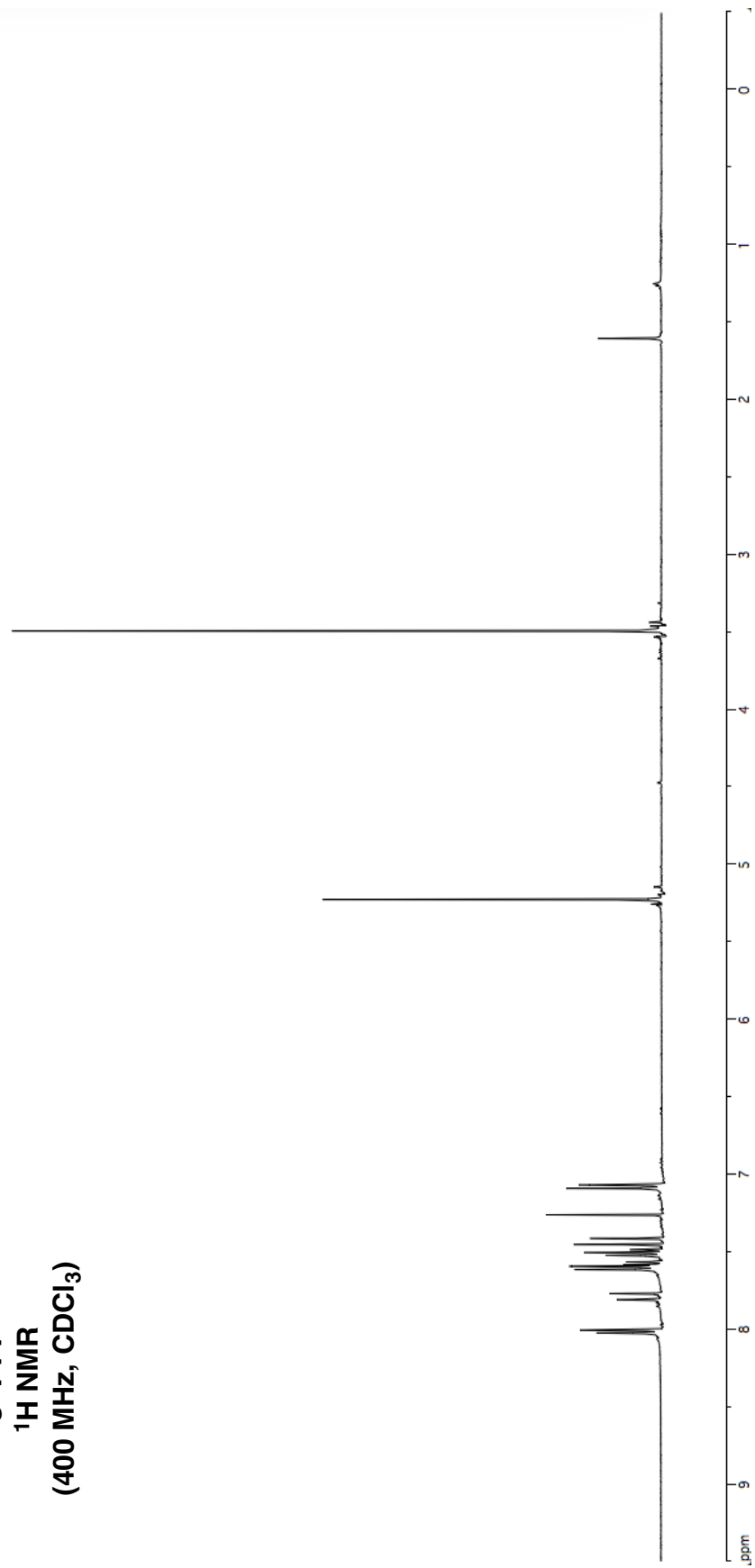


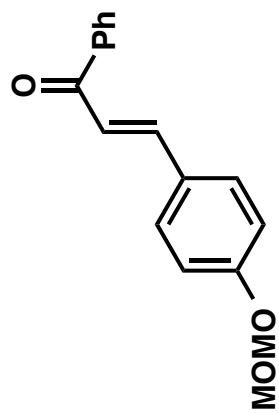
**5-143**  
**<sup>13</sup>C NMR**  
**(100 MHz, CDCl<sub>3</sub>)**



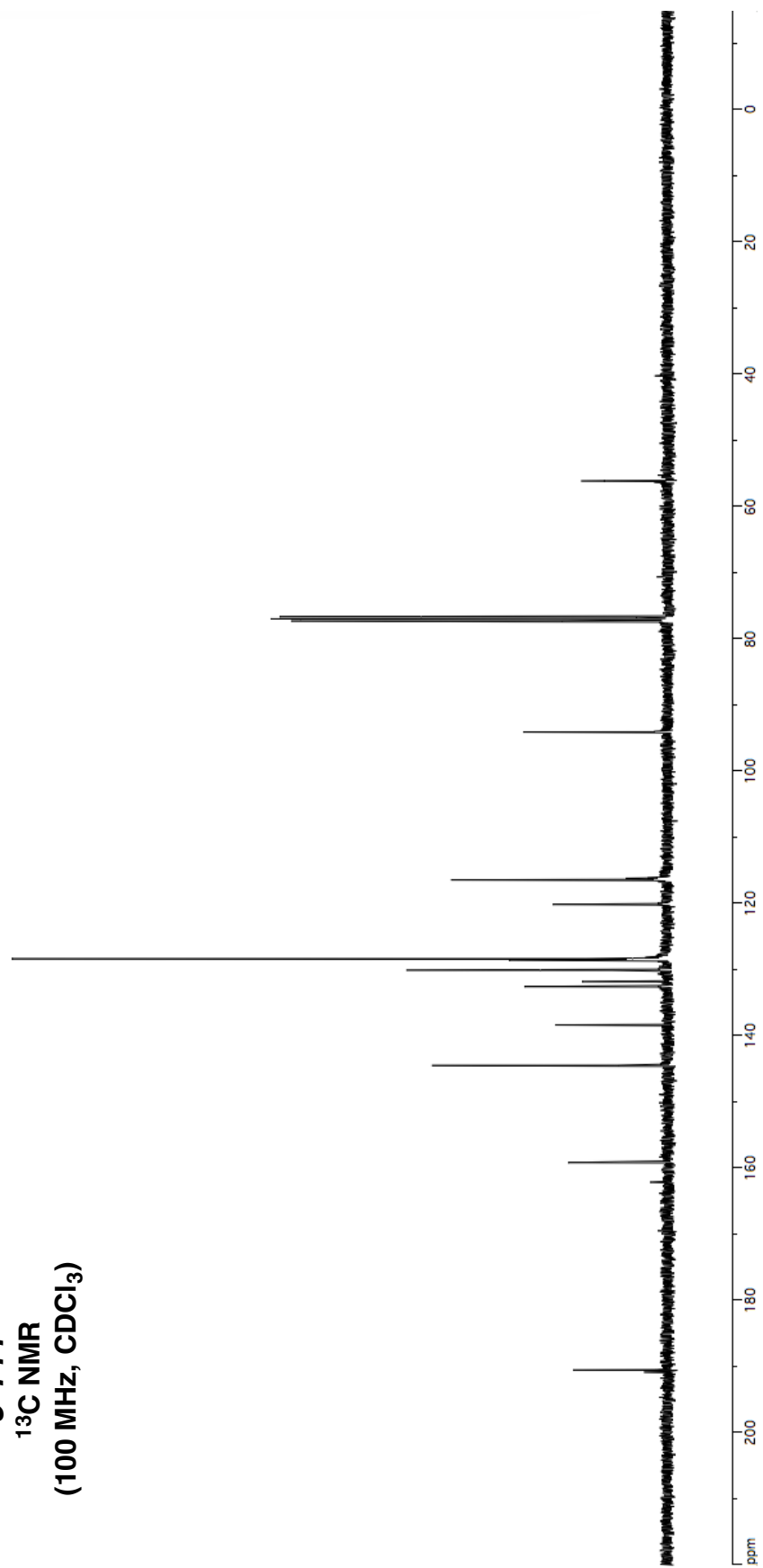


5-144  
<sup>1</sup>H NMR  
(400 MHz, CDCl<sub>3</sub>)



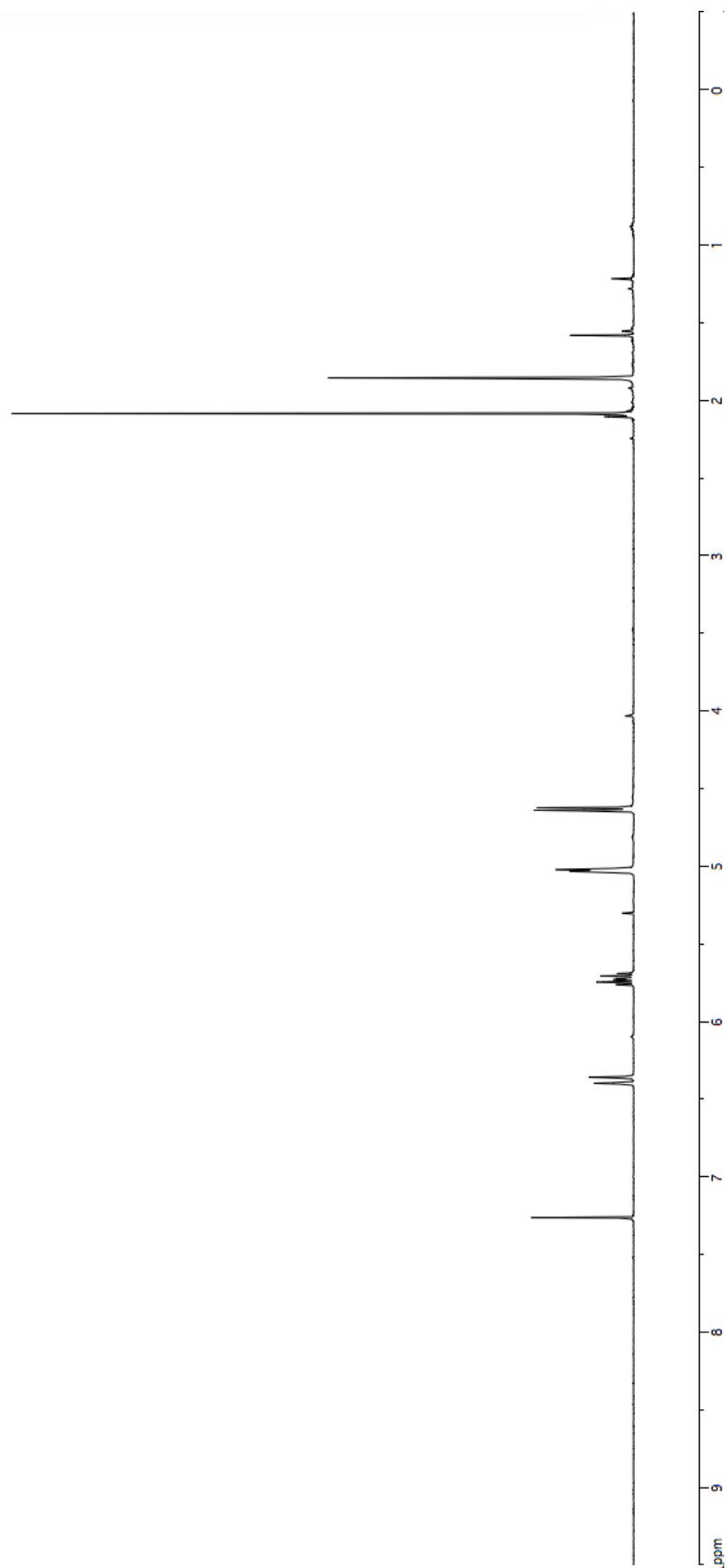


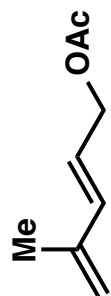
**5-144**  
**<sup>13</sup>C NMR**  
**(100 MHz, CDCl<sub>3</sub>)**





**5-149**  
**<sup>1</sup>H NMR**  
**(400 MHz, CDCl<sub>3</sub>)**

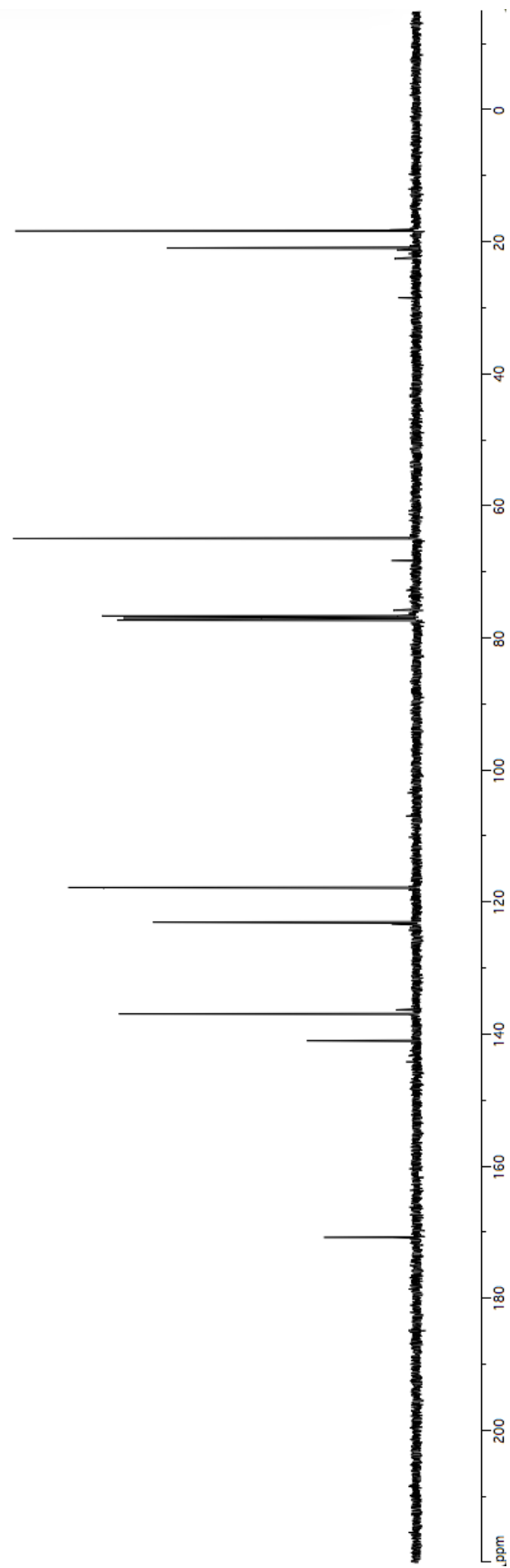


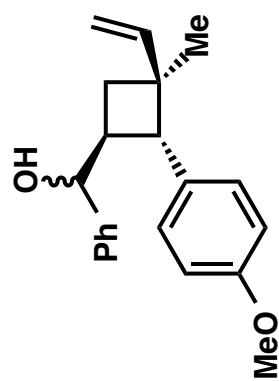


**5-149**

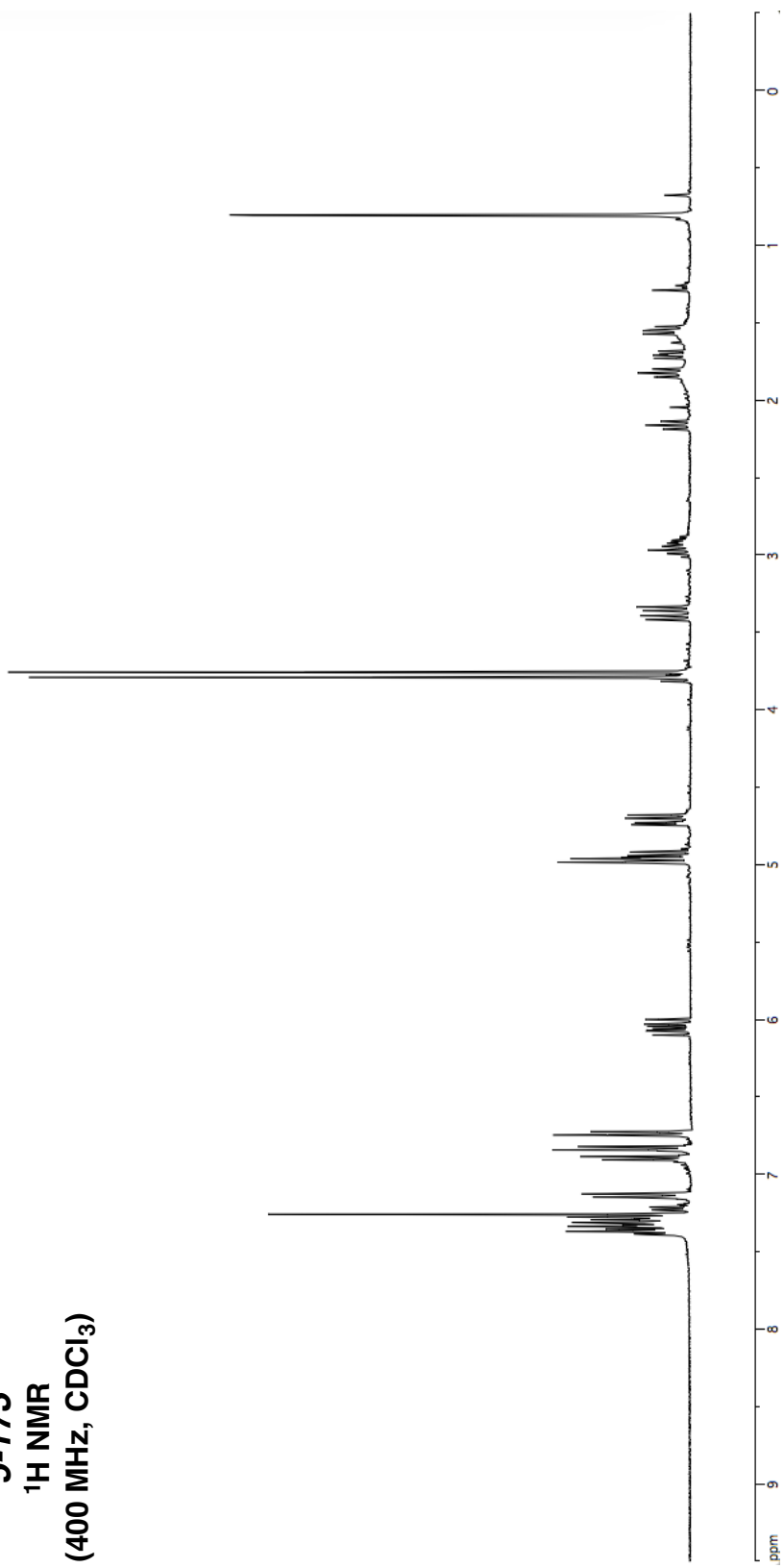
<sup>13</sup>C NMR

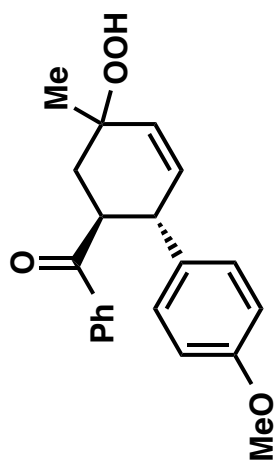
(100 MHz, CDCl<sub>3</sub>)





**5-173**  
**<sup>1</sup>H NMR**  
**(400 MHz, CDCl<sub>3</sub>)**

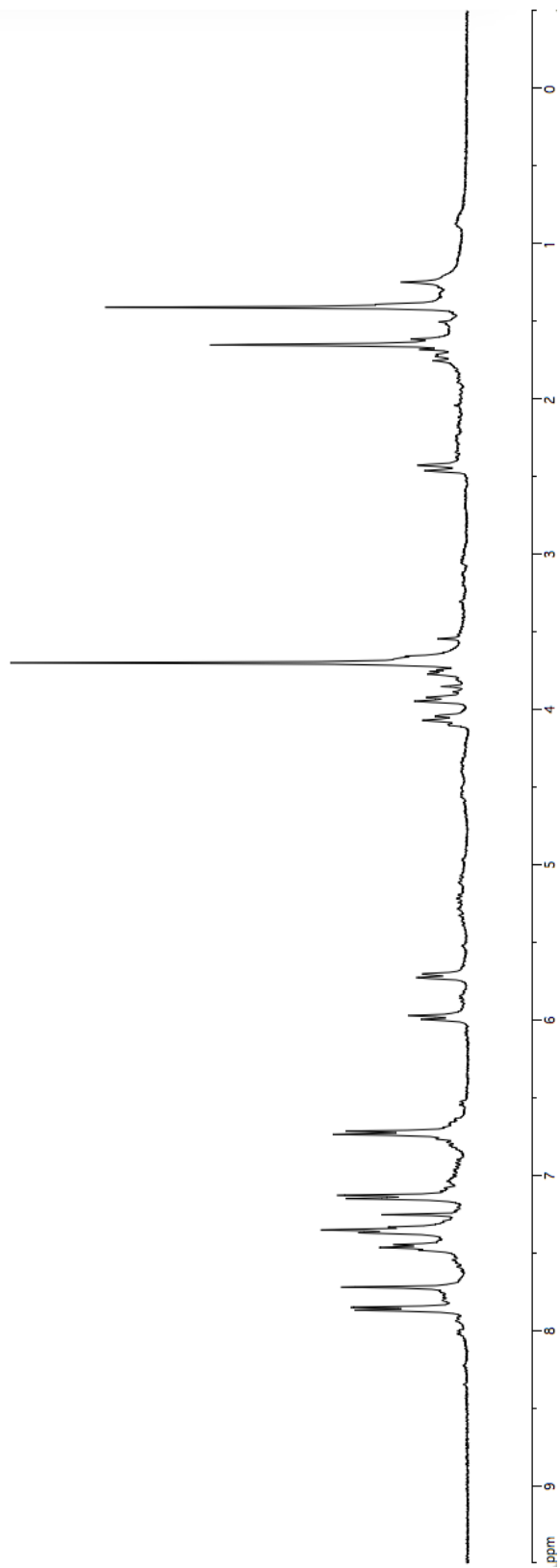


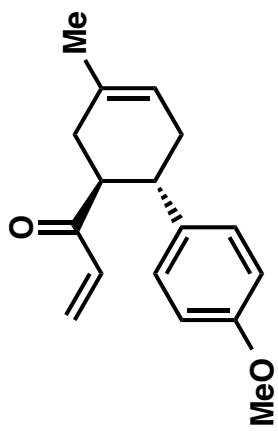


5-10

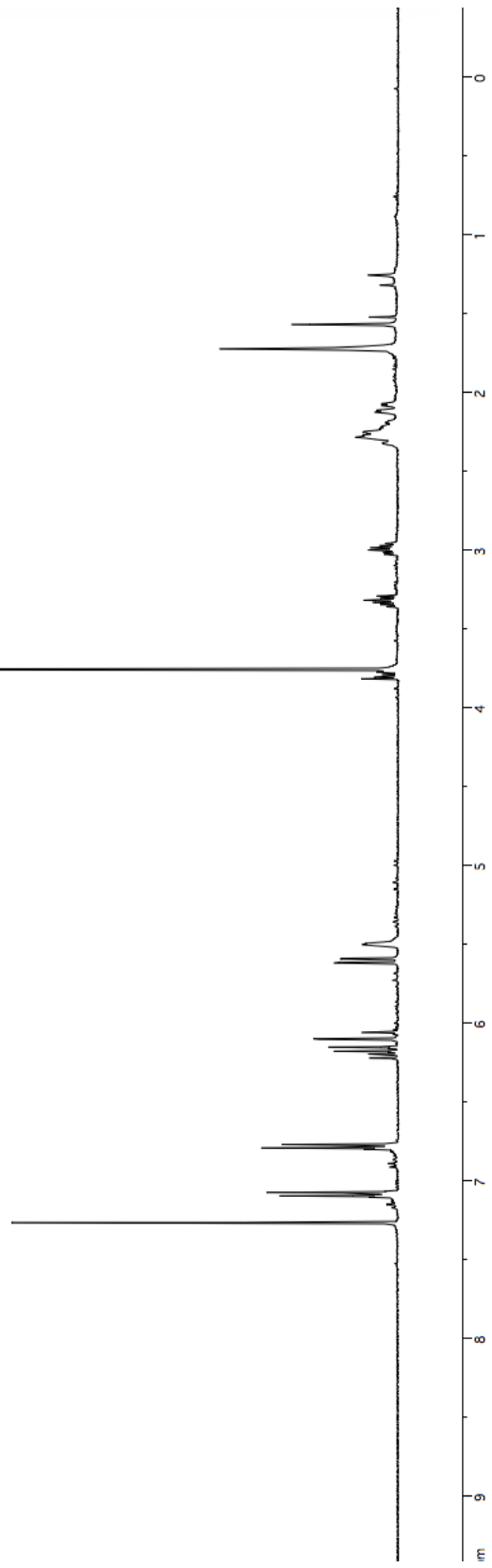
<sup>1</sup>H NMR

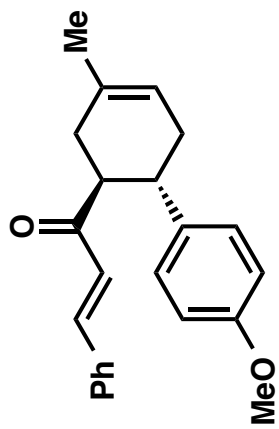
(400 MHz, CDCl<sub>3</sub>)



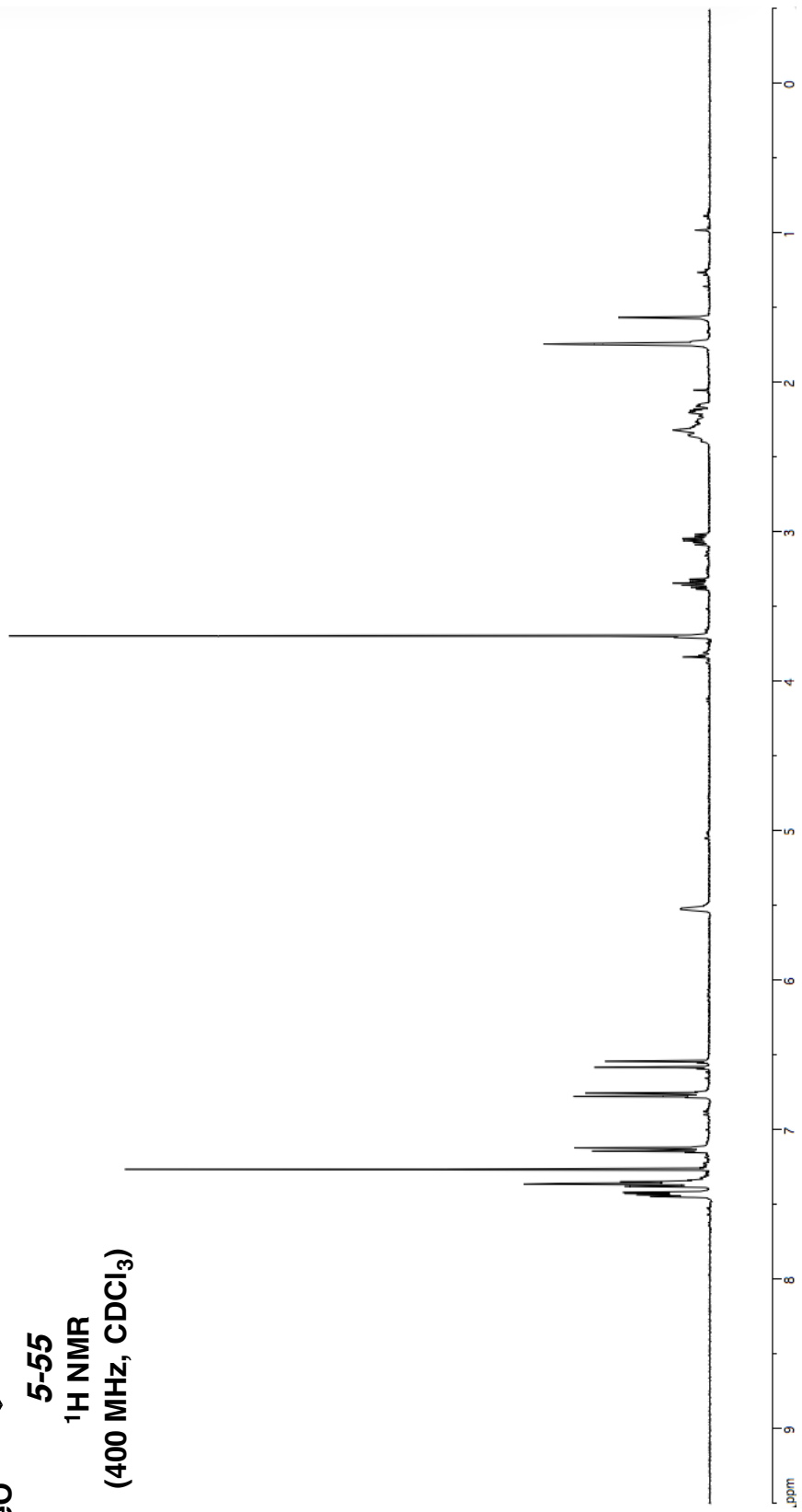


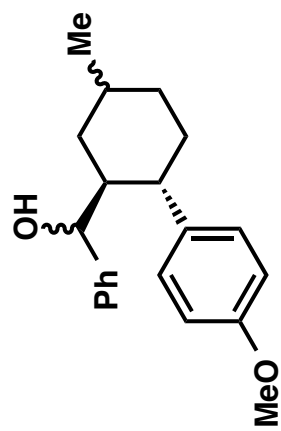
**5-54**  
**<sup>1</sup>H NMR**  
**(400 MHz, CDCl<sub>3</sub>)**



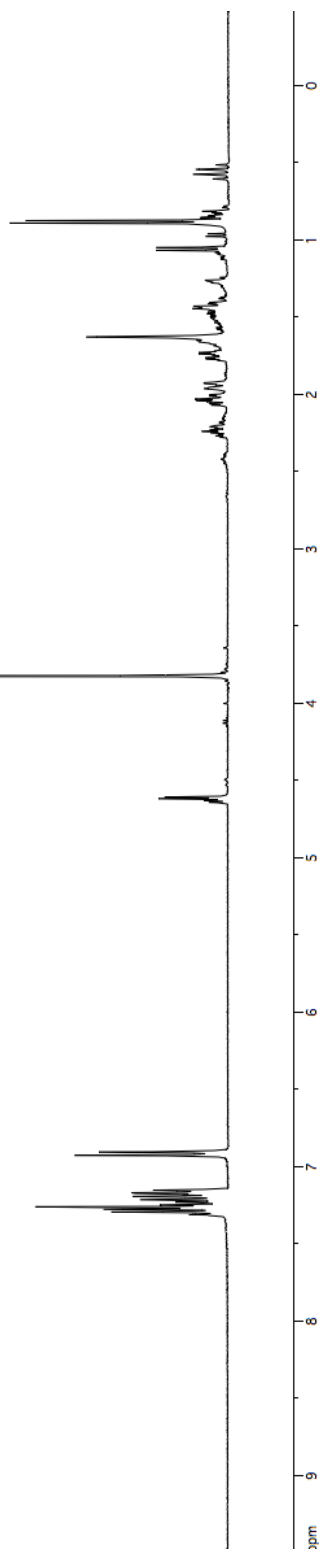


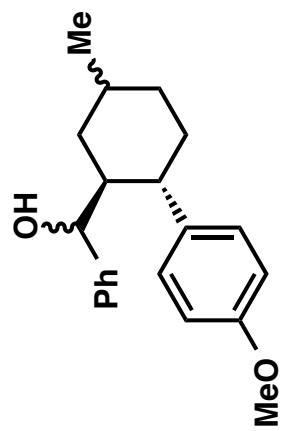
5-55  
<sup>1</sup>H NMR  
(400 MHz, CDCl<sub>3</sub>)



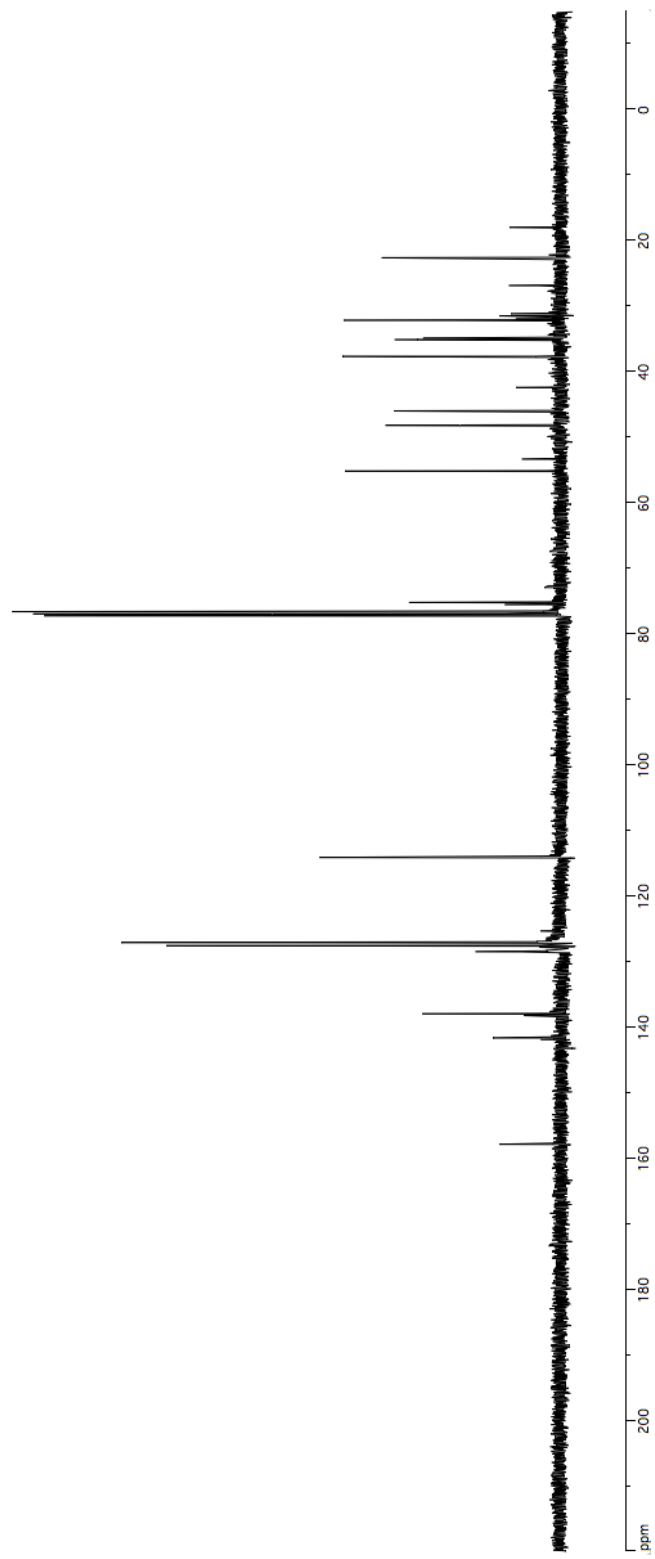


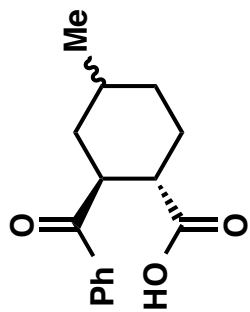
5-175  
<sup>1</sup>H NMR  
(400 MHz, CDCl<sub>3</sub>)





**5-175**  
**<sup>13</sup>C NMR**  
**(100 MHz, CDCl<sub>3</sub>)**

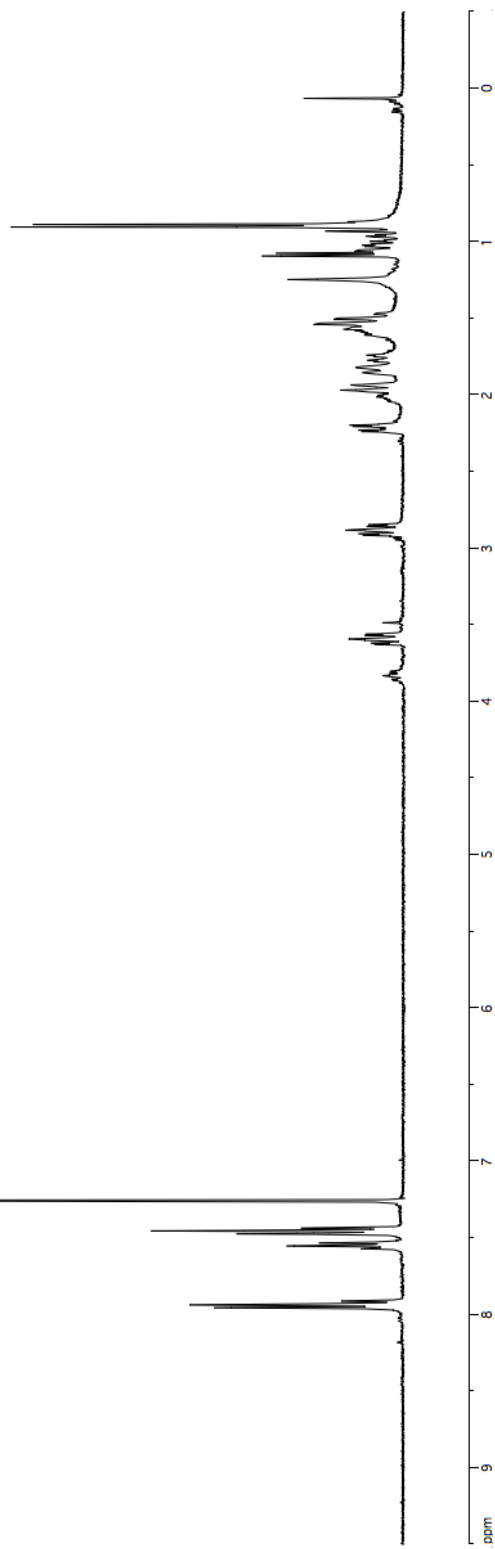


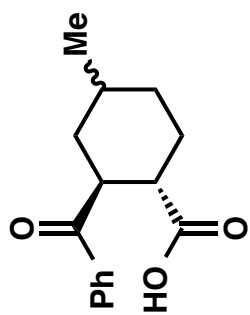


5-99

<sup>1</sup>H NMR

(400 MHz, CDCl<sub>3</sub>)

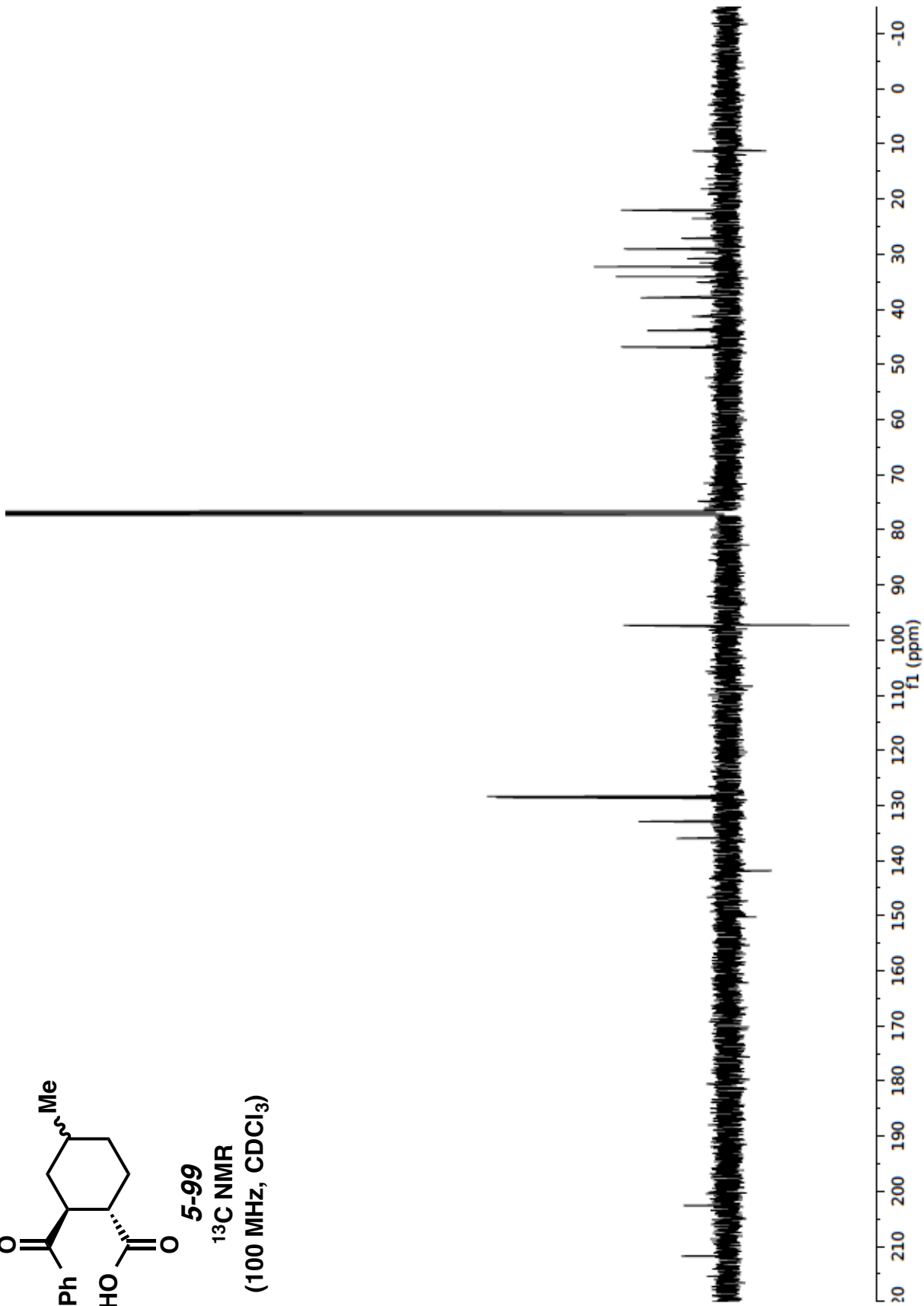


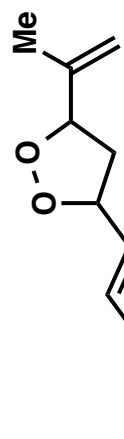


5-99

<sup>13</sup>C NMR

(100 MHz, CDCl<sub>3</sub>)





**5-135**  
**<sup>1</sup>H NMR**  
**(400 MHz, CDCl<sub>3</sub>)**

